Czech Lighting Society

Slovak Lighting Society

PROCEEDINGS

of the
14th European Lighting Conference

LUX EUROPA 2022

LIGHTING AT THE DAWN
OF THE NEW ERA

20 – 22 September 2022
PRAGUE – CZECH REPUBLIC – HEART OF EUROPE

with kindful support of golden sponsor

YD ILLUMINATION

PROCEEDINGS

14th European Lighting Conference

LUX EUROPA 2022

20 – 22 September 2022
Prague, Czech Republic

ISBN 978-80-11-02269-3


YD® ILLUMINATION | Since 1984
3D Printed Luminaires:
• Any color, any size & shape, any texture
• Anti-UV
• Flame retardant V-0
• Could be used in outdoor application
• Personal customization and unique
• Can be reuse, reprint and recycle
YDSIGN
CONTACT INFORMATION
Mobile: +8618867506219
WeChat/WhatsApp: +86 18867506219
E-mail: info@ydsign.com
Add:No.587,kangxin Road,District,Hangzhou.Zhejiang,China
www.ydsign.com

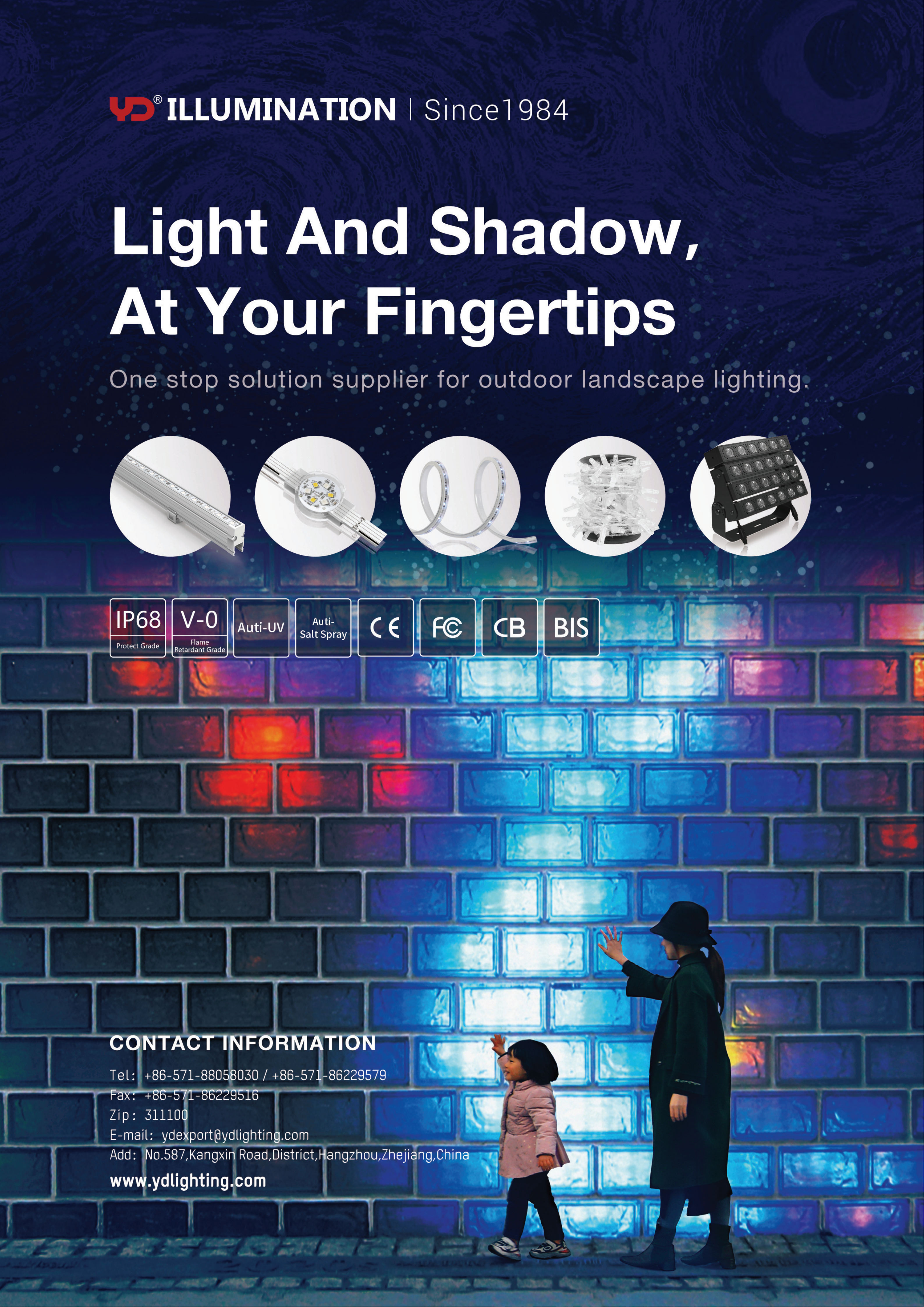
YD® ILLUMINATION | Since1984
Light And Shadow,
At Your Fingertips
One stop solution supplier for outdoor landscape lighting.
IP68 Protect Grade
V-0 Flame Retardant Grade
Auti-UV
Auti-Salt Spray
CE
FC
CB
BIS
CONTACT INFORMATION
Tel: +86-571-88058030 / +86-571-86229579
Fax: +86-571-86229516
Zip: 311100
E-mail: ydexport@ydlighting.com
Add: No.587,Kangxin Road,District,Hangzhou,Zhejiang,China
www.ydlighting.com

LUX EUROPA 2022

Proceedings of the
14th European Lighting Conference

Publishing house:
Česká společnosť pro osvětlování, z.s.
17. listopadu 2172/15, 708 00 Ostrava – Poruba, Czech Republic
Tel.: +420 602 724207, E-mail: tomas.novak1@vsb.cz

1st Edition
Prague (Czech Republic), September 2022

412 pages
200 pcs on USB stick

ISBN 978-80-11-02269-3
EAN 9788011022693

PART I

Scientific papers

The Influence of Light on Alertness when Walking or Driving in the Evening

Nima Hafezparast Moadab
School of Architecture
University of Sheffield
Sheffield, UK
n.hafezparastmoadab@sheffield.ac.uk

Aysheh AM Alshdaifat
School of Architecture
University of Sheffield
Sheffield, UK
a.alshdaifat@sheffield.ac.uk

Steve Fotios
School of Architecture
University of Sheffield
Sheffield, UK
steve.fotios@sheffield.ac.uk

***Abstract*—This paper reports an experiment conducted to investigate the effect of light on alertness in a context intended to represent driving or walking in the evening. Four lighting conditions were employed, darkness, typical road lighting, and increases in illuminance and short wavelength content to enhance circadian stimulation. Analyses of melatonin levels and responses (reaction times) to an acoustic stimulus did not suggest any significant effects.**

Keywords—road lighting, alertness, walking, driving

I. Introduction

One key purpose of road lighting is to allow road users to proceed safely [1]. For the motorist, a role of road lighting is to reveal extraneous objects that suddenly appear on the road, in particular those beyond the reach of vehicle headlights, with the aim of giving sufficient time to allow evasive action to be taken without resorting to an abrupt manoeuvre [1]. For the pedestrian, road lighting helps to reveal trip hazards [2], helps to reveal the approach of oncoming vehicles, and helps to raise the visibility of pedestrians to oncoming vehicles.

There is some evidence that higher levels of light enhance hazard detection [3,4] or, reduce road traffic collisions (RTC) [5,6], but there remains uncertainty as to whether current standards deliver optimal recommendations [7]. For those studies testing vision directly, such as experiments of visual detection, one limitation is that alertness has not been considered. Alertness, also known as vigilance, arousal or sustained attention [8], describes the activation states of the cerebral cortex and affects ability to process information. Decrement in alertness means a decline in the performance of tasks requiring attention over an extended period [9] and can increase the risk of an RTC [10].

Alertness is subject to diurnal variation as controlled by circadian pacemaker and homeostatic process of sleep [11, 12]. In the evening, for normal chronotypes, we might therefore expect in reduction in alertness with the passing of time towards habitual time of sleep. Lighting of enhanced short wavelength content more strongly stimulates the ipRGC, the photoreceptor which feeds into the circadian system. Enhanced short wavelength content might be achieved by common white light sources of higher luminance, or, sources with a blue-rich spectrum.

This was examined by Bhagavathula et al., 2021 [13] in the context of motorists, with participants driving for two hours (01:00 to 03:00) on a closed loop road after a two-hour adaptation period (23:00 to 01:00) under normal home-indoor lighting levels. They included five lighting conditions, these resembling conditions typical of road lighting:

- HPS, 2100K, 1.5 cd/m^2
- LED, 4000K, 1.5 cd/m^2
- LED, 4000K, 1.0 cd/m^2
- LED, 4000K, 0.7 cd/m^2
- No road lighting (<0.05 cd/m^2).

Their findings did not suggest a statistically significant impact of lighting condition on either of their measures - melatonin levels derived from saliva samples (see Fig. 1), self-report of sleepiness, nor response to a visual reaction time test. CIE suggest that circadian stimulation is modelled using equivalent daylight illuminance (EDI) melanopic lux [14]. The adaptation phase presented an EDI of 87 lx. The four lit test phases presented EDIs of 0.3 to 0.8 lx. It is possible that using lighting giving a higher EDI, rather than using only lighting typical of current practice, would lead to a significant effect of lighting on measured alertness.

An experiment was conducted to investigate the degree to which road lighting mediates sleepiness and alertness when driving or walking. This was conducted in the laboratory to have better control over exposure (duration and visual stimulus) and with lighting giving a higher level of EDI.

II. Method

The experiment was designed to explore the impact of lighting on alertness in a context designed to simulate a typical evening: two hours sitting at home exposed to lighting of typical domestic characteristics (the adaptation phase) followed by one-hour exposure to outdoor lighting (the test phase). A one-hour test phase was chosen following analysis of typical journey times for walking and driving.

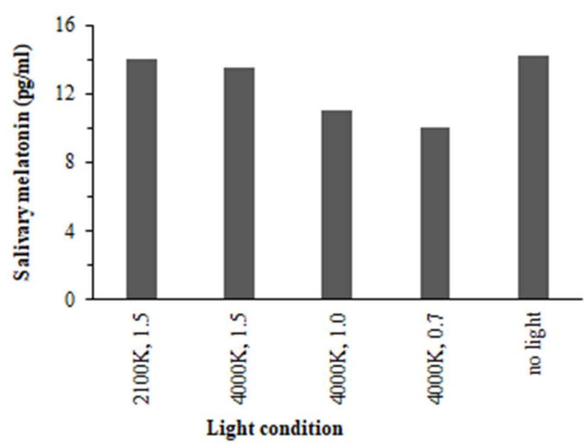

Fig. 1. Mean melatonin levels for different light conditions as estimated from Figure 13 in Bhagavathula et al. [13]). Light condition labels are CCT and photopic luminances.

This work was conducted within the LightCap project. The LightCap project has received funding from the European Union's Horizon 2020 research and innovation programme under the Marie Skłodowska-Curie grant agreement No. 860613.

Participants conducted the experiment in pairs. For the adaptation phase both participants were seated. For the test phase, one participant changed from being seated to walking on a treadmill to simulate pedestrian activity: the other participant remained seated. The trials were conducted in the evenings, with the test phase scheduled to be the hour before the participants' normal time of sleep and hence the adaptation period started 3 hours before the participant's normal sleep time. Participants were asked to arrive 45 min before the adaptation period to confirm and sign the consent to participate form, to check their visual acuity and color vision, to fix the skin temperature sensors and to establish their hearing threshold.

The test sample comprised 40 people aged 18-30 years. Participants were required to be (and, confirmed by self-report) healthy (including no short and long-term medication, regular sleep, and being a non-smoker), having habitual bedtime not later than midnight, not having been employed for night-time shift work in the past year, and not traveled over one or more time zones in the past 3 months. Participants were asked to keep a steady sleep-wake schedule for a week prior to the experiment. On the day of the experiment participants were asked to avoid consuming after midday any alcohol or caffeine and to refrain from napping.

The experiments were conducted in the laboratory shown in Fig. 2. During the adaptation phase, all participants were exposed to the same lighting condition (25 lx at the eye, 2700 K, 10.7 EDI lx). The sample was split into four groups of ten, with each group exposed to one of four lighting conditions during the test phase (Table 1):

- C1: Illuminance and spectrum representative of typical road light.
- C2: Same photopic illuminance as C1 but with increased short-wavelength content to better simulate the circadian system.
- C3: Same SPD as C1 but with the illuminance increased to give same melanopic EDI as C2. This is also the same condition as used in the adaptation phase.
- C4: a near-unlit environment.

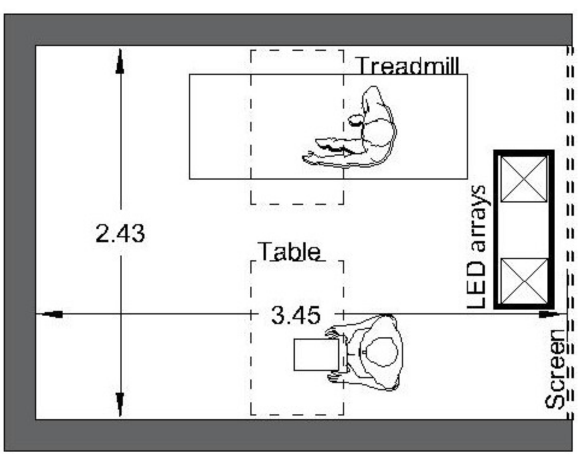

Fig. 2. Plan diagram of the laboratory. Room dimensions in metres.

TABLE I. ILLUMINANCE AND CCT FOR EACH OF THE TEST CONDITIONS

Condition	Illuminance [a] (lx)	CCT (K)	Melanopic EDI (lx)
C1	8	2700	3.4
C2	8	5800	10.4
C3	25	2700	10.7
C4	<0.5	2700	< 0.5

[a] Vertical illuminances at eye level (1.5 m above the floor)

At intervals of approximately 30 minutes throughout the adaptation and test phases, four measures of alertness were recorded: self-report of sleepiness, reaction time to an acoustic stimulus, skin temperature, and melatonin levels.

Melatonin levels were determined from saliva samples captured using Salivettes at five intervals during the adaptation phase (Ad1 to Ad5) and three intervals during the test phase (T1 to T3) giving eight samples in total. These require participants to chew a cotton bud for 1 to 2 minutes. The samples were stored at -20°C, then packaged in dry ice for transport to the Chorono@work laboratory (University of Groningen) for analysis.

Alertness was measured using an auditory Psychomotor Vigilance Test (PVT) conducted in the three-minute intervals before and after saliva sampling. This measures reaction time (RT) to detection of an acoustic stimulus. A 1000 Hz tone was played for 0.5 second at randomized intervals ranging from 2 to 10 seconds: test participants were instructed to press the response button as soon as they heard a stimulus. The loudness of the tone was determined separately for each participant according to their audibility threshold as measured during the pre-experiment period.

Subjective evaluation of alertness was recorded using the Karolinska Sleepiness Scale (KSS). Skin temperature was measured continuously using four temperature sensors (iButtons) attached to each participant at four locations - neck, scapula, hand, and shin.

The analyses are ongoing. This paper presents results established from salivary melatonin, suggested to be the most promising and accurate measure for revealing underlying non-visual physiological impacts of light [15] and for the PVT test, which is among the most sensitive tests to sleepiness and lack of alertness, most reliable with no evidence of learning over repeated administration, and most practical test to use in an operational environment [16].

III. RESULTS

Fig.3 shows median melatonin levels at each test interval. Measures of central tendency and dispersion, graphical representations and statistical tests indicated that these data were not drawn from a normally distributed population.

Fig. 3 shows a steady increase in melatonin levels with time during the experiment Analysis using the Friedman test suggested a statistically significant (p<0.0001) effect of interval. Pairwise tests confirmed a tendency for significant increase compared with the previous test interval.

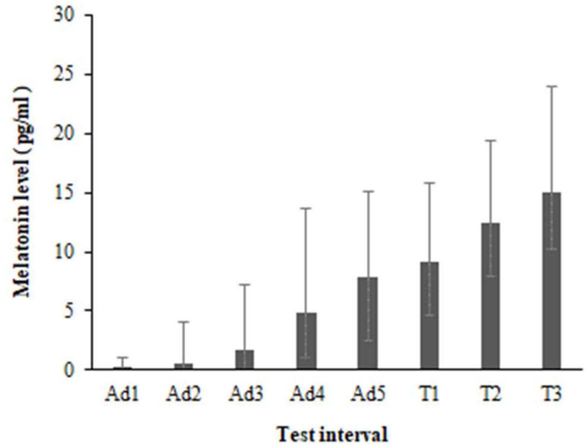

Fig. 3. Median melatonin levels (and interquartile range) at each test interval

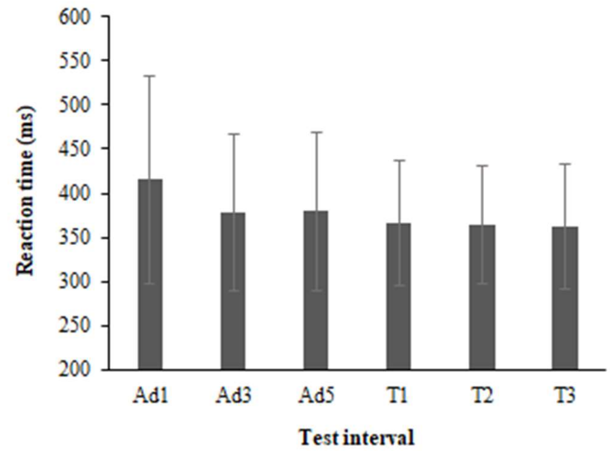

Fig. 5. Mean reaction time (ms) and standard deviations at each test interval

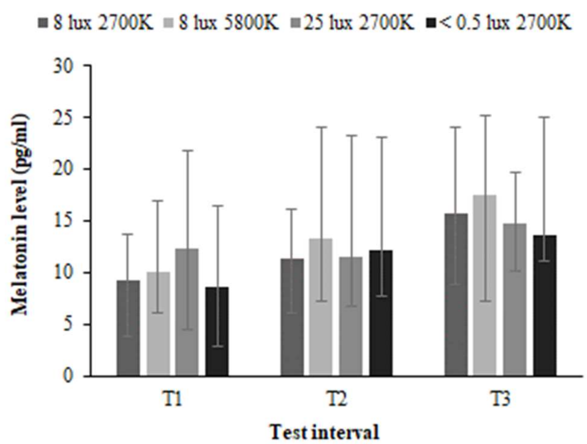

Fig. 4. Median melatonin levels (and interquartile range) for each lighting condition during the test phase

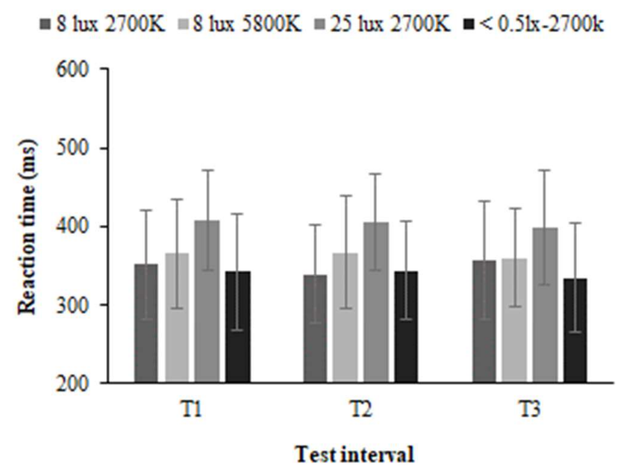

Fig. 6. Mean reaction time (ms) and standard deviations for each lighting condition during the test phase

Fig. 4 shows the melatonin levels recorded during the test phase for each of the four conditions shown in Table 1. Comparison of these using the Kruskal-Wallis test did not suggest significant differences between the lighting conditions (p>0.83). The Kruskal-Wallis test also failed to reveal a significant effect of posture (p>0.44).

Fig.5 shows mean RTs to the PVT stimulus at each test interval and Fig.6 shows the mean RTs in each lighting condition during trials in the test phase.

In a given PVT trial, each test participant responded to approximately 60 acoustic stimuli. The data were cleaned by omitting assumed errors of omission (twice the median RT) and errors of assumed commission (RT<100 ms). Of the remaining responses, analysis of the data did not suggest they were drawn from a normal distributions and hence each was characterised by the median level. This reduced the RT data to 40 responses (one per participant) at each of the six test intervals, and these data were suggested to be normally distributed.

Analyses were conducted using repeated measures ANOVA. This suggested a significant effect of interval (p=0.003) (suggested by pairwise tests to be significant differences between Ad1 and either T1 or T2) but did not suggest significant effects of lighting condition (p=0.22) nor posture (p=0.84).

IV. DISCUSSION

These findings suggest that light intervention had no significant effect on either reaction time or melatonin levels, a finding which is in line with Bhagavathula et al. [13] despite the use of lighting with higher melanopic content.

However, these findings are not in line with the findings of some other studies [17,18].

Phipps-Nelson et al. [17] compared the impact of a narrow band blue light (peak wavelength 460 nm, 1 lx) and a broad spectrum ambient light (0.2 lx) on subjective and objective indices of sleepiness during prolonged nighttime performance testing (23.30 to 05.30). Their results suggest that the method of measurement matters. Measurement of driving performance using a driving simulator did not show any effect of lighting: In contrast, other measurements suggested the blue light led to faster reaction times using a PVT, reduced slow eye movements, and decreased EEG delta and theta activity. Their results also suggests that the time of exposure matters.

Plitnic et al. [18] investigated the impact of nighttime exposure to LED lighting labelled blue (peak wavelength 470 nm) and red (peak wavelength 630 nm) at two illuminances, 10 and 40 lx (vertical illuminances at the eye). These conditions reduced self-reports of sleepiness and slightly increased alertness using objective measures (power in the beta frequency range of EEG) compared with the lower illuminance (<1 lx, red light peak wavelength 630nm) of the dim phases before and after the test period.

The current work and that of Bhagavathula et al. used brighter lighting in the adaptation period than in the test period: Phipps-Nelson et al. and Plitnic et al. used instead dark adaptation. This suggests that the adaptation conditions matter. In terms of practical relevance, the current work and that of Bhagavathula et al. attempted to represent natural situations and found suggest no effect of lighting on alertness: we must instead we might need to use conditions (dark adaptation) not typical of natural situations in order to reveal an effect.

V. CONCLUSION

This results of this experiment did not suggest an effect of light condition on alertness as measured using saliva-derived melatonin levels and response to an acoustic reaction task. This confirms the conclusion drawn by Bhagavathula et al [13] and in the current work this conclusion was tested by using a higher EDI (~10 lx) than used by Bhagavathula et al (<1 lx).

If confirmed, these findings have two implications for evening travel. First, that lighting, within the range of conditions typical of current outdoor lighting practise, does not raise the alertness of drivers or pedestrians. Second, that lighting does not adversely affect circadian cycle of pedestrians.

Further work is required to test whether the no-effect findings are real. This might include repeating the current experiment with a greater range of lighting conditions, specifically lighting of higher EDI; increasing the walking speed of the participants (hence increasing their cognitive load), recruiting test participants of older age or who are sleep deprived. It is also important to investigate the impact of such conditions on target detection as such changes may affect target visibility and adaptation of the eye.

REFERENCES

[1] Commission Internationale de l'Éclairage. "Lighting of roads for motor and pedestrian traffic", Vienna, CIE 115, 2010.

[2] Commission Internationale De L'Éclairage. "Lighting for pedestrians: a summary of empirical data", Vienna, CIE 236, 2019.

[3] Y. He, M. Rea, A. Bierman, J. Bullough, "Evaluating light source efficacy under mesopic conditions using reaction times", J. Illum. Eng. Soc., Vol. 26, pp. 125-138, Jan 1997.

[4] R. Lingard, M. S. Rea, "Off-axis detection at mesopic light levels in a driving context". J. Illum. Eng. Soc., Vol. 31, pp. 33–39, Jan 2002.

[5] J. M. Sullivan, M. J. Flannagan, "The role of ambient light level in fatal crashes: inferences from daylight saving time transitions", Accid. Anal. Prev., Vol. 34, pp. 487-498, Jul 2002.

[6] C. J. Robbins, S. Fotios, "Motorcycle safety after-dark: the factors associated with greater risk of road-traffic collisions". Accid. Anal. Prev., Vol. 146, p. 105731, Oct 2020.

[7] S. Fotios, R. Gibbons, "Road lighting research for drivers and pedestrians: the basis of luminance and illuminance recommendations", Light. Res. Technol., Vol. 50, pp. 154-186, Jan 2018.

[8] B. S. Oken, M. C. Salinsky, S. Elsas, "Vigilance, alertness, or sustained attention: physiological basis and measurement". Clin. Neurophysiol., Vol. 117, pp.1885-1901, Sep 2006.

[9] J. F. Mackworth, "Performance decrement in vigilance, threshold, and high-speed perceptual motor tasks". Can. J. Psychol., Vol. 18, p.209, 1964.

[10] S. Bioulac, J. A. Franchi, M. Arnaud, P. Sagaspe, N. Moore, F. Salvo, P. Philip, "Risk of motor vehicle accidents related to sleepiness at the wheel: a systematic review and meta-analysis". Sleep, Vol. 40, Oct 2017.

[11] T. Åkerstedt, S. Folkard, "Validation of the S and C components of the three-process model of alertness regulation". Sleep, Vol. 1, pp. 1-6, Jan 1995.

[12] A. A. Borbély, S. Daan, A. Wirz - Justice, T. Deboer, "The two - process model of sleep regulation: a reappraisal", J. sleep Res., Vol. 25, pp.131-43, Apr 2016.

[13] R. Bhagavathula, R. Gibbons, J. Hanifin, G. Brainard, "LED roadway lighting: impact on driver sleep health and alertness", 2021.

[14] Commission Internationale de l'Éclairage, "CIE system for metrology of optical radiation for ipRGC-influenced responses to light", Vienna, CIE S 026/E, 2018.

[15] P. R. Boyce, "Human Factors in Lighting" 3rd ed. Boca Raton, FL: CRC Press, 2014.

[16] T. J. Balkin, P. D. Bliese, G. Belenky, H. Sing, D. R. Thorne, M. Thomas, D. P. Redmond, M. Russo, N. J. Wesensten, "Comparative utility of instruments for monitoring sleepiness - related performance decrements in the operational environment". J. Sleep Res., Vol. 13, pp. 219-227, Sep 2004.

[17] J. Phipps-Nelson, J. R. Redman, L. J. Schlangen, S. M. Rajaratnam, "Blue light exposure reduces objective measures of sleepiness during prolonged nighttime performance testing" Chronobiol. Int., Vol. 26, pp. 891-912, Jan 2009.

[18] B. Plitnick, M. G. Figueiro, B. Wood, M. S. Rea, "The effects of red and blue light on alertness and mood at night", Light. Res. Technol., vol. 42, pp. 449-458, Dec 2010.

Development of Floodlighting Design System Based on Raster Images

Rafał Krupiński
Faculty of Electrical Engineering, Electrical Power Engineering Institute Lighting Technology Division Warsaw University of Technology
Warsaw, Poland
rafal.krupinski@pw.edu.pl

Wolfgang Scherzer
Information Technologist (Freelance) and Computer Graphics Specialist
Garching, Germany
it@wolfgangscherzer.de

Piotr Pracki
Faculty of Electrical Engineering, Electrical Power Engineering Institute Lighting Technology Division Warsaw University of Technology
Warsaw, Poland
piotr.pracki@pw.edu.pl

Andrzej Wiśniewski
Faculty of Electrical Engineering, Electrical Power Engineering Institute Lighting Technology Division Warsaw University of Technology
Warsaw, Poland
andrzej.wisniewski@pw.edu.pl

Krzysztof Skarżyński
Faculty of Electrical Engineering, Electrical Power Engineering Institute Lighting Technology Division Warsaw University of Technology
Warsaw, Poland
krzysztof.skarzynski@pw.edu.pl

***Abstract*—The article describes the next stage of work on a system for designing floodlighting objects using computer graphics. Contrary to the currently used visualisation tools, the developed computer application is based on the daytime photography of the object and not on its three-dimensional geometric model. The advantage is the high photorealism of the simulation, with no need to create a collage of visualisation with photography. The designer uses the photometric data of luminaires, and its photometric and colorimetric parameters are defined. It is possible to perform a precise lighting analysis - the distribution of illuminance and luminance, both for the entire facility and in any plane or point. The system's operation is presented as an example in the form of a case study. The example shows the features of the system and the further expected development direction.**

Keywords—lighting technology, floodlighting, lighting simulations, lighting analysis, computer graphics

I. Introduction

Currently, the design of floodlighting is primarily done using simulation methods. Various computer software is used for this purpose, ranging from relatively simple to technically very advanced [1]–[12]. In any case, however, it is a laborious and time-consuming process. This is mainly due to the need to build a three-dimensional geometric model of the object to be illuminated. The final effect of the simulation work depends on the quality of the 3D model [13]–[17]. It is estimated that making a three-dimensional geometric model of an object used as a basis for a lighting design is about 70% of the overall designer's working time [18]. Another problem is the time of photometric calculations. In illumination projects, a large amount of lighting equipment is often used. The computation is thus becoming a hefty burden on computing units in terms of graphics. The rendering time, i.e. the conversion of vector graphics into raster graphics, also depends on the resolution of the raster image. It can be said that with HD resolution (1920x1080) and the number of luminaires of several dozen pieces, the time of lighting calculations, the final effect of which is photorealistic visualisation, is several hours for an average computer currently used.

In the case of floodlighting objects, a collage of computer graphics and evening photography is also made to obtain photorealism. This requires the use of dedicated digital image processing tools and additional time to create the collage. In such cases, for the simulation process to run correctly, the computer graphics must be matched to the evening photography taken. Matched in terms of camera parameters, its position and orientation, but also in terms of photometric and colorimetric properties. Generally, the lighting designer needs to measure the luminance distribution when taking evening photography. The measured luminance levels and distributions should be transferred to a virtual environment. All camera data should also be shared.

The surrounding of the facility is often a big problem. The landscaping around it especially objects with organic shapes: trees, shrubs, and figures walking around the object are challenging to recreate geometrically or transfer from a photography. This is the reason why these objects are very often removed from the final collage. Therefore, it should be borne in mind that what is presented on such visualisations, despite correctly performed photometric calculations, will differ from what a human observes after the project is implemented. Figure 1 shows a three-dimensional computer simulation made in the form of a collage, while Figure 2 shows a post-implementation photograph of the illumination project. Although the object has the same luminance levels and distributions, the images are significantly different. Research shows [18], [19] that traceability, whether computer graphics or reality, results only from how the college is conducted. When analysing the images in Figure 1, if we are only guided by the idea of the object generated by the computer and the real object, without taking into account the surroundings, the differences between the building in the simulation and the photography are not noticeable. The luminance levels and distribution measurements also indicate a high convergence of the results [19]. So the collage technique is a problem. It is the collage that makes graphics different from reality.

Fig. 1. Floodlighting project of the object was made using the collage technique of three-dimensional computer graphics and evening photography.

Fig. 2. Post-realization photography of the object floodlighting.

All this means that a lighting designer, especially floodlighting, who wants to perform a photorealistic computer simulation of lighting becomes a computer graphic designer. In addition to the ability to create a geometric model, he must also have a good command of digital image processing. The designer's graphic skills determine whether the simulation will attract the human eye. This is a big problem because the designer should focus on his task - designing a technically correct floodlighting, not just graphically attractive. It may also happen that an excellent illumination concept will not be presented in a photorealistic way, which is the only reason the project will be rejected.

The described problems are known in the lighting industry; therefore, lighting designers, especially architects, use applications for digital image processing in their work. Using daytime photos, they create eye-catching simulations. In the picture, luminance distributions are made using various techniques. Usually, it consists of "painting" with colour with brushes and the so-called using a mouse or stylus to complete the stamps. This design process, by definition, leads to photorealistic simulations, but unfortunately technically incorrect. It is easy to create the desired luminance distribution in this way; it is more difficult to execute it with actual lighting equipment. Without the use of lighting simulations, it is difficult to predict how the light will behave on the facade of the building and what the actual levels and distributions of illuminance and luminance will be. After all, it depends on many factors. Of course, with the extensive experience of the designer, who makes the graphics and selects luminaires whose task is to achieve the intended effect, this design process can be completed. Practice shows, however, that the differences in the final implementation of the project can be significant. This means that, regardless of the technique of developing the floodlighting project, the work results may be affected by many errors. In the case of the 3D model, they result from the limited time, i.e. the use of model simplifications, and in the case of photography - due to the lack of professional tools for this purpose.

The work aims to present the next stage of development of an IT system for fast, technically correct design of floodlighting objects without the need to build a geometric model of the object and perform post-production in the form of a collage of computer graphics with photography. Work on the system has been going on for several years, and the preliminary results were presented at the LumenV4 conference in 2018 [20].

II. System Development

As already mentioned, the system's assumption is to use a dedicated computer application and daytime photography of the object to design floodlighting. Figure 3 shows the interface of the application. No significant changes have been made to the first version. New IT algorithms have been improved and developed. They allow you to simulate the illumination design regardless of the surroundings of the building.

In addition to defining the reflective properties of the illuminated object and its surroundings, the application allows you to mask any areas. Masks create layers and can apply to both areas of the photo that are not subject to lighting and the object's body. These layers are assumed to be parallel to each other. Each mask has defined properties: dimension, reflection, transmission, and displacement. This way, a lighting scene is created, marked as 2.5D in computer graphics. You can also meet the term pseudo-three-dimensionality of such a scene because the layers formed in this graphic are intended to evoke the three-dimensional illusion using the axonometry theory.

The developed system enables the correction of basic photometric parameters: editing of photometric files, luminous flux, the luminous intensity in various directions, colour temperature and colour filters. A complete lighting analysis is also possible based on the illuminance and luminance distributions generated in the false-colour scale and measurements in points or planes.

The assumption is that the application is intended for designing the floodlighting of objects with classical architecture. The system uses a raster file (day photo), and, like most currently used on the market, the calculations are based on Lambert's cosine law. All materials are therefore perceived as diffusive by the application. Therefore, design errors will appear if you try to simulate an object made of glossy materials. This is a computer application limitation.

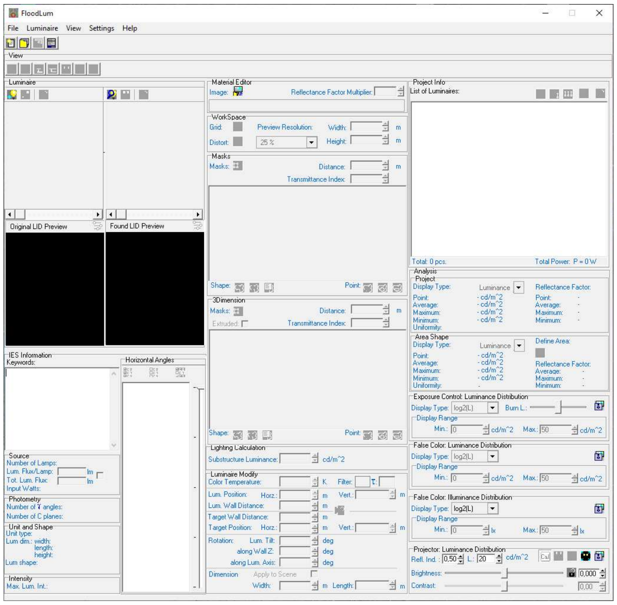

Fig. 3. The interface of computer software for designing floodlighting based on daytime photography of the object.

III. Case Study and Discussion

A photography of the Palace building in Słupia in Poland was used to analyse the operation of the application (Fig. 4). It is a classic two-floor building that meets the application's requirements and its behaviour tests in cases of simulating floodlighting projects with an organic environment. In the photo, both on the right and left sides of the object, we can see trees whose branches overlap the object. In addition, there is also low vegetation at ground level. It would be difficult to recreate such a state in a three-dimensional computer simulation photo-realistic. The photo was taken in perfect lighting conditions, but there are no shadows from the sun's rays on the facade. This is due to the northern direction of the illuminated facade of the building. If, however, there were shadows in the photography, they would have to be removed graphically. Otherwise, the daytime play of chiaroscuro would automatically be transferred to the floodlighting project. This would disrupt the realism and, above all, the correctness of the project. When using this system, you should take care of the correct input data for the project - first of all, good daytime photography. However, it should be remembered that currently used tools have the same limitation.

The first step in creating a project using this method is to select the sky and the surrounding area in front of the object to eliminate these parts of the image from lighting. The software allows you to move the masks and make them transparent. Figure 5 shows the orange mask of the sky and the tree standing on the side of the object.

The next step in the simulation is to create masks that define three-dimensional space. In Figure 6, these masks are marked in blue, with the distinction of the colour tone for the mask under editing (portico). As with masks that exclude the selected area from under the lighting, 3D masks have a defined distance between themselves. You can also

Fig. 4. Palace in Słupia (Poland) - daytime photography was used for the 2.5D simulation.

Fig. 5. Masking the sky in day photography.

Fig. 6. 3D Masks are responsible for the three-dimensionality of the object.

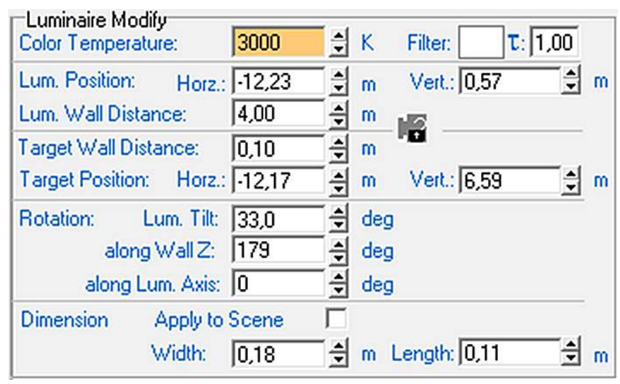

Fig. 7. The Luminaire Modify section of the system allows you to define the light source's colour temperature, colour filters and the exact positioning and orientation of the luminaires.

give them a transmission factor if the selected part of the object is transparent

The Luminaire Modify section of the computer application (Fig. 7) allows you to define the colour temperature of light sources, colour filters, and luminaires' exact positioning.

The test project of the floodlighting of the building assumes illumination in a planar method [21]–[24] with the use of ground-based luminaires and highlighting the pilasters in the central part. The tympanum will be illuminated from a long distance using two luminaires with a narrow luminous flux distribution. This will allow the roof plane to be emphasised at the same time. Figure 8 shows a 2.5D computer simulation according to the assumed lighting concept.

Compared to the application initially developed in 2018, computational algorithms have been developed for accurate lighting analysis. In addition to the illuminance or luminance distribution made in the false-colour technique for the entire lighting scene, along with the object's surroundings (Fig. 9), the system allows you to select any area (Area Shape) and check the local values, both luminance (Fig. 10) and illuminance. The system calculates the luminance or illuminance value at any point. It also gives the average value in the marked area, the maximum, minimum, uniformity (quotient of the minimum and average values), and the reflection factor's average, maximum and minimum values (Fig. 11).

When analysing the final luminance distribution, both in the form of classic visualisation (Fig. 8) and made in the false-colour technique (Fig. 9, 10), it should be stated that the system works very well in the case of objects covered by

Fig. 8. Floodlighting design of the Palace in Słupia was made in the 2.5D technique.

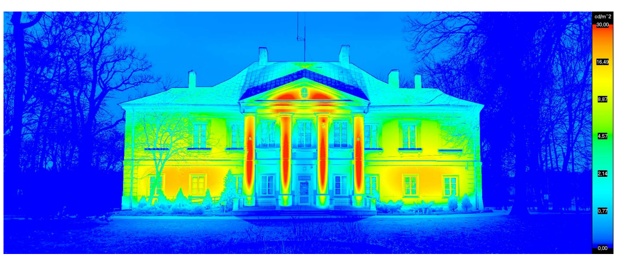

Fig. 9. Luminance distribution of the palace and surrounding.

Fig. 10. Local analysis of luminance distribution and illuminance. The marked area on the facade where the system is performing calculations.

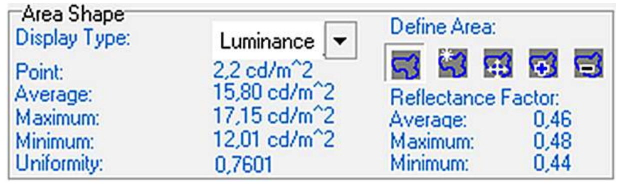

Fig. 11. Numerical analysis of the luminance distribution in the selected area.

trees. It would be difficult to achieve such an effect with a 3D simulation using a collage with evening photography.

The authors' research proves that the developed system shortens the time of creating the floodlighting concept to a large extent. Depending on the architecture of the building and its size, the process is even several hundred times faster compared to the classic design approach using a 3D model. The process is faster while maintaining the same simulation quality and, most importantly, technical correctness. The simulation development presented in Figure 8 takes about one hour of work.

Unfortunately, the system also has limitations. It is possible to properly create the depth of the image and the play of chiaroscuro, provided that the planes making up the object are parallel to each other and to the screen on which the project is presented. In fact, the luminance gradient on the palace roof planes will be more significant as they are rotated concerning the elevation plane by an angle of 60 to 70 deg. Due to this rotation, the shadows created from the tympanum will also be longer. Therefore, it should be borne in mind that the system generates errors in such cases. The authors are currently working on eliminating this limitation of the software.

IV. Conclusions

The developed IT system enables fast, technically correct implementation of the floodlighting concept of the object. The design process is based on the daytime photography of the object, so there is no need to build its geometric model. This significantly reduces the project development time and, therefore also, costs. The software's algorithms allow you to simulate the object’s lighting regardless of its obscuration, which is currently a big problem in the case of 3D simulation with the use of a collage with evening photography. The computer application enables complete lighting analysis based on illuminance and luminance distributions generated in the false-colour scale and measurements in points or planes. So it is the system that solves the problem described. It can be said that it is a universal and useful tool in the hands of a designer of object floodlighting.

Acknowledgment

Publication based on research funded by the Warsaw University of Technology grant supporting scientific activity in the discipline of Automatic Control, Electronics and Electrical Engineering, No. 504/04675/1041/43.020008

References

[1] D. Fernandez-Prieto and H. Hagen, "Visualization and Analysis of Lighting Design Alternatives in Simulation Software," Appl. Mech. Mater., vol. 869, pp. 212–225, 2017.
[2] B. Jiménez Fernández-Palacios, D. Morabito, and F. Remondino, "Access to complex reality-based 3D models using virtual reality solutions," J. Cult. Herit., vol. 23, pp. 40–48, 2017.
[3] K. P. Mansfield, "Architectural lighting design: A research review over 50 years," Light. Res. Technol., vol. 50, no. 1, pp. 80–97, 2018.
[4] M. Moeck, "Constraint satisfaction software for architectural lighting design: A case study," Leukos, vol. 1, no. 1, pp. 101–127, 2004.
[5] K. Nassar, "Integrating discrete event and lighting simulation for analyzing construction work zones lighting plans," Autom. Constr., vol. 17, no. 5, pp. 561–572, 2008.
[6] W. Natephra, A. Motamedi, T. Fukuda, and N. Yabuki, "Integrating building information modeling and virtual reality development engines for building indoor lighting design," Vis. Eng., vol. 5, no. 1, 2017.
[7] M. Navvab, F. Bisegna, and F. Gugliermetti, "Evaluation of historical museum interior lighting system using fully immersive virtual luminous environment," Opt. Arts, Archit. Archaeol. IV, vol. 8790, no. May 2013, p. 87900F, 2013.
[8] E. Y. Y. Ng, L. K. Poh, W. Wei, and T. Nagakura, "Advanced lighting simulation in architectural design in the tropics," Autom. Constr., vol. 10, no. 3, pp. 365–379, 2001.
[9] T. Schielke, "The Language of Lighting: Applying Semiotics in the Evaluation of Lighting Design," LEUKOS - J. Illum. Eng. Soc. North Am., vol. 15, no. 2–3, pp. 227–248, 2019.
[10] M. Schwarz and P. Wonka, "Procedural Design of Exterior Lighting for Buildings with Complex Constraints," ACM Trans. Graph., vol. 33, no. 5, pp. 166:1--166:16, 2014.
[11] M. Scorpio et al., "Virtual Reality for Smart Urban Lighting Design: Review, Applications and Opportunities," Energies, vol. 13, no. 15, p. 3809, 2020.
[12] L. Valetti, F. Floris, and A. Pellegrino, "Renovation of Public Lighting Systems in Cultural Landscapes: Lighting and Energy Performance and Their Impact on Nightscapes," Energies, vol. 14, no. 2, p. 509, 2021.
[13] R. Krupinski, "Simulation and analysis of floodlighting based on 3D computer graphics," Energies, vol. 14, no. 4, 2021.
[14] N. Mantzouratos, D. Gardiklis, V. Dedoussis, and P. Kerhoulas, "Concise exterior lighting simulation methodology," Build. Res. Inf., vol. 32, no. 1, pp. 42–47, 2004.
[15] M. Tural and C. Yener, "Lighting monuments: Reflections on outdoor lighting and environmental appraisal," Build. Environ., vol. 41, no. 6, pp. 775–782, 2006.
[16] H. Wachta, K. Baran, and M. Leśko, "The meaning of qualitative reflective features of the facade in the design of illumination of architectural objects," AIP Conf. Proc., vol. 2078, no. March, pp. 1–6, 2019.
[17] J. Whyte, N. Bouchlaghem, A. Thorpe, and R. McCaffer, "From CAD to virtual reality: Modelling approaches, data exchange and interactive 3D building design tools," Autom. Constr., vol. 10, no. 1, pp. 43–45, 2000.
[18] R. Krupiński, H. Wachta, W. M. Stabryła, and C. Büchner, "Selected issues on material properties of objects in computer simulations of floodlighting," Energies, vol. 14, no. 17, pp. 1–24, 2021.
[19] R. Krupiński, "Evaluation of Lighting Design Based on Computer Simulation," 7th Light. Conf. Visegr. Countries, LUMEN V4 2018 - Proc., 2018.
[20] R. Krupiński, "The Floodlighting Design System Based on the Object's Daytime Photography," 7th Light. Conf. Visegr. Countries, LUMEN V4 2018 - Proc., 2018.
[21] "External Artificial Lighting, Guidance Note," Colchester Brgh. Counc., 2012.
[22] CIE, "A Guide To Urban Lighting Masterplanning," 2019.
[23] CIE Technical Report, "Guide for Floodlighting," 1993.
[24] G. O'Farrell, "External Lighting for Historic Buildings," English Herit., vol. 04, pp. 1–14, 2007.

The Effect of Darkness on Cycling Rates - A Multi-Country Comparison

Jim Uttley
School of Architecture
University of Sheffield
Sheffield, United Kingdom
j.uttley@sheffield.ac.uk

Steve Fotios
School of Architecture
University of Sheffield
Sheffield, United Kingdom
steve.fotios@sheffield.ac.uk

Maan Balela
School of Architecture
University of Sheffield
Sheffield, United Kingdom
mbalela1@sheffield.ac.uk

***Abstract*—Cycling has a range of benefits and should be encouraged but darkness is likely to deter people from cycling. Lighting could potentially offset this negative effect of darkness. A first step in understanding how to design lighting to encourage cycling after dark is to measure the effect of darkness on cycling rates. Cyclist counts from cities in three countries are used to measure the effect darkness has on cycling rates, using a case / control method. Darkness was shown to significantly reduce cycling rates in all three locations, supporting similar previous findings. Further work is needed to understand the role lighting can play in helping reduce this negative impact of darkness on the willingness to cycle.**

Keywords—cycling, road lighting, outdoor lighting, active travel

I. Introduction

The current climate emergency requires a significant reduction in the anthropogenic emission of greenhouse gases. The transport sector is one of the largest contributors to carbon emissions globally, accounting for 24% of direct CO_2 emissions from fuel combustion alone. Road vehicles account for almost three quarters of these emissions [1]. Although these emissions have begun to reduce in recent years due a growing shift towards electric vehicles, the carbon cost of the electricity generated for these vehicles will remain high for many years [2].

There is a health cost in addition to the environmental cost of motorised transport. A switch from petrol or diesel to electric vehicles is only a partial mitigation because electric vehicles continue to contribute towards poor air quality in urban areas through the release of non-exhaust particulate matter due to tyre, brake and road wear [3]. They will also continue to negatively impact public health through road deaths and reduced physical activity. An estimated 1.35 million people around the world are killed in road traffic collisions annually [4]. Research has also suggested every hour per day spent travelling by car can increase the risk of obesity by 6% [5].

There is a need to reduce society's reliance on powered vehicles for everyday transportation. Pedal cycles offers an efficient, healthy and environmentally friendly alternative to powered vehicles. Despite the range of health [6], economic [7] and environmental benefits [8] of cycling there are relatively few countries in the world where it is a popular mode of transport. A survey of cycling behaviour in 35 countries across six continents showed that only two of these countries (Netherlands and Japan) had a mode share for cycling above 10% [9]. Denmark, one of few other countries where cycling has a relatively high modal share, was not included in this survey.

A range of factors contribute towards the low take-up of cycling globally. These include the perceived risk of involvement in a crash, a fear of being a victim of crime, and adverse weather conditions [10,11]. The 2012 British Social Attitudes Survey found that 48% of existing cyclists and 65% of non-cyclists think it is too dangerous to cycle on UK roads [12]. Another factor that may dissuade someone from using a bicycle is the potential need to travel after dark. The need to travel is usually influenced by the time of day rather than ambient light conditions, meaning people frequently have to or want to travel after dark. For example, a person's commute to or from their workplace usually takes place around the same time each day, regardless of whether it is daylight or after dark. The decision to cycle or use another mode of transport may be influenced by whether that trip will take place partly or entirely during hours of darkness. After dark conditions make hazards such as potholes or kerbs harder to see, make the cyclist less visible to other road users, and can increase fear of being a victim of crime - all reasons why someone may want to avoid cycling after dark if they can. This is confirmed by research on the deterrents to cycling, which suggest being able to make the trip in daylight hours is one of the top motivators to cycle [11]. Darkness is a greater deterrent to cycling for some demographic groups, particularly women. For example, only 23% of women reported feeling safe to cycle during hours of darkness, compared with 36% of men [13].

Appropriate use of road or cycle path lighting could reduce the deterrent effect of darkness. This may particularly be the case when trying to encourage new people to cycle. When surveying people about the motivators and deterrents to cycling, Winters et al [11] found that cycling on a route that is not well lit after dark was a major deterrent for all types of cyclist, but particularly for people who cycle infrequently or not at all (see Figure 1). Lighting after dark has the potential to make hazards easier to detect, increase the visibility of cyclists, and create greater reassurance and feelings of personal security. Understanding this relationship between lighting and cycling propensity can help optimise lighting conditions to encourage cycling after dark whilst avoiding energy waste and environmental harm through excessive light pollution. A necessary step in understanding how lighting affects cycling after dark is to first quantify the effect ambient darkness has on cycling rates; we can then compare quantitative changes in lighting characteristics such as illuminance or uniformity against this quantitative effect of darkness on cycling rates.

This research is part of the SATURN project funded by EPSRC, grant reference EP/V043463/1

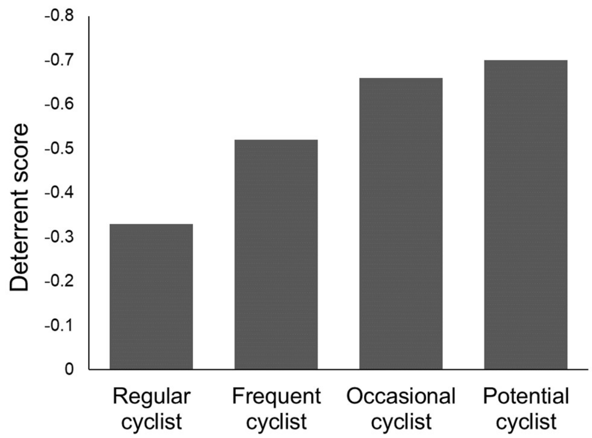

Fig.1. Deterrent effect of having to cycle on a route that is not well lit after dark, by type of cyclist. A more negative deterrent score means a greater deterrent. Regular cyclist = 52+ trips by cycle per year; Frequent cyclist = 12-51 trips by cycle per year; Occasional cyclist = 1-11 trips by cycle per year; Potential cyclist = never cycled in the past year. Data from Fig. 2 in Winters et al [11].

Previous research [14-16] has used counts of cyclists in the same hour when it is in daylight or darkness to quantify the effect darkness has on cycling propensity. This research used a case / control method to isolate the effect of darkness from other confounding factors such as weather conditions and seasonal variations of cycling behaviour. Darkness was found to significantly reduce cycling rates, with this effect being defined as small-to-medium based on the odds ratios calculated from the cyclist counts in the case and control periods. However, this research was carried out in a limited number of locations (Arlington, in the United States, and Birmingham, in the UK), and these locations have similar baseline levels of cycling (the mode share of cycling is 1-2% in both countries [9]). Here we present work to firstly confirm whether the effect of darkness on cycling rates found in previous studies can be replicated, and secondly to understand if this effect varies between different countries. In particular, we are interested in knowing whether a country's latitude and cycling culture is correlated to any differences in the effect of darkness on cycling propensity. Identifying any variation between countries, and factors that might explain such variation, can inform lighting strategy for cycling. For example, locations that show a greater reduction in cyclists after dark may benefit from a more developed lighting strategy for cycling.

We use the same case / control method applied to cyclist counts in previous work [14-16] to compare the effect of darkness on cycling rates in three different countries - Canada, Germany and Finland. These countries vary in latitude and in cycling culture, as defined by the mode share of cycling in those countries.

II. METHOD

A case / control method is used to compare counts of cyclists in daylight and after dark during the same hour across the year. This approach was originally proposed by Johansson, Wanvik & Elvik [17] for assessing the risk of a road traffic collision associated with darkness and has since been adapted to examine the association between darkness and cycling rates.

A 'case' hour is selected such that it is in darkness for part of the year and in daylight for part of the year, due to variation in the duration of daylight hours across the year. A comparison can be made between the counts when the case hour is in darkness and when it is in daylight. Comparing counts within the same hour across the year ensures that the time of day is not a confounding factor. The case hour is defined as being in darkness if the sun's altitude is at or below -6° at the end of that hour. The case hour is defined as being in daylight if the sun's altitude is at or above 0° at the beginning of that hour. Dates where the sun's altitude at any point during the case hour is between -6° and 0° are defined as being in twilight and are excluded from the analysis.

A 'control' hour is also selected such that it is in the same ambient light condition throughout the year. Counts in this hour can be compared for the periods when the case hour is in darkness or daylight, to account for other factors that may influence cyclist numbers and co-vary with changes in ambient light across the year, such as weather conditions.

Counts in the case and control hours during the periods when the case hour is in daylight or darkness are incorporated into an odds ratio equation (see Equation 1) which provides an estimate of the effect of darkness on cyclist numbers. A 95% confidence interval can be calculated for this odds ratio using Equation 2. An odds ratio significantly greater than one suggests darkness reduces the number of people cycling, after accounting for other factors such as time of day and seasonal changes in weather conditions.

$$OddsRatio = \frac{\frac{Case_{Day}}{Case_{Dark}}}{\frac{Control_{Day}}{Control_{Dark}}} \quad (1)$$

$$95\%\ CI = exp\left(\ln(OddsRatio) \pm 1.96\sqrt{\frac{1}{Case_{Day}} + \frac{1}{Case_{Dark}} + \frac{1}{Control_{Day}} + \frac{1}{Control_{Dark}}}\right) \quad (2)$$

Where:

CaseDay = Count of cyclists in case hour when it is defined as being in daylight

CaseDark = Count of cyclists in case hour when it is defined as being in darkness

ControlDay = Count of cyclists in control hour when case hour is defined as being in daylight

ControlDark = Count of cyclists in control hour when case hour is defined as being in darkness

TABLE I. DETAILS OF LOCATIONS AND CYCLE COUNTER DATA USED IN ANALYSIS.

Location	Number of counters	Years of data	Latitude	Modal share of cycling
Helsinki, Finland[a]	21	2014-2019	+60.17°	7.8%[d]
Munster, Germany[b]	10	2019	+51.96°	9.3%[d]
Montreal, Canada[c]	37	2019	+45.50°	1.6%[e]

[a] Data source: https://tinyurl.com/4ydzakek

[b] Data source: https://tinyurl.com/27x2jakd

[c] Data source: https://tinyurl.com/3hthenyr

[d] [9]

[e] [18]

This analysis used open access data from automated cycle counters in three different countries: Finland (Helsinki), Germany (Munster) and Canada (Montreal). Table 1 shows details of the years and number of counters included in these datasets, and their online sources. Data for years after 2019 were available but these have not been included in the analysis due to the potential influence on cycling behavior of travels restrictions and lockdowns associated with Covid-19.

Some counters at each location did not provide full data for each year either because they had not been commissioned yet or because there were dates with missing data, for example due to maintenance issues with the counter. This is assumed not to have influenced the results however as any dates with missing data will affect both the case and control hours and will therefore be accounted for in the odds ratio calculation.

The case and control hours selected for each location are shown in Table 2. The number of days per year the case hour is classed as being in daylight or darkness is also shown.

Counts of cyclists in the case and control hours, during the periods when the case hour was in daylight and darkness, were summed across all years available. These summed counts were used to calculate odds ratios for each counter in each location, and an overall odds ratio for each location.

TABLE II. CASE AND CONTROL HOURS, AND NUMBER OF DAYS PER YEAR THE CASE HOUR WAS IN DAYLIGHT AND DARKNESS, FOR EACH LOCATION.

Location	Case hour	Control hour	Number of days per year case hour in daylight[a]	Number of days per year case hour in darkness[a]
Helsinki, Finland	19:00-19:59	14:00-14:59	114	189
Munster, Germany	19:00-19:59	14:00-14:59	157	142
Montreal, Canada	19:00-19:59	14:00-14:59	101	157

[a.] Remaining days of year the case hour is in twilight

TABLE III. TOTAL COUNTS OF CYCLISTS IN CASE AND CONTROL HOURS AND BY LIGHT CONDITION OF CASE HOUR, FOR EACH LOCATION

Location	CaseDay	CaseDark	ControlDay	ControlDark
Helsinki, Finland	1,074,185	392,503	1,896,776	957,708
Munster, Germany	504,856	360,959	583,258	464,618
Montreal, Canada	377,963	74,790	386,202	95,172

III. RESULTS

The total counts of cyclists by case or control hour and by light condition of the case hour are shown for each location in Table 3.

Overall odds ratios for each location and their upper and lower 95% confidence intervals are shown in Table 4. The range of individual odds ratios for each counter at each location is also shown. In each case the odds ratio is greater than 1.0 ($p<0.001$) which indicates a statistically significant reduction in the numbers of cyclists after dark.

IV. DISCUSSION

There is a range of evidence from subjective methods suggesting darkness deters people from cycling [11, 13, 19]. Recent studies using objective, behavioural methods have also demonstrated that darkness deters people from cycling [14-16]. The research outlined in the current paper extends this exploration of the relationship between darkness and cycling rates using behavioural methods by analysing the cyclist counts in three different countries that vary in latitude and cycling culture. Odds ratios were calculated using the cyclist counts in case and control hours in each country. This use of case and control hours helps to account for factors such as time of day and weather conditions that may also influence cyclist numbers alongside ambient light conditions. The odds ratio is a measure of the effect of darkness on cycling rates: when determined according to equation 1, an odds ratio greater than one suggests fewer people cycle when it is dark, after controlling for time of day and other seasonal influences.

The overall odds ratios for each of the three countries included in this analysis were all significantly greater than one. This confirms the deterrent effect of darkness that has been found in previous work [14-16].

TABLE IV. OVERALL ODDS RATIOS AND RANGE OF INDIVIDUAL COUNTER ODDS RATIOS FOR EACH LOCATION.

Location	Overall odds ratio (95% CI)	P-value, for significant difference from 1.00	Range of odds ratios for individual counters
Helsinki, Finland	1.38 (1.38-1.39)	< .001	1.18 – 2.25
Munster, Germany	1.11 (1.11-1.12)	< .001	1.09 – 1.99
Montreal, Canada	1.25 (1.23-1.26)	< .001	0.54 – 5.31

The odds ratios vary between the three countries, the lowest being 1.11 in Munster, Germany and the highest being 1.38 in Helsinki, Finland. This suggests the effect of darkness may not be consistent across different locations and countries. A range of odds ratios was also found between individual counters at each of the locations (Table 4). Although some of the differences between individual counters is likely due to random variation in counts caused by smaller samples, the local environment at each counter may also influence the effect darkness has on cycling propensity. For example, previous research suggests a link between the size of the effect of darkness on cycling rates (i.e. the size of the odds ratio) and the lighting at that counter location. The presence of lighting (compared with an absence of lighting) is likely to reduce the odds ratio [14], and higher illuminances may also reduce the odds ratio [15].

This article has discussed the effect of darkness on cyclists. Similar analyses have also shown reductions in the numbers of pedestrians after dark [14, 15]. If people are not cycling or walking after dark, what are they doing instead? One option is that people deterred from cycling and walking use instead motorised transport. However, an analysis of the influence of darkness on numbers of cyclists, pedestrians and motorised vehicles in the same city (Cambridge, UK) found no significant effect on motorised vehicles despite the reduction in pedestrians and cyclists [20].

A second option is that transport decisions depend on the purpose of the journey. For destination trips (those with a motivation to arrive at a specific destination [21]), the practicality or viability of cycling/walking, flexibility in the times of arrival and/or departure, availability of other transport modes, and accessibility (i.e., distance) may affect the choice between cycling, walking or driving. For leisure-related trips (those which are optional, without particular destinations, such as cycling undertaken for exercise or fresh air), feasibility and safety factors may affect the choice between taking a walk, changing the time at which a walk is taken, or not leaving the house at all.

Demographic factors may also influence decisions about travel and travel mode after dark. Research based on self-report methods suggest women are less likely to cycle after dark than men [13], and observational research also suggests older people are less likely to walk after dark than younger people [20].

If there is a desire to promote cycling as a means of transport, and if darkness is a barrier to cycling, then road lighting after dark should help to achieve that desire. What lighting conditions are sufficient to support cycling? This remains uncertain: as recently concluded "it is not at all clear that the current lighting regulations and recommendations are the best that can be achieved or are even adequate." [23].

V. CONCLUSION

The work presented here provides further evidence of the relationship between light conditions and cycling rates. Further work is required to understand the factors that influence this relationship, such as national cycling culture and local lighting conditions. This work would help inform future cycling policy and lighting design guidance to encourage more cycling after dark.

REFERENCES

[1] IEA, "Tracking Transport 2020", IEA: Paris, 2020.

[2] N. Rietmann, B. Hügler, T. Lieven, "Forecasting the trajectory of electric vehicle sales and the consequences for worldwide CO2 emissions.", J. of Clean. Prod., 261:121038, 2020.

[3] R.M. Harrison, J. Allan, D. Carruthers, M.R. Heal, A.C. Lewis, B. Marner, T. Murrells, A. Williams, "Non-exhaust vehicle emissions of particulate matter and VOC from road traffic: A review." Atmos. Environ., 262:118592, 2021.

[4] World Health Organisation, "Global status report on road safety 2018", Geneva: World Health Organisation, 2018.

[5] L.D. Frank, M.A Andresen, T.L. Schmid, "Obesity relationships with community design, physical activity, and time spent in cars." Am. J. Prev. Med., 27(2):87-96, 2004.

[6] P. Oja, S. Titze, A. Bauman, B. De Geus, P. Krenn, B. Reger - Nash, T. Kohlberger, "Health benefits of cycling: a systematic review." Scand. J. Med. Sci. Spor., 21(4):496-509, 2011.

[7] S. Gössling, A.S. Choi. "Transport transitions in Copenhagen: Comparing the cost of cars and bicycles." Ecol. Econ., 113:106-13, 2015.

[8] C. Brand, E. Dons, E. Anaya-Boig, I. Avila-Palencia, A. Clark, A. de Nazelle, M. Gascon, M. Gaupp-Berghausen, R. Gerike, T. Götschi, F. Iacorossi, "The climate change mitigation effects of daily active travel in cities." Transport Res. D – Tr. E., 93:102764, 2021.

[9] R. Goel, A. Goodman, R. Aldred, R. Nakamura, L. Tatah, L.M. Garcia, B. Zapata-Diomedi, T.H. de Sa, G. Tiwari, A. de Nazelle, M. Tainio, "Cycling behaviour in 17 countries across 6 continents: levels of cycling, who cycles, for what purpose, and how far?" Transport Rev., 42(1):58-81, 2022.

[10] R. Félix, F. Moura, K.J. Clifton. "Maturing urban cycling: Comparing barriers and motivators to bicycle of cyclists and non-cyclists in Lisbon, Portugal." J. Transp. Health, 15:100628, 2019.

[11] M. Winters, G. Davidson, D. Kao, K. Teschke, "Motivators and deterrents of bicycling: comparing influences on decisions to ride." Transportation, 38(1):153-68, 2011.

[12] Department for Transport. British Social, "Attitudes Survey 2012: Attitudes to Transport." London: Department for Transport, 2013.

[13] SUSTRANS, "Bike life: All cities publication." SUSTRANS, 2018.

[14] J. Uttley, S. Fotios, "Using the daylight savings clock change to show ambient light conditions significantly influence active travel." J. Environ. Psychol., 53:1-10, 2017.

[15] S. Fotios, J. Uttley, S. Fox, "A whole-year approach showing that ambient light level influences walking and cycling." Lighting Res. Technol., 51(1):55-64, 2019.

[16] J. Uttley, S. Fotios, R. Lovelace. "Road lighting density and brightness linked with increased cycling rates after-dark." PloS one, 15(5):e0233105, 2020.

[17] O. Johansson, P.O. Wanvik, R. Elvik, "A new method for assessing the risk of accident associated with darkness." Accident Anal. Prev., 41(4):809-15, 2009.

[18] C. Morency, H. Verreault, A. Frappier. "Estimating latent cycling and walking trips in Montreal." Int. J. Sustain. Transp., 14(5):349-60, 2020.

[19] H. Strömberg, I.M. Karlsson, "Enhancing utilitarian cycling: a case study." Transp. Res. Proc., 14:2352-61, 2016.

[20] S. Fotios, C.J. Robbins, "Effect of ambient light on the numbers of motorized vehicles, cyclists and pedestrians." Transportation Res. Rec., 2676(2): 593-605, 2022.

[21] S.L. Handy, "Urban Form and Pedestrian Choices: Study of Austin Neighborhoods." Transportation Res. Rec., 1552: 135–144, 1996.

[22] S. Fotios, J. Uttley, S. Gorjimahlabani, "Extending observations of ambient light level and active travel to explore age and gender differences in reassurance." Lighting Res. Technol., published online June 2020.

[23] S. Fotios, H.F. Castleton, "Lighting for cycling in the UK – A Review." Lighting Res. Technol., 49(3); 381-395, 2017.

Photometric Characterization of Pavements Under Different Wetting Conditions

Valérie Muzet
ENDSUM research team
Cerema
Strasbourg, France
valerie.muzet@cerema.fr

Guillaume Gublin
ENDSUM research team
Cerema
Strasbourg, France
guillaume.gublin@cerema.fr

Corentin Meyer
ENDSUM research team
Cerema
Strasbourg, France

***Abstract*— Depending on the climatic region, the road surface may be wet or moist for a large part of the year, which reduces lighting performance. The luminance uniformity is degraded, and mirror reflection generates glare. These phenomena are not usually taken into account when designing lighting installations. With the current technological developments introduced by LED luminaires, it now seems possible to adapt lighting to the surface condition of pavements, in order to better meet energy and safety requirements. However, the photometric characterisation of wet pavements is very difficult to carry out because their surface condition evolves rapidly, whereas table-r measurements carried out in the laboratory are generally long. In this paper, we propose a simple and pragmatic wetting protocol which, associated with the COLUROUTE rapid portable device, allows the characterisation of pavements for different wetting conditions. The first results obtained on 13 samples showed that the use of the standard CIE W wetting tables is not relevant for all pavement types and different wetting states. In addition, we found a correlation between Q0 and S1 for the different wetting conditions.**

***Keywords*— pavement photometry, r-table, state of wetting, adaptative lighting**

I. Introduction

The design of road lighting installation requires a combination of the photometric properties of the road surface and the optical characteristics of the luminaires to guarantee the visual comfort for the driver while ensuring road safety and minimum energy consumption. Road lighting installations are designed by calculating performance in terms of luminance distribution as defined in EN13201 standard [1]. As the photometric characteristics of the pavements are generally not measured, a reference *r*-table as defined in CIE reports [2], [3] is often used for lighting design and represents the dry condition.

However, depending on the climatic region, the road surface may be wet or damp for much part of the year, resulting in reduced lighting performance. The overall uniformity of luminance decreases, and mirror reflection generates glare. These phenomena are generally not taken into account when designing lighting installations. With the current technological developments provided by LED luminaires, it now seems possible to adapt lighting to the surface condition of pavements, in order to better respond to energy and safety issues. However, to be able to adapt the optics of the luminaires, and thus achieve such adaptive lighting, it is first necessary to characterise the photometry of the pavements in a wet and damp state.

In CIE report 47: 1979 report [4], standard wet *r*-tables are given. They are more than 40 years old and the proposed wetting method does not allow to characterise a pavement under different wetting states. The measurement of different wetting conditions is rather difficult to achieve because the surface state evolves quickly, while laboratory measurements of r-tables are usually long (from 30 minutes to several hours) [5].

In this paper we propose a simple and pragmatic wetting protocol which, associated with a rapid portable device, allows the measurements of pavements for different wetting conditions. With this approach, we would like to have first elements to answer the following research question. Is the use of the standard W tables relevant for different pavement types and several wetting conditions?

We first present a state of the art with the basics of road photometry in dry and wet state and a short literature review. The material and method section includes a description of the COLUROUTE portable device, the wetting protocol and the collection of sample to be characterised. In the results section, the validation of the protocol is presented, followed by a specific study on 3 samples and finally the analysis of the measurements obtained on the complete database of 13 pavement samples.

II. State of the Art

A. *Basics of road photometry*

The surface of a pavement is described according to its reflection properties [6]. The most characteristic parameter is the luminance coefficient *q*, given as:

$$q(\beta,\varepsilon) = L(\beta,\varepsilon)/E_h \qquad (1)$$

It is the ratio between the observed luminance L in cd.m^{-2} that the observer sees, and the illuminance E_h in lux incident on the surface.

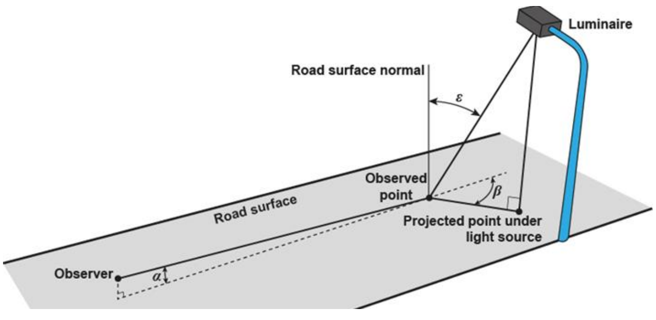

Fig. 1. The photometric characteristics of the road surface depend on the angles of observation α, deviation β and incidence ε (picture from [5]).

The standardised viewing height is 1.5 m and the angle of observation α is constant at 1°, corresponding to an observation distance of 86 m. The lighting standards use the area of the road between 60 m and 160 m ahead of the driver, because it is considered an important area for the detection of obstacles. Since the 1980s, for practical reasons the luminance coefficient was replaced by the reduced luminance coefficient r in cd.m^2.lx^{-1}, which is derived from q:

$$r(\beta,\varepsilon) = q(\beta,\varepsilon) \times cos^3\varepsilon \qquad (2)$$

A reduced coefficient table called r-table was defined, where the luminance coefficient r is given for a combination of fixed lighting angles β and ε (Fig. 1). The average luminance coefficient Q0, represents the degree of lightness of the measured surface. It is computed as the average of the luminance coefficients over the specified solid angle, Ω_0.

$$Q0 \;\; = \frac{1}{\Omega_0}\int q \, d\Omega \qquad (3)$$

The specular factor S1 represents the degree of specularity (shininess) of the observed surface. It is defined as the ratio between the reduced luminance coefficients of two specific illumination conditions defined in (4)

$$S1 = \frac{r(\beta=0, \tan\varepsilon=2)}{r(\beta=0, \tan\varepsilon=0)} \qquad (4).$$

According to the CIE144 report [3], the road photometry of a pavement shall be measured in a dry state and different set of standard r-tables for a pavement in its dry state are directly available in all lighting design software [7].

B. Basics of road photometry in the wet state

In the presence of moisture or water, the variations of photometry are very important, depending on the amount of water. If the road surface is flooded, the luminance coefficients depend mainly on the luminance and size of the light source providing the illumination [8]. The “wetness” depends on the quantity of water on the surface and the composition and texture of the pavement. There is a combination of two optical mechanisms [9]. Sub-scattering by water within the material increases absorption and the material becomes darker. There is also a reflection from the water film covering the macrotexture. The reflection is therefore more directional and the surface appears both darker and more reflective.

In annex C of CIE 47 [4], a wet protocol has been described for a road surface sample. The “wet condition” is measured 30 minutes after uniformly spreading water at a rate of 5 mm of rain per hour in a draught-free room at a temperature of 25° and a relative humidity of 50 %. A classification system for wet road surfaces based on the specularity value of the standard wet condition is defined. As for the dry tables, the boundaries between the classes WI to WIV are established with the specularity value S1 and sthe tandard tables W1 to W4 are given with the corresponding Q0 and S1 values (Table 1). A 2D projection of two CIE standard wet r-tables is shown in Fig. 2.

TABLE I. THE CLASSIFICATION SYSTEMS DEFINED BY THE CIE FOR THE WET TABLES WITH THE NAME OF THE CLASS DEFINED WITH LATIN NUMBERS AND THE NAME OF THE STANDARD TABLES DEFINED WITH ARABIC NUMBERS TO AVOID CONFUSION.

Class name	Class limits on S1	Class standard tables	standard Q0	standard S1
WI	S1 < 4.5	W1	0.114	3.2
WII	4.5 ⩽ S1 <7.2	W2	0.15	5.7
WIII	7.2 ⩽ S1 < 9.8	W3	0.196	8.7
WIV	9.8 ⩽ S1 <12	W4	0.247	10.9

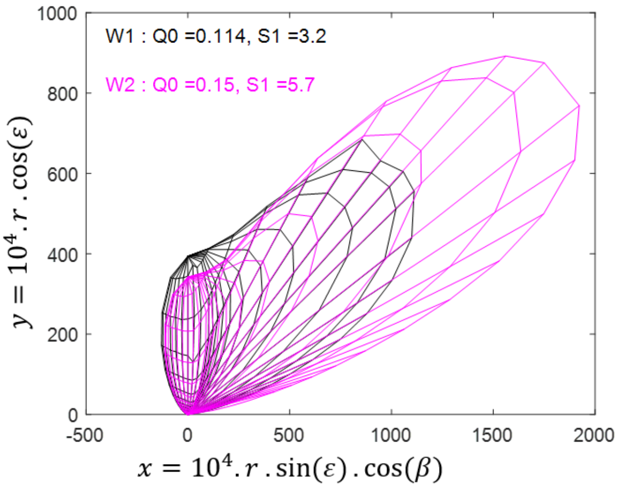

Fig. 2. Reflection indicatrix of the CIE standard r-tables W1 and W2 projected in a 2D space.

However, for wet but not flooded surfaces, the luminance coefficients are defined in [4] and luminance calculations are possible using the standard wet r-table W1 to W4. In the road lighting standard EN13201-2 [1], for wet roads, the minimum recommended value for overall luminance uniformity is 0.15.

For the majority of pavements, there is a very important increase of Q0 and S1 factors in the wet conditions [4]. To our knowledge, no relationship has been found between the photometric characteristic in dry and wet state. In CIE 47 [4] a specific specular factor S'_1 was defined for the wet condition. It was called the corrected specular factor S'_1. It is calculated by using the factors $S1_{wet}$ and $Q0_{wet}$ according to the following formula:

$$S'1 = 0.147 \times \exp\left[\frac{log\left(^{S1wet}/_{0.147}\right)}{1-\left(^{Q0wet}/_{0.687}\right)}\right] \qquad (5)$$

There seems to be a correlation between $S'1$ and luminance uniformity. However, as $S'1$ is calculated with Q0 and S1 in the wet state, it cannot be used to predict the wet photometric behaviour of a pavement from its dry state.

C. Review of the state of the art

As stated in Bommel [8], there is a clear need for further research on wet road surface conditions based on current road surfaces. Very little research has been conducted on the photometry of wet road pavements since the eighties. The S'_1 factor is not used, probably because it depends on the standard wet condition which is quite complicated to achieve.

Ekrias [10] used a video luminance photometer in different weather conditions and confirmed that in a wet condition the luminance distributions of road surfaces change significantly compared to a dry condition. Some areas of the road surface with specular reflection towards the observation point become very bright and may cause discomfort glare. On the other hand, the luminances of the darker areas of road surface decrease. This results in lower luminance uniformities and worse visibility conditions for the driver. However, the average luminance of wet road surfaces is usually higher than in normal, dry conditions. In wet conditions, the luminance of the bright areas can be over ten times higher compared to the dry conditions. Taking into account climatic conditions on road luminance is an opportunity to save energy while improving visibility and therefore safety.

In 2017, Li [11] used a CIE 47 [4] compliant rain simulator to wet 20 road samples. Each sample was put into the wet treatment area for 15 minutes with a flow set at 5 mm per hour achieve full wetting. As the reflection properties change rapidly with time, a segmented measured process was defined and applied. The *r*-table was divided into 10 groups according to the β angle and each time there was only the measurement of one group (corresponding to two column of the *r*-table). This measurement was done in less than 30 minutes assuming that the reflection properties would not differ much. After each group of measurements, the sample was again fully wetted and left to dry naturally for a set period of time, ready for a new set of measurements. Considering that the standard wet condition defined by the CIE is after 30 minutes of drying, 13 out of the 20 pavements are within WI class, 6 in WII and 1 in the WIII class.

Since the wetness condition changes very quickly, several authors measured the photometry of wet pavements at a few angles corresponding to those used for the calculation of the specularity factor S1 (illumination angle $\beta = 0°$, tan $\varepsilon = 2°$ and also $\varepsilon = 0°$). Pattanapakdee [12] and Dumont [9] measured S1 as a function of drying time starting from an flooded state. In Dumont [9] and Basset [13], a steady peak was observed in both a saturated and dry mode. The question of defining the wet and humid state at inflection points was raised by Dumont. For Pattanapakdee [12] experiment, the evolution of S1 with time while drying is very different between each pavements type and differ from the other studies presented. The rough asphalt samples have very high specular factor in the short term and a slightly decreasing one in the long term. The fine asphalt and concrete samples have a longer rise time and a lower specular factor.

The wetting protocol proposed in the CIE 47 report [4] requires a specific installation and does not consider different states of wetness. The approach of Li [11] is very interesting but time consuming. In this paper, we will present a different wetting protocol and the first results obtained on several road samples.

III. Material and Methodology

A. Description of COLUROUTE device

The portable measurement device named COLUROUTE [14] (french acronym "COefficient de LUminance des ROUTEs"), was developed by the Cerema and complies with the specifications of the CIE 144 [6]. With this instrument (Fig. 3), the luminance coefficients of a road surface are measured on site, in daylight and without extracting pavement cores.

COLUROUTE is equipped with a sensor directed at the measurement surface with an observation angle of 1° and has twenty-seven sources set to illuminate successively this surface with different combinations of angles β and ε. These angles were chosen judiciously to allow the calculation of the specularity factor S1 and to reconstruct by interpolation the complete reflection table of the road surface. Calibration is performed using reference plates measured with the Cerema laboratory goniophotometer [15]. The outputs of COLUROUTE comprise the reduced luminance coefficient table (*r*-table), the average luminance coefficient Q0 and the specularity factor S1. With this portable device it is possible to analyse a great number of areas on site and increase the number of interventions without damaging the road. This enables the photometric characteristics of the road surface to be monitored over time [16] and to take into account the heterogeneity of the surface [17]. It is also possible to caracterise samples of pavements, using it the over way round (Fig. 3 right). Since the measurement is conducted quickly (less than 1 minute), it could be used to measure different wetness state of a pavement.

Fig. 3. Picture of the COLUROUTE device in site (left) and for the measurement of road samples (right).

B. Presentation of the protocol

A specific protocol was therefore developed and evaluated. It is possible to generate 4 different moisture states of a sample: dry, moist, wet and soaked. At each state of the protocol, at least two successive measurements of the *r*-tables are conducted with COLUROUTE.

- Dry state: reference measurements.
- Soaking state: the wetting protocol consists in immersing the sample in a basin containing 2 cm of water. A second set of two measurements is performed immediately after removing the sample from the basin to characterize the soaked state.
- Wet state: a third set of measurements is performed after a 5 minutes of natural draining to characterize the wet state.
- Moist state: finally, after absorbing the excess water with a tissue, a last set of measurements is conducted to characterize the moist state.

To validate this protocol, it was used several times with different operators on the same samples.

C. The selection of pavements

After its validation, the protocol was implemented on a representative panel of pavements in order to characterise their photometry in different wet states. A set of 13 cores extracted from conventional and innovative pavements was used in this study. These included a cement concrete, three raw asphalt pavements aged one year or less, aged classic raw asphalt pavements, initially treated asphalt pavement with water scrubbing or sand blasted, and innovative pavements with porcelain chips or with a synthetic binder. The type, age and characteristics of the samples measured are shown in TABLE II.

IV. Results

A. *Evaluation of the wetting protocol*

In order to assess its relevance, the protocol was used several times by different operators. It was repeated twice (2021 and 2022) on a sample extracted of one year old classic asphalt pavement and three times (2020, 2021, 2022) on a 30 months core of innovative pavement including porcelain chips. Each year, a different operator conducted the experiment. The results of the corresponding Q0 and S1 factors are represented in Fig. 4 for the first pavement and in Fig. 5 for the second pavement.

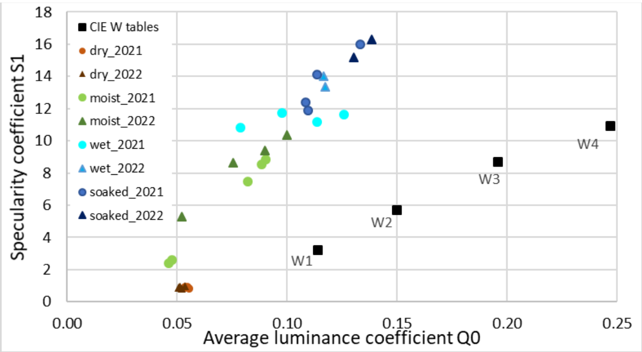

Fig. 4. Representation of the photometric characteristic's Q0 and S1 of a one year classic asphalt pavement under different wet state. The same experiment was conducted in 2021 (circles) and 2022 (triangles). The CIE 47 [4] standard wet tables are represented with black squares.

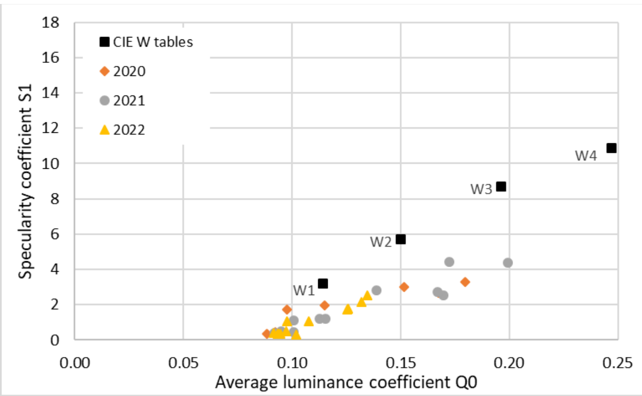

Fig. 5. Representation of the photometric characteristic's Q0 and S1 of an innovative asphalt pavement under different wet state. The same experiment was conducted in 2020 (losange), 2021 (circles) and 2022 (triangles).

For the first pavement, there is a very important increase in specularity with the increase level of wetness and the measurements points are really above the wet standard CIE *r*-tables. For the second pavement, there is a moderate increase in specularity with increasing wetness level and all measurement points are below the wet CIE *r*-tables.

Despite the pragmatic and non-controlled approach of the protocol, the same behaviour was observed each year with significant differences between the two samples.

B. *Results for three samples with different surface treatment*

A specific study was conducted on the same asphalt concrete formulation with three different surface treatments: raw for the untreated surface, shot blasted and waterjet scrubbed (pictures on Fig. 6). The aim of the treatment is to remove the initial asphalt layer to decrease the initial specularity and make the white stones visible (and if possible increase Q0). The corresponding photometry of each pavement are shown in Fig. 7 and Fig. 8 in the different moisture states of our wetting protocol.

Fig. 6. Pictures of the same formulation for a raw pavement (a), waterjet scrubbing (b) and shot-blasted (c) initial treatment.

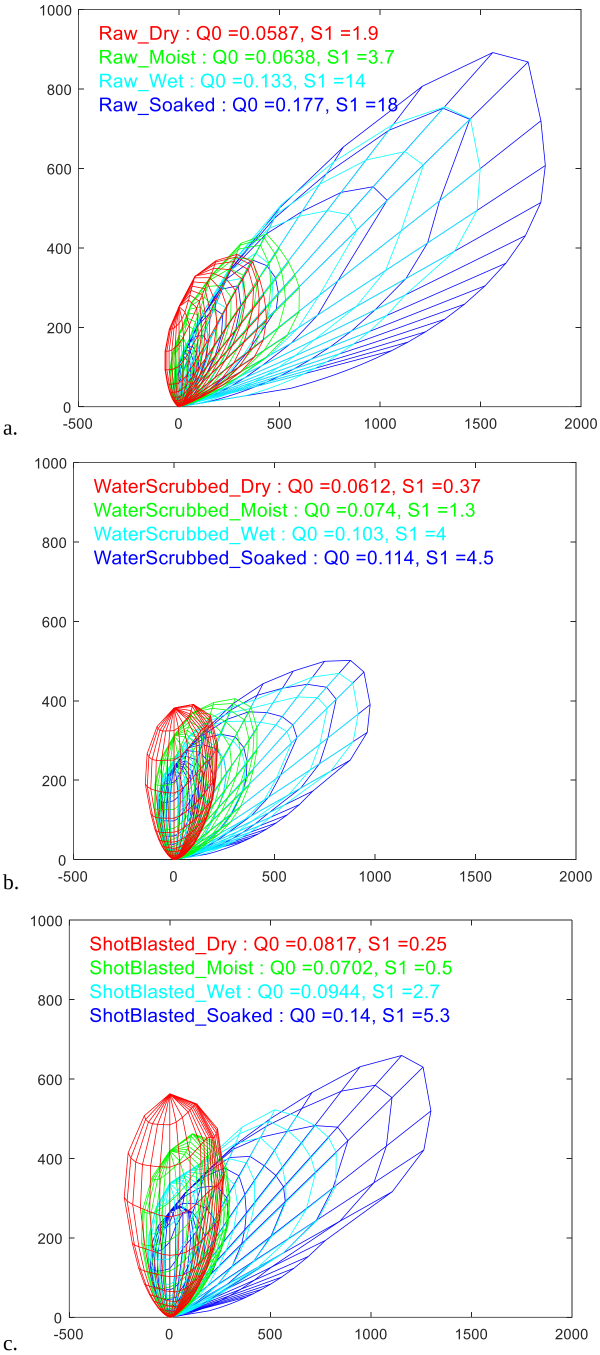

Fig. 7. Reflection indicatrix for the dry state (in red), humid in green, wet in light blue and soaked in blue for the raw (a), waterjet scrubbing (b) and shot-blasted (c) pavements.

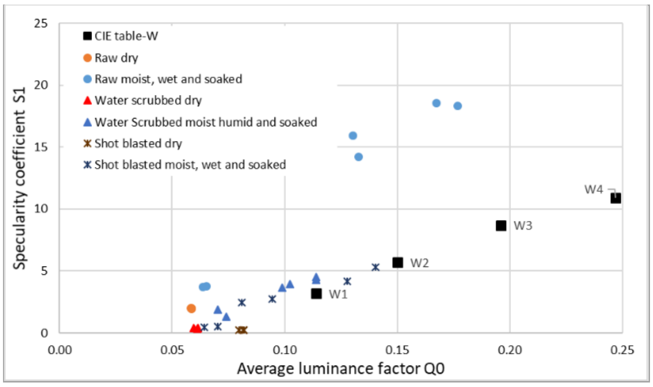

Fig. 8. Representation of the photometric characteristic's Q0 and S1 of three samples under the different wet state. The dry state are in orange, red and brown and the wet states in different blue. The results of the raw sample are represented with circle, the water jet core with triangles and the shot blasted one with stars.

As already shown in the evaluation study and in the former CIE report [4], there is no direct relationship between the wet and dry state. For the raw road surface, the specularity increases greatly in the presence of water, resulting in an important increase in Q0. For the initially treated surface, the increase in specularity is less important, and for the shot-blasted sample, Q0 decreases between the dry and moist state. These results show the influence of the asphalt layer, that is usually not very permeable. Its removal probably has an influence on the porosity of the pavement that could explain the differences between the three pavements.

C. *Results for all the measured samples*

Our wetting protocol was applied on all pavement samples described in TABLE II. and several measurements were made with the COLUROUTE device for all samples under each wetness condition. All specularity measurements are plotted as a fonction of the average luminance factor Q0 for the dry state and the different wet states in Fig. 9. The results are plotted with the previous 1975 Sorensen database [18] were the wet state was generated according to the CIE 47 specification. As in the previous database of 1975, the differences between the pavements of our dataset are huge.

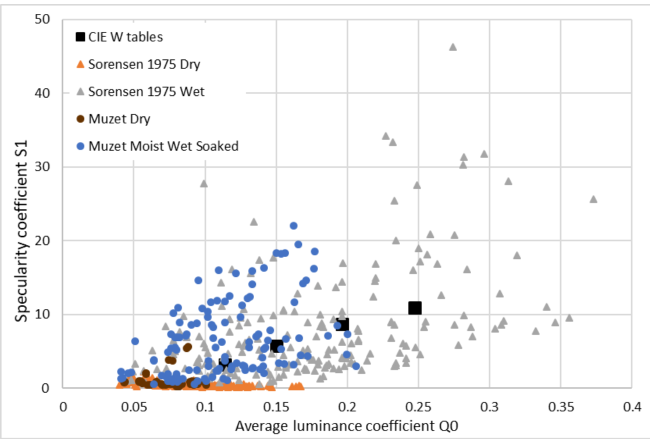

Fig. 9. Representation of the photometric characteristic's Q0 and S1 of our pavements database under dry (in dark brow), humid, wet and soaked state (in blue). The results of the 1975 Sorensen database [18] are presented in orange triangles for the dry state and grey triangles for the wet state.

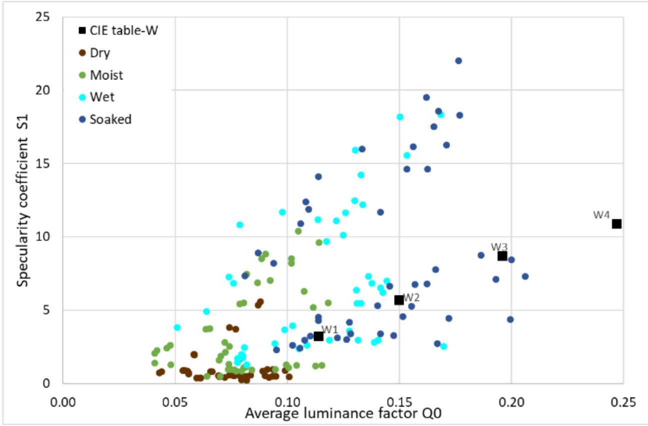

Fig. 10. Representation of the photometric characteristic's Q0 and S1 of our pavements database under dry (in dark brow), moist (in green), wet (in blue) and soaked state (in dark blue).

In Fig. 10, the different wet states are represented for all the 13 samples. In most cases, the average luminance factor Q0 and specularity S1 increase strongly with increasing wetting. Our measurements show a great variability in the evolution of pavement photometry as a function of the wetting condition. For some roads, the W1 to W4 CIE *r*-tables describe the pavements quite well, for others, the specularity is largely underestimated. This confirms the need for both wet and dry state measurement to design optimal lighting with acceptable uniformities both in the dry and wet state.

For the different samples presented in the Fig. 4, Fig. 5 and Fig. 8, there seems to be a linear relationship per sample between Q0 and S1 for the different states of wetness. To confirm this phenomenon, a correlation factor was calculated for each sample. The results are presented in the TABLE II. Since the correlation coefficient is always higher than 0.8, this relation is confirmed for all our pavements.

TABLE II. DESCRIPTION OF THE 13 CORES OF PAVEMENTS WITH THEIR DESCRIPTION, AGE AND THE CORRELATION FACTOR BETWEEN Q0 AND S1 UNDER THE DIFFERENT WET CONDITIONS. **AC** STANDS FOR ASPHALT CONCRETE, **VT** FOR VERY THIN AND **CC** FOR CEMENT CONCRETE.

Road type	Age in year	Specificity	Granular		Correlat° factor
			Size (mm)	Colour	
CC	0.5	Desactivate cement concrete	0 – 14	light	0.89
VTAC	2	synthetic binder + TiO2	0 - 10	white	0.96
VTAC	3	water jet scrubbing	0 - 10	light	0.87
VTAC	3	water jet scrubbing	0 - 10	grey	0.98
VTAC	1	none (raw)	0 - 10	grey	0.82
VTAC	3	none (raw)	0 - 10	grey	0.96
VTAC	2	projection of white granular	0 - 6	white	0.85
VTAC	New	none (raw)	0 - 6	white	0.94
AC	New	water jet scrubbing	0 - 14	light	0.96
AC	New treated	shot blasted	0 - 14	light	0.94
AC	New treated	water jet scrubbing	0 - 14	light	0.95
AC	2.5	porcelain chips	0 - 10	grey	0.81
AC	2.5	porcelain chips	0 - 10	grey	0.87

V. CONCLUSIONS

A simple road sample wetting protocol was proposed and used to characterise the road photometry of a set of 13 pavement samples at different moisture states. The protocol was validated and the first results are promising.

We confirmed that the presence of water increases specularity as already shown in [4], [11], [12], [18] and that there are large differences between pavements. The use of the W standard tables does not seem to be relevant for all pavement types and different wetting conditions. For some asphalt pavements, especially new ones but not only, the increase of specularity is really bigger than the four standard W tables. For others, the standard wet tables are quite appropriate.

Since photometric properties can differ greatly from one road surface to another, it would be best to measure the pavement in place in both its dry and wet states and use the results to design adaptive lighting for the different weather conditions. This methodology has been used in an innovative weather adaptive lighting project [19]. The road surface was characterised with our method, which allowed to have different *r*-tables according to the wetting state and thus to design an adaptive lighting system able to consider the evolution of the reflective properties of the pavements according to their moisture state.

Another wetting protocol will be proposed for on-site measurements. Then, the next steps will be to carry out further measurements in the laboratory and in the field in order to build up a photometric database on dry and wet pavements.

With this study, we found that there is a linear relation of Q0 and S1 between the different wet conditions. This result of course needs to be confirmed with more data. If we could better understand the difference in behaviour between pavements, it would then be possible to predict the evolution of road photometry as a function of wetting condition, by making a single measurement in a single wet and dry condition.

ACKNOWLEDGMENT

We would like to thank Thibaut Rohmer who carried out the 2022 measurements, Florian Greffier for his advices and comments and Kai Sorensen for access to his database of measurements.

REFERENCES

[1] 'EN 13201-2:2015. Road lighting - Part 2: Performance requirements'. CEN, 2015.

[2] CIE, 'CIE 066:1984 Road surfaces and lighting (joint technical report CIE/PIARC)', 1984.

[3] CIE, 'CIE 144:2001 Road Surface and Road Marking Reflection Characteristics', CIE, 2001.

[4] CIE, 'CIE 047:1979 Road lighting for wet conditions'. CIE, 1979.

[5] V. Muzet, J. Bernasconi, P. Iacomussi, S. Liandrat, F. Greffier, P. Blattner P *et al.*, 'Review of road surface photometry methods and devices – Proposal for new measurement geometries', *Lighting Research & Technology*, 2021; 53: 213-229, doi: 10.1177/1477153520958454.

[6] CIE 144, 'CIE 144:2001 Road Surface and Road Marking Reflection Characteristics', CIE, 2001.

[7] CIE 140, 'CIE 140:2000 Road Lighting Calculations'. CIE, 2000.

[8] W. van Bommel, *Road Lighting: Fundamentals, Technology and Application*. Springer International Publishing, 2015. doi: 10.1007/978-3-319-11466-8.

[9] E. Dumont, E. Saint-Jacques, and V. Muzet, 'Photometric properties of wet road surfaces', presented at the Contribution to CIE TC 4.50, Sep. 2012.

[10] A. Ekrias, M. Eloholma, and L. Halonen, 'Analysis of Road Lighting Quantity and Quality in Varying Weather Conditions', *LEUKOS*, vol. 4, no. 2, pp. 89–98, Oct. 2007, doi: 10.1582/LEUKOS.2007.04.02.001.

[11] W. Li, X. Zheng, X. Zhu, G. Whang, and H. Shen, 'Measurement system and method for reflection properties of wet road surfaces', Manchester, UK, 2017, pp. 294–302.

[12] K. Pattanapakdee and S. Chotigo, 'Experimental investigation of pavement light reflection characteristics in wet conditions', in *Proceedings of the 29th Quadrennial Session of the CIE*, Washington DC, USA, Jun. 2019, pp. 1790–1795. doi: 10.25039/x46.2019.PO187.

[13] M. G. Bassett, D. Dmitrevsky, and P. C. Kremer, 'Measurement of Reflection Properties of Wet Pavement Samples', *Journal of the Illuminating Engineering Society*, vol. 17, no. 2, pp. 99–104, Jul. 1988, doi: 10.1080/00994480.1988.10748730.

[14] V. Muzet, J.-L. Paumier, and Y. Guillard, 'COLUROUTE : a mobile gonio-reflectometer to characterize the road surface photometry', TURIN, ITALY, Jul. 2008, vol. CIE x033:2008.

[15] V. Muzet, M. Colomb, M. Toinette, P. Gandon-Leger, and J.-P. Christory, 'Towards an optimization of urban lighting through a combined approach of lighting and road building activities', in *Proceedings of the 29th Quadrennial Session of the CIE*, Washington DC, USA, Jun. 2019, pp. 789–800. doi: 10.25039/x46.2019.PP23.

[16] V. Muzet, F. Greffier, A. Nicolaï, A. Taron, and P. Verny, 'Evaluation of the performance of an optimized road surface/lighting combination':, *Lighting Research & Technology*, vol. 51, no. 4, pp. 576–591, Oct. 2018, doi: 10.1177/1477153518808334.

[17] F. Greffier, V. Muzet, V. Boucher, F. Fournela, L. Lebouc, and S. Liandrat, 'Influence of Pavement Heterogeneity and Observation Angle on Lighting Design: Study with New Metrics', *Sustainability*, vol. 13, no. 21, Art. no. 21, 2021, doi: 10.3390/su132111789.

[18] K. Sorensen and B. Nielsen, 'Road surfaces in traffic lighting'. Report n°9, the Danish Illumination Engineering Laboratory, Sep. 1974.

[19] F. Greffier, V. Boucher, R. Dronneau, and V. Muzet, 'Design of an adaptative road lighting installation taking into account the evolution of pavement reflection properties according to the weather conditions.', Praha, CZ, Sep. 2022.

Virtual Plant Models as a Tool in Horticultural Luminaire Design

Jens Balasus
Laboratory of Adaptive Lighting Systems and Visual Processing
Technical University of Darmstadt
balasus@lichttechnik.tu-darmstadt.de

Tran Quoc Khanh
Laboratory of Adaptive Lighting
Systems and Visual Processing
Technical University of Darmstadt
office@lichttechnik.tu-darmstadt.de

***Abstract*— To satisfy the hunger in a growing world population, plants must be grown more and more efficiently. Trends such as vertical farming rely on LED lighting for this and still come with a huge amount of need for electrical energy. As lighting engineers, we address the following question: How must the luminaire be designed to support plant growth best? Growth experiments are both costly and time-consuming, and looking at many different conditions requires exceptionally good laboratory equipment. One way to investigate on those problems is to rely on simulation models. Studies in the field of horticultural lighting using virtual plants are presented in this work. So far, however, the optical properties of the plant's organs have only been considered in a rudimentary way in these studies, and no spectrally resolved simulation has been carried out. Therefore, a measurement setup to measure those is introduced and finally a simulation using a virtual plant is carried out to demonstrate the use of virtual plants to investigate on spectral variations in the canopy.**

Keywords—horticultural lighting, virtual plants, transmission, reflection, optical leaf properties

I. Introduction

In central Europe, year-round cultivation of plants, especially in the winter months, is not possible without artificial lighting. In cultivation under glass, artificial lighting on the one hand increases the intensity of light, but on the other hand it also serves to extend the daytime. Thus, year-round cultivation of plants such as tomatoes, cucumbers or peppers is possible. In closed cultivation, in so-called plant factories or vertical farms, plants are grown under exclusively artificial lighting. Unlike cultivation under glass, only LED lights are used here. With the future replacement of the high-pressure sodium lamp by LEDs, there are many lighting design possibilities in horticultural lighting. LED lights allow a specific variation of the spectral composition of the light, the intensity and due to the small dimensions of the quasi-monochromatic light sources, different, also spectrally dependent radiation characteristics are conceivable.

The present work deals with a solution approach for the following lighting engineering question in plant illumination: Which characteristics must a horticultural luminaire have for the best possible plant support? So far, horticultural luminaires have mainly been compared in growth experiments - which are time-consuming and cost-intensive and require appropriate laboratory equipment.

To evaluate the long-term light effect on the plant side and thus the production of biomass, it is necessary to know the Light Use Efficiency (LUE) and the Light Interception. From these two data, the production of biomass can be calculated. The light use efficiency depends on various factors, including the plant species and the irradiance spectrum used. It is determined from the ratio of the biomass accumulated over a period of time and the photosynthetically active radiation encountered during that period [1].

The light interception describes the amount of photons impinging on the entire leaf surface, thus it is also dependent on the leaf area. For energy-efficient cultivation of plants, increasing light interception therefore appears to be particularly interesting - after all, it tends to increase the biomass produced. The exact determination of light interception in practice involves considerable effort. Another measure of particular interest for evaluating a lighting installation is the ratio between light interception and the photons emitted by the luminaire. In the optimum case, each photon emitted by the luminaire encounters a leaf - and not, for example, on the floor or a wall. For the application of plant luminaires, this means: Light use efficiency can be significantly influenced by the choice of spectrum and intensity. However, effects are only apparent in the long term via the biomass produced. An increase in light interception generally leads to increased biomass. For an improved effect of plant luminaires, an increase in light interception can therefore be aimed at

Evaluating plant luminaires requires quite elaborate observations - if not extensive field studies. The photon yields of individual luminaires can easily be measured, but the long-term effect of these on plants cannot. The problems are manifold and require a systematic approach. In the following part of the article, such an approach is summarized from various studies

II. Virtual Plants And Their Use With Horticultural Luminaires

One way of investigating and understanding the complex relationships in horticultural lighting is to use simulation models. In the field of plant simulation, various models are coupled together for this purpose. For example, geometric models and their optical properties with a ray tracing method and various biological models. The biological models include models for photosynthesis, water transport, temperature distribution and light receptors. Among the geometric models, a distinction must be made between static and dynamic plant models, which are explained in more detail below. Static structural models describe a 3D geometry of the plants that is constant during the simulation. This can be determined, for example, from a 3D scan of the plant. The digitization of the plant varies in complexity depending on the species. Small

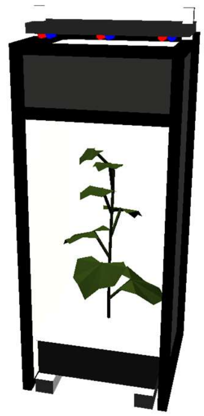

Figure 1 Example of a virtual cucumber plant in a grow box.

plants such as lettuce can be digitized without difficulty using existing 3D scanners, but overlapping leaves can be problematic. With larger plants such as tomatoes, this is often difficult. Here, points have to be captured manually. An alternative to the generation of plant models is a successive programming approach. Here, a plant model is created from individual components according to defined production rules. For example, in the first step a stem (cylinder) is defined with a bud (sphere) attached. In the next step, all spheres are replaced by two cylinders, which stand at a certain angle to each other, and so on. These production rules lead then after several program steps to models, which can be changed very simply in their characteristics. Of course, the geometric possibilities go far beyond the example given here. Leaves can consist of simple parallelograms, or of digitized, real leaves. With plants constructed in this way, it is possible, for example, to change all the leaf angles in the system by changing just one parameter. A freely available software that can be used to simulate plants is the "Growth Grammar-related Interactive Modeling Platform" (GroIMP) [2]. The software has an integrated spectral ray tracing algorithm [3]. In Figure 1, a plant constructed in this software is shown. In addition to static structures, dynamic structures are also used. Output variables of the stored biological models such as photosynthesis rates can be fed back by means of production rules and thus influence the virtual plant in its development. However, this work deals exclusively with the consideration of static states. The plant structures created with it are deposited with measured optical properties.

The majority of previous work in the field of virtual plants deals with outdoor or protected cultivation under glass. Questions in this work are often of a plant physiological nature. The virtual models support a targeted investigation of influencing parameters on the plant side. No luminaire characteristics are varied, but physiological effects are investigated. However, the study presented below investigates a hybrid lighting system that varies different properties of LED luminaires and is therefore included in the selection. In 2014, de Visser et al [4] published a study that investigated the lighting of tomatoes in a greenhouse using 3D models. Motivated by the enormous effort involved in investigating different lighting strategies, the lighting conditions here included sunlight, high-pressure sodium lamps, and an inter-row LED fixture shining laterally on the foliage wall. A photosynthesis model was incorporated into the models, the parameters of which were determined in real experiments. The virtual tomato plants were constructed statically, but in the different scenarios a variation of the leaf angles was performed to evaluate their influence. In addition to the tomatoes, the complete greenhouse was modeled with its optical properties [4]. One effect detectable in the model is that the high-pressure sodium lights used lead to a higher photosynthetic rate per leaf area in the upper leaf layers - this can be justified by an increased photosynthetic capacity of the leaves there. In contrast, the interrow LED fixtures resulted in a higher proportion of photons absorbed by the leaves. This was higher than the proportion of the high-pressure sodium lamp. Regarding the LED illumination, it was also shown that the beam angle of the luminaire had a strong effect on light absorption and light use efficiency. On the plant side, different leaf angles resulted in different light use efficiencies [4]. Overall, this study demonstrated that virtual models of plants can be a useful tool for understanding plant lighting and its design. It should be noted that spectral dependent effects were not investigated in this study. In addition to this study in the greenhouse, other studies exist on horticultural lighting in closed systems such as climate chambers or vertical farms under exclusively artificial lighting.

Besides using the GroIMP software, other programs have been used for light simulation in recent years. Kim et al [5] used OptisWorks to simulate the photon flux density on lettuce plants. Here, the digitization of the plants was done by 3D scanning. The aim of the work was to realistically represent the light conditions in a growth chamber for lettuce plants in a virtual experiment. This was to quantitatively determine light interception as well as photosynthesis and to compare certain scenarios with real measurements. An investigation of the effect of light design on light interception and photosynthesis is thus possible. The parameters for the simulation of photosynthesis were determined by means of photosynthesis measurements on real plants. The model set up in this way, consisting of a 3D scan of the plant and the photosynthesis parameters determined in real life, was used to simulate different lighting conditions [5]. In the virtual experiment, lighting was provided by linear luminaires positioned either above or between the plants. The height of the lights was varied in a range between 20 and 40 cm in 5-cm increments. The effects of different optical soil properties (non-reflective, highly reflective) were also studied. The following is a summary of the results on the effect on light interception from [5]:

1) At low luminaire height (less than 30 cm): light interception mainly on leaves directly under the light source, hardly any light interception on the other leaves
2) At luminaire heights between 30 and 40 cm: little effect on light interception by luminaire height and arrangement, generally more evenly distributed
3) Use of the highly reflective soil material increases light interception by about 3.6% on average.
4) At the leaf level: light interception depends on the angle of light incidence and thus also on the leaf angle.

The study shows that optical simulations and a plant model can be used to address various issues of plant illumination

such as luminaire height. In addition to the previous study with lettuce, Saito et al [6] investigated digitized canola plants in closed cultivation in order to use them in the virtual model to optimize horticultural lighting. The optical simulations were done in Radiance software. The coefficient of variation of the light absorption of the individual plants was evaluated, as well as the coefficient of light utilization. The simulation started with the calculation of the light absorption of the individual plants, followed by the calculation of the coefficient of variation. The coefficient of light utilization was formed from the ratio of total radiation absorbed by the plants and the radiation emitted by the lights - it thus represents a measure of the proportion of photons impinging on leaves. The following properties of the illumination were varied and the two quantities were calculated: (1) number of luminaires (2) luminaire spacing (3) luminaire height (4) photon current (5) radiation characteristics. It was noticed during the simulation that a homogeneous light distribution in the empty shelf did not result in a uniform light distribution on plant leaves. The photon flux density on leaves directly under a luminaire was significantly higher than on the rest. By selectively changing the radiation pattern, a lower coefficient of variation of light utilization could be achieved using luminaires with focused radiation [6].
This study shows that prior simulation of luminaire configurations can be performed using optical simulations. As in the previously mentioned studies, luminaire parameters could be specifically evaluated in their effect on plants using a simulation approach. However, spectral composition and photosynthesis were not considered.

III. Measuring Setup

From the current state of research, the previous simulations only consider a few spectral effects, but these are also important for plant development. If spectrally dependent effects, such as that of shade avoidance (red/far-red) [7], or blue light response [8] are to be simulated in the virtual plant models, a simulation with separate spectral regions is required. In this work, a real cucumber plant is digitized as an example and virtual experiments are performed with it. For this purpose, the measurement setup of optical leaf properties is presented. Subsequently, the simulation environment for the photometric experiments is digitized and calibrated. The geometry of a young cucumber is measured and digitized in the simulation environment - then a simulation of the spectral conditions is performed.

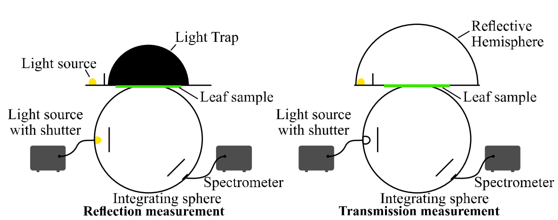

Figure 2 Experimental setup for measuring hemispherical spectral reflectance (left) and transmittance (right). For the reflectance measurement, the light source outside the sphere is shadowed by the light trap; for the transmittance measurement, it is coupled in via a reflective hemisphere. The light source with shutter is then shadowed for the transmission measurement.

The optical measurement of the cucumber leaves is performed with a test rig on which both the spectral hemispherical transmittance and reflectance can be measured under diffuse illumination using an integrating sphere (ISP-REF from *Ocean Insight*) (see **Chyba! Nenašiel sa žiaden zdroj odkazov.**). Of particular importance in this measurement is that the leaves can be measured in-situ, since depending on the water content of leaves their reflectance spectrum changes [9]. The experimental setup consists of an integrating sphere to which a spectrometer and an external light source with a shutter are connected. A sample port allows the measurement sample to be placed on the sphere. Outside the sphere, above the sample port, there is the possibility to place a light trap for reflection measurements, or alternatively a place hemisphere for transmission measurements, which brings diffuse light to the top of the leaf. The two light sources used can be shaded so that they are in a stable state even during measurement series. The leaf reflectance and transmittance spectrum is recorded on a leaf. This data is going to be used in the next section to setup the virtual experiment.

IV. Experimental Results

The light simulation is performed with the GroIMP software. In order to validate the light simulation, an empty growth chamber is reconstructed in the first step, which also exists in the same form in the authors' laboratory. The spectral irradiance was measured at two different heights (440 mm, 90 mm). The measurement at 440 mm (directly below the lighting fixture, see **Chyba! Nenašiel sa žiaden zdroj odkazov.**) was used to calibrate the virtual chamber - the virtual LED powers were adjusted so that the spectral irradiances in simulation and reality matched (the relative deviation in the end was less than 0.01%). The spectral reflectance of the walls was measured with the setup described in Section III and adjusted in the model. With the correct reflectance, a second simulation followed at height 2 (90 mm) (see Fig. 3). The simulated value of irradiance was 18.174 Wm^{-2} compared to the measured 18.455 Wm^{-2} (relative deviation < 2 %). With a simulated reflectance of the walls of 0 %, the simulated value of the irradiance is 2.657 Wm^{-2}, corresponding to a large indirect illumination component in the measurement point and thus a correct simulation of it is assumed.

In the next step, a static cucumber model is set up in the growth chamber. The basis for this is a six-week-old cucumber plant whose geometry is measured in the laboratory. This provides the necessary information on the number of leaves, leaf size, leaf position, leaf angle, stem length and stem angle.

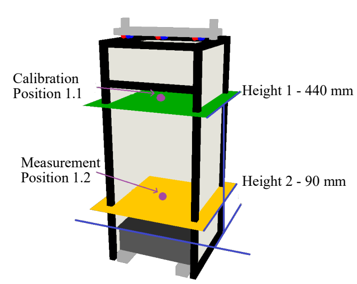

Figure 3 Simulated empty grow chamber, with two sensor points. The calibration is done at height 1 on position 1.1. The measurement is performed afterwards and simulated at position 1.2.

With these, the plant is programmed in GroIMP, it is assumed that all leaves have the same spectral reflectance and transmittance and that there are no inhomogeneities on the leaf surface. Sensors are placed both above and below the leaves to measure the spectral irradiance (see **Chyba! Nenašiel sa žiaden zdroj odkazov.**).

These are used to measure how the leaves change the spectrum. The light source is a Lambertian radiator placed centrally above the plant. The spectrum is composed of several LED spectra (450, 660, 730 nm) and corresponds to the wavelength ranges commonly used in plant lighting. The light simulation with the plant is performed in two different setups: Once in the white growth chamber and once in a black one. The results at the different measurement points are listed in Table *1* for the adaxial leaf side and Table *2* for the abaxial leaf side.

$$r_{\mathrm{r:b}} = \frac{\int_{440\,\mathrm{nm}}^{460\,\mathrm{nm}} E_{\mathrm{e},\lambda}(\lambda)\mathrm{d}\lambda}{\int_{650\,\mathrm{nm}}^{670\,\mathrm{nm}} E_{\mathrm{e},\lambda}(\lambda)\mathrm{d}\lambda} \tag{1}$$

$$r_{\mathrm{r:fr}} = \frac{\int_{650\,\mathrm{nm}}^{670\,\mathrm{nm}} E_{\mathrm{e},\lambda}(\lambda)\mathrm{d}\lambda}{\int_{720\,\mathrm{nm}}^{740\,\mathrm{nm}} E_{\mathrm{e},\lambda}(\lambda)\mathrm{d}\lambda} \tag{2}$$

The calculated spectral ratios in *Table 1* show that, especially for the white boxes, hardly any spectral differences were measured in the different leaf ranks. The largest deviations occurred here adaxially for the $r_{\mathrm{r:fr}}$ ratio, as well as abaxially for the $r_{\mathrm{r:b}}$ ratio at the fifth leaf. Especially for the $r_{\mathrm{r:fr}}$ ratio, hardly any differences between adaxial and abaxial side are measurable in a white growth chamber, this can be explained by a high proportion of diffuse light, which provides for a good spectral mixing. In the simulations, which were carried out with an absorbing (black) box, a clear deviation of the spectral ratios from those in the other leaf layers can be seen, especially in the first (lowest) leaf. This can be explained by the fact that this leaf is shaded by others above it, and thus the illumination spectrum is largely determined by the transmission of the leaves above it. This also shows the importance of the use of geometries within those simulation, as those cases cannot be captured with a single radiation equation.

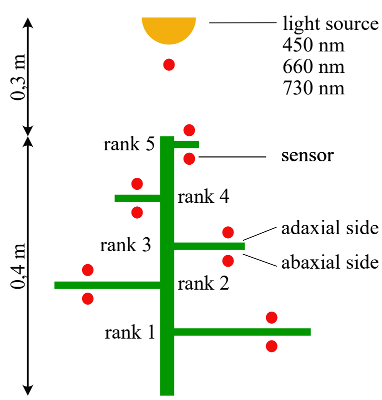

Figure 4 Schematic overview of the experimental setup. Above the plant a light source with lambertian emission characteristics and LED-spectra at 450, 660 and 730 nm (typically used in horticultural applications) is placed. On each leaf, two virtual sensors are placed with approximately 5 mm between the leaf surface and the sensor. Below the light source, a reference sensor is placed to measure the emission spectrum.

The abaxial side of all leaves is influenced by the transmission of the leaves, especially in a black environment, only light passes through the leaves to the sensors due to the absorbing environment. This is shown by ratios varying with leaf rank. In particular, the first leaf shows a very low red component. The differences between the individual leaves are significantly greater here than in the white environment, due to the lack of diffuse and direct light.

Table 1 Experimental results for the adaxial leaf side. Calculated are the spectral ratios for a simulated white and black box.

Rank (adaxial)	red:blue ($r_{\mathrm{r:b}}$) (white box)	red:far-red ($r_{\mathrm{r:fr}}$) (white box)	red:blue ($r_{\mathrm{r:b}}$) (black box)	red:far-red ($r_{\mathrm{r:fr}}$) (black box)
1	1.16	1.04	7.38	0.15
2	1.13	1.15	1.08	1.22
3	1.12	1.18	1.17	1.27
4	1.16	1.11	1.12	1.28
5	1.13	1.37	1.15	1.20

Table 2 Experimental results for the abaxial leaf side. Calculated are the spectral ratios for a simulated white and black box.

Rank (abaxial)	red:blue ($r_{\mathrm{r:b}}$) (white box)	red:far-red ($r_{\mathrm{r:fr}}$) (white box)	red:blue ($r_{\mathrm{r:b}}$) (black box)	red:far-red ($r_{\mathrm{r:fr}}$) (black box)
1	1.10	1.14	0.23	0.1
2	0.98	1.16	2.93	0.16
3	1.06	1.15	2.38	0.16
4	1.08	1.16	1.73	0.16
5	1.37	1.14	1.42	0.14

V. Conclusion

As a result, this example can be used to show the potential of a simulation with virtual plants. When using plant lighting, similar cases can quickly occur: Using a horticultural luminaire with directional light, spectral inhomogeneity will develop in the plant body - but less so with diffuse lighting. A simulation - even of several plants in different growth stages with different phenotypic characteristics is relatively easy to implement. In reality, measurements within the plant canopy are a major challenge, as the radiation itself within the plant is affected by the measuring instruments.

This technology becomes particularly interesting when other factors besides spectral ratios are added. For example, the total absorption on the individual leaf surfaces can be calculated - a simulative determination of light use efficiency and light interception (see above) is thus possible. The evaluation of plant illumination thus becomes more quantifiable.

The authors plan to use virtual plant models as examples in further work, for example to investigate suitable luminaire positions, luminaire spectra, luminous intensity distributions, calculations of light use efficiency or the effects of LED degradation on plants. The long-term goal is to create a tool for luminaire development with virtual plant models.

References

[1] P. Kusuma, P. M. Pattison, and B. Bugbee, 'From physics to fixtures to food: current and potential LED efficacy', *Hortic. Res.*, vol. 7, no. 1, p. 56, Dec. 2020, doi: 10.1038/s41438-020-0283-7.

[2] O. Kniemeyer, G. Buck-Sorlin, and W. Kurth, 'Groimp as a Platform for Functional-Structural Modelling of Plants', in *Functional-Structural Plant Modelling in Crop Production*, J. Vos, L. F. M. Marcelis, P. H. B. De Visser, P. C. Struik, and J. B. Evers, Eds. Dordrecht: Springer Netherlands, 2007, pp. 43–52. doi: 10.1007/1-4020-6034-3_4.

[3] M. Henke and G. H. Buck-Sorlin, 'Using a Full Spectral Raytracer for Calculating Light Microclimate in Functional-Structural Plant Modelling', *Comput. Inform.*, vol. 36, no. 6, pp. 1492–1522, 2017, doi: 10.4149/cai_2017_6_1492.

[4] P. H. B. de Visser, G. Buck-Sorlin, and G. W. A. M. van der Heijden, 'Optimizing illumination in the greenhouse using a 3D model of tomato and a ray tracer', *Front. Plant Sci.*, 2014, doi: 10.3389/fpls.2014.00048.

[5] J. Kim, W. H. Kang, and J. E. Son, 'Interpretation and Evaluation of Electrical Lighting in Plant Factories with Ray-Tracing Simulation and 3D Plant Modeling', *Agronomy*, 2020, doi: 10.3390/agronomy10101545.

[6] K. Saito, Y. Ishigami, Y. Ishigami, and E. Goto, 'Evaluation of the Light Environment of a Plant Factory with Artificial Light by Using an Optical Simulation', *Agronomy*, 2020, doi: 10.3390/agronomy10111663.

[7] K. Kahlen, D. Wiechers, and H. Stützel, 'Modelling leaf phototropism in a cucumber canopy', *Funct. Plant Biol.*, vol. 35, no. 10, p. 876, 2008, doi: 10.1071/FP08034.

[8] T. Hitz, 'Exploring and modelling the influence of spectral light composition on soybean (Glycine max (L.) Merr.)', Feb. 2021, Accessed: June 1, 2022. [Online]. Available: http://opus.uni-hohenheim.de/volltexte/2021/1844/

[9] G. A. Carter, 'PRIMARY AND SECONDARY EFFECTS OF WATER CONTENT ON THE SPECTRAL REFLECTANCE OF LEAVES', *Am. J. Bot.*, vol. 78, no. 7, pp. 916–924, Jul. 1991, doi: 10.1002/j.1537-2197.1991.tb14495.x.

Interactions Between Light and Environments – Impact on Non-visual Effects Evaluation

Laura Bellia
Department of Industrial Engineering
University of Naples "Federico II"
Naples, Italy
bellia@unina.it

Urszula Błaszczak
Department of Photonics, Electronics and Lighting Technology
Politechnika Białostocka
Bialistok, Poland
u.blaszczak@pb.edu.pl

Francesca Diglio
Department of Industrial Engineering
University of Naples "Federico II"
Naples, Italy
francesca.diglio@unina.it

Francesca Fragliasso
Department of Industrial Engineering
University of Naples "Federico II"
Naples, Italy
francesca.fragliasso@unina.it

***Abstract*—Knowing the characteristics of light reaching the occupants' eyes is fundamental to evaluate the human non-visual responses. These characteristics depend on the interactions between light and the built environment. To deeply analyze this effect, the spectral irradiance at the eye level were measured and the related circadian responses were calculated in a test room where 21 different light scenes are set, combining 7 different wall colors and 3 CCTs. Variations of circadian stimulus (CS) for colored walls in comparison to neutral configurations were found. Furthermore, lighting simulations were performed. Spectral irradiance was obtained by means of both basic and accurate computational approaches. The outputs were compared to measurements. It was found that, despite more accurate lighting simulations perform better than the basic ones, results are not always completely reliable.**

Keywords—non-visual effects of light; spectral measurements; spectral simulations; materials reflectance; circadian light; circadian stimulus.

I. Introduction

Light is crucial for human life as it influences us through both visual and non-visual pathways. On one hand, it enables to see and interact with the environment and the other people around us. On the other hand, light affects human well-being and general health, inducing instantaneous and long-term responses. Indeed, it is well known that light can influence body temperature [1], heart rate [2], alertness state [3], mood [4], and work performances [5], also, it influences human circadian rhythm entraining or phase-shifting the human biological clock and affecting the sleep-wake cycle [6]. These effects, called non-image-forming (NIF) or non-visual (NV), mainly depend on the intrinsically photosensitive retinal ganglion cells (ipRGCs) [7].

Even if knowledge about the non-visual effects of light is not fully conclusive yet, recent discoveries have increased the interest in lighting design conceived to support circadian rhythms. To this end, many studies have tried to understand which characteristics of light most affect the circadian responses. New metrics for the evaluation of circadian potential of lighting are emerging, of which the Circadian Stimulus (CS) is often used [8]. It varies from 0.1 to 0.7 and represents the effectiveness of the spectrally weighted irradiance of the cornea in terms of melatonin suppression. CS is linked to the Circadian Light (CLA) which is the irradiance of the cornea weighted to reflect the spectral sensitivity of the human circadian system as measured by acute melatonin suppression after a 1-hour exposure [9].

The traditional lighting design is conceived to satisfy only the merely visual needs (e.g., an adequate color rendering and illuminance level linked to the required task, a restrained glare index, safety requirements). In contrast, lighting design for the entrainment of the circadian system considers the characteristics of light playing a key role in non-visual responses, which are the spectrum, illuminance level at the eye [10], time and duration of light exposure [11], and previous photic history [12] [13]. This approach moves the designer's attention from the light levels on the horizontal surfaces to those on the vertical plans.

For estimating metrics related to NIF effects a crucial first step is to define the spectral irradiance reaching the occupants' eyes [8]. Since it results from the multiple reflections from the surfaces limiting the space its definition is a complex task. The topic would be even more complex, considering the integration of daylight and electric light. Here, we focus only on electric lighting.

Some studies have already dealt with this topic. In [14], [15], a reduction of CS is always found considering yellow, orange, red, grey, and blue walls as compared to white or neutral walls in daylit environments; in [16] the reduction and the increase of the Circadian Action Factor (CAF) are observed for red and blue walls in electric lit environments.

Having said that, it becomes clear that lighting designers need proper tools to calculate the spectral irradiance at the eye, and then infer the corresponding circadian responses. Nowadays, software like ALFA [17] or Lark [18] enable to compute the spectral irradiance at the eye level, considering the spectral modifications of light due to its reflection from the surfaces, but their use has not spread among designers yet.

An alternative approach is to perform traditional simulations considering the total photometric quantities (not the spectral ones) by using any lighting design software to calculate the illuminance at the eye level. Then, it is assumed that the shape of the spectrum at the eye coincides with the one emitted by the light source, so the spectral irradiance at the eye could be calculated by scaling the spectrum of the source to fit it with the calculated illuminance. Hence, the interaction between light and materials is partly considered. Materials can increase or decrease light levels at the eye, but their capacity of modifying the shape of the light spectrum is neglected (since the most common lighting software do not consider the spectral characteristics). This approximation could be acceptable or not based on the properties of the surfaces, i.e., if they are neutral or chromatic.

In this research we try to answer three questions: 1) What is the impact of the spectral reflectance of walls in varying the shape of the spectrum of light reaching the eye and consequently the circadian response? 2) Is this significant? 3) Is it possible to correctly simulate the interaction between light and materials during design phases?

Thus, to study the impact of the indoor features to the descriptors of non-visual responses, we measure the spectral irradiance of light reaching the eye in a test room for different color finishes of the wall facing the observer under three CCTs. Then, to estimate the need of complex calculations during the lighting design including NIF effects, we compare measurements' results with those gained through the two aforesaid calculation approaches:

- Simulation approach 1 - the spectral irradiance at the eye level is simulated by scaling the spectra emitted by the light source to fit it with the illuminances resulting from simple lighting simulations;
- Simulation approach 2 - the spectral irradiance at the eye level is simulated by using accurate lighting simulations accounting for spectral interaction between light and materials.

II. Method

In this study, the Laboratory of Photometry of the Department of Industrial Engineering – University of Naples Federico II (hereafter called Test Room), is used as a simple case study. The room (3.48m by 2.80m) is equipped with 2 white-tuning LED panels and a desk is placed in it (see Fig. 1). Since our aim is to analyze the impact of the walls' color finish on non-visual response to light, regardless of the illuminance values on the work plane, the luminaires are set to emit the 100% of the luminous flux. This brings to very high illuminance levels achieved on the work plane, ranging from 894 lx to 1093 lx depending on the specific light scene.

We assume an observer is sitting at the desk, facing the wall, whose color is changed by covering it with 7 different panels: white, grey, black, blue, red, light blue, and pink. For each color of the wall, three CCTs (3000 K, 4000 K and 6000 K) are set one at a time, so, a total of 21 scenes are considered. Hereafter, each scene will be denoted indicating the CCT and the color of the wall facing the observer, assuming WH for white, GR for gray, BL for black, BU for blue, RE for red, LB for light blue, and PI for pink. For example, "3000K-WH" denotes the scene characterized by CCT equal to 3000 K and the white finish in front of the observer.

First (see results in MEASUREMENTS section), using a Konica Minolta CL500A spectroradiometer (placed as shown in Fig. 1a), we measure the spectral irradiance at the eye level for all the 21 scenes. Then we compute the related CLA and CS values using the CS Calculator released by the Lighting Research Center (LRC) [9].

Then, (see results in SIMULATION APPROACH 1 section), the CS values are calculated with the CS Calculator [9] using as inputs the spectra directly emitted by the light sources, measured with a Konica Minolta CS 2000 spectroradiometer, and reported in Fig. 2 and the illuminance values at the eye level gained by modelling the test-room in DIALux and assigning the surfaces' total reflectance values (see Table I). These are obtained considering the surfaces' spectral reflectance and the actual incident luminous flux for the three CCTs. Illuminances, spectra, and CS values gained with this approach are compared to those arising from measurements.

Finally, (see results in SIMULATION APPROACH 2 section), the CS values are calculated with the CS Calculator [9] considering the spectral irradiance and the illuminance values at the eye level resulting from ALFA simulations. To this end, the Test Room is modelled in Rhinoceros 3D and simulations are performed using the plug-in ALFA. Then, the obtained illuminance values, spectra, and CS are compared to those resulting from measurements.

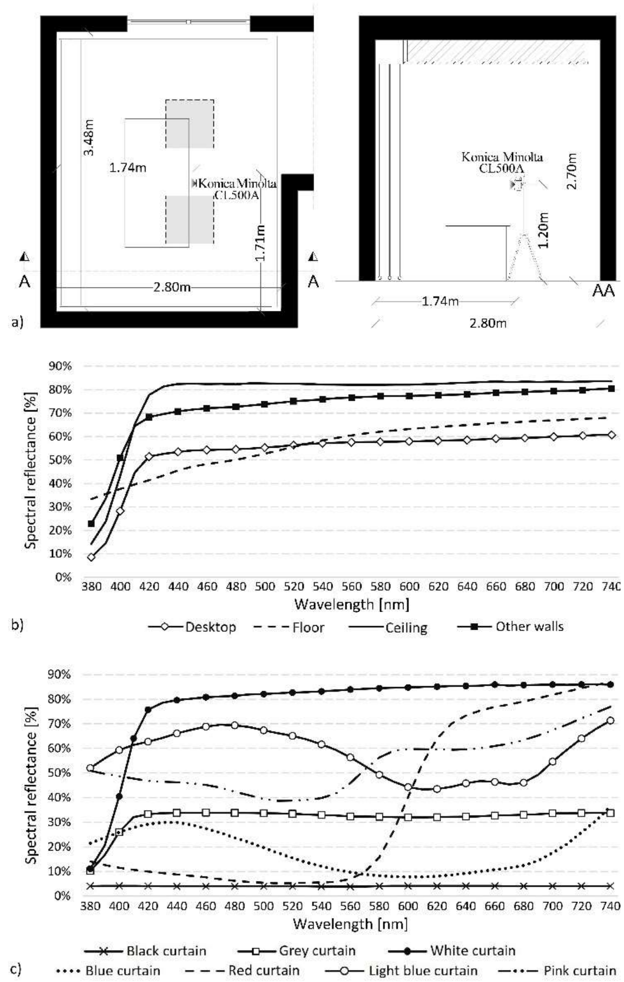

Fig. 1. Test Room's plan and section (a), spectral reflectance of room's surfaces (b) and of the wall facing the observer for various finishes (c).

The comparisons of the two simulation approaches against measurements are based on the relative error (RE) computed as in (1), where "X" is the considered parameter, i.e. CLA, CS, illuminance, and spectral irradiance values alternately.

$$RE\ [\%] = (X_{sim} - X_{meas}) / X_{meas} * 100 \qquad (1)$$

Currently, a standard or a common reference to assess if simulations are reliable as compared to measurements does not exist. However, likewise in [19], RE within ±10% will be considered acceptable in the following.

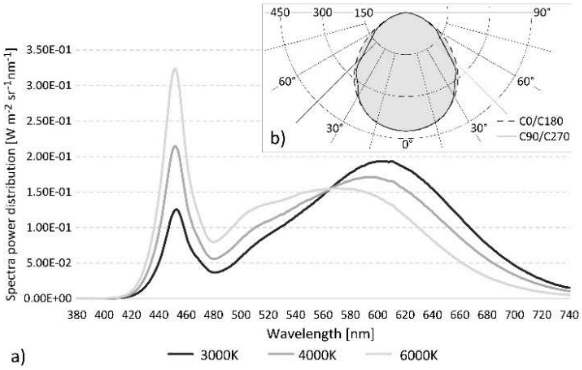

Fig. 2. LED panes' spectral power distribution (a) and photometry (b).

TABLE I. SURFACES' TOTAL REFLECTANCE UNDER DIFFERENT CCTs

surface	Total reflectance		
	3000K	*4000K*	*6000K*
ceiling	0.82	0.82	0.82
walls	0.77	0.77	0.76
floor	0.61	0.60	0.60
desk	0.58	0.57	0.57
white curtain (WH)	0.84	0.84	0.84
light blu curtain (LB)	0.53	0.54	0.56
pink curtain (PI)	0.51	0.50	0.48
grey curtain (GR)	0.32	0.33	0.33
red curtain (RE)	0.23	0.20	0.17
blue curtain (BU)	0.10	0.11	0.11
black curtain (BL)	0.04	0.04	0.04

The comparison of outputs resulting from measurements against those obtained through both simulation approaches allows to analyze the reliability of the lighting simulation software, and the specific comparison of CS values resulting from the three approaches allows to define if complex calculations are always needed when the design of light from a circadian point of view is considered.

III. RESULTS

A. Measurements

Fig. 3 shows the CS and CLA values calculated for the spectral irradiance measured at the eye level for each one of the 21 scenes. As suggested by the LRC, being exposed to a CS equal to or greater than 0.3 for at least one hour in the morning can effectively stimulate the circadian system, leading to better sleep and improved mood and behaviour [8]. Thereby, here, the CS values gained for the 21 scenes are compared against CS=0.3 (indicated with the dashed black line in Fig. 3).

CS values range from 0.18 to 0.43, observed in the "4000K-BL" and "6000K-LB" conditions respectively. In these scenes the lowest and the highest CLA values, equal to 137 and 529 respectively, occur as well.

The impact of the wall's color is significant. CS values are always greater than 0.3 if the wall in front of the observer is light blue, independently from the CCT; considering the white, grey, and pink walls, CS values greater than 0.3 occur for CCTs equal to 3000 K and 6000 K; conversely, CS values are always lower than 0.3 if the black wall faces the observer. At last, for the red and the blue walls, CS values are greater than 0.3 only for CCTs equal to 4000 K and 6000 K.

The CCT is crucial as well: as it can be inferred from Fig. 3, for a fixed wall's color, the lowest CS and CLA values are attained for CCT equal to 4000 K, while the highest CS and CLA values occur for CCT equal to 6000 K. The only exception is the red wall for which the highest CS and CLA values occur for CCT equal to 4000 K.

To better understand these results, it must be underlined that CS values depend on both the amount of light reaching the eye and on the shape of the spectrum.

Similar CS values can be obtained both combining a more stimulating spectrum (energy concentrated in wavelengths around the sensitivity peak of the ipRGCs) with a lower illuminance value and a less stimulating spectrum with a higher illuminance value.

For this reason, it is useful to consider separately the illuminance values at the eye (giving information about the quantity of the received visible radiation) and the shape of the spectra (giving information about the quality of the received visible radiation). Since measured spectra correspond to different illuminance values, they have been scaled to fit a unique value equal to 300 lx (the mean measured eye illuminance collected among the 21 scenes).

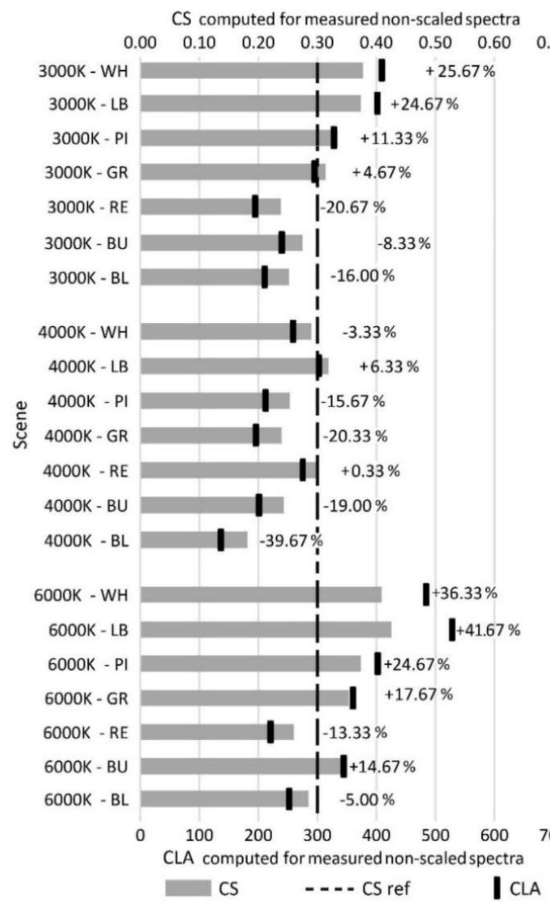

Fig. 3. CS (grey bar) and CLA (black bar) values computed for measured spectral irradiance; percentages refer to the comparison of CS value for each scene against CS = 0.3 (dashed black line).

In this way, all the spectra are compared while providing the same visual stimulus. The scaled spectra are shown in Fig. 4a.3, 4b.3, 4c.3 and Fig. 5a.3, 5b.3, 5c.3.

As expected, considering the white, grey, and black walls (neutral colors) the spectra of light reaching the eye are very similar to the one emitted by the lighting source (see Fig. 2) and nearly overlap each other except in the 450-460 nm interval whatever the CCT (see Fig. 4). Conversely, for blue, red, light blue, and pink walls (strongly characterized from a chromatic point of view) the spectra reaching the eye deviate from the one emitted by the lighting source (see Fig. 2 and 5). In particular, the broadest deviation is observed for the red wall whatever the CCT, while minimal deviations occur for the blue wall for CCTs equal to 3000 K and 6000 K and for the pink wall for CCT equal to 4000 K.

Evaluating the weight of the spectrum shape in altering the circadian response is difficult by simply observing it. For this reason, the CLA for each one of the scaled spectra (CLA_{300lx}) is calculated. It can be considered a good parameter to describe the weight of the shape of the spectrum in defining the CS. Indeed, since all the scaled spectra provide the same visual stimulus, the CLA_{300lx} reflects the potential to vary the circadian response caused only by the differences of the shape of the spectra. The so calculated CLA_{300lx} values are shown in Fig. 6 together with the measured illuminance values and CS values calculated considering the non-scaled spectra (already reported in Fig. 3).

Illuminance values at the observer's eye range between 230 lx and 483 lx observed in the "3000K-BU" and "6000K-WH" conditions respectively. They follow the decreasing order WH>LB>PI>GR>RE>BL>BU for CCTs equal to 4000 K and 6000 K, while for 3000 K the only difference is that the PI illuminance value is a little bit higher than the LB one. Therefore, WH and LB colors bring to higher illuminance values whereas BL and BU colors lead to the lowest ones.

CLA_{300lx} values range between 155 and 436 observed in the "4000K-PI" and "6000K-BU" conditions respectively. They follow the decreasing order BU>LB>GR>BL>WH>PI>RE for CCTs equal to 3000 K and 6000 K, while for 4000 K the only difference from the aforesaid order is that the RE color provides the highest CLA_{300lx} value. Therefore, blue and light blue provide the most stimulating spectra whereas pink and red provide the less stimulating ones, except for CCT equal to 4000 K. It is interesting to note that if the same illuminance value at the eye were provided in the test room conditions, the grey, blue, and black walls would be more stimulating than the white one.

As can be inferred from Fig. 6, very similar CS values occur in the "3000K-WH" and "3000K-LB" conditions, and in the "6000K-WH" and "6000K-LB" conditions. These similar CS values are obtained in two different ways: both for 3000 K and 6000 K, if the white wall faces the observer, it results from a less stimulating spectrum shape combined with a high illuminance value, while, considering the light blue wall, it results from a more stimulating spectrum shape combined with a lower illuminance value.

It can be observed that CLA_{300lx} values are always higher for CCT equal to 6000 K and lower for CCT equal to 4000 K (except for the red wall). Therefore, the spectra shapes are more stimulating from a circadian point of view if a CCT equal to 6000 K is considered and less stimulating for a CCT equal to 4000 K, whatever the color of the wall.

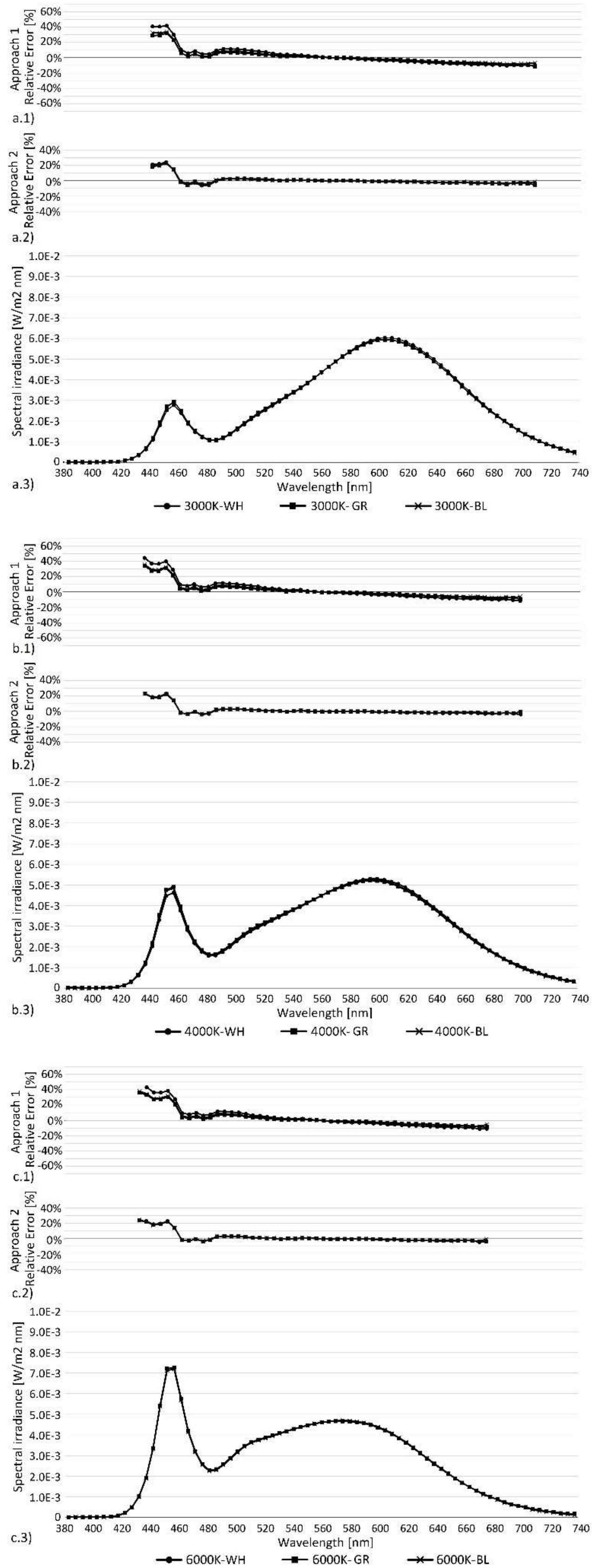

Fig. 4. Spectral irradiance at the eye level for a fixed Ev=300lx resulting from measurements (a.3, b.3, c.3) and relative errors observed applying the simulation approach 1(a.1, b.1, c.1) and simulation approach 2 (a.2, b.2, c.2) for the white, grey, and black walls facing the observer.

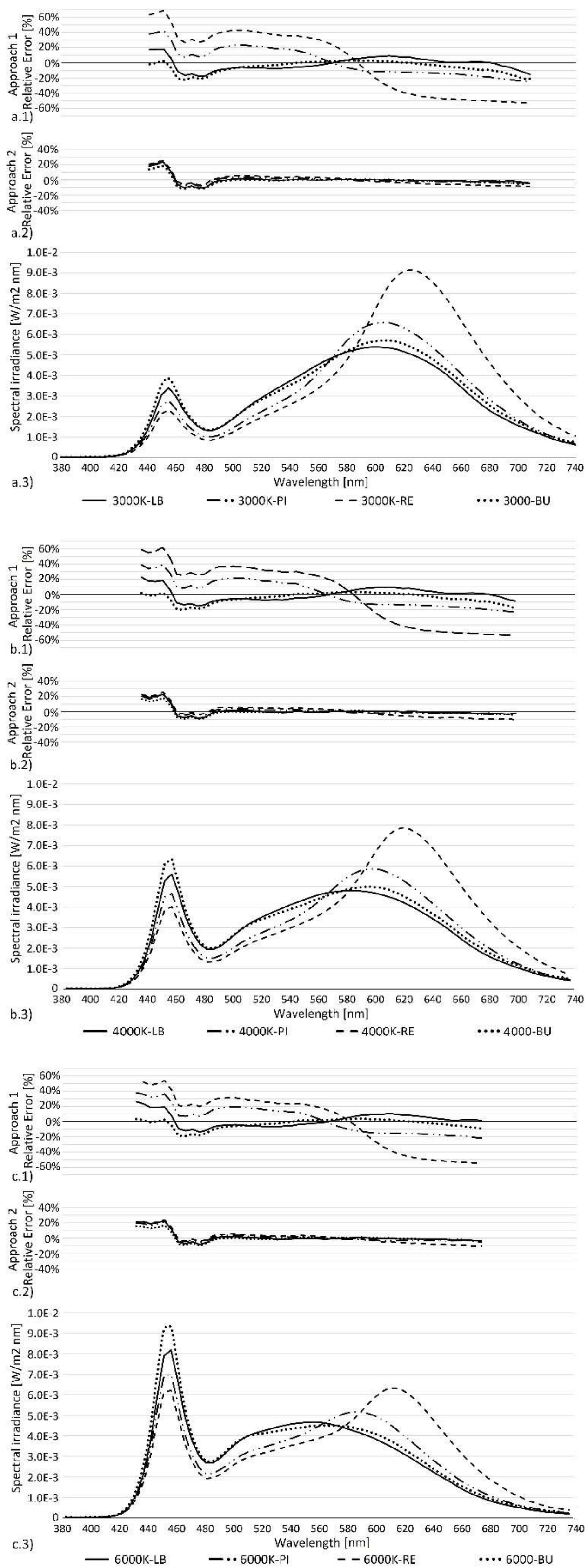

Fig. 5. Spectral irradiance at the eye level for a fixed Ev=300lx resulting from measurements (a.3, b. 3, c. 3) and relative errors observed applying the simulation approach 1(a.1, b. 1, c. 1) and simulation approach 2 (a.2, b. 2, c. 2) for the light blue, pink, red, and blue walls facing the observer.

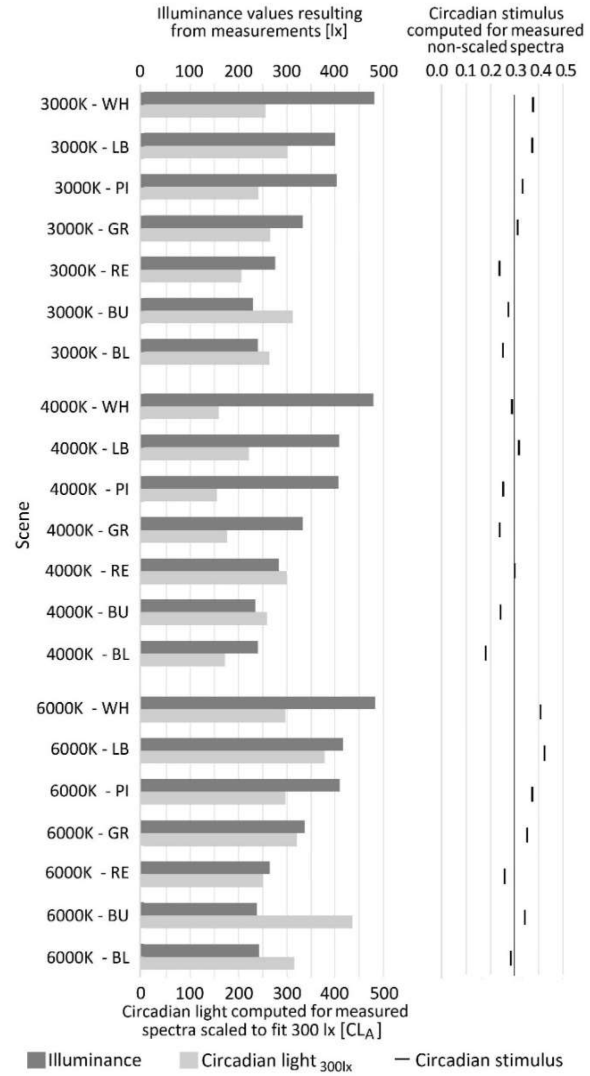

Fig. 6. Measured illuminances (dark grey bar), circadian light computed for spectra scaled to fit the illuminance value equal to 300 lx (light grey bar) and circadian stimuli (black dashes) computed for non-scaled spectra.

This explains why CS values are always higher for CCT equal to 6000 K and lower for CCT equal to 4000 K (except for the red wall) even if, for fixed wall color, the illuminance values are similar among the three CCTs.

The contribution of the spectrum shape is crucial in the definition of the circadian response: for the white and pink walls for CCT equal to 4000 K, CS values are lower than 0.3 since the related CLA_{300lx} are very low, even if high illuminance values are achieved in these conditions. Also, for the blue and black walls, even if the illuminance values are similar, CS values for the BU case are higher due to the higher CLA_{300lx}. Specifically, for 6000 K CCT, a CS value greater than 0.3 is achieved even with low illuminances.

B. Simulation Approach 1

Table II shows the illuminance, CLA_{300lx} values and CS values resulting from DIALux simulations, and the related relative errors computed in comparison to the corresponding measured quantities. The values trespassing ±10% are highlighted in bold type. CLA_{300lx} is computed considering the spectra emitted by the lighting source scaled to fit 300 lx illuminance, whereas CS values are computed considering the illuminances resulting from DIALux simulations and the spectra emitted by the lighting source scaled to fit them.

CS values range from 0.23 to 0.49, observed in the "4000K-BL" and "6000K-WH" scenes respectively. Neither the highest and the lowest CS values, nor the scenes where they occur correspond to those noted for the measurements except for the scene in which the lowest CS value occur. CS values computed applying the simulation approach 1 are always higher than those resulting from measurements except in the "4000K-RE" scene. The minimum (+0.41%) and the maximum (+40.0%) relative errors occur in the "4000K-BU" and "6000K-RE" scenes respectively.

Considerable relative errors occur in 13 scenes over the considered 21 scenes: for the white, pink, and red walls whatever the CCT, and for the grey and black walls for CCTs equal to 4000 K and 6000 K. These errors can be ascribed both to illuminance at the eye and the shape of the spectrum.

As regards illuminance, values obtained by performing DIALux simulations range between 249 lx and 573 lx observed in the "4000K-BL", "6000K-BL" and "3000K-WH" conditions respectively. As expected, the illuminances follow the decreasing order WH>LB>PI>GR>RE>BU>BL whatever the CCT, according to the decreasing order of the wall's total reflectance.

If compared to measurements, DIALux always provides higher illuminances, showing the minimum (+3.06%) and maximum (+19.14%) relative errors in the "6000K-BL" and "3000K-WH" scenes respectively. In particular, considerable relative errors occur for the white, blue, and light blue walls whatever the CCT, and for "3000K-RE" and "3000K-PI".

As for the shape of the spectra, the relative errors calculated for normalized spectral irradiance are shown in Figg. 4 and 5. A clarification is needed about the RE computed for the spectral irradiance. Since spectral irradiance values are often equal to 0 in the extremes of the interval 380 nm-740 nm, the related RE are very high but not significant and misleading. So, we compute them only for spectral irradiance values greater than 10-3 Wm-2nm-1.

Considerable relative errors occur in the short-wavelength interval [≈430 nm-455 nm] whatever the color of the wall in front of the observers, and for the pink and red walls, for all the wavelengths (see Fig. 4 and 5). In more detail, the maximum relative errors occur for λ=450 nm in the "4000K-RE", "4000K-PI", and in all the 3000 K scenes whatever the color of the wall, except for the blue wall. In this last case, the maximum relative errors occur for λ=465 nm whatever the CCT. For white, grey, black, and light blue walls, for CCT equal to 4000 K, and in the "6000K-WH" scene, the maximum relative errors are observed for λ=435 nm. At last, the maximum relative errors occur for λ=430 nm for grey, black, red, light blue, and pink walls for CCT equal to 6000 K. Among the aforesaid maximum relative errors, the highest (+68.72%) and the lowest (+17.70%) values occur in the "4000K-RE" and "3000K-LB" scenes respectively.

The observed differences are confirmed by the CLA_{300lx} shown in Table II. Since DIALux does not simulate the spectral interreflections between light and materials, CLA_{300lx} vary only depending on the CCT. In particular, CLA_{300lx} values are equal to 288, 225, and 393 for CCTs equal to 3000 K, 4000 K, and 6000 K respectively.

TABLE II. COMPARISON OF THE RESULTS OBTAINED BY APPLYING THE SIMULATION APPROACH 1 AGAINST THE CORRESPONDING QUANTITIES GAINED FROM MEASUREMENTS

Light scene	Simulation approach 1					
	***Ev* [lx]**	***RE_{Ev}* [%]**	***CLA_{300lx}***	***$RE_{CLA300lx}$* [%]**	***CS***	***RE_{CS}* [%]**
3000K-WH	573	**+19.14**	288	**+12.50**	0.43	**+14.85**
3000K-LB	456	**+14.26**	288	-4.64	0.39	+4.28
3000K-PI	446	**+10.54**	288	**+19.50**	0.39	**+15.57**
3000K-GR	357	+7.16	288	+8.27	0.34	+9.24
3000K-RE	319	**+15.75**	288	**+39.81**	0.32	**+34.87**
3000K-BU	268	**+16.46**	288	-7.69	0.29	+4.73
3000K-BL	252	+5.15	288	+9.09	0.28	+9.92
4000K-WH	567	**+18.27**	225	**+41.51**	0.39	**+33.79**
4000K-LB	456	**+11.86**	225	+1.81	0.35	+8.15
4000K-PI	437	+7.32	225	**+45.16**	0.34	**+32.81**
4000K-GR	358	+7.40	225	**+27.84**	0.30	**+24.27**
4000K-RE	304	+7.33	225	**-25.00**	0.27	**-11.63**
4000K-BU	269	**+14.68**	225	**-13.13**	0.24	+0.41
4000K-BL	249	+3.56	225	**+30.81**	0.23	**+27.07**
6000K-WH	566	**+17.18**	393	**+32.32**	0.49	**+19.07**
6000K-LB	466	**+11.98**	393	+3.97	0.45	+6.59
6000K-PI	427	+4.49	393	**+32.32**	0.44	**+16.84**
6000K-GR	358	+6.38	393	**+22.43**	0.40	**+14.45**
6000K-RE	292	+10.32	393	**+56.57**	0.36	**+40.00**
6000K-BU	269	**+12.85**	393	-9.86	0.35	+1.16
6000K-BL	249	+3.06	393	**+24.76**	0.33	**+16.49**

As regards CLA_{300lx}, considerable relative errors occur for the white, pink, and red walls whatever the CCT, for the grey and black walls for CCTs equal to 4000 K and 6000 K, and in the "4000K-BU" condition.

Given all these considerations, it is worthy to note that considerable relative errors for CS values occur always when considerable relative errors for CLA_{300lx} values occur (both with considerable errors for illuminance values or not), that is for the white, pink, and red walls whatever the CCT, and for the grey and black walls for CCTs equal to 4000 K and 6000 K. Conversely, considerable relative errors noted only for the illuminance values do not correspond to considerable errors for the related CS values. Nevertheless, considering the "4000K-BU", considerable relative errors occur both for illuminance and CLA_{300lx} values but not for CS values.

However, the obtained results seem to prove that errors in CLA are more relevant in the definition of CS rather than the errors in illuminance values. So, it seems that in simulations it is more crucial to consider the correct shape of the spectrum at the eye rather than the exact illuminance value.

Simulation Approach 2

Table III shows the illuminance, CLA_{300lx} values and CS values resulting from ALFA simulations, and the related relative errors computed in comparison to the corresponding measured quantities. The values trespassing ±10% are highlighted in bold type. CLA_{300lx} is computed considering the spectra resulting from simulations scaled to fit 300 lx illuminance, whereas CS values are computed considering the illuminance values and the non-scaled spectra resulting from ALFA simulations.

CS values range from 0.18 to 0.45, noted in the "4000K-RE" and "6000K-WH" scenes respectively. Neither the maximum CS value, nor the scenes when it occurs correspond to the one noted for measurements. The same minimum CS value (0.18) occurs both for measurements and simulation approach 2, but it is observed in different scenes ("4000K-BL" and "4000K-RE" respectively).

CS values computed applying the simulation approach 2 are higher than those arising from measurements except for "4000K-RE". The minimum (+1.50%) and the maximum (-39.20%) relative errors occur in the "3000K-PI" and "4000K-RE" scenes respectively. Considerable relative errors occur for the black wall whatever the CCT, for the grey and red walls for 4000 K and 6000 K CCTs, and for "4000K-WH".

As for illuminance, values obtained by means of ALFA simulations range from 248 lx to 530 lx, noted in the "3000K-BU" and "3000K-WH" scenes respectively. As expected, the illuminance values follow the decreasing order WH>LB>PI>GR>RE>BU>BL whatever the CCT, according to the decreasing order of the wall's total reflectance.

TABLE III. COMPARISON OF THE RESULTS OBTAINED BY APPLYING THE SIMULATION APPROACH 2 AGAINST THE CORRESPONDING QUANTITIES GAINED FROM MEASUREMENTS

Light scene	Simulation approach 2					
	Ev [lx]	*RE_{Ev} [%]*	*CLA_{300lx}*	*$RE_{CLA300lx}$ [%]*	*CS*	*RE_{CS} [%]*
3000K-WH	530	+10.30	265	+3.52	0.40	+6.63
3000K-LB	414	+3.74	307	+1.66	0.38	+2.67
3000K-PI	393	-2.61	249	+3.32	0.34	+1.50
3000K-GR	364	+9.38	276	+3.76	0.34	+7.96
3000K-RE	291	+5.74	217	+5.34	0.25	+6.72
3000K-BU	248	+7.98	312	0.00	0.29	+5.09
3000K-BL	272	**+13.38**	273	+3.41	0.28	**+11.51**
4000K-WH	527	+9.89	185	**+16.35**	0.34	**+16.21**
4000K-LB	416	+1.94	242	+9.50	0.34	+6.90
4000K-PI	400	-1.84	177	**+14.19**	0.27	+8.30
4000K-GR	364	+9.08	203	**+15.34**	0.28	**+17.15**
4000K-RE	296	+4.63	143	**-52.33**	0.18	**-39.20**
4000K-BU	250	+6.60	272	+5.02	0.26	+8.64
4000K-BL	272	**+13.15**	199	**+15.70**	0.22	**+23.76**
6000K-WH	526	+8.84	336	**+13.13**	0.45	+9.54
6000K-LB	419	+0.62	413	+9.26	0.44	+4.24
6000K-PI	405	-0.98	332	**+11.78**	0.39	+4.28
6000K-GR	363	+7.97	362	**+12.77**	0.39	**+10.76**
6000K-RE	276	+4.39	289	**+15.14**	0.29	**+13.08**
6000K-BU	253	+6.03	458	+5.05	0.37	+6.10
6000K-BL	267	+10.33	356	**+13.02**	0.33	**+14.74**

If compared to measurements, ALFA always provides higher illuminances except for the pink wall, showing the minimum (+0.62%) and maximum (+13.38%) relative errors in the "3000K-BL" and "6000K-LB" scenes respectively.

Considerable relative errors occur only for the black wall facing the observer for CCT equal to 3000 K and 4000 K.

As for the shape of the spectra, considerable relative errors occur only in the short-wavelength interval [≈430 nm-455 nm] (see Fig. 4 and 5). In more detail, the maximum relative errors occur for λ=450 nm for almost all the scenes, except in "6000K-WH", "6000K-GR", "4000K-BL", and "6000K-BL" scenes, in which they are observed for λ=435 nm, λ=430 nm, λ=435 nm, and λ=430 nm respectively. Among the aforesaid maximum relative errors, the highest (+25.54%) and the lowest (+17.22%) values occur in the "4000K-RE" and "6000K-BU" scenes respectively.

The observed differences are confirmed by the CLA_{300lx} shown in Table III. They range from 143 to 458 observed in the "4000K-RE" and "6000K-BU" scenes respectively. They follow the decreasing order BU>LB>GR>BL>WH>PI>RE whatever the CCT. As regards CLA_{300lx}, considerable relative errors occur for CCTs equal to 4000 K and 6000 K for the white, pink, grey, red, and black walls.

As seen in simulation approach 1 section, considerable relative errors for CS values are observed if considerable relative errors occur for CLA_{300lx} values, that is for "4000K-WH", and for grey, red, and black walls with 4000K and 6000K CCTs. Nevertheless, in "3000K-BL", a considerable relative error for CS value is observed even if considerable relative error occurs only for illuminance. At last, for "4000K-PI", "6000K-PI", and "6000K-WH" considerable relative errors do not occur even if considerable relative errors are observed for CLA_{300lx} values.

IV. Discussion and Conclusion

In this paper, the influence of walls' color on circadian responses, evaluated through the CLA and CS, has been analyzed considering 7 different walls' color and 3 CCTs.

We found that the alteration of CLA and CS strongly depends on the color of the walls, the luminaires' CCT and their combination. In particular, we proved that the white color (characterized by high total reflectance) provides high illuminance values at the eye level and ensures the achievement of a sufficient CS value whatever the luminaire's CCT, even for a low stimulating spectrum shape occurring for CCT equal to 4000 K. Conversely, reducing the total reflectance of the surface, it is crucial to consider the interaction between colors and CCT. Indeed, the grey color (characterized by intermediate total reflectance) provides intermediate illuminance values at the eye level and ensures the achievement of a sufficient CS value only for high stimulating spectra shapes occurring for CCTs equal to 3000 K and 6000 K. In addition, the black color (characterized by low total reflectance) provides very low illuminance values at the eye level and never ensures the achievement of a sufficient CS value, even though the spectra shapes would be more stimulating than those related to the white color, if the same eye illuminance value would be provided. Similarly, as for the pink, red and blue, the provided illuminances ensure the achievement of sufficient CS values only for stimulating spectra shapes occurring for both CCTs equal to 3000 K and 6000 K for the pink, and for 4000 K and 6000 K for red and blue respectively. Considering the light blue (blue with high brightness), it ensures the achievement of a sufficient CS value whatever the luminaire's CCT, likewise the white case discussed before. In sum, white walls always ensure the achievement of CS values greater than 0.3 and further increases up to 0.43 (for CCT equal to 6000 K) can be obtained by painting the walls with the light blue color. On the other hand, reductions of CS, up to 0.18 (specifically for CCT equal to 4000 K), can be obtained by painting the walls with the black color.

Also, this paper investigates what is the most proper approach to simulate the interactions between light and materials during the design phase when the light-induced circadian response is considered. To this end, two simulation approaches have been compared each other and against measurements, taking into account the reliability of the two simulation approaches in predicting spectral irradiance, illuminance values and light-induced circadian responses.

We proved that the software ALFA provides very reliable illuminance values for almost all the considered light scenes. In addition, spectra resulting from simulations nearly overlap those resulting from measurements (except in the short-wavelength interval) whatever the CCT is, both for neutral walls and those strongly characterized from a chromatic point of view. On the other hand, significant relative errors are often observed considering the CLA_{300lx} values calculated for the normalized spectra resulting from ALFA simulations, and, consequently, for CS values as well.

However, considering the simulation approach 1, reliable outputs are observed in very few scenes, concerning all illuminance, CLA_{300lx}, and CS values. Therefore, performing simulations with ALFA ensure to achieve more reliable results rather than using DIALux to obtain the illuminance values and scaling the spectra emitted by the lighting source to fit them. This underlines the need to use proper lighting simulation software when the design of light from a circadian point of view is considered. Indeed, considering the "3000K-WH" scene (the condition when the highest relative error for illuminance value occurs), CS value computed for measurements' outputs is equal to 0.38 while the one computed for simulation approach 1 is equal to 0.43. Moreover, considering the "6000K-RE" scene (the condition when the highest relative error for CLA_{300lx} value occurs), CS value calculated for measurements' outputs is equal to 0.26 while the one computed simulation approach 1 is equal to 0.36. On the other hand, considering the "6000K-LB" scene (the condition when the lowest relative error for illuminance value occurs), CS value calculated for measurements' outputs is equal to 0.43 while the one computed for simulation approach 2 is equal to 0.44. Moreover, considering the "3000K-BU" scene (the condition when the lowest relative error for CLA_{300lx} value occurs), CS value calculated for measurements' outputs is equal to 0.28 while the one computed for simulation approach 2 is equal to 0.29.

Putting together the results of measurements and simulations, we can conclude that the shape of the spectra is crucial for the definition of CS values, therefore the alteration of the spectra emitted by the light source needs to be considered by proper lighting simulation software accounting for spectral interreflection between light and materials.

Further studies are needed to deepen the specific weight of spectra and illuminance on the light-induced circadian response. They should consider proper illuminance values on the work plan (i.e. that meet standard's requirements), other light sources' spectra, other colors of the walls and/or other distributions of the color in the space (e.g. covering with colored cardboards all walls, only the wall on the left of the observer, only the one on the right, and so on).

REFERENCES

[1] M. Te Kulve, L. Schlangen, and W. van Marken Lichtenbelt, "Interactions between the perception of light and temperature," Indoor Air, vol. 28, no. 6, pp. 881–891, 2018.

[2] C. Cajochen et al., "High sensitivity of human melatonin, alertness, thermoregulation, and heart rate to short wavelength light," J. Clin. Endocrinol. Metab., vol. 90, no. 3, pp. 1311–1316, 2005.

[3] S. W. Lockley, E. E. Evans, F. A. J. L. Scheer, G. C. Brainard, C. A. Czeisler, and D. Aeschbach, "Short-wavelength sensitivity for the direct effects of light on alertness, vigilance, and the waking electroencephalogram in humans," Sleep, vol. 29, no. 2, pp. 161–168, 2006.

[4] M. B. C. Aries, J. A. Veitch, and G. R. Newsham, "Windows, view, and office characteristics predict physical and psychological discomfort," J. Environ. Psychol., vol. 30, no. 4, pp. 533–541, 2010.

[5] O. Keis, H. Helbig, J. Streb, and K. Hille, "Influence of blue-enriched classroom lighting on students′ cognitive performance," Trends Neurosci. Educ., vol. 3, no. 3–4, pp. 86–92, 2014.

[6] J. F. Duffy and C. A. Czeisler, "Effect of Light on Human Circadian Physiology," Sleep Med. Clin., vol. 4, no. 2, pp. 165–177, 2009, doi: 10.1016/j.jsmc.2009.01.004.

[7] G. C. Brainard et al., "Action spectrum for melatonin regulation in humans: evidence for a novel circadian photoreceptor," J. Neurosci., vol. 21, no. 16, pp. 6405–6412, 2001.

[8] M. G. Figueiro, K. Gonzales, and Da. PeDLer, "Designing with circadian stimulus," Ld+ a, vol. 8, pp. 30–34, 2016.

[9] Lighting Research Center, "CS calculator." https://www.lrc.rpi.edu/cscalculator/ (accessed Jun. 07, 2022).

[10] K. W. Houser, P. R. Boyce, J. M. Zeitzer, and M. Herf, "Human-centric lighting: Myth, magic or metaphor?," Light. Res. Technol., vol. 53, no. 2, pp. 97–118, 2021.

[11] J. J. Gooley, S. M. W. Rajaratnam, G. C. Brainard, R. E. Kronauer, C. A. Czeisler, and S. W. Lockley, "Spectral responses of the human circadian system depend on the irradiance and duration of exposure to light," Sci. Transl. Med., vol. 2, no. 31, pp. 31ra33-31ra33, 2010.

[12] A. Chang, F. A. J. L. Scheer, and C. A. Czeisler, "The human circadian system adapts to prior photic history," J. Physiol., vol. 589, no. 5, pp. 1095–1102, 2011.

[13] C. Vetter et al., "A review of human physiological responses to light: Implications for the development of integrative lighting solutions," Leukos, pp. 1–28, 2021.

[14] J. Hraška and P. Hartman, "Daylighting: Prediction of circadian effects of different spectral filters," in Advanced Materials Research, 2014, vol. 1041, pp. 386–389.

[15] P. Hartman, L. Maňková, P. Hanuliak, and M. Krajčík, "The influence of internal coloured surfaces on the circadian efficiency of indoor daylight," in Applied Mechanics and Materials, 2017, vol. 861, pp. 493–500.

[16] I. T. Kim, A. S. Choi, and M. K. Sung, "Accuracy evaluation of a calculation tool based on the spectral colour property of indoor luminous environments," Build. Environ., vol. 139, pp. 157–169, 2018.

[17] Solemma, "ALFA - Adaptive Lighting for Alertness," 2018. https://www.solemma.com/alfa (accessed Jun. 07, 2022).

[18] M. Inanici & ZGF Architects LLP, "Lark Spectral Lighting." 2015.

[19] I. A. Rahman, J. C. P. Putra, and A. Asmi, "Modelling of Particle Dispersion in Mechanically Ventilated Space," Mod. Appl. Sci., vol. 8, no. 3, p. 60, 2014.

Dynamic Road Lighting Using Image-Based Traffic Intensity Sensors; System Considerations and Practical Results on Energy Savings

Eduardo Pereira
Segment & Product Mgmt Outdoor
*Tridonic AG**
Ennenda, Switzerland
eduardo.pereira@tridonic.com

Markus Wagenseil
Segment & Product Mgmt Outdoor
*Tridonic GmbH & Co KG**
Dornbirn, Austria
markus.wagenseil@tridonic.com

***Abstract*— This paper will present the results obtained on a test installation where low bandwidth edge processing imaging sensors were deployed for traffic intensity measurements. The comparison of energy consumption data between astronomical clock based on and off and dynamic lighting, based on the traffic information, scenarios will be presented and extended to a citywide case. The innovative sensors were deployed directly into the lighting system via Zhaga interface allowing seamless integration. Data was collected using DALI D4i based LED drivers.**

Keywords—Smart Street lights, adaptive street lighting, smart cities, vision system, traffic, image sensors.

I. Introduction

Across the globe, more than 90 million streetlights are installed turning it into a ubiquitous facility in urban and country areas [1]. Properly designed street lighting can reduce illegal activities and improve road safety [2]**Chyba! Nenašiel sa žiaden zdroj odkazov.** resulting in a positive effect on human behavior by facilitating social and economic activities at night. Even though having innumerous benefits, the financial and environmental impacts of street lighting is a major concern to local authorities. Almost 40% of a city's electricity costs is used by street lighting [4]. Overall energy consumption figures are up to 114TWh resulting in 64 million tons of carbon dioxide dissipated in the atmosphere [1]. The economical and environmental concerns will not ease in short term given the predicted growth in the number of streetlights was over 300% in the last decade [5].

Normally on streetlights, lamps are turned on continually overnight. Several systems allow controlling the start and the end of this period via fixed time schedules or integrated photocells. Nevertheless, this approach can result into higher power consumption. There is still a latent need to reduce brightness in periods when it is not required. Typical examples of such periods include later hours of the night when traffic of persons and vehicles is reduced. Time-based dimming approaches are well established whereby selected streetlights are switched off or dimmed at specific hours. In a typical city with circa 150.000 habitants the annual savings can reach up to $900.000 and the amount carbon dioxide spread is reduced by 3.000 tons just with time-based control of the installation[6]. Despite solid savings both financially and environmentally, time-based dimming profiles ignores the original purpose of having street lighting. The reduction of street lighting at some specific periods could cause impairment on road users' skills to navigate or to avoid obstacles [7], leaving the environment prone to have more accidents or crimes.

Recently, new sensing and communication technologies have gained space on streetlight control and monitoring allowing fine management of streetlight infrastructure [8][9][10]. This remote-managed and sensor-controlled approach offers more potential for energy savings as the capability of continual adjusts of light level is possible. With this solution a control center, in some cases remotely, is responsible for management and control of the installation including dimming to save energy and monitoring of the streetlight assets. In more advanced installations, light levels are adjusted according to environment conditions including weather and traffic conditions that are collected by local sensors.

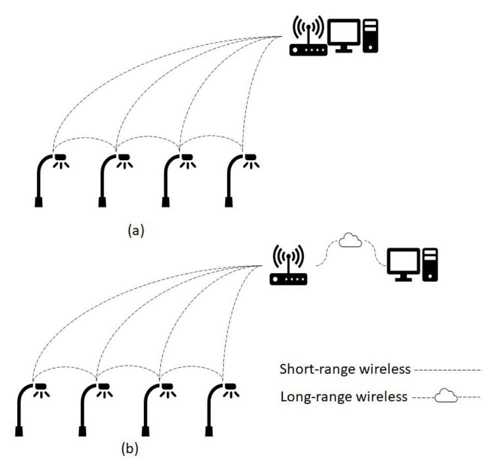

Fig. 1. Common network topologies.

The majority of the proposed remote- and sensor-controlled street lighting uses short range wireless to establish a communication between poles and local gateways see Fig.1(a) while remote wireless communication networks are used when the installation is intended to be remotely controlled Fig.1(b).

The rest of the paper is organised as follows. Section 2 discusses the proposed vision sensor considering the minimization of the required data transfer. Section 3 presents practical results from the deployment of the proposed sensor. Finally, section 4 concludes the paper.

*Member of the Zumtobel Group.

II. Vision Based System for Traffic Detection

The most straightforward way to minimize energy consumption on streetlights is to turn them off. Unfortunately, this goes against its purpose. Well operated streetlights enable road users to see clearly, better and further. Some studies even consider psychological needs [11]. Combining safe roads with energy saving s is then only possible by using sensors that can detect the actual level of traffic and adjust light levels accordingly. Adaptive dimming control strategies for smart streetlights has been investigated under various aspects. For example, studies in [12-15] focus on pedestrian-based methods, [16-19] focus on road traffic, while [20-22] consider both methods.

In this section, we focus on how to generate the actual traffic density information using image based sensor considering the practical aspects.

A. *Edge deployment of vision sensors*

In a dimming according to traffic street light system, the main target of the vision sensor is to count the average number of cars in each road section over a time window. The optimal parameters are subject of some studies [23][24]. Algorithms are responsible for video analytics and later the data is presented for the final user or used as input to generate automatic commands to the streetlight system. With this setup, the light levels can be adjusted according to traffic.

When deploying a vision sensor that needs connection to the cloud for data analytics and, in this case, sending commands back to the streetlight system, three basic ways are possible, see Fig.2.

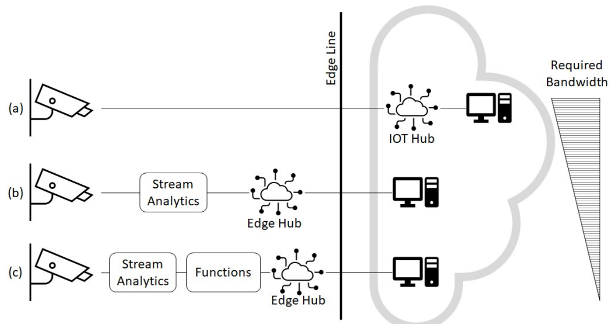

Fig. 2. Possible ways to connect a sensor to the cloud.

Fig.2(a) shows a typical arrangement when the vision sensor has built in network connection capabilities. In this case, the video analytics is performed by computing units placed on the cloud. The processing power contained in the sensor is relatively low since the complexity has been shifted to cloud premises. The sensor streams video footage directly to the network resulting in high demand for bandwidth on the communication channel. The high bandwidth requirements in this arrangement limits the type of network protocol to be used. High latency choices, e.g., LoRaWAN, are not possible in this scenario.

The first alternative to minimize the amount of data being transferred over the communication channel is performing basic functionality at the sensor, see Fig.2(b). Processing complexity in the sensor is increased and data generated by the sensor is still a video stream with video compaction allowing lower bandwidth requirements. In this scenario, the data from many sensors can also be concentrated into an "Edge Hub" and a single broadband connection can be shared within several sensors in the installation.

Fig.2(c) shoes the arrangement of the so called "Edge deployed" sensor. All the expected functionalities are now implemented in the vision sensor unity. This allows massive reduction on the amount of data required to be transmitted since, instead of a video stream, the sensor broadcasts short data packets informing the average of cars that crossed the road on the last time window.

B. *Privacy considerations*

Looking at Fig.2(a) the data going to the cloud is a video stream. Therefore, privacy is not guaranteed since the system can now be attacked and the video stream can be seen, and stored, by third persons. The same is also valid for Fig.2(b) arrangement. Full privacy is only ensured with the arrangement presented in Fig.2(c). For this arrangement, no video, nor pictures, leaves the device and the implementation of the device is done in a way that no internal memory is used to store privacy relevant data. Individual frames are processed and not stored in the device.

C. *Implemented system*

For the practical results the system components show in Fig.3 were used.

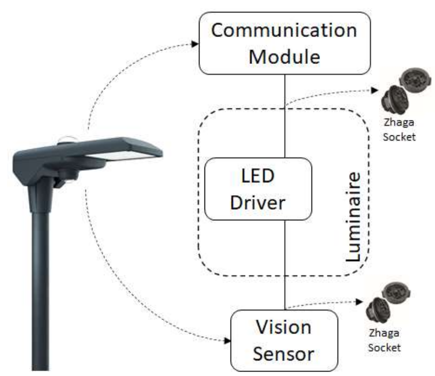

Fig. 3. Sytem components with power and data connections

A total of 12 video sensors were deployed in different street segments in the city of Glostrup, Denmark. Each luminaire is equipped with a 120W LED driver with Zhaga D4i interface allowing the measurement of consumed power of each device. Data was logged and transmitted by communication modules working on IPv6/6LoWPAN protocols using narrow band 868MHz frequency. Data was logged over a period of one year. See Fig.4 for a picture of one of the sensors installed.

Fig. 4. One of the luminaires under test.

III. PRACTICAL RESULTS

Several data collection campaigns were performed for collecting data. For each luminaire the following data was tracked:

- Switch-on and switch-off time.
- Date (dd.mm.yyyy).
- Total energy consumption from the last hour.
- The number of cars crossing the road in the last hour.

Fig.5 shows the average number of cars per hour on sensor number 12 over the period of one year.

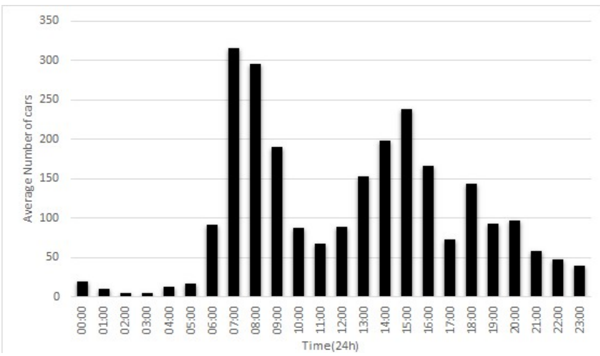

Fig. 5. Average number of cars counted by sensor 12 over one year.

The typical traffic pattern with peaks coinciding with office times, 7:00h and 16:00h. Interesting to note that on the period from 00:00h to 05:00 there is a drastic drop on the number of cars passing. That time interval is the perfect spot for reducing the light intensity to minimum levels. For this work the presence of pedestrians were not considered.

On average for the location under investigation, when operating under time-controlled scheme, the average switch-on time was around 18:00h whilst turn-off time was 07:00h. Lights were completely off outside this time window. Bad weather days when lights are turned on during storms were not accounted. When operating under time-controlled the drivers are operating at full power consuming 120W in average. For the time the system was then operating with dynamic levels according to the traffic the dim level was proportional to the traffic intensity from the last hour. In this condition maximum power was applied on the period when the maximum number of cars was reached. That scheme results on the following diagram from Fig.6.

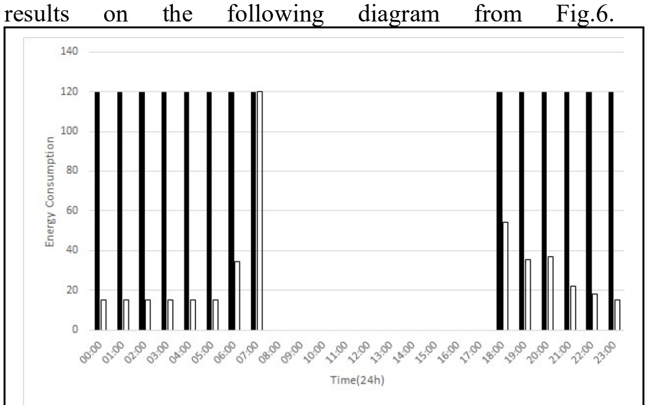

Assuming the costs of the MWh of May 22 which was €168.51 the traffic dimmed systems shows its proposition. The table below shows the calculated values for a single luminaire. Per year one luminaire can save up to €76.00. on practical basis one vision sensor will control an average of about 5 streetlights. That means, assuming and average price of €600.00 per sensor, including the communication infrastructure, the return of investment period can be as short as 2 years

	Time based	Traffic Dimm
Energy consumption per year (kWh)	604,8	153,7
Energy costs per year (€)	101,9	25,90
Savings		**74,59%**

Fig. 6. Total energy consumption comparison

IV. CONCLUSIONS

The growing penetration of smart streetlights in urban environments results in a variety of challenges and opportunities. This paper aimed at providing an overview of the possibilities to install camera sensors that are not privacy intrusive checking the bandwidth requirements of possible solutions to optimize costs of operation as well. As smart streetlight systems are anticipated to grow rapidly across the globe, there will be a growing interest in the topic, and at the same time, increased need to provide sensors that are, at the same time, easy to install, privacy neutral and cost effective.

Future work is ongoing to extend the functionalities of the existing platform. The next natural implementation will be the detection of pedestrians to combine energy savings and safety for both actors.

Given the advantages of smart streetlights, such as energy-saving, system visibility and controllability enhancement, service quality enhancement, and CO2 emission decrease, it is anticipated that more smart streetlights systems will be installed across the globe. In addition, smart streetlight systems can serve as a mainstay for smart city networking and therefore offer a foundation for smart city applications with planning and traffic supervision, mobility outline identification, and emergency assistance. Yet, deploying smart streetlight systems play a fundamental part in enhancing the effectiveness, security, flexibility, reliability, and resiliency of a smart city.

REFERENCES

[1] International Energy Agency, Light's Labour's Lost: Policies for Energy-efficient Lighting, France: IEA, 2006

[2] Pease, K. (1999). A review of street lighting evaluations: Crime reduction effects. Crime prevention studies, 10(1), 47-76.

[3] Wanvik, P. O. (2009). Effects of road lighting: An analysis based on Dutch accident statistics 1987–2006. Accident Analysis & Prevention, 41(1), 123-128.

[4] Echelon, Monitored outdoor lighting: Market, Challenges, Solutions and Next steps, 2007, 19 p

[5] Northeast Group, LLC, Global LED and Smart Street Lighting: Market Forecast (2014 – 2025), Washington: Northeast Group, LLC, 2014

[6] Warwickshire County Council, Part-Night Lighting. [Online]. Available:https://www.warwickshire.gov.uk/strategies-policies-legislation/street-lighting-standards/2 [Accessed: 16 June. 2022].

[7] A. Mayeur, R. Brémond and J. Bastien, "The Effect of the Driving Activity on Target Detection as A Function of the Visibility Level:

Implications for Road Lighting," Transportation Research Part F, vol. 13, pp. 115-128, 2010

[8] S. I. Hong, H. S. Ryu, D. H. Yoon, C. G. In, J. C. Park and C. H. Lin, "A Development of LED-IT-Sensor Integration Streetlight Management System on Ad-hoc," in *Proc. IEEE Region 10 Conf.*, Bali, 2011, pp 1331-1335.

[9] A. Siddiqui, A. Ahmad, H. K. Yang and C. Lee, "ZigBee based energy efficient outdoor lighting control system," in *Proc. 14th Int. Conf. Advanced Communication Technology*, Pyeong Chang, 2012.

[10] J. Zhang, G. F. Qiao, G. M. Song, H. T. Sun and J. Ge, "Group decision making based autonomous control system for street lighting," *Measurement*, vol. 43, no. 1, pp. 108 - 116, 2013.

[11] Y. Lin, W. Cheng, C. Wu and Y. Sun, "An Intelligent Lighting Control System Based on Ergonomic Research," in Proc. Int. Conf. Consumer Electronics, Communications and Networks (CECNet), XianNing, 2011, pp.4744-4747.

[12] Jin, D., Hannon, C., Li, Z., et al.: 'Smart street lighting system: a platform for innovate smart city applications and a new frontier for cyber-security', Electr. J., 2016, 29, (10), pp. 28–35

[13] Atıcı, C., Özçelebi, T., Lukkien, J.J.: 'Exploring user-centered intelligent road lighting design: a road map and future research directions', IEEE Trans. Consum. Electron., 2011, 57, (2), pp. 788–793

[14] Lau, S.P., Merrett, G.V., White, N.M.: 'Energy-efficient street lighting through embedded adaptive intelligence'. IEEE Int. Conf. on Advanced Logistics and Transport (ICALT), Sousse, Tunisia, May 2013

[15] Sun, J., Su, J., Zhang, G., et al.: 'An energy-saving control method based on multi-sensor system for smart streetlightsar street lamp'. IEEE Int. Conf. on Digital Manufacturing and Automation (ICDMA), Changsha, China, December 2010

[16] Todorović, B.M., Samardžija, D.: 'Road lighting energy-saving system based on wireless sensor network', Energy Effic., 2017, 10, (1), pp. 239–247

[17] Mustafa, A.M., Abubakr, O.M., Derbala, A.H., et al.: 'Towards a smart highway lighting system based on road occupancy: model design and simulation'. Applications for Future Internet, Puebla, Mexico, May 2016

[18] Lavric, A., Popa, V., Sfichi, S.: 'Street lighting control system based on largescale WSN: a step towards a smart city'. IEEE Int. Conf. and Exposition on Electrical and Power Engineering (EPE), Iasi, Romania, October 2014

[19] Novak, T., Pollhammer, K., Zeilinger, H., et al.: 'Intelligent streetlight management in a smart city'. Emerging Technology and Factory Automation (ETFA), Barcelona, Spain, September 2014

[20] Zotos, N., Pallis, E., Stergiopoulos, C., et al.: 'Case study of a dimmable outdoor lighting system with intelligent management and remote control'. Int. Conf. on Telecommunications and Multimedia (TEMU), Chania, Greece, August 2012

[21] Kaleem, Z., Ahmad, I., Lee, C.: 'Smart and energy efficient LED street light control system using ZigBee network'. 12th Int. Conf. on Frontiers of Information Technology, Islamabad, Pakistan, December 2014

[22] Beccali, M., Bonomolo, M., Ciulla, G., et al.: 'Improvement of energy efficiency and quality of street lighting in South Italy as an action of sustainable energy action plans. The case study of Comiso (RG)', Energy, 2015, 92, pp. 394–408

[23] Pereira, M., Baykas, P. B., Kulcsár, B., & Lang, A. (2022). Parameter and density estimation from real-world traffic data: A kinetic compartmental approach. Transportation Research Part B: Methodological, 155, 210-239.

[24] Janrao, A., Gupta, M., Chandwani, D., & Joglekar, U. A. (2017). Real Time Traffic Density Count Using Image Processing. International Journal of Computer Applications, 162(10).

Pitfalls in Low Power Measurement of Smart Lighting Products

Jan, Krüger
Department of Lighting and Multimedia
TÜV SÜD Product Service GmbH
Garching, Germany
jan.krueger@tuvsud.com

Josef, Schütz
Department of Lighting and Multimedia
TÜV SÜD Product Service GmbH
Garching, Germany
josef.schuetz@tuvsud.com

***Abstract*—With the advent of the new directive on eco-design requirements for light sources and separate control gears more stringent requirements for standby power and networked standby power were introduced. This paper exemplifies that low power measurement is by no means a trivial task and it discusses how pitfalls can be avoided from a metrological point of view. In addition, an approach is proposed which can serve as a guide for correct measurement of standby power. Furthermore, products with characteristic power consumption profiles are presented.**

Keywords*—*standby, low power, measurement, eco-design, energy consumption, smart lighting

I. Introduction

The framework regulation 2009/125/EC addresses the energy efficiency requirements for energy-related products [1]. Detailed requirements regarding the power consumption in off-mode and in networked standby mode are governed in product specific regulations.

Since the 1st of Sept. 2021 the regulation (EU) 2019/2020 entered into force and regulates the ecodesign requirements for light sources and separate control gears [2]. Currently the upper limit of the standby power of a light source or a control gear is 0,5W.

In the field of home appliances, the regulation (EU) 1275/2008 defines the requirements for standby power consumption [3]. This regulation is supplemented by the (EU) 801/2013 which deals with requirements for connected home appliances [4].

Already on the 7th of January 2022 the EU published a draft of a new regulation regarding the ecodesign requirements for off mode, standby mode, and networked standby energy consumption of electrical and electronic household and office equipment. This draft estimates the energy consumption of household equipment in standby mode at 59,4 TWh a year, which corresponds to 23,8 million of tons of CO2 [5].

A study by Clement et al. [6] investigated the standby energy consumption of home appliances in Denmark, Greece, Portugal, and Italy. This study estimates an annual energy consumption of 439 kWh per household [6]. This should make up 14% of the total energy used. Furthermore, Clement emphasizes that these findings are representative for Europe.

In the field of lighting the situation is even more drastic. In a Swedish study the power consumption of 57 office rooms was examined. The study shows that 30% of the total energy of the lighting system can be attributed to the standby mode [7]. These findings demonstrate that low power consumption of many individual components can add up to a significant amount of energy.

Wang et al. [8] draws the attention to the fact, that the trend of decreasing energy consumption for LED lamps is reversed in the case of smart LED lamps. Wang explains that traditional LED lamps do not consume any energy when they are switched off, whereas networked lighting products draw energy permanently.

Page et al. [9] puts it in a nutshell and describes that smart lighting products jeopardise their technological lead in the field of energy efficiency by standby energy consumption. Page et al. substantiates his claim by a sample calculation. He calculates the annual energy consumption of 11 smart light bulbs for a daily utilization cycle of “2 hours on” and “22 hours off” [9]. In this example a classical compact fluorescent lamp outperforms 10 out of 11 of the latest smart LED lamps.

Another study examined the standby power consumption of 30 current smart lamps in the Canadian market according to IEC 62301 [10]. Eight out of these 30 models exceeded the European limit of 0,5W and would thus not meet the EU requirements [11]. Page et al. comes to comparable results in the US market. Fife out of eleven models revealed higher standby power than 0,5W [9].

One reason for the significant standby energy consumption of smart lighting products is, that these products incorporate additional features. That includes the adjustment of dimming status, correlated colour temperature, colour of light as well as presence sensing and timer functions. The incorporation of necessary communication technologies like WiFi, Bluetooth or Zigbee affect the power consumption. Even if these features bring advantages for the user, they come with the hidden disadvantage of increased standby power consumption.

II. Background and Motivation

Against this background the precise measurement of low power gains in importance. Also, the European Commission points to this fact in its draft on “ecodesign requirements for off mode, standby mode, and networked standby energy consumption of electrical and electronic household and office equipment”: “the relevant product parameters should be measured using reliable, accurate and reproducible methods. Those methods should take into account recognised state-of-the-art measurement methods.” (p. 3)[5].

Often the idea about the measurement of low power is to connect a power meter to the product and to read off the value after a stabilization phase or to start a wizard which automatically conducts the measurement after the input of some parameters. Unfortunately, this is a misconception.

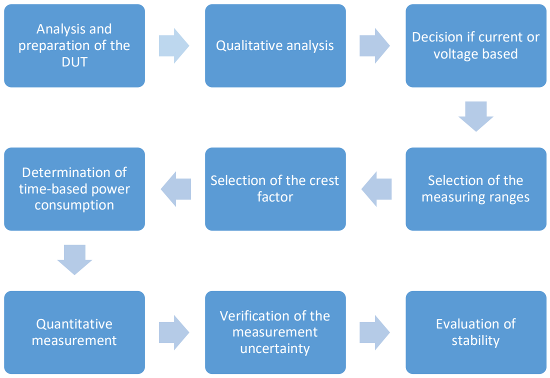

Figure 1: Flowchart of the sub-steps for low power measurement

Bucci et al. [12] points out, that there are two problems with the measurement of low power. On the one hand, power meters are designed to measure high power, especially the small currents are often outside the approved range. On the other hand, the low sampling rate often leads to problems with the detection of peaks and rapid changes in the time series [12].

III. Method

The relevant standard for "Non-active power measurement" of lighting equipment is IEC 63103 [13]. The measurement of low power consumption is further described in IEC 62301 [10] as well as in DIN EN 50564 [14], which is a modification of IEC 62301 [10]. IEC 63103 [13] is concerned with topics that are not are not dealt with in IEC 62301 but the measurement procedure was adapted from IEC 62301 [10]. Furthermore, IEC 63103 [13] remains unspecific about the execution and calculation methods, including the required accuracy, whereas IEC 62301 [13] goes into further details. The following approach is in accordance with all the above-mentioned standards.

Our approach incorporates a two-stage procedure involving the qualitative analysis of the current consumption profile and the quantitative measurement of standby power. The flowchart is shown in fig. 1. It includes the following sub-steps:

A. Analysis and preparation of the product

First, the manual of the device under test (DUT) should be consulted, to find out if sensors, accumulators, or special operating modes should be considered. Attached light sensors, temperature sensors, motion detectors or an active charging process can confound the measurement results.

B. Qualitative Analysis

The qualitative analysis intends to investigate the current consumption profile with an instrument of high sampling rate to derive the right selection of the current measurement range and the crest factor.

For the determination of small currents, a resistor is needed to evoke a voltage drop just large enough to measure the current indirectly but small enough to keep the measurement uncertainty low. As a rule, currents in the order of a few milliamperes can be measured which should be displayed on an oscilloscope.

Furthermore, the correct wiring is emphasized where a decision needs to be taken whether a current-based or a voltage-based circuit must be chosen. From the analysis of the time-based power consumption the duration of measurement period can be derived depending on a cyclical or stable power draw.

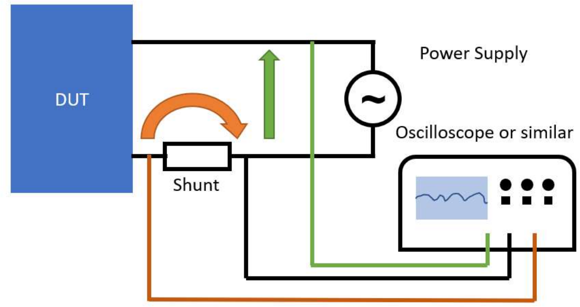

Figure 2: Measurement setup for qualitative Analysis

C. Current-based or voltage-based circuit

The choice of a current-based or voltage-based circuit can be made with the help of formula B.4.1 in DIN EN 50564 (p. 24) [13]. For low power the effective current should not exceed the following limit:

$$I_m \leq V_S * \sqrt{\frac{1}{(R_a * R_v)}}$$

$$I_m = measured\ effective\ current\ of\ DUT$$
$$V_S = supply\ voltage$$
$$R_a = resistance\ of\ the\ shunt$$
$$for\ the\ chosen\ current\ range$$
$$R_v = internal\ resistance\ of\ the\ voltmeter$$

With a supply voltage of 230V and a shunt of $50m\Omega$ as well as an internal resistance of the voltmeter of $2M\Omega$ the calculation results in a limit of 727mA. The estimation shows that DUTs with a current consumption of less than 727mA should be measured in a current-based circuit. The current- and voltage-based measurement circuits are depicted in figure 3.

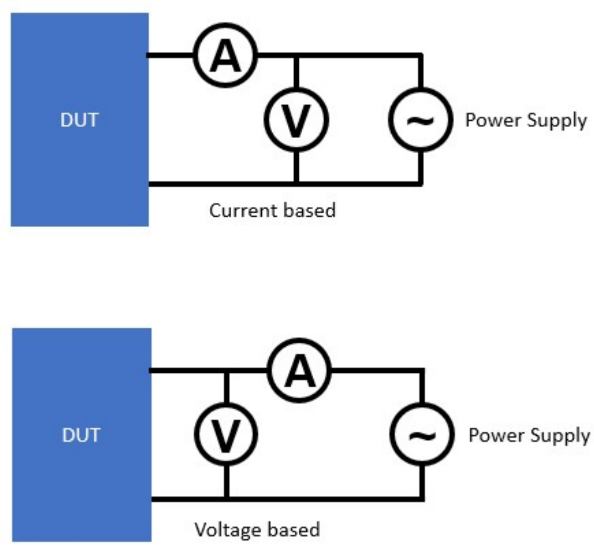

Figure 3: Current- and voltage-based measurement circuits

D. Current measurement range

The choice of the right current measurement range is of particular importance for the measurement uncertainty. The uncertainty of the power meter usually depends on a combination of the reading value with the peak value of the measuring range. Thus, for example a measuring range of 2,5mA and a crest factor of 6 leads to a peak value of 15mA, whereas a measuring range of 10mA and a crest factor of 6 leads to a peak value of 60mA which affects the measurement uncertainty more strongly.

E. Selection of crest factor

From the analysis of the current consumption profile conclusions regarding the crest factor can be drawn. The high sampling rate is of special significance for the detection of transient bursts and peaks. The crest factor relates exclusively to the current measurement because the voltage crest factor is already covered by stability requirements of the power supply.

The crest factor describes to what extend current peaks are allowed to exceed the chosen measuring range. In figure 4 the measuring range is defined by the green lines, the extended measuring range, which is covered by the crest factor, is defined by the red lines. Peaks that exceed the red lines will not be detected by the instrument. Therefore, the crest factor of the power meter must be larger than the crest factor of the DUT. Otherwise, current peaks will be cut-off which would distort the integration of the power consumption [14].

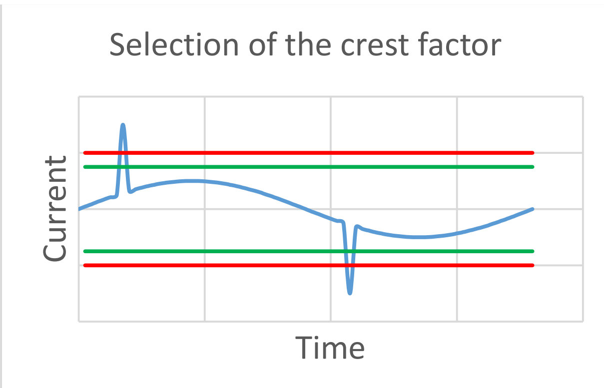

Figure 4: Selection of the crest factor

F. Determination of the time-based variations

Another essential aspect of the qualitative analysis is the determination of the time-based variations in the power consumption. As a result, three conditions can be distinguished:

- A power profile that is stable over time
- Cyclical changes of the power profile
- Non-cyclical changes of the power profile

The temporal variation determines the duration of the measuring period. In the case of cyclic changes, the period duration must be identified. The assessment period should incorporate at least two cycles. In any case the sampling method is recommended for all types of time-based variations. Thereby, a logging of electrical parameters at short time intervals takes place over the entire measuring period.

G. Quantitative Measurement

Once the steps of the qualitative analysis have been completed and the parameters have been set in the power meter the measurement can be started. During the measurement the following parameters must be logged:

- IRMS – Current (RMS)
- URMS – Voltage (RMS)
- Ipeak – Peak Current
- UTHD – Total harmonic distortion of the voltage
- F - Frequency
- PF – Power Factor
- P – Power

The logging has to be conducted over three equal periods of time, whereas one period shall not be shorter than 5 minutes.

H. Measurement uncertainty

Besides the determination of the standby power the recorded data is needed for the estimation of the maximum permissible measurement uncertainty of the power meter. Using Ipeak and IRMS a crest factor for the DUT can be calculated. Together with the power factor this crest factor is used to calculate the current ratio (MCR). From the current ratio the maximum permissible measurement uncertainty of the power meter can be determined. Based on the determined value, it has to be checked if the power meter meets the minimum requirements regarding the measurement uncertainty.

In addition to the measurement uncertainty of the power meter the following contributing factors should be controlled for the consideration of the overall measurement uncertainty:

- High stability of the power supply with limited portion of harmonics
- Air movement of less than 0,5m/s and specific ambient temperature
- Reduction of contributing factors from the wiring by keeping the wires short and twisting the cables of the circuit

I. Stability assessment

Finally, the logged power consumption must be verified using a stability criterion before the standby power consumption can be derived. For this purpose, a regression line is calculated over the last two evaluation periods. If the slope of the regression line does not exceed 10mW the stability criterion is met.

IV. Results

In the following section two examples are given where irregularities could be uncovered by the application of the proposed method which otherwise have remained concealed and may have led to false results.

The examples involve two smart LED lamps with a standard base and different communication technologies. The first sample relates to a E14 lamp that was connected via WiFi to a wireless network router. The second sample incorporates a GU10-lamp which could be controlled via Bluetooth by the smartphone of the operator without using a separate gateway device.

During the measurement of standby power of smart lighting products, it should be considered that lamps or sensors often wait for activation. For this purpose, they are sending communication impulses. Thus, lamps with WiFi-communication show a peak-shaped power consumption of a few milliseconds during the sending process of the beaconing status, which also depends on the signal strength of the access point [15]. In the case of Zigbee lamps it must be distinguished between a start-up phase and the networked standby mode, which show different profiles of power consumption [15].

The following figure shows the current consumption of the E14 WiFi-Lamp which was connected to the wireless network and switched into standby mode by the app of the manufacturer. The graph can be divided into three sections. The first section (0s-25s) shows the networked standby current consumption. In the second section the connection to the wireless network was interrupted (28s-50s). The third section (50s-80s) presents the current consumption in the disconnected state. It becomes clear that the power consumption increased after the disconnection. In networked standby mode the power consumption was 0,51W whereas the consumption increased by 0,18W to 0,69W after the disconnection. Changes in the connection state cannot be immediately detected by the operator.

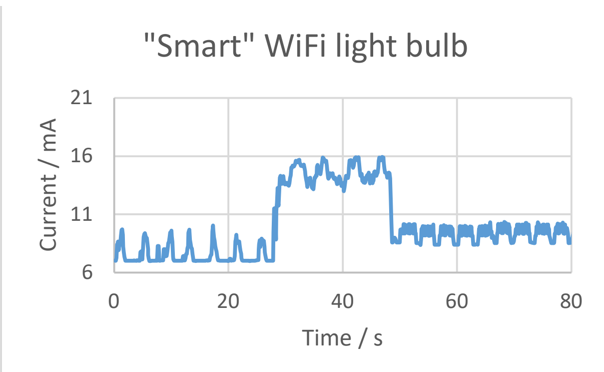

Figure 5: Current consumption profile of a WiFi lamp after connection loss

The second example shows the current consumption profile of a GU10 lamp. In the first third of the graph the current consumption during networked standby is presented. During this measurement period the app of the manufacturer was opened on the smartphone. After closing the app by the operator, the power consumption increased by 20mW. In the last section of the graph the app was opened again, and the current profile returned to its initial level. With an opened app a connected standby power of 0,60W was measured, with closed app 0,62W was measured. This example also shows a higher power consumption in disconnected state.

V. Discussion

The preliminary considerations about the proportion of the total power consumption that can be assigned to the standby mode illustrate the significance of this issue. This is also evident from the upcoming European regulations which attach more importance to this topic in the future. Simultaneously, there is a growing need for precise and reproducible measurements. Against this background, this paper shows the complexity of these measurements. Bedsides the pitfalls that must be considered regarding the measurement circuit and the selection of proper settings at the power meter, potential pitfalls during the operation of the DUT must be avoided. This is by no means a trivial task. The proposed approach and the overview of the electrical parameters can serve as guidance for correct measurements of standby power.

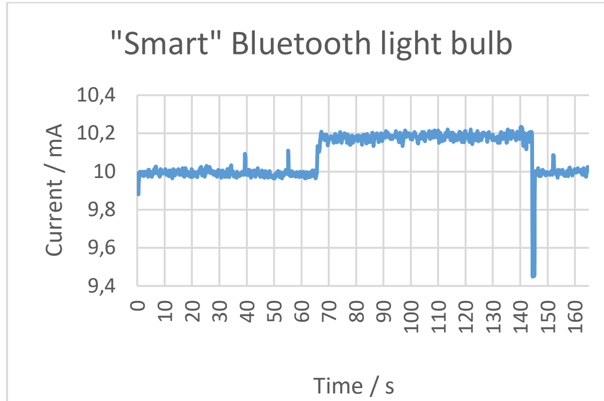

Figure 6: Current consumption profile of a Bluetooth lamp after opening and closing the app

References

[1] 2009/125/EC, “Framework for the setting of ecodesign requirements for energy-related products”, European Union, Official Journal of the European Union, Vol. 285, p. 10–35, 2009.

[2] (EU) 2019/2020, “Ecodesign requirements for light sources and separate control gears”, European Union, Official Journal of the European Union, Vol. 315, p. 209–240, 2019.

[3] (EU) 1275/2008, “Ecodesign requirements for standby and off mode electric power consumption of electrical and electronic household and office equipment”, European Union, Official Journal of the European Union, Vol. 339, p. 45–52, 2008.

[4] (EU) 801/2013, “Amending Regulation (EC) No 1275/2008 with regard to ecodesign requirements for standby, off mode electric power consumption of electrical and electronic household and office equipment”, European Union, Official Journal of the European Union, Vol. 225, p. 1–12, 2013.

[5] European Commisson, “Draft on ecodesign requirements for off mode, standby mode, and networked standby energy consumption of electrical and electronic household and office equipment”, p. 1-8, 07.01.2022 retrieved from: https://op.europa.eu/s/wl8J.

[6] K. Clement, I. Pardon and J. Driesen, "Standby Power Consumption in Belgium," in 9th International Conference on Electrical Power Quality and Utilisation, 2007, pp. 1-4.

[7] N. Gentile, M.-C. Dubois, “Field data and simulations to estimate the role of standby energy use of lighting control systems in individual offices”, Energy and Buildings, Vol. 155, pp. 390-403, 2017.

[8] W. Wang, J. Su, Z. Hicks, B. Campbell, (2020). “The Standby Energy of Smart Devices: Problems, Progress, & Potential” in Fifth International Conference on Internet-of-Things Design and Implementation, 2020, pp. 164-175.

[9] E. Page, S. Beletich, S. Jeffcott, E. Kummert, “Not so clever when they are off: standby power use in smart lamps”, in Proceedings of the 2015 ECEEE Summer Study on Energy Efficiency, 2015, 1479-1485.

[10] IEC 62301, Household electrical appliances - Measurement of standby power, VDE Verlag, Berlin, pp. 1-87, 2011.

[11] E. Dikel, Y. Li, M. Vuotari, S. Mancini, “Evaluating the standby power consumption of smart LED bulbs”, Energy and Buildings, vol. 186, pp. 71-79, 2019.

[12] G. Bucci, E. Fiorucci, F. Ciancetta, M. Luiso, “Measuring System for Microelectric Power. Instrumentation and Measurement”, IEEE Transactions, vol. 63, pp. 410-421, 2014.

[13] IEC 63103, Lighting equipment – Non-active mode power measurement, International electrotechnical commission, Geneve, pp. 1-33, 2020.

[14] DIN EN 50564, Electrical and electronic household and office equipment - Measurement of low power consumption, Beuth, Berlin, pp. 1-36, 2011.

[15] Y. Chen and Q. Wu, "Power consumption measurement and clock synchronization on low-power wireless sensor networks" in 14th International Conference on Advanced Communication Technology (ICACT), 2012, pp. 406-409.

Design of an Adaptive Road Lighting Installation Taking into Account the Evolution of Pavement Reflection Properties According to the Weather Conditions

Greffier Florian
Light and Lighting Team
Cerema
Les Ponts-de-Cé, France
florian.greffier@cerema.fr

Boucher Vincent
Light and Lighting Team
Cerema
Les Ponts-de-Cé, France
vincent.boucher@cerema.fr

Muzet Valérie
ENDSUM Research Team Cerema
Strasbourg, France
valerie.muzet@cerema.fr

Dronneau Romain
Light and Lighting Team Cerema
Les Ponts-de-Cé, France
romain.dronneau@cerema.fr

***Abstract*— The optimization of road lighting installations is nowadays mainly considered from the point of view of reducing energy costs by using the advantages of LED technology when designing or renovating lighting installations. Knowing the actual reflection properties of the road to be illuminated enables further optimization but these are too often not measured. Moreover, the evolution of the pavement reflection properties according to the surface state of the road (dry, moist, wet, soaked) is never considered. This paper proposes a methodology to design an adaptive lighting system that takes into account the optical properties of the pavement according to the weather conditions in order to optimize the visibility offered to users. This methodology is based on numerous simulations of potential surface states and associated *r*-tables to develop luminaire photometry and define a set of lighting scenarios. The selection of the best lighting scenario according to the surface condition is then simulated. The process is mainly based on the measurement of *r*-table using a virtual ILMD. By comparing on a test case the developed adaptive lighting system with a conventional lighting system, it is shown that the overall optimization of the lighting installation is achieved both on photometric and on energy aspects.**

Keywords—adaptive lighting system, road lighting simulation, pavement reflection properties, surface state, weather conditions

I. Introduction

The optimization of road lighting installations is a very interesting lever for adapting cities to the requirements of the ecological transition. Optimized lighting allows the saving of energy and the limitation of light pollution while ensuring satisfactory visibility conditions for users. The use of LED in road lighting makes a significant contribution to these energy-related issues, particularly if the optical properties of the road are taken into account when designing the lighting installation [1], [2]. LED technology also offers new possibilities for designing smart lighting, capable for example of adapting in real time to the traffic volume or the presence of pedestrians [3]. However, one aspect remains difficult to address. It is the evolution of the optical properties of the road surface according to the weather conditions. The moisture state of the pavement (dry, moist, wet or soaked) has an important effect on the light reflection. It can significantly disturb the average luminance levels and the associated luminance uniformities. CIE technical reports [4] or European standardization [5] consider this evolution of the performance of lighting installations when the pavement is wet by proposing only to reduce the requirements on the overall uniformity, to the detriment of the visibility of the users. It has been shown [6] that a lighting installation with fixed parameters cannot offer equivalent performance when the pavement is dry or when it is wet. The change in pavement brightness and specularity [6], [7] with the degree of wetting would require changes in the photometry of the luminaires, both in terms of the outgoing flux and the distribution of this flux on the pavement.

In this paper, we present the approach used to design an adaptive lighting system that takes into account the evolution of pavement reflection properties as a function of weather conditions. A specific luminaire has been developed from measured *r*-tables and CIE *r*-tables of type "wet" [7]. It is equipped with two different photometries, one dedicated to the dry state of the pavement and one dedicated to the wet states, with the possibility of combining these two photometries together. Different lighting scenarios have been determined from numerous lighting calculations performed on multiple random linear combinations of the available *r*-tables. These combinations were constructed to consider the spatial heterogeneity of the pavement [8] and to anticipate its potential surface states under different weather conditions. The relevance of the set of lighting scenarios is evaluated numerically in a simulation of the overall operation of the adaptive lighting installation. New random combinations of *r*-tables are generated and the selection of the best lighting scenario is performed by simulating a measurement of the *r*-table with an ILMD [9]. The contributions of our adaptive lighting system are evaluated by comparing its operation with that of a conventional lighting installation on a test case.

II. Road Lighting Basics

In road lighting design, the nominal position of the grid points at which calculations are made is defined in [10], [11]. In the longitudinal direction, the measurement field shall enclose two luminaires in the same row. In the transversal direction, the measurement field is positioned over the entire width of the road and can include several driving lanes as shown in Fig. 1 on the left.

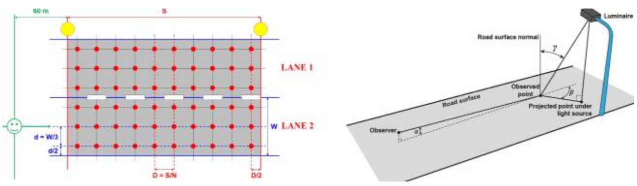

Fig. 1. Normative grid points for lighting calculations or measurements (on the left); Angles of observation α, deviation β and incidence γ to characterize the photometry of the road surface (on the right).

For luminance evaluation, the position of the observer is 1.5 m above the road surface and at 60 m ahead the field of the relevant area. In the transverse direction, the observer shall be positioned in the center of each lane in turn. From luminance values on the normative grid, average luminance (L_{ave}), overall uniformity (U_0) and longitudinal uniformity (U_l) are computed [10], [11].

The reflection properties of the road surface are used for the design of a lighting installation. The most characteristic parameter is the luminance coefficient q, which is the ratio between the luminance L in cd/m² seen by an observer and the illuminance E in lux incident on the surface (1).

$$q = L/E \tag{1}$$

Since the 1980s, for practical reasons, the luminance coefficient was replaced by the reduced luminance coefficient r in cd/m²/lux, which is derived from q (2) and given for a combination of fixed lighting angles β and tan(γ) (see Fig. 1 on the right).

$$r = q.(cos\,\gamma)^3 \tag{2}$$

The standardized viewing height is still 1.5 m and the angle of observation α is constant at 1°, corresponding to an observation distance of 86 m.

To simplify the calculation, two indicators are defined by the CIE [7]. The average luminance coefficient Q0 represents the degree of lightness of the measured surface. It is computed as the average of the luminance coefficients over the specified solid angle Ω_0 which only depends of β and γ values (3).

$$\text{Q0} = \frac{1}{\Omega_0}\int q d\Omega \tag{3}$$

The specular factor S1 represents the degree of specularity (shininess) of the observed surface. It is defined as the ratio between the reduced luminance coefficients of two specific illumination conditions (4).

$$\text{S1} = \frac{r(\beta=0;\,\tan\gamma=2)}{r(\beta=0;\,\tan\gamma=0)} \tag{4}$$

In CIE 144:2001 [7], a classification system groups different surfaces according to the value of the specular factor S1. Surfaces within a class are represented by a predefined *r*-table as well as values of Q0 and S1. Typical *r*-tables are defined for the dry state and for the wet state (called respectively R and W *r*-tables).

III. Development of the Adaptive Lighting Luminaire

A. *Description of the experimental set up*

The site that will host the adaptive lighting demonstrator is located in Limoges, France. The pavement is an asphalt mix with a granular fraction composed of 30% crushed porcelain, which, in addition to industrial recycling issues, allows the pavement to be lightened and thus limits the amount of light power installed [12]. This pavement was completed in June 2017 and can therefore be considered photometrically stabilized in 2021 [1]. It is a 7 m wide street consisting of two traffic lanes. It is mainly intended for motorized vehicles and the maximum speed limit is 50 km/h. These characteristics correspond to a lighting class M3 [4], [5].

B. *Pavement reflection properties measurements*

To optimally design a lighting installation, it is necessary to know the pavement reflection properties [1], [2]. Since the aim of this work is to design road lighting that adapts to different road surface states, the optical properties of the pavement were measured in the dry state and for different degrees of wetting (moist, wet and soaked). The wetting method proposed in the CIE technical report 47:1979 [6] does not allow a pavement to be characterized for these different conditions because they require rapid measurements. A specific protocol was therefore developed [13] and the measurements were carried out with the COLUROUTE device [14], [15] which allows to obtain a complete *r*-table in less than 1 minute. Eight samples were taken by coring the pavement in place in Limoges. The number and locations of the samples (four in the central track noted CT1, CT2, CT3, CT4 and four in the wheel track noted WT1, WT2, WT3, WT4) were chosen to consider the spatial heterogeneity of the road surface [8]. The pavement reflection properties were measured in the dry state for the eight samples and then at different degrees of wetting for two of them (CT2 and WT2). The wetting protocol consists in immersing the sample in a basin containing 2 cm of water. A first measurement is performed immediately after removing the sample from the basin to characterize the soaked state. A second measurement is performed after a 5 minutes of natural draining to characterize the wet state. Finally, after absorbing the excess water with a tissue, a last measurement is conducted to characterize the moist state. This protocol was repeated several times.

Fig. 2 shows the Q0 and S1 values associated with the COLUROUTE measurements and the standard CIE *r*-tables type R and W. The samples measured in the dry state are slightly to very slightly specular with a S1 value between 0.37 and 0.53. The pavement has an average lightness coefficient Q0 of 0.098 which is quite high for an asphalt mix. This behavior confirms the interest of the addition of the porcelain residues to increase Q0 without any drawback of an increase of specularity.

In the different wetting conditions, the specularity S1 increases as expected, with a small increase in the moist state, a large increase in the wet state and a very large increase in the soaked state. Measurements in the wet and soaked states

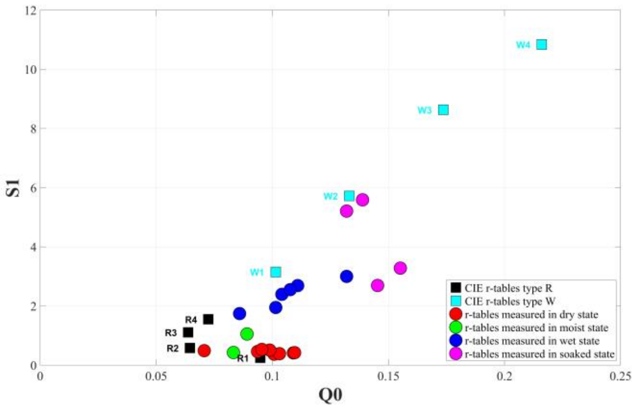

Fig. 2. Representation of Q0 and S1 values associated with the standard *r*-tables R (black squares) and W (cyan squares) and with the *r*-tables measured by COLUROUTE (red circles for dry state, green for moist state, blue for wet state and magenta for soaked state).

generate values of Q0 and S1 close to those associated with typical *r*-tables W1 and W2.

C. Characteristics of the adaptive road lighting installation

Design calculations, using ULYSSE 3.5.2 software [16] for the lighting class M3 (L_{ave}=1.00 cd/m²; $U_0 \geq 0.40$; $U_l \geq 0.60$) [4], [5], led to a one-sided lighting installation with luminaires 8 m high and 29 m apart. Concerning the design of the luminaire, it was composed of two different photometries, one designed for the dry state and one for the wet states.

The so-called “dry photometry” was designed using the *r*-tables measured by COLUROUTE in the dry state. It is a module consisting of 24 LED each equipped with an optic that optimizes the luminance/uniformity ratio. The maximum flux associated with this photometry is 6058 lm in order to satisfy the normative requirements for all the measured samples.

The so-called “wet photometry” dedicated to moist, wet and soaked states has been developed based on the W1 and W2 *r*-tables since they are close to the measurements performed by COLUROUTE on the two samples submitted to our wetting protocol. The main issue for this photometry was to obtain for these states good overall uniformity values as the requirements of the dry state. The wet photometry was obtained with two modules of 24 and 16 LED respectively. The 24 LED of the first module are equipped with a specific optic different from the one used for dry photometry. The 16 LED of the second module are equipped with an optic oriented at 90° with respect to the previous one. The maximum flux associated with this photometry is 8955 lm.

All the dimensioning calculations carried out to develop the luminaire and its two photometries are presented in TABLE I. In terms of average luminance, overall uniformity and longitudinal uniformity obtained, the luminaire developed enables the requirements of class M3 [4], [5] for dry pavement to be met, whatever the experimental *r*-table used. Thanks to the presence of the second photometry dedicated to wet conditions, the luminaire can achieve lighting performance corresponding to the requirements of a dry pavement for the W1 *r*-table. This is also almost the case for the W2 *r*-table. Only the overall uniformity is slightly lower than the requirement while remaining two times better than the standard requirement for a wet pavement. Calculations were also conducted with the W3 *r*-table. The uniformities are then slightly more degraded since this *r*-table corresponds to a very

TABLE I. CALCULATIONS WITH THE DEVELOPED LUMINAIRE

r-table	Photometry	Flux	L_{ave}	U_0	U_l
CT1	DRY	6058 lm	1.00 cd/m²	0.57	0.79
CT2	DRY	4248 lm	1.00 cd/m²	0.57	0.72
CT3	DRY	4036 lm	1.01 cd/m²	0.59	0.73
CT4	DRY	4766 lm	1.02 cd/m²	0.58	0.72
WT1	DRY	4248 lm	1.01 cd/m²	0.58	0.72
WT2	DRY	4248 lm	1.00 cd/m²	0.55	0.81
WT3	DRY	3929 lm	1.00 cd/m²	0.58	0.74
WT4	DRY	4559 lm	1.02 cd/m²	0.60	0.75
W1	WET	8955 lm	1.00 cd/m²	0.46	0.68
W2	WET	7515 lm	1.00 cd/m²	0.33	0.62
W3	WET	6626 lm	1.01 cd/m²	0.23	0.55

important wetting condition with a high degree of specularity which impacts the overall uniformity [8], [17], [18]. Even if the COLUROUTE measurements on the soaked samples do not suggest that the pavement in place can achieve such properties, it was still interesting to evaluate the performance of the luminaire under these extreme conditions.

IV. LIGHTING SCENARIOS

On the experimental site, the luminaire will be installed on the entire street with the objective of continuously adapting the outgoing lighting fluxes and the spatial distribution of these fluxes according to the weather conditions. The adaptive lighting installation operating requires the programming of predefined lighting scenarios in the luminaire control system. As shown in TABLE I, the presence of two photometries in the luminaire provides an optimal setting (activation of the right photometry and optimization of the outgoing flux) for each *r*-table used during the dimensioning. However, these *r*-tables remain punctual measurements. Due to the heterogeneity of road surface on real site [8], the pavement reflection properties could differ from those used to design the luminaire and the lighting installation. Therefore, in addition to the initial settings exposed in TABLE I, a new set of lighting scenarios is proposed to consider the variability of the actual pavement reflection properties by activating the two on-board photometries separately or simultaneously. It is mainly assumed that the pavement will exhibit intermediate properties among those used for designing. Numerous lighting simulations have therefore been carried out with the Ecl_R the lighting calculation engine developed by Cerema [8]: 100,000 to build the different scenarios and 100,000 to validate them.

A. Construction of lighting scenarios

The simultaneous activation of the two photometries of the luminaire in varying proportions will be necessary on the real site. Eleven basic configurations (denoted A to K) are therefore proposed by varying the flux of each photometry between 0% and 100% of its maximum value (6058 lm for the dry photometry, 8955 lm for the wet photometry) by steps of 10%. The configurations A and K correspond respectively to the extreme settings [F_{DRY}=100%; F_{WET}=0%] and [F_{DRY}=0%; F_{WET}=100%]. Configuration F corresponds to the middle setting [F_{DRY}=50%; F_{WET}=50%] (see Fig. 3). These 11 basic configurations were used in the first 100,000 simulations performed using the following process:

1. A uniform random selection of a surface state (dry, moist, wet or soaked) is made and a simulated *r*-table corresponding to this state is generated as explained later on.

2. The average luminances and uniformities associated with this r-table are calculated for the 11 basic configurations.

3. For each basic configuration, an adjustment coefficient is calculated and applied to F_{DRY} and F_{WET} to obtain an average luminance of 1.05 cd/m².

4. For each basic configuration, the calculated overall and longitudinal uniformities are compared to the normative requirements of class M3 in the dry state. Configurations that do not meet the requirements are discarded.

5. The best configuration is the one minimizing the total flux (F_{DRY}+F_{WET}) adjusted (see step 3). If after step 5 no configuration meets the normative requirements, the best configuration is the one maximizing the overall uniformity.

6. The best basic configuration and the adjusted fluxes are stored.

Concerning step 1, the generation of a simulated r-table is based on the following assumptions:

- Dry state: the simulated r-table is a linear combination of the eight r-tables measured by COLUROUTE in the dry state by randomly weighting them at each simulation. The objective here is to consider the spatial heterogeneity of the pavement by following the recommendations proposed in [8].

- Moist state: the simulated r-table is a random linear combination of an r-table obtained on the same principle as in the dry state with the W1 r-table. This assumption seems reasonable in view of the measurements shown in Fig. 2.

- Wet state: the simulated r-table is a random linear combination of the W1 and W2 r-tables. This assumption also seems reasonable in view of the measurements shown in Fig. 2.

- Soaked state: the simulated r-table is a random linear combination of the W2 and W3 r-tables to represent an extreme wetting behavior.

Fig. 3 represents the initial fluxes associated with the basic configurations and the adjusted fluxes based on the basic configurations selected in the simulations. As expected, the simulation process generated a set of intermediate surface states requiring the simultaneous activation of both photometries of the luminaire in varying flux proportions. For each basic configuration, the adjusted fluxes are lower than the initial fluxes, the latter having been chosen as a percentage of the maximum flux associated with each photometry. For each configuration, the dispersion of the adjusted fluxes could be small (configurations C to I) or very important (configurations A and K). TABLE II presents the mean, minimum and maximum values of adjusted fluxes obtained as well as the associated standard deviation for each basic configuration and each photometry. Assuming that the standard deviation associated with the dispersion of the fluxes for a same scenario should not exceed 50 lm, the adjusted mean fluxes associated with basic configurations B to I can become new additional lighting scenarios (see TABLE II). We assume that this value of 50 lm is relatively arbitrary. It was chosen to have a common dispersion criterion for all scenarios, also taking into account that the luminaire control system allows the programming of up to 50 scenarios.

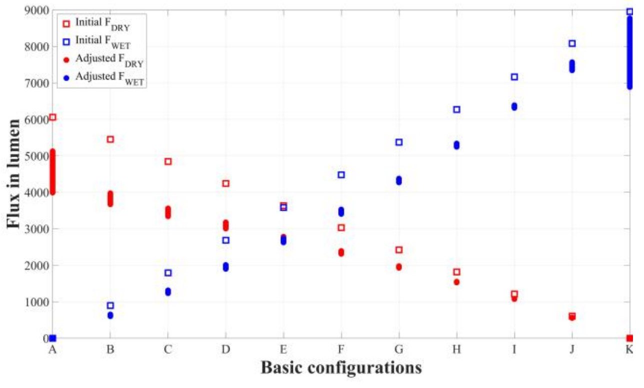

Fig. 3. Initial fluxes associated with basic configurations (red and blue squares) and adjusted fluxes based on basic configurations selected in the simulations (red and blue disks).

TABLE II. MEAN, MINIMUM AND MAXIMUM VALUES OF ADJUSTED FLUXES (IN LUMEN) AND ASSOCIATED STANDARD DEVIATION FOR EACH BASIC CONFIGURATION AND EACH PHOTOMETRY

Config	F_{DRY}				F_{WET}			
	mean	*min*	*max*	*std*	*mean*	*min*	*max*	*std*
A	4548	3991	5126	181	0	-	-	-
B	3785	3671	3975	43	621	602	652	7
C	3433	3342	3558	36	1266	1233	1312	13
D	3077	3005	3176	29	1945	1900	2008	18
E	2713	2669	2784	20	2669	2625	2739	19
F	2340	2309	2392	13	3452	3407	3529	19
G	1949	1929	1977	7	4313	4270	4376	17
H	1532	1524	1551	3	5274	5247	5338	11
I	1077	1070	1082	3	6356	6314	6386	19
J	561	553	570	5	7453	7341	7567	66
K	0	-	-	-	7764	6884	8770	543

On the same principle of a fluxes dispersion below 50 lm, 11, 2 and 14 intermediate lighting scenarios were constructed from the fluxes associated with the basic configurations A, J and K, respectively. To establish the complete set of lighting scenarios, it was chosen to complete the scenarios obtained by simulation with the settings used to design the luminaire and generate the values presented in TABLE I. Finally, two other scenarios, necessary for the programming of the luminaire control system, were introduced. They correspond respectively to 100% and 0% of both photometry. In the end, 37 scenarios were programmed to control the adaptive lighting installation (the flux settings are shown in TABLE III).

TABLE III. FINAL LIGHTING SCENARIOS (FLUXES IN LUMEN)

	F_{DRY}	F_{WET}		F_{DRY}	F_{WET}		F_{DRY}	F_{WET}
S1	6058	8955	**S14**	3433	1266	**S27**	0	7490
S2	3929	0	**S15**	3077	1945	**S28**	0	7515
S3	4036	0	**S16**	2713	2669	**S29**	0	7664
S4	4160	0	**S17**	2340	3452	**S30**	0	7839
S5	4248	0	**S18**	1949	4313	**S31**	0	8012
S6	4322	0	**S19**	1532	5274	**S32**	0	8184
S7	4521	0	**S20**	1077	6358	**S33**	0	8358
S8	4559	0	**S21**	561	7426	**S34**	0	8530
S9	4676	0	**S22**	561	7542	**S35**	0	8693
S10	4766	0	**S23**	0	6626	**S36**	0	8955
S11	4832	0	**S24**	0	6971	**S37**	0	0
S12	6058	0	**S25**	0	7143			
S13	3785	621	**S26**	0	7318			

B. Validation of the lighting scenarios on a test case

The validation process of the lighting scenarios and more globally of the adaptive lighting system is carried out from a global simulation of the installation operation on a test case that represents the site that will host the demonstrator.

On site, the lighting scenario the most adapted to the surface state of the road shall be activated. This requires the ability to measure the actual pavement reflection properties in real time. The measurement of the actual *r*-table will be performed with an ILMD according to the method detailed in [9]. This method consists in performing a principal component analysis (PCA) on a database of *r*-tables that provides a set of eigen *r*-tables. For this study, we added to the initial database used in [9] the eight *r*-tables measured by COLUROUTE in the dry state and the four standard CIE *r*-tables of type wet. Knowing the characteristics of the lighting installation, these eigen *r*-tables can be used to compute eigen luminance maps. The experimental luminance map provided by the ILMD is decomposed onto the set of eigen luminance maps. The *r*-table that generated the experimental luminance map is then estimated as the combination of the eigen *r*-tables weighted by the decomposition coefficients.

The validation of the proposed lighting scenarios and the selection of the best scenario was carried out following a similar approach to the one conducted to construct the scenarios. 100,000 new simulations were performed in the following steps:

1. A uniform random selection of a surface state (dry, moist, wet or soaked) is performed and a simulated *r*-table corresponding to this state is generated according to the process previously presented.
2. A uniform random selection of a lighting scenario (between S2 and S36, see TABLE III) is performed. The random scenario (S_{random}) and the simulated *r*-table are used to generate a simulated experimental luminance map as if we had an ILMD.
3. Knowing S_{random} and the experimental luminance map, the *r*-table corresponding to the road surface state is estimated according to the principle summarized above and described in [9].
4. The average luminances and uniformities associated with this estimated *r*-table are calculated for the 37 lighting scenarios in TABLE III.
5. For each scenario, the calculated average luminance, overall uniformity and longitudinal uniformity are compared to the normative requirements (Class M3 in the dry state). Scenarios that do not meet the requirements are discarded.
6. The best scenario is selected as the one minimizing the total flux (F_{DRY}+F_{WET}). If at the end of step 3 no scenario reached the normative requirements, the best scenario is the one maximizing the overall uniformity among those that meet the requirement on the average luminance.
7. The surface condition, the simulated *r*-table, the estimated *r*-table, the best scenario, and the values for average luminance, overall uniformity, and longitudinal uniformity are stored to represent our results.

Fig. 4 shows four examples of simulated and estimated *r*-tables, one for each surface state. These representations are called photometric solids and consist in projecting on a plane the *r*-table values. The photometric solids are visually very close regardless of surface state, suggesting that the performance of our *r*-table estimate from an experimental luminance map is maintained even in weather conditions. The Fig. 5 confirms this robustness. For each of the 100,000

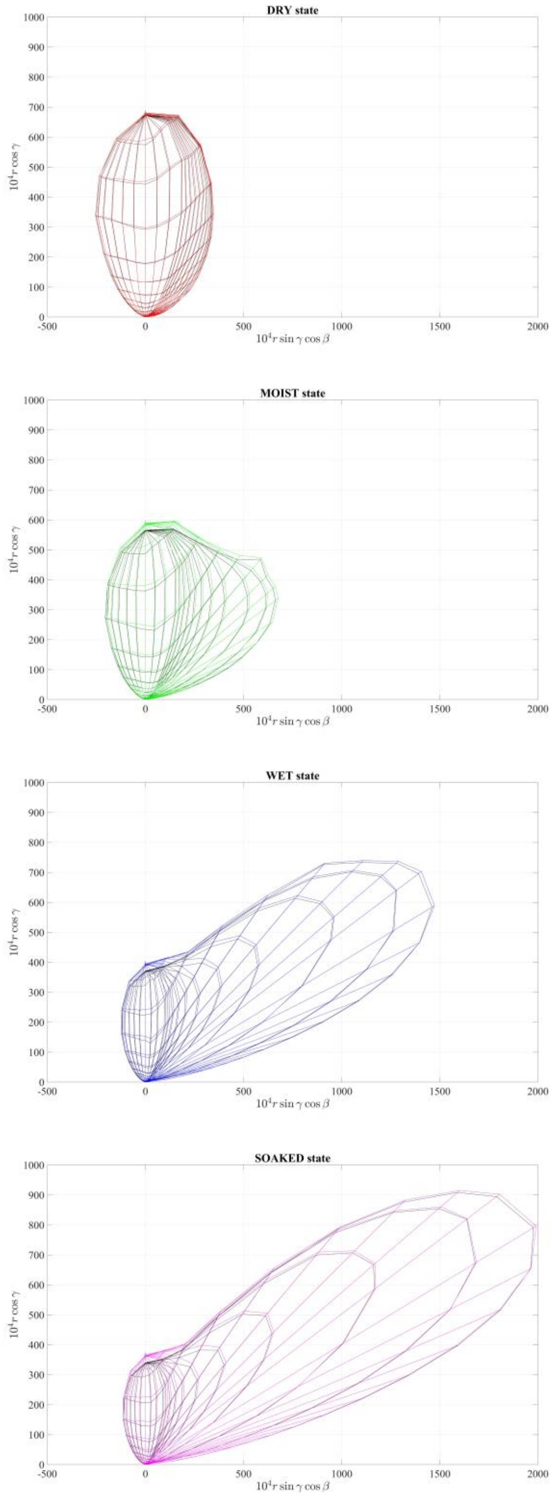

Fig. 4. Comparisons between simulated *r*-tables (black solids) and estimated *r*-tables (red solid for dry state, green solid for moist state, blue solid for wet state and magenta solid for soaked state).

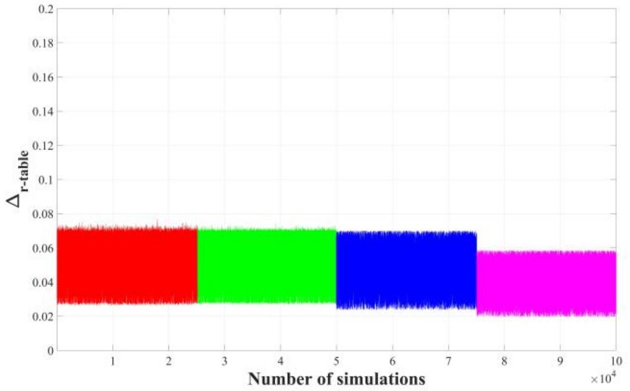

Fig. 5. Evolution of $\Delta_{r\text{-}table}$ between simulated r-tables and estimated r-tables. Red values correspond to the dry state, green to the moist state, blue to the wet state and magenta to the soaked state.

simulations performed, we computed $\Delta_{r\text{-}table}$ value (5) between the simulated r-table and the estimated r-table.

$$\Delta_{r-table} = 2\,\frac{\sqrt{N\sum_i (R_{\text{est},i} - R_{\text{sim},i})^2}}{\sum_i R_{\text{est},i} + \sum_i R_{\text{sim},i}} \qquad (5)$$

where $R_{\text{est},i}$ (resp. $R_{\text{sim},i}$) represents the i-th element of the estimated (resp. simulated) r-table and N is the total number of elements in the r-tables (usually N=580).

As stated in [8], [9], $\Delta_{r\text{-}table}$ is a comparison metric between two r-tables directly correlated to the performance of a lighting installation. If $\Delta_{r\text{-}table}$ is less than 0.1, the difference between the two r-tables will not affect the performance of the lighting installation and the r-tables can be considered similar.

Fig. 6 represents the probability of occurrence of the scenarios for these 100,000 new lighting simulations. The scenarios 1 and 37, added for operational reasons, are never used as expected. Scenarios 10, 11, 12, 22 and 23 are rarely used. After examination, they correspond in the random generation process to r-tables almost identical to those used to develop the luminaire. Scenarios 10, 12 and 23 are in fact directly derived from the initial designing calculations. Concerning scenario 7, it could be highlighted that it was well adapted for both dry and moist states. It is therefore regularly used for these two states, which explains its greater occurrence.

During this second series of simulations, the average luminance, overall uniformity and longitudinal uniformity are

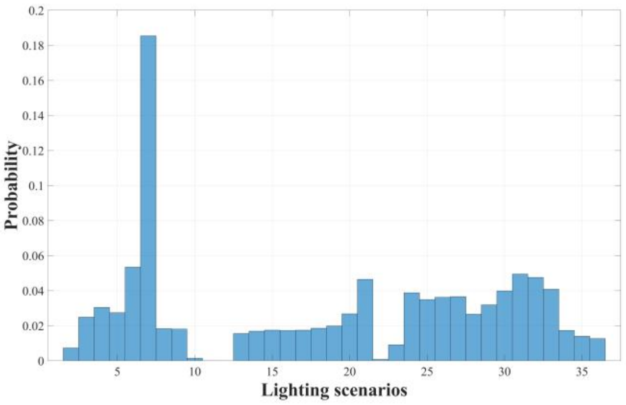

Fig. 6. Probability of lighting scenario using.

calculated for each estimated r-table using the best of our 37 scenarios. The same computations are conducted with a conventional lighting installation, i.e. designed in a standard way (one typical CIE pavement, one photometry and a constant flux). The CIE standard R2 r-table (Q0=0.070; S1=0.85) is used because it corresponds to the original pavement formulation and confirmed by the COLUROUTE measurements. Only the dry photometry of the luminaire is used and the corresponding outgoing flux to meet the M3 requirements is 7064 lm.

Fig. 7 presents for the second set of simulations the evolution of the average luminance, the general uniformity and the longitudinal uniformity obtained in the case of the lighting functioning in adaptive mode (3 top graphs) and in classical mode (3 bottom graphs). The results are represented by different colors for the four surface states (dry, moist, wet, soaked). For the adaptive road lighting, the average luminance remains very well contained whatever the surface state generated, which indicates a good mastering of the outgoing fluxes. The overall uniformity decreases with the increase of the degree of wetting but it remains above the requirement of 0.40 for the dry and moist states, relatively close to 0.40 for the wet state and largely higher than 0.15 for the soaked state. The longitudinal uniformity also tends to decrease for the wet and soaked states, presenting values below the requirement of 0.60 in the soaked state. These elements agree with the analysis of the calculations presented in TABLE I.

The conventional road lighting design based on R2 r-table leads to significant overlighting (around 60% in the dry state). The luminance increases strongly with the degree of wetting, while the overall uniformity decreases significantly in the moist state. The combination of these two observations indicates potential visibility problems for users with the cohabitation of very bright and very dark areas on the road. On the other hand, the longitudinal uniformity is very well maintained. It remains above the normative requirements for all surface states and presents higher values than those obtained for adaptive lighting. This suggests that in the strategy chosen for the adaptive lighting installation, the overall uniformity is favored to the detriment of the longitudinal uniformity, even if the latter remains systematically higher than 0.60 for the dry, moist and wet states and acceptable for the soaked state.

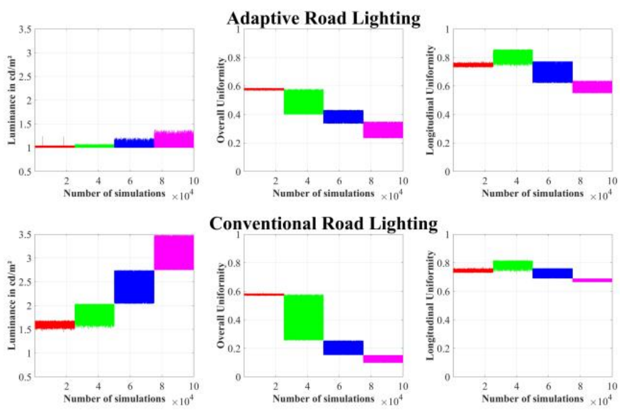

Fig. 7. Evolution of average luminance, overall uniformity and longitudinal uniformity for the case of adaptive lighting functioning (3 top graphs) and standard lighting functioning (3 bottom graphs). Red values correspond to the dry state, green to the moist state, blue to the wet state and magenta to the soaked state.

TABLE IV. COMPARISON OF PERFORMANCE OF THE ADAPTIVE AND CONVENTIONAL ROAD LIGHTING SYSTEMS

		Surface state			
		Dry	***Moist***	***Wet***	***Soaked***
Adaptive	L_{ave}	1.02 (+/- 0.01)	1.03 (+/- 0.02)	1.04 (+/- 0.04)	1.08 (+/- 0.08)
	$\%_{Lave\geq1.00}$	*100%*	*100%*	*100%*	*100%*
	U_0	0.58 (+/- 0.00)	0.45 (+/- 0.05)	0.39 (+/- 0.03)	0.29 (+/- 0.03)
	$\%_{U0\geq0.40}$	*100%*	*100%*	*49%*	*0%*
	$\%_{U0\geq0.15}$	*100%*	*100%*	*100%*	*100%*
	U_l	0.75 (+/- 0.01)	0.82 (+/- 0.02)	0.68 (+/- 0.04)	0.59 (+/- 0.02)
	$\%_{Ul\geq0.60}$	*100%*	*100%*	*100%*	*32%*
Conventional	L_{ave}	1.60 (+/- 0.04)	1.82 (+/- 0.13)	2.39 (+/- 0.20)	3.11 (+/- 0.21)
	$\%_{Lave\geq1.00}$	*100%*	*100%*	*100%*	*100%*
	U_0	0.58 (+/- 0.00)	0.40 (+/- 0.09)	0.20 (+/- 0.03)	0.12 (+/- 0.02)
	$\%_{U0\geq0.40}$	*100%*	*47%*	*0%*	*0%*
	$\%_{U0\geq0.15}$	*100%*	*100%*	*100%*	*4%*
	U_l	0.74 (+/- 0.01)	0.80 (+/- 0.01)	0.73 (+/- 0.02)	0.68 (+/- 0.01)
	$\%_{Ul\geq0.60}$	*100%*	*100%*	*100%*	*100%*

TABLE IV compares the performance of the adaptive and conventional lighting systems by providing the average luminance and uniformities and the associated standard deviations obtained for the four surface states. The values given in italic percentage represent a compliance rate, i.e. the percentage of simulations that met the normative requirement noted in subscript of the *%* symbol. The TABLE IV confirms the interpretations of the Fig. 7. The more the pavement is wet, the more the values of Q0 and S1 are important (see Fig. 2), which leads to an increase in the average luminance and a decrease in the overall uniformity. These results are in accordance with the analyses presented in [8] that have shown correlations between the average luminance and the brightness coefficient Q0 as well as between the overall uniformity and the specularity factor S1. It is also observed that the evolution of S1 values has no influence on the longitudinal uniformity since these quantities are not correlated [8].

Finally, a calculation of relative deviation in percentage was performed between the outgoing fluxes taking the adaptive lighting installation as a reference. Fig. 8 shows the evolution of this deviation as a function of the surface state. The average deviations are respectively -57% for the dry state, -46% for the moist state, +12% for the wet state and +6% for the soaked state. Considering all the simulations, the total flux associated with the adaptive lighting installation is -22%. In addition to the improved overall uniformity achieved, the proposed adaptive lighting system allows potential energy savings compared to a conventional lighting installation designed with a standard *r*-table.

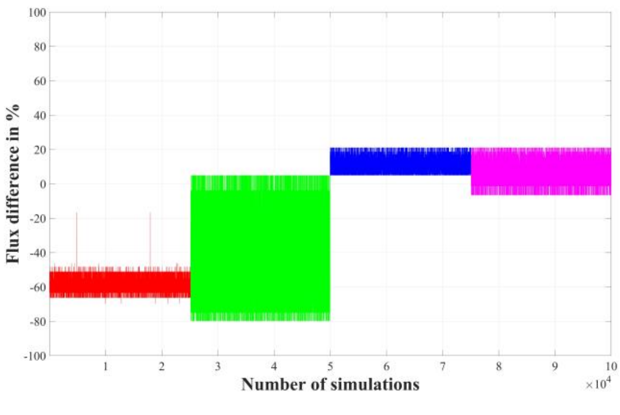

Fig. 8. Evolution of the relative deviation in % between the outgoing fluxes.

V. CONCLUSION AND PERSPECTIVES

This paper presents a complete methodology for the design of an adaptive lighting installation, from the development of a specific luminaire to the definition of a set of lighting scenarios allowing to continuously adjust the average luminance and uniformities according to the road surface state. The development of the lighting scenarios was based on the random generation of numerous *r*-tables from actual measurements of pavement reflection properties and CIE *r*-tables of type wet. A global simulation of the adaptive lighting system operation was also performed. A novel method to measure the actual *r*-table from a luminance map was used to determine the best lighting scenario for the pavement surface state. By comparing the adaptive lighting installation with a conventional lighting installation, it has been shown that the lighting functioning is globally optimized both on photometric and on energy aspects.

These results remain purely computational and need to be confirmed in the field. The experimental monitoring of the real performance of this demonstrator, named LUMI'NOV and financed by Limoges Métropole, started in April 2022. The adaptive lighting installation was built according to the work detailed in this paper with two lighting photometries in luminaires and the 37 associated lighting scenarios. To activate the right lighting scenario according to the weather conditions, a dedicated ILMD was added to the installation, providing real-time information on the actual pavement reflection properties and continuous measurements of average luminance and uniformities. A specific device using a laser sensor was also installed to measure the road surface condition and make the whole system more robust.

Evaluation of the photometric and energy performance of this adaptive lighting installation is planned for the next three years. The data collected will also be used for research aimed at predicting the evolution of pavement reflection properties according to weather conditions.

ACKNOWLEDGMENT

Authors acknowledge Gautier Monnet from Comatelec-Schréder, Patrick Tardieux from Limoges Métropole and Paul Verny from Cerema for their technical support.

ADDITIONAL INFORMATION

The methodology described in this paper is the subject of a patent application.

REFERENCES

[1] V. Muzet, F. Greffier, A. Nicolaï, A. Taron, et P. Verny, « Evaluation of the performance of an optimized road surface/lighting combination », Lighting Research & Technology, vol. 51, no 4, p. 576-591, 2019, doi: 10.1177/1477153518808334.

[2] V. Muzet, S. Liandrat, V. Bour, J. Dehon, et J.-P. Christory, « Is it possible to achieve quality lighting without considering the photometry of the pavements? », in Proceedings of the Conference CIE 2021, NC Malaysia online, sept. 2021, p. 11-21. doi: 10.25039/x48.2021.OP01.

[3] R. B. Gibbons et al., « Approaches to Adaptive Lighting on Roadways », Transportation Research Record, vol. 2485, no 1, p. 26-32, janv. 2015, doi: 10.3141/2485-04.

[4] CIE, « CIE 115:2010 - Lighting of roads for motor and pedestrian traffic », International Commission on Illumination (CIE), 2010.

[5] CEN, « EN 13201-2:2015. Road lighting - Part 2: Performance requirements », European Committee for Standardization (CEN), 2015.

[6] CIE, « CIE 47:1979 Road lighting for wet conditions », International Commission on Illumination (CIE), 1979.

[7] CIE, « CIE 15 supp 2 - Recommandations on uniform colour spaces, colour-difference equations, psychometric colour terms », International Commission on Illumination (CIE), 1978.

[8] F. Greffier, V. Muzet, V. Boucher, F. Fournela, L. Lebouc, et S. Liandrat, « Influence of Pavement Heterogeneity and Observation Angle on Lighting Design: Study with New Metrics », Sustainability, vol. 13, no 21, p. 11789, 2021, doi: 10.3390/su132111789.

[9] V. Boucher et F. Greffier, « Space of Basis Functions to Retrieve Road Surface Reflection Tables from Luminance Maps », Lighting Research & Technology, 2022 (in press).

[10] CIE, « CIE 140:2019 Road Lighting Calculations, 2nd Edition », International Commission on Illumination (CIE), 2019. doi: 10.25039/TR.140.2019.

[11] CEN, « EN 13201-3:2015. Road lighting - Part 3: Calculation of performance », European Committee for Standardization (CEN), 2015.

[12] « La porcelaine, une affaire qui roule », 17 mars 2017. https://www.lemoniteur.fr/article/la-porcelaine-une-affaire-qui-roule.594974.

[13] V. Muzet, G. Gublin, et C. Meyer, « Photometric characterization of pavements under different wetting conditions », Prague, Czech Republic, 2022.

[14] V. Muzet et al., « Review of road surface photometry methods and devices – Proposal for new measurement geometries », Lighting Research & Technology, vol. 53, no 3, p. 1-16, 2021, doi: 10.1177/1477153520958454.

[15] V. Muzet, J.-L. Paumier, et Y. Guillard, « COLUROUTE : a mobile gonio-reflectometer to characterize the road surface photometry », in 2nd CIE Expert Symposium on « Advances in Photometry abd Colorimetry », Turin, Italy, juill. 2008, vol. CIE x033:2008.

[16] https://za.schreder.com/en/ulysse-352

[17] K. Sørensen et B. Nielsen, « ROAD SURFACES IN TRAFFIC LIGHTING ». Report n°9, the Danish Illumination Engineering Laboratory, septembre 1974.

[18] A. Erbay, « Of the reflection properties of road surfaces », Technische University of Berlin, 1974.

A Study On a Parametric Model that Interrelate Lighting Parameters Based on Methods of Data Analysis

Asterios K. Tolidis
School of Electrical and Computer Engineering
Aristotle University of Thessaloniki
Thessaloniki, Greece
atol@auth.gr

***Abstract*—Lighting designers would find it very useful to obtain a parametric model that could link lighting design parameters like position, orientation, size, or intensity of the luminaires with parameters describing, in a measurable way, the visual objective, the scene in general that is desired to be perceived and its characteristics relevant to light and lighting.**

The study of the present paper concerns the creation of a parametric model that intends to set the lighting design parameters and the ones describing the visual results as input and output in a function and to express their interrelation in an as much as possible deterministic way. It is extremely difficult though to determine the correlation of these parameters in terms of mathematical functions or formulas in general. Thus, an alternative approach will be followed to find and express the interrelation of these parameters, by means of data analysis methods. Drawing inspiration from fields like Artificial Intelligence and Machine Learning, methods ranging from Regression to Deep Learning will be used for the construction of the parametric model. As a prior process, there will be a selection of the appropriate lighting parameters that describe on one hand and influence on the other hand the visual result, according to relevant well-established principles. Especially for the parameterization of the visual result optics and perception principles are involved. Then data will be collected as values of these parameters by means of computer simulations. Finally, the model will be constructed and trained through machine learning methods and afterwards it will be tested and assessed. The final goal in this whole process is to create a tool with which, there could be a control on the lighting parameters to achieve a desired visual result in a more automated and systematic way, and less following a kind of trial-and-error way.

Keywords—Lighting design, Parametric design, Algorithms, Data Analysis

I. Introduction

Objects and the surrounding space are perceived by humans mainly via the visual system. It is clear that light plays the leading role in this, although the procedure of visual perception includes more than the construction of an image on the surface of the eye retina [1], [2]. Light, as it falls on surfaces and is reflected to the eye, transmits information about the environment concerning not only the geometric characteristics like shape, size, and position but also quality characteristics like color or transparency and even more abstract ones like freshness or vividness or having to do with the perceivable atmosphere of the environment. All these combined and processed by the human brain lead to a visual result, or better to a perceptual result in a more general sense. There are principles that govern the way these characteristics are perceived. These principles concern not only the obvious fields like optics or the physics of light but also fields like psychology. An example for the latter is the "Gestalt" theory which originates in psychology and deals with visual perception. This theory suggests that the human mind tend to organize the visual information in integrated ensembles implementing specific principles [3].

The scope of the present study is the creation of an algorithm, in the form of a parametric model, that would take a desired visual result, as an input and give the proper lighting design to attain this result, as an output. The algorithm will accept values to specific input parameters that describe the visual objective. These input parameters are related one way or another with variations of the luminous intensity coming from the visible surfaces of the environment and the objects in it [4], [5]. After all, whatever the visual perception process might be, the trigger is always the light intensity that stimulates the cones and rods of the eye. According to visual perception principles the visual characteristics of the environment can be parameterized to absolute or relative values of light intensity. In other words, the visual objective can be described as a 2D "luminous intensity image", where each pixel represents the intensity coming from the corresponding projected point of the field of view i.e., a 2D matrix of intensity values.

After obtaining the 2D matrix as input, the algorithm, based on data analysis methods, will assign the proper values to the output parameters which determine the lighting design plan. These output parameters are basically geometric like the number, position, and orientation of the luminaires, but there are others like their luminous intensity. The data analysis and machine learning methods give the opportunity to interrelate the lighting design parameters and the visual result parameters, based on data, either from simulations or from real cases, rather than on mathematical expressions which are very hard to determine.

It must be mentioned that there are well established rendering techniques that use mathematical equations to describe the relation between the lighting parameters and the visual result, but first they give simulations with restricting assumptions, and second they treat each case individually directly on implementation without facing the equations as generalized descriptions of the interrelations between the lighting parameters.

II. The Parametric Model

A. Method

There are two stages in the present study of the realization of the parametric model. First the creation of the data base needed for the data analysis methods and second the creation of the model that will interrelate the input and output data and finally give the proper output for the relative input.

The data base will be set up for a specific case of a simplified environment, the lighting of which will be simulated. For the creation of the data base, a selection of features in the form of lighting parameters is needed, such as the position and orientation of the luminaires and the observer, the position and orientation of the reflecting surfaces, reflectance characteristics, light intensity etc. Assigning values to these parameters and according to physics-based principles, the viewing result can be derived as a luminous intensity image which was described in the introduction. The basic idea is to take as reference the general rendering equation [6]:

$$L_o(\omega_o, x) = \int_\Omega L_i(\omega_i, x) f_r(\omega_o, \omega_i, x)(\omega_i \cdot n) d\omega_i \qquad (1)$$

Where L_o, x, n, ω_i, ω_o, L_i, f_r are observed light luminance, surface location, surface normal, light direction, view direction, incident light luminance, and Bidirectional Reflectance Distribution Function (BRDF), respectively. It can be seen here that there are parameters referring to the surfaces of the scene reflecting light to the observer and not only parameters that refer to light, incident or observed.

During implementation, BRDF is expressed by a simulation model like the "Phong" model which is simple but adequate [7]. Equation (1) is simple and general at its form and its main principle is that the light coming to the observer's eye from a surface depends on the incident light on the surface, the way the surface reflects this light, and the incidence angle. Each of the components is represented by a function describing the impact of specific parameters like position or direction to its contribution to the final luminance observed. The general form of the functions is adapted to the specific case of study, for the final equation to be implemented for every microfacet i.e., every elemental part of the surface, and the luminous intensity image to be extracted. For the final data base to be constructed, the whole routine is iterated as many times as possible, assigning different combinations of values to the input parameters, to obtain as many different luminous intensity images as possible.

As soon as an adequate data base exists, a machine learning model is created. The model should accept the data from the luminous intensity images as an input and assign the proper values to the output parameters i.e., the lighting design parameters which by these values will lead to the desired visual result. According to the description of the problem, the construction of the model at first glance is recognized as a regression type of problem, due to the continuous output parameter values desired. A suitable kind of method must be used to construct and train the model to predict in the most reliable way possible the values that the lighting design parameters like number, position, orientation, intensity of the luminaires etc. should have to give the desired visual result. This method shall be searched among multi-label regression solutions, because the number of output parameters is bigger than one. These solutions resemble the ones used for image analysis and pattern recognition, because the input is a series of values like pixel values in an image.

B. Construction of the data base

For the construction of the data base, an algorithm has been developed in MathWorks® MATLAB® for a particular example of space. It calculates parametrically, for a certain cylindrical space under a semispherical dome, the luminous intensity on a certain point of the floor of the cylindrical space (viewer's position), that comes from one point source located at another point of the floor by reflection on every microfacet of the inner surface of the dome. The calculation takes place for every microfacet of the semispherical surface and thus a 2D matrix with the values of the luminous intensity is made. Supposedly, the viewer will be situated within the boundaries of the floor of the cylindrical space looking up at the dome, for all the microfacets to be visible, and the luminous intensity image to be whole.

The inspiration came from the case of an orthodox church dome with a tessellated surface. Parameters like the size, position, orientation, color, or the existence of glaze of the tiles of the mosaic influence the way that light is reflected on them and produces a certain visual effect. There are pieces of evidence mentioned in relevant literature [8] that middle age mosaic artists in Ravenna, Italy were putting deliberately the little pieces of their mosaics in a well-studied manner regarding the position and orientation to reflect light in a certain way and produce specific visual effects. Besides tessellation, the geometric characteristics in general like size and curvature of the dome of an orthodox church could also influence the visual result and produce specific effects [9], [10].

The algorithm is quite simplified for the particular case. Only the contribution of the dome and not the cylindrical space is considered, the light source is single, and the interreflections between points of the dome surface are not taken into account. This is because the data base must be as controllable and assessable as possible, at least at a first stage, to facilitate the construction and assessment of the machine learning model. Besides, the data base results from a simulation and the values are not supposed to be real measurements.

Specifically for the case, the parameters used as inputs in the algorithm are:

- the dome radius,
- the distance of the center of the dome from the floor (height),
- the distance of the light source from the axis of the cylinder underneath the dome,
- the distance of the viewer's position from the axis of the cylinder and
- the angle around the axis on the horizontal plane between the source and the viewer.

From the above parameters, via trigonometric equations, parameters like the light direction ω_i, the view direction ω_o and the BRDF can be derived and finally the resulting luminous intensity coming from each microfacet of the dome can be determined. The dome's inner surface is divided into microfacets for every degree of azimuthal angle and every degree of polar angle. Thus, the algorithm finally calculates a 360 x 90 matrix of luminous intensity values. The implementation of the general rendering equation for the present specific case is done using the "Phong" simulation model with some adaptations due to the aforementioned simplifications, e.g., there is no ambient light coefficient because the interreflections between points of the dome surface are neglected at this stage. Equation (3) describes the simulation model:

$$I_o = I_i \left(k_d (\boldsymbol{n} \cdot \boldsymbol{l}) + k_s (\boldsymbol{r} \cdot \boldsymbol{v})^n \right) \qquad (3)$$

Where I_o and I_i are the observed and incident luminous intensities, k_d, k_s and n are coefficients relevant to the "Phong" model, $\boldsymbol{n}$ is the normal vector of each microfacet, $\boldsymbol{I}$ and $\boldsymbol{v}$ are the incident and viewing direction vectors and $\boldsymbol{r}$ is the mirroring vector of the incident direction with respect to the normal vector [7]. The above vectors and the positions of the light source and the viewer can be seen in Fig. 2.

Fig. 1 shows a screenshot of the Graphical User Interface (GUI) of the application facilitating the calculating algorithm. At the left side of the image there are fields where the inputs for the algorithm, described in the above bullet list, are inserted. At the left side there is the graphical representation of the output in the form of a 3D mesh in a cylindrical coordinate system. The angular coordinate and the radial distance of every microfacet are translated into cartesian coordinates x and y and are represented by the corresponding point on the x-y plane, while the height on the vertical z axis represents the luminous intensity value coming from the corresponding microfacet to the viewer as a rate of the absolute intensity of the light source. For a better understanding there is also another representation of the output in the form of a contour plot containing isolines of the same luminous intensity values on the x-y plane. It can be regarded as a top view of the 3D mesh.

Fig. 3 shows a part of the 2D matrix with the intensity values of the specific example of the previous graphical representation.

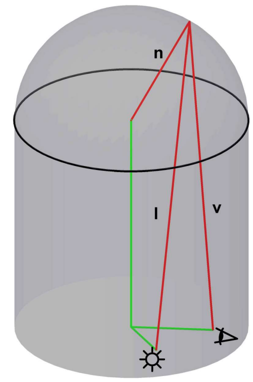

Fig. 2. A drawing of the hypothetical case of the illuminated dome at the particular example with the relevant vectors of the simulation model and the positions of the light source and the viewer (author's sketch).

In Fig. 5 there is a rendering image simulating the lighting of the dome for the above example, using the same simulation model. It is produced by a program made by the author in "Processing" language for the proper comparisons with the results of the MATLAB® application. Both the "Processing" program and the MATLAB® application for the graphical representation are constructed to help making a first rough visual assessment of the data base. Visualizing the data somehow in spatial terms could offer some first useful indications.

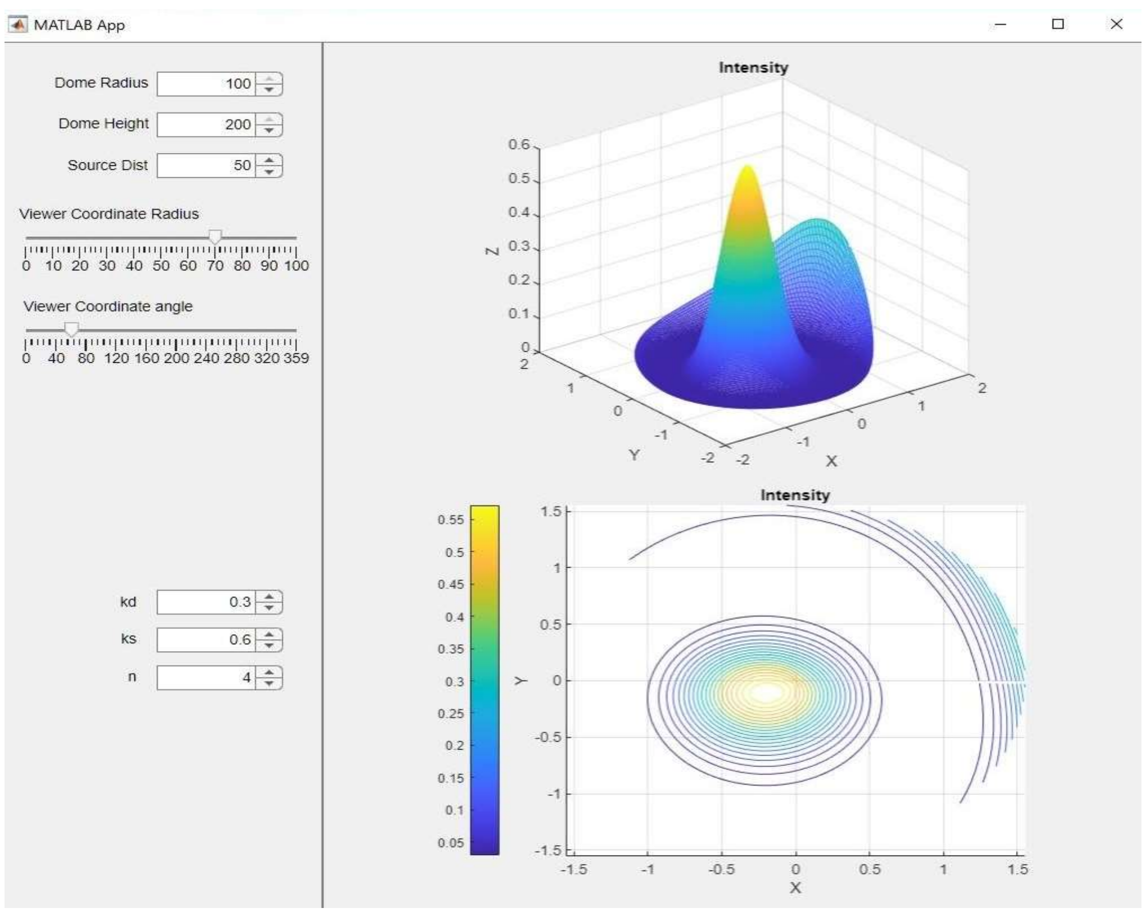

Fig. 1. The GUI of the application facilitating the calculating algorithm, with the input fields and the output plots.

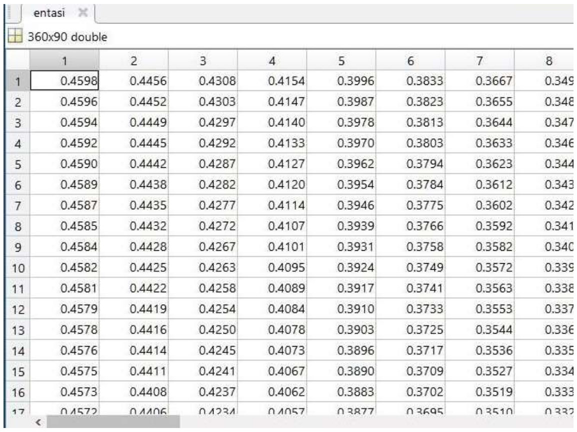

entasi
360x90 double

	1	2	3	4	5	6	7	8
1	0.4598	0.4456	0.4308	0.4154	0.3996	0.3833	0.3667	0.349
2	0.4596	0.4452	0.4303	0.4147	0.3987	0.3823	0.3655	0.348
3	0.4594	0.4449	0.4297	0.4140	0.3978	0.3813	0.3644	0.347
4	0.4592	0.4445	0.4292	0.4133	0.3970	0.3803	0.3633	0.346
5	0.4590	0.4442	0.4287	0.4127	0.3962	0.3794	0.3623	0.344
6	0.4589	0.4438	0.4282	0.4120	0.3954	0.3784	0.3612	0.343
7	0.4587	0.4435	0.4277	0.4114	0.3946	0.3775	0.3602	0.342
8	0.4585	0.4432	0.4272	0.4107	0.3939	0.3766	0.3592	0.341
9	0.4584	0.4428	0.4267	0.4101	0.3931	0.3758	0.3582	0.340
10	0.4582	0.4425	0.4263	0.4095	0.3924	0.3749	0.3572	0.339
11	0.4581	0.4422	0.4258	0.4089	0.3917	0.3741	0.3563	0.338
12	0.4579	0.4419	0.4254	0.4084	0.3910	0.3733	0.3553	0.337
13	0.4578	0.4416	0.4250	0.4078	0.3903	0.3725	0.3544	0.336
14	0.4576	0.4414	0.4245	0.4073	0.3896	0.3717	0.3536	0.335
15	0.4575	0.4411	0.4241	0.4067	0.3890	0.3709	0.3527	0.334
16	0.4573	0.4408	0.4237	0.4062	0.3883	0.3702	0.3519	0.333

Fig. 3. The first 16x8 cells of the 2D matrix with the luminous intensity values which give the relevant plots of Fig. 1.

C. *Construction of the model*

The second stage, this of the creation of the final parametric model starts after obtaining the corresponding data base from the first stage. This final parametric model will be a machine learning model that will take as input the luminous intensity values and give as output the values for the lighting design parameters. At the beginning, a preparation of the data is made. The input data of the luminous intensity image i.e., the 360x90 matrix with the intensity values is modified to a proper format for the machine learning model to be trained and tested. The same applies also to the output data of the lighting design parameters. The number of sample images for the training and testing of the model was decided to be 1000, 800 to provide the training data and 200 the testing data.

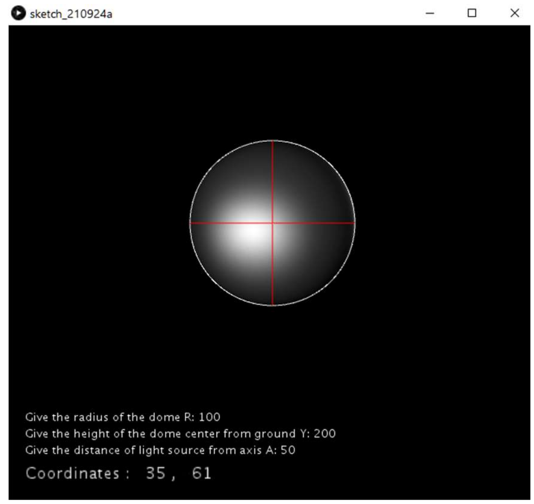

Fig. 5. The simulation of the lighting of the dome for the previous example. The surface of the dome is supposed to have no texture or colour variations.

An application of MATLAB® that applies several algorithms for regression and assess them, is used for the implementation of the machine learning model. One of its main tasks is to provide the accuracy of each algorithm, for the user to be able to choose the one that better meets the requirements. Fig. 4 shows this regression learner application interface with the results for the root mean square error (RMSE) as a measure of accuracy of each model algorithm. The user can use several plots like predicted vs actual plot etc. to assess the algorithms.

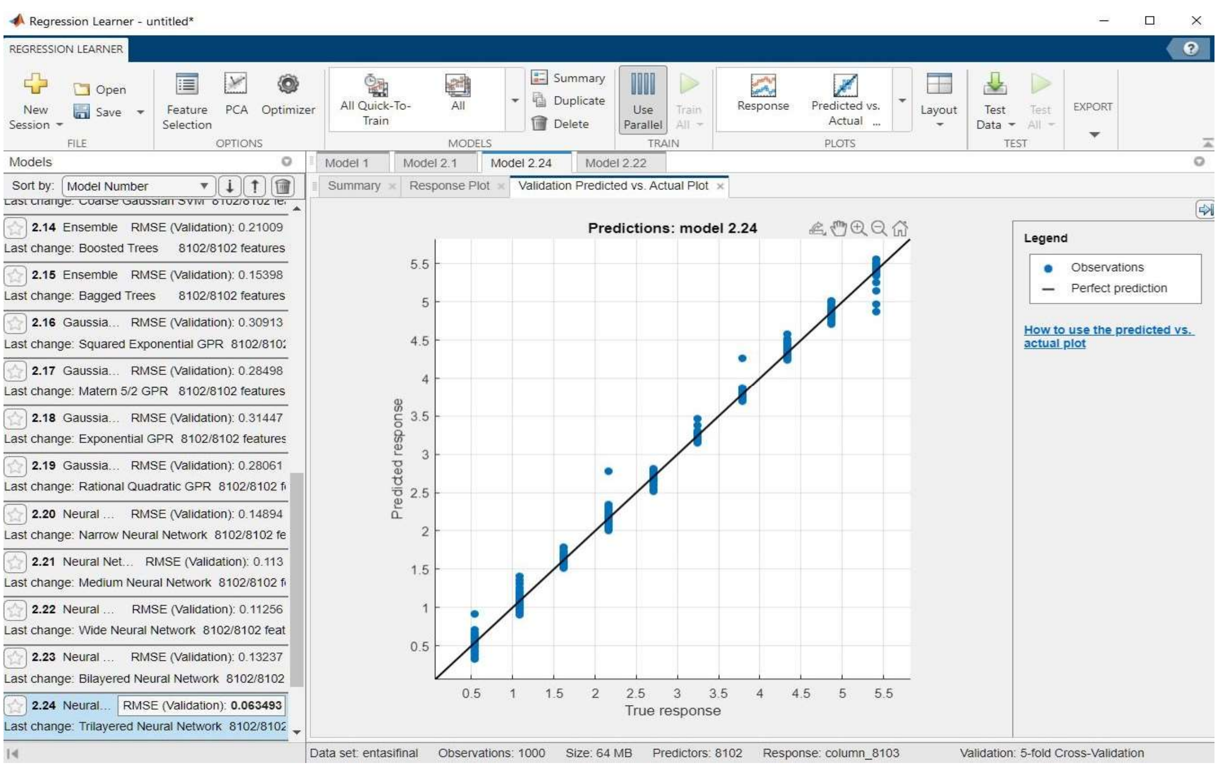

Fig. 4. The regression learner application interface.

Apart from the validation with the testing data, a cross-validation is made automatically by the application during the training procedure of the algorithms. It must be mentioned here that the algorithms applied and assessed by the regression learner at a first stage are single target regression algorithms which at a second stage are to be combined in regressor chains or ensembles to be utilized for our multi-target regression problem.

D. Results

After running on a computer with a quad-core CPU, in parallel mode, the application gave the results for 26 regression algorithms. The one with the best accuracy i.e., the lowest RMSE was the Trilayered Neural Network with RMSE equal to 0.063493, which is quite satisfactory. The above can be seen in Fig. 4. These were the results of the implementation of the final machine learning model and its assessment. A comparison between a rendering image related to the true parameter values and one related to the predicted ones showed really small differences.

III. Conclusions – Discussion

One main and quite important conclusion of the implementation of the parametric model is the verification of its feasibility. The model is actually attainable and can lead to acceptable results. Although the data base used to train the model is resulting from a simplified simulated example, the model can work with data from real cases. The concept and method used rely on physics-based principles and formulas, therefore the model does not lose its generality. Thus, one can use a model like this to find out the proper lighting installation for achieving a particular desired visual result in terms of light brightness and contrast of a specific scene.

Instead of artificial data from simulations, real-life data collected from real spaces e.g., orthodox churches with domes can be used. A Future work could be to light domes like these in a certain controlled way and measure the luminous intensity at various viewpoints arriving from each microfacet of the surface of the dome. The data of the lighting installation together with the luminous intensity values would constitute the data base for the model. Testing with various machine learning algorithms is needed for assessment because the real-life data may prove other algorithms as better for real cases. Of course, the final scope is the use in whichever case and not only for church domes.

The parametric model of this study could be used either as a standalone application for lighting design or as a routine embedded in programs for lighting design or rendering. For example, programs like Relux® and DIALux could include it as a plug-in, for lighting designers to find solutions for specific more complex lighting schemes. The designers could form the space and the lighting conditions in terms of brightness and contrast at certain points and the program would propose not only the number and position of the luminaires but also luminaires with certain lighting specifications such as intensity and light beam characteristics. The procedure and especially the selection of the luminaires would be more automated and less following a kind of trial-and-error way.

Another use of the parametric model, beyond the study of how the lighting design parameters relate to the final visual result parameters, is also to study how the lighting design parameters relate to and influence each other to lead to a specific visual result.

Conclusively this model could constitute a great tool for lighting design, giving the professionals the opportunity to create special visual effects e.g., particular impressions in places like churches that have an emotive character. Theaters where light plays a major role or cultural monuments could benefit too and the list could go on. A tool like this could give an impulse to creativity.

References

[1] R. Arnheim and I. Potamianos, Art and visual perception : a psychology of the creative eye, 3rd ed. Athens: Themelio, 2005.

[2] J. J. Gibson, The ecological approach to visual perception., 1st ed. Athens: Gutenberg, 2002.

[3] A. Desolneux, L. Moisan, and J.-M. Morel, From Gestalt Theory to Image Analysis, vol. 34. New York, NY: Springer New York, 2008.

[4] M. Stokkermans, I. Vogels, Y. de Kort, and I. Heynderickx, "Relation between the perceived atmosphere of a lit environment and perceptual attributes of light," Light. Res. Technol., vol. 50, no. 8, pp. 1164–1178, Dec. 2018.

[5] D. L. Loe, K. P. Mansfield, E. Rowlands, "A step in quantifying the appearance of a lit scene," Light. Res. Technol., vol. 32, no. 4, pp. 213-222, Dec. 2000.

[6] K. Zhang, F. Luan, Z. Li, and N. Snavely, "IRON: Inverse Rendering by Optimizing Neural SDFs and Materials from Photometric Images," IEEE Conf. Comput. Vis. Pattern Recog., Apr. 2022, unpublished, arXiv:2204.02232.

[7] T. Theoharis, G. Papaioannou, N. Platis, and N. M. Patrikalakis, Graphics and Visualization - Principles and Algorithms. Athens: Symmetria, 2012.

[8] M. De Luca, Il mosaico per immagini, Italy: Essegi, 1989.

[9] W. Jabi and I. Potamianos, "Geometry, Light, and Cosmology in the Church of Hagia Sophia," Int. J. Archit. Comput., vol. 5, no. 2, pp. 303–319, 2007.

[10] W. Jabi and I. Potamianos, "Parameterizing the geometry and visualizing the lighting method of byzantine church domes," in Lecture Notes in Computer Science (including subseries Lecture Notes in Artificial Intelligence and Lecture Notes in Bioinformatics), 2016.

[11] Y. Tao, H. Lin, F. Dong, C. Wang, G. Clapworthy, and H. Bao, "Structure-aware lighting design for volume visualization," IEEE Trans. Vis. Comput. Graph., vol. 18, no. 12, pp. 2372–2381, 2012.

[12] M. Moeck, "Constraint Satisfaction Software for Architectural Lighting Design: A Case Study," LEUKOS - J. Illum. Eng. Soc. North Am., vol. 1, no. 1, pp. 101–127, Jan. 2005.

[13] R. Shacked and D. Lischinski, "Automatic Lighting Design using a Perceptual Quality Metric," Comput. Graph. Forum, vol. 20, no. 3, pp. 215–227, Sep. 2001.

[14] T. Schielke, "Influence of Lighting Design on Marketing Communication," LEUKOS - J. Illum. Eng. Soc. North Am., vol. 11, no. 3, pp. 109–124, 2015.

[15] W. Van Bommel, "Visual, biological and emotional aspects of lightings: Recent new findings and their meaning for lighting practice," LEUKOS - J. Illum. Eng. Soc. North Am., vol. 2, no. 1, pp. 7–11, 2005.

[16] J. A. Veitch, "Psychological processes influencing lighting quality," J. Illum. Eng. Soc., vol. 30, no. 1, pp. 124–140, 2001.

[17] T. Edensor, "Light design and atmosphere," Vis. Commun., vol. 14, no. 3, pp. 331–350, Aug. 2015.

[18] X. Y. Liu, M. R. Luo, and H. Li, "A study of atmosphere perceptions in a living room," Light. Res. Technol., vol. 47, no. 5, pp. 581–594, Aug. 2015.

[19] M. Moeck, "On Computer Aided Architectural Lighting Design: Lighting Design Techniques," J. Illum. Eng. Soc., vol. 28, no. 2, pp. 33–41, Jul. 1999.

[20] D. Forsyth and J. Ponce, Computer vision : a modern approach. Englewood Cliffs, N.J.: Prentice Hall, 2003.

[21] M. Turrin, P. Von Buelow, and R. Stouffs, "Design explorations of performance driven geometry in architectural design using parametric modeling and genetic algorithms," Adv. Eng. Informatics, vol. 25, no. 4, pp. 656–675, 2011.

[22] W. O. Parker and R. C. Wolf, Scene design and stage lighting, 7th ed. Harcourt Brace College Publishers, 1996.

[23] Y. Dobashi, K. Kaneda, H. Nakatani, H. Yamashita, and T. Nishita, "A Quick Rendering Method Using Basis Functions for Interactive Lighting Design," Comput. Graph. Forum, vol. 14, no. 3, pp. 229–240, Aug. 1995.

[24] A. C. Costa, A. A. Sousa, and F. Nunes Ferreira, "Lighting Design: A Goal Based Approach Using Optimisation," in Rendering Techniques' 99, D. Lischinski and G. W. Larson, Eds. Granada, Spain: Springer, 1999, pp. 317–328.

[25] A. Mahdavi and H. Eissa, "Subjective Evaluation of Architectural Lighting via Computationally Rendered Images," J. Illum. Eng. Soc., vol. 31, no. 2, pp. 11–20, Jul. 2002.

[26] M. J. Murdoch, M. G. M. Stokkermans, and M. Lambooij, "50.3: Invited Paper : Perceptual Accuracy in the Visualization of Lighting Scenes," SID Symp. Dig. Tech. Pap., vol. 46, no. 1, pp. 758–761, Jun. 2015.

[27] J. Lai, X. Li, and P. Ge, "Designing double freeform surfaces for point source and extended sources using a construction, iteration and optimization process," Light. Res. Technol., vol. 0, no. 0, pp. 0–10, Oct. 2018.

[28] C. Cuttle, "A fresh approach to interior lighting design: The design objective – direct flux procedure," Light. Res. Technol., vol. 50, no. 8, pp. 1142–1163, Dec. 2018.

[29] K. P. Mansfield, "Architectural lighting design: A research review over 50 years," Light. Res. Technol., vol. 50, no. 1, pp. 80–97, Jan. 2018.

[30] B. Mildenhall, P. P. Srinivasan, M. Tancik, J. T. Barron, R. Ramamoorthi, and R. Ng, "NeRF: Representing Scenes as Neural Radiance Fields for View Synthesis," IEEE Conf. Comput. Vis. Pattern Recog., Mar. 2020, unpublished, arXiv:2003.08934.

[31] Procopius of Caesarea, On Buildings, General Index, Translated by H. B. Dewing, Glanville Downey, Loeb Classical Library 343, Cambridge, MA, Harvard University Press, 1940.

The Measurement Uncertainty of the Imaging Luminance Measurement Device based on the DSLR Camera

Ing. Martin Motyčka, Ph.D.
Department of Electrical Power Engineering
Brno University of Technology
Brno, Czech Republic
motyckam@vutbr.cz

Ing. Jan Škoda, Ph.D.
Department of Electrical Power Engineering
Brno University of Technology
Brno, Czech Republic
skoda@vutbr.cz

Ing. Petr Baxant, Ph.D.
Department of Electrical Power Engineering
Brno University of Technology
Brno, Czech Republic
baxant@vutbr.cz

***Abstract*—This article describes the measurement uncertainties of imaging luminance measurement device based on the DSLR camera. These devices are suitable for outdoor measurements for its practicality. They are capable of fast and reliable measurement and proved as valuable instrument for the measurement of glare index and the luminance of roads, traffic signs and night sky. However, calibration of these devices are more difficult than for the ordinary luminance meter and therefore it is necessary to evaluate measurement uncertainties for the comparison with the conventional luminance meters and cameras. The expanded measurement uncertainty also depends on the camera settings e.g. f-number, shutter speed or ISO parameter. This article describes all important uncertainties of the camera and lens and propose their measurement and estimation.**

***Keywords*—Luminance camera, DSLR camera, measurement uncertainty, luminance distribution measurement**

I. Introduction

The luminance camera based on DSLR is a type of imaging luminance measuring device that is capable of the luminance measurement in every pixel of captured image. The conventional luminance meter only measures average luminance in its defined viewing angle in one direction. The imaging luminance measuring devices offer more flexibility and complexity to the luminance analysis of captured scenes. However, these devices are very complex in order of hardware and software calibration and the uncertainty analysis is therefore more difficult than in case of the conventional luminance meters. Among the key benefits of using DSLR camera as an imaging luminance measuring device is the practicality of capturing images when companies like Nikon or Canon has been improving ergonomics and reliability of the camera over the decades. There is also possibility to change lenses for specific application. For the UGR evaluation of the scene and light pollution measurement it is necessary to use the FishEye lens with the half-space viewing angle. On the contrary in case of the measurement of street luminaires it is appropriate to use the lens with longer focal length in order to achieve more detailed luminance distribution map. Due to the spectral sensitivity of standard photometric observer these devices can be also used for the measurement of traffic signs and illuminated advertisement without significant spectral errors.

This research work has been carried out in the Centre for Research and Utilization of Renewable Energy (CVVOZE). Authors gratefully acknowledge financial support from the Technology Agency of the Czech Republic (project No. CK03000154)).

The main benefit is also possibility of capturing images with the camera without necessity of connected controlling computer and therefore is well suited for outdoor quick measurement. The calibration procedure is more complicated than in case of ordinary luminance camera with monochromatic sensor. The expanded measurement uncertainties are higher due to variable aperture in the camera lens and mechanical parts inside the camera like mechanical shutter. Moreover, it is more difficult to achieve the spectral sensitivity of a standard photometric observer. Before the description of individual standard uncertainties, the basic theory of uncertainty estimation is explained.

II. Uncertainty of mesurement

According to GUM (Guide to the expression of uncertainty) term uncertainty means doubt about validity of the measured value [1]. The measurement uncertainty characterizes dispersion of measured values. In other words, the measurement uncertainty defines an interval, where the true value is found within certain probability. Uncertainties can be divided according to type of calculation. Standard uncertainty is expressed as a standard deviation from repeated measurements and it is associated to type A evaluation of uncertainty. Type B evaluation is not using statistical analysis of repeated measurements. In most cases type B evaluation covers the measurement errors of the measuring devices or the uncertainties of calibration. According to GUM all systematic errors of the measuring device or method must be corrected and the uncertainties type A should be calculated for each correction. However, in some cases it not possible to measure correction in whole range or image and therefore the fitting with appropriate function is necessary. Then it is necessary to calculate uncertainty of the fitting with both the uncertainty evaluation of type A and B. The uncertainties calculated from type A and B calculation are used for the calculation of combined uncertainty that is multiplied with the coverage factor to obtain the expanded uncertainty [1].

A. Type A evaluation

Type A evaluation uses statistical analysis of the series of measurements. Such uncertainty is defined as the standard uncertainty of measurement and is calculated as the experimental standard deviation of the mean given by.

$$u(x) = \frac{1}{\bar{x}}\sqrt{\frac{1}{n(n-1)}\sum_{n=1}^{n}(x_n - \bar{x})^2} \qquad (1)$$

Where n is the number of independent measurements, x_n is the input estimate and $\bar{x}$ is the arithmetic mean of measured values. The standard deviation of the mean only covers 68.3 % of normal probability distribution and should be calculated from 20 values at least. The standard deviation of the mean can be decreased with higher number of measurements.

B. Type B evaluation

Type B uncertainty is not calculated with the statistical analysis and its variance is assumed from manufacturer's specification, calibration reports and certificates. When expanded uncertainty of the measuring device is known the standard uncertainty can be calculated given by

$$u(i) = \frac{U_i}{z} \tag{2}$$

Where U_i is the expanded uncertainty of measuring device from calibration certificate and z is the conversion factor. Conversion factor is similar to coverage factor in case of normal probability distribution. For rectangular probability distribution the conversion factor equals $z = \sqrt{3}$.

C. Combined uncertainty

The combined uncertainty is calculated with the law of propagation of uncertainty and it is combining all variances of the measurands. It is calculated with the formula given by

$$u_c = \sqrt{\sum_{i=1}^{n} C_i^2 u_i^2 + 2 \cdot \sum_{i=1}^{n-1} \sum_{k=i+1}^{n} C_{k,i} C_{i,k} u_i u_k r_{j,k}} \tag{3}$$

Where $r_{j,k}$ is the correlation coefficient and $c_{j,i}$ is the sensitivity coefficient that converts measurement uncertainty from one quantity to other. The sensitivity coefficient can be calculated with the formula given by

$$c_i = \frac{\partial f}{\partial x_i} \tag{4}$$

The correlation coefficient only applies when standard uncertainties are correlated. Two quantities are correlated when change in one quantity also creates change in the second quantity. The correlation coefficient describes scale from -1 to 1 of correlation of two quantities [1].

D. Expanded uncertainty

The combined uncertainty only covers 68.3 % of normal probability distribution and therefore it shall be expanded by coverage factor for increasing the probability of true value to be found within the interval defined by the uncertainty. The expanded uncertainty can be calculated with the equation given by

$$U = k \cdot u_c \tag{5}$$

Where Coverage factor equals $k = 2$ for the normal probability distribution. In this case the probability of finding true value inside interval defined by the expanded uncertainty is 95.5 %.

III. Measurement uncertainties of luminance camera

The standard uncertainties of ILMD can be divided into two groups. The first group relates to the camera. There are uncertainties of spectral sensitivity and linearity of the detector, repeatability of the shutter and temperature dependency of the sensor [2].

A. Spectral uncertainty

The luminance camera must be adapted to have spectral sensitivity of a standard photometric observer in order to measure the luminance correctly for the all possible spectra. Every photometer can be characterized by the mismatch index f_1' that statistically describes goodness of fit to $V(\lambda)$ curve. The mismatch index f_1' can be calculated with the equation given by

$$f_1' = \frac{\sum_{380\,nm}^{780\,nm} |s_{rel}^*(\lambda) - V(\lambda)| \Delta\lambda}{\sum_{380\,nm}^{780\,nm} |V(\lambda)|\, \Delta\lambda} \tag{6}$$

Where $s_{rel}^*(\lambda)$ is the normalized spectral responsivity of the photometer. When spectral sensitivity of the photometer and spectrum used during the calibration is known it is possible to calculate spectral mismatch correction for specific spectra with equation given by

$$a^*(s_Z(\lambda)) = \frac{\dfrac{\sum_{380\,nm}^{780\,nm} s_Z(\lambda) \cdot s_{rel}(\lambda) \Delta\lambda}{\sum_{380\,nm}^{780\,nm} s_Z(\lambda) \cdot V(\lambda) \Delta\lambda}}{\dfrac{\sum_{380\,nm}^{780\,nm} s_A(\lambda) \cdot s_{rel}(\lambda) \Delta\lambda}{\sum_{380\,nm}^{780\,nm} s_A(\lambda) \cdot V(\lambda) \Delta\lambda}} \tag{7}$$

Where $s_{rel}(\lambda)$ is the relative responsivity of the photometer calibrated with the spectra $s_A(\lambda)$ that is defined as CIE standard illuminant A and $s_Z(\lambda)$ is the spectra of tested light source [2]. When the correction is not carried out it is possible to estimate spectral error with the equation given by

$$f_1(s_Z(\lambda)) = a(s_Z(\lambda)) - 1 \tag{8}$$

To calculate the standard uncertainty of spectral error (furthermore spectral uncertainty) it is necessary to use conversion factor z in equation given by

$$u_s = \frac{f_1(s_Z(\lambda))}{z} \tag{9}$$

Conversion factor depends on the probability distribution of the error and for this case the rectangular distribution can be used with the conversion factor $z = \sqrt{3}$ [1,2].

The spectral sensitivity of the ILMD should be measured for individual lenses and settings of the camera e.g. f-number, focus distance and ISO parameter. Moreover, it is necessary to measure the uniformity of spectral sensitivity across the sensor due to possible angular differences in spectral transparency of the optical system. Therefore, in the calibration certificate there should be presented spectral sensitivity examples for the center of the image and for its corner for specific setting of the camera [3].

B. Linearity uncertainty

The linearity uncertainty is related to the linearity error of the detector or the uncertainty of its correction. When using an DSLR camera for luminance measurement the linearity is internally corrected by a manufacturer. However, it is recommended to verify linearity with the measurement described in the CIE 237:2020 where superposition method (flux doubling) and combinatorial method is described [4]. The most commonly used superposition method uses the light source L and two controllable shutters. Three measurements must be made. The first one only with the shutter S_1 opened, the second one only with the shutter S_2 opened and the last one with the both shutters opened. Scheme of the double aperture method is shown in the figure 1 [4].

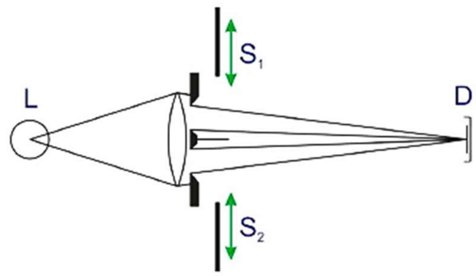

Fig. 1. Double aperture method [4]

An ideal linear detector should have sum of responses for each opened shutter equal to the response when both shutters are opened. When this ratio is significantly larger or smaller than 1 beyond uncertainty of linearity measurement then the correction should be made or the uncertainty of “not performing linearity correction” should be calculated. The uncertainty of linearity correction can be estimated with the formula given by

$$u_{lin} = \sqrt{u_{S1}^2 + u_{S2}^2 + u_{S1+S2}^2} \tag{10}$$

Where u_{S1} is calculated with type A uncertainty evaluation from sequence of measurements when the shutter S1 is opened. Analogically other standard uncertainties are calculated. The systematic errors are neglectable due to the estimation as a ratio of measurements. However, to do so the conditions in the laboratory must be maintained during the measurement and the light source must be stabled and powered with the high quality current source [4].

C. Calibration uncertainty

The calibration of the ILMD is the same as for the ordinary luminance camera. The substitution method is the most common where uniform target is measured with calibrated luminance meters with the traceability to primary standard. The integrating sphere with incandescent lamp can be used as luminance target. However, the spectral power distribution of these systems are slightly different from the standard illuminant A and should be recorder for spectral mismatch corrections [2,3]. In order to limit transfer uncertainty, the evaluated region should be the same as viewing angle of the calibrated luminance meter. In case of circular target, it is advised to set evaluation circle to have half of the target diameter as it is shown in figure 2.

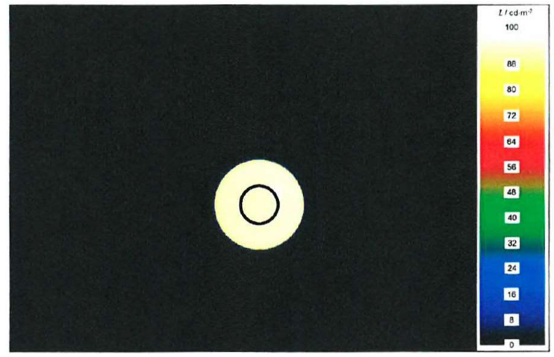

Fig. 2. Evaluation region during the calibration [3]

It is also possible to use the luminance standard that is composed of the integrating sphere and the light source with the current stabilized source [5]. Then the whole unit is often calibrated at national laboratory with expanded uncertainty that is then adopted in the uncertainty of calibration of ILMD based on the DSLR camera. During the calibration the camera should be set to ISO 100 and the smallest aperture number (f/1.4 or f/1.8). Focus distance should be also set at minimum but possible unwanted light reflection on the surface of lens should be checked. The distance of camera should be increased in case of unwanted stray light coming back on the target of luminance standard. This effect only occurs with the lens with small focal length especially for the Fish Eye type lens. The uncertainty of the calibration can be estimated with the formula given by

$$u_{cal} = \sqrt{\begin{matrix} u_{LS}^2 + u_{CAM}^2 + (c_{CS} \cdot u_{CS})^2 + (c_{LS_{AT}} \cdot u_{AT})^2 \\ +(c_{CA\_AT} \cdot u_{AT})^2 + 2 \cdot c_{LS_{AT}} \cdot c_{CA\_AT} \cdot u_{AT}^2 \cdot r_{LS,CAM} \end{matrix}} \tag{11}$$

Where u_{LS} is the standard uncertainty of luminance standard, u_{CAM} is the uncertainty of repeatability of the camera calculated with the type A uncertainty evaluation, u_{CS} is the standard uncertainty of the current source of the luminance standard and c_{CS} is the sensitivity coefficient of the luminous flux of the lamp inside luminance standard to current, u_{AT} is the standard uncertainty of the thermometer and c_{LS_AT} is the sensitivity coefficient of the lamp to ambient temperature, c_{CAM_AT} is the sensitivity coefficient of the camera sensor to ambient temperature, $r_{LS,CAM}$ is the correlation coefficient of ambient temperature uncertainty for the sensitivity of the detector and the luminous flux of the lamp inside the luminance standard. The correlation term may have minus sign and can slightly decrease the uncertainty of calibration. This only occurs when the sensitivity coefficients have different signs. When the uncertainty of thermometer is very small the correlation term can be neglected. Practically uncertainties related to ambient temperature are often neglected because of difficult measurement of the sensitivity coefficients for other quantities. When the reference luminance meter is used instead of the calibrated luminance standard it is necessary to calculate type A uncertainty of sequence of measurements.

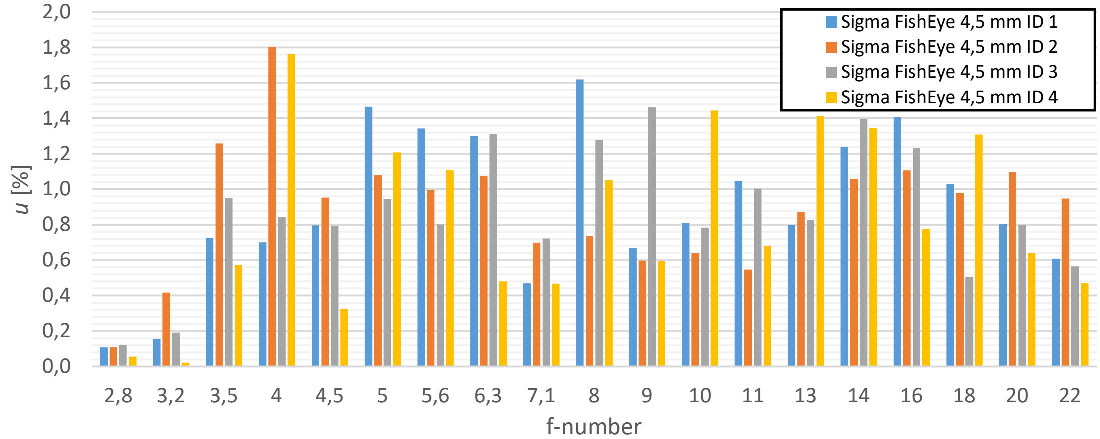

Fig. 3 Aperture uncertainty (repeatability) of the lenses Sigma FishEye 4.5 mm DG

D. Ambient temperature uncertainty

Luminance camera based on the DSLR camera is mainly used in outdoor measurement for its practicality. However, this device is calibrated at ambient temperature 25 °C and in lower temperatures the sensitivity of sensor may be slightly different which then causes error in measurement. Dependency of camera sensitivity can be measured in the climate chamber with transparent window and by measuring the luminance standard while changing ambient temperature. Then the correction coefficients can be estimated. These correction coefficients should be stated in the calibration certificate or error caused by not performing correction should be taken into account in the estimation of expanded uncertainty [1,5].

E. Aperture uncertainty

The aperture uncertainty is related to the mechanical repeatability of the aperture inside the lens which causes variance in repeated measurements. This uncertainty is unique for each lens and aperture f-number. Generally smaller f-number (widely opened aperture) have smaller standard uncertainty. Mechanical variance in aperture area causes higher variance for exposure of the sensor when the area is only few millimeters in diameter. Even the same type of lenses might have slightly different variances due to manufacturing tolerances. Moreover, this uncertainty may change in time because of mechanical wearing of the aperture. The aperture uncertainty can be also named aperture repeatability and it is calculated as type A uncertainty. In the following figure 3 there is the aperture uncertainty of the lens Sigma FishEye 4.5 mm. Totally 4 brand new lenses are tested with repeated twenty measurements of stabilized luminance standard and the results confirms that every lens is unique and should be measured separately. The luminance camera used for this test is based on the Nikon DSLR camera D7500. The lowest values are for the aperture number f/2.8 as presumed. Very precise measurement e.g. linearity of detector should be done with the smallest aperture number. This uncertainty should be also taken into account when calculating correction coefficients e.g. for nonuniformity of the image or focus distance [4]. In this case Method Monte Carlo is more useful tool to estimate impact of this uncertainty on the correction and calibration coefficients and its standard uncertainties.

F. Uniformity uncertainty

The uncertainty of uniformity is related to important correction of the vignetting effect of the optical system. Vignetting causes signal drop-off from the center of image to its corners. It is also often symmetrical around the center of image. Vignetting is mainly caused by the blockage of light inside the lens and by the angular sensitivity of the sensor pixels [6]. There are two appropriate methods of the measurement of vignetting. The first method uses uniformly illuminated surface where luminance distribution is known. Therefore, the vignetting function is calculated simply as a ratio of captured image and the measured luminance distribution in the image with equation given by

$$f_{vnorm}(x,y) = \frac{\frac{s(x,y)}{L_v(x,y)}}{\max\left(\frac{s(x,y)}{L_v(x,y)}\right)} \qquad (12)$$

Where $s(x,y)$ is the camera response in the region of known luminance $L_v(x,y)$. The second method uses luminance standard with known luminance and uncertainty that is traceable to manufacturer of standard or laboratory that calibrates the standard instead. The camera is then moved around its nodal point and the response for certain position within image is recorded [6]. The measured data are then fitted with 3rd order polynomial at least. Both method have its advantages and disadvantages. The uniformly illuminated surface in the first method must be large enough in order to measure vignetting function for all focus distances. Moreover, its time stability and uniformity must be excellent. The second method needs the luminance standard with good uniformity and time stability. There is also slightly higher uncertainty in fitting the measured points by polynomial function. It is also necessary to have very precise positioning system to move the camera. The second method is more suitable for the luminance camera based on DSLR camera because of variable focus distance and necessity of measuring vignetting function for each focus distance and aperture f-number. Thus the measurement of the vignetting is one of the biggest challenges in calibration process of the luminance camera. When vignetting function is measured it is possible to calculate vignetting correction with equation given by

$$k_{vnorm}(x,y,f/x,FD) = \frac{1}{f_{vnorm}(x,y,f/x,FD)} \qquad (13)$$

Where f_{vnorm} is the normalized vignetting function for the aperture number *f/x* and focus distance *FD*. The standard uncertainty of uniformity is then calculated with formula given by

$$u_{uni} = \sqrt{u_{rep}^2 + u_{stab}^2 + u_{fit}^2} \tag{14}$$

Where u_{rep} is the standard uncertainty calculated with type A from sequence of repeated measurement, u_{stab} is the standard uncertainty of time stability of the luminance standard and u_{fit} is the standard uncertainty calculated with B type calculation from the error of the fitting by the polynomial function. The standard uncertainty of luminance standard is not taken into account due to comparative measurement of the method. The most important is the stability of the luminance standard. The standard uncertainty of ambient temperature is neglected due to small fluctuations of ambient temperature during one cycle of measurement.

G. Focus distance uncertainty

The standard uncertainty of focus distance is related to quantized steps of focus distances in DSLR camera where the correction is made for discrete focus distances. However, the real distance of the camera (position of the focusing ring) can be in the middle of two discrete focus distances and it is almost impossible to predict this uncertainty in practical measurement. An experiment can be carried out to estimate the uncertainty by measuring the luminance standard with focus distances that are in the middle of near-by discrete focus distances. From the measured deviations it is possible to estimate standard uncertainty with type B evaluation. This uncertainty can be neglected when measuring with focus to infinity that applies almost for the most cases in outdoor measurement.

H. Other uncertainties

The errors of measurement may be also caused by known phenomena e.g. smear effect, bleeding effect, blur effect, moiré effect or even impurities in the optical system like dust particles. These errors and standard uncertainties estimated from them are difficult to predict because they vary with the position of light sources within the image. Blur effect can also influence only more distant objects depending on the focus distance. However, an experienced photograph should know how to set the camera to limit those effect and therefore to limit the uncertainties.

I. Expanded uncertainty

The expanded uncertainty is calculated with equation 3-5 from the standard uncertainties described above. Since some standard uncertainties are spatially correlated and some are not it is not possible to express expanded uncertainty with one value as for ordinary photometer. Spatially correlated uncertainty is the same for all pixels of the image [3]. To this category belongs the standard uncertainty of linearity, calibration, aperture number and ambient temperature. The standard uncertainty of uniformity and spectral sensitivity is uncorrelated and therefore specific for each pixel. Therefore, the expanded uncertainty can be best presented as a 3D surface as it shown in the figure 3. In this figure the expanded uncertainty is shown for luminance camera based on the Nikon D7500 with lens Sigma 135mm (aperture number *f*/1.8 and measurement of LED with neutral white). In this case the expanded uncertainty is not higher than 10 % in the corners and in the middle of image is around 7 %. However, this 3D surface of expanded uncertainty changes drastically with the aperture number when for smaller aperture numbers (f/1.8) the expanded uncertainty is higher in the corners due to the higher standard uncertainty of uniformity (vignetting). With higher aperture numbers e.g. f/16 (small surface of the aperture) the expanded uncertainty is smaller in the corners, but it is higher in the middle of the image due to the higher standard uncertainty of aperture repeatability.

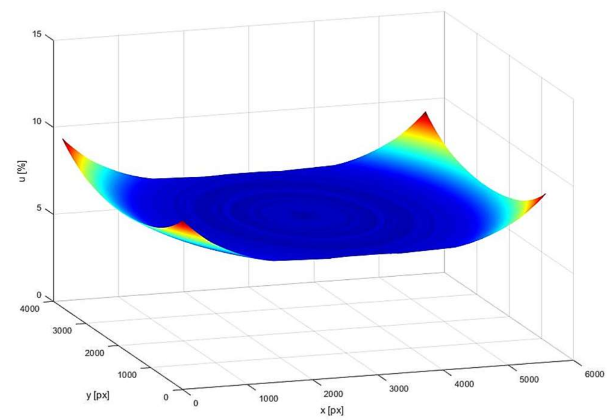

Fig. 3 Expanded uncertainty of luminance measurement of ILMD based on the DSLR camera (Nikon D7500, lens Sigma 135 mm)

IV. Conclusion

The luminance camera based on DSLR camera has many advantages for outdoor measurements for its practicality. However, the calibration process and uncertainty estimation is more challenging. The expanded uncertainty of luminance measurement cannot be presented with one value but with uncertainty map or 3D surface. The smallest uncertainty is generally in the middle of the image and increases towards the corners symmetrically. The 3D shape of expanded uncertainty shape mainly depends on the aperture number and used lens. Many uncertainties are spatially correlated and therefore only add an offset to the surface of expanded uncertainty. It is also possible to make the uncertainty budged for recommended settings of the camera and for the several position in the image.

References

[1] Bureau International des Poids et Mesures, "Evaluation of measurement data — Guide to the expression of uncertainty in measurement", JCGM 100:2008. 2008.

[2] Commission Internationale de l'E´ clairage, "Determination of measurement uncertainties in photometry", CIE 198:2011, Vienna: CIE, 2011

[3] Commission Internationale de l'E´ clairage, "Characterization of Imaging Luminance Measurement Devices (ILMDs) ", CIE 244:2021, Vienna: CIE, 2021, CIE 244 – 2021.

[4] Commission Internationale de l'E´ clairage, "Non-Linearity of Optical Detector Systems", CIE 237:2020, Vienna: CIE, 2020, CIE 244 – 2021.

[5] Y. Zong, "NIST Measurement Services Photometric Calibrations", NIST Special Publication 250-95, 2018, NIST.

[6] A. Kordecki, H. Palus, and A. Bal, "Practical vignetting correction method for digital camera with measurement of surface luminance distribution", Signal, Image and Video Processing, vol 21, July 2016.

Non-visual Effectiveness of Light at Night as a Function of the Light Direction

Kai Broszio
Lighting Technology
Technische Universität Berlin
Berlin, Germany
ORCID 0000-0002-8269-8654
kai.broszio@tu-berlin.de

Martine Knoop
Lighting Technology
Technische Universität Berlin
Berlin, Germany
ORCID 0000-0002-5097-3623
martine.knoop@tu-berlin.de

Stephan Völker
Lighting Technology
Technische Universität Berlin
Berlin, Germany
stephan.voelker@tu-berlin.de

Ljiljana Udovicic
Unit 2.2 "Physical Agents"
Federal Institute for Occupational Safety and Health (BAuA)
Dortmund, Germany
ORCID 0000-0002-6035-8309
udovicic.ljiljana@baua.bund.de

***Abstract*— In industrialized countries with their 24h-societies humans are increasingly exposed to light at night. More and more people are working at night or in evening shifts in times when the circadian system expects darkness to function smoothly. On one hand, light at night is necessary for work and safety reasons, on the other side it can lead to negative health consequences. In this study we investigate the research question, if it is possible to design the spectral and spatial features of a lighting installation for night shift workers to minimize the melatonin suppression and at the same time to support acute alertness. This paper focuses on the applied method because it is an ongoing study and results are planned to become available from late summer 2022 on. The results can be used to derive recommendations for health-promoting lighting during the night shift, for example for control centers, control rooms or similar workplaces.**

Keywords—non-image-forming effects, alertness, melatonin suppression, light direction, night shift, control rooms

I. Introduction

Light at night for night shift work is a topic with conflicting interests. Working in evening- and night-shifts is usually connected to light exposure during circadian night. Light is necessary at the workplace to perform tasks. A higher light intensity increases alertness and, as a result, safety. At the same time, light at night suppresses the release of the hormone melatonin. Light at night for prolonged night-shift work, e.g. working night shift for several years, has been associated with numerous adverse health outcomes, including obesity, cardiovascular problems, and cancer [1–9]. Mechanisms contributing to these consequences are related to the disruption of circadian rhythms, e.g. the sleep-wake cycle and the melatonin secretion. In 2007 the International Agency for Research on Cancer classified night-shift work as potential carcinogenic according to the above-mentioned context [10]. With reducing the melatonin suppression during nighttime work, one could make use of its oncostatic capabilities and possibly reduce adverse health effects [11].

This paper describes a study on lighting for night work. With subjects, it is investigated how the lighting conditions can be optimized. The aim is to achieve a high level of alertness and sufficient visual stimulation to perform the visual task. At the same time, melatonin suppression should be minimized. If successful, recommendations for health-promoting lighting during the night shift could be derived, for example for control rooms in industry and health care or similar workplaces.

II. State of Research

Over the last decades of research on non-image-forming (NIF) effects of light it has been shown that five main parameters are to consider: the irradiance at the eye, the spectral composition (spectral power distribution, SPD), the duration of exposure, the (circadian) time, and (daily) temporal pattern [12, 13]. The international standard CIE S026, based on the work of Lucas et al. (2014), introduced an SI-compliant system of metrology. Further, it combines the illuminance and the spectral composition with the photoreceptors' sensitivities as α-opic values which equal to photopic illuminance for natural daylight (α-opic equivalent daylight illuminance, α-opic EDI) [14, 15].

Recently, Brown [16] performed a comprehensive study evaluating the spectral sensitivity and illuminance levels of several laboratory studies. The resulting publication showed that melanopic equivalent daylight illuminance (MEDI) has the best fitting correlation of any α-opic EDIs and photopic illuminance for the nighttime light effect on melatonin suppression and for subjective sleepiness (Karolinska Sleepiness Scale, KSS). This means that the MEDI can be increased either at a constant spectral power distribution with higher illuminance levels or at a constant illuminance level with a higher short wavelength (blue-cyan) content in the spectrum. Higher MEDIs result in both higher melatonin suppression and a reduction of subjective sleepiness. Other research supports the (moderate) evidence that nightly light exposure increases cognitive performance and alertness while reducing sleepiness [17, 18].

Whereas the intensity and spectral composition of the light has been subject of a large number of studies focusing on cognitive performance and alertness (reviews in e.g. [19–21]), the direction of light entering the eye has been less studied. The influence of the spatial light distribution on NIF effects was investigated by only a few studies over the last 30 years. While the study design, stimuli sources, SPD, illuminances, method of shading the retina partially, duration, etc. varied they all examined the effect on melatonin suppression (reviews in [22, 23]). These studies examining the influence of field of view (FOV) related effects like mono- vs. binocular observation, the size of the light source and nasal vs. temporal retinal exposure on melatonin secretion, found higher facilitation of melatonin suppression for binocular and nasal illumination while results for size depended effects remained inconclusive [24–29]. Five studies compared differences between superior and inferior retinal parts [29–32]. Among these, two studies found a higher sensitivity of the inferior retina for melatonin suppression [30, 31]. Additionally, the work by Piazena et al. (2014) confirmed these findings [32, 33]. For subjective sleepiness in nighttime, Rüger et al. (2005) did not find an inferior-superior difference, whereas Broszio (not published yet) did find a positive effect and reduced subjective sleepiness, when light was coming from the upper field of view [28]. Thus, it might be possible to influence the extent of melatonin suppression at a constant vertical illuminance without tuning spectra just via setting the direction of light entering the eye, e.g. by arranging the luminaires. Liedtke et al. (2013) discussed the light incidence and Broszio et al. (2018) variety of different lighting settings for constant illuminance. [22, 34, 35].

For alertness-promoting effects of light there is an increasing number of studies showing positive impact of blue-depleted light with low melanopic daylight efficacy ratio, (MDER), usually meaning low correlated color temperature, without nocturnal melatonin suppression. Suggesting a second pathway which might circumvent the Retinohypothalamic Tract (RHT) and the Suprachiasmatic Nucleus (SCN) of the well investigated common path for immediate nocturnal melatonin suppression causing higher alertness levels [36–42]. Hence, there might be the possibility to decouple alertness and melatonin effects via tuning the spectral composition of light.

III. Research question and hypotheses

In the previous section, it was shown that:

1. melatonin suppression generally increases with increasing illuminance (increasing MEDI),
2. there is preliminary evidence that illumination of the lower half of the retina causes greater melatonin suppression than does similar illumination of the upper half of the retina,
3. nocturnal acute attention usually correlates with greater melatonin suppression,
4. sustained nocturnal melatonin suppression is a health risk,
5. light with higher red content and low MEDI can increase acute alertness without having effects on melatonin concentration.

The research question is therefore:
Can a lighting solution be designed using the spectral properties and spatial arrangement of luminaires to maintain melatonin production while supporting acute alertness in night shift workers?

This leads to the following hypotheses:

1. For nighttime NIF effects in general it is hypothesized that:
   a. lighting situations with higher MEDI result in higher melatonin suppression and higher acute alertness than lighting situations with lower MEDI.
   b. lighting situations with a low MDER result in less melatonin suppression and similar acute alertness as lighting situations with a higher MEDI.
2. For nighttime effects and lighting situations with the same MEDI and the same illuminance of which 50 % comes either from upper and lower FOV it is hypothesized that:
   a. lighting situations in which 80 % of the MEDI is coming from the upper half of the FOV result in higher melatonin suppression and higher acute alertness than lighting situations in which 80 % of the MEDI is coming from the lower half of the FOV.

The aim of the study with subjects is to investigate how the light sources can be optimally arranged considering their spectral power distributions.

IV. Materials and method

A. Experimental conditions and apparatus

The 3-week study was conducted on weekdays (except Monday, to exclude influence of the weekends light history) in a test room at the Technische Universität Berlin (TU Berlin). Trial nights took place between October 12th 2021 and July 28th 2022 on Tuesdays, Wednesdays, Thursdays and Fridays between 22:00 and approx. 03:20 Central European Time (CET), respectively Central European Summer Time (CEST). The study used a within-subjects experimental design to minimize the effects of individual differences among study participants. Each participant had own trial days and was accompanied by one person of the study personnel who stayed outside the test room.

The test room is an office like room (approx. 5 m x 4 m x 2.8 m) without daylight openings, and with a heating, ventilation and air conditioning (HVAC) system to maintain air quality. The test room is equipped with gray carpet and diffusing material as walls and ceiling. For this study we used in total 12 three-channel-luminaires (60 cm x 60 cm) in the middle part of the ceiling (7) and wall (5). These were especially designed to optimize NIF effects, offering a CCT range between 1,900 K and 20,000 K, using warm white (1,900 K), neutral white (4,000 K) and blue LEDs (peak wavelength 475 nm).

The participants sat at a desk with light gray/white surface in the middle of the room facing one of the long sides, usually dressed according to the respective season. The utensils needed to conduct the study were located on the table. These were a desktop computer (Intel NUC BXNUC10I5FNHN2, Intel Corporation) running Ubuntu, a white washable keyboard, a mouse (InduProof, GETT Gerätetechnik GmbH) and a centrally placed 19-inch LCD monitor with a matte screen (ThinkVision L1900pA, Lenovo Ltd.). To minimize the contribution of short-wave light, the operating system's night mode for the monitor was activated. To the right of the monitor there was the audio test device (AuReTim v2, TU Berlin), to which the headphones and the pushbutton was connected [43]. In addition, the air quality measuring device (BZ30, Trotec GmbH & Co KG, measuring minutely ambient air CO_2 concentration, temperature and humidity) and two laminated DIN A4 pages with instructions for the subjects were on the table to the left of the monitor. Figure 1 shows a schematic top view drawing with the positions of the

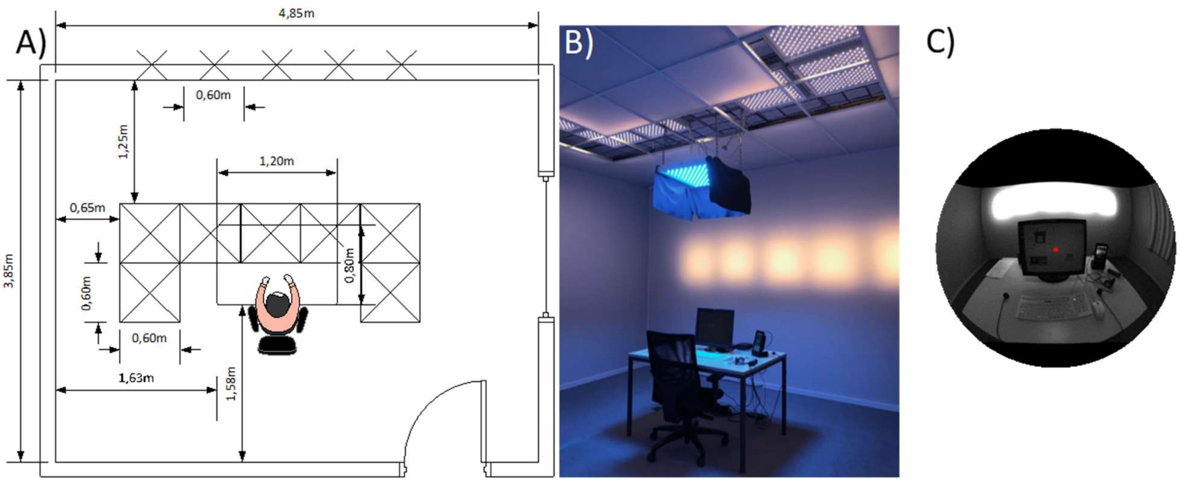

Figure 1 A) Schematic drawing of the setup in the light simulator room; crosses indicate the position of the used luminaires in the ceiling and wall (by Fabian Hirschmiller); B) color photograph showing the setup in the light simulator room and C) gray scale photograph showing the setup in the light simulator room and C) gray scale photograph of the view from the participant's eye position

luminaires indicated, a photograph of the setup in the test room and a fisheye picture from the participants viewpoint.

The three lighting conditions differ in terms of illuminance and MEDI at the subject's eye. Two of the three lighting conditions (LS2 and LS3) elicit the same vertical illuminance (E_v = 140 lx) and MEDI ($E_{v,mel}^{D65}$ = 200 lx) at the eye. However, the proportion of visual and NIF stimulation of the upper and lower retina is different (see Table I).

The spectral irradiance was measured by means of a spectroradiometer (model specbos scb1211UV, JETI, Jena; S/N 2011303, calibration date July 19th 2017) at the eye position in the direction of gaze (height 1.2 m; gaze tilted approx. 25° below the horizontal direction). The spatial distribution of illuminance and melanopic irradiance was measured at the eye position in the direction of gaze using an imaging luminance measurement device (ILMD), model LMK5color, TechnoTeam, Ilmenau; S/N TTF8829, calibration date 11/2017. This luminance camera (imaging luminance measurement device; ILMD) is equipped with different filters, e.g. V(λ), V'(λ) and s_{mel}. We used an improved but in principle previously described method to measure and describe the lighting conditions [22, 44, 45]. The current method incorporates the not-normative recommendations on considering the human field of view in measurements of quasi fixed gaze conditions from the CIE S026/E:2018 [46]. The spectral power distribution (spectral irradiance) at the observers' eye is shown in Figure 2. Table 1 gives an overview of the most important measured values; α-opic values were calculated the CIE S 026 alpha-opic Toolbox [47]. Figure 3 shows the fish-eye pictures of lighting conditions; for LS2 and LS3 separate for V(λ)- and melanopic-measurements.

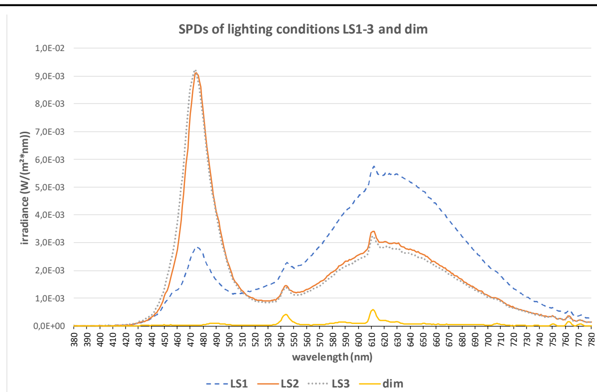

Figure 2 Spectral power distribution of the three investigated lighting conditions (including irradiance from displays)

TABLE I. LIGHTING CHARACTERISTICS

		lighting conditions			
		dim	*LS1*	*LS2*	*LS3*
E_v ^a.^[lx]		**7.4**	**214**	**140**	**140**
	upper retina [%]	45	18	50	50
	lower retina [%]	55	82	50	50
$E_{v,mel}^{D65}$ ^a.^[lx]		**3**	**100**	**200**	**200**
	upper retina [%]	45	50	19	79
	lower retina [%]	55	50	81	21
MDER ^a.^		**0.42**	**0.43**	**1.43**	**1.43**
	upper retina	0.42	1.30	0.54	2.26
	lower retina	0.42	0.28	2.31	0.60
CCT ^a.^ [K]		**2750**	**2300**	**5100**	**6400**
α-opic EDI ^a.^ [lx]	S-cone-opic	1.7	62	168	148
	melanopic	2.9	100	205	198
	rhodopic	0.8	109	175	172
	M-cone-opic	1.1	156	136	140
	L-cone-opic	1.7	218	143	150
E_v ^b.^ [lx]		**7.6**	**180**	**345**	**360**

[a.] measured values at the eye position perpendicular to the direction of gaze

[b.] measured horizontally on the desk

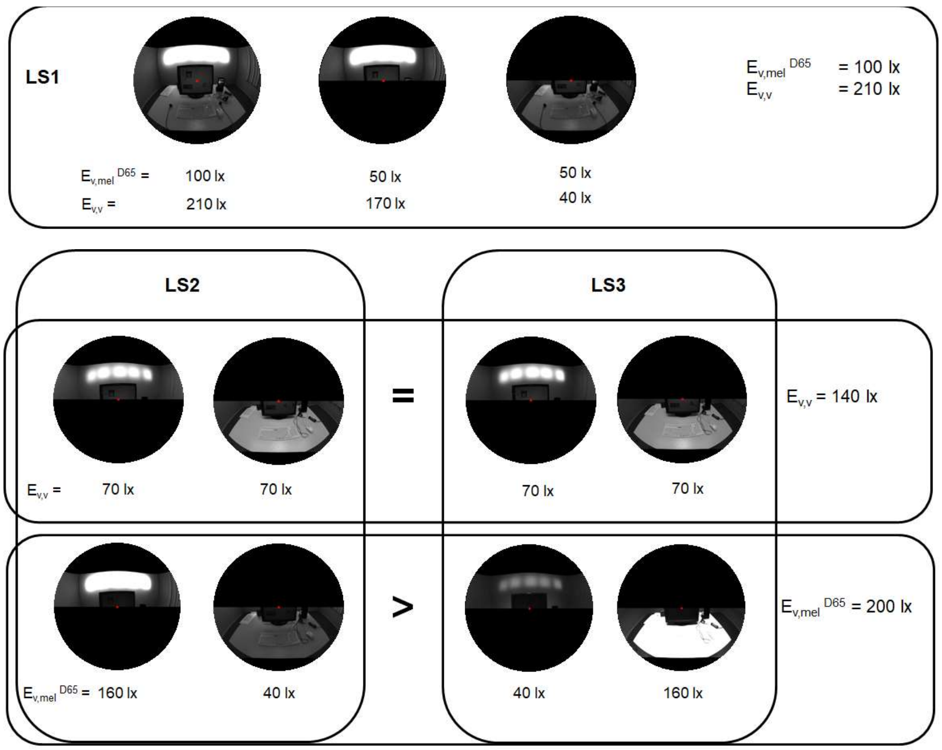

Figure 3 fish-eye pictures of lighting conditions LS1) taken with an imaging luminance measurement devices (ILMD) here V(l)- and melanopic-measurements (indicated by $E_{v,v}$ and $E_{v,mel}$) are shown, in picture only V(l)-measurement is shown LS2) and LS3) taken with a ILMD either with a V(l)- (upper part; indicated by $E_{v,v}$) and a smel-filter (lower part; indicated by $E_{v,mel}^{D65}$). Gray scale representation: lower values represented by darker gray value. Restricted field of view fish-eye pictures of lighting conditions according to CIE S026 recommendation and additionally split into superior and inferior parts; "Equal" and "greater than" sign refers to the above outlined hypotheses on NIF effects: "equal" would hold for just considering photopic illuminance as "greater than" considers the portions of the MEDI from upper and lower field of view.

B. Selection of participants

Prospective participants were recruited via the institution's study subject portal. Only individuals who were between 18 and 35 years old, had not worked as night and/or shift workers or traveled across time zones in the last 3 months, had a native level of German, are not color vision deficient, nor have eye diseases or artificial lenses and were either normally sighted or corrected to normal vision were eligible. In addition, validated questionnaires were used to screen for covariates that had to be within certain limits: general health (SF-12 within normal range), depressiveness (PHQ-9 $\leq$ 10), sleep quality (PSQI $\leq$ 5), and chronotype (D-MEQ/MCTQ no extreme types) [48–56]. These potential participants were again screened by a preventive checkup (preventive occupational medical care G37) including tests for visual acuity (far and near), stereopsis, heterophoria, color vision (Ishihara color blindness tests) and the central visual field [57, 58]. The selected participants were instructed to maintain their regular sleep-wake rhythm during the weeks of participation and to wear a calibrated light dosimeter (Philipps Respironics Actiwatch Spectrum) at the chest to record the light history 24 h before each study night [59]. In addition, they were asked not to consume caffeinated beverages after 15:00 on trial days. The participants were asked to wear the same spectacles or contact lenses at all trial dates if they usually use any.

The study complies with the standards of the World Medical Association's Declaration of Helsinki and international ethical standards [60]. It was reviewed and approved by the ethics committee of the Charité - Universitätsmedizin Berlin. Informed consent was obtained from all study participants. The design aims for the collection of complete study data from a total of 36 study participants.

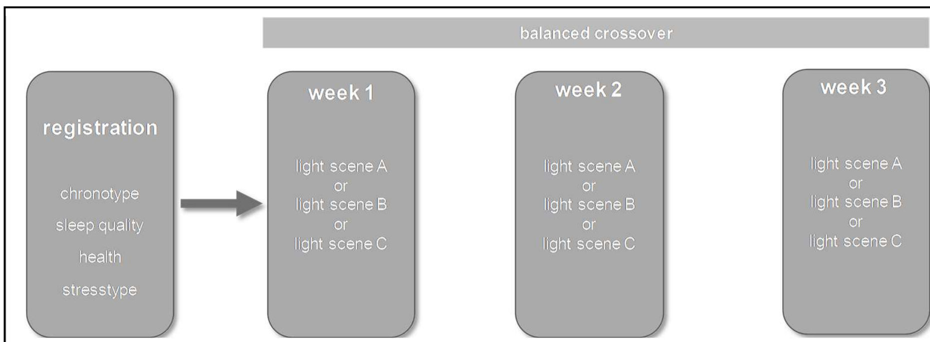

Figure 4 Study protocol - sequence of important steps and trial dates for each participant

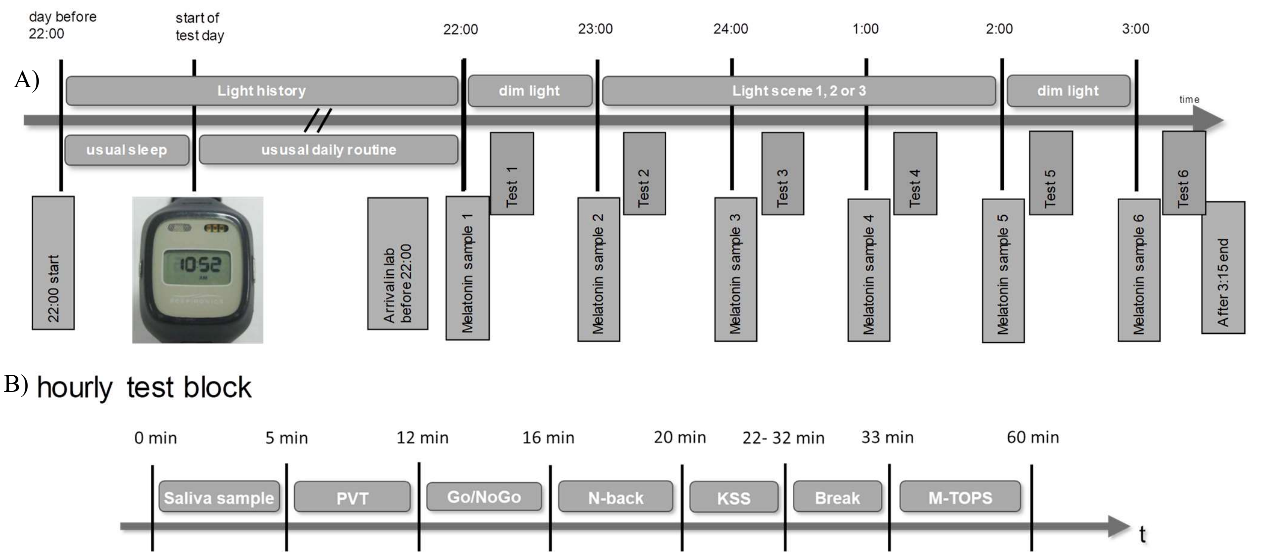

Figure 5 Study protocol - A) procedure of a trial date; B) procedure of the hourly test block consisting of saliva sample, PVT, Go/NoGo, N-Back test, KSS and M-TOPS

C. *Study protocol*

Participants arrived until 22:00 at the lab. From 22:00 they were exposed to dim light (illuminance 7 lx; MEDI 3 lx) for 60 min until at 23:00 the 180 min exposure of one of the three experimental conditions was switched on, followed by approx. 80 min dim light again until the end of the trial session. Usually at 03:20 the participants were released from the laboratory (see Figure 5 A).

The sequence of light conditions for the participant was counterbalanced using a balanced latin square design to minimize the carry over effects on the evaluation [61]. At intervals of at least one week, the five-hour nocturnal sessions took place for each subject on the same working day. On each experimental date, participants were exposed to a different experimental condition, as shown in .

To ensure that the viewing direction is kept constant and the appropriate regions of the retina are illuminated the participants had to process a modified PC-based control room simulation. This Multi-Task Operator Performance Simulation (M-TOPS) demands in this modified version two tasks to be executed in parallel for 27 min each hour [62]. Additionally, the hourly questionnaires were completed on the computer as well, giving additional 2 min – 12 min of defined exposure conditions each hour.

Between 22:00 and 03:00 hourly test blocks consisting saliva sample taking, cognitive tests and questionnaires were conducted (see Figure 5A)). These test blocks took about 22 min – 32 min, leaving a 1 min – 11 min hourly window for a break directly after answering the questionnaire. The time of the break differs between the first and all other hours because within the first questionnaire some additional questions were asked, e.g. on the daily routine, the Harvard Light Exposure Questionnaire (H-LEA) and the Pittsburgh Sleep Quality Index (PSQI) [52, 63]. While in the break, the participant was allowed to drink and if necessary go to the toilet. The rest of the time only small movements on the chair were allowed to not negatively influence saliva sampling quality [64].

The saliva samples (1 ml) were collected by using the Salivette® Cortisol system (Sarstedt, Nümbrecht, DE). Participants directly spitted into the Polypropylene (PP) tubes which was then immediately frozen (-60 °C). Saliva samples at 23:00 and 02:00 were collected in duplicate to allow for separate analysis. This duplicate sample for preliminary analysis was always taken as a second saliva sample so as not to interfere with the overall procedure and analysis. This second saliva samples were analyzed by Enzyme-Linked Immunosorbent Assays (ELISA) using the Melatonin ELISA Kit (Enz-Kit150-0001; Enzo Life Sciences, Inc., USA). The overall analysis is done by liquid–liquid extraction (LLE) followed by liquid chromatography coupled to electrospray tandem mass spectrometry (LC–ESI–MS/MS). It features the lowest available limit of detection (LOD) with 4.11 pmol/l for melatonin and the lowest inter- and intra-assay-variability and hence is best for detecting also small changes in the suppression of melatonin [65].

The cognitive tests (see Figure 5 B)) consisted of the psychomotor vigilance task (PVT), the Go/NoGo task, and the n-back test followed by a questionnaire. The PVT is a simple reaction time test with randomized inter-stimulus intervals to test for sustained attention [66], the Go/NoGo is a test of inhibitory reaction time [67], and the n-back test checks working memory performance [68]. These cognitive tests were performed in the auditory version to rule out effects of light conditions on visual performance. In addition, participants rated their subjectively perceived sleepiness on the Karolinska Sleepiness Scale (KSS) [69], their mood and well-being on the Multidimensional Mood State Questionnaire (MDMQ) [70] and the perceived task load on the NASA-TLX [71].

V. Results and Conclusion

Results are not yet available since at the moment of writing the data collection has just been finished and data preparation and evaluation is ongoing.

The outcome of this study will provide information if the inferior FOV can be illuminated with light with higher MDER than the superior FOV, to meet the initially set criteria to contribute to the maintenance of health during night shift work. This could influence lighting design and lead to guidelines for night shift workplaces, especially for workplaces where main viewing directions are known and constant for prolonged periods.

Acknowledgment

K.B. would like to thank the Federal Institute for Occupational Safety and Health (BAuA) for initiating and financing this project (F 2496). Further, he thanks the team of the BAuA Unit 2.2 "Physical Agents" for provision and support of the Actiwatch spectrum devices and especially Hannah Rolf and Andreas Wojtysiak for scientific discussions. K.B. would like to acknowledge the work done by the bachelor and master thesis writing students Fabian Hirschmiller, Jenny Lichtenstein, Maximilian Lutz, Yannic Nießen, Noah Pütz and Ruochen Tang, as well as the contribution by student workers Moritz Dölle, Noah Pütz, Max Hellberg and Felix Patge.

References

[1] R. M. Lunn *et al.,* "Health consequences of electric lighting practices in the modern world: A report on the National Toxicology Program's workshop on shift work at night, artificial light at night, and circadian disruption," *The Science of the total environment*, 607-608, pp. 1073–1084, 2017, doi: 10.1016/j.scitotenv.2017.07.056.

[2] E. S. Schernhammer, C. H. Kroenke, F. Laden, and S. E. Hankinson, "Night work and risk of breast cancer," *Epidemiology*, vol. 17, no. 1, pp. 108–111, 2006, doi: 10.1097/01.ede.0000190539.03500.c1.

[3] C. Ramin, E. E. Devore, W. Wang, J. Pierre-Paul, L. R. Wegrzyn, and E. S. Schernhammer, "Night shift work at specific age ranges and chronic disease risk factors," *Occupational and Environmental Medicine*, vol. 72, no. 2, pp. 100–107, 2015, doi: 10.1136/oemed-2014-102292.

[4] E. S. Schernhammer *et al.,* "Rotating night shifts and risk of breast cancer in women participating in the nurses' health study," *Journal of the National Cancer Institute*, vol. 93, no. 20, pp. 1563–1568, 2001, doi: 10.1093/jnci/93.20.1563.

[5] P. Razavi *et al.,* "Shift Work, Chronotype, and Melatonin Rhythm in Nurses," *Cancer Epidemiology Biomarkers & Prevention*, vol. 28, no. 7, pp. 1177–1186, 2019, doi: 10.1158/1055-9965.EPI-18-1018.

[6] S. Davis, D. K. Mirick, and R. G. Stevens, "Night shift work, light at night, and risk of breast cancer," *Journal of the National Cancer Institute*, vol. 93, no. 20, pp. 1557–1562, 2001, doi: 10.1093/jnci/93.20.1557.

[7] J. Hansen, "Light at night, shiftwork, and breast cancer risk," *Journal of the National Cancer Institute*, vol. 93, no. 20, pp. 1513–1515, 2001, doi: 10.1093/jnci/93.20.1513.

[8] J. Hansen, "Increased breast cancer risk among women who work predominantly at night," *Epidemiology*, vol. 12, no. 1, pp. 74–77, 2001, doi: 10.1097/00001648-200101000-00013.

[9] D. E. Blask, "Melatonin, sleep disturbance and cancer risk," *Sleep medicine reviews*, vol. 13, no. 4, pp. 257–264, 2009, doi: 10.1016/j.smrv.2008.07.007.

[10] *Painting, Firefighting, and Shiftwork*. [Place of publication not identified]: [publisher not identified], 2010.

[11] E. L. Haus and M. H. Smolensky, "Shift work and cancer risk: potential mechanistic roles of circadian disruption, light at night, and sleep deprivation," *Sleep medicine reviews*, vol. 17, no. 4, pp. 273–284, 2013, doi: 10.1016/j.smrv.2012.08.003.

[12] *Ocular lighting effects on human physiology and behaviour: Technical report*, 158:2009 (incl. Erratum 1), Internationale Beleuchtungskommission, Vienna, 2009.

[13] *Light and lighting — Integrative lighting — Non-visual effects*, TR 21783, Aug. 2022.

[14] R. J. Lucas *et al.,* "Measuring and using light in the melanopsin age," *Trends in neurosciences*, vol. 37, no. 1, pp. 1–9, 2014, doi: 10.1016/j.tins.2013.10.004.

[15] *CIE system for metrology of optical radiation for ipRGC-influenced responses to light*, S 026/E:2018.

[16] T. M. Brown, "Melanopic illuminance defines the magnitude of human circadian light responses under a wide range of conditions," *Journal of Pineal Research*, e12655, 2020, doi: 10.1111/jpi.12655.

[17] C. Cajochen, "Alerting effects of light," *Sleep medicine reviews*, vol. 11, no. 6, pp. 453–464, 2007, doi: 10.1016/j.smrv.2007.07.009.

[18] P. M. Pattison, J. Y. Tsao, G. C. Brainard, and B. Bugbee, "LEDs for photons, physiology and food," *Nature*, vol. 563, no. 7732, pp. 493–500, 2018, doi: 10.1038/s41586-018-0706-x.

[19] M. A. Siraji, V. Kalavally, A. Schaefer, and S. Haque, "Effects of Daytime Electric Light Exposure on Human Alertness and Higher Cognitive Functions: A Systematic Review," *Front. Psychol.*, vol. 12, p. 765750, 2021, doi: 10.3389/fpsyg.2021.765750.

[20] J. L. Souman, A. M. Tinga, S. F. Te Pas, R. van Ee, and B. N. S. Vlaskamp, "Acute alerting effects of light: A systematic literature review," *Behavioural brain research*, vol. 337, pp. 228–239, 2018, doi: 10.1016/j.bbr.2017.09.016.

[21] R. Lok, K. C. H. J. Smolders, D. G. M. Beersma, and Y. A. W. de Kort, "Light, Alertness, and Alerting Effects of White Light: A Literature Overview," *Journal of Biological Rhythms*, vol. 33, no. 6, pp. 589–601, 2018, doi: 10.1177/0748730418796443.

[22] K. Broszio, M. Knoop, M. Niedling, and S. Völker, "Effective Radiant Flux for Non-image Forming Effects – is the Illuminance and the Melanopic Irradiance at the Eye Really the Right Measure?," *Light & Engineering/Svetotekhnika*, vol. 26, no. 2, pp. 68–74, 2018.

[23] P. Teikari, "Spectral Modulation of Melanopsin Responses: Role of Melanopsin Bistability in Pupillary Light Reflex," PhD Thesis, Universite Claude Bernard - Lyon 1, Lyon, France, 2012.

[24] P. Novotny, P. Paulick, M. J. Schwarz, and H. Plischke, "The Solid Angle of Light Sources and Its Impact on the Suppression of Melatonin in Humans," in *Lecture Notes in Computer Science*, vol. 8008, *Human-computer interaction: Towards intelligent and implicit interaction ; 15th international conference, HCI International 2013, Las Vegas, NV, USA, July 21 - 26, 2013 ; proceedings, part V*, M. Kurosu, Ed., Berlin: Springer, 2013, pp. 454–463. Accessed: Jul. 3 2017.

[25] E. K. Visser, D. G. Beersma, and S. Daan, "Melatonin suppression by light in humans is maximal when the nasal part of the retina is illuminated," *J Biol Rhythms*, vol. 14, no. 2, pp. 116–121, 1999, doi: 10.1177/074873099129000498.

[26] G. C. Brainard, M. D. Rollag, and J. P. Hanifin, "Photic regulation of melatonin in humans: Ocular and neural signal transduction," *Journal of Biological Rhythms*, vol. 12, no. 6, pp. 537–546, 1997, doi: 10.1177/074873049701200608.

[27] M. Spitschan and C. Cajochen, "Binocular facilitation in light-mediated melatonin suppression?," *Journal of Pineal Research*, vol. 67, no. 4, e12602, 2019, doi: 10.1111/jpi.12602.

[28] M. Rüger, M. C. M. Gordijn, D. G. M. Beersma, B. de Vries, and S. Daan, "Nasal versus temporal illumination of the human retina: effects on core body temperature, melatonin, and circadian phase," *J Biol Rhythms*, vol. 20, no. 1, pp. 60–70, 2005, doi: 10.1177/0748730404270539.

[29] M. S. Rea, R. M. Nagare, and M. G. Figueiro, "Relative light sensitivities of four retinal hemi-fields for suppressing the synthesis of melatonin at night," *Neurobiology of Sleep and Circadian Rhythms*, p. 100066, 2021, doi: 10.1016/j.nbscr.2021.100066.

[30] T. A. Lasko, D. F. Kripke, and J. A. Elliot, "Melatonin suppression by illumination of upper and lower visual fields," *J Biol Rhythms*, vol. 14, no. 2, pp. 122–125, 1999, doi: 10.1177/074873099129000506.

[31] G. Glickman, J. P. Hanifin, M. D. Rollag, J. Wang, H. Cooper, and G. C. Brainard, "Inferior retinal light exposure is more effective than superior retinal exposure in suppressing melatonin in humans," *J Biol Rhythms*, vol. 18, no. 1, pp. 71–79, 2003, doi: 10.1177/0748730402239678.

[32] H. Piazena, L. Franke, B. Thomsen, I. Kamenzky, R. Uebelhack, and S. Völker, "Melatoninsuppression mit Weißlicht-LEDs – erste Ergebnisse," in *Proceedings des 8 Symposiums Licht*, pp. 39–52.

[33] R. Uebelhack, L. Franke, H. Piazena, and I. Fietze, "NIVIL, Teilvorhaben: "Einfluß von Lichtspektrum, Bestrahlungsstärke und Alter auf die Melatoninsuppression" : Schlußbericht zum BMBF-geförderten Forschungsprojekt : Laufzeit des Vorhabens: 01.12.2014 bis 31.07.2018,"

[34] C. Liedtke, S. Völker, and M. Knoop, "The Light Direction and Directional Light — Towards a new Quantification of an Essential Lighting Quality Criterion," in *Proceedings of CIE Centenary Conference "Towards a New Century of Light": April 15/16, 2013, Paris, France : (including addendum 1)*, Paris, 2013, 542-551.

[35] C. Liedtke, "Quantifizierung der räumlichen Lichtverteilung," Technische Universität Berlin, Berlin, 2019.

[36] M. G. Figueiro, A. Bierman, B. Plitnick, and M. S. Rea, “Preliminary evidence that both blue and red light can induce alertness at night,” *BMC Neuroscience*, vol. 10, no. 1, p. 105, 2009, doi: 10.1186/1471-2202-10-105.

[37] J. Lin and S. Westland, “Effect of long-wavelength light on electroencephalogram and subjective alertness,” *LR&T*, vol. 52, no. 6, pp. 763–774, 2020, doi: 10.1177/1477153520902255.

[38] M. Canazei, W. Pohl, H. R. Bliem, and E. M. Weiss, “Acute effects of different light spectra on simulated night-shift work without circadian alignment,” *Chronobiology International*, vol. 34, no. 3, pp. 303–317, 2017, doi: 10.1080/07420528.2016.1222414.

[39] L. Sahin and M. G. Figueiro, “Alerting effects of short-wavelength (blue) and long-wavelength (red) lights in the afternoon,” *Physiology & behavior*, 116-117, pp. 1–7, 2013, doi: 10.1016/j.physbeh.2013.03.014.

[40] M. G. Figueiro, L. Sahin, B. Wood, and B. Plitnick, “Light at Night and Measures of Alertness and Performance: Implications for Shift Workers,” *Biological Research For Nursing*, vol. 18, no. 1, pp. 90–100, 2016, doi: 10.1177/1099800415572873.

[41] M. G. Figueiro and D. Pedler, “Red light: A novel, non-pharmacological intervention to promote alertness in shift workers,” *Journal of safety research*, vol. 74, pp. 169–177, 2020, doi: 10.1016/j.jsr.2020.06.003.

[42] M. G. Figueiro and M. S. Rea, “The effects of red and blue lights on circadian variations in cortisol, alpha amylase, and melatonin,” *International Journal of Endocrinology*, vol. 2010, p. 829351, 2010, doi: 10.1155/2010/829351.

[43] Yannic Nießen, “Extension of an Inexpensive Open-Source Platform for Cognitive Tests with Visual and Auditory N-Back Test to Measure Alertness,” bachelor thesis, Lighting Technology, Technische Universität Berlin, Berlin, 2021.

[44] M. Knoop *et al.,* “Methods to Describe and Measure Lighting Conditions in Experiments on Non-Image-Forming Aspects,” *LEUKOS*, vol. 15, 2-3, pp. 163–179, 2019, doi: 10.1080/15502724.2018.1518716.

[45] M. Moeck and S. Anaokar, “Illuminance Analysis from High Dynamic Range Images,” *LEUKOS*, vol. 2, no. 3, pp. 211–228, 2006, doi: 10.1582/LEUKOS.2006.02.03.005.

[46] “CIE SYSTEM FOR METROLOGY OF OPTICAL RADIATION FOR IPRGC-INFLUENCED RESPONSES TO LIGHT,” 2018.

[47] L. Price, *CIE S 026 alpha-opic Toolbox*: International Commission on Illumination.

[48] J. Ware, M. Kosinski, and S. D. Keller, “A 12-Item Short-Form Health Survey: construction of scales and preliminary tests of reliability and validity,” *Medical Care*, vol. 34, no. 3, pp. 220–233, 1996, doi: 10.1097/00005650-199603000-00003.

[49] K. Gräfe, S. Zipfel, W. Herzog, and B. Löwe, “Screening psychischer Störungen mit dem “Gesundheitsfragebogen für Patienten (PHQ-D)“,” *Diagnostica*, vol. 50, no. 4, pp. 171–181, 2004, doi: 10.1026/0012-1924.50.4.171.

[50] R. L. Spitzer, K. Kroenke, and J. B. Williams, “Validation and utility of a self-report version of PRIME-MD: the PHQ primary care study. Primary Care Evaluation of Mental Disorders. Patient Health Questionnaire,” *JAMA*, vol. 282, no. 18, pp. 1737–1744, 1999, doi: 10.1001/jama.282.18.1737.

[51] K. Kroenke, R. L. Spitzer, and J. B. Williams, “The PHQ-9: validity of a brief depression severity measure,” *Journal of General Internal Medicine*, vol. 16, no. 9, pp. 606–613, 2001, doi: 10.1046/j.1525-1497.2001.016009606.x.

[52] D. J. Buysse, C. F. Reynolds, T. H. Monk, S. R. Berman, and D. J. Kupfer, “The Pittsburgh sleep quality index: A new instrument for psychiatric practice and research,” *Psychiatry Research*, vol. 28, no. 2, pp. 193–213, 1989, doi: 10.1016/0165-1781(89)90047-4.

[53] Horne JA and Östberg O., *A self-assessment questionnaire to determine morningness-eveningness in human circadian rhythms. Int J Chronobiol 4: 97–110, 1976.*

[54] B. Griefahn, C. Kunemund, P. Brode, and P. Mehnert, “Zur Validitat der deutschen Ubersetzung des Morningness-Eveningness-Questionnaires von Horne und Ostberg. The Validity of a German Version of the Morningness-Eveningness-Questionnaire Developed by Horne and Ostberg,” *Somnologie*, vol. 5, no. 2, pp. 71–80, 2001, doi: 10.1046/j.1439-054X.2001.01149.x.

[55] T. Roenneberg, A. Wirz-Justice, and M. Merrow, “Life between clocks: daily temporal patterns of human chronotypes,” *Journal of Biological Rhythms*, vol. 18, no. 1, pp. 80–90, 2003, doi: 10.1177/0748730402239679.

[56] A. L. Stewart, J. E. Ware, A. Stewart, and J. Ware, Eds., *Measuring functioning and well-being // Measuring Functioning and Well-Being: The Medical Outcomes Study Approach: The medical outcomes study approach,* 2nd ed. Durham: Duke University Press, 1993 // 1992.

[57] J. Schönenborn, Ed., *Guidelines for occupational medical examinations,* 2nd ed. Stuttgart: Gentner, 2014.

[58] Verwaltungs-Berufsgenossenschaft, *DGUV Grundsatz für arbeitsmedizinische Untersuchungen „Bildschirmarbeitsplätze“ G 37 (mit Kommentar): Bildschirmarbeit,* 5th ed. Hamburg: VBG, 2015. [Online]. Available: http://www.vbg.de/SharedDocs/Medien-Center/DE/Broschuere/Themen/Bildschirm_und_Bueroarbeit/DGUV_Grundsatz_Bildschirmarbeitsplaetze_DGUV_Information_250_007.pdf?__blob=publicationFile&v=10

[59] L. L. Price, M. Khazova, and J. B. O'Hagan, “Performance assessment of commercial circadian personal exposure devices,” *Lighting Research & Technology*, vol. 44, no. 1, pp. 17–26, 2012, doi: 10.1177/1477153511433171.

[60] F. Portaluppi, M. H. Smolensky, and Y. Touitou, “Ethics and methods for biological rhythm research on animals and human beings,” *Chronobiology International*, vol. 27, 9-10, pp. 1911–1929, 2010, doi: 10.3109/07420528.2010.516381.

[61] J. V. Bradley, “Complete Counterbalancing of Immediate Sequential Effects in a Latin Square Design,” *Journal of the American Statistical Association*, vol. 53, no. 282, pp. 525–528, 1958, doi: 10.1080/01621459.1958.10501456.

[62] D. Manzey, N. Gérard, and R. Wiczorek, “Decision-making and response strategies in interaction with alarms: the impact of alarm reliability, availability of alarm validity information and workload,” *Ergonomics*, vol. 57, no. 12, pp. 1833–1855, 2014, doi: 10.1080/00140139.2014.957732.

[63] A. Bajaj, B. Rosner, S. W. Lockley, and E. S. Schernhammer, “Validation of a light questionnaire with real-life photopic illuminance measurements: the Harvard Light Exposure Assessment questionnaire,” *Cancer epidemiology, biomarkers & prevention : a publication of the American Association for Cancer Research, cosponsored by the American Society of Preventive Oncology*, vol. 20, no. 7, pp. 1341–1349, 2011, doi: 10.1158/1055-9965.EPI-11-0204.

[64] S. W. Lockley, “Journal of Pineal Research guideline for authors: Measuring melatonin in humans,” *Journal of Pineal Research*, vol. 69, no. 2, e12664, 2020, doi: 10.1111/jpi.12664.

[65] M. A. Jensen, A. M. Hansen, P. Abrahamsson, and A. W. Nørgaard, “Development and evaluation of a liquid chromatography tandem mass spectrometry method for simultaneous determination of salivary melatonin, cortisol and testosterone,” *Journal of chromatography. B, Analytical technologies in the biomedical and life sciences*, vol. 879, no. 25, pp. 2527–2532, 2011, doi: 10.1016/j.jchromb.2011.07.005.

[66] R. T. Wilkinson and D. Houghton, “Field test of arousal: a portable reaction timer with data storage,” *Human factors*, vol. 24, no. 4, pp. 487–493, 1982, doi: 10.1177/001872088202400409.

[67] F. C. Donders, “On the speed of mental processes,” *Acta Psychologica*, vol. 30, pp. 412–431, 1969, doi: 10.1016/0001-6918(69)90065-1.

[68] W. K. KIRCHNER, “Age differences in short-term retention of rapidly changing information,” *Journal of Experimental Psychology*, vol. 55, no. 4, pp. 352–358, 1958, doi: 10.1037/h0043688.

[69] T. Åkerstedt and M. Gillberg, “Subjective and Objective Sleepiness in the Active Individual,” *International Journal of Neuroscience*, vol. 52, 1-2, pp. 29–37, 1990, doi: 10.3109/00207459008994241.

[70] R. Steyer, *Der mehrdimensionale Befindlichkeitsfragebogen: (MDBF)*. Göttingen: Hogrefe Verl. für Psychologie, 1997.

[71] S. G. Hart and L. E. Staveland, *Development of NASA-TLX (Task Load Index): Results of Empirical and Theoretical Research,* Advances in Psychology: Elsevier, vol. 52.

Comparison Between CIE 2° and 10° Field Photopic Luminosity Functions V(λ) for Calculating Daylight Discomfort Glare Metrics

Sneha Jain
Laboratory of Integrated Performance in Design (LIPID)
École polytechnique fédérale de Lausanne EPFL
Lausanne, Switzerland
sneha.jain@epfl.ch
https://orcid.org/0000-0001-7981-2754

Jan Wienold
Laboratory of Integrated Performance in Design (LIPID)
École polytechnique fédérale de Lausanne EPFL
Lausanne, Switzerland
jan.wienold@epfl.ch ORCID

Marilyne Andersen
Laboratory of Integrated Performance in Design (LIPID)
École polytechnique fédérale de Lausanne EPFL
Lausanne, Switzerland
marilyne.andersen@epfl.ch ORCID

***Abstract*— The spectral sensitivity of the average human eye in photopic conditions is represented by the photopic luminosity function V (λ). The CIE has established the photopic luminosity functions for the 2° and 10° visual fields for a standard observer applicable for foveal and para-foveal light sources, respectively. These functions differ in short wavelength region where $V_{10°}$(λ) has higher sensitivity. However, $V_{10°}$(λ) function is not implemented in any of the discomfort glare metrics even though, for most glare scenarios, the glare source is located further than 2° from the fovea. This can result in an underestimation of the short wavelength contribution of the glare sources' spectra, and, a fortiori, in the blue-colored light sources. In this paper, we aim to determine the impact of replacing $V_{2°}$(λ) with $V_{10°}$(λ) in the daylight discomfort glare metrics for scenarios where the visible sun disk lies very much outside the 2° zone and acts as a glare source through blue-tinted and color-neutral tinted low transmittance glazing. We compare three types of colored glazed façade: color-neutral glazing, blue-tinted electrochromic (EC) glazing and an extreme case of saturated blue-tinted glazing. We found that the difference in derived glare source luminance and discomfort glare metrics is statistically significant only for the saturated blue glazing with an average 70% increase in luminance and 20% increase in DGP (i.e. one category higher discomfort) and 9% increase in CGI, when using $V_{10°}$(λ). We conclude that the impact of replacing $V_{2°}$(λ) with $V_{10°}$(λ) is negligible for standard EC or color-neutral glazing types in commercial buildings. However, specific cases of saturated blue light sources that peaks at 450nm are more accurately quantified by $V_{10°}$(λ), that produces higher values of glare metrics.**

Keywords—Discomfort glare, Spectral sensitivity, Glazing color, photopic luminosity function, Daylight

I. INTRODUCTION

Photopic luminous efficiency function *V*(λ) is the spectral weighting function that defines the average spectral sensitivity of the human visual perception of brightness [1]. The photopic human vision state applies to the scenarios having luminance higher than 5cd/m^2 that typically includes discomfort glare scenarios under daylight. Photopic luminosity function is derived experimentally based on user studies of side-by-side matching task or alternate matching (flicker photometry) [2], [3]. A relative subjective brightness perception of the lights at different wavelengths in visible spectrum is determined under constant and neutral adaptation. *V*(λ) was proposed by CIE in 1923 for a 2 degree visual field, which continues to be used in practice for most of the photometric measurement tasks and other practical lighting applications [2].

It was first investigated by Stiles and Burch in 1958 and later proved by several studies that the spectral sensitivity of human eye changes from the center towards the periphery of the retina [4]. Between the foveal and parafoveal fields, the difference in sensitivity to light is attributed to the presence of blue-light absorbing macular pigments in the foveal region of the macula [5]. The yellow macular pigments in the eye are located in front of photoreceptors and are concentrated within 3 degrees of fovea and declines in parafovea, therefore, not effecting the 10 degree field sources [6]. The absorption spectrum of macula lies between 400nm to 550nm and peaking around 460nm [7]. Following these results, CIE established photopic spectral sensitivity function CIE $V_{10°}$(λ) for parafoveal light sources up to 10 degree visual field [8]. Studies have indicated that the ratio $V_{2°}$(λ) / $V_{10°}$(λ) results in a function which is characteristic of the absorption spectrum by the macula [9].

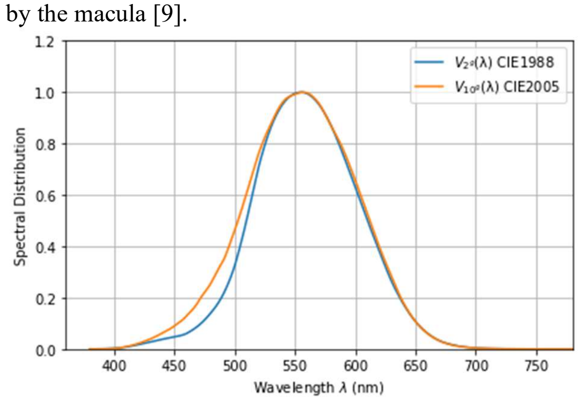

Figure 1 Comparison of 2 and 10-degree photopic luminous efficiency functions

Fig. 1 shows the 2 degree and 10-degree functions. It can be observed from Figure 1 that the difference between $V_{2°}$(λ) and $V_{10°}$ (λ) functions becomes significant between the wavelengths 450nm to 500nm where $V_{10°}$ (λ) has increased sensitivity compared to $V_{2°}$ (λ). It can be inferred that the replacing one function with the other have higher impact in case of blue light sources emitting higher quantity in short wavelength region. Previous studies have emphasized on the use of $V_{10°}$ (λ) instead of $V_{2°}$ (λ) for the measurement of luminance for large field sources under both photopic and mesopic adaptations [9]–[11]. Furthermore, there are ongoing discussions in the lighting community to replace $V_{2^\circ}(\lambda)$ with $V_{10^\circ}(\lambda)$ for extending the applicability to parafoveal sources in discomfort glare scenarios where often the glare source lies outside the fovea. However, $V_{10^\circ}(\lambda)$ is not implemented in any discomfort glare metrics and there are no studies investigating the impact of using $V_{10^\circ}(\lambda)$ instead of $V_{2^\circ}(\lambda)$ for the calculation of luminance and illuminance in discomfort glare metrics for blue and non-blue light sources.

To fill this gap, this study aims to compare what difference the use of either of these two luminosity functions makes when glare metrics are applied under daylit conditions. We calculate glare from the sun visible behind three different colored glazings that have blue, saturated deep blue and color-neutral tints using $V_{2^\circ}(\lambda)$ with $V_{10^\circ}(\lambda)$ and compare the results within each glazing color.

II. Method

A. Test setup

The setup is done in a lab facility located in Lausanne, Switzerland (46°31'00.4"N 6°33'47.1"E) that is arranged to resemble an office space (Fig. 2). The test room has a south façade which provides an unobstructed view to the sun at low altitudes in winter months (mid-October to mid-March) until late afternoon. The south façade is the test façade which we manipulate to create a glare source (sun) of different spectral power distribution by installing colored glazings. The sun is the only glare source visible through the glazing in parafoveal field of view of the observer (ranges of angles of the sundisk, relative to the gaze direction were 20° to 40°). We conducted vertical illuminance measurements using a LMT pocketlux2 lux sensor and high dynamic range (HDR) imaging using a calibrated luminance camera LMK for glare metric calculation, the setup is shown in left part of Fig. 2. These measurements were done under three types of glazing colors on sunny days. The viewing direction towards sun was maintained by adjusting the desk position, so that the eye, the center of the screen(task) and sun position are lying within a plane. Further details of the test room and equipment can be found in [12]. All the measurements were conducted under stable weather conditions with clear sky.

B. Glazing selection

The criteria of choosing three types of glazing spectrum (color) was to have a representation of commercially available and employed glazing types that also exhibit enhanced spectral transmittance under shorter wavelength region where we expect to find the highest impact of replacing $V_{2^\circ}(\lambda)$ with $V_{10^\circ}(\lambda)$. An additional requirement of the glazing characteristic was to reduce the overall transmittance to a level, that one can expect a certain glare protection function (=low transmittance glazing, τ_{vis} ~0.3-2.5%). Due to the characteristics of $V_{10^\circ}(\lambda)$ function, we know that the change in luminance and illuminance (and therefore discomfort glare metrics) of the scene due to the visible sun will only be observed with the glazing that must transmit between 400nm to 550nm. To achieve this, we selected three types of glazing as shown in fig. 2: 1) a color-neutral glazing often used in buildings with glass façade, 2) EC glazing that has blue-tint in its darker state, 3) a saturated deep blue tinted glazing which is meant for specific use cases but have highest sensitivity under short wavelengths compare to the other two types. These three types of glazing are referred as color-neutral glazing, EC glazing and blue glazing in this paper.

The color-neutral glazing was installed as an adhesive film over the window. The film was chosen in a way to not alter the daylight spectrum and maintain natural looking environment inside and outside the room but also has peaks in the short wavelength region where we could expect to see a prominent difference in glare source spectra when using $V_{10^\circ}(\lambda)$.

For the second glazing type, we installed a commercially available electrochromic glazing for its blue tint. EC glazing offers switchable transmittance technology to facilitate daylight modulation. EC material used in such glazing exhibit a spectral shift towards short wavelength region in their darkened state, causing them to appear blue.

For the third type, another blue-colored glazing was installed as an extreme test case having a saturation of 100%, calculated using HSL color model. This type of glazing has limited and specific usage in buildings compared to other two. However, the glazing spectrum was chosen to have peak sensitivity in the region where $V_{2^\circ}(\lambda)$ and $V_{10^\circ}(\lambda)$ differ from each other in order to determine a maximum possible discrepancy in calculation of discomfort glare metrics under daylit conditions ("extreme case").

C. Glazing properties

Spectral transmittance of all the glazings were measured in a glazing and Nano-technology laboratory on its window

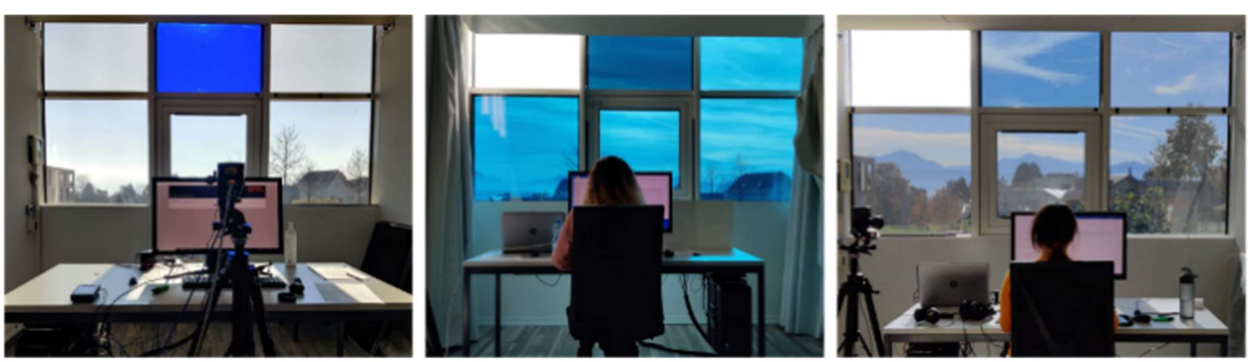

Blue glazing Electrochromic glazing Color-neutral glazing

Figure 2 Tested glazing colors: Saturated blue glazing (left), EC Blue glazing (center), color-neutral glazing (right) test bench. Fig. 3 shows the normalized measured spectral transmittance under visible range for color-neutral, EC and blue glazings. We tested two levels of visible light transmittances for each glazing type listed in Table 1 to evaluate the glare metric variations over a range of conditions. The spectral profile of the glazings are similar for both the transmittances, therefore, we plot normalized spectral transmittance in Fig.3. We report the normal-hemispherical visible light transmittances ($\tau_{v,n\text{-}h}$) of tested windowpane from where the sun was visible. It can be observed from the figure 3 that all our glazing types transmit in the wavelength range (~400nm-525nm) where $V_{10°}(\lambda)$ differs from $V_{2°}(\lambda)$ function.

TABLE 1 Glazing color and tint properties of all three glazing types

Glazing Type	Chromaticity coordinates		HSL values			$\tau_{v,n\text{-}h}$
	x	y	Hue	Saturation	Lightness	
Color-neutral	0.33	0.34	0	0	3.9	0.36%, 1.25%
EC glazing	0.24	0.30	189	65%	5.7	0.6%, 1.6%
Blue Glazing	0.14	0.05	240	100 %	3.3	0.39%, 2.25%

Fig. 4 shows the CIExy chromaticity diagram for all three glazing types depicting how they render the sun in reference to D65 illuminant representing the white point. Chromaticity defines the quality of color on two parameters: its hue and colorfulness, regardless of its luminance. Colorfulness is approximately similar to 'saturation' in HSL color model. Table 1 lists the chromaticity coordinates for each glazing type corresponding to the Fig. 4. It also lists the hue, saturation and lightness value of HSL color model. The saturation or the purity of color is highest for blue glazing at 100%.

It should be noted that these three glazing colors are of different low visible light transmittance from each other as reported in Table 1. These transmittances were designed for other independent experimental studies. Since in this study we only compare the glare metric and luminance values within each glazing color and not across, therefore, the different transmittances are not of concern. Also, within each glazing spectrum, the spectral profile remains the same for different transmittances.

D. Glare metrics

Discomfort glare metrics for daylit conditions generally account for either contrast or saturation effects or both effects in case of hybrid metrics. Both contrast and saturation terms in the glare metrics are affected by the replacement of $V_{2°}(\lambda)$ with $V_{10°}(\lambda)$ function due the change in photometrics quantities: glare source and background luminance and the vertical illuminance at eye (E_v). We evaluate two glare metrics- Daylight Glare Probability (DGP) [13] and CIE Glare index (CGI) [14] based on hybrid and contrast effects, respectively, and compare the values weighted using $V_{2°}(\lambda)$ with $V_{10°}(\lambda)$ functions. The glare metric equations are shown in the Eq. 1 and 2, where we replaced the Luminance, E_v and E_{dir} in the equation weighted by $V_{10°}(\lambda)$. Studies have shown that these two metrics are reliable in predicting glare in typical daylit workplace conditions and also under electrochromic glazing [12], [15].

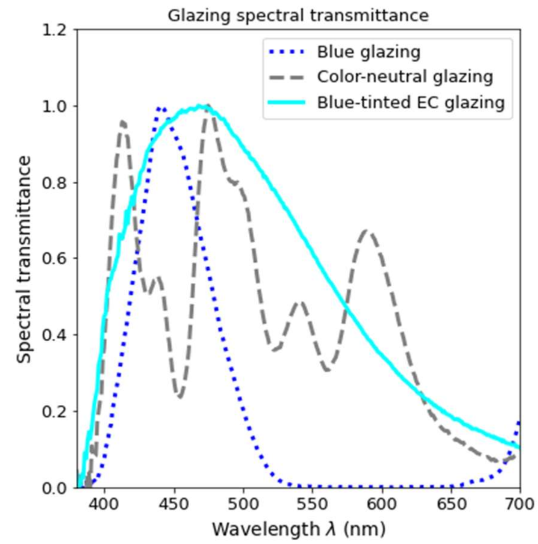

Figure 3 Normalised spectral transmittance of color-neutral, EC and blue glazing under visible range

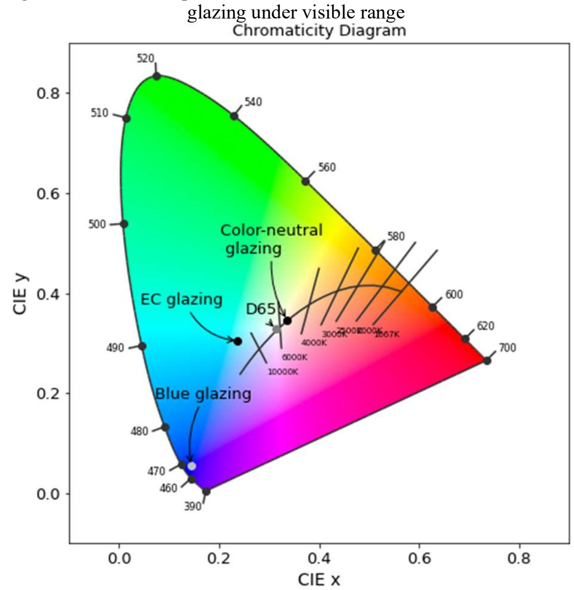

Figure 4 CIE xy chromaticity coordinates of the sun filtered by all three glazings in reference to illuminant D65

Equation 1:

$$DGP = 5.87e^{-5}\,\boldsymbol{E_v} + 9.18e^{-2}\log\left(1 + \sum \frac{L^2\omega_{5.8°}}{E_v^{1.87}P^2}\right) + 0.16$$

Equation 2:

$$CGI = 8 * \log 2 * \frac{1+E_{dir}/500}{E_v}\left(\sum \frac{L^2\omega_{5.8°}}{P^2}\right)$$

where E_v is vertical illuminance at eye level, L is luminance of glare source weighted by $V_{2°}(\lambda)$ or $V_{10°}(\lambda)$ functions, ω is solid angle of the glare source (=0.00804651 sr), P is the position index of the glare source, E_{dir} is the direct vertical illuminance at eye level.

E. Photometric measurements and calculations

Measurements of vertical illuminance and HDR capture of glare scenes were conducted on sunny days. For color-neutral glazing, we collected 50 datapoints under two transmittances (total 100 datapoints), for blue glazing 25 datapoints for two transmittances (total 50 datapoints) and for EC glazing 20 datapoints were collected under two transmittances (total 40 datapoints). Discomfort glare was calculated for the low sun position indices (P<4) to have sun always within central visual field but not in the fovea. This was chosen to create critical glare scenarios in workplace environment where we could observe the maximum difference, if any, between $V_{2^\circ}(\lambda)$ and $V_{10^\circ}(\lambda)$ weighted glare metrics.

Since the measuring equipment used in this study employ a $V_{2^\circ}(\lambda)$ function to measure illuminance and capture HDR imaging, and due to the lack of spectral imaging and measurements, a reference standard solar spectra provided by ASTM G173-03 [16] was used to create the sun spectrum. We used the standard direct solar (+circumsolar) spectrum defined by ASTM G173 for 5.8° diameter (solid angle ω= 0.00804651 steradians) around the sun. The integrated power density of this spectrum is 855 W/m^2 which was scaled to match the on-site measured solar irradiance at the time of measurements for a range of 400nm to 2700nm. The resulted solar spectra were then integrated with the measured spectral transmittances of the glazings. The sun luminance weighted over $V_{2^\circ}(\lambda)$ and $V_{10^\circ}(\lambda)$ was calculated as per Equation 1.

$$L_{2^\circ or\ 10^\circ} = K_m \int_{380}^{780} E_\lambda * T_\lambda * V_{2^\circ or\ 10^\circ}(\lambda) d\lambda$$

Equation 1

where $L_{2^\circ or\ 10^\circ}$ is luminance of the glare source weighted by $V_{2^\circ}(\lambda)$ and $V_{10^\circ}(\lambda)$ K_m is the photopic luminance efficacy value, E_λ is the scaled spectral irradiance of the sun based on ASTM spectra [16], T_λ is the measured spectral transmittance of glazing.

To further validate this method, we compared the above calculated luminance values using $V_{2^\circ}(\lambda)$ weighting function with the luminance derived from the HDR images captured with a luminance camera that employs $V_{2^\circ}(\lambda)$ filter. We found that the normalized RSME errors stayed within an acceptable range of 15%.

In a similar way, we also calculated the vertical illuminance at eye level weighted by $V_{2^\circ}(\lambda)$ and $V_{10^\circ}(\lambda)$ functions. For calculating the direct part of vertical illuminance which is contributed solely by the sun, we followed same approach as mentioned above for the sun luminance calculation. Direct vertical illuminance values derived from the HDR images using the Evalglare [17] tool in Radiance [18] for a 5.8° sun were scaled by a factor of L_{10°/L_{2° to get the illuminance weighted by $V_{10^\circ}(\lambda)$ function. For the total vertical illuminance at eye level, we incorporated measured spectral irradiance profile at eye level for all the glazing configuration using the spectrophotometer data and weighted the total spectral irradiance by $V_{2^\circ}(\lambda)$ and $V_{10^\circ}(\lambda)$ and scaled it to match the measured vertical illuminance at eye.

Evalglare was further used to derive the position index P of the sun from the HDR images. The adjusted glare metrics (DGP and CGI) were calculated as per Eq. 1 and 2 by replacing the illuminance and source luminance values in the equations with the adjusted values weighted based on $V_{2^\circ}(\lambda)$ and $V_{10^\circ}(\lambda)$ functions.

III. Results

A. Relative spectral power distribution

Fig. 5-7 shows the normalized spectral power distribution of the sun (serving as glare source) visible through the color-neutral glazing, EC glazing and blue glazing, respectively. It can be observed from the figures that the difference between the glare source spectra weighted with $V_{2^\circ}(\lambda)$ and $V_{10^\circ}(\lambda)$ is maximum in case of blue glazing (fig. 7). In case of EC glazing, even though it has blue-tint we do not observe significant difference between the two functions (fig. 6). Similarly, for color-neutral the difference is not significant.

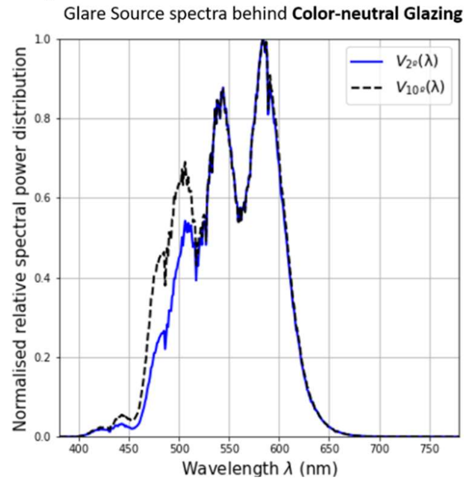

Figure 5 Normalised relative spectral power distribution for color-neutral glazing weighted by $V_2(\lambda)$ and $V_{10}(\lambda)$ functions

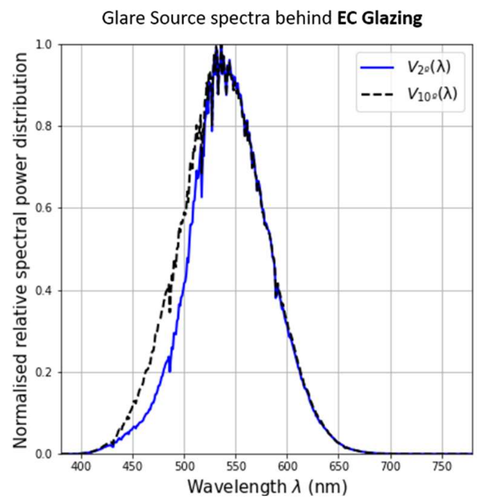

Figure 6 Normalised relative spectral power distribution for EC glazing weighted by $V_2(\lambda)$ and $V_{10}(\lambda)$ functions

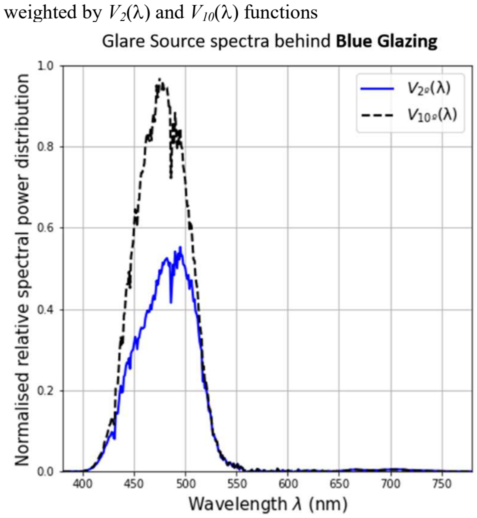

Figure 7 Normalised relative spectral power distribution for blue glazing weighted by $V_2(\lambda)$ and $V_{10}(\lambda)$ functions

TABLE 2 Mean values of glare metrics and sun luminance based on $V_{2°}(\lambda)$ and $V_{10°}(\lambda)$ functions

Glazing type	*Mean DGP*		Mean CGI		Mean Sun Luminance	
	$V_{2°}(\lambda)$	$V_{10°}(\lambda)$	$V_{2°}(\lambda)$	$V_{10°}(\lambda)$	$V_{2°}(\lambda)$	$V_{10°}(\lambda)$
Color-neutral	0.32	0.33	28.6	28.8	67583	70448
EC glazing	0.34	0.35	35.4	35.7	94283	98494
Blue Glazing	0.34	0.41	33.2	36.2	98467	166883

Table 3 Wilcoxon p-values and mean relative differences between the two groups based on $V_{2°}(\lambda)$ and $V_{10°}(\lambda)$ functions for evaluates metrics under three glazing colors

Glazing type	*DGP*		CGI		Sun Luminance	
	p-value	Mean relative diff.	p-value	Mean relative diff.	p-value	Mean relative diff.
Color-neutral	0.27	3%	0.6	0.7%	0.18	4%
EC glazing	0.54	3%	0.7	0.8%	0.36	4.5%
Blue Glazing	***1.6e-5***	***20%***	***3.6e-3***	***9%***	***2.4e-5***	***70%***

B. Luminance

Fig. 8 presents the comparison of the luminance of the visible sun calculated based on $V_{2°}(\lambda)$ and $V_{10°}(\lambda)$ for all three glazing colors with the median values in the boxplots. Table 2 reports the mean values of each evaluated metric for $V_{2°}(\lambda)$ and $V_{10°}(\lambda)$ functions. The observed spread in the boxplots are due to two levels of visible light transmittances being tested in each of the glazing spectra.

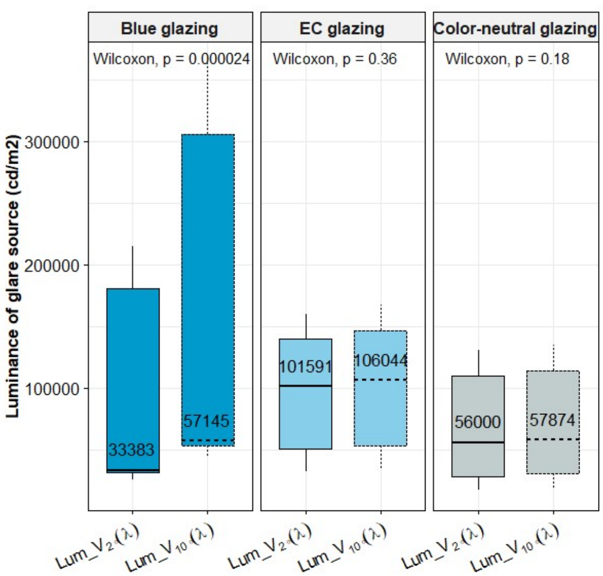

Figure 8 Box plots with median values showing the comparison between $V_2(\lambda)$ and $V_{10}(\lambda)$ functions in quantifying luminance

We applied Wilcoxon ranked sum test [19] to perform pairwise comparison between the two groups of luminance values weighted by $V_{2°}(\lambda)$ and $V_{10°}(\lambda)$ to determine if there is a significant difference at α=0.05 between these two groups in each glazing category (Fig. 8 and Table 3). We also calculated a mean relative percentage difference between these two groups as reported in Table 3.

The difference of the sun luminance is not significant for color-neutral (p=0.18) and EC glazing (p=0.36), however, it is statistically significant for the blue glazing with a p=0.00024 with an effect size of 0.44 indicating a moderate effect. The mean relative percentage differences between the luminance are around 4% for EC and color-neutral glazing, whereas for blue glazing the difference is 70%. These results indicate that for color-neutral and EC glazing, that are more often employed in buildings, replacing $V_{2°}(\lambda)$ with the $V_{10°}(\lambda)$ has minimal impact on the luminance. However, same doesn't hold true for saturated blue glazing where we observe highly substantial difference in luminance that can entirely transform the glare scenario.

C. Discomfort glare

Fig. 9 and 10 demonstrate the comparison of glare metrics DGP and CGI based on $V_{2°}(\lambda)$ and $V_{10°}(\lambda)$ functions under three different glazing spectra. Similar to luminance results, we observe a statistically significant difference ($p<0.05$) only in the blue glazing for both the glare metrics. The difference is not significant for EC and color-neutral glazing. Wilcoxon p-values are reported in Table 3 along with the mean relative difference which are again negligible for color-neutral and EC glazing compared to the blue glazing. In case of blue glazing, the difference in mean DGP values (Table 2) between the $V_{2°}(\lambda)$ and $V_{10°}(\lambda)$ are equivalent to one category difference of achieved comfort from glare as defined by EN17037 [20]. Similarly, for CGI the difference in mean metric values can create a large difference of 9%. In comparison to the relative luminance differences, the impact of replacing $V_{2°}(\lambda)$ with $V_{10°}(\lambda)$ on glare equations are rather small due to the logarithmic function over the luminance in the glare equations.

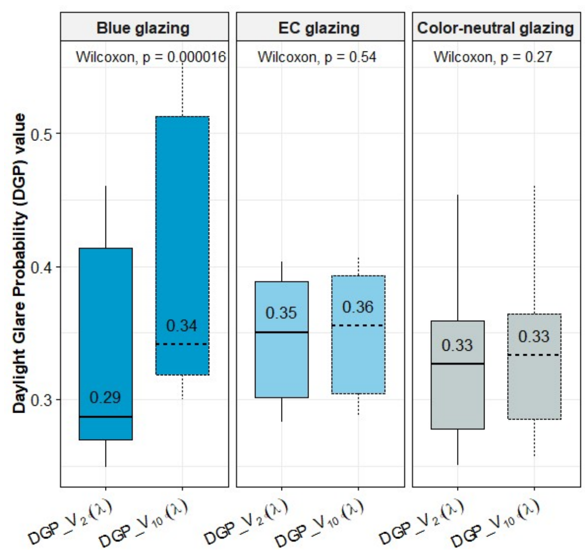

Figure 9 Box plots with median values showing the comparison between $V_2(\lambda)$ and $V_{10}(\lambda)$ functions in quantifying DGP metric

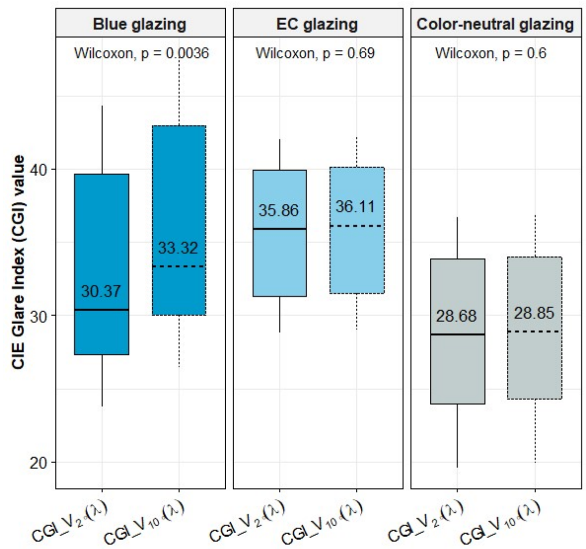

Figure 10 Box plots with median values showing the comparison between $V_2(\lambda)$ and $V_{10}(\lambda)$ functions in quantifying CGI metric

IV. Discussions

It should be noted that in this paper we purely focus on the quantitative difference between using 2 degree and 10-degree functions. The subjective perception of occupants under colored glazing and glare sources should be evaluated to determine if any of these two functions are applicable under non-neutral daylit conditions. Previous studies with vehicular headlamps have suggested the inability of conventional photopic luminosity functions (both $V_2(\lambda)$ and $V_{10}(\lambda)$) in defining the glare perception of users under blue colored LEDs and possibility of including s-cone sensitivity to modify the $V(\lambda)$ for both 2- and 10-degree glare sources [22]–[26]. There is a need to evaluate impact of color under daylit glare scenarios to further elucidate on these findings.

Some limitations of this study are that due to the lack of measuring instruments and measurements available based on $V_{10}(\lambda)$, we implement a calculation method that uses standard sun spectra that could differ from actual onsite sun spectra due to the atmospheric conditions and this can create discrepancies to some extent in the calculated glare metric values using this method. However, since we perform a relative comparison between the glare metrics based on $V_2(\lambda)$ and $V_{10}(\lambda)$, these discrepancies can be ignored. We also made sure to conduct the measurements only during stable weather conditions with clear sky.

It should also be noted that the results found in this study are only applicable for the broad-spectrum daylight sources and can vary for narrow spectrum and monochromatic light sources. Although the method described in this paper can be extended to electric light scenarios as well. The spectrum profile of the luminaries and the peak wavelength of the spectra play a key role in determining whether using $V_{10}(\lambda)$ would make a large impact on glare metrics.

V. Conclusion

We found that the mean relative difference between the sun luminance calculated using $V_2(\lambda)$ and $V_{10}(\lambda)$ ranges between 4% to 5% for the color-neutral and EC glazing, whereas the difference lies between 68% to 70% for the saturated blue glazing and is statistically significant. The mean difference in daylight glare probability (DGP) calculated using $V_2(\lambda)$ and $V_{10}(\lambda)$ is 3% for both color-neutral and EC glazing, whereas for the blue glazing the difference is 20%. Calculated CGI metric values differ by 0.7% and 0.8% in case of color-neutral and EC glazing, whereas for the blue glazing the difference between CGI calculated based on $V_2(\lambda)$ and $V_{10}(\lambda)$ is 9% and is statistically significant.

From these results, we can conclude that even though the $V_{10}(\lambda)$ luminosity function represents a physiologically more accurate quantification of the luminance in the parafoveal field, the difference in achieved discomfort glare metrics based on this function for the more often employed color-neutral and EC glazing are negligible compared to the conventionally used $V_2(\lambda)$. However, the user perception of glare under blue EC glazing in comparison to color neutral glazing is suggested to be higher [27] which is not explained by the replacement of $V_2(\lambda)$ with $V_{10}(\lambda)$ in the glare equations as shown in this study. We need further modification into photopic luminosity function and thereby in the current glare metrics to include the impact of color on glare perception. We also found that if the sun is filtered by saturated blue glazing that peaks at 450nm, the $V_{10}(\lambda)$ function provides much higher discomfort glare metrics values and therefore, indicate high level of perceived discomfort which needs further investigation through subjective assessment under such glazing spectrum.

Acknowledgment

This study is funded by Swiss National Foundation project (SNF) grant for the project "Visual comfort without borders: interactions on discomfort glare" number 200020_182151. We would like to thank M. Lagier and A. Schüler for conducting the spectral transmittance measurements..

References

[1] CIE 086-1990, "CIE 1988 2° spectral luminous efficiency function for photopic vision | CIE," 1988. Accessed: Apr. 30, 2022. [Online]. Available: https://cie.co.at/publications/cie-1988-2-spectral-luminous-efficiency-function-photopic-vision

[2] K. S. Gibson and E. P. T. Tyndall, *Visibility of radiant energy*, vol. 19. US Government Printing Office, 1923.

[3] J. J. Vos, "Colorimetric and photometric properties of a 2-deg fundamental observer," *Color Research and Application*, vol. 3, no. 3, pp. 125–128, 1978.

[4] W. S. Stiles and J. M. Burch, "N.P.L. Colour-matching Investigation: Final Report (1958)," *Optica Acta: International Journal of Optics*, vol. 6, no. 1, pp. 1–26, Jan. 1959, doi: 10.1080/713826267.

[5] CIE, "Fundamental Chromaticity Diagram with Physiological Axes - Part 1," Technical Report 170–1, 2006.

[6] J. M. Stringham, P. V. Garcia, P. A. Smith, L. N. McLin, and B. K. Foutch, "Macular Pigment and Visual Performance in Glare: Benefits for Photostress Recovery, Disability Glare, and Visual Discomfort," *Invest. Ophthalmol. Vis. Sci.*, vol. 52, no. 10, p. 7406, Sep. 2011, doi: 10.1167/iovs.10-6699.

[7] CIE 170-2: 2015, "Fundamental Chromaticity Diagram with Physiological Axes – Part 2: Spectral Luminous Efficiency Functions and Chromaticity Diagrams | CIE," Commission Internationale de

l'éclairage, 978-3-902842-05–3, 2015. Accessed: Apr. 30, 2022. [Online]. Available: https://cie.co.at/publications/fundamental-chromaticity-diagram-physiological-axes-part-2-spectral-luminous-efficiency

[8] CIE publication 165:2005, "CIE 10 Degree Photopic Photometric Observer," Commission Internationale de l'éclairage, Vienna, Austria (2005), 2005.

[9] W. Adrian, "Spectral sensitivity of the pupillary system," *Clin Exp Optom*, vol. 86, no. 4, pp. 235–238, Jul. 2003, doi: 10.1111/j.1444-0938.2003.tb03111.x.

[10] J. Ding, Q. Yao, and L. Jiang, "Comparisons of Scotopic/Photopic Ratios Using 2- and 10-Degree Spectral Sensitivity Curves," *Applied Sciences*, vol. 9, no. 20, Art. no. 20, Jan. 2019, doi: 10.3390/app9204471.

[11] A. Stockman and L. T. Sharpe, "Human cone spectral sensitivities: a progress report," *Vision Research*, vol. 38, no. 21, pp. 3193–3206, Nov. 1998, doi: 10.1016/S0042-6989(98)00060-1.

[12] S. Jain, C. Karmann, and J. Wienold, "Behind electrochromic glazing: Assessing user's perception of glare from the sun in a controlled environment," *Energy and Buildings*, vol. 256, p. 111738, Feb. 2022, doi: 10.1016/j.enbuild.2021.111738.

[13] J. Wienold and J. Christoffersen, "Evaluation methods and development of a new glare prediction model for daylight environments with the use of CCD cameras," *Energy and Buildings*, vol. 38, no. 7, pp. 743–757, Jul. 2006, doi: 10.1016/j.enbuild.2006.03.017.

[14] H. D. Einhorn, "Discomfort glare: a formula to bridge differences," *Lighting Research & Technology*, vol. 11, no. 2, pp. 90–94, Jun. 1979, doi: 10.1177/14771535790110020401.

[15] J. Wienold *et al.*, "Cross-validation and robustness of daylight glare metrics," *Lighting Research & Technology*, p. 147715351982600, Mar. 2019, doi: 10.1177/1477153519826003.

[16] ASTM (2020), ASTM G173, "Standard Tables for Reference Solar Spectral Irradiances," Standards. Accessed: Apr. 29, 2022. [Online]. Available: https://www.astm.org/g0173-03r20.html

[17] J. Wienold, "Evalglare–A new RADIANCE-based tool to evaluate daylight glare in office spaces," 2004.

[18] G. J. Ward, "The RADIANCE lighting simulation and rendering system," in *Proceedings of the 21st annual conference on Computer graphics and interactive techniques - SIGGRAPH '94*, New York, New York, USA, 1994, pp. 459–472. doi: 10.1145/192161.192286.

[19] F. Wilcoxon, "Individual Comparisons by Ranking Methods," *Biometrics Bulletin*, vol. 1, no. 6, pp. 80–83, 1945, doi: 10.2307/3001968.

[20] European Committee for Standardization CEN, "EN17037:2019 Daylight in buildings," 2019.

[21] S. Carlucci, F. Causone, F. De Rosa, and L. Pagliano, "A review of indices for assessing visual comfort with a view to their use in optimization processes to support building integrated design," *Renewable and Sustainable Energy Reviews*, vol. 47, no. 7491, pp. 1016–1033, Jul. 2015, doi: 10.1016/j.rser.2015.03.062.

[22] M. Sivak, B. Schoettle, T. Minoda, and M. J. Flannagan, "Short-Wavelength Content of LED Headlamps and Discomfort Glare," *LEUKOS*, vol. 2, no. 2, pp. 145–154, Oct. 2005, doi: 10.1582/LEUKOS.2005.02.02.006.

[23] M. Flannagan, M. Sivak, M. Ensing, and C. Simmons, "Effect of wavelength on discomfort glare from monochromatic sources.," *undefined*, 1989, Accessed: May 16, 2022. [Online]. Available: https://www.semanticscholar.org/paper/Effect-of-wavelength-on-discomfort-glare-from-Flannagan-Sivak/b59b3dd819fe43ccd1c2a1c1cbf7fc1aae137c23

[24] J. D. Bullough, "Spectral sensitivity for extrafoveal discomfort glare," *Journal of Modern Optics*, vol. 56, no. 13, pp. 1518–1522, Jul. 2009, doi: 10.1080/09500340903045710.

[25] J. Fekete, C. Sik-Lányi, and J. Schanda, "Spectral discomfort glare sensitivity investigations," *Ophthalmic and Physiological Optics*, vol. 30, no. 2, pp. 182–187, Mar. 2010, doi: 10.1111/j.1475-1313.2009.00696.x.

[26] W. Huang, Y. Yang, and M. R. Luo, "Discomfort glare caused by white LEDs having different spectral power distributions," *Lighting Research & Technology*, vol. 50, no. 6, pp. 921–936, Oct. 2018, doi: 10.1177/1477153517704996.

[27] S. Jain and J. Wienold, Eds., *Glare behind blue (electrochromic) glazing*. 2021.

General Lighting Solutions for the Required Ceiling, Wall and Cylindrical Illumination in Interiors

Piotr Pracki
Lighting Technology Division,
Electrical Power Engineering Institute
Warsaw University of Technology
Warsaw, Poland
piotr.pracki@pw.edu.pl

Paulina Komorzycka
Doctoral School No. 3
Warsaw University of Technology
Warsaw, Poland
paulina.komorzycka.dokt@pw.edu.pl

***Abstract*— The new standard 2021 on lighting of interior workplaces, raises the requirements for maintained average illuminances on the ceiling, walls and cylindrical on the horizontal reference plane, compared to the requirements of the old standard 2011. In the course of computer simulation studies, 432 situations of general lighting in interiors were analyzed, varying in room size and reflectance, luminaire class and downward luminous intensity distribution, and luminaire layout. In the analyzed situations, in accordance with the old standard, in 96% of cases the requirement of the average ceiling illuminance was met, in 92% of cases the requirement of the average wall illuminance was met, and in 89% of cases the requirement of the average cylindrical illuminance was met. In accordance with the new standard, in 90% of cases the requirement of the average ceiling illuminance was met, in 91% of cases the requirement of the average wall illuminance was met, and in 88% of the cases the requirement of the average cylindrical illuminance was met. The use of direct lighting significantly reduced the normative ceiling illumination, and the use of luminaires with very narrow downward luminous intensity distribution significantly reduced the normative wall and cylindrical illumination.**

Keywords—interior lighting, ceiling illumination, wall illumination, cylindrical illumination, lighting solutions

I. INTRODUCTION

Assessment of the interior luminous environment is based on the verification of normative criteria [1][2]. The assessment includes i.e. illumination on the task, immediate surrounding and background areas [3], illumination on the walls [4] and ceiling [5], illumination in the interior space [6], glare [7], color of light [8], color rendering [9], flicker and stroboscopic effects [10], illumination of work stations with display screen equipment [11]. After more than 10 years of use in the EU, the "old" standard: EN 12464-1:2011 [1] has been replaced by the "new" one: EN 12464-1:2021 [2]. A significant difference in requirements is in the increase for the average illuminance on the ceiling and walls, and the average cylindrical illuminance on the horizontal reference plane in interiors. These changes mean that some existing lighting solutions, correct in terms of the old requirements, may not meet the new ones. The need to verify this supposition was the motivation to undertake the research.

II. CEILING, WALL AND CYLINDRICAL ILLUMINATION

The ceiling and walls occupy a significant part of the visual field of interior users. Their illumination is important in creating the desired luminance distribution in order to create a stimulating and attractive luminous environment in interiors. The desired illumination of the ceiling and walls limits glare by reducing excessive brightness and contrasts, and at the same time should not lead to monotony by avoiding too low brightness and contrasts. The ceiling and walls illumination should therefore be properly balanced and not lead to extreme luminance distributions.

In the interior space there are various three-dimensional objects, including people - users of interiors, which are made visible due to the light falling. Then, lighting in the interior space can be used to highlight the object, reveal its form or texture. Lighting in interiors where people work and live is useful for recognizing the objects and for visual communication.

According to the old standard [1], in interiors the maintained average illuminance should be higher than 50 lx on the walls and higher than 30 lx on the ceiling. In some enclosed places, where higher brightness is expected, it is recommended to increase these values to 75 lx on the walls and to 50 lx on the ceiling. For good visual communication and recognition of objects within the interior space the maintained average cylindrical illuminance in the activity areas should be not less than 50 lx. In some areas, where visual communication is crucial, it is recommended to increase this value to 150 lx.

According to the new standard [2], the requirements for the ceiling, walls and cylindrical illumination in interiors are strongly connected with the required maintained average illuminance on the task area. In general, the higher the requirement for the task area illuminance, the higher the requirement for the ceiling, walls and cylindrical illuminances in interiors.

Tab. I summarizes the requirements for maintained average illuminance levels on the ceiling (EC), walls (EW) and cylindrical on the horizontal reference plane (EZ), for the required task area illuminance levels (E): 100 – 150 – 200 – 300 – 500 – 750 – 1000 lx. For the new standard [2], in Tab. I, the highest requirements for the given task area illuminance levels are presented.

Comparing the old and new requirements for the ceiling, walls and cylindrical illuminances, it can be observed that for the task area illuminance levels 100 lx and 150 lx the requirements do not change. For the task area illuminance level 200 lx and higher, the requirements of the new standard [2] are higher. For the task area illuminance levels 500 lx and higher, the requirements of the new standard [2] are three levels higher than the requirements of the old standard [1].

The research objective was to determine differences in meeting the lighting requirements when using both the old [1] and new [2] standards, as well as to determine general lighting solutions at which the compliance with the considered standard requirements were limited. This work is a continuation of the research on lighting solutions for high quality lighting in interiors [12][13][14].

TABLE I. COMPARISON OF REQUIREMENTS FOR EC, EW AND EZ, FOR THE REQUIRED E LEVELS IN INTERIORS

E [lx]	Standard	EC [lx]	EW [lx]	EZ [lx]
100	Old [1]	30[a]	50[a]	50[b]
	New [2]	30	50	50
150	Old [1]	30[a]	50[a]	50[b]
	New [2]	30	50	50
200	Old [1]	30[a]	50[a]	50[b]
	New [2]	50	75	75
300	Old [1]	30[a]	50[a]	50[b]
	New [2]	75	100	100
500	Old [1]	30[a]	50[a]	50[b]
	New [2]	100	150	150
750	Old [1]	30[a]	50[a]	50[b]
	New [2]	100	150	150
1000	Old [1]	30[a]	50[a]	50[b]
	New [2]	100	150	150

a. For higher brightness in interiors, it is recommended [1] to increase EC to 50 lx and EW to 75 lx.

b. For better visual communication and object recognition in interiors, it is recommended [1] to increase EZ to 150 lx.

III. METHOD

The realization of the research objectives was based on computer simulation, for reference, empty interior lighting situations. Models of rooms, lighting systems and calculations were made in an online available and verified [15] DIALux 4 software. The results were analyzed in Statistica package.

The reference interior lighting situations were elaborated to consider a wide range of general lighting scenarios. The following assumptions were taken:

- Room size: 3 room indices (RI): 1.5 (relatively small rooms), 3.0 (moderate rooms), 4.5 (relatively large rooms).
- Room reflectance (RO): 3 sets: 752 (0.7 for ceiling, 0.5 for walls, 0.2 for floor), 753 (0.7 for ceiling, 0.5 for walls, 0.3 for floor) and 772 (0.7 for ceiling, 0.7 for walls, 0.2 for floor).
- Luminaire characteristic: 4 lighting/luminaire classes (CL): I (direct lighting), II (semi-direct lighting), III (direct-indirect lighting), IV (semi-indirect lighting).
- Luminaire characteristic: 4 downward luminous intensity distributions (LID): 1 (the widest distribution), 2 (wide distribution), 3 (narrow distribution), 4 (the narrowest distribution).
- Luminaire layout: 3 spacing-to-height ratios (SH): 0.5 (small spacing relative to suspension height), 1.0 (moderate spacing relative to suspension height), 1.5 (large spacing relative to suspension height).

The luminaire luminous intensity distributions and layouts selected for the study are presented in Fig. 1 and Fig. 2 respectively. In Table II more information on rooms and luminaire layouts is presented.

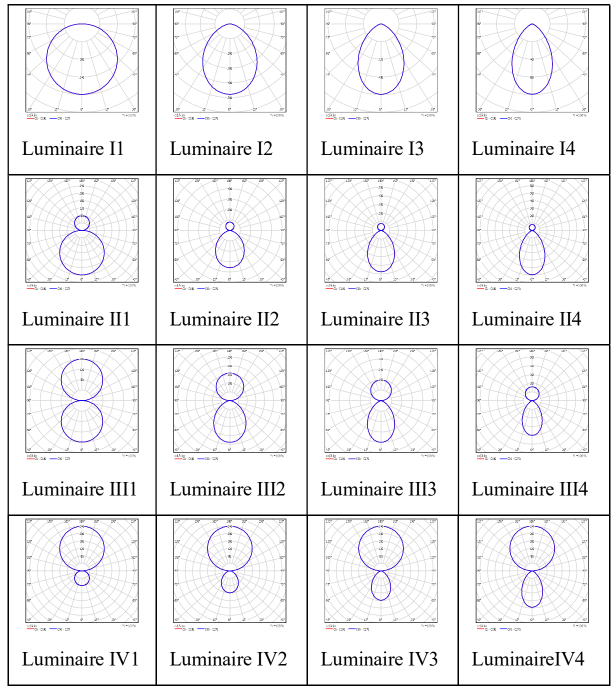

Fig. 1. Luminaire luminous intensity distributions selected for the study

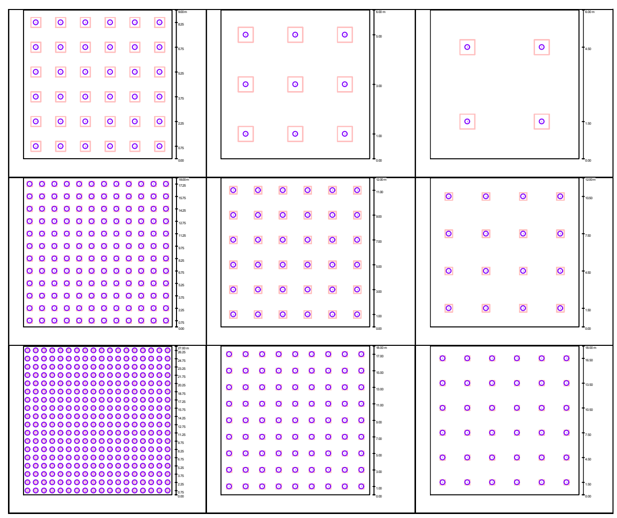

Fig. 2. Luminaire layouts selected for the study (floor views of rooms are not in scale)

TABLE II. INFORMATION ON ROOMS AND LUMINAIRE LAYOUTS

RI	SH	H	N	L
1.5	0.5	3	36(6x6)	9
	1.0	2	9(3x3)	6
	1.5	2	4(2x2)	6
3.0	0.5	3	144(12x12)	18
	1.0	2	36(6x6)	12
	1.5	2	16(4x4)	12
4.5	0.5	3	324(18x18)	27

	1.0	2	81(9x9)	18
	1.5	2	36(6x6)	18

The room heights (H), lengths/widths (L) and luminaire numbers (N) were specified to get appropriate RI and SH. The task area for illuminance calculation was assumed to be located at 0.75 m above the floor. The reference plane for cylindrical illuminance calculation was assumed to be located at 1.20 m above the floor. Both, the task area and reference plane were extended between the walls. The luminaire CL I were located directly on the ceiling, and the ones of CL II, CL III and CL IV were suspended by 0.5 m from the ceiling. The spacing (S) between the centers of the adjacent luminaires in the lines was twice as large as the spacing between the centers of the outermost luminaires from the nearest wall.

There were 432 lighting situations considered for a given average illuminance on task area. The analysis of the results covered the maintained average illuminances: on task area (E), on ceiling (EC), on walls (EW) and cylindrical on horizontal reference plane (EZ). Also, a useful in the analysis illuminance ratios were included: for ceiling (EC/E), for walls (EW/E) and for horizontal reference plane (EZ/E). The maintenance factor was assumed to be equal 0.8.

IV. Results and Analysis

A. *Illuminance ratios*

In the first stage of the research, the illuminance ratios EC/E, EW/E and EZ/E were calculated for each situation. The luminaires luminous flux in each situation was adjusted to obtain E level of exactly 500 lx. The results for all 432 lighting situations are summarized in Tab. III.

For all the considered cases, the largest dispersion of relative illuminances occurred on the ceiling, EC/E between 0.1540 and 1.6520, substantially smaller on the walls, EW/E between 0.2960 and 0.7080 and the smallest on the reference plane, EZ/E between 0.3320 and 0.5760.

There were also the Pearson's correlation coefficients calculated, presented in Tab. IV, to demonstrate the level and direction of the impact of room parameters, luminaires and their layouts on the EC/E, EW/E and EZ/E values. The bolded correlations are significant at $p<0.01$. For the considered range of parameters characterizing the rooms and luminaires, the luminaire class (N4 index) has the largest impact on the EC/E level, and the luminaire downward luminous intensity distribution (N1 index) has the largest impact on both the EW/E and EZ/E levels.

TABLE III. Illuminance ratios EC/E, EW/E and EZ/E, for all the considered cases (N=432)

Var.	Mean	Min	Max	SD
EC/E	0.7304	0.1540	1.6520	0.4151
EW/E	0.5107	0.2960	0.7080	0.0925
EZ/E	0.4707	0.3320	0.5760	0.0579

TABLE IV. Pearson's correlations, for all the considered cases (N=432)

Var.	RI	ROA	N4	N1	SH
EC/E	**-0.1573**	0.0804	**-0.9654**	-0.0648	-0.0220
EW/E	**-0.1453**	**0.1533**	**-0.4681**	**-0.7310**	**-0.2167**
EZ/E	**0.1440**	**0.2893**	**-0.3721**	**-0.7769**	-0.0002

Luminaire class (CL) strongly determined the EC/E level (see Fig. 3). Use of direct lighting (CL I) enabled to get very low EC/E levels, within a narrow range (Mean=0.2367, Min=0.1540, Max=0.3440). The higher the class, the higher levels and wider range of the EC/E values were obtained. For CL II: Mean=0.5115 (Min=0.4260, Max=0.6500) and for CL III: Mean=0.8591 (Min=0.7220, Max=1.0960). The use of CL IV enables to get EC level higher than E level (Mean=1.3142, Min=1.1020, Max=1.6520).

Luminaire downward luminous intensity distribution (LID) strongly determined the EW/E level (see Fig. 4). Use of the widest distributions (LID 1) enabled to get relatively high EW/E levels: Mean=0.6169, Min=0.5380, Max=0.7080. For the narrower LID, the lower levels and wider range of the EW/E values were obtained. For LID 2: Mean=0.5198 (Min=0.4220, Max=0.6560) and for LID 3: Mean=0.4689 (Min=0.3460, Max=0.6260). Using the narrowest LID 4 enabled to get EW/E in the range between Min=0.2960 and Max=0.6060, with Mean=0.4371.

Luminaire downward luminous intensity distribution (LID) strongly determined the EZ/E level (see Fig. 5). The EZ/E changes were similar to that of the EW/E. The narrower LID, the lower levels and wider range of the EZ/E values were obtained. For LID1: Mean=0.5390 (Min=0.4740, Max=0.5760), for LID2: Mean=0.4806 (Min=0.4200, Max=0.5440), for LID3: Mean=0.4439 (Min=0.3700, Max=0.5260), and for LID4: Mean=0.4193 (Min=0.3320, Max=0.5160). The range of EZ/E values is narrower than the range of EW/E values.

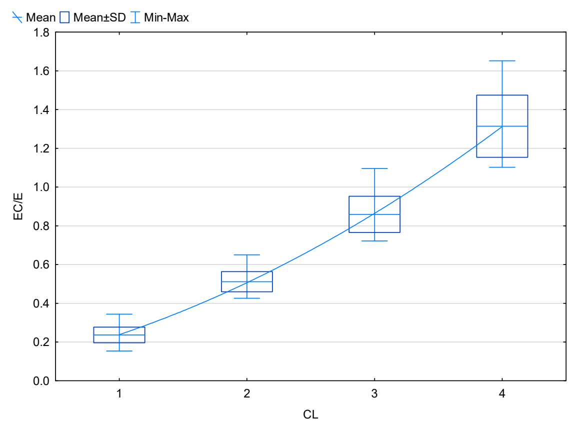

Fig. 3. EC/E distribution for the considered luminaire classes CL

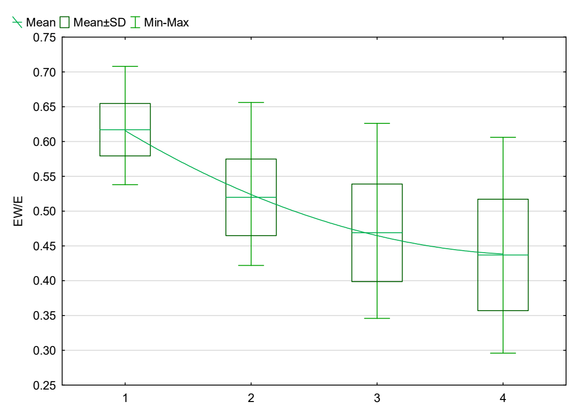

Fig. 4. EW/E distribution for the considered luminaire downward LID

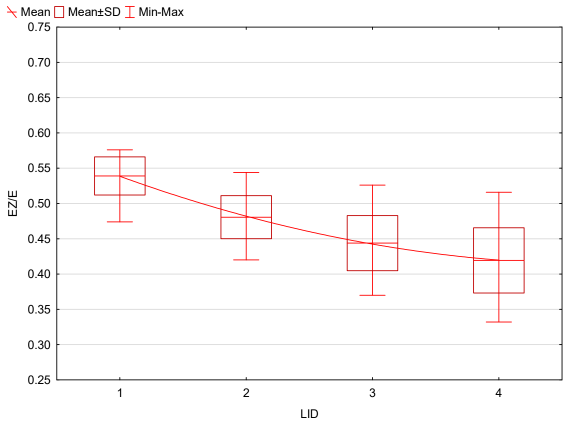

Fig. 5. EZ/E distribution for the considered luminaire downward LID

B. Average illuminances

In the second stage of the research, the maintained average illuminances EC, EW and EZ were calculated, for E levels: 100 - 150 - 200 - 300 - 500 - 750 - 1000 lx, for each of 432 lighting situations.

Fig. 6 shows the EC values for: E = 100 lx - designation EC (100), E = 150 lx - designation EC (150), E = 200 lx - designation EC (200), E = 300 lx - designation EC (300) and E = 500 lx - designation EC (500). The normative EC levels are marked with horizontal lines: 30 - 50 - 75 - 100 lx. Tab. V summarizes the percentage of cases meeting the normative EC levels for the analyzed E levels.

According to the requirements of the old standard [1], in 76% of cases the EC≥30 lx requirement was met for E=100 lx, and in 95% of cases the EC≥30 lx requirement was met for E=150. For levels of E≥200 lux, the requirement of EC ≥30 lux was always met. For the recommended level of EC ≥50 lx, this requirement was met in 63% of cases for E=100 lx, in 75% of cases for E=150 lx and in 85% of cases for E=200 lx. For levels of E≥300 lx, the recommendation EC≥ 50 lx was always fulfilled.

In total, according to the requirements of the old standard [1], in 96% of cases the EC≥30 lx requirement was met and in 91% of cases the EC≥50 lx recommendation was met.

According to the requirements of the new standard [2], in 76% of cases the EC≥30 lx requirement was met for E=100 lx, in 95% of the cases the EC≥30 lx requirement was met for E=150 lx, in 85% of the cases the requirement was met EC ≥ 50 lx for E=200 lx, in 85% of cases the EC ≥ 75 lx requirement was met for E=300 lx and in 95% of cases the EC ≥100 lx requirement was met for E=500 lx. In 100% of cases, the EC ≥ 100 lx requirement was met for E=750 lx and E=1000 lx.

In total, according to the requirements of the new standard [2], in 90% of cases the EC requirement was met.

Fig. 7 shows the EW values for: E = 100 lx - designation EW (100), E = 150 lx - designation EW (150), E = 200 lx - designation EW (200), E = 300 lx - designation EW (300) and E = 500 lx - designation EW (500). The normative EW levels are marked with horizontal lines: 50 - 75 - 100 - 150 lx. Tab. VI summarizes the percentage of cases meeting the normative EW levels for the analyzed E levels.

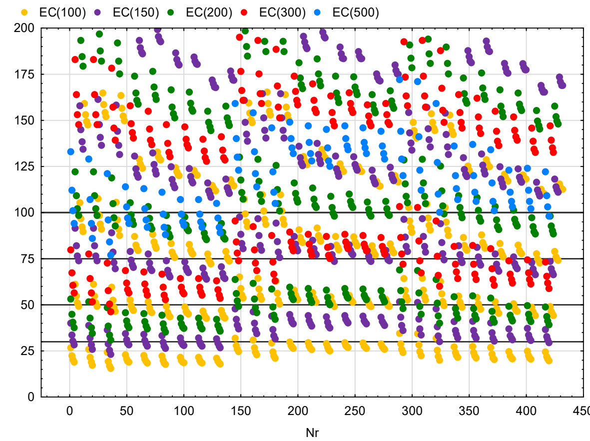

Fig. 6. EC distribution for E on task area: 100-150-200-300-500 lx

TABLE V. PERCENTAGES OF CASES MEETING THE REQUIRED EC FOR THE ANALYZED E ON TASK AREA

E [lx]	EC [lx]			
	30	50	75	100
100	76%	63%	48%	28%
150	95%	75%	63%	50%
200	100%	85%	75%	63%
300	100%	100%	85%	75%
500	100%	100%	100%	95%
750	100%	100%	100%	100%
1000	100%	100%	100%	100%

According to the requirements of the old standard [1], in 54% of cases the EW≥50 lx requirement was met for E=100 lx, and in 98% of cases the EW≥50 lx requirement was met for E = 150 lx. For levels of E≥200 lx, the requirement of EW ≥50 lux was always met. For the recommended level of EW ≥75 lx, this requirement was not met in any case for E=100 lx, in 54% of cases for E=150 lx and in 92% of cases for E=200 lx. For levels of E≥300 lx, the recommendation EW ≥75 lux was always fulfilled.

In total, according to the requirements of the old standard [1], in 92% of cases the EW≥50 lx requirement was met and in 82% of cases the EW≥75 lx recommendation was met.

According to the requirements of the new standard [2], in 54% of cases the EW≥50 lx requirement was met for E=100 lx, in 98% of cases the EW≥50 lx requirement was met for E=150 lx, in 92% of the cases the requirement EW≥75 lx was met for E = 200 lx and in 98% of cases the EW≥100 lx requirement was met for E = 300 lx. In 100% of cases, the EW ≥150 lx requirements were met for E=500 lx, E=750 lx and E = 1000 lx.

In total, according to the requirements of the new standard [2], in 91% of cases the EW requirement was met.

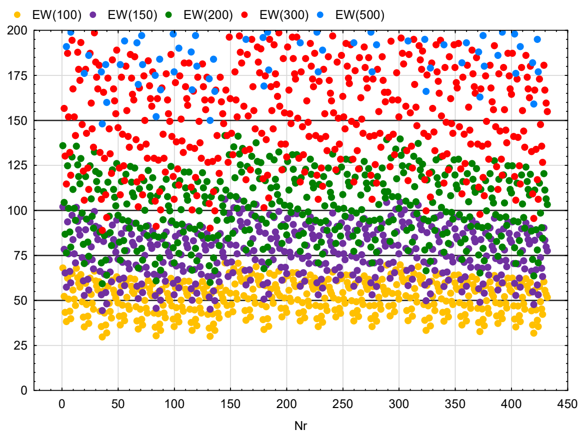

Fig. 7. EW distribution for E on task area: 100-150-200-300-500 lx

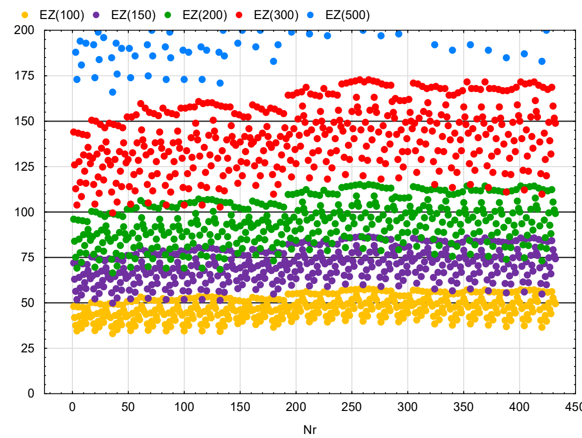

Fig. 8. EZ distribution for E on task area: 100-150-200-300-500 lx

TABLE VI. PERCENTAGES OF CASES MEETING THE REQUIRED EW FOR THE ANALYZED E ON TASK AREA

E [lx]	EW [lx]			
	50	75	100	150
100	54%	0%	0%	0%
150	98%	54%	3%	0%
200	100%	92%	54%	0%
300	100%	100%	98%	54%
500	100%	100%	100%	100%
750	100%	100%	100%	100%
1000	100%	100%	100%	100%

TABLE VII. PERCENTAGES OF CASES MEETING THE REQUIRED EZ FOR THE ANALYZED E ON TASK AREA

E [lx]	EZ [lx]			
	50	75	100	150
100	34%	0%	0%	0%
150	100%	34%	0%	0%
200	100%	95%	34%	0%
300	100%	100%	100%	34%
500	100%	100%	100%	100%
750	100%	100%	100%	100%
1000	100%	100%	100%	100%

Fig. 8 shows the EZ values for: E = 100 lx - designation EZ (100), E = 150 lx - designation EZ (150), E = 200 lx - designation EZ (200), E = 300 lx - designation EZ (300) and E = 500 lx - designation EZ (500). The normative EZ levels are marked with horizontal lines: 50 - 75 - 100 - 150 lx. Tab. 8 summarizes the percentage of cases meeting the normative EZ levels for the analyzed E levels.

According to the requirements of the old standard [1], in 34% of cases the EZ⩾50 lx requirement was met for E = 100 lx, and for E⩾150 lx levels, the EZ⩾50 lx requirement was always met. For the recommended level of EZ⩾150 lx, this recommendation was not met in any case for E=100 lx, E=150 lx and E=200 lx. In 34% of cases, the EZ ⩾ 150 lx recommendation was met for E=300 lx, and for E⩾500 lx levels, the EZ⩾150 lx recommendation was always met. In total, according to the requirements of the old standard [1], in 89% of cases the EZ⩾50 lx requirement was met, and in 56% of cases the EZ⩾150 lx recommendation was met.

According to the requirements of the new standard [2], in 34% of cases the EZ⩾50 lx requirement was met for E=100 lx, and in 100% of cases the EZ⩾50 lx requirement was met for E=150 lx. In 95% of cases, the requirement of EZ⩾75 lx was met for E=200 lx. In 100% of cases, the EZ⩾100 lx requirement was met for E = 300 lx, and also the EZ⩾150 lx requirement was met for E=500 lx, E=750 lx and E=1000 lx. In total, in accordance with the requirements of the new standard [2], in 88% of cases the EZ requirement was met.

C. Luminaire CL and LID limitations

In the third stage of the research, the CL and LID of luminaires were determined, at which obtaining the required ceiling, wall and cylindrical illumination in interiors, according to the new standard [2], was limited.

In the case of ceiling illumination, the use of CL II, III and IV always guaranteed the compliance with the normative EC requirement [2]. The use of CL I limited meeting the EC requirement, mainly for E=100 lx, but also for E=200 lx and E=300 lx. In some cases, it also limited meeting the EC requirement for E=150 lx and E=500 lx. The limitations for meeting the EC requirements are presented in Tab. VIII.

In the case of wall illumination, the use of LID 1 always guaranteed compliance with the normative EW requirement [2]. In the case of implementing the E levels 200 lx and higher, the use of LID 1 and LID 2 always guaranteed compliance with the normative EW requirement [2]. The use of LID 4 is the strongest limiting factor in meeting the EW requirement. The greatest limitation of meeting the EW requirement occurred for E=100 lx, for LID 4, but also for LID 3 and LID 2. For E levels between 150 lx and 300 lx, the limitation of meeting the requirement was not that strong. The use of CL I and II was less favorable than CL III and IV in meeting the EW requirement. The limitations for meeting the EW requirements are presented in Tab. IX.

TABLE VIII. LIMITATIONS FOR MEETING EC REQUIREMENTS IN GENERAL INTERIOR LIGHTING

E [lx]	Ceiling illumination
100	24% of cases do not meet the EC⩾30 lx requirement. This applies to almost all CL I luminaires use.
150	5% of cases do not meet the EC⩾30 lx requirement. This mainly applies to the CL I luminaires use, in rooms with RO 752.
200	15% of cases do not meet the EC⩾50 lx requirement. This applies to approx. 60% of cases where CL I luminaires are used.
300	15% of cases do not meet the EC⩾75 lx requirement. Same cases as for E=200 lx.
500	5% of cases do not meet the EC⩾100 lx requirement. Same cases as for E=150 lx.

TABLE IX. LIMITATIONS FOR MEETING EW REQUIREMENTS IN GENERAL INTERIOR LIGHTING

E [lx]	Wall illumination
100	46% of cases do not meet the EW⩾50 lx requirement. This applies to the LID 2 (CL I and II), and LID 3 and LID 4 (CL I, II and III) luminaires use
150	2% of cases do not meet the EW⩾50 lx requirement. This applies to the LID 4 (CL I) luminaires use.
200	8% of cases do not meet the EW⩾75 lx requirement. This applies to the LID 4 (CL I and II) and also LID 3 (CL I and II) luminaires use.
300	2% of cases do not meet the EW⩾100 lx requirement. Same cases as for E=150 lx.

TABLE X. LIMITATIONS FOR MEETING EZ REQUIREMENTS IN GENERAL INTERIOR LIGHTING

E [lx]	Cylindrical illumination
100	67% of cases do not meet the EZ⩾50 lx requirement. This applies to the LID 1 (in small rooms, RI=1.5), LID 2 and LID 3, and almost all LID 4 luminaires use.
200	5% of cases do not meet the EZ⩾75 lx requirement. This applies to LID 4 (CL I and II) luminaires use.

In the case of cylindrical illumination, the biggest problem of meeting the requirement (as in the case of wall and ceiling illumination) concerned the E levels of 100 lx and 200 lx, see Tab. X. The use of LID 4 was the strongest limiting factor in meeting the normative EZ requirement [2]. For E=100 lx, also the other distributions LID 3, LID 2 and LID 1 did not guarantee meeting the EZ requirement in most cases. The use of CL I and II was less favorable than CL III and IV in meeting the EZ requirement. The limitations for meeting the EZ requirements are presented in Tab. X.

D. Regression models

In the last stage of the research, the linear multiple regression models for dependent variables EC/E, EW/E and EZ/E were elaborated. The impact of independent variables RI, ROA, N4, N1 and SH was considered. ROA is the weighted average of the reflectances of ceiling, walls and floor, over the surface areas of these planes. N4 and N1 are the CIE luminous flux code the 4th and 1st indices, characterizing the luminaire class (CL) and downward luminous intensity distribution (LID) respectively.

Assuming a linear relationship between the considered variables, the models were developed with the use of the backward stepwise method of multiple regression. The final regression models are presented in Tab. XI for EC/E, in Tab. XII for EW/E and in Tab. XIII for EZ/E.

The bolded correlations were significant at $p<0.05$. On the basis of the results, it was found out that the developed linear regression models made it possible to explain around 96% of variability of EC/E, about 83% of variability of EW/E, and about 88% of variability of EZ/E. The values of the F statistics and the corresponding p probability levels confirmed the statistically significant linear relationships. In addition, the values of the t statistics indicated that intercepts and regression coefficients were significantly different from zero. The standard error of estimate did not exceed 0.09 for EC/E, 0.04 for EW/E and 0.03 for EZ/E. The developed multiple linear regression equations should enable a quick and practical prediction of relative EC, EW and EZ values based on the room, luminaire and luminaire layout parameters.

TABLE XI. REGRESSION SUMMARY FOR EC/E VARIABLE

N =432	R= .98029772 R2= .96098363 Adjusted R2= .96071015 F(3,428)=3513.9 p<0.0000 Std.Error of estimate: .08227					
	b*	Std. Err. of b*	b	Std. Err. of b	t(426)	p-value
Int.			**1.9196**	**0.0241**	**79.678**	**0.0000**
RI	**-0.1573**	**0.0096**	**-0.0533**	**0.0032**	**-16.476**	**0.0000**
N4	**-0.9654**	**0.0096**	**-1.4320**	**0.0142**	**-101.115**	**0.0000**
N1	**-0.0648**	**0.0096**	**-0.2169**	**0.0310**	**-6.790**	**0.0000**

TABLE XII. REGRESSION SUMMARY FOR EW/E VARIABLE

N =432	R= .91250573 R2= .83266671 Adjusted R2= .83070270 F(5,426)=423.96 p<0.0000 Std.Error of estimate: .03805					
	b*	Std. Err. of b*	b	Std. Err. of b	t(426)	p-value
Int.			**0.8647**	**0.0327**	**26.4123**	**0.0000**
RI	**-0.1113**	**0.0208**	**-0.0084**	**0.0016**	**-5.3486**	**0.0000**
SH	**-0.2205**	**0.0198**	**-0.0499**	**0.0045**	**-11.1166**	**0.0000**
N4	**-0.4644**	**0.0198**	**-0.1535**	**0.0066**	**-23.4148**	**0.0000**
N1	**-0.7300**	**0.0198**	**-0.5440**	**0.0148**	**-36.8820**	**0.0000**
ROA	**0.1112**	**0.0208**	**0.3081**	**0.0578**	**5.3356**	**0.0000**

TABLE XIII. REGRESSION SUMMARY FOR EZ/E VARIABLE

N =432	R= .93613065 R2= .87634059 Adjusted R2= .87518219 F(4,427)=756.51 p<0.0000 Std.Error of estimate: .02047					
	b*	Std. Err. of b*	b	Std. Err. of b	t(426)	p-value
Int.			**0.3976**	**0.0175**	**22.6959**	**0.0000**
RI	**0.2521**	**0.0179**	**0.0119**	**0.0008**	**14.1064**	**0.0000**
N4	**-0.3602**	**0.0170**	**-0.0746**	**0.0035**	**-21.1538**	**0.0000**
N1	**-0.7769**	**0.0170**	**-0.3628**	**0.0070**	**-45.6524**	**0.0000**
ROA	**0.3542**	**0.0179**	**0.6148**	**0.0310**	**19.8057**	**0.0000**

The final linear regression equations are given: Eq. 1 for EC/E, Eq. 2 for EW/E, and Eq. 3 for EZ/E respectively.

$$EC/E=1.91961-0.05325\cdot RI-1.43201\cdot N4-0.21694\cdot N1 \qquad (1)$$

$$EW/E=0.864654-0.008397 \cdot RI-0.049882 \cdot SH-0.153457 \cdot N4+-0.544981 \cdot N1+0.308108 \cdot ROA \quad (2)$$

$$EZ/E=0.397485+0.011911 \cdot RI-0.074571 \cdot N4-0.362839 \cdot N1++0.614776 \cdot ROA \quad (3)$$

V. Conclusions

For the analyzed general lighting solutions in interiors the largest dispersion of relative illuminances (in relation to E on the task area) occurred on the ceiling, substantially smaller on the walls and the smallest for the cylindrical illuminance on the reference plane.

Luminaire class CL had the biggest impact on the EC/E and luminaire downward luminous intensity distribution LID had the biggest impact on both the EW/E and EZ/E values.

In the analyzed lighting situations, in accordance with the requirements of the old standard [1], in 96% of cases the EC ⩾30 lx requirement was met, and in 91% of cases the EC⩾ 50 lx recommendation was met. On the other hand, in accordance with the requirements of the new standard [2], in 90% of cases the EC requirement was met.

In the analyzed lighting situations, in accordance with the requirements of the old standard [1], in 92% of cases the EW ⩾50 lx requirement was met, and in 82% of cases the EW⩾ 75 lx recommendation was met. On the other hand, in accordance with the requirements of the new standard [2], in 91% of cases the EW requirement was met.

In the analyzed lighting situations, in accordance with the requirements of the old standard [1], in 89% of cases the EZ ⩾50 lx requirement was met, and only in 56% of cases the E ⩾150 lx recommendation was met. On the other hand, in accordance with the requirements of the new standard [2], in 88% of cases the EZ requirement was met.

The use of CL I luminaires significantly reduced the fulfillment of the EC requirement [2] for E=500 lx level. The greatest limitations with meeting the EC requirement existed for E=100 lx, but also for E=200 lx and E=300 lx. The use of LID 4 luminaires reduced the fulfilment of the EW requirement [2] for E=300 lx. Also, the use of LID 3 luminaires, and to a lesser extent LID 2 luminaires, limited the fulfillment of the EW requirements for luminaires of CL I and CL II. The use of LID 4 luminaires also limited the fulfillment of the EZ requirement [2] for E=100 lx, and to a much lesser extent also for E=200 lx. For E=100 lx, also the LID 3, LID 2 and LID 1 luminaires did not guarantee the fulfillment of the EZ requirement in many cases.

The developed multiple linear regression models should enable a quick and practical prediction of average illuminances on the ceiling, walls and cylindrical on the reference plane, for general lighting in interiors.

References

[1] European Standard EN 12464-1:2011, Light and lighting – Lighting of work places – Part 1: Indoor work places, CEN, 2011.

[2] European Standard EN 12464-1:2021, Light and lighting – Lighting of work places – Part 1: Indoor work places, CEN, 2021.

[3] G. Newsham, C. Arsenault, J. Veitch, A.M. Tosco and C. Duval. "Task Lighting Effects on Office Worker Satisfaction and Performance, and Energy Efficiency," LEUKOS, vol. 1(4), pp. 7-26, 2005.

[4] A. de Vries, J. Souman, B. de Ruyter, I. Heynderickx, and Y. de Kort, "Lighting up the office: The effect of wall luminance on room appraisal, office workers' performance, and subjective alertness," Building and Environment, vol. 142, pp. 534-543, 2018.

[5] A. de Vries, I. Heynderickx, J. Souman, and Y. de Kort, "Putting the ceiling center stage – The impact of direct/indirect lighting on room appraisal," Building and Environment, vol. 201, pp. 107989, 2021.

[6] C. Cuttle, Lighting Design: A Perception-based Approach, Routledge, London, 2015.

[7] S. Słomiński, "Identifying problems with luminaire luminance measurements for discomfort glare analysis," Lighting Research & Technology, vol. 48(5), pp.573-588, 2016.

[8] W. Tantanatewin and V. Inkarojrit, "Effects of color and lighting on retail impression and identity," Journal of Environmental Psychology, vol. 46, pp. 197-205, 2016.

[9] K. Houser, M. Mossman, K. Smet and L. Whitehead, "Tutorial: Color Rendering and Its Applications in Lighting," LEUKOS, vol. 12(1-2), pp. 7-26, 2016.

[10] M. B. Kobav and M. Colarič, "Flicker experimental set up and visual perception of flicker," 2018 Seventh Balkan Conference on Lighting (BalkanLight), pp. 1-6, 2018.

[11] M. Helland, G. Horgen, T.M. Kvikstad, T. Garthus, J. R. Bruenech, and A. Aarås, "Musculoskeletal, visual and psychosocial stress in VDU operators after moving to an ergonomically designed office landscape," Applied Ergonomics, vol. 39(3), pp. 284-295, 2008.

[12] P. Pracki, "The impact of room and luminaire characteristics on general lighting in interiors,", Biluetyn, vol. 68(3), pp. 447-457, 2020.

[13] P. Pracki, M. Dziedzicki and P. Komorzycka, "Ceiling and Wall Illumination, Utilance, and Power in Interior Lighting," Energies, vol. 13(18), pp. 4744, 2020.

[14] P. Pracki and R. Krupiński, "Brightness and Uniformity Perception of Virtual Corridor with Artificial Lighting Systems," Energies, vol. 14(2), pp. 412, 2021.

[15] R.A. Mangkuto, "Validation of DIALux 4.12 and DIALux evo 4.1 against the Analytical Test Cases of CIE 171:2006," Leukos, vol. 12, pp. 139–150, 2016.

A Study of the Relationship Between Lighting Levels and Vehicle Speed

Lanlan Wei
University of Ljubljana
Faculty of Electrical Engineering
Ljubljana, Slovenia
lanlan.wei@fe.uni-lj.si

Grega Bizjak
University of Ljubljana
Faculty of Electrical Engineering
Ljubljana, Slovenia
grega.bizjak@fe.uni-lj.si

Matej Bernard Kobav
University of Ljubljana
Faculty of Electrical Engineering
Ljubljana, Slovenia
matej.kobav@fe.uni-lj.si

***Abstract*—The paper presents the results of two road experiments conducted over a year where vehicle speed was measured under different lighting conditions. On two roads, Parmova ulica and Zaloska cesta, with speed limits of 30 km/h and 50 km/h respectively, speed cameras were located to find out if the lighting level influences the speed of the vehicles. Both roads are located in Ljubljana, Slovenia. At both locations, a speed of a total of 4 191 956 vehicles (Parmova ulica: 2 777 591; Zaloska cesta: 1 414 265). There were 68 % cars, 17 % vans, 10 % trucks, 5 % semi-trucks. The analysis of average speed related to the lighting level is based on all detected vehicle data, excluding two-wheeled vehicles. Besides the speed and type of vehicle also daytime data (the data based on the time of sunrise and sunset) and weather data (the data based on the Centre for Meteorological Monitoring in Slovenia) were included to limit the analysis to the nighttime without rain.**

Results obtained on the first road (Parmova ulica, speed limit 30 km/h) show that the speed of the vehicles has been slightly reduced by reducing the level of lighting. When the level of lighting was first reduced from 100 % luminance (road lighting standard is M4 (EN 13201)) to 80 % luminance average speed decreased from 33.32 km/h to 31.68 km/h. After the second reduction of luminance level from 80 % to 60 %, the average speed dropped again from 31.68 km/h to 31.93 km/h. The observed decrease in speed was slightly more pronounced when the lighting level was reduced from 100 % to 80 %, and not so much with the lighting level reduction from 80 % to 60 %. In this case, the speed camera was positioned near traffic lights and intersections with speed bumps.

The results obtained on a second road (Zaloska cesta, speed limit 50 km/h) show that the vehicle speed was not following the trend observed in the first location. Also here the lighting level was modified in the same way as at the Parmova ulica first from 100 % to 80 % luminance and then from 80 % to 60 % luminance. With these three lighting levels (100 %, 80 %, 60 %), the measured average speed was 50.74 km/h, 50.05 km/h and 50.68 km/m respectively. The speed on this road does not show the same trend as on the other road, and the changes between the three lighting levels are small to negligible. In this second experiment, the speed camera was placed on a road with no intersections but with pedestrian crossing with traffic lights. All obtained speed differences are statistically significant ($p \leqslant 0.001$).

Keywords*—*Road lighting, Luminance levels, Vehicle speed

I. Introduction

A. *Effect of road lighting on vehicle speed and road accidents*

Some comparisons of vehicle speed between daytime and night time in literature gave mixed results: higher speed in daytime compared to night time, vehicle speed at daytime higher by approximately 3 % compared with dark time [1], lower speed during the day [2], or no difference [3]. A study conducted in Sweden at 25 locations showed that analysis of vehicle speed and speed differences between daylight, twilight, and darkness, with and without street lighting, revealed no differences attributable to lighting conditions [4]. Another study showed that the average speed was decreased under low illumination, but the decrease was not significant compared to the decrease caused by the loss of visual recognition because of other reasons such as age [5].

A study on road safety has estimated that between 750 and 880 thousand people die each year in road accidents and that between 23 and 34 million are injured. 14 % of these deaths take place in Europe, and 86 % occur outside Europe, with Asia accounting for nearly half the total [6]. The risk of accidents increases significantly with darkness [7]. Many studies have proved that road lighting improves the visual environment of drivers and pedestrians at night, reducing the number and frequency of traffic accidents [8]. On the other hand, studies have also shown that there is no evidence that a reduction in lighting levels is associated with road traffic injuries at night [9]. Some studies even showed that brighter lamps may compromise safety rather than reduce harm [10].

On the other hand, a fast-moving vehicle requires a longer stopping distance than a slow-moving vehicle [11], and better lighting conditions help the driver to better assess distance with surroundings. Higher luminance increases visual acuity and helps to see small details [12]. Properly designed lighting environments contribute to better visual acuity.

B. *Effect of posted speed limit on vehicle speed*

Results of a study [13] show that the speed limit has a high correlation with the average speed of traffic flow. With the speed limits of 80 km/h, 100 km/h and 120 km/h, the coefficients of determination are as high as 0.84, 0.85 and 0.92 respectively. In a free-flow state, when the posted speed limit is increased the average speed also increases by approximately the same magnitude. The mentioned posted speed limit values correspond to the 90, 88 and 97 percentile speeds of the traffic flow, respectively. The other study examined the effect of posted speed limit changes on free-flow speed on urban roads. The posted speed limit was changed from 50 km/h to 40 km/h or 60 km/h. The results showed that a decreased posted speed limit (50 km/h to 40 km/h) caused a small (1.6 km/h) but significant decrease in mean free-flow speed and speed dispersion, while increasing the speed limit (50 km/h to 60 km/h) resulted in a 2.6 km/h increase in mean free-flow speed but in no change in speed dispersion [14].

C. *Effect of weather on vehicle speed*

The effect of road lighting on vehicle speed is not a critical factor compared to other parameters such as rain, snow, fog [4], the posted speed limit and traffic density [14], [13], etc.. One study suggests that when roads are covered with snow, lighting output can be reduced to meet lighting standards and reduce energy consumption [15], however, it is unclear how this affects traffic accidents.

D. *General hypotheses*

Using the proper lighting level can lead to unnecessary energy consumption while providing the best possible safety [16], [17]. As our review of past research has revealed, the effect of road lighting on speed is uncertain, and if the environment is dark, drivers may reduce their speed and improve their concentration, especially when visibility is low on urban roads. Considering that in the urban areas the speed limit is 50 km/h on main roads and 30 km/h on some secondary roads or within conflict areas, the question arises whether a change in lighting levels will affect the speed of vehicles at a prescribed speed limit?

In this paper, we used vehicle speed data recorded continuously for 12 months at 2 locations in Ljubljana urban area for the period from June 2020 to May 2021. A total the speed of 43 053 928 (Parmova ulica: 41 639 663; Zaloska cesta: 1 414 265) vehicles were measured. The analysis of lighting levels and speed relation is based on all detected vehicle data, excluding two-wheelers. The data analysis focuses mainly on the relationship between lighting levels and speed, the speed difference between daytime and nighttime, and the effects of speed limits on the vehicles' speed. The speed difference between wet and dry pavements was not taken into account, so the data studied and analysed do not include data on wet pavements.

II. MATERIAL AND METHODOLOGY

A. *Experiment location description*

In this study, the speed of vehicles was investigated in two different locations: Road 1 is Parmova ulica with a single lane in both directions, each lane is 3.5 m wide, and there is a bicycle lane on both sides of this road (Fig. 1). Road 2 is Zaloska cesta with two lanes in both directions, each lane is 3.5 m wide, and the bicycle lane is separated from the vehicle road with a green stripe (Fig. 2). The speed limit on Road 1 where the camera was located was 30 km/h at the time of our experiment and the speed limit on Road 2 is 50 km/h.

Fig. 1. Parmova ulica (Road 1), with a speed limit of 30 km/h, Ljubljana, Slovenia. © google map

Fig. 2. Zaloska cesta (Road 2), with speed limit of 50 km/h, Ljubljana, Slovenia. © google map

Road 1 is classified as a class M4 road (based on CEN/TR 13021-1) with a recommended maintained luminance of L_{ave} = 0.75 cd/m². The road lighting consists of LED lamps with 90 W, the colour temperature is 3000 K, and Ra is 75. Road 2 is classified as a class M3 road with a recommended luminance of L_{ave} = 1.00 cd/m². The road lighting consists of HP Sodium lamps with 150 W.

We used three different luminance levels: 1.0 (full lumen output), 0.8 (80 % lumen output) and 0.6 (60 % lumen output) in our study. The levels were set on the LED driver and the luminance levels were not measured.

B. *Data collection*

Data structure and processing are shown in Fig. 3. There are four groups of main related variables, including traffic volume, road lighting level, precipitation, sunrise and sunset time.

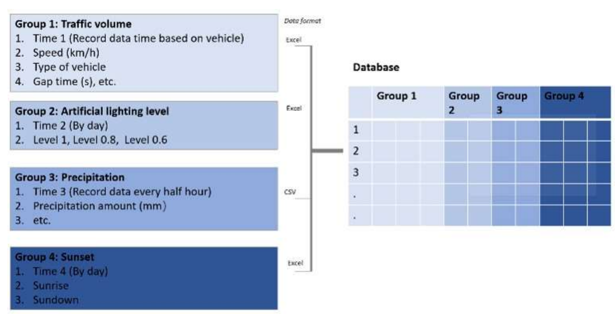

Fig. 3. Data structure and process of merging

The first set of data comes from a speed camera. The brand of the speed camera is VIACOUNT II. The camera captures and records the data on speed, vehicle types (car, semi-truck, truck, van, two-wheeler), vehicle length, gap time, etc. The lighting level data includes the output level of road lighting: 1.0, 0.8 or 0.6. We opted for data from June 2020 to May 2021, with a duration of approximately 12 months on each road. Weather data is data about precipitation, which is recorded every half hour on the website of the Slovenian Meteorological Monitoring Department (SMMD). The data comes from the weather station Ljubljana Bezigrad, which is located 1 km away from Road 1, and 6 km away from Road 2. Weather data are recorded locally in a half-hourly interval, and precipitation is measured in mm. The fourth group of data set contains sunrise and sunset times. Both times were calculated using Excel and based on the geographic location of the speed camera. The calculation formula was based on data from NOAA Solar Calculator.

In this study, lighting conditions are divided into 'daytime' and 'nighttime'. The 'daytime' is defined as the time between sunrise and sunset. The 'nighttime' is defined as the time between sunset and sunrise and includes three road lighting levels: 1.0, 0.8, and 0.6.

C. *Data analysis*

Before analysis, we checked the distribution of the vehicle speed data to ensure that there was an approximately normal distribution. To test the difference in vehicle speed at different lighting levels and to determine if there is a significant difference between daytime and nighttime, the first step is to analyse the variance of each parameter, and then the Tukey-Kramer HSD test is used to compare the differences between lighting levels.

Since vehicle speed is inevitably affected by vehicle density, only vehicles with a gap time greater than 6 seconds are used in this study to ensure that traffic data, used for analysis, is under free-flow conditions [18]. The gap time is the distance between the rear end of the vehicle and the front end of the next vehicle, which is used to describe the distance between the two vehicles.

III. RESULTS AND DISCUSSIONS

A. *Road 1, Parmova unica*

a. *General distribution of vehicle speed*

Overall, the passenger cars (N = 2 285 661, 82.3 % of total) had the highest average speed of 32.04 km/h (SD = 8.29), vans (N = 338 298, 12.2 % of total) had the second highest average speed of 30.32 km/h (SD = 7.67), trucks (N = 101 521, 3.7 % of total) had the average speed of 29.31 km/h (SD = 7.37), and semi-trucks (N = 52 111, 1.8 % of total) had the lowest average speed of 28.09 km/h (SD = 5.30). The speed limit had the significant impact on all types of vehicles. The highest average speed (passenger cars) was 32.04 km/h, which is 6.8 % above 30 km/h, and the lowest average speed (semi-trucks) was 28.09 km/h, which is 3.4 % below 30 km/h speed limit.

b. *Correlation between lighting level and vehicle speed*

In general, when we check all the nighttime vehicle data (considering all four types of vehicles in one group) speed could be correlated with lighting levels. One-way ANOVA analysis showed that the differences in average speed at three lighting levels were significant. Table I presents the average speed under the three lighting levels, the data include all the nighttime data with the vehicle gap time > 6 s. The results of speed distribution under three lighting levels showed that there were significant differences in speed between lighting levels 1.0 and 0.8 and between 1.0 and 0.6 (*p-value* < 0.0001). Table II shows details of paired differences between lighting levels and vehicle speed. For vans, the average difference in speed between levels 1.0 and 0.8 was 3.26 km/h and between levels 1.0 and 0.6 was 3.11 km/h. For trucks, these differences were 1.46 km/h (between levels 1.0 and 0.6) and 1.39 km/h (between levels 1.0 and 0.8) respectively. Even smaller differences were obtained for cars between levels 1.0 and 0.8 was 1.30 km/h, and between levels 1.0 and 0.6 was 1.26 km/h. For semi-trucks, the average difference in speed between levels 1.0 and 0.6 was 1.46 km/h and for levels 1.0 and 0.8 was 1.39 km/h. These difference pairs have a *p-value* < 0.0001. For the other pairs, the differences are not statistically significant. Mostly, the average speed difference between levels 0.8 and 0.6 is not significant except for semi-trucks. The average speed of passenger cars was 35.16 km/h at 1.0 light level, and the speed decreases by 4 % at 0.8 level. This change caused the largest decrease in the speed of vans from 35.25 km/h to 31.99 km/h (10 % decrease).

To exclude the influence of high traffic volume, pedestrians, cyclists, etc. on the speed of vehicles, we repeated the analyses on the data from 22:00 to 23:00 only. As shown in Table II, only $p < 0.0001$ was obtained between levels 1.0 and 0.6 with trucks, where the difference is 5.82 km/h. The other comparisons of the speed differences give *p-values* greater than 0.0001, which means there is no statistical difference.

In summary, from the analysis of the two sets of data, the first data set reveals that the lighting levels have a certain impact on the speed. If the lighting level decreases (from 1.0 to 0.8 or from 1.0 to 0.6), the speed also decreases. However, when we extract a small amount of data at a specific time (22:00 – 23:00), this effect almost does not exist (Table II).

c. *The difference in speed between day and nighttime*

We first compare day to night time differences using all the data with a gap time > 6 s. Analysis of the one-way ANOVA shows that the average speed of passenger cars at night time is 34.00 km/h (SD =8.24) and during the day, the average speed is 31.51 km/h (SD =8.22). Night time speed is 8 % higher than daytime. The average speed of vans at night is 32.50 km/h (SD =7.93) and is 9 % higher than during the day (29.73 km/h, SD =7.49). Similarly, the nighttime speed of trucks is 6 % higher than daytime speed and with Semi-trucks, the speed at night is 2 % higher than during the day. All types of vehicles in the data show that their daytime speeds are lower than at night time.

The low speed during the day may be due to the high residential density around this road. This means more cyclists and pedestrians on the sidewalk and the bicycle lanes which are close to the vehicle paths. In addition, the data distribution shows the traffic density in this area during the day is more than twice that during the night.

To test that the low speed during the day may be caused by large traffic volume and driver habits, we compared the data within the same period from 17:00 to 18:00 in the week before the 2020 winter time change (October 7, 2020, to October 13, 2020) and in the week after (November 21, 2020, to November 27, 2020). As shown in Fig. 4, the blue bar represents the average speed at night time, the red bar represents the speed during daytime. In general, the speed during the nighttime is higher than during the daytime. The biggest speed difference is with semi-trucks, which are at night about 10 % faster. The difference is the smallest with the trucks, which are at nighttime about 5 % faster than at daytime. This further reinforces the previous conclusion that all types of vehicles have lower daytime speeds than nighttime speeds on this road.

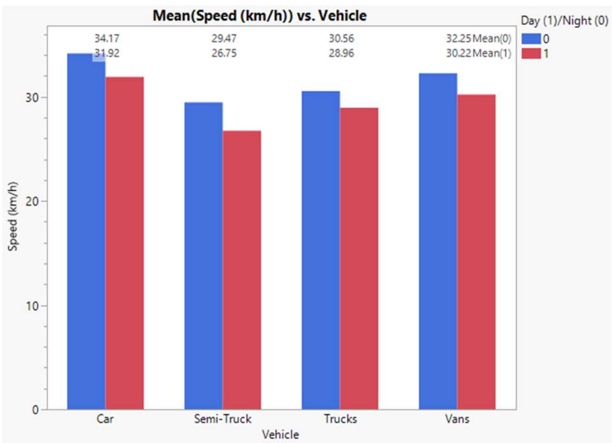

Fig. 4. Distribution of nighttime and daytime speed (only data with gap time greater than 6 s, the data from 17:00 to 18:00)

B. *Road 2, Zaloska cesta*

a. *General distribution of vehicle speed*

On this road, the passenger cars (N = 558 989, 41% of total) have the average speed of 50.66 km/h (SD = 9.97), average speed of vans (N = 367428, 23 %) is 50.23 km/h (SD = 8.63), and of trucks (N=332 588, 27 %) is 48.07 km/h (SD = 9.02). Semi-trucks (N = 155 260, 10 %) have the lowest average speed of 43.77 km/h (SD=12.32).

b. *Correlation between lighting level and vehicle speed*

One-way analysis of the correlation between speed and lighting level considering all types of vehicles shows that speed changes with lighting level. A significant difference in speed ($p < 0.001$) was found for passenger cars with all pairs of lighting level changes (from 1.0 to 0.8, from 1.0 to 0.6, and from 0.8 to 0.6) With semi-trucks, trucks and vans the significant difference with *p-value* > 0.0001 was found only at the change of lighting level from 1.0 to 0.8. The results are presented in Table III. The speed of passenger cars increased by 3 % (from 51.13 km/h to 52.64 km/h) when the lighting level was decreased from 1.0 to 0.6. Trucks and vans show the same trend. Semi-trucks show different trends. When the lighting level drops from 1.0 to 0.6, the speed of the semi-truck decreases by 6 % from 43.99 km/h to 41.38 km/h. Table IV shows details of the effects of lighting levels and vehicle speeds together with the *p-value.*

Additional analysis was made also for this road. The data were extracted, and only the data from 22: 00 to 23: 00 were analysed to avoid the influence of congestion, pedestrians and cycling on the results. As shown in Table IV, the only $p < 0.0001$ was found at a change in lighting level from 1.0 to 0.6 with cars (difference = 2.34 km/h), trucks (difference = 1.76 km/h), and vans (difference = 1.81 km/h).

c. *The difference in speed between day and nighttime*

Using the same method as for Road 1, only the vehicles with a gap time > 6 s were analysed. Single-factor analysis of variance showed that the average speed of passenger cars during the day was 52.13 km/h (SD = 10.71), and the average speed at night was 51.29 km/h (SD = 11.43), which gives a 1.6 % decrease. The average daytime speed of the trucks was 50.40 km/h (SD = 9.68), and the nighttime speed was 48.54 km/h (SD = 10.36, 3.7 % decrease). The speed of vans was 52.18 km/h during the daytime (SD = 8.81) and 51.33 km/h at night (SD = 9.10, 1.6 % decrease). The average speed of semi-trucks was 42.15 km/h (SD = 14.68) in the daytime and 39.79 km/h at night (SD = 15.27, 6 % decrease).

Additional analysis was done comparing the data within the period from 17:00 to 18:00 in the week before the 2020 winter time change (October 7, 2020, to October 13, 2020) and in the week after (November 21, 2020, to November 27, 2020). As shown in Fig. 5, the speed of all types of vehicles is higher in the daytime than at night.

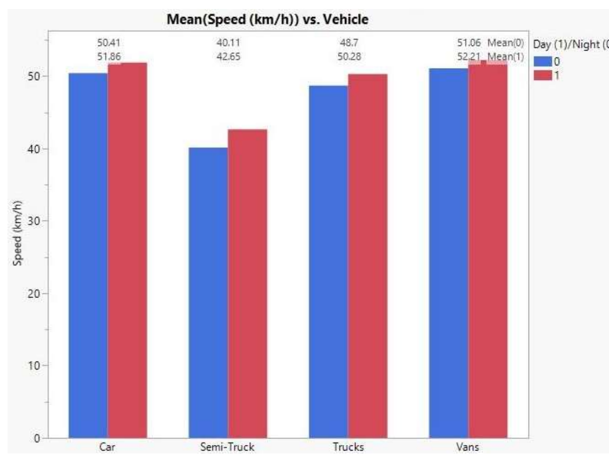

Fig. 5. Distribution of nighttime and daytime speed (only data with gap time greater than 6 s, the data from 17:00 to 18:00)

IV. CONCLUSION

In this study, the traffic speed data, obtained on two different roads in Ljubljana urban area in one year, were analysed. the results can be summarized in the following conclusions:

a. Vehicle speed always depends on the maximum speed limit. Both roads with a speed limit of 30 km/h and 50 km/h confirmed this result.

b. Vehicle speed is not always lower at night than in the daytime. Results from Road 1 (speed limit 30 km/h, bicycle lanes on both sides) indicate that nighttime speeds are higher than daytime. On the other hand, results from Road 2 (speed limit 50 km/h, two lanes, dual carriageway separated with median strip, bike path separated from the carriageway by a green lane) show higher speeds during the day.

TABLE I. SPEED DISTRIBUTION UNDER THREE LIGHTING LEVELS (ROAD 1)

Name of the road	Type of the vehicle	Lighting level 1.0			Lighting level 0.8			Lighting level 0.6		
		Number	Average speed (km/h)	SD	Number	Average speed (km/h)	SD	Number	Average speed (km/h)	SD
Road 1, Parmova ulica all nighttime data	Cars	473680	35.16	8.32	4722245	33.89	8.28	2454562	33.86	8.08
	Semi-Trucks	21572	29.39	4.33	179188	29.08	4.79	94746	27.83	4.66
	Trucks	44980	31.86	6.50	239007	30.46	7.00	148070	30.39	6.84
	Vans	110202	35.25	7.56	591683	31.99	7.92	331832	32.15	7.78
Road 1, Parmova ulica 22:00 - 23:00 data	Cars	2104	35.49	8.18	4843	35.83	8.50	1744	36.29	8.50
	Semi-Trucks	12	27.33	13.07	27	25.22	6.97	38	18.53	6.73
	Trucks	136	34.03	7.11	116	29.86	8.81	56	28.21	9.16
	Vans	666	34.58	6.46	508	33.04	8.38	200	33.91	9.32

TABLE II. PAIRED COMPARISON OF VEHICLE SPEED DIFFERENCES UNDER ALL THREE LIGHTING LEVELS (ROAD 1)

Name of the road	Type of the vehicle	Lighting level	All night data			22:00 - 23:00 data		
			Difference in average speed	Std Err Dif	p-Value	Difference in average speed	Std Err Dif	p-Value
Road 1, Parmova ulica	Cars	1.0 - 0.8	1.30	0.08	<0.0001	0.35	0.22	0.258
		1.0 - 0.6	1.26	0.07	<0.0001	0.80	0.27	0.010
		0.8 - 0.6	0.03	0.04	0.631	0.45	0.24	0.131
	Semi-Trucks	1.0 - 0.8	0.31	0.18	0.212	2.11	2.80	0.453
		1.0 - 0.6	1.56	0.19	<0.0001	8.81	2.67	0.002
		0.8 - 0.6	1.25	0.10	<0.0001	6.70	2.03	0.002
	Trucks	1.0 - 0.8	1.39	0.20	<0.0001	4.17	1.03	0.000
		1.0 - 0.6	1.46	0.21	<0.0001	5.82	1.30	<.0001
		0.8 - 0.6	0.07	0.13	0.842	1.65	1.33	0.431
	Vans	1.0 - 0.8	3.26	0.15	<0.0001	1.54	0.45	0.002
		1.0 - 0.6	3.11	0.16	<0.0001	0.67	0.62	0.528
		0.8 - 0.6	0.16	0.10	0.228	0.87	0.64	0.361

TABLE III. SPEED DISTRIBUTION UNDER THREE LIGHTING LEVELS (ROAD 2)

Name of the road	Type of the vehicle	Lighting level 1.0			Lighting level 0.8			Lighting level 0.6		
		Number	Average speed (km/h)	SD	Number	Average speed (km/h)	SD	Number	Average speed (km/h)	SD
Road 2, Zaloska cesta all nighttime data	Cars	7647	51.13	11.36	17319	51.78	11.08	26902	52.64	10.24
	Semi-Trucks	1777	43.99	13.94	3925	42.55	14.56	6210	41.38	14.91
	Trucks	4900	49.82	9.95	11352	49.89	9.69	16092	50.95	9.56
	Vans	6386	51.70	8.91	14147	51.80	8.98	21109	52.59	8.65
Road 2, Zaloska cesta 22:00 - 23:00 data	Cars	1842	50.71	10.88	1717	51.97	10.31	2771	53.05	9.74
	Semi-Trucks	289	38.60	14.33	305	37.60	15.09	602	38.56	13.67
	Trucks	951	48.07	9.92	805	49.62	9.31	1295	49.83	8.78
	Vans	1395	50.89	8.74	1347	52.02	8.34	2123	52.71	8.23

TABLE IV. PAIRED COMPARISON OF VEHICLE SPEED DIFFERENCES UNDER ALL THREE LIGHTING LEVELS (ROAD 2)

Name of the road	*Type of the vehicle*	*Lighting level*	*All night data*			*22:00 - 23:00 data*		
			Difference in average speed	*Std Err Dif*	*p-Value*	*Difference in average speed*	*Std Err Dif*	*p-Value*
Road 2, Zaloska cesta	***Cars***	**1.0 - 0.8**	0.65	0.15	<0.0001	1.26	0.34	0.001
		1.0 - 0.6	1.50	0.14	<0.0001	2.34	0.31	<.0001
		0.8 - 0.6	0.86	0.10	<0.0001	1.08	0.31	0.002
	Semi-Trucks	**1.0 - 0.8**	1.44	0.42	0.001	1.00	1.17	0.666
		1.0 - 0.6	2.61	0.39	<0.0001	0.04	1.02	0.999
		0.8 - 0.6	1.17	0.30	<0.0001	0.96	1.00	0.598
	Trucks	**1.0 - 0.8**	0.07	0.17	0.675	1.54	0.44	0.002
		1.0 - 0.6	1.13	0.16	<0.0001	1.76	0.40	<.0001
		0.8 - 0.6	1.06	0.12	<0.0001	0.21	0.42	0.865
	Vans	**1.0 - 0.8**	0.10	0.13	0.744	1.12	0.32	0.001
		1.0 - 0.6	0.89	0.13	<0.0001	1.81	0.29	<.0001
		0.8 - 0.6	0.79	0.10	<0.0001	0.69	0.29	0.047

c. Changes in lighting level (from 100 % output to 80 %, and then to 60 %) caused only minor or no change in vehicle speed.

Road lighting changes the visual environment. The construction of road lighting is justified by an improved vision and better visibility which should contribute to road traffic safety. The current road lighting standardizations and regulations define lighting level as a function of various influencing factors, including speed. However, our results show that in urban speed limit areas (30 km/h, 50 km/h), lighting level has almost no effect on drivers' habits or at least on the speed of driving. This means that, even with the reduced lighting level, the visual performance is good enough to provide drivers with enough confidence at a speed close to the speed limit. It might so be necessary to rethink the use of vehicle speed or its limits as a weight in lighting level selection in road lighting standards.

In the next step of further research, we plan to place the speed detectors in other locations. We plan to choose the surrounding environment with fewer factors affecting the speed, and further explore the influence of lighting level on the speed.

V. FUNDING

This work was supported by a Slovenian Research Agency ARRS as a part of the research program Electric Power Systems, P2-356.

VI. ACKNOWLEDGEMENT

The authors would like to thank the company Javna Razsvetljava d.d., which took care of reducing the luminous flux of luminaires on Parmova ulica and Zaloska cesta during the research period.

VII. REFERENCES

[1] T. Assum, T. Bjørnskau, S. Fosser, and F. Sagberg, “Risk compensation， the case of road lighting,” *Accid. Anal. Prev.*, vol. 31, no. 5, pp. 545–553, 1999, doi: 10.1016/S0001-4575(99)00011-1.

[2] M. Bassani and G. Mutani, “Effects of environmental lighting conditions on operating speeds on Urban Arterials,” *Transp. Res. Rec.*, no. 2298, 2012, doi: 10.3141/2298-09.

[3] Ridwan B. Quaium, “A comparison of vehicle speed at day and night rural horizontal curves,” Virginia Polytechnic Institute and State University, USA, 2010.

[4] A. K. Jägerbrand and J. Sjöbergh, “Effects of weather conditions, light conditions, and road lighting on vehicle speed,” *Springerplus*, vol. 5, no. 1, 2016, doi: 10.1186/s40064-016-2124-6.

[5] D. A. Owens, J. M. Wood, and J. M. Owens, “Effects of age and illumination on night driving: A road test,” *Hum. Factors*, vol. 49, no. 6, pp. 1115–1131, Dec. 2007, doi: 10.1518/001872007X249974.

[6] “Road transport lighting for develping countries,” 2007, Accessed: May 25, 2022. [Online]. Available: http://www.cie.co.at/.

[7] Ö. Johansson, P. O. Wanvik, and R. Elvik, “A new method for assessing the risk of accident associated with darkness,” *Accid. Anal. Prev.*, vol. 41, no. 4, pp. 809–815, Jul. 2009, doi: 10.1016/J.AAP.2009.04.003.

[8] F. R. Beyer and K. Ker, “Street lighting for preventing road traffic injuries,” *Cochrane Database Syst. Rev.*, no. 1, 2009, doi: 10.1002/14651858.CD004728.PUB2/INFORMATION/EN.

[9] C. Perkins *et al.*, “What is the effect of reduced street lighting on crime and road traffic injuries at night? A mixed-methods study,” *Public Heal. Res.*, vol. 3, no. 11, pp. 1–108, Sep. 2015, doi: 10.3310/phr03110.

[10] P. Marchant, J. D. Hale, and J. P. Sadler, “Does changing to brighter road lighting improve road safety? Multilevel longitudinal analysis of road traffic collision frequency during the relighting of a UK city,” *J. Epidemiol. Community Health*, vol. 74, no. 5, pp. 467–472, May 2020, doi: 10.1136/JECH-2019-212208.

[11] J. L. Nasar and S. Bokharaei, “Lighting modes and their effects on impressions of public squares,” *J. Environ. Psychol.*, vol. 49,

2017, doi: 10.1016/j.jenvp.2016.12.007.

[12] J. L. Nasar and S. Bokharaei, “Impressions of Lighting in Public Squares After Dark,” *Environ. Behav.*, vol. 49, no. 3, pp. 227–254, Apr. 2017, doi: 10.1177/0013916515626546.

[13] C. Gao, J. Xu, Q. Li, and J. Yang, “The effect of posted speed limit on the dispersion of traffic flow speed,” *Sustain.*, vol. 11, no. 13, 2019, doi: 10.3390/su11133594.

[14] A. P. Silvano and K. L. Bang, “Impact of speed limits and road characteristics on free-flow speed in urban areas,” *J. Transp. Eng.*, vol. 142, no. 2, 2016, doi: 10.1061/(ASCE)TE.1943-5436.0000800.

[15] A. Ekrias, M. Eloholma, and L. Halonen, “Analysis of road lighting quantity and quality in varying weather conditions,” *LEUKOS - J. Illum. Eng. Soc. North Am.*, vol. 4, no. 2, pp. 89–98, 2007, doi: 10.1582/LEUKOS.2007.04.02.001.

[16] U.S. Department Transportation, “Guidelines for the Implementation of Reduced Lighting on Roadways,” no. June, pp. 1–46, 2014.

[17] A. Peña-García, A. Hurtado, and M. C. Aguilar-Luzón, “Impact of public lighting on pedestrians’ perception of safety and well-being,” *Saf. Sci.*, vol. 78, 2015, doi: 10.1016/j.ssci.2015.04.009.

[18] K. Vogel, “What characterizes a ‘free vehicle’ in an urban area?,” *Transp. Res. Part F Traffic Psychol. Behav.*, vol. 5, no. 1, pp. 15–29, 2002, doi: 10.1016/S1369-8478(02)00003-7.

Simulating CIE LED Illuminants With a Low-Cost Six-Channels LED System

Maria Tejada-Casado
Department of Optics
University of Granada
Granada, Spain
mariatejadac@ugr.es

Luvin M. Ragoo
Department of Computer Science
Norwegian University of Science and Technology
Gjøvik, Norway
luvin.m.ragoo@ntnu.no

Luis Gómez-Robledo
Department of Optics
University of Granada
Granada, Spain
luisgrobledo@ugr.es

Manuel Melgosa
Department of Optics
University of Granada
Granada, Spain
mmelgosa@ugr.es

***Abstract*— A low-cost (below 250 Euros) tunable light source has been built from six commercially available LEDs, one white plus five colored (blue, cyan, lime, amber and red) with peaks at 450, 515, 569, 595 and 635 nm, and average ± standard deviation Full Width at Half Maximum of 38 ± 35 nm. Since each LED intensity can be adjusted independently, our system allows simulations of the relative spectral power distributions (SPDs) of different illuminants or light sources. The specific objective of the current work is to report on the accuracy of the simulations of the nine LED illuminants recently proposed by the International Commission on Illumination (CIE) using our system. We have developed two different methods to obtain the optimal intensities of the six LEDs such that the combined output would match each one of the nine LED illuminants proposed by the CIE: One based on spectral match and the other based on colorimetric match. Our algorithms started with measurements of the SPDs of each one of the six LEDs (380-780 nm at steps of 1 nm) from minimum to maximum intensities at 10% intervals, and used constrained non-linear optimizations, looking for minimization of two spectral metrics, in the case of the spectral method, and minimization of differences in CIE 1931 *x,y* chromaticity coordinates, in the case of the colorimetric method. The performance of our system in comparison with CIE LED illuminants can be measured as average differences ± standard deviations of the values of the following parameters: Root Mean Square Error (RMSE), Goodness-of-fit (GFC) coefficient of normalized (*Y*=100) SPDs, distance in the CIE *u'v'* chromaticity system, general CIE color rendering index (R_a), CIE 2017 color fidelity index (R_f), and correlated color temperature (CCT). Specifically, the averages ± standard deviations between the values of parameters obtained from our system and those of the CIE LED illuminants (in this order) were as follows: RMSE 0.3645 ± 0.2473 and 0.4276 ± 0.2492; GFC 0.8793 ± 0.1183 and 0.8434 ± 0.1341; CIE *u'v'* distances 0.0037 ± 0.0062 and 0.0009 ± 0.0019; R_a index 8.2 ± 5.9 and 8.7 ± 2.8; R_f index 8.0 ± 3.9 and 8.4 ± 2.4; CCT 130 ± 411 K and 15 ± 24 K, for our spectral and colorimetric matching methods, respectively. These results seem encouraging because, for example, the typical size of just noticeable color differences (3 times the size of MacAdam achromatic ellipses) is 0.0033 *u'v'* units. From current results, we also conclude that our six LEDs system does not accurately simulate CIE standard illuminants D65, D50 and A. However, in some applications our current system may be a useful alternative to other commercial expensive devices simulating the CIE LED illuminants.**

Keywords—Low-cost lighting, CIE LED illuminants, CIE illuminants, spectral matching, colorimetric matching.

I. Introduction

Traditionally, artificial light has been generated with light sources of fixed spectral power distributions (SPDs), such as incandescent, fluorescent, halogen or gas-discharge lamps. These light sources have their own specific and relatively constant SPDs [1]. In recent years, several researchers have been introducing numerous approaches for the development of tunable light sources with tailored SPDs, through the use of Liquid Crystal Tunable Filters (LCTF), Digital Micromirror Devices (DMDs) and LEDs [2–4].

One of the most beneficial recent advancements in terms of lighting is the advent of solid state lighting, in particular LEDs. Now, the research focus has shifted to the design of intelligent LED lighting systems due to their advantages (e.g., low–cost, variability of spectral bands, and energy–efficiency), and the fact that the LEDs can be easily combined with other electronics, such as micro controllers, and a variety of sensors and wired or wireless communication devices [5].

While LEDs are already quite popular for commercial applications due to their efficiency and long life, it seems that their full potential is not being fully exploited. Perhaps in the field of colorimetry and lighting research, the main feature of interest would be their extremely fast switching time and low power consumption. With multiple channels of primary emitters and intelligence of digital systems, the number of possible light combinations are virtually limitless.

LED tunable light sources have proved to be useful in many photometric and colorimetric applications. Different studies [6-8] have shown that it is possible to compute the contribution of each individual LED to the final spectra that would match a desired illumination. However, these studies use a large number of narrow band LEDs, which result in devices that are difficult to design or develop and usually very expensive. Therefore, the objectives of this paper are (1) the construction of a six-channels low-cost LED tunable light source and (2) to compute the contribution of each channel for the simulation of different CIE illuminants.

II. MATERIAL AND METHODS

A. Tunable light design and characterization

A custom light engine circuit board was designed and printed, consisting of six LEDs from the Luxeon Rebel series. Out of a total of six channels, five were chromatic with wavelengths peaks at 450, 515, 569, 595, and 635 nm. The last channel featured a cool white LED with a correlated color temperature of 6500 K. The light engine was driven with a custom-built power module consisting of six independently controlled CAT4101 LED driver chips. Each CAT4101 driver has a Pulse Width Modulation (PWM) dimming functionality, where an external signal can be sent to adjust the current flowing through each LED channel, effectively allowing a precise control of its brightness. An Arduino Mega microcontroller was then used to send PWM signals to the driver chips.

After assembling, each channel was turned on individually at 100% intensity, and its corresponding SPD was measured, normalized (peak values equal to 1) and plotted, as shown in Figure 1.

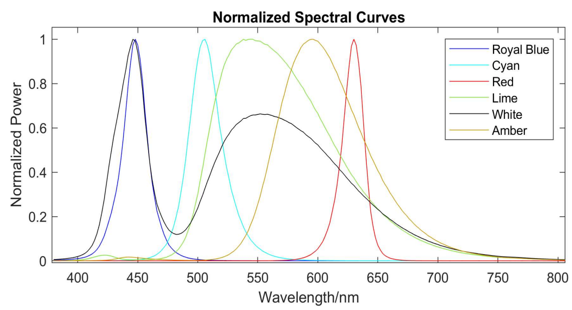

Fig.1. Normalized spectral power distributions of the LED channels.

The SPD of a certain illuminant or light source can be represented as a linear combination of the SPDs of monochrome LEDs. Considering a tunable lighting system with N-colored channels, the spectrum of the compound light $P(\lambda)$ can be described as:

$$P(\lambda) = \sum_{i=1}^{N} w_i e_i(\lambda) \tag{1}$$

where λ is the wavelength, and w_i and $e_i(\lambda)$ are the weight and SPD of the i-th color LED of the lighting system, respectively. The weights are defined to be $0 \leq w_i \leq 1$, where, $w_i = 0$ and $w_i = 1$ correspond to LEDs being fully turned off and on, respectively. The SPD of the i-th color LED, $e_i(\lambda)$, is calculated as shown in Equation 2. So, by adjusting the values of $w = [w_i, \ldots, w_N]$, considering that our system has N=6 LED channels, each having 255 intensity levels, this amounts to 255^6 (roughly 270 trillions) possible combinations.

In an attempt to match a target light source, one could proceed by adjusting the LED intensities manually, measure the resulting light characteristics between each adjustment and finally compare with the target in an iterative manner. However, this approach would be highly impractical and error prone. A better method would be to run an optimization algorithm to find the intensity coefficients of each channel that would best match the target light source in the desired characteristics. For example, the optimization algorithm could seek to find the best combination of LED intensity coefficients that would present the best spectral match of the target light source. However, we need to ensure that the combinations generated by the optimization process are realistic i.e., reachable with our light system. For this reason, the LED channel responses need to be characterized, and the light system calibrated.

From characterization, the LEDs seemed to exhibit an approximately linear relationship between input current level and luminance. Thus, it might be safe to assume that if the SPD at maximum intensity is known, then the resulting SPD at a lower intensity could be estimated by interpolation using a scaling factor. However, this approach proved to be insufficiently accurate, due to the compounding effect of the errors in each of the 6 channels that adds up in the final combined curve. In order to minimize these errors, the spectral curves of each channel were measured from 0 - 100% at every 10% intensity intervals and later compiled into a look-up table. These SPDs were measured in the range from 380 to 780 nm at 1 nm intervals using a spectroradiometer (Konica Minolta CS-2000) with a 0º/45º geometry (see Figure 2). For these measurements, the light was mounted around 40 cm above a nearly lambertian white surface, and the spectroradiometer was set at a 45º angle with the optical head around 60 cm away.

Then, an algorithm was developed to first calculate the resulting percentage intensity from an input value (0-255), select the most appropriate characterized curve, $S_{(10\cdot n)\%}$, for each channel, and combine them to obtain the simulated light as shown in next Equation 2:

$$e_i(\lambda) = \frac{x}{10 \cdot n} S_{(10 \cdot n)\%}(\lambda) \tag{2}$$

where x is the intensity in percentage of the input bit level and n is an integer from 1-10 that specifies the closest measured spectral curve to that input bit level.

The next step was to ensure that the simulated light sources correspond to their measured physical counterparts once the intensity coefficients found by the algorithm are set in the system. As a first step to do so, five random light sources were created and their simulated SPDs were compared to their measured spectra. These spectra were measured using the CS-2000 spectroradiometer in the lab, in a similar setup to the one used to characterize the LEDs. Performance metrics, such as Root Mean Square Error (RMSE) and Goodness-of-fit coefficient (GFC) [9] were calculated to assess how well the simulated light sources matched their physical counterparts. For a perfect match RMSE = 0 and GFC = 1. For our five selected light sources the mean RMSE was 0.00007 and the mean GFC was 0.99998, which confirms the validity of the calibration of the system and the method to accurately generate the SPDs of randomly selected target light sources.

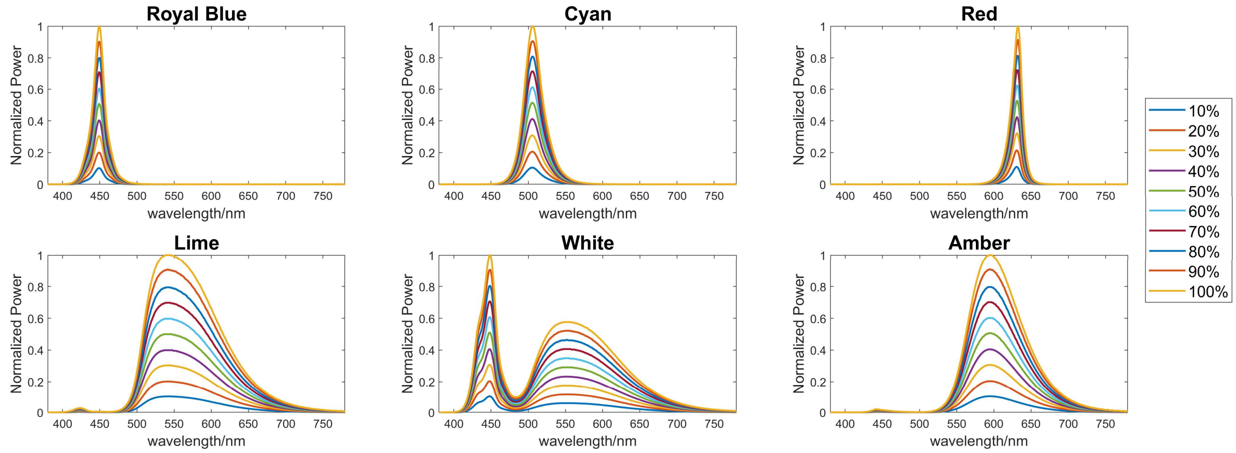

Fig. 2. Measured SPDs of the six LED channels at every 10% intensity interval.

B. Algorithm description

After system calibration, an algorithm based on constrained non-linear multivariable optimizations was developed to find the intensity values that would be set to find the desired lights, based on two different optimization objectives, which we treated as two separate methods here, namely a "spectral method" and a "colorimetric method". One would look for the best possible spectral match, while the other would aim to find the best colorimetric match instead.

For the spectral method, the goal was to find the combination of intensities of 6 LEDs that will result in a SPD as similar in shape as possible to those proposed by the CIE illuminants. To do so, the algorithm was set to look for the minimization of RMSE and maximization of GFC spectral metrics. Thus, the following cost function, $f_{spec}(w_i)$ was minimized:

$$f_{spec}(w_i) = RMSE\big(P_{CIE}, P_T(w_i)\big) - GFC\big(P_{CIE}, P_T(w_i)\big) \quad (3)$$

where w_i are the intensity input values of the six LED channels, P_{CIE} is the SPD of the target CIE illuminant and $P_T(w_i)$ is the SPD generated from the method described in the previous section (Equation 1).

In the case of the colorimetric method, the algorithm would instead find the intensities' combination of the 6 LEDs corresponding to a light source with chromatic characteristics as close as possible to the ones of the target CIE illuminant. Therefore, the cost function, $f_{color}(w_i)$ would minimize the differences in CIE 1931 x,y chromaticity coordinates and is defined as follows:

$$f_{color}(w_i) = |\Delta x\big(P_{CIE}, P_T(w_i)\big)| + |\Delta y\big(P_{CIE}, P_T(w_i)\big)| \quad (4)$$

where the symbols Δ mean differences between the chromaticity coordinates associated to the two SPDs indicated in parentheses, which are the same used in Equation (3).

To minimize the cost functions $f(x)$ of each objective (Equations 3 and 4), the *fmincon* function from the MATLAB's optimization toolbox [10] was used.

C. Performance indices

The performance of our system has been evaluated with different metrics. The spectral indices used were the RMSE and GFC, to assess the accuracy of the spectral match between the normalized (Y=100) SPDs of our sources and those proposed by the CIE illuminants. As for the colorimetric performance, four color indices were used; Euclidean distance in the u',v' chromaticity diagram, general CIE color rendering index (R_a) [11], CIE 2017 color fidelity index (R_f) [12] and correlated color temperature (CCT) [13]. These four indices were used to assess the colorimetric performance of the light generated from our system with respect to their corresponding CIE illuminants.

III. Results and Discussion

The above proposed methods were implemented for the simulation of the nine LED-illuminants recently proposed by the CIE (named as B1, B2, B3, B4, B5, BH1, RGB1, V1 and V2), as well as, six of the most important and traditional CIE illuminants (D50, D65, A, F2, F7 and F11) [14]. Specifically, D65, A and D50 are currently considered as the main CIE illuminants, and are designed as "CIE standard illuminants", while F2, F7 and F11 are the three main fluorescent CIE illuminants [14]. Table I shows the values of RMSE and GFC spectral indices between each one of the CIE illuminants and sources found using our two methods. Table II shows the values of the four color indices (CCT, $Du'v'$, R_a and R_f) for the CIE illuminants and the sources from our two optimization methods. Finally, Table III, shows the average values of differences between the indices for the three groups of CIE illuminants considered here (CIE standard illuminants, main CIE fluorescent illuminants and CIE LED illuminants) and their colorimetric and spectral matches using our system of 6 LEDs.

Figures 2 and 3 show the SPDs of the target illuminants [14] with their corresponding matches obtained by each of our two proposed methods (colorimetric and spectral), for the nine CIE LED illuminants and six CIE traditional illuminants mentioned above, respectively.

Table I denotes better results of RMSE and GFC for the simulations using the spectral method, being the RMSE values always smaller and the GFC values always higher than the ones obtained with the colorimetric method. This was expected since these two spectral indices were the ones used as the constraint in the cost function, $f_{spec}(w_i)$ (see Equation 3). It is worth highlighting the simulation of LED B3 by the spectral method, with RMSE = 0.0999 and GFC = 0.9890, which are very close to 0 and 1, respectively. However, the simulations of LEDs V1 and V2, are clearly worse compared to the ones for others CIE LED simulations, with RMSE and GFC values around 0.4 and 0.9, respectively. These poor simulations are probably due to the lack of LEDs with emissions below 450 nm in our system, which makes it impossible to simulate, in terms of their spectral shape, the peaks of the V1 and V2 CIE LED illuminants in the very short wavelength region of the visible spectrum.

Speaking of spectral shape simulations, it is worth noting the strong difference between the simulations of the CIE LED illuminants (Figure 3) and those of other CIE traditional illuminants (Figure 4), with the latter ones being clearly worse. This is probably due to the LEDs selected for our system, as broadband LEDs are known to help in matching smooth and continuous spectra, evenly spaced narrowband LEDs are necessary for matching highly structured spectra. Current results compared to the ones obtained in other studies [8], show a worse performance of our system, however, it is important to consider that whereas the system proposed in [8] uses 13 color LEDs and 4 white LEDs, our system uses only 5 color and 1 white low-cost LEDs.

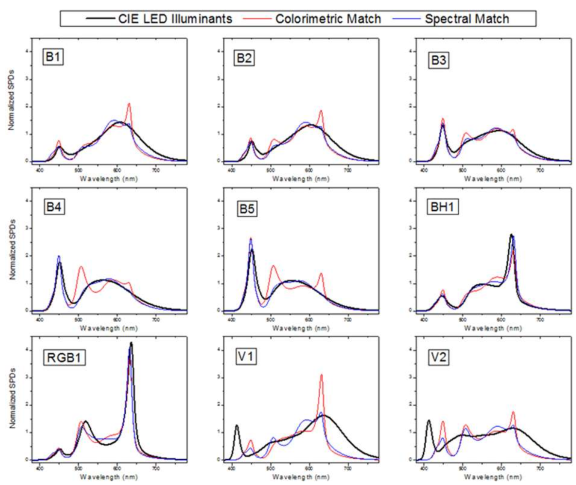

Fig. 3. SPDs of the nine CIE LED illuminants [14] and their colorimetric and spectral matches.

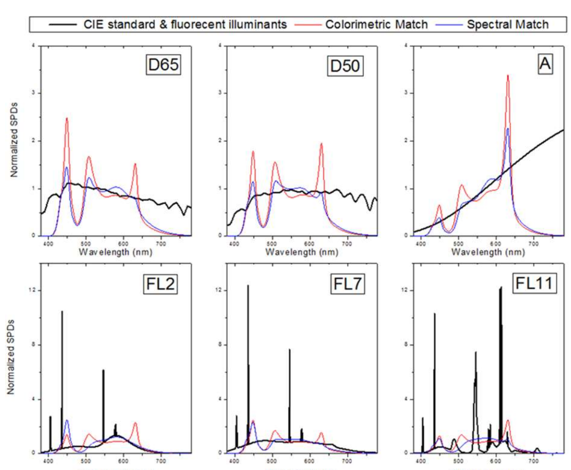

Fig. 4. SPDs of six traditional CIE illuminants [14] and their colorimetric and spectral matches.

TABLE I. RMSE AND GFC BETWEEN ILLUMINANTS PROPOSED BY THE CIE [14] AND THE SOURCES FOUND WITH OUR TWO METHODS.

	Spectral Method		**Colorimetric Method**	
	RMSE	**GFC**	**RMSE**	**GFC**
D50	0.4653	0.8318	0.5165	0.7942
D65	0.4564	0.8443	0.5224	0.8026
A	1.0565	0.5732	1.1055	0.5259
FL2	0.4036	0.8427	0.4756	0.7839
FL7	0.3983	0.8677	0.4726	0.8253
FL11	0.6998	0.6667	0.7958	0.5786
B1	0.1544	0.9765	0.2079	0.9575
B2	0.1497	0.9767	0.1906	0.9626
B3	0.0999	0.9890	0.1257	0.9831
B4	0.1231	0.9842	0.2773	0.9289
B5	0.1684	0.9747	0.2911	0.9342
BH1	0.1703	0.9740	0.1900	0.9677
RGB1	0.2987	0.9549	0.3064	0.9537
V1	0.4403	0.8627	0.5148	0.8103
V2	0.3831	0.8715	0.4225	0.8437

Considering that it is very hard to obtain a perfect spectral match, and that CCT, D_{uv} and color rendering indices are the most important parameters widely used in general lighting applications, it is important for any proposed multi-channel LED source to optimize the values for these parameters. It is well known that a perfect spectral match imply an accurate colorimetric matching, but the reverse is not true. Perfect colorimetric matches do not necessary reproduce a spectral match, since different SPDs can produce the same CIE x,y color coordinates, as observed with metamers. In this sense, if only colorimetric indices are considered to evaluate the quality of our simulations, the performance of our system improves considerably. Comparing the results obtained from both methods, it can be observed that the simulations obtained from the colorimetric method perform better (Table III). As in the previous case, this was somehow expected, since the constraint used in the cost function for this method is based on the minimization of differences of CIE x,y colorimetric coordinates. Moreover, the average CIE u',v' differences obtained for the colorimetric method were 0.0003, 0.0003 and 0.0001 for the CIE standard, fluorescent and LED illuminants, respectively, below the typical size of just noticeable color differences (around 3 times the size of MacAdam achromatic ellipses), which is 0.0033 $u'v'$ units [15]. Furthermore, in most cases the R_a and R_f indices of the sources found with the colorimetric method are higher than the ones of the CIE illuminants, which implies a better color reproduction. This is especially true for corresponding sources of the CIE

TABLE II. CHARACTERISTICS (CCT, $D_{u'v'}$, R_a AND R_f) OF MAIN CIE (STANDARD, FLUORESCENT AND LED) ILLUMINANTS AND THEIR CORRESPONDING COLORIMETRIC AND SPECTRAL MATCHES USING OUR SET OF 6 LEDS.

	CIE illuminants				**Colorimetric Match**				**Spectral Match**			
	CCT(K)	**$D_{u'v'}$**	**R_a**	**R_f**	**CCT(K)**	**$D_{u'v'}$**	**R_a**	**R_f**	**CCT(K)**	**$D_{u'v'}$**	**R_a**	**R_f**
D50	5002	0.0033	99.9	99.9	5042	0.0034	91.0	91.0	4934	0.0187	80.0	85.1
D65	6502	0.0032	100.0	100.0	6573	0.003	92.0	91.8	5261	0.0113	83.0	85.7
A	2856	0	100.0	100.0	2888	0.0005	87.0	87.8	2806	0.0074	87.0	88.2
FL2	4224	0.0018	70.1	70.1	4247	0.0023	90.0	90.7	4975	-0.0101	73.0	69.3
FL7	6495	0.0032	91.5	91.5	6548	0.0032	92.0	91.7	6609	0.0025	81.0	80.9
FL11	3999	0.0001	79.9	79.9	4014	0.0005	89.0	90.2	4096	0.0074	72.0	75.0
B1	2733	-0.0007	82.0	84.1	2728	-0.0008	82.0	80.7	2691	0.0006	72.0	75.7
B2	2998	-0.001	83.0	84.3	2993	-0.0011	87.0	85.8	2925	0.0004	74.0	76.9
B3	4103	-0.0007	85.0	85.3	4108	-0.0007	87.0	86.1	3979	-0.0004	80.0	80.7
B4	5109	0.0005	77.0	76.9	5099	0.0002	92.0	90.4	4799	0.0008	72.0	72.5
B5	6598	0.0009	80.0	79.5	6606	0.0008	93.0	92.0	5997	0.0007	76.0	75.1
BH1	2851	-0.0003	92.0	85.2	2855	-0.0003	85.0	82.7	2877	0.002	88.0	83.5
RGB1	2840	0.0043	57.0	71.0	2836	0.0041	77.0	79.0	2894	0.0059	75.0	80.5
V1	2724	-0.0019	95.0	87.3	2722	-0.0019	93.0	85.3	2647	0.0021	81.0	85.1
V2	4070	0.001	96.0	94.1	4071	0.001	95.0	92.2	3655	0.0066	88.0	89.7

TABLE III. AVERAGE DIFFERENCES BETWEEN MAIN PARAMETERS OF 3 GROUPS OF CIE ILLUMINANTS (STANDARD, FLUORESCENT AND LED) AND THEIR COLORIMETRIC AND SPECTRAL MATCHES USING OUR SET OF 6 LEDS.

	CIE - Colorimetric Match						CIE - Spectral Match					
CIE illuminants	**RMSE**	**GFC**	**ΔCCT (K)**	**$\Delta u'v'$**	**ΔR_a**	**ΔR_f**	**RMSE**	**GFC**	**ΔCCT (K)**	**$\Delta u'v'$**	**ΔR_a**	**ΔR_f**
Standard	0.7148	0.7076	48	0.0003	10.0	9.8	0.6594	0.7498	453	0.0103	16.7	13.6
Fluorescent	0.5813	0.7293	30	0.0003	11.3	10.4	0.5005	0.7924	321	0.0066	3.6	5.4
LED	0.2807	0.9269	5	0.0001	4.8	5.1	0.2209	0.9516	191	0.0019	4.5	5.2

fluorescent illuminants. It is worth noting (see Table III) that the light sources obtained from the colorimetric method have CCTs that closely match those of the CIE illuminants, while this is not the case with the light sources obtained from the spectral method. In particular, the CCT of the D65 illuminant, particularly important in many applications, is poorly emulated from the spectral method.

In contrast to the results of the spectral method, the colorimetric method for source optimizations can result in very good color rendering properties while nearly exactly matched a desired combination of CIE x,y chromaticity coordinates, demonstrating its usefulness.

IV. CONCLUSIONS

The 6 LEDs low-cost proposed system performed fairly well in the simulation of the CIE LED illuminants [14], both spectrally and colorimetrically. However, it is worth noting that for LED illuminants V1 and V2, the results were not as good because an additional peak in the violet region (~400 nm region) was unreachable with our system.

Unfortunately, the proposed LED system does not accurately simulate CIE standard illuminants D65, D50 and A. This is expected, given that our LEDs have narrow spectral curves. More channels would be needed if those illuminants are to be simulated spectrally. As for the three main CIE fluorescent illuminants, their very narrow peaks makes it problematic to be spectrally simulated using our LEDs.

It is important to mention that the LEDs in our system were only loosely selected to more or less cover the visible spectrum. As future research, an optimization to select the most effective channels in spectral reconstruction could be performed. Perhaps a combination of wider-band and narrow band LEDs would be better suited for this objective.

Nevertheless, with the advent of more new LEDs, the accuracy of the spectral matching method will surely be upgraded in the future.

ACKNOWLEDGMENT

THIS RESEARCH WAS SUPPORTED BY THE MINISTRY OF SCIENCE AND INNOVATION OF THE NATIONAL GOVERNMENT OF SPAIN (PID2019-107816GB-I00 / AEI / 10.13039/501100011033) AND BY FEDER/JUNTA DE ANDALUCÍA-CONSEJERÍA DE TRANSFORMACIÓN

ECONÓMICA, INDUSTRIA, CONOCIMIENTO Y UNIVERSIDADES/ PROYECTO A-FQM-30-UGR20.

REFERENCES

[1] U. J. Blaszczak, L. Gryko, and A. Zajac, "Tunable white light source for medical applications," in *Photonics Applications in Astronomy, Communications, Industry, and High-Energy Physics Experiments 2017*, R. S. Romaniuk and M. Linczuk, Eds. Wilga, Poland. SPIE, 2017. Accessed: Jun. 6, 2022. https://doi.org/10.1117/12.2281095

[2] M. Litorja and B. Ecker. "Use of a spectrally tunable source to explore improvement in chromatic contrast for illumination of tissues." *Emerging Digital Micromirror Device Based Systems and Applications II*. Vol. 7596. International Society for Optics and Photonics, 2010. https://doi.org/10.1117/12.846096

[3] R.P. Francis, K. J. Zuzak, and R. Ufret-Vincenty, "Hyperspectral retinal imaging with a spectrally tunable light source." *Emerging Digital Micromirror Device Based Systems and Applications III*. Vol. 7932. SPIE, 2011. https://doi.org/10.1117/12.873891

[4] P. Bartczak, A. Gebejes, P. Falt, and M. Hauta-Kasari, "An LED-Based Tunable Illumination for Diverse Medical Applications," in *2016 IEEE 29th International Symposium on Computer-Based Medical Systems (CBMS)*, Belfast and Dublin, Ireland, Jun. 20–24, 2016. IEEE, 2016. https://doi.org/10.1109/cbms.2016.33

[5] Y. S. Cho, J. Kwon, and H.-Y. Kim, "Design and Implementation of LED Dimming System with Intelligent Sensor Module," *Journal of information and communication convergence engineering*, vol. 11, no. 4, pp. 247–252, Dec. 2013. https://doi.org/10.6109/jicce.2013.11.4.247

[6] S. W. Brown, "LED-based spectrally tunable source for radiometric, photometric, and colorimetric applications," *Optical Engineering*, vol. 44, no. 11, p. 111309, Nov. 2005. https://doi.org/10.1117/1.2127952

[7] M. Lukovic, V. Lukovic, I. Belca, B. Kasalica, I. Stanimirovic, and M. Vicic, "LED-based Vis-NIR spectrally tunable light source-the optimization algorithm," *Journal of the European Optical Society-Rapid Publications*, vol. 12, no. 1, Oct. 2016. https://doi.org/10.1186/s41476-016-0021-9

[8] F. Zhang, H. Xu, and Z. Wang, "Spectral design methods for multi-channel LED light sources based on differential evolution," *Applied Optics*, vol. 55, no. 28, p. 7771, Sep. 2016. https://doi.org/10.1364/ao.55.007771

[9] J. Hernández-Andrés, J. Romero, and R. L. Lee, "Colorimetric and spectroradiometric characteristics of narrow-field-of-view clear skylight in Granada, Spain," *Journal of the Optical Society of America A*, vol. 18, no. 2, p. 412, Feb. 2001 https://doi.org/10.1364/josaa.18.000412

[10] The Help document of Optimization Toolbox, included in MATLAB 6.5 help, Mathwork, www.mathwork.com , html, 2003.

[11] CIE 13.3-1995. Method of measuring and specifying colour rendering properties of light sources. CIE Central Bureau, 1995. (ISBN 3 900 734 57 7).

[12] CIE 224:2017. CIE 2017 Colour Fidelity Index for accurate scientific use. CIE Central Bureau, 2017 (ISBN 978-3-902842-61-9)

[13] C. Li et al., "Accurate method for computing correlated color temperature," *Optics Express*, vol. 24, no. 13, p. 14066, Jun. 2016. https://doi.org/10.1364/oe.24.014066

[14] CIE 015:2018. Colorimetry, 4th Edition. CIE Central Bureau, 2018. (ISBN: 978-3-902842-13-8. DOI: 10.25039/TR.015.2018).

[15] CIE TN 01:2014. Chromaticity difference specification for light sources. CIE Central Bureau, 2014. Accessed: Jun. 6, 2022. http://files.cie.co.at/738_CIE_TN_001-2014.pdf

Evaluating Non-visual Effects of Light: An Open Challenge for Designers

Laura Bellia
Department of Industrial Engineering
University of Naples "Federico II"
Naples, Italy
bellia@unina.it

Francesca Fragliasso
Department of Industrial Engineering
University of Naples "Federico II"
Naples, Italy
francesca.fragliasso@unina.it

Matteo Seraceni
Hera Luce
Bologna, Italy
matteo.seraceni@gruppohera.it

Giulia Sodano
Department of Industrial Engineering
University of Naples "Federico II"
Naples, Italy
giulia.sodano@unina.it

***Abstract* — Light is a powerful stimulus capable of influencing and altering physiological, psychological, and behavioural dynamics such as endocrine and cardiovascular functions, alertness, and circadian rhythms. Despite extensive researches on human-centred lighting and on potential applications of integrated design, many attempts to combine design-specific demands for the visual task with circadian metrics are not immediately useful for designers. Considering morning hours, a typical office has been simulated with three LED luminaires settings (direct, direct/indirect, indirect), three correlated colour temperatures (CCTs) and three different wall reflectances to evaluate two different approaches to lighting design: in the first (called "visual design") luminous fluxes were set to be compliant with EN 12464-1 standard and then the circadian effects were assessed; in the second (called "non-visual design"), luminous fluxes were modified in order to meet the minimum circadian metrics, suggested by The Lighting Research Center (LRC) and the WELL Building Institute, and the illuminance on the task area, as defined by EN 12464-1 standard, were assessed. The obtained results show how lighting sources spectral and spatial distributions, together with the environmental characteristics are to be carefully considered by designers to comply both visual and non-visual requirements.**

Key Words: Circadian light, human centric lighting, integrative lighting, non-visual effects of light, circadian stimulus, equivalent melanopic.

I. INTRODUCTION

How are lighting scenarios designed today? How important is light for people's lives? Is it possible to create an environment that improves well-being? Since the invention of the electric light, human life has changed and along with the evolution of lighting, spaces and work systems have been reshaped. Today people spend more time inside buildings and, instead of being exposed to a varied light - both in terms of spectrum and intensity - they are exposed to a light that is always the same and with much lower intensity. A study conducted in Chicago estimated that a typical office worker receives about 2.5 h of intense outdoor light (>1000 lx) on summer workdays, but only about half of it on winter workdays [1].

The exposition to daylight is fundamental for human wellness. The combination of light stimuli, composed of the variation of intensity and spectrum during the various hours of the day, plays a major role in defining human non-visual (NV) responses [2], which, as the name suggest, relate to melatonin production, alertness, cognition, and other functions, rather than vision. These responses impact the regulation of the circadian system and have multiple effects on behaviour, mood, and health [3]. NV responses to light depend primarily on melanopsin-expressing retinal ganglion cells (ipRGCs) [4].

One of the best known NV response is the light-induced suppression of endogenous melatonin, that it is alleged to desynchronize our circadian rhythm from the sleep wake-cycle [5]. It has been established that there is a link between the type of light stimulus we undergo and the nocturnal production of melatonin [4][6].

Improper administration of light can have negative effects, such as:

- Physiological Effects (increased risk of): daytime sleepiness, cardiovascular disorders, infections, cancer, abnormal metabolism, diabetes, psychosis.
- Cognitive Effects (decompensation in): performance, ability to multitask, memory, attention, concentration, communication, productivity.
- Emotional Effects (increase in): mood changes, irritability, anxiety, loss of empathy, frustration, impulsivity, depression.

Therefore, it is essential that humans receive the right dosage of light at the right time and, due to the reduced exposure to natural light, electric light should play a major support role. The introduction of LED sources and the improvement of intensity and spectral controls changed the way artificial light is designed, making possible to overcome the static nature of electric light and to design the so-called integrative lighting. "The essence of human-centric lighting is integrated thinking about light and lighting as mediators of visual, biological and behavioural responses in humans" [7] Furthermore, as Boyce et al. say while "light is still for vision, and lighting for visibility, visual comfort and visual amenity is as important as ever" [7].

Currently, there are different approaches to evaluate the NV responses: the most known are the model of human circadian phototransduction developed by Rea et al. at the Lighting Research Center (LRC) [8] and the model by Lucas et al. [9]. Since no model seems to offer a complete and exhaustive view on NV effects, no legislator has made any effort to insert these indications in a standard.

The mathematical model of human circadian phototransduction developed by Rea et al. [8][10][11][12] is based on the neuroanatomy and neurophysiology of the retina and on the nocturnal suppression of melatonin using a certain quantity and power of light. The model uses the spectral irradiance distribution at the eye's level to generate circadian light (CLA), expressed in weighted W/m^2, that is the spectrally weighted retinal irradiance according to photoreceptors sensitivity. The Circadian Stimulus (CS), calculated on the basis of CLA, is a non-linear function and is defined as the relative effectiveness of light to produce a meaningful response of the human circadian system in terms of melatonin suppression. The model considers the role of ipRCGs, rods and cones in circadian phototransduction via neural connections, including spectral opposition in the outer layer of the retina. It allows to quantitatively predict how the circadian system responds to different light exposures. This model is usually applied to calculate the efficacy of a light stimulus for the suppression of nocturnal melatonin, but it is also used for assessing daytime lighting conditions that can properly entrain the circadian rhythms. According to [13], the minimum circadian stimulus (CS) to be achieved - for a good balance of circadian rhythms - should be at least 30 % during morning. There is an usable online tool called CS Calculator[14] to calculate the CS, that requires as input data the source SPD and the illuminance at the eye.

The mathematical model of human circadian phototransduction developed by Lucas et al. [9] [15], is based on the spectral response of photopigments in the ipRGC photoreceptors, cones, and rods. Starting from the spectral irradiance at the eye's level, it calculates the optical equivalent illuminance values - "α-opic" illuminance - for each of the 5 photopigments in the human eye: Cyanotic illuminance, Melanopic illuminance, Rhodopic illuminance, Chloropic illuminance, Erythropic illuminance. The average values of the optical density of the photopigment at the absorption peak were considered about 0.40 for rods, 0.30 for S cones and 0.38 for the other cones. This approach is used to evaluate non-visual effects of light as the equivalent melanopic to photopic ratio M/P [16], calculated as the melanopically weighted content of an SPD compared to the photopically weighted content, which means that it helps to evaluate the circadian potential of a light source without assessing its impact on humans. This approach allows to evaluate the Equivalent Melanopic Illuminance, expressed in Equivalent Melanopic Lux (EML), which is obtained as the product of the photopic illuminance and the melanopic ratio, so it is linearly dependent on the photopic illuminance. This model has been adopted by the CIE [17] and a calculation tool (Irradiance Toolbox) is available for free online and it requires as input data the spectral irradiance at the eye. Likewise, the International WELL Building Institute has developed a certification system [18], that uses EML to assess minimum requirements for circadian lighting design and identifies limits for different lighting conditions (in the presence or absence of daylight). In the absence of natural light, two limits value are proposed, 150 EML and 275 EML should be achieved from 9 to 13 every day of the year to gain 1 point and 3 points respectively. Current standards do not give specific indications about integrative light, but the last version of the EN 12464-1 "Lighting of Workplaces" [19], in the appendix B refers to the CEN/TR 16791 [20] that quantifies irradiance for eye-mediated non-image-forming (NIF) effects of light in humans.

Various researches [21][22][23][24][25][26] have also focused on the lighting design of circadian light in different types of lit environments with the use and comparison of different calculation models and different metrics. However, they don't provide any kind of guidelines for the designers. The designer projects the environments for the visual tasks by applying the EN 12464-1 [19], that specifies the requirements for good lighting solutions focusing on visual comfort, without integrating circadian metrics.

The aim of this work is therefore to define an integrated design approach, and to evaluate the differences between the two design approaches and the two circadian models. Starting from a simple case study, different lighting system solutions will be presented. They are designed based on the fulfilment of visual comfort requirements applying the EN 12464-1. Then the circadian parameters are evaluated to verify if non-visual comfort is achieved as well. Finally, the lighting system configurations useful to fulfil thresholds limits for circadian parameters are identified. In this way it is possible to highlight current models' issues and which parameters must be considered for an integrated design.

II. METHOD

The work is divided into two parts. In the first phase different lighting configurations for an office are released to respect the limits reported in the EN 12464-1 [19] for the visual tasks and then the circadian parameters are evaluated. In the second phase, the opposite approach is followed, evaluating how to design the system starting from the circadian metrics, to obtain the CS = 30% [8] and the Equivalent melanopic illuminance = 150-275 EML [18].

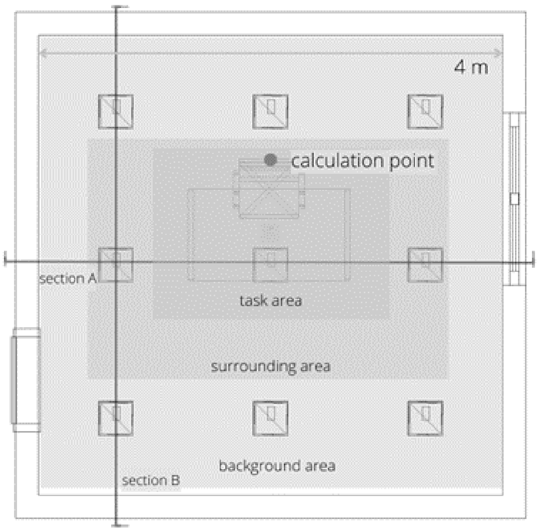

Fig. 1. Plan of the office (with the direct light)

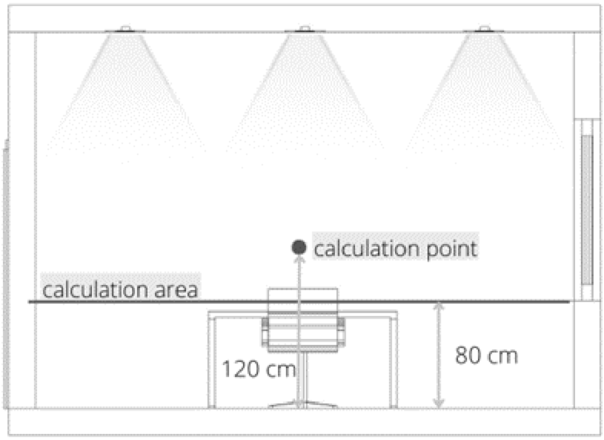

Fig. 2. Section A

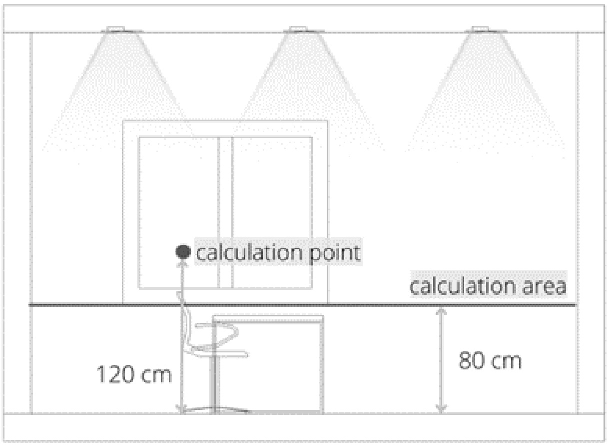

Fig. 3. Section B

The office space considered, modelled with Dialux, was 4.0 m wide, 4.0 m deep and 3.0 m high, and it is equipped with a single window (see Figg. 1,2,3). The case study represents a cellular office intended for a single occupant, sitting behind a desk with a view direction parallel to the window (although the presence of natural light was not considered for this first study). The office environment conforms to a simple and aseptic type of environment. The reflectance of the ceiling is always set at 70% and the one of the floor always at 20%, while the reflectance values of the walls have been modified to simulate three different values 30%, 50%, 70%. It must be underlined that the standard advises reflectance values in the range 50% - 80%, but also 30% was considered to analyse an unfavourable condition.

The task area has been set at 80 cm above the floor for the calculation of the horizontal illuminance $\bar{E}$. The position of the observer's eye was set at a height of 120 cm above the floor, in correspondence of which the UGR and the vertical illuminance Ev (necessary for the circadian effects assessment) were calculated.

Three luminaire types with different photometries were taken into consideration for the calculations:

- a luminaire with direct light (Φ=1800 lm, P=18W);
- a luminaire with direct / indirect light (Φ=4240 lm, P=31W);
- a luminaire with indirect light (Φ=4030 lm, P=26W).

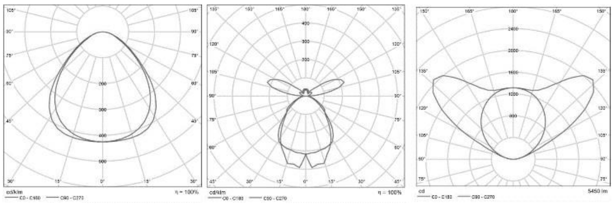

1 2 3

Fig. 4. 1) direct light 2) direct - indirect light 3) indirect light

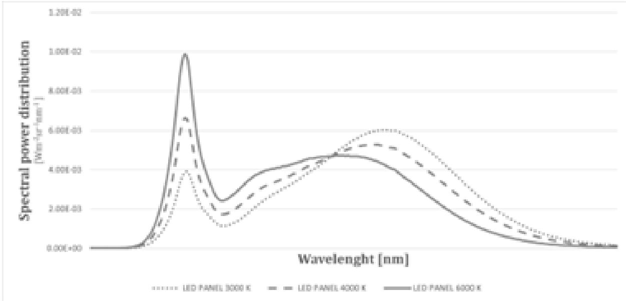

Fig. 5. Normalized spectral power distribution

Furthermore, three different typical LED spectral power distributions (Fig. 5) corresponding to three correlated colour temperatures (CCTs) (3000 K - 4000 K - 6000 K) have been considered for each photometry.

Therefore, using each luminaire in turn, the lighting system was designed to achieve the requirements prescribed for office activities by the EN 12464-1 [19], with the worst condition, i.e. wall reflectance 30%. Specifically for the visual task "writing, typing, reading, data processing" the following prescription are given:

- Average maintained illuminance on the task area, the immediate surrounding area and backgroundarea ≥ 500 lx, 300 lx and 100 lx respectively;
- CIE Unified Glare Rating (UGR) ≤ 19;
- colour rendering index ≥ 80;
- illuminance uniformity at the task area and on walls ≥ 0,60, ≥ 0,10 respectively;
- maintained illuminance on walls ≥ 150 lx;
- maintained illuminance on ceiling ≥ 100 lx.

To obtain and respect these values, considering the maintenance factor set at 80%, the devices were positioned in the office as follows (Fig. 6):

- the direct light luminaire : 9 devices;
- the direct / indirect light luminaire: 4 devices;
- the indirect light luminaire : 6 devices.

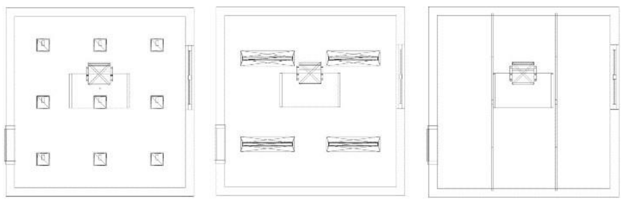

1 2 3

Fig. 6. 1) direct light 2) direct - indirect light 3) indirect light

So, considering all the described variables, in total 27 different light scenes have been developed (three walls reflectances, three photometries, three spectral power distributions), Fig. 7.

In the first phase of the work, for this light scene the worktop Ē and vertical Ev illuminances have been calculated and the ratio of Ev to Ē has been obtained. Furthermore luminaires were dimmed to obtain illuminances at the task area equal to 300 lx and 500 lx. That was made to take into consideration two factors: it is possible to apply the lumen maintenance strategy to keep constant the illuminance prescribed by the standard over time (500 lx) and thus save energy. In addition, for office activities, the standard provides different requirements for different tasks, for example 300 lx on the worktop are required for "filing, copying, etc.". Thus, it is possible to dim the luminaires for different conditions. For these two cases (Ē= 500 lx, Ē= 300 lx), we calculated the illuminances Ev - in relation to the illuminances on the work plan, based on the Ev/ Ē ratio. Then starting from Ev and the spectral power distribution of the sources, we calculate the CS and EML values for all the conditions.

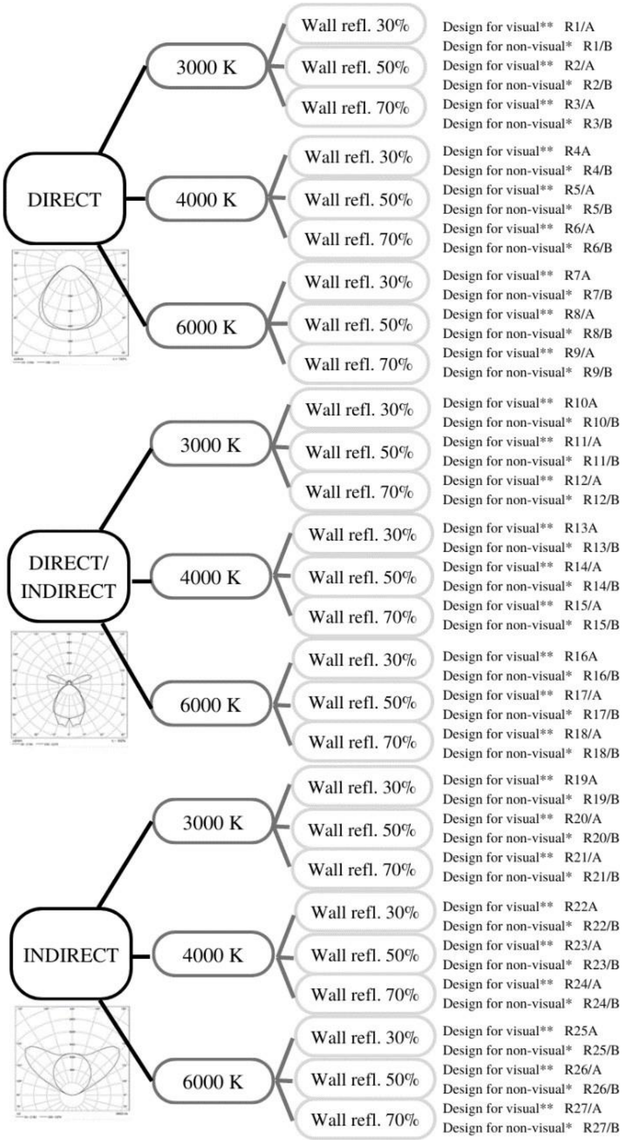

* By setting the threshold values of CS and EML
** Complying with EN 12464-1

Fig. 7. Methodology flowchart

TABLE I. LIMITS FOR THE TWO CIRCADIAN METRICS

Parameters	Limit values		Note
Circadian stimulus (CS)	≥ 30% [a]		Minimum of 4 h. and at least between the hours of 9 a.m. and 1 p.m.
Equivalent melanopic Illuminance (EML)	Requirements for 1 point	≥150 [a]	
	Requirements for 3 points	≥ 275 [a]	

[a.] Whit the electric light only

In the second phase, starting from the limit values of circadian parameters, as reported in table I, the corresponding illuminances at the eye are calculated and consequently the values of illuminance Ē on the work plan.

The two models/tools that will be used for the calculation of the circadian parameters, previously illustrated, are:

- Model of Human Circadian Phototransduction proposed by the LRC - CS Calculator Tool.
- Irradiance Toolbox - WELL Standard

III. RESULTS

A. Phase 1

In the Fig. 8 the illuminance values Ē calculated on the worktop, 80 cm from the ground, the illuminance values to the eye measured at 1.20 m from the ground, the relationship between the vertical illuminance Ev and the horizontal illuminance Ē are shown.

With direct lighting the Ē on the worktop has the highest values compared to the other two types of luminaires. Furthermore, the ratio between Ē and Ev changes from fixture to fixture and the highest values are in the case of the luminaire with direct/indirect light distribution.

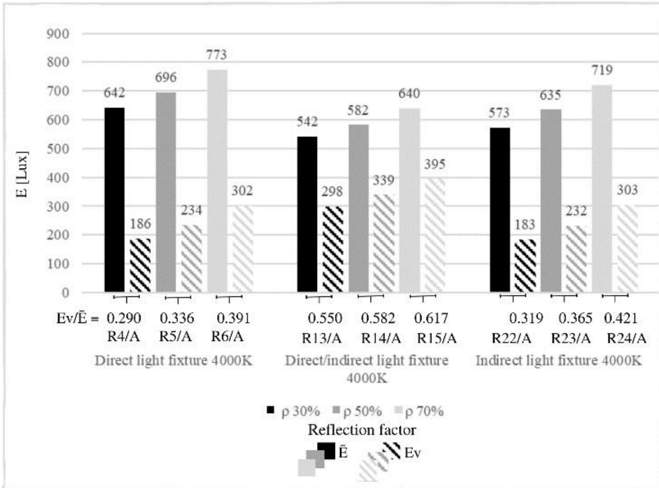

Fig. 8. Average illuminance values on the work plane (Ē) and illuminance at the eye (Ev)

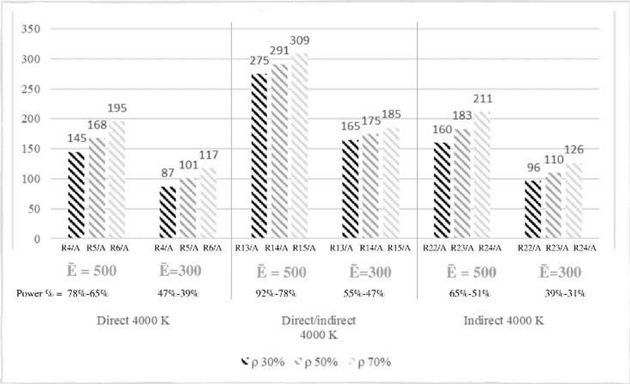

Fig. 9. The eye illuminance (Ev) with the maintained illuminance on the work plan ($\bar{E}_m$) of 500 lx and 300 lx

In the bar plot (Fig. 9) the eye illuminance values calculated for the three photometries and the three environmental conditions are shown, setting 500 lx and 300 lx as the maintained average illuminance on the worktop. Naturally, when the reflectance is great, we have greater Ev values, and this is an important first fact that highlights how significant it is to choose more reflective rather than absorbent materials and colours to have a greater illuminance to the eye and therefore a greater luminous stimulus.

In the scatter chart in Fig. 10, the CS values - calculated with the maximum flux of the appliance and with a maintenance factor of 80% - are illustrated. The lowest values are observed with the CCT equal to 4000 K. For this CCT only the case with ρ = 70% and direct/indirect light exceeds the limit. In the case of CCT equal to 6000 K, the CS value of 30% is exceeded in all configurations, with the highest values attained with the direct/indirect fixture. With the 3000 K direct light the 30% CS value is reached only with ρ = 70%, the other two photometries satisfy the requirement, except with indirect light and ρ = 30%.

In the scatter chart in Fig. 11, the CS values - calculated with the average maintained illuminance Ē= 500 lx are illustrated. It is evident that the value of 30% CS is reached only with the direct / indirect light with CCT values equal to 3000 K and 6000 K. Specifically, for 3000 K, the CS limit value is not reached when the wall reflectance is low.

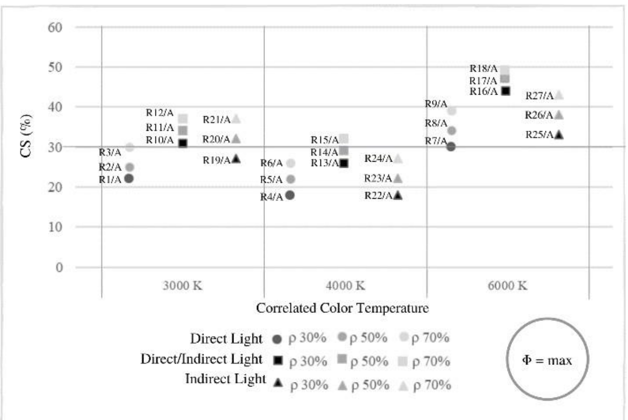

Fig. 10. CS calculated with the maximum luminous flux of the luminaire

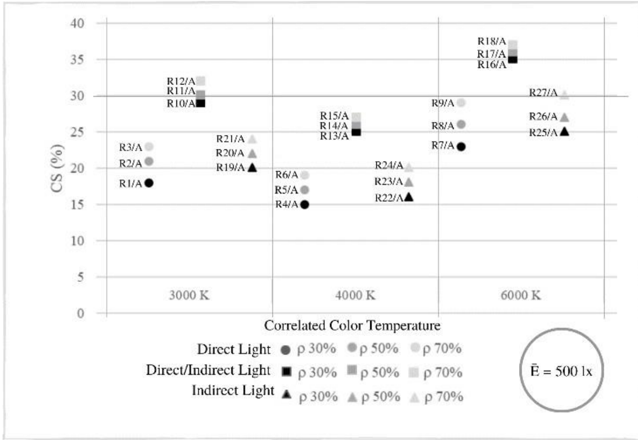

Fig. 11. CS calculated with the average maintained illuminance Ē =500 lx

In the scatter chart in Fig. 12, the CS values - calculated with the average maintained illuminance Ē= 300 lx - are illustrated. It should be noted that, having lower illuminances on the work plan and consequently lower illuminances to the eye, the value of CS = 30% is not reached in any case.

In the scatter chart in Fig. 13, the Equivalent Melanopic Illuminance values - calculated with the maximum flux of the appliance and with a maintenance factor of 80% - are illustrated. It should be noted that two limit values are highlighted because of the WELL standard limits. It is evident that the combination giving the lowest values is direct light with 3000 K, that even with the highest reflectance, fails to obtain 150 EML. Furthermore, the direct / indirect luminaire manages to obtain the best results, but the upper limit is never obtained. With 4000 K, most cases are between the two limits, with the exceptions of direct/indirect and ρ = 70% which exceeds 275 EML and direct and indirect cases with ρ = 30%, which provide values below the lower limit. With 6000 K the best results are obtained, always above the lower limit.

In the scatter charts in Figg. 14 and 15, the Equivalent Melanopic Illuminance values calculated with the average maintained illuminance Ē= 500 lx and Ē= 300 lx respectively are shown.

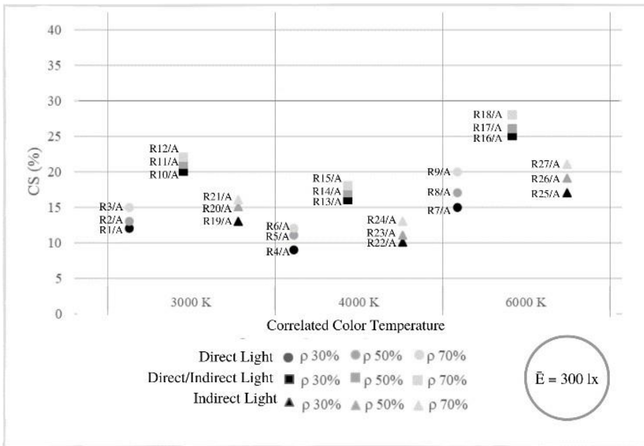

Fig. 12. CS calculated with the average maintained illuminance Ē =300 lx

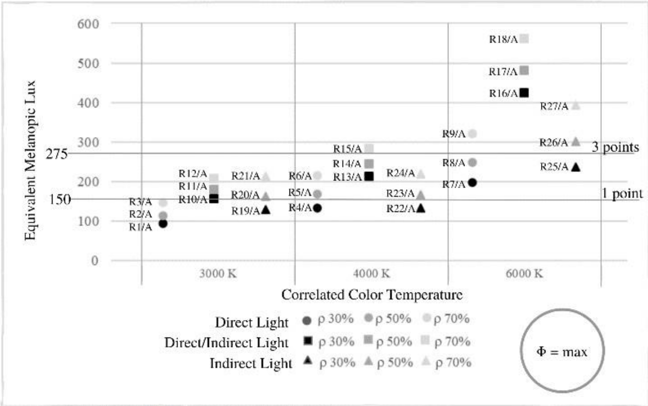

Fig. 13. EML calculated with the maximum luminous flux of the luminaire

It could be noted that the trend is very similar to the one observed in Fig.13, but the lower photopic illuminance values induce lower Equivalent Melanopic Illuminance values. Indeed, in the case of Ē= 300 lx, the limit of 275 EML is never attained and in most cases neither the 150 EML one.

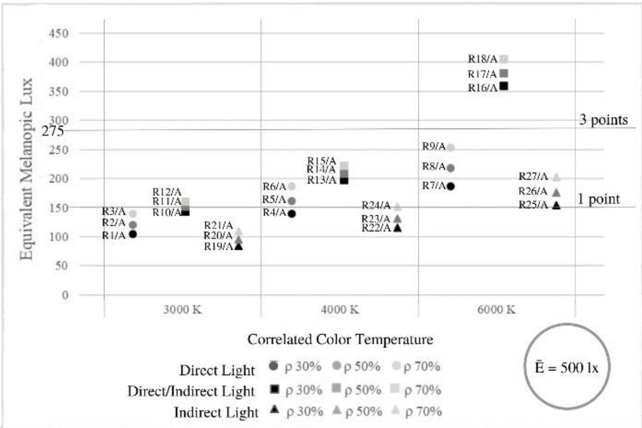

Fig. 14. EML calculated with the average maintained illuminance Ē =500 lx

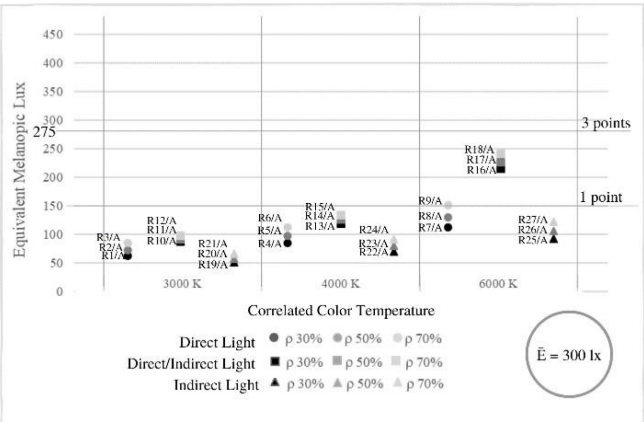

Fig. 15. EML calculated with the average maintained illuminance Ē =300 lx

B. Phase 2

In this section the illuminance values at the eye Ev are calculated by setting the threshold values of CS and EML:

- 150 EML for a point WELL v2
- 275 EML for three points WELL v2
- 30% CS according to the LCR prescriptions

Then, from the Ev/Ē ratio, the illuminances on the work surface corresponding to the calculated Ev are obtained. They are reported in Figg. 16, 17 and 18, respectively calculated with 30% CS value, 150 EML and 275 EML.

According to previously seen results, the graph in Fig. 16 shows that illuminances on the work plan are in almost cases higher than 500 lx, with the exception of direct/indirect light at 3000 K and 6000 K. In some cases illuminances are very high, as for 4000 K with direct light and ρ = 30%, with a value higher than 1200 lx.

As expected from previous results, Figg.17 and 18 show higher illuminance values for the direct luminaire and the indirect luminaire.

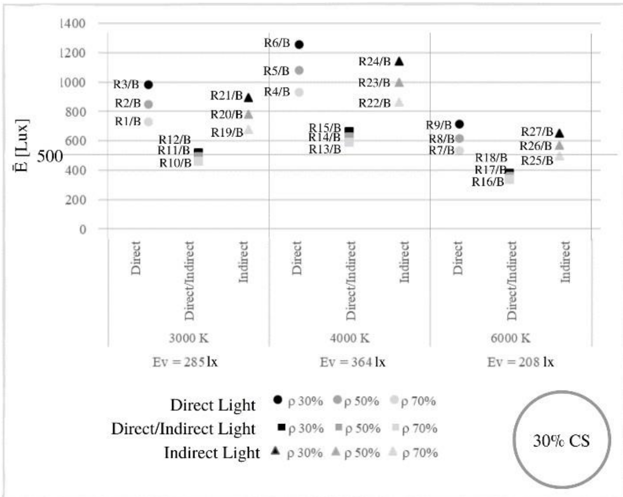

Fig. 16. The average maintained illuminance on the work plan calculated with 30% CS

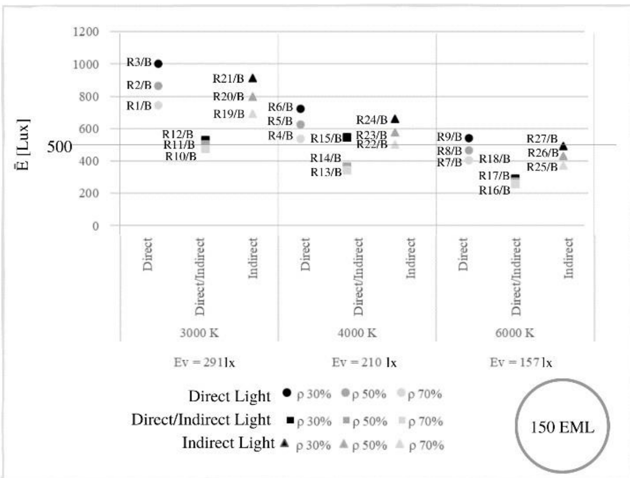

Fig. 17. The average maintained illuminance on the work plan calculated with 150 EML

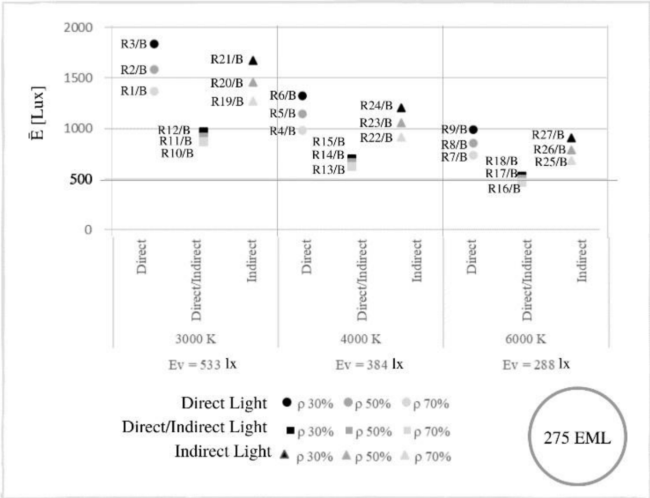

Fig. 18. The average maintained illuminance on the work plan calculated with 275 EML

What is immediately noticeable is the request for illuminances higher than those calculated in the first phase. As for the direct light fixture, to obtain 150 and 275 EML there is an excessive increase in the illuminance values on the work plan. These values are respectively double (with 150 EML) and almost four times bigger (with 275 EML) of those recommended by the EN 12464-1. The lowest illuminance values are obtained with 150 EML. In cases where the value of 30% CS is set, there is a corresponding value of about 200 EML which is however an optimal value and halfway between 150 EML and 275 EML.

IV. Discussion and Conclusions

As highlighted in previous sections, visual requirements and non-visual aspects may be in conflict with each other, so lighting designers could face many obstacles before finally reaching satisfactory results. Starting from two of the available calculation models - better known and developed - we performed various simulations in an office environment with different photometries, SPDs and walls reflectance to evaluate circadian parameters and their corresponding threshold values. From the obtained results, the following observations can be inferred:

- As for the photometries, the choice should be made considering a proper ratio between the illuminance at the eye and at the workplan.
- Once fixed the illuminance at the workplan, the most effective photometries for non-visual effects are those for which the illuminance at the eye is higher.

In the reported examples, the best was the direct/indirect one.

The SPD of light sources has a relevant role: in the case of 6000 K CCT, non-visual requirements are fulfilled in most cases, but, in the case of 3000 K CCT, the compliance of non-visual requirement is strictly linked to environmental characteristics, as wall reflectances.

The two main circadian approaches, respectively based on CS and EML values, provide different results and consequently different environmental conditions. Specifically, it has been observed that results in terms of illuminance at the workplan, with 3000 K and 6000 K for CS = 30% and 150 EML are rather similar, whereas with 4000 K in order to obtain CS = 30%, illuminance values on the workplan higher than those necessary to reach 150 EML are needed. So, precisely with 4000 K CCT which is the most often used, the two models provide very different results due to the spectral opposition which is central to the Rea et al.[8] model. This because colour opposition forms before the retinal gaglion cell layer [27], and also recent discoveries by Figueiro et al. [28] show evidence of spectral opposition blue/yellow in the nocturnal suppression of melatonin.

The three SPDs adopted were LED’s typical ones, but different results could be achieved with same CCTs but different spectra. For this reason further investigation is required. The adopted threshold limits for the circadian parameters are referred to daytime conditions (i.e. from 9:00 to 13:00) neglecting daylight contribution. It’s obvious that in presence of daylight, these thresholds for electric light could be reduced, according to its availability. Even for this reason, further research is required, considering also that different limit values for circadian parameters should be adopted during other periods of the day, as in the afternoon and in the evening.

References

[1] M. Andersen, S. J. Gochenour, and S. W. Lockley, “Modelling ‘non-visual’effects of daylighting in a residential environment,” *Build. Environ.*, vol. 70, pp. 138–149, 2013.

[2] L. Bellia and F. Fragliasso, “Good Places to Live and Sleep Well: A Literature Review about the Role of Architecture in Determining Non-Visual Effects of Light,” *Int. J. Environ. Res. Public Health*, vol. 18, no. 3, p. 1002, 2021.

[3] C. Blume, C. Garbazza, and M. Spitschan, “Effects of light on human circadian rhythms, sleep and mood,” *Somnologie*, vol. 23, no. 3, pp. 147–156, 2019.

[4] G. C. Brainard *et al.*, “Action spectrum for melatonin regulation in humans: evidence for a novel circadian photoreceptor,” *J. Neurosci.*, vol. 21, no. 16, pp. 6405–6412, 2001.

[5] R. G. Foster, “Fundamentals of circadian entrainment by light,” *Light. Res. Technol.*, vol. 53, no. 5, pp. 377–393, 2021.

[6] S. R. Pandi-Perumal *et al.*, “Dim light melatonin onset (DLMO): a tool for the analysis of circadian phase in human sleep and chronobiological disorders,” *Prog. Neuro-Psychopharmacology Biol. Psychiatry*, vol. 31, no. 1, pp. 1–11, 2007.

[7] K. W. Houser, P. R. Boyce, J. M. Zeitzer, and M. Herf, “Human-centric lighting: Myth, magic or metaphor?,” *Light. Res. Technol.*, vol. 53, no. 2, pp. 97–118, 2021.

[8] M. S. Rea, M. G. Figueiro, J. D. Bullough, and A. Bierman, “A model of phototransduction by the human circadian system,” *Brain Res. Rev.*, vol. 50, no. 2, pp. 213–228, 2005.

[9] R. J. Lucas *et al.*, “Irradiance toolbox.” Oxford, 2013.

[10] M. S. Rea, M. G. Figueiro, A. Bierman, and R. Hamner, “Modelling the spectral sensitivity of the human circadian system,” *Light. Res. Technol.*, vol. 44, no. 4, pp. 386–396, 2012.

[11] M. G. Figueiro, “An overview of the effects of light on human circadian rhythms: Implications for new light sources and lighting systems design,” *J. Light Vis. Environ.*, vol. 37, no. 2_3, pp. 51–61, 2013.

[12] M. G. Figueiro, “Future directions for lighting environments,” in *Circadian Rhythm Sleep-Wake Disorders*, Springer, 2020, pp. 221–240.

[13] M. S. Rea and M. G. Figueiro, “Light as a circadian stimulus for architectural lighting,” *Light. Res. Technol.*, vol. 50, no. 4, pp. 497–510, 2018.

[14] LRC, “Cs calculator.” https://cscalc.light-health.org/.

[15] R. J. Lucas *et al.*, "Measuring and using light in the melanopsin age," *Trends Neurosci.*, vol. 37, no. 1, pp. 1–9, 2014.

[16] N. J. Miller and A. L. Irvin, "M/P ratios–Can we agree on how to calculate them," *IES Illum. Eng. Soc.*, vol. 27, 2019.

[17] S. Cie, "026/E: 2018 CIE System for Metrology of Optical Radiation for ipRGC-Influenced Responses to Light," *CIE Cent. Bur. Vienna, Austria*, 2018.

[18] Well, "Well certified." https://v2.wellcertified.com/en.

[19] "EN 12464-1." https://landingpage.bsigroup.com/LandingPage/Undated?UPI=000000000030081826&utm_campaign=pdfdoi.

[20] "CEN/TR 16791." https://landingpage.bsigroup.com/LandingPage/Undated?UPI=000000000030310356&utm_campaign=pdfdoi&utm_medium=pdf&utm_source=pdfdoi.

[21] P. H. Ewing, J. Haymaker, and E. A. Edelstein, "Simulating circadian light: Multi-dimensional illuminance analysis," in *Proceedings of the 15th IBPSA Conference*, 2017, pp. 2363–2371.

[22] J. Potočnik and M. Košir, "Influence of commercial glazing and wall colours on the resulting non-visual daylight conditions of an office," *Build. Environ.*, vol. 171, p. 106627, 2020.

[23] A. Sánchez-Cano and J. Aporta, "Optimization of lighting projects including photopic and circadian criteria: A simplified action protocol," *Appl. Sci.*, vol. 10, no. 22, p. 8068, 2020.

[24] I. Acosta, J. F. Molina, and M. Á. Campano, "Analysis of Circadian Stimulus Provide by Daylighting in Educational Uses."

[25] L. Bellia, I. Acosta, M. Á. Campano, and F. Fragliasso, "Impact of daylight saving time on lighting energy consumption and on the biological clock for occupants in office buildings," *Sol. Energy*, vol. 211, pp. 1347–1364, 2020.

[26] M. Andersen, J. Mardaljevic, and S. W. Lockley, "A framework for predicting the non-visual effects of daylight–Part I: photobiology-based model," *Light. Res. Technol.*, vol. 44, no. 1, pp. 37–53, 2012.

[27] D. M. Dacey, "Circuitry for color coding in the primate retina.," *Proc. Natl. Acad. Sci.*, vol. 93, no. 2, pp. 582–588, 1996.

[28] M. G. Figueiro, J. D. Bullough, R. H. Parsons, and M. S. Rea, "Preliminary evidence for spectral opponency in the suppression of melatonin by light in humans," *Neuroreport*, vol. 15, no. 2, pp. 313–316, 2004

.

How to Design a Proper Daylight Control System? An Example of Calibration Under Overcast Sky Conditions

Remedios M. López-Lovillo
Department of Architectural Constructions I
University of Seville
Seville, Spain
rllovillo@us.es

Laura Bellia
Department of Industrial Engineering
University of Naples "Federico II"
Naples, Italy
bellia@unina.it

Francesca Fragliasso
Department of Industrial Engineering
University of Naples "Federico II"
Naples, Italy
francesca.fragliasso@unina.it

Ignacio Acosta
Department of Architectural Constructions I
University of Seville
Seville, Spain
iacosta@us.es

Samuel Domínguez-Amarillo
Department of Architectural Constructions I
University of Seville
Seville, Spain
sdomin@us.es

Juan José Sendra
Department of Architectural Constructions I
University of Seville
Seville, Spain
jsendra@us.es

***Abstract*—Despite the benefits that lighting control systems provide in terms of energy saving and improving user comfort, these systems are not very spread due to several factors. Furthermore, one of the main challenges to overcome in the configuration of these systems is the adaptation to natural lighting, due to its continuous variations. With this paper it is proposed to give the keys to obtain a simple automatic control system, which gives good results and low cost. To do this, it is proposed to find the existing correlation value between the photosensor signal and the work plane illuminance to calibrate the system under overcast sky conditions. For this, a private office in Naples is considered as a case study. Specifically, three calibration strategies were compared, respectively based on 1) data referred to the entire year, 2) data referred to each month and 3) data depending on sun position. The results obtained show that the best calibration strategy for this case located in Naples and facing south, is considering the position of the sun. This is so because it has been demonstrated that despite being an analysis under overcast sky condition, there is an influence of the incidence of the sun.**

***Keywords*—Daylight linked control systems, daylight availability, daylight linked control systems calibration strategies, overcast sky**

I. INTRODUCTION

In the design of a building, daylight-linked controls (DLC) play a key role since, in addition to ensuring comfort conditions for users, they contribute significantly to energy savings [1].

The use of DLC is beginning to spread, although the results are not always auspicious due to difficulties from design to commissioning [2].

One of the main problems is related to the integration of daylight. Daylight has multiple proven benefits ranging from ensuring user performance [3] to improving their mental [4] and biological health [5], even affects the circadian rhythm [6]. However, the control of daylighting is quite complex due to the continuous changes depending on the type of sky, the position of the sun (direct radiation), etc.

Daylighting in the DLC system is often incorporated using photosensors. These elements report the amount of daylight available to adjust electric lighting to the required lighting conditions. The type [7][8][9], position [8][10][11][12][13][14], and number [13][15][14] of photosensors will condition the performance of DLCs, so their configuration has been a field of in-depth study in recent years.

The main objective of the DLC system is to ensure that the illuminance at the work plane is optimal for each specific task [16]. To guarantee that this occurs, it is necessary to know the level of illumination at these points to cover with electric lighting the desired level that cannot be achieved with daylighting. To guarantee that is a complicated task since the lighting conditions in a space are not constant. Interior daylight is affected by static factors such as the morphology of windows [17][18], the orientation [18][19] or the reflectance of the surfaces [18][20], but also by dynamic factors such as the period of year [21], the type of the sky [22] or the solar radiation [23] which make it necessary to check the lighting levels from time to time.

Ideally, to have this information, a photosensor should be placed on the working plane. However, the information perceived by the sensors placed in this position can be interfered with by objects or the movement of users [16][24]. Some methodologies rely on alternative configurations such as user-ported sensors [25] or sensorless systems [26]. However, the most traditionally used option is the placement of sensors on the ceiling plane [16]. This configuration requires a calibration process. This is again a challenge, as the calibration is based on establishing a correlation between the illuminance measured by the photosensor in the ceiling or a wall plane and the one established at the working plane, which is conditioned by the variation in the indoor lighting environment [27][14].

The DLCs calibration will determine how the system works and it depends on the type of control strategy. To obtain this value, some methodologies use monitoring campaigns with photosensors on the work plane and on the ceiling or wall[14][27][28]. With this information, it is possible to obtain the typical correlation (E/S) between the illuminance at the work plane (E) and the photosensor signal (S). However, this is not always possible, or it is difficult to obtain a large amount of data to get reliable results. An alternative to monitoring is the use of simulation tools to determine these values [15][29][30].

Several methodologies have stated that calibration cannot be considered standard due to the aforementioned changes in the indoor lighting environment [8][31]. In an attempt to address this gap, Chiogna et al. [14] have proposed seasonal calibration functions. Li et al. [22] established different calibration strategies depending on the type of sky: overcast and non-overcast and they found satisfactory calibration results in the absence of direct sunlight.

All these conditions cause that the use of the DLC system is not very widespread [2]. Therefore, the motivation of this work is to deepen the effects of calibration strategy on DLCSs functioning in order to give a contribute in overcoming the limits preventing the spread of the control systems.

The objective of this paper is to propose a reliable calibration strategy for DLC systems in a Mediterranean climate (Naples) under overcast sky conditions. At this latitude, it is relatively easy to achieve adequate illumination levels on the working plane only with daylight under non-overcast sky conditions, so DLCs are mostly activated under overcast sky. For this, it is proposed to consider three calibration strategies based on simulated data: annual, monthly, and depending on the position of the sun.

II. Methodology

To determine the best calibration strategy, we must first be acquainted with the illuminance values at the working plane and those detected by a photosensor placed on the ceiling. For this reason, it is necessary to find a relationship between the daylight value detected at the ceiling and the illuminance on the work plane. To do this, a set of simulations will be performed, under overcast sky.

In these conditions it is more complex to obtain adequate values for the development of the task. A reference value of 500 lux on the working plane will be taken as a reference value considering that there is an office where tasks are writing, typing, reading, data processing [32]. Thus, it will be understood that the system should work when the illuminance on the work plane is less than 500 lux.

A. *Case study description*

This research is supported by a case study located in Naples. It is a single office of a building of Federico II University (Latitude 40° 51′ 22 N, Longitude 14° 14′ 47 E) located at the seventh floor and its dimensions are 4.0 m x 4.0 m x 3.0 m. In this room there is a south-oriented window that is 1.5 m large and 2.4 m high. With respect to furniture, there is a cabinet in front of the window and a desk near the window.

There are three sensors that measure the illuminance on the work plane placed on the desk and a photosensor located on the ceiling as indicated in Fig. 1.

B. *Simulation*

For the simulations, the case study described in Section 2.1 has been considered as a model. The geometry of the space corresponds to the real model and the three illuminance calculation points simulating the sensors are placed on the working plane and one simulating the photosensor on the ceiling, as shown in Fig. 1.

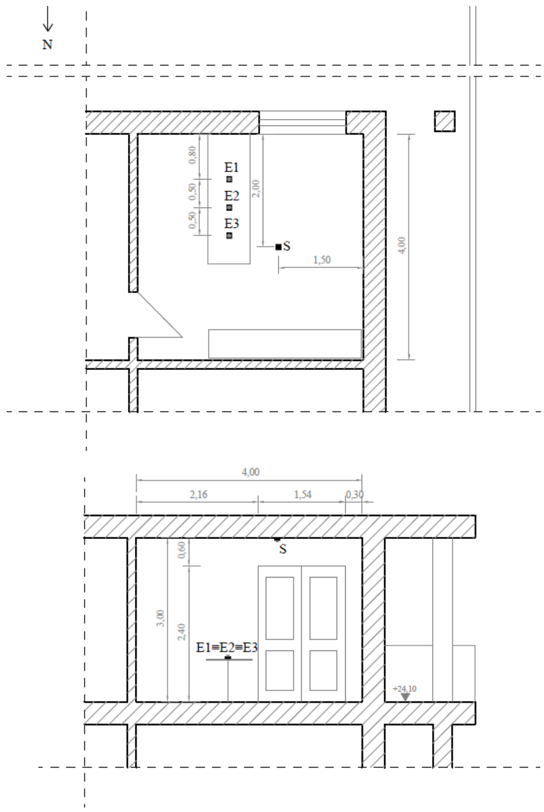

Fig. 1. Room configuration with sensors (E1, E2, E3) and photosensor (S) position

Regarding the reflectance or transmittance of surfaces, those listed in TABLE I have been considered.

First, a static simulation is performed with the DIALux tool version 4.13. In this case, we only want to consider daylight, so no luminaires are incorporated. We select a typical overcast day for each month. The illuminance values obtained on the ceiling (S) and on the work plane (E) are different for each day. However, due to the sky model adopted (standard overcast sky), the E/S ratio remains constant for each moment of the year. Therefore, we assume this value as the annual calibration ratio.

In addition, to consider an analysis closer to reality, a dynamic simulation is performed with the Climate Studio for Rhino tool version 1.2.7796.19900. The selected simulation parameters for this are listed in TABLE III.

To determine the days with overcast sky conditions, we used the global horizontal irradiance (Eglobal) and diffuse horizontal irradiance (Ediffuse) values from the climate file. With these data, the sky ratio (SR = Ediffuse /Eglobal) was analyzed. Those days in which the sky ratio was greater than

TABLE III. Characteristics of the surfaces

Material	Reflectance or transmittance
Interior walls	0.84
Ceiling	0.82
Floor	0.67
Window frame	0.85
Glazing	0.50
Furniture	0.68

TABLE IV. RADIANCE CALCULATION PARAMETERS

Radiance calculation parameters	
Ambient Bounces	6
Ambient divisions	1500
Ambient super samples	100
Ambient resolution	300
Ambient accuracy	0.05

or equal to 0.8 were selected because this implies that they present overcast sky conditions [33].

C. *Calibration strategies*

The most common calibration strategy is based on determining a single value of the E/S ratio for the whole year. Considering a perfect overcast sky, this statement could be fulfilled. However, it has already been mentioned that conditions such as the time of year influence the calibration of the system. Furthermore, in a previous analysis it was found that, despite considering values of SR⩾0.8 in the dynamic simulation and in the real data —therefore overcast skies, the direct component of the sun was affecting the illuminance values measured by the sensors.

Considering this, 3 calibration strategies will be analyzed in this work. The same procedure has been followed for all 3 strategies. First, the data measured by the sensors (obtained through simulation) will be taken hour by hour from 8 am to 7 pm. To find the E value, the average of the data taken by the three illuminance sensors placed on the desk was considered. From this average value, only values below 500 lux have been extracted. The 3 strategies are described below:

- For the first one, the E/S value for a standard overcast sky is calculated. For this, the illuminance data of the static simulation are used as described in Section 2.2.1, obtaining an annual calibration ratio.

- Several methodologies have shown the importance of seasonal/monthly calibration [14][19]. In this way, we propose a monthly analysis considering the dynamic simulation with Climate Studio. We extracted the conditions with SR⩾0.8 and in these cases, the E/S ratio is analyzed for each month, obtaining one calibration ratio value for each month.

- The third strategy is based on the observation that, even whit overcast conditions the position of the sun in the sky vault can affect the calibration ratio. To determine the number of different calibrations created by this phenomenon, all the values of the dynamic simulation for SR⩾0.8 were analyzed by means of a graph. It was observed that 3 trend lines could be distinguished and that these lines correspond to different time slots (see Fig. 2). The correlation in the 3 lines is significant, as for each one, the R2 value is 0.98, 0.97 and 0.99 respectively. In this way, the incidence of the sun entering through the window was checked graphically as a function of its hourly position (mainly influenced by the azimuth), and it was found that these ranges corresponded to different times when the sun's radiation affected one or another area of the room. It was concluded that there were 3 different time ranges that could correspond to 3 periods of the day (different positions of the sun in the sky): 8 a.m. – 11 a.m., 12 p.m. – 1 p.m., 2 p.m. – 7 p.m.

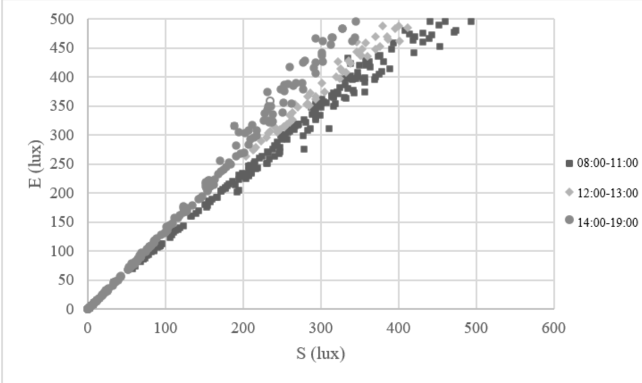

Fig. 2. Work-plane illuminance (S) vs. photosensor signal (E)

TABLE V summarizes the three strategies.

The efficacy of a calibration strategy is evaluated by comparing the actual illuminance at the work plane with the one predicted by the controller according to the calibration ratio and the photosensor signal. The lower are the differences the better the performance.

The predicted illuminance values depending on the photosensor signal at each moment t, $E_{exp,t}$, are calculated as the product of the calibration ratio to the simulated photosensor signal:

$$E_{exp,t} = E/S*S_t \quad (1)$$

where $E_{exp,t}$, is the expected illuminance at the work plane according to photosensor detections and S_t is the photosensor signal.

To analyze which strategy allows the system to work better, the so-obtained values were compared with the simulated ones. So, the error is:

$$Error = (E_{exp,t} – E_{sim,t})/E_{sim,t} *100 \quad (2)$$

where $E_{exp,t}$ is the expected illuminance at the work plane according to photosensor detections and $E_{sim,t}$ is the simulated illuminance on the work plane.

Furthermore, we evaluate the MSE values for each strategy.

III. RESULTS AND DISCUSSION

Considering the first calibration strategy, the initial analysis was performed by static simulation with DIALux. In this case, the E/S ratio is 0.86.

To check the efficiency of the system operating throughout the year with this value, the error between the values obtained in the work plane applying this calibration and the work plane

TABLE VI. TYPE OF CALIBRATION STRATEGIES

Strategy type	Simulation type	Overcast sky determination	Calibration type caracterization
Annual	Static	CIE standard overcast sky	One value
Monthly	Dynamic	SR⩾0.8	12 values - 1 per month

Depending on the sun position	Dynamic	SR⩾0.8	3 values - 1 per range (8 a.m.-11 a.m., 12 p.m.-1 p.m., 2 p.m.-7 p.m.)

TABLE IV. MONTHLY RATIO E/S

Month	E/S
January	1,22
February	1,19
March	1,22
April	1,23
May	1,24
June	1,25
July	NO DATA
August	1,28
September	1,15
October	1,21
November	1,24
December	1,15

illuminance values of the dynamic simulation was analyzed. In this case, most of the error are between 34% and 54%, so the system would not be operating efficiently.

Considering the second calibration strategy, monthly calibration, the ratio E/S is set for all months except July, since there are no data on days with overcast sky in this month. TABLE IV shows the ratio for each month.

In this case, when checking the errors, i.e., how the system would work if each ratio was taken in the corresponding month the bulk is concentrated between 3%, which is an acceptable value, and 13%, which is still a high value.

With the third strategy, the ratios are obtained for the whole year, which vary according to the position of the sun during the day. The values obtained for each range are shown in TABLE IV.

In this case, the error between the values obtained from the calibration and the simulated values is smaller; it is between 3% and 9%. Thus, although this last calibration is unique for the whole year, the incidence of direct radiation has more weight in the operation of the system than the time of the year.

Comparing the MSE of the 3 strategies between the expected results and those obtained, it is confirmed that the strategy based on the position of the sun presents a lower value (528 sun position; 1568 monthly; 8524 annual).

IV. CONCLUSIONS

The aim of this work was to find the best calibration strategy that would allow a DLC system to work in a simple and economical way using a ceiling photosensor under overcast sky conditions.

For this reason, three calibration strategies have been proposed based on static and dynamic simulations: annual, monthly, and depending on the sun position.

In this research, it is demonstrated that the incidence of the sun influences the operation of the system despite considering overcast sky. Therefore, the best calibration strategy will be based on solar position for this case study with a window oriented to the south.

A solar position-based calibration strategy is proposed improving performance of the present system against other calibration methods. Further development of this strategy must analyse the constraints of the specific case.

TABLE V. RATIO E/S DEPENDING ON THE SUN POSITION

Time range depending on the sun position	E/S
8 a.m. – 11 a.m.	1,11
12 p.m. – 1 p.m.	1,25
2 p.m. – 7 p.m.	1,46

This approach allows the system to perform almost 95% better than conventional (annual) calibration strategies and 13% better than monthly strategies. In this way, this strategy will also allow greater energy savings to be achieved because the system will work more efficiently.

The calibration based on the position of the sun proposed in this research allows to approach the problem for other sky conditions, extending the procedure to general cases, as will be considered in future research.

ACKNOWLEDGMENT

The authors would like to thank the Government of Spain for financing the predoctoral contract (FPU18/04889) and the research stay at the Federico II University of Naples for Remedios M. López-Lovillo, which has made this joint research possible. In addition, they would like to thank the Federico II University of Naples for giving the space of the case study. Also thank the support of the Doctorate Program in Architecture of the University of Seville and the Research group TEP-130: Architecture, Heritage and Sustainability: Acoustics, Lighting, Optics and Energy.

REFERENCES

[1] M. Á. Campano, I. Acosta, S. Domínguez, and R. López-Lovillo, “Dynamic analysis of office lighting smart controls management based on user requirements,” in Autom. Constr., vol. 133, 2022, doi: 10.1016/j.autcon.2021.104021.

[2] L. Bellia, F. Fragliasso, and E. Stefanizzi, “Why are daylight-linked controls (DLCs) not so spread? A literature review,” Build. Environ., vol. 106, 2016, pp. 301–312, , doi: 10.1016/j.buildenv.2016.06.040.

[3] M. G. Figueiro, M. S. Rea, A. C. Rea, and R. G. Stevens, “Daylight and Productivity – A Field Study,” ACEEE Summer Study Energy Effic. Build., no. January 2002, pp. 69–78, 2002.

[4] M. G. Figueiro et al., “The impact of daytime light exposures on sleep and mood in office workers,” Sleep Heal., vol. 3, no. 3, pp. 204–215, 2017, doi: 10.1016/j.sleh.2017.03.005.

[5] M. S. Rea and M. G. Figueiro, “Quantifying light-dependent circadian disruption in humans and animal models,” Chronobiol. Int., vol. 31, no. 10, pp. 1239–1246, 2014, doi: 10.3109/07420528.2014.957302.

[6] M. S. Rea, A. Bierman, M. G. Figueiro, and J. D. Bullough, “A new approach to understanding the impact of circadian disruption on human health,” J. Circadian Rhythms, vol. 6, pp. 1–14, 2008, doi: 10.1186/1740-3391-6-7.

[7] A. Bierman and K. M. Conway, “Characterizing daylight photosensor system performance to help overcome market barriers,” J. Illum. Eng.

Soc., vol. 29, no. 1, pp. 101–115, 2000, doi: 10.1080/00994480.2000.10748486.

[8] R. G. Mistrick and J. Thongtipaya, "Analysis of daylight photocell placement and view in a small office," J. Illum. Eng. Soc., vol. 26, no. 2, pp. 150–160, 1997, doi: 10.1080/00994480.1997.10748199.

[9] S. Ranasinghe and R. Mistrick, "A Study of Photosensor Configuration and Performance in a Daylighted Classroom Space A Study of Photosensor Configuration and Performance In a Daylighted Classroom Space," vol. 4480, 2013, doi: 10.1080/00994480.2003.10748412.

[10] S. Subramaniam, L. Chen, and R. Mistrick, "Annual Performance Metrics for Photosensor Controlled Daylight-Responsive Lighting Control Systems Dissertation work : Parametric Modeling Strategies for Efficient Annual Analysis of Daylight in Buildings View project Repurposing Radiance for non-visual a," 2013. [Online]. Available: https://www.researchgate.net/publication/325248660

[11] S. Y. Kim, H. H. Alzoubi, and P. Ihm, "Determining photosensor settings for optimum energy saving of suspended lighting systems in a small double-skinned office," Int. J. Energy Res., vol. 33, no. 6, pp. 618–630, 2009, doi: 10.1002/er.1501.

[12] R. Mistrick and A. Sarkar, "A study of daylight-responsive photosensor control in five daylighted classrooms," LEUKOS - J. Illum. Eng. Soc. North Am., vol. 1, no. 3, pp. 51–74, Mar. 2005, doi: 10.1582/LEUKOS.2005.01.03.004.

[13] N. H. M. R. Khairul Rijal Wagiman, Mohd Noor Abdullah, Mohammad Yusri Hassan, "A-new-optimal-light-sensor-placement-method-of-an-indoor-lighting-control-system-for-improving-energy-performance-and-visual-comfortJournal-of-Building-Engineering.pdf."

[14] M. Chiogna, R. Albatici, and A. Frattari, "Electric lighting at the workplace in offices: Efficiency improvement margins of automation systems," Light. Res. Technol., vol. 45, no. 5, pp. 550–567, Oct. 2013, doi: 10.1177/1477153512461372.

[15] A. Tsangrassoulis, L. Doulos, and A. Mylonas, "Simulating the impact of daytime calibration in the behavior of a closed loop proportional lighting control system," Energies, vol. 14, no. 21, Nov. 2021, doi: 10.3390/en14217056.

[16] F. Rubinstein, G. Ward, and R. Verderber, "Improving the Performance of Photo-Electrically Controlled Lighting Systems".

[17] I. Acosta, M. Á. Campano, and J. F. Molina, "Window design in architecture: Analysis of energy savings for lighting and visual comfort in residential spaces," Appl. Energy, vol. 168, pp. 493–506, 2016, doi: 10.1016/j.apenergy.2016.02.005.

[18] R. A. Mangkuto, M. Rohmah, and A. D. Asri, "Design optimisation for window size, orientation, and wall reflectance with regard to various daylight metrics and lighting energy demand: A case study of buildings in the tropics," Appl. Energy, vol. 164, pp. 211–219, 2016, doi: 10.1016/j.apenergy.2015.11.046.

[19] L. Bellia and F. Fragliasso, "Automated daylight-linked control systems performance with illuminance sensors for side-lit offices in the Mediterranean area," Autom. Constr., vol. 100, no. December 2018, pp. 145–162, 2019, doi: 10.1016/j.autcon.2018.12.027.

[20] L. Bellia, F. Bisegna, and G. Spada, "Lighting in indoor environments: Visual and non-visual effects of light sources with different spectral power distributions," Build. Environ., vol. 46, no. 10, pp. 1984–1992, Oct. 2011, doi: 10.1016/J.BUILDENV.2011.04.007.

[21] M. Beccali, M. Bonomolo, G. Ciulla, and V. Lo Brano, "Assessment of indoor illuminance and study on best photosensors ' position for design and commissioning of Daylight Linked Control systems . A new method based on arti fi cial neural networks," Energy, vol. 154, pp. 466–476, 2018, doi: 10.1016/j.energy.2018.04.106.

[22] D. H. W. Li and E. K. W. Tsang, "An analysis of measured and simulated daylight illuminance and lighting savings in a daylit corridor," Build. Environ., vol. 40, no. 7, pp. 973–982, 2005, doi: 10.1016/j.buildenv.2004.09.007.

[23] V. Čongradac, M. Prica, M. Paspalj, D. Bojanić, and D. Čapko, "Algorithm for blinds control based on the optimization of blind tilt angle using a genetic algorithm and fuzzy logic," Sol. Energy, vol. 86, no. 9, pp. 2762–2770, Sep. 2012, doi: 10.1016/j.solener.2012.06.016.

[24] D. Caicedo and A. Pandharipande, "Daylight and occupancy adaptive lighting control system: An iterative optimization approach," Light. Res. Technol., vol. 48, no. 6, pp. 661–675, Oct. 2016, doi: 10.1177/1477153515587148.

[25] M. G. Figueiro, R. Hamner, A. Bierman, and M. S. Rea, "Comparisons of three practical field devices used to measure personal light exposures and activity levels," Light. Res. Technol., vol. 45, no. 4, pp. 421–434, 2013, doi: 10.1177/1477153512450453.

[26] N. Lee, J. Kim, C. Jang, Y. Sung, and H. Jeong, "Comparison of sensorless dimming control based on building modeling and solar power generation," Energy, vol. 81, pp. 15–20, 2015, doi: 10.1016/j.energy.2014.10.027.

[27] D. Caicedo, S. Li, and A. Pandharipande, "Smart lighting control with workspace and ceiling sensors," Light. Res. Technol., vol. 49, no. 4, pp. 446–460, Jun. 2017, doi: 10.1177/1477153516629531.

[28] B. C. Park, A. S. Choi, J. W. Jeong, and E. S. Lee, "A preliminary study on the performance of daylight responsive dimming systems with improved closed-loop control algorithm," LEUKOS - J. Illum. Eng. Soc. North Am., vol. 8, no. 1, pp. 41–59, Jul. 2011, doi: 10.1582/LEUKOS.2011.08.01.003.

[29] L. Bellia, A. Pedace, and F. Fragliasso, "The impact of the software's choice on dynamic daylight simulations' results: A comparison between Daysim and 3ds Max Design®," Sol. Energy, vol. 122, pp. 249–263, 2015, doi: 10.1016/j.solener.2015.08.027.

[30] I. Acosta, J. Navarro, and J. J. Sendra, "Towards an analysis of daylighting simulation software," Energies, vol. 4, no. 7, pp. 1010–1024, 2011, doi: 10.3390/en4071010.

[31] R. Mistrick, C. H. Chen, A. Bierman, and D. Felts, "A comparison of photosensor-controlled electronic dimming systems in a small office," J. Illum. Eng. Soc., vol. 29, no. 1, pp. 66–80, 2000, doi: 10.1080/00994480.2000.10748483.

[32] "Light and lighting - Lighting of work places - Part 1: Indoor work places, EN 12464-1, 2021."

[33] D. DiLaura, K. Houser, R. Mistrick, and G. Steffy, "ESNA Lighting Handbook 10th edition," Illum. Eng. Soc. North Am., 2011.

Bringing Daylighting to the Fore: Advances in Integral Control Concepts, Simulation Tools, and Evaluation Metrics

David Geisler-Moroder
Research & Development
Bartenbach GmbH
Aldrans, Austria
david.geisler-moroder@bartenbach.com

Martin Hauer
Research & Development
Bartenbach GmbH
Aldrans, Austria
martin.hauer@bartenbach.com
Unit for Energy Efficient Buildings
University of Innsbruck
Innsbruck, Austria
martin.hauer@uibk.ac.at

Christian Knoflach
Research & Development
Bartenbach GmbH
Aldrans, Austria
christian.knoflach@bartenbach.com

Wilfried Pohl
Research & Development
Bartenbach GmbH
Aldrans, Austria
wilfried.pohl@bartenbach.com

***Abstract*—Daylighting plays a key role in providing a biologically effective and energy efficient lighting of indoor spaces with highest visual and thermal comfort. In this article, we summarize key findings from research projects conducted in this area. We focus on three important areas in the field of daylighting design and technology:**

(i) We present an integral control concept that promotes individual lighting of workplaces, the so-called IndiLight-Module (ILM). This simulation-based control kernel calculates the optimum shading configuration of each contributing façade opening depending on the current exterior situation (incident radiation, ambient temperature) as well as the workplace-individual interior situation and demands (visual comfort, electric lighting). First results from a Living Lab installation and simulation studies show the ILM's potential to reduce a building's primary energy demand to a minimum by optimizing solar gain and daylight utilization respectively solar shading individually for individual façade parts and workplaces.

(II) We show recent advances in daylight simulation possibilities which allow a better support through digital models and tools in design and evaluation of daylighting projects. This includes the detailed representation of daylighting systems in the software tools through correct application of their so-called bidirectional scattering distribution function (BSDF). Additionally, we present a novel algorithm that allows improved simulations of direct solar contributions through daylighting systems and thus more accurate evaluation of resulting luminance distributions and subsequently evaluation of glare effects.

(iii) We highlight shortcomings and challenges in the evaluation of daylight performance metrics with a special focus on the assessment of daylight glare. Glare metrics – regardless of whether for daylight or electric lighting – penalize small and bright light sources excessively. In the case of daylight, this is especially problematic for situations with the sun in the field of view, even if the luminance is sufficiently reduced through a shading system. We present an approach to solve this problem and make daylight glare evaluations easier to apply in practical daylighting design projects.

Keywords—daylight, integral control, simulation, daylight glare evaluation

I. Introduction

Electric lighting accounts for 5% of the global CO2 emissions and 15% of the total electricity consumption and thereby causes a significant ecological "carbon" footprint with a direct impact on global warming. Moreover, in the transition to mainly electricity-based energy systems, lighting faces direct and strong competition from new consumers (heat pumps, e-mobility, new electronic devices, etc.) and existing devices (HVAC utilities, office equipment, household appliances, and entertainment electronics). Against this background, daylighting of buildings is coming more and more to the focus as a renewable, efficient, unlimited, and freely available resource.

In January 2019, the Solar Heating and Cooling Technology Collaboration Programme of the International Energy Agency, IEA SHC, published a position paper titled "Daylighting of Non–Residential Buildings" [1] to highlight why the use of daylight in the built environment needs to be extensively and widely supported, expanded and promoted. The advent of new standards (e.g., the European standard EN 17037 Daylight in Buildings) and further development of certification schemes also towards non-visual, biological effects of (day-)lighting (LEED, WELL building standard, etc.), brings daylight even more to the fore.

At Bartenbach, we are continuously working on several projects to gain new insights in the field of daylighting and to drive innovations in the field of efficient and healthy daylighting of buildings. From these projects, we report results in three important areas: integrated day- and electric lighting controls, advanced daylighting simulations taking into account complex fenestration systems, and the evaluation of daylight glare as an essential measure of visual comfort.

II. The IndiLight-Module (ILM) Control Strategy

A. Trends in control concepts

In real applications, control strategies for day- and artificial lighting systems are still mainly rule-based and less integrated, as mostly both systems are operated separately. A review of literature published between 2015 and 2020 on integral control strategies for day- and artificial lighting for office application highlights a clear trend in research towards addressing multiple trades for achieving a maximum improvement in user comfort and energy efficiency [2]. The review mentions user acceptance as a decisive factor to achieve the targeted effectiveness of complex control routines also in real-world applications. In general, the trend is moving towards decentralized control concepts with appropriate occupancy detection and space zoning, which are able to address both, high user centeredness and optimal user comfort through individual configurations, while optimizing the building's energy demand by space- or façade-specific control. In this context, integral control concepts based on simulations or learning systems offer suitable methods to achieve these requirements.

To evaluate the impact of integral control solutions for day- and artificial lighting in a more general view, a simulation-based case study was elaborated based on a simple shoebox model for three locations, testing different control approaches in combination with multiple façade configurations and artificial lighting operating modes [3]. The investigated cases show significant differences between the applied lighting control strategies in terms of energy demand when the availability of natural daylight is considered, and in terms of visual comfort if an appropriate blind control strategy is used that takes glare problems into account. The results also clearly show that energy optimization acts partly contradictory to the needs in visual comfort, which strives again for integrative control approaches capable to optimize among different trades.

B. The ILM-concept

Within a cooperative research project together with the University of Innsbruck and HELLA Sonnen- und Wetterschutztechnik, we developed an integral control concept that promotes individual lighting of workplaces – the so-called IndiLight-Module (ILM). This simulation-based control kernel applies a full-factorial design to evaluate all possible states of the façade system to determine the optimum shading configuration for each contributing façade opening depending on the current exterior situation (incident radiation, ambient temperature) as well as the workplace-individual interior situation and demands (visual comfort, electric lighting). To apply a melanopic optimization, the vertical illuminance values for the occupants of the respective façade configurations are summed up to calculate a daily light dose. The configuration with the maximum value is chosen. In this way, a compromise between comfort and energy optimization is realized. In addition, daylight exposure of the occupants can be improved which represents an important factor for the melanopic effect.

For a defined time-interval, the ILM provides the dimming value for the artificial lighting as well as the optimum setting of the daylighting system (i.e., blind position and slat angle in the case of a venetian blind) in real time depending on the external conditions. Therefor it uses a dataset of pre-calculated factors for the day- and artificial light calculation as well as the EN 13790 algorithms for the quasi-static energy balancing. This allows a time- and computationally efficient application, which can be integrated in real operating control systems. The kernel is developed in MATLAB and can be easily implemented as compiled DLL in existing building management systems. Fig. 1 shows the conceptual input/output scheme of the ILM control.

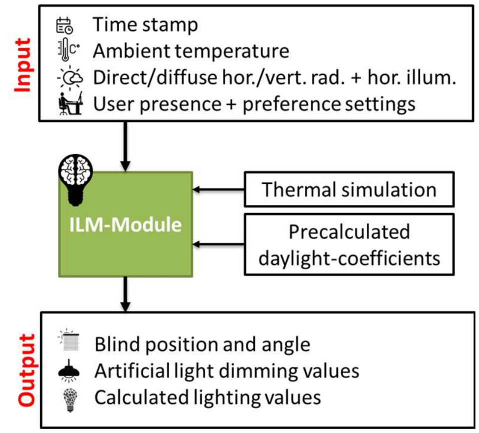

Fig. 1. Input/Output scheme of the IndiLight module.

In contrast to conventional control strategies and referring to the name "Indi", the ILM is a workstation-specific control system that optimizes day- and artificial lighting as well as the comfort situation individually for each occupant. This requires a specific configuration of the module for each building and room setup. A configuration workflow (the so-called "Honeybee2ILM" script) allows to extract datasets required for setting up the ILM from the simulation model as it is used in the design phase. This offers several advantages: i) the same simulation model used for the planning of a building is also applied to configure the control module, thus minimizing the performance gap between planning and operation; ii) beside design decisions, also a control approach for the building can be provided already within the planning phase; and iii) the control strategy can be optimized and tested within a simulation environment already before the commissioning starts. In this context, BIM-based methods hold the chance to improve the practice of implementing building control strategies drastically by providing all needed data from a single source.

Results of an earlier simulation study [4] show that the ILM strategy has a significant influence on the total energy demand of buildings, with up to 30 % savings in total primary energy demand compared to conventional sun protection controls.

C. Current ILM investigations

To evaluate the benefits of the ILM concept in real applications, an implementation was tested in a Living Lab installation at HELLA Sonnen- und Wetterschutztechnik premises in July and August 2021. First results from the four-week testing period show the ILM's potential to reduce a building's primary energy demand to a minimum by optimizing solar gains and daylight utilization or solar shading individually for individual façade parts and workplaces. A detailed description of the office room and the results of the investigation are presented in [5]. The test office has a south-oriented façade with a double-glazing window and an exterior venetian blind system. The artificial lighting is realized with four dimmable LED tubes that can be switched separately. The office has in total three workplaces.

A comparison of the target illuminance levels on the work plane with the monitored data shows a good agreement. Also, an occupant survey conducted during the study phase confirms that operating the lighting and shading system depending on individual workplace preferences is perceived as very positive. For this particular study it was found that the standard target values for the horizontal illuminance of Eh = 500 lx on the desk and the glare limit of L = 3000 cd/m^2 were too stringent. Based on logged overruling entries by the users, a horizontal illuminance of Eh = 390 lx and a glare limit of L = 3800 cd/m² could be determined in average as subjective preferred values for this study setting. However, it is questionable whether the subjective perception then also corresponds to an objective good visual environment to support performance and health.

A further test implementation is planned at the University of Innsbruck, where one office room will be equipped with the ILM for applying and monitoring the control under real conditions. A half-year extensive testing phase is planned from July 22 to December 22. The results will be directly compared to a parallel installation in a neighboring office equipped with a state-of-the-art, rule-based blind control and dimmable artificial lighting controlled by a look-down sensor.

In addition to those practical implementations also simulation case studies applied on simple show box models as well as an open plan office with multiple façade sections are currently under investigation. This allows to optimize the control algorithm as well as to test the potential in enhancing a building's overall energy demand in larger models on full building scale.

III. BSDF Characterization of Daylighting Systems and BSDF Peak Extraction

A. BSDF Characterization of Daylighting Systems

Standardized methods for characterizing angle-dependent, solar-optical properties of transparent glazing for windows are well established, i.e., visible and solar transmittance, absorptance, reflectance, and solar heat gain coefficient. Standardized methods do not exist however for "optically complex" or light scattering shading and daylighting systems, which in turn makes objective evaluation of energy performance, daylighting, comfort, and other building performance qualities almost impossible. Simplified methods for characterizing complex fenestration systems (CFS) have been developed based on normal/normal, normal/hemispherical, and diffuse/hemispherical transmittance measurements. These methods have found their way into European standards [6] but are of limited use for CFS and can contribute to significant error in evaluations of certain aspects of building performance. To overcome these restrictions, so-called bidirectional scattering distribution functions (BSDF) are used to describe how light from each incident direction is scattered (reflected and transmitted) by a simple or composite surface, such as a window shade. BSDFs are used in design practice to represent optically complex daylighting and solar control systems in lighting and energy simulation software. An example is shown in Fig. 2 for a 3D shaped highly reflective solar protection louver system.

In the recently finished IEA SHC Task 61 [7] an international group of experts summarized the current state of the art in the field of measurement and simulation characterization of daylighting systems by BSDFs [8]. The document also provides recommendations broken down by classes of systems and use cases and describes proposed procedures for the measurement of angle-dependent transmittance and reflectance properties of daylighting and shading systems, and the generation of tabular BSDF data sets from measurement data for use as input to simulation tools.

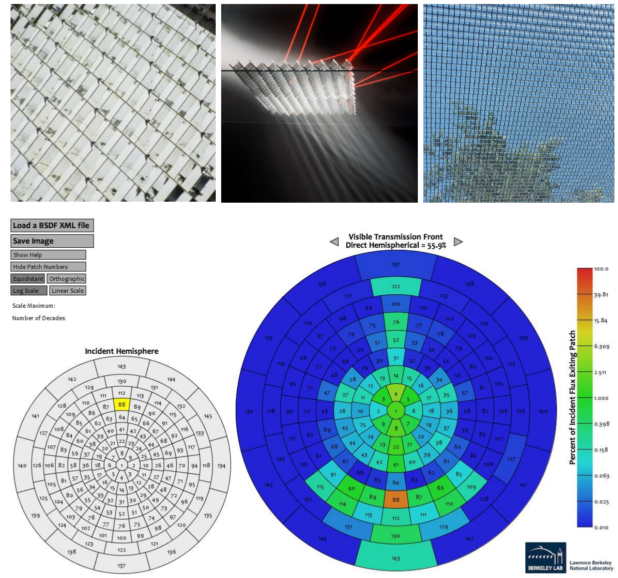

Fig. 2. Three-dimensionally shaped highly reflective solar control louver (top) and resulting BSDF in Klems resolution, showing the exiting distribution for irradiation from patch around 50° (bottom).

While BSDF representations using a coarse subdivision of incident and exiting hemispheres (145x145 Klems, or 145x1297 IEA21, cf. e.g. [8]) are suitable for illuminance or SHGC calculations, visual comfort assessments (e.g., daylight glare) require accurate determination of luminance and corresponding solid angle of glare sources. For the sun, the necessary resolution of the BSDF would cause problems both in terms of data volume and computational effort. Sunlight, whether transmitted, scattered, or reflected, needs to be predicted at highest accuracy due to its high intensity. An accurate representation of the direct solar contribution is critically important when it comes to luminance-based output. This includes evaluation of visual comfort (e.g., using the daylight glare probability (DGP) metric [9, 10]) as well as realistic appearance of physically-based renderings (e.g., sun in the field of view or sharp shadow patterns).

B. Peak Extraction from BSDF Data

With the "peak extraction" (PE) concept [11], a new method was developed that simulates the direct solar contribution at its real size and spread, while efficiently using the underlying BSDF data set for the scattered light. The algorithm analyzes tabulated BSDF data for every ray that hits the respective daylighting or shading system surface and determines whether the underlying distribution has a peak in the tested direction (e.g., peak in the distribution shown in Fig. 2, bottom, describing the direct-through component). By checking surrounding directions, the algorithm determines if there is a strong local peak in the distribution. If so, the peak is replaced with a direct specular component where the transmission is calculated from the local BSDF value.

In Radiance, the leading software package for daylighting simulations [12], the PE method has been implemented in the *aBSDF* material ("a" for "aperture") [13]. By assigning this material, the user tells the software to look for a possible peak in direct transmission. This results in well-defined shadow contours as well as a sharp view through the fenestration system modeled by *aBSDF* (Fig. 3), the view being of particular importance in contrast-based glare evaluations. PE thus enables practitioners to evaluate daylight performance metrics for their designs at improved accuracy.

Fig. 3 shows the effect of the PE method in simulations of a simple test room. The window is equipped with a fabric shade with 2% openness factor, and a tree is placed in front of the window. The renderings in Fig. 3 show the differences between the simulations not applying the PE method (top) and applying the method (bottom). Using the novel PE method generates an undistorted view through the perforated and thus partially open fabric (note the tree and horizon). Also, the interior shadow patterns appear sharp as expected from such a system instead of being blurred when not using PE.

C. *Impact of the BSDF Peak Extraction Method*

The PE method was applied for a test case mimicking a real-world office application (Fig. 4). The glare protection system attached to the upper window is the same fabric shade as in the example space in Fig. 3, i.e. a gray fabric with 2% openness factor. Here the simulations also show the difference in both the visual appearance of the shadow patterns in the room and the size and luminance of the direct sun in the field of view. While the vertical illuminance evaluated from the image remains equal except for minor stochastic effects (Ev = 542lx and Ev = 544lx, respectively) and thus gives evidence for the correctness of the implementation of the algorithm, the maximum luminance in this example changes from 163K cd/m^2 without PE (Fig. 4, top) to 4,260K cd/m^2 with PE (Fig. 4, bottom). The corresponding DGP value (evaluated using the *evalglare* tool [14]) increases from 0.248 (classification "imperceptible" glare) to 0.359 ("noticeable" glare).

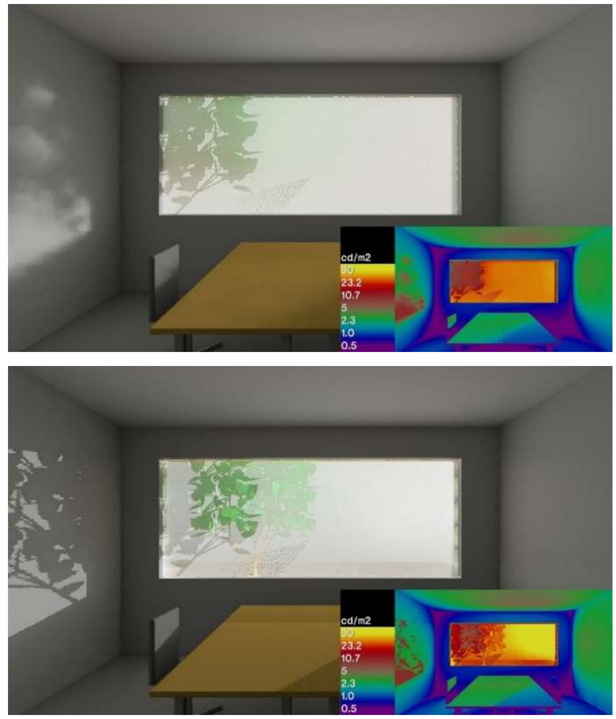

Fig. 3. Simulation of a room with a window equipped with a fabric glare protection system without applying the PE method (top) and with applying the PE method (bottom). The differences are in the view through the system and in the interior shadow patterns.

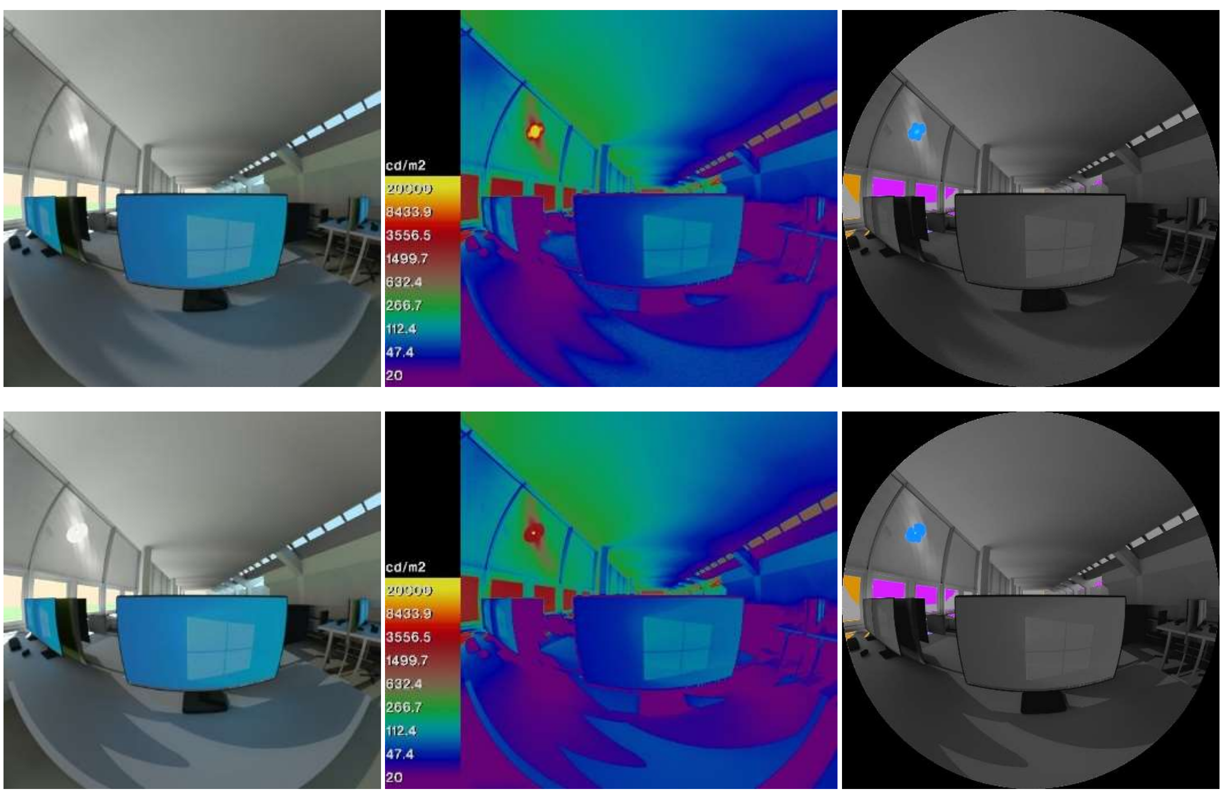

Fig. 4. Simulation of an office space equipped with fabric glare protection systems. Renderings (left column), luminance falsecolor images (center column) and glare sources reported by *evalglare* (right column) resulting from simulation without applying the PE method (top row) and with applying the PE method (bottom row). Note the differences in the sharpness of the interior shadow patterns and the size of the solar disk (sunspot).

A second example shows a single office space with a south oriented façade where the window is again equipped with the glare protection fabric with 2% openess factor. The images in Fig. 5 show the resulting differences from using the BSDF data directly in the simulation (top), and using the BSDF data with the PE algorithm (bottom) for a direct view to the façade. The vertical illuminance at the observer position evaluated from the images matches again with some minor simulation variation (Ev = 971 lx and Ev = 946lx, respectively). However, the maximum luminance again rises dramatically when using PE, from 437K cd/m^2 without PE (Fig. 5, top) to 9,560K cd/m^2 with PE (Fig. 5, bottom). Thereby, also the DGP again increases – despite the small decrease in Ev – from 0.352 (classification "noticeable" glare) to 0.403 (classification "disturbing" glare) and thus into the next DGP class.

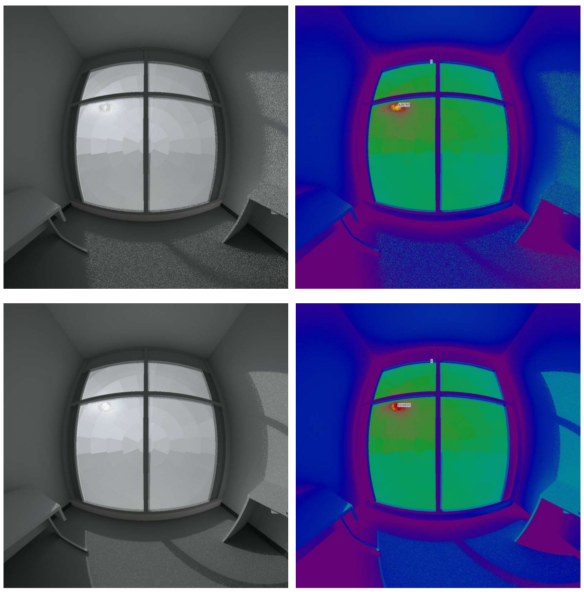

Fig. 5. Simulation of a single office space with south facing façade and window equipped with fabric glare protection. The top row shows the result from a simulation and falsecolor evaluation without applying the PE method, the bottom row with applying the PE method. The differences are in the size of the solar disk (sunspot) and the sharpness of the interior shadows from the window frames.

Summarizing, the new PE algorithm clearly improves accuracy and quality of daylighting simulations with BSDF data of daylighting systems that have a view, or "direct-through transmission", component. This includes many of the widely-used window attachments in buildings as e.g., glare protection fabrics with some openness fraction, blinds, perforated louvers, expanded metal meshes, or even clear and solar protection or electrochromic glazing.

IV. Daylight Performance Metrics for Visual Comfort – Investigations into the Evaluation of Daylight Glare

A. Daylight Glare Evaluation

The evaluation of glare caused from electric lighting is well standardized and normatively anchored through the "Unified Glare Rating" (UGR) calculation methodology. The standard for the lighting of workplaces (EN 12464-1) [15] specifies UGR requirements for all types of interiors, visual task areas and activities. Due to the extensive technology transformation towards LED technology, changes in the calculation methodology are currently being discussed [16], but the specifications in the application remain.

In the daylighting sector, the European standard for daylight in buildings EN 17037 has been published in 2018 and sets out requirements for glare caused by daylight [17]. It is proposed to use the "Daylight Glare Probability" (DGP) [9,10] for the evaluation, however, in the daylight standard also explicit reference is made to shortcomings of the method. This includes two main issues: besides the fact that (i) the DGP should not be applied for the assessment of daylight glare in rooms with horizontal daylight openings, (ii) the probably more important and more critical point is that DGP cannot be applied in situations where vertical illuminance is not a good indicator of glare perception.

In indoor office situations this can e.g. be the case whenever a sun shading or glare protection device is applied that reduces the overall luminous flux, but still leads to high contrast scenarios. A typical example is a fabric glare protection device with a non-negligible openness factor (cf. the simulated fabric in section III). In such setups the primary glare source is the sun disk, which is a tiny (about 2 × 0.26 degrees aperture angle) but very bright (luminance in the order of about 1e9 cd/m^2, possibly only reduced through the glazing transmittance).

Looking at the DGP formula as developed by Wienold and Christoffersen [9], one can notice that in the contrast term (the sum over all glare sources) the luminance of the glare source is squared while the solid angle is linear:

$$\mathrm{DGP} = 5.87 \times 10^{-5} E_{\mathrm{v}} + 9.18 \times 10^{-2} \log\left(1 + \sum_i \frac{L_{\mathrm{s},i}^2 \omega_{\mathrm{s},i}}{E_{\mathrm{v}}^{1.87} P_i^2}\right) + 0.16$$

This is in also line with other contrast-based glare metrics (e.g., UGR). However, for UGR a lower limit for the size of the glare source is specified to maintain the validity of the formula. This limit is given with 0.0003sr, which corresponds to a cone with 2 × 0.56 degrees aperture angle, or about five times the solid angle of the sun. The question is therefore whether a comparable lower limit is also needed for the DGP metric.

B. Investigation of the detectability of the size of glare sources

This led us to investigate in a small pre-study what magnitude a difference in the size of a glare source must have in order to still be detected. if vertical illuminance at the eye is maintained.

A circular disc on an ultra-high bright LED screen serves as a visual stimulus. The diameter and the luminance of this disc in the center of the screen are changed simultaneously in such a way that the vertical illuminance at the eye remains constant. The goal is to determine a size difference above which subjects can detect this change in the peripheral visual field. The assumption is, that below this threshold, the term $L^2\,\omega$ leads to an overestimation of glare from small sources. Illustration with a simple example: The human eye cannot distinguish two squares in the periphery where the larger square has four times the area but only a quarter of the luminance (see Fig. 6). Then it makes no sense to use $L^2\,\omega$ for describing glare.

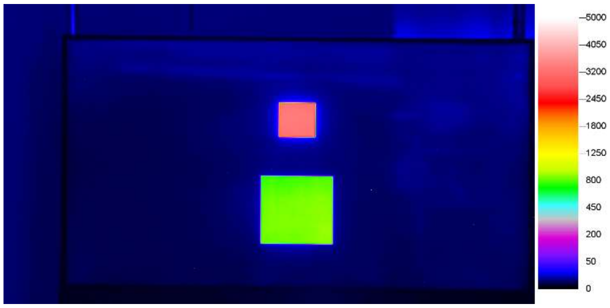

Fig. 6. The lower square has twice the side length, but only 1/4 the luminance of the upper square.

The effect that luminance does not adequately represent the brightness of tiny light stimuli is well known from astronomy when using the apparent magnitude to measure the brightness of a star. Magnitude is not based on luminance (or radiance with a spectral filter) but on illuminance (or spectrally filtered irradiance). The same basic concept of using the illuminance at the observer's eye is frequently used when evaluating glare from small light sources in artificial lighting.

In CIE 147:2002 "Glare from Small, Large and Complex Sources" [18] it is suggested to replace L^2 ω by 200 I^2/r^2 when calculating the UGR for small sources. This corresponds to replacing the real-world geometry of the luminous parts by a sphere with a diameter of 80 mm and thus a projected area of 1/200 m^2. This approach implies that the source is mounted at the ceiling in a typical office room.

This method is specially designed for standard situations in artificial lighting. In contrast to this the aim of our preliminary study is to find out the minimum solid angle (cone $2 \times \gamma_{threshold}$) to justify an evaluation with L^2 ω when applying the DGP-formula for daylighting situations. The concept of an adapted glare rating is then to replace the solid angle for sources smaller than $2 \times \gamma_{threshold}$ by $\omega = 2\,\pi\,(1 - \cos(\gamma_{threshold}))$ or apply a corresponding Gaussian filter on the luminance picture before calculating DGP. This approach generalizes the method described for artificial lighting in CIE 232:2019 "Discomfort Caused by Glare from Luminaires with a Non-Uniform Source Luminance" [16].

The tests are performed for horizontal viewing directions at 30°, 45°, 60°, 75° and 90° to the source and for vertical viewing directions at 30°, 45° and 55° to the source (cf. setup in Fig. 7).

The study on the adaptation of the DGP-formula by means of experiments is currently the subject of research within the framework of the project GLARE.

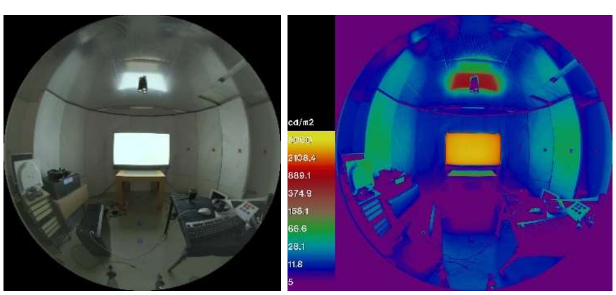

Fig. 7. Experimental setup with an ultra-high bright LED screen.

C. First results

One test run consists of a rough calibration of the size of discs a subject can distinguish for each of the 8 viewing directions considered. Afterwards, highly randomized sequences of four different disc sizes each with double solid angle and 8 viewing directions are presented to prevent learning effects. The test person must guess whether the circular disk is increasing or decreasing in size, or whether the size of the circular disk is not changing. A total of 96 situations are presented for each viewing direction resulting in 768 answers of a single subject.

To date, 14 subjects have participated in the experiment, with a total of 30 runs made resulting in 23040 answers. Typically, a subject participates in the trials twice to be able to respond to the first trial run. Fig. 8 shows an example of the evaluation for a subject for a single viewing direction (horizontal 45° to the source).

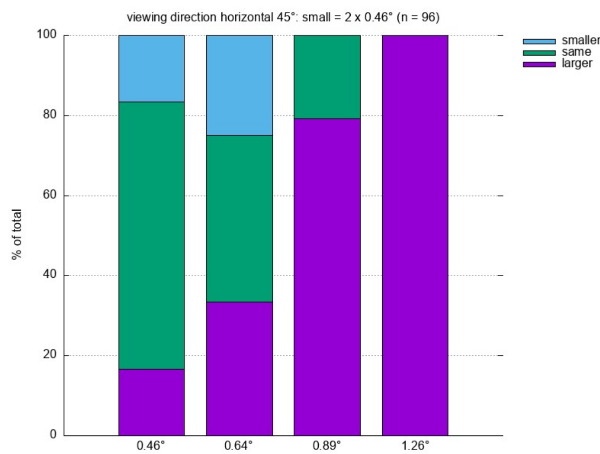

Fig. 8. Statistic for subject DGM3, horizontal viewing direction 45°, resulting in $\gamma_{threshold} = 0.89°$.

Summing up for all subjects so far, the results of these experiments provide a good estimate of the threshold angles $\gamma_{threshold}$ for all eight viewing directions. Fig. 9 and Fig. 10 show the resulting threshold angles for the five horizontal (Fig. 9) and three vertical (Fig. 10) viewing directions investigated.

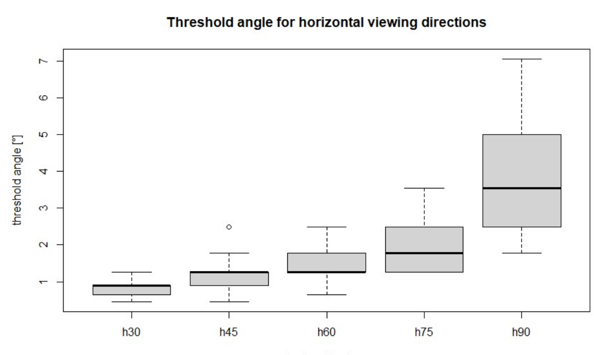

Fig. 9. Threshold angles $\gamma_{threshold}$ for five horizontal viewing directions.

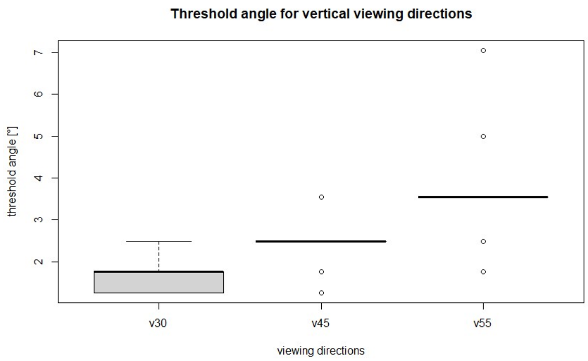

Fig. 10. Threshold angles $\gamma_{threshold}$ for three vertical viewing directions.

According to these experiments the threshold angles for vertical viewing directions $\gamma_{threshold,\ vertical}$ are significantly larger than the threshold angles for horizontal viewing directions $\gamma_{threshold,\ horizontal}$. The visual acuity angles used in CIE 232 are much smaller than the angles $\gamma_{threshold,\ vertical}$. Moreover, the angles calculated according to the method proposed in CIE 147 are smaller than the angles $\gamma_{threshold,\ vertical}$. Fig. 11 compares the threshold angle findings of our first small study with angles according to CIE proposals.

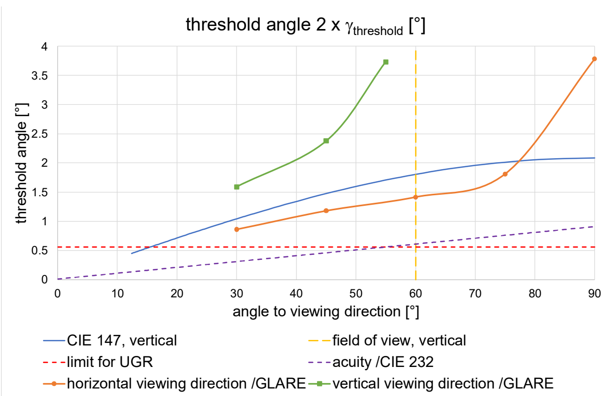

Fig. 11. Comparison of threshold angles (GLARE) with visual acuity (CIE 232) and the angles calculated from the method proposed in CIE 147.

When evaluating discomfort glare for daylighting it is essential to consider human perception in the peripheral field of view. Comparable to the application of the Unified Glare Rating UGR for artificial lighting, the evaluation of small glare sources is particularly problematic. The new method that will be elaborated in detail within project GLARE should lead to a more consistent model.

V. Conclusions

We presented results from projects in the field of efficient and healthy daylighting of buildings. The ILM module was introduced as simulation-based integral control concept. Evaluations of simulation studies and monitoring of a real-world Living Lab installation demonstrate that the cross-trade and individualized concept offers high potential to increase energy efficiency and user comfort in buildings. The PE algorithm was presented as methodology to extract the direct-through solar component in simulations. Further, an envisaged adjustment of the application of the DGP metric through pre-processing the luminance pictures before performing the calculations was introduced. These are important steps forward in enabling practitioners to correctly evaluate daylighting and visual comfort in buildings taking into account the planned or installed system technologies.

Acknowledgments

Funding through the research projects "BIM2IndiLight", financed by the Province of Tyrol and the European Regional Development Fund (EFRE) under grant EFRE K-Regio 10033, and „Early Stage: Tageslicht-Blendung und Virtual Reality" (GLARE), financed through the Austrian Research Promotion Agency FFG under grant 878958, are gratefully acknowledged.

References

[1] IEA Solar Heating and Cooling Technology Collaboration Programme, "Daylighting of Non-Residential Buildings. Position Paper.", January 2019, https://www.iea-shc.org/Data/Sites/1/publications/IEA-SHC-Daylighting-Non-Residential-Buildings-Position-Paper.pdf, accessed June 10, 2022.

[2] D. Plörer, S. Hammes, M. Hauer, V. v. Karsbergen, R. Pfluger, "Control Strategies for Daylight and Artificial Lighting in Office Buildings – A Bibliometrically Assisted Review", Energies 2021, 14, 3852. https://doi.org/10.3390/en14133852

[3] M. Hauer, D. Geisler-Moroder, W. Pohl, „Impact of Integral Day- and Artificial Lighting Solutions on Energy Demand and User Comfort", ISEC 2022, 5th – 7th of April, Graz.

[4] D. Plörer, M. Werner, M. Hauer and D. Geisler-Moroder., "Effect of blind control strategies on energy demand of office buildings and melanopic effect for occupants", IBPSA Italy Building Simulation Application 2017 Conference.

[5] V. v. Karsbergen, S. Moser, D. Plörer, R. Weitlaner, M. Hauer, R. Pfluger, "An experimental investigation of the IndiLight-Module – a multi-objective occupant-centric day- and artificial lighting control strategy", Advanced Building Skins Conference 2021, Bern.

[6] EN 14501:2021, Blinds and shutters - Thermal and visual comfort - Performance characteristics and classification, 2021.

[7] IEA SHC Task 61 / EBC Annex 77: Integrated Solutions for Daylighting and Electric Lighting, https://task61.iea-shc.org/, accessed June 9, 2022.

[8] D. Geisler-Moroder, E.S. Lee, G. Ward, B. Bueno, L.O. Grobe, T. Wang, B. Deroisy, H.R. Wilson, "BSDF generation procedures for daylighting systems. White paper.", T61.C.2.1 – A Technical Report of Subtask C, IEA SHC Task 61 / EBC Annex 77. 2021. https://task61.iea-shc.org/publications, accessed June 9, 2022.

[9] J. Wienold, J. Christoffersen, "Evaluation methods and development of a new glare prediction model for daylight environments with the use of CCD cameras", Energy and Buildings 38 (7), 2006.

[10] J. Wienold, T. Iwata, M. Sarey Khanie, E. Erell, E. Kaftan, R.G. Rodriguez, J.A. Yamin Garretón, T. Tzempelikos, I. Konstantzos, J. Christoffersen, T.E. Kuhn, "Cross-validation and robustness of daylight glare metrics". Lighting Research & Technology 51(7): 983-1013, 2019.

[11] D. Geisler-Moroder, G. Ward, T. Wang, E.S. Lee, "Peak extraction in daylight simulations using BSDF". Proceedings of Building Simulation 2021, Bruges, 1-3 September, 2021.

[12] Ward, G., Shakespeare, R., Rendering with RADIANCE. The Art and Science of Lighting Visualization. Morgan Kaufmann Publishers, 1998.

[13] Radsite, m_bsdf.c. https://www.radiance-online.org/, Radiance Source Code, Head Release, m_bsdf.c, v.2.63, accessed June 9, 2022.

[14] Radsite, evalglare.c. https://www.radiance-online.org/, Radiance Source Code, Head Release, evalglare.c, v.2.11, accessed June 9, 2022.

[15] EN 12464-1:2021, Light and lighting - Lighting of work places - Part 1: Indoor work places, 2021.

[16] CIE 232:2019, Discomfort Caused by Glare from Luminaires with a Non-Uniform Source Luminance, Technical Report, 2019.

[17] EN 17037:2018, Daylight in buildings, 2018.

[18] CIE 147:2002, Glare from Small, Large and Complex Sources, Technical Report, 2002.

The Outputs of SURFACE Project: Pavement Surface Characterisation for Smart and Efficient Road Lighting

Paola Iacomussi
Coordinator of SURFACE Project
INRIM
Torino, Italy
P.Iacomussi@inrim.it

Valerie Muzet
CEREMA Strasbourg, France
Valerie.Muzet@cerema.fr

Peter Blattner, Johanna Bernasconi
METAS Bern, Switzerland
Johanna.Bernasconi@gmail.com
Peter.Blattner@metas.ch

Mikael Lindgren
RISE
Sweden
Mikael.Lindgren@ri.se

***Abstract*—Pavement surface characteristics are crucial for functional quality and safety of roads, related not only to its mechanical and dynamic performance, but also to its visual performance under artificial lighting conditions and to design road lighting systems for the safety at night of all road users. The luminance coefficient, q (or reduced luminance coefficient r that is the q values multiplied by the cube of the cosine of the angle of light incidence) is a physical parameter describing the reflective behavior of road pavements used to design road lighting systems to ensure a given road surface luminance and uniformity. To do these calculations, designers use reference data r values (called r-tables) published in the CIE 144 document. However, these r-tables are derived from measurements carried out more than 40 years ago: the photometric properties of the road materials have evolved over time and reference data are no longer representative and their uncertainty is not known. A European funded project international consortium, SURFACE, worked for three years on the topic and this paper presents the main achievements.**

Keywords— Road lighting, road surface characterization, luminance coefficient, r-tables, asphalt

I. Introduction

Pavement surface characteristics are crucial for functional quality and safety of roads, related not only to its mechanical and dynamic performance, but also to its visual performance and the safety at night of all road users. In Europe there are 5 Million kilometres of roads, about the 40% of them are lit using lighting systems designed in compliance with the directives of the European Road Lighting Standards EN 13201. The EN standard specifies the average luminance of the road that must be maintained by the lighting system in order to ensure safety and proper visibility conditions for the assigned road class to all road users. The road luminance is calculated from a physical property of the pavement describing its reflective behaviour: the luminance coefficient, q (or reduced luminance coefficient r that is the q values multiplied by the cube of the cosine of the angle of light incidence) and from the luminous intensity emission (in a given direction) of road lighting luminaires.

Designers determine the required number and spacing of road luminaires in a road to fulfil the requirements for road luminance and quality parameters values, given in the EN Standard 13201 with the additional goal of energy optimization. To do these calculations, designers use reference data r values (called r-tables) published in the CIE 144 document. However, these r-tables are derived from measurements carried out more than 40 years ago. The photometric properties of the road materials have evolved over time and reference data are no longer representative. Furthermore, the reliability of these published data is unknown, because no statement about measurement uncertainty is presented.

Within the Horizon 2020 research and innovation programme, EURAMET [1] (the association of National Metrology Institutes of Europe) financed with the EMPIR programme the project SURFACE "16NRM02 SURFACE, Pavement surface characterisation for smart and efficient road lighting" [2] with the task to provide to CIE and EU standard organization the metrological support on road surface characterization for road lighting, providing also new traceable reference data (q values and r-tables) representative of current road surfaces used in EU. The project was presented at Lux Europa 2017 Conference and this paper presents the most relevant results achieved during the 42 months duration of the project.

SURFACE project was able to build an international metrology structure in support to the measurement of q, ensured a progress beyond the state of art in the measurement of q by publishing several guidelines and arranging the first interlaboratory comparison, and investigated new measurement geometries.

II. SURFACE Project tasks

SURFACE project was lead by the National Metrological Institute (NMI) of Italy (INRIM) and includes NMI of Estonia (Metrosert), France (LNE), Finland (Aalto), Sweden (Rise) and Switzerland (Metas), plus a National French Research Centre (Cerema) and two industrial companies (Proce-Q, measuring instruments and Ansys-Optis, software simulation), with the support of CEN, CIE and National Standardisation Organisation, road Authorities as well a group of more than forty Stakeholder. The project had several main tasks:

- To define new optimized geometrical conditions for the characterization of photometric quantities (*q* and *r*) or road surfaces, useful for the new needs of smart and LED lighting and to improve measurement accuracy;

- To establish a metrological structure in Europe for the measurement of photometric properties of road surfaces, establishing traceability through an intercomparison and ensuring uncertainty evaluation;
- To provide input to the International Commission on Illumination CIE and CEN through guidelines and reference data of current road surfaces properties;
- To provide guidelines on metrological specification for instruments, characterization methods and uncertainty evaluation

In addition, SURFACE defined a method and a reference set of conditions to evaluate the energetic impact of current road lighting design procedures based on reference outdated r- tables versus the new reference data of current road pavements and patented a set of Reference materials for the calibration of instruments.

III. SURFACE MAIN RESULTS

A. *Optimized measurement geometries*

Specifications concerning road lighting and photometry of road surfaces were established in the seventies [3]. Road lighting design and road marking visibility were developed primarily for drivers of motorised vehicles as well the geometrical measurement condition of reflectance properties of pavements.

The design of a road lighting system includes determination of the optimal combination of lamp power, height, spacing and luminaire optics to provide the desired road surface luminance, based on vision model, and reflectance properties of road pavements. The method for characterizing pavements photometrically was developed in the nineteen-seventies and updated in 1982 and 2001 [4]. The quantities used in road lighting characterization are described in additional CIE reports [6][7]: the most relevant parameter is the luminance coefficient q, is the ratio between the luminance L in cd/m², which the observer sees, and the illuminance E in lux which is incident on the surface. This parameter is measured for a viewing condition of 1° of observation angle along the road length, namely the height of the eye of the observer is set at the nominal value of 1.5 m for viewing distance of 86 m. This geometry is well adapted for a speed of 90 km/h, on motorways for example. However, nowadays, except in tunnels, there are few interurban lighted roads in Europe. Illuminated areas are located in urban environments where there are several types of road users (vehicle drivers, but also cyclists and pedestrians), travelling at different speeds.

To define new observation angles, SURFACE consortium approached also to stopping distance in EU countries. Typical stopping distances are presented in the following Table 1. For road safety, good visibility of obstacles within the stopping distance is very important.

TABLE 1 Stopping distance at different driving speeds in some EU countries and Switzerland

		Stopping distance on dry pavement in official documents (m)			
	Speed (km/h)	**France**	**Italy**	**Sweden**	**Switzerland**
Urban driving	**30**	13	22	16	16 - 22
	50	28	55	38	34 - 48
Interurban driving	**90**	70	136	121	88 - 115
	120	112	235	222	144 - 189

TABLE 2 SURFACE recommendations for new observation angles.

Road environment condition	Nominal observation angle recommendation
Extra-urban road	1°, viewing distance of 85,9 m
Urban road	2,29°, viewing distance of 37,5 m

SURFACE consortium recommended different nominal observation angles (Table 2) for different driving conditions and road users: for urban environment 2,29° (consistent with road marking standards and stopping distances in urban environment), for extra-urban environment 1° (consistent with previous geometries). The angle of 5°, corresponding to a viewing distance of 17 m, is an interesting complement, suitable for urban driving at low speed, cycling and for scooters. The angles of 10° and 20° are submitted to CIE TC4-50 for consideration as condition for describing the boundary between diffuse and specular behaviour.

B. *Metrological Structure and support*

Reliable and traceable data of q and r coefficients are unquestionable needs not only for EU standards, but also for industrial and lighting engineering communities. NMI have a well-established traceability chain for the photometric units in the absolute definition of q coefficient, but never had the chance to arrange an interlaboratory comparison on the

Luminance coefficient. As well the industrial laboratories providing measurement services. SURFACE consortium organized the first interlaboratory comparison on Reduced Luminance coefficient *r,* to compare and ensure EU measurement reproducibility and uncertainty evaluation. Absolute measurement methods of an r-table require a direct calibration of luminance and illuminance meters in absolute units: these methods are usually used in laboratory goniophotometers. While relative methods are based on the calibration of Reference Materials (RM) , usually generic tiles previously calibrated in goniophotometers are used as RM. The project developed dedicated RM based on IoT especially designed considering the peculiarities of road surfaces and engineered to ensure high stability (also in time) and easy alignment to provide high reproducibility and repeatability. These RM were patented and used in the interlaboratory comparison. Regarding uncertainty evaluation, SURFACE deeply investigated the impact of geometrical aperture of the lighting beam and of the luminance detector: illuminance should be measured at a given point (i.e. within an infinitesimal small area) and luminance, at the same point, in a given direction (i.e. within an infinitesimal small solid angle), but this is not possible as finite apertures are necessary to emit and collect light. Furthermore, road surfaces are highly non-uniform, hence the luminance coefficient will vary at each point and averages over a certain surface area need to be taken. The freely available software LUMCORUN (on the project website [7]) allows to calculate the errors due to aperture effects for any measurement system, given its optical characteristics.

The intercomparison data analysis showed that instruments have a low compatibility index when only the standard deviation of data is considered, but the targeted uncertainty of 10% produces satisfactory results for the S1 Values, and for the lighting directions less affected by aperture effect systematic errors (namely $\tan\varepsilon=0$ and $\beta=0$) and ensures measurement compatibility and for the most relevant samples.

LUMCORUN software highlighted that measurement systems suffer from different systematic effects due to the extended apertures of viewed and illuminated area of the measuring devices. Using as input the instrument characteristics (lens apertures, detector sensitive area and lit area), the software is able to calculate these systematic effects. Unluckily, the software demonstrated that for high values of illumination directions (namely $\tan\varepsilon > 2$ and $\beta => 15$) measuring devices, not equipped with telecentric lenses, have the largest errors. This means that where the road pavements have high luminance coefficient values, the measurement errors are larger.

C. CIE TC4-50 input

Unfortunately CIE TC4-50 has been not able to provide the necessary data and research, to revise publication 144: the TC started the revision in 2010 and was not able to end its work. SURFACE activities were integrated with the CIE TC4-50 working plan. SURFACE results brought new energies and technical expertise to the CIE TC and finally the new revision of CIE 144 is expected in 2024. In particular, SURFACE launched an international call to collect full r-tables of current road surfaces and built a database that includes about 250 different types of road surfaces. The database and its differences from CIE reference data is shown in Figure 1.

Data have been classified in clusters, and a champion for each cluster was used as reference for road lighting calculations. The results published in [8] highlight the differences among current road surfaces and CIE 144 published road data. To compare performances a SURFACE Test Set was defined as a given road of lighting class M3 and a set of pavement data of the SURFACE database.

Results shown in Table 3 and [8] highlighted that if the lighting system is designed considering a reference CIE pavement, but the installed pavement differs from the selected CIE reference, large erroneous evaluations can occur: a relevant luminance underestimation (more than 40 %) for a very dark road surface and luminance overestimation for a bright pavement (more than 100 %) and only a luminous flux controller allows to fulfill normative requirements.

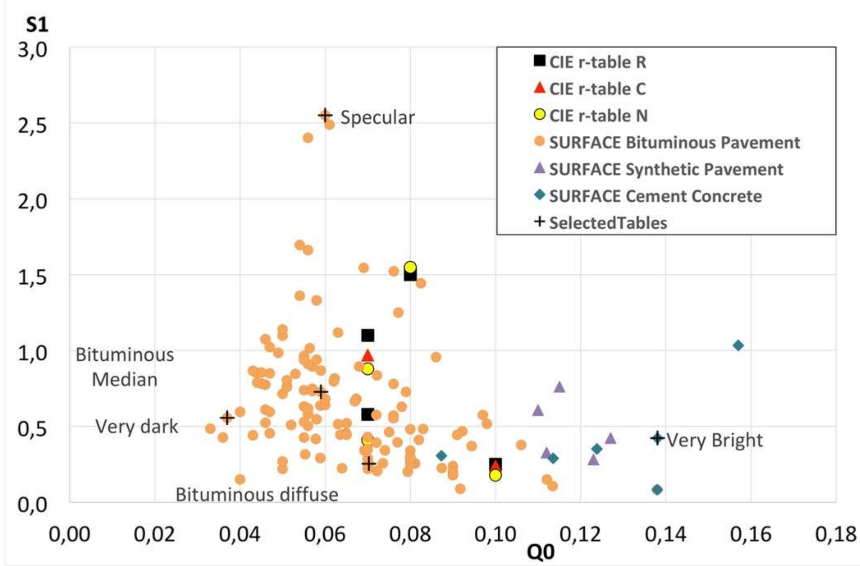

FIGURE 1: Q0 and S1 values of CIE road surface reference r-tables and SURFACE current database composed of 138 stabilized pavements.

TABLE 3: Road lighting values for the given pole-luminaire arrangement and for different road pavements (* no normative fulfillment of the calculated values)

Road Pavement	L [cd m^{-2}]	U_0 [-]	U_i [-]	f_{TI} [%]	E [lx]
Reference C2 (Q_0=0,070 S_1=0,970)	1,01	0,60	0,64	13	14
SURFACE Very bright (Q_0=0,138 S_1=0,410)	2,06	0,62	0,63	7	14
SURFACE Bituminous Diffuse (Q_0=0,070 S_1=0,253)	1,05	0,71	0,52*	13	14
SURFACE Bituminous Median (Q_0=0,059 S_1=0,730)	0,91*	0,62	0,64	14	14
SURFACE Specular (Q_0=0,060 S_1=2,550)	0,96*	0,38*	0,32*	14	14
SURFACE Very dark (Q_0=0,037 S_1=0,560)	0,57*	0,69	0,67	20*	14

TABLE 4: Energy performance indicators of road lighting calculated from the rescaled values of Table 3.

	Rescaled values to fulfil normative requirements				Energy performance Indicators			
Road Pavement	**Luminaire luminous Flux [lm]**	**Luminaire Power [W]**	**L [cd m^{-2}]**	**E [lx]**	**q_{inst} [-]**	**D_p [mW /lx m^2]**	**D_E [Wh/m^2]**	**Diff. vs. C2 [%]**
Reference C2	12064	78,2	1	13,9	1,03	18	1016	-
SURFACE Very Bright	5915	38,3	1	6,8	2,1	18	498	-51
SURFACE Bituminous Diffuse	11605	75,2	1	13,3	1,07	18	977	-3,8
SURFACE Bituminous Median	13390	86,8	1	15,4	0,92	18	1127	11
SURFACE Specular	12693	82,3	1	14,6	0,98	18	1069	5,2
SURFACE Very Dark	21377	138,6	1	24,6	0,58	18	1800	77,2

D. *Guidelines*

Guidelines are focused on metrological performances of instruments and measuring requirements and procedures, guidelines were put in a form to be incorporated directly into the new revision of CIE TR144. In particular regarding instrument characteristics, SURFACE consortium suggests to have instrument with observation angles of 1° and 2,29°, a good collimation, i.e. small angular subtense of the light source (<0.2°), small detector angular subtense, i.e. good telecentricity of the detector (<0.08°) [5]. The measured area should be at least 100 cm^2

Regarding on site measurements, it is necessary to choose a planar area without defects, and to use a contour gauge to identify convexities, pavement must be dry, unsalted and all measurement shall be done in the direction of circulation. Several sampling areas should be chosen, at least six measurements should be done on each lane of circulation, three in the centre track and three in the tyre tracks, with the advice to make the same number of measurements in the tyre track and in the centre track. Six measurements seem to be the minimum required to be representative of the road heterogeneity and to enable statistics. It is always possible to make characterization at specific area, but it shall be noted

Data analysis: it is always better to avoid to average different r-table values because the results may not be representative of a physical surface, then it is necessary to identify the usage of data to choose the best data analysis approach. If measured data are used to scale CIE r-table (scaling of Q0), the measured r-table is used only to calculate Q0 and S1 factors and it is possible to average them. If measured data are used to identify the actual *r*-table of the road surface, it is recommended to choose the most representative measured r-table as the closest to the average of the S1 factor, this table has physical sense and can be scaled according to the average of the Q0 factor.

To characterize the heterogeneity of the road, it is always necessary provide different measured values (the most representative and the extremes) and differentiate the statistics for the centre track and tyre track.

For devices measuring only Q0 and S1, it possible to provide the mean value and standard deviation

Acknowledgment

Project "16NRM02 Surface, Pavement surface characterisation for smart and efficient road lighting" has received funding from the EMPIR programme. EMPIR programme is co-financed by the Participating States and from the European Union's Horizon 2020 research and innovation programme.

References

[1] https://www.euramet.org/

[2] https://www.euramet.org/research-innovation/search-research-projects/details/project/pavement-surface-characterisation-for-smart-and-efficient-road-light

[3] "CIE 030:1976 Calculation and Measurement of Luminance and Illuminance in Road Lighting." CIE, 1976.

[4] CIE 144:2001 Road Surface and Road Marking Reflection Characteristics," CIE, 2001

[5] CIE 066:1984 Road surfaces and lighting (joint technical report CIE/PIARC)," CIE, 1984. Accessed: Mar. 12, 2020

[6] CIE 140:2000 Road Lighting Calculations." CIE, 2000, Accessed: Mar. 18, 2020.

[7] https://surface-nrm02.eu.

[8] H. Gidlund, M. Lindgren, V. Muzet, G. Rossi, and P. Iacomussi, "Road Surface Photometric Characterisation and Its Impact on Energy Savings," Coatings, vol. 9, no. 5, Art. no. 5, May 2019, doi: 10.3390/coatings9050286

Evaluation and Improvement of Lighting Ergonomy in Home-Office Area

Ayşegül Tereci
KTO Karatay University
Architecture Department
Konya, Turkey
0000-0001-5989-9565

Dilay Kesten Erhart
Fraunhofer Institute for Manufacturing Engineering and Automation IPA
Stuttgart, Germany
dilay.kesten.erhart @ipa.fraunhofer.de

Uçman Tan
AEP Architekten Eggert Generalplaner GmbH
Stuttgart, Germany
u.tan@aep-p.de

***Abstract*— Working from home is becoming more recognized and this practice has accelerated with the pandemic. However, in this process, the employees did not have the professional equipment and infrastructure to provide sufficient ergonomic conditions. One of the differences between home and office environments is that the lighting conditions are not appropriate enough for work. Ergonomics is the arrangement of environmental conditions in a way that positively affects human physiology and psychology. In most office buildings, ergonomics arrangements in terms of lighting are managed at the architectural design phase, whereas office spaces are rarely considered in the preliminary design stage in residential designs. Visual performance and comfort issues should be evaluated together as lighting ergonomics in the home-office environment. Ergonomically, personal preferences should be considered in the lighting organization. Within the scope of this study, a home-office area, which is considered as a working environment during the pandemic process, was evaluated in terms of lighting ergonomics. The home-office area is in Stuttgart, Germany. In the simulations, it was evaluated whether the lighting conditions determined by the standards were adequately provided. In addition, users were asked to evaluate the lighting problems they experienced with their personal experiences. Suggestions for the improvement of lighting were developed by evaluating user opinions. Human Centric Lighting was chosen as the recommendation for home office appliances in this study to maximize people's well-being and performance.**

Keywords*— *Lighting ergonomics, home-office, human centric lighting

I. Introduction

Working conditions are constantly changing and developing as a result of national and international competition with globalization. Work from home is defined by the ILO (International *Labour* Organization)'s Home Work Convention (No. 177) and Recommendation (No. 184), 1996, as "work carried out by a person … (i) in his or her home or in other premises of his or her choice, other than the workplace of the employer; (ii) for remuneration; (iii) which results in a product or service as specified by the employer, irrespective of who provides the equipment, materials or other inputs used" (Convention No. 177, Art. 1) [1]. Alongside the opportunity to work from home, there is increasing acceptance of working from home, and this process has accelerated with the pandemic. It is estimated that around 40% of office professionals in the EU work from home during the COVID-19 pandemic [2]. Before COVID-19, around 5% of workers in Europe continually worked from home, this figure has now risen to 12.3% [3]. It is also projected that employment in the home-office sectors in the EU is approximately 25% of all employment. Considering that only 15% of workers in the EU had ever worked remotely before the pandemic, many workers and employers are likely to face difficulties in coping with the sudden shift to remote work.

The sales of home-office furniture and appliances have generally increased with its users trying to suit up with the new home-office environment. Individuals trying to adapt to the home-office environment seek to conduct the work that needs to be done by communicating with all working stakeholders over digital platforms in the remote working model. However, it was noted that they did not have the professional equipment and infrastructure to provide enough ergonomic conditions in this extremely unprepared process. Furthermore, one of the differences between home and office environments is the lack of lighting conditions. As the post-COVID new normal home has created a niche for work environments, a new requirement has emerged for lighting systems that enhance health, well-being, and productivity.

The International Ergonomics Association defines ergonomics as "the scientific discipline concerned with the understanding of interactions among humans and other elements of a system, and the profession that applies theory, principles, data, and methods to design in order to optimize human well-being and overall system performance. [4]" It can be stated that the organization of environmental conditions in a way that positively affects human physiology and psychology.

One of the essential elements of ergonomics is lighting. Since we perceive 80% of all impressions through eyesight, lighting is one of the most important factors that make things visually easier in the working environment. Lighting, which significantly affects work efficiency [5], is a primary factor especially to see the details in all works. In all types of environments or activities, a little or a lot of lighting will affect vision and perception levels. As light affects the sense of sight, it affects people physically and psychologically. [6, 7] Studies have shown that lighting leads to an increase in concentration and motivation, and thus an increase in performance in employees.

Ergonomics arrangements in terms of lighting are considered at the architectural design stage in most office buildings. Since offices mostly have daytime uses, the area is organized for the working environment most effectively, from facade designs to space organization. All fixed space elements (wall, ceiling, floor) and movable elements within the space are also evaluated in terms of office lighting. On the other hand, office spaces are rarely considered in the preliminary design phase of residential designs. Unless there is a specially designed office room, working areas in residences remain only a niche so it is considered as part of a large space. For this reason, the office areas in the house should be illuminated as a part of the whole space and also as a special area as a working area.

II. HOME-OFFICE LIGHTING

Lighting should be designed considering visual performance, visual environment and visual comfort as described in Table1. Lighting requirements in-home office places can be determined according to daylighting and artificial lighting properties and some personal features. While there are guides for home-offices in terms of lighting, there are not any standards specifically for these areas. On the contrary, there are lighting standards for indoor working environments and daylighting.

TABLE I. PARAMETERS OF ILLUMINATION [8]

Illumination		
Visual performance	*Visual comfort*	*Visual environment*
Illumination level Glare	Light intensity Color rendering	Shadiness Direction of light Light color

EN 12464-1:2021 [9]- Lighting of workplaces specifies requirements for lighting solutions for most indoor workplaces and their associated areas in terms of quantity and quality of illumination. This standard highlights the minimum illuminance requirements of an actual working area rather than the entire room. Home office work is based on desk and visual displays. According to standards, home offices require 500 lux for task lighting on desks and illuminances on the wall should be 0.5 of the task area illuminances. Ensuring comfortable workplace illumination, a minimum color display is 80 at workplaces and the UGR (Unified Glare Rating) level is 19. It is recommended to plan diffuse background lighting to avoid disturbing lighting to create glare on working places such as computer screens and desks.

In addition to the artificial lighting standard, it is emphasized in the EN 17037 [10] that sufficient sunlight is taken indoors, and minimum sun exposure criteria are met in all places where sunlight intake is important, such as residential buildings. According to this standard, the daylight provision corresponds to "a level of illuminance achieved across a fraction of a reference plane for a fraction of daylit hours within a space". Building users should have a large, clear view of the outside. EN 17037 considers the width and outside distance of the view, as well as landscape layers and the view, should be perceived to be clear, undistorted and neutrally colored. While these standards are the criteria to ensure minimum lighting quality in home-office areas, many other ergonomic aspects should also be considered.

As lighting ergonomics in a home-office environment, it is necessary to evaluate the distribution of lighting and contrasts in the whole space, together with the problems that will occur in the working plane. At this point, lighting, where the relationship with the external environment is not broken and daily changes are felt as in office buildings, is the most important element in home-office areas. In particular, the maximum use of daylight not only increases the concentration of employees but also positively affects their health. In conjunction with lifestyle, working rhythm and many personal biological factors, daylight determine the work of our body in the first place [11]. Despite the important positive effects of daylight, artificial lighting can harm people's circadian rhythms while providing the continuation of activities in situations where daylight is insufficient. Light causes several physiological and behavioral responses in humans, including hormone production, alertness, and cognitive performance. Many lighting systems are not specifically developed as anthropocentric lighting does not provide sufficient light for circadian rhythm or to stimulate other physiological and behavioral responses [12]. At this point, one of the important factors is the color temperature. In particular, it is aimed to capture the cyclic color temperatures of daylight in this lighting. There is an inconsistency between natural and electric light in terms of intensity, color and dynamics of light. For this reason, the use of light sources or systems suitable for this rhythm is supported in human-centered lighting design. The proper illuminance level in the working plane must be provided to work areas. In cases where this cannot be achieved with natural lighting during the day, support should be given to human-centric artificial lighting in accordance with the characteristics of daylight. Illumination level, glare and color rendering on the working plane should be arranged by the standards. Concerning the environment, the light distribution and the absence of contrasts are the elements that are considered in lighting. It would be a better solution to have different lighting options for the user. After the daylight is maximized, it is important to control the artificial lighting with different elements in the space, especially the general lighting coming from the ceiling, as well as a floor lamp that can create a transition in the atmosphere and table lamp for task lighting.

Ergonomically, another factor in the arrangement of the work area is the introduction of the individual characteristics of the person. At this juncture, in addition to the relationship between the eye level and lighting that occurs with the sitting action of the person's body, it is also necessary to provide adequate lighting required by the age-related vision. Window orientation, lighting level, and lighting distribution need to be evaluated regarding age and personal characteristics. In line with their personal preferences, desk positioning, lighting fixtures and room configuration should be determined with some questions and determinations, and action should be taken according to this.

In order to create ergonomically appropriate lighting in-home office areas, it is necessary to consider visual factors and comfort factors in the organization phase [8]. Reflectance between a task and its background, intensity range, spectrum and direction of light should be controlled as visual factors. Contrast, glare, lightness, luminous texture, spectrum and direction of light, controlling intensity could also be organized according to the user.

III. EVALUATION OF VISUAL PERFORMANCE

Within the scope of this study, a home-office area, which is considered as a working environment during the pandemic process, was evaluated in terms of lighting ergonomics. The home-office space considered in this study is in Stuttgart, Germany (48.7758° N, 9.1829° E). There is an average of 1776 hours of sunlight per year and solar irradiance is 1116 KWh/m2a. The modelled area is a living area of 4.5m*6.5m. There is a desk as a working corner in the space. There is a desk as a working corner in the space. The desk is white lacquered. In the living area, the reflectance factor of the ceiling is 70%, that of the walls is 50%, and that of the floor is 30%. In addition, all the other furnishing elements used are defined in the model together with their reflectivity values. The application area receives daylight with windows facing Northwest, along with general lighting for the living area and desk lighting for the office corner. The office model in this context is shown in Figure 1.

Fig. 1. Plan of case study home-office space.

A line of sight to the outside is an important quality featurefor indoor spaces. It provides information about the local environment,weather changes and the time of day. According to DIN EN 17037 [10], the line of sight should be evaluated concerning the whereabouts of the user. To assess the view, the room including the spatial organization of use was considered. The horizontal viewing angle is determined here by calculating the width angles between the perpendicular to the window and a line to the right and right view-limiting edges of the window. On the right side, the outside of the window frame represents the view-limiting edge, while the outside of the window reveals limits the view on the right side of the window. As Figure 2 shows, the horizontal angle of view for the user is 22.

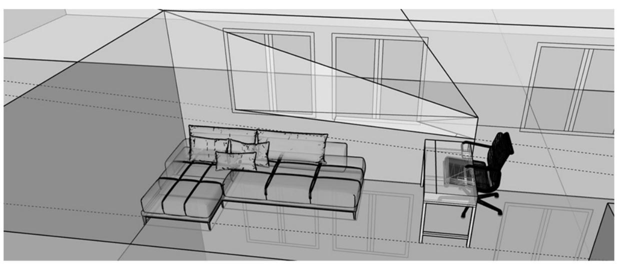

Fig. 2. The drawing of the external visual range.

The external visual range is the distance from the inside of the wall surface of the room in question to the building opposite the window. The external visual range, in this case, is 10 m. The proportion of the usable floor area from which the sky can be seen can be determined with the help of the "no-skyline". This identifies the area of the room from which the sky can be seen from a height of 1.20 m above the floor. Based on these boundary conditions, the sky can be seen from an area of the room on the façade with a depth of 0.37 m. This means that the sky can be seen from 90 % of the floor space. Since the required proportion of 75 % of the area is reached, the "sky" level is counted as a visible level. The proportion of the usable floor area with a view of the ground can be determined with the help of the "No-Ground-Line". In this home office conditions, the ground can be seen from a room area on the facade with a depth of 0.80 m. This means that the ground can be seen from 20% of the usable area. The level of the floor is therefore not counted as the level visible from the usage area. The results were summarized in the Table II.

TABLE II. DAYLIGHT ILLUMINANCE DATA FOR 21 MARCH, 21 JUNE AND 23 SEPTEMBER, AND 21 DECEMBER FOR MORNING, NOON AND EVENING HOURS.

level	*Horizontal viewing angle*	*Outside visibility*	*Number of planes that can be seen from at least 75% of the space used: sky/landscape/ground*
Small amount	*≥ 14°*	*≥ 6m*	*1 landscape*
Middle	*≥ 28°*	*≥ 20m*	*2 Landscape and sky or ground can be seen through the same aperture*
High	*54°*	*ÿ 50m*	*3 All levels can through the same opening can be seen*

At this point, it was verified whether the lighting conditions determined by the standards were adequately provided in the simulations performed using the Grasshopper plugin Ladybug/Honeybee Tools and VELUX [13, 14]. Annual daylight simulations were made for daylight factor and illumination level. Calculations were compared monthly for 8.00 a.m, 12 noon and 06:00 p.m. In the evaluations, daylight simulations were made for Stuttgart without an artificial lighting system.

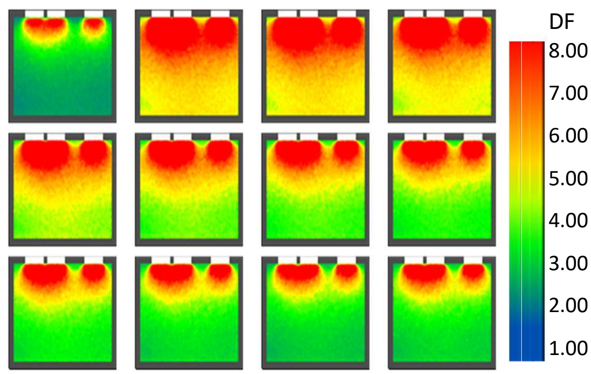

Fig. 3. Monthly average daylight factor at noontime.

The result of monthly daylight factors based on the CIE overcast Sky for noon time is presented in Figure3. In the daylight factor calculations for the living area, the daylight factor, which can be below 2% in the morning and evening hours, except in summer months, was determined in the depths of the room, while the daylight factor was determined above 5% in the areas very close to the window. According to this result, artificial lighting generally is not required near the window. On the other hand, the rest of the room needs to support by artificial light. It would be more accurate to place the working desk in the areas close to the window to benefit more from daylight.

The result of monthly illumination of room level for noontime is presented in Figure4. In this area, a high level of illumination is achieved especially near the window, while the remaining areas in the living room must be supported with artificial lighting. In the table area, the lighting distribution is good enough with a 0.65 ratio and the overall illuminance distribution in the room is not appropriate with a 0.10 ratio. Therefore, people can notice different lighting levels.

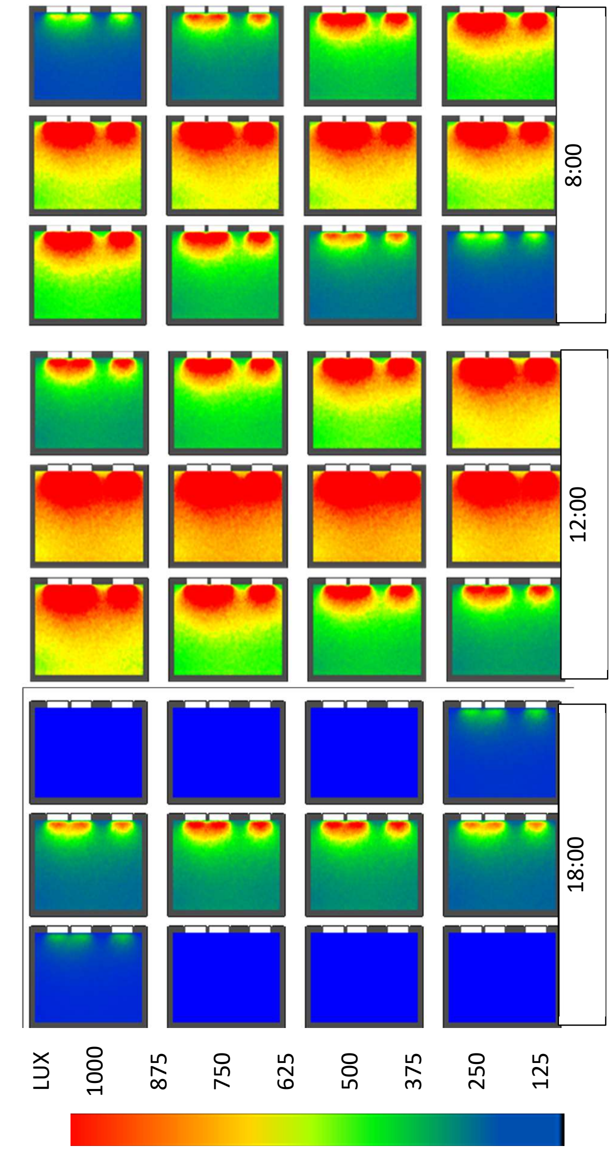

Fig. 4. Monthly illumination level for 8:00,12:00 and 18:00

Similar to illuminance in a desk area, luminance on the surrounded surfaces has a considerable effect on visual comfort and performance. The monthly luminance level of walls and ceiling for noontime is shown in Figure 5. The walls and the ceiling have a higher luminance level for nearly the whole year, which is appropriate for visual comfort. The critical factors that influence the level of visual comfort and quality in daylit rooms include glare, window luminances and luminance ratios within the field of view. To evaluate the glare situation, the luminance distribution within the field of view was simulated, which can be seen in Figure 4. Glare perception can differ from season to season. In order to prevent the lighting situation from changing significantly with different weather conditions, the glare assessment was performed with a constant overcast sky. No artificial lighting was added during the simulation(s). The windows were recognized as a source of glare (especially the first window, over 500 cd/m2 in overcast conditions). This means that solutions should be integrated to overcome the visual difficulties due to perceived glare.

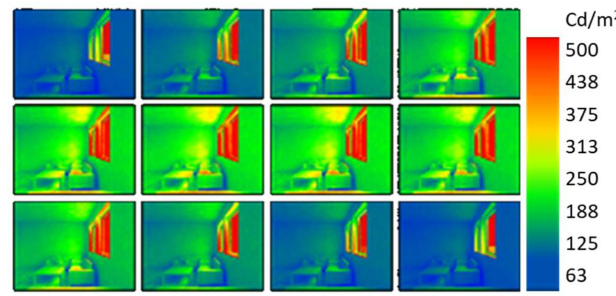

Fig. 5. Monthly luminance level at noontime.

Discomfort Glare can result from direct or reflected glare and can be caused by daily bright sunlight. Unpleasant glare occurs in varying degrees of intensity, but even the milder degrees of unpleasant glare cause visual disturbances that often manifest as fatigue or eye pain. Depending on light sensitivity, this glare can also be uncomfortable regardless of weather or time of day. The unprotected eye reacts to unpleasant glare by blinking and constricting the pupil. Discomfort glare analysis at 8:00,12:00 and 18:00 on 21 June is presented in Figure 6. DGP value is varied between 0,19-0,44 on this day.


Fig. 6. Discomfort glare analysis at 8:00,12:00 and 18:00 on 21 June

The illumination levels obtained with daylight on the working plane for specific design days (21 March, 21 June, 23 September, and 21 December) are shown in Table III. Artificial lighting, except for the simulation at noon for the months of March, September and December, must support the working area. However, only in June, an illuminance level above 500 lux was achieved on the table during the day.

TABLE III. DAYLIGHT ILLUMINANCE DATA FOR 21 MARCH, 21 JUNE AND 23 SEPTEMBER, AND 21 DECEMBER FOR MORNING, NOON AND EVENING HOURS.

Date/Time	Emin (room)	Emax (room)	Eort (working plane)
21March/08:00	25	725	280
21March/12:00	60	1830	720
21March/18:00	25	585	250
21June/08:00	50	1400	550
21June/12:00	50	1570	530
21June/18:00	135	500	102
23Sept/08:00	30	860	350
23Sept/12:00	75	1900	760
23Sept/18:00	20	550	185
21Dec/08:00	0.4	13	5
21Dec/12:00	35	1060	450
21Dec/18:00	0	0	0

The data taken with the lighting results facing the table area in the space was converted into TIF formatted images with the converter elements in Grasshopper and 'False Color' maps were created. The simulation data obtained for the brightness distribution and the ratio of photopic and melanopic values were examined in terms of compliance with human-centered lighting design criteria at the working plane level. RGB (Red, Green, Blue) values of the determined point on the table were found and this ratio was calculated with the transformation matrices [15]. The situation in this area was evaluated in terms of human-centric lighting by calculating the color temperatures in Kelvin at the points determined on the surface and it was determined that the values vary between 0.87 to 1.

IV. EVALUATION OF VISUAL COMFORT

The home office users were interviewed for their opinion on lighting conditions in their home office. Two adult users are interviewed about their experience, opinions, and perceptions of the space, windows, and lighting during work hours in their home office where they performed various office-like tasks.

The questions about the lighting conditions in the home office are divided into three parts: personal questions such as age, gender and whether he/she has vision problems (wear glasses or contact lenses). The second part of the questions was related to the type of tasks to be done and the daily working hours. In the third part, general impressions of the room were asked.

The users are 41 (female) and 43 (male) years old. One of them wears glasses; the other has no vision problems. Both works from home for more than 2 days and their working hours vary between 08:00-08:30 and 17:00-17:30.

The typical activities they perform in the home office are reading and writing on a digital screen and a computer, reading and writing (partly digital, partly on paper) and participating in digital meetings. They state that both have sufficient daylight most of the time, except in December (mornings and evenings) and March mornings. The outside view from the window satisfies them both, but they report that the overall level of lighting in the room is not sufficient. They complain about direct sunlight causing glare between May and September. They do not have reflection problems in the work area, especially on screens.

V. IMPROVEMENT OF LIGHTING ERGONOMY IN HOME-OFFICE AREA

The user of this place is around 41 years old it is older than the 32 years old accepted by the standard observer. According to DIN SPEC 5031-100 [16], age dependent correction factor for spectral light transmission and pupil diameter is applied as 0,83 for illuminance level. The task lighting illuminance level is suggested 600 lux on the desk area and at the eyelevel illuminance is defined 150 lux for 2700 K light temperature in the morning time . Higher illuminance levels and light colours above 5500 K help to sustain concentration during daytime. It is proposed that 850 lux iilumination level on the desk area for afternoon period.

To maximize the well-being and performance of people, Human Centric Lighting was chosen as a recommendation for home office appliances in this study. Technical specifications of selected lighting are presented in Table IV.

TABLE IV. TECHNICAL SPECIFICATIONS OF SELECTED LIGHTING [17]

Height	300 mm – 900 mm
Radius	100 mm – 700 mm
Lamp base	250 mm × 250 mm × 8 mm
LEDs	2 cold white & 2 warm White
LEDs Power consumption	10,5 W
Nominal luminous flux	neutral white 680 lm | Boost 900 lm
Light intensity	neutral white 566 cd | Boost 746 cd
Illuminance	1,000 lux at a height of 75 cm
Colour temperature (CCT)	2.700 K <--------> 6.500 K
Colour reproduction index	≥ 80
Burning lifeover	50,000 hours

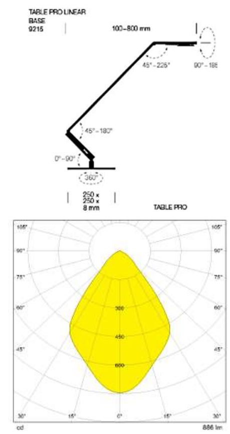

In this direction, a human-centered table lamp is designed to provide the desired values in the desk area, and a human-centered lamp arrangement that can be controlled from the ceiling for better distribution of lighting in the room. The light source changes the color temperature and adapts to the circadian rhythm. In this direction, while it works in a cooler color temperature to support being more active and brisker in the morning hours, it offers warm color light to help rest and relax towards the afternoon hours. Although it is a new and expensive system, it is thought that its use will become widespread in a short time.

In this direction, besides the health benefit, the economic depreciation of this equipment, which is used by comparing a human-centered lamp with a standard 60 W table lamp, has been evaluated to provide the desired values in the desk area. It has been calculated that the proposed system in terms of energy expenditures can pay for itself at the end of 6 years. When the repair costs come into play, this value decreases up to 5 years.

VI. CONCLUSION

Ergonomics arrangements enable the person to do the work comfortably with minimum physical and psychological effort. Working from home is increasing, as well as the problems related to the use of furniture, problems related to lighting affect the work efficiency. Lighting ergonomics should be considered in all areas as it helps prevent Computer Vision Syndrome (CVS) and improve quality of life and productivity.

At this point, lighting ergonomics must be taken into account when arranging home-office areas. In this study, the compliance of a case-study area with lighting standards has been evaluated and an example of ways to organize a more efficient workspace with personal characteristics has been established.

As a result, the steps to be followed in such arrangements can be listed as follows:

- Especially when determining home-office working areas, places that will receive maximum daylight should be preferred.
- Visual communication with the environment should be established by considering the perspective from the window.
- As in office lighting, the location of the work area should be arranged so that it does not face glare problems that may occur throughout the year due to long working hours.
- Even if daylight is received, artificial lighting supports should be added to the area for different weather conditions. In this selection, human-centered lighting should be preferred.
- It should use dimmable lighting options depending on the age factor of the users and different types of work. In this way, the lighting design should be arranged in such a way that personal satisfaction can be controlled.

References

[1] ILO, "Working from home,From invisibility to decent work,Executive summary," 1 12 2021. [Online]. Available: https://www.ilo.org/wcmsp5/groups/public/---ed_protect/---protrav/---travail/documents/publication/wcms_765896.pdf.

[2] Ballarımo M. (JRC-ISPRA), "Telework in the EU before and after the COVID-19: where we were,where we head to," 6 15 2021. [Online]. Available: https://joint-research-centre.ec.europa.eu/system/files/2021-06/jrc120945_policy_brief_-_covid_and_telework_final.pdf.

[3] EU-eurostat, "Working from home across EU regions in 2020," 23 9 2021. [Online]. Available: https://ec.europa.eu/eurostat/web/products-eurostat-news/-/ddn-20210923-1.

[4] Human Factors and Ergonomics Society, "About HFES," [Online]. Available: https://www.hfes.org/About-HFES/What-is-Human-Factors-and-Ergonomics#:~:text=Ergonomics%20(or%20human%20factors)%20is,being%20and%20overall%20system%20performance.. [Accessed 2022].

[5] Y. Al Horr, M. Arif, A. Kaushik, A. Mazroei, M. Katafygiotou and E. Elsarrag, "Occupant productivity and office indoor environment quality: A review of the literature," Building and Environment, pp. 369-389, 2016.

[6] C. Vetter, P. M. Pattison, K. Houser, M. Herf, A. J. K. Phillips, K. P. Wright, D. J. Skene, , G. C. Brainard and D. B. Boivi, "A Review of Human Physiological Responses to Light: Implications for the Development of Integrative Lighting Solutions," *LEUKOS,* pp. 387-414, 2022.

[7] J. A. Veitch, "Psychological Processes Influencing Lighting Quality," Journal of the Illuminating Engineering Society, pp. 124-140, 2013.

[8] Skansi, Ranko ; GE Lighting, "Ergonomics of Light," in *Balkanlight*, Belgrade, Serbia, 2021.

[9] CEN, «EN 12464-1 Light and lighting - Lighting of work places - Part 1: Indoor work places,» CEN, 2021.

[10] CEN, «EN 17037 Daylight in Building,» CEN, 2018.

[11] W. J. M. van Bommel ve G. van den Beld, «Lighting for work: a review of visual and biological effects,» *Lighting Research & Technology,* pp. 36(4):255-266., 2004.

[12] M. Amundadottir , S. Lockley ve M. Andersen , «Unified framework to evaluate non-visual spectral effectiveness of light for human health,» Lighting Research & Technology. , pp. 49(6):673-696., 2017.

[13] "Honeybee," ladybug tools, [Online]. Available: https://www.ladybug.tools/honeybee.html. [Accessed 2022 05 30].

[14] VELUX A/S, «Velux,» [Online]. Available: https://www.velux.com/. [Accessed 2022 05 30].

[15] B. Jung & M. İnancı, «Measuring circadian lighting through high dynamic rangephotography,» *Lighting Research & Technology,* cilt 5, no. 51, pp. 742-763, 2019.

[16] DIN, «DIN SPEC 5031-100 Strahlungsphysik im optischen Bereich und Lichttechnik - Teil 100: Über das Auge vermittelte, melanopische Wirkung des Lichts auf den Menschen - Größen, Formelzeichen und Wirkungsspektren,» 2021.

[17] LUCTRA, «Table Lamps,» [Online]. Available: https://www.luctra.eu/en/products/table-lamps. [Accessed 2022 05 30]

An Overview of the Adverse Effects of Outdoor Light at Night and the Research Methods Used in Different Areas

Annika K. Jägerbrand
School of Business, Innovation and Sustainability
Halmstad University
Halmstad, Sweden
ORCID 0000-0001-8016-0124

Maria Nilsson Tengelin
Department of Measurement Science and Technology
RISE Research Institutes of Sweden
Borås, Sweden
ORCID 0000-0002-0909-626X

Dorukalp Durmus
Department of Architectural Engineering
Pennsylvania State University
University Park, USA
ORCID 0000-0001-9809-2406

***Abstract*— Light is imperative to achieve viable conditions for human activity at night. However, for the lighting to be sustainable, it is crucial to reduce unwanted and harmful side-effects of light at night (LAN). These unwanted effects and impacts are often referred to as light pollution. Hitherto, it has been somewhat unclear how all these adverse effects can be described in a systematic way and whether light pollution is similarly defined among different scientific disciplines and contexts. Therefore, in this review, we present an overview of the identified areas where light pollution can be confirmed from the scientific literature and the methods commonly used within these areas. We have identified three key areas: astronomical light pollution (ALP), ecological light pollution (ELP), and impacts of LAN on humans in two subareas; impacts on human health (physiology and behaviour) and impacts on humans in terms of obtrusive light that can be perceived as negative, for example, discomfort, annoyance, nuisance and distractions. Methods used in various disciplines are partly similar, e.g., satellite-based sensor collected data are used in all three areas to study impacts, but specific methods are also used within each field.**

Keywords*— ALAN, astronomical light pollution, ecological light pollution, physiology and behaviour, health

I. Introduction

Humans need light at night for an active lifestyle and relies on adequate visual performance for many important activities in our daily life, such as transportation, work and exercise. Light is imperative to achieve viable conditions for human activity at night. Therefore, the use of outdoor lighting enables many night-time activities and is beneficial, especially in urban environments, but the use of light at night (LAN) also results in an increase in outdoor illumination. For the outdoor lighting to be sustainable it should fulfil the functional needs of the users, be cost- and energy-efficient, and result in minimal environmental impact [1]. The use of outdoor lighting during night-time can result in various unwanted and harmful side-effects and such unwanted consequences are often referred to collectively as light pollution. Examples of unwanted effects of the use of outdoor LAN are:

- Increase of human-made sky glow (the diffuse luminance of the night sky) [2],
- Degradation of ground-based astronomical observatories operating in the optical range [3] and a decreased ability to observe the stars due to the brightening of the night sky,
- Increase of obtrusive light [4] causing nuisance and discomfort glare for humans,
- Adverse health outcomes, such as circadian disruption, mood effects, and increased breast cancer incidence risk in humans [5],
- Disturbances and negative impacts on species, ecosystems and wildlife conservation areas [6, 7].

The unwanted side-effects are measured through response variables which are determined by the focus of the investigation and the response variable will therefore vary significantly depending on the research discipline and the study objects. In astronomy the response variable can be sky brightness or upward emitted light. For impacts on human health the response variable can be human behaviour or various health outcomes, for example, sleep quality, melatonin suppression or risk of cancer. In ecology the response variable is usually restricted to appropriate study variables for the specific study species or the spatial scale or ecosystem of the investigation.

Measurements of the independent variable light will also vary significantly between disciplines since it is dependent on the data used in the experiments or observations. For example, if you are conducting an indoor experiment, you will most likely measure illuminance or luminance and exposure levels. In most disciplines light at night over larger geographical areas can be assessed via ground-based or aerial light measurements or through satellite-based measurements of the upward emitted light.

Hitherto, it has been unclear if all these various adverse effects can be described in a systematic way and whether light pollution is similarly defined and measured between different scientific disciplines, spatial scales and contexts (see e.g., [8]). Therefore, in this review, we present an overview of the identified areas where light pollution can be confirmed from the scientific literature and the methods commonly used within these areas.

This paper is organised as follows: section II is a literature overview that describes and defines light pollution; section III describes the methods used for this study. Section IV presents the results of our systematic review and Section V discusses the results. The paper ends with conclusions in Section VI.

II. DEFINITION OF LIGHT POLLUTION

Historically, it seems that light pollution as a concept have been used more commonly in the context of degradations of astronomical observations and a reduced ability to observe the stars (e.g., [3]). In astronomy, the adverse effect of LAN is proportional to the emitted light because there is a causal linear relationship between ability to observe the night sky and stars and the light emitted into the atmosphere. For example, when a city, town or a region emits light in the surroundings, and especially upward emitted light, it propagates through the atmosphere and is scattered by molecules, aerosols and clouds giving rise to man-made sky glow. This has a direct negative consequence for star gazing and the ability to experience the natural sky since it reduces the contrast between stellar objects and the background. This underlying causal relationship between the amount of emitted light and reduced ability to observe stars is also demonstrated in the many definitions of light pollution that has been proposed by astronomical organizations and researchers. For example, the International Astronomical Union defines light pollution as *"artificial light that shines where it is neither wanted, nor needed"* [9] and globe at night writes that light pollution "*is excessive, misdirected, or obtrusive artificial (usually outdoor) light*" [10] (Table 1). The International Dark-Sky Association similarly describes light pollution as "*the inappropriate or excessive use of artificial light*" [11] (Table 1).

In various disciplines such as human health, biology, and economy, light pollution is described as the presence of, for example, unnecessary/annoying or excessive/intrusive or consequences of poorly designed and injudiciously used artificial lighting in the outdoor environment (Table 1). Cinzano et al. [12] states that light pollution can be defined as "*the alteration of natural light levels in the outdoor environment owing to artificial light sources*" and argues that increases of night sky brightness is an example of the most noticeable effects of light pollution. Longcore & Rich [13] suggests separating astronomical light pollution ("*obscures the view of the night sky*") from ecological light pollution that "*alters the natural patterns of light and dark in ecosystems*".

TABLE I. DEFINITIONS OF LIGHT POLLUTION AND ADVERSE EFFECTS OF OUTDOOR LIGHT AT NIGHT FROM DIFFERENT SCIENTIFIC FIELDS.

Definition of light pollution	**Field**	**Source**
sum total of all adverse effects of artificial light	International standardization body within light and lighting	International Lighting Vocabulary, International Commission of Illumination [14].
Artificial light that shines where it is neither wanted, nor needed	Astronomy	International Astronomical Union (IAU) [9].
Is excessive, misdirected, or obtrusive artificial (usually outdoor) light.	Astronomy	Globe at night [10].
The inappropriate or excessive use of artificial light	Dark sky association	International Dark-Sky Association [11].
…can be defined as the alteration of natural light levels in the outdoor environment owing to artificial light sources	Astronomy	Cinzano et al. [12].
…when artificial outdoor lighting becomes inefficient, annoying, and unnecessary	Human health	Chepesiuk [15].
Artificial light that alters the natural patterns of light and dark in ecosystems	Ecology	Longcore & Rich [13].
Excessive, intrusive, or prominent artificial light in the environment	Biology	Alaasam et al. [16].
The unintended consequences of poorly designed and injudiciously used artificial lighting	Economy	Gallaway [17].

Unfortunately, most of the existing definitions in the literature do not clearly separate the origin of the pollutant or the presence of light in space from the actual adverse or negative impacts and effects of lighting on humans or organisms. The International Commission of Illumination (CIE), the only internationally recognized standardization body within light and illumination, defines light pollution as the "*sum total of all adverse effects of artificial light*" in the International Lighting Vocabulary (ILV) [14] (Table 1). This definition is in line with other definitions of pollutants in environmental science since the word pollutant is only used when a substance or energy is introduced into the environment and causes an undesired or negative effect or adversely effects the use of a resource. Most well-known pollutants have been studied extensively for many decades to establish their toxicity and dose-effect responses on organisms, humans and the environment. Such evidence-based knowledge is crucial to be able to establish threshold values for toxicity and to combat pollutants with policies and international regulations. In lighting research, controlled evidence-based research of high quality on dose-effect responses realistic for outdoor condition is mainly lacking, apart from a few controlled studies on individual species that incorporate more than one light level in their experiments.

One of the main challenges is the lack of clarity in the light pollution definition across scientific disciplines, organisations and authors. For example, light pollution has different definitions in astronomy and ecology (see Table 1) resulting in a high risk of miscommunication and misunderstanding. However, none of the definitions of light pollution found in the literature and online are in accordance with the internationally established definition in ILV [14]. One common misunderstanding is that light pollution is equated with the presence of "artificial" light, without acknowledging the adverse effects or impacts of the light. Most do not use a scientific definition for light pollution but instead a rather subjective definition which is centred around what is needed or not needed for humans.

III. METHODS

We conducted a systematic literature search using online databases for aspects considered to be correlated with light pollution and for measuring aspects of relevance in the field. The literature search was performed in the bibliographic databases Scopus and Web of Science on 1 March 2021 and included hits for all years and until 2020. The search in Scopus was executed in the title, abstract and keywords and included all years, document types and languages available. The search in Web of Science was conducted by searches in "topic" which includes title, abstract, keywords), and was restricted to articles or reviews and the English language. Searches were subsequently imported to an Endnote library to enable identification and exclusion of duplicates.

Searches terms were created by use of two different search strings. One search string consisted of Group I search terms, representing light pollution, and the other consisted of Group II terms for words representative for methods, units and various measuring techniques for the various research areas (Table 1). Searches were conducted by construction of search queries such as: ("light pollution" OR "artificial light at night"…(group I terms) AND (lux OR illuminance OR…). Search terms in both groups was identified based on the current research literature in the field and from well-established definitions. Truncations (*) in the searches were used to include varied endings of words, for example, a search on "light*" resulted in hits on both "light" and "lighting". The function for identifying exact phrase matches was used for all search terms that consisted of more than one word in both database searches.

TABLE II. SEARCH TERMS AND GROUPS USED IN THE DATABASE LITERATURE SEARCH.

Group I	Group II			
Light pollution	Instrument*	Radiance	Meter	Unit
Artificial light at night	Drone-gonio-photometer	Kilolumen	Drone	UAS
Night-time light* / night time light*	Illuminance	Gigalumen	Lumen	Flux
Obtrusive light*	Luminance	Megalumen	Imag*	Lux
Spill light* / light* spill	Night sky brightness	Monitor*	Metrol*	
Light* trespass	Sky quality meter	Measur*	SI unit	
Skyglow / sky glow	Goniophotometer	Satellite	Method	
Lightscape*	Unmanned aerial systems	Detect*	LMK	
Light* nuisance	Irradiance	Photomet*	SQM	

We excluded invasive light as a search term since it did not yield more than one or a few hits and because indoor lighting was outside the scope of the review. Stray light was also excluded since it yielded a vast number of articles in the optic field which was not relevant for this review. We decided to not include brightness or bright* or ALAN (a common abbreviation used for artificial light at night) or glare because these search terms yielded a huge amount of irrelevant hits since researchers commonly use these words in other contexts.

The literature was screened according to the PRISMA 2009 flow diagram to begin with, first by title, secondly by abstract and thirdly, full-texts were read and assessed for eligibility [18]. The relevance for inclusion was evaluated based on the following criteria: the environmental impact is a verified consequence by LAN and if not, that an ecological or environmental impact is likely to occur from LAN or that LAN causes an adversely effect on the use of a resource.

Our systematic literature search yielded 1704 hits, which was reduced to 1522 after duplicates were removed (Table 3). All records were imported into Rayyan to evaluate them for inclusion and for labelling of the content to organize the review. Rayyan is free web-tool designed to help researchers conduct systematic reviews and synthesis projects by functions of screening and selecting studies in real time by joint access for the authors/members [19].

After excluding studies that were deemed as irrelevant for our study, 877 records remained (Table 3). For example, studies conducted with high illuminance levels were determined to be unrealistic for this study due to the focus on outdoor LAN. We only included primary research in our review and excluded secondary studies to avoid repetition, pseudo replication and also because we in our review of methods needed access to the original method description. Decision on inclusion was taken using Rayyan, of those were 35% of the decisions made by at least two researchers and 6% had at least three researchers. In cases of uncertainty all three researchers were involved in the decision. This review is a part of a larger project investigating effects of light pollution and the methods for measuring light pollution. In this article we present an overview of our main findings across scientific fields and we do not aim to present a full systematic review covering all hits in the literature search. As a part of this project, a separate systematic literature review of studies investigating light pollution and its impact on human physiology and behavior has previously been performed [5]. More detailed systematic reviews within additional relevant fields will be published in the future.

TABLE III. LITERATURE SCREENING PROCEDURE, PARTLY ACCORDING TO THE PRISMA 2009 FLOW DIAGRAM.

Records identified through database searching (Scopus and WOS)	**Records after duplicates removed and records screened**	**Records excluded**	**Records included and assessed for eligibility**
1704 (Scopus 640 Wos 1064)	1522	646	877

In Rayyan we used the labelling function to organise the records in categories based on scientific field of the study (see Table 4). We found most papers in ecology (ecosystems) which was sometimes overlapping with animal category if the study concerned animal species. In astronomy, we divided the studies in three areas: sky brightness, astronomy and satellite. However, satellite studies could be found in all other areas as well (i.e., ALP, ELP and impact on humans) and were not restricted to astronomical studies. Similarly, studies labelled as measurements also covered all fields.

TABLE IV. LABELLING OF THE RECORDS INTO CATEGORIES. *SOME RECORDS WERE CLASSIFIED AS MORE THEN ONE CATEGORY.

Category	**Number of records***	**Type of light pollution**
Sky brightness	187	ALP
Astronomy	45	ALP
Satellite	101	ALP, ELP, impact on humans
Ecosystem	330	ELP
Animals	115	ELP, impact on humans
Health	94	Impact on humans
Measurements	79	ALP, ELP, impact on humans

IV. RESULTS

Based on our systematic literature review, we have identified three key areas for light pollution impacts: I) astronomical light pollution (ALP), ecological light pollution (ELP) and impacts on humans, see Figure 1. Impacts on humans consists of two subareas: impacts on human health in physiology and behaviour and impacts on humans in terms of obtrusive light that can be perceived as negative or obtrusive, for example, discomfort, annoyance, nuisance and distractions. Astronomical light pollution includes studies performed on sky brightness, sky glow and has astronomical focus (for example investigations of light pollution at sites of importance for astronomical observations), while ecological light pollution studies study impact of LAN on various organisms (for example animals, plants or microorganisms) or ecosystems. Studies performed on human health investigates the impact of LAN on humans.

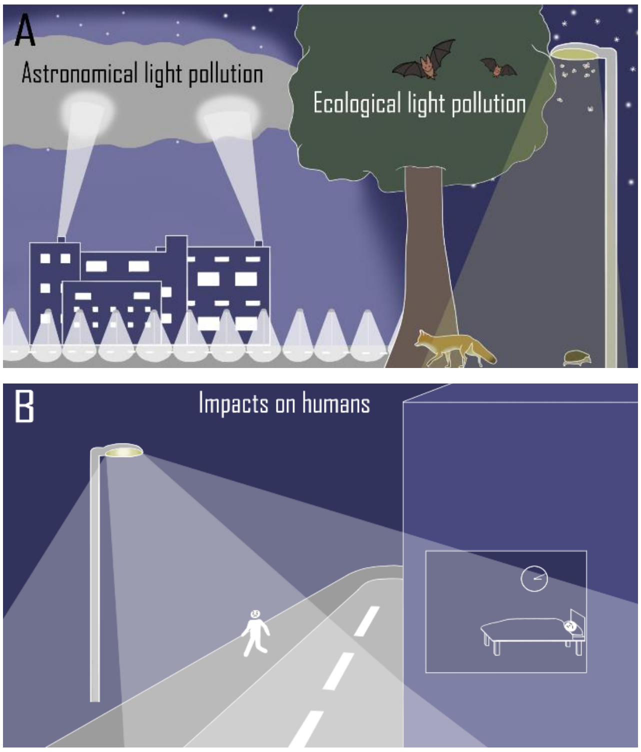

Fig. 1. Illustrations of the identified three key areas of light pollution: A) Astronomical light pollution and ecological light pollution, and B) Impacts on humans.

Based on the literature review it was identified that light pollution could have direct impacts and effects as well as indirect. For example, LAN can result in increased man-made sky glow and sky brightness which can reduce the ability for astronomical observations and degrade the ability to observe stars (see Table 5). Similarly, in ecology, we have identified impacts that directly affect organisms, such as, disturbances on migration and disruption of natural rhythms. The indirect consequences of such impacts can be increased mortality and changes in population sizes. Increased vision for diurnal species may result in increased predation which can lead to higher mortality of the prey. Barrier effects of light can result in, for example, reduced home ranges, smaller feeding areas and decreased number of nesting sites. For humans, disruption of natural rhythms and changed activity patterns can result in health impacts. Our results therefore demonstrate that light pollution can be both direct and indirect resulting in very complicated processes and possibly also in feedback loops.

TABLE V. EXAMPLES OF DIRECT IMPACTS OF LIGHT POLLUTION. NUMBER OF RECORDS WAS COUNTED THROUGH THE USE OF A SEARCH FUNCTION IN RAYYAN AND COVERED VARIOUS CATEGORIES.

Impacts of light pollution	**Number of records (search string)**	**Type of light pollution**
Sky glow	74	ALP
Sky brightness	179	ALP
Upward emitted light	16	ALP
Reduced ability for astronomical observations	54 (astronomical observations)	ALP
Degraded star observations	14 (star observations)	ALP
Disturbances on migration and activity	42 (migration) 229 (activity)	ELP
Disruption of natural rhythms	27 (natural rhythm)	ELP
Increased vision	16 (vision¤)	ELP
Attraction	72	ELP
Barrier	10	ELP
Alertness	1	Impact on humans
Disruption of natural rhythms	27 (as above)	Impact on humans
Changed activity pattern	121 (behaviour°)	Impact on humans
Decreased visibility	75 (visibility°)	Impact on humans
Discomfort	3	Impact on humans
Glare	14	Impact on humans
Annoyance	1	Impact on humans
Distraction	2°	Impact on humans
Nuisance	6	Impact on humans

¤ most records were not found in ecology. ° included records in all fields.

Our systematic review also shows that a number of studies focuses on measurements and development of measurements of light pollution (see Table 4). However, the response variables in each scientific area are rather unique for the specific scientific discipline (astronomy, ecology and human) so studies should be categorized according to the specific scientific field of application. For the measurement of the independent variable (light) the general scientific classification of measurements is more consistent, because even though the applications are different, the same units and methods for measurements can be used.

A. *Astronomical light pollution (ALP)*

1) *Studies of the sky, stellar objects and phenomena*

The studies in the field of astronomical light pollution include measurements of night sky brightness, both natural and anthropogenic, (at zenith and spatial distribution), observation of celestial objects and phenomena and the disturbance from man-made sky glow, observation of night-time lights from earth reaching satellites and modelling of light propagation and scattering through the earth atmosphere.

2) Methods

The methods used in the publications covered by this review include both experimental and theoretical simulations and combination of the two. Ground based measurements include astronomical photometry and spectroscopy at large observatories, wide-field photometry using all-sky cameras with fish-eye lenses, narrow angle measurements (typically in only one band) using e.g., sky quality meters (SQM). Naked eye observations of stellar objects where citizen observations can be used to get large coverage of the observations. For light emitted through the earth atmosphere, remote sensing is carried out with radiance measurements by satellite-based sensors and photographs taken from the international space station (ISS).

In the earlier studies mostly telescopes and naked eye observations were used. From the year 2000 and onwards satellite based radiometry has been used in the studies of light pollution, starting with the Defense Meteorological Satellite Program (DMSP) Operational Linescan System and later with the higher resolution of the monthly cloud-free night-time imagery from the Suomi National Polar-Orbiting Partnership (Suomi NPP) Visible Infrared Imaging Radiometer Suite Day/Night Band, and most recently the Chinese satellite Jilin-1, claiming to have a spatial resolution below 1 m. With the development of wide-angle photometry, from 2010 and onwards the number of studies using camera-based measurements have increased. From 2012 onwards, studies using sky quality meters started to appear.

The number of records assigned at least one of the labels Sky brightness, Satellite, Astro, Simulation, Modelling and Camera, were 324. The earliest paper is published in 1978. Out of those 324, 32 studies used sky quality meters, 42 camera-based measurements and 130 used modelling. The process of sky glow and the measurement of the sky brightness is highly influenced by meteorological conditions and the influence of clouds on the measurement of light pollution is analysed in 34 of the 324 studies.

Based on a sample of 45 publications (label Astro) 28 were observational, 4 were theoretical simulations and 13 used a combination of observations and modelling. The publications spanned between 1991 and 2020.

In astronomical studies different units are used depending on the experimental technique. It is common to report the sky brightness in the astronomical magnitude system mag/arcsec^2. This can be approximately compared to luminance in mcd/m^2, but the different measurement techniques and bands used make it difficult to compare results from different studies.

B. Ecological light pollution (ELP)

1) Organisms studied

In ecology, studies have been conducted on many different species, taxa and groups. An analysis of the 491 scientific publications labelled in Rayyan as ecosystem, animals, fish or measurements of light pollution (published during all years until 2020), shows that most research has been done on birds, insects, bats, fish, plants, invertebrates and mammals (see Table 6). Most of the studies state that they show a significant negative impact of LAN, and very few studies show no impact at all or positive impacts.

Our result shows that birds are the most well-studied group in the field of ecology and there is a large variety of species of birds studied, for example great tits (32), songbirds (26), seabirds (13), petrels (12), blackbirds (11), sparrows (6), owls (6), and pigeon (4). Another well-studied group is insects which has been mainly focused on moths (19), although several studies have been performed on invertebrates in general (22), arthropods (10), spiders (9), beetles (8), diptera (6), mayflies (6), crickets (4), worms (3) and fireflies (3). Bats are also a well-represented in ecological light pollution studies with 48 records in our search. Fish has been relatively well investigated (37) and examples of well-studied species are perch (11), and roach (5). Some studies also incorporate plants (29), vegetation (21), leaves (6), either in individual studies, for example on trees (18) and sometimes plants or vegetation are included or mentioned when performing studies on insects and pollination.

At a first glance, mammals (22) seem to be a well-studied group, however most of the studies are on bats and there seems to be a general lack of studies done on other mammals including primates. For example, we found only two studies on primates (nocturnal strepsirrhines and grey mouse lemur *Microcebus murinus*).

Turtles (22) are well-studied and involves loggerhead turtles (9), sea turtles (16), green sea turtles (6), flatback turtles (4), and marine turtles (4).

Rats (11), mice (10), and rodents (5) are also represented in studies investigating light pollution. Few studies have been performed on amphibians (10), toads (8), reptiles (4), frogs (3) and lizards (3). There have been studies performed on the ecological impacts of LAN on corals (9), parasites (9), and microbial organisms (9). Very few studies (3) have been found that involves hedgehogs, viruses, daphnia and plankton. In general, non-flying mammals and microorganisms seems to be understudied.

TABLE VI. STUDY ORGANISMS IN ECOLOGICAL LIGHT POLLUTION AND THE NUMBER OF RECORDS FOUND IN THE SYSTEMATIC LITERATURE REVIEW.

Study organisms	Number of records
Birds	112
Insects	58
Bats	48
Fish	37
Plants	29
Invertebrates	22
Mammals	22
Turtles	22
Rats	11
Amphibians	10
Mice	10
Corals	9
Parasites	9
Microbial	9
Frog, hedgehog, worms, viruses, lizards, fireflies, daphnia, primates, plankton	3 (each)

Our literature review shows that responses of the organisms was studied primarily on investigating ecologically relevant dependent variables such as reproduction (94), interactions (85), behaviour (81), distribution (69), foraging (48), prey (39), migration/migrating (39), movement (29), life cycle (19), biomass (15), phenology (14), collisions (8), pollination (6). Many studies mentioned biodiversity (68), but few was actually investigating diversity or impacts on diversity of LAN. Studies also investigated physiological response variables such as rhythm (58), stress (34), melatonin (31), sleep (26), body mass (16), immunology (11), glucocorticoids (6), pigments (6) and photosynthesis (6).

The ecosystems and areas of the research in ecological light pollution were mainly aerial because the majority of species and groups was flying organisms (birds, bats, insects). Areas for other studies involved aquatic (42), terrestrial (35), marine (32), coastal (31), freshwater (28) environments, but also streams (13), grasslands (10) and rivers (8).

2) Methods

Methods used in ecological light pollution studies are plentiful because of the many different kinds of organisms that are studied. Therefore, the methods will be reviewed based on the largest groups (identified in the previous section).

LAN impacts on birds have been studied through observational studies in the field that correlated bird responses (e.g. migration) to satellite-based light measurements or to ground-based measurements, but also through controlled indoor experiments or through experiments using bird enclosures outdoor. Studies also include introducing light sources and studying the behaviour after the intervention in comparison with an unlit control. Biologgers on birds have been used to correlated exposure of LAN to movement patters.

The effects of LAN on insects (or invertebrates) have been studied in observational studies, often by comparing the number of trapped insects, with and without lighting (often using light as a source of attraction for the insects), or by introducing different kinds of interventions in unlit or lit areas. Insect responses have also been studied by introducing LAN in previously unlit areas in manipulative field experiments and observing the responses. Insect responses have also been studied in more controlled conditions such as in compartments in greenhouses or indoors. Common response variables include the number of insects, species and diversity, but ecological and behaviour variables have also been studied.

Bats have only been studied through field experiments. Observational studies have been performed that compares the bats movements and frequency of activity without any intervention. Field experiments varies much in their design but some use already lit areas for introducing interventions (e.g. changed light sources, or light intensity or light distribution) and others use previously unlit areas to introduce LAN and study impacts on behaviour. Behaviour is most often studied by the use of echolocation making it possible to put up detectors in the field for several days and collect the data afterwards. Measurements of echolocation gives data on which species are in the area, number of species (and diversity), and how frequent they are in the area. LAN impact on bats can be studied by colony size and in roosts, hibernation sites and in foraging and commuting routes.

Fish responses to LAN can be studied in field experiments, mesocosms, enclosures or in laboratory studies. Field experiments can be conducted to study both lit or unlit conditions with or without interventions. Use of mesocosms, enclosures or laboratory environments will improve the scientific reliability of the study since it will be more controlled, and the influence of external factors will be minimised. Fish is studied through many different ecological or physiological response variables as well as behaviour patterns. Various life stages can be used in the experiments to investigate impacts on different ages.

Responses of plants can be investigated through controlled field experiments manipulating various light conditions. Studies can also be performed as observations in unlit or lit areas with or without interventions. Tree phenology can be correlated with satellite-based measurements or with ground-based measurements. Responses to LAN can also be investigated through the use of enclosures or laboratory experiments and use different life stages of the plant or tree. Responses can be studied through ecological and physiological variables.

Turtles have mainly been studied in their natural habitats and in the field. Studies are often observations of behaviour before/after interventions have been introduced. Studies focuses on hatchlings, but also adult turtles have been under investigation.

Responses of rats, mice and rodents have been investigated in controlled laboratory studies where lighting manipulations can be fully controlled and measured. Field experiments of mice and rats in natural environments or in more controlled enclosures have also been performed. Response variables includes behaviour, ecological relevant variables and physiological measurements.

Many studies are conducted without including data on environmental factors that may influence the results. Especially field experiments are very poor in reporting the lighting condition, for example light source, light intensity and light distribution. Only a few studies report enough information on light distribution to be able to repeat the study. Light sources are often mentioned but rarely with enough information to replicate the study. For example, data of the spectral power distribution of the light sources used is rarely included. Even during controlled conditions, measurement details were not clearly stated or reported. For example, exposure levels for the organism are rarely reported.

C. Impact on humans

Apart from affecting the ability to view stars and make astronomical observations (see section on astronomical light pollution), light pollution can have significant impact on humans. The impact of light pollution on humans can be visual (e.g., glare, obtrusive light) and non-visual (e.g., circadian entrainment). While circadian and sleep research studies utilized a range of lighting conditions in often controlled conditions (i.e., laboratory), realistic outdoor scenes are often observed in short periods and under low lighting conditions. Therefore, it is likely that light pollution has lower impacts on non-visual mechanisms, such as circadian entrainment, sleep quality, alertness, and mood. A separate systematic literature review of studies investigating light pollution and its impact on human physiology and behavior indicates that there are four areas of health outcomes and two types of experimental methodologies [5].

1) Health outcomes of LAN

Cancer: Light pollution studies primarily focused on the breast cancer incidence in humans, followed by prostate cancer. While most studies collected data through self-reported questionnaires and medical databases, only two studies collected tissue samples to connect LAN to cancer. The primary outcome of the studies was a positive correlation between LAN and cancer, but one study found no effect of light pollution. In addition, there was no effect of LAN on any other cancer type besides breast and prostate cancer.

Sleep: The impact of LAN on sleep quality was the second most investigate parameter. Similar to cancer, most studies utilized self-report surveys and databases, and a small portion collected tissue or used imaging or other observation techniques. The primary outcome was the relationship between poor sleep quality and LAN.

Depression: A quarter of studies were observational, while the rest were conducted on animal models (mice, rats, and hamsters). Studies with human subjects found a negative impact of LAN on depression. Rodent model studies found depression-like symptoms in test subjects, but two studies found positive effects of LAN on learning and memory tasks, and anxiety-like behaviour. Results suggest that the effects of LAN can be task specific.

Obesity: A small number of studies investigated obesity in humans over a long period of time and found a higher likelihood of developing obesity with the increased LAN exposure.

2) Methods

Observational studies: An observational study which draws causal inferences from a population sample, is often run with a large sample size over a longer period. These are often used to investigate complex problems and require a large dataset to be collected from realistic settings. In light pollution literature, the primary measurement method was self-report (i.e., surveys, questionnaires, and information from existing databases). The response variables were physical (e.g., weight, height, body mass index (BMI), behavioural (e.g., sleep), and physiological (e.g., melatonin, gene expression) parameters. The controlled variables included age, smoking, alcohol consumption, socioeconomic status, income, BMI, weight, obesity, education, urbanization, population density, ethnicity, race, diet, gender, sex, physical activity, and family history, menopausal status, and other factors, such as viewing TV, chronic conditions, folate intake, and coffee consumption. Unfortunately, observational studies lacked a consideration for the environmental factors. Also, none of the studies controlled all the variables at the same time. Reporting of the lighting conditions were often poor (i.e., missing control groups, measurement details were not reported in detail, light source spectra and exposure duration were not known).

Lab studies: Controlled laboratory studies are conducted to isolate individual parameters and to establish firm connections between independent and dependent variables. Although lab studies cannot account for real-world environment complexities, they can provide robust understanding on human physiology and behaviour in a specific context. Most light pollution studies used animal models (primarily rodents). Physical (e.g., BMI) and physiological measures (e.g., tumour size, gene expression) were the most common responses. Although experimental methods were reported more thoroughly, none of the studies reported spectral power distributions or circadian metrics. Only five studies reported light measurement equipment and their model, while a majority did not report any information related to the measurement device.

V. DISCUSSION

This systematic literature review shows that light pollution consists of three main fields: astronomical light pollution, ecological light pollution and impacts on humans. Other studies have hitherto not been able to identify these three fields. This is probably because other systematic reviews have been conducted with a narrow focus (e.g., restricted to ecological impacts or very specific health outcomes) but may also be due to the widespread use of inaccurate definitions of the term light pollution, which has resulted in confusion and difficulties in separating the presence of LAN with the impacts and effects of LAN. In this study, we used the standardized definition of light pollution [14] which resulted in a more efficient evaluation process in the systematic literature review.

Our systematic review of impact of LAN in ecology and on human health demonstrates that study design and reporting of lighting conditions were not very robust. All relevant and influencing parameters must be reported to be able to repeat a study and to validate the results. Observational studies, field studies, experimental manipulations and laboratory studies have limitations in controlling and reporting lighting parameters. In ecology, for example, it is very rare to report light exposure levels for the organisms studied. Inadequate reporting of lighting conditions in studies claiming to show significant effects of LAN makes the results and conclusions questionable since the studies cannot be repeated and because it is unknown whether effects can be attributed to LAN or to other influencing or confounding parameters.

In all three fields, a plethora of methods are used for measuring the dependent and independent variables. This has unfortunately resulted in significant difficulties in comparing responses between geographical areas, species, and effects of LAN on human health. For example, despite the large number of studies performed on LAN impacts in all three fields, it is very challenging to assess if the lighting in a specific location has a negative impact and if so, how to reduce it to avoid inducing light pollution. However, because many studies show negative impacts of LAN for organisms and humans it is essential to establish standardized ways of evaluating light pollution. This includes standardizing experimental procedures as well as methods and metrics used for collecting data of dependent and independent variables. This should therefore be of high priority for international standardization efforts, for example, in technical committees in CIE concerning light pollution.

VI. CONCLUSION

In this systematic review of light pollution, we identified three key areas: astronomical light pollution (ALP), ecological light pollution (ELP), and impacts of LAN on humans in two subareas; impacts on human health (physiology and behaviour) and impacts on humans in terms of obtrusive light that can be perceived as negative, for example, discomfort, annoyance, nuisance and distractions. Methods used in various disciplines are partly similar, e.g., satellite-based sensor collected data are used in all three areas to study impacts, but specific methods are also used within each field. This study shows that the study design and reporting of lighting conditions were not robust and there is an urgent need for establishing standardized experimental procedures, and for collecting data for the dependent and independent variables as well as for environmental and confounding factors that can influence the results in significant ways.

REFERENCES

[1] A. K. Jägerbrand, "Development of an Indicator System for Local Governments to Plan and Evaluate Sustainable Outdoor Lighting," Sustainability, vol. 13, no. 3, Art. no. 1506, 2021.

[2] C. C. M. Kyba et al., "Worldwide variations in artificial skyglow," Scientific Reports, vol. 5, no. 1, Art. no. 8409, 2015.

[3] K. W. Riegel, "Light pollution," Science, vol. 179, no. 4080, pp. 1285-1291, 1973.

[4] CIE 150:2017, "Guide on the limitation of the effects of obtrusive light from outdoor lighting installations, 2nd edition.," Commission Internationale de l'Éclairage, Vienna, Austria, 2017.

[5] D. Durmus, M. Nilsson Tengelin, and A. K. Jägerbrand, "Investigating the methods and health outcomes of research studies on light pollution and human physiology and behaviour: a systematic review," unpublished, presented at the 17th International Symposium on Science & Technology of Lighting, Toulouse, France, 2022.

[6] D. Sanders, E. Frago, R. Kehoe, C. Patterson, and K. J. Gaston, "A meta-analysis of biological impacts of artificial light at night," Nature Ecology and Evolution, vol. 5, no. 1, pp. 74-81, 2021.

[7] A. K. Jägerbrand and C. A. Bouroussis, "Ecological Impact of Artificial Light at Night: Effective Strategies and Measures to Deal with Protected Species and Habitats," Sustainability, vol. 13, no. 11, Art. no. 5991, 2021.

[8] A. K. Jägerbrand, D. Gasparovsky, C. A. Bouroussis, L. J. M. Schlangen, S. Lau, and M. Donners, "Correspondence: Obtrusive light, light pollution and sky glow: Areas for research, development and standardisation," Lighting Research and Technology, vol. 54, pp. 191-194, 2022.

[9] International Astronomical Union. Controlling Light Pollution. [Online]. Available: https://www.iau.org/public/themes/light_pollution/

[10] Globe at night. What is light pollution? [Online]. Available: https://www.globeatnight.org/light-pollution.php

[11] International Dark-Sky Association. Light Pollution. [Online]. Available: https://www.darksky.org/light-pollution/

[12] P. Cinzano, F. Falchi, C. D. Elvidge, and K. E. Baugh, "The artificial night sky brightness mapped from DMSP satellite Operational Linescan System measurements," Monthly Notices of the Royal Astronomical Society, vol. 318, no. 3, pp. 641-657, 2000.

[13] T. Longcore and C. Rich, "Ecological light pollution," Frontiers in Ecology and the Environment, vol. 2, no. 4, pp. 191-198, 2004.

[14] CIE S 017/E:2020. "ILV: International lighting vocabulary, 2nd edition," Commission Internationale de l'Éclairage, Vienna, Austria, 2020.

[15] R. Chepesiuk, "Missing the dark: Health effects of light pollution," Environmental Health Perspectives, Article vol. 117, no. 1, pp. A20-A27, 2009.

[16] V. J. Alaasam, M. E. Kernbach, C. R. Miller, and S. M. Ferguson, "The Diversity of Photosensitivity and its Implications for Light Pollution," Integrative and Comparative Biology, vol. 61, no. 3, pp. 1170-1181, 2021.

[17] T. Gallaway, "On light pollution, passive pleasures, and the instrumental value of beauty," Journal of Economic Issues, vol. 44, no. 1, pp. 71-88, 2010.

[18] D. Moher, A. Liberati, J. Tetzlaff, and D. G. Altman, "Preferred reporting items for systematic reviews and meta-analyses: the PRISMA statement," BMJ (Online), vol. 339, no. 7716, pp. 332-336, 2009.

[19] M. Ouzzani, H. Hammady, Z. Fedorowicz, and A. Elmagarmid, "Rayyan—a web and mobile app for systematic reviews," Systematic Reviews, vol. 5, no. 1, Art. no. 210, 2016.

NLITED - New Level of Integrated Techniques for Daylighting Education: Premilinary Data on the Use of an E-learning Platform

Federica Guliani
Faculty of Engineering
University "Niccolò Cusano"
Rome, Italy
federica.giuliani@unicusano.it

Natalia Sokol
Faculty of Architecture,
The Gdansk University of Technology,
Gdansk, Poland
natalia.sokol@pg.edu.pl
ORCID: 0000-0002-0269-1701

Niko Gentile
Div. of Energy and Building Design
Lund University
Lund, Sweden
niko.gentile@ebd.lth.se
ORCID: 0000-0001-5721-6644

Mandana Sarey Khanie
International Center for Indoor Environment and Energy, Department of Environment and Resource Engineering
Technical University of Denmark
Copenhagen, Denmark
masak@byg.dtu.dk
ORCID: 0000-0001-8096-4261

Valerio R.M. Lo Verso
Dept. of Energy 'Galileo Ferraris',
TEBE Research Group
Politecnico di Torino
Turin, Italy
ORCID: 0000-0003-0065-3178

Federica Caffaro
Dept. of Education
University "Roma Tre"
Rome, Italy
federica.caffaro@uniroma3.it
ORCID 0000-0003-3911-5924

***Abstract*— Project NLITED – New Level of Integrated Techniques for Daylighting Education - is an educational project for students and professionals. The project's objective is to create and develop an online eLearning platform with 32 eModules dedicated to daylight knowledge. The project also offers e-learners two summer school training where the theory is put into practice. The platform was launched on January 31, 2022. The paper analyses the participation during the first four months of online activity until May 31, 2022. It discusses which eModules have received the highest participation rate and which have the lowest. These data are compared to the preferences on modules expressed by different panels of experts. The experts expressed their recommendations for specific educational content during workshops conducted in 2021, which led to the definition of the curriculum. Furthermore, participants also fill out an evaluation test on the quality and the usability of the eModule(s) they have taken. This information leads to the amendments of the ePlatform which are in the scope of action for the final year of the NLTED project.**

Keywords - NLITED, daylight, eLearning platform, eModules, online education, an evaluation test

I. Introduction

The project NLITED – New Level of Integrated Techniques for Daylighting Education - is a 3-year educational project aiming to increase daylighting knowledge for students and professionals in the building sector. The eLearning platform was built, and a summer school with specialist teachers is offered yearly. The project was funded with the support of the Erasmus+ Programme of the European Union and involved four countries: Italy (leader), Denmark, Poland, and Sweden. Four universities are the collaborative partners: Università Niccolò Cusano, Danmarks Tekniske Universitet (DTU), Politechnika Gdańska, and Lunds Universitet. For the project's definition of the goals, a strategic role was played by networks each partner built at a national level. These include other universities, consulting and design firms, manufacturing companies and trade associations, (day)lighting associations, and technical publishing houses.

The NLITED eLearning platform was launched on January 31, 2022. Data about participants in the various eModules have been collected for four months of activity until May 31, 2022, and trends have been analyzed. This paper describes the first results observed on how the eLearning platform has been used, compared to the input received during the definition stage, which led to the construction of the curriculum.

II. The NLITED eLearning platform

A. Creation of a shared curriculum

The curriculum of the NLITED ePlatform was created through the involvement of representatives from the national networks built by four partners. It allowed a better understanding of their needs and ensured appeal to potential target groups. This fact-finding investigation was conducted through supplementary questionnaires during workshops with experts. A detailed description of the methodology applied to develop the curriculum is reported in the conference paper [1].

Fourteen workshops were held between January and February 2021, and 63 experts participated. There were 98 responses to the questionnaires, 53 generated during workshops and an additional 45 via a survey posted on the social media platforms.

Based on all the information obtained, the structure and content of the final curriculum of the NLITED platform were defined. Figure 1 shows the structure of the NLITED platform.

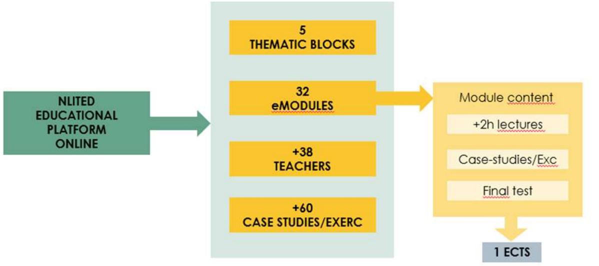

Fig. 1. Schematic structure of the NLITED ePlatform

The final curriculum presents five thematic areas (called "blocks") that represent the main macro-topics of interest in daylighting: (1) heath; (2) daylighting design; (3) energy aspects; (4) daylight assessment; and (5) daylighting simulation. For each block, there are consistent and coordinated lectures (called 'eModules') to provide all the knowledge on that specific topic. Each eModule contains two or three hours of lectures to provide theoretical knowledge on a specific topic and one hour of case studies to show theory applications to real projects. Following good practices in online learning, several 'eTivities' have been introduced in eModules: these are interactive self-assessment exercises to help participants assess their progress in their understanding. eTivity is a dynamic and interactive learning framework developed in the early 2000s in eLearning pedagogy [2].

This framework was designed to achieve the workload of 1 ECTS based on proper learning outcomes. Therefore, each module includes a final assessment test on the acquired knowledge. This test needs to be passed to get the credit.

Users are also asked to fill an "eModule evaluation" (EE): this consists of 29 items that address different aspects of the eModules related to:

- learning expectations, e.g. "*the eModule covered the content I was expecting*", "*the eModule content was consistent with the learning outcomes?*"
- the time needed, e.g., "*the amount of time it took to complete the eModule was appropriate*
- eModules structure and contents, e.g., "*the eModule workload was adequate," "etivities helped me gain a clearer understand of the subject", "the number of multimedia used in the eModule was adequate*",, "*the quality of multimedia used in the eModule was good*"; "*the audio of the eModule had a good quality*"; *the quality of the overall visual design of eModule content and materials was good*"; "*the case-studies were pertinent/inspiring*"; "*the links to external resources were useful*"; "*the tutoring service was useful*"; "*the eModule content was arranged clearly and logically*"; "*the final test adequately covered the content of the eModule*")
- engagement, *e.g.,* "*I would recommend the eModule to my colleagues*"; "*I enjoyed the eModule"; "the eModule was inspiring*",; *"I am confident about the knowledge I gained after attending the eModule*".

All the items were evaluated on a 4-point rating scale, labelled as 1 =, not at all agree; 2 = partially agree; 3 = quite agree; 4 = completely agree. For the subsequent analyses, the responses were then categorized into two groups: scores 1-2 = low agreement; scores 3-4 = high agreement.

B. ePlatform's architecture

A total of 32 modules were designed, involving lecturers from the strategic network. The production phase of the modules is still ongoing: it is expected to be completed by the end of June 2022. Figure 2 shows the active eModules (as of May 31, 2022) within the NLITED platform.

Some of the key features of the curriculum that have determined the architecture of the platform were:

- *the curriculum was designed for heterogeneous users.* Within each block is a basic knowledge eModule '0' and other eModules with increasingly advanced knowledge. In this way, the ePlatform is suitable for a broader audience ranging from neophytes to researchers and professionals.
- *The eModules are independent of each other.* Therefore, users are not required to follow the entire learning path but can fill their knowledge gaps through a flexible and tailored curriculum. To facilitate the recognition of users' knowledge gaps, an 'admission test' is mandatory as the first step after registering into the platform. The test covers all knowledge areas of the curriculum and directs users to the modules whose answers were incorrect. It avoids taking modules that may be too easy or too difficult. The results from this test only suggest which modules to pick from the catalogue, but users are left free to choose the modules they prefer or are interested in
- *the eModules are self-paced*. No deadline is given for the completion of a module, and lectures and case studies are pre-recorded. It means that participants can attend every module and get the ECTS credit at their best convenience in terms of time; furthermore, they can re-attend parts of a module for more in-depth analysis and understanding.

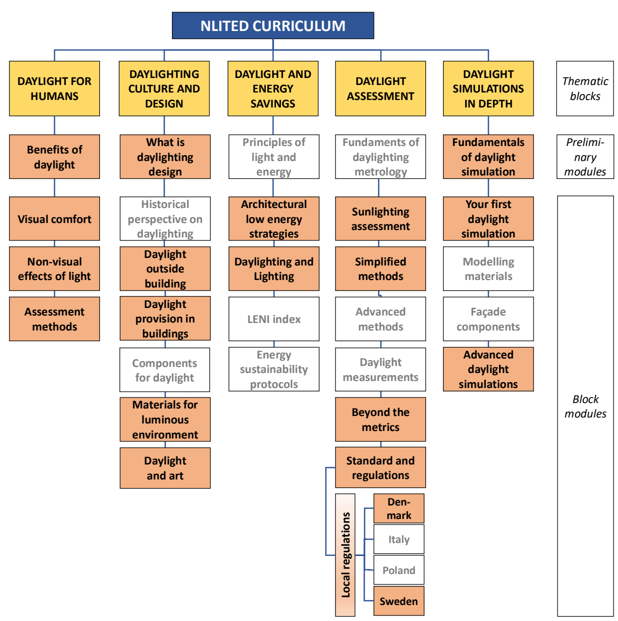

Fig. 2. eModules that are active (orange background) within the entire NLITED platform. eModules due to be released by June 2022 have a white background.

III. EARLY DATA ON THE USAGE OF THE EPLATFORM

A. *Launch of the ePlatform*

An online event was created on January 31, 2022, to launch the platform officially. One hundred thirty-nine people were booked to attend the event, and 98 took part in the event.

The number of eplatform registrations has been rising, with an initial peak and a steady trend of 3.69 registrations per day. Over 120 days of activity (as of May 31, 2022), 443 people have enrolled on the platform.

The enrollees should be drastically scaled-down because only 244 users (53%) are currently active on the platform. The remaining 47% of people registered in the platform never completed the ‘admission test’, which would have made them active users within the platform.

B. *Most and least selected eModules.*

Although not all eModules are active, users can sign up for the eModules they prefer while waiting for them to become active. Figure 6, at the end of the paper, shows in detail the number of registered users in each module.

Based on the preferences extracted after the first 120 days of operation, the five most selected modules are shown in Table I. Data show that more than half of the active users in the platform enrolled in the basic module B1.0 - Benefits of daylight: this can be considered quite logical, as users can see the module as a general introduction to the potential effects of daylight over a vast range of aspects. However, the ‘most selected’ eModules cover different topics, including traditional topics such as ‘visual comfort’ (B1.1) and new topics such as ‘non-visual effects of light’ (B1.2). Besides, a technical eModule, ‘first simulations with Ladybug and Grasshopper’ (B5.1), has also been diffusely selected.

TABLE I. EMODULES WITH THE HIGHEST NUMBER OF SUBSCRIPTIONS

eMODULES			
CODE	***TITLE***	***Sub-scribed***	***%***
B1.0	Benefits of daylight	123	50.4%
B1.1	Visual comfort	87	35.7%
B5.1	Your first daylight model with Ladybug. tools in Rhino+Grasshopper	72	29.5%
B1.2	Non-visual effects of light	66	27.0%
B1.3	Assessment methods	60	24.6%
B4.6	Beyond the metrics	50	20.5%

Conversely, Table II illustrates the modules with the lowest number of subscriptions: as one could expect, the least picked modules concern daylighting legislation and regulations at a national level, as these address a more limited audience. Other topics among the least selected concern the energy aspects regarding more specific topics, such as daylight and electric light (through the LENI index) and modelling of materials for simulations, but also general topics such as simplified methods to assess daylight and measures.

TABLE II. MODULES WITH THE LOWEST NUMBER OF SUBSCRIPTIONS

e-MODULES			
CODE	***TITLE***	***Sub-scribed***	***%***
B4.5b	Italian Standard and Regulations	11	4.5%
B4.5c	Polish Standard and Regulations	11	4.5%
B3.3	LENI index	17	7.0%
B4.5d	Swedish Standard and Regulations	17	7.0%
B4.4	Daylight measurments	19	7.8%
B4.2	Daylighting assessments - simplified methods	21	8.6%
B5.2	Modelling materials	21	8.6%

In both Tables I and II, the percentage column shows the percentage of platform learners enrolled on each eModule. 50.4% of active learners (one out of two) are enrolled in the basic B1.0 module, and 35.7% in B1.1 (more than 1/3).

C. *Average eModule frequency*

Figure 3 shows the average eModule frequency rate from the beginning to the end of the eModules. This analysis considers only the number of learners who watched the introductory video and followed the rest of the eModule content.

About 29% of those who started a course have completed it. The most significant number of dropouts occur before they have passed 1/4 of the module, while most students who have passed this threshold make it to the end of the module. 67% of those who have passed 1/4 of the module complete it.

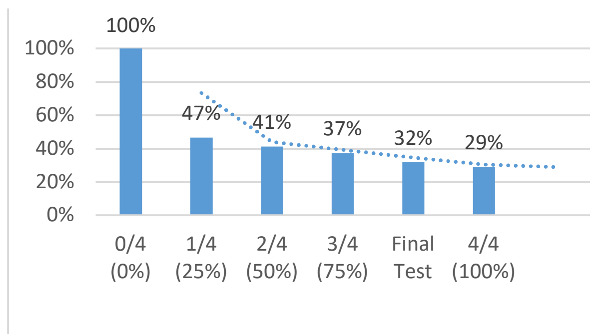

Fig. 3. The average percentage of completion of eModules vs progressive course progressions.

D. *Most completed modules*

Table III shows the rate of users who completed an eModule, compared to the number of active users who registered into that module.

It is worth stressing that the module with the highest completion rate (B4.1, ‘Sunlighting assessment’) is not among the eModules with the highest number of subscriptions (see Table I). The same applies to the third eModule (B1.2, ‘non-visual effects of light’), the third one in the completion rate list but not among the most selected courses.

TABLE III. EMODULES WITH THE HIGHEST COMPLETION RATE

eMODULES				
CODE	*TITLE*	*Sub-scribed*	*Completed*	*%*
B4.1	Sunlighting assessment	47	10	21.3%
B1.0	Benefits of daylight	123	23	18.7%
B1.2	Non-visual effects of light	66	6	18.2%
B4.6	Beyond the metrics	50	9	18.0%
B5.1	Your first daylight model with Ladybug.tools in Rhino+Grasshopper	72	10	13.9%
B1.3	Assessment methods	60	5	13.9%
B1.1	Visual comfort	87	12	13.9%

E. A download of certificates of participation

In order to obtain a certificate of participation in a module, users must pass the final test and complete the EE on the quality of the module delivered. As shown in Fig. 3, on average, 3% of learners who have completed the final test have not proceeded to download the certificate of attendance. Although it is a marginal number, this value shows that not all participants are interested in obtaining training credits or proving that they have participated in the course.

F. Quality of the modules

Figure 6 summarizes the main finding from the e-module evaluations: EEs.

The following considerations can be drawn based on the scores provided by the participants in eModules (1-2: low agreement; 3-4: high agreement):

- *the eModule covered the content I was expecting*
  For half of the emodules (5 out of 10), respondents gave low agreement scores (1-2); B4.1 (sunlight assessment) leads with 34% of respondents, while the other modules are: B2.3 (daylight provision in buildings) and B4.6 (beyond the metrics), around 20% (all scores being ‘2’ for eModule B.4.1 and ‘1’ for eModule B2.3); B1.1 (visual comfort), around 15%, and B1.0 (benefits of daylight), around 5%

- *the amount of time it took to complete this eModule was appropriate*
  For half of the modules evaluated (5 out of 10), respondents attributed low agreement scores (1 or 2), stating that they found that the time needed to complete a module was too long. Particularly module B4.1 (sunlight assessment) received 37% of low agreement scores. A low agreement score was attributed by 20-22% of respondents to modules B2.3 (Daylight provision in building, with all scores ‘2’ and no score ‘1’), B5.1 (Your first daylight model with Ladybug, with an equal number of scores '2' and '1'), and B4.6 (beyond the metrics, with all scores ‘1’). Finally, module B1.0 (benefits of daylight) was judged too long by 10% of respondents, with an equal number of scores '2' and '1.'

- *the eModule content was consistent with the learning outcomes*
  Most courses (8 out of 10, 80%) were rated with high agreement scores on this issue. No course received the lowest agreement score of 1, whilst two courses only received the low agreement scores of 2: module B4.1 (sunlight assessment), 18% of respondents; and B1.0 (benefits of daylight), 5% of respondents

- *the eModule workload was adequate*.
  Unlike the previous question about the time needed to complete an eModule, the workload of the module was generally assessed as adequate through high agreement scores (3 and 4). Four modules out of 10 (40%) received low agreement scores (1 and 2): B2.3 (daylight provision in a building) from 40% of respondents; B4.6 (beyond the metrics), 20% of respondents; B5.1 (your first daylight model with Ladybug), 12% of respondents; and B1.0 (benefits of daylight), 8% of respondents

- *I would recommend the eModule to colleagues.*
  Most courses (7 out of 10, 70%) were judged positively with high agreement scores (3-4), which shows that users would recommend the module. On the other hand, three courses also received low agreement scores (1-2) by a low rate of users: B2.3 (daylight provision in buildings, with all scores ‘1’), 20% of respondents; B4.1 (sunlight assessment, with all scores ‘1’), 18% of respondents, and B5.1 (your first daylight model with Ladybug), 14% of respondents

- *attending the module was inspiring*
  Six courses out of 10 (60%) received high agreement scores (3-4), while 4 (40%) also received low agreement scores (1-2): B3.2 (daylighting and electric lighting), 36% of respondents; B2.3 (daylight provision in buildings, all scores ‘1’) and B4.1 (sunlight assessment, all scores ‘2’), 20% of respondents; and B1.1 (visual comfort), 12% of respondents

- *I feel confident about the knowledge I gained after attending this eModule*
  Mainly, respondents assessed positively the knowledge they gained through a module: 70% of them (7 courses out of 10) received high agreement scores (3-4). Three courses also received low agreement scores (1-2): B1.0 (benefits of daylight) from 20% of respondents and B1.1 (visual comfort), and B5,1 (your first daylight model with Ladybug), 12% of respondents.

Overall, it is worth pointing out that the low agreement scores (1-2) generally remained relatively low (20% on average), never exceeding 40% of the respondents. The general trend is therefore positive: most respondents judged positively the module they attended, attributing scores of 3 and 4. In this regard, Fig. 6 summarizes the scores that were attributed in each question of the EE. As shown in the figure, 17 questions out of 27 (63%) received at least 90% of high agreement scores (3-4). Tables IV and V summarize the questions that obtained the highest and the lowest agreement scores, distinguished for aspects concerning the quality of the content of an eModule and its usability.

TABLE IV. QUESTIONS THAT OBTAINED THE HIGHEST POSITIVE SCORES

Questions on the quality of eModules’ content	*% of ‘higher agreement’ scores (3-4)*
For my professional development, it is a way to increase values	100%

Questions on the quality of eModules' content	*% of 'higher agreement' scores (3-4)*
The emodule content was consistent with the learning outcomes	96%
The case studies presented in the emodule were pertinent/inspiring	94%
Attending the emodule was inspiring	93%
The concepts learned are helpful for my academic curriculum	92%
The title of the emodule was representative of the content	92%
After this experience, I will attend another NLITED emodule	92%
Design for daylighting is a pleasant task to work with	91%
I feel confident about the knowledge I gained after attending this emodule	91%
the eModule workload was adequate	90%
the eModule content covered the topics I was expecting	90%
I enjoyed the eModule	90%
Questions on the usability of eModules	*% of positive scores*
the number of multimedia used in the eModule was adequate	96%
the text and fonds used in the eModule are legible	94%
the quality of the audio had a good quality	92%

TABLE V. QUESTIONS THAT OBTAINED THE LOWEST SCORES

Questions on the quality of eModules' content	*% of positive scores*
Legal requirements for daylight standards	38%
Etivities helped me gain a clearer understanding	25%
The content is arranged in a logical way	15%
The amount of time needed was appropriate	15%
The module was easy to attend, based on my previous knowledge of the topic	15%
I enjoyed the module	11%
I feel confident about the knowledge I gained	11 %
Questions on the usability of eModules	*% of positive scores*
Link to external resources was useful	30%
The tutoring service was useful	21%
Rate the overall visual design of the module	13%
The quality of the multimedia was good	12%

IV. DISCUSSION

Data collected from the first four months of activity within the NLITED platform led to some considerations about the specialized platform dealing with daylighting and its users.

A. Dropout from the platform

Some considerations could be made considering data on active platform users and eModules completion rates. More than 50% of the enrollees are active on the platform, while the eModules have an average completion rate of about 29%. This decrease may be interpreted by considering the present dynamics of education. In the world of training, increasing the success rate of learners is a significant challenge. It has become particularly relevant with the advent of eLearning activities since, in this case, the success rate often remains tiny compared to the number of registrants. It usually runs around 10% [3].

The literature highlights two main reasons for such high dropout rates. One is that the platform's function design or content quality cannot satisfy users [4]. The other is that many users only selectively acquire the knowledge they want according to their needs. They just take eLearning as one of the many ways of learning, and the eLearning platform is only one of the platforms used by such users [5]. Motivations to follow a course or training are numerous and varied, ranging from curiosity for the general theme of a course to the desire to acquire knowledge and skills without being engaged or adopting a steady pace of work [6]. Results from Onah et al. (2014) [6] indicate that many participants who may be classified as dropouts (for example, because they do not complete the necessary components to gain a certificate) are still participating in the course in their preferred way (either at a slower pace or with selective engagement).

The present data on active platform users and eModules completion rates are higher than those reported in the literature for other eLearning platforms. However, they will still be monitored, and further considerations will be made after the next four months of using the platform to point out critical issues and possible corrective interventions.

B. Comparison with indications provided by daylighting experts during the workshops

As mentioned earlier, the NLITED curriculum was built after consultations and workshops with a panel of daylighting experts from universities, professional design studios, and lighting associations [1,7]. They expressed their judgment on the initial version of the curriculum. They commented on each module proposed if that module was to be included in the curriculum or not. Tables VI-VII report the most and the least voted modules by the panel of daylighting experts [1].

Most of the 'most voted' modules by experts are in line with the eModules with the highest number of registrations, particularly: 'visual comfort' (B1.1), which comprises visual comfort and visual perception (first and sixth most voted) and 'benefits of daylight' (B1.0). The second most voted module (example of good design through actual case studies) was spread across several eModules in the NLITED curriculum by adding 1 hour of case study in each eModule. Therefore, a direct comparison between experts' indications and the participants' preferences in the NLITED platform is impossible. The same applies to the fourth most voted topic ('daylighting at various scales'), subdivided into several eModules inside the NLITED curriculum.

TABLE VI. COMPARISON OF PREVIOUSLY REQUESTED AND ACTUALLY **HIGHEST SELECTED** MODULES IN THE PLATFORM

RANKING	*PREVIOUSLY REQUESTED*	*ACTUALLY SELECTED*
1st	Visual comfort: assessments and methods	Benefits of daylight (B1.0)
2nd	Example of good design (real case studies)	Visual comfort (B1.1)
3rd	Daylighting benefits	Your first daylight model with Ladybug. tools in Rhino+Grasshopper (B5.1)
4th	Daylight at various scales, from urban to building and a single room	Non-visual effects of light (B1.2)
5th	Daylight design elements: materials,	Assessment methods (B1.3)

	components, and devices	
6th	Visual perception	Beyond the metrics (B4.6)

TABLE VII. COMPARISON OF PREVIOUSLY REQUESTED AND **LOWEST SELECTED** MODULES IN THE PLATFORM

RANKING	*PREVIOUSLY REQUESTED*	*ACTUALLY* **SELECTED**
1st	Advanced simulations (BSDF data	Italian/Polish Standard and Regulations
2nd	Modelling devices (solar pipes, sunlight mirrors, etc.);	LENI index
3rd	Daylighting for exhibition spaces	Swedish Standard and Regulations
4th	Energy protocols	Daylight measurements
5th	Modelling components (windows, light pipes, etc.);	Daylighting assessments - simplified methods

As for the 'least voted' topics, some were dropped from the NLITED platform, such as '*daylighting for exhibition spaces*'. Other topics concerned with advanced daylighting modelling and simulating were retained in the eplatform but are not available yet. This analysis will be carried out in the next stage of the eplatform when all eModules are available and evaluated. The topic of 'energy protocols (LENI and LEED)' was also retained in the NLITED platform, as it was conceived as strategic in the frame of an extensive analysis of the global energy demand for a building. The corresponding eModule (3.2 'daylighting and electric lighting') was among the ones that received some low scores in terms of excessive workload and time needed to complete the eModule.

C. *Platform user type*

As demonstrated in Table I and Figure 4, the eModules with the highest enrollees are mainly related to knowledge and simulation of visual well-being.

Specifically, 50.4% of active participants in the platform selected the basic module "Benefits of daylight". It might suggest that there are many neophytes on daylighting in the platform, people who are attracted to the conceptual rudiments on the topic. Even the simulation module “Your first daylight model with Ladybug. tools in Rhino+Grasshopper” (30% of subscribers) is a beginner module.

These data suggest that the platform is mainly attractive to people who know little about the topic and want to learn the rudiments. Overall, this is encouraging data for a publicly funded platform created to expand knowledge on a topic that can give a counterpart to well-being and energy conservation.

D. *Limits of the current analysis*

The data on which the current analysis was made refer only to the first 4-month period of activity of the NLITED platform. At that time, 50% of the curriculum (16 modules out of 32) were uploaded. This figure may have affected some user behaviour within the platform. However, the platform rules allow enrolment even if the module has not yet been activated, so the reported analysis can be considered reliable. Nevertheless, the fact remains that the data are still few, and it will be necessary to see how they will vary when the entire platform is uploaded.

E. *User evaluation of the quality of the modules*

Overall, the users who completed an eModule and filled the FT (final test) and the EE (eModule evaluation) expressed favourable judgments on the quality of the eModule itself.

‘Higher agreement’ judgments (scores 3-4) concerned the consistency with learning outcome (‘*the eModule content was consistent with the learning outcomes*) and the competencies users gained through an eModule (‘*I feel confident about the knowledge I gained after attending this eModule*’ and ‘*the eModule was inspiring*’). Besides, most users feel at ease recommending the eModule they passed to colleagues (‘*I would recommend the eModule to my colleagues*’).

Most negative judgments concerned a mismatch between the content expected by a participant and the content provided within the module (‘*the eModule covered the content I was expecting*’) and the duration of the eModule (‘*the amount of time it took to complete this eModule was appropriate*’).

In general, users who completed the modules and filled out the evaluation questionnaires found the modules' quality satisfactory. It should be mentioned that negative ratings can be derived from the dropout rate of the modules.

F. *Time duration of eModules*

As already pointed out earlier, excessive duration of eModules was one of the most critical issues reported by the participants, who complained about the time needed to complete an eModule for over 70% of the eModules.

On the one hand, the modules adhere to a teaching framework equal to the workload required for recognizing 1 ECTS (1 ECTS = 25 hours of work) as determined by *ECTS Users' Guide* [8]. On the other hand, eModules are programmed to be listened to several times, according to users' individual wishes for a better understanding. It is, therefore, possible that the "effective" duration of a module can reach between 2.5 and 4 hours of recorded material. This aspect is one of the weaknesses that could link to the dropout rate. Therefore, a future revision of the emodule structure is planned.

Another aspect that was observed (and found surprising) is the number of users who completed an eModule, (the final test) but did not go through the ‘eModule evaluation’ to complete the module and thus download the certificate of attendance, which is necessary for the recognition of 1 ECTS. For some users, the motivation to attend an eModule is more related to acquiring personal skills and competencies on daylighting than obtaining proof of attendance.

Based on the first findings, the need to revise the length of the modules emerged. Besides, the number of certificates not downloaded suggests that this platform may offer some alternative to 1 ECTS module.

CONCLUSIONS

NLITED: New Level of Integrated Techniques for Daylighting Education – is an Erasmus Plus educational project for students and professionals. Within the project, an online eLearning platform on daylighting was built, with 28 eModules on five main topics: ‘daylight for humans, ‘daylight culture and design’, ‘daylight and energy saving’, ‘daylight assessment’, and ‘daylight simulation’. Besides, a summer school is offered with qualified daylighting experts. The platform was launched on January 31, 2022. The paper mainly analyzed the first four months of activity, until May 31, 2022: which types of participants (students or professionals, from which country they are from, etc.) and which eModules participants have selected and they have signed in, thus highlighting which eModules resulted more interesting or competing, and which ones less. These selection data were then compared to the preferences on modules expressed by different panels of experts during the construction of the NLITED curriculum [1]. Furthermore, at the end of each eModule, participants must pass a final test and then fill an evaluation test on the quality and the usability of the eModule(s) they attended. After completing these tests, they can receive recognition of 1 ECTS.

During the first four-month activity since the ePlatform launch, 443 people have enrolled in the platform, and 244 (53%) are currently active inside the platform, meaning they have signed into at least an eModule, either completed o still in progress in terms of attendance. The remaining 199 users registered into the ePlatform but have not completed the entrance test (an orientation test to suggest eModules participants may be interested in attending without any strict constraint). They, therefore, have not signed into any eModules yet.

The most selected eModules were: Benefits of daylight; Visual comfort; Your first daylight model with Ladybug tools in Rhino+Grasshopper; Non-visual effects of light; Assessment methods; Beyond the metrics. Conversely, the eModules with the lowest number of subscriptions were: local standards and regulations (Italian, Polish, and Swedish), LENI index, daylight measurements, daylighting assessments - simplified methods, and modelling materials.

So far, there has been an average module completion rate of 29%, far higher than that of online educational platforms, usually around 10%.

Based on data from the first four months of activity, the NLITED platform is promising. The enrolment number is still increasing (more than 500 users at the end of June 2022), and the dropout is higher than the values reported in the literature.

Considering that such knowledge is non-mandatory and based on free courses is a great result. However, there are factors conditioning the results (incomplete curriculum), it is possible to affirm that the trend is positive, and there is a great need for specialized teaching on daylighting.

Acknowledgement

The NLITED project (New Level of Integrated TEchniques for Daylighting education Project) is funded with support from the European Commission. Ref: 2020-1-IT02-KA203-079527.

References

[1] N. Gentile, et. al., A shared curriculum for daylighting education to meet the educational needs of society, Accepted for publication in proceedings of PLEA 2022 Conference, Santiago de Chile, Chile, November 23-25, 2022.

[2] L. Rai, D. Chunrao, Influencing Factors of Success and Failure in MOOC and General Analysis of Learner Behavior, Int. J. Inf. Educ. Technol. 6 (2016) 262–268. https://doi.org/10.7763/ijiet.2016.v6.697.

[3] J. Goopio, C. Cheung, The MOOC dropout phenomenon and retention strategies, J. Teach. Travel Tour. 21 (2021) 177–197. https://doi.org/10.1080/15313220.2020.1809050.

[4] T. Sun, S. Shen, An analysis of factors affecting MOOC learners' continuous learning: A review of CNKI's empirical research (2011-2016), Distance Educ. China. 10 (2017) 55–62. https://doi.org/10.13541/j.cnki.chinade.20171019.

[5] Y. Mourali, M. Agrebi, H. Ezzedine, R. Farhat, M. Jemni, M. Abed, A review on e-learning: Perspectives and challenges, in: 15th Int. Conf. Internet Web Appl. Serv., Vienna, Austria, 2019.

[6] D.F.. Onah, J. Sinclair, Boyatt, Dropout Rates of Massive Open Online Courses: Behavioural Patterns MOOC Dropout and Completion: Existing Evaluations, in: Proc. 6th Int. Conf. Educ. New Learn. Technol., Barcelona, Spain, 2014: pp. 5825–4834. https://doi.org/10.13140/RG.2.1.2402.0009.

[7] S. Khanie, F. Giuliani, M.S. Khanie, N. Sokół, N. Gentile, Discussing daylight simulations in a proposal for online daylighting education, in: B. Abstr. BuildSim Nord. 2020 – Int. Conf., Oslo Metropolitan University (OsloMet), Oslo, 2021: pp. 89–93. https://lucris.lub.lu.se/ws/portalfiles/portal/85337926/BuildSim_Nordic_FinalPaper.pdf.

[8] European Union, ECTS Users' Guide, (2015). https://doi.org/:10.2766/87192.

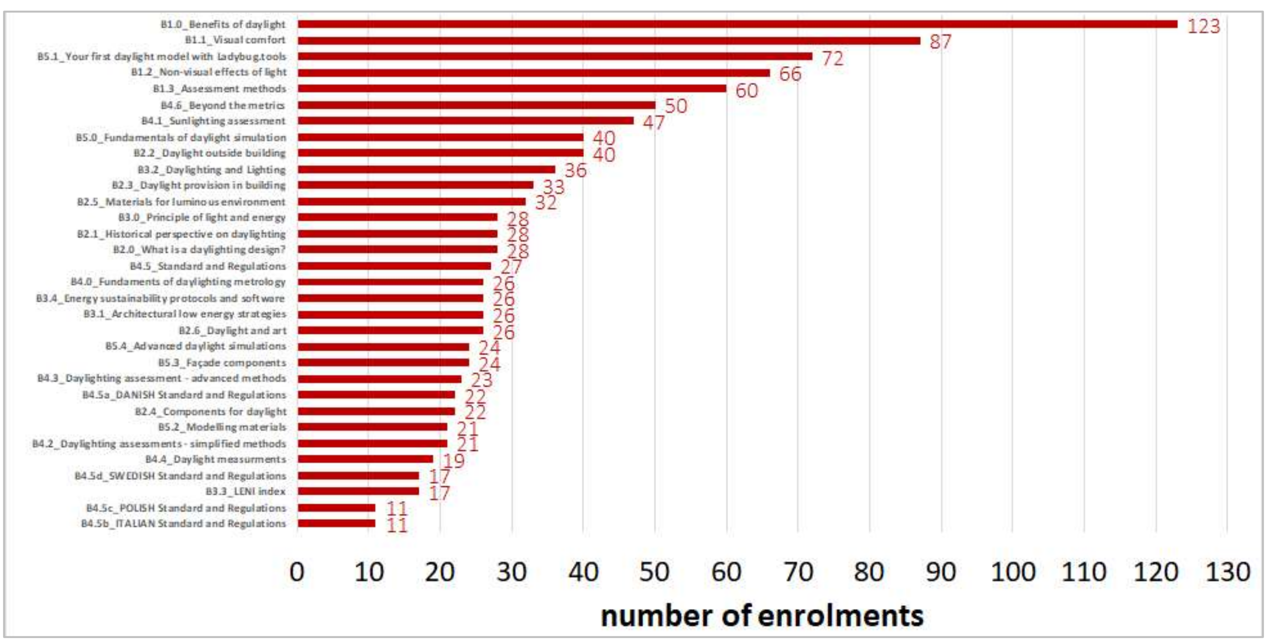

Fig. 4. Users registered into the NLITD eModules (NOTE: registration is allowed for active and non-active courses).

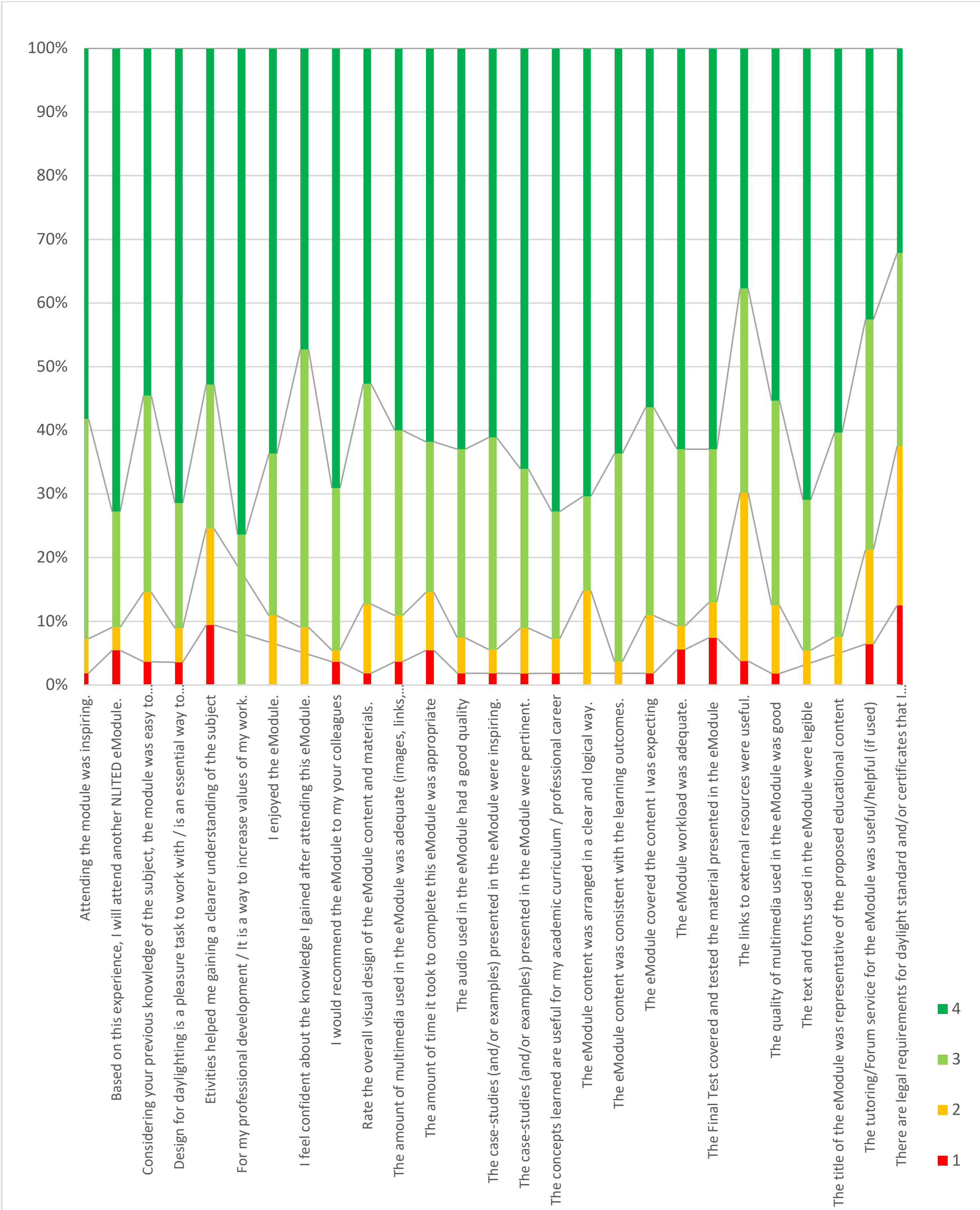

Fig. 5. Scores attributed by respondents in all the questions of the 'eModule evaluation' (EE). (1-2: low agreement; 3-4: high agreement)

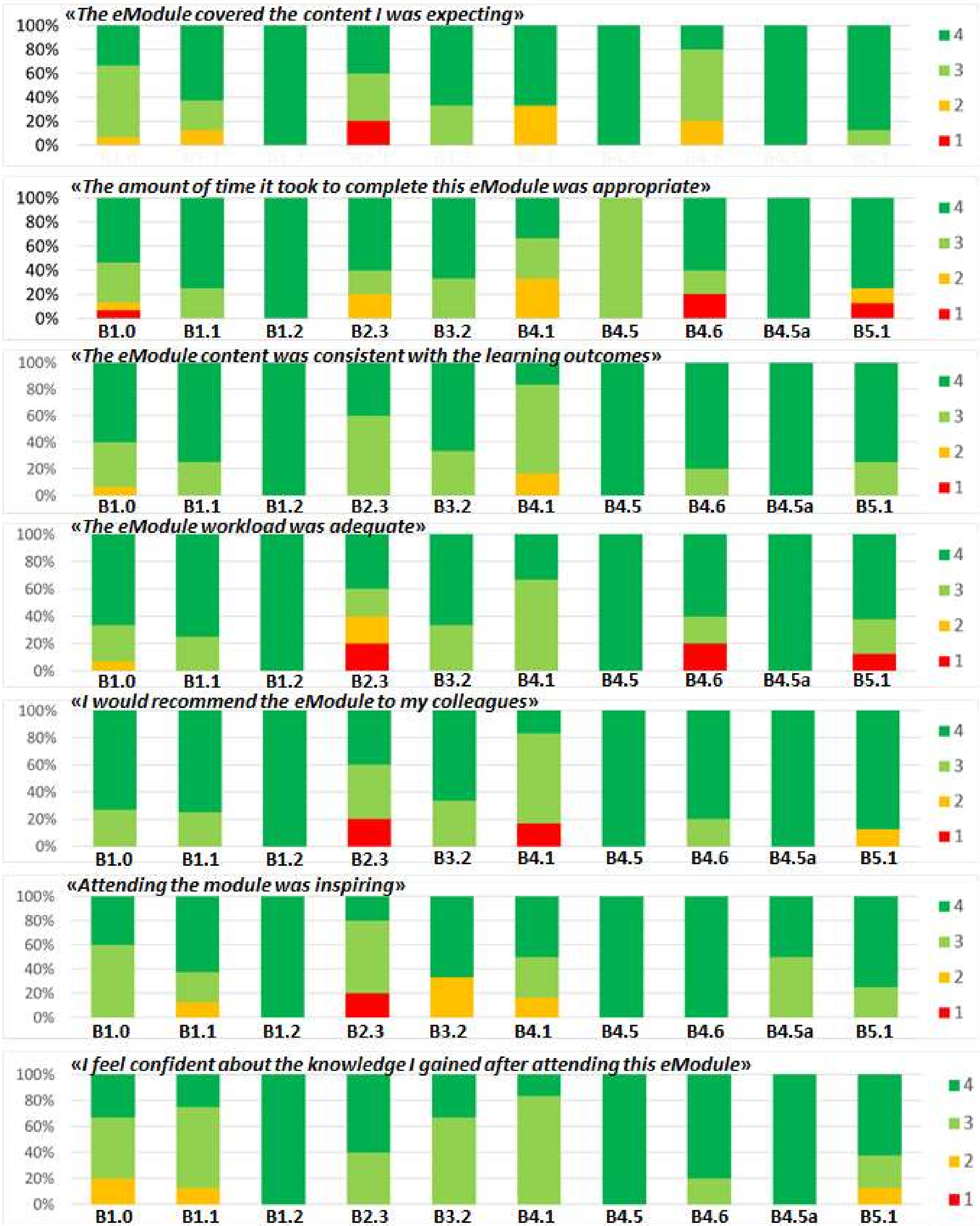

Fig. 6. Findings from the EE 'eModule evaluation' filled after having attended an eModule (1-2: low agreement; 3-4: high agreement):

Spectral Mismatch Corrections of Illuminance Meters for Field Measurements of Indoor Workplaces

Roman Dubnička, Marek Mokráň, Peter Janiga
Institute of Power and Applied Electrical Engineering
Faculty of Electrical Engineering and Information Technology STU in Bratislava
Bratislava, Slovakia
roman.dubnicka@stuba.sk

***Abstract*— Every indoor workplace lighting design shall follow rules stated in European standard EN 12464-1 Part 1: Indoor workplaces. In some European countries are basic rules for some parameters defined in Decrees of the Ministry of Health in combination with parameters of the mentioned standard above. Verification of parameters listed in standard of every lighting design is performed by field measurement of workplaces.**

In the paper are presented results of various field measurement situations according to relevant standards of lighting parameters of indoor workplaces with knowledge about spatial spectral data of LED luminaires represented by luminous intensity distribution installed and impact to measured values of illuminance values regarding to spectral mismatch factor for various illuminance meters with different quality indicated by their qualitative parameters and compared to old approach assuming CIE illuminant A and spectral power distribution of defined CIE illuminant L for measurements of lighting systems with LED luminaires and lamps to be installed. Furthermore, the paper also presents a depiction of assumption of spectral mismatch error based on tests of luminaires or lamps in photometric testing laboratories, where by means of spectroradiometric systems measurement of luminous intensity distribution is performed.

Keywords*— *Spectral mismatch factor, Spectral power distribution, Field measurement of illuminance, Spectrogoniophotometry.

I. INTRODUCTION

One of the important parameters is also spectral power distribution of installed luminaires. Emphasis of this problem emerged by installing luminaires with new LED technology, especially for smart lighting systems, where the spectrum of radiated light can be changed dynamically by means of drivers. The knowledge of relative spectral power distribution of light at field measurement is very important, because of the shape of various LED products, which was presented in many papers all over the world. This well-known knowledge is very important for precision of measured values, because the shape of spectral power distribution can vary in every point of the measurement grid. The problem was described for LED luminaires also by spectrogoniophotometric measurement that spectrum is changing by angles in the polar coordinate system. Therefore, lack of this information can lead to interpretation wrong results, which can negatively influence some permissions e.g. permission of Public Health Authority in Slovakia for particular indoor workplace [1]. For spectral correction is theoretically well-known stated mathematical formula describing spectral-mismatch error f1, when lighting source with other spectral power distribution is measured than at was illuminance meter was calibrated related to CIE illuminant A, because of imperfection matching relative spectral responsivity of photometer head to V(λ) by means of optical filters. Very often this parameter for illuminance meters is underestimated by users performing field measurements. Even more, these days the international scientific community at CIE organisation has an interest to re-define mathematical formula of spectral mismatch factor f_1 which should be connected to spectral power distribution of standardised LED lighting sources.

II. THEORETICAL BACKROUND

A. *Spectral mismatch factor of illuminance meters*

The spectral response of the photometer head of illuminance meter should be as much as close to the tabulated CIE function V(λ). However the matching to the CIE function can't be achieved because deviations at the particular wavelength occur (Fig. 1). The quality of the matching is expressed by means of the quality index f1' related to the CIE illuminant A [2], which cannot be used as correction, but in the uncertainty budget shall be assumed. Error is not so significant in the measurement of the light environment where spectral power distribution of light sources are close to the calibration source. At present, the significant influence of this mismatch occur especially in the measurement of the lighting installations of indoor workplaces with LED luminaires. In most cases, this error can be reduced by the theoretical approach represented by relationship

$$f_1(Z) = 1 - \frac{\dfrac{\int_{\lambda 1}^{\lambda 2} S_Z(\lambda).r(\lambda).\mathrm{d}\lambda}{\int_{\lambda 1}^{\lambda 2} S_Z(\lambda).V(\lambda).\mathrm{d}\lambda}}{\dfrac{\int_{\lambda 1}^{\lambda 2} S_A(\lambda).r(\lambda).\mathrm{d}\lambda}{\int_{\lambda 1}^{\lambda 2} S_A(\lambda).V(\lambda).\mathrm{d}\lambda}} \qquad (1)$$

where:

- $S_A(\lambda)$ is spectral power distribution of calibration source (CIE A),
- $S_Z(\lambda)$ is spectral power distribution of measured source (e.g. CFL, LED)
- V(λ) is tabulated function of spectral responsivity of human eye
- r(λ) is the spectral responsivity of photometer head of illuminance meter.

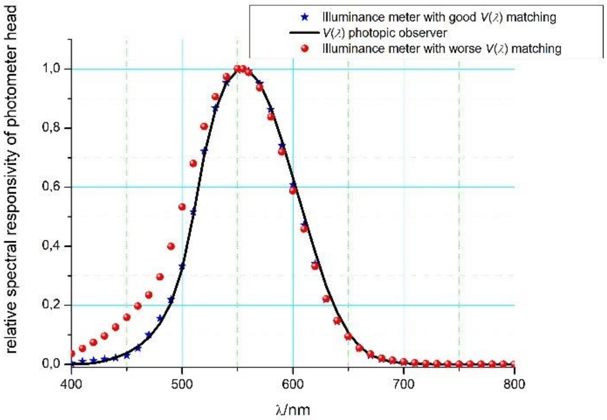

Fig. 1. Relative spectral responsivities of illuminance meters to V(λ)

The formula (1) expresses error from the "real" value of the measured illuminance E (lx). From relationship can be derived correction factor so called „actinity“ of the source.

$$a(Z)=\frac{\dfrac{\int_{\lambda 1}^{\lambda 2} S_Z(\lambda).r(\lambda).\mathrm{d}\lambda}{\int_{\lambda 1}^{\lambda 2} S_Z(\lambda).V(\lambda).\mathrm{d}\lambda}}{\dfrac{\int_{\lambda 1}^{\lambda 2} S_A(\lambda).r(\lambda).\mathrm{d}\lambda}{\int_{\lambda 1}^{\lambda 2} S_A(\lambda).V(\lambda).\mathrm{d}\lambda}} \tag{2}$$

By the factor shall be multiply result of measurement of measured value of the illuminance when the spectral power distribution is different to the calibration source. Both relationships can be transformed to the sums beside integrals for simplification of calculations. As it was mentioned above at the present in mostly cases at field measurements of lighting instalations are LED luminaires installed, especially, in new lighting installations or at reconstruction of old lighting systems of indoor workplaces. Therefore as $S_A(\lambda)$ can be replaced by $S_L(\lambda)$ what is spectral power distribution of LED calibration source or standardised CIE illuminant L which in the future shall supplement standardised illuminants defined by CIE and research work about this topic is still undergoing at present with impact to the uncertainty of the measurement [3]. or was instrument calibrated (usually it is CIE illuminant A), r(λ) is spectral responsivity of the instrument and V(λ) is tabulated spectral sensitivity of human eye [3]. When multiplication to the result is done it can be reduced error which can occur in the field measurement. The knowledge of the spectral power distribution of the light source to be measured shall be known before calculation of this correction (2) to the result. This is not unrealistic condition because in the present producers of the light sources provided spectral power distribution in the datasheet with supplied sources or it can be found in relevant standards, scientific papers, technical reports or recommendations. At the worst case it is possible to measure one type of source by spectroradiometer and in the process of quality assessment can be measured by used illumance meter. Also user of the illuminance meter shall be known spectral responsivity of photometer head (Fig. 2).

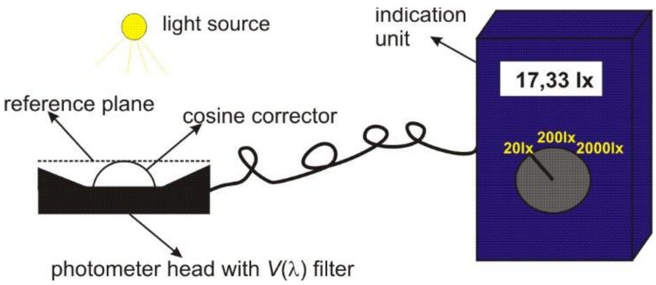

Fig. 2. Scheme of illuminance meter using for the field measurement

Spectral responsivity of photometer heads of illuminance meters in Slovakia is mandatory to provide to the user by performing calibration as one of the part of verification at characterisation of performance of illuminance meters which are officially used for field measurements according to the Decree of Ministry of Health in connection to the standard EN 12461-1.

B. Spectral changes in the angles of radiation of luminaires

A goniophotometer is needed to measure the luminous intensity distribution of luminaires. The results from goniophotometric measurements are very important for lighting engineers who are using these results in lighting calculation of photometric parameters of the various lighting systems. At the present is discussion among scientific community to provide that interchangeable photometric data where spectral power distribution information regarding to angle radiation of light will be included. Spatial characteristics of the luminaire are expressed by luminous intensity distribution curves (LIDC) which represent particular distribution of the luminous flux in particular direction from light sources installed in the luminaire. These curves are also used in lighting design calculations of photometric parameters of the indoor workplace lighting system. Photometric parameters, including the spatial luminous intensity characteristics of the luminaires are defined in the interchangeable photometric data files (e.g. LDT, IES, CIE etc.) for the C plane where the luminous intensity in particular direction is defined by means of the angles C, γ. However, this approach does not consider possible dependence of spectral power distribution of luminaire light radiation on changing angle what was shown in some scientific papers treating goniospectroradiometry of luminaires regarding to indoor lighting systems [4]. Therefore, it is needed to use gonio-spectroradiometers for proper spatial radiant characteristics of the luminaire. Example of the spectrogoniophotometer system is depicted in figure 3, where instead of photometer head is placed spectroradiometer.

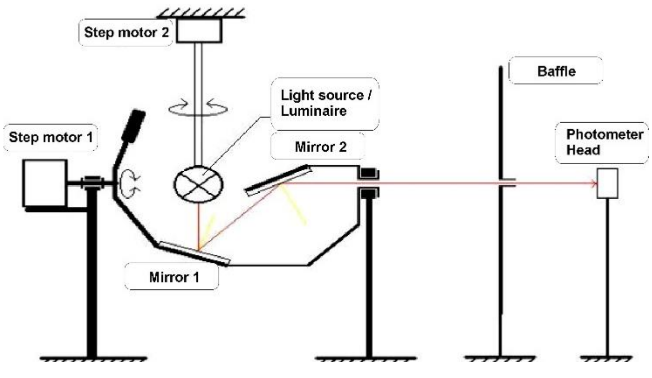

Fig. 3. Photograph of the examined room

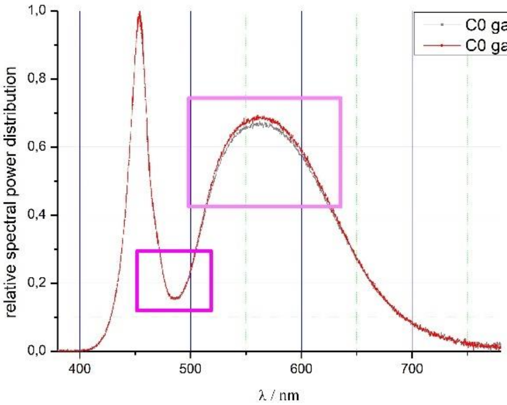

Fig. 4. Photograph of the examined room

Change of spectral power distribution of sample LED luminaire measured by the system is shown in figure 4 for two angles in the same C-plane. Therefore the neediness of knowledge about spectral characteristic is very important to provide information both designers and persons who perform verification field measurement. Then measured spectral data can be transformed into photometric data files for lighting calculation purposes by lighting tools used usually in practice or using corrections at the field measurements with defined topology of luminaires in the room.

III. Experiment

Chosen experimental indoor workplace was office space at the Faculty of electrical engineering and information technology of Slovak university of technology in Bratislava (Fig. 5, Fig. 6). The subject of the field measurement was the measurement of general illuminance level in combination of the measurement of illuminance level on visual tasks (table office) as it is depicted in the figure 6. The measurement of spectral power distribution was performed in the stated points of measurement grid with some extra points according to the new standard of indoor workplaces EN 12464-1:2021, where design photometric criteria of illuminance of surfaces i.e. walls and ceiling is stated and at some critical verification field measurements e.g. for justice purposes can be performed.

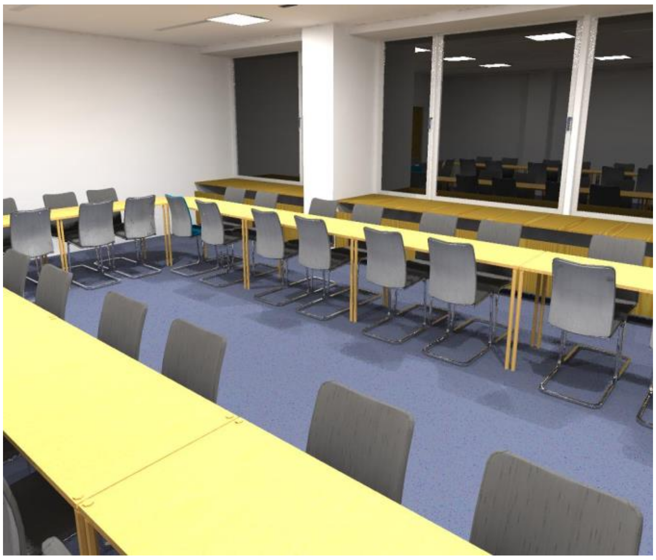

Fig. 5. Visualization of the experimental indoor working place

Fig. 6. Real photography of the experimental room

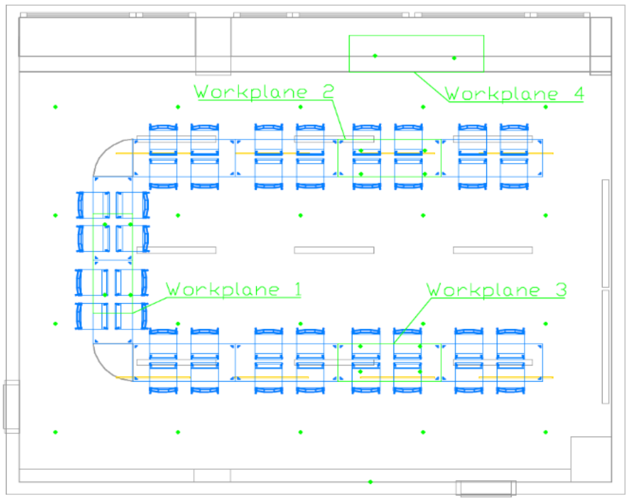

Fig. 7. Layout plan of the experimental room from the top view

For the measurement of spectral power distribution at defined points was used portable spectroradiometer (Fig. 8) with cosine correction on the input port, which was chronologically placed in the grid points and points on the selected wall at the different height to investigate how the spectra is changed. At the same place and at the same height insured by tripod were placed two types of illuminance meters with different relative spectral responsivity what was presented in the graph above (Fig. 1). The purpose of investigation of two illuminance meters with different quality indeces were performed, because for the field measurement very oftenly are used instruments which are so called low-cost illuminance meters with no good V(λ) function matching. Illuminance meter with good quality and relatively good matching to the V(λ) function is marked as A illuminance meter. The second illuminance meter with worse quality was marked as B for the evaluation purposes. Both illuminance meters had cosine correction by the diffuser and they were characterised in the photometric laboratory for linearity, cosine error as well with relative spectral responsivities.

Fig. 8. Portable spectroradiometer UPRtek MK350S

The measured horizontal general illuminances with spectral measurements on the reference plane stated at height 0,85m above the floor, vertical illuminances on the wall were defined in three points placed in the line of vertical plane from the floor to the ceiling at heights 0,6m, 1,2m, 1,86m and 2,2m. The dimension of the measurement grid for the general illuminance was 5x4 points and for the workplace 2x2 points according to the formula stated in the standard EN 12464-1. For the experiment were used linear LED luminaires positioned in two rows in variations CASE A and CASE B experiment which distance from the wall was measured by laser distance meter with resolution of 0,001m.

IV. Results

In tables I. and II. are presented results of the experiment in the office where relative difference in the measured values to the reference values measured by portable spectroradiometer in the measurement grid points. Linear LED luminaires with CCT 4000K were installed on the ceiling by magnets which allowed perform experiment for various position of luminaires. Therefore in the tables are presented results for the CASE A was 1st row of luminaires from the wall placed at 1,677m from the wall and 2th row of the luminaires at 5,270m and for the CASE B was 1st row of luminaires from the wall placed at 1,077m from the wall and 2th row of the luminaires at 5,270m from the same wall opposite to the windows plane as it is shown in the visualisation (Fig. 5). In the CASE B it was shown influence and change of spectral power distribution on the measurement results when luminaires are approaching to the wall. On the opposite side the window were not results so significant due to the reflection part of the light is not so significant to the results therefore for the presentation of values these investigated cases were chosen.

The results of the difference related to the measurements by portable spectroradiometer by which was possible to measure illuminance level related to the spectral irradiance saved into the instrument marked as E_G (%) as relative difference in the measurement gird, E_v (%) as relative difference at chosen visual task Workplane 1 and E_w (%) as relative difference at wall points. It shows that, in the case of using a linear LED luminaire, significant changes were observed for the general illuminance E_G = -14,7%, walls E_W = 20,8% and E_V = 6,8% in the CASE A and for the general illuminance E_G = -15,1%, walls E_W = 29,2% and E_V = 8,9% in the CASE B, both for illuminance meter B. Result with minus sign means that measured value with illuminance meter is lower than reference value measured by spectroradiometer. The uniformity of the illuminance was not investigated at the assumption when field measurement is performed with same error then overall uniformity is not affected. The change in of the correlated colour temperature in the experiments were from 2894 K (the bottom of the wall) to 4033 K depending on position and measurement point.

TABLE I. Measured relative differences in the measurement grid, at the workplace and walls – CASE A

	E_G [%] in the measurement grid					E_V [%] at visual task (workplace)		E_w [%] walls
Illum. meter A	-0,1	-2,1	-1,7	-1,7	-2,3			1,1
	-0,2	-1,9	-1,5	-1,4	-1,7	1,3	0,8	0,8
	0,3	-1,5	-1,2	-0,7	-0,9	1,1	0,6	0,5
	0,1	-0,8	-0,7	0,1	-0,3			0,2
Illum. meter B	1,2	2,3	-9,1	-5,5	2,5			20,8
	2,1	-5,4	4,2	-6,9	1,5	6,8	5,2	16,0
	1,6	-14,0	5,7	-10,7	2,9	4,5	3,3	9,8
	2,9	-14,7	2,0	-11,7	-1,4			3,7

TABLE II. Measured relative differences in the measurement grid, at the workplace and walls – CASE B

	E_G [%] in the measurement grid					E_v [%] at visual task (workplace)		E_w [%] walls
Illum. meter A	-0,1	-2,0	-1,6	-1,6	-2,2			2,2
	-0,2	-1,8	-1,4	-1,3	-1,6	1,2	0,5	1,2
	-0,1	-1,4	-1,1	0,9	-1,1	1,0	0,7	0,7
	0,2	-0,8	-0,7	0,1	-0,6			0,3
Illum. meter B	1,5	2,4	-9,8	-4,9	2,8			29,2
	2,2	4,1	3,3	-7,2	0,8	8,9	5,8	22,3
	2,6	-8,0	6,2	-5,8	-7,8	8,0	7,5	13,4
	3,9	-15,1	8,2	-12,6	-2,6			4,1

V. CONCLUSION

The results of the experiment show that the photometric parameters are sensitive to the spectral power distribution changes of the radiated light from luminous part of the luminaire related to the angle of radiation. Results of performed experiment in administration space of shown also importance of using photometers with higher precision with good matching of V(λ) because values of differences for the illuminance meter A shown consistency with assumed measurement uncertainty of field measurement of experiment. It should be mentioned that results were evaluated from three repeated independent measurements nearly at the same condition where stability of LED lighting system shown negligible differences between trials. Attention should be focused on measurement surfaces were expectations of bigger differences was proved.

ACKNOWLEDGMENT

„This publication was created thanks to support under the OP Integrated Infrastructure for the project: International Center of Excellence for Research on Intelligent and Secure Information and Communication Technologies and Systems - II. stage, ITMS code: 313021W404, co-financed by the ERDF“. This work was also supported by the Slovak Research and Development Agency under the contract No. APVV-20-0157.

REFERENCES

[1] STN EN 12464-1. Light and lighting - Lighting of work places - Part 1: Indoor work places. 2021.

[2] CIE S 023/E:2013: Characterization of the Performance of Illuminance Meters and Luminance Meters , ISBN 9783901906329

[3] Bizjak G., Kobav M., New CIE Standard Illuminant L and its Affect on Measurement Uncertainty, 2020 Fifth Junior Conference on Lighting (Lighting), DOI:10.1109/Lighting47792.2020.9240587

[4] David B. Moyano,Silvia B. Moyano,Miguel G. López,Alejandro S. Aznal,Roberto A. González L. Photometric and colorimetric analysis of light emitting diode luminaires for interior lighting design, COLOR Resarch and Technology, February 2021, https://doi.org/10.1002/col.22616

The Issue of Obtrusive Light Control

Petr Žák
Dept. of Electrical Power Engineering
Czech Technical University in Prague,
Faculty of Electrical Engineering
Prague, Czech Republic
zakpetr@fel.cvut.cz

Marek Bálský
Dept. of Electrical Power Engineering
Czech Technical University in Prague,
Faculty of Electrical Engineering
Prague, Czech Republic
balskmar@fel.cvut.cz

Michal Kozlok
Dept. of Electrical Power Engineering
Czech Technical University in Prague,
Faculty of Electrical Engineering
Prague, Czech Republic
kozlomi1@fel.cvut.cz

***Abstract*— Currently, the issue of undesirable effects of artificial outdoor lighting on the surrounding environment is a very widely discussed topic. In individual countries, there is an effort to solve this issue within the framework of documents that take different forms, from recommendations to technical standards to legal regulations. Most of these documents are based on the international recommendations of the CIE, which relate to limiting the undesirable effects of so-called obtrusive light on the surrounding environment. In practice, this concept is not widespread among the general public, and is often referred to as light pollution. In spite of the considerable efforts made to address this issue, there is no simple visible consensus in practice on how to deal with it. There are probably several possible reasons. The primary and fundamental one is the issue of terminology and definitions. In practice, one term is used to refer to a number of different phenomena, and at the same time, several terms are used for one phenomenon. Already in current documents, obtrusive light refers to phenomena that are not, by definition, obtrusive light. Clarity and consistency in the use of terms and adherence to their definitions is a prerequisite for mutual understanding when dealing with a particular issue. If definitions are not respected and terminological discipline is not observed, it is very difficult to deal with the issues related to the terms and definitions. The following paper also deals with other possible causes of the mentioned situation.**

Keywords—obtrusive light, light pollution, spill light, environmental zone, useful light

I. Introduction

The issue of light pollution, or obtrusive light is nowadays a much discussed topic, to which not only a large number of professional articles and publications are devoted, but also popular educational programs on television or contribution on social networks. Although this topic is given a relatively large amount of attention by the professional public and there was partial agreement on its solution, this agreement was only partially reflected in practice and technical standards. This situation leads to the fact that, within the national states, there is an effort to solve this issue with own national technical standards [1] and legal regulations [2] and thus there are different approaches that deviate from the original agreement at the international level. The following paper tries to identify the possible causes of this situation.

II. Background

Astronomers were probably the first to draw attention to the problem of the disturbing effects of artificial lighting, for whom outdoor artificial lighting began to worsen observation conditions. One of the first mentions dates back to 1908, when astronomers at the Mount Wilson Observatory in California noticed a decrease in the performance of their telescope. The cause was the outdoor lighting of a small town that grew up in today's Los Angeles.

One aspect on which progress in astronomy depends is the possibility of observing very weak cosmic objects and bodies that can only be observed with large telescopes against a dark background, i.e. at a low level of brightness of the night sky. The higher level of brightness of the night sky, called sky glow [3], which can be caused by natural and man-made light sources, limits such observations, or makes it impossible. The source of the man-made sky glow is the direct light from the luminaires and lighting systems emitted upwards as well as the light reflected from the earth's surface or the surfaces of buildings.

Since the 1940s, the man-made sky glow began to be taken into account when locating astronomical observatories, but despite the careful selection of locations, the problem grew relatively quickly due to the expansion of outdoor lighting. This growth reached a rate of up to 20% per year and ultimately meant a 38-fold increase in the man-made sky glow over the course of 20 years. As a result of this unfavorable trend, in 1976 the General Assembly of the International Astronomical Union (IAU) adopted a resolution expressing concern over the increase in interference with astronomical observations caused by artificial lighting of the night sky, radio transmissions, air pollution and aircraft traffic over observation sites. At the same time, in its statement, it asked state and local government authorities to take appropriate measures to protect current and planned observatories from these forms of interference [4]. In response to the IAU resolution, the International Commission on Illumination (CIE) issued a statement in June 1978 recognizing the problems caused by uncontrolled outdoor lighting in the vicinity of astronomical observatories and agreeing to take the necessary steps to protect them. On the basis of cooperation between the IAU and the CIE, technical reports [4],[5] were published, which deal with the description and solution of this issue. The first measures related to limiting the disturbing effects of artificial outdoor lighting on astronomical observations began to be taken in the USA since the 1970s at the local (Flagstaff, Tuscon, Richland), regional (Coconino, Pima, Jefferson Davis) and national levels (Arizona, Hawaii) [4].

As part of the detailed solution to the disturbing effect of outdoor lighting on astronomical observations, undesirable effects in other areas were also described. Due to the fact that the observed undesirable effects became more widespread, the term light pollution, spoken “light smog”, defined as "sum total of all adverse effects of artificial light" began to be used to denote them [3]. In such a general concept, the problem of light pollution is difficult to solve, and therefore it is advisable to analyze it in detail. In principle, the light emitted by outdoor lamps can be divided into useful light and spill light [3]. Useful light is the luminous flux that falls on the illuminated area and its size is related to the purpose of the given area. Spill light is the light emitted by the lighting system that falls outside the boundaries of the property for which the lighting system is designed.

In principle, useful light is not disruptive, as it reaches its destination and fulfills a specific purpose. The problem is its reflected component from the surfaces of the illuminated area, which can already be obtrusive. If the solution of light pollution is not a complete switching off of outdoor lighting, then this component cannot be removed, as it is directly related to the purpose of the lighting system. In this case, the solution is to optimize the solution and operation of the lighting system (e.g. adaptive road lighting).

Spill light can theoretically be completely eliminated without impacting the purpose of outdoor lighting, however, complete elimination would be associated with disproportionate costs of implementation, so it is generally more appropriate to talk about its minimization. Increased attention has been paid to the minimization of useless light since the 1990s. When solving this problem in practice, the problem arose of how to control it, what evaluation parameters to use and how to set their limit values. To solve this problem, the areas in which spill light has a undesirable effect were named, controlled light technical parameters and their limit values were established for these areas, and at the same time the term obtrusive light was introduced [3]. Methods for the reduction of disturbing light are given in the publication CIE [6]and its 2nd edition [7].

III. Motivation

Currently, the Czech Standardization Agency is working on a draft of a Czech national standard on reducing the undesirable side effects of outdoor lighting. The draft of this standard is based on the methodology presented in document CIE [7]. The requirements stated in this document are tried to be modified for the conditions in the Czech Republic and to supplement the methodology with additional parameters. In addition to the draft standard, in accordance with the rules of CEN (European Committee for Standardization), it respects the requirements for the reduction of obtrusive light specified in the European standards [8], [9], which are based on the requirements in the publication CIE [6]. As part of the preparation of the national standard, a number of ambiguities and contradictions were discovered in the current methodology. Knowledge and experience with the drafting of the national standard is part of the following paper. They can serve as a basis for discussion on modifications of the existing methodology to limit the undesirable effects of artificial light in night environment.

IV. Terms and definitions

In order to solve a certain problem, it is necessary to have established terms and their definitions and to respect these terms and definitions. In the area of obtrusive light, this principle is violated. This may be one of the possible reasons for the relatively unsatisfactory state of affairs in solving this issue. Basic terms and definitions that are used in the field of obtrusive light include:

- *light pollution* - sum total of all adverse effects of artificial light.
- *obtrusive light* - spill light which, because of quantitative or directional attributes, gives rise to annoyance, discomfort, distraction, or a reduction in ability to see essential information such as transport signals.
- *spill light* - light emitted by a lighting installation that falls outside the boundaries of the property for which the lighting installation is designed.
- *sky glow* - brightening of the night sky that results from the reflection of radiation (visible and non-visible), scattered from the constituents of the atmosphere (gas molecules, aerosols and particulate matter), in the direction of observation.
- *man-made sky glow* - part of the sky glow that is attributable to man-made sources of radiation (e.g. outdoor lighting).

Currently, several parameters are used to describe obtrusive light that do not correspond to the definition of this term. The first is the R_{UF} parameter, which is used to control obtrusive light in relation to limiting man-made sky glow [7]. This parameter indicates the proportion of the luminous flux of the lamp emitted into the upper half-space both directly and by reflection from the illuminated area and from the non-illuminated area. This parameter cannot be used for the evaluation of obtrusive light, since by definition, obtrusive light is only the light emitted by the lighting system outside the boundaries of the property for which the lighting system is designed. Next parameters are the building facade luminance L_b and the sign luminance $L_s$ing. Both parameters characterize the useful luminous flux falling on the illuminated area, not the luminous flux falling outside the illuminated area. The use of the above parameters, i.e. R_{UF}, L_b and L_s for the control of obtrusive light is incorrect and misleading from the point of view of the definition of obtrusive light.

V. Sources of obtrusive light

The light emitted by lighting systems into the outdoor environment can be divided into two components, useful light and spill light (Fig. 1).

Useful light is not defined within the terminology of lighting engineering, but can be understood as the light falling on the area for which the lighting system is designed (illuminated area). The illuminated area includes areas prescribed in the framework of technical standards (e.g. SR surrounding of roads) or specified in the project documentation, for which lighting requirements are specified. Primarily, useful light, like spill light, is defined geometrically, not quantitatively. From a quantitative point of view, useful light can be divided into the limiting and over-limiting parts. The limiting part includes the luminous flux needed to ensure the maintained values (E_m, L_m), the coverage of light losses caused by the aging of the lighting system and the coverage of tolerances related to measurement uncertainties, product tolerances and product power level. The over-limiting part is the light that is not needed to ensure the required lighting parameters.

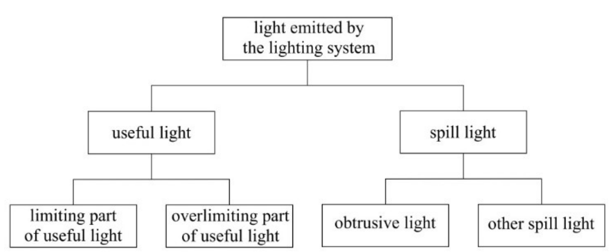

Fig. 1. Components of light in the outdoor environment

Spill light is light falling outside the area for which the lighting system is designed. Given that the existing technical means do not allow this component of outdoor lighting to be completely removed, it is controlled by means of parameters describing the degree of disturbance to the surrounding environment (obtrusive light). Other spill light is not checked.

The source of artificial lighting in the outdoor environment at night are lighting systems, which can be divided according to their location and application area into the following groups:

Outdoor lighting

- road lighting;
- lighting of outdoor work places;
- lighting of outdoor sports grounds;
- architectural lighting;
- advertising lighting;
- outdoor lighting of residential buildings and buildings for accommodation.

Indoor lighting

- lighting of indoor work spaces;
- lighting of indoor sports grounds;
- lighting of residential buildings.

A number of these application areas have lighting requirements (i.e. useful light) specified in relevant technical standards [8], [9], [10] or recommendations [11]. Some of these standards include requirements to limit obtrusive light. Currently, the issue of obtrusive light is addressed in standards for outdoor work places [8] and outdoor sports grounds [9]. This issue is mentioned in the standard for road lighting [10], but its solution is relatively insufficient. In other outdoor application areas, the issue of obtrusive light is not addressed within the framework of the technical standards. As is clear from the list of application area, the source of obtrusive light is not only outdoor lighting systems, but also indoor lighting systems operated at night, where artificial light penetrates through windows or rooflights into the outdoor environment (e.g. parking houses, greenhouses). The solution to this issue is significantly different from that of outdoor lighting, as it is tied to the use of shading technology and is more of a construction issue than a lighting engineering. In order to solve the problem of obtrusive light from indoor lighting systems, it would be advisable to create a technical standard or a technical report that would contain requirements to limit the adverse effects of light from indoor lighting systems penetrating from through windows or rooflights into the outdoor environment at night.

In connection with the definitions in the field of obtrusive light, it should be noted that the oversizing of the lighting system is not currently being addressed. Spill light, and therefore useful, is limited spatially, but not limited by its quantity. At the same time, oversizing the lighting depending on the degree can significantly contribute to the increase of undesirable effects of artificially light on the surrounding environment in the night. Therefore, in order to be able to define oversizing in all application areas, it would be appropriate to define the lighting requirements for all application areas. If the requirements are given, it is possible to control the degree of oversizing. If the requirements do not exist, we cannot talk about the degree of oversizing.

VI. Specific Effects and Relevant Light Technical Parameters

In the current methodology for the reduction of obtrusive light [7], four disturbing effects are listed. For these effects, parameters (Fig. 2) are determined by which they are assessed and limit values are determined according to the environmental zones or lighting classes.

A. *Effects on residents*

The effect on residents is assessed in terms of their disturbance in residential buildings and two aspects are used for its assessment. The first consideration is the amount of light that penetrates or can potentially penetrate into the living rooms of buildings. The illuminance of the vertical surfaces of the E_V is used to evaluate this aspect. The second aspect is the possible glare of residents in their homes by the disproportionately high brightness of the lighting parts of luminaires. Luminous intensity I is used to evaluate this aspect. To determine the limit values of the parameters, environmental zones linked to the district brightness are used. The question is whether this principle is suitable for determining limit values

B. *Effects on transport system users*

The effect of obtrusive light on traffic safety is primarily considered for drivers of motor vehicles on roads. Effects on road users (e.g. motor vehicle drivers, cyclists, pedestrians) are usually manifested by reduced vision caused by disability glare from bright light sources. Disability glare reduces the apparent contrast of objects against their background, reducing their visibility, and when the level of glare reaches a certain threshold, objects are not visible. The aspect used to assess this impact is the degree of disability glare of drivers from other lighting systems that are not used to illuminate the road on which the impact on safety is assessed. The threshold increment TI (%) is used to evaluate this effect. Lighting classes are used to determine the limit values of the threshold increment.

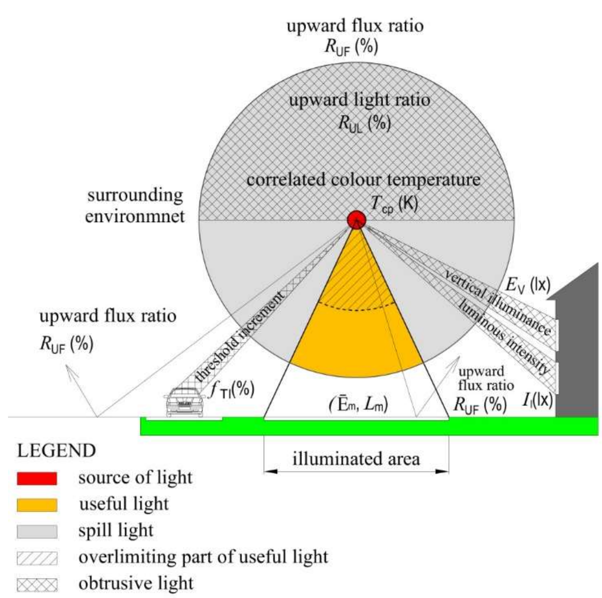

Fig. 2. Light technical parameters for evaluation of obtrusive light

C. Effects on sightseers

Architectural and advertising lighting with too high brightness or inappropriate color characteristics can be perceived by tourists and visitors to the city as disturbing, which inappropriately affects the night atmosphere of public spaces. To evaluate the degree of this effect, the building façade luminance L_b and the sign luminance L_s are used. To determine the limit values of the parameters, environmental zones linked to the district brightness are used.

D. Effects on astronomical observations

The effects of obtrusive light on astronomical observations are manifested by a change in the conditions for observing the night sky, caused on the one hand by an increase in the brightness of the dark sky caused by the scattering of light from lighting systems in the atmosphere (man-made sky glow) and on the other hand by direct light from lighting systems falling on the observatory. To assess this effect, the proportion of overhead light R_{UL} (%) is used. To determine the limit values of the parameters, the environmental zones linked to the distances of the boundaries of the environmental zones from the reference point (astronomical observatories) are used.

E. Other effects of obtrusive light

Undesirable effects, which are listed in the current methodology for evaluating obtrusive light, could be supplemented by other effects, in particular, the effect on the natural environment (fauna, flora) and the effect on the landscape, as well as the parameters by which these effects are controlled.

1) Effect on the natural environment

The effect on the natural environment (fauna and flora) is currently probably the most discussed effect of disturbing light on the surrounding environment. The regular alternation of light and darkness during day and night is demonstrably a basic factor of the natural environment, to which the energy balance and reproductive cycles of all organisms (plants and animals) of the temperate zone and tropics are developmentally linked, and many types of behavior leading to the preservation of the species. Artificial lighting disrupts the night environment and has a negative effect both directly in the immediate vicinity of the artificial light source and indirectly, due to the spread of light to the distant surroundings, which creates a man-made sky glow and thus increases the overall sky glow.

The basic problem with the impact on the natural environment is the overall load of the outdoor environment with artificial light in the night. This effect can be solved by reducing the total amount of artificial light in the night environment by optimizing useful light (i.e. light falling into the illuminated area) and minimizing spill light (i.e. light falling outside the illuminated area). Given that the influence of light on the natural environment is related to the spectral composition of the luminous flux, it would be desirable to introduce a parameter to control the spectral properties of light sources (e.g. correlated color temperature). This parameter needs to be addressed in coordination with the lighting requirements specified in the technical standards and recommendations. The following procedures can be used to optimize useful light:

- verification of the possibility of reducing requirements for outdoor lighting levels in relation to new light sources, or other aspects;
- elimination of oversizing of lighting systems;
- designing lighting systems enabling the regulation of luminous flux;
- use of adaptive lighting classes and the possibility of reducing lighting in accordance with regulatory requirements;
- introduction of a parameter to control the spectral properties of lighting sources.

In the area of minimizing spill light, it would be appropriate to propose a parameter that would control the utilization of the luminous flux of luminaire in relation to the illuminated area. One of the possible auxiliary parameters in the case of roads could be the use of luminaire classification according to CIE [12]. A similar classification is used in the USA, it is not used in Europe. The limit values of the controlled parameters should be determined according to the environmental zones linked to the district brightness.

2) Effect on the landscape

Another possible controlled effect, which is not mentioned much, is the effect on the landscape character, i.e. the effect of obtrusive light on the appearance of the landscape with settlement at night. In addition to the proportion of the luminous flux emitted into the upper half-space, which increases the level of sky glow, two other aspects affect the landscape character in a more fundamental way:

- luminous parts of luminaires visible at great distances;
- luminance of large areas of building facades unintentionally illuminated by stray light.

One of the parameters that is used to limit the visibility of the luminous parts of luminaire in the case of roadways is the installed luminous intensity classes G* [10]. For other lighting systems, it would be possible to use the luminous intensity of the luminaires relative to a defined reference point in the landscape.

The luminance of large areas of building facades unintentionally illuminated by stray light is caused by luminaires that are placed directly on these buildings or in their immediate surroundings. These are mainly buildings of business and logistics centers, and agricultural and industrial sites. These large illuminated areas disrupt the landscape, especially at the border of the settlement and the surrounding free landscape. A parameter that could be used to control this effect could be the luminance or illumination of these areas. However, it is necessary to set a reference plane and controlled values (maximum, average...). The limit values of the controlled parameters should be determined according to the environmental zones linked to the district brightness.

VII. Public Interest

The complexity of solving the problem of obtrusive light is due, among other things, to fact that it interferes with several public interests. As a rule, common standards and recommendations address only one public interest, e.g. the standard for road lighting primarily addresses the issue of safety. However, the problem of obtrusive light affects a number of public interests, including:

- human health;
- environment protection;
- transport safety;
- energy consumption;
- landscape character;
- appearance of public spaces.

Individual public interests are the responsibility of different ministries. For that reason, enforcement of requirements to limit the undesirable effects of lighting on the surrounding environment is difficult in practice. For example, if the control of obtrusive light is handled by the Ministry of the Environment, then effect on traffic safety, residents or energy consumption are not within its competence. The requirements and priorities of individual ministries can be contradictory, and the preparation of a legal document that would include all public interests can be quite complicated.

VIII. Restriction and prohibition of lighting

Technical standards and recommendations state the lighting requirements for individual activities and spaces so that a lighting system can be designed. These requirements are of a technical nature and serve for situations where lighting can or must be provided. Technical standards or reports should not prescribe whether a given space or surface must or must not be lit. This is a matter of public interest, which is a political issue. The fact that something must or must not be illuminated, or in what period of time, is within the competence of legal regulations. From this point of view, a very problematic part of the requirements for the control of obtrusive light, when architectural or advertising lighting is indirectly prohibited by prescribing zero (or almost zero) values of building façade luminance L_b or sign luminance L_s [7].

IX. Conclusion

Based on the experience and knowledge gained during the drafting of the draft Czech national standard for the reduction of undesirable effects of artificial outdoor lighting, it is possible to open the following topics for discussion on the methodology for the reduction of obtrusive light or, more generally, light pollution:

- addition or modification of terms and definitions and discussion on the use of parameters R_{UF}, L_s and L_b;
- development of a methodology for the control of obtrusive light from indoor lighting systems;
- revaluation of current undesirable effects (e.g. sightseers, astronomical observations) and addition of new undesirable effects (e.g. natural environment, landscape) of artificial lighting on the environment;
- introduction of new parameters for the control of useful and spill light (oversizing of the lighting system, utilization of the luminous flux of luminaire in relation to the illuminated area, spectral properties of lighting sources, luminance of unintentionally lit surfaces and others);
- updating or creating new recommendations or technical standards with lighting requirements (architectural lighting, advertising lighting, outdoor lighting of residential buildings and others) to control the oversizing of lighting systems;
- modifications of existing procedures for determining limit values for individual disturbing effects (environmental zones, lighting classes, etc.);
- arrangement of controlled parameters, or disturbing effects according to public interests;
- reassessment of restriction and prohibition of lighting.

[1] Önorm O1052, Light pollution – Measurement and evaluation, Vienna, June 2016.

[2] NOR : TREP1831126A , Arrêté du 27 décembre 2018 relatif à la prévention, à la réduction et à la limitation des nuisances lumineuses, Ministre de la transition écologique et solidaire, France, December 201.

[3] IEC 60050-845, International Electrotechnical Vocabulary (IEV) – Part 845: Lighting, 2nd edition, Geneva, December 2020.

[4] Joint Publication IAU/CIE CIE 001-1980, Guidelines for minimizing urban sky glow near astronomical observatories, Vienna, 1980.

[5] CIE Publication 126-1997, Guidelines for minimizing sky glow, Vienna, 1997.

[6] CIE Publication 150-2003, Guide on the Limitation of the Effects of Obtrusive Light from Outdoor Lighting Installations, Vienna, 2003.

[7] CIE Publication 150-2017, Guide on the Limitation of the Effects of Obtrusive Light from Outdoor Lighting Installations, 2nd edition, Vienna, 2017.

[8] EN 12464-2 Light and lighting – Lighting of work places – Part 2: Outdoor work places, Brussels, 2014.

[9] EN 12193, Light and lighting – Sports lighting, Brussels, December 2018.

[10] EN 13201-2, Road lighting – Part 2: Performance requirements, Brussels, December 2015.

[11] CIE Publication 094-1993, Guide for Floodlighting, Vienna, 1993.

[12] CIE Publication 034-1977 Road lighting lantern and installation data: photometrics, classification and performance, Vienna, 1977.

Procedure for Establishing Environmental Zones

Petr Žák
Dept. of Electrical Power Engineering
Czech Technical University in Prague, Faculty of Electrical Engineering
Prague, Czech Republic
zakpetr@fel.cvut.cz

Simona Vondráčková
Department of Urban Design, Town and Regional Planning
Czech Technical University in Prague, Faculty of Civil Engineering
Prague, Czech Republic
simona.vondrackova@fsv.cvut.cz

***Abstract*—Within the framework of the problematics of undesirable side effects of artificial lighting on the environment, the surroundings are classified in terms of environmental zones. At present, two classifications are used in practice: the earlier system, which contains 4 classes designated as E1 through E4, and the newer one, which contains 5 classes designated as E0 through E4. The earlier classification is used in certain applications of EU technical standards for outdoor lighting, while the newer one is used in the CIE international recommendations. The original delineation of these zones was based on the positions of important astronomical observatories. Currently, the problem of obtrusive light is being addressed with great intensity in from the standpoint of protection of nature and the environment, in other words the influence of artificial light on fauna, flora, and the landscape.**

In terms of current recommendations for addressing the question of obtrusive light, the delineation of the environmental zones is described quite generally, and there are no clear rules for how to proceed in establishing them in practice.

Keywords— environmental zone, obtrusive light, protected area, national park, protected natural area, natural park

I. Introduction

In the framework of the CIE international recommendations, two approaches are used for establishing environmental zones. The first approach is based on the district brightness This approach is relatively general, and the individual zones are described using examples, which over the course of methodical development have changed. The second approach is derived from setting the so-called “reference points” sensitive to the undesirable side effects of outdoor lighting (e.g., major astronomical observatories, national parks, etc.). For a number of territories, this second approach may be too strict considering that it does not differentiate between natural and urban environments. The proposal of a procedure for determining environmental zones within a specific territory (district, region or state) requires a more detailed analysis of the landscape and settlement structure of this territory.

II. BACKGROUND

One of the basic tools for limiting the undesirable side effects of outdoor lighting on the environment is environmental zoning. This tool is relatively commonly applied in environmental legislation. In situations where it is not possible to remove the sources influencing the environment, the environment should be divided into several zones based on sensitivity towards the influencing source. The parameters and requirements in these zones, in turn, are set in relation to the human activities that are the source of the undesirable side effects.

First to draw attention to the obtrusive effects of artificial lighting at night time were astronomers starting in the early part of the 20th century. The first mention of zoning with respect to undesirable side effects of lighting in night time appeared in a CIE publication from 1980 [1] , where the zoning is mentioned as one of the regulatory tools for legislation concerning this problem. The first zoning system, in turn, appeared in a CIE publication from 1997 [2], based on the zoning used in Great Britain (Pollard 1996). In this publication, two approaches are used in zoning: district brightness and by reference points. In the case of the district brightness, the environment is divided into four environmental zones, expressed on a scale of intrinsically dark - low brightness - medium brightness – high brightness. In the case of reference points, the boundaries between environmental zones are determined by the distance from a specified reference point (e.g. astronomical observatory).

Another document where zoning is used in relation to undesirable side effects of artificial lighting in night time is CIE publication 150-2003 [3]. In this document, environmental zones are defined according to the district brightness. It no longer works with the distances between reference points and zone boundaries, yet it also makes reference to the previous document CIE 126-1997. The most recent zoning system is given in the updated document CIE 150 from 2017 [4]. This document expands the environmental zones to include a new class E0 and no longer refers to the document CIE 126 -1997.

In comparing these three mentioned documents, the environmental zones can be divided into two groups: first group concerning built-up areas (Table I) and second group concerning non-built-up areas (Table II).

TABLE I. Environmental Zones for Built-Up Areas

Zone	**Lighting environment**	**Description**		
		CIE 126-1997	***CIE 150-2003***	***CIE 150-2017***
E2	Low	Outer urban and rural residential areas	Industrial or residential rural areas	Sparsely inhabited rural areas
E3	Medium	Urban residential areas	Industrial or residential suburbs	Well inhabited rural and urban settlements
E4	High	Urban areas having mixed residential and commercial land use with high night-time activity	Town centres and commercial areas	Town and city centres and other commercial areas

From the Table I, there is a clear shift particularly in the zones E2 and E3. While in the first document, it was possible to apply zone E2 to villages or even towns, in the second and third documents it is applied exclusively in rural areas. Zone E3 could be applied in the first two documents only in towns, but in the third also in villages.

As we see, there is a definite trend in which, in uninhabited or sparsely inhabited areas, the use of zones is expanded in essence from E0 up through E2 and for cities, the extent is narrowed to E3 and E4. In natural, low-settlement areas, the strictest requirements should be invoked, i.e., E0 and E1. By contrast, in settlements, as per character and size, there should be a possibility of using the entire range of zones, for instance E0 through E3 for smaller towns and E0 through E4 for larger towns and cities.

Zones primarily involving the natural environment include zone E1 and, in the new document CIE150-2017 [4], also zone E0. From a comparison of the documents, it is not entirely clear whether zone E0 has been added or whether zone E0 corresponds to the original zone E1 and a new E1 has been inserted. The description of zones E0 and E1 is shown in Table II.

TABLE II. ENVIRONMENTAL ZONES FOR NON-BUILT-UP AREAS

Zone	Description				
	Lighting env.	***CIE 126-1997***	***CIE 150-2003***	***Lighting env.***	***CIE 150-2017***
E0	x	x	x	Intrinsically dark	Sparsely inhabited rural areas
E1	Intrinsically dark	National Parks, Areas of outstanding natural beauty	National parks or protected area	Dark	Town and city centres and other commercial areas

III. MOTIVATION

The reason for the proposal of environmental zones at the national level is the newly prepared draft of the national standard for reducing the undesirable side effects of outdoor lighting on the surrounding environment. The national methodology is based on the natural conditions and settlement structure in the Czech Republic and tries to find a balance between the natural environment and urban settlements.

IV. ANALYSIS OF THE TERRITORY OF THE CZECH REPUBLIC

The Czech Republic is an inlands state with a total area of 78,866 km^2 and a population of 10.5 million, in size placing it among Europe's smaller states. Yet the landscape of the Czech Republic is quite diverse, both in natural conditions and its settlement structure. Bearing in mind the diversity of natural conditions in the territory and the values of the landscape characteristics, the Czech settlement structure is itself specific, based on the possibilities of making a living. The character of the landscape has shaped the spatial and functional composition as well as the visual appearance of settlements. In the Czech Republic, practically all the land consists of a cultivated landscape, where most settlements have significant links to the "open" landscape. Found in the Czech Republic are both landscapes with basic (common) protection of landscape character as well as protected areas with a concentration of specific values. In the Czech Republic, protected areas in the field of nature and landscape protection are defined in Act No. 114/1992[6].

A. Protected Areas in the Czech Republic

National legislation [6] establishes, alongside general territorial and species protection for nature and landscapes, protection of vegetation, caves and paleontological finds, a category of so-called "specially protected areas", which form scientifically or aesthetically highly significant or unique elements of living or non-living nature. Belonging to the category of specially protected areas are: national parks, protected natural areas, national nature reserves, nature reserves, national natural heritage and natural heritage [6]. In terms of environmental zoning for purposes of limiting undesirable side effects of outdoor lighting, particularly significant are the categories with a large physical area. In the Czech context, these are national parks and protected natural areas (Fig. 1).

National parks are extensive areas with noteworthy outlines and geological formation, with a predominant occurrence of natural or at least low-human-impacted ecosystems. The long-term goal of protection of national parks is the preservation or gradual renewal of natural ecosystems, including the assurance of the undisturbed course of natural events in their expected succession in the prevailing land area of national parks, and the preservation or gradual improvement of the condition of ecosystems for which their existence is conditional for human activity or are significant in terms of biodiversity, in the remaining area of national parks. Czech legislation [6], in turn, sets the basic protective conditions for national parks, among them a ban within the entire area of national parks on situating light sources outside of enclosed buildings, which direct the luminous flux above the horizontal plane passing through the center of the light source. This forms, at present, the only legislative limitation on outdoor lighting in the Czech Republic.

Protected Natural Areas are also large terrain areas, yet in this case consisting of harmonically shaped landscapes marked by a developed outline and a significant share of natural ecosystems of forest and perennial grass growth, with ample tree representation and, in certain instances, with preserved landmarks of historical settlement. Economic and agricultural use of these areas is performed as per zones of increasing protection levels, in order to maintain and improve the natural state and preserve and create optimal ecological functions for the said area.

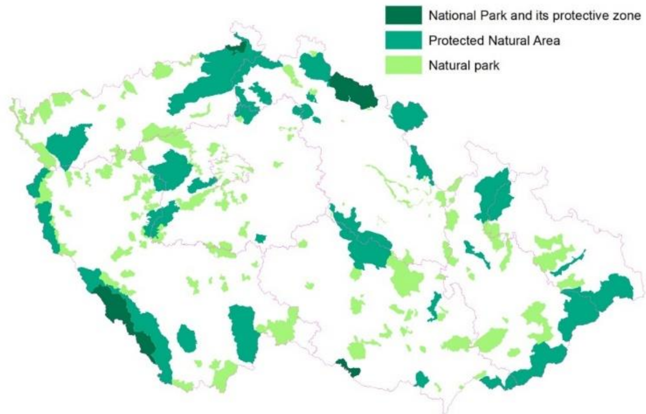

Fig. 1. Protected Areas and Natural Parks in Czech Republic

For protection of the landscape character of an area with a significant concentration of aesthetic and natural values but that is not specifically protected (Fig.1), there is the status of natural park (Fig. 1) and the creation within them of limitations on such a use of the land that would imply the destruction, damaging, or disruption of the current state of the said area.

Other categories of strongly protected areas are usually smaller areas of exceptional or concentrated natural value, sites of mineral finds, or habitats of rare or endangered species in fragmented ecosystems.

B. Settlement Structure of the Czech Republic

The settlement of the Czech Republic developed in dependence on natural conditions and highly complex historical processes. Its settlement structure is the outcome of a long-term development, with evidence of internal and external influences. Settlement in the Czech Republic forms a specific structuring of settlements, which in dependence on the natural environment and morphological shaping arose predominantly in medieval times. Its main characteristic is a noteworthy dense presence of settlements and a high share of small settlements. According to the document PPÚP [5] a settlement is a place with a concentration of dwellings and economic activities, in which the majority of functions associated with human life are brought together. On the territory of the Czech Republic, there occur settlements of urban and rural type in a total number of 6 258 municipalities. Rural settlements form the great majority of all settlements (86 %), though they contain just under one-fourth of the population.

1) Rural settlement

Villages, rural settlement, have, or in the past had, a primarily agricultural and productive function, now primarily replaced by functions as residential, recreational, or a combination of the two. The village is a traditional urbanistic ensemble of agricultural-economical and residential structures on individual parcels. Villages of most urbanistic types may display a public space and public buildings (chapel, church, parish house, school, magistrate's house). Villages can have a variety of spatial layouts and organisations (clumped, street-based, field-based, green-centred etc.). For agricultural villages, a characteristic is the immediate accessibility of cultivated land from the plots of the farmsteads and the economic dependence of the settled area on the cultivated land [5]. Small settlements without statutes (villages) have close ties with the landscape, not only functional but also spatial, influencing the landscape framework including its living components.

2) Urban settlement

Towns and cities have their unique spatial, functional, and social structures. They have a primarily residential function, yet also contain areas serving for facilities, manufacturing, recreation, or transport. As the town is an environment for human life, it should – along with the surrounding landscape – satisfy the spatial, functional, and aesthetic demands of its residents, throughout the course of time in which these needs are continually changing. Among the characteristic signs of towns are the following:

- A complete and diverse composition of public urban spaces, density and urban construction types, an architectonic form of buildings and groups that matches the town character, a unique external and internal image, panorama, or silhouette, squares, embankments, street networks etc.;
- A complex and balanced functional composition satisfying the needs not only of permanent residents of the town, residents of rural settlements in the catchment area, other daytime inhabitants, but also visitors and tourists;
- A characteristic diverse social composition of inhabitants, an urban way of life, a smaller number of employees in agriculture and higher total population [5].

TABLE III. DIVISION OF MUNICIPALITIES ACCORDING TO NATIONAL LEGISLATION

Statute	Designation	Description
No statute	O1	Settlements that do not have the status of a township, town, statutory city, or the capitol city of Prague.
Township	O2	A municipality is a township if at its request it is authorised by the speaker of the Chamber of Deputies pursuant to a cabinet ruling.
Town		A municipality with at least 3,000 residents is a town, if at its request it is authorised by the speaker of the Chamber of Deputies pursuant to a cabinet ruling.
Statutory City	O3	Statutory cities are Kladno, České Budějovice, Plzeň, Karlovy Vary, Ústí nad Labem, Liberec, Jablonec nad Nisou, Hradec Králové, Pardubice, Jihlava, Brno, Zlín, Olomouc, Přerov, Chomutov, Děčín, Frýdek-Místek, Ostrava, Opava, Havířov, Most, Teplice, Karviná, Mladá Boleslav, Prostějov and Třinec.
Capitol		The capitol city is Prague.

Reaching a certain population figure or surface area does not make a village a town, or the reverse. What is decisive here are the urbanistic indicators, i.e., the spatial, functional, and social organisation. In urban theory, though, there are visible differences in these indicators related to city size, hence for the needs of environmental zoning the criterion of the municipality's statute is applied.

A municipality is understood in Czech law as a territorially bounded, self-governing land unit with legal subjectivity and its own property. For national legislation, a municipality is the basic self-government unit of the association of its citizens; it forms a territorial unit that is outlined by the territorial boundaries of the municipality **Chyba! Nenašiel sa žiaden zdroj odkazov.**. For purposes of environmental zoning, settlements are divided per the municipalities act for reasons of greater simplicity (Table III, Fig.2)

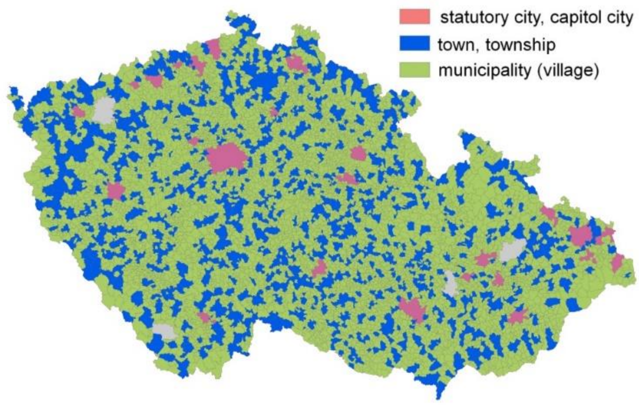

Fig. 2. Settlement Structure in the Czech Republic

V. Application of Environmental Zones in the Czech Republic

In the initial considerations about the zoning system in the Czech Republic, a method of zoning using reference points was tested according to the recommendations in the publication CIE 150-2017. When it is applied, it would be possible to use only zones E0, E1 and E2 in the Czech Republic, and a number of large cities, including Prague, would be in zones E0 and E1, which is unusable in the current real situation (Fig. 3). For this reason, a method based on the brightness of district was chosen for design the system of environmental zones in the Czech Republic.

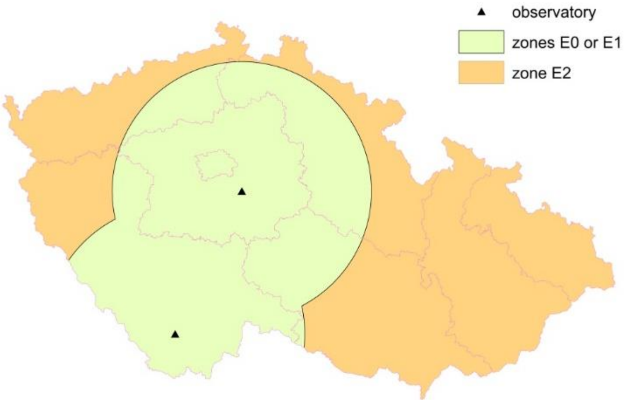

Fig. 3. Environmental Zone in the Czech Republic based on reference points

Based on the analysis of the CIE approach to environmental zoning and the analysis of the Czech environment with respect to its protected areas and settlement structures, five environmental zones have been defined as per CIE 150-2017 [4], with alterations reflecting the specifics of the Czech environment. Zones E0 and E1 are usually assigned to non-built-up areas, zones E2, E3 and E4 are defined for the areas of settlements (their built-up areas).

Zone E0, reflecting the CIE recommendations, includes the territories of national parks including their restrictive zones, territories of protected natural areas, and territories of natural parks, but does not include built-up areas of settlements. Beyond the framework of national legislation, it also includes so-called “dark sky reserves”. In the other parts of non-built-up land, the setting is zone E1, which furthermore applies to large areas of vegetation of natural character inside built-up areas. Settlements, for the needs of zoning, are divided into three basic groups, from small settlements through medium-sized ones up to larger ones (Table IV). Villages (municipalities without statute) are assigned, considering their close ties to the landscape, their smaller area, and their relatively simple organisation, in zone E2. Medium-sized and larger settlements are differentiated further. Medium-sized settlements (townships and towns) can have their centres assigned to zone E3, but other areas to zone E2. Larger settlements and cities have their centres assigned to E4, inner sections of cities with a certain level of public facilities fall within zone E3, and peripheral or remote urban areas (often of residential character, but also e.g., industrial complexes at the edge of a city or freestanding logistics or shopping centres) are assigned to zone E2.

At the same time, certain rules apply for zoning to achieve the maximum possible limitation of undesirable side effects of light pollution. If settlements are situated in a protected area (zone E0), the defined environmental zones are reduced by one level downward (e.g., from zone E3 to E2). At the same time, for other protected areas [6], and for proposals subject to environmental impact assessment per Act no. 100/2001 [7], the relevant administrative body may, in specifically justified cases, set different zones than those in the regular method (e.g., the presence of an endangered species particularly sensitive to light in night time etc.). To ensure that the least amount of light pollution escapes into the open landscape and areas with more benevolent parameters for lighting systems do not obtrude on immediately sensitive (non-built-up) areas, a condition has been imposed that zones E3 and E4 may not adjoin any non-built-up areas.

TABLE IV. Proposed Environmental Zones for the Czech Republic

Zone	**Lighting environment**	**Specification**
E0	Intrinsically dark	Non-built-up areas in protected regions (national parks including their restrictive zones, protected natural areas, natural parks) and dark-sky reserves
E1	Dark	Other non-built-up areas (areas outside settlements) and large areas of vegetation of a natural character
E2	Low brightness	Built-up areas and potential building areas in O1 municipalities and peripheral or remote sections of O2 and O3 municipalities
E3	Medium brightness	Built-up areas and potential building areas in compact inner sections and centres of O2 and O3 municipalities
E4	High brightness	Built-up areas and potential building areas of city-wide importance in centres of O3 municipalities

VI. Conclusion

The proposed zoning system is part of the proposal for a new national standard to limit the undesirable side effects of outdoor lighting on the surrounding environment. New national standard is based on the international recommendations of the CIE and on the analysis of the settlement and landscape structure of the Czech Republic. The zoning system tries to find a balance between the requirements for the protection of the natural environment and the requirements of the night environment of cities with a number of specific functions and requirements. The requirements of the new national standard are to be incorporated into the newly prepared national legislation in the field of construction law.

References

[1] CIE (1980). CIE 001-1980 Guidelines for minimizing urban sky glow near astronomical observatories (Joint Publication IAU/CIE). Vienna: CIE.

[2] CIE (1997). CIE 126-1997 Guidelines for minimizing sky glow. Vienna: CIE.

[3] CIE (2003). CIE 150-2003 Guide on the Limitation of the Effects of Obtrusive Light from Outdoor Lighting Installations. Vienna: CIE.

[4] CIE (2017). CIE 150-2017 Guide on the Limitation of the Effects of Obtrusive Light from Outdoor Lighting Installations, 2nd Edition. Vienna: CIE.

[5] Institute for Spatial Development: PPÚP – Ústav územního rozvoje, 2022. Principy a pravidla územního plánování. Ministry for Local Development.

[6] Act No. 114/1992 Coll., Act of the Czech National Council on Nature and Landscape Protection.

[7] Act No. 128/2000 Coll., Act on Municipalities (municipal establishment)

[8] Act No. 114/1992 Coll., Act of the Czech National Council on Nature and Landscape Protection.

Using Lighting to Offset the Influence of Driver Distraction on Hazard Detection

Steve Fotios
School of Architecture
University of Sheffield
Sheffield, UK
steve.fotios@sheffield.ac.uk

Yichong Mao
School of Architecture
University of Sheffield
Sheffield, UK
yichong.mao@sheffield.ac.uk

***Abstract*—Typical laboratory studies of visual detection are designed for the test participant to give their attentional only to that task. A limitation of applying the results of such work to driving is that it does not account for the detrimental effect of distraction. The distracted driver pays less attention to the primary task of safe driving leading to greater risk of involvement in a road traffic collision. This work investigates the impact of distraction upon detection of peripheral targets and the possibility to counter this using lighting. The first stage was a literature review to establish predominant in-vehicle distractions to driving. This was followed by a pilot study comparing detection performance under different levels of distraction. On-going work is investigating the relationship between lighting, distraction and peripheral detection.**

Keywords—road lighting, driving, hazard detection, distraction

I. Introduction

One key purpose of road lighting is to allow road users to proceed safely [1]. For the motorist, a role of road lighting is to reveal extraneous objects that suddenly appear on the road, in particular those beyond the reach of vehicle headlights, with the aim of giving sufficient time to allow evasive action to be taken without resorting to an abrupt manoeuvre [1].

One approach to establishing optimal lighting conditions is to investigate object detection with changes in the luminance, spectrum and uniformity of road lighting [2]. Typically, this is done by measuring the probability of detecting obstacles that suddenly appear in the field of view and/or the reaction time from onset of the object to detection.

For those studies conducted in the laboratory the driver is able, and is usually so encouraged, to direct their complete attention toward the detection task. Put another way, the test participant does their best to follow the experimenter's instructions and there is nothing else for them to do anyway.

See, for example, the detection experiment reported by He *et al* [3] where test participants looked through an aperture in a viewing chamber into which were projected small discs (the detection target) at on-axis and off-axis locations on an otherwise uniform wall. This is not the natural situation when driving. In addition to the visual search, detection and identification tasks necessary for driving, drivers are frequently distracted by tasks not associated with safe driving.

This same limitation may also be applied to experiments conducted on closed roads or using simulators, albeit perhaps to a lesser extent. A detection experiment using a scale model of a road scene [4] employed a secondary task (focus on a moving fixation mark and state aloud the randomly appearing digits) to promote on-axis vision towards the fixation mark and hence that detection targets were in peripheral vision. This was, however, a known task rather than being a randomly occurring event. Trials using a test track or a closed road enhance context validity [5]. Since these drivers know they are being observed, and are possibly accompanied in the vehicle by an experimenter, and furthermore that there are no other vehicles, the potential for distraction is less than likely in a natural setting.

Distractions can be as extreme as conducting office administration tasks whilst driving [6] and when distracted, drivers are less responsive to hazards [7]. Mobile phone use can lead to reaction times significantly slower than those associated with driving at the legal limit for blood alcohol [8]. Clearly, distraction is likely to be a contributory factor to road traffic crashes (RTCs). Note, for example, that distracted driving was reported to be a factor in 8.5% of fatal RTCs in the USA in 2019 [9].

Distractions can be visual, acoustic, cognitive or a combination. Some key distractions are acoustic (see below). Acoustic distraction, which can substantially impair driving [10], is a mind-off-road problem; even if a driver's gaze is directed towards the hazard, they may not be able to process it or react to it in an appropriate time frame - the 'looked-but-failed-to-see' phenomenon [11]. Acoustic distraction is particularly problematic for peripheral targets, since it normally causes a focus and increase of gaze concentration towards the road centre [12] and away from hazards in the peripheral field of view such as a pedestrian about to step into the road. Lighting of higher luminance and S/P ratio may be able to offset this by enhancing peripheral vision [13]. Therefore the cognitive demand of distraction needs to be considered when drawing the luminance vs detection curve.

Fig. 1. This image is not relevant to lighting and hazard detection, the focus of this article, but it will have distracted some people from giving their attention to the text. Image: PIXNIO .com, CC0 license.

The HAROLD (HAzards, ROad Lighting and Driving) project was conducted with support from EPSRC grant ref EP/S004009/1

This article describes the preliminary studies carried out to then enable an experiment investigating lighting, distraction and detection.

II. Critical Distractions

The first task was to identify the critical distraction(s) that occur in natural settings so that these could be represented in a detection experiment. This was done by a literature review [14].

In the first place, the review considered studies reporting distractions at the time of an RTC, with this being captured either through in-vehicle cameras or self-report. In five studies [15-19] conversing with passengers was the most frequently reported distraction, with mobile phone use being second ranked in three [16-18]. In the final study [20] listening to music was the most prevalent distraction, with passenger conversation being the second most prevalent.

That disagrees with a widespread public opinion that mobile phones are the main distraction to driving. There are a number of reasons why those studies did not reveal mobile phone use to be more prevalent. Despite being reported in 2006 or later, it may be the case that mobile phone use was not so widespread at that time. It may be the case that the categories into which distractions were binned led to phone use frequency being de-emphasised. We considered an alternative explanation, that the use of mobile phones whilst driving was prohibited to some extent, and hence that in self-reports drivers chose not to mention this, or when knowingly being observed by an in-vehicle camera that drivers changed their behaviour.

The review was therefore extended to a second method, studies using roadside observation of driver distraction. Of seven studies using this method, conversing with passengers was again found to be the most frequent distraction in six studies [21-26]: in the seventh study [27] mobile phone use was the most frequent distraction with conversation placed third after eating and drinking. A limitation of this approach is that some distractions cannot be observed, such as listening to music.

It was therefore concluded that conversing with passengers was widely found to be the most prevalent distraction [14]. However, subsequent to that publication, disagreement was found in a further study. From roadside observation of vehicles in Norway, Sagberg *et al*. [28] found that hand-held mobile phone use was the most prevalent distraction: conversing with passengers was second, followed by eating and drinking.

A key feature of Sagberg *et al* [28] was that the observations were conducted of vehicles on a motorway. All but one of the roadside observation studies included in the review [14] were conducted on minor roads [21-26]. The remaining roadside observation study [27] was observations of drivers on major roads and a signalised intersection: their observation on major roads found mobile phone use to be more prevalent than conversing with passengers, which agrees with Sagberg *et al*. [28]. Those studies using self-report and in-vehicle cameras to record distractions at the time of an RTC did not tend to report road type,

It was therefore proposed that the prevalence of driver distraction varies according to road type. This was tested using a third approach to quantifying in-vehicle distractions, the distraction reported in national records of RTCs [29].

To be useful for this analysis, an RTC database needed to include data regarding the attribution of fault to one or other driver for a specific RTC, categorise the type of distraction, and identify the type of road (major or minor) on which the RTC occurred. Two databases were found: the Fatality Analysis Reporting System (FARS) from the USA and the Crash Analysis System (CAS) from New Zealand.

With FARS, data were drawn from the eight-year January 2011 to December 2018: distractions were not reported prior to 2011 and data were not published online after 2018. While CAS reports RTCs from January 1980, the current analyses used data from January 2011 to December 2018 to match the FARS data. There are differences between these databases, with a key difference being injury severity – fatalities-only in FARS and all severities in CAS. There are also differences in the nature of the road network in the two nations represented.

Note that neither FARS nor CAS include a category labelled ‘conversing with a passenger’. We instead assumed that this was represented by the alternative category labels distraction ‘by other occupant(s)’ (FARS) or ‘attention diverted by passengers’ (CAS).

Comparisons of the prevalence of specific distractions in RTCs on major and minor roads were investigated using Odds Ratios determined using Equation (1).

$$OR = (A/B) / (C/D) \tag{1}$$

Where

A = RTCs reporting type of distraction on major roads

B = RTCs reporting type of distraction on minor roads

C = RTCs reporting no distraction on major roads

D = RTCs reporting no distraction on minor roads

In terms of overall distraction frequency, while the CAS data suggested conversing with passengers to be the most prevalent, followed by use of a mobile phone, the FARS data suggested a reverse order, with conversation with passengers being ranked second below mobile phone use. Both databases were consistent, however, in the change of distraction revealed according to road type: the Odds Ratios (Table I) show that distraction by conversing with passengers was significantly lower on major roads than on minor roads, while using mobile phone was significantly higher on major roads than on minor roads.

III. Standardised Distraction Task

From these investigations [14,29] it was concluded that, in terms of overall frequency, passenger conversation is the more frequent distraction. It was also recognised that this varies with road type: passenger conversation is the more frequent distraction on minor roads, and mobile phone use is the more frequent distraction on major roads.

TABLE I. Odds Ratios, 95% Confidence Interval and Difference from 1.0 for Comparisons of Distraction Frequency by Road Type

Type of distraction	Database	OR	95% CI	Sig.
Conversing with passengers	FARS	0.80	0.71-0.90	p<0.001
	CAS	0.66	0.60-0.73	p<0.001
Using mobile phone	FARS	1.11	1.01-1.23	p<0.05
	CAS	3.66	2.92-4.59	p<0.001

Having labelled passenger conversation as a distraction, it is important to clarify the impact. For RTCs involving two or more vehicles, the presence of passengers offers a protective effect [30-33]. In other words, RTC risk is higher for those who drive alone. Passengers may provide a protective effect, for example by alerting drivers to approaching hazards, or by withdrawing from the conversation. A caveat to passenger protection is the effect of age. For young drivers, commonly defined as <24 years, passengers (in particular if these are also young) reduce the protective effect and may even lead to an increase in RTC risk [30-35]. For this purpose, the young are defined as less than 24 years.

While passenger conversation, for example, could be repeated in a controlled experiment, it would be difficult to ensure a consistent level of distraction on repeated trials, and it might be difficult to control and report the level of distraction imposed. A distraction task used in an experiment is ideally standardised, meaning that when repeated in successive trials it maintains the same level of distraction, and also that the degree of distraction is easily characterised and can be varied in controlled steps. The n-back task meets this need. This is a delayed letter (or digit) recall task, in which an audible series of letters is played to participants who are then required to report this sequence by repeating aloud either the last letter heard (n0), the last letter heard but one (n1), or the last letter heard but two (n2).

IV. PILOT STUDY

A pilot study was conducted to investigate the influence on target detection of three variables: observer age, response mode, and type of distraction [36], this being done to help establish an experimental design for subsequent work to investigate changes in lighting.

A screen-based distraction task was used, with a central fixation mark surrounded by a target (discs subtending 0.88° at the eye) appearing at one of four locations 15° to 18° peripheral to the fixation mark toward each corner of the screen being. The targets appeared at random intervals for 250 ms, and were grey (5.5 cd/m^2) against a dark background (0.23 cd.m^2). Detection performance was investigated using reaction times and error rates.

The 89 participants were drawn from older (60+ years) and younger (18-25 years) groups, the young group representing those for whom there is a high casualty rate and the older group associated with the onset of significant impairment to visual functions [37].

To indicate detection of a target, two response modes were used, simple and choice. Simple response involved pressing the space bar on a keyboard when a target was detected at any location. This was used with one group of young participants (n=30). Choice responses used a box with four buttons, one button per target location: for correct detection, the button corresponding to the target location needed to be pressed. The choice response was used by young (n=30) and old (n=29) participants.

The detection task was conducted alongside a parallel distraction task, in separate blocks. These distraction tasks were the n-back task (with three levels of increasing difficulty, n0, n1 and n2), a word generation task, a number fixation task and a control (no distraction task). The letters (n-back task) and words were played to participants via the laptop speakers. Here, results from the n-back and control tasks are reported.

In the n-back task a sequence of letters was played over a speaker, and the test participant repeated this sequence, but with their response delayed by 'n' intervals of the sequence. The least distraction is imposed by n=0, where the participant repeats the digit immediately heard; for n=1, the participant repeats the digit one before the most recent, and thus successful performance demands greater attention (and hence less attention is allocated to driving).

The results are shown in Figs. 2 and 3.

There was a significant effect of age (p<0.01). For the choice response mode, the older group responded slower (a longer reaction time) than did the younger group and detected fewer targets.

There was a significant effect of response mode (p<0.001) when measured using reaction time but not with error rate. Comparing across the two groups of young participants, participants were generally slower at responding with the choice response than the simple response but this did not lead to a greater number of errors (missed targets).

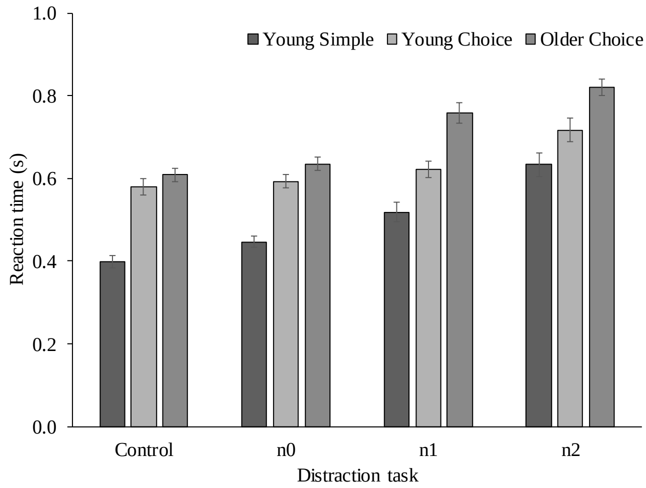

Fig. 2. Mean reaction times to detection of a peripheral target according to age, response mode and distraction. Error bars show standard error [36].

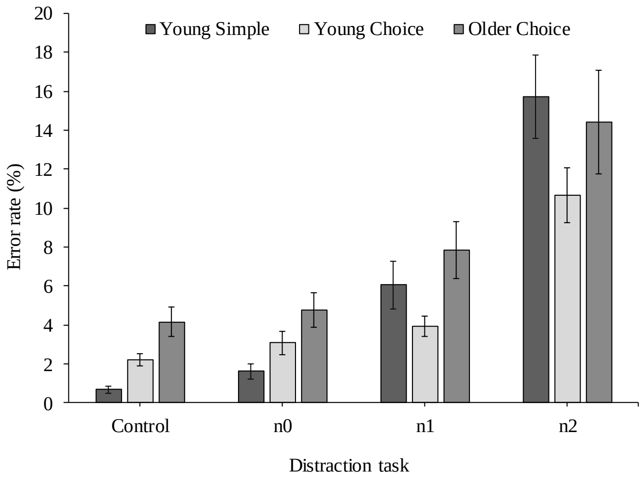

Fig. 3. Mean error rate for detection of a peripheral target according to age, response mode and distraction. Error bars show standard error [36].

There was a significant effect of distraction (p<0.001) with similar conclusions reached when using either reaction time or error rate. The difference between the control condition (no distraction) and n-back with no delay (n0) was not suggested to be significant. n2 led to significant slower responses and more errors than n1, and this in turn significantly slower responses and more errors than n0 (p<0.001). In other words, the more demanding the distraction task, the harder it was to detect peripheral visual targets.

The n2 task displayed a similar impairment to detection as did a word generation task. In this task a sequence of English language words was played over the speaker at a random interval of between 4 to 6 seconds, and after each word participants were required to say aloud a word beginning with the last letter of that word. The word generation task might be thought of as a reasonable representation of natural discussion (listen, comprehend, respond) and therefore that the n2 task is a suitable standardised distraction to represent conversation with passengers.

V. ONGOING WORK

Having established the nature of distractions when driving, and tested a standardised task for that distraction, then next step is to determine the degree to which road lighting can offset that distraction. Specifically, whether lighting of higher S/P ratio offsets the tendency to focus on the central vision field when distracted [12].

This is being investigated in an ongoing experiment. The apparatus is a scale model road scene as used in previous work [4,38] but with the detection targets extended from vehicle lane change and a road surface obstacle to include two additional surface obstacles and a 2D model pedestrian moving along the edge of the carriageway. Changes in lighting conditions are characterised by road surface luminance and S/P ratio of the light source. Distraction is imposed by an oral n-back task to represent conversation with a passenger, a digit identification task with responses given using a key pad to resemble the physical distraction of phone use, and a control.

Fig.4 shows the mean reaction times recorded with the control and n-back distractions. These data are for ten test participants (independent samples for each level of the n-back task), averaged across trials at three lighting conditions: a horizontal surface luminance of 0.5 cd/m^2 with S/P=1.0, the same luminance but with an S/P ratio increased to 1.8 and the original S/P ratio but with luminance increased to 1.6 cd/m^2. These data do not suggest any impact of distraction upon reaction time to detection, which contradicts the results found in the pilot study (Fig. 2) and a similar situation was found when the results were analysed by detection rate.

It was noted that performance of the n2 task was only about 55%, which might result from participants giving more attention to performance on the detection task than on the distraction task. The next pilot study will investigate this by incentivising performance on the distraction task.

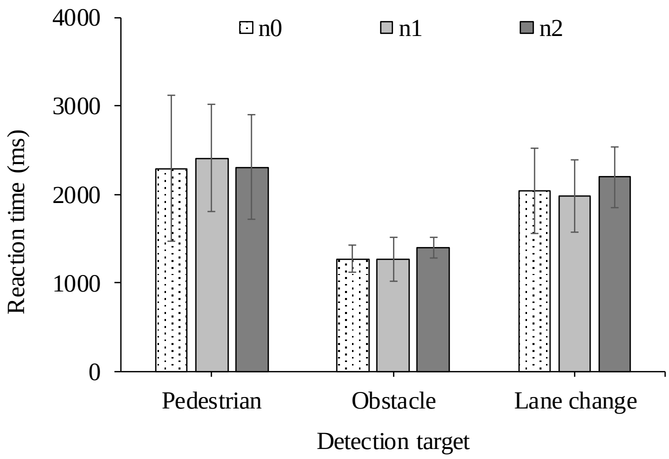

Fig. 4. Mean reaction time to detection of a moving pedestrian, a suddenly appearing road surface obstacle, and a vehicle changing lanes, for distraction imposed by the n-back task for n = 0, 1 and 2. Error bars show one standard deviation above and below the mean

REFERENCES

[1] Commission Internationale de l'Éclairage, CIE 115:2010 Lighting of roads for motor and pedestrian traffic, 2nd ed. Vienna: CIE, 2010.

[2] S. Fotios and R. Gibbons, "Road lighting research for drivers and pedestrians: The basis of luminance and illuminance recommendations." Light. Res. Technol. vol. 50(1), pp. 154-186, 2018.

[3] Y. He, M. Rea, A. Bierman and J. Bullough, "Evaluating light source efficacy under mesopic conditions using reaction times," J. Illum. Eng. Soc., vol. Winter, pp. 125-138, 1997.

[4] S. Fotios, C. Cheal, S. Fox and J. Uttley, "The effect of fog on detection of driving hazards after dark," Light. Res. Technol. vol. 50(7), pp. 1024-1044, 2018.

[5] J. M. Wood, G. Isoardi, A. Black and I. Cowling, "Night-time driving visibility associated with LED streetlight dimming," Accid. Anal. Prev., vol. 121, pp. 295-300, 2018.

[6] E. Laurier, "Doing office work on the motorway," Theor. Cult. Soc., vol. 21(4/5), pp. 261-277, 2004.

[7] T. Horberry, J. Anderson, M. A. Regan, T. J. Triggs and J. Brown, "Driver distraction: the effects of concurrent in-vehicle tasks, road environment complexity and age on driving performance," Accid. Anal. Prev., vol. 38, pp. 185-191, 2006.

[8] P. C. Burns, A. Parkes, S. Burton, R. K. Smith and D. Burch, "How dangerous is driving with a mobile phone? Benchmarking the impairment to alcohol," TRL Rep. 547, Crowthorne, 2002.

[9] National Highway Traffic Safety Administration (NHTSA), Detailing the Factors Behind Traffic Fatalities on our Roads, 2020.

[10] A. Chaparro, J. M. Wood and T. Carberry, "Effects of age and auditory and visual dual-tasks on closed road driving performance," Hum. Factors Ergon. Soc., pp. 2319-2322, 2004.

[11] M. B. Herslund and N. O. Jørgensen, "Looked-but-failed-to-see-errors in traffic," Accid. Anal. Prev., vol. 35(6), pp. 885-891, 2003.

[12] G. Kountouriotis and N. Merat, "Leading to distraction: driver distraction, lead car, and road environment," Accid. Anal. Prev., vol. 89, pp. 22-30, 2016.

[13] R. Lingard and M. S. Rea, "Off-axis detection at mesopic light levels in a driving context," J. Illum. Eng. Soc., vol. 31, pp.33–39, 2002.

[14] C. J. Robbins and S. Fotios, "Road lighting and distraction whilst driving: establishing the significant types of distraction," Light. Res. Technol., vol. 53(1), pp. 30-40, 2021.

[15] V. Beanland, M. Fitzharris, K. L. Young and M. G. Lenné, "Driver inattention and driver distraction in serious casualty crashes: data from the Australian national crash in-depth study," Accid. Anal. Prev., vol. 54, pp. 99-107, 2013.

[16] T. A. Dingus, F. Guo, S. Lee, J. F. Antin, M. Perez, M. Buchanan-King and J. Hankey, "Driver crash risk factors and prevalence evaluation using naturalistic driving data," Proc. Natl. Acad. Sci., vol. 113(10), pp. 2636-2641, 2016.

[17] T. A. Dingus, S. G. Klauer, V. L. Neale, A. Petersen, S. E. Lee, J. Sudweeks, M. A. Perez, J. Hankey, D. Ramsey, S. Gupta and C. Bucher, "The 100-car naturalistic driving study. Phase 2: results of the 100-car field experiment," United States: Department of Transportation. National Highway Traffic Safety Administration, 2006.

[18] C. Gordon, "Driver distraction: An initial examination of the attention diverted by contributory factor codes from crash reports and focus group research on perceived risks," IPENZ Technical Conference, Auckland: Institution of Professional Engineers New Zealand, September 2005.

[19] S. P. McEvoy, M. R. Stevenson and M. Woodward, "The prevalence of, and factors associated with, serious crashes involving a distracting activity," Accid. Anal. Prev., vol. 39(3), pp. 475-482, 2007.

[20] M. Née, B. Contrand, L. Orriols, C. Gil-Jardiné, C. Galéra and E. Lagarde, "Road safety and distraction, results from a responsibility case-control study among a sample of road users interviewed at the emergency room," Accid. Anal. Prev., vol. 122, pp. 19-24, 2019.

[21] M. E. Gras, M. Planes, S. Font-Mayolas, M. J. Sullman, M. Jiménez and F. Prat, "Driving distractions in Spain. driver behaviour and training," vol. 4, L. Dorn, Eds. Farnham: Ashgate Publishing Ltd., 2012.

[22] C. Huisingh, R. Griffin and G. McGwin Jr., "The prevalence of distraction among passenger vehicle drivers: a roadside observational approach," Traffic Inj. Prev., vol. 16(2), pp. 140-146, 2015.

[23] F. Prat, M. Planes, M. E. Gras and M .J. Sullman, "An observational study of driving distractions on urban roads in Spain," Accid. Anal. Prev., vol. 74, pp. 8-16, 2015.

[24] J. T. Sabzevari, A. R. Nabipour, N. Khanjani, A. M. Tajkooh and M. J. Sullman, "An observational study of secondary task engagement while driving on urban streets in Iranian safe communities," Accid. Anal. Prev., vol. 96, pp. 56-63, 2016.

[25] M. J. Sullman, F. Prat and D. K. Tasci, "A roadside study of observable driver distractions," Traffic Inj. Prev., vol. 16(6), pp. 552-557, 2015.

[26] M. J. Sullman, "An observational study of driver distraction in England," Transp. Res. F: Traffic Psychol. Behav., vol. 15(3), pp. 272-278, 2012.

[27] D. G. Kidd, J. Tison, N. K. Chaudhary, A. T. McCartt and T. D. Casanova-Powell, "The influence of roadway situation, other contextual factors, and driver characteristics on the prevalence of driver secondary behaviors," Transp. Res. F: Traffic Psychol. Behav., vol. 41, pp. 1-9, 2016.

[28] F. Sagberg, O. J. Johansson and H. B. Sundfør, "Combining roadside interviews and on-road observation for assessing prevalence of driver inattention," Transp. Res. F: Traffic Psychol. Behav., vol. 62, pp. 305-315, 2019.

[29] C. J. Robbins and S. Fotios, "The prevalence of in-vehicle driving distractions in road traffic collisions as a function of road type," Transp. Res. F: Traffic Psychol. Behav., vol. 84, pp. 211-222, 2022.

[30] M. Vollrath, T. Meilinger and H. P. Krüger, "How the presence of passengers influences the risk of a collision with another vehicle," Accid. Anal. Prev., vol. 34(5), pp. 649-654, 2002.

[31] J. A. Geyer and D. R. Ragland, "Vehicle occupancy and crash risk," Transp. Res. Rec., vol. 1908(1), pp. 187-194, 2005.

[32] C. Lee and M. Abdel-Aty, "Presence of passengers: does it increase or reduce driver's crash potential?" Accid. Anal. Prev., vol. 40(5), pp. 1703-1712, 2008.

[33] I. Engström, N. P. Gregersen, K. Granström and A. Nyberg, "Young drivers—reduced crash risk with passengers in the vehicle," Accid. Anal. Prev., vol. 40(1), pp. 341-348, 2008.

[34] C. Orsi, P. Marchetti, C. Montomoli and A. Morandi, "Car crashes: the effect of passenger presence and other factors on driver outcome," Saf. Sci., vol. 57, pp. 35-43, 2013.

[35] M. C. Ouimet, A. K. Pradhan, A. Brooks-Russell, J. P. Ehsani, D. Berbiche and B. G. Simons-Morton, "Young drivers and their passengers: a systematic review of epidemiological studies on crash risk," J. Adolesc. Health, vol. 57(1), pp. S24-S35, 2015).

[36] S. Fotios, C. J. Robbins, S. R. Fox, C. Cheal and R. Rowe, "The effect of distraction, response mode and age on peripheral target detection to inform studies of lighting for driving," Light. Res. Technol., vol. 53(7), pp. 637-656, 2021.

[37] G. Haegerstrom-Portnoy, M. E. Schneck and J. A. Brabyn, "Seeing into old age: vision function beyond acuity," Optom. Vis. Sci., vol. 76(3), pp. 141-158, 1999.

[38] S. Fotios, C. Cheal, S. Fox and J. Uttley, "The transition between lit and unlit sections of road and detection of driving hazards after dark," Light. Res. Technol., vol. 51(2), pp. 243-261, 2019.

Measurement of Light-technical Parameters of Public Lighting with Regard to Simulated Atmospheric Conditions

1st Jan Latal
Dept. of Telecommunications, FEECS
VSB–Technical University of Ostrava
Ostrava-Poruba, Czech Republic
jan.latal@vsb.cz

2nd Stanislav Hejduk
Dept. of Telecommunications, FEECS
VSB–Technical University of Ostrava
Ostrava-Poruba, Czech Republic
stanislav.hejduk@vsb.cz

3rd Tomas Stratil
Dept. of Telecommunications, FEECS
VSB–Technical University of Ostrava
Ostrava-Poruba, Czech Republic
tomas.stratil@vsb.cz

4th Tomas Novak
Dept. of Electrical Power Engineering, FEECS
name of organization (of Aff.)
Ostrava-Poruba, Czech Republic
tomas.novak1@vsb.cz

5th Pavel Valicek
Dept. of Electrical Power Engineering, FEECS
name of organization (of Aff.)
Ostrava-Poruba, Czech Republic
pavel.valicek@vsb.cz

***Abstract*—The aim of this article is to introduce an implementation of Visible Light Communication (VLC) into the public lighting network within a testbed in the University campus. Also, this article deals with the VLC technology and therefore with the transmission of data using visible light as well as with tests of the selected modulation formats and their abilities to transmit data under different atmospheric conditions. The results of the work are evaluated with the regards to the different modulation formats under different atmospheric conditions simulated in the acrylate box.**

***Index Terms*—VLC; Simulation; Atmospheric conditions; Modulation; Visible Light Communication**

I. Introduction

Currently, there is pressure to cover various locations with sufficient connectivity to the internet network. This is causing difficulties for most operators as mobile networks are reaching their limits. This is in view of the availability of smart mobile phones and the associated internet usage on these devices [1]. This is leading to new types of communication technologies being developed that operate, as far as possible, in licence-free bandwidth while providing low requirements with respect to transmitted message and power consumption per 1bit. This has led to a shift of attention to public lighting networks, which have a large number of applications [2].

As such, public lighting has made great strides in development over the years and its innovations are helping to improve the surrounding environment and reduce light pollution. Especially compared to the older high pressure sodium lamps. In the Czech Republic, the most common type of public lighting is sodium vapour lamp, which has many advantages such as high luminous efficiency, up to 70–130lm/W, high lifetime of about 16000 hours and small size with affordable price. The main disadvantages are mainly high light pollution, typical orange colour of light and inaccurate colour rendering [3]. However, this is changing over time, especially with the developing LED solid-state lighting (SSL) technology [4], where advances in this industry are slowly, but surely improving the availability of this type of lighting and thus reducing the previously higher prices. LED lighting then offers better colour rendering, often better ambient illumination and excellent luminous efficiency.

This paper attempts to elucidate the effects of simulated atmospheric phenomena for VLC communication through the luminous flux in the visible spectrum of radiation generated by public lighting (similar to [6], [7]). Sequentially, background information is presented including a description of the testbed and as well as the outputs obtained from the measurements.

II. Parameters of SMART Public Lighting

A. Lighting technical parameters

Luminous flux is a parameter that indicates the amount of light that a light source emits. Luminous flux is given in lumens (lm). It is one of the main parameters that indicates the output of a light source. For LED lights it is the total luminous flux and not the sum of the individual fluxes of each LED in the matrix. Brightness is primarily the main measure that determines the human eye's response to light. The unit of brightness is Candela per square meter (cd/m^2). Illuminance, or light intensity, is another measure of the luminous flux that falls on the area to be illuminated. It is given in lux (lx). For example, for the roads with pedestrians or cyclists, an illuminance of 2 to 50 lx is expected. The specific power represents the efficiency of the process of converting electricity into light. In simple terms, it is the ratio of luminous flux to electrical input. The unit of specific power is lumen per watt (lm/W), where again, for LED luminaires, specific power is given as a total number. Chromaticity temperature expresses the white tone of the emitted light. It has the designation T_c and is given in Kelvin (K). Basically, we can say that we have 3 groups of temperatures, below 3300K we refer to as warm tone, 3300K to 5300K where it is a neutral tone and above 5300K we refer to a cool tone with a tinge of blue [8].

B. Communication parameters

When implementing the communication interface in public lighting luminaires, it is necessary to define how the addition of communication will affect the parameters of the luminaire itself [9], [10]. Compared to conventional lighting, the spectrum temperature did not change by more than 150K. (The spectrum shifted to higher values due to the response of the phosphor of the white LEDs). So, if the luminaire was operating at 4150K by default, then with the implementation of communication (in the worst case scenario of OOK 50%On / 50%Off) the temperature dropped to approximately 4000K.

The second part is then the behavior of such communication in outdoor environments where we are beyond the calm conditions of indoors [2]. Inhospitable atmospheric influences can easily limit or even make communication impossible.

The primary problem in the communication domain is the lack of power for communication. Especially in the case of public lighting, the requirements for lighting intensity are relatively low. As the power decreases, the usable frequency bandwidth, communication distance, etc. logically decreases [5]. The problem is also the varying level of influence on the modulation schemes used. Basic on-off keying (OOK) modulation is in principle more robust to amplitude fluctuations than, for example, multi-state QAM etc.

C. Qualitative parameters of modulations

There are some parameters, which enables us to evaluate how the modulated optical wave was affected by negative effects from the transmission environment. These parameters are Modulation Error Ratio (MER) and Error Vector Magnitude (EVM) or SNR (Signal to Noise Ratio) [12], [13], [14]. Both these parameters (EVM, MER) are related to constellation diagram

. In the ideal constellation diagram, there are only two ideal points. In real there are plenty of points around ideal point therefore the point seems to be spread, see Fig. 1.

- Parameter MER

Parameter MER is defined as a ratio of sum of amplitude square of ideal symbol vectors to sum of amplitude square of error symbol vectors. This parameter is analog to SNR in digital modulated signal and it is usually expressed in dB units.

$$MER = \frac{\sum_{j=1}^{N}\left(\widetilde{I}_j^2 + \widetilde{Q}_j^2\right)}{\sum_{j=1}^{N}\left[(I_j - \widetilde{I}_j)^2 + (Q_j - \widetilde{Q}_j)^2\right]}, \qquad (1)$$

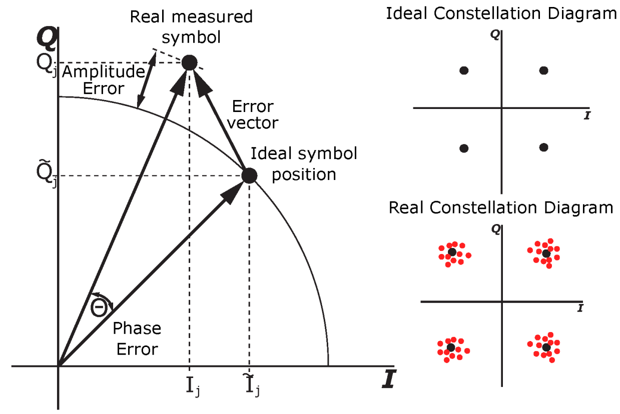

Fig. 1. Graphics representation of error vector.

where: $\widetilde{I}_j$ is component size of ideal symbol on axis I of constellation diagram, I_j is component size of real symbol on axis I of constellation diagram, $\widetilde{Q}_j$ is component size of ideal symbol on axis Q of constellation diagram, Q_j is component size of real symbol on axis Q of constellation diagram.

- Parameter Signal to noise ratio (SNR)

Another measured parameter is SNR. This is a signal-to-noise ratio measurement whose main objective is to determine the desired signal level relative to the normal background noise in the broadcast. If the measurement indicates a higher dB than 0dB then it most often indicates that we have a signal level greater than the noise level. The SNR is typically calculated using the following formula:

$$SNR = \frac{P_{Signal}}{P_{Noise}} \qquad (2)$$

where P_{Signal} represents the power of the signal and P_{Noise} represents the power of the noise. However, in our case we calculate SNR using a different formula, where LABVIEW uses two analyses. One is the SINAD (Signal-to-Noise and Distortion Ratio) analysis. It is a signal noise and distortion analysis and if we put this value from the second analysis and subtract it from the power of THD (Total Harmonic Distortion), which is actually the distortion value from the second signal analysis, we can use the subtracted result for further calculations. The next procedure is that we get the signal-to-noise value, which we add to the denominator in the formula $1/x$ and subtract the next value to get the SNR.

III. Atmospheric Simulations HW Tools

The fundamental question is how the communication parameters will change under adverse atmospheric conditions [6]. In the first place, one can consider an increase in environmental attenuation (which negatively affects any form of communication). For real simulations of atmospheric phenomena was used following set-up (shown in Fig. 2).

As a result, the atmospheric chamber has been built. (see Fig. 3). It allows "realistic" measurements of settled atmospheric conditions, which are mainly rain, turbulence (wind blowing), or fog. And of course their combinations. This

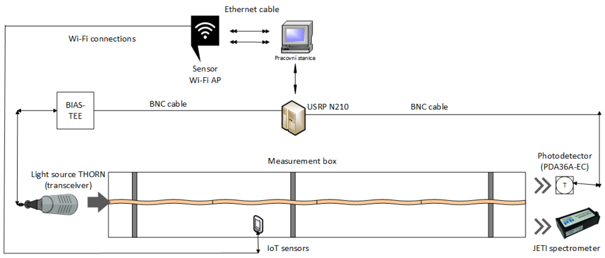

Fig. 2. A diagram of the experimental set-up.

configuration freedom is especially suitable for testing above mentioned communication parameters. At the one side of the acrylate box (with dimensions: length 5 m, height 0.5 m and width 0.5 m) with 120 mm openings on all sides (separated from each other by 625 mm), to position ventilators or allow air conduction. The upper side of the set-up is removable to allow for the placement of the measurement box into the apparatus during experimentation. On the front part was placed a public lighting as a source by the THORN - Model ISARO 36L35 BP (with modulation unit NI-USRP N210 and communication part). And on the other side is a photodetector (PDA36A-EC) connected to the computer, so we can compare transmitted and received data streams. During all measurements, the simulated box was hermetically sealed (only when we simulated rainy the upper part of the box was removed) to ensure uniform decomposition conditions inside the box and at the same time to maintain stable conductions.

Fig. 3. Atmospheric box for weather simulations.

IV. Results

Measurements were performed in different modulation schemes ranging from classical On-Off-Keying (OOK) to more complex modulations such as m-QAM and m-PSK. For each scheme, data were evaluated to calculate SNR and MER under different atmospheric conditions. That is, more precisely for normal environment, turbulent environment, rainfall simulation and finally fog.

A. SNR for different conditions

In the case of the results (Figs. 4, 5, 6, 7) for a normal (steady state) environment without significant simulated atmospheric external effects, we can observe that the OOK modulations in their various forms (non-return to zero, return to zero, pulse position modulation and Manchester coding) maintain very stable values. The explanation is very simple, because a suitably chosen decision level always evaluates only log 1 or 0. In contrast, modulations that require deeper detection of the signal waveform itself to operate are at a slight disadvantage. In a real environment, where in addition the transmitter and receiver can move mutually, the dispersion of values is even larger. However, in multi-state modulations we transmit more data, so the decision levels are closer to each other, and the noise has a much larger effect.

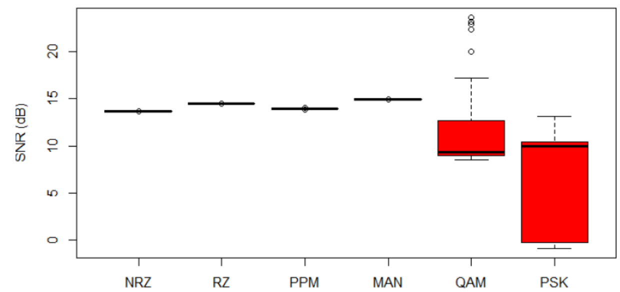

Fig. 4. SNR for different modulations in normal conditions @ 1MHz carrier.

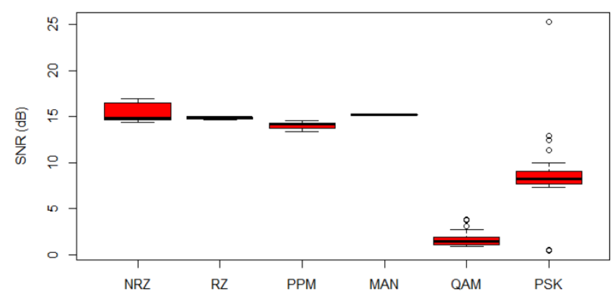

Fig. 5. SNR in turbulent (windy) conditions.

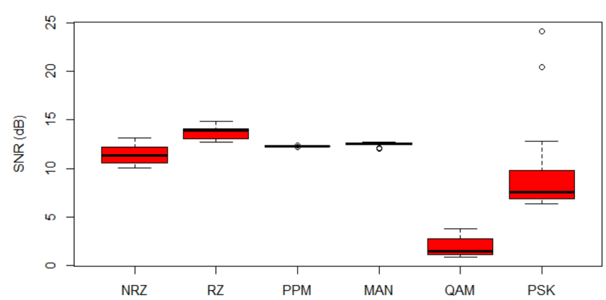

Fig. 6. SNR in rainy conditions.

The greatest influence on communication is undoubtedly the simulation of the atmospheric phenomenon in the form of fog (Fig. 7), which affected all tested modulation schemes almost symmetrically. When light radiation passes through a foggy environment, large scattering losses occur, which cause a reduction in power level and the breakdown of communication

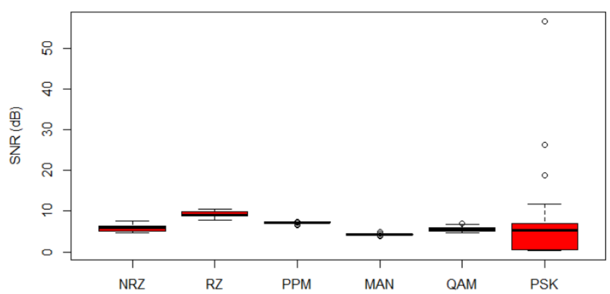

Fig. 7. SNR in foggy conditions.

itself, regardless of the modulation scheme. For the very existence of the communication, the 3dB limit (50% loss of signal power) is important for SNR. If we exceed this limit, we will have a problem with demodulation of the signal itself, because it will no longer be easy to separate the useful signal from the noise.

B. MER for different conditions

The second qualitative communication parameter observed was MER. The following box plots, see (Figs. 8, 9, 10, 11), express the statistical analysis for the already above-mentioned conditions.

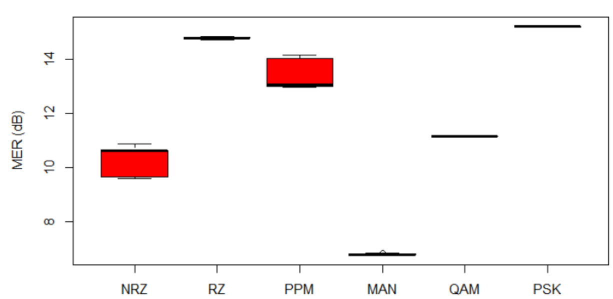

Fig. 8. MER for different modulations in normal conditions @ 1MHz carrier.

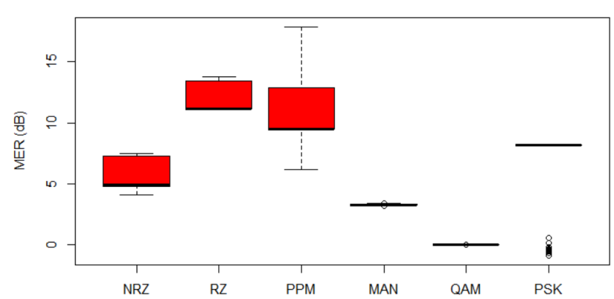

Fig. 9. MER in turbulent (windy) conditions.

It can be seen, that for QAM modulation, MER is reaching almost zero values for all non-normal atmospheric conditions. It is logical since the SNR values from previous graphs are as well close or under 3dB level.

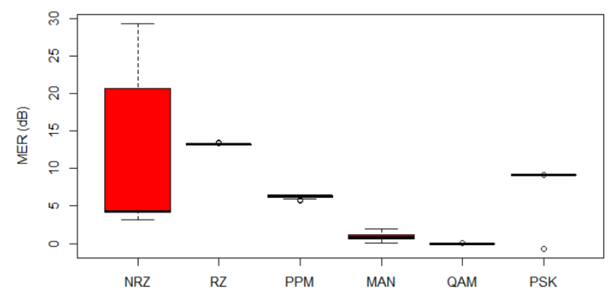

Fig. 10. MER in rainy conditions.

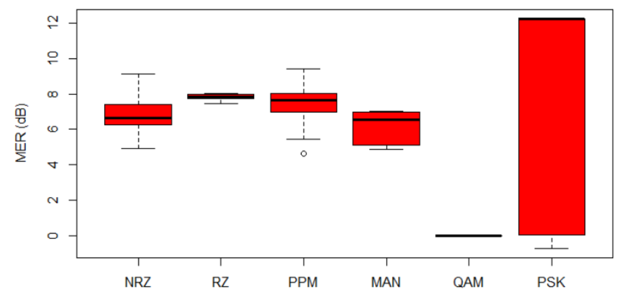

Fig. 11. MER in foggy conditions.

C. Conclusion

Atmospheric conditions have a high influence on communication parameters of VLC systems. More or less, it is always necessary to count with atmospheric influences during the system design. There are two ways to deal with this problem.

- Use higher output power. However, an outdoor area is not always suitable for installation of the street lamps radiating for example 400lx.
- Lower the communication speed. With slower signal changes, it is possible to increase photodetector sensitivity, but in this case the noise will be amplified together with the useful signal [15].

Although the VLC communication is always a compromise between optical power and sensitivity, atmospheric influences make outdoor communications quite a challenge. Main problems are usually with sophisticated amplitude dependent modulations. It is because amplitude changes caused by external influences (or movement of the mobile station itself) are difficult to compensate for in real time.

Acknowledgment

The work has been partially supported by Projects no. SP2022/18, SP2022/21, CZ.1.07/2.3.00/20.0217. This work was also supported by the European Regional Development Fund in the Research Centre of Advanced Mechatronic Systems project, project number CZ.02.1.01/0.0/0.0/16_019/0000867.

References

[1] G. A. Ma, R. Ramogomana, L. Marata, B. Basutli, A. S. Khan and J. M. Chuma, "Indoor Visible Light Communication: A Tutorial and

Survey ," in *Wireless Communications and Mobile Computing*, vol. 2020, Article ID 8881305, pp. 1–46, 2020.

[2] A. Memedi and F. Dressler, "Vehicular Visible Light Communications: A Survey," in *IEEE Communications Surveys* & *Tutorials*, vol. 23, no. 1, pp. 161–181, 2021.

[3] C. R. B. S. Rodrigues, P. S. Almeida, G. M. Soares, J. M. Jorge, D. P. Pinto and H. A. C. Braga, "An experimental comparison between different technologies arising for public lighting: LED luminaires replacing high pressure sodium lamps," 2011 IEEE International Symposium on Industrial Electronics, 2011, pp. 141-146, doi: 10.1109/ISIE.2011.5984147.

[4] Y. Zhang, J. XU, M. Ding, D. Zhao, H. Huang, G. Lu, Z. Miao, Y. Qi, B. Zhang and Y. Cai. "Wafer-Level Light Emitting Diode (WL-LED) Chip Simplified Package for Very-High Power Solid-State Lighting (SSL) Source," IEEE Electron Device Letters, vol. 37, no. 2, pp. 197-200, Feb. 2016, doi: 10.1109/LED.2015.2509462.

[5] T. Novak et al., "Case study – Modelling of Visible Light Communication on Luminous Intensity Distribution Curve of LED Low Beam Car Headlamps," 17th International Symposium on the Science and Technology of Lighting, 2022, pp. 1–5.

[6] B. Liu, P. Tang, Y. Yin, J. Zhang and L. Xia, "Measurement-based Analysis of Atmospheric Attenuation by Considering Different Weather Types for Visible Light Communications," 16th European Conference on Antennas and Propagation (EuCAP), 2022, pp. 1-5, doi: 10.23919/EuCAP53622.2022.9769424.

[7] G. Singh, A. Srivastava and V. A. Bohara, "Impact of Weather Conditions and Interference on the Performance of VLC based V2V Communication," 21st International Conference on Transparent Optical Networks (ICTON), 2019, pp. 1-4, doi: 10.1109/ICTON.2019.8840164.

[8] CIE Commission Internationale de l'Éclairage. CIE 121. In The Photometry and Goniophotometry of Luminaires; International Commission on Illumination: Vienna, Austria, 1996.

[9] J. Latal et al., "Implementation of VLC Within a Public Lighting Network," 2020 22nd International Conference on Transparent Optical Networks (ICTON), 2020, pp. 1-5, doi: 10.1109/ICTON51198.2020.9203074.

[10] P. Kurniawan, K. Sujatmoko and B. Pamukti, "Performance of OOK-RZ and NRZ Modulation Techniques in Various Receiver Positions for Li-Fi," 2019 IEEE International Conference on Signals and Systems (ICSigSys), 2019, pp. 173-177, doi: 10.1109/ICSIGSYS.2019.8811047.

[11] National Instruments, Modulation Error Ratio (MER) and Error Vector Magnitude (EVM). http://www.ni.com/white-paper/3652/en/.

[12] F. Knobloch, "Channel gain and frame error rate for optical street lighting communication," 2015 13th International Conference on Telecommunications (ConTEL), 2015, pp. 1-5, doi: 10.1109/ConTEL.2015.7231194.

[13] Seok-Ju Lee and Sung-Yoon Jung, "A SNR analysis of the visible light channel environment for visible light communication," 2012 18th Asia-Pacific Conference on Communications (APCC), 2012, pp. 709-712, doi: 10.1109/APCC.2012.6388286.

[14] B. Turan, E. Kar and S. Coleri, "Vehicular Visible Light Communications Noise Analysis and Autoencoder Based Denoising," 2022 Joint European Conference on Networks and Communications 6G Summit (EuCNC/6G Summit), 2022, pp. 19-24, doi: 10.1109/EuCNC/6GSummit54941.2022.9815630.

[15] A. Assabir, J. Elmhamdi, A. Hammouch, L. Belhaf and A. Akherraz, "The effects of the field of view and reflections on the optical wireless channel," 2017 International Conference on Electrical and Information Technologies (ICEIT), 2017, pp. 1-5, doi: 10.1109/EITech.2017.8255218.

Image-based Material Characterization for Daylight Simulation Using Illuminance-proxy and Artificial Neural Networks

Nima Forouzandeh
Faculty of Architecture & the Built Environment
Delft University of Technology
Delft, Netherlands
ORCID: 0000-0001-7025-5509

Eleonora Brembilla
Faculty of Architecture & the Built Environment
Delft University of Technology
Delft, Netherlands
ORCID: 0000-0003-1800-8660

J. Alstan Jakubiec
John H. Daniels Faculty of Architecture, Landscape and Design
University of Toronto
Toronto, Canada
ORCID: 0000-0002-8534-6902

***Abstract*—A key aspect of daylight modeling is the definition of material optical properties. Characterization of such properties in existing indoor spaces with current methods is a labour-intensive and time-consuming task, especially in surfaces with considerable visual complexity. Faster and more accurate estimations of such properties will lead to more efficient workflows. Towards this direction, the present work studied the feasibility of using two novel approaches i.e. illuminance-proxy and probabilistic image based material characterization methods for implementation in daylight modeling. These approaches are compared with two common techniques, namely the manual selection from a measured dataset and the use of illuminance/luminance measurements. According to the results, both novel techniques are able to predict spatially-averaged Daylight Autonomy, continuous Daylight Autonomy, and Useful Daylight Illuminance in 300-3000 lx range with less than 5% error.**

***Keywords*—on-site, field, measurement, visual, Digitalization, Optical.**

I. Introduction

Sufficient and proper daylight in indoor spaces lead to more energy-efficient buildings and has a significant impact on users' satisfaction and well-being[1, 2].

Numerical simulation of daylight has been extensively implemented in recent decades as a reliable tool to assess the performance of buildings for improving existing indoor spaces and designing future buildings. Such a numerical model is not only applied for design and retrofit purposes, but it is also capable of acting as a virtual representation of a building which can potentially be applied for making several kinds of real-time to long-term decisions during the building life-cycle. The key to constructing this so-called "digital twin" is, on one hand, dependent upon the calculation and estimation algorithms, and on the other hand, accurate and reliable inputs, based on which making such informed decisions will be feasible. As far as daylight is concerned, the optical properties of different surfaces within an indoor space are important determinants of its short-term and long-term performance[3]. While this information can be defined roughly according to design specifications in the pre-construction phases, measurements are, in most cases, necessary for creating an accurate model. With current methods, however, this demands a considerable on-site field measurement effort followed by manual modeling, which makes daylight analyses costly for many applications and real-time decision-making impossible.

To tackle these limitations, two image-based techniques for pixel-wise and patch-wise material characterization are tested in estimation of material properties in a real indoor space. These results are then implemented for daylight simulation and calculation of annual performance.

II. Background

A. Illuminance-proxy method

Characterization of dense, pixel-wise reflectance maps of arbitrarily complex diffuse surfaces using High Dynamic Range Imaging (HDRI) has been studied by Mardaljevic, Brembilla, and Drosou [4], [5]. This approach derives an illuminance map, based on interpolation of sparsely known reflectance values on a surface. Since it requires only a few known reflectance values on a surface, this method can reduce the field measurement labor, while giving a pixel-wise reflectance map.

B. Probabilistic material characterization

The existing body of literature on probabilistic material characterization in computer vision attempts to minimize the measurement cost by probabilistic characterization of material optical properties. This is done with the help of supervised learning algorithms, mainly Convolutional Neural

Networks (CNN) trained with labeled datasets of materials. These datasets can be categorized according to acquisition method, including real-world images (e.g., MINC[6] and OpenSurfaces[7]), synthesized sets of images, and measured datasets (e.g., BTF material database[8] and SVBRDF database Bonn[9]). Another example of measured datasets, relevant to the daylighting field, is Spectral Materials Database (SpectralDB), a work done by Jakubiec [10]. This is extensively used by daylight modellers and researchers to define materials in simulation models for evaluation of daylight provision, visual comfort and non-visual effects of light on building occupants. However, the applicability of this dataset for image-based probabilistic estimation of key material information for daylight simulation (i.e., reflectance$_{\mathrm{RGB}}$, specularity, and roughness) is not yet studied, which is one of the objectives of the present work.

III. Objectives

This study investigates the feasibility of using the illuminance-proxy method as an efficient characterization approach for pixel-wise reflectance calculation for modeling daylight in existing indoor spaces.
Moreover, it aims to study the feasibility of using a learning-based approach for estimating material optical properties with only a small-size (128*128 pixels) rectangular RGB patch from an image taken with a regular camera. This is an effort towards automation of daylight modeling in existing indoor spaces, and to address the lack of coordination with other related fields, such as geomatics and scan-to-BIM [11].

IV. Methods

Four material characterization scenarios are considered for the purpose of this study, each applied to the same daylight model of a case study room.
The results of annual daylight simulations obtained using these methods are then compared and discussed. The following subsections describe the case study room, simulation parameters, material characterization scenarios, and data analysis methods.

A. The case study room

The studied room is a 5.8 m by 4.3 m meeting room located at the Faculty of Architecture in Delft, The Netherlands. The room is oriented towards South-East with a 4 degrees angle from due South. Pictures from the room are presented in Fig. 1

B. Material characterization scenarios

The following four methods for characterizing material optical properties are considered:

1) Manual selection from a material database: Material properties were manually selected based on color and type from *SpectralDB*.

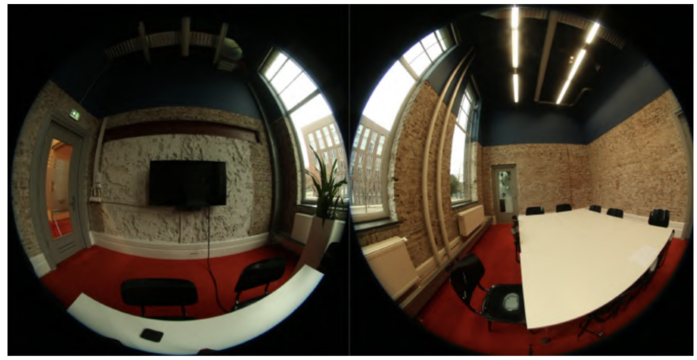

Fig. 1. The case study room

2) Average Hemispherical Reflectance (AHR): Reflectance values for each sub-surface were calculated based on luminance and illuminance measurements, assuming the following relation:

$$\rho = \pi * (L/E) \quad (1)$$

where ρ is diffuse reflectance, L is luminance, and E is illuminance.
This method, known as Average Hemispherical Reflectance (AHR), is assumed as the ground truth method for material characterization in this study. Specularity and roughness values were assigned a value of zero.

3) Illuminance-proxy method: HDR images of five main surfaces, i.e. walls and ceiling, were captured. The validity of the resulting luminance map was tested against measured luminance values of three spots in the Field of View (FOV).
A list of sparse points of known reflectance values, measured with the AHR method, was created. A mask, indicating the area of interest in each HDR image was created as the third input of this method. In Fig. 3 these inputs for calculating the mean reflectance in one of the walls are visualized. Knowing the luminance and reflectance, an illuminance map is generated. The resulting list of illuminance values and their pixel location is then fed into a Kriging interpolation algorithm, as previously implemented by Mardaljevic et. al. [12]. The resulting illuminance map and the input luminance map are used to generate the reflectance map. Finally, the reflectance is calculated by averaging the pixel-wise reflectance values across the area of interest, indicated by the mask, e.g., brick parts, plinth (see Fig 3).
An additional outlier removal step, which includes the removal of 0-5$^{\mathrm{th}}$ and 95-100$^{\mathrm{th}}$ percentiles is applied to the list of output reflectance values for one of the surfaces (*wall 3*). This was only done on this wall because for other surfaces this did not significantly change the result (less than 5%).
A geometrically simplified model was also created by approximating a big surface, e.g. a wall, with many sub-surfaces, such as pipes and ducts, to a single polygonal surface. This is visualised for two example surfaces in Fig. 2.
Like the AHR method, specularity and roughness are assumed to be zero in this characterization scenario. For the definition of the floor, reflectance from the measurements is used for

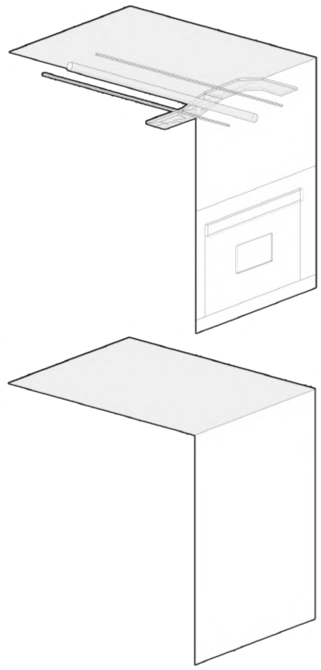

Fig. 2. Geometrical simplification adopted in the illuminance-proxy method.

simulation, since it was not possible to capture a full image of the floor.

4) Image-based probabilistic estimation: An Artificial Neural Networks model was constructed to quantitatively characterize material properties under random daylight conditions, consisting of an input layer with the shape of 128*128*3 (pixels*pixels*channels), one hidden layer, and an output layer with five neurons, for estimation of the following variables:

1) Reflectance in the red channel
2) Reflectance in the green channel
3) Reflectance in the blue channel
4) Specularity
5) Roughness

Mean squared error (MSE) was selected as the loss function to optimize the ANN model. Number of neurons was fine-tuned in from a search space of 1 to 400 neurons. 16 is shown to give the least loss (0.05). This neural network model was trained by a rendered data set with 1288 materials measured with a reflectance spectrophotometer [10](see Fig. 4). Each material was labeled with the above-mentioned information to define the material optical properties. The Radiance rendering engine [13] was used to generate a dataset of images of a flat surface perpendicular to the virtual camera for training. The rendered views were compressed from a four-channel HDR image to JPG images with three color channels to be read by the ANN model. A set of 16 random rendered samples are presented in Fig. 5.

The training data set is split into two training and validation sets with 1159 and 129 samples, respectively. Seven images of surface materials – including an exposed brick wall – from the studied room under random daylight illumination were cropped from images of the room to estimate the optical properties with the ANN model (see Fig. 6).

Fig. 5. Rendered samples for training the ANN.

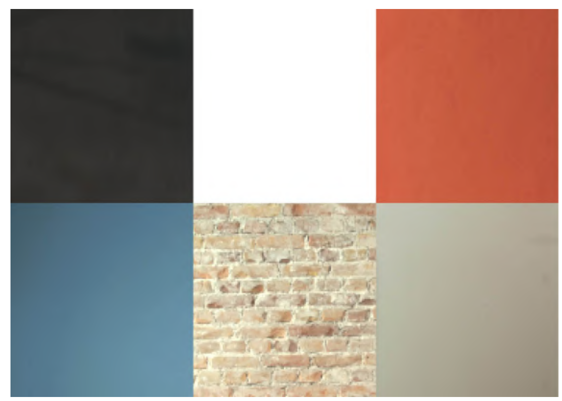

Fig. 6. Input samples of materials as real-world test cases. Top row from left to right: black screen, white desk, and orange floor. Bottom row from left to right: painted blue walls and ceiling, brick walls, opaque parts of the doors

C. Daylight performance simulation

The Radiance 2-phase method was chosen to run annual daylight simulations, using Honeybee [14] as the interface. Five daylight performance metrics are used in this study, including Daylight Autonomy (DA), continuous Daylight Autonomy (cDA), and three Useful Daylight Illuminance (UDI) values representing under-lit, well-lit, and over-lit areas. The thresholds for calculating these metrics are 300 lux for DA and UDI (lower threshold), and 3000 lux as the upper threshold for UDI.

The output of each material characterization scenario is applied on a single room described in section IV-A. Other information necessary for daylight calculations, including context and transmittance of windows, are maintained constant for all scenarios.

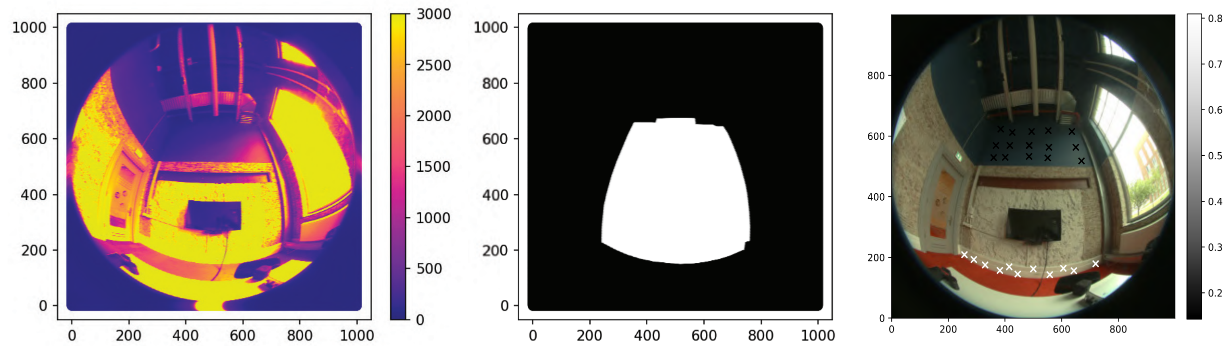

Fig. 3. Inputs for the illuminance-proxy method. From left to right: luminance map [cd/m^2], masked area, spots of known reflectance

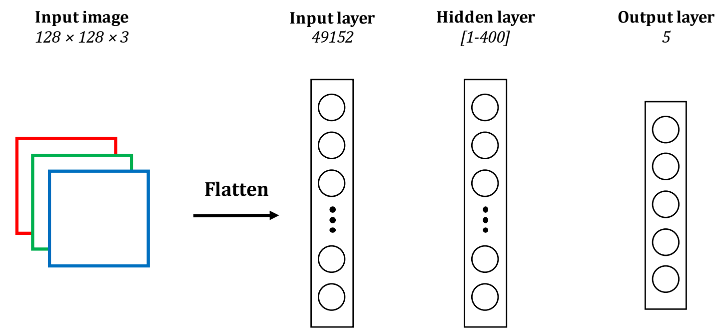

Fig. 4. Representation of the simple ANN used in this study.

V. RESULTS

Firstly, the results from the various material characterisation methods are presented and compared against the AHR method. Secondly, the corresponding daylight simulation results are presented.

A. Material properties

The visible reflectance values given by the AHR, SpectralDB (manual selection), illuminance proxy, and ANN methods are presented in Fig. 7. Since specularity is assumed to be zero in AHR and illuminance proxy, only the estimation of specularity resulting from ANN and SpectralDB are presented in Fig. 8. The results show that SpectralDB predicts reflectance more accurately compared to ANN, however, this prediction resulted in significant error in characterizing the reflectance of *White desk*, *Floor*, *Windows sill*, and *Flower box*. Reflectance results from the illuminance-proxy method gives the reflectance for *brick* and *plaster*, as well as the minor sub-surfaces including *black screen* and *red beam* with less than 5% absolute error. Errors are considerable for *white pipes*, *silver ducts*, and *radiators*. The results for radiators is above 1, even with outlier removal.

The output illuminance map, reflectance map, and the final mean reflectance values from the illuminance-proxy method corresponding to the model with geometrical simplification, for five surfaces including four walls and the ceiling, are presented in Table I. These mean values range from 0.36 for the ceiling to 0.481 for *wall1*. As mentioned in Section IV-B3, for *wall3* the initial mean reflectance output was 1.48, so an outlier removal was applied (removal of lowest and highest five percentiles), and the resulting value, 0.42, is considered for the daylight simulation.

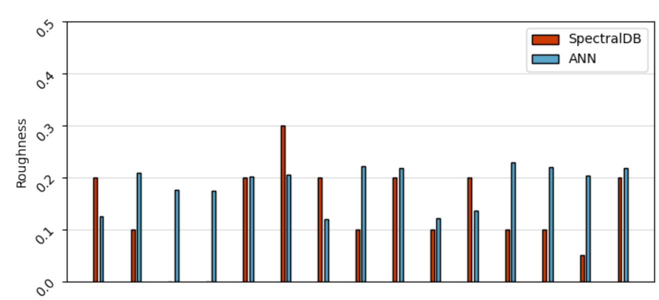

Fig. 8. Comparison of specularity values from ANN and SpectralDB

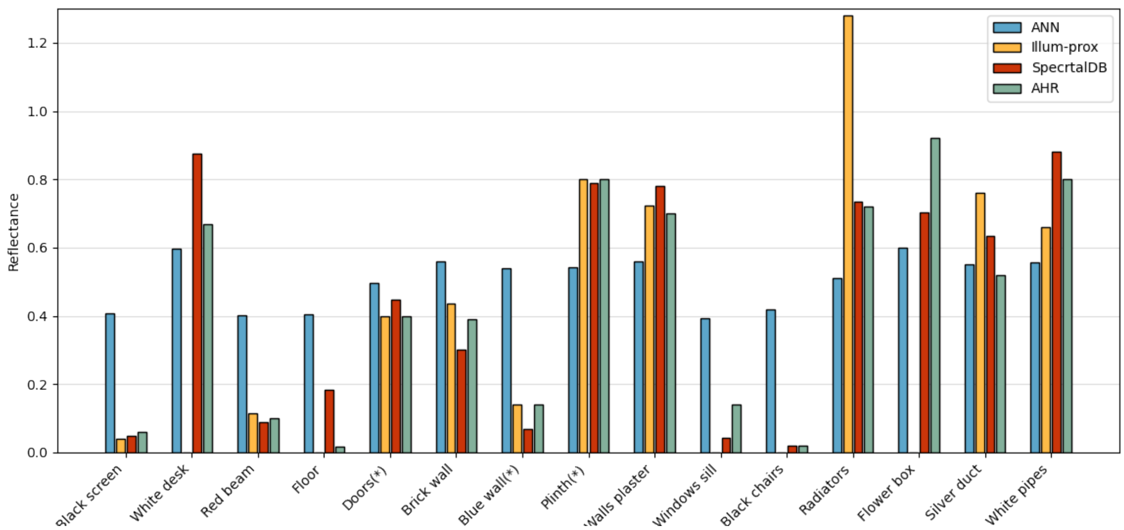

Fig. 7. Visible reflectance values from AHR, SpectralDB, illuminance proxy, and ANN. Reflectance values corresponding to the surfaces indicated by (*) are include the spots with known reflectance as the input for illuminance-proxy methods, thus are equal to AHR.

B. Annual daylight performance metrics

The spatially averaged performance values corresponding to each of the four material characterization scenarios are presented in Fig. 9. A more detailed comparison was done to capture the deviation of each annual performance metric from the AHR scenario across all the points on the simulation grid. The RMSE values resulting from this comparison are presented in Fig. 10.

According to the daylight results in Fig. 9, the performance metrics from the illuminance proxy method with and without geometrical simplification falls within 5% error range for DA, cDA, and $UDI_{\text{well-lit}}$ and it predicts $UDI_{\text{over-lit}}$ with less than 10% error. Nevertheless, the error in calculation of $UDI_{\text{under-lit}}$ is more than 15%.

Comparing the annual results across grid points (Fig. 10) shows that, while illuminance proxy results agrees the most with the ground truth model, geometrical simplification causes significant errors in predicting $UDI_{\text{under-lit}}$ and $UDI_{\text{well-lit}}$, and while performing almost similarly with ANN in calculating cDA, it is considerably more accurate than ANN overall.

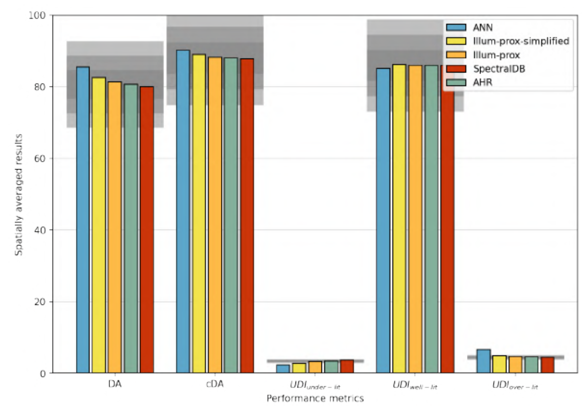

Fig. 9. Average values of annual daylight performance metrics with 5, 10, and 15% error range relative to AHR

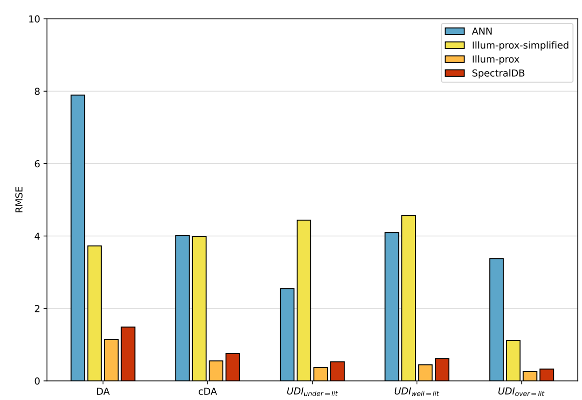

Fig. 10. Root Mean squared error (RMSE) of annual performance values across the simulation grid range relative to AHR

VI. Discussion

Annual daylight results (Fig. 9 and 10) indicate that illuminance-proxy performs better that the other methods, showing less than 10% error relative to the model corresponding to AHR technique. However, significant errors exist when geometrical simplification is applied.SpectralDB also shows good agreement with the ground truth, however, significant errors exist when this comparison is done for visible reflectance values as shown in Fig. 7.Such errors are more than 10% for a few surfaces, namely *White desk*, *Floor*, *Plinth*, *Walls-plaster*, *Windows-sill*, and *Flower box*.

TABLE I
INTERPOLATED ILLUMINANCE MAP, REFLECTANCE MAP, AND MEAN REFLECTANCE FOR FIVE MAIN SURFACES OF THE STUDIED ROOM

Surface name	**Input HDR map [cd/m^2]**	**Illuminance map[lx]**	**Reflectance map[0-1]**	**Mean reflectance**
Wall1	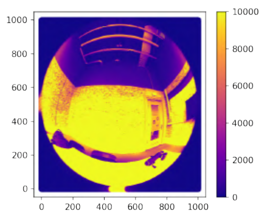	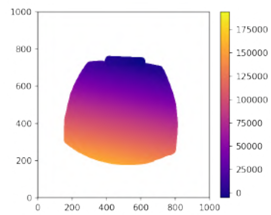	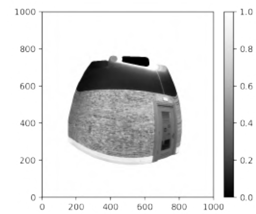	0.481
Wall2	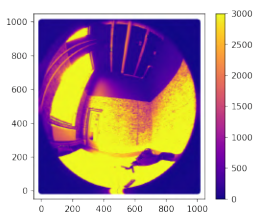	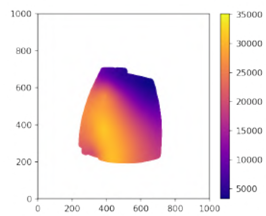	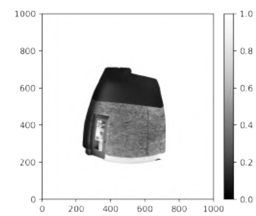	0.361
Wall3	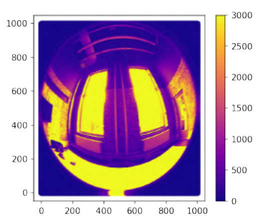	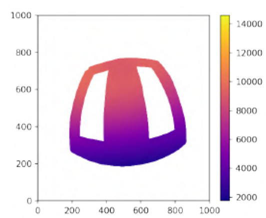	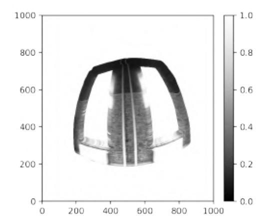	0.42
Wall4	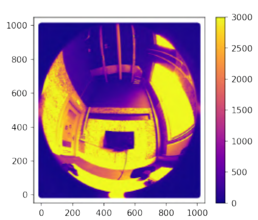	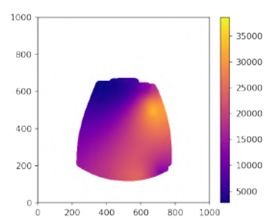	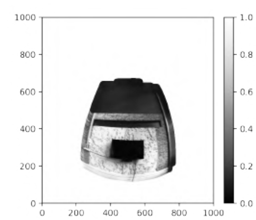	0.44
Ceiling	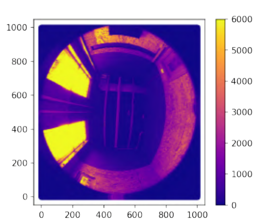	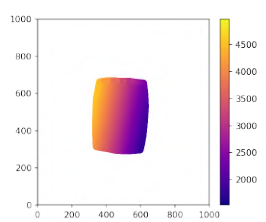	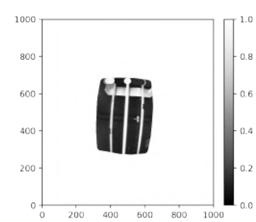	0.36

There are three underlying assumptions in the illuminance-proxy method:

1) The area of interest does not have significant protrusions and is flat.
2) The light that falls onto each surface has smooth illuminance variations.
3) All of the surfaces and materials in the FOV are diffuse.

Any geometrical and lighting conditions deviating from these assumptions will cause error in the final results. A possible source of errors in many cases is the existence of specular surfaces, resulting in over-prediction of average reflectance, and consequently, daylight results. This over-prediction has been significant for two specular surfaces, namely *silver ducts*, *radiators* (see Fig. 7) and *wall3*(see Section IV-B3). This outliers might also be partly caused by abrupt changes in the illuminance levels on the areas close to the windows, which can be the result of inaccurate masking of the opening areas. According to annual average results, ANN has less than 5% error in the calculation of DA, cDA, $UDI_{under-lit}$ (Fig.9).

Fig. 11. Rendered scene corresponding to each measurement scenario, from left to right: (1) AHR, (2)SpectralDB, (3)Illuminance-proxy, (4) Illuminance proxy with geometrical simplification,and (5)ANN

However, except for *White desk*, *Doors*, *Walls-plaster*, and *Silver duct*, it estimated the visible reflectance with significant error. The predicted specularity results are not realistic, while seven (out of fifteen) predictions for roughness are close to those suggested by SpectralDB for a similar material (Fig. 8). Five renderings of the room (Fig. 11), corresponding to each scenario reveals the inaccurate predictions of ANN.
Inaccurate predictions of ANN is also confirmed by analysing hourly illuminance values for all the grid points with RMSE of31.62 for illuminance-proxy, 98.52 for illuminance proxy(simplified), 44.02 for SpectralDB, and 270.75 for ANN.

VII. Conclusion

In this study, four material characterization scenarios are implemented to define material properties of opaque surfaces in a single meeting room. Accuracy of these methods are evaluated both by comparing the reflectance values, and by annual daylight provision metrics. Illuminance-proxy has shown promising results for pixel-wise reflectance characterization and proved to be a powerful alternative for manual point-by-point measurements of luminance and illuminance (AHR) as a common approach. Nevertheless, this method is prone to error specially when a specular surface is in the FOV. Manual selection of materials from SpectralDB has also shown to give accurate results compared to ANN. Still, all the scenarios showed acceptable results in predicting average annual performance metrics, i.e., DA, cDA, and $UDI_{\text{well-lit}}$ with less than 5% error, while significant error exists in calculation of material properties, namely reflectance and specularity. Both methods have potentials in digitizing the process of daylight modeling. Illuminance proxy reduces the measurement costs by reducing the number of AHR and offers pixel-wise material reflectance map of areas within the FOV. This is a good solution for complex surfaces.
This project is limited in some aspects, which will be described in the next paragraphs. Future research will address these limitations.

- *Reliable ground truth measurement.* Average Hemispherical Reflectance (AHR) technique is used as the ground truth value for visible reflectance in this study. Since this method does not capture detailed information regarding the five key optical properties, a similar material from a measured data set (SpectralDB) is used to check the validity of the ANN outputs for specularity and roughness (see Fig. 8). Even in that data set, the roughness values assigned to each material are not coming from accurate measurements and are based on a rule of thumb introduced by Jones and Reinhart [15]. A more reliable data measured in the studied space is needed to check the validity of the outcomes. This can be done using reflectance spectrophotometers [16].
- *Error measurement for illuminance proxy.* In this study, daylight results were used to quantify the errors associated with the uncertainties in the illuminance proxy method (see Section VI). To do this task more reliably, a predicted mean reflectance should be calculated based on accurate measurements.
- *Improved learning approaches.* In this study a simple neural network, consisting of one hidden layer with 16 neurons, with linear activation is used. This simple architecture does not capture the capabilities of probabilistic methods. In future research, this will be addressed by generating other training datasets under a certain lighting condition, which is reproducible in the indoor space. This will be done to reduce the uncertainties concerning the lighting conditions. Furthermore, other learning architectures proven to perform well on material classification task will be adapted to the problem of this research [17, 18]. Lastly, based on the reliable results from manual selection of materials (SpectralDB), approaching the learning-based material characterization as a classification, rather than regression (as done in this study) might give more accurate results and will be further developed in the future studies.

VIII. Acknowledgement

We thank Dr. Stef Lhermitte for useful discussions.

References

[1] Ann R. Webb. “Considerations for lighting in the built environment: Non-visual effects of light”. In: *Energy and Buildings* 38.7 (July 2006), pp. 721–727. ISSN: 03787788. DOI: 10.1016/J.ENBUILD.2006.03.004.

[2] *EU Buildings Database*. URL: https : / / ec . europa . eu / energy / eu - buildings - database_en (visited on 01/17/2022).

[3] Eleonora Brembilla, Christina J Hopfe, and John Mardaljevic. “Influence of input reflectance values on climate-based daylight metrics using sensitivity analysis”. In: *Journal of Building Performance Simulation* 11.3 (2018), pp. 333–349.

[4] John Mardaljevic, Eleonora Brembilla, and Nafsika Drosou. “Illuminance-proxy high dynamic range imaging: a simple method to measure surface reflectance”. In: (2015).

[5] Nafsika Drosou and John Mardaljevic. *Real World Complexity in Reflectance Value Measurement for Climate-Based Daylight Modelling - Data*. 2016. DOI: 10.17028/rd.lboro.3364747.v2.

[6] Sean Bell et al. “Material Recognition in the Wild with the Materials in Context Database”. In: *Proceedings of the IEEE Computer Society Conference on Computer Vision and Pattern Recognition* 07-12-June (Dec. 2014), pp. 3479–3487. ISSN: 10636919. DOI: 10.48550/arxiv.1412.0623. arXiv: 1412.0623. URL: https://arxiv.org/abs/1412.0623v2.

[7] *OpenSurfaces - A Richly Annotated Catalog of Surface Appearance*. URL: http://opensurfaces.cs.cornell.edu/ (visited on 05/04/2022).

[8] Michael Weinmann, Juergen Gall, and Reinhard Klein. “Material Classification Based on Training Data Synthesized Using a BTF Database”. In: *Lecture Notes in Computer Science (including subseries Lecture Notes in Artificial Intelligence and Lecture Notes in Bioinformatics)* 8691 LNCS.PART 3 (2014), pp. 156–171. ISSN: 16113349. DOI: 10.1007/978-3-319-10578-9_11. URL: https://link.springer.com/chapter/10.1007/978-3-319-10578-9_11.

[9] B Andres et al. “Vision, Modeling, and Visualization (2021) Capturing Anisotropic SVBRDFs”. In: (2021). DOI: 10.2312/vmv.20211372. URL: https://diglib.eg.org.

[10] Alstan Jakubiec. *Spectral Materials Database*. URL: http://spectraldb.com/ (visited on 03/28/2022).

[11] Rabia Rashdi et al. “Scanning Technologies to Building Information Modelling: A Review”. In: *Infrastructures* 7.4 (2022), p. 49.

[12] John Mardaljevic et al. “A hybrid measurement-simulation approach to determine the reflectance map of a historic tapestry”. In: *Building Simulation 2021 Conference: BS2021*. International Building Performance Simulation Association. 2021.

[13] Gregory J Ward. “The RADIANCE lighting simulation and rendering system”. In: *Proceedings of the 21st annual conference on Computer graphics and interactive techniques*. 1994, pp. 459–472.

[14] Mostapha Sadeghipour Roudsari, Michelle Pak, Adrian Smith, et al. “Ladybug: a parametric environmental plugin for grasshopper to help designers create an environmentally-conscious design”. In: *Proceedings of the 13th international IBPSA conference held in Lyon, France Aug*. 2013, pp. 3128–3135.

[15] Nathaniel L Jones and Christoph F Reinhart. “Experimental validation of ray tracing as a means of image-based visual discomfort prediction”. In: *Building and Environment* 113 (2017), pp. 131–150.

[16] Greg Ward and Rob Shakespeare. *Rendering with Radiance: the art and science of lighting visualization, Chapter 5*. Randolph M.Fritz, 1998.

[17] Hanxiao Liu et al. *Hierarchical Representations for Efficient Architecture Search*. 2017. DOI: 10.48550/ARXIV.1711.00436. URL: https://arxiv.org/abs/1711.00436.

[18] Adrian de Wynter. “On the Bounds of Function Approximations”. In: *Artificial Neural Networks and Machine Learning – ICANN 2019: Theoretical Neural Computation*. Springer International Publishing, 2019, pp. 401–417. DOI: 10.1007/978-3-030-30487-4_32. URL: https://doi.org/10.1007%2F978-3-030-30487-4_32.

Color Rendering Evaluation Using Metameric Pairs and D&H Color Rule

1st Michal Vik
Dept. of Material Engineering
Technical University of Liberec
Liberec, Czech Republic
ORCID: 0000-0002-1170-2388

2nd Martina Viková
Dept. of Material Engineering
Technical University of Liberec
Liberec, Czech Republic
ORCID: 0000-0002-6254-4834

3rd Azmary Akter Mukthy
Dept. of Material Engineering
Technical University of Liberec
Liberec, Czech Republic
ORCID: 0000-0003-3949-432X

***Abstract* — The color rendering methods of light sources are a very important criterion in assessing their quality. Apart from the color rendering itself, which can be assessed for example by color constancy, the biggest concern for the end customer is the metameric effect. This can be assessed by simple tools such as selected metameric pairs of samples. In this paper, attention is paid to the use of the Davidson and Hemmendinger Color Rule (D&H color rule) as a simple aid to assess the quality of light sources. The D&H color rule consists of two strips of approximately constant brightness, one going from purple at one end to grey to green at the other end and the other from blue to grey to brown. From the code on the back of the rule, it is possible to read out the areas in which an object matches the colors of the two slides under the illumination tested. By knowing the spectral reflectance of each part of the two strips and the spectral composition of the radiation emitted by the light sources tested, the minimum color difference can be calculated and compared with the results of the visual judgements. The results obtained are then compared with existing standard color rendering evaluation methods such as Ra and TM-30-2020 Rf.**

Keywords—metamerism, color, light source, color rendering, color difference

I. Introduction

The evaluation of the color rendering quality of different artificial light sources is carried out using several indices based on two different principles. The first is the direct evaluation of the color differences of a selected set of samples under a reference and tested light source, such as CIE Ra [1], CIE CFI [2], ANSI/IES TM-30-20 [3]. In the second case, the position of the preferred color of the object is included in the calculation of the respective color difference, this includes the Sanders color index Rp [4], Judd's Flattery index [5], Thorton index [6], or Smet index MCRI [7]. Basically, two different aspects of color perception are evaluated. On the one hand, there is the somewhat adapted perception of a particular color induced by the light source under investigation and, on the other hand, there are mainly memory colors and their influence on the human psyche, whether conscious or unconscious. However, the user encounters another phenomenon related to the confusion of light sources, namely metamerism. If we use the International Electrotechnical Dictionary [8], we can state that metamerism is the property of spectrally different color stimuli having the same tristimulus values in a specified colorimetric system. But what does this mean in practice. In many applications we encounter the need to achieve identical color in products or parts of products when these are made of different materials. For this reason, the use of different dyes or color pigments is necessary. The consequence is that color stimuli with different spectral reflectance result in parts appearing to be identical in color under certain lighting and viewing conditions and then appearing to be different in color when these conditions are changed (change of light source or observer). Metameric colors, on the other hand, allow the assessment of color differences or color matching only for the light source under test, without the need for a reference light source. This also has the advantage of allowing the user to verify the quality of the light source using a simple visual tool.

Normal color vision is known to be trichromatic. Any color stimulus can be defined by three quantities that correspond to the quantum yield of the three types of cones in the retina. Thus, the human visual system reduces the physical information contained in the light spectrum to three signals - spectral responses. This explains metamerism, the property of colored stimuli that are spectrally different and yet can be perceived as identical, i.e., having the same tristimulus values. In the case of metameric pairs, these are pairs of samples that usually appear to be identical under a certain comparative illumination, such as CIE D65, A or F11.

To assess the magnitude of the metameric color difference, pairs of samples were developed on different substrates such as fabrics, coated paper, or coatings. Several metameric samples such as the Garner test [9] or the Glenn Colorule test [10] are a special case. Both the Garner test and Glenn Colorule were produced as a series of dyed textiles, which is not very practical due to easy soiling and lower stability. Therefore, the Davidson and Hemmendinger Color Rule (D&H Color Rule) was prepared as series of coated patches in the 1960s [11]. D&H Color Rule is a rectangular tool measuring 36.7 X 7.8 cm. In the center is a rectangular hole measuring 3.2 X 3.5 cm. Through this hole, you can see part of the two-color slides that are the working mechanisms of the rule. Observers are asked to move the slides back and forth until the two halves visible through the hole look the same or nearly the same, essentially creating a metameric match. One slide contains samples marked on the back with the letters A through U, which change color from purple to green through neutral gray. The other slice contains samples varying in color from blue to brown through neutral grey, which are marked on the reverse side with the numbers 1 to 21. The observer places a D&H Color Rule under the appropriate illuminant and adjusts the slides back and forth until the top and bottom halves match in color. The D&H Color Rule is then rotated to determine the combination of numbers and letters for which there is a metameric match.

II. Materials and Methods

For the initial test, 4 light sources with a CCT of approximately 4000 K were selected. These were two triband fluorescent lamps (Osram L 18W/840 Hellweis Lumilux Cool White 840, Phillips Master TLD 30W/840) and two LED linear sources (a Voltolux LED SMD2835-T8-60-MAT-9W retrokit and a YUJILEDS CRI 98 8.6 W LED linear module).

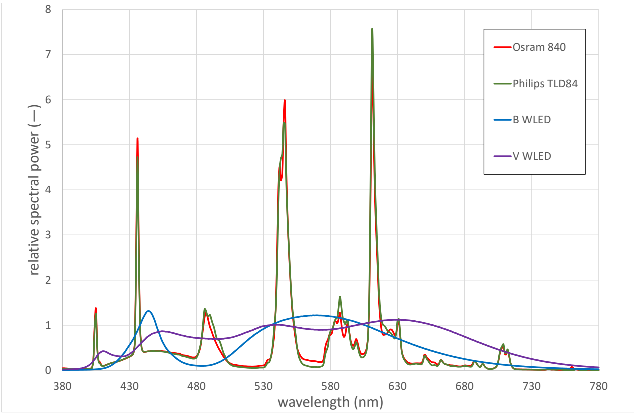

Fig. 1. Map of color differences in CIELAB – Osram 840/2°

The light technical parameters of these light sources are shown in Table 1 and spectral power distribution is visible on graph in Figure 1 above.

TABLE I. PARAMETERS OF TESTED LIGHT SOURCES

Color coordinates	4000 K light sources			
	Osram Lumilux 840	*Philips Master TLD840*	*Voltolux B WLED*	*YujiLEDS V WLED*
X	98.54	101.09	97.40	100.16
Y	100	100	100	100
Z	58.98	57.56	59.79	71.87
x	0.3827	0.39083	0.3787	0.3682
y	0.3883	0.38663	0.3888	0.3676
u'	0.2220	0.22795	0.2193	0.2206
v'	0.5069	0.5074	0.5065	0.4957
Tcp	4033	3804.7	4129	4290
Duv	0.0047	0.0017	0.0065	-0.0005
CIE Ra	81	83	65	98
R9	12	13	-47	92
TM-30-18 Rf	79	82	68	97
TM-30-18 Rg	98	100	92	101

All light sources were placed in a light box, the walls and sample holder of which were painted with an achromatic light grey paint N7 according to Munsell's nomenclature. A D&H Color Rule was placed in the sample holder. The observer made visual judgements in a 45°:0° geometry at approximately 40 cm distance. Eight observers with normal color vision, superior and average color discrimination, respectively, participated in the visual assessment according to the FM 100 Hue color vision test. Visual assessments were performed repeatedly on different days, with each observer performing three baseline sessions for each light source, where they were asked with finding the position of the D&H Color Rule slides at which the samples appeared to be in color match. The observer then had to determine the maximum acceptable slide displacement in both the left and right directions to maintain an approximate color match in the viewing window. In principle, this produced 5 individual judgments of a single light source at each session, for a total of 480 individual judgments.

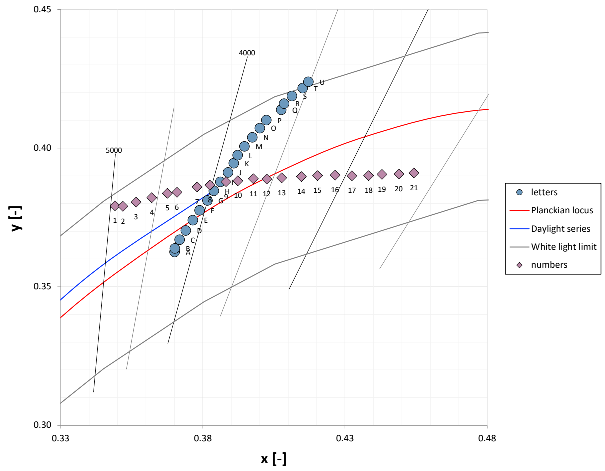

Fig. 2. D&H Color Rule patches in CIE x,y diagram – Osram 840/2°

III. Results and Discussion

In the case of metameric samples, the metameric index is usually used as a measure to evaluate the variation in color difference that occurs between two samples under two different illuminations. Since in our case the subject of evaluation was the relative position of the D&H Color Rule slide (Fig. 2 and Fig. 3), the frequency of occurrence of each position was observed for the observed light sources in the case of visual judgments, and the relative color differences of each D&H Color Rule position for the respective illuminations were calculated in the case of objective evaluation. For each light source, a map of the color deviations that may occur for the D&H Color Rule was thus created. The color differences were calculated for both the CIELAB color space and CIECAM16 because the CIELAB system is often criticized for incorrect application of the von Kries adaptation.

The graphs in Figures 3, 4, 5 and 9 show the color difference maps, if the smaller color difference induced by a given light source, the easier it will be to visually identify such a metameric match. In other words, a higher slope of contours marking the same color difference means a higher focus on the metameric color match. In the case of both triband fluorescent lamps and the blue pumped white LED retrokit from Voltolux (B WLED), the color difference maps are similar. On the other hand, the linear violet pumped white LED module made by YUJILEDS (V WLED), which shows a high color rendering index or TM-30-18 rating, shows both the lowest color difference achieved, but also the highest slope of the individual color difference contours.

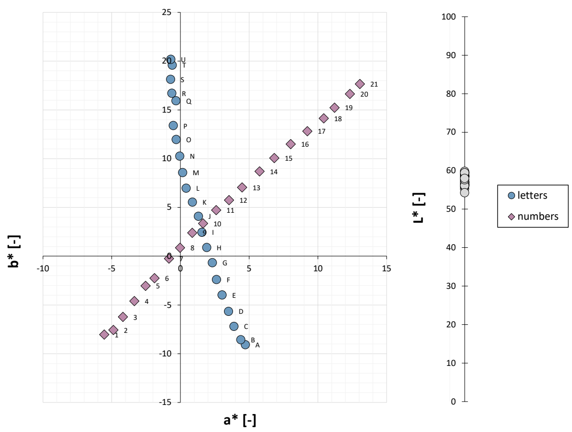

Fig. 3. D&H Color Rule patches in CIELAB – Osram 840/2°

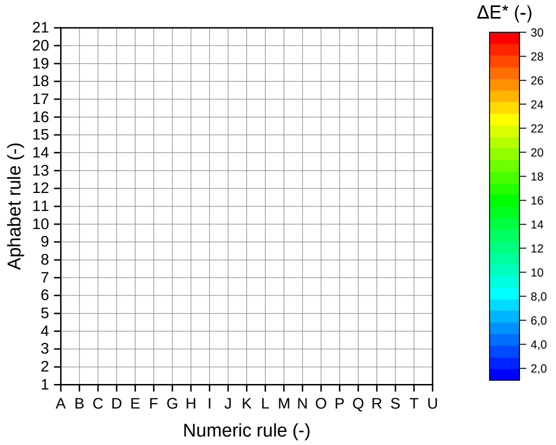

Fig. 4. Map of color differences in CIELAB – Osram 840/2°

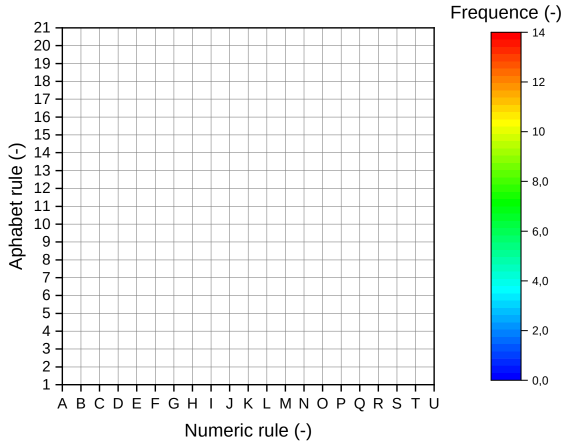

Fig. 7. Map of color visual match – Osram 840

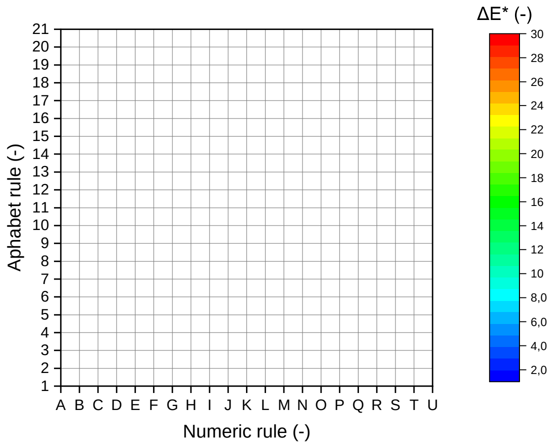

Fig. 5. Map of color differences in CIELAB – Philips TLD840/2°

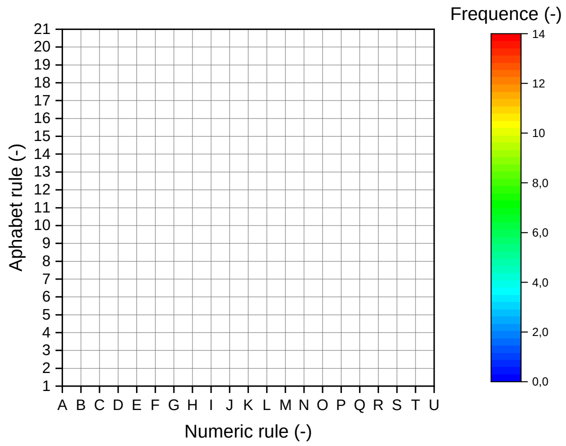

Fig. 8. Map of color visual match – Philips TLD840

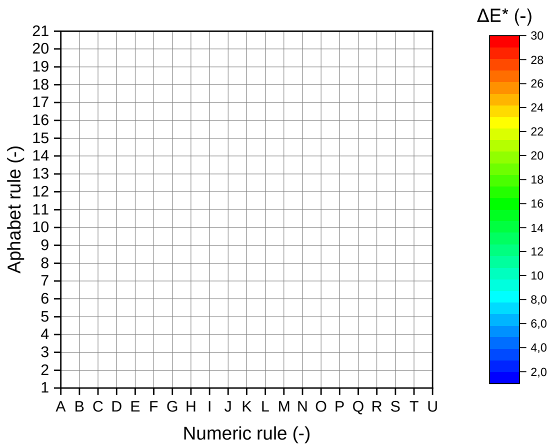

Fig. 6. Map of color differences in CIELAB – B WLED/2°

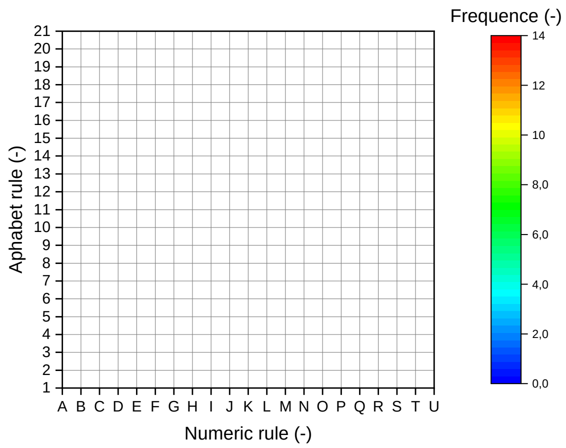

Fig. 9. Map of color visual match – B WLED

A similar result can be seen in the graphs in Figures 6, 7, 8 and 10, which show frequency maps documenting the number of metameric matches for each sample combination produced by the D&H Color Rule shift. It is also apparent that some outlier visual ratings (small indents in the maps) follow a diagonal direction, as do the color difference maps.

All the plots, both the color difference maps and the metameric match frequencies in the visual assessment, document the diagonal shift of the focal point as a function of the CCT of the source under test. The Philips TLD840 triband fluorescent lamp, which exhibits a CCT of approximately 3800 K, has a focal point of judgments at position H8.

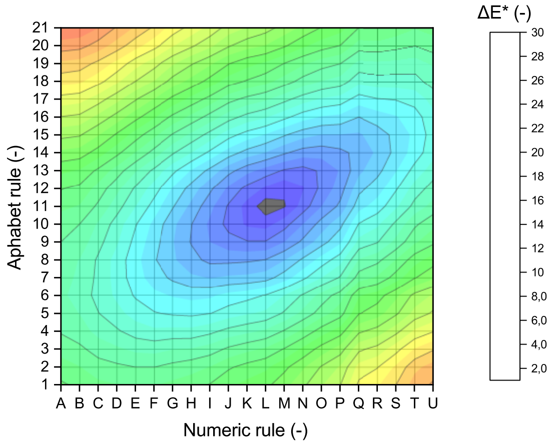

Fig. 10. Map of color visual match – V WLED

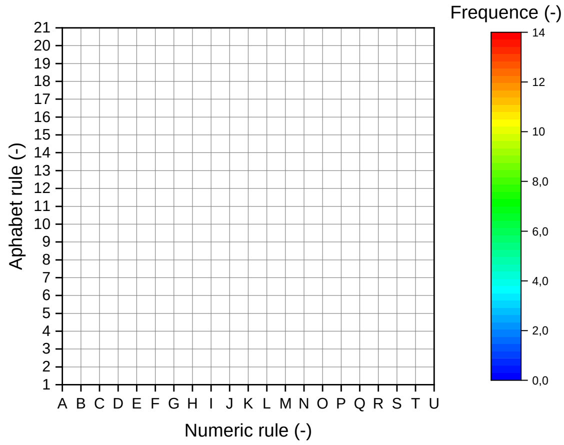

Fig. 11. Map of color visual match – V WLED

Osram 840 triband fluorescent lamp with a CCT of approximately 4000 K at position H9, the blue pumped white LED with a CCT of approximately 4100 at position I10, and the violet pumped white LED with a CCT of approximately 4300 K at positions L11 and K11, respectively. This demonstrates the sensitivity of the D&H Color Rule to both the color rendering quality of the tested light sources and the respective CCT.

IV. Conclusion and Future Work

Metamerism as a phenomenon poses a great challenge in terms of the development and production of the final product, whether it is a fashion clothing collection or a car interior. On the other hand, it has been documented here that a relatively simple tool like the D&H Color Rule can be very useful for lighting technology. The D&H Color Rule was shown to be a convenient tool for diagnosing the various manifestations defective color vison, here it was demonstrated that the D&H Color Rule allows for a qualitative evaluation of light sources and that these results agree with the evaluation according to both the TM-15-20 methodology and the CIE color rendering index Ra.

Future work should include a theoretical analysis of the long-term repeatability of visual judgments for individual raters, and it is also planned to extend the research to a larger number of light sources involving a wide range of surrogate chromaticity temperatures and color rendering quality.

Unfortunately, it must be stated that the D&H Color Rule is no longer in production and its availability is thus significantly limited, however the authors believe that this research could provide some challenge to potential manufacturers.

Acknowledgment

This publication was written at the Technical University of Liberec as part of the Student Grant Competition under the project number SGS-2020-6038, as provided by the Ministry of Education, Youth and Sports of the Czech Republic in the year 2020.

References

[1] CIE, "CIE 13.3-1995 method of measuring and specifying colour rendering properties of light sources," (Commission Internationale de l'Eclairage), 1995.

[2] CIE, CIE 224:2017 CIE 2017 Colour Fidelity Index for Accurate Scientific Use (CIE Central Bureau), 2017.

[3] ANSI/IES TM-30-20+E1 *IES Method for Evaluating Light Source Color Rendition*, Illuminating Engineering Society, 2020.

[4] C.L. Sanders, Colour preferences for natural objects. *Journal of the Illuminating Engineering Society*, (54), 452–456, 1959.

[5] D. B. Judd, Flattery Index for Artificial Light Illuminants, *Illuminating Engineering*, 593-598, 1967

[6] W.A. Thorton, Luminosity and Color-Rendering Capability of White Light, *J. Opt. Soc. Am.* 61 (9), 1155-1163, 1971

[7] K. Smet, W. R. Ryckaert, M. R. Pointer, G. Deconinck, and P. Hanselaer, "Correlation between color quality metric predictions and vis- ual appreciation of light sources," *Opt. Express* 19, 8151–8166, 2011.

[8] IEC 60050-845, *International Electrotechnical Vocabulary (IEV) – Part 845: Lighting*, 2020

[9] W. Garner, Colour Matching and Colour Blindness, J. Soc. D. Col. 58 (4), 65-71, 1942

[10] M. W. Ballard, Measuring your color vision with a Glenn Colorule, *The Textile Specialty Group Postprints*, American Institute for Conservation of Hystoric and Artistic Works, 40th Annual Meeting, Albuquerque, New Mexico, 2012

[11] H. Hemmendinger and H. R. Davidson, ''Color measurement in industry,'' *Proc. Symp. on Colour Measurement in Industry*, Imperial College, London, 1967.

A Mixed Methods Approach to Measuring Pedestrian Reassurance

Steve Fotios
School of Architecture
University of Sheffield
Sheffield, UK
steve.fotios@sheffield.ac.uk

Jim Uttley
School of Architecture
University of Sheffield
Sheffield, UK
j.uttley@sheffield.ac.uk

Shahab Gorjimahlabani
School of Architecture
University of Sheffield
Sheffield, UK
sgorjimahlabani1@sheffield.ac.uk

***Abstract*—This paper discusses three methods that might be used to measure the effect of road lighting on pedestrian reassurance, research needed to ensure robust guidance for pedestrian lighting. The three methods are quantitative subjective evaluations (reassurance ratings), qualitative subjective evaluations (interviews) and observation of activity. Given the advantages and disadvantages of any one of these methods, it is suggested that a mixed methods approach is needed. It is further suggested that the effect of lighting on crime needs to be considered in parallel to determine that the apparent enhancement of reassurance does not give false confidence that it is safe to walk.**

***Keywords*—road lighting, pedestrians, reassurance**

I. Introduction

One aim of lighting on minor roads is that pedestrians are reassured that it is safe to walk after dark [1]. People tend to walk less when they do not feel safe [2,3], contributing to an increase in motorised traffic. While some lighting is good for reassurance, and more lighting is better, any recommendations need to consider that for other reasons (such as reductions of energy use or sky glow) there is a preference for less, or even no lighting after dark. There is therefore a need to optimise the provision of lighting after dark.

The optimal lighting conditions for pedestrian reassurance have yet to be established [4], along with identification of the critical factors of influence. One problem in establishing optimal conditions is that measurement is not straightforward. Here we describe three different methods for measuring the degree of reassurance offered to pedestrians by road lighting: quantitative subjective evaluations (reassurance ratings), qualitative subjective evaluations (interviews) and observation of activity.

II. Quantitative Subjective Evaluations

The most widely used method is to ask pedestrians to describe how safe they feel using a rating scale, where a low feeling of safety might be given the value of 1 and a high feeling of safety the value of 6. The evaluation is repeated in multiple roads of different illuminance to test whether a change in illuminance changes the feeling of safety [5-7]. We focus discussion here on illuminance, the most commonly targeted attribute of lighting, but spectrum-derived characteristics and spatial variation in illuminance (e.g. uniformity) have also been considered.

Within any one particular study, with this method it is generally found that higher light levels lead to a higher feeling of safety [8].

Three key limitations of this method are the use of questionnaires, stimulus range bias, and changes in the local environment.

Unless they are designed carefully, questionnaires may not be measuring what the experimenter intended. The ease with which it is possible to type out a list of questions, to make a large number of photocopies, and to gain a large number of responses is perhaps an attractive offer for the busy researcher, but may be leading to misleading findings [9-11]. Questionnaire design is rarely mentioned in previous studies. What is needed are measures with which to objectively verify response credibility, such as attention checking questions, repeated use of identical (or, near identical) questions, and inclusion in the test procedure of test conditions predicted a-priori to give negligible and extreme responses.

Stimulus range bias is the tendency for respondents to map the range of observed scenes onto the range of available options [12,13]. If the observed scenes range from 1 lx to 10 lx and are evaluated with the 6-point scale described above, then 1 lx will tend towards a low feeling of safety and 10 lx to a high feeling of safety. If instead the observed scenes range from 10 lx to 20 lx then then 10 lx will tend towards a low feeling of safety and 20 lx to a high feeling of safety. In these two examples, 10 lx is associated with low and high feelings of safety, according to the experimenter's choice of the stimulus range. The influence of stimulus range has been demonstrated directly in evaluations of perceived safety [8], it has been demonstrated indirectly by comparing the results of different studies evaluating the same issue but using different ranges of illuminance [8], it has been demonstrated to explain the results of previous experiments [14,15] and has been shown to affect evaluations of preferred light level and discomfort from glare [16-20]. Stimulus range bias produces confusions when interpreting experimental results. Within any one experiment, it means a tendency to reach the conclusion that the higher illuminance is better, regardless of what illuminances were evaluated. If the experimenter interprets an absolute meaning from the results (e.g. 10 lx will mean evaluations of high safety) then studies using different ranges will disagree. Instead, we should draw only relative conclusions.

Typically, evaluations are carried out in locations of different illuminance. In which case, there may be observable changes in the environment other than the lighting, such as those informing evaluations of prospect, refuge and signs of incivility. This method therefore confounds the underlying physical environment of a location with any effect of lighting.

The day-dark method introduced by Boyce et al [21] and used subsequently by others [22] overcomes some of these problems. In this method, evaluations are sought in daylight and darkness at the same location: analyses are conducted using the difference between these evaluations, with good lighting identified by a smaller day-dark difference. The day evaluations provide a datum for dark evaluations at that same location, therefore offsetting differences due to location. It may mitigate stimulus range bias but that remains to be validated.

A limitation of the day-dark method is that the two evaluations are carried out at different times of day. However, time of day may influence other factors which influence reassurance, such as the types and numbers of other pedestrians and vehicular traffic. A different approach would be to conduct day and dark evaluations at the same time of day, but take advantage of the daylight savings clock change to provide a rapid transition from daylight to darkness.

A field study was conducted to test this proposal. 56 test participants were asked to evaluate reassurance at six urban residential roads in Sheffield, UK. This was done over the six days before and after clock changes in Autumn 2021 and Spring 2022. Consider the Autumn 2021 clock change. Evaluations in the week before clock change were carried out from 25th to 30th October at 12:00pm to 1:15pm and 5.00pm to 5:45pm, with both evaluations being conducted in daylight as defined by a solar altitude of greater than 0°. Evaluations in the week after clock change, 1st to 6th November, were carried out at 5.00pm to 5:45pm, with this period now being defined as darkness by a solar altitude of less than -6°. The small time windows are essential to avoid inclusion of civil twilight in either the day or dark periods, and this limited the number of locations that could be evaluated. The experiment followed a repeated measures design and the six locations were evaluated in randomised orders by participants in groups of six or less.

Participants evaluated the degree of reassurance (and other factors) at a certain location condition using a series of category scales. For reassurance, the four questions were:

1. *How risky do you think it would be to walk alone here at night?*
2. *How safe do you think this street is?*
3. *How anxious do you feel when walking down this street?*
4. *I would rather avoid this street if I could.*

Responses were given using a 6-point response scale with the end points labelled (e.g.) *not at all risky* and *very risky* subsequently coded for analysis so that 6 indicates the greater degree of reassurance. The response scales for some questions were reversed to counter the assumption that one or other end of the scale was always the more positive response. Bogus questions [23] were included to test for attentive responding.

Analysis of these data are ongoing. Fig. 1 shows the mean differences between daylight (mid-day or evening) and dark evaluations, as averaged across the 56 test participants and the four reassurance questions, for each of the six roads, and for the two methods of defining daylight conditions. For four of the six roads, the day-dark difference is greater when the daylight evaluations were given at mid-day than when given at the same time of day as the dark evaluations: for one road the direction of this difference is reversed and in one road there is no difference. In any case, the error bars do not suggest a significant difference: this is the focus of ongoing analysis.

By explicitly focussing participants' attention on road lighting, and revealing differences between different lighting conditions, questionnaires force a conclusion that road lighting matters. The next two methods, much less widely used, were established in an attempt to avoid that explicit focus.

III. OBSERVATION OF ACTIVITY

The second method is to count the number of people participating in a certain activity, here, walking. Assuming that a greater feeling of reassurances means more people choose to walk [24], this would measure the reassurance benefit of higher illuminance if counts were made in locations of different illuminance and if the counts were made at moments of time strategically chosen to isolate the effect of light from other factors.

This method has been used mainly, to date, to test the influence of ambient light level on walking – for a given time of day, do fewer people walk when it is dark than when it is daylight? [25-27]. Those studies have used the daylight savings clock change, or the seasonal variation in daylight hours, to distinguish between daylight and darkness for the same time of day, and have used control hours (permanently daylight, or, permanently dark) within an odds ratio to account for other changes such as season and weather. The numbers of pedestrians passing each of a series of specific locations were recorded using publically-available data from automated counters installed by others, these giving access to large data sets. Analyses have been conducted for 14 locations in Cambridge (UK) and about 22 locations (from 5 to around 30, depending on year and season) in Arlington (Virginia, USA): the results confirm, as expected, that fewer people walk in darkness than in daylight [25-27].

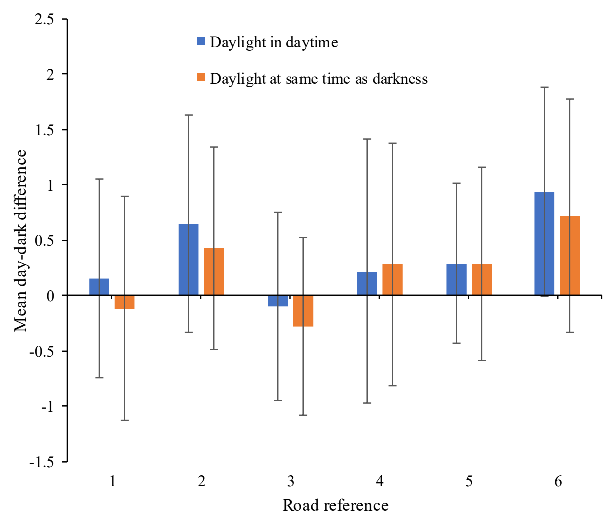

Fig. 1. Mean differences between daylight and dark evaluations of reassurance. These are the means of the 56 test participants in the autumn and spring field studies. Error bars show one standard deviation above and below the mean.

To show the effect of changes in illuminance it is possible to plot the ORs for each location against the illuminance at that location. Whilst this has been done for cyclists [28], using aerial images to estimate light levels, this has yet to be done for pedestrians.

There are however some limitations of the data from automated counters. One is that the data reveal the numbers of pedestrians but do not reveal their characteristics, and age and gender are expected to affect walking decisions [29-31].

To reveal these latter data a travel count survey was conducted using on-road observers rather than automated counters [32]. This enabled the apparent age and gender of each pedestrian to be recorded. The counts were made at eight urban locations in Sheffield, for six days before (Monday 22/3/2021 to Saturday 27/3/2021) and six days after (Monday 29/3/2021 to Saturday 3/4/2021) the spring 2021 clock change. The case hour was 19:00 to 19:59, with this hour being predominantly in darkness before the clock change (the latest end of civil twilight during the week before the clock change being 19:07) and in daylight after the clock change (the earliest onset of civil twilight in the week after the clock change being 19:34). The control hour was 16:00-16:59, this hour remaining in daylight during the entire data collection period. Observed pedestrians were allocated into one of three age groups, <30, 30-59, and >59 years: comparisons of age were drawn by comparing the older and younger of these groups.

The odds ratios were calculated as shown in equation (1).

$$\text{Odds Ratio} = \frac{\text{CaseDay/CaseDark}}{\text{ContolDay/ControlDark}} \quad (1)$$

Where

- CaseDay is the number of pedestrians in the case hour after the Spring clock change
- CaseDark is the number of pedestrians in the case hour before the Spring clock change
- ControlDay is the number of pedestrians in the control hour on days when the case hour would be in daylight
- ControlDark is the number of pedestrians in the control hour on days when the case hour would be in darkness

The results are shown in Table 1. The overall odds ratio of 1.56 shows that darkness led to significantly fewer pedestrians in the case hour. This lies between the odds ratios of 1.29 and 1.62 found using automated counters in previous studies in Cambridge [27] and Arlington [25] respectively: the use of on-site observation and resulting smaller samples does not appear to have distorted this overall estimate.

The odds ratios for younger (1.58) and older (3.38) pedestrians were suggested to be significantly different (p<0.001), indicating that darkness is a greater deterrent to old pedestrians than to young pedestrians.

The odds ratios for males (1.55) and females (1.59) were not suggested to be significantly different (p=0.302), which agrees with analysis of self-reported walking behaviour [30]. It disagrees, however, with conclusions drawn in studies using subjective evaluations of reassurance, which is that darkness leads to a significantly greater reduction in reassurance for females than for males [29,30].

TABLE I. ODDS RATIOS, 95% CONFIDENCE INTERVAL FOR THE EFFECT OF AMBIENT LIGHT LEVEL ON PEDESTRIAN COUNTS AND SIGNIFICANCE OF DIFFERENCE FROM 1.0

Pedestrian category	**Odds Ratio**	**95% CI**	***p***
Overall	1.56	1.49-1.64	p<0.001
Male	1.55	1.46-1.66	p<0.001
Female	1.59	1.48-1.71	p<0.001
Young	1.58	1.49-1.66	p<0.001
Old	3.38	2.29-5.00	p<0.001

IV. INTERVIEWS

The third method is to ask people about their experience of walking, using open-ended questions carefully scripted to stimulate discussion but without explicit focus on road lighting or fear [33]. If test participants were taken to different locations for these interviews, changes in lighting conditions may force their focus on lighting. Instead, they are first invited to submit photographs of places where they would and would not be happy to walk alone after dark. Clearly, asking for locations where you are not happy to walk alone *after dark* may prompt the participant to focus on lighting: it would be useful to establish a different way of asking this question.

The photographs are then used in a follow-up interview in which the experimenter asks the participant to explain their choice. To be clear, this is not an evaluation of how safe the pedestrian feels in the scene presented in the photograph, but instead the photograph is used as a prompt to remind them of their choice. The interviews are then transcribed and participants explanations are searched for themes as to why people might choose to walk along some paths but not others. The results have been used to compare the frequency with which lighting (or darkness) and other factors were raised during the interviews.

Fig. 2 shows the results from two studies using this method, the original work reported by Fotios *et al* [33] using 53 participants drawn from older and younger age groups, and a recent repetition [34] using twenty younger people (mean age 21 years). Both studies were carried out in Sheffield, UK. The data shown are the percentages with which each type of explanation was used. It can be seen that road lighting tends to be one of the more frequently given factors.

V. CRIME

One further aspect is the effect of lighting on those crimes committed in outdoor environments. There is little benefit in enhancing reassurance that it is safe to walk if there is no concurrent reduction in crimes against pedestrians, indeed that might just offer more potential victims.

Research about lighting and crime widely used as a source of evidence in the UK [35] is now out of date. Of the eight studies from the USA, seven were published in the 1970s; the remaining USA study, and the five from the UK were published in the 1990s. Characteristics of road lighting and crime have since changed.

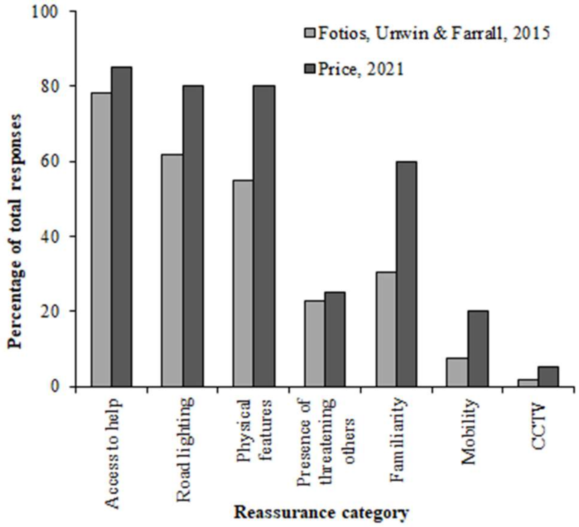

Fig. 2. Frequencies with which reasons were given for the choices of locations in which respondents were happy or not to walk alone after dark [33,34].

More recent research conducted in the UK [36] is hampered by the limited crime location data reported by UK police in the interest of preserving victim anonymity. Accurate date, time and location data are available for crimes reported in a sample of cities in the USA and this has been used in recent studies [37,38] albeit the effect of ambient light level rather than road lighting. A change in ambient light level is an interesting intervention because it reveals the impact on crime counts of a change in visibility but says nothing about community pride. A decrease in ambient light level, from daylight to darkness, for a given time of day, was suggested to bring a statistically significant increase in robbery but did not have significant effect on any other type of crime, including assault. Unless the enhanced community pride gained by the installation of new or improved road lighting offers significant and long term mitigation to assaults, then such installations may be giving false reassurance that it is safe to walk.

Further research is needed to establish the crime reduction effect of road lighting, in conjunction with the low probability of being involved in such a crime and the high probability that promoting walking is a great and broad benefit to public health.

VI. DISCUSSION

Three methods have been described for exploring the reassurance offered to pedestrians by road lighting that it is safe to walk after dark.

The first method asks participants to evaluate how safe they feel, a quantitative subjective evaluation, and this is repeated under lighting of different characteristics. Whilst this method is the most widely used, the degree to which responses are influenced by the forced focus on lighting and stimulus range bias remains to be validated. One improvement to this method is the day-dark analysis, and here we describe an experiment comparing two approaches for defining the daylight part of that analysis.

The second method overcomes the influence of subjectivity by observing people rather than asking them – a revealed preference rather than a stated preference. Specifically, the numbers of pedestrians passing a location at a certain time of day are counted when this time of day is either daylit or in darkness. To date, this method has been used to influence the impact of ambient light level on pedestrians, revealing that there are fewer pedestrians after dark: while the data can be extended to compare the effect of different lighting conditions, this has been done for cyclists [28] but not pedestrians. For cyclists, higher light levels reduce the deterrent effect of darkness, although there is a ceiling to this effect. Here we describe a study using in-person observation of pedestrians rather than data from automated counters which enabled age and gender to be recorded. The results revealed the surprising conclusion that the deterrent effect of darkness for women is not greater than that for males, as would otherwise be expected from subjective evaluations.

Observation of activity does not reveal any information about why there may be fewer pedestrians in some locations than in others. This can be explored in the third method, interviews. Data from two previous studies using this method reveal that the presence (or absence) of road lighting is one of the more frequent factors in the choices of routes pedestrians are happy to use (or avoid) after dark. This is a useful finding because the method aims to not force a focus on lighting, although the degree to which that is achieved remains to be shown. This method could be used to investigate the benefit of different lighting characteristics if the conditions at each location chosen by participants were recorded. However, such comparison may be trivial if each participant chooses different locations. If instead the experimenter asks about specific locations, then this brings a risk of forcing a focus on lighting.

The different methods of experiment enable different types of conclusions to be drawn about lighting and pedestrian reassurance: they each display different advantages and disadvantages. To establish optimal lighting conditions for pedestrian reassurance will require a mixed methods approach.

REFERENCES

1. British Standards Institution (BSI), "Code of practice for the design of road lighting part 1: Lighting of roads and public amenity areas," BS 5489-1:2020, London: BSI, 2020.
2. S. Foster, P. Hooper, M. Knuiman, H. Christian, F. Bull, and B. Giles-Corti, "Safe residential environments? a longitudinal analysis of the influence of crime-related safety on walking," IJBNPA, vol. 13(1), pp. 1-9, 2016.
3. P. Mason, A. Kearns, and M. Livingston, ""Safe going": the influence of crime rates and perceived crime and safety on walking in deprived neighbourhoods," Soc. Sci. Med., vol. 91, pp. 15-24, 2013.
4. Commission Internationale De L'Éclairage (CIE), "Lighting for pedestrians: A summary of empirical data," CIE 236:2019, Vienna: CIE, 2019.
5. L. J. Loewen, G. D. Steel, and P. Suedfeld, "Perceived safety from crime in the urban environment," J. Environ. Psychol., vol. 13, pp. 323-331, 1993.
6. A. Peña-García, A. Hurtado, and M. C. Aguilar-Luzón, "Impact of public lighting on pedestrians 'perception of safety and well-being," Saf. Sci., vol. 78, pp. 142-148, 2015.
7. A. Svechkina, T. Trop, and B. A. Portnov, "How much lighting is required to feel safe when walking through the streets at night?," Sustainability, vol. 12, pp. 3133, 2020.
8. S. Fotios, and H. Castleton, "Specifying enough light to feel reassured on pedestrian footpaths," Leukos, vol. 12, pp. 235-243, 2016.
9. S. Fotios, "Using category rating to evaluate the lit environment: Is a meaningful opinion captured?," Leukos, vol. 15, pp. 127-142, 2019.
10. J. Annett, "Subjective rating scales: science or art?," Ergonomics, vol. 45, pp. 966-987, 2002.

11. P. M. Boynton, and T. Greenhalgh, “Selecting, designing, and developing your questionnaire,” BMJ, vol. 328, pp. 1312-1315, 2004.
12. E. C. Poulton, “Bias in quantifying judgements”. London: Lawrence Erlbaum Associates Ltd., 1989.
13. E. C. Poulton, “Quantitative subjective assessments are almost always biased, sometimes completely misleading,” Br. J. Psychol., vol. 68:, pp. 409-425, 1977.
14. S. Fotios, “Review of a published article (Kakitsuba N. Comfortable indoor lighting conditions evaluated from psychological and physiological responses.),” Leukos, vol. 12, pp. 173-17, 2016.
15. S. Fotios, “Comment on of empirical evidence for the design of public lighting,” Saf. Sci., vol. 86, pp. 88-91, 2016.
16. S. A. Fotios, and C. Cheal, “Stimulus range bias explains the outcome of preferred-illuminance adjustments,” Light. Res. Technol., vol. 42, pp. 433-447, 2010.
17. Á. Logadóttir, J. Christoffersen, and S. A. Fotios, “Investigating the use of an adjustment task to set preferred illuminance in a workplace environment,” Light. Res. Technol., vol. 43, pp. 403-422, 2011.
18. Á. Logadóttir, S. A. Fotios, J. Christoffersen, S. S. Hansen, D. D. Corell and C. Dam Hansen, “Investigating the use of an adjustment task to set preferred colour of ambient illumination,” Col. Res. Appl., vol 38(1), pp. 46-57, 2013.
19. J. Uttley, S. Fotios, and C. Cheal, “Satisfaction and illuminances set with user-controlled lighting,” Archit. Sci. Rev., vol. 56, 306-314, 2013.
20. M. G. Kent, S. Fotios, and T. Cheung, “Stimulus range bias leads to different settings when using luminance adjustment to evaluate discomfort due to glare,” Build. Environ., vol. 153, pp. 281-287, 2019.
21. P. R. Boyce, N. H. Eklund, B. J. Hamilton, and L. D. Bruno, “Perceptions of safety at night in different lighting conditions,” Light. Res. Technol., vol. 32, pp. 79-91, 2000.
22. S. Fotios, A. Liachenko Monteiro, and J. Uttley, “Evaluation of pedestrian reassurance gained by higher illuminances in residential streets using the day-dark approach,” Light. Res. Technol., vol. 51, pp. 557-575, 2019.
23. A. W. Meade, and S. B. Craig, “Identifying careless responses in survey data,” Psychol. Methods, vol. 17, pp. 437–455, 2012.
24. J. Hong, and C. Chen, “The role of the built environment on perceived safety from crime and walking: examining direct and indirect impacts,” Transportation, vol. 41, pp. 1171-1185, 2014.
25. J. Uttley, and S. Fotios, “Using the daylight savings clock change to show ambient light conditions significantly influence active travel.,” J. Environ. Psychol., vol. 53, pp. 1-10, 2017.
26. S. Fotios, J. Uttley, and S. Fox, “A whole-year approach showing that ambient light level influences walking and cycling,” Light. Res. Technol., vol. 51, 55-64, 2019.
27. S. Fotios, C. J. Robbins, “Effect of ambient light on the numbers of motorized vehicles, cyclists and pedestrians,” Transp. Res. Rec., vol. 2676, pp. 593-605, 2022.
28. J. Uttley, S. Fotios, and R. Lovelace, “Road lighting density and brightness linked with increased cycling rates after dark,” PlosONE, vol. 15, e0233105, 2020.
29. A. R. Gover, E. A. Tomsich, W. G. Jennings, and G. E. Higgins, “An exploratory study on perceptions of safety, fear of crime, and victimization experiences among faculty and staff at an urban university: a focus on gender,” Crim. Justice Stud., vol. 24, pp. 37-55, 2011.
30. C. Foster, M. Hillsdon, and M. Thorogood, “Environmental perceptions and walking in English adults,” J. Epidemiol. Community Health, vol. 58, pp. 924-928, 2004.
31. I. M. Bernhoft, and G. Carstensen, “Preferences and behaviour of pedestrians and cyclists by age and gender,” Trans. Res. F, vol. 11, pp. 83–95, 2008.
32. S. Fotios, J. Uttley J, and S. Gorjimahlabani, “Extending observations of ambient light level and active travel to explore age and gender differences in reassurance,” Light. Res. Technol., in press, DOI: 10.1177/14771535221080657.
33. S. Fotios, J. Unwin, and S. Farrall, “Road lighting and pedestrian reassurance after dark: a review,” Light. Res. Technol., vol. 47, pp. 449-469, 2015.
34. T. Price, “The architecture of pedestrian reassurance”. Year 3 Special Study, School of Architecture, The University of Sheffield, 2021.
35. B. C. Welsh, and D. P. Farrington, “Effects of improved street lighting on crime,” Campbell Syst. Rev., vol. 13, 2008.
36. R. Steinbach, C. Perkins, L. Tompson, S. Johnson, B. Armstrong, J. Green, C. Grundy, P. Wilkinson, and P. Edwards, “The effect of reduced street lighting on road casualties and crime in England and Wales: controlled interrupted time series analysis,” J. Epidemiol. Community Health, vol. 69, pp. 1118-1124, 2015.
37. S. Fotios, C. J. Robbins, and S. Farrall, “The effect of lighting on crime counts,” Energies, vol. 14, p. 4099, 2021.
38. S. Fotios, C. J. Robbins, and S. Farrall, “Research note: variation of the effect of ambient light level on crime frequency with type of crime and location,” Light. Res. Technol., in press, DOI: 10.1177/14771535221100671.

Developing Light Pollution Reduction Guidelines for Switzerland

1st Dr. David Michael Kretzer
Non-Ionising Radiation Section
Swiss Federal Office for the Environment
Bern, Switzerland
david.kretzer@bafu.admin.ch

2nd Alexander Reichenbach
Non-Ionising Radiation Section
Swiss Federal Office for the Environment
Bern, Switzerland
alexander.reichenbach@bafu.admin.ch

Abstract: *This paper outlines the process and outcome of developing official guidelines to reduce light pollution in accordance with Swiss legislation such as the Environmental Protection Act (EPA) and the Nature and Cultural Heritage Act (NCHA). This process had begun in February 2015 and resulted in the publication of the law enforcement aid 'Recommendations for limiting light emissions' (German title: 'Empfehlungen zur Vermeidung von Lichtemissionen') in October 2021 by the Swiss Federal Office for the Environment (FOEN). On the one hand, this paper provides an overview of how the FOEN approached the development of these guidelines in a 2-step approach. During step 1, expert groups for a variety of topics related to light emissions including lighting design, public safety, street lighting, limiting values, and disturbing reflections during daytime were set up. The findings of these expert groups were compiled in a baseline report. Based on this report, a first version of the law enforcement aid was created and then released for public consultation. This resulted in over 70 written feedbacks, which included, for example, comments of private persons, environmental organizations, public authorities, members of the expert groups, academics, and associations such as the Swiss Olympic Association. This great number of feedbacks illustrates the huge diversity of viewpoints on the topic of light pollution. Several of the most contradicting feedbacks are presented and discussed in this paper. During step 2, these feedbacks were bilaterally reviewed with their authors and considered for the final version of the law enforcement aid. The challenges of this 2-step process, for example, harmonizing the conflicting interests and targets of different stakeholders are portrayed. On the other hand, the main content of the law enforcement aid, namely a 7-point-approach as well as a relevance matrix for lighting installations is presented in this paper. Moreover, the FOEN's recommended limiting values for luminaire glare and light trespass are outlined and discussed in relation to existing limiting values suggested by other bodies such as the Commission Internationale de l'Éclairage and the European Committee for Standardization. The law enforcement aid further contains information for authorities that need to assess light emissions within the scope of project approvals or in the event of complaints. It defines, for instance, the required information and documentation that needs to be submitted for the approval of a certain lighting project. Moreover, an additional tool that supports the application of the law enforcement aid, the so-called 'Lichttoolbox' (light toolbox), is presented. It constitutes a moderation tool kit that can be used by municipalities to develop 'eco-friendly' regional lighting concepts in collaboration with the different relevant lighting stakeholders. This paper concludes by arguing that the development process of the Swiss law enforcement aid seems in general applicable in other European countries, even though it may require some adaptation depending on the specific political structure and legal system of a country. Moreover, that the 7-point-approach, the relevance matrix as well as the light toolkit represent promising tools for addressing light pollution across Europe*.

Keywords: *light pollution, guidelines, law, sustainability*

I. Introduction

In October 2021, the Swiss Federal Office for the Environment (FOEN) published the enforcement aid 'Recommendations for limiting light emissions' (German title: 'Empfehlungen zur Vermeidung von Lichtemissionen') based on the Environmental Protection Act (EPA) **[1]** and the Federal Act on the Protection of Nature and Cultural Heritage (NCHA) **[2]**.

These recommendations for limiting light emissions should enable those involved in the planning, evaluation, approval and operation of lighting installations to take the measures required to avoid or minimise light emissions. On the one hand, this paper outlines the legal basis of these recommendations and provides an overview of how the FOEN approached the development of the enforcement aid. On the other hand, the main content of these guidelines are outlined and discussed.

II. Legal basis - the protection concept of the EPA

The EPA is intended to protect humans, animals and plants, their biotic communities and habitats against harmful effects or nuisances (Art. 1 para. 1 EPA). Impacts that could become harmful or a nuisance must be limited at an early stage as a precautionary measure (Art. 1 para. 2 EPA). According to Art. 7 para. 1, *«radiation»* that is generated by the construction and operation of installations is also considered to be such an impact within the meaning of the EPA. The Swiss government, the so-called Federal Council, described what is meant by radiation in its dispatch on the draft of the EPA in 1979, namely non-ionising radiation such as bright light, flashes of light, ultraviolet, infrared or laser radiation and microwaves. Artificially generated light at night or sunlight that is altered (e.g. reflected) by the construction or operation of installations thus falls within the scope of the EPA.

Emissions within the scope of the EPA are to be limited by measures at the source (Art. 11 para. 1 EPA). And the EPA provides a two-stage concept for this:

- As a first stage, Art. 11 para. 2 EPA requires emissions to be limited as far as it is technically and operationally feasible as well as economically viable (precautionary emission limitations), irrespective of existing environmental pollution.
- In a second stage, the emission limitations have to be tightened if it is established or can be expected that the immissions will become harmful or a nuisance, taking into account the existing environmental pollution (Art. 11 para. 3 EPA). Such immissions are considered excessive. For the assessment of whether an immission

is harmful or a nuisance, the Federal Council sets immission limiting values by means of an ordinance (Art. 13 para. 1 EPA).

In contrast to other environmental sectors, the Federal Council has never specified the protection against light immissions with an ordinance or binding limiting values. For the assessment of the harmfulness or nuisance of light and lighting, there are no binding immission limiting values in Switzerland so far. Therefore, the authority applying the law has to assess on a case-by-case basis, directly based on the EPA, whether light immissions need to be classified as harmful or a nuisance. In doing so, it can rely on information from experts and specialist bodies or it can also take into account binding and recommended limiting values of private or foreign regulations, provided that their assessment criteria are compatible with those of Swiss environmental law. The recommended limiting values of the new implementation aid are supposed to be used to assess disturbing effects of light and lighting on humans.

The EPA aims in particular to protect humans and animals, plants and habitats in general. If natural habitats requiring protection, habitats of light-sensitive animal groups or landscapes are affected, the requirements of the Federal Act on the Protection of Nature and Cultural Heritage (NCHA; SR 451) must be fulfilled **[2]**.

The extinction of indigenous animal and plant species must be prevented by preserving sufficiently extensive habitats (biotopes) and by other appropriate measures (Art. 18 para. 1 NCHA). Such habitats include riparian zones and bogs, as well as other sites that play a role in preserving the ecological balance or that provide especially favourable conditions for biocoenoses (Art. 18 para. 1bis NCHA).

If, after due consideration of the interests of all parties, damage by technical interventions (such as light emissions) to habitats that deserve protection is unavoidable, the party responsible must take measures to ensure the best possible protection or restoration. If this is not possible, appropriate compensation must be provided as an alternative measure (Art. 18 para. 1ter NCHA).

III. Enforcement of the law

In Switzerland, three political levels share power, namely the Confederation, the 26 cantons and 2172 communes. According to Art. 36, the cantons and communes are responsible for enforcing the EPA. They are in charge of approving the lighting installations of, for example, cantonal or communal streets, other public spaces (such as squares), public buildings, industrial premises, illuminated signs, private premises and sports infrastructures. The aim of the new enforcement aid is to support the different cantons and communes to enforce the EPA (as well as the NCHA).

In general, Swiss *«[e]nforcement aids are published by the FOEN in its role as supervisory authority and are primarily aimed at cantonal enforcement authorities. They substantiate the provisions of federal environmental legislation (regarding unclear legal concepts and scope/exercise of discretion) and are designed to foster uniform practice in enforcing environmental law. By respecting the guidelines, the authorities can assume that they are acting in accordance with federal law; however, other solutions are permissible, so long as they are legally compliant. Enforcement aids are therefore primarily an instrument with which the federal government can supervise enforcement of federal law by the cantons.»* **[3]**

A canton can also contact the FOEN directly in order to ask for advice (regarding specific lighting installations) on how to enforce the environmental laws. Moreover, the FOEN is in charge of evaluating the light emission reduction measures of installations for which the Confederation is responsible – such as the lighting of national streets, army logistic sites and railway stations.

Still, the aim of the new enforcement aid 'Recommendations for limiting light emissions' was not only to support cantonal enforcement authorities, but to enable anyone involved in the planning, evaluation, approval and operation of lighting installations to take the measures required to avoid or minimise light emissions. This implementation aid is intended to help limit light emissions in accordance with legislation such as the Environmental Protection Act (EPA) **[1]** and the Federal Act on the Protection of Nature and Cultural Heritage (NCHA) **[2]**.

IV. Development process

The main goal of developing the new enforcement aid was to define concrete recommendations for lighting installations based on the rather unspecific content (regarding light and lighting) of the Environmental Protection Act (EPA) and the Federal Act on the Protection of Nature and Cultural Heritage (NCHA). What are the effects of light and lighting *«which could become harmful or a nuisance»* - and what are adequate *«[e]arly preventive measures (...) to limit»* them as well to limit them *«more strictly if the effects are found or expected to be harmful or a nuisance»* (Art. 11 para. 2/3 EPA)? To address these relevant questions, the development of the implementation aid was approached in two steps.

During step 1, expert groups for a variety of topics related to light emissions including public safety, lighting design, street lighting, limiting values, and disturbing reflections during daytime were set up. The members of these different expert groups included, for example, public authorities, lighting installation operators, lighting designers, experts in urban safety and a representative of Dark-Sky Switzerland. In order to provide a knowledge base for the work of the expert groups, reports about the current state of research (e.g. regarding the impact of light emissions on human health) or about specific technical questions (e.g. what vertical illuminance values on façades are common in street lighting settings) were created by external partners such as research institutes and lighting design practices. The outcome of the expert group meetings was finally compiled in a baseline report. Interesting during this step was that the biggest disagreements were not observed between different stakeholder groups but within the same group (namely lighting designers).

Based on this report, a first version of the law enforcement aid was created and then released on the FOEN's website for public consultation. This resulted in over 70 written feedbacks, which included, for example, comments of private persons, environmental organizations, public authorities, members of the expert groups, academics, and associations such as the Swiss Olympic Association. This great number of feedbacks illustrates the huge diversity of viewpoints on the topic of light pollution. The comprehensive approach to the topic and the predominantly correct summary of technical information was appreciated by the feedbacks. However, the cantonal environmental authorities criticised that the preliminary draft was not sufficiently suitable for enforcement because the document was too long and the structure too complex. Furthermore, aids such as instructions and checklists were missing. The sports associations and sports authorities (including the Swiss Olympic Association) criticised the recommendations on the assessment of discomfort glare from sports infrastructures and the definition of the environmental zones. While these organisations were afraid that the recommendations would be too strict (and hence could hinder the use of sports facilities at night), other organisations complained the recommendations were not strict enough: Especially several environmental organisations demanded that more explicit recommendations and restrictions should be made (for instance, it was recommended to use the term *«is prohibited»* instead of *«is not recommended»* regarding the installation of luminaires in natural environments and the use of sky beamers). There were also requests for additions on the topics of obstacle lighting (aircraft warning lights) and reflection of sunlight (caused, for example, by photovoltaic panels). Moreover, it was requested to address possible target conflicts more strongly (for example, regarding night-time safety).

During step 2, these feedbacks were bilaterally reviewed with their authors and considered for the final version of the law enforcement aid:

The FOEN organised workshops with the cantonal and municipal environmental authorities in order to find solutions for the different issues they had pointed out. One of the outcomes was the development of a relevance matrix (see Fig. 2). Furthermore, it was decided to produce a short brochure for municipal authorities that summarises the most important content of the enforcement aid. Various discussions were also held with different sports stakeholders. Furthermore, the FOEN commissioned an additional study that analysed the degree of discomfort glare caused by a typical lighting installation for a football and tennis pitch. Finally, countless small editorial comments were implemented, if they were technically justified and contributed to a better understanding of the enforcement aid.

V. The Outcome

The outcome was a 170-page long document (the implementation aid), an 8-page long brochure for municipalities, and a ‘light toolbox’ (the so-called ‘Lichttoolbox’). These three instruments are available in German, French and Italian respectively, since those are official languages in Switzerland.

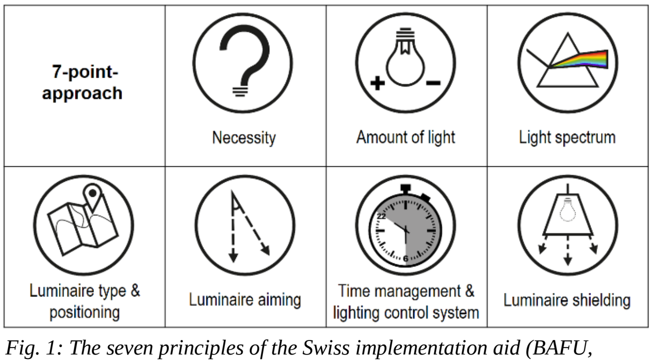

Fig. 1: The seven principles of the Swiss implementation aid (BAFU, 2021)

The core of the implementation aid is a 7-point-approach as well as a relevance matrix for lighting installations.

The 7-point-approach outlines seven principles (see Fig. 1):

1. ***Necessity****: One should only light something or an area, if this is necessary.*
2. ***Amount of light****: One should only use as much light as needed for the visual task.*
3. ***Light spectrum:*** *One should adapt the light spectrum to the lighting purpose and the environment.*
4. ***Luminaire type & positioning:*** *One should light as precisely as possible in order to avoid light spill by selecting the right luminaire (especially having an adequate luminous intensity distribution) and installation location.*
5. ***Luminaire aiming:*** *The light should be emitted downwards and the luminaire should be carefully adjusted during the installation process.*
6. ***Time management & lighting control system:*** *One should reduce or switch off the light according to different times of the day/year or presence detection.*
7. ***Luminaire shielding:*** *One should consider additional shielding of a luminaire in problematic situations.*

In the annex of the implementation aid, it is then shown how to apply these basic seven principles in concrete lighting situations such as street lighting, sports lighting and façade lighting.

The relevance matrix (see Fig. 2) was developed for the implementation aid in order to help authorities determine the impact of a certain lighting installation in a certain local context as well as subsequent measures. The greater the number (0 to 4), the higher the relevance - and hence the more urgent are the measures to reduce light emissions:

0: measures are out of proportion
1 to 3: measures need to be determined depending on the individual case (the greater the number, the more justified is the complexity of each measure)
4: lighting is not allowed

If authorities have to assess in a particular case whether artificial light entering an interior space from outside (light trespass) is significantly disturbing to people according to the EPA, they can rely on the recommended limiting values of the enforcement aid. If necessary, stricter measures to limit emissions must be set until the immissions are no longer obtrusive.

Two effects of outdoor lighting installations that can become harmful or a nuisance to human beings were defined, namely glare (perceived especially in interior spaces) and light trespass (essentially light entering windows). Moreover, corresponding recommended limiting values were determined.

Two different methods are used in practice to assess the discomfort glare. On the one hand, the index k_s is used, which was developed by the LiTG and presented in its publication no. 12.3 **[4]**. On the other hand, a method is applied that evaluates the luminous intensity (in candela) in the direction

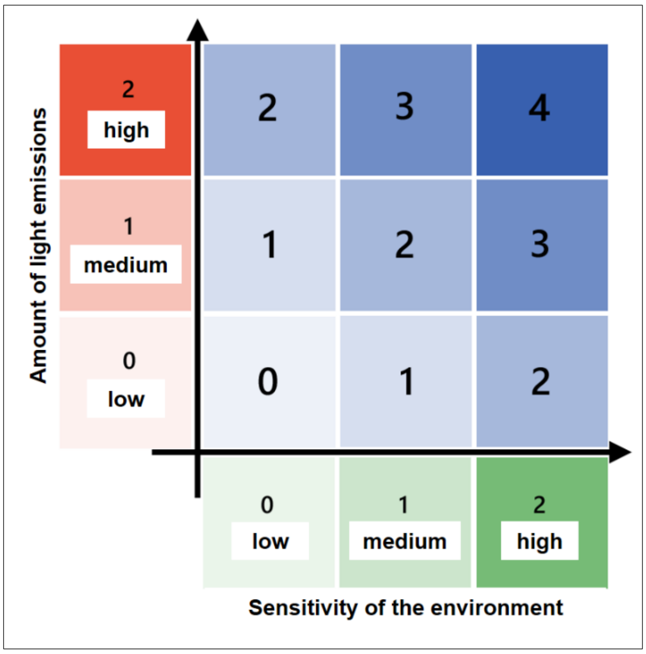

Fig. 2: The Swiss relevance matrix (BAFU, 2021)

of an immission location. Regarding the assessment of the discomfort glare caused by a light source, the index k_s is basically more suitable than merely the luminous intensity value, because the index k_s considers a light source's luminance as well as its background luminance (which both combined represents more accurately the brightness perceived by humans). For this reason, the enforcement aid generally recommends the use of the glare index k_s. The specific recommended limiting values were derived from Annex C of the CIE's technical report 150:2017 **[5]**. However, sports field lighting constitutes an exception, since there seems to be no empirical basis for the determinations of realistic background luminance values for the calculation of k_s. For the time being, it is therefore recommended to apply the luminous intensities method in order to assess discomfort glare caused by sports field luminaires.

In order to assess the disturbing effect of artificial light entering an interior space from outside (light trespass) the vertical illuminance E_v on the window of an affected interior space is determined. The period after 10 pm is considered to be particularly relevant, since this is the sleeping time for a large part of the population. Therefore, the recommended limiting values for assessing light trespass refer to this sleeping time between 10 pm and 6 am. Regarding light trespass, the limiting values for vertical illuminance on properties of the CIE technical report 150:2017 were adopted **[5]**.

Furthermore, the law enforcement aid contains information for authorities that need to assess light emissions within the scope of project approvals or in the event of complaints. It defines, for instance, the required information and documentation that needs to be submitted for the approval process of a certain lighting project.

Due to the decentralised organisaton of the Swiss state, the implementation aid also provides information on governmental responsibilities. If, for example, a person feels disturbed by the outdoor lighting installation of his neighbour, he/she can find in the implementation aid what specific authority needs to be contacted.

Finally, the implementation aid summarizes the state of research with regards to the impact of artificial light on human beings, animals and plants.

The brochure for municipalities is an 8-page long summary of the implementation aid. The reason for creating this additional brochure was that the workshops with the cantonal and communal authorities had shown that a shorter version of the 170-page long implementation aid would be supportive. This brochure focuses on the 7-point-approach as well as the relevance matrix.

The 'light toolbox' is a moderation tool kit that can be used by municipalities to develop 'eco-friendly' regional lighting concepts in collaboration with the different relevant lighting stakeholders in a workshop. During the first step of the workshop, the light 'toolbox' helps analyzing how a specific region will develop during the next 10 to 15 years regarding its society, economy and ecology. The main lighting challenges of that region are then determined during the second step. The light 'toolbox' contains many examples of common measures to tackle common lighting challenges. Hence, during the third step, appropriate measures are defined for the specific lighting challenges of that region based on the measures provided by the light 'toolbox'.

VI. Discussion and Conclusion

The aim of releasing a new implementation aid in Switzerland was to enable those who are involved in the planning, evaluation, approval and operation of lighting installations to take the measures required to avoid or minimise light emissions. In order to reach this goal, many different stakeholders were involved in its development process to facilitate that their diverse viewpoints on light pollution could be incorporated as best as possible.

The Swiss EPA requires precautionary measures: even effects of light and lighting that could become harmful or a nuisance must be limited at an early stage (without having caused any harmful effects yet). This precautionary principle constitutes an effective 'lever' for the authorities to order concrete measures that limit light emissions, and to do so at an early stage - according to the motto 'prevention is better than cure'.

Since the first version of the enforcement aid had been released for public consultation, every person and organization in Switzerland had the chance to influence these guidelines. In Switzerland, there is direct democracy – hence, people are used to participate directly in political processes. Still, the development process of the implementation aid seems (if applied in an adapted way) also beneficial for countries whose political structures are less participative and whose legal systems are more condensed, because this process seems to foster the acceptance of the different lighting stakeholders. Moreover, it makes it difficult to challenge the content of the implementation aid after its publication. An important Swiss organization related to tourism, for example, contacted the FOEN in order to ask how they could influence the implementation aid's content regarding night-time skiing (because the organization was afraid of certain night-time restrictions). In this case, the FOEN could refer to the fact that the public consultation phase had been officially over for a long time already (and that the organization had in consequence missed the opportunity to change the implementations aid's content).

Legal regulation of light emissions in Europe is rather diverse: while some countries such as Slovenia have decrees that are legally binding, other countries only have technical standards **[6]**. Some content of the Swiss implementation aid is Switzerland specific - especially when it comes to the governmental responsibilities (because it is a federal state). However, the core of the Swiss implementation aid constitutes the 7-point-approach and the relevance matrix. This relevance matrix supports people that may not be lighting experts (for example civil servants representing the authorities) to determine quickly the impact of a certain lighting installation in a specific local context as well as to specify how urgent the required subsequent measures are. On the one hand, the 7-point-approach facilitates lighting experts to define and apply concrete measures to reduce the negative impact of light emissions. On the other hand, the 7-point-approach can be used by the authorities as a checklist to control whether all relevant points have been considered and implemented. In addition, the moderation toolkit 'Lichttoolbox' (light toolbox) can be applied by municipalities to develop large-scale lighting concepts in collaboration with the different relevant stakeholders. Hence, especially the 7-point-approach, the relevance matrix as well as this moderation toolkit represent promising tools to support the reduction of light pollution also in other European countries, because these instruments seem to address many common environmental problems in Europe. Furthermore, their recommended measures and principles are not too rigorous and hence leave some space for local regulatory adaptation.

REFERENCES

[1] The Federal Assembly of the Swiss Confederation. (1983 (Status as of 1 January 2022)). *Federal Act on the Protection of the Environment (Environmental Protection Act, EPA)*. Retrieved from https://www.fedlex.admin.ch/eli/cc/1984/1122_1122_1122/en

[2] The Federal Assembly of the Swiss Confederation. (1966 (Status as of 1 January 2022)). *Federal Act on the Protection of Nature and Cultural Heritage (NCHA)*. Retrieved from https://www.fedlex.admin.ch/eli/cc/1966/1637_1694_1679/en

[3] Federal Office for the Environment (FOEN). (2022, Mai 05). *Enforcement aids and notices to applicants*. Retrieved from https://www.bafu.admin.ch/bafu/en/home/topics/law/enforcement-aids.html

[4] Deutsche Lichttechnische Gesellschaft e.V. (LiTG). (2011). *Empfehlungen für die Messung, Beurteilung und Minderung von Lichtimmissionen künstlicher Lichtquellen.* Berlin : Deutsche Lichttechnische Gesellschaft e.V. (LiTG) (Hrsg.).

[5] CIE. (2017). Guide on the Limitation of the Effects of Obtrusive Light from Outdoor Lighting Installations. Vienna: Commission International de l'Eclairage (CIE).

[6] Swiss Institute of Comparative Law. (2015). Gutachten über Lichtimissionen: Belgien, Deutschland, Frankreich, Italien, Niederlande, Österreich, Slowenien, Spanien, Tschechische Republik und Vereinigtes Königreich. Lausanne: Swiss Institute of Comparative Law.

An Innovative Adaptive Lighting Smart City Project: Life Diademe

P. DI LECCE
Revetec srl
Castelnovo né Monti, Italy
paolo.dilecce@revetec.it

M. FRASCAROLO
Università Roma 3
Rome, Italy
marco.frascarolo@uniroma3.it

S. GIANSANTE
Revetec srl
Castelnovo né Monti, Italy
sonny.giansante@revetec.it

The LIFE Diademe project, funded by the European Union, is measuring the relevant influence parameters, in order to dim Public Lighting, according to adaptive lighting concept, to demonstrate that an energy saving of at least 30% (compared to the state-of-the-art dimming techniques) is possible. The European LIFE Diademe Project installed about 1000 devices on each lamp of different areas of Rome, Piacenza and Rimini. The results show how Adaptive Distributed Lighting is not only a sustainable investment, but also a harbinger of significant reductions in CO2 emissions, ensuring traffic safety conditions, correlated to lighting levels.

Besides, the devices, distributed in a dense network of strategically identified points, allow the measurement of various environmental parameters (noise levels, air quality, traffic flow etc.).

Adaptive Street Lighting, Smart Lighting, IoT, noise, air quality, CEN 13201

I. Introduction

A low voltage network, that extends for 7956 km, with 224480 light sources, powers the public lighting of ROMA CAPITALE. ROMA CAPITALE municipality owns these systems, fed by approximately 4,200 control panels. Rome is the largest city in Italy, an important European Capital, having the typical complexity of a modern city.

The technical report EN 13201-1: 2015 and the CIE recommendation TR 115: 2010, have introduced specific chapters related to new approaches to Adaptive Lighting. With the available technology, both the ESCOs and the Municipalities are now able to manage the Public Lighting Remote Management Systems in real time, through sensors installed within their territories, with benefits in terms of energy saving and road safety.

II. Background

The new Italian standard UNI 11248, referring to the technical report CEN EN 13201-1: 2015, defines a series of parameters (speed of dimming, maximum lighting levels, number and frequency of sampling of environmental parameters, calculation and measurement methods, control strategies, etc.), to ensure, in different situations, measured in real time, adequate safety for night driving, compatible with traffic conditions. The Italian standard introduces two adaptive lighting strategies for street lighting: TAI (Traffic Adaptive Installation), in which only the traffic volume is measured and FAI (Full Adaptive Installation), where weather conditions and luminance of the road are monitored as well. When the FAI strategy is implemented to guarantee safety conditions, UNI 11248 allows the level to be reduced up to three lighting categories, often corresponding to the 75% reduction of the luminous flux required by the project lighting class.

This standard requires specific measurements in real time. This is probably the reason that pushes some operators towards simpler dimming systems, capable of detecting only the presence of traffic (for example pedestrians) or movements. Such simple dimming lighting systems is suitable for applications such as parks, gardens or pedestrian areas. The situation regarding motorized traffic roads is different. In these, the driver's main visual task lies in identifying a possible obstacle on the roadway. In this scenario, safety is guaranteed by a correct street lighting luminance, directly related to the detection of the real traffic flow (not to be confused with a simpler identification of lane occupation).

III. Motivation

The LIFE Diademe project, thanks to the LIFE European funding program, has been able to experiment in the cities of ROME (within the EUR and Pietralata districts), PIACENZA and RIMINI, an innovative approach to dim the road lighting. The project places these cities at the forefront in the creation of Smart City IoT (Internet of Things), which is perceived as the only possibility to reconcile the typical safety needs of a city (variability of the conditions of use of the road, presence of events, difficult weather conditions, etc.), with the environmental advantages deriving from energy saving.

Figure 1 - Diademe installed in EUR (Rome)

Today, IoT technology makes it possible to install low-cost sensors on each pole and related lighting fixture, capable of detecting the luminance of the road surface, the flow of traffic and weather conditions. To obtain a wide range of typical street lighting situations, the tests conducted so far have considered residential urban areas, with a prevalence of offices, shops, public administration, universities, etc. Expert systems on site analyze road data and adapt street lighting levels in real time: measurements and adjustments of the systems are performed every minute.

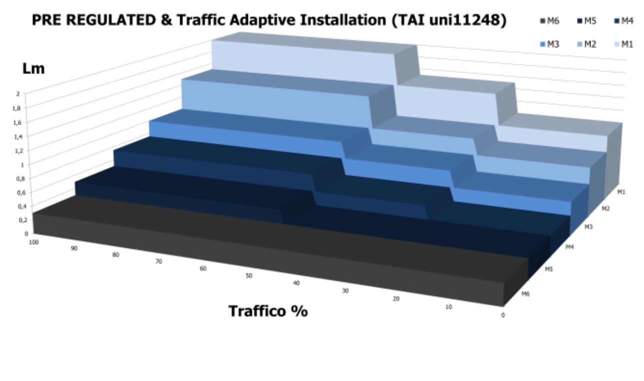

Figure 2 - Dimming expected by UNI 11248 for a scheduled pre-programmed cycle or TAI system

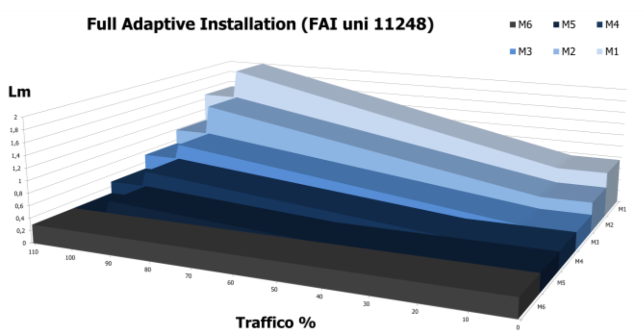

Figure 1 - Dimming expected by UNI 11248 for a FAI system

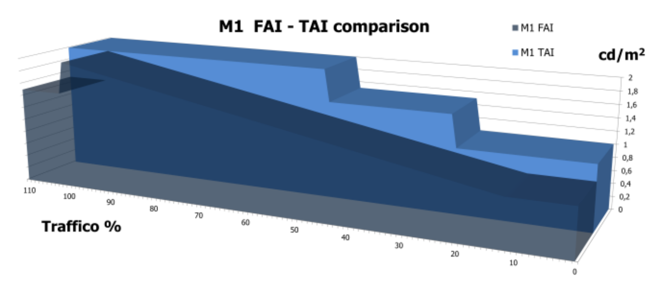

Figure 2 – Comparison example between FAI and TAI systems

One of the reasons why adaptive lighting did not find great diffusion was to be found in the lack of technologically advanced sensors, able to reliably measure, on the road, the flow of traffic and luminance, combined with weather conditions. Today, with the help of computer vision technology, this is possible.

There are sensors, such as LTM (Luminance, traffic, meteo) which uses computer vision techniques, capable of measuring, on site, traffic, with an accuracy of 10%, the average value of the luminance of the road surface, with an accuracy of 8% and is also able to estimate the weather conditions. This type of equipment has a single disadvantage: the cost. This is the reason why it is difficult to install them in a widespread manner on the territory. They have perfect application in the areas identified by the lighting designers as strategic.

The UNI 11248 standard assigns the lighting designer the possibility of identifying homogeneous areas from the point of view of traffic flows and luminance measurement, in order to allow the use of LTM for the control and command of different plants.

It is clear, however, that technological evolution must provide more diffused measures in the area, in order to arrive at extensive and precise real-time assessments DAI (Diffuse Adaptive Installation).

At the end of 2016 the consortium formed by Revetec srl and Agire (agency of the Province of Mantua), to which ROMA CAPITALE, the Municipality of Rimini, the municipality of Piacenza, Enel Sole and Citelum SA were added, obtained a co-financing of the project called Diademe, relating to the installation in Rome at the EUR district, in Piacenza at via Primo Maggio and Rimini in viale Losanna of about 1000 low-cost devices capable of measuring the parameters necessary to correctly manage adaptive lighting (FAI), on a widespread territory (DAI). Thanks to the active contribution of all the aforementioned actors and of Roma 3 University, INRIM and RSE, new delocalized adaptive systems were installed.

IV. METHODS

With the LIFE Diademe project, a total of 962 devices were installed, divided as follows: 825 within the perimeter of Rome, in detail 746 in the EUR area and the remaining 79 along the Pietralata district. The project also had the opportunity to test the replicability of the system thanks to the interest also shown by the municipalities of Piacenza and Rimini. 76 LIFE Diademe devices have been installed in the city of Piacenza, while in the city of Rimini the installed park is 61 devices.

Figure 5 – installation in Roma EUR neighborhood

Within the test sites, the LIFE-DIADEME consortium installed devices, developed ad hoc, with basic functions for monitoring light, traffic flow, noise pollution and inclination. Thanks to the IoT concepts, for each light point, the data relating to the light present on the road surface, the luminous flux emitted by the light point, the traffic volume, the noise and the inclination of the poles are collected. Furthermore, every 20 light points, the air quality was monitored through a special control unit. In practice, a neuronal network spread over the urban area was created.

Figure 6 - Diademe device in operation

With regard to adaptive regulation, each single LIFE-DIADEME light point is able to detect the conditions of traffic and the light present under it.
The information acquired from the individual points is essential to understand how to adjust the light based on real traffic conditions and how a dimming implementation affects the luminance present below the light point.

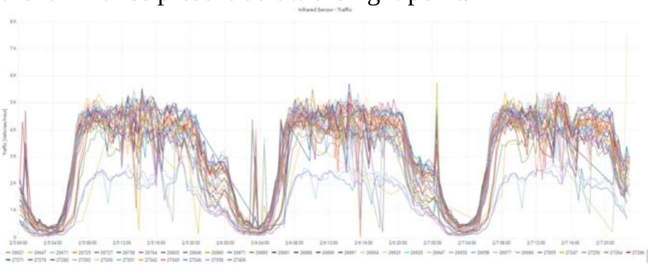

Figure 7 - Traffic measurement with Diademe detector on Via Cristoforo Colombo

In addition to the basic sensors, 30 light points were also equipped with an LTM sensor capable of operating as a precision reference for analyses relating to adaptive lighting, vehicular traffic and weather conditions.
As previously mentioned, 50 poles (1 every 20 light points) were equipped, again in addition to the basic functions, with a control unit capable of detecting the concentrations of 3 different types of gas (CO_2, NO_2, O_3), using an experimental technology based on electrochemical sensors. The electronic board was redesigned for industrial use starting from an experimental electronics made by the EU JRC of Ispra (Joint Reserach Center). This is the first massive installation of this type of sensors, with the further particularity of being located in southern Europe. This is because, so far, the most active researchers have turned out to be linked to countries in Northern Europe, with a trend that continues to push in this direction. The availability of so many data in a Mediterranean context has proved useful to understand the functioning of electrochemical sensors in an environment that is climatically different from the Nordic one, typically cooler.
The collaboration with ARPA LAZIO has made it possible to use validated references in order to develop a machine learning analysis, useful in finding an algorithm capable of calibrating the different electrochemical sensors on board the gas detection units.
Thanks to this type of network installation, the previous scenario is revolutionized, were a few high-precision control units monitor the data locally and then the system extends its validity over an area of several square kilometers. Thanks to low-precision but widespread sensors, it is possible to collect information relating to air quality in a more widespread and selective manner.

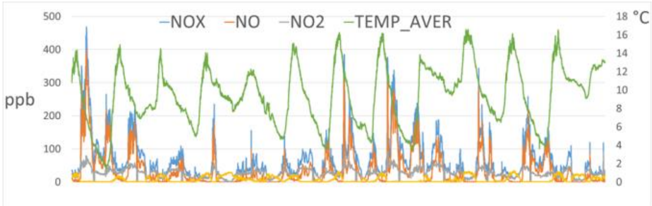

Figure 8 – Data example collected by a control unit on air quality in Cinecittà neighborhood

Noise sensors allow municipalities to have a useful tool for complying with the directives issued by the EU on the subject of noise pollution mapping, ensuring extensive and continuous monitoring.
For the evaluation of the noise along the test sites, LIFE-DIADEME has chosen to use the results provided by another project funded by the European Community, LIFE-HARMONICA. This project aimed to find a noise index, according to the standards, that was easy to use for ordinary citizens.
The final result of this work led to the creation of a Harmonic index that makes it intuitive to evaluate the noise level within an area. LIFE-DIADEME has decided to use this data presentation methodology precisely to make the noise level perceived by people easily understandable at different times of the day.
In order to interface with all this amount of data, a total of 26 gateways were installed along the roads involved in the LIFE-DIADEME test site.
The connection with the light points and with the LIFE-DIADEME devices was chosen on the basis of the system characteristics. All the data collected in near real time by the gateway were then downloaded to a server.
It was necessary to carry out a measurement campaign of the pre-existing conditions in order to evaluate scientifically the energy saving results. The Roma3 University carried out the survey of the lighting conditions of the roads involved in the experiment, at the beginning of the project.
Following the commissioning of the devices, about a hundred interviews were conducted, both with citizens on the street and with professionals who, directly or indirectly, are familiar with adaptive lighting. The results of these surveys appeared interesting to understand, within these groups, what perceptions they have of adaptive technology.

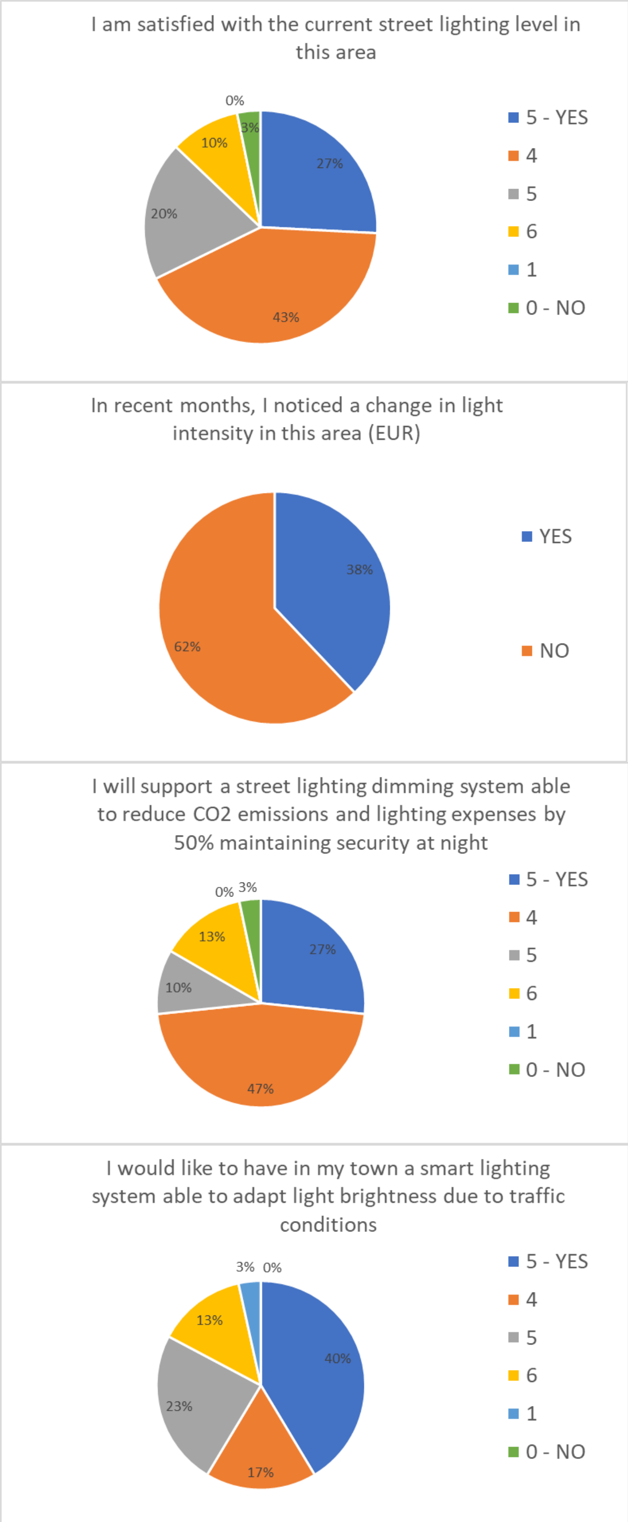

Figure 9 – Analysis of the interviews conducted on EUR inhabitants

Expert systems, on site, analyse road data and adapt street lighting levels in real time: measurements and adjustment are performed every minute. It is essential that the measurement and command are performed locally, to avoid a large flow of data to and from a remote controller, which would have no use, indeed would make the system vulnerable and relatively slow.

Thanks to expert software which, based on the analysis of BIG DATA, have self-learning capabilities (machine learning), it is possible to reconstruct precise measurements based on correlations with cheap sensors. In this way, the metrological performance of the sensors was checked, ensuring the accuracy of the measurements throughout the monitored area, without the need for periodic calibration interventions on all sensors.

From cheap sensors installed on a single light point, capable of measuring traffic with an accuracy of 20% and luminance with an accuracy of 15%, it is possible to derive more precise data, with accuracies comparable to those declared by LTM.

V. RESULTS

To determine the "base-line", a complete campaign of lighting measures on the lighting points of EUR was carried out by the University of Rome 3 and by Revetec. Parameters relating to luminance, glare, uniformity (transverse and longitudinal), the lighting levels of the pedestrian area and the power absorbed according to the different types of lighting fixtures were measured.

Figure 10 – measurements campaign conducted by Università Roma 3

Data collected by the light points installed show that it is possible to obtain, thanks to a distributed FAI adaptive lighting (DAI), an energy saving of more than 40% when compared to a system with pre-regulated cycles. Savings of 60% are exceeded when compared to a non-regulated system.

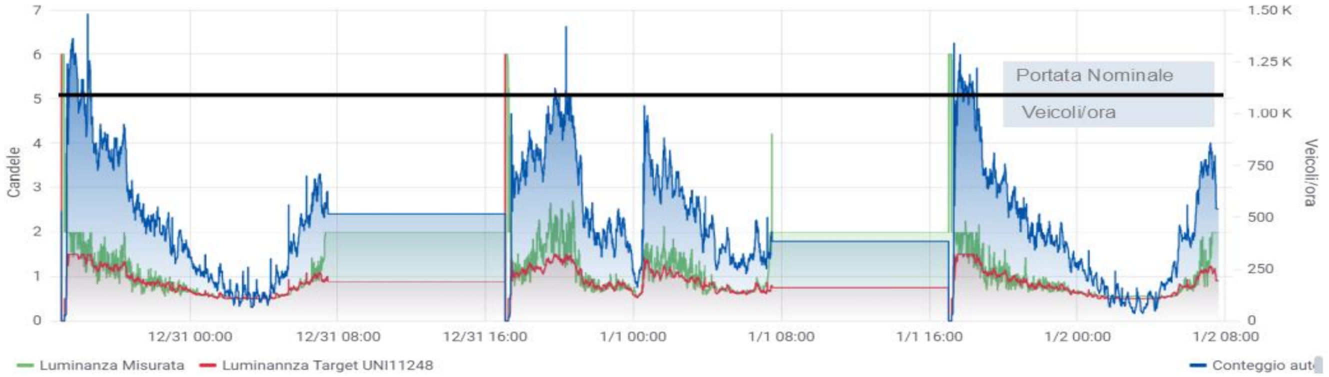

Figure 11 – Traffic volume in Via Laurentina example of measurement and level and attended power levels of the lighting system: comparison 31/12, 1/1 and 2/1

RSE (Research Electric System, a company of the MISE Ministry of Economic Development) has completed an LCCA (Life Cycle Cost Analysis) and an LCA (Life-Cycle Assessment) study.

The two distinct analyzes have shown that the payback of a LIFE-DIADEME investment is very close to 4 years. As regards the environmental contribution of a project such as LIFE-DIADEME, the numbers indicate an absolute advantage in using adaptive systems both on large systems and on systems consisting of a few light points.

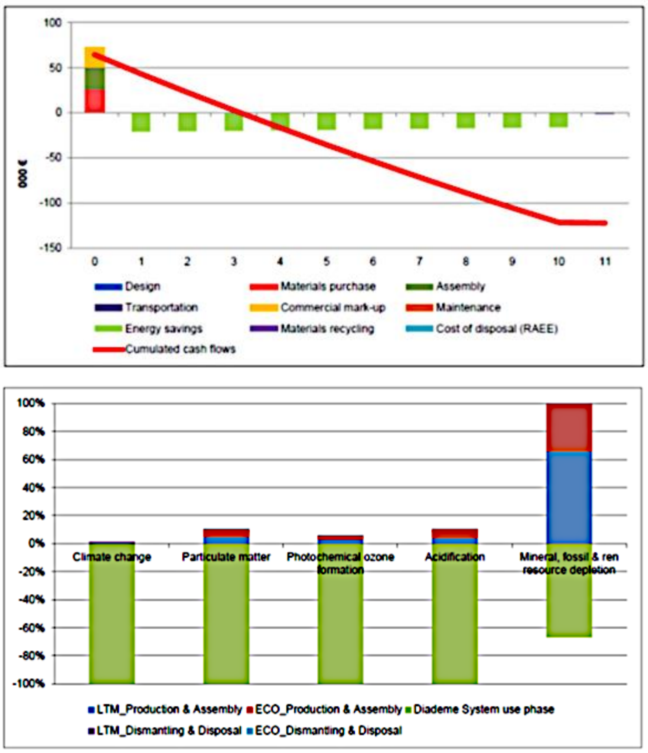

Figure 12 – LCCA study, payback calculation

Assuming to install a system such as DIADEME along the streets of a city with more than 200,000 light points, over the lifetime of the lighting fixtures, the environmental savings would translate into a reduction of emissions into the air equal to 40,000. tons of CO2eq and 8 tons of PM2.5.

Then, the calculations inherent to the formation of ozone, which would produce a saving of 48,000 kg equivalent and a lower acidification estimated at 95,000 molc H + equivalent should be added.

Having to produce a system that requires the use of electronic components, the contribution of approximately 160 kg of minerals and fossils necessary for industrial production cannot be eliminated. This contribution is amply repaid by all the environmental benefits quantitatively listed above.

In the end, LIFE-DIADEME has proven to be an effective and efficient system, aimed at reducing the environmental impact for public lighting installations.

During the project, attention was also paid to the perception, by users, of how adaptive technology, declined in public lighting, is experienced. The results of the interviews showed that road users did not perceive any change in lighting (63%). A high percentage of respondents say they are in favor of switching to adaptive lighting (70%)

Professionals have shown themselves to be very favourable to the use of these technologies.

The data, which were collected throughout 2020, passed under the management of the Municipalities involved in the project from 1 January 2021. In this regard, Roma Capitale is preparing a platform for the collection and analysis of data, called "City Data Platform", in which data from the Diademe project will also be integrated. This platform aims to make available, for internal and external operators to the administration, a data lake in which to aggregate both data from the ERP systems of the various departments (mobility, tourism, environment, culture, etc.) and data from external sources. , possibly also in Big-Data mode. The platform is built in Fiware technology, an open environment promoted by the European Commission, which today sees a community of over 170 cities, 1000 startups and 15 innovation hubs to share modules and experiences for the development of IoT, Big-Data, Open- Date and, more generally, dashboard for the data governance of the reference area. This platform, together with other strategic infrastructural elements, such as the PagoPA system, the CRM shared with the in-house, the digital identification system with SPID and CIE and the Smart Citizen Wallet project, represents a key digital asset available to the city as indicated. in the guidelines of Rome Smart City, the strategic digital development plan for improving the quality of life with a view to environmental sustainability.

VI. CONCLUSIONS

The Diademe project undoubtedly shows the interest and results achievable from FAI (UNI 11248) adaptive lighting with distributed sensors (DAI): 40.6 % compared to pre-programmed dimming profiles, 57% compared to no dimming. It has to be emphasized that not only the energy saving is a relevant result, but as well the expected reduction in the volume of waste is important, due to the lengthening of the life of the lighting fixtures. The investment can pay off in less than 4 years, and today, with energy prices going up, in less than 3 years. In addition to the economic aspect, the importance of a reduction in expected CO2 emissions, the main among GHG (greenhouse gas), is guaranteed.

Finally, the distributed measurement system has proved efficient and effective, because it reduces the initial investment compared to a non-distributed system and has the ability to support the collection of numerous other environmental data, such as noise, traffic flows and air quality data.

Some results of the DIADEME project have been analyzed and used by the UNI working group that manages the revision of the UNI 11431: 2011 standard, in order to set new highest targets for street lighting dimming.

Beside, data are currently evaluated in CIE Technical Committee TC62, under the coordination of Division 4.

VII. ACKNOWLEDGMENTS

Many thanks to EASME -now CINEA- (European Commission Executive Agency for Small and Medium-sized Enterprises) trusting in the credibility of the project, ROMA CAPITALE, Piacenza and Rimini Municipalities , Citelum SA and Enel Sole for the technical support on their installations.

[1] Ministry of Transport , Transport Research Center, The Netherlands – Dynamic Public Lighting –Cover Report – Marzo 1999

[2] CEN 2014. CEN TR13201-1:2014. Road lighting - Part 1: Guidelines on selection of lighting classes. Brussels: CEN.

[3] CEN 2015a. EN 13201-4:2015. Road lighting - Part 4: Methods of measuring lighting performance. Brussels: CEN.

[4] CEN 2015b. EN 13201-5:2015. Road lighting - Part 5: Energy performance indicators. Brussels: CEN.

[5] CEN 2015c. EN 13201-5:2015. Road lighting - Part 2: Performance requirements. Brussels: CEN.

[6] CEN 2015d. EN 13201-5:2015. Road lighting - Part 3: Calculation of performance. Brussels: CEN.

[7] CIE 2001. CIE 144:2001. Road Surface and Road Marking Reflection Characteristic. Vienna: CIE.

[8] CIE 2003. CIE 154:2003. The Maintenance of Outdoor Lighting System. Vienna: CIE.

[9] CIE 2010. CIE 115:2010 2nd Edition. Lighting of Roads for Motor and Pedestrian Traffic. Vienna: CIE.

[10] ISO/CIE 2014. ISO/CIE 19476:2014. Characterization of the Performance of Illuminance Meters and Luminance Meters. Joint ISO/CIE International Standard. Geneva: ISO.

[11] UNI 2011. UNI 11431:2011. Luce e illuminazione - Applicazione in ambito stradale dei dispositivi regolatori di flusso luminoso. Milano: UNI

[12] UNI 2016. UNI 11248:2016. Illuminazione stradale - Selezione delle categorie. Milano: UNI

[13] Paolo Di Lecce "Illuminazione adattiva: Italia sempre un passo avanti" U&C (Unificazione & Certificazione, rivista ufficiale di UNI) - n.7 Luglio Agosto 2016 pagine 32-33

[14] ADAPTIVE SYSTEMS IN ROAD LIGHTING INSTALLATIONS Rossi, G.1, Iacomussi, P.1, Mancinelli, A.2, Di Lecce, P. 2 INRIM, Torino, ITALY, 2. REVERBERI Enetec, Castelnuovo ne' Monti (RE), ITALY LIGHT & ENGINEERING 2015 VOL.23 #4

[15] ADAPTIVE SYSTEMS IN ROAD LIGHTING INSTALLATIONS Rossi, G.1, Iacomussi, P.1, Mancinelli, A.2, Di Lecce, P. 2 INRIM, Torino, ITALY, 2. REVERBERI Enetec, Castelnuovo ne' Monti (RE), ITALY CIE 216:2015: Proceedings of the 28th Session of the CIE, 28 June – 4 July 2015, Manchester, United Kingdom.

[17] Paolo Di Lecce, Alain Mazzocchi, Andrea Mancinelli, Giuseppe Rossi "Illuminazione adattiva: l'Italia fa sul serio" LUCE - n.322 2021 pages 90-94

[18] Paolo Di Lecce Alain Mazzocchi, Andrea Mancinelli, Giuseppe Rossi., Marco Frascarolo " ADAPTIVE LIGHTING IN MOTORIZED TRAFFIC ROAD: REAL INSTALLATIONS SHOW THAT IOT TECHNOLOGIES CAN SUPPORT THE CORRECT USE OF STANDARDS " CIE 2018 Topical Conference on Smart Lighting in Taipei, Chinese Taipei, April 26–27, 2018

[19] Paolo Di Lecce, Andrea Mancinelli, Alberto Scarlatti, Giuseppe Rossi, Marco Frascarolo IL PROGETTO LIFE-DIADEME: ROMA SPERIMENTA TECNOLOGIE INNOVATIVE IOT NELLA ILLUMINAZIONE ADATTIVA DELLA SMART CITY. Congresso AIDI Rome June 2022

[20] Paolo Di Lecce Alain Mazzocchi, Andrea Mancinelli, Giuseppe Rossi., Marco Frascarolo Commissione Europea Greenlight Program – Improving Energy Efficiency in Commercial Buildings and Smart Communities Frankfurt March2018

A Method to Estimate Road Optical Reflection Properties from Luminance Map

Boucher Vincent
Light and Lighting Team
Cerema/DTerOuest
Les Ponts de Cé, France
vincent.boucher@cerema.fr

Greffier Florian
Light and Lighting Team
Cerema/DTerOuest
Les Ponts de Cé, France
florian.greffier@cerema.fr

***Abstract*— A basis of functions is obtained by Principal Component Analysis of an *r*-tables dataset. Thus an *r*-table can be described as a linear combination of the basis functions (or eigenvectors) using weighting factors (or eigenvalues). This decomposition is applied to the calculation of pavement luminance to create "eigen luminance maps" used for decomposing a measured luminance map. The resulting weighting factors are used to estimate the *r*-table that generated the measured luminance map. To assess the validity of the estimate, the Normalized Root Mean Square Deviation is computed as well as quality criteria used in road lighting. A dry pavement (R2) and a wet one (W2) are taken to evaluate the accuracy of the estimated retrieved *r*-table. An unknown *r*-table not belonging to the dataset is also retrieved. The method remains robust and reliable with a noisy input luminance map simulating a real camera measurement.**

***Keywords*— road lighting, r-table estimation**

I. Introduction

The optical reflective properties of pavement are essential to know when designing a road lighting installation or optimising lighting over time [1]–[3]. Studies [4]–[7] have shown that it is not possible to be satisfied with CIE standard tables, which are not representative of recent materials, and that it is necessary to take into account the evolution of optical properties with age and weather in order to properly estimate perceived luminance. But there is no simple way today to measure these properties for a whole street at once, nor in real time. The first way to measure these optical properties is to take a core sample of pavement and characterise it in laboratory using a gonioreflectometer [8]–[10]. This method is destructive, and also spatially and temporally punctual. Portable devices have been developed in order to avoid the destructive aspect [11]–[15], but the punctual drawback in space and time remains true. Finally, camera-based methods have been developed, but some of them require the estimation of many parameters in order to reach the correct *r*-table [16], [17], or for others, specific street lighting are required to access certain elements of the *r*-table [18]. We propose here a method for estimating the whole *r*-table, based on a luminance map that can be measured by an Image Luminance Measurement Device (ILMD) and the knowledge of the lighting system.

II. METHOD

Road surface reflection tables (*r*-tables) are arrays describing the relative efficiency of light reflection on a road surface. It relates scene illuminance to luminance seen by an observer's eye. They are depending on two angles (β, γ), the two others (α, δ) being fixed and they are commonly used in road lighting calculations to compute a luminance map defined at some points given by the CIE grid [19] (Fig.1).

A. Principal Component Analysis

The dataset is composed of 14 standard CIE *r*-tables (C1,

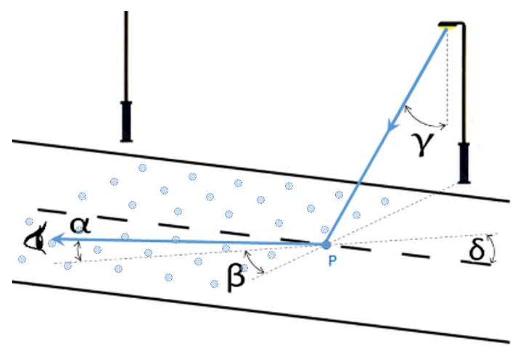

Fig. 1. Mesh grid and angles used for luminance calculations.

C2, R1..R4, N1..N4,W1..W4). The full method has been exposed in [19] with a database of experimental non-public *r*-tables. To allow others to replicate the results obtained and for operational applications for road operator teams, we expose here the method with standard well known *r*-tables. Photometric coefficients Q0, S1 of the database are gathered in Table I.

TABLE I. PHOTOMETRIC COEFFICIENTS Q0, S1 OF THE DATABASE

	C1	C2	R1	R2	R3	R4	N1
Q0	0.100	0.070	0.101	0.070	0.070	0.080	0.100
S1	0.24	0.97	0.25	0.58	1.11	1.55	0.18
	N2	**N3**	**N4**	**W1**	**W2**	**W3**	**W4**
Q0	0.070	0.070	0.080	0.114	0.150	0.196	0.247
S1	0.41	0.88	1.61	3.15	5.72	8.63	10.84

A Principal Component Analysis (PCA) is performed on the 14 *r*-tables, each constituted of 580 elements (29x20 elements array). PCA is a dimensionality-reduction method that is often used to reduce the dimensionality of a large data set, by transforming it into a smaller one that still contains most of the information from the large set. It allows to reduce dimensionality without losing much information. Here our objective is to reduce the 580 dimensionality in order to solve more easily a linear system containing N_G equations (number of luminance map points). Once the PCA has been computed, r-tables can then be decomposed as:

$$\mathbf{R} = \boldsymbol{\lambda}\, \mathbf{M} \tag{1}$$

where $\mathbf{R}$ is a 1 x 580 r-table vector (29x20 elements row aligned), $\boldsymbol{\lambda} = [\lambda_1, \ldots, \lambda_D]$ is a 1 x D weighting vector, D corresponding to the space dimensionality (here 13, corresponding to the dataset size minus one), $\mathbf{M}=[\mathbf{M_1},\ldots,\mathbf{M_D}]^T$ is D x 580 eigenvectors matrix. That representation allows for describing r-tables with 13 scalar numbers without losing their β and γ original dependencies.

B. Luminance Map Calculation

Given an intensity of luminaires I and a point P at a position p, reflection r-table elements relate light intensity to luminance at P through the following expression :

$$L_p = \sum_{i=1}^{N_S} \frac{r_{i,p} \cdot I_{i,p}}{h^2} \tag{2}$$

where L_p is the luminance at the point P, N_S is the number of luminaires, $r_{i,p}$ are the reduced luminance coefficients (r-table elements to be found), $I_{i,p}$ are the intensity of luminaires at the point P, h is the mounting height of the luminaires. $r_{i,p}$ are interpolated depending on β and $\tan\gamma$ through the position p.

As each element $r_{i,p}$ is a linear combination of $m_1,..,m_D$, the elements of eigenvectors $\mathbf{M_1},..,\mathbf{M_D}$ (cf eq. 1). Equation (2) can then be written in a matrix form:

$$\mathbf{L} = \boldsymbol{\lambda}\, \mathbf{A} \tag{3}$$

where $\mathbf{L}$ is a 1 x N_G vector of luminance map, $\mathbf{A}$ is a D x N_G matrix. $\mathbf{A}$ matrix can be seen as a set of “eigen luminance maps” acting as a basis to decompose the luminance map $\mathbf{L}$. Elements of $\mathbf{A}$ are constructed according to the following equations:

$$a_{d,j} = \sum_{i=1}^{N_S} \frac{m_{d,i,p} \cdot I_{i,p}}{h^2},\ d = 1..D,\ j = 1..N_G \tag{4}$$

where $m_{d,i,p}$ are the elements of the eigenvector $\mathbf{M_d}$, N_G is the number of points defined by the CIE calculation grid. For an experimental application of this model, $\mathbf{L}$ can be given by Imaging Luminance Measurement Device (ILMD) data and we need the knowledge of the scene geometry and the intensity distribution function of the luminaires.

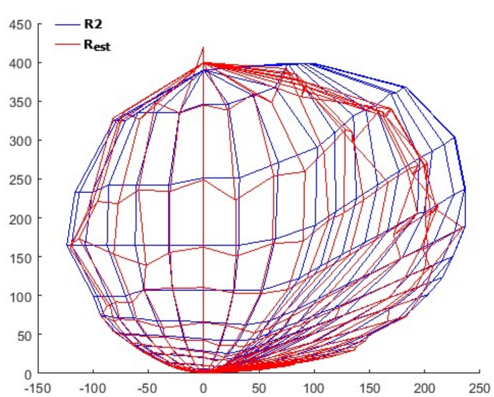

Fig. 2. R_{est} (red curve) vs R2 (blue curve)

C. Model inversion

With D unknowns (here 13) and N_G equations (from 60 to 162 depending on CIE situation given in [19]), system (3) is easily solved by pseudo-inverse:

$$\boldsymbol{\lambda} = \mathbf{L}\, \mathbf{A}^{-1} \tag{5}$$

The resolution of this over-determined system leads to a least-squares solution vector $\boldsymbol{\lambda}$. The estimated r-table R_{est} can then be retrieved with $\boldsymbol{\lambda}$ and (1).

III. RESULTS

A. r-table estimation

A luminance map has been generated from the R2 table and the previous procedure has been applied. Figure 2 shows R_{est} (in red) in comparison with R2 (in blue), calculated from a luminance map of $N_G = 60$ grid points corresponding to CIE situation 1 referenced in [19] and for one observer’s position in the slow lane. Table II shows Q0, S1 values of R_{est} tables calculated for the seven CIE situations of [19].

TABLE II. Q0, S1 OF R_{est} IN THE 7 SITUATIONS

Sit	**1**	**2**	**3**	**4**	**5**	**6**	**7**	**R2**
Q0	0.070	0.069	0.074	0.074	0.078	0.074	0.073	**0.070**
S1	0.55	0.55	0.59	0.57	0.54	0.61	0.57	**0.58**

Q0 and S1 values are well retrieved, regardless of installation geometry. Even if the photometric coefficients (Q0, S1) are close, a better quantification of the deviation can be obtained using all the r-table elements by calculating the Normalized Root Mean Square Deviation (NRMSD):

$$NRMSD(R_{est}) = 2\,\frac{\sqrt{N \sum_i (R_{\text{est}\,i} - R_{0\,i})^2}}{\sum_i R_{\text{est}\,i} + \sum_i R_{0\,i}} \tag{6}$$

NRMSD is computed between the r-table found by our method and the R2 reference. Results are presented in Table III for the seven CIE situations.

TABLE III. NRMSD(R) IN THE 7 CIE SITUATIONS

Sit.	**1**	**2**	**3**	**4**	**5**	**6**	**7**
NRMSD	0.148	0.151	0.112	0.118	0.132	0.123	0.113

A NRMSD value inferior to 0.1 stands for a pretty good approximation of the original r-table. In Table III, values are about twice greater those found in [20] because of lower dimensionality (here 13 against 33 in [20]) leading to a less accurate reconstruction.

B. Luminance Map estimation

However r-table deviations do not translate directly how they act upon luminance maps. To estimate the influence of the estimated r-table on luminance distribution, it can be injected into (2). Then the original luminance map calculated from standard R2 table can be compared with one calculated from the estimated r-table as shown in figure 3 for the CIE situation 1.

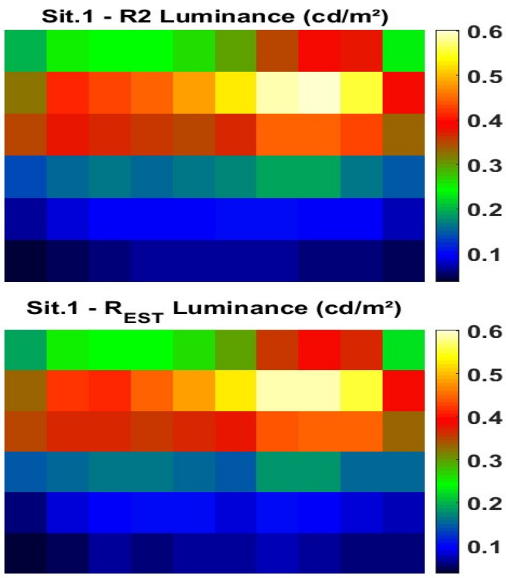

Fig. 3. Luminance maps generated with R2 (top) and R_{est} (bottom)

Deviations between luminance maps are quantified via NRMSD of luminance values. Results are gathered in Table IV.

TABLE IV. NRMSD(L) IN THE 7 CIE SITUATIONS

Sit.	1	2	3	4	5	6	7
NRMSD	0.028	0.043	0.029	0.029	0.026	0.022	0.026

Recomputed luminance maps are very close to the originals (NRMSD<0.05) and results are independent on the number of points in the grid (from 60 to 162 according to situations) on the number of luminaires (varying from 5 to 12), on light arrangement and on road width. Accessing to luminance map allows to compute the standardized and largely used criteria, defining quality of road lighting installations: Average Luminance L_{ave}, Overall Uniformity U0 and Longitudinal Uniformity Ul (for definitions, see [19]). Table V presents relative deviations of those criteria defined by:

$$\Delta Y_{est} = 100 \,.\, (Y_{est} - Y) / Y \tag{7}$$

where Y_{est} is the estimated value and Y the true value.

TABLE V. LIGHTING CRITERIA DEVIATIONS

Situation	1	2	3	4	5	6	7
ΔL_{ave} (%)	0.1	0.2	-0.1	-0.1	0.0	-0.0	-0.0
ΔU0 (%)	-1.4	0.3	2.2	-0.6	2.7	0.0	-6.2
ΔUl (%)	-8.4	4.8	2.2	2.9	-2.2	0.1	-3.7

Results in Table V are very good for average luminance (the model currently fits the luminance map). As expected, results for overall and longitudinal uniformities are more sensitive due to their definitions as a ratio of two specific values.

C. *Retrieving a wet r-table*

In this section, the starting point is a luminance map generated from the W2 table. The procedure of section II is followed. Knowing the luminaires geometry and their distribution curves, the model **A** is constructed with eq. (3) and eq.(4). Weighting factors **λ** are determined solving the system (5). The *r*-table is then estimated using eq.(1). An example of retrieved *r*-table for the CIE situation 1 is exposed in figure 4. All the metrics and road lighting criteria are also gathered in the table VI. Q0 and S1 values standing in the table VI are to be compared with W2's Q0 =0.150 and S1=5.70.

TABLE VI. CRITERIA FOR A WET R-TABLE (W2)

Situation	1	2	3	4	5	6	7
Q0	0.150	0.149	0.155	0.155	0.158	0.154	0.153
S1	5.54	5.17	5.70	5.72	5.50	5.77	5.64
NRMSD(R)	0.078	0.080	0.059	0.062	0.070	0.065	0.060
NRMSD(L)	0.009	0.013	0.009	0.011	0.016	0.007	0.008
ΔL_{ave} (%)	0.03	0.09	-0.03	-0.04	-0.02	0.00	-0.01
ΔU0 (%)	-1.96	-4.32	-1.64	-3.36	-0.52	0.85	-6.42
ΔUl (%)	-16.0	1.88	-2.05	1.07	-2.38	0.98	-4.41

We find that the estimation is very close to the truth for *r*-table elements, luminance map, average luminance and overall uniformity. All the deviation values are very small except for uniformities, again due to their definitions that make them sensitive to small deviations.

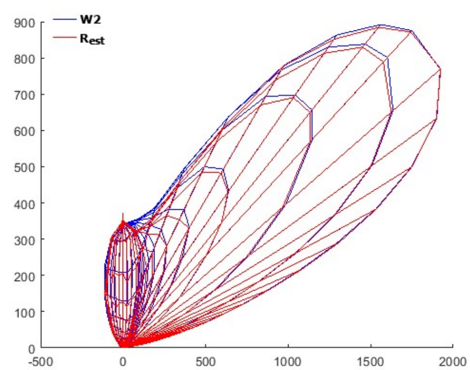

Fig. 4. R_{est} (red curve) vs W2 (blue curve)

D. *Retrieving an unknown r-table*

A Belgian *r*-table (called Asphalt 300, Q0 = 0.097, S1 = 0.85) has been found in [21]. Figure 5 presents the photometric solid of the original asphalt *r*-table (blue) and of the estimated one R_{est} (red) in the CIE situation n°1. Statistical and road lighting quality criteria are also summed up in Table VII:

TABLE VII. CRITERIA FOR ASPHALT300 R-TABLE

Situation	1	2	3	4	5	6	7
Q0	0.098	0.095	0.101	0.101	0.110	0.099	0.100
S1	0.79	0.73	0.81	0.80	0.76	0.87	0.81
NRMSD(R)	0.19	0.20	0.14	0.13	0.17	0.15	0.17

Situation	1	2	3	4	5	6	7
NRMSD(L)	0.04	0.06	0.04	0.04	0.04	0.03	0.03
ΔL_{ave} (%)	0.01	0.37	-0.02	-0.19	-0.01	0.04	0.12
ΔU0 (%)	6.03	-12.3	0.71	-14.1	-4.02	2.29	-7.05
ΔUl (%)	-13.8	3.95	3.72	4.44	1.64	0.63	0.24

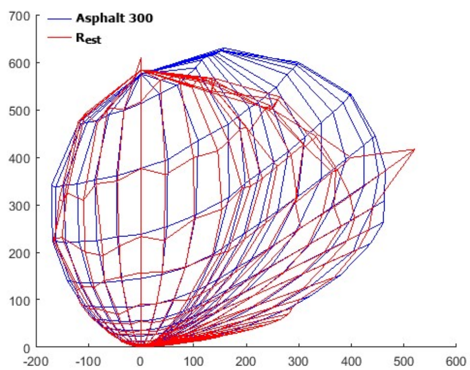

Fig. 5. R_{est} (red curve) vs $R_{asphalt300}$ (blue curve)

E. *Model robustness*

Finally to test the model robustness, a Gaussian noise σ_p has been added into the input luminance map:

$$L_p' = L_p (1+\sigma_p) \tag{12}$$

where σ_p is a random number from a normal law centred in zero with a standard deviation of 0.1, corresponding to large experimental uncertainties (20 % of relative uncertainty with a coverage factor k=2). The same process as previously has been followed with R2 as reference: constructing the model (A matrix) from scene geometry, luminaires intensity distributions and eigenvectors, then generating the noisy luminance map, calculating estimated *r*-table R_{est}, regenerating a luminance map from R_{est}, evaluating statistical and road lighting quality criteria. The following results are the median of 10^6 repetitions of this process to be reliable with respect to randomization. All computed criteria are gathered in Table VIII.

TABLE VIII. ALL CRITERIA DEVIATIONS WITH NOISE

Situation	1	2	3	4	5	6	7
median Q0	0.070	0.069	0.074	0.075	0.078	0.074	0.073
median S1	0.55	0.55	0.59	0.57	0.54	0.61	0.57
median NRMSD(R)	0.26	0.19	0.18	0.16	0.17	0.20	0.21
median NRMSD(L)	0.08	0.06	0.05	0.04	0.04	0.04	0.05
median ΔL_{ave} (%)	0.19	0.25	-0.03	-0.11	-0.03	0.05	0.09
median ΔU0 (%)	0.60	-0.98	-0.11	-3.81	0.38	-0.62	-6.93
median ΔUl (%)	-8.16	2.69	1.13	1.64	-3.12	-1.51	-7.19

Q0 and S1 are well estimated (here the reference is R2 with a Q0 value of 0.070 and S1 = 0.58), even with noisy luminance maps. The *r*-table estimations are also near the reference with NRMSD values from 0.16 to 0.26 and the associate luminance maps also (NRMSD(L) between 0.04 and 0.08). Moreover the average luminance is very well retrieved (less than 1% in all situations) as the overall uniformity (mostly less than 4%). The longitudinal uniformity is more badly retrieved (up to 8% of deviation) as it depends on two specific values in the map. Even with input data tainted with a 0.1 standard-deviation noise, the model remains stable. It is related to the highly over-determined system of equations (3) : $\mathbf{L}=\boldsymbol{\lambda}\ \mathbf{A}$. The model confirms its robustness and is also applicable with experimental data.

IV. CONCLUSION

From a database of 14 classical *r*-tables, a Principal Component Analysis has been performed. The *r*-tables can then be described in a 13-dimensional space in keeping good accuracy. That representation allows for a description of any *r*-table with 13 scalar numbers (and 13 eigenvectors) without losing its β, γ dependency. That description has been used to retrieve *r*-tables from luminance maps. On the one hand, the model requires the knowledge of the scene geometry and luminaire intensity curves. On the other hand, an input luminance map is needed, derived here from simulation as described in CIE road lighting reports. Luminance maps can also be based on ILMD images. The major benefit of our model lies in dealing with luminaires being currently in place without a limiting number. To assess the reliability of the model, statistical and road lighting quality criteria have been computed and analysed. Retrieved *r*-tables have been evaluated for seven road lighting CIE reference situations with very good agreement according to the NRMSD metric. A wet *r*-table and one not belonging to the database have also been retrieved with a good accuracy. Noise has been added into the input luminance map in order to evaluate the model robustness. Results have confirmed its stability and make it potentially applicable with ILMD data in real-time to modify the illumination with respect to estimated *r*-tables, to adapt the lighting to the real on site conditions [22].

ADDITIONAL INFORMATION

The methodology described in this paper is subject of a patent application.

REFERENCES

[1] V. Muzet, F. Greffier, A. Nicolaï, A. Taron, and P. Verny, ‘Evaluation of the performance of an optimized road surface/lighting combination’:, Lighting Research & Technology, vol. 51, no. 4, pp. 576–591, Oct. 2018, doi:10.1177/1477153518808334.

[2] V. Muzet, F. Greffier, and P. Verny, ‘Optimization of road surface reflections properties and lighting: learning of a three-year experiment’, in Proc. of the 29th Quadrennial Session of the CIE, Washington DC, USA, Jun. 2019, p. 525-535. doi: 10.25039/x46.2019.OP72.

[3] H. Gidlund, M. Lindgren, V. Muzet, G. Rossi, and P. Iacomussi, ‘Road Surface Photometric Characterisation and Its Impact on Energy Savings’, *Coatings*, vol. 9, nº 5, p. 286, Apr.. 2019, doi: 10.3390/coatings9050286.

[4] E. Dumont, J.-L. Paumier, V. Ledoux, ‘Are standard r-tables still representative of road surface photometric characteristics in France? ’, in CIE International symposium on road surface photometric characteristics, Torino, Italy, 2008, p. 8.
[5] C. Chain, F. Lopez, and P. Verny, ‘impact of road photometry on public lighting design’, in Proc. of the 26th session of the CIE, Beijing, China, 4-11 July 2007.
[6] V. Muzet, J. Abdo, ‘On site photometric characterisation of concrete pavements with coluroute device’, in Proc. of Lux Europa , Ljubljana, Slovenia, 2017, pp.164-168.
[7] I. Petrinska, D. Ivanov, D. Pavlov, et K. Nikolova, ‘Road Surface Reflection Properties of Typical for Bulgaria Pavement Materials’, in Proc. of Lux Junior, 2015, p. 7.
[8] E. Saint-Jacques, E. Dumont, and C. Villa, ‘Characterisation of the reflection properties of road surfaces using an in-lab gonioreflectometer’. in Proc. of the CIE midterm session, 2017, Jeju, South Korea. p. 433-442. doi: 10.25039/x44.2017.WP03.
[9] F. Greffier, V. Muzet, V. Boucher, F. Fournela, L. Lebouc, and S. Liandrat, ‘Influence of Pavement Heterogeneity and Observation Angle on Lighting Design: Study with New Metrics’, *Sustainability*, vol. 13, nº 21, Art. nº 21, 2021, doi:10.3390/su132111789.
[10] M. G. Bassett, S. Dmitrevsky, P. C. Kremer, and F. W. Jung, ‘Automated Facility for Measurement of Pavement Sample Reflectance Characteristics’, in Higway Information Systems, Visibility, and Pedestrian Safety, Transportation Research Record, 1983, pp.87-91.
[11] V. Muzet, J.-L. Paumier, Y. Guillard, ‘Coluroute : a mobile gonio-reflectometer to characterize the road surface photometry’, in CIE International Symposium on Road Surface Characteristics, Torino, Italy, 2007.
[12] D. Schreuder, ‘A portable reflectometer for on the road measurements. Experiences from The Netherlands’, in CIE International symposium on road surface photometric characteristics, Torino, Italy, 2008, p. 4.
[13] N. Strbac-Hadzibegovic, S. Strbac-Savic, and M. Kostic, ‘A new procedure for determining the road surface reduced luminance coefficient table by on-site measurements’, Light. Res. Technol., vol. 51, nº 1, p. 65-81, Jan. 2019, doi: 10.1177/1477153517736804.
[14] M. Frankinet, M. Gillet, V. Lang, J.L. Longueville, L. Maghe, C. Marville, C. Castellana, N. Debergh, J.J. Embrechts, ‘Memphis, characterization of road surfaces using a mobile gonio-reflectometer’, Report Memphis Project, 2005.
[15] L. Maghe, ‘Characterization of Road Surfaces using a Mobile Gonio-reflectometer’, CIE NEWS, 2006, 78: 5-6.
[16] W. Li, X. Zeng, H. Demirdes, X. Zhu, H. Shen, S. Fan, ‘New achievements in practical determination of road surface reflection table from in-situ measurement data’, in Proc. of the 28th Session of the CIE, 2015, 1676-1681.
[17] A. Ogando-Martínez, F. Troncoso-Pastoriza, P. Eguía-Oller, E. Granada-Álvarez, and A. Erkoreka, ‘Model Calibration Methodology to Assess the Actual Lighting Conditions of a Road Infrastructure’, Infrastructures, vol. 5, nº 1, p. 2, déc. 2019, doi:10.3390/infrastructures5010002.
[18] S. Buschmann, S. Völker, and J. Steblau, ‘New Image Based Measurement Method of Reflective Properties of Road Surfaces’, in Proc. of the CIE midterm session, 2017, Jeju, South Korea., Jan. 2018, p.284-293. doi:10.25039/x44.2017.OP39.
[19] CIE 2019, ‘Road Lighting Calculations, 2nd Edition’, Publication No. 140, Vienna: CIE, 2019.
[20] V. Boucher, F. Greffier, ‘Space of basis functions to retrieve road surface reflection tables from luminance maps’, in Press.
[21] N. Debergh and J. Embrechts, ‘Mathematical modelling of reduced luminance coefficients for dry road surfaces’, Light. Res. Technol., vol. 40, nº 3, p. 243-256, Sept.2008, doi:10.1177/1477153508095129.
[22] F. Greffier, V. Boucher, R. Dronneau, and V. Muzet, ‘Design of an adaptive road lighting installation taking into account the evolution of pavement reflection properties according to the weather conditions.’, LUX EUROPA 2022, Praha, CZ, Sep. 2022.

Methods to Determine Photosynthetic Photon Flux Density (PPFD) Using Low-Cost Spectral Sensors in Daylight

Tim Hegemann
Laboratory of Adaptive Lighting Systems and Visual Processing
Technical University of Darmstadt
Darmstadt, Germany
0000-0002-9451-3944

Khanh Quoc Tran
Laboratory of Adaptive Lighting Systems and Visual Processing
Technical University of Darmstadt
Darmstadt, Germany
0000-0003-1828-2459

Precise determination of the photosynthetic photon flux density (PPFD) is important for illumination in modern horticultural systems. Most systems for measuring PPFD are very expensive or lose the spectral properties of the incident light. Spectral sensors provide an intermediate solution. By using a large number of channels, the spectral information can be preserved and at the same time the PPFD can be determined with a low-cost sensor. In this paper, three methods for the determination of the PPFD using spectral sensors are presented and reviewed. It is shown that it is possible to determine the PPFD in daylight using suitable models.

Keywords—Photon Flux Density, PPFD, spectral sensing, regression models, Daylight

I. INTRODUCTION

Plant growth is mostly influenced by temperature, humidity, nutrient supply, water supply and light. In modern horticulture, growers are increasingly supported by technology to use these parameters to make cultivation as efficient as possible. For example, decisions about heating or watering in the greenhouse are supported by common sensors.[2] Likewise, sensors help measure the fertilizer status of the plant or the concentration of fertilizer in the substrate.

The light relevant for plants, i.e. the light that contributes to the photosynthesis of the plant, is defined according to McCree in 1972 as photosynthetically active radiation (PAR) for the range from 400nm to 700nm [2]. Within the PAR range, all photons are summed without further *weighting*. Growers and farmers measure photosynthetically active photon flux density (PPFD) in $\mu molm^{-2}s^{-1}$, which indicates how many photons are received in the spectral range of PAR radiation per area and per area per time unit. By continuously recording the PPFD, it is possible to determine the light sum of an area element over the entire day, which is called the day light integral (DLI).

If the day light integral is documented over the lifespan of the plant, a prediction of growth as well as flowering, can be made using appropriate crop-dependent models. Prediction models for the DLI based on solar radiation are proposed by Albright et al..[3]

For measurement of the PPFD different approaches were made in previous works. Summed up, it can be done with several techniques, as stated by Ross and Sulev using: (1) spectroradiometers; (2) pyranometers covered with hemispherical glass filters; or (3) sensors based on silicon photodiodes (quantum sensors) [4-18].

Measuring with spectrometers preserves the spectral composition as information, but spectrometers are too expensive for most applications or are inappropriate for the weather at the measurement location. Pyranometers are used to measure solar radiation, including the IR range. In today's horticulture, quantum sensors are used which use photodiodes to detect incident light. For this purpose, an optical filter set is used to weight the incident spectrum based on the photon energy as well as the spectral sensitivity of the receiver. The information about the spectral composition of the incident light is hereby lost. The accuracy of quantum sensors varies widely and is largely dependent on the spectral sensitivity of the sensor as well as the light source. For example, Barnes et al. show that higher accuracy is achieved with broad spectra. Errors of more than 30% could be determined by Blonquist et al. as well as LI-COR in experiments of different sensor light source pairings [19-21].

Recent work has already demonstrated the potential of spectral sensors for the measurement of PPFD. [22-24]

Due to their design, spectral sensors allow only a narrow portion of the incident spectrum to be viewed at a time. For this purpose, arrays of photodiodes are usually coated with individual optical filters. In combination with the filter characteristics and the sensitivity of the semiconductor, optical bandpass filters are created. Depending on the number and distribution of the different photodiode-filter combinations (channels), the loss of spectral information can be reduced. Depending on the application, optical filters are used to adjust the sensitivity function and to (1) spectral measurements, (2) an adaptation to the color sensitivity curves of the eye, (3) an adaptation to the luminous efficiency function for photopic vision V(λ), and (4) a fit to calculate the R-G-B components. None of these filters allows direct measurement of the PPFD, but these filters can be used to provide information about the spectrum. This allows the calculation of a conversion factor to calculate the PPFD from the measured irradiance calculation.

II. METHODS

In this work, different methods for the calculation of PPFD are verified in practice. For this purpose, daylight measurements were carried out simultaneously on several days with a spectral sensor and a spectrometer. The spectral sensor has 8 channels in the visible range as well as one channel in the IR range and one without filter optics.[25]

Due to the IR sensitivity of some spectral channels of the spectral sensor, an IR filter was connected upstream. To make the measurements comparable, the integration time was kept constant for each gain stage. Between each measurement, a dark current measurement with the spectrometer and a gain adjustment of the spectral sensor were performed.

For the first method, a reduced PAR weighting function is used to calculate the PPFD. For the second, the CIE daylight model is used to estimate the PPFD, and the third method relies on a gaussian model to calculate the PPFD. For these methods, the spectral response curves of the channels of the spectral sensor are needed. These are determined using a monochromator and a xenon light source in an integrating sphere. A spectrometer is used as a reference. The sensitivity curves shown in Figure 1 are determined for the spectral sensor using the simple estimation method according to HP Laboratories. [26,27]

With the help of the spectrum of the incident light and the sensitivity curves of the channels, the spectral irradiance relevant for the channel can be calculated. The conversion of the spectral irradiance into PPFD can be done with the help of a PAR weighting curve W(λ) and conversion factors. [24]

W(λ) is a function for weighting the spectral irradiance according to the energy content of photons at the specific wavelength λ and shown in Figure 2. The conversion the energy related quantity W m^{-2} into the quantity µmol m^{-2} s^{-1} is done by Planck's quantum of action h (6.6261×10^{34} J s), Avogadro's constant NA (6.0221×10^{23} mol^{-1}) and the speed of light c (299 792 458 m s^{-1}).

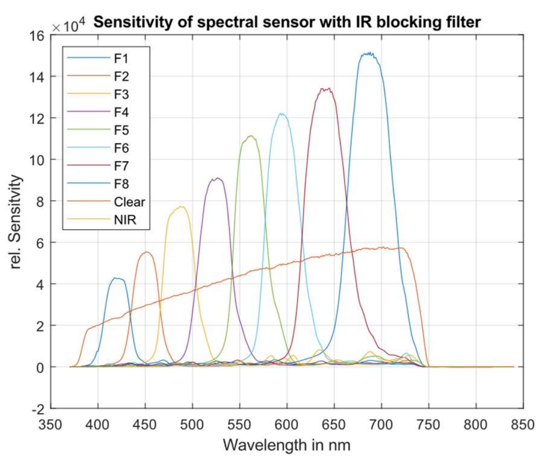

Figure 1: Channel sensitivity of spectral sensor with IR filter. Outside the PAR region the function is equal to zero

$$W(\lambda) = \frac{\lambda}{h \cdot c \cdot N_A} \quad (1)$$

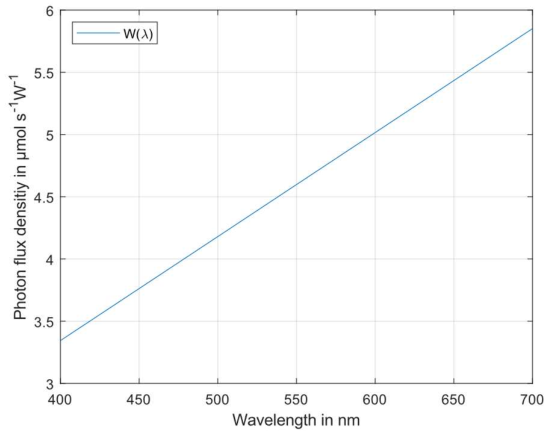

Figure 2: Weighting function W(λ). Outside the PAR region the function is equal to zero.

The first method to approximate the PPFD using spectral sensors is based on the sensitivities $S_n(\lambda)$ of the channels. Thus, the W(λ) function is simulated using the sensitivities and a factor which depend on the value of the W(λ) function at the center-wavelength of each channel. By integrating the incident spectra ($E_e(\lambda)$) with the sensitivity curve of each channel $S_n(\lambda)$ and weight it with the value of the W(λ)-curve at the corresponding center-wavelength of each channel a simulated channel PPFD ($PPFD_n$) can be found.

$$PPFD_n = \mathrm{W}(\lambda_{\mathrm{center}}) \int_{400}^{700} S_n(\lambda) \cdot E_e(\lambda)\, d\lambda \quad (2)$$

By dividing the $PPFD_n$ value and the measured channel value F_n the scaling factor α_n for each channel can be found.

$$\alpha_n = \frac{PPFD_n}{F_n} \quad (3)$$

$$PPFD = \sum_{n=1}^{8} F_n \cdot \alpha_n \quad (4)$$

Summing up these factorized channels gives the PPFD of the incident spectra. Because of overlapping of the channels an offset for correction is needed. To find the values of α_n, the Data were split into training data (80%) and test data (20%).

In the second method, the chromaticity coordinate is calculated from the channels of the spectral sensor using a regression model. Based on the chromaticity coordinates and the conversion according to McCamy, the color temperature CCT can be calculated.[28] With the help of the CIE daylight spectrum, a corresponding daylight spectrum with the calculated color temperature can be generated and by using the W(λ)-curve the PPFD can be calculated.[29]

Also, a model is used to directly approximate the CCT from the measured values of the channels of the spectral sensor.

For the third method, a regression model is used to directly map the measured values of the sensor channels to the PPFD.

III. Results

For this work, only measured values of one gain factor with fixed integration time were used to exclude nonlinearities between gain stages. The data set has 276 measurement points and was split into 80% training data and 20% test data.

Method 1

Figure 3 shows the predicted PPFD by using Eq. 4 versus the PPFD measured with the reference instrument. It can be clearly seen that it is possible to estimate the PPFD, but it has a high variance. Using this method, an R^2 of 0.92 and an RMSE of 86.75 are obtained. The factors used to weight the channel readings are shown in Table I.

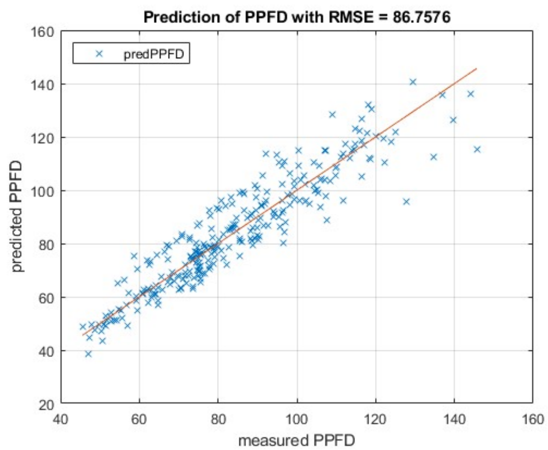

Figure 3: Prediction of PPFD in µmol m^{-2} s^{-1} with Method 1 using all 8 Channels of the spectral sensor in visual spectral range.

TABLE I. FACTORS FOR EACH CHANNEL OF THE SPECTRAL SENSOR UNSING METHOD 1

Channel	Center wavelength in λ	W(λ) in µmol W^{-1} s^{-1}	α_n
1	415	3.452	0.056
2	445	3.703	0.063
3	480	3.995	0.056
4	515	4.204	0.059
5	555	4.539	0.057
6	590	4.915	0.056
7	630	5.249	0.055
8	680	5.751	0.054

Method 2

For the second method, first color locus (x, y, z) is calculated using the spectral channels. A regression model is used to calculate the chromaticity coordinate. Channels 3, 5 and 8 are used for modeling. These cover one channel from the red, blue and green spectral regions. Using all channels for modeling did not yield significant improvements. Various approaches e.g., linear regression, regression trees, support vector machines, Gaussian process regression (GPR), and neural networks were reviewed. A model from Gaussian process regression was shown to be the best model.

Figures 4 and 5 show the color coordinates (x, y) calculated using the model versus those of the reference. With an RMSE of 0.0014 for x and 0.0012 for y, the color coordinates can be predicted in a sufficiently good way.

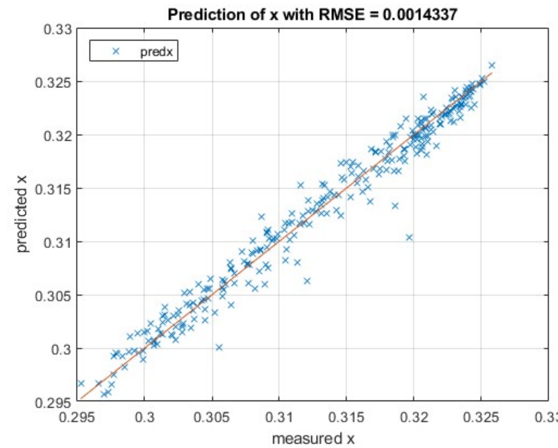

Figure 4: Prediction of color coordinate x by using a GPR-Model.

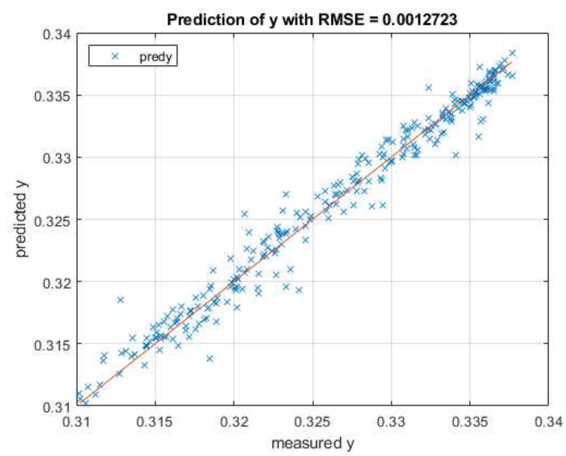

Figure 5: Prediction of color coordinate y by using a GPR-Model.

The color temperatures calculated from the color coordinates using McCamy are shown in Figure 6.

In comparison, another GPR model shows the direct calculation of the color temperature from the channel values (Figure 7). By modeling the CCT directly from the Channel values (RMSE=79.2), the prediction of the CCT is better than modeling the color coordinates and calculating the CCT (RMSE=92.44).

For calculating the CIE-daylight spectra by using the CIE-daylight model with an absolute value a scaling factor is needed. This scaling factor could be found by using the reference spectra and split the data in training and test data.

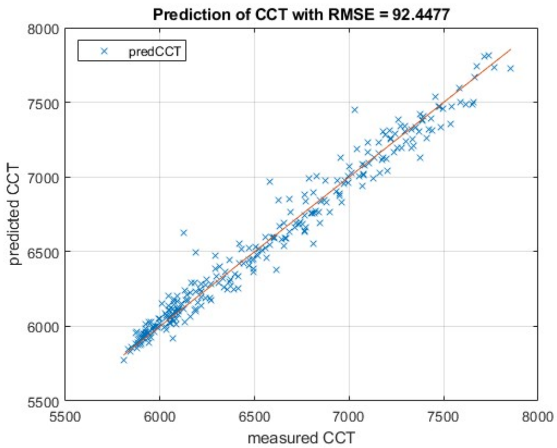

Figure 6: Prediction of CCT by using color coordinates and McCamy.

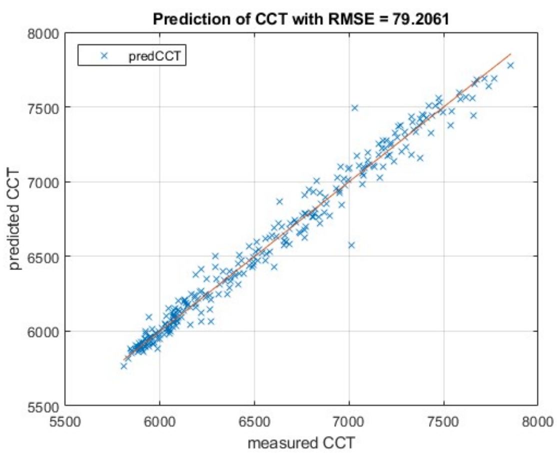

Figure 7: Prediction of CCT by using the channel values and a GPR-Model.

The PPFD is calculated using the two calculated CCT as well as the CIE daylight model. For both calculations of PPFD, the results are compared in Figures 8 and 9. While the direct calculation of the CCT from the channel values is more

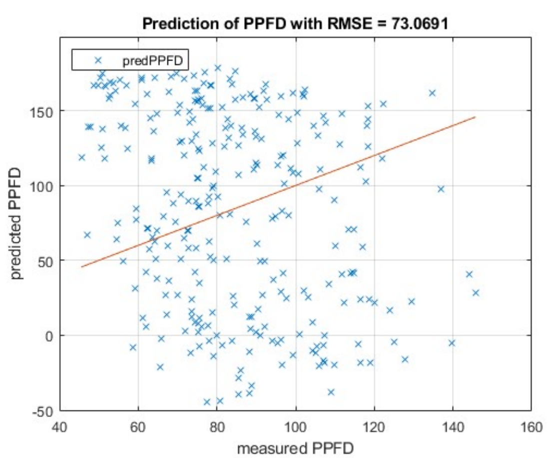

Figure 8: PPFD prediction in µmol m^{-2} s^{-1} by using the CCT calculated from the color coordinates x and y.

accurate than the calculation via the chromaticity coordinate, both methods show approximately the same accuracy in the calculation of the PPFD. The calculation via the chromaticity coordinate is minimally better with an RMSE=73 than that via the channel values with an RMSE=74.2. Both determinations show a high variance and are not suitable for a precise PPFD determination.

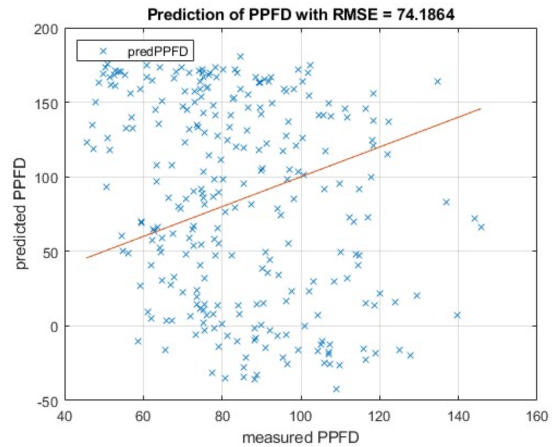

Figure 9: PPFD prediction in µmol m^{-2} s^{-1} by using the CCT calculated directly from the measured channel values.

Method 3

In the third method, various linear regression approaches, regression trees, support vector machines, Gaussian process regression, and neural networks were also used to determine the PPFD directly from the channel values. Again, a GPR approach performed best.

Figure 10 again shows the comparison of the calculated PPFD and the measured reference.

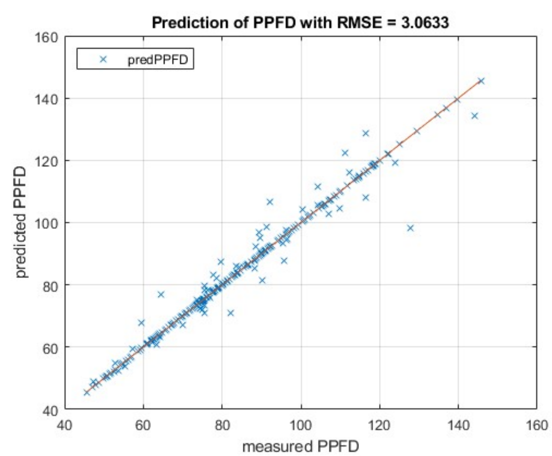

Figure 10: Predicting the PPFD in µmol m^{-2} s^{-1} by using the measured channel values and a GPR-model.

IV. Discussion

With method 1 and 3 it is possible to determine the PPFD. Whereby the third method allows the most accurate determination (see Table II). Method 1 requires an accurate spectrometer and monochromator for the calculation of the $PPFD_n$ as well as a light laboratory to record the sensitivity curves of the spectral channels. The resulting accuracy in the PPFD estimation is not ultimately accurate enough to justify this effort. Method two uses the CIE daylight model, and the CCT or color coordinates (x, y, z) to determine the PPFD. Determining the CCT via both methods is insufficiently accurate to determine the PPFD accurately afterwards. Another weakness of this method is the CIE daylight model, which involves a purely color temperature dependent spectral distribution. However, due to location, clouds, shadows or particles in the atmosphere, the spectral distribution can deviate significantly from the model. Adding location and cloudiness can help to model the daylight spectrum better. The use of true xyz sensors could also improve the determination of the CCT.

For the third method, a model can be found that can determine the PPFD based on the channel values. For the model building computing power is needed, but afterwards the model can also be done on a microcontroller basis, which combines a low-cost sensor with a low-cost computer and thus provides a cost-efficient measurement system.

TABLE II. Comparision of the thre Methods for PPFD determination by using low-cost spectral sensors

	Method 1	Method 2 (xyz)	Method 2 (CCT)	Method 3
RMSE	86.75	73.0	74.0	3.06

References

[1] van Iersel MW, Chappell M, Lea-Cox JD. Sensors for improved efficiency of irrigation in greenhouse and nursery production. HortTechnology 2013; 23: 735–746. DOI: 10.21273/HORTTECH.23.6.735.

[2] McCree K. Test of current definitions of photosynthetically active radiation against leaf photosynthesis data. Agricultural Meteorology 1972; 10: 443–453. DOI: 10.1016/0002-1571(72)90045-3.

[3] Albright LD, Both AJ, Chiu AJ. Controlling greenhouse light to a consistent daily integral. Transactions of the ASAE 2000; 43: 421–431. DOI: 10.13031/2013.2721.

[4] Pinho P, Hyt¨onen T, Rantanen M, Elomaa P, Halonen L. Dynamic control of supplemental lighting intensity in a greenhouse environment. Lighting Research and Technology 2013; 45: 295–304. DOI: 10.1177/1477153512444064.

[5] Schwend T, Beck M, Prucker D, Peisl S, Mempel H. Test of a par sensor-based, dynamic regulation of led lighting in greenhouse cultivation of helianthus annuus. European Journal of Horticultural Science 2016; 81: 152–156. DOI: 10.17660/eJHS. 2016/81.3.3.

[6] van Iersel MW, Gianino D. An adaptive control approach for light-emitting diode lights can reduce the energy costs of supplemental lighting in greenhouses. HortScience 2017; 52: 72–77. DOI: 10.21273/HORTSCI11385-16.

[7] Federer CA, Tanner CB. Sensors for measuring light available for photosynthesis. Ecology 1966; 47: 654–657. DOI: 10.2307/1933948.

[8] McCree KJ. A solarimeter for measuring photosynthetically active radiation. Agricultural Meteorology 1966; 3: 353–366. DOI: 10.1016/0002-1571(66)90017-3.

[9] Biggs WW, Edison AR, Eastin JD, Brown KW, Maranville JW, Clegg MD. Photosynthesis light sensor and meter. Ecology 1971; 52: 125–131. DOI: 10.2307/1934743.

[10] Muchow RC, Kerven GL. A low cost instrument for measurement of photosynthetically active radiation in field canopies. Agricultural Meteorology 1977; 18: 163–239. DOI: 10.1016/0002-1571(77) 90036-

[11] Woodward FI. Instruments for the measurement of photosynthetically active radiation and red, far-red and blue light. Journal of Applied Ecology 1983; 20: 103–115. DOI: 10.2307/2403379.

[12] Mims FM III. A 5-year study of a new kind of photosynthetically active radiation sensor. Photochemistry and Photobiology 2003; 77(1): 30–33. DOI: 10.1562/0031-8655(2003)0770030AYSOAN2.0.CO2.

[13] Caya MVC, Alcantara JT, Carlos JS, Cereno SSB. Photosynthetically active radiation (par) sensor using an array of light sensors with the integration of data logging for agricultural application. In: 2018 3rd International Conference on Computer and Communication Systems (ICCCS). Piscataway, NJ: IEEE, 2018: 377–381. DOI: 10.1109/ ccoms.2018.8463321.

[14] Yadav D, Sumesh M, Beno T, Karanth S, Sadashivappa G. Design of photosynthetically active radiation sensor. Examines in Physical Medicine and Rehabilitation 2018; 1(5). DOI: 10.31031/ epmr.2018.01.000521.

[15] Rajendran J, Leon-Salas WD, Fan X, Zhang Y, Vizcardo MA, Postigo M. On the development of a low-cost photosynthetically active radiation (par) sensor. In: 2020 IEEE International Symposium on Circuits and Systems (ISCAS). Piscataway, NJ: IEEE, 2020: 1–5. DOI: 10.1109/iscas45731.2020. 9181220.

[16] McCree K. The measurement of photosynthetically active radiation. Solar Energy 1973; 15: 83–87. DOI: 10.1016/0038-092X(73)90010-8.

[17] Norman JM, Tanner CB, Thurtell GW. Photosynthetic light sensor for measurements in plant canopies. Agronomy Journal 1969; 61: 840–843. DOI: 10.2134/agronj1969.00021962006100060004x.

[18] Ross J, Sulev M. Sources of errors in measurements of PAR. Agricultural and Forest Meteorology 2000; 100: 103–125.DOI: 10.1016/S0168-1923(99)00144-6.

[19] Barnes C, Tibbitts T, Sager J, Deitzer G, Bubenheim D, Koerner G, et al. Accuracy of quantum sensors measuring yield photon flux and photosynthetic photon flux. HortScience 1993; 28: 1197–1200. DOI: 10.21273/HORTSCI.28.12.1197.

[20] Biosciences LC. Comparison of quantum sensors with different spectral sensitivities. LI-COR Biosciences Technical Note 2018, Retrived from, Spectral sensors to determine photosynthetic photon flux density 11 Lighting Res. Technol. 2022; 0: 1–12 https://www.licor.com/ documents/oi26ib7eb6wm5y5u9ebv4b3jodm09tf9.

[21] Blonquist M, Johns J. Accurate PAR measurement: comparison of eight quantum sensor models. Apogee Instruments Research Report 2018, Retrived 20th August 2021 from, https://www.apogeeinstruments.com/content/Comparison-of-Eight-Quantum-Sensor-Models.pdf.

[22] Bäumker E, Zimmermann D, Schierle S,Woias P. A novel approach to obtain PAR with a multi-channel spectral microsensor, suitable for sensor node integration. Sensors 2021; 21: 3390. DOI: 10.3390/ s21103390.

[23] Leon-Salas WD, Rajendran J, Vizcardo M, Postigo-Malaga M, Postigo-Malaga M. Measuring photosynthetically active radiation with a multichannel integrated spectral sensor: 2021 IEEE International Symposium on Circuits and Systems (ISCAS), Daegu, South Korea, May 22–28:2021. DOI:10.1109/iscas51556.2021.9401321.

[24] Hegemann T, Balasus J, Trinh Q, Herzog A, Khanh T. Using spectral sensors to determine photosynthetic photon flux density in daylight – A theoretical approach. Lighting Research & Technology. April 2022. doi:10.1177/14771535221077881

[25] AMS. AS7341 11-channel multi-spectral digital sensor. Retrived 20th August 2021 from, https://ams.com/documents/ 20143/36005/ AS7341_DS000504_3-00.pdf.

[26] Vora PL, Farrell JE, Tietz JD, Brainard DH. Digital color cameras - 2 - spectral response. HP Laboratories Technical Report 1997: 97–54.

[27] Hubel PM, Sherman D, Farrell JE. A comparison of methods of sensor spectral sensitivity estimation. HP Laboratories Technical Report 1994: 45–48.

[28] McCamy CS. Correlated color temperature as an explicit function of chromaticity coordinates. Color Research & Application 1992; 17(2): 142–144. DOI: 10.1002/col.5080170211

[29] CIE. Technical Report 015:2008 Colorimetry. 4th Edition. Vienna: CIE, Central Bureau, 2018. ISBN 978-3-902842-13-8. DOI: 10.25039/TR.015.2018

Home as the New Office: Considerations of Interior Lighting Including Occupancy Scenarios of Ongoing Covid-19

Banu Manav
Department of Interior Architecture and Environmental Design
Faculty of Art and Design
Kadir Has University
Istanbul, Turkey
banu.manav@khas.edu.tr

Egemen Kaymaz
Department of Architecture
Faculty of Architecture
Bursa Uludag University
Bursa, Turkey
ekaymaz@uludag.edu.tr

***Abstract*—This study aims to assess how to apply melanopic (non-visual) requirements together with photopic (visual) requirements and energy performance requirements to lighting scenarios for residential spaces. Two living rooms in different orientations, one facing to the North and the other facing to the South-east direction, are evaluated according to the visual comfort parameters together with the human-centric lighting (HCL) concept and equivalent melanopic lux (EML) metrics in WELL Building standard v2:2022. The visual and non-visual aspects of lighting are analyzed and evaluated by using different simulation programs, DIALux Evo and DesignBuilder. Also, the effect of wall reflectance values on energy performance is analyzed for four different values. The results of computer simulations demonstrate that depending on the occupancy pattern and façade orientation, the application of LEDs and dimming control together with the increase in wall reflectance value can improve lighting energy performance by up to 37% in comparison to manually controlled luminaires with CFL lamps. The melanopic lux calculations indicate that higher illuminance is necessary on the vertical plane than the proposed lighting scenarios to satisfy the HCL concept and EML metrics in the WELL standard. This may lead to a higher installed power and correspondingly an increase in lighting energy consumption.**

***Keywords*—residences, visual comfort, lighting energy performance, building simulation, Covid-19, human-centric lighting**

I. Introduction

Lighting shall meet visual comfort, while energy efficiency and environmental factors shall be satisfied together with human needs [1]. As a result of industrialization, our daytime light exposure decreases. We benefit from less daylight during the day and less darkness during the nighttime. Electric lighting is considered the dominant lighting source which is a critical design factor for our health as well. Recent research highlights that light does more than enable vision; besides supporting visual perception, it influences our physiology and behavior including our circadian system, mood, and even cognitive functions [2]. It is well known that with emerging lighting technologies, different lighting scenarios can promote psychological wellbeing, improve performance and consider energy efficiency [2,3].

Today, wellbeing is closely linked to proper lighting design which satisfies visual comfort, efficiency, and psychological comfort [4,5,6]. As Viola et al. [7], Arendt [8], Do and Yau [9], Jarboe, Snyder, and Figueiro [10] suggest, light is effective in generating a non-image-forming, biological response affecting the human circadian clock.

The home-bound period urged many citizens to stay in their homes while, remote working policies and digital technologies have gained wider acceptance that changed our modes of working, teaching, and learning from in-person to virtual conditions. The pandemic crisis has had various impacts on the way we live in our homes and the way we evaluate the design of our living habitat and it forward the "home office" idea again. More attention has been given to spatial organization, and functionality, to improve indoor environmental quality and promote productivity during homestays. In this sense, lighting has a great influence on our mood, circadian rhythm, visual acuity, and alertness as well as the quality of interiors.

On the other hand, with the extended residential occupancy, energy consumption has increased since the beginning of the pandemic. According to the energy policy review of IEA in 2021 [11], 21.1% of the total electricity consumption in Turkey is attributed to the residential sector which has also experienced significant growth with 38% since 2000. Similarly, according to the Energy Market Regulatory Authority monthly reports which also include the energy statistics of the case study area, Bursa increased by an average of 8.2% from the beginning of the COVID-19 pandemic in March 2020 until the controlled normalization process in March 2021 compared to the same period of the previous year [12].

Residential lighting becomes a significant contributor to energy costs in most industrialized countries [13,14]. Therefore, it is worth studying design variables that are effective in lighting energy consumption. As in the design of almost all building types, the first and the common principle is to benefit daylight in residences. In this regard, various researchers have performed experimental studies, field measurements, and computational simulations particularly focusing on maximizing daylight availability indoors [15-23].

As suggested by Aman et al. [24] and Attia et al. [25], the choice of light source and luminaire has a decisive impact on the annual total electricity consumption of buildings. The lighting literature supports that by controlling the regulation of the lighting power gradually (dimming) or completely (on/off), potential energy savings can be achieved. Similarly, Dubois and Blomsterberg [26] highlight the importance of lighting control system applications for energy conservation. Makaremi et al. [27] and Frascarolo et al. [28] have also investigated energy savings by incorporating LED technology with lighting control strategies that are up-to-date and also advisable to adapt to interior lighting systems.

Another design variable is the light reflectance of surfaces. Most of the prior research has emphasized that the reflective property of interior materials can contribute to achieving the required illuminance, thus operating less artificial lighting and lowering the overall energy consumption [29-34].

R. Singh and R. Rawal [35] and Yu and Su [36] state that the function of a space, its daylight potential, and occupancy rate also determine daytime electric lighting load and energy savings. In this regard, Das and Paul [37] analyzed daylight availability and artificial lighting requirement in residential buildings considering the floor plan, the location and orientation of the building, and the interior design of various plan typologies. Occupant behavior and lifestyle preferences regarding internal illuminance were also studied within the scope of the research.

In addition to the previous articles on occupancy patterns in building energy consumption [31, 35, 38, 39], Rinaldi et al. [40] focus on the influence of occupant behavior on the characteristics of the built environment, while Gerhardsson et al. [41] conducted a survey to explore occupants' experiences with their residential lighting. Zhang et al. [42] argued that not only technology but also humans' energy-related behavior in buildings shall be included in energy performance studies to achieve building energy conservation goals. Recent research [43, 44, 45] has reviewed the impacts of "stay-home living patterns" on energy consumption in residential buildings.

This study aims to evaluate the hybrid mode of working schedules on visual comfort, occupancy patterns, and energy efficiency. In this context, the impact of interior lighting design and technology, lighting operation schedules, together with manual and daylight integrated lighting control strategies are analyzed for a residential building with a special focus on human-centric lighting (HCL).

II. Method

A. Field Study and the Participant Group

For the case study, a multi-story residential site located in a temperate climate zone in Bursa (Turkey) was selected which exemplifies a recently constructed gated community for high-income groups. The housing complex holds B class building energy certification according to Turkish building energy performance regulation [46]. The six-story high apartment blocks were constructed on 21,500 m², with two flats (each having 232 m² area of use) on each story.

The shadow analysis of 3D apartment blocks for morning and noon hours on summer and winter solstices is given in Fig 1. Block VII, the living space that faces to the North, is the most unfavorable case; whereas, Block II, the living space that faces to the South-east, is the best among all buildings in terms of annual lighting energy consumption. In the study, these two cases are studied and compared.

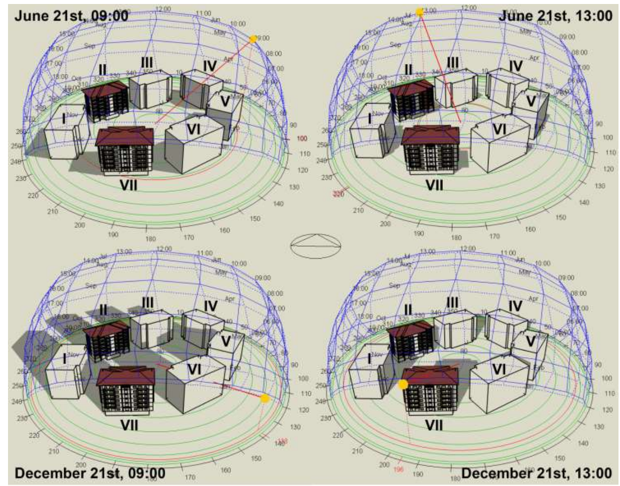

Fig. 1. 3D model of selected buildings and shadow analysis of the study site on solstice dates

By referring to the importance of occupancy patterns in previous research [40-42], in the present study, we referred to the results of a questionnaire that investigates user preferences. It is a part of a face-to-face survey that was conducted by the authors in 2020 before the pandemic. The questionnaire results were also evaluated to estimate occupancy rates and lighting operation hours and set up the lighting design and occupancy scenarios. The 56 feedbacks out of 84 questionnaires are used as valid data in simulation models. The results are summarized below:

- Gender and age range distribution; 33.9 % were male and 66.1 % were female with the age ranges between 18 to 66 and above, (3.6 % were between 18-25 age, 35.7 % were between 26-35, 26.8 % were between 36-45, 26.8 % were between 46-55, and 7.1 % were 56 years old and/or above).
- Education level distribution; 67.9 % are university graduates.
- The average household size is 4 persons (42.9 %), followed by 3 members (28.6 %). It was recorded that 50 % have two children, followed by 26.7 % with one child. Nearly all of the participants have been living in the same residences (96.4 %) between 1-5 years.
- Occupational status; 53.6 % are employed, 33.9 % are unemployed, 10.7 % are retired and 1.8 % are students.
- Average time spent at home; on weekdays and weekends is recorded. The living room is stated to be the most frequently used residential space (44.6 %) followed by the kitchen (28.6 %).

As seen in Fig. 2, the participants preferred various lighting fixtures while the majority of them prefer pendant luminaires. For the lamp type, light-emitting diodes (LED) were preferred by 63.6 %, compact fluorescent lamps (CFL) by 20.6%, and other lamp types by 15.6 %. The breakdown of the responses for correlated color temperature (CCT) indicates that neutral white (3000-4500K) is more commonly used than warm white (2700-3000K) and cool white/daylight (4500-6000K) option indoors.

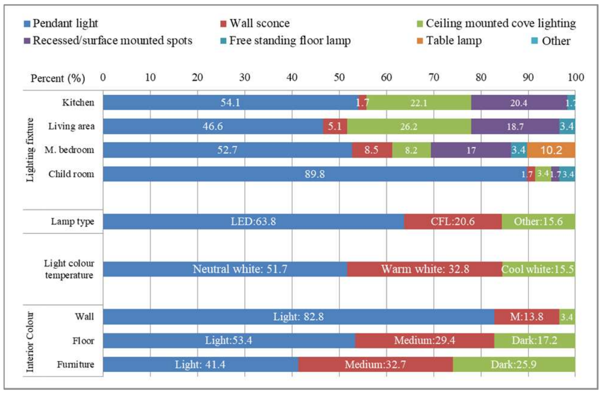

Fig. 2. User preferences; lighting fixtures, lamp type, color temperature, interior color preferences

B. Lighting and Building Energy Performance Simulations

In the study, the reference building's occupancy scenario, artificial lighting system, and operation schedule were created considering the field study and the questionnaire results. Static and annual-based dynamic simulations were run including the EML approach.

Two computer programs with considerable accuracy were adopted for the simulation of interior lighting considering energy and visual comfort. In line with the mean of occupants' responses for lighting fixtures, lamp type, light color temperature, and interior color preferences, lighting scenarios were modeled; daylight and artificial lighting conditions are simulated in DIALux Evo software. Based on the architectural plans and national building energy performance regulation [46], the reference building energy model was created in DesignBuilder which is a graphical interface of the EnergyPlus simulation engine.

a) Artificial Lighting Scenarios: Lighting scenarios are proposed for the living room of a sample apartment. It is based on both the user preferences in Fig. 2 and the up-to-date technology that is LED lamps. Artificial lighting proposals are summarized below;

- L_1 scenario is a conventional lighting solution designed by CFL lamps. The system is managed by independent switches.
- L_2 scenario is a dynamic lighting scenario designed by dimmable LED lamps which are also suitable for color adjustment from warm to cool white (2700 K to 6500 K). The luminaries are selected with efficacy of a minimum of 70 lm/W for general lighting. The system is operated by brightness-related lighting automation.

The light reflectance coefficients are set by r=0.4, r=0.5, r=0.8 and r=0.6 for r_{floor}, r_{wall}, $r_{ceiling}$ and $r_{furniture}$; total solar heat gain coefficient (SHGC) and visible light transmittance (T_{vis}) of windows are assumed as t=0.75, and t=0.80 respectively.

Visual Approach: The lighting simulations are run for 0.80 m above the floor level with 0.5 m away from the room perimeter for the horizontal working plane. The average illuminance (E_{av}), uniformity of lighting (U_o: E_{min}/E_{av}) and unified glare ratio (UGR) are recorded as well. L_1 and L_2 scenarios are designed by considering the recommended thresholds in EN 12464-1 [47] and IESNA lighting guide [48]. Light distribution and specifications of luminaires together with lighting system layouts are presented in Table 1. Detailed technical data about the selected products can be reached from the DIALux Evo library [49].

A central pendant luminaire (b: diffused for L_1 and direct/indirect for L_2 in Table 1) is used above the seating area together with strip lights (a: indirect) installed as cove lighting. Similarly, the dining area is lit by a pendant luminaire with direct-indirect light distribution (c: for L_1 and b: for L_2).

TABLE I. LIGHTING SCENARIOS WITH LUMINAIRES' TECHNICAL DATA

Type	Light distribution and specifications of luminaires used			
	L₁: CFL		***L₂: LED***	
a. Ceiling mounted	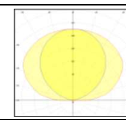	φ: 1230 lm P: 14 W Tc: 3000 K CRI: 85	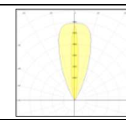	φ: 1288 lm P: 15.1 W Tc: 3000 K CRI: 80
b. Pendant	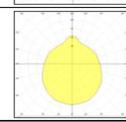	φ: 3200 lm P: 42 W Tc: 2700 K CRI: 84	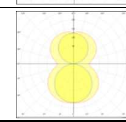	φ: 1258 lm P: 17 W Tc: 2687 K CRI: 92
c. Pendant	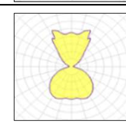	φ: 3200lm P: 42W Tc: 2700 K CRI: 84	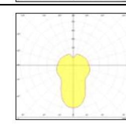	φ: 3587 lm P: 41 W Tc: 4000 K CRI: 90
d. Portable floor lamp	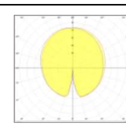	φ: 3200 lm P: 42 W Tc: 2700 K CRI: 84	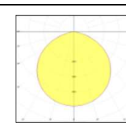	φ: 800 lm P: 10 W Tc: 2689 K CRI: 90
e. Table lamp	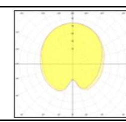	φ: 3200 lm P: 42 W Tc: 2700 K CRI: 84	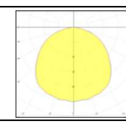	φ: 75 lm P: 2.7 W Tc: 3000 K CRI: 80
Living room lighting system layout L_1: CFL	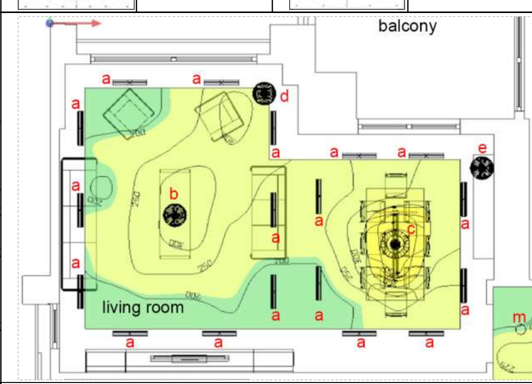			
Living room lighting system layout L_2: LED	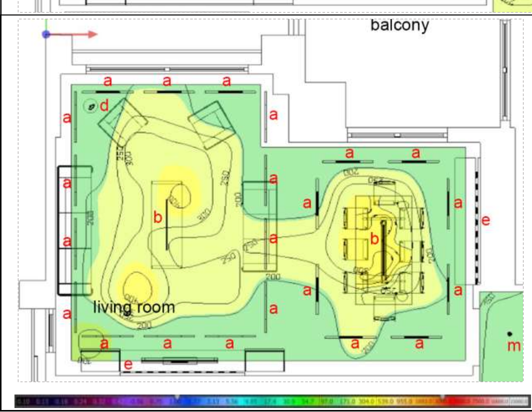			

Portable floor lamps (d) and table lamps (e) are placed in the living room to improve occupant flexibility and make individual lighting possible in both lighting proposals.

EML Approach: The biological and non-visual effects of light are calculated as equivalent melanopic lux (EML) according to the toolbox of IWBI International Well Building Institute [50] and WELL building standard v2 [5]. To calculate EML, firstly electric lighting simulations are run for 09:00 and 13:00 hours on the 21st of June (CIE clear sky) and on the 21st of December (CIE overcast sky). Melanopic light values are calculated for the sample living rooms located on the 1st floor according to the equation below [6,48]:

$$EML = L \times R \tag{1}$$

L is the simulated illuminance on the working plane and R is the melanopic ratio of the light source. Simulations are performed for the vertical plane in the center of the living room facing toward the walls (h:1.2 m for the day and h: 0.76 for the night). For the working and learning areas, the illuminance on the vertical plane facing forward (h: 1.2 m) is calculated. The melanopic ratio of 2700 K LED, 3000 K Fluorescent and 6500 K daylight are 0.45, 0.45, and 1.1 respectively [48].

Occupancy Scenarios and Lighting Schedules: The occupancy scenarios are applied to general and task lighting including weekdays and weekends (Fig. 3). Based on the previous research on residential occupancy and electricity consumption in households [12, 43, 44, 45], we assumed that the room has been used more frequently during and after the Covid-19. The artificial lighting operation schedules are summed up as follows;

- S_1 pre-pandemic scenario; is based on the survey results. It is assumed that each residence has at least one working member between 08:00 – 18:00,
- S_2 stay-at-home scenario; is developed according to the increased use of residential space during the governmental restrictions and COVID-19 lockdown conditions,
- S_3 post-pandemic scenario; is based on today's hybrid working conditions.

The occupancy fraction is a value between 0 and 1, where "0" indicates that the lights are off for an hour and "1" represents they are fully on.

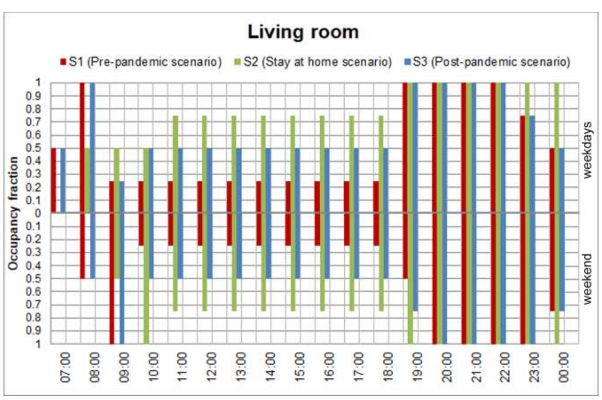

Fig. 3. Lighting system operation schedules regarding the occupancy rates

b) Lighting System Control Scenarios: Besides the artificial light source, daylight availability and user behavior, one other possible efficiency measure related to lighting energy in buildings refer to the use of lighting system automation. In this regard, four lighting control scenarios that are explained below are simulated:

- C_0 scenario; Lights are fully-on due to user presence in a zone.
- C_1 scenario; Lights are controlled by manual switching through the occupancy schedule. Electric lights are switched off when the target light level can be maintained on certain work planes by daylight alone.
- C_2 scenario; the artificial lighting system is operated with LED lamps suitable for lighting automation. In the stepped lighting control scenario, the general light level can be dimmed by four steps and finally switched on/off according to daylight availability by a photo sensor installed in the center of the room.
- C_3 scenario; In the linear/off lighting control scenario, the light level can be dimmed continuously and linearly from maximum electric power to minimum light output as daylight illuminance increases. LED lamps are switched off completely when the necessary set point value is guaranteed by natural light.

III. Results and Discussion

A. Lighting Simulation Results in DIALux Evo

As addressed in WELL Standard, the calculated melanopic light intensity for the work area and in the living environments together with the simulated visual lighting design metrics are presented. Table II indicates daylighting results including EML calculations. Due to the change in working habits and the extended and shifted working hours with the Covid-19 pandemic, simulations were iterated for the night-time scenario. The results for electric lighting in Table III are considered the same for two living spaces with equivalent architectural features and interior lighting design.

TABLE II. Daylighting and Electric Lighting Simulation Results for L_1 and L_2 Scenarios on Dec 21st and June 21st

Daylighting + Electric Lighting			**Visual (lx)**				**EML**			
			General lighting (lx)		Task Lighting (lx)		Living area		Working area	
Scenario			**L_1**	**L_2**	**L_1**	**L_2**	**L_1**	**L_2**	**L_1**	**L_2**
December 21st	**09:00**	*VII (N)*	260	252	372	365	207	212	307	266
		II (SE)	258	246	371	365	200	222	219	218
	13:00	*VII (N)*	350	341	392	385	235	240	323	284
		II (SE)	342	331	389	384	221	272	199	218
June 21st	**09:00**	*VII (N)*	407	398	422	415	268	272	365	327
		II (SE)	484	471	435	431	380	410	313	355
	13:00	*VII (N)*	400	391	417	410	263	267	355	318
		II (SE)	530	531	448	448	482	548	342	387

TABLE III. ELECTRIC LIGHTING SIMULATION RESULTS FOR L_1 AND L_2 SCENARIOS

Electric Lighting (No daylight)	Visual (lx)				EML			
	General lighting (lx)		Task Lighting (lx)		Living area		Working area	
Scenario	L_1	L_2	L_1	L_2	L_1	L_2	L_1	L_2
$E_{av\ (lx)}$	235	220	367	360	68	89	85	107
U_o	0.44	0.41	0.77	0.63				
UGR	15.6	20.7	14.4	16.8				

a) Average illuminance on the working plane (E_{av}): Considering the recommended thresholds in EN 12464-1 [47] and IESNA [48], a minimum of 150 lx for the living room and 300 lx for the possible workstations such as horizontal plane on the dining table are achieved in terms of sufficient lighting for the day and the nighttime. Therefore, the room is comfortable depending on the illuminance levels.

b) Unified glare ratio (UGR): Maximum threshold of 19 is provided for the workstation and 22 for the living room with artificial lighting (Table 3). Discomfort glare limits, one of the visual comfort criteria, are met for the room.

c) Illuminance distribution uniformity (U_o): On the working planes for general lighting, U_o values are higher than the 0.40 limit. 0.60 is achieved for the task lighting (Table 3). Therefore, it can be said that minimum uniformity values are provided.

d) Color rendering index (CRI): Light source quality of rendering colors is selected with a minimum of 80.

e) EML in the living area: In the presence of daylight, 200 EML is achieved in the living environment (Table 2); however, proposed lighting systems (L_1, L_2) fail to comply with the minimum threshold independently with electric lighting (Table 3). Therefore, integrated lighting seems to be the best solution to achieve the target EML levels. Also, it is advisable to use dynamic lighting systems.

During the nighttime, when all lights are on, the illuminance is above the maximum threshold of 50 EML (Table 3). On the other hand, this target can be achieved by switching ceiling mounted or pendant lights off in L_1 scenario with CFL lamps. In the L_2 scenario with LED lamps, light fixtures can be dimmed to the required illuminance after 20:00 and visual comfort conditions can be satisfied as recommended in the WELL v2 Building standard [5].

f) EML in the working and learning area: Together with electric lighting, 200 EML is reached on the vertical plane (at the eye level of the occupant) for at least 4 hours per day (between 9:00 - 13:00 hours) to stimulate the circadian system (Table 2). Yet, L_1 and L_2 don't comply with the minimum criteria of 150 EML for work areas and 125 EML in learning areas alone according to the WELL standard [5], therefore a supplementary light source is needed to support the system in the absence of daylight (Table 3).

B. Annual Lighting Energy Analysis in DesignBuilder

DesignBuilder is used to analyze the annual lighting energy results for the lighting scenarios, that are operated by different lamps, luminaires, and lighting control strategies as presented in Fig. 4.

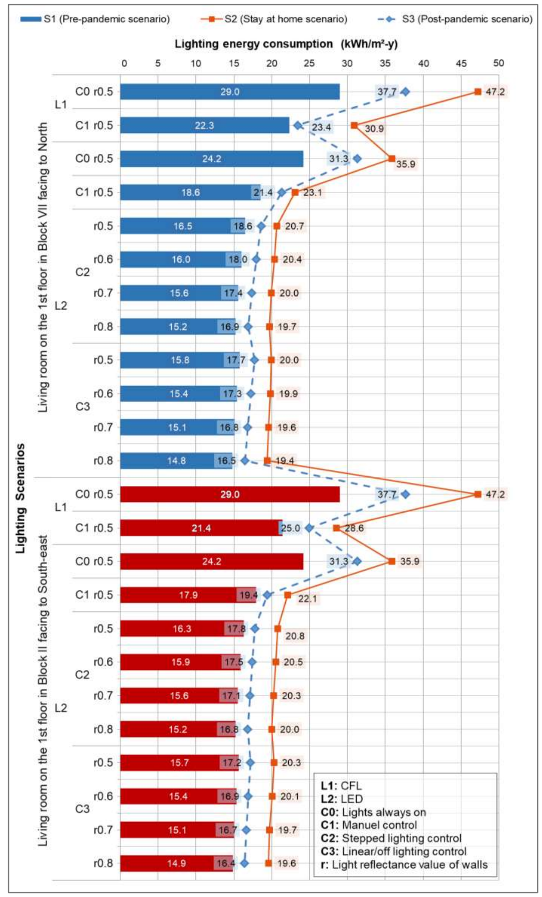

Fig. 4. Annual lighting energy consumption for the proposed scenarios

Furthermore, various wall reflectance cases (r_1=0.5, r_2=0.6, r_3=0.7, r_4=0.8) are evaluated for L_2 (LED lamps) scenario as an additional parameter of visual comfort and for lighting energy performance as discussed by Stephen and Coley [29], Mohelnikova Hirs [30] and Mangkuto et al. [31].

a) Artificial Lighting System Scenarios: Two lighting scenarios are analyzed regarding the total lighting energy consumption of apartment blocks. The results in Fig. 4 show that the annual lighting energy consumption of the building is higher in L_1 than L_2. Since LEDs are lower in power density yet higher in light output than the selected CFLs, they became more economical in lighting energy consumption. Together with the luminous efficiency of lamps, the light fittings efficiency factor is also higher in L_2 scenario which is meaningful in terms of the luminous flux emitted per watt of electrical power.

b) Occupancy Scenarios and Lighting Schedules: L_1 (CFL lamps) and L_2 (LED lamps) are analyzed for the pre-pandemic survey scenario (S_1), stay-at-home scenario (S_2) and based on the occupancy predictions [44, 45] for post-pandemic scenario (S_3). According to the survey, lighting system operating time includes mostly morning and night hours. As seen in Fig. 4, depending on the long-lasting working hours during nighttime, annual lighting energy consumption in S_2 is the highest, followed by S_3 and S_1 scenarios in all cases.

c) Lighting System Control Scenarios: The lighting automation system is effective in energy efficiency by reducing lighting system operation hours. The annual lighting energy consumption of the north-facing living room is ~4% higher than that of the south-facing room, and this difference has decreased with the use of lighting automation. When photo-sensors and dimmers are integrated to modulate LED lamps according to daylight level, 6 – 9% and 10.5 – 12.8% improvements are achieved by stepped-dimming control (L_2-C_2) compared to LEDs with manual control (L_2-C_1) for Block II and Block VII respectively. In this regard, a reduction in lighting energy consumption between 23.9 – 28.7% and 20.5 – 33.1% can be achieved by using the stepped lighting strategy with LEDs (L_2-C_2) instead of a manually controlled CFL (L_1-C_1) scenario. Likewise, linear/off dimming control (L_2-C_3) decreases lighting energy consumption by 26.8 – 31.1% for Block II and by 24.3 – 35.4% for Block VII in comparison to L_1-C_1 scenario.

Depending on occupant behavior, constant use of artificial lighting may result in higher energy consumption through excessive use of the lighting system. Furthermore, over-lighting the zone can also cause glare during the daytime. When the simulation results are analyzed, significant differences are computed in energy loads between lights controlled by the automation (C_2, C_3) and lights in fully-on mode (C_0). The greatest difference occurs in the scenario by linear/off dimming strategy (L_2-C_3) during COVID-19 limitations (S_2). Also, this scenario leads to electric savings of up to 57,0 % for Block II and 57,7% for Block VII in comparison to L_1-C_0 scenario through photosensor-controlled use of LEDs.

Finally, the impact of light reflectance values of walls on lighting energy consumption is analyzed. In parallel to the research by Bourgeois et al [17], Tian et al [19] and Meugheuvel et al [20], the findings verify that increasing surface reflectance is effective on energy consumption without changing the number of light sources. For instance, for the post-pandemic scenario (S_3) in Block VII, the annual lighting energy can be decreased by 9.3% for L_2-C_2 and by 7% for L_2-C_3 scenarios only by changing the wall reflectance from 0.5 to 0.8. Annual lighting energy saving rates are compared and summarized in Table IV.

TABLE IV. LIGHTING ENERGY SAVING RATES OF THE RESEARCH SCENARIOS

LIGHTING SCENARIO	LIGHTING CONTROL SCENARIO	OCCUPANCY SCENARIO					
		S1		S2		S3	
		II (SE)	VII (N)	II (SE)	VII (N)	II (SE)	VII (N)
Lighting energy saving (%) compared to L1 - C1 r:0.5							
L2	C0 r:0.5	-12.8	-8.4	-25.7	-16.1	-25.5	-33.7
	C1 r:0.5	16.4	16.8	22.5	25.2	22.1	8.8
	C2 r:0.5	23.9	26.1	27.1	33.1	28.7	20.5
	C3 r:0.5	26.8	29.3	29.0	35.4	31.1	24.3
Lighting energy saving (%) compared to L2 - C1 r:0.5							
L2	C2 r:0.5	9.0	11.2	6.0	10.5	8.5	12.8
	C2 r:0.6	11.2	13.6	7.2	11.7	10.2	15.8
	C2 r:0.7	13.2	15.9	8.4	13.6	11.8	18.6
	C2 r:0.8	15.1	17.9	9.5	14.8	13.4	20.9
	C3 r:0.5	12.5	15.1	8.3	13.6	11.5	17.0
	C3 r:0.6	14.3	16.8	9.3	14.1	13.0	19.2
	C3 r:0.7	15.9	18.6	11.2	15.2	14.2	21.1
	C3 r:0.8	16.9	20.2	11.5	16.1	15.5	22.8

IV. CONCLUSION

The pandemic crisis has had various impacts on the way we live in our homes, and the way we evaluate the design of our living habitat and it put forward the "home office" idea again. This study addresses the lighting planning aspects such as lighting system and lighting operating hours together with occupancy scenarios in residences. We focused on the living area which is assumed to function as an office during and after the pandemic. Our results provide evidence for potential lighting energy savings by using different lighting control strategies that can be adapted to the lighting scenarios. Besides adjusting the light output by photo sensors, we examined three occupancy patterns including the HCL concept in LED lighting scenarios with light color and illuminance flexibility. In this way, it is intended to design a dynamic inner atmosphere stimulating the circadian rhythm throughout the day via changing the color and distribution of artificial lighting.

As the circadian stimulus is different than the visual stimulus of the light sources, it shall also be taken into account in lighting design. In this regard, the two living rooms facing opposite directions are assessed with visual comfort and EML metrics in the WELL v2 standard. The simulation results demonstrated that a higher light level is required to meet WELL requirements than the proposed lighting scenarios, which comply with EN 12464-1 standard and IESNA guidelines. This may lead designers to search for flexible lighting solutions for home offices.

In the study, due to the limitations in face-to-face surveys during and ongoing COVID-19 pandemic, it is difficult to renew the questionnaire and to evaluate the changes in occupancy patterns with a projection of post-pandemic conditions. The energy simulations confirm that the annual residential lighting energy consumption is higher than it was before the pandemic. In this sense, the findings of this study are valuable while the changes in living, working and learning habits are expected to be continued even after the resolution of this health crisis. In addition to the calculations for yearly lighting energy demand, analyzing daylight availability of residential spaces by annual climate-based dynamic metrics is also desirable for future research.

REFERENCES

[1] IESNA Illuminating Engineering Society of North America. Light and Design A Guide to Designing Quality Lighting for People and Buildings IES-DG-18-08, New York, 2008.

[2] T. M. Brown, G. C. Brainard, C. Cajochen, C. A. Czeisler, J. P. Hanifin, S. W. Lockley, R. J. Lucas, et al., “Recommendations for daytime, evening, and nighttime indoor light exposure to best support physiology, sleep, and wakefulness in healthy adults,” Plos Biology, vol. 20 (3), 2022, e3001571.

[3] M. Awada, B. Becerik-Gerber, S. Hoque, Z. O’neill, G. Pedrielli, J. Wen, and T. Wu, “Ten questions concerning occupant health in buildings during normal operations and extreme events including the COVID-19 pandemic,” Building and Environment, vol. 188, 2021, pp. 1–11.

[4] A.T.P So and L.M Leung, “Indoor Lighting Design Incorporating Human Psychology,” Architectural Science Review, vol. 41, 1998, pp. 113–124.

[5] IWBI International Well Building Institute. WELL building standard v2 Q1 2022 version. Section L03: circadian lighting design, 2022. Accessed 2 January 2022 from https://v2.wellcertified.com/v/en/light/feature/3

[6] CIE S 026/E. CIE System for Metrology of Optical Radiation for ipRGC-Influenced Responses to Light (e.). Commision. Vienna, Austria, 2018.

[7] A. U. Viola, L. M. James, L. J. M. Schlangen and D. J. Dijk, “Blue-enriched white light in the workplace improves self-reported alertness, performance and sleep quality,” Scandinavian Journal of Work, Environment and Health, vol. 34 (4), 2008, pp. 297–306.

[8] J. Arendt, “Shift work: Coping with the Biological Clock,” Occupational Medicine vol. 60(1), 2010, pp. 10–20.

[9] M. T. H. Do and K.-W. Yau, “Intrinsically Photosensitive Retinal Ganglion Cells,” Physiological Reviews vol. 90, 2010, pp.1547–1581.

[10] C. Jarboe, J. Snyder and M. G. Figueiro, “The effectiveness of light-emitting diode lighting for providing circadian stimulus in office spaces while minimizing energy use,” Lighting Research and Technology vol. 52, 2020, pp. 167–188.

[11] IEA International Energy Agency. Energy Policy Review - Turkey Country Report, March 2021. Accessed 29 March 2022. https://www.iea.org/reports/turkey-2021

[12] EPDK - Electricity Market Sector Report 2022. Ankara: Republic of Turkey Energy Market Regulatory Authority, Strategy Development Department, 2022. Accessed 21 April 2022. https://www.epdk.gov.tr/Detay/Icerik/1-1271/electricityreports

[13] N. Makaremi, S. Schiavoni, A. L. Piselloa, F. Asdrubalic and F. Cotana, “Quantifying the effects of interior surface reflectance on indoor lighting,” Energy Procedia vol. 134, 2017, pp. 306–316.

[14] A. A. Baloch, P. H. Shaikh, F. Shaikh, Z. H. Leghari, N. H. Mirjat, M. A. Uqaili, “Simulation tools application for artificial lighting in buildings,” Renewable and Sustainable Energy Reviews, vol. 82(3), 2018, pp. 3007–3026.

[15] M. Krarti, P. M. Erickson and T. C. Hillman, “A simplified method to estimate energy savings of artificial lighting use from daylighting,” Building and Environment vol. 40(6), 2005, pp. 747–754.

[16] D. H.W. Li, T. N. Lam and S. L. Wong, “Lighting and energy performance for an office using high frequency dimming controls,” Energy Conversion and Manag. vol. 47 (10), 2006, pp. 1133–1145.

[17] D. Bourgeois, C. Reinhart and I. Macdonald, “Adding advanced behavioural models in whole building energy simulation: A study on the total energy impact of manual and automated lighting control,” Energy and Buildings vol. 38, 2006, pp. 814–23.

[18] M. C. Singh and S. N. Garg, “Illuminance estimation and daylighting energy savings for Indian regions,” Renewable Energy vol. 35(3), 2010, pp. 703–711.

[19] C. Tian, T. Chen and T. Chung, “Experimental and simulating examination of computer tools, Radlink and DOE2, for daylighting and energy simulation with venetian blinds,” Applied Energy, vol. 124, 2014, pp. 130–139.

[20] N. Meugheuvel, A. Pandharipande, D. Caicedo and P. P. J. Hof, “Distributed lighting control with daylight and occupancy adaptation,” Energy and Buildings vol. 75, 2014, pp. 321–329.

[21] E. J. Gago, T. Muneer, M. Knez and H. Köster, “Natural light controls and guides in buildings. Energy saving for electrical lighting, reduction of cooling load,” Renewable and Sustainable Energy Reviews, vol. 41, 2015, pp. 1–13.

[22] L. Xu, Y. Pan, Y. Yao, D. Cai, Z. Huang and N. Linder, “Lighting energy efficiency in offices under different control strategies,” Energy and Buildings, vol. 138, 2017, pp. 127–139.

[23] L. Van Thillo, S. Verbeke and A. Audenaert, “The potential of building automation and control systems to lower the energy demand in residential buildings: A review of their performance and influencing parameters,” Renewable and Sustainable Energy Reviews, vol. 158, 2022, 112099.

[24] M. M. Aman, G. B. Jasmon, H. Mokhlis, A. H. A. Bakar, “Analysis of the performance of domestic lighting lamps,” Energy Policy vol. 52, 2013, pp. 482–500.

[25] S. Attia, M. Hamdy and S. Ezzeldin, “Twenty-year tracking of lighting savings and power density in the residential sector,” Energy and Buildings, vol. 154, 2017, pp. 113–126.

[26] M. C. Dubois, and Å. Blomsterberg, “Energy saving potential and strategies for electric lighting in future North European, low energy office buildings: A literature review,” Energy and Buildings vol. 43(10), 2011, pp. 2572–2582.

[27] N. Makaremi, S. Schiavoni, A. L. Pisello and F. Cotana, “Effects of surface reflectance and lighting design strategies on energy consumption and visual comfort,” Indoor and Built Environment vol. 28(4), 2019, pp. 552–563.

[28] M. Frascarolo, S. Martorelli and V.Vital, “An innovative lighting system for residential application that optimizes visual comfort and conserves energy for different user needs,” Energy and Buildings, vol. 83, 2014, pp. 217–224.

[29] S. Stephen and D. Coley, “The relationship between wall reflectance and daylight factor in real rooms,” Architectural Science Review vol. 54(4), 2011, pp. 329–334.

[30] J. Mohelnikova and J. Hirs, “Effect of externally and internally reflective components on interior daylighting,” Journal of Building Engineering, vol. 7, 2016, pp. 31–37.

[31] R. A., Mangkuto, M. Rohmah and A. D. Asri, “Design optimisation for window size, orientation, and wall reflectance with regard to various daylight metrics and lighting energy demand: A case study of buildings in the tropics,” Applied Energy vol.164, 2016, pp. 211–219.

[32] M. Boubekri, Daylighting Design: Planning Strategies and Best Practice Solutions, Basel: Birkhäuser, 2014.

[33] S. Swinal, “A critical review of articles published on atrium geometry and surface reflectances on daylighting in an atrium and its adjoining spaces,” Architectural Science Review, vol. 53(2), 2010, pp. 145–156.

[34] M. C.Dubois, F. Bisegna, N. Gentile, M. Knoop, B. Matusiak, W. Osterhaus and E. Tetri, “Retrofitting the electric lighting and daylighting systems to reduce energy use in buildings: a literature review,” Energy Research Journal, vol. 6 (1), 2015, pp. 25–41.

[35] R. Singh, and R. Rawal, “Effect of surface reflectance on lighting efficiency in interiors,” In 12th Conference of International Building Performance Simulation Association, 2011, pp. 2301–2308. Sydney, Australia.

[36] X. Yu and Y. Su, “Daylight availability assessment and its potential energy saving estimation–A literature review,” Renewable and Sustainable Energy Reviews vol. 52, 2015, pp. 494–503.

[37] A. Das and S. K. Paul, “Artificial illumination during daytime in residential buildings: Factors, energy implications and future predictions,” Applied Energy, vol. 158, 2015, pp. 65–85.

[38] F. Rubinstein, N. Colak, J. Jennings and D. Neils, “Analyzing occupancy profiles from a lighting controls field study” In Proceedings of CIE Session, 2003, San Diego, California.

[39] J. Mardaljevic, L. L. Heschong and E. S. Lee, “Daylight metrics and energy savings,” Lighting Research and Technology, vol. 41(3), 2009, pp. 261–283.

[40] A. Rinaldi, M. Schweiker and F. Iannone, “On uses of energy in buildings: Extracting influencing factors of occupant behaviour by means of a questionnaire survey,” Energy and Buildings, vol. 168, 2018, pp. 298–308.

[41] K. M. Gerhardsson, T. Laike and M. Johansson, “Leaving lights on – A conscious choice or wasted light? Use of indoor lighting in Swedish homes,” Indoor and Built Environment, vol. 30(6), 2020, pp. 745-762.

[42] Y. Zhang, X. Bai, F. P. Mills, J. C.V. Pezzey, “Rethinking the role of occupant behavior in building energy performance: A review,” Energy and Buildings, vol. 172, 2018, pp. 279–294.

[43] M. Krarti and A. Mohammad, “Review analysis of COVID-19 impact on electricity demand for residential buildings,” Renewable and Sustainable Energy Reviews, vol. 143, 2021, 110888.

[44] T. Mehdi and R. Morisette, “Working from home after the COVID-19 pandemic: An estimate of worker preferences, economic and social reports,” StatCan COVID-19: Data to Insights for a Better Canada vol. 1(5), 2021, Statistics Canada Catalogue no. 36-28-0001.

[45] A. Brodeur, I. Grigoryeva and L. Kattan, “Stay-at-home orders, social distancing, and trust,” Journal of Population Economics, vol. 34, pp. 1321-1354.

[46] BEP Building Energy Performance Regulation. Ankara: Turkish Republic Ministry of Public Works and Settlements, Turkish Official Gazette, 5/12/2008.

[47] EN 12464-1. Lighting of work places - Part 1: Indoor work places. European Committee for Standardization, 2011.

[48] IESNA Illuminating Engineering Society of North America. The Lighting Handbook Reference and Application, 10th Edition. Editors: D.L. DiLaura, K.W. Houser, R.G. Mistrick, G.R. Steffy. New York, 2011.

[49] Lumsearch, DIALux lighting products database, 2022. Accessed 8 February 2022. https://lumsearch.com/en#0

[50] IWBI International Well Building Institute, 2019. EML Toolbox. Accessed 3 December 2021. https://standard.wellcertified.com/tables#melanopicRatio

On the Applicability of Obtrusive Light Assessment Parameters – Upward Light Ratio and Upward Flux Ratio

Krzysztof Skarżyński
Lighting Technology Division,
Electrical Power Engineering Institute,
Warsaw University of Technology
Warsaw, Poland
krzysztof.skarzynski@pw.edu.pl

***Abstract*— This paper is related to light pollution, an actual problem widely commented on in contemporary literature. It concerns the parameters of the quantitative assessment of light pollution at the design stage, which were defined in standards and technical reports, especially the Upward Light Ratio (ULR) and Upward Flux Ratio (UFR). The primary motivation for this research was the observation of certain inaccuracies related to the applicability and interpretation of the selected parameters mentioned above in practice. Therefore, the computer simulations of the lighting system of an exemplary large outdoor parking lot in the city were conducted. Over four hundred cases of lighting systems were analyzed. Individual cases differ in the shape of the task area, luminaires arrangement, mounting height, luminous intensity distribution, aiming, and maintenance factor. The results confirmed that for the modern luminaires, the criterion values of ULR and UFR are overestimated in many cases. Suppose luminaires' luminous flux is emitted only in the bottom hemisphere, which is currently the most used luminaires type. In that case, the ULR and UFR values do not exceed the criterion values specified for zones with lower ambient brightness, even in extreme cases. Thus, even lighting solutions with lower energy efficiency easily meet the requirements of these parameters. This situation is not rational. So, it is crucial to improve it by making the requirements more stringent for both the ULR and UFR in all environmental zones.**

Keywords—outdoor lighting, light pollution, obtrusive light, energy efficiency, upward light ratio, upward flux ratio

I. Introduction

Light pollution is an issue that has been studied by scientists and engineers around the world for at least 30 years. In the literature, many works presenting various essential aspects of this phenomenon can be found. The influence of light pollution on changes in the broadly understood natural environment is the most frequently analyzed nowadays. The works mainly concern the influence of lighting on living organisms. Research is carried out to show how light pollution affects the population and functioning of various species of insects, birds, and bats [1]–[3].

Another group of works is related to astronomical issues [4], [5]. One of the disadvantages of light pollution is the formation of skyglow. It causes the night sky, which should be dark, to be brightened. As a result, many celestial bodies are impossible to observe, and the work of people engaged in astronomy is difficult or even impossible to perform (Fig. 1). Additionally, there was some difference in the definition of surface brightness by engineers and astronomers. Therefore, some works also concern the derivation of appropriate mathematical formulas enabling the transition from the luminance scale to the magnitude scale, taking into account the luminous efficiency function of the human vision [6].

Fig. 1. An example of the lack of stars visibility over the city of Warsaw due to skyglow

Many of the papers relate to measurement techniques and light pollution monitoring. Appropriate hardware solutions are created, sometimes combined into entire measurement networks that enable the analysis of the surface brightness of the night sky [7], [8]. The influence of weather conditions on the obtained results is also analyzed [9]. There is also great interest in using unmanned aerial vehicles for quick analysis of light pollution in a given area [10], [11].

In the works related to light pollution, one can also find analyzes related to its impact on economic issues, civilization development, and the impact on the human well being [4], [12], [13]. Some papers are also devoted to more technical issues related to the lighting design process to obtain an optimal, sustainable solution for various types of outdoor lighting [14]–[18].

It can be easily observed that the problem of light pollution is present all over the globe and many people analyze it in many various aspects. Its main reason is the use of various electric lighting installations at night. However, not all outdoor lighting installations are correctly designed and implemented to minimize light pollution and maximize energy efficiency. This problem of light pollution is so severe that some countries have also decided to tighten the requirements related to light pollution to reduce it [19]. There are associations whose main task is protecting the dark sky, e.g, International Dark-Sky Association [20].

They define a framework by which light pollution can be reduced. Lighting installations must be: useful, adequately targeted, realize low brightness levels, be controllable, and the appropriate spectral power distributions (especially for LED equipment) must be selected. The correctness of light pollution of a given lighting installation can be determined based on appropriate quantitative parameters, e.g., Upward Light Ratio and Upward Flux Ratio. Definitions and derivation of these parameters can be found in the CIE reports [21]. However, the literature lacks a thorough analysis of the criteria values of these parameters concerning the state of the art of the currently used lighting equipment and the lighting design process. Therefore, the main goal of this work is to try to fill this gap and present some thoughts of the Author related to the applicability of using the Upward Light Ratio and Upward Flux Ratio parameters in design practice.

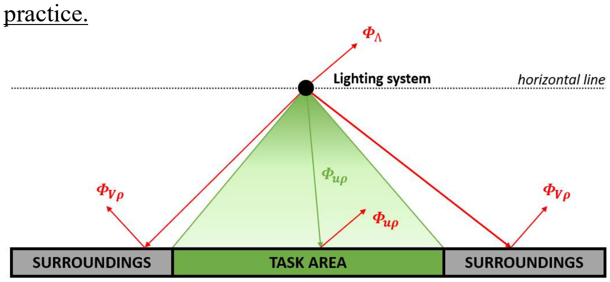

Fig. 2. A basic and typical situation of outdoor lighting

II. Upward Light Ratio and Upward Flux Ratio

A typical situation in outdoor lighting is shown in Figure 2. Part of the luminous flux from the lighting system can be directly emitted into the upper hemisphere. Some parts may reach the task field, some to the surroundings and may be reflected. The described situation is the simplest case and does not consider other objects that may be present in the vicinity of, e.g. residential buildings. However, on its basis, it is possible to define some quantitative parameters for assessing light pollution related to the emission of the luminous flux into the upper hemisphere: Upward Light Ratio and Upward Flux Ratio. Their brief definitions of these parameters are presented below.

Upward Light Ratio (ULR) – it is the ratio of the luminous flux of luminaires emitted directly into the upper hemisphere (above the horizon) ϕ_Λ and the total luminous flux of these lighting luminaires ϕ_{lum} (1).

$$ULR = \frac{\phi_\Lambda}{\phi_{lum}} \cdot 100\ [\%] \quad (1)$$

Upward Flux Ratio (UFR) – while the ULR only considers the luminous flux of the luminaires emitted directly upwards, the UFR also considers the luminous flux reflected upwards from the substrate, both from the area intended for illumination (task area) and the area that is not (surroundings). Thus, it can be defined as the ratio of the maximum luminous flux emitted upwards for a given lighting solution to the minimum value of the luminous flux emitted upwards in an ideal situation. The ideal situation should be understood as obtaining 100% of the utilization factor and the average illuminance value equal to the criterion value adopted based on the relevant lighting standard.

$$UFR = \frac{\phi_{up,max}}{\phi_{up,min}}[-] \quad (2)$$

Examples of ULR and UFR criterion values for individual environmental zones are presented in Table I. They were taken from the CIE report "Guide on the Limitation of the Effects of Obtrusive Light from Outdoor Lighting Installations, 2nd edition" from 2017 [21]. It is worth noting that the UFR criterion values were presented only for amenity lighting because only this type is analyzed by the case study presented in this article. The UFR criterion values for sports lighting and road lighting are different. Moreover, the calculation procedure of this parameter for road lighting is also slightly different, depending on the geometry of the illuminated road [21].

TABLE I. ULR and UFR criterion values ind each environmental zone for amenity lighting

Parameter	Environmental zone				
	E0	*E1*	*E2*	*E3*	*E4*
ULR [%]	0	0	2,5	5	15
UFR [–]	- [a]	- [a]	6	12	35

[a] not defined in this zone

III. Methods of Simulation Studies

The research methods are based on the computer simulation of lighting using dedicated software. Therefore, the DIALux 4.13 was used as it is pretty reliable for lighting calculations [22]. When analyzing the primary sources of light pollution in urban areas, it was determined that one of them is large-area parking lots. The area for illumination in such a facility may be several thousand square meters. Therefore, it was decided to simulate the lighting for such an object with an area of 10,000 m2 in a variant approach. The highest requirements for the luminous environment for the parking lot have been adopted following the European standard for outdoor workplaces [23]. As these facilities are located in the urban zone (high ambient brightness), the requirements for the ULR and UFR parameters will be the same as in the environmental zone E4. Calculations of the UFR parameter were made assuming that the task field reflectance is the same as for the surroundings and is 20%. In addition, it was decided to analyze the obtained values of utilance (4) and normalized power density power (5). As there are no formal requirements related to the values of these parameters for the lighting of parking lots, it was decided that the utilance should aim at one and the normalized power density to zero. The summary of the adopted all assumed requirements is presented in Table II.

TABLE II. Setted requirements for particular parameters

E_m $[lx]$	U_0 $[-]$	*GR* $[-]$	*Zone*	*ULR* [%]	*UFR* [–]	U [–]	*NPD* $[W/m^2\|100\ lx]$
20	*0,25*	*50*	*E4*	*15*	*35*	**→ 1**	**→ 0**

Utilinace – it is the ratio of the useful luminous flux reaching the task area ϕ_u and the total luminous flux of all used luminaires ϕ_{lum}.

$$U = \frac{\phi_u}{\phi_{lum}} \cdot 100\ [\%] \quad (3)$$

Normalisaed Power Denisty (NPD) – it is the lighting power density related to the level of 100 lx. This parameter is a classic measure of energy efficiency for various types of lighting installations [24].

$$NPD = LPD \cdot \frac{100}{E_m}[\frac{W}{m^2}|100\ lx] \quad (4)$$

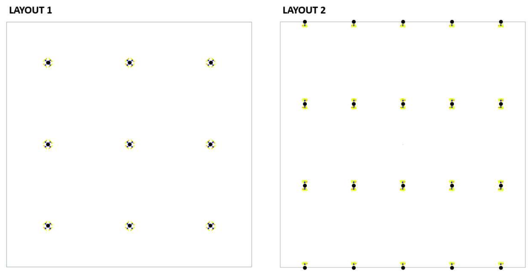

Fig. 3. Schematic layout of poles on the area of analyzed parking lots

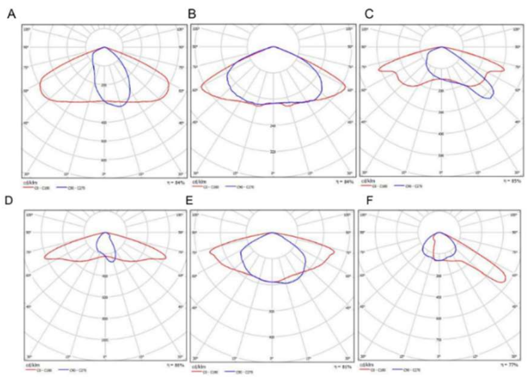

Fig. 4. Used luminous intensity distrubutions of lumianires

A As mentioned earlier, the lighting simulations were carried out in a variant approach, assuming the following variables:

- Two parking lots with the area of 10 00m2: 100 m x 100 m, 50m x 200m,
- Two arrangements of luminaires: poles located on the edges of the parking lot and the parking lot surface; poles located only on the parking lot surface. In both cases, the arrangement of poles is even and symmetrical concerning the symmetry axis of the parking lot shape (Fig. 3).
- Six different luminous intensity distributions (Fig. 4),
- Three titls of the luminaires: 0°, 15°, 30°,
- Three mounting heights of luminaires: 9 m, 12 m, 15m,
- Two maintenance factors 0,71 and 0,91 correspond to a relatively small (110%) and relatively large (140%) oversizing of lighting level.

Calculations of the luminous environment parameters were made following the European standard for outdoor lighting [23]. The dimension of the calculation grid is 4 m, and the calculation points have been evenly distributed over the area of both parking lots. <u>In total, 432 lighting solutions were obtained, for which all the previously discussed parameters of the luminous environment, light pollution, and energy efficiency were calculated</u>. Then, the results were compared, presenting histograms of the relevant parameters. Finally, it was decided to investigate whether there is a linear correlation between the UFR parameter and the utilance and the normalized power density, and if so, what level it is.

TABLE III. GENERAL LIGHTING REQUIREMENTS RESULTS

Parameter	Number of cases that fulfill the requirements	Percent of all cases
$\boldsymbol{E_m[lx]}$	431	99,8 %
$\boldsymbol{U_0[-]}$	389	90,0 %
$\boldsymbol{GR[-]}$	417	96,5 %

IV. Results and Discussion

In the beginning, the obtained results were analyzed to meet the normative requirements for the luminous environment. The results are shown in Table III. In almost 100% of cases, the value of the average maintained illuminance was obtained following the normative requirements. The illuminance uniformity in 90% of cases exceeds the value of 0.25 and most often has a value from 0.30 to 0.50. Solutions with very high uniformity of over 0.5 (51 cases) were also obtained, corresponding to 12% of all cases. For 96% of all cases, the maximum value obtained in the calculation point of the glare (GR) is less than or equal to 50, which is a condition for meeting the normative requirements for this parameter. The GR values exceeding 50 are obtained for cases where the luminaires are installed in the lowest analyzed working position (9m) and are tilted by 30 degrees. This result is in line with the predictions based on the definition of glare and design practice for outdoor workplaces [23], [25].

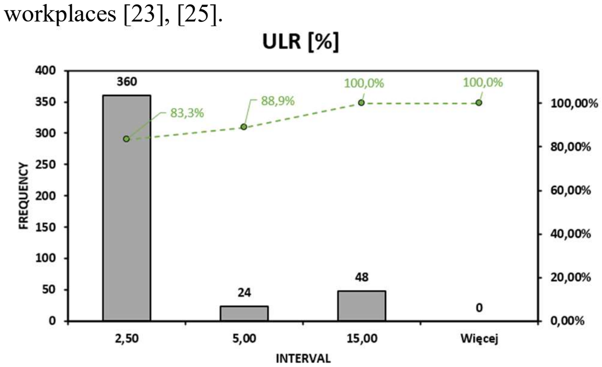

Fig. 5. The histogram of Upward Light Ratio results

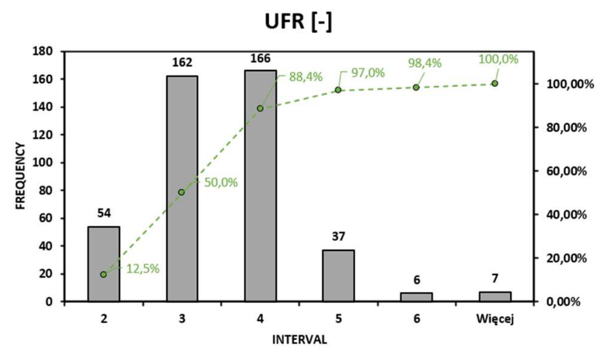

Fig. 6. The histogram of Upward Flux Ratio results

The distributions of the results of calculations of the ULR and UFR parameters are presented in Figures 5 and 6. For 360 cases (approx. 84% of all cases), the value of the ULR parameter does not exceed 2.5%, which means that these solutions meet the requirements for this parameter in the environmental zone E2. The ULR parameter for only 48 lighting solutions ranges from 5% to 15%. The maximum value obtained is 7.5%, linked to the luminaires' tilt of 30 degrees. It is worth emphasizing that in no case did the ULR value exceeds 15%, and it means that all lighting solutions meet the requirements of the high-brightness environmental zone E4.

Taking into account the obtained results of the UFR parameter, it should first of all be noted that the obtained values, even for extensive lighting oversize (140%, MF = 0.71) and large tilt of the luminaires, are lower than the requirements for zone E4

The UFR values are most often in the range from 2 to 4. Only in 13 cases of the obtained values exceed 5. It means that 97% of the cases meet the requirements for the E2 zone, and 100% are suitable for the E3 and E4 zones. It can be assumed that this is because, in all the luminaires used, the emission of the luminous flux occurs only and exclusively in the lower hemisphere. Relatively large tilts, even by 30 degrees, causes the value of the UFR parameter increases. However, it still does not exceed the requirements for zones with high ambient brightness.

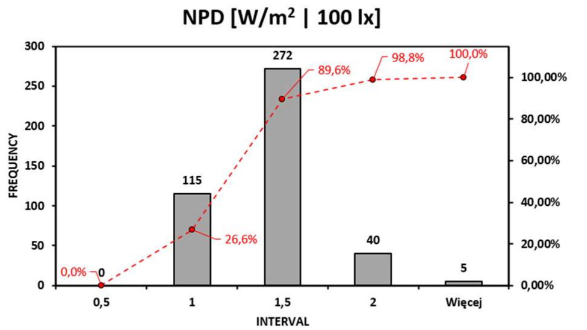

Fig. 7. The histogram of Normalised Power Deinsity results

Figure 7 shows the distribution of the calculation results for the normalized power density. In 90% of all cases, the value obtained shall not exceed 1.5 W/m2 | 100 lx, while for 27%, this value does not exceed 1 W/m2 | 100 lux. The lowest obtained value of this parameter is 0,81 W / m2 | 100 lx, while the highest is 2,42 W / m2 | 100 lx. It should be emphasized that higher values of NPD are most often associated with higher values of the UFR parameter. This observation aligns with the generally accepted assumption that light pollution is related to the energy efficiency issue.

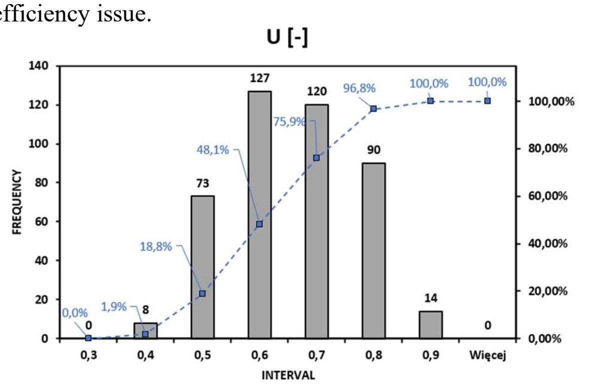

Fig. 8. The histogram of utilance results

The histogram of the obtained values of the utilance is shown in Figure 8. Interestingly, in 369 cases, the value of this parameter is greater than or equal to 0.5. It means that 85% of all cases are characterized by 50% or more of the luminous flux of all luminaires reaching the task area. The distribution of the obtained lighting efficiency values resembles the normal distribution. Both weak cases in terms of luminaires' luminous flux usage and those in which the losses are minimal can be distinguished. In the worst case, the utilance reached the value of 0.31. It was achieved with luminaires installed on poles with a height of 15 m and a tilt of 30 degrees. In this case, the highest value of the UFR (7.5) and the normalized power density (2.42 W/m2 | 100 lx) were also obtained.

In contrast, the case with the best luminous flux usage (utilance equals 0,86) was achieved for mounting the luminaires at 9m and a tilt of 0 degrees. In this case, the UFR is 2,35, and the normalized power density is 0.81 W/m2 | 100 lx. However, this case does not meet the requirements of a luminous environment because the uniformity value is 0.11. Thus, this lighting solution could not be implemented despite the fair values of quantitative parameters related to light pollution and energy efficiency. It is also worth emphasizing that the parameter of utilance determines the engineering correctness of a given lighting solution. Therefore, to eliminate light pollution, it is recommended to analyze it at the design stage, during which one should strive to ensure that its value for a given lighting solution is close to 1. When a value close to 1 is obtained, it means that the total luminous flux of all luminaires reaches only and exclusively the area intended for the task area. However, this may not always be the best lighting solution due to light pollution. It will also depend on the adopted oversizing lighting level (maintenance system). The designed lighting does not increase light pollution to a greater extent than the minimum that is impossible to eliminate only if the adopted value of the maintenance system is rational or if an appropriate control system is used (e.g., constant lumen output).

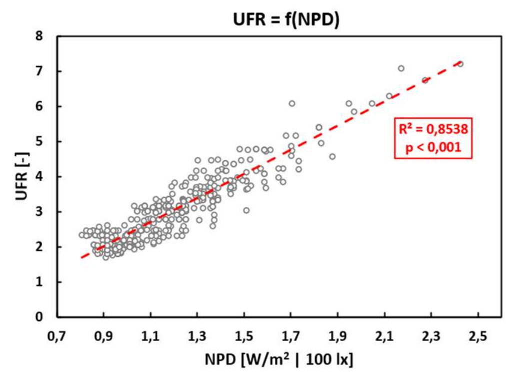

Fig. 9. The linear correlation between Upward Flux Ratio and Normalised Power Denisty

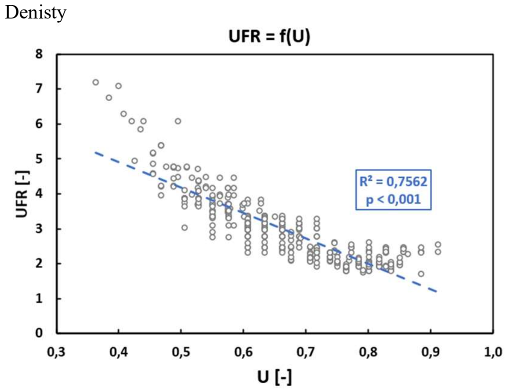

Fig. 10. The linear correlation between Upward Flux Ratio and utilance

Because the highest UFR values correspond to both the highest NPD values and the lowest values of utilance, it was decided to investigate the correlation between these parameters. The scatter plots of the relationship between UFR and NPD and the UFR, and the utilance are presented in Figures 9 and 10. A trend line was determined for the obtained values based on linear regression for a given set of values. The value of the R2 parameter, which specifies the square of Pearson's linear correlation coefficient, was also calculated. The obtained results determined that between the UFR parameter and the NPD, there is a strong positive linear correlation of 0,92 (with a significance level of $p < 0.001$).

On the other hand, there was a strong negative linear correlation of -0,87 between the UFR and the utilance (with a significance level of $p < 0.001$). Therefore, it is possible to quantify the issue of light pollution from a given lighting installation based on the accurate calculation of NPD or utilance. However, it requires proposing an adequate scale, including, e.g., energy efficiency classes for outdoor lighting.

V. Conclusion

The paper presents considerations related to the usefulness and applicability of parameters for quantitative assessment of light pollution at the design stage - Upward Light Ratio and Upward Flux Ratio. It presents the results of a variant lighting simulation of a typical outdoor lighting facility - a large city parking lot. The obtained results confirmed the predictions that the criteria values of these parameters are too high in the case of amenity lighting and not adapted to the capabilities of the currently used standard lighting equipment. Therefore, revising the current approach and making the requirements much stricter is necessary.

Moreover, it should be emphasized that the conducted research, despite the high number of cases, was limited to only one type of object. In order to accurately define the new criteria values of ULR and UFR, a more significant number of cases should be analyzed as well as other types of outdoor lighting installations such as sports lighting and road lighting. It will be the basis for further research conducted by the author of this article.

Finally, there are two critical observations. First of all, the UFR is very complicated, especially regarding its calculations. Not all commercial simulation programs commonly used can directly show the UFR value. An alternative approach to using the UFR parameter is to create an appropriate scale based on the normalized power density, which is easier to understand and more commonly used by engineers. Additionally, to ensure that a given lighting installation is adequately designed, it is necessary to analyze the obtained utilance during the design process. Secondly, whether the criterion values of the parameters for the quantitative assessment of light pollution should be different in individual environmental zones (except for the E0 protection zone) should also be considered. Assigning an area to a given zone is problematic and may result in some unfair design practices or simply mistakes. From the view of engineering correctness, understood as the lack of intensification of light pollution and obtaining solutions with high energy efficiency, it seems that the requirements should be standardized regardless of where the illuminated object is located.

References

[1] A. Wakefield, M. Broyles, E. L. Stone, S. Harris, and G. Jones, "Quantifying the attractiveness of broad-spectrum street lights to aerial nocturnal insects," *J. Appl. Ecol.*, 2018, doi: 10.1111/1365-2664.13004.

[2] J. Q. Ouyang *et al.*, "Restless roosts: Light pollution affects behavior, sleep, and physiology in a free-living songbird," *Glob. Chang. Biol.*, 2017, doi: 10.1111/gcb.13756.

[3] J. Pauwels, I. Le Viol, Y. Bas, N. Valet, and C. Kerbiriou, "Adapting street lighting to limit light pollution's impacts on bats," *Glob. Ecol. Conserv.*, vol. 28, p. e01648, 2021, doi: 10.1016/j.gecco.2021.e01648.

[4] F. Falchi *et al.*, "The new world atlas of artificial night sky brightness," *Sci. Adv.*, 2016, doi: 10.1126/sciadv.1600377.

[5] J. C. Barentine *et al.*, "Skyglow changes over Tucson, Arizona, resulting from a municipal LED street lighting conversion," *J. Quant. Spectrosc. Radiat. Transf.*, 2018, doi: 10.1016/j.jqsrt.2018.02.038.

[6] I. Fryc, S. Bará, M. Aubé, J. C. Barentine, and J. Zamorano, "On the Relation between the Astronomical and Visual Photometric Systems in Specifying the Brightness of the Night Sky for Mesopically Adapted Observers," *LEUKOS - J. Illum. Eng. Soc. North Am.*, vol. 00, no. 00, pp. 1–12, 2021, doi: 10.1080/15502724.2021.1921593.

[7] A. Hänel *et al.*, "Measuring night sky brightness: methods and challenges," *Journal of Quantitative Spectroscopy and Radiative Transfer*. 2018, doi: 10.1016/j.jqsrt.2017.09.008.

[8] A. Bertolo, R. Binotto, S. Ortolani, and S. Sapienza, "Measurements of night sky brightness in the Veneto Region of Italy: Sky quality meter network results and differential photometry by digital single lens reflex," *J. Imaging*, 2019, doi: 10.3390/jimaging5050056.

[9] T. Ścieżor, "The impact of clouds on the brightness of the night sky," *J. Quant. Spectrosc. Radiat. Transf.*, vol. 247, p. 106962, 2020, doi: 10.1016/j.jqsrt.2020.106962.

[10] P. Tabaka, "Pilot measurement of illuminance in the context of light pollution performed with an unmanned aerial vehicle," *Remote Sens.*, vol. 12, no. 13, 2020, doi: 10.3390/rs12132124.

[11] C. A. Bouroussis and F. V. Topalis, "Assessment of outdoor lighting installations and their impact on light pollution using unmanned aircraft systems - The concept of the drone-gonio-photometer," *J. Quant. Spectrosc. Radiat. Transf.*, vol. 253, p. 107155, 2020, doi: 10.1016/j.jqsrt.2020.107155.

[12] T. Gallaway, R. N. Olsen, and D. M. Mitchell, "The economics of global light pollution," *Ecol. Econ.*, 2010, doi: 10.1016/j.ecolecon.2009.10.003.

[13] M. A. Contín, M. M. Benedetto, M. L. Quinteros-Quintana, and M. E. Guido, "Light pollution: The possible consequences of excessive illumination on retina," *Eye*, vol. 30, no. 2, pp. 255–263, 2016, doi: 10.1038/eye.2015.221.

[14] P. Pracki and K. Skarżyński, "A multi-criteria assessment procedure for outdoor lighting at the design stage," *Sustain.*, 2020, doi: 10.3390/su12041330.

[15] K. Skarżyński and W. Żagan, "Quantitative Assessment of Architectural Lighting Designs," *Sustainability*, vol. 14, no. 3934, 2022, doi: https://doi.org/10.3390/su14073934.

[16] S. Słomiński and R. Krupiński, "Luminance distribution projection method for reducing glare and solving object-floodlighting certification problems," *Build. Environ.*, 2018, doi: 10.1016/j.buildenv.2018.01.019.

[17] R. Krupiński, H. Wachta, W. M. Stabryła, and C. Büchner, "Selected issues on material properties of objects in computer simulations of floodlighting," *Energies*, vol. 14, no. 17, pp. 1–24, 2021, doi: 10.3390/en14175448.

[18] L. T. Doulos, I. Sioutis, P. Kontaxis, G. Zissis, and K. Faidas, "A decision support system for assessment of street lighting tenders based on energy performance indicators and environmental criteria: Overview, methodology and case study," *Sustain. Cities Soc.*, 2019, doi: 10.1016/j.scs.2019.101759.

[19] J. S. Cha et al., "Policy and status of light pollution management in Korea," Light. Res. Technol., 2014, doi: 10.1177/1477153513508971.

[20] Website of International Dark-Sky Association:, https://www.darksky.org/; Retrived on 22 June 2022

[21] CIE Technical Report no. 150, "Guide on the Limitation of the Effects of Obtrusive Light from Outdoor Lighting Installations, 2nd edition," CIE, Vienna, 2017," 2017.

[22] K. Skarżyński, A. Rutkowska, "A comparison of the calculations and measurements for a lighting design of the same room," *Przegląd Elektrotechniczny*, vol. 96, no. 11, pp. 11–14, 2020, doi: 10.15199/48.2020.11.03.

[23] European Standard "EN 12464–1:2022, Light and lighting – Lighting of work places – Part 1: Interior work places", CEN, Brussels, 2022.

[24] P. Pracki, M. Dziedzicki, and P. Komorzycka, "Ceiling and wall illumination, utilance, and power in interior lighting," *Energies*, vol. 13, no. 18, 2020, doi: 10.3390/en13184744.

[25] D. Sawicki and A. Wolska, "Objective assessment of glare at outdoor workplaces," *Build. Environ.*, vol. 149, no. December 2018, pp. 537–545, 2019, doi: 10.1016/j.buildenv.2018.12.049.

Influence of Road Surfaces on Target Visibility: Experimental Measurements

Laure LEBOUC
Technical Direction
Spie batignolles malet
Portet-sur-Garonne, France
laure.lebouc@spiebatignolles.fr

Vincent BOUCHER
Light and Lighting Team
Cerema
Angers, France
vincent.boucher@cerema.fr

Florian GREFFIER
Light and Lighting Team
Cerema
Angers, France
florian.greffier@cerema.fr

Sébastien LIANDRAT
STI Research Team
Cerema
Clermont-Ferrand, France
sebastien.liandrat@cerema.fr

Aurélia NICOLAÏ
Technical Direction
Spie batignolles malet
Portet-sur-Garonne, France
aurelia.nicolai@spiebatignolles.fr

Paul RICHARD
LARIS – SFR MATHSTIC
University of Angers
Angers, France
paul.richard@univ-angers.fr

***Abstract*— Street lighting ensures visibility and legibility for road users. In this paper, performances of the lighting installation of two road sections with different type of road surface are measured in accordance with guidelines and road lighting standards. Then, the calculation of the visibility level of a target according to the Adrian's model is included considering the light reflections on the road. We compare the results obtained for each section with and without considering the light reflections and conclude that there is an incidence of the nature of the road surface on the target luminance. However, the effect on the visibility level of the target is not so straightforward. This depends on whether it is close to the visibility threshold, and it is therefore important to consider the reflective properties of the road surface. Moreover, we see that the visibility level provides us more information than the classical descriptors. The same luminance distribution for two pavement/lighting couples does not necessarily lead to the same distribution in terms of target visibility. It seems necessary to us to reinstate the visibility level in the performance criteria defined by the standard because it would act as a local descriptor of the performance of the pavement/lighting combination and would thus make it possible to avoid safety problems.**

Keywords—Road Lighting Calculation, Road Surface, Visibility Level, Road Surface Reflections Properties.

I. Introduction

The optimization of public lighting installations is a major challenge for the adaptation of urban areas to climate change. The increasing use of LED technology in road lighting is a very interesting lever for reducing energy costs. Another equally interesting lever is rarely considered: taking into account the actual pavement reflection properties in the design of lighting installations. Recent studies [1, 2] have shown that the combined optimization of lighting and pavement reflection properties made it possible to go much further in reducing energy consumption and limiting the amount of artificial light at night.

In addition to these concerns, the pavement reflection properties also play a central role in what is one of the historical reasons for lighting a road: to provide sufficient visibility conditions for users to detect an obstacle on the road [3]. Since this detection is based on the contrast between the luminance of the target to be avoided and that of the roadway, the optical properties of the road surface are directly involved since they constitute the pavement luminance. More indirectly, they can participate in the target luminance after reflection of the light on the portion of pavement located in front of the target [4]. The difference between these two luminances (target and pavement) can then be compared to a threshold difference, using for example the Adrian's visibility model [5], in order to evaluate the detectability of the target. This approach, which has long been a performance criterion for lighting installations [6-8], has been abandoned in the last ten years [9]. Only the more immediate performance criteria (average luminance, overall uniformity and longitudinal uniformity) remain [10]. They are indeed more easily calculated in software and measured in the field [11]. However, since they are based on luminance averages (mean luminance, overall uniformity) or a preferred direction (longitudinal uniformity), they do not allow us to examine locally the ability of the pavement/lighting combination to reveal the presence of an obstacle on the road [12].

In this paper, we propose to use Adrian's visibility model as a criterion for the performance of a lighting installation by examining the effect of the road surface on the visibility of a target. For this purpose, we conducted a measurement campaign on an experimental site equipped with two distinct pavements, each illuminated by a different lighting installation. We then evaluated the performance of these two urban configurations using only the classical criteria and then by evaluating the visibility level of a standard target placed at each point of the standardized grid [10, 11]. The effect of the road surface on the visibility was also examined by experimentally annihilating its influence on the target luminance. Finally, on one of the configurations, we studied the influence of a power reduction on lighting installation again by the classical criteria and by visibility measurements.

II. Road Lighting Basics

Guidelines [9, 13] and road lighting standards in Europe [10, 14] define the performance requirements that are specified in the form of lighting classes for street lighting. They consider the visual needs of road users and the environmental aspects of street lighting. They specify the mathematical conventions and procedures to be adopted for calculating the photometric performance of road lighting installations.

Especially, they give threshold minimum values for illuminance and luminance and their distribution on the road surface according to a grid of points whose number N depends on the pole spacing S and the number of traffic lanes (Fig. 1). Three performance criteria are defined in luminance: the

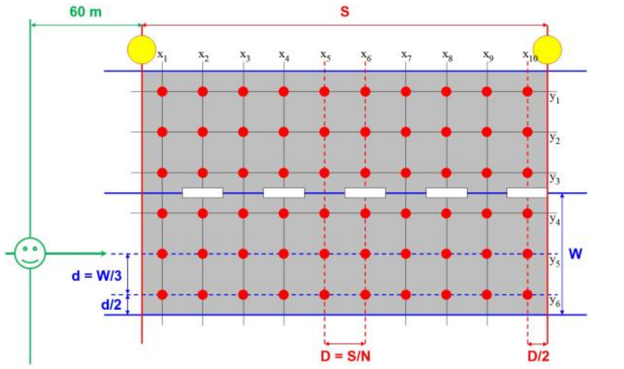

Fig. 1: Example of a calculation grid of points (in red) in road lighting design, according to the European standard [10]. The "smiley" represents the driver's eyes, and each measurement point is marked by its column 'x' and row 'y'.

average luminance (L_{ave}) (1), the overall luminance uniformity ratio (U_O) (2) and the longitudinal luminance uniformity ratio (U_l) (3). For a 2x2 lane road, the average luminance is the arithmetic mean of the luminances of the points of the calculation grid.

$$L_{ave} = \frac{1}{6\times N}\sum_{i=1}^{N}\sum_{j=1}^{6} L(x_i, y_j) \tag{1}$$

where x_i, y_j are the coordinates of the CIE grid points (related to the Fig.1) and N the number of points in the longitudinal direction.

The overall uniformity is calculated as the ratio of the lowest luminance, at any point on the CIE grid, to the average luminance.

$$U_O = \min(L(x_i, y_j))/L_{ave} \tag{2}$$

Longitudinal uniformity is the ratio of the lowest luminance to the highest luminance along the centerline of the roadway where is located the observer. For an observer placed in slow lane,

$$U_l = \min(L(x_i, y_5))/\max(L(x_i, y_5)) \tag{3}$$

III. Experimental Setup and Addition of Adrian's Visibility Model

To go further than the classical photometric quantities (average luminance, overall and longitudinal uniformities), in our opinion, a visibility calculation is a necessary complement, especially since one of the main functions of lighting is to make an obstacle on the road visible and thus enable a user to avoid it. We propose to use Adrian's well-known visibility model for road lighting applications, a model that was included in the CIE documents a few years ago [6] and then removed [9].

A. *Adrian's Model of Visibility Level*

From 1972 to 2010, a supplementary criterion to those specified in the CIE performance requirements was used: the Visibility Level (VL). We will focus on the model of Adrian who adapted it for road applications in order to characterize a lighting installation quality.

The visibility calculation model presented by Adrian [5] draws on laboratory research of Blackwell [15] and Aulthorn [16]. He defines the VL as the ratio of the actual contrast C of a target with its background over a threshold contrast C_{th} (4).

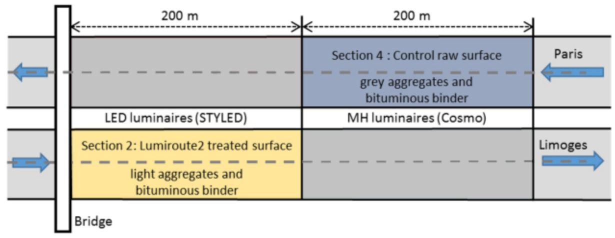

Fig. 2: Framework of the implementation of the two sections in Limoges, France.

$$VL = C/C_{th} = \Delta L/\Delta L_{th} \tag{4}$$

where ΔL is the actual luminance difference in cd/m^2 between the target and its background, ΔL_{th} is the threshold luminance difference in cd/m^2 required to detect a target as a function of background luminance.

The calculation of the threshold luminance difference is based on Ricco's and Weber's laws (5).

$$\Delta L_{th} = 2.6 \times (\Phi^{1/2}/\alpha + L^{1/2})^2 \times AF \times TF \times F_{CP} \tag{5}$$

where α is the angular size of the target in minutes of arc, Φ is a luminous flux function that determines perception, characteristic of the Ricco's process, L is a luminance function, translating Weber's law.

Adrian used some factors in this formula (5) to take into account the impact of the observer's age (AF), the observation time (TF) and the contrast polarization (F_{CP}) on the visibility of a target in an illuminated road (defined in [5]). Moreover, he replaced the background luminance by an adaptation luminance to consider the presence of glare sources in the visual field.

B. *Experimental Setup*

The experimental site is located on a suburban road in Limoges, France [17]. This is a 2 × 2 lanes road 6.50 meters wide and 400 meters long. The 4.25 meters wide central reserve is equipped with a 9 meters high lighting system with twin central arrangement and a spacing of 30 meters between luminaires. The surfacing of the entire road is a very thin asphalt concrete with a 0/10 mm gradation.

The experimental area consists of two sections of 200 meters (Fig. 2). Section 2 is an innovative section called Lumiroute® section and section 4 is an ordinary control section. Section 4 is a raw section while the surface of section 2 is treated with high-pressure water jet to remove the thin bituminous layer from the surface.

The control section 4 composed of ordinary road surface is lit by metal halide lighting while the Lumiroute® section composed of light surface is lit by adjustable LED lamps.

The experimental measurements were carried out on sections 2 and 4 at night for 3 different configurations. The resulting three combinations of road surface and lighting are summarized below:

- Section 2a consists of Lumiroute® road surface (water jet scrubbed road surface with light aggregates and a bituminous binder) combined with a LED illumination of 103 W (STYLED lamp, color temperature 4000 K). The luminaire flux is 4600 lumens.

- Section 2b is the same as section 2a but the flux of the STYLED luminaires is lowered by approximately 48%, i.e. equal to 2392 lumens.
- Section 4 is composed of a raw road surface (current road surface with grey aggregate and a bituminous binder) combined with traditional lighting consisting of a 140 W metal halide discharge source (COSMO lamp, color temperature of 2811 K) with a flux of 6270 lumens.

IV. Experimental Measurements

A. Classical measurements

For each configuration, luminance measurements are made with an Imaging Luminance Measurement Device (ILMD) placed 60 m in front of the measurement area (CIE grid). The average luminance (L_{ave}), the overall luminance uniformity ratio (U_O) and the longitudinal luminance uniformity ratio (U_l) are then deduced and reported in TABLE I. The results show that the performance criteria are respected for each of the configurations and that the lighting installations therefore comply with the EN 13201 standard [14] (classes M3 and M5 in TABLE II).

B. VL measurements

We first worked with the measurements obtained for sections 2b and 4 since they obtain similar values for classical performance criteria. We will then compare the results obtained for sections 2a and 2b to study the influence of a power reduction.

1) Study for sections with the same classical performance

To complete our measurements and evaluate locally the capacities of the pavement/lighting couple on target visibility, for each configuration, measurements of road surface luminance and target luminance were made for all positions defined by the CIE grid [13]. The target used for the VL measurements was a 25 cm square spectralon with a reflectance of 20%. For each position, the target was placed vertically, an image was captured, then a 1 m x 1 m black cloth was placed on the ground at the foot of the target to eliminate light reflections from the road surface and a second image was taken (Fig. 3). The target is cropped on each image to deduce its luminance (Fig. 4). For each section, we calculate the target luminance deviation with and without light reflections for each point of the CIE grid in order to study the influence of the road surface on target luminance (Fig. 5).

In Fig. 5, we see that the blue curves (section 2b) show almost always larger differences (in absolute terms) than the red curves (section 4). When we look at the average of all the luminance differences in absolute terms, we obtain an average of about 10% for section 2b and 5% for section 4, i.e. twice less. This suggests that the nature of the road surface has a greater or lesser impact on the luminance of the target.

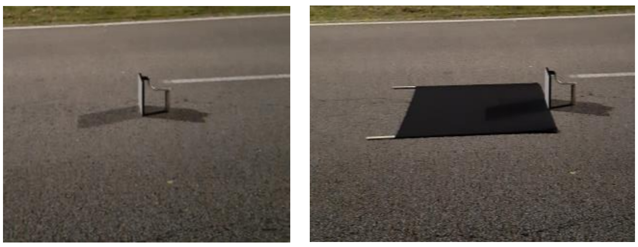

Fig. 4: Elimination of light reflections on the road surface by placing a black cloth of 1 m^2 at the foot of the target.

TABLE I. MEASURED VALUES FOR CLASSICAL PERFORMANCE CRITERIA.

Section number	Flux (in lumen)	L_{ave} (in cd/m^2)	U_O	U_l
2a	4600	1.22	0.49	0.71
2b	2392	0.64	0.50	0.73
4	6270	0.64	0.52	0.76

TABLE II. M CLASSES USED FOR ROAD LIGHTING WITH THEIR ASSOCIATED PERFORMANCE CRITERIA. WE ALSO REMINDED THE VALUES OF THE VISIBILITY LEVEL (VL) THAT APPEARED IN THE PREVIOUS VERSION OF THE CIE PUBLICATION 115 [6].

Class	L_{ave} (in cd/m^2)	U_O	U_l	VL
M1	2.00	0.40	0.70	7.5
M2	1.50	0.40	0.70	7.0
M3	1.00	0.40	0.60	6.5
M4	0.75	0.40	0.60	6.0
M5	0.50	0.35	0.40	5.5

On the other hand, we deduce the VL of the target for each position of the CIE grid for each section, with and without light reflections. For the background luminance, the luminance on the side of the target (Fig. 4) that maximizes the contrast is used because it was shown in a comparison between contrast computation and human detection that it is better correlated to target detection performance [18]. Considering that a target with $|VL| \geq 5.5$ is visible and one with $|VL| < 5.5$ is not [6] (see class M5 in TABLE III), we look if the target visibility changes somewhere in the grid after the addition of light reflections (Fig. 6).

By analyzing Fig. 5 and Fig. 6 in a cross-sectional way, it can be seen that it is not necessarily the largest deviations in target luminance that lead to a change in target visibility. For example, the target placed on the section 2b at (x_4, y_4) receives 6.1% more luminance due to the light reflections on the road surface and becomes invisible (red on the Fig. 6), whereas the target placed at (x_1, y_4) has a luminance difference of over 20% and its visibility does not change (blue on the Fig. 6). On the other hand, 5% more luminance is enough for the target placed at (x_5, y_4) to become visible (green on the Fig. 6). This is easily explained: when the VL of the target is close to the threshold of 5.5 before considering light reflections, then a small amount of additional luminance can bring the VL below this threshold. On the contrary, when the VL is much higher (or much lower) than 5.5 (in absolute terms), even a large addition of luminance does not cause a change in visibility in most cases.

Fig. 3: Left: Image captured from the observer's point of view with the target positioned at a point of the CIE grid. Right: We crop the area corresponding to the target (in green) and the areas used for the background luminance in the calculation of the VL (in red).

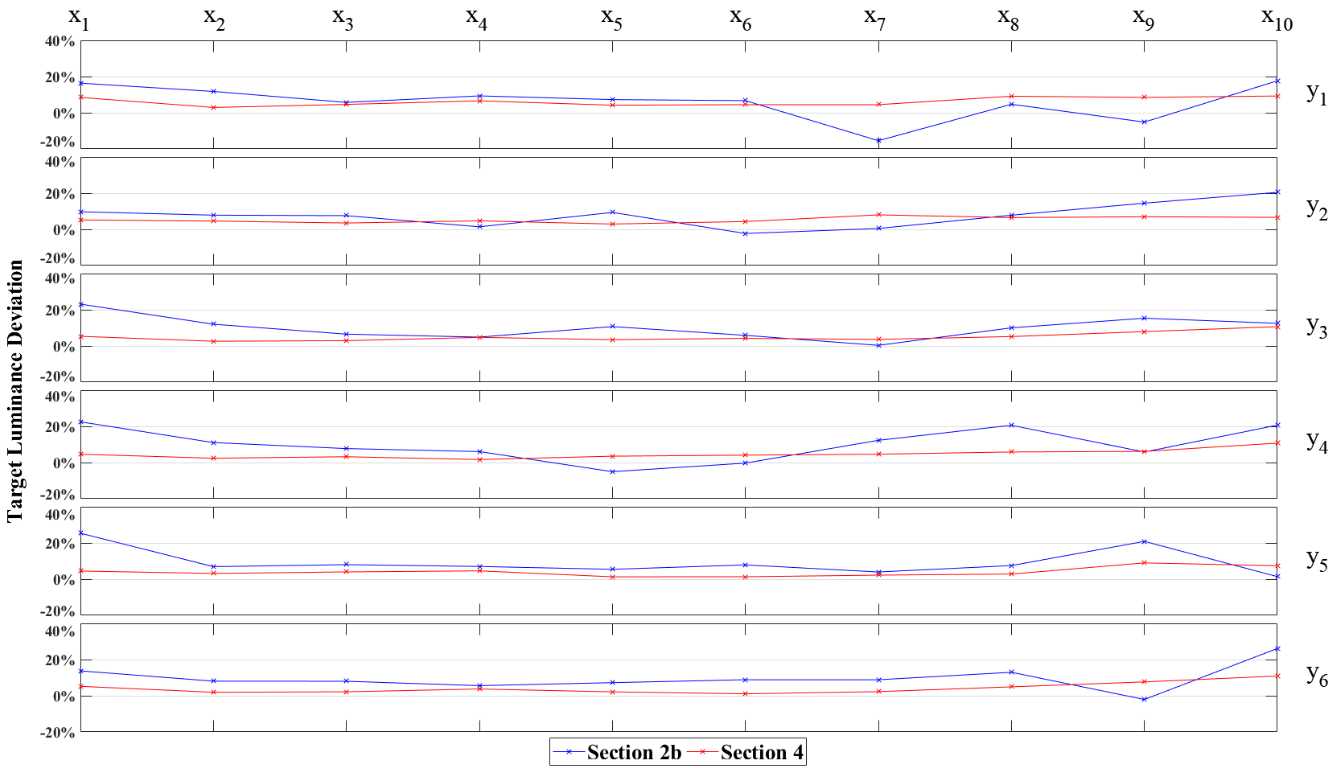

Fig. 5: Target luminance deviation between with and without consideration of light reflections on road surface for the sections 2b and 4. The x and y coordinates correspond to the measurement points of the CIE grid in Fig. 1.

Also, we see in Fig. 6 that the majority changes in visibility that occur are "become invisible". This is because the target is actually in negative contrast with the road, i.e. its luminance is lower than that of the road. Thus, when the reflections of light from the road are taken into account, the luminance of the target may increase and it approaches that of the background, so the VL decreases, approaching the critical threshold.

Finally, we can see the need to reinvest Adrian's visibility model as a performance criterion for a lighting installation. Indeed, despite the good results obtained for the classical criteria (luminance uniformities in TABLE II), the local performances are not at all comparable when we look at the Fig. 7 representing the visibility of the target in each point of the CIE grid. It can be seen that the target is not visible (red cell on Fig. 7) for every point of the CIE grid whatever the section considered, which may pose some local safety problems. Moreover, despite their similar classical performance, sections 2b and 4 do not provide at all the same distribution of target visibility on the grid. For the configuration of section 2b, the target is visible for 70.00% (42/60) of the CIE grid positions while this is only the case for 11.67% (7/60) for the pavement/lighting couple in section 4.

2) Study of the influence of a lowering of the lighting flux

To study the influence of a power reduction, we will now compare the measurements for sections 2a and 2b. First, we can see in TABLE I that the reduction of 48% of the luminaire flux between configurations 2a and 2b only affects the average luminance L_{ave} measured on the CIE grid. The luminance uniformities are similar, which is a typical behavior for a lighting installation equipped with LED lamps.

Furthermore, we consider the influence of power reduction on the VL. Fig. 8 represents the visibility of the target on the section 2 with a luminaire flux of 4600 lumens (so before the lowering) considering a VL threshold of 6.5 (TABLE III). The target is visible for 81.67% (49/60) of the CIE grid positions whereas it is for 70% when the flux is lowered (Fig. 7, left).

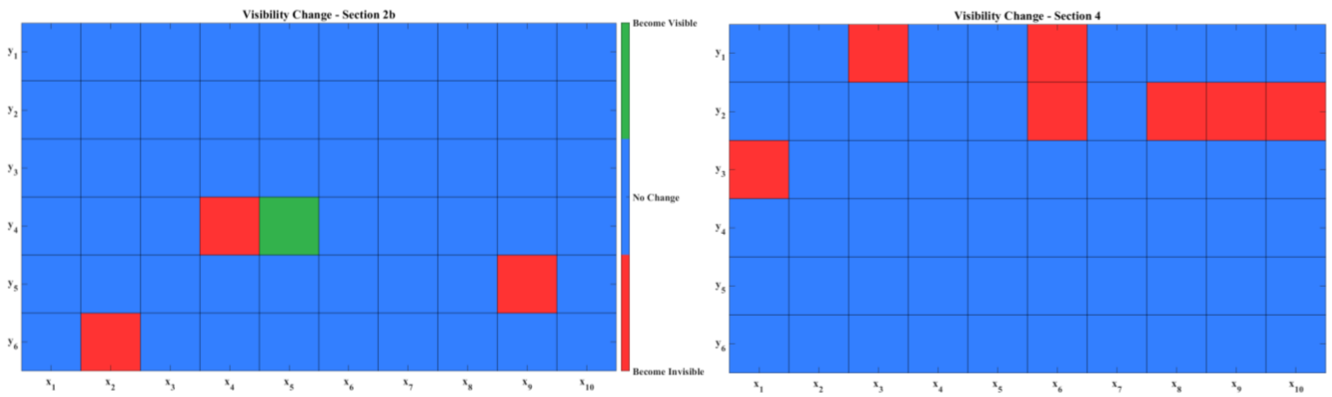

Fig. 6: Target visibility change for each point after considering light reflections on road surface for the section 2b (on the left) and the section 4 (on the right). The x and y coordinates correspond to the measurement points of the CIE grid in Fig. 1.

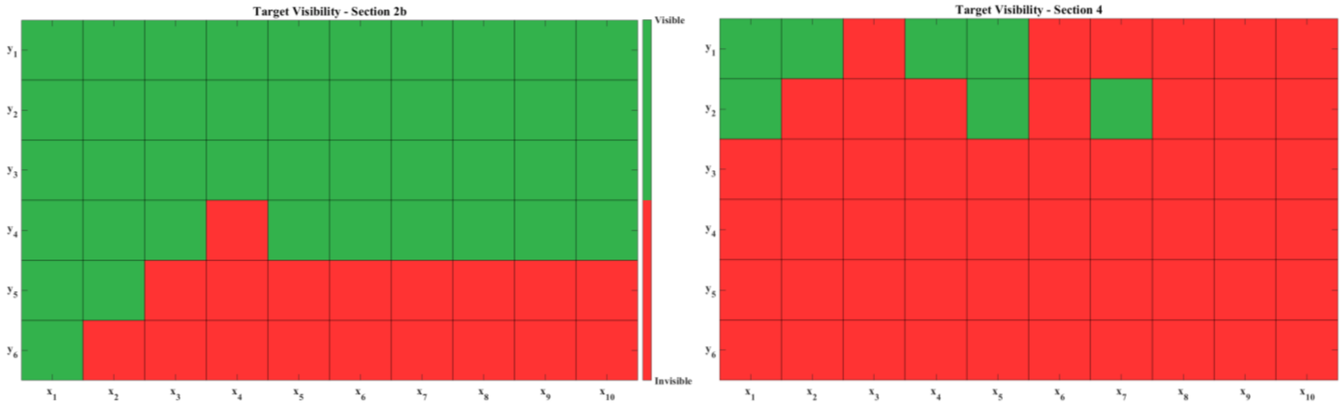

Fig. 7: Target visibility for each point after considering light reflections on road surface for the section 2b (on the left) and the section 4 (on the right). The x and y coordinates correspond to the measurement points of the CIE grid in Fig. 1.

Despite similar luminance uniformities, the visibility distribution of the target on the grid is not the same when the luminaire flux is changed. Contrary to the usual reasoning, the power reduction does not only lead to a decrease of the average luminance but also to a local modification of the visibility. This seems to be especially true since we compared our visibility measurements with different VL threshold values (6.5 for M3 and 5.5 M5). The requirement was more stringent for full power and the results are nevertheless better. This result confirms the need to add a visibility metric to the classical performance criteria in order to account locally for pavement/lighting performances.

V. Conclusion

To study the influence of the pavement on the target visibility, on-site measurements were performed for two different lighting situations with different road surfaces. We first evaluated the performance of these two urban configurations using only the classical criteria and then by evaluating the visibility level of a standard target placed at each point of the standardized grid. To see the effect of the road surface on the visibility, we have experimentally annihilated its influence on the luminance of the target by placing a black cloth at its foot. Finally, on one of the configurations, we studied the influence of a power reduction again by the classical criteria and by visibility measurements.

The results for the two road sections obtained with and without taking into account the light reflections allow us to state that there is an incidence of the nature of the road surface on the target luminance. A road surface that tends to reflect light better will increase the luminance of the target. However, it is not necessarily a large amount of additional light that will change the visibility of the target. A small addition of luminance is sufficient to bring the VL above or below the threshold when it is close to the threshold.

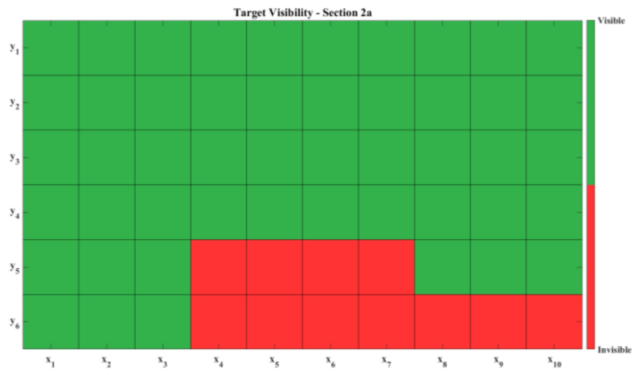

Fig. 8: Target visibility for each point after considering light reflections on road surface for the section 2a. The x and y coordinates correspond to the measurement points of the CIE grid in Fig. 1.

Moreover, we can see that the VL provides us more information than the classical descriptors. Both sections have similar conventional performance and comply with the standard. It is therefore expected to be compliant in terms of visibility as well. However, the two configurations do not give us the same target visibility distribution. One of them gives us 70% of visibility area while the other one has only 11% of the CIE grid positions where the target is visible. Also, when a power reduction is performed, not only a decrease of the average luminance appeared but also a local modification of the visibility.

In our opinion, it is necessary to reintegrate the visibility level into the performance criteria defined by the standard since it would have a role of local descriptor of the performance of the pavement/lighting couple and would thus make it possible to avoid safety problems.

Finally, the photometry of light and road have an important impact on the visibility level of a target. In order to better quantify and separate the effects of the lamps and the road, measurements and calculations with the same luminaires and same power for each section will be conducted.

References

[1] V. Muzet, F. Greffier, A. Nicolaï, A. Taron, P. Verny, “Evaluation of the performance of an optimized road surface/lighting combination”. Lighting Research and Technology, vol. 51, no. 4, pp. 576–591, June 2018.

[2] V. Muzet, S. Liandrat, V. Bour, et al. “Is it possible to achieve quality lighting without considering the photometry of the pavements?” In: Proceedings of the Conference CIE 2021. NC Malaysia online, sept. 2021, p. 11–21. https://doi.org/10.25039/x48.2021.OP01.

[3] R. Brémond. “Visual Performance Models in Road Lighting: A Historical Perspective”. LEUKOS, 17:3, 212-241, 2021. DOI: 10.1080/15502724.2019.1708204

[4] R. B. Gibbons. Influence of Pavement Reflection on Target Visibility. University of Waterloo, 1998. Available online: https://uwspace.uwaterloo.ca/handle/10012/244

[5] W. Adrian, “Visibility of targets: model for calculation”. Lighting Research and Technology, vol. 21, pp. 181-188, 1989.

[6] CIE, CIE 115:1995. Recommendations for the Lighting of Roads for Motor and Pedestrian Traffic. International Commission on Illumination (CIE): Vienna, Austria, 1995.

[7] AFE. Recommandations relatives à l'éclairage des voies publiques. (*in French*), Paris : Association Française de l'Eclairage. 2002.

[8] IESNA. American national standard practice for roadway lighting. RP-8-00. New York, NY: Illuminating Engineering Society of North America. 2000.

[9] CIE, CIE 115:2010. Lighting of Roads for Motor and Pedestrian Traffic. International Commission on Illumination (CIE): Vienna, Austria, 2010.

[10] CEN, EN 13201-3:2015. Road Lighting - Part 3: Calculation of Performance. CEN: Brussels, Belgium, 2015.

[11] CEN, EN 13201-4:2015. Road Lighting - Part 4: Methods of Measuring Lighting Performance. CEN: Brussels, Belgium, 2015.

[12] J. M. Waldram, "The revealing power of street lighting installations". In: Lighting Research and Technology 3, pp. 173–186, 1938.

[13] CIE, CIE 140:2019. Road Lighting Calculations, 2nd Edition. Vienna: CIE, 2019.

[14] CEN, EN 13201-2:2015. Road Lighting - Part 2: Performance Requirements. CEN: Brussels, Belgium, 2015.

[15] H. R. Blackwell, "Contrast thresholds of the human eye". Journal of The Optical Society of America, vol. 36, pp. 624-643, 1946.

[16] E. Aulthorn, "Über die beziehung zwischen lichtsinn und sehschärte" (*in German*). Graefes Archiv für Ophthalmologie, vol. 167, pp. 4 -75, 1964.

[17] V. Muzet, M. Colomb, M. Toinette, P. Gandon-Léger, J.-P. Christory, "Towards an optimization of urban lighting through a combined approach of lighting and road building activities". Proceedings of the 29th Quadrennial Session of the CIE. Washington DC, USA. pp. 789–800, 2019.

[18] R. Brémond, E. Dumont, V. Ledoux, A. Mayeur, "Photometric measurements for visibility level computations, Lighting Research and Technology, 43(1), pp. 119–128, 2011.

Life Cycle Assessment on Conversion to LED in Road Lighting

Ezgi Berberoğlu
Energy Institute
Istanbul Technical University
Istanbul, Turkey
ezgiiberberoglu@gmail.com

Sermin Onaygil
Energy Institute
Istanbul Technical University
Istanbul, Turkey
onaygil@itu.edu.tr

M. Berker Yurtseven
Energy Institute
Istanbul Technical University
Istanbul, Turkey
byurtseven@itu.edu.tr

***Abstract*—Nowadays, the environment, economies and social issues affect each other and cannot be considered separately. For this reason, sustainability is an issue that is gaining importance day by day. Life cycle sustainability assessments should be done with a holistic approach, taking into account the environment, economies and social factors.**

In this study, as a sample application, road lighting design was done using high-pressure sodium vapor lamps (HPSVL) and LED luminaires on an existing road, and the luminaires used in the design were evaluated in terms of environmental, economic and social aspects. For this purpose, calculations and evaluations have been carried out on an existing M2 lighting class road for which the LED conversion project was done. The requirements for EN road lighting standards that were valid in Turkey were fulfilled to a minimum extent within the scope of energy saving. In practice, the conversion to LED was taken as a basis by simply changing the luminaire, without changing the lighting poles in the existing installation. The use of HPSVL and LED luminaires in an existing road lighting through a sample application has been evaluated in terms of environmental greenhouse gas emissions, the economics of the life cycle cost approach and the social effects by forming opinions. From the evaluations made regarding raw materials, supply and process information, the data was obtained from a domestic manufacturer and evaluation was made in accordance with field studies. As a result, it has been determined that the global warming potential of the installation with HPSVL is 44% higher than the installation with LED. In addition, as a result of the LCA for HPSVL and LED luminaires, it was calculated that the operating cost is much higher than the maintenance and repair, investment and **salvage value** ***costs.***

***Keywords*—Life Cycle Assessment; Economy; Environment and Energy; Energy Efficiency; Road Lighting; Conversion to LED**

I. INTRODUCTION

The environment, energy and economies are three essential topics that cannot be thought of separately, and they affect each other and influenced by one other, have never ceased to be important from the past until now. Historical developments show that the rate of pollution in the environment increases whenever there is an economic crisis. Together with increasing levels of welfare, rapid population growth and developing technology, the energy demand is also increasing and getting harder to meet. With this in mind, energy efficiency applications that have a high impact on emission reduction, become more important. Today, the effects of climate change have led to the most critical environmental problems. The main anthropogenic cause of climate change is greenhouse gas emissions from the combustion of fossil fuels. To reduce this effect, radical changes are required regarding energy production and consumption. On the other hand, a long-term solution also should be affordable and cost-effective to enable technological development to proceed in a climate-friendly manner. In energy efficiency studies, lighting installations are seen as a highly significant topic because of their efficiency in saving a high amount of electric energy in a short period of time, while being cost-effective.

Turkey is a developing country and energy demand is increasing rapidly in this respect. Considering the international agreements of which Turkey is a party, it is necessary to meet the energy need reliably and economically by minimizing its negative environmental effects. In order to alleviate the impact of the energy cost burden on the economy, and to improve efficiency for environmental benefit, the "National Energy Efficiency Action Plan (NEEAP)" was published in 2017, and targets were set for 2023, regarding energy efficiency. In the National Energy Efficiency Action Plan, "E7: Improve Energy Efficiency Public Lighting" action was also implemented. Within the scope of the relevant action, activities such as evaluating and planning the transition from HPSVL luminaires to LEDs, in terms of efficiency, time and benefit/cost, ensured the integration of innovative technologies into the legislation, and the development of domestic production and design in the field of efficient lighting were carried out [1]. In this study, the aim was to create a sample application and evaluation that could guide these activities.

II. METHODOLOGY AND CASE STUDY

Today, with the development of LED technology, conversion studies to LED in road lighting have increased. While LED conversion applications in lighting provide benefits in terms of both energy efficiency and cost, significant gains have also been obtained in terms of environmental impact, which has become mandatory with national and international commitments and practices. It is thought that the high savings expected from energy efficiency studies can be achieved as a result of cost-effective replacement of inefficient systems in existing installations. For this reason, it was planned that the LED conversions on the existing road lighting would be carried out only by replacing the luminaire without any installation changes. For this purpose, calculations and evaluations were carried out for an existing M2 lighting class road for which the LED conversion project was implemented. In Denizli, Turkey, a road defined as an M2 lighting class was chosen as an example and an evaluation was made on completely real data. Both HPSVL and LED installation designs were carried out using the DIALux lighting design program, in order to provide the lighting quality criteria in accordance with TS EN 13201 standards [2], by changing only the luminaire without changing the pole. The road has 2 lanes with a width of 3.5 meters in two direction, and the width of the median is 1.5

meters. Calculations were made by only changing the luminaire without changing the pole. The lighting installation includes 12 meter high poles positioned in the middle median with 30 meter intervals. The poles with double consoles in both directions, have a console length of 2 meters. Luminaires were mounted on the consoles at a 15° angle so that they were parallel to the road's surface. The road map is shown in Figure 1.

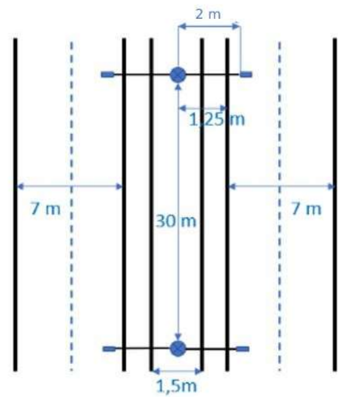

Fig. 1. Road map

The road surface was considered as an R3 class, the maintenance factor was taken as 0.80 and lighting designs were carried out. Taking this into account, the possibility of replacing old HPSVL luminaires, which have low lighting quality and are inefficient, with new HPSVL luminaires that meet the lighting criteria in accordance with the standards, or LED luminaires that provide the same road lighting quality, were examined. In terms of energy efficiency, the design is based on ensuring that the average luminance level is not exceeded by 1.2 times. The aim was to find 2 equivalent solutions that provide the required lighting quality values optimally, and to make a life cycle assessment (LCA) by accessing all possible data during production and use. In the evaluations, domestically manufactured lighting luminaires were selected in accordance with the national legislation. Considering the possibility of accessing the necessary data, the luminaire data of the same domestic lighting luminaire manufacturer was used in the designs. The electrical and photometric properties of the luminaires used in the design of the comparative HPSVL and LED road lighting installations were carried out in the study are given in Table1.

TABLE I. THE ELECTRICAL AND PHOTOMETRIC PROPERTIES OF THE LUMINAIRES

	Electrical and Photometric Properties of Luminaires					
Luminaire	***Light source power (W)***	***Ballast loss (W)***	***Luminaire luminous flux (lm)***	***Efficacy factor (lm/W)***	***Colour temperature (K)***	***Colour rendering***
HPSVL	150	18	12261	72.98	2000	~20
LED	93	-	13759	148	4000	>70

In this case HPSVL and LED luminaires were used on the road installation, and the road lighting quality criteria and calculation results are given in Table 2.

TABLE II. M2 CLASS ROAD LIGHTING QUALITY CRITERIA AND APPLICATION EXAMPLE CALCULATION RESULTS

	M2 Class Road Lighting Quality Criteria and Application Sample Calculation Results		
	M2 class road lighting quality criteria	***Values obtained as a result of using 150 W HPSVL luminaires***	***Values obtained as a result of using 93 W LED luminaires***
L_{ave} (cd/m^2)	≥ 1.5	1.62	1.76
U_o	≥ 0.40	0.49	0.6
U_l	≥ 0.70	0.84	0.94
f_{TI} (%)	<10	7	8
R_{EI}	> 0.35	0.87	0.86

III. LIFE CYCLE ASSESMENT AND IMPLEMENTATION

In Tähkämö et al.'s study (2012) in which LEDs of light sources were analyzed, it was noted that light sources could be efficient, long-lasting, repairable, easily disassembled, recyclable, free from hazardous substances, and be environmentally friendly, provided that they contain the lowest possible amount of pollutants. When traditional light sources and LEDs are compared, it is stated that the environmental effects of LEDs in production and raw material purchase are higher, but their lifetime effects are low due to their low energy consumption, and consequently their total life cycle effects are lower. In the study, it was also emphasized that the scope of the LCA should be chosen carefully so that the LED luminaires and conventional light sources are comparable [3]. Bazzana et al. (2012) evaluated the process effects of LED luminaires in their study and concluded that the environmental effects of LED luminaires during the usage phase and the hazardous/non-hazardous waste effects during the manufacturing phase are dominant. It was determined that the environmental effects caused by the LED array, driver and aluminum parts were seen during the manufacturing phase, while the installation, transportation and service life had very little effect on the LCA. It was said that the environmental impact of 50000 hours of life were on average 17% lower than those of 36000 hours of life. Depending on the impact category, aluminum parts such as heatsinks had an environmental impact of 11%-42%, the driver had an environmental impact of 19%-66%, and the LED array had an environmental impact of 4% to 50% [4]. A cradle-to-grave approach for Ceramic Discharge Metal Halide Lamps (CDMHL) and LED street lighting in Abu Dhabi, the United Arab Emirates, covering raw material acquisition, luminaire production, service life and usage stages, was carried out by Hadi et al. (2013). In that study, it was realized that the environmental effects of LEDs, which were high during the production phase, were balanced due to their low energy consumption during use. When the analyses were made for the road lighting luminaires used with photovoltaic panels, it was seen that the battery production, fossil fuel use for energy and transportation stages were dominant on the environmental impact. Their conclusions indicated that LEDs have lower effects than CDMHLs in all scenarios powered by photovoltaic panels with and without battery recycling [5].

In another study by Tähkämö et al. (2015), based on a HPSVL and LED comparison, it was confirmed in the LCA analyses concerning road lighting technology that HPSVL and LED luminaires when used, the environmental effects mostly arise from the usage phase. It was observed that LEDs had a 26% lower effect per luminaire and a 17% lower effect per light amount (lumen-hours). On the other hand, since the amount of lumen hours and luminaires do not define the actual function of the luminaires, the difference between the luminaires compared to a 1 kilometer road is only 3% on average. In addition, it was pointed out that studies should be conducted to evaluate the environmental, social and economic effects of road lighting fixtures with an appropriate functional unit in order to evaluate the total sustainability perspective of the products [6]. Tannous et al. (2018) in their study comparing two streets' lighting in Lebanon with a cradle-to-grave approach, came to the conclusion that the use of solar street luminaires with 70 Watt LED is environmentally better than a conventional system with 150 Watt HPSVL. It has been stated that recycling after the end of the life of the systems is even more positive for LED. Since the assembly stage of short-lived and old-designed luminaires with HPSVL requires significant amounts of aluminum and metal; this is a dominant stage in their environmental impact [7]. Richter et al. (2019) explain the comprehensive LED review they carried out for LEDs between 2012-2017 in their study. The lifetime of the LEDs was evaluated as a sensitivity analysis. From an environmental point of view, it was worth noting that it was more advantageous to replace the existing product with new products in its category, in contrast to products with a long service life. It was also stated that this effect will decreased with the maturation of LED technology [8]. Finally, in the study done by Dzombak et al (2020), which analyzed the circular economy model, which optimized both the environmental effects and the cost of street lighting in terms of cost assessment, stated that the cost-effective method is not the most suitable, from an environmental point of view, and it was noticed that cost savings and management strategies should be developed. They emphasized the need for extensive research on the use of long-lasting products should be cost-effective and reusable. It was observed that the use of new technological products was also advantageous in terms of efficiency gain [9]. When the literature is reviewed, it is seen that the results differ depending on the developments in LED technology. From this, it is understood that Life Cycle Assessment analyses, which require detailed data analyses, should be made on a project basis, based on the latest available technologies.

In the light of these requirements, energy efficiency analyses, greenhouse gas emission calculations, and then life cycle cost (LCC) calculations for lighting installation alternatives with HPSVL and LED designed for a sample road, were evaluated. In recent years, the focus has been to carry out these analyses under the name of the Life Cycle Sustainability Assessment (LCSA), including environmental life cycle assessments, life cycle costs and social life cycle assessments. Within the framework of our approach, greenhouse gas emission assessments and the environment, purchasing costs and economy were analyzed. However, in the third dimension, the social life cycle assessment, since impact analyses based on long-term multi-parameter field studies are required, possible reversals could only be identified to guide future research.

A. Environmental Life Cycle Assesment

An environmental impact assessment was done in terms of energy efficiency and greenhouse gas emission reduction and global warming potential of the use of luminaires with HPSVL and LEDs with total powers of 168 W (including ballast loss) and 93 W respectively, designed with the life cycle assessment approach. Evaluations were made using real production and usage data of the luminaires in both alternative solutions. The calculations of greenhouse gas emissions were carried out with the data obtained from the local luminaire manufacturer. The evaluations were made for a single luminaire. The functional unit was determined as the amount of electrical energy in kWh saved within the scope of energy efficiency. Considering the economic life of the luminaires to be used and the light sources inside, the evaluations were made on a 15-year basis. In the emission calculations made for both alternative luminaires, emissions from vehicles for transportation purposes (raw material/component supply, in-plant transportation, delivery of the product to the final usage point), and emissions from combustion and electrical energy used in production processes during the pre-production, production and post-production stages, were taken into account.

In accordance with the "IPCC Guidelines for National Greenhouse Gas Inventories" [10], CO_2, N_20 and CH_4 emissions were included in the calculation. The emission factor for electrical energy use was calculated with reference to the emission factor of the "Turkish National Electricity Network Emission Factor Data Sheet" [11]. Global warming potential was accepted as 1 for CO_2, 21 for CH_4 and 298 for N_2O.

The electricity, diesel and natural gas carbon dioxide equivalent emission factors used in the calculation are outlined in Table 3.

The calculations of greenhouse gas emissions from combustion and from vehicles were based on the Tier 1 method specified in the "IPCC Guidelines for National Greenhouse Gas Inventories". The calculation is based on the source category and fuel quantity for the fuel and a default emission factor. The amount of greenhouse gas emissions from combustion in tons was calculated by using equation 1.

Combustion emission amount (tonnes) = Fuel consumption (kg) * Cycle coefficient (TJ/kg) * Emission factor (ton/TJ) (1)

TABLE III. EMISSION FACTORS

	Emission Factors		
Source	***CO_2***	***CH_4***	***N_20***
Electric	0.7258 ton/MWh	-	-
Natural gas	56.1 ton/TJ	1 kg/TJ	0.1 kg/TJ
Diesel	74.1 ton/TJ	3.9 kg/TJ	3.9 kg/TJ

Energy indirect greenhouse gas emissions calculations were based on the Tier 2 method, which uses the amount of fuel burned in the source category and a country-specific emission factor for each fuel written in the "IPCC Guidelines for National Greenhouse Gas Inventories". The amount of greenhouse gas emission originating from electricity was calculated with equation 2.

Emission amount (tonnes) = Electricity consumption (kWh) * Emission factor (tons/kWh) (2)

In the production process of the polycarbon-bodied HPSVL luminaire, 0.097 m^3 of natural gas was only consumed for the painting of metal console parts. Calculations were made for CO_2, CH_4 and N_20. The emission amount caused by natural gas combustion during the production phase of the luminaire with HPSVL was calculated as 0.00018810 tons of CO_2.

In LED luminaires, 1.687 m^3 of natural gas was consumed, including the injection process, in the production of body and console parts. Calculations were made for CO_2, CH_4 and N_20. The emission amount caused by natural gas combustion during the production phase of the LED luminaire was calculated as 0.00327132885 tons of CO_2.

Based on the information obtained from the domestic manufacturer, emissions from transportation were calculated at the raw material procurement stage. The raw material supply of the luminaire with HPSVL was realized from a distance of 19300 km by ship and 2759 km by truck. The raw material supply of the LED luminaire was realized from a distance of 19000 km by ship, 1623 km by truck and 3800 km by semi-trailer. The calculation results performed by proportioning the luminaire volume to the total volume of the transport vehicle, are given in Table 4.

The distance between the pilot road in Denizli and the luminaire production facility, which was chosen as a sample application, is 560.5 km. The products came to the assembly site by pickup truck; the greenhouse gas emission from the vehicles due to product delivery was calculated as 0.000361728 tons of CO_2 when rated against the volume of the luminaire with HPSVL, and as 0.00021436 tons of CO_2 when rated against the volume of the luminaire with LED.

Electric vehicles were generally used to transport products within the factory. Transportation was done with the help of electric forklifts or electric reach-rucks. For diesel fuel forklifts used outdoors, 0.0009 lt/product of fuel was used per product. It was concluded that 0.000002420 tons of CO_2 were generated within the scope of these in-plant transports for both luminaires. Total greenhouse gas emissions from transportation are given in Table 5.

TABLE IV. GREENHOUSE GAS EMISSIONS FROM VEHICLES DURING THE RAW MATERIAL SUPPLY OF LUMINAIRES WITH HPSVL AND LED

	Greenhouse Gas Emissions from Vehicles During Raw Material Supply of Luminaires with HPSVL and LED	
Vehicle	***HPSVL Luminaire***	***LED Luminaire***
Truck	0.0016025	0.0005586
Ship	0.2078966	0.1212831
Semi-trailer	-	0.0021254
Total	0.2094991	0.1239671

TABLE V. GREENHOUSE GAS EMISSIONS OF HPSVL AND LED LUMINAIRES DURING RAW MATERIAL SUPPLY, IN-PLANT TRANSPORTATION AND DELIVERY TO THE DELIVERY POINT

	Greenhouse Gas Emissions Occurring During Raw Material Supply, In-plant Transportation and Delivery to the Delivery Point of Luminaires with HPSVL and LED	
Process	***HPSVL Luminaire***	***LED Luminaire***
Raw material supply	0.2094992	0.12338742
In-plant transport	0.00000242	0.00000242
Move to point-of-use	0.00036173	0.00021436
Total	0.20986335	0.1236042

The total amount of electrical energy consumed during the production phase of the luminaire with HPSVL is 2.1 kWh. In addition to this value, the amount of electrical energy consumed by the luminaire with HPSVL, which draws a total power of 168 W, including ballast loss, during the 15-year evaluation period, at 4000 hours per year, was also calculated. A total of 10080 kWh of electrical energy was consumed for 15 years, at 672 kWh per year. The total of 372 kWh of electrical energy consumed for the production phase of the LED luminaire, which is 4 kWh, and the amount of electrical energy consumed by the 93 W LED luminaire at the end of 15 years with an annual use of 4000 hours, were also calculated. By multiplying these consumption amounts with the emission factor, greenhouse gas emissions originating from electrical energy consumption were calculated. The results are given in Table 6.

Total greenhouse gas emissions were calculated by adding up total direct vehicle emissions, total direct combustion emissions, and total indirect electricity energy consumption emissions. The values obtained as a result of the calculations are given in Table 7.

TABLE VI. GREENHOUSE GAS EMISSION METRICS AND AMOUNTS DUE TO ELECTRICAL ENERGY CONSUMPTION FOR LUMINAIRES WITH HPSVL AND LED

	Greenhouse Gas Emission Metrics and Quantities from Electrical Energy Consumption for Luminaires with HPSVL and LED				
Phase	***Consumption (kWh)***	***Emission Factor (t/mWh)***	***Year***	***Emission (ton)***	***Total emission (ton)***
Luminaire production phase with HPSVL	2.1	0.7258	-	0.0015	7.3176
HPSVL luminaire usage phase	672	0.7258	15	7.3161	
Luminaire production phase with LED	4	0.7258	-	0.0029	4.0529
LED luminaire usage phase	372	0.7258	15	4.05	

TABLE VII. EMISSION VALUES CALCULATED FOR LUMINAIRES WITH HPSVL AND LED

	Calculated Emission Values	
	HPSVL	***LED***
Direct - greenhouse gas emissions from combustion	0.000188097	0.003271329
Direct - greenhouse gas emissions from vehicle	0.209863352	0.123604205

Total direct greenhouse gas emissions	0.210051449	0.1268755334
Indirect - greenhouse gas emissions from electrical energy consumption	7.31758818	4.0528672
Total greenhouse gas emissions	7.527639629	4.179742733

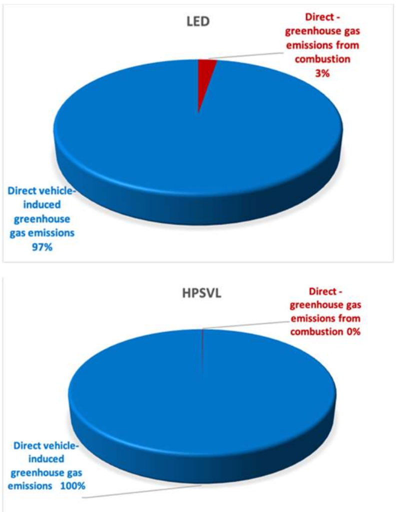

Fig. 2. Direct greenhouse gas emission rates of luminaires with LED and HPSVL

The global warming potential of the luminaire with HPSVL was determined as 7.528 tons CO_2e, and that of the luminaire with LED was determined as 4.180 tons CO_2e. Direct greenhouse gas emission rates of luminaires with LED and HPSVL are given in Figure 2. Of the direct greenhouse gas emissions, vehicle-induced greenhouse gas emissions constitute 97%, while the amount of emissions caused by combustion during the production phase constitutes 3%. Almost all of the direct greenhouse gas emission of the luminaire with HPSVL was caused by the greenhouse gas emissions from the vehicle. Life Cycle Cost

The life cycle cost (LCC) of the sample road lighting using 150 W HPSVL luminaire and 93 W LED luminaires were evaluated. The luminaire-based cost analyses were carried out in two stages. First of all, a cost analysis was made with the net present value method and it was determined which application was better in terms of cost. In the second stage, evaluations were made by comparing different expenses within the total cost.

The interest rate was determined by taking into account the interest data of the Turkish Central Bank dated 20.05.2022. The value of 23.27, in TL, which was valid for commercial loans (excluding corporate overdraft accounts and corporate credit cards), was accepted as the interest rate [12]. The prices of the luminaires were obtained from the domestic manufacturer. The LED luminaire is \$120 and the HPSVL luminaire is \$52. The HPSVL price is accepted as \$3 based on the TEDAŞ (Turkey Electricity Distribution Inc.) unit price book, which included the unit prices valid as of January 1 [13]. An assessment was made for a 15-year amortization period. Although summer and winter are different, calculations are made on the assumption that road lighting installations are used 10-12 hours a day in Turkey, based on 4000 hours of use per year. According to the TEDAŞ specification, LED luminaires and/or components would not be replaced during the 15-year evaluation period, since all components of LED luminaires have a 60000-hour lifetime commitment condition. At the end of this period, LED luminaire salvage value cost would occur. A 15-year usage period was also valid for the luminaire with HPSVL, but the economic life of the transparent tube high-pressure sodium vapor lamp inside the luminaire was 24000 hours. During the 15-year depreciation period, lamps needed to be changed twice in six-year periods, and at the end of the period, the cost of HPSVL luminaire salvage value would occur. The maintenance and repair cost was accepted as \$21 per luminaire and was taken into account in the calculations, assuming that it would be done every year. The unit electricity energy consumption price was taken as 0.1371 \$/kWh, which is the value under the "lighting" title, from the activity-based electricity tariffs table published by EPDK (Republic of Turkey Energy Market Regulatory Authority) on 31.05.2022 and effective until 1.06.2022. The annual operating time of the luminaires was considered as 4000 hours, and the annual total electrical energy consumption and operating cost were calculated over the power and operating time.

According to the information obtained from the domestic manufacturer, the salvage value and waste price of the luminaire with HPSVL is \$0.48, the salvage and waste price of the luminaire with LED is \$1.16. This value was included in the total salvage value cost, as disassembly would also be done at the salvage stage of the luminaires. Income and expenses for the application example are given in Table 8.

The cash flow chart of the luminaire with HPSVL and the luminaire with LED for 15 years per luminaire are given in Figure 3 and Figure 4. Cost calculations were made with the NPV method as indicated in the flow chart.

TABLE VIII. INCOME AND EXPENSES FOR THE APPLICATION EXAMPLE

	Income And Expenses For The Application Sample (\$)	
Cost	***HPSVL***	***LED***
Investment cost	85	153
Operating cost	92158	51016
Salvage value cost	6	7
Maintenance and repair cost[a.]	21	21
Interest rate	23.27	23.27

a.It is price given by the electricity distribution company (TEDAŞ) in Turkey for the year 2022 [13].

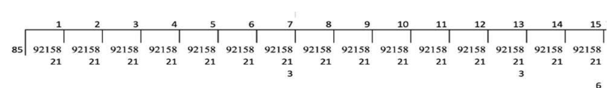

Fig. 3. Flow chart of HPSVL luminaire in \$.

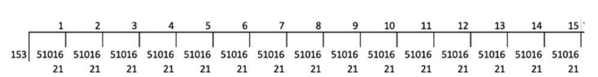

Fig. 4. Flow chart of LED luminaire in \$.

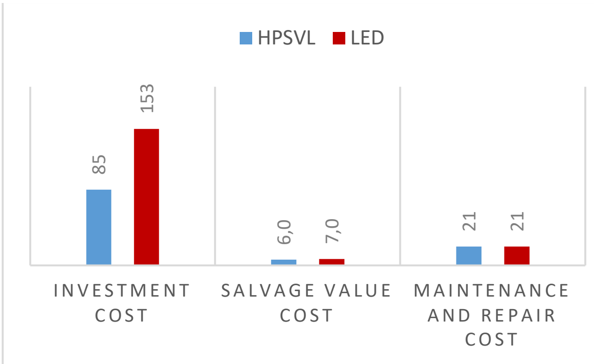

Fig. 5. Comparison of investment, salvage value and maintenance-repair costs of HPSVL and LED luminaires.

At the end of the 15-year period, when the specified expenses were included in the calculation with the determined interest rate, operating expenses were calculated as $378865 in the use of HPSVL and $209729 in the use of LED. It was concluded that the total costs were $379038 for HPSVL and $209969 for LED, respectively. When the costs were evaluated with the net present value method, it is seen that the use of LED luminaires is preferable.

LCC is a method in which different stages of design and projects are evaluated in terms of cost in order to arrived at the best decision in decision making stages. Applying LCC for $ type HPSVL and LED luminaires, it was seen that the operating cost was much higher than the maintenance and repair, investment and salvage value costs. This result is consistent with the results in the literature [9]. The comparison of investment, salvage value, maintenance and repair costs of HPSVL and LED luminaires as a result of LCC has been graphed in Figure 5. It has been concluded that the least expense is the salvage value cost, followed by the maintenance and repair cost, and the highest value is the investment cost for both types of luminaires. As can be seen from the comparison of luminaires with HPSVL and LED, the initial investment cost of LED luminaires is still higher than luminaires with HPSVL in today's conditions.

B. *Social Impact Assesment*

Social impact assessment aims to evaluate the potential impact, social and socio-economic aspects of products on users throughout their lives. It analyses the social and socio-economic performance that may affect the stakeholders in all processes of the product from raw material acquisition, processing, production, distribution, use and final disposal. It can be applied with an environmental life cycle assessment or remain alone. However, the decisions made within the scope of the social life cycle assessment (SLCA) are generally insufficient. These analyses can document the benefits that can be obtained from the product, but cannot give clear information about whether the product is produced or not. In the current assessments, the environmental dimension has been developed and can be comprehensively addressed. Moreover, basic scientific developments, consistent and robust indicators and methods are still needed for social dimension assessment. Since semi-quantitative and qualitative data are used, it becomes difficult to express the effects on the functional unit with the SLCA analysis. When applying the SLCA analysis, it is recommended to focus on the stage with the highest potential and the most important improvement in the life cycle stages [14].

It is also significant to determine the target and scope in the evaluations at the first stage, and to make all analyses within the same scope. In our study, in the analyses designed within the framework of energy efficiency studies, the functional unit was determined as the amount of electrical energy saved in kWh. As a socio-economic effect, the most important benefit can be explained as the energy saving value that can be achieved throughout the country with efficient road lighting installations, reducing Turkey's total energy consumption and foreign dependency on energy. On the other hand, with the road lighting designs made in accordance with the regulations and standards, the number of traffic accidents and the death rate can be reduced. Considering that possible crime rates can be reduced in outdoor environments at night and night life opportunities in cities can be increased by improving security conditions, other socio-economic contributions of the life cycle assessment carried out within the scope of the study can also be described. The controlled use of limited resources and the reduction of greenhouse gas emissions through energy efficiency studies have environmental benefits as well as improving the quality of life of societies.

IV. DISCUSSION

When the environmental impact is evaluated in terms of direct carbon emissions for the processes from raw material procurement to production, installation at the end of the 15-year usage period for HPSVL and LED luminaires in alternative designs realized on the current pilot road, it was noticed there was little difference between them. On the other hand, when only the emissions caused by indirect electrical energy consumption during the usage process are taken into account, it is seen that the LED luminaire, which consumes less electrical energy, has a superior position with less emission.

When life cycle cost evaluation is done in order to examine the lifetime cost of luminaires with HPSVL and LED, the investment cost of luminaires with LED is higher than luminaires with HPSVL, but due to less energy consumption during operation, considering all life cycle steps of the products, the cost of using LEDs was found to be more advantageous.

It is seen that the use of LED luminaires in road lighting is more appropriate in terms of social aspects compared to luminaires with HPSVL. These applications will both reduce foreign dependency for energy due to low energy consumption and contribute positively to human health and the environment by reducing greenhouse gas emissions.

V. CONCLUSION

Road lighting installation design with equivalent performance was made for luminaires with HPSVL and LED through the sample application. This design was evaluated using the life cycle sustainability assessment approach. Evaluations are based on actual usage data. Environmental life cycle assessment was examined in terms of greenhouse gas emissions during the production and usage stages of the luminaires. A lifetime cost evaluation of the luminaires was also carried out. Finally, social impact assessment was attempted to be understood. Since long-term multivariate field studies or healthy and comprehensive data that can be obtained from different sources are needed to concretely reveal the social effects of the use of luminaires with HPSVL and LED in road lighting with numerical values, in this study, only possible socio-economic benefits that could guide further research could be identified.

In conclusion, it was determined that the global warming potential of the installation with HPSVL is 44% higher than the installation with LED. Using the LCC for HPSVL and LED luminaires, it was calculated that the operating cost is much higher than the maintenance and repair, investment and salvage value costs. On the other hand, it was seen that the initial investment cost of LED road lighting fixtures is still higher than present HPSVL luminaires.

Life cycle sustainability assessment studies are difficult to do as accurate and comprehensive data analysis is required. For this reason, there is a need for exemplary and guiding studies in the literature in which project and technology-based life-cycle sustainability are analyzed.

References

[1] ETKB Department of Energy Efficiency and Environment, "National Energy Efficiency Action Plan 2017-2023". Ankara, 2017.

[2] CEN, EN 13201-2 :2015-Road lighting-Part 2 : Performance Requirements, Brussels

[3] Tähkämö, L., Puolakka, M., Halonen, L., & Zissis, G. (2012). Comparison of life cycle assessments of LED light sources. Journal of Light & Visual Environment, 36(2), 44-54.

[4] Bazzana, M., Ravel, P., Grannec, F., & Martinsons, C. (2012), Life cycle assessment of light-emitting diode downlight luminaire-a case study.

[5] Hadi, S. A., Al Kaabi, M. R., Al Ali, M. O., & Arafat, H. A. (2013). Comparative Life Cycle Assessment (LCA) of streetlight technologies for minor roads in United Arab Emirates. *Energy for Sustainable Development*, *17*(5), 438-450.

[6] Tähkämö, L., & Halonen, L. (2015). Life cycle assessment of road lighting luminaires–comparison of light-emitting diode and high-pressure sodium technologies. *Journal of Cleaner Production*, *93*, 234-242.

[7] Tannous, S., Manneh, R., Harajli, H., & El Zakhem, H. (2018). Comparative cradle-to-grave life cycle assessment of traditional grid-connected and solar stand-alone street light systems: A case study for rural areas in Lebanon. *Journal of Cleaner Production*, *186*, 963-977.

[8] Richter, J. L., Tähkämö, L., & Dalhammar, C. (2019). Trade-offs with longer lifetimes? The case of LED lamps considering product development and energy contexts. *Journal of cleaner production*, *226*, 195-209.

[9] Dzombak, R., Kasikaralar, E., & Dillon, H. E. (2020). Exploring cost and environmental implications of optimal technology management strategies in the street lighting industry. *Resources, Conservation & Recycling: X*, *6*, 100022.

[10] IPCC , "Guidelines for National Greenhouse Gas Inventories," 2006.

[11] ETKB, "Turkish National Electricity Network Emission Factor Information Form", Access Address: https://enerji.gov.tr/evced-cevre-ve-iklim-turkiye-ulusal-elektrik-sebekesi-emisyon-faktoru Accessed date: 29.05.2022

[12] Interest statistics. TCMB, 2022. [Online]. Available: < https://evds2.tcmb.gov.tr/index.php?/evds/portlet/0QRrRj0ew0Y%3D /tr>

[13] TEDAŞ, "Unite price book", 2022. [online] Available: https://birimfiyat.tedas.gov.tr/ Accessed date:22.05.2022

[14] UNEP, "Guidelines For Social Life Cycle Assessment Of Products", UNEP, 2009.

The Importance of Luminous Intensity Distribution in Adaptive Road Lighting for Twin Bracket Central Arrangement Systems

M. Berker Yurtseven
Energy Institute
Istanbul Technical University
Istanbul, Turkey
byurtseven@itu.edu.tr

Sermin Onaygil
Energy Institute
Istanbul Technical University
Istanbul, Turkey
onaygil@itu.edu.tr

Önder Güler
Energy Institute
Istanbul Technical University
Istanbul, Turkey
gulerond@itu.edu.tr

***Abstract*—To increase energy savings, adaptive road lighting (ARL) systems that can provide dynamic lighting by the change in the parameters on the road are recommended by international standards. According to CEN/TR 13201-1 "Road lighting - Part 1: Guidelines on selection of lighting classes", adaptive road lighting is defined as "temporal controlled changes in luminance or illuminance in relation to traffic volume, time, weather or other parameters". With the changes in the parameters considered, the initial design average luminance can be changed by reducing it, usually. The most important parameters in this respect are, traffic volume (vehicle density), traffic speed, traffic composition (motorized, pedestrian, etc.), real-time reflection properties, and the current state of the road surface. Also, the variable effect of ambient luminosity can be considered. While applying adaptive lighting, it is also important that changes in the average lighting level do not affect other required quality parameters on the road.**

When the roads with different luminaire arrangements are taken into consideration, especially roads with a median separating two directions and the poles with twin bracket arrangement are hard to design for adaptive road lighting scenarios. If both directions are to be adjusted to different levels of lighting classes, the designer should make detailed calculations since depending on the luminous intensity distribution of the luminaire, the contribution of one luminaire to the other side should be analyzed. Especially as the median width gets shorter, the contribution of the luminaire will increase. And if a one-sided dimming scheme is used, the contribution to the other side will decrease proportionally to the dim level. Thus, different luminous intensity distribution types (in 270° plane) should be analyzed for different scenarios, and energy efficiency calculations should be done using these different scenarios.

In this paper different luminous intensity distributions (in 270° plane) will be evaluated against different median widths for a sample M2 lighting class road illuminated with the twin bracket arrangement on the median. For both directions, different couples of lighting classes will be simulated using Dialux lighting simulation software ie. M2-M2 (base), M2-M4 (static), and also M2-10% (dynamic) level for no traffic "night" scenario for one side. Using the M2-M2 scenario as a base, how much the luminaires' luminous output should be increased or dimmed will be calculated and energy saving calculations for different scenarios will be done against the standard operation scenario which is M2-M2 lighting classes for both sides. As a result, depending on the 270° plane distribution of the luminaire power to be selected during the design, it will be determined how much more should be selected according to the base scenario.

Keywords—Adaptive Road Lighting, Luminous Intensity Distribution, Lighting Simulation

I. INTRODUCTION

The main purpose of road lighting is to create the necessary lighting conditions and ensure traffic safety. Organizations that develop international standards and recommendations prepare publications that will guide based on scientific research and past experiences on this subject. Many countries in the world publish their standards and regulations based on these international publications. Adaptive road lighting applications are still being studied. "CEN/TC169/WG12 – Joint Working Group with CEN/TC226 – Road Lighting" started to work in 2020 to contribute to EN 1301 standards [1]. Also, The International Commission on Illumination's (CIE) technical committee of "TC 4-62 Adaptive Road Lighting" works on technical reports [2]. According to CEN/TR 13201-1; the design speed or speed limit of the road, traffic density, whether there is a median that separates the roundtrip lanes on the road, where the traffic is mixed with motor vehicles only or with non-motorized vehicles and pedestrians, junction density, presence of parked vehicles, ambient luminosity and navigational task are considered while selecting the road lighting class [3].

Some parameters like the speed of vehicles, traffic density and ambient luminosity may change in time. So, the adaptive road lighting systems that can change the lighting scheme depending on these parameters are very popular topics nowadays. In CEN/TR 13201-1, adaptive lighting is defined as "temporary controlled changes in luminance or illuminance based on traffic density, time, weather conditions or other parameters".

Static and dynamic methods may be used for adaptive road lighting. Static methods can be described as simple time-based schedule control systems where some future parameters can be predicted from the historical data (like traffic volume, speed or meteorological conditions). In dynamic methods, sensors are used for real-time data and the road is monitored. With the developments in LEDs, sensor technologies, wireless communication and cloud technologies, ARL applications are easier in theory. The most important aspect of ARL should be not to endanger traffic safety while aiming at energy efficiency.

In practice, especially roads with a median separating two directions and poles placed on the median with twin brackets arrangements are analyzed, when both directions are to be adjusted to different lighting levels, a careful design should be done considering the contribution of one side to the other side.

Depending on the luminous intensity distribution of the luminaire, the contribution of one luminaire to the other direction should be simulated, accordingly. As the median width gets shorter, the contribution of the luminaire will increase depending on the 270º plane luminous intensity distribution of the luminaire. Also, if one-sided dimming schemes are of concern, the contribution will decrease proportionally to the dim level. Thus, detailed simulations should be done to calculate the contribution of the other side with different scenarios.

In this study, firstly different luminous intensity distributions are explored using online databases. A sample 2x2 lane M2 lighting class road was selected. For both directions, different couples of lighting classes will be simulated using Dialux lighting simulation software ie. M2-M2, M2-M4, and also M2-10% level for no traffic scenario for one side. 10% luminous flux as the "night" level to be used in the hybrid automation strategy is the 10% of the luminous flux of the distribution in the M2-M2 scenario. Using the M2-M2 scenario as a base, how much the luminaires' luminous output should be increased or dimmed will be calculated and power calculations for different scenarios will be done against the standard operation scenario which is M2-M2 lighting classes for both sides.

II. METHODOLOGY AND CASE STUDY

The sample road selected for the analysis has two lanes going and two lanes return and a twin bracket arrangement on the median (Figure 1). Luminaires are mounted on 2 meters long consoles on 12 meters high poles with 30 meters distance between the poles. The road surface class is taken as R3.

To investigate the effect of luminous intensity distribution, different luminaires are evaluated using Dialux lighting simulation software [4] and an online luminaire database. To differentiate distributions, 270° plane of the distributions are analyzed. Two distributions were selected as given in Figure 2.

As can be seen from the figure, the light distribution in the 270° plane of Distribution 2 is higher than that of Distribution 1. The distributions are imported into Dialux for simulations. Firstly, the median is set to 1 meter and console length to 2 meters resulting in 1.5 meters of overhang. Simulations for two distributions are done for both sides for M2-M2 lighting classes. The luminous flux of the distributions is changed to satisfy the M2 lighting class requirements given in Table 1 as given in CEN/TR 13201-2:2016 "Road Lighting – Part 2: Performance Requirements" [5].

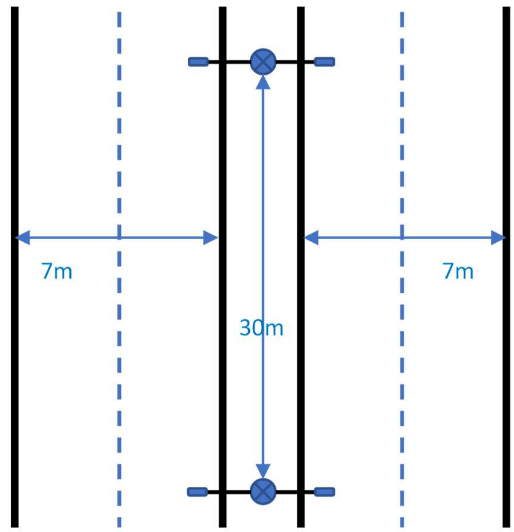

Fig. 1. Sample Road

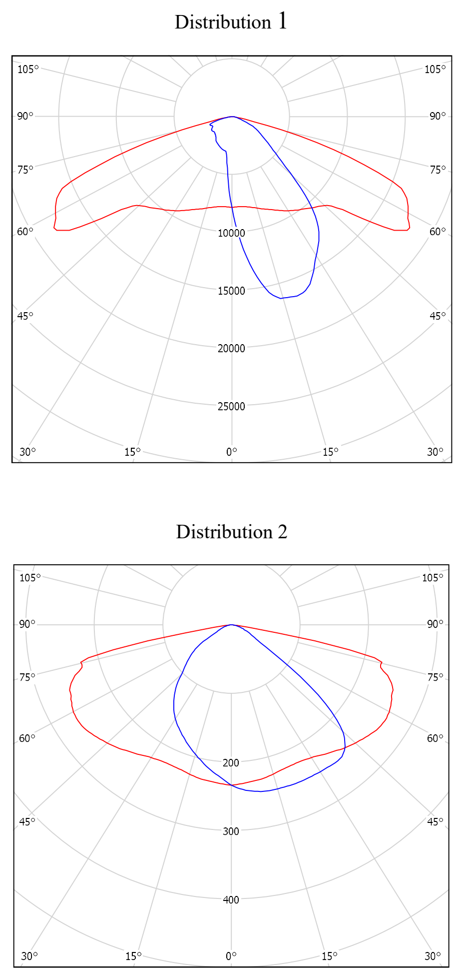

Fig. 2. Selected Distributions

TABLE I. LIGHTING QUALITY CRITERIA FOR M2 ROAD LIGHTING CLASS

L_{ave} (cd/m^2)	U_o	U_l	f_{TI} (%)	R_{EI}
≥ 1,5	≥ 0,40	≥ 0,70	<10	> 0,35

Then by changing the luminous flux of both sides M2-M4 and M2-10% scenarios are satisfied using both distributions. To normalize the power values, it is assumed that both distributions have an efficacy of 125 lm/W and power level changes linearly with luminous flux. After finding minimum luminous flux values for the distributions power values are calculated for considered lighting classes as given in Table 2.

As seen from Table 2 for 1 meter median width Distribution 1 needs 10.9% more power for M2 side whilst Distribution 2 needs a 35% increase in power. For the night scenario Distribution 1 needs 17.4% more power whilst Distribution 2 needs a 37.5% increase in power. The calculations are repeated for 2 meters of median width and are given in Table 3.

TABLE II. CALCULATIONS FOR 1 METER MEDIAN

	Distribution 1			Distribution 2		
	Luminous Flux (lm)	Power (W)	Power Increase for M2 side	Luminous Flux (lm)	Power (W)	Power Increase for M2 side
Direction 1 M2	11500	92.0	-	12180	97.4	-
Direction 2 M2	11500	92.0		12180	97.4	
Direction 1 M2	12750	102.0	10.9%	16443	131.5	35%
Direction 2 M4	4500	36.0		1914	15.3	
Direction 1 M2	13500	108.0	17.4%	16748	134.0	37.5%
Direction 2 10%	1150	9.2		1218	9.7	

TABLE III. CALCULATIONS FOR 2 METER MEDIAN

	Distribution 1			Distribution 2		
	Luminous Flux (lm)	Power (W)	Power Increase for M2 side	Luminous Flux (lm)	Power (W)	Power Increase for M2 side
Direction 1 M2	11500	92.0	-	12615	100.9	-
Direction 2 M2	11500	92.0		12615	100.9	
Direction 1 M2	12500	100.0	8.7%	16443	131.5	30.3%
Direction 2 M4	4750	38.0		2610	20.9	
Direction 1 M2	13000	104.0	13.0%	16965	135.7	34.5%
Direction 2 10%	1150	9.2		1262	10.1	

As seen from Table 3 for 2 meters median width Distribution 1 needs 8.7% and 13% more power for M2-M4 and M2-10% scenario whilst Distribution 2 needs 30.3% and 34.5% increase in power, respectively. The results for 3 meters of the median are given in Table 4.

TABLE IV. CALCULATIONS FOR 3 METER MEDIAN

	Distribution 1			Distribution 2		
	Luminous Flux (lm)	Power (W)	Power Increase for M2 side	Luminous Flux (lm)	Power (W)	Power Increase for M2 side
Direction 1 M2	12000	96.0	-	13050	104.4	-
Direction 2 M2	12000	96.0		13050	104.4	
Direction 1 M2	12300	98.4	2.5%	16313	130.5	25%
Direction 2 M4	5000	40.0		3263	26.1	
Direction 1 M2	13000	104.0	8.3%	16965	135.7	30%
Direction 2 10%	1200	9.6		1305	10.4	

As the width of the median increases, the power difference for M2 is less pronounced since the contribution from the other lane also decreases. For Distribution 1 the power differences are 2.5% and 8.3% whilst they are 25% and 30% for Distribution 2.

III. CONCLUSION

Two different luminous intensity distributions are evaluated for a sample M2 road illuminated from the median with a twin brackets arrangement. The distributions selected as one of them sends more light to the rear while the other sends less to compare their contributions to the other lane. Three different median widths are selected as 1, 2 and 3 meters. The simulations are done with Dialux software. Firstly, the luminous fluxes of the distributions are calculated to satisfy M2 lighting criteria for both lanes. After the simulations are done, one of the lanes' lighting criteria changed to M4 class and the luminous fluxes for the M2-M4 scenario is calculated. Lastly, for the night scenario M2-10% is simulated and Luminous fluxes are calculated. To normalize power levels, it is assumed that the luminous flux and power changes linearly and all the distributions have 125 lm/W efficacy.

For all scenarios, the increase in power for the M2 side is calculated and given in Tables 2, 3 and 4. Especially for 1 meter median width power increase rate in the M2-M4 scenario is calculated as 35% and for M2-10% flux scenario 37.5%, respectively.

To conclude, for static or dynamic adaptive road lighting applications, while designing an installation of luminaires with twin bracket arrangement lighting designs on the median, luminaires with less light in the 270° plane should be chosen as much as possible. If there is more light in the 270° plane, depending on the distribution of the luminaire selected according to the base scenario, a luminaire with 37.5% more power should be selected, which means initial investment costs increases.

REFERENCES

[1] European Committee for Standardization (CEN), www.cencenelec.eu, Accessed: 25.05.2022

[2] International Commission on Illumination (CIE), http:// cie.co.at/, Accsed: 25.05.2022

[3] CEN/TR 13201-1: 2014, Road lighting – Part 1: Guidelines on selection of lighting classes.

[4] Dialux, http://www.dial.de, Accessed 25.05.2022

[5] CEN/TR 13201-2: 2016, Road lighting – Part 2: Performance requirements.

Measurement and Analysis of Luminance Values and Ratios on a Road with an Adaptive Lighting System

Filip Novák, Petr Baxant, Martin Motyčka
Faculty of Electrical Engineering and Communication
Brno University of Technology
Brno, Czech Republic
xnovak1x@vutbr.cz, baxant@vut.cz, motyckam@vut.cz

***Abstract*—Light has an effect not only on the formation of visual perception itself, but also on other biological functions of humans - especially the endocrine system, which in this case mainly includes the pineal gland and the melatonin it produces. This hormone influences not only sleep and the associated processes of biological renewal, but also the secretion of other hormones and thus the human organism. An inappropriately designed lighting system (both in terms of the intensity of the lighting and the spectral composition of the light emitted) can adversely affect the secretion of this hormone, which can then be reflected in poor quality sleep or depression, or even diabetes or certain types of cancer. Moreover, humans are not the only living beings to be affected by disruptive light (and especially its blue component) - the negative effects of this phenomenon have been demonstrated in a wide range of animals, from insects, fish and amphibians to birds and higher mammals. In addition, ALAN (artificial light at night) also affects plant growth, typically affecting growth changes in deciduous trees, for example. For these and other reasons not mentioned here (mainly excessive energy consumption), so-called adaptive or biodynamic lighting systems, i.e., lighting that typically changes its luminous flux, the spectrum of light emitted, and thus the correlated color temperature, or both, with time, have been gaining prominence, especially in recent years. It is also possible to relate the light output of such a lighting system to the detection of the presence of people in the illuminated space. For example, a reduction of the luminous flux by up to 50 % and a shift of the correlated color temperature from 2700 K to 1800 K are typical. The requirements for road lighting are mainly dealt with in the standard ČSN EN 13201. The purpose of the measurements was mainly to compare the individual phases of adaptive (or biodynamic) lighting with each other and with a lighting system based on high pressure sodium lamps (HPS) and LEDs, in terms of luminance distribution and its uniformity on the road surface in the sense of ČSN EN 13201. The measurements were carried out on a less busy two-lane roads, probably class M4, and a luminance analyzer was used. This was followed by the evaluation of the luminance maps and the determination of the luminance values and their uniformities and finally the comparison itself.**

Keywords—luminance, luminance camera, luminance analyzer, ALAN, stray light, obtrusive light, skyglow, biodynamic lighting, adaptive lighting, LED, streetlight

I. Introduction

A. Uniformity

In addition to the illuminance or luminance value, the uniformity of illumination is also a key and evaluated factor of any lighting system. For outdoor lighting systems, this importance is particularly emphasised by the need to provide a background against which objects occurring on the road can be observed [1, 2]. Another, equally important reason for sufficient uniformity is also the desire not to expose the human eye to excessive changes in the luminance perceived by the eye - the visual organ is adapted to a certain level of luminance in each situation, and rapid, exaggerated changes in the luminance of a scene will lead to eye fatigue or the appearance of glare.

In the context of the Czech Republic, the lighting of outdoor roads is dealt with in particular by the standard ČSN EN 13201. Its third part (Road lighting - Part 3: Calculation of performance) defines two variables, referred to as uniformity. The first is Overall uniformity, referred to as U_O. This value is determined as the ratio of the minimum luminance value to its average value, i.e.

$$U_O = \frac{L_{min}}{\bar{L}} \tag{1}$$

The average here means the arithmetic mean. The second quantity is the Longitudinal uniformity with the symbol U_l [3]. This value is determined by measuring the luminance values in the axis of each lane and then calculating the ratio of the minimum luminance value to the maximum value, i.e.

$$U_l = \frac{L_{min,l}}{L_{max,l}} \tag{2}$$

The number and location of measuring points on the road is described in Chapter 7 of the standard. In general, the distance between the points where measurements are taken must not exceed 3 m. The factors that determine the position of the measuring points are in particular the distance between the individual luminaires and the width of the lane [3]. Due to the fact that a luminance analyzer was used for the described measurement, we can choose the distance of the measuring points to be almost infinitely small. The described standard also specifies the position of the observer as 1.5 m above the road surface and 60 m in front of the evaluated section. However, the latter condition was not fully met in this case due to space constraints, so the measurements described are not fully compliant with the standard, even though it allows the use of a luminance analyser for lighting assessment.

B. Lighting classes of road lighting

In order to define the lighting requirements for outdoor roads, it is first necessary to determine the category and class of the road. This is the subject of the second chapter of the aforementioned standard EN 13201 (Road lighting - Part 2: Performance requirements). The first thing to do is to determine which category of road it is. If it is a road for motor vehicles, it is category M. Pedestrian and cyclist roads fall into category P. If the area is assessed as a conflict area, i.e. if there is a crossing of traffic flows or high traffic density

(Commercial avenues, complex intersections, roundabouts or areas with frequent traffic jams), category C is used. Roads or sections of roads that would otherwise fall into category P may also fall into category C if the local situation requires it - typically, for example, underpasses, underpasses or other traffic risk locations. The standard also defines HS, SC and EV categories.

In the following, we will deal only with the description of category M, as all the roads measured here fall into this category. Once the category has been determined, the class of the road must also be determined. The first part of the technical report mentioned above - Road lighting - Part 1: Guidelines on selection of lighting classes - serves as a guide for this classification. In order to determine the class, the road must be evaluated using the defined parameters listed in Table I.

TABLE I. PARAMETERS FOR THE SELECTION OF A LIGHTING CLASS M [5]

Parameter	Options	Weighting value V_W
Design speed	Very high ($v \geq 100$ km/h)	2
	High ($70 < v < 100$ km/h)	1
	Moderate ($40 < v \leq 70$ km/h)	-1
	Low ($v \leq 40$ km/h)	-2
Traffic volume	High	1
	Moderate	0
	Low	-1
Traffic composition	Mixed with high percentage of non-motorized	2
	Mixed	1
	Motorized only	0
Separation of carriageways	No	1
	Yes	0
Junction density	High	1
	Moderate	0
Parked vehicles	Present	1
	Not present	0
Ambient luminance	High	1
	Moderate	0
	Low	-1
Navigational task	Very difficult	2
	Difficult	1
	Easy	0

All V_W parameters are then added together to give the sum of the values - V_{WS}. The communication class is then determined as

$$M\ class = 6 - V_{WS} \quad (3)$$

If the sum of the V_{WS} weights is < 0, $V_{WS} = 0$ is used. If the resulting lighting class number M $\leqslant 0$, the lighting class M1 shall be used.

Once we know the category and class of the road, we can proceed to check the requirements for the minimum values of illuminance, luminance, uniformity, or other parameters required by the technical report. In Table II we find the values of the minimum required luminances and uniformity values for the lighting classes of category M, which are valid for a dry road surface.

This research work has been carried out in the Centre for Research and Utilization of Renewable Energy (CVVOZE). Authors gratefully acknowledge financial support from the Technology Agency of the Czech Republic (project No. SS05010159).

TABLE II. REQUIREMENTS FOR LIGHTING CLASSES M FOR MOTORIZED TRAFFIC [4]

Class	$\bar{L}$ (cd.m^{-2})	U_O (-)	U_l (-)
M1	2,00	0,40	0,70
M2	1,50	0,40	0,70
M3	1,00	0,40	0,60
M4	0,75	0,40	0,60
M5	0,50	0,35	0,40
M6	0,30	0,35	0,40

In the case of a wet road surface, the only requirement is a minimum Overall Uniformity value of 0.15 for all classes. In addition, the standard for motor vehicle roads also specifies a maximum Threshold Increment value and a minimum Edge Illuminance ratio value.

C. Adaptive lighting systems

Adaptive lighting systems (also known as biodynamic lighting systems) are lighting systems that change their spectrum (and consequently their correlated color temperature), luminous flux, or both, over time. The main motivation for this approach is to eliminate the negative effects of artificial lighting, which are mainly caused by inappropriate choice of spectrum, luminous intensity distribution, or time intervals when the respective light source or lighting system will be switched on.

As already mentioned, outdoor lighting has negative effects in addition to the positive effects of increased safety, improved orientation, aesthetic benefits and more. For example, the economic impact of increased electricity consumption in the event of excessive lighting or lighting at inappropriate times, but the negatives do not end there.

Through the intrinsically photosensitive retinal ganglion cells (ipRGCs), located on the retina, the blue light component in particular acts on the secretion of the photopigment melanopsin, which in turn acts mainly on the suprachiasmatic nuclei in the hypothalamus and thus influences the circadian rhythms of the human organism [6]. If these natural cycles are disrupted by artificial lighting, sleep disturbances, seasonal depression, psychological disorders, and some research has even suggested a link to the occurrence of diabetes or certain types of cancer [7].

Disruptive lighting or ALAN can also have negative effects on other living organisms. A significant proportion of these animals studied so far have also been shown to be adversely affected by light of shorter wavelengths [8], demonstrating the advantage of using luminaires with a lower correlated color temperature. Insects, such as moths, are typically attracted to light in the blue part of spectrum, which leads to exhaustion and eventual death when flying chaotically around outdoor sources artificial light [9].

Given that in scotopic vision, human vision is most sensitive to short wavelengths around 500 nm and due to Rayleigh scattering, it is evident that light sources and systems with higher correlated color temperature will have a greater impact on the skyglow in the atmosphere, which among other things makes astronomical observations more difficult [10]. Another factor is that in the case of astronomical observations, the relatively narrow-spectrum emission of discharge light sources could be filtered out by appropriate filters, whereas this is a much greater problem for the much more broad-spectrum LED light sources, if the spectrum of interfering light in the atmosphere allows it at all.

However, these examples of the negative impacts of artificial lighting are only part of the reasons for more environmentally friendly lighting, of which adaptive lighting systems, when configured and set up appropriately, are undoubtedly a representative.

II. Measured lighting systems

All measured roads are located in the area of Brno - Královo Pole. Parameters of the adaptive lighting system, on which a large part of the measurements were carried out, are given in Table III.

TABLE III. Parameters of the Measured Adaptive System

Height of the poles	Pole spacing	Number of masts
5 m	20 m	7
Length of the section	Width of the road	Slope of the road
130 m	10 m (incl. sidewalks)	4°

The luminaires used are from the manufacturer Tungsram, from the SLBT LED series. These Luminaires contain two kinds of LED chips, neutral white LEDs with correlated color temperature of 4000 K and PC Amber LEDs with CCT around 1800 K. The luminaires do not have an integrated real time clock, ethernet connection or any other means of communication, rather it just averages times of last three turn-ons and then switches to the next phase of lighting, therefore the exact switching time varies slightly each day. This deviation is in the range of minutes – the time of the first change was measured between 19:57 and 20:06 on the days the measurement took place. The approximate switching times that have been programmed into the units can be seen in Table IV.

TABLE IV. Switching Schedule of Installed Adaptive Luminaires

4000 K	PC Amber	Time
Φ (lm)	Φ (lm)	
3000	1000	Sunset - 20:00
1500	1500	20:00 - 21:00
0	1500	21:00 - 4:00
1500	1500	4:00 - 5:00
3000	1000	5:00 - Sunrise

The measured spectra for each of the stages can be seen on Figure 1.

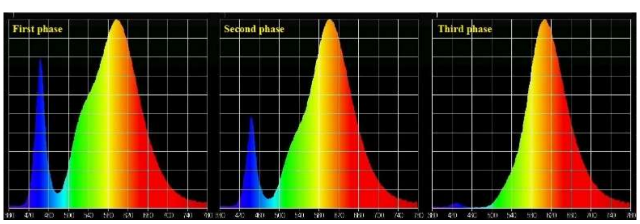

Figure 1. Spectra measured on the adaptive lighting system.

As you can see from Figure 1., the amount of blue light is dropping significantly with time. The CCTs measured for all three phases were 3157 K, 2552 K and 1799 K respectively.

The other three measured lighting systems were equipped with unknown HPS and LED light sources.

III. The measured data

The following data were captured with a luminance analyzer.

Figure 2. Luminance map of a road illuminated by an adaptive lighting system – first stage of switching.

On Figure 2, you can see the illuminated street in false colors – each color represents a certain luminance, as seen on the color palette on the top of the photo. There is a rectangular strip detector placed on the road between two poles of public lighting. We will take a closer look at the columns A and B (second and fifth one), because these represent the center of each traffic lane. If we divide the space in each column in 15 equal parts, we will get the following values of luminance.

TABLE V. Luminance Values During the First Phase

n (-)	L_A (cd.m^{-2})	L_B (cd.m^{-2})
0	2,881	1,327
1	2,472	1,332
2	2,112	1,164
3	1,617	1,073
4	1,527	0,955
5	1,576	0,967
6	1,605	0,972
7	1,696	1,032
8	1,753	0,977
9	1,721	0,967
10	1,804	1,052
11	1,927	1,120
12	2,212	1,254
13	2,495	1,285
14	2,774	1,185

If we then divide the columns into 100 parts each (for a more precise data presentation) and then plot the results, we will get the following graph.

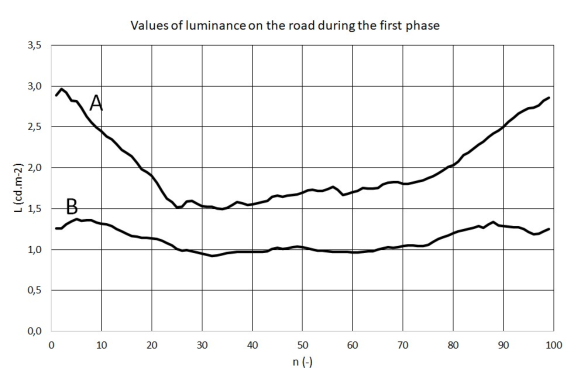

Figure 3. Plotted values of luminance during the first phase

From this data, we can then calculate the average luminance for each traffic lane and find the minimal and maximal value. For lane A, the average value of luminance comes out at 2,00 cd.m^{-2}, the minimum is 1,48 cd.m^{-2} and the maximum is 2,99 cd.m^{-2}. For lane B, these values are 1,11 cd.m^{-2} for the average and 0,92 cd.m^{-2} and 1,38 cd.m^{-2} for the minimum and maximum. Using these values, we can now calculate the overall and longitudinal uniformity:

$$U_{O,A} = \frac{L_{min.A}}{\overline{L}_A} = \frac{1{,}48}{2{,}00} = 0{,}74$$

$$U_{l,A} = \frac{L_{min,l,A}}{L_{max,l,A}} = \frac{1{,}48}{2{,}99} = 0{,}49$$

The same process can then be repeated for lane B:

$$U_{O,B} = \frac{L_{min.A}}{\overline{L}_A} = \frac{0{,}92}{1{,}11} = 0{,}83$$

$$U_{l,B} = \frac{L_{min,l,B}}{L_{max,l,B}} = \frac{0{,}92}{1{,}38} = 0{,}67$$

Now, we can perform the same analysis for the data acquired between 20:00 and 21:00 – for the second stage of switching.

Figure 4. Luminance map of a road illuminated by an adaptive lighting system – second stage of switching.

Then we can again table the acquired data.

TABLE VI. LUMINANCE VALUES DURING THE SECOND PHASE

n (-)	L_A (cd.m^{-2})	L_B (cd.m^{-2})
0	2,236	1,006
1	1,926	1,018
2	1,644	0,905
3	1,267	0,828
4	1,192	0,762
5	1,202	0,767
6	1,237	0,768
7	1,285	0,822
8	1,380	0,785
9	1,362	0,767
10	1,419	0,836
11	1,488	0,862
12	1,680	0,975
13	1,918	1,000
14	2,128	0,906

The data can then be plotted again.

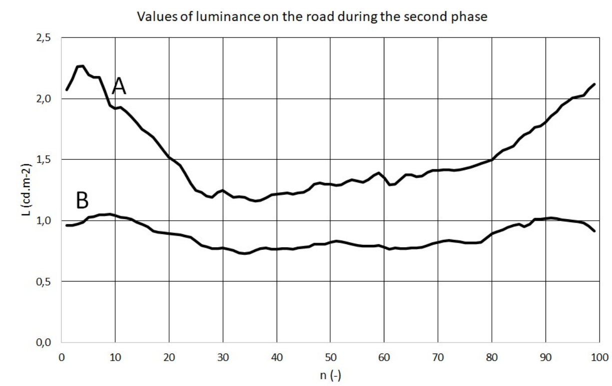

Figure 5. Plotted values of luminance during the second phase

Now, we can again find the average, minimal and maximal value of luminance for both lanes. For lane A, the average luminance value during the second phase is 1,54 cd.m^{-2}, the minimum is 1,16 cd.m^{-2} and the maximum 2,30 cd.m^{-2}. For lane B, these values are 0,87 cd.m^{-2}; 0,73 cd.m^{-2}; 1,07 cd.m^{-2}. Now we can calculate the uniformities:

$$U_{O,A} = \frac{L_{min.A}}{\overline{L}_A} = \frac{1{,}16}{1{,}54} = 0{,}75$$

$$U_{l,A} = \frac{L_{min,l,A}}{L_{max,l,A}} = \frac{1{,}16}{2{,}30} = 0{,}50$$

And for lane B:

$$U_{O,B} = \frac{L_{min.A}}{\overline{L}_A} = \frac{0{,}73}{0{,}87} = 0{,}84$$

$$U_{l,B} = \frac{L_{min,l,B}}{L_{max,l,B}} = \frac{0{,}73}{1{,}07} = 0{,}68$$

The process now can be repeated for the last phase of switching.

Figure 6. Luminance map of a road illuminated by an adaptive lighting system – third stage of switching.

During this phase, only the PC Amber LEDs are active, and the luminous flux of each luminaire is 1500 lm approximately.

We will now table the data in the same manner as before:

TABLE VII. LUMINANCE VALUES DURING THE THIRD PHASE

n (-)	L_A (cd.m^{-2})	L_B (cd.m^{-2})
0	1,145	0,482
1	0,976	0,540
2	0,871	0,482
3	0,727	0,459
4	0,647	0,421
5	0,592	0,418
6	0,629	0,438
7	0,680	0,470
8	0,690	0,460
9	0,712	0,447
10	0,748	0,486
11	0,769	0,471
12	0,830	0,537
13	0,934	0,556
14	1,045	0,533

And the graphical representation of measured data is as follows:

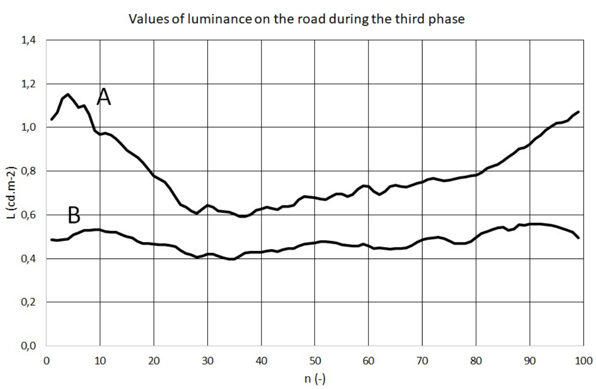

Figure 7. Plotted values of luminance during the third phase

We will now find the average, minimum and maximum value for each lane. For lane A, these values are 0,80 cd.m^{-2}; 0,59 cd.m^{-2}; 1,16 cd.m^{-2}. For lane B, they were measured at 0,48 cd.m^{-2}; 0,39 cd.m^{-2}; 0,56 cd.m^{-2}. This will allow us to calculate the uniformities again.

$$U_{O,A} = \frac{L_{min.A}}{\overline{L}_A} = \frac{0{,}59}{0{,}80} = 0{,}74$$

$$U_{l,A} = \frac{L_{min,l,A}}{L_{max,l,A}} = \frac{0{,}59}{1{,}16} = 0{,}48$$

And for lane B:

$$U_{O,B} = \frac{L_{min.A}}{\overline{L}_A} = \frac{0{,}39}{0{,}48} = 0{,}81$$

$$U_{l,B} = \frac{L_{min,l,B}}{L_{max,l,B}} = \frac{0{,}39}{0{,}56} = 0{,}70$$

Apart from the adaptive lighting system, also a traditional public lighting system were selected for comparison – one based on LED lighting, one based on HPS. These lighting systems were installed on one-way street with similar class (according to ČSN EN 13201), so only one lane was evaluated.

The following lighting system is based on LED lighting.

Figure 8. Luminance map of a road illuminated by a conventional LED lighting system.

The illuminated road was evaluated in a similar manner. The detector was once again placed between two lamp posts to read the luminance values.

TABLE VIII. LUMINANCE VALUES ON A ROAD ILLUMINATED BY CONVENTIONAL LED LUMINAIRES

n (-)	L_A (cd.m^{-2})
0	0,472
1	0,442
2	0,453
3	0,423
4	0,381
5	0,401
6	0,391
7	0,407
8	0,438
9	0,485
10	0,514
11	0,577
12	0,597
13	0,614
14	0,611

The graphical representation of measured data:

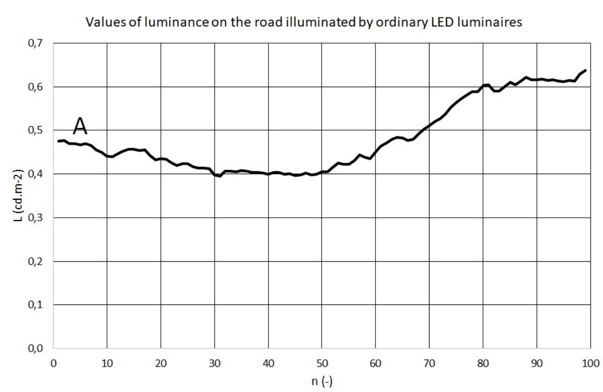

Figure 9. Plotted values of luminance under ordinary LED based system

The average luminance was calculated to be 0,48 cd.m^{-2}, the minimal value was 0,39 cd.m^{-2} and the maximum was found to be 0,64 cd.m^{-2}. Using these values, we can now calculate the uniformities.

$$U_{O,A} = \frac{L_{min.A}}{\overline{L}_A} = \frac{0,39}{0,48} = 0,81$$

$$U_{l,A} = \frac{L_{min,l,A}}{L_{max,l,A}} = \frac{0,39}{0,64} = 0,61$$

At last, a HPS lighting system was evaluated.

Figure 10. Luminance map of a road illuminated by a conventional HPS lighting system.

During evaluation of the measured data, it turned out that there was a complication in a form of significant lens glare that appeared near the center of the road. Due to this it would be impossible to accurately evaluate the uniformities. This road is again one way only, meaning there is only one lane to evaluate. This required a small change of methodology. A detector with a width of five columns was again placed between two lamp posts, but the middle column was not fit for the evaluation due to the problem mentioned. Instead, we opted out to average the data from second and fourth column for every row of the detector. This should give us luminance values very similar to the center of the lane, but unaffected by the lens glare.

TABLE IX. LUMINANCE VALUES ON A ROAD ILLUMINATED BY HPS LIGHTING SYSTEM

n (-)	L_{AB} (cd.m^{-2})
0	0,259
1	0,267
2	0,249
3	0,216
4	0,196
5	0,183
6	0,177
7	0,168
8	0,154
9	0,166
10	0,163
11	0,184
12	0,208
13	0,221
14	0,231

These values are the average of columns A and B, as stated above. We can again plot the results.

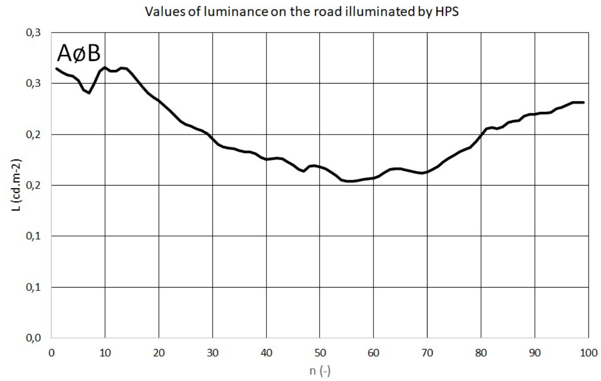

Figure 11. Plotted values of luminance under HPS based system

We will now find the principal three values from the averaged data. The average luminance was found to be 0,20 cd.m^{-2}, the minimum is 0,15 cd.m^{-2} and the maximum 0,27 cd.m^{-2}. Now we can calculate the uniformities.

$$U_{O,AB} = \frac{L_{min.AB}}{\overline{L}_{AB}} = \frac{0,15}{0,20} = 0,75$$

$$U_{l,AB} = \frac{L_{min,l,AB}}{L_{max,l,AB}} = \frac{0,15}{0,27} = 0,56$$

IV. CONCLUSION

The presented data shows that on a road illuminated by an adaptive lighting system both the overall uniformity and longitudinal uniformity changes very little – almost negligibly – during the changing of luminous flux and spectrum. This follows the theoretical assumptions, because even though the source of light inside the luminaire changes, the geometry of it stays the same, so a significant change in the uniformity should not be expected. This would not apply in a place where an adaptive lighting system meets a conventional one, because there could be a significant change in the average luminance of the road, resulting in a disproportionately low uniformity. The overall luminance of the road dropped during the changeover of phases as expected, because the luminous flux dropped as well.

In comparison with conventional lighting systems, it was found that the road in question is overlit, because the standard ČSN EN 13201 demands significantly lower values of luminance on a road such as this. For a significant positive impact on human health and the environment this should not be the case. The uniformities calculated were comparable for the adaptive lighting system and the conventional ones.

It is worth noting that some of the measured roads did not seemingly fulfill the requirements set by the ČSN EN 13201. This could be caused by multiple reasons, such as the effect of nearby objects (for instance, trees on Figure 10.). The methodology for measurement and subsequent evaluation of data was also not completely according to the instructions of the standard aforementioned, but it is expected that this fact should not have a huge impact on the results measured.

REFERENCES

[1] Commission Internationale de l'Eclairage. Lighting of Roads for Motor and Pedestrian Traffic; CIE 2010:115; CIE: Vienna, Austria, 2010

[2] Wänström Lindh, U.; Jägerbrand, A.K. Perceived Lighting Uniformity on Pedestrian Roads: From an Architectural Perspective. Energies 2021, 14, 3647. https:// doi.org/10.3390/en14123647

[3] EN 13201-2:2015 Road lighting – Part 3: Calculation of performance. 2015

[4] EN 13201-2:2015. Road lighting - Part 2: Performance requirements. 2015.

[5] STOCKMAR, Axel. Dynamic Light: Handbook about interpretation of EN 13201 [online]. [cit. 2022-06-30]. ISBN 978-3-947929-07-8. Available from: https://www.interreg-central.eu/Content.Node/Dynamic-Light/04-DL-Handbook-about-interpretation-of-EN-13201.pdf

[6] PROVENCIO, Ignacio a Daniel M. WARTHEN. Melanopsin, the photopigment of intrinsically photosensitive retinal ganglion cells. *Wiley Interdisciplinary Reviews: Membrane Transport and Signaling* [online]. 2012, **1**(2), 228-237 [cit. 2022-03-14]. ISSN 2190460X. Available from: doi:10.1002/wmts.29

[7] TOUITOU, Yvan, Alain REINBERG a David TOUITOU. Association between light at night, melatonin secretion, sleep deprivation, and the internal clock: Health impacts and mechanisms of circadian disruption. *Life Sciences* [online]. 2017, **173**, 94-106 [cit. 2022-03-14]. ISSN 00243205. Available from: doi:10.1016/j.lfs.2017.02.008

[8] Longcore, T, Rodríguez, A, Witherington, B, Penniman, JF, Herf, L, Herf, M. Rapid assessment of lamp spectrum to quantify ecological effects of light at night. *J Exp Zool*. 2018; 329: 511– 521. https://doi.org/10.1002/jez.2184

[9] BREHM, Gunnar, Julia NIERMANN, Luisa Maria JAIMES NINO, David ENSELING, Thomas JÜSTEL, Jan Christoph AXMACHER, Eric WARRANT a Konrad FIEDLER. Moths are strongly attracted to ultraviolet and blue radiation. *Insect Conservation and Diversity* [online]. 2021, **14**(2), 188-198 [cit. 2022-03-14]. ISSN 1752-458X. Available from:10.1111/icad.12476

[10] LUGINBUHL, Christian B., Paul A. BOLEY a Donald R. DAVIS. The impact of light source spectral power distribution on sky glow. *Journal of Quantitative Spectroscopy and Radiative Transfer* [online]. 2014, **139**, 21-26 [cit. 2022-03-14]. ISSN 00224073. Available from: doi:10.1016/j.jqsrt.2013.12.004

Glare Evaluation of Outdoor Lighting Systems using a Luminance Analyser

Jan Škoda
Faculty of Electrical Engineering and Communication
Brno University of Technology
Brno, Czech Republic
skoda@vut.cz

Martin Motyčka
Faculty of Electrical Engineering and Communication
Brno University of Technology
Brno, Czech Republic
motyckam@vut.cz

Filip Novák
Faculty of Electrical Engineering and Communication
Brno University of Technology
Brno, Czech Republic
xnovak1x@vut.cz

Petr Baxant
Faculty of Electrical Engineering and Communication
Brno University of Technology
Brno, Czech Republic
baxant@vut.cz

***Abstract*— This article describes the possibilities of glare evaluation of outdoor lighting systems using a luminance analyser. Determining the level of glare from luminaires intended for road lighting, or from luminaires intended for lighting outdoor work areas is a challenging task, as lighting situations in outdoor environments range at several extremes. In the first case, it is the background (or road) luminance, which in many cases is very low, in contrast to the luminaire luminance, which is high. In addition, outdoor luminaires are often relatively smaller in size and therefore occupy a relatively small spatial angle in the scene, which places great demands on the resolution of the measurement technique. These extremes can therefore very realistically adversely affect the measurement result. The EN 13201 standard for the evaluation of glare from luminaires for road lighting uses the so-called TI threshold increment, which is determined practically by calculation on an ideal road section. In a real situation, the condition is often far from ideal, as real conditions enter into the assessment. Although the above mentioned standard allows for measurements using luminance cameras, the difference between calculation and measurement may in some cases give different results. This paper will present the results of several experiments in which more than 2000 images were taken and these images were then thoroughly analysed and correlated with the theoretical assumption. The results show that the theoretical values are in order of magnitude with the measured ones, but in certain situations these measurements are different due to unexpected situations. The calculation often considers a flat scene with regularly repeating light points, illuminating an ideally flat homogeneous surface. In addition, luminaires that may distort the result, such as luminaires from adjacent lighting systems, billboards, shiny building facades, etc., are often not included in the calculation. This paper is therefore intended to highlight the potential pitfalls of realistic glare assessment using luminance analysers.**

Keywords—glare , luminance analyser, luminance camera

This research work has been carried out in the Centre for Research and Utilization of Renewable Energy (CVVOZE). Authors gratefully acknowledge financial support from the Technology Agency of the Czech Republic (project No. TK03020094).

I. Introduction

The glare from outdoor luminaires can be divided according to its origin into two basic categories, namely:

- Discomfort Glare
- Disability Glare

The difference between these two categories is that the "discomfort" glare is more psychological in nature, causing the driver's attention to be distracted by the glare, which can play a role, for example, in averting the driver's eyes and subsequently overlooking an obstacle on the road. This situation can play a significant role, especially for younger drivers who lack experience and foresight. This type of glare does not cause physical limitation of vision.

In contrast, "disability" glare has a negative consequence associated with an effect in which the visual acuity is already physiologically reduced. It could be said that disability glare is a higher degree than discomfort glare. The reduction in visual acuity is due to light scattering on the structure of the eye, where a strong glare results in a so-called increase in veil luminance, which reduces the contrast between the object to be discriminated and the background, thereby increasing the threshold for discriminating the object. For the assessment of glare from luminaires for road lighting, it is the disability glare that is evaluated, since in the vast majority of cases, due to the dark background, the discomfort glare state almost always transitions to the disability glare state. Numerically, the permissible level of glare is then expressed by the so-called Threshold Increment (TI), which expresses how much the threshold below which the eye is no longer able to distinguish an object.

On the basis of Holladay's experiments from 1927 [1], it was found that the veiling luminance, or the threshold increment, is influenced by the illuminance of the eye, the angle between the direction of sight and the glare source, and the age of the observer. The calculation of the veiling luminance involves luminaires that are located in an area defined by a plane passing through the eye, whose inclination is 20° and whose horizontal projection is transverse to the road (see Figure 1).

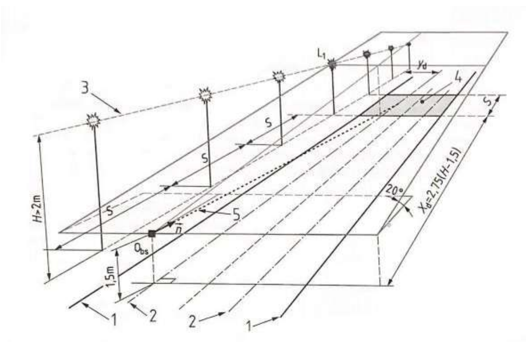

Fig. 1 – Drawing for calculation of veil luminance or glare [3]

Luminaires above this inclined plane are not included in the calculation (these luminaires are usually shielded by the car cab). The veil luminance, denoted Lv, is then calculated according to the empirical equation (1).

$$L_{vi} = k_v \frac{E_i}{\vartheta_i^2} \qquad (\text{cd·m}^{-2}; -, \text{lx}, °) \qquad (1)$$

where E_i is the direct illuminance of eye's observer in perpendicular plane to the direction of view caused by the i-th luminaire

ϑ_i is the angle between the direction of view and the line from the eye to luminaire

k_v is the constant dependent on the age of the observer.

Calculation of the constant k_v is made with equation:

$$k_v = 9{,}86 \left[1 + \left(\frac{V}{66{,}4}\right)^4\right] \qquad (-; \text{year}) \qquad (2)$$

where V is the age of the observer. For the design of lighting systems, the standard age of the observer is taken as 23 years.

Relationship (1), using relationship (2), subsequently changes to the form (3), in which it is also given in the standard EN 13201-3, and which is also recommended by the International Commission on Illumination CIE.

$$L_{vi} = 9{,}86 \frac{E_i}{\vartheta_i^2} \left[1 + \left(\frac{V}{66{,}4}\right)^4\right] \qquad (\text{cd·m}^{-2}; \text{lx}, °, \text{year}) \qquad (3)$$

The validity of this relationship is within the range of angles $1{,}5° < \vartheta_i \leq 60°$.

For installations of luminaires less than 6 m above the ground, situations may arise where the ϑ_i angle drops below 1.5°. Based on this finding, the International Commission on Illumination issued a recommendation in 2002 and updated it in 2019, recommending in CIE140:2019 [2] that a modified relationship be used to calculate the veiling luminance (4).

$$L_{vi} = 5 \left[1 + \left(\frac{A}{62{,}5}\right)^4\right] \frac{E_i}{\vartheta_i^2} + 10 \frac{E_i}{\vartheta_i^3} \qquad (\text{cd·m}^{-2}; \text{lx}, °, \text{year}) \qquad (4)$$

which is valid in the range of angles $0.1° < \vartheta_i \leqslant 1.5°$. However, It should be noted that such lighting systems are rare.

The resulting value of the equivalent veil luminance is then the sum of all partial contributions, as indicated by relation (5)

$$L_v = \sum_{i=1}^{n} L_{vi} \qquad (\text{cd·m}^{-2}; \text{cd·m}^{-2}) \qquad (5)$$

All luminaires which are defined by their respective angles and inclined plane up to a distance of 500 m in each row of luminaires shall be included in the total and the counting shall cease when the contribution of the veil luminance from any one luminaire falls below 2 % of the total veil luminance of the preceding luminaires in that row.

The resulting value of the threshold increment is estimated from the relationship (6)

$$\text{TI} = 65 \frac{L_v}{L_{av}^{0{,}8}} \qquad (\%; \text{cd·m}^{-2}, \text{cd·m}^{-2}) \qquad (6)$$

where L_v the veiling luminance for an observer at a height of 1,5 m above the roadway, looking forward in a direction parallel to the axis of the roadway with his view directed to the centre of the field as shown in Figure 1

L_{av} the initial average roadway luminance (for new luminaires and sources of rated luminous flux), which represents the background luminance in the glare calculation.

The observer shall then be positioned on the axis of each lane and longitudinally positioned in front of the array of control points at the beginning of each evaluation at a distance determined by the relationship 2,75(H 1,5), where H is the height of the luminaire above the ground. The observer shall then move along the axis with a step corresponding to the spacing of the control points in the calculation field. From all the threshold increments of TI, the maximum value is found which is decisive for the control and comparison with the maximum permissible TI value for the specific road class.

The result of the evaluation is therefore the f_{TI} function whose maximum value in the evaluated section must not exceed the specified limit.

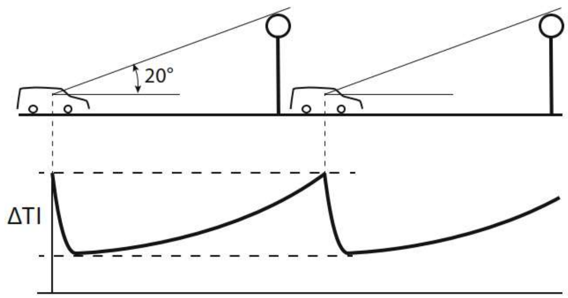

Fig. 2 – Representation of the function f_{TI} [1]

It should also be noted that the validity of this calculation is limited to an average roadway luminance of 0.05 cd·m^{-2} to 5 cd·m^{-2}, which is a realistic value under normal conditions.

II. Measuring of TI

Measuring threshold increment is not as easy as it might seem at first sight. If the measurement is to correspond to the above relationships, we need to correctly measure the direct illuminance to the eye induced from potentially glare-producing luminaires. Measuring this quantity with a conventional luxmeter is virtually impossible, so modern techniques based on luminance analysis from image luminance measurement devices (ILMDs) must be used for this purpose. This device provides information about the luminance in the area of the captured scene, divided into millions of elementary areas, displayed as image pixels [5]. If each point is an image of an elementary luminance area, it is possible to convert luminance to illuminance using the trivial relation (7).

$$L = \frac{d^2\Phi}{d\Omega \cdot dA \cdot cos\vartheta} = \frac{dE}{d\Omega \cdot cos\vartheta} \Rightarrow$$
$$\Rightarrow dE = L \cdot d\Omega \cdot cos\vartheta \qquad (7)$$

(lx; cd·m^{-2}, sr, -)

If the photometric quantities are to be measured correctly, the measuring equipment must be adapted to the spectral sensitivity of a normal photometric observer V (λ), be absolutely calibrated and provide sufficient resolution for correct determination of the solid angle. Focusing on the possible difficulties of the measurement cycle, we encounter possible problems in the evaluation of the individual quantities.

A. Measurement of luminance

In order to calculate the threshold increment, it is necessary to provide measurements of both the ambient luminance, represented by the roadway luminance, and the luminance of the glaring luminaires. Considering that the luminance of a normal roadway is on the order of tenths cd·m-2 and that the luminance of glaring luminaires is on the order of hundreds of thousands to millions, it is necessary to analyse luminance differences of 1:10,000,000, which would require a huge dynamic range at the level of at least a 24 bit A/D converter. Such a dynamic range is not yet achievable with conventional CMOS sensors, so it is necessary to take a so-called HDR image, which is a high dynamic range image composed of several images taken with different exposures. By composing such images, it is therefore possible to cover both very low and very high luminance values. The condition is that the scene does not change during the exposure. Subsequently, algorithms must be applied to combine all the images into one in a suitable way to suppress noise at low luminance and light scattering and sensor oversaturation at high luminance.

B. Measurement of plane and solid angle

The image of the measured scene is transferred to the sensor surface by the optics, which itself defines the area of the solid angle that is captured by the sensor. By dividing the sensor into millions of areas (pixels), the elementary solid angle $d\Omega$ and the angle ϑ of the incident light can be calculated for each pixel area. An important requirement for the correct determination of these quantities is a precise calibration of the image distortion of used lens. Using the principle described in relation (7), it is then possible to determine the direct illuminance of the eye from the individual luminaires, and then, using the relations described above, it is possible to evaluate the threshold increment, assuming knowledge of the road luminance in the defined field, which can also be measured by ILMD.

C. Determination of the maintenace factor

According to EN 13201-3, the threshold increment should be determined for new light sources at the rated luminous flux. If a new lighting system is being built together with the road surface, it can be assumed that the measured TI results are likely to be the highest, since light sources providing the full rated luminous flux will be used and the road surface will still be deep black, i.e. its reflectance will be low and therefore the L_{av} will be very low and the results according to relation (6) will take the maximum values. However, if the system is measured after some time of operation, the maintenance factor should be used to calculate the luminous flux at the beginning of the life of the light source. No prescription exists yet for the surface reflectance over time. It is assumed that TI measurements will be checked when new luminaires are approved, so the need for recalculation using a maintenance factor is not usually considered.

III. Control Measurement

To test the functionality of the above relationships to determine TI, two streets were selected. One with high-pressure sodium lamps and one with LEDs. Both systems were not new, but since this was a comparison of glare levels at a specific time between the two systems, recalculation using a maintenance factor was not considered. Both systems had the same luminaire height above the roadway and approximately the same mast spacing. In terms of subjective evaluation, the sodium lamp lighting system gave a more pleasant non-glaring impression, whereas the LED system was subjectively evaluated as glaring.

Fig. 3 – HDR image of the road illuminated by the high-pressure sodium lamps

The same measurement and evaluation procedure was used for both systems. The measuring apparatus was placed at a height of 1.5 m and set at a distance to cover the luminaire area within the defined area (20° vertically) described in Figure 1.

Subsequently, the area of the luminaires was defined and the limit for masking areas was defined. Anything above 500 cd·m^{-2} was considered as a luminaire region and the solid angle required in relation (7) was also calculated in this region. Since the luminaires reach luminance many times greater than the background luminance, finding the luminaire regions is relatively easy and setting a different limit around 500 cd·m^{-2} does not have a significant effect on the result. If the limit were set very low (on the order of about 5 cd·m^{-2}), the algorithm would risk including the area of diffuse light around the luminaire in the luminaire region. This diffuse light is only visible in the image due to HDR and the non-linear color palette. Some of this scattered light is also produced on the optical path inside the eye, but it is quite difficult to quantify.

On the other hand, more distant luminaires, which already have the light source shielded and whose luminance is lower relative to the observer, are not detected above the selected boundary.

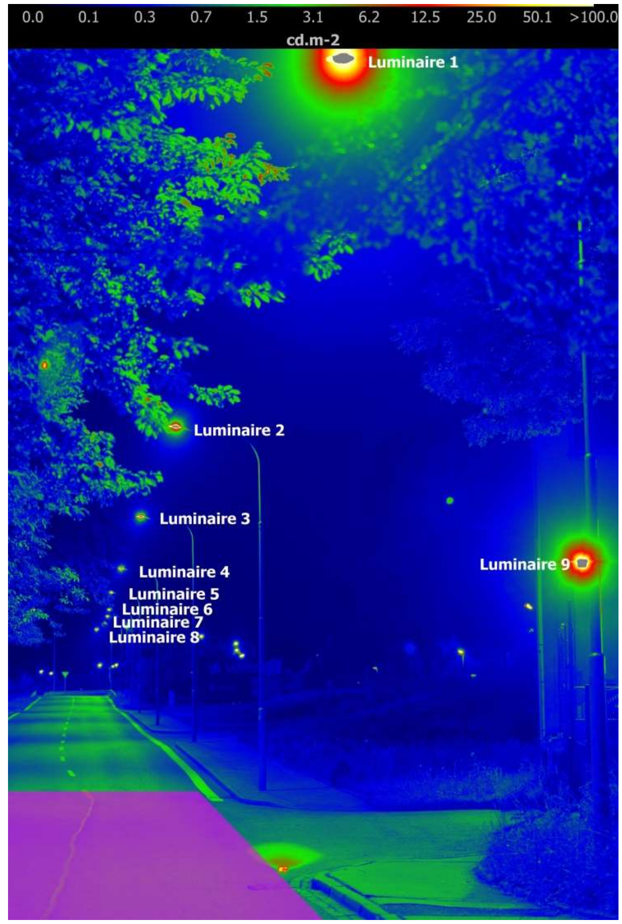

Fig. 4 – HDR image of road illuminated by LED luminaires

The final but crucial question is which luminaires to specifically include in the TI calculation. If the lighting system to be evaluated is one in which only luminaires that were considered in the design of the lighting system are present, the procedure is fairly straightforward. Only luminaires that are within the defined range of angles and contribute more than 2 % to the overall TI value will be included in the measurement (see Chapter I). An example of such a system is shown in Figure 3. The resulting TI for this system is shown in Table 1. For comparison, the illuminance under luminaire 1 was also measured, which was 5.7 lx.

TABLE I. TI FOR HPS LUMINAIRES

Detector	ϑ (°)	E_i (lx)	L_{vi} (cd.m^{-2})	TI increase (%)
Luminaire 1	21.6	1.5554	0.0333	
Luminaire 2	9.7	0.0389	0.0041	7.29
Luminaire 3	5.9	0.0097	0.0028	4.91
Luminaire 4	4.3	0.0092	0.0049	8.55
Luminaire 5	3.4	0.0019	0.0016	2.86
Luminaire 6	2.7	0.0014	0.0019	3.41
Luminaire 7	2.3	0.0014	0.0026	4.51
Luminaire 8	1.9	0.0007	0.0019	3.42
Luminaire 9	1.6	0.0005	0.0018	3.14
Luminaire 10	1.5	0.0004	0.0018	3.19
L_v (cd.m^{-2})			**0.0568**	
L_{av} (cd.m^{-2})			**0.2359**	
TI (%)			**11.7**	

However, if a situation arises where a luminaire that the designer did not count on is in the field of view (Luminaire 9 from the private lighting system in Fig. 4), it should be considered whether to exclude this luminaire from the evaluation. Logically, if I want to evaluate only a lighting system designed to illuminate a specific roadway, I will only include luminaires that are designed for that purpose in the analysis. However, if we want to assess glare at a particular location as a whole, it is appropriate to include all significant luminaires in the analysis.

TABLE II. TI FOR LED LUMINAIRES WITHOUT LUMINAIRE 9

Detector	ϑ (°)	E_i (lx)	L_{vi} (cd.m^{-2})	*TI* increase (%)
Luminaire 1	21.3	5.3207	0.1178	
Luminaire 2	8.9	0.0616	0.0077	4.4%
Luminaire 3	6.0	0.0136	0.0038	2.2%
Luminaire 4	4.3	0.0042	0.0023	1.3%
Luminaire 5	3.5	0.0003	0.0002	0.1%
Luminaire 6	3.0	0.0002	0.0003	0.2%
Luminaire 7	2.8	0.0002	0.0002	0.1%
Luminaire 8	2.4	0.0006	0.0010	0.6%
L_v (cd.m^{-2})			**0.1294**	
L_{av} (cd.m^{-2})			**1.2862**	
***TI* (%)**			**6.87**	

Tab. II shows the case when TI is evaluated only from luminaires 1 - 8 (Fig. 4), while for the actual calculation only luminaires 1 - 3 are considered, because according to the rules for TI calculation the calculation is terminated when the luminaires do not contribute more than 2% to the result.

TABLE III. TI FOR LED LUMINAIRES WITH LUMINAIRE 9

Detector	ϑ (°)	E_i (lx)	L_{vi} (cd.m^{-2})	*TI* increase (%)
Luminaire 1	21.3	5.3207	0.1178	
Luminaire 2	8.9	0.0616	0.0077	4.4%
Luminaire 3	6.0	0.0136	0.0038	2.2%
Luminaire 4	4.3	0.0042	0.0023	1.3%
Luminaire 5	3.5	0.0003	0.0002	0.1%
Luminaire 6	3.0	0.0002	0.0003	0.2%
Luminaire 7	2.8	0.0002	0.0002	0.1%
Luminaire 8	2.4	0.0006	0.0010	0.6%
Luminaire 9	15.5	1.0139	0.0422	24.6%
L_v (cd.m^{-2})			**0.1716**	
L_{av} (cd.m^{-2})			**1.2862**	
***TI* (%)**			**9.12**	

Comparing the results from Tab. II and Tab. III it is clear that luminaire 9 has a very significant effect on the glare level. Subjectively, this luminaire appeared to be very glaring, which is confirmed by the measurement results. For the sake of completeness, it should be added that the illuminance under luminaire 1 was 25.7 lx.

However, the comparison of the results of lighting systems with HPS and LED is very surprising. According to the subjective evaluation it was expected that numerically the LED system would be more glaring, but according to the results it seems that the situation is exactly the opposite.

IV. SEARCHING FOR THE CAUSE OF THE DISCREPANCY BETWEEN THE OBJECTIVE AND SUBJECTIVE EVALUATION

If we compare both cases in terms of TI at the observation point, the system with HPS is worse, but this does not correspond with the subjective evaluation, where it is obvious that the system with LED was more glaring. There may be several reasons for this discrepancy.

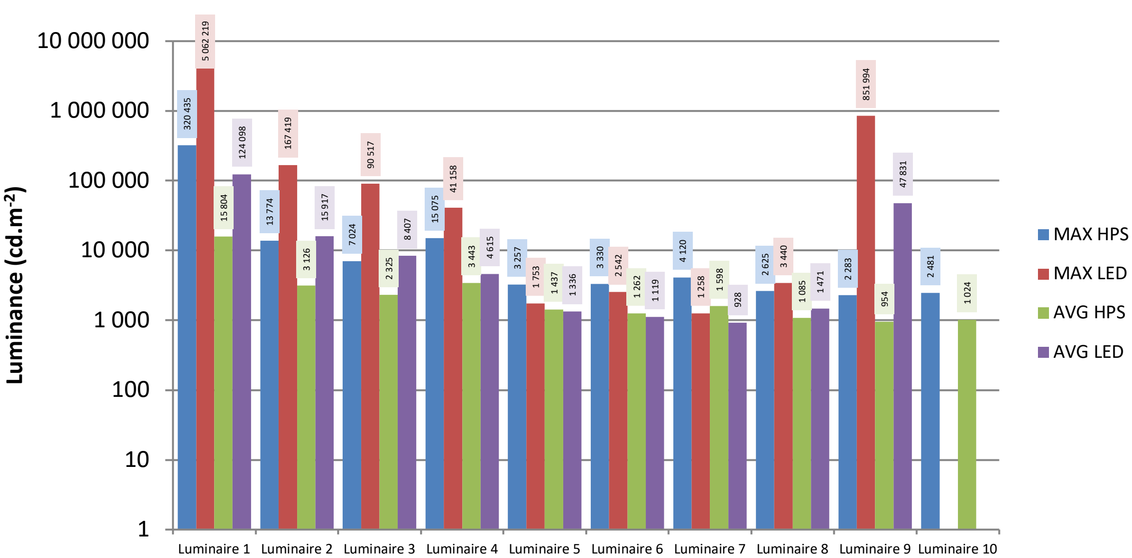

Fig. 5 – Comparison of average and maximum luminance of individual luminaires

A. Absolute value of luminaire luminance and small emitting area

One of the reasons why the LED system appears to be inferior in terms of subjective glare assessment is the fact that these luminaires, or light sources, have many times higher luminance than HPS luminaires, see Fig. 5.

In addition, the light flux from the luminaire is emitted unevenly from a relatively small area, which contributes to a subjectively greater sense of glare.

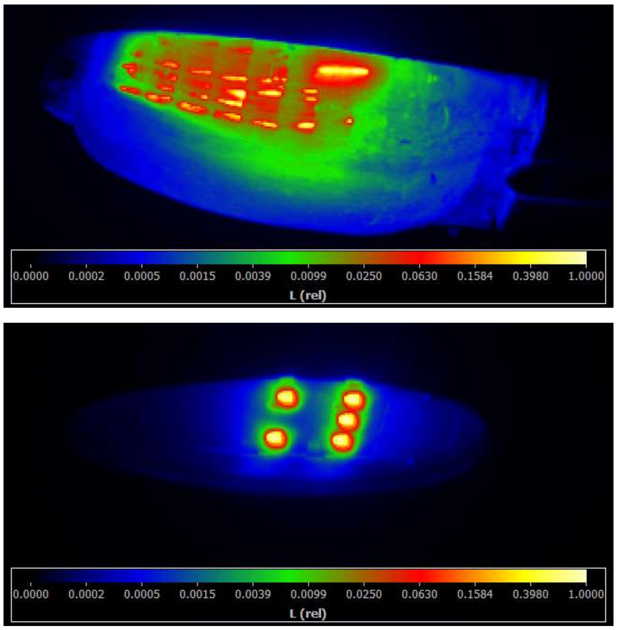

Fig. 6 – Comparison of radiating areas for Luminaire 1 (HPS top image, LED bottom image)

This fact can be seen in Fig. 6, which shows the two luminaires No. 1 for each lighting system. The luminaires are measured at the same angle, from the same distance and the color palette is normalised to the maximum luminance value.

B. Luminance of the road in the defined field

For the purpose of evaluating the threshold increment, the reference value shall be the luminance of the road within the defined roadway field. This has a certain logic because it is assumed that there may be an obstacle on the roadway that can be overlooked due to glare. However, it must also be taken into account that the driver's eyes are not fixed on one place and his eyes are constantly moving and scanning the scene in front of him, and the brain then assembles this information into a coherent picture. This happens in addition to the relatively high speed of the moving driver, and his eyes are forced to constantly adapt to new lighting conditions. The question then arises as to whether it would not be better to set the L_{av} reference luminance value over a wider area to better accommodate the lighting situations to which the driver's vision is exposed. In addition, glare is an important visual stimulus in terms of information and the defence mechanisms of the visual system subconsciously try to avoid direct vision and direct the eye to 'safer' places. The question then is what value to take for the adaptive luminance.

If we evaluate the luminance in the defined field specifically for these two lighting systems, we find that the luminance of the roadway illuminated by LED sources is approximately 5 times greater than the luminance of the roadway illuminated by HPS (this corresponds approximately with the measured illuminance under the luminaires, 25 lx vs. 5 lx) This fact significantly contributes to the reduction of TI and thus to the numerical expression of the level of glare on the roadway. However, the question remains whether the values in this case correspond to reality.

C. Chromaticity of light and other influences

From the point of view of the subjective perception of the pleasantness of light, the substitute chromaticity temperature of the light source will certainly play a role, but this phenomenon is not yet included in the evaluation methodologies.

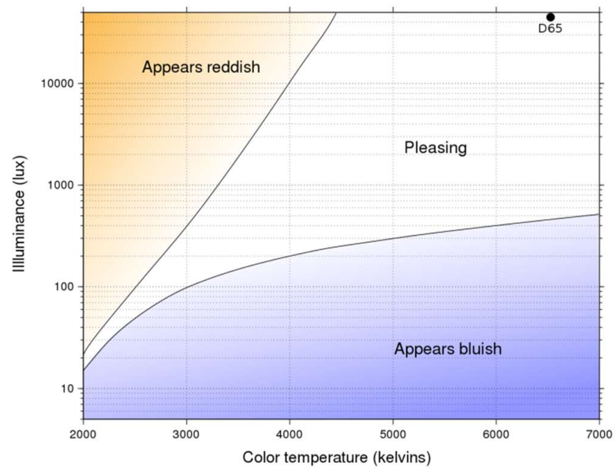

Fig. 7 – Kruithof curve [4]

In general, the pleasantness or unpleasantness of light seems to depend on the balance between illuminance and the correlated color temperature. This fact is expressed by the so-called Kruithof diagram shown in Fig. 7.

By measuring our two lighting systems, it was found that the correlated color temperature was measured with CCT = 2000 K for the HPS and CCT = 3000 K for the LED. This may in some way also affect the perception of the pleasantness or unpleasantness of the light, and hence the level of glare, as 3000 K is perceived as unpleasant at these intensities.

Since the evaluation of sensations can be influenced by factors other than the actual light intensity, it can be assumed that other factors will also influence the phenomenon of perceived light pleasantness or glare. Consideration should be given to the previous state of vision (what the vision has been adapted to), at what time of day the lighting system is evaluated, or at what ambient temperature the subjective evaluation was made.

V. Conclusion

Determining the level of glare on roads using an objective method is a rather complex task. The expression of the threshold increment of TI is currently used to assess glare on roads. The measurement of this quantity is carried out by an indirect method by calculating from the direct illuminance of the eye, the direction of incidence of light from individual luminaires and the background luminance. To determine these quantities, it is convenient to use luminance cameras (luminance analysers), which nowadays provide sufficiently reliable data to evaluate the level of glare. However, it is necessary to take into account that the measured data may differ from the theoretical data, especially since the lighting system is set in a real environment. For example, trees around the luminaires, luminaires from neighbouring systems, unevenness of the road, etc. may affect the measurement results. However, in some cases, it may be encountered that the numerical glare level (threshold increment TI) may not correspond to the subjective perception, especially when the roadway is quite strongly illuminated and the luminous flux from the luminaire is emitted from a relatively small area.

References

[1] BOMMEL, W. Road Lighting – Fundamentals, Technology and Application, Springer Cham Heidelberg, New York Dordrecht London, 2015, ISBN 978-3-319-11465-1

[2] CIE 140:2019. Technical Report, Road Lighting Calculations, 2nd Etition, ISBN 978-3-902842-56-5

[3] ČSN EN 13201-3. Osvětlování pozemních komunikací - Část 3: Výpočet. Brusel: CEN, 2016.

[4] Kruithof curve [online]. [cit. 2022-06-30]. Available at: https://en.wikipedia.org/wiki/Kruithof_curve

[5] List of Applicalion - LumiDISP [online]. [cit. 2022-06-30]. Available at: https://lumidisp.eu/list-of-application/

Effects of Dappled Light Patterns on Preference, Fascination, and Restoration in an Online Study

Kynthia Chamilothori
Human Technology Interaction
School of Innovation Sciences
Eindhoven University of Technology
Eindhoven, the Netherlands
k.chamilothori@tue.nl

Özge Karaman Madan
Human Technology Interaction
School of Innovation Sciences
Eindhoven University of Technology
Eindhoven, the Netherlands
o.karaman.madan@tue.nl

Renate Lemmens
Human Technology Interaction
School of Innovation Sciences
Eindhoven University of Technology
Eindhoven, the Netherlands
r.m.m.lemmens@student.tue.nl

Yvonne de Kort
Human Technology Interaction
School of Innovation Sciences
Eindhoven University of Technology
Eindhoven, the Netherlands
y.a.w.d.kort@tue.nl

***Abstract*— The present work examines, for the first time, the effect of the spatial and temporal composition of dappled light (i.e., sunlight falling through a tree canopy) on preference, fascination, as well as restoration from stress and attention fatigue. In a within-subject online study, 45 participants performed an Auditory Oddball task while one out of three different stimuli was projected to the background of their computer: a grayscale video of dappled light (dynamic dappled light), a single frame from the video (static dappled light), and a grayscale image with the same average luminance as the single frame (control condition). The results of this study show a significant effect of condition on how much participants liked the task background, how fascinating and complex they rated it, and how much it reminded them of nature. Condition did not influence restoration from stress nor improved performance on the Auditory Oddball task. The outcomes of this study show that exposure to both the static and the dynamic dappled light conditions led to a significant increase in reported preference, fascination, association with nature, and perceived complexity compared to the control condition. The dynamic dappled light was also more preferred, more fascinating, and more strongly associated with nature than the static dappled light, showing an effect of temporal variation in the displayed pattern. The results of this study pave the way for further research on identifying the spatial and temporal qualities of daylight that can contribute to the design of indoor environments that support the psychological wellbeing of occupants.**

Keywords—dappled light, preference, naturalness, complexity, stress restoration, attention restoration, fascination

I. INTRODUCTION

Access to daylight and nature is crucial for our wellbeing and has been shown to positively influence our mental and physical health [1]. Humans have a strong preference for daylight compared to electric light, and the perceived naturalness of the light plays an important role for this preference [2]. Moreover, occupants have a higher tolerance for mild degrees of glare from daylight compared to electric lighting [3], [4]. This tolerance and preference for daylight is not well understood [5], and might be attributed to the presence of an accompanying view or to the particular attributes of daylight. Daylight shows unique variations in intensity and in spatial and spectral distribution, which might explain its emotional appeal [6]. Nevertheless, we know little about how this dynamic character of daylight contributes to occupant perception and preference. Understanding and translating these unique attributes of daylight to electric lighting could be a way to create artificially lit environments that are more accepted and more pleasant.

Similar to daylight, humans have a strong preference for natural elements and perceive nature to be aesthetically attractive [7]. Contact with nature has also been consistently shown to contribute to restoration from stress and attention fatigue by positively influencing emotion, cognition, and physiology in laboratory and field studies [8]. Two central theories in environmental psychology, the Stress Reduction Theory (SRT; Ulrich, 1983) and the Attention Restoration Theory (ART; R. Kaplan & Kaplan, 1989; S. Kaplan, 1995, p. 199) aim to explain the mechanism behind these restorative effects by postulating, respectively, that nature induces an immediate positive emotional response (SRT) or that it replenishes our depleted resources for voluntary attention by inducing effortless attention, also called fascination (ART). Apart from explicit access to nature, it has been argued that bringing natural elements and attributes indoors [12] or schematically imitating nature [7] can contribute to the design of built environments that have restorative capabilities. To use these insights in the field of lighting, and particularly in lighting design, we first need to examine which characteristics of daylight could be promising as a source of preference, interest, and association with nature.

Studies in simulated environments show that the spatial composition of building openings and of the resulting sunlight patterns can affect the experience of a space [13]–[18]. Irregularity in the façade geometry and the resulting light pattern has been shown to render the same space more interesting, pleasant, and exciting [13], and decrease the participants' heart rate, although this physiological effect was not replicated in a follow up study [14]. The degree to which the light composition resembles nature seems to also be important and might explain the high preference towards certain façade and sunlight patterns [14]. In a similar vein, Abboushi et al. [18] found that light patterns with a medium fractal complexity, which is prevalent in nature, led to higher visual interest towards visualizations of an indoor sunlit space projected on a wall. On the other hand, contrary to these findings, studies in real environments where the same patterns were applied to the glazing of offices using black film showed no effect of façade pattern on visual interest when workers were preoccupied with performing typical office work, and workers were more satisfied with the outside view in a clear glazing condition [19]. These results show that it is necessary to examine further the effect of light patterns that resemble nature on human experience when one's attention is focused on a particular task. In addition, separating the light pattern from the façade geometry would allow us to disentangle the two factors and remove the potentially confounding effects of obstructing the outside view.

Sunlight filtered through a tree canopy, called dappled light, has been argued to be a source of pleasure for humans [20], and is expected to be strongly associated with nature. Similarly, "the motion of the leaves in the breeze" has been suggested as an element that induces fascination, holding our attention effortlessly and giving an opportunity for our minds to wander [11], and is thus promising as a source of stress restoration. To the authors' knowledge, no previous research has been conducted on the effects of dappled light or its temporal dynamics on human experience. The present study aims to examine, for the first time, how exposure to static and dynamic dappled light patterns influences preference, fascination, subjective stress restoration, and attentional performance.

This article presents the outcomes of an online study where participants performed a cognitive task while their computer screen showed either a control condition, a static image of dappled light, or a video of dappled light as the task background. By comparing these three conditions, the present study examines the following research question:

1. What is the influence of static and dynamic dappled light patterns on preference, fascination, stress restoration, and attentional performance?

In addition, we aim to better understand the mechanism behind human responses to dappled light, and particularly to dynamic dappled light conditions. As a result, we also examine effects of the presented stimuli on perceived complexity and perceived associations with nature:

2. What is the influence of static and dynamic dappled light patterns on perceived complexity and perceived association with nature?

II. METHOD

A. Experimental Design

The study followed a within-subjects design, with the task background as the within-subjects factor with three conditions: a grayscale image (control), an image of dappled light (static dappled light pattern) and a video of dappled light (dynamic dappled light pattern), shown in Fig. 1b-d. These conditions were shown to the participants in random order.

B. Participants

The sample consisted of 45 participants (21 male, 24 female) aged between 18 and 40 years (M = 25.3 years, SD = 5.11 years). Participants were recruited using the online participant database Prolific (www.prolific.co). Prolific allows for screening participants according to certain criteria of choice. The eligibility criteria to participate in the study were fluency in English, normal or corrected-to-normal vision, age between 18 and 40 years old (to decrease the occurrence of presbyopia), and absence of hearing difficulties given the use of an auditory task. Participants were also required to conduct the study on a computer (e.g., not on a phone or tablet); 11 participants reported using a desktop and 35 participants reported using a laptop computer.

C. Equipment, Stimuli, and Stressor Task

The video of dappled light consists of a continuous recording of sunlight falling through leaves on a white background (see Table I, a). The material was recorded using a tripod and a Nikon camera (Nikon Coolpix P510; Fig. 1a) with a resolution of 1920 by 1080 pixels and a frame rate of 30 frames per second. The resulting recording was edited with VideoPad Video Editor by converting the video to grayscale, increasing the contrast so that the lit parts of the video became white (Table I, b) and cropping the frames to 1440 by 810 pixels to remove reflections at the top and left of the image (Table I, c). A single frame was extracted to be used as the static dappled light condition (Table I, c). Last, the control condition was created using the average luma value [21] of the static dappled light image (Table I, d), calculated in MATLAB 2020b.

TABLE I. GENERATION OF EXPERIMENTAL STIMULI

a. Frame from original video.	
b. Frame from edited video (grayscale, high contrast)	
c. Frame from the edited and cropped video (static dappled light pattern)	
d. Grayscale image with the mean luma value of the static dappled light pattern	

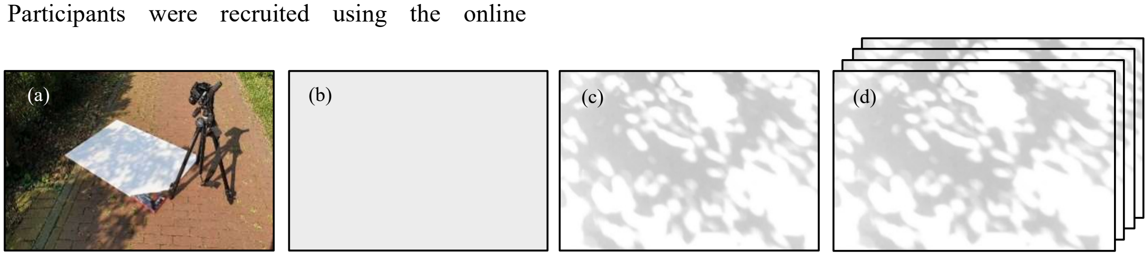

Fig. 1. Illustration of the video recording setup (a), and of the control (b), static dappled light pattern (c), and dynamic dappled light pattern (d) within-subjects stimuli. The dappled light video can be found here. Note that the stimulus appeared in full screen without a black border during the auditory task.

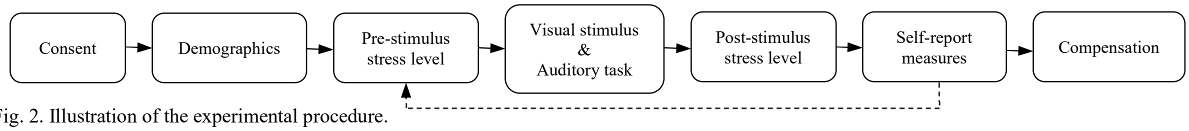

Fig. 2. Illustration of the experimental procedure.

An Auditory Oddball Task from Millisecond Software, based on Williams and colleagues [22], was used as a stress and attention fatigue induction task. This is a task which involves vigilance behavior, i.e., focusing one's attention on detecting small changes in the environment during a certain time period [23]. In this task, participants heard two different tones (176 instances of 500 Hz and 24 instances of 1000 Hz) in random order and were instructed to press a key when they heard the high tone (500 Hz, baseline tone; 'Go' trial) and to not do anything when they heard the low tone (1000 Hz, oddball tone; 'No-go' trial). The task consisted of 200 trials and had a duration of 3 minutes and 20 seconds. The stimuli were presented as a full screen background during the task and thus had the same duration as the task.

D. Measures

In addition to performance on the Oddball task, assessed as mean reaction time to 'Go' trials (mean latency) and accuracy (hit rate), we probed multiple variables through self-report. Table II presents an overview of the questionnaire items used in this study. Participants were asked to rate their perceived stress level before and after the auditory task. In addition, they were asked to evaluate their preference and fascination towards the background during the task. Perceived fascination was measured with the three items of the Fascination factor from the shortened version of the Perceived Restorativeness Scale PRS-11 [24]. The PRS-11 items were modified slightly so that the subject of the question was the background of the task, rather than the environment (see Table II). The Cronbach's alpha for the three items of perceived fascination was 0.87, showing high internal consistency. Participants were also asked to evaluate the characteristics of the task background, and in particular the complexity of the background and the degree to which they associated it with nature.

TABLE II. QUESTIONNAIRE ITEMS

Attribute	**Questionnaire item (scale from 0 "Not at all" to 10 "Very much")**
Preference	I liked the background of the screen during the task.
Fascination (mean of three items)	The background of the screen during the task had fascinating qualities.
	During the task, my attention was drawn to many interesting things.
	The background of the screen during the task was boring. (reversed item)
Association with nature	The background of the screen reminded me of nature.
Complexity	The background of the screen during the task was complex.
Perceived stress	How much stress do you experience at this moment?

All questionnaire items used a 11-point rating scale ranging from 0 ("Not at all") to 10 ("Very much"). The order of the questionnaire items was not randomized, but questions appeared separately depending on their content. Perceived stress, affective responses towards the task background (e.g., preference and fascination) and task background characteristics (e.g., complexity and association with nature) were presented in three different parts of the questionnaire, shown separately. Lastly, participants were asked demographic questions such as their age, gender, country of residence, and screen resolution.

E. Procedure

This study was conducted online using the platform Inquisit 6 Web. Before conducting the experiment, each participant was asked to download the Inquisit app, which could be deleted after participation in the study. During the experiment, the participant's computer would only show the Inquisit app in full screen, and blocked access to other applications.

A schematic overview of the experimental procedure is shown in Fig. 2. The study was conducted in experimental sessions of around 25 minutes. Each participant signed an informed consent form before starting the study. After providing consent, the participant were asked to answer demographic questions, and then performed fifteen test rounds of the Auditory Oddball task to familiarize themselves with it. After this, the participant was asked to provide their current stress level. In the next step, the participant performed the Auditory Oddball task while being exposed to one of the three stimuli, projected as the background of their screen. During the task, the stimulus was covering the full screen of the participants' computer, and they were instructed to pay attention to the screen.

After completing the Auditory Oddball task and the simultaneous exposure to the presented stimulus, the participant was asked to provide answers to several questionnaire items (shown in Table II), the first of which was to rate their stress level at that moment. All questions appeared once for each of the three within-subjects conditions, except for the stress level measurement which was measured before and after the simultaneous exposure to the auditory task and the visual stimuli. The order of the three conditions was randomized. After completing the study, the participant was thanked and compensated for their participation with £3.13. This experimental study was approved by the Human Technology Interaction Ethical Review Board and complied with the tenets of the Declaration of Helsinki.

III. RESULTS

Fig. 3 presents the distribution of ratings for preference, fascination, association with nature, and complexity per stimulus. In each boxplot of Fig. 3, the middle line indicates the median, and the edges of the box show the 25th (top edge) and 75th (bottom edge) percentiles, respectively. The same figure shows the pairs of stimuli with significant differences between them according to the pairwise comparisons of the three conditions.

A one-way Friedman's ANOVA showed a statistically significant effect of condition on preference ($\chi^2(2) = 28.65$, $p < 0.0001$). Post-hoc pairwise comparisons with a Wilcoxon Signed-Ranks Matched-Pairs test showed that the dynamic dappled light condition was preferred more than both the control ($W = 75.5$, $p < 0.0001$, $r = 0.69$) and the static dappled

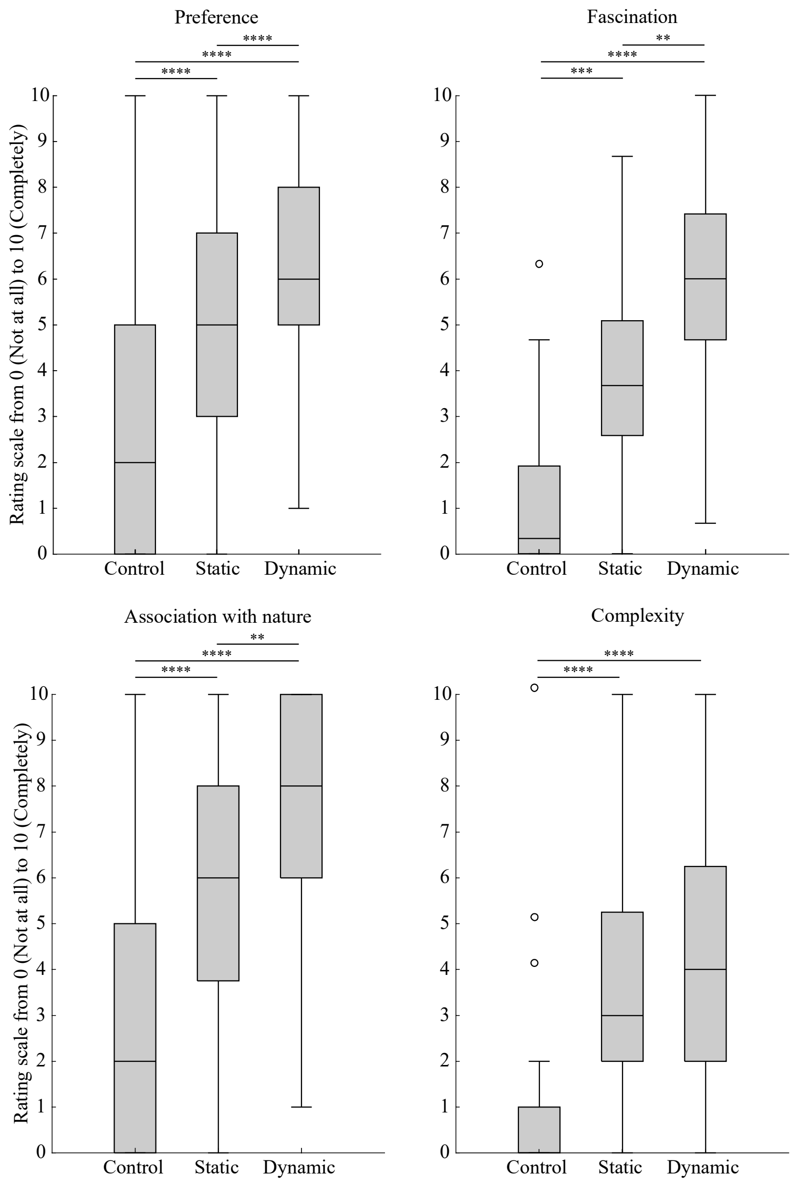

Fig. 3 Boxplots showing the distribution of responses and pairwise comparison outcomes for ratings of preference, fascination, association with nature, and complexity across three within-subjects conditions: control, static dappled light (static), and dynamic dappled light (dynamic). Note that fascination represents the mean of three items. Significance levels are marked as follows: ** = $p < 0.01$, *** = $p < 0.001$, **** = $p < 0.0001$.

light condition (W = 97.5, $p < 0.01$, r = 0.49). Similarly, the static dappled light condition was preferred over the control condition (W = 157.5, $p < 0.001$, r = 0.51).

Results showed that condition also significantly influenced ratings of fascination ($\chi^2(2) = 65.84$, $p < 0.0001$). Follow-up paired comparisons showed that the dynamic dappled light condition was rated as more fascinating than the control (W = 0, $p < 0.0001$, r = 0.87) and the static dappled light condition (W = 52.5, $p < 0.0001$, r = 0.74). As was the case for preference, the static condition was rated as more fascinating than the control (W = 63, $p < 0.0001$, r = 0.74).

Similar results were found for the association with nature, with a main effect of condition on the degree to which the presented stimulus reminded the participants of nature ($\chi^2(2) = 46.5$, $p < 0.0001$). The dynamic dappled light condition was associated more strongly with nature than both the control (W = 50, $p < 0.0001$, r = 0.75) and the static dappled light condition (W = 125, $p < 0.01$, r = 0.49). The static dappled light condition was more strongly associated with nature than the control condition (W = 71.5, $p < 0.0001$, r = 0.70).

The presented condition also influenced ratings of complexity ($\chi^2(2) = 52.14$, $p < 0.0001$). Paired comparisons showed that both the static (W = 35, $p < 0.0001$, r = 0.75) and the dynamic dappled light condition (W = 22, $p < 0.0001$, r = 0.77) were rated as more complex than the control condition. However, the static and dynamic dappled light conditions did not differ in perceived complexity (W = 171.5, $p = 0.08$, r = 0.26).

Fig. 4 shows the distribution of reported stress restoration, defined as the difference when subtracting the ratings of perceived stress after the task from the ratings before the task, per condition. A one-way Friedman's ANOVA showed no significant effect of condition on reported stress restoration ($\chi^2(2) = 0.26$, $p = 0.88$).

Attentional performance was also not influenced by the presented task background. One-way Friedman's ANOVA tests showed no significant effect of condition on either mean latency in 'Go' trials ($\chi^2(2) = 1.20, p = 0.55$) nor the proportion of correct responses ($\chi^2(2) = 0.63, p = 0.73$).

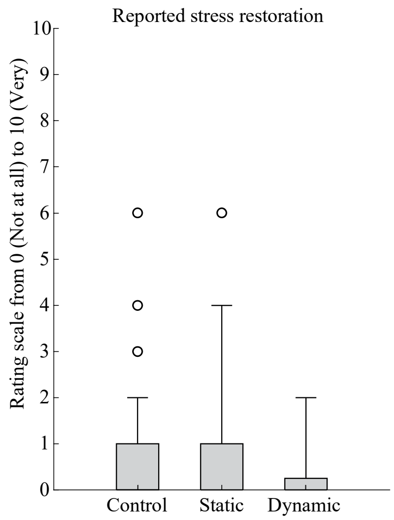

Fig. 4. Boxplots showing the distribution of reported stress restoration, calculated as the difference between ratings of stress before and after the stressor, across the within-subject conditions of control, static dappled light pattern (static), and dynamic dappled light pattern (dynamic).

IV. DISCUSSION AND CONCLUSION

A. Overview of Main Findings

The present study investigated, for the first time, preference, fascination, and restoration of attention and perceived stress induced by dappled light patterns in an online experiment. Participants were exposed to three grayscale stimuli, each displayed in full screen on their computer while they were performing an Auditory Oddball task: a control image, a static image of dappled light, and a video of dynamic dappled light. In addition to the aforementioned effects on preference, fascination, and restoration, we also examined the influence of the presented stimuli on ratings of perceived complexity and association with nature.

Findings showed a significant effect of condition on preference, fascination, complexity, and association with nature, but no significant effect on reported stress restoration or attention performance. However, performance on the task was also not hindered by the visual stimuli that were presented in parallel. Based on the effect size thresholds by Ferguson [25], results showed that exposure to the dynamic dappled light condition led to a moderate-to-strong increase in how much participants liked the background of the screen compared to the control condition, and a small-to-moderate increase compared to the static dappled light condition. Participants rated the dynamic dappled light condition as more fascinating than the control (strong effect) and the static dappled light condition (moderate-to-strong effect). The static dappled light condition was also more preferred (moderate effect) and rated as more fascinating (moderate-to-strong effect) than the control condition.

Regarding the characteristics of the stimuli, as expected, both the static and the dynamic dappled light condition led to higher ratings of association with nature and to higher ratings of complexity compared to the control condition (moderate-to-strong effects). The dynamic dappled light reminded participants of nature more than the static dappled light (small-to-moderate effect), showing that the temporal variation in the dappled light distribution influenced the degree of association with nature. Contrary to this finding, the static and dynamic dappled light conditions did not differ in perceived complexity (small non-significant effect), showing that the dappled light pattern that was changing over time was not perceived as more complex than the static dappled light pattern.

Contrary to previous research that employed stimuli with light patterns resulting from façade openings [13]–[18], the present study used recordings of dappled light found in nature in order to create visual stimuli that resemble the natural patterns as closely as possible. The experimental findings show that changing the background of the screen from a light gray image to either a static image or a video of a dappled light pattern can lead to a substantial increase in how much participants like the background ($M_{control} = 2$, $M_{static} = 5$, $M_{dynamic} = 6$), how fascinating they find it ($M_{control} = 0.33$, $M_{static} = 3.5$, $M_{dynamic} = 6$), and how much it reminds them of nature ($M_{control} = 2$, $M_{static} = 6$, $M_{dynamic} = 8$). While further research is necessary to test these effects for actual lighting conditions in a room, rather than stimuli presented on a computer screen, the outcomes of the present study are very promising for the use of dappled light as a means to induce positive responses to occupants.

To our knowledge, the present study is the first to examine restoration relevant responses to the dynamic element of simulated daylight and shadows found in nature. The significant differences between the static and dynamic dappled light conditions show that the dynamic behavior of recorded dappled light leads to higher preference, fascination, and association with nature, as only the temporal variability of the pattern was manipulated between these two conditions. The outcomes of this study show that movement in light patterns is a promising area for future research, and can elicit positive responses, at least in the context of the present work.

B. Limitations and Future Research

Although the present findings are an important first step for future research using light distributions found in nature, they are limited in their generalizability. The employed conditions were visual stimuli displayed on the participants' computer screen, rather than actual, more immersive lighting conditions. Ongoing research by the authors examines occupant responses to projected dappled light indoors, and will examine whether the current findings are replicated in real conditions and for longer exposure times. Nevertheless, the present findings showed that significant effects occur even when using dappled light images and videos as a screen background, and are thus promising for future applications, either screen-based or in physical spaces.

Moreover, the static and dappled light stimuli used in the present study were generated from a single recording of dappled light in real conditions. In this particular recording, there is little wind, and, as a result, little variation in the light pattern over time. Future research could employ multiple stimuli with varying spatial and temporal characteristics in order to differentiate these two effects further and perhaps also assess the boundaries of complexity that could be introduced without inducing negative distraction.

As the study was conducted online, screen characteristics may have differed between participants and confounded the outcomes. Even though participants were asked to report their screen resolution (which is not reported here for brevity), almost one fourth of them were unable to do so, and present analyses did not account for potential variations in this screen attribute. In addition to resolution, screen attributes such as the gamma response curve of the display or its maximum luminance were not controlled and could have confounded the current findings. The use of an online protocol also means that there was no experimental control in the participants' surroundings and options to induce emotional stress and cognitive fatigue were limited. This limitation also influenced the effectiveness of the stressor task and hence decreased the potential for restorative effects to be found.

Last, participants performed the Auditory Oddball task (stressor) while being simultaneously exposed to the stimulus shown on their screen, rather than them being presented sequentially as is more common in restoration research. This protocol was chosen to emulate realistic conditions (such as exposure to dappled light when one is conducting office work), but does not allow to differentiate the effect of the task from the effect of the exposure to the light stimulus, which could have reduced the effectiveness of the task as stressor. As a result, future research is encouraged to induce a higher level of attention fatigue or emotional stress.

C. Conclusion

This study examined human responses towards static and dynamic dappled light stimuli in an online experiment with 45 participants. Participants were exposed to a control condition, a grayscale image of dappled light (static condition), and a grayscale video of dappled light (dynamic condition) in a within-subjects design. Stimuli were presented as the screen background while participants performed an Auditory Oddball task. Attentional performance and self-report ratings regarding momentary stress before and after the stimulus exposure, preference, fascination, association with nature, and perceived complexity were measured for each stimulus.

Findings showed that the presented condition influenced ratings of preference, fascination, association with nature, and perceived complexity, but did not result in restoration of perceived stress nor improved objective performance. On the bright side, the presented condition also did not induce negative effects or distract participants from the attention task. The outcomes of this study show that both the static and the dynamic dappled light conditions led to higher ratings of how much participants liked the task background, how fascinating they found it, and how much it reminded them of nature compared to the control condition. In addition, the dynamic dappled light condition led to higher ratings on these attributes than the static dappled light condition, showing that the temporal variation of the presented stimulus had a significant positive influence and confirming the suggested emotional appeal of the temporal variability of daylight.

By examining, for the first time, the effect of dappled light characteristics on human experience, the results of this work aim to pave the way for the design of lit environments with fascinating qualities that contribute to occupant wellbeing.

REFERENCES

[1] F. Beute and Y. A. W. de Kort, "Salutogenic Effects of the Environment: Review of Health Protective Effects of Nature and Daylight: Health Protective Effects of Nature and Daylight," *Appl. Psychol. Health Well-Being*, vol. 6, no. 1, pp. 67–95, Mar. 2014.

[2] A. Haans, "The natural preference in people's appraisal of light," *J. Environ. Psychol.*, vol. 39, pp. 51–61, Sep. 2014.

[3] P. Chauvel, J. Collins, R. Dogniaux, and J. Longmore, "Glare from windows: current views of the problem," *Light. Res. Technol.*, vol. 14, no. 1, pp. 31–46, 1982.

[4] R. G. Hopkinson, "Glare from daylighting in buildings," *Appl. Ergon.*, vol. 3, no. 4, pp. 206–215, Dec. 1972.

[5] M. Knoop *et al.*, "Daylight: What makes the difference?," *Light. Res. Technol.*, vol. 52, no. 3, pp. 423–442, May 2020.

[6] K. W. Houser, "Cloudy with a Chance of Sunbeams," *LEUKOS*, vol. 14, no. 3, pp. 107–110, Jul. 2018.

[7] Y. Joye, "Architectural Lessons from Environmental Psychology: The Case of Biophilic Architecture," *Rev. Gen. Psychol.*, vol. 11, no. 4, pp. 305–328, Dec. 2007.

[8] T. Hartig, R. Mitchell, S. de Vries, and H. Frumkin, "Nature and Health," *Annu. Rev. Public Health*, vol. 35, no. 1, pp. 207–228, Mar. 2014.

[9] R. S. Ulrich, "Aesthetic and Affective Response to Natural Environment," in *Behavior and the Natural Environment*, Springer, Boston, MA, 1983, pp. 85–125.

[10] R. Kaplan and S. Kaplan, *The Experience of Nature: A Psychological Perspective*. Cambridge University Press, 1989.

[11] S. Kaplan, "The restorative benefits of nature: Toward an integrative framework," *J. Environ. Psychol.*, vol. 15, no. 3, pp. 169–182, 1995.

[12] S. R. Kellert, J. H. Heerwagen, and M. L. Mador, *Biophilic Design : The Theory, Science, and Practice of Bringing Buildings to Life*. New Jersey: John Wiley & Sons, Inc., 2008.

[13] K. Chamilothori, G. Chinazzo, J. Rodrigues, E. S. Dan-Glauser, J. Wienold, and M. Andersen, "Subjective and physiological responses to façade and sunlight pattern geometry in virtual reality," *Build. Environ.*, vol. 150, pp. 144–155, Mar. 2019.

[14] K. Chamilothori, J. Wienold, C. Moscoso, B. Matusiak, and M. Andersen, "Subjective and physiological responses towards daylit spaces with contemporary façade patterns in virtual reality: Influence of sky type, space function, and latitude," *J. Environ. Psychol.*, vol. 82, p. 101839, Aug. 2022.

[15] S. F. Rockcastle, M. L. Amundadottir, and M. Andersen, "Contrast measures for predicting perceptual effects of daylight in architectural renderings," *Light. Res. Technol.*, vol. 49, no. 7, pp. 882–903, Apr. 2017.

[16] K. Chamilothori, J. Wienold, C. Moscoso, B. Matusiak, and M. Andersen, "Regional Differences in the Perception of Daylit Scenes across Europe Using Virtual Reality. Part II: Effects of Façade and Daylight Pattern Geometry," *LEUKOS*, vol. 18, no. 3, pp. 316–340, Jul. 2022.

[17] S. F. Rockcastle, K. Chamilothori, and M. Andersen, "Using Virtual Reality to Measure Daylight-Driven Interest in Rendered Architectural Scenes," presented at the Conference of International Building Performance Simulation Association, San Francisco, CA, USA, Aug. 2017.

[18] B. Abboushi, I. Elzeyadi, R. Taylor, and M. Sereno, "Fractals in architecture: The visual interest, preference, and mood response to projected fractal light patterns in interior spaces," *J. Environ. Psychol.*, vol. 61, pp. 57–70, Feb. 2019.

[19] B. Abboushi, I. Elzeyadi, K. Van Den Wymelenberg, R. Taylor, M. Sereno, and G. Jacobsen, "Assessing the Visual Comfort, Visual Interest of Sunlight Patterns, and View Quality under Different Window Conditions in an Open-Plan Office," *LEUKOS*, vol. 17, no. 4, pp. 321–337, 2021.

[20] S. Augustin, N. Frankel, and C. Coleman, *Place advantage: Applied psychology for interior architecture*. John Wiley & Sons, 2009.

[21] S. Bezryadin, P. Bourov, and D. Ilinih, "Brightness calculation in digital image processing," in *International symposium on technologies for digital photo fulfillment*, 2007, vol. 2007, no. 1, pp. 10–15.

[22] L. Williams, E. Simms, C. Clark, R. Paul, D. Rowe, and E. Gordon, "The test-retest reliability of a standardized neurocognitive and neurophysiological test battery:'neuromarker,'" *Int. J. Neurosci.*, vol. 115, no. 12, pp. 1605–1630, 2005.

[23] T. Paus *et al.*, "Time-related changes in neural systems underlying attention and arousal during the performance of an auditory vigilance task," *J. Cogn. Neurosci.*, vol. 9, no. 3, pp. 392–408, 1997.

[24] M. Pasini, R. Berto, M. Brondino, R. Hall, and C. Ortner, "How to measure the restorative quality of environments: The PRS-11," *Procedia-Soc. Behav. Sci.*, vol. 159, pp. 293–297, 2014.

[25] C. J. Ferguson, "An effect size primer: A guide for clinicians and researchers," *Prof. Psychol. Res. Pract.*, vol. 40, no. 5, pp. 532–538, 2009.

Architectural Lighting in the Context of Visual Comfort and Environmental Aspects of Artificial Light at Night

Patrik Kučera
Faculty of Civil Engineering
Czech Technical University in Prague
Prague, Czech Republic
ORCID: 0000-0003-3943-5442
patrik.kucera@fsv.cvut.cz

Romain Lapujade
University Centre for Energy Efficient Buildings
Czech Technical University in Prague
Prague, Czech Republic
romain.lapujade@gmail.com

Jaroslav Vychytil
Faculty of Civil Engineering
Czech Technical University in Prague
Prague, Czech Republic
ORCID: 0000-0001-6786-2690
jaroslav.vychytil@fsv.cvut.cz

Lenka Maierova*
University Centre for Energy Efficient Buildings
Czech Technical University in Prague
Prague, Czech Republic
ORCID: 0000-0002-7303-8232
lenka.maierova@fsv.cvut.cz

***Abstract*— The paper is focused on the light produced by architectural lighting in urban environments, and its impacts on the aesthetic perception of both, the building and the whole urban composition of spaces, the effect on the visual comfort of users, and the environmental aspects.**

The case study is located in the Namesti Miru, Prague Czech Republic. It provides data on properties and the effects of public lighting and architectural lighting on the historical facades and their surroundings. It identifies the over-illuminated or high contrast zones, assess glare risk, visual comfort of the users. Further, based on the virtual model, scenarios for the lighting optimalisation are suggested.

Keywords—ALAN, glare, spectrum, disturbing light, light pollution, urban area, energy savings

I. Introduction

Public lighting is an important part of public spaces. Light makes a place interesting, safe and clear. Excess or lack of light directly affects the quality and usability of the space. The main function of public lighting is to ensure the safety of the space at night, promoting good orientation in the space, identifying people's faces, and revealing important parts of the space [1]. If these conditions are met, the environment becomes subjectively safe for the user. Public lighting must also make it easier for pedestrians to identify potential obstacles and make them visible when moving on and around the road [2].

The main requirements for artificial night lighting are specified in the European standard [2] in order to provide visual comfort. They consist of minimal required intensity, uniformity, duration of illumination and avoidance of misdirected disturbing light or potential glare from light sources. Once these basic requirements are met, further increasing the site lighting has no positive effect. It not only results in unnecessary energy consumption, which is the main reason for optimizing lighting systems in last decades. Excessive lighting may have a disturbing effect on its surroundings. A more positive effect than increasing the illuminance is to ensure the quality of the lighting, and particularly to avoid glare. For better illumination and visual comfort in the night urban environment, attention should be paid to better orientation of the light, which should fall only on the area to be illuminated. This measure reduces the occurrence of light pollution [3] and protects the night starry sky. Misdirected light flux can produce glare and hinder the eye from adapting to lower night-time illuminance. The use of an adequate spectrum of illumination is also important. In nighttime environments, the most adequate use of lighting is warm white chromaticity temperature (K < 3000 K), since lighting in this spectrum has been shown to have less negative effect on nature [4]. Modern light sources with low correlated color temperature (CCT), despite the limited portion of long wavelength spectral component, can provide reasonable color rendering quality, its color rendering index (CRI) values exceeded 50, that is in line with nighttime lighting requirements.

Another aesthetically important part of night lighting is architectural lighting. Architectural lighting is only a supplementary part of public lighting, which does not have to meet the technical requirements for conventional artificial night lighting and is primarily intended to contribute to the aesthetical quality of the area [5,6]. Properly designed architectural lighting should harmonize with the place and support its genius loci, to illuminate objects or significant historical or cultural values in the area, such as statues, landmarks, spatially important elements within the city [7]. For this type of lighting, it is very important to find the right level of light [8] and balance its quantity in relation to the surroundings.

Lighting buildings at night is unjustified in the historical context - the building was not designed for it. In the past, buildings were primarily designed to be lit by daylight, i.e. from above. In the historical night environment, artificial light

* Corresponding author

This research was partially funded by SGS22/085/OHK1/2T/11 – Visual comfort variables measurement indoors and outdoors and RVO36000, specific research funds from the Czech Technical University in Prague.

The research was carried out using a brightness distribution analyser, which was purchased from the grant CZ.02.2.67/0.0/0.0/16_016/0002526 provided by the Ministry of Education, Youth and Sports of the Czech Republic and the European Union.

was a valuable and expensive commodity, technically difficult to create and safely keep. As a result, environments were lit sparingly and only used where it was absolutely needed. With the advent of electricity and new technologies, this trend gradually began to change, and light became more affordable and more present in the night environment. There is no existing principle for lighting historical building, that could be used today. Thanks to very rapid development of powerful light sources, new ways of working with light are emerging. The only limitation to the further expansion of architectural lighting is the increasing pressure to on energy consumption. Current energy crisis, which is rapidly increasing the cost of electricity, seems to be powerful tool to optimize architectural lighting and consider smart system of control and operation [9].

In recent decades, the question of the impact of artificial lighting on nature has been raised. Meanwhile there is already existing strong evidence [10] that artificial light at night (ALAN) has a demonstrable negative effect on wildlife and flora. High intensity and color of light in short wavelengths were identified as the main disturbing parameters. This excessive light emission has a negative effect not only on nature, animals and insects, but also on humans themselves. Despite this finding there is currently no document in Czech or European legislation that would regulate maximal lighting levels used in the public space. Few existing documents, in general older than 10 years, cannot be used effectively in view of the rapid development of lighting technology. As a result, global light pollution levels are increasing by 4-6% per year and the short wavelengths have increasing proportion in its spectrum. In several EU countries, legislation of this type is being introduced [11]. The topic of light smog is also becoming an important issue for the general public [12].

To summarize, lighting in the historical urban areas is a complex task, that must satisfy needs of many cultural, technical, environmental domains.

II. Study objectives and setup

The aim of this study is to qualify and quantify the state of artificial night lighting within the urban area and to provide a critical analysis using measurements that can serve as a basis for optimizing a new lighting concept.

A. Location

To investigate various parameters of the lighting environment quality in the urban area, we performed a case study in Náměstí Míru see Fig. 1), a central plaza of Prague's popular residential and business district of Vinohrady, which originated in 18. – 19. century.

The area is dominated by the neo-Gothic church of St. Ludmila, which is located in the middle of the square. In front of the church there is a pedestrian zone surrounded by the greenery of the city's public park. The area is crossed by important arteries of individual and public transport. The intersection of the tram, bus and metro lines makes it busy throughout the whole day and night. Other culturally significant buildings, such as the Vinohrady Theatre and the National House, are located around the perimeter of the square. Each facade of these important buildings is illuminated by independent architectural lighting. The site contributes significantly to the long-distance views, which are assessed as part of the UNESCO World Heritage Site, and to the overall expression of the city of Prague.

Figure 1: Night view of the Náměstí Míru with St. Ludmila church

The main source of lighting in the area is public lighting, installed along the roadways, tram tracks and pedestrian walkways on the plaza. Light is provided by high pressure sodium discharge lamps. For the roadways, light head is placed on the boom on the road lighting pole, park lighting is produced by lanterns with top shading.

Public lighting is greatly complemented by several types of architectural lighting directed at the façade of the Church of St. Ludmila, the National House and the Vinohrady Theatre. The facades and towers of the church are illuminated by reflectors placed on poles in the park. In addition, the side facades of the church are illuminated by reflectors placed in the pavement in a form of line following the church side façade. The light beam of these lights is directed fully vertically to the sky. The facades of the National House and the Vinohrady Theatre are regularly illuminated by pairs or quadruples of spotlights placed on high poles in the park and behind the church. Their light is directed at an angle close to the horizontal and may potentially interfere with the pedestrian's field of vision.

B. Field measurements

During the multi-criteria evaluation of the space we data on many lightings technical parameters were collected, and their effects on visual comfort were assessed. All the measurements were carried out in the winter period of the year, at night, at least two hours after sunset.

Subjective assessment of the visual comfort has been performed in the area. A total of 7 positions were identified, where potential discomfort may arise from high contrasts between the surfaces or glare from the light sources in the field of vision, see Fig. 2. To assess visual comfort and glare risks objectively, individual measurements were taken at these locations using a luminance analyzer LDA. Images of the lighting environment were taken, placing the camera in the horizontal direction at the position of the eye (height of 150 cm). The device was calibrated to the spectral sensitivity of the human eye and equipped with a full-frame sensor and fisheye lens to capture the total field of vision of a pedestrian. Produced high dynamic range images (HDRI) were processed with LumiDISP software [13] to compile brightness maps describing luminance on individual surfaces and UGR analysis.

The luminance on the paved surface at the square was recorded with a lux meter calibrated for low light measurements. The data obtained were compared with the technical requirements of the legislation for the lighting in the traffic service areas according to [2]. The luminance on the surfaces has been obtained by a recording of the brightness of the square's surfaces taken from an overhead perspective.

Further measurements were carried out using a radiospectrometer Spectis to record the spectral composition, correlated color temperature (CCT), and color rendering index (CRI) of the installed light sources and the spectral reflectance and absorbance of the surfaces. The instrument was also used to determine the illuminance values of the surface to be illuminated.

In addition to the above measurements, local greenery was periodically monitored. This monitoring aimed to provide information on the effect of light during wintertime and at the beginning of the growing season.

C. Virtual model

A virtual model of the area was created within the project. The computer model was built in Dialux software [14]. Data from the freely accessible online land registry was used as the ground plan. The height dimensions were derived from the geoportal of the City of Prague, which contains the necessary data and a 3D model of the entire city. The exact location of the lighting infrastructure, detailed data on the light points (type, color correlated temperature, installed luminous power of the source) were provided by the company Technologie hlavního města Prahy, which manages public lighting.

For an accurate and close-to-reality modelling, confirmation field measurements with a radio spectrometer and a laser meter were performed. These instruments provided more accurate data on the height of the light source location and the light flux dominant direction in both, horizontal and vertical angle. Reflectance properties of the surfaces were obtained by radio spectrometer extended with luminance probe. In addition, surface photography was performed to accurately map onto the surfaces of objects in the model. Based on this data and all the detected parameters, the model was successfully validated with the real situation and resulted in the mean absolute percentage deviation of 10% (Fig. 3).

Figure 2: Overview of the measurement positions

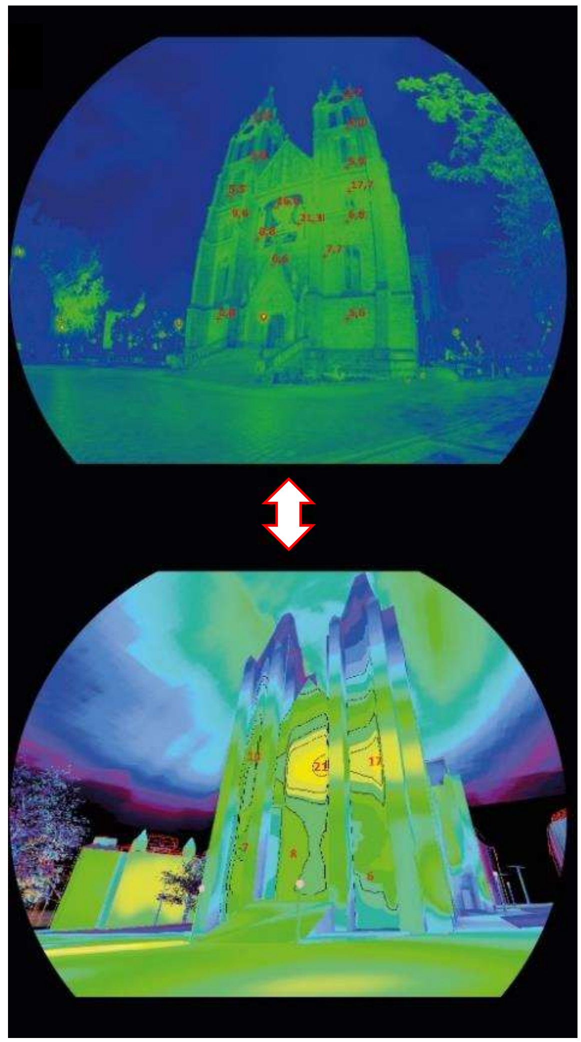

Figure 3: Comparison of field measurements (above) and virtual model (below) values during validation, viewpoint 6.

III. RESULTS - MEASUREMENTS

A. Illuminance on the ground

In the area, the real illuminance of the pavement was verified using the radio spectrometer. According to the standard [2], the pedestrian areas of the plaza are classified into the P3 lighting class and requires the average illuminance $E_m = 7.5$ lx and at the minimum surface illuminance of $E_{min} = 1.5$ lx. The real average value on the paved surface of the plaza reaches $E_{m,real} = 15$ lx. This means that the actual surface illuminance exceeds twice the standard requirement.

Areas designated for motorized traffic are classified by the standard as Class M. The requirements of the standard specify an illuminance class of M1 for the roadways on the site. The minimum maintained average roadway surface luminance value $L_m = 2$ cd*m^{-2}, the actual value measured using the luminance map $L_{m,real} = 2.08$ cd*m^{-2} reasonably meets the requirements of the standard.

B. Luminance on facades

To evaluate the luminance on the facades of the objects, luminance analyses were performed using luminance maps of

HDR images. The comparison of the individual images resulted in a summary assessment of the luminance on the façades of the important objects on the plaza (Table 1). High values of surface global luminance indicate problematic over-illumination of the surface that may create undesirable contrast to the other objects and disturb adaptation of the visual system. Masive overlighting increases risk of glare. Another consequence is higher energy consumption. The greatest over-illumination within the site occurs in the lighting of the National House and the Vinohrady Theatre, where the façade luminance exceeds 10 cd*m^{-2}.

The Table 1 further describes the luminance of the surface compared to the average background luminance (adaptation luminance) at the site, i.e. the luminance contrast. Low luminance contrast indicates poor resolution of the object in the scene, while too high values indicate a risk of glare. The luminance on the National House facade relative to the surroundings are 100 times brighter that the adaptation background and more than 8 times higher compared to the facades of surrounding buildings. This illumination is dazzling and causes other architecture in the area to enter the background or motivates the others to use higher light intensities as well.

In addition to the overall comparison, individual luminance maps were also evaluated. For example, Figure 4 demonstrates the luminance on the church main façade. Light flux is unevenly distributed, with the highest luminance in the central area, at the rosette window (on the photo temporarily covered by an opaque screen). Luminance of light at the central spot reaches L_{max} = 29.22 cd*m^{-2}. Directing the light beam on the rosette window is inefficient and different lighting approach should be chosen to highlight the architectural element of the rosette. Another deficiency identified is the uneven luminance distribution of the church towers.

C. *Visibility of details*

Architectural lighting of buildings is designed to support the aesthetic value of the building in the night environment. To support the character of the historical construction, it is important to point out details and surface structures. Next to the lighting intensity, the degree of visibility of the facade details is related to the position and directivity of the light illuminating the surface. Light directed perpendicular to the surface does not create shadows of the structure. This result in the low contrast and flat appearance of the surface due to the low contrast between the luminance of the details and its surrounding.

There are significant buildings on the site with a different approach to lighting. The National House building is lit by high intensity lights positioned perpendicular to the façade. The resulting appearance of the lighting is flat, not supporting self-cast shadows. This method of lighting does not enhance the architectural detail (Fig. 5). The principle of church lighting is different – the lighting is not chosen perpendicular to the façade and the spotlights are predominantly placed in the corner of the illuminated area.

D. *Glare risk*

As part of the evaluation, a calculation of the glare within the visual field was carried out. The architectural lighting has been identified as the main source of glare. These sources are in both vertical (pointing up towards the sky) and horizontal directions.

TABLE 1: COMPARSION OF BRIGHTNESSES ON SURFACES

object	$L_{O,average}$	$L_{B,average}$	Background to surface luminance
	(cd*m^{-2})	(cd*m^{-2})	ratio
st. Ludmila church – front view	7.301	0.082*	1:89
st. Ludmila church – side view	1.728		1:21
National House	11.272		1:137
Vinohrady theatre	9.981		1:121
non-illuminated objects	1.353		1:16

* average number from more views

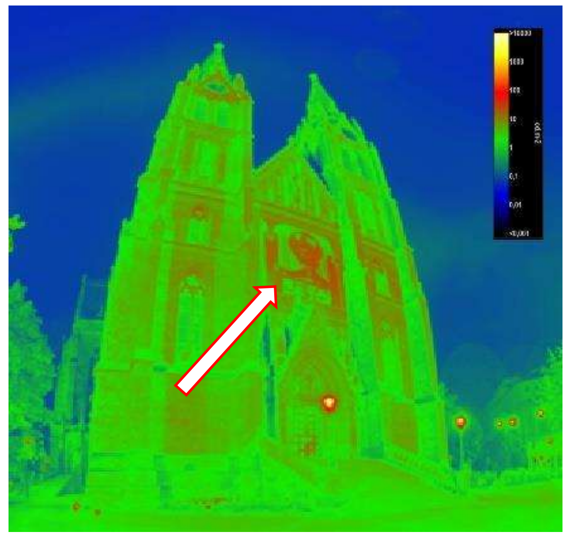

Figure 4: Luminance map on the front façade of the Church of St. Ludmila, viewpoint 5.

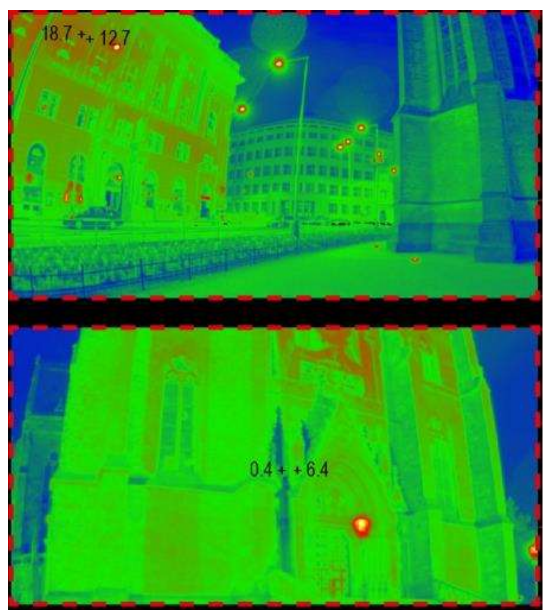

Figure 5: Visibility of architectural details on illuminated buildings in Náměstí Míru: National House, viewpoint 3 (top), St. Ludmila Church front view, viewpoint 5 (bottom).

The glare occurs is mainly due to the positioning of light sources coinciding with the direction of view of the user of the space and at the same time the light sources are in the center of visual vision (Fig. 6, 7) The proposed lighting does not reflect the source position index, which reflects the changes in glare with respect to the angular displacement of the light source from the observer.

The glare mainly occurs due to positioning the light sources in the opposite direction then the view, and mainly, when these light sources occur close to the observers' central visual field – i.e. with the high position index. Figures. 6 and 7 document glare situations in the investigated area. If expressed as UGR based on luminance analyses of the visual field in situation at figure 6, the total calculated value of glare reached 36.59. This value far exceeds the limits of acceptable glare risks, according to the standards it must not exceed 28, to achieve good visual comfort should preferably stay below 19.

E. Color temperature

The typical color correlated temperature (CCT) of public lighting in the area is 2100 K. This lower CCT value is provided by using sodium lamps as a source of light. The CCT of architectural lighting is higher. Lighting integrated in the ground along the church has warm light of 3000 K. Neutral white light of 4300 K is installed in the powerful reflectors directing light onto facades.

In the historical context, sources with lower values of chromaticity temperature were used for lighting, especially candles and torches, which are resembling the color of fire. With the advent of artificial lighting, color of exterior lighting always has been in alike color. Only recently outdoor lights become closer to neutral or even cold white with CCT above 4000 K. For an environmental setting, this temperature is not appropriate and less natural for the night environment. In respect to the historical context of illuminated buildings, warm soft lighting with CCT below 2500 K should be applied.

F. Greenery

Long-term, regular monitoring the impact of the installed façade lighting on the greenery proved the negative influence of the powerful light sources on the nearby trees. At the branches where the light cone collides with the tree canopy, trees are notably desynchronized with the natural seasonal changes. The delay phase of the leaf fall in autumn and leaf emergence in spring weakens the plants, which are at risk of gradual dieback. Brightly illuminated leaves are visible at the nighttime records at Fig. 6 and 7. Delayed phase of leaf emergence in the light cone of the architectural lighting is documented at Figure 8.

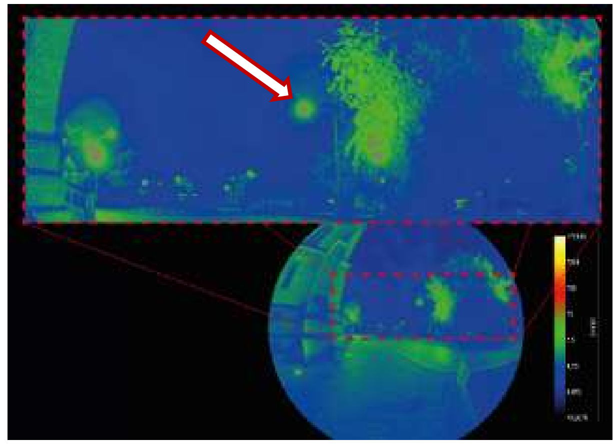

Figure 4: Position of glare reflectors at the front façade of St. Ludmila's Church extending into the greenery - side view (viewpoint 4). Arrow indicatea source of glare, UGR above 36.

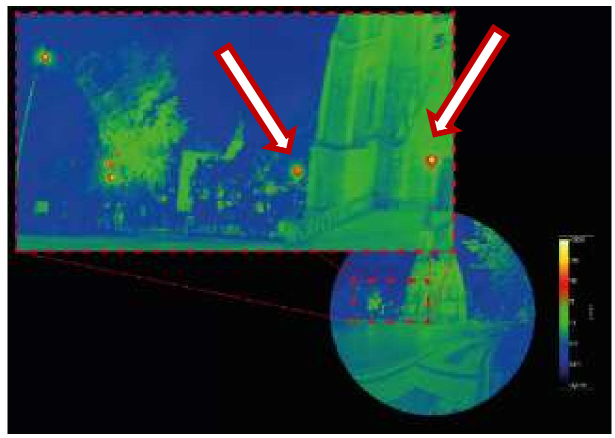

Figure 5: Position of glare reflectors at the front facade of St. Ludmila's Church extending into the greenery - view from the square, viewpoint 6. Arrows indicate sources of glare,

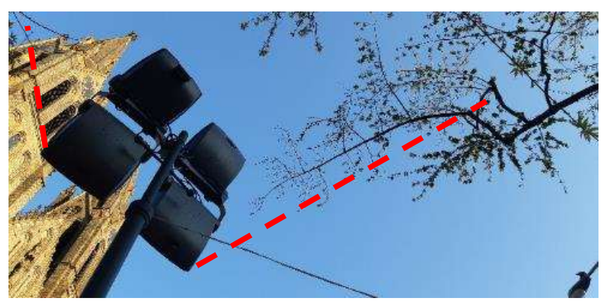

Figure 8: Reflectors illuminating the church affecting the greenery in the early spring 2022.

IV. VIRTUAL MODEL - OPTIMALISATION POTENTIAL

Validation of the virtual model to the real-life measurements resulted in very similar values, with maximal mean error not exceeding 10%. Also the other parameters in the model and in the reality provide comparable results, such as the UGR value in the viewpoint 7 calculated the virtual model reached of 39, while the field measurement was 36.59. Therefore, the model was used for lighting calculations and optimization of the lighting system.

The optimization of the lighting environment was focused on the identified deficiencies and monitoring the effect on energy efficiency. Using the virtual model, we reduced over-illuminating of the facades and obstructive light from the vertical lighting, that causes light pollution and glare.

High UGR values calculated in some areas of the plaza can be reduced and at the same time better lighting efficiency can be achieved by better directing the light flux precisely to the facades of buildings. As an example of such optimalization could be the lights installed in the in the ground along the St. Ludmilla Church. These luminaires direct light directly upwards. In the virtual model the angle of the metal grid above

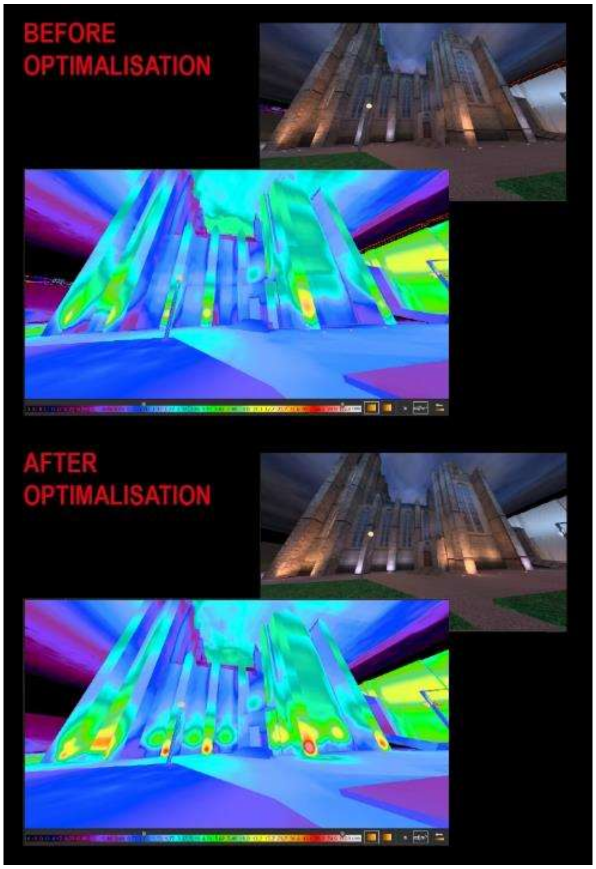

Figure 9: Effect of the inclination of shading grids to adjust the direction of vertical beams of illumination on the side wall of St. Ludmila's Church, viewpoint 7.

the light sources was tilted from the vertical position to 22.5 degrees in the direction to the wall of the building. In comparison with the original condition, the luminance on the surface significantly increased, glare from the light sources decreased and higher light efficiency has been achieved, see figure 9. At the same time, lighting makes the façade more plastic, while the structural elements cast their own shadows.

Thanks to the validated model, different lighting optimization options can be tested. As part of the optimization, basic modes of temporal regulation of both, the street lighting and the architectural lighting system could be manipulated to calculate the effect on energy consumption and costs. An example of 4 lighting scenarios were created, see Table 2. The scenarios were carefully selected based on the insights gained from the previous detailed analyses. The lighting mode adjustments are designed to reduce the amount of light in the space and to limit the risk of glare, while promoting visual comfort and aesthetic impact of the lighting.

- Scenario 1 represents the current lighting setup with 100% power of both street and architectural lighting
- Scenario 2 slightly reduces the public lighting, namely 100% illumination until 22:00 with a subsequent dynamic switch to 75% power until 5:00 or dawn. Architectural lighting remains on at full intensity.
- Scenario 3 keeps full use of public lighting throughout the night but reduces the architectural lighting. namely full lighting power until 22:00, power reduced to 75% from 22:00 to 1:00, and then switching off the architectural lighting completely, which is objectively redundant.
- Scenario 4 combines the optimization of public lighting from Scenario 2 and architectural lighting from Scenario 3 to achieve maximal savings. This optimization can achieve up to almost 32% savings.

V. Discussion

From the observed illuminance parameters of the area, we can conclude that the brightness values on pedestrian areas exceed the standard requirements and can be reduced. This reduction would mean a more environmentally friendly lighting approach and the elimination of light pollution. Due to the higher required illuminance on the nearby motor traffic areas, setting significantly lower illuminance in adjacent pedestrian zones may create uncomfortable contrast and create subjective discomfort to the users. Therefore, the reductions should be applied with discretion.

The study has shown that brightness on building facades is set inappropriately high. Given the average background luminance values, the surfaces are illuminated with inadequate intensity. The contrast to the adaptation luminance by more than 100 times is excessive and a reduction of these values should be considered. At such high illuminance levels, façades create large contrasts with the surroundings and reduce the eye adaptation to the low light condition during the nighttime. Attention should also be taken to distribute the light evenly over the area to be illuminated not to create points that are over-illuminated.

At the same time, high-intensity architectural lighting degrades the level of legible detail; legibility of detail is also closely related to the direction of the light flux and the positioning of the reflectors. To highlight architectural elements (e.g. the rosette of St. Ludmila Church), a different lighting method should be chosen that also reflects the material properties of the illuminated, works with the inherent shadows of the architectural details etc.

Further, some of the façade lights are positioned and its light is directed so that it causes discomfortable or unbearable glare situations. The glare should be reduced by using luminaires with adequate beam angle and using shading elements to direct the light flux precisely towards the illuminated surface.

TABLE 2: CALCULATION OF POTENTIAL ENERGY SAVING

	zone	*scenario 1*	*scenario 2*	*scenario 3*	*scenario 4*
Energy (kWh/year)	Public lighting	35 693	30 015	35 693	30 015
	Architectural lighting	49 706	49 706	28 242	28 242
Price* (€/year)	Public lighting	7 774	6 537	7 774	6 537
	Architectural lighting	10 826	10 826	6 151	6 151
	Whole installation	18 600	17 363	13 925	12 688
	Savings	0 %	6,6 %	25,1 %	31,8 %

* 0,218 (€/kW) … actual price (spring 2022)

The positioning of architectural lighting in the park area is also not appropriate regarding the mature greenery surrounding the plaza and the church - light cones that encroach into the tree canopy not only cannot reach the surface they aim to illuminate, but negatively affect the trees and its temporal synchronization to the seasons.

Installed hue of the public lighting is warm or neutral white. This is ensured by the application of sodium lamps, which provide light in warmer shades that are more acceptable to the environment and to the human user of the space. The architectural lighting is neutral white with CCT higher than 4000 K, which corresponds daytime lighting and is not appropriate for night lighting. It does not enhance the historical context of buildings, since in the history, if any, then warm light has been used in the night environment. Finally, white light is more disturbing to the living organisms.

Simulation on the virtual model suggests that the lighting values can be dynamically changed during the night, providing a more acceptable environmental environment, but also financial savings of around a third of the total energy consumption.

VI. Conclusion

Based on the on-site measurement we evaluated many important aspects affecting the space and its light environment can run multicriterial analysis. Modern measurements techniques, such as luminance analyses, can provide detailed and objective information on the visual comfort and suitability of lighting. Parameters of virtual models can reach close to reality, making the virtual model to become valuable tool for optimalization of the lighting system.

The analyses revealed low quality of visual comfort when moving around the square. This fact is not caused by the low quantity of lighting, but by the considerable unevenness in distribution of the light in the area, and especially by the positioning of several light sources in such a way that they glare pedestrians passing by. Directivity of the light is further is important for the aesthetic appearance of the building. This indicates the potential of improving the lighting environment by precise design of the lighting system, without the need to increase quantity of light. In contrary with such approach, quantity of light can be reduced, nature preserved, and energy and cost can be saved.

VII. References

[1] Fotios, Steve, and R. Gibbons. "Road lighting research for drivers and pedestrians: The basis of luminance and illuminance recommendations." *Lighting Research & Technology* 50.1 (2018): 154-186.

[2] *EN 13201 Standards for Road lighting*, Brusel: European Committee for Standardization (CEN), 2016.

[3] F. Falchi, "The new world atlas of artificial night sky brightness", *Science Advances*, vol. 2016, 2016.

[4] L. Maierová, "Public Lighting, Public Health", in *VII. Lighting Conference of the Visegrad Countries (Lumen V4)*, 2018, pp. 1-5.

[5] P. Žák, "Venkovní architekturní osvětlení", *Časopis Světlo*.

[6] L. Monzer, *Venkovní osvětlení architektur*, 1. Prague: SNTL - Nakladatelství technické literatury, n.p., 1980.

[7] P. Pavelec and P. Slavko, "Metodika pro přípravu a realizaci historicky poučených festivit v prostředí hradů a zámků - I.". National Institute for the Protection and Conservation of Monuments and Sites, Prague, 2015.

[8] *CIE 094-1993: Guide for floodlighting*, 1. Vienna: Commission Internationale de L'Eclairage, 1993.

[9] A. Bejšovec, "Praha plánuje omezit dobu nasvícení památek. Reaguje tak na nárůst cen elektřiny", *iROZHLAS*, 2022.

[10] S. Schroer, B. Huggins, C. Azam and F. Hölker, "Working with Inadequate Tools: Legislative Shortcomings in Protection against Ecological Effects of Artificial Light at Night", *Sustainability*, vol. 2020, no. 126, p. 2551, 2020.

[11] CSN 36 0459 - Omezení rušivých účinků umělého světla ve venkovním prostředí". Czech Office for Standards, Metrology and Testing, Prague, in preparation.

[12] S. Kolařík, "Petice za lepší světlo v Praze", *petice.com*. [Online]. Available: https://www.petice.com/svetlo. [Accessed: 2022-04-24].

[13] VUT LIGHT LABORATORY. *LumiDISP* [Computer software]. (2021). Retrieved from: https://lumidisp.eu/luminance-analyser/

[14] DIAL GMBH. *DIALux evo 10.1* [Computer software]. (2022). Retrieved from: https://www.dialux.com/en-GB/download

Optimization of Spatial Photon Irradiance Distribution for Indoor Vertical Farms

László Balázs
Department of Microelectronics and Technology, *Kálmán Kandó Faculty of Electrical Engineering, Óbuda University*
Budapest, Hungary
balazs.laszlo@kvk.uni-obuda.hu

József Nádas
Department of Microelectronics and Technology, *Kálmán Kandó Faculty of Electrical Engineering, Óbuda University*
Budapest, Hungary
nadas.jozsef@kvk.uni-obuda.hu

Zsolt Molnár
Department of Microelectronics and Technology, *Kálmán Kandó Faculty of Electrical Engineering, Óbuda University*
Budapest, Hungary
molnar.zsolt.vil@.uni-obuda.hu

Tamás Páva
Agritech |Division
Tungsram Operations Kft.
Budapest, Hungary
tamas.pava@tungsram.com

Zoltán Sejpes
Agritech |Division
Tungsram Operations Kft.
Budapest, Hungary
zoltan.sejpes@tungsram.com

***Abstract*—Vertical farms are gaining popularity because of the increasing need for localized food production. The economics of indoor crop cultivation largely depends on the operating cost of electrical lighting illuminating the plant canopy. We present a designed experiment aimed at mapping the useful photosynthetic photon flux (PPF) and spatial distribution of the photosynthetic photon irradiance (PPFD) measured at the canopy level. We showed that a single uniformity measure used in general lighting (minimum/average or minimum/maximum) is not adequate to describe the subtle differences in the histogram of the spatial PPFD distributions relevant for horticultural lighting. Both the width and the skewness of the histograms change with the three input parameters. The ultimate challenge of the optimization was to find the tradeoff between the utilization factor and light uniformity. The location of the optimum depends on the relative weights of the two objective functions in the optimization. Additional design parameters need to be incorporated in the optimization to further reduce edge effects and increase the productivity of the lighting installation.**

Keywords—horticultural lighting, PPFD distribution, utilization factor, uniformity, vertical farm

I. Introduction

In vertical farms or plant factories electric lighting provides the sole source of light for plant growth and development. The plants are cultivated in vertically stacked layers and luminaires are placed in close proximity to the illuminated crop[1].

There are several advantages of indoor cultivation over traditional open field farming. Since all environmental parameters affecting crop yield (temperature, humidity, lighting environment, nutrients) are controlled, vertical farms can operate at any geographical location allowing year-round production of food. Vertical farms can be built in urban areas close to the consumers enabling the transportation costs to be reduced. During the times of disrupted supply chains food security is significantly increased by localized crop production in controlled environment agriculture (CEA)[2].

Lighting has the highest share in the electricity consumption of CEA applications limiting the economics of indoor cultivation[3], [4]. Light-emitting diodes (LED) have significantly increased the photon conversion efficiency of horticultural lighting systems approaching the theoretical limits of photon efficacy for phosphor converted white (3.4 μmol J^{-1}) and narrowband blue + red fixtures (4.1 μmol J^{-1}) There is limited room for further improvement in fixture efficacy after decades of intensive developments of all subsystems of LED luminaires[5].

Some plants are tolerant to fluctuating light intensity. This means that irradiance in a vertical farm can vary over time without reducing the crop yield, in case the total amount of photosynthetically active photons absorbed during the daily photoperiod, defined as daily light integral (DLI), is constant. Implementing load shifting in vertical farms operated from an electricity grid with time dependent tariffs offers substantial cost saving[6], but the extent of electricity cost reduction and the profitability of the cultivation is still limited by the nature of the electricity price variations.

Optimizing the lighting environment is another opportunity for increasing the profitability of vertical farms[7]. The rate of photosynthesis depends both on the intensity and the spectral distribution of irradiance impinging on plant leaves[8]. As a quantitative parameter of light photosynthetic photon irradiance or with another commonly used name, photosynthetic photon flux density (PPFD) is used in horticultural lighting[9]. PPFD is defined by the following equation.

$$E_{PPFD} = \frac{10^6}{hcN_A} \int_{\lambda_{min}}^{\lambda_{max}} \lambda E_e(\lambda)\, d\lambda \qquad (1)$$

In (1) E_{PPFD} is the photosynthetic photon irradiance expressed in μmol· m^{-2}·s^{-1}, h is the Planck constant, c is the speed of light, $E_e(\lambda)$ is the spectral irradiance measured in W·m^{-2}·nm^{-1} at wavelength λ. N_A denotes the Avogadro constant. $\lambda_{min} = 400$ nm is the lower, $\lambda_{max} = 700$ nm is the upper bound of the waveband defined as photosynthetically active radiation (PAR). The crop yield increases with increasing photon irradiance up to the light saturation point where the photosynthetic activity reaches a saturation level. At excessive illumination photodegradation reduces the photosynthetic activity. More than the necessary light required for plant growth and development increases the operation cost and reduces the productivity of the vertical farms.

From productivity perspective the objective of the lighting design is to focus the light emitted by the luminaires to the target area and ensure the spatial uniformity of the photon irradiance over the plant canopy. If the photon irradiance received by a plant is less than the PPFD value of the light saturation point, the crop yield will be below the entitlement and the cultivation capacity is underutilized.

In general lighting the parameters associated with these two criteria are the utilization factor and the illuminance uniformity [10]. In horticultural lighting the utilization factor, U_f, can be defined as the quotient of photon flux received by the target area and the total amount of photons emitted by the luminaires illuminating the target area.

Despite several decades of investigations highlighting the sensitivity of plant growth to the variability of lighting conditions, there is still no generally accepted protocol to characterize the photon irradiance uniformity in horticultural applications[11]. Research papers generally refer to single PPFD values without any variability statistics while characterizing the lighting conditions of plant growth experiments[12]. This practice makes the comparison and reproduction of research data difficult or impossible.

Guidelines for growers recommend reporting the minimum, maximum average and standard deviation of PPFD readings measured on a regularly spaced grid, but there is no standard protocol to evaluate the spatial variability[12] of data. Following the general lighting practice, the overall uniformity, U_o, defined as the quotient of minimum PPFD and the average PPFD or the diversity, U_d, the minimum to maximum ratio, often appears in specifications, though these extreme value based metrics are prone to the sampling error and can hide important characteristics of the spatial distribution.

The objective of this research was to optimize photon irradiance distribution on a 1 m × 1 m target area. Ensuring high spatial uniformity over the canopy level and achieving sharp cut-off at the boundaries of the target area were the key challenges of the lighting design. We applied the methodology of designed experiment to map the design criteria as a function of the geometrical position and the beam angle of the luminaires.

II. Materials and Methods

We used 8 parallel LED lightbars (Tungsram TUAS VFPM)) incorporating three narrowband LEDs with emission peaks at 450 nm, 660 nm and 730 nm as well as a broadband white phosphor LED. The relative photon flux of the channels, consequently the spectral power distribution of the emitted light was held constant during the experiment. The arrangement of the lightbars and the experimental setup is shown in **Chyba! Nenašiel sa žiaden zdroj odkazov.**.

We placed a measurement grid made of black PVC foam with regularly spaced perforations (red crosses in Fig. 1b) defining the locations where spectral irradiances were captured by an AvaSpec-2048 spectroradiometer in the 380-780 nm wavelength range. The distance between the adjacent points on the grid was 10 cm both in x and y direction.

The light probe equipped with a cosine corrector was pointing upwards in the grid. The collected light was transferred by an optical fiber to the optical bench of the spectrometer. Each spectrum ($E_e(\lambda)$) comprising 698 data

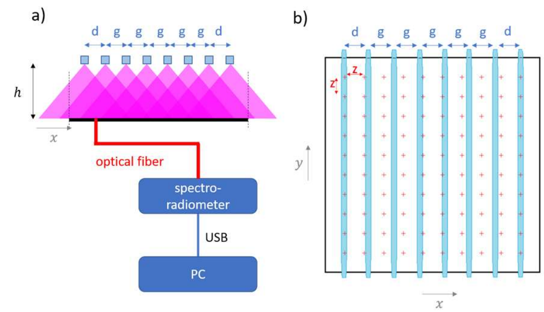

Fig. 1. Schematic of the experimental setup, a) sideview b) top view. The first factor in the experiment was the height of the luminaires above the measurement grid, h. The second factor was the horizontal position defined by parameter d. The third factor was the beam angle of light emission. Red crosses indicate the measurement grid regularly spaced by z=10 cm.

points was saved as an excel file and processed separately following the measurements.

We used 8 lightbars in the same plane parallel with the reference plane to illuminate the target area. The mounting height, h, measured from the plane of the measurement grid was the first factor in the experiment.

The horizontal positions of the leftmost and rightmost light bars were fixed above the leftmost and rightmost columns of the measurement grid. The distance between the 1st and 2nd and the 7th and 8th lightbars (d) was the second factor. The gap between the remaining adjacent lightbars was the same value, g, adjusted according to the actual value of d.

The third factor of the experiment was the type of secondary optics of the lightbars. Two versions were compared denoted by N, for no secondary optics except the cover glass of the luminaire, and F for arched Fresnel lens expanding the beam angle of the light emission along the x axis of the experimental setup. The light distribution curves shown in Fig. 2 indicate that the Fresnel lens significantly increased the beam angle of light distribution. There was no difference in the total photon flux of the two cases.

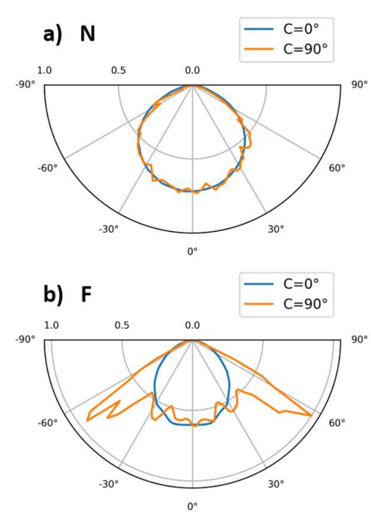

Fig. 2. Light distributions along the x (C=90°) and y (C=0°) of the lightbars with no secondary optics, N a) and with arched Fresnel lens, F b). The Fresnel lens broadened the light distribution in the x direction.

TABLE I. FACTORS AND RESPONSE VALUES OF THE EXPERIMENT

#	O	Factors h [mm]	d [mm]	Response values U_o	U_d	U_f	W [%]	s
1	N	100	64	0.73	0.50	0.75	39	0.69
2	N	100	128	0.70	0.58	0.75	40	-0.36
3	N	200	64	0.76	0.66	0.48	58	-0.71
4	N	200	128	0.60	0.48	0.52	67	-0.31
5	N	300	64	0.55	0.45	0.41	95	-0.60
6	N	300	128	0.58	0.44	0.43	86	-0.25
7	F	100	64	0.76	0.57	0.69	41	0.15
8	F	100	128	0.73	0.54	0.74	39	0.29
9	F	200	64	0.68	0.57	0.63	50	-0.55
10	F	200	128	0.52	0.41	0.66	60	-0.33
11	F	300	64	0.64	0.50	0.51	66	-0.16
12	F	300	128	0.56	0.43	0.56	68	-0.22

The photosynthetic photon irradiance values were calculated by numerical integration according to (1) using the rectangle rule.

III. DESIGN OF EXPERIMENTS

The 10×10 spectra were captured in 12 experimental runs in two major steps (TABLE I). In the first step lightbars with no secondary lens (N) were tested. The mounting height, h, was set at three levels, 100 mm, 200 mm and 300 mm relative to the reference plane. The spacing parameter of the luminaires, d, was changed at two levels. In case of $d = 64$ mm, the 2nd and the 7th lightbar was shifted to the left and right edge, whereas in case of $d = 128$ mm all the gaps between the adjacent lightbars were uniformly $d = g = 128$ mm. In the second half of the experiment the settings were the same as in the first one, but the lightbars were equipped with Fresnel lenses (F).

All other parameters were held constant throughout the experiment. Lightbars were switched on one hour prior to each step to allow sufficient time for thermal stabilization of the light output.

IV. RESULTS AND DISCUSSION

Fig. 3a) shows the photosynthetic photon irradiance (PPFD) histogram measured for run #3 (O=N, $h = 200$ mm, $d = 64$ mm) along with the contour plot of the spatial PPFD distribution (Fig. 3b). The PPFD values (E) were normalized to the average value (E_{ave}) of the experimental run. The scale of the x axis on the histogram and the scale of the color bar are the same.

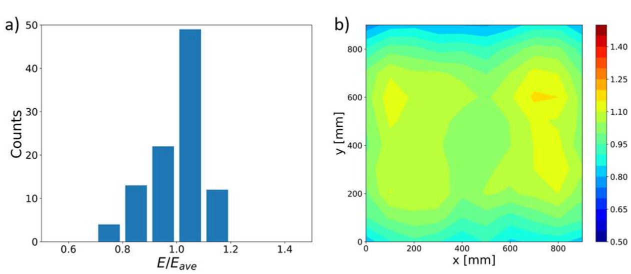

Fig. 3. a) Histogram of the PPFD distribution measured for the 10×10 grid points in case of experimental run #3. The PPFD values were normalized to the average of the experimental run. b) Contour plot visualizing the spatial distribution of relative PPFD values. The x axis of the histogram and the color are on the same scale.

Run #3 delivered the tightest distribution in the entire experiment. 84% of the illuminated area was within the ±10% ($0.9 < E/E_{ave} < 1.1$) range of the average and only 12 % of data was found in the ($1.1 < E/E_{ave} < 1.2$) and 4% in the ($0.8 < E/E_{ave} < 0.9$) interval.

The contour plot is a good qualitative tool to visualize spatial distribution of the light intensity and reveal deviations in the accuracy of the fixture positioning. High end PPFD values are split into two domains appearing on the left and on the right half of the target area in Fig. 3b). This feature of the distribution is the consequence of the 2nd and the 7th lightbars positioning close to the leftmost 1st and rightmost 8th lightbars which enabled the drop of photon intensity on the edges to be reduced. Most of the low end values of the PPFD distribution appear on the upper edge of the target area indicating a slight asymmetry in the positioning of the lightbars along the y axis.

Histograms related to configurations with no secondary optics are shown in Fig. 4, whereas histograms associated with the Fresnel lens series are shown in Fig. 5. The first observation while comparing histograms of group N and F is that distributions look taller and narrower in case of O=N and broader in case of O=F. This is due to the wide beam angle of the lightbars equipped with the Fresnel lens. We want to stress that the data presented here are limited to two levels in factor d. We cannot draw a general conclusion that light distribution is worse in case of Fresnel optics. On the contrary, with less than 8 lightbars over the 1 m^2 area and wider separations in factor d and g high spatial uniformity can also be achieved. The statement we can make is that in this experiment we did not set horizontal and vertical positions in the range where the highest spatial uniformity could have been achieved with the wide beam optics[13].

Another observation we want to highlight is that histograms can be rather asymmetric, skewed to the lower or higher values as in case of runs #1 (N100_64) and #5 (N300_64). The consequence for indoor cultivation is that crops growing under the same average photosynthetic photon irradiance can behave differently depending on whether under

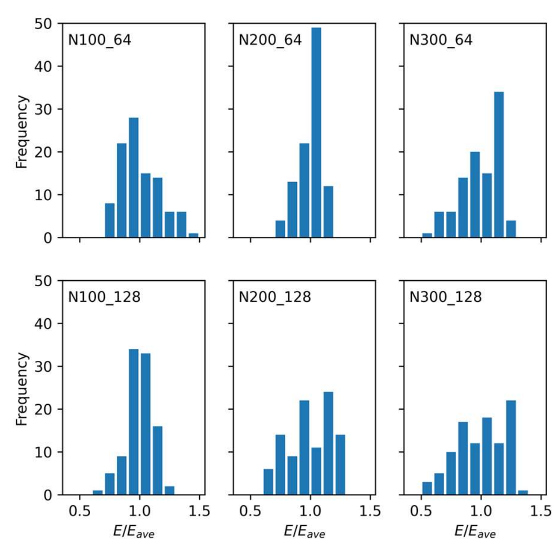

Fig. 4. PPFD histograms for experimental runs 1-6. The code in each pane is composed of the 3 factors: optics, parameter h and parameter d.

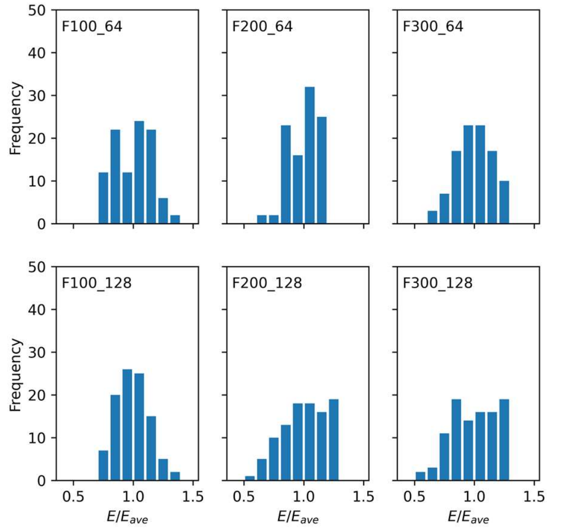

Fig. 5 PPFD histograms for experimental runs 7-12. The code in each pane is composed of the 3 factors :o ptics, parameter h and parameter d.

or over illuminated points dominate the spatial PPFD distribution.

For the optimization we need quantitative figures of merit which can be incorporated into an objective function. We need to consider how well the light emitted by the luminaires is focused on the target area and how uniformly is the light distributed over the target area.

On top of the calculated values of the overall uniformity, U_o , diversity, U_d and the utilization factor, U_f already described in the Introduction, we list two additional quantitative parameters, W and s in TABLE I. W denotes a dimming level relative to the nominal power, required to set the minimum PPFD value to 250 µmol m^{-2} s^{-1}. The parameter s stands for the skewness of the PPFD histogram. We will provide a detailed description of these parameters later in this chapter.

We start our discussion with the spatial variability of the photon irradiance over the illuminated area. The overall uniformity U_o was plotted against the mounting height of the lightbars in Fig. 6. The decreasing trend in uniformity might be surprising for engineers trained in general lighting. The common expectation is that uniformity of the illumination is increasing with distance between the light source and the illuminated surface. This is generally true if the size of the light source is significantly smaller than the mounting height of the luminaire. In our vertical farm scenario, the 8 lightbars cannot be regarded as a point like light source and both the vertical and the horizontal arrangement have a significant effect on the spatial uniformity. The interaction between h and d are pronounced at $d = 64$ mm, $h = 200$ mm. For the O=N lightbars without secondary optics the uniformity reaches a maximum, whereas the uniformity is at the minimum at $d = 128$ mm, $h = 200$ mm in case of O=F.

Comparison of U_o values in TABLE I with the associated histograms in Fig. 6 reveals the ambiguity about the use of overall uniformity as a figure of merit. In runs #3 and #7 $U_o = 0.76$ was calculated which is the highest value for this parameter in our measurements. The width of the PPFD distribution, however, is smaller in case of #3 (N200_64) realtive to #7 (F100_64), therefore these two spatial distributions cannot have the same uniformity. This contradiction is the result of the definition of the overall uniformity as the minimum/average ratio the of data points. The value of $U_o$is sensitive to the shape of the distribution and does not take into consideration the spread of data points above the average. Therefore U_o can overrate uniformity if the distribution is skewed to the left and underestimate uniformity if the distribution is skewed to the right.

The diversity, U_d, defined as the minimum / maximum ratio is better suited to quantify the width of the histograms. Its value is 0.66 for #3 and only 0.57 for #7 indicating that the spread of the data points is smaller in case of #3 (N200_64). Fig. 7 exhibits the more realistic trend of the spatial uniformity as a function of the mounting height, h. U_d determines the width of the distribution independently from its shape. The narrow PPFD distribution implies that there will be less variance in the development of individual plants grown in the cultivation cell.

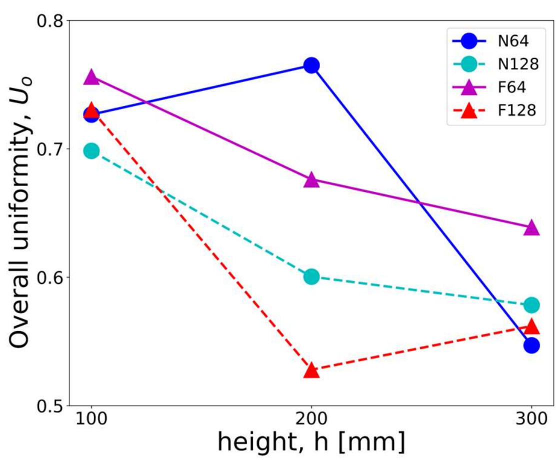

Fig. 6 The overall uniformity, U_o, as a function of the mounting height of the lightbars, h, for all experimental runs. Circle markers denote no secondary optics, triangles represent Fresnel lens data points. Solid lines connect data points related to $d = 64$ mm, whereas dotted lines connect $d = 128$ mm data.

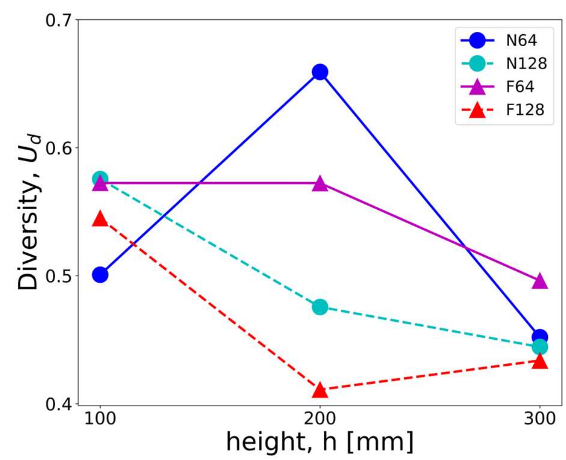

Fig. 7. The diversity, U_d, as a function of the mounting height of the lightbars, h, for all experimental runs. Circle markers denote no secondary optics, triangles represent Fresnel lens data points. Solid lines connect data points related to $d = 64$ mm, whereas dotted lines connect $d = 128$ mm data.

Being a parameter based on extreme values, U_d is also sensitive to sampling and measurement errors, therefore it can be advantageous to use other dispersion measures, e.g. the complement of the coefficient of variation[14]. In our investigation we accepted the diversity as the figure of merit for spatial uniformity and the run #3 (N200_64) was considered to be the most uniform experimental setting.

The skewness trend shown in Fig. 8 also reveals interesting features. Three out of the four data points at $d = 100$ mm has positive values indicating that these distributions are tilted to the lower values, meaning that majority of the target area is slightly under illuminated and a minority of data points are in over illuminated hot spots. A change in the sign of the skewness is between $h = 100$ and 200 mm.

Uniformity of the PPFD distribution is not the only design parameter influencing the crop yield in the vertical farm.

The second metric we used to characterize the PPFD distribution is the utilization factor (U_f) defined as the quotient of the photosynthetic photon flux (PPF) incident on the target area and the total photosynthetic photon flux emitted by the 8 lightbars in total. Not all the photons emitted by the luminaires will reach the surface of the work plane as illustrated by the vertical dotted lines in Fig. 1a). Illuminating regions beyond the perimeter of the target area is regarded as a loss, reducing the productivity and efficiency of cultivation.

The useful photon flux Φ_p was determined by summing up the measured 10 × 10 PPFD values followed by the multiplication of the sum by the area of the unit cell (ΔA= 0.01 m^2) about the reading positions marked with red crosses in Fig. 1b).

$$\Phi_p = \Delta A \sum_{i=1}^{10} \sum_{j=1}^{10} E(x_i, y_j) \tag{2}$$

Dividing Φ_p by the total PPF of the 8 lightbars yields the quotient U_f. The dependence of the utilization factor on the mounting height is shown in Fig. 9.

The trend is similar to what we have seen while analyzing uniformity in Figs. 6 and 7. The highest utilization factor values are at $h = 100$ mm. The slope of the decrease as a function of increasing mounting height is different between the two types of optics used. The rate of decrease was lower in case of lightbars equipped with Fresnel lens relative to fixtures without secondary optics. The best utilization factor was achieved at run #2 (N100_128) closely followed by #1 (N100_64) and #8 (F100_128). This order is markedly different from the uniformity ranking where #3 (N200_64) was on the top.

There is no single maximum for the utilization factor and the uniformity within the variable space investigated. By taking into account exclusively lighting design parameters we cannot optimize the position of the luminaires. To find a tradeoff between these two parameters we would need to define the relative weights of U_d and U_f in an objective function of the optimization.

To identify the weights for a profit-driven optimization, we would need a transfer function which takes light response of the crop, electricity tariff, sales price of the crop as input variables and yields the profit generated during a cultivation cycle as an output.

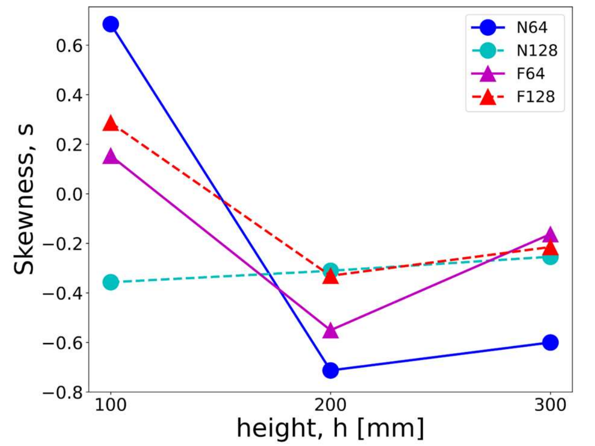

Fig. 8. The skewness of the histograms, s, as a function of the mounting height of the lightbars, h, for all experimental runs. Circle markers denote no secondary optics, triangles represent Fresnel lens data points. Solid lines connect data points related to $d = 64$ mm, whereas dotted lines connect $d = 128$ mm data.

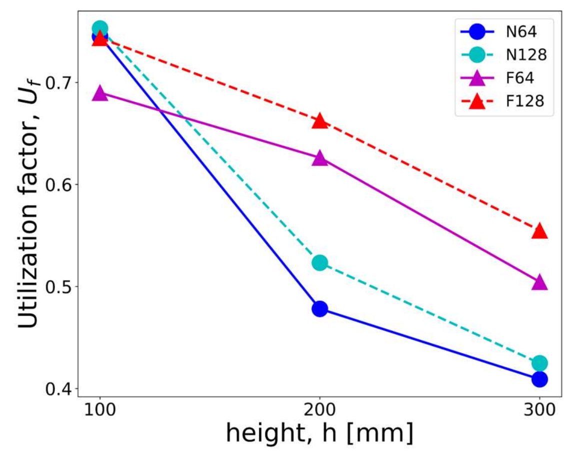

Fig. 9. The quotient of the useful and the total photon flux, U_f, as a function of the mounting height of the lightbars, h, for all experimental runs. Circle markers denote no secondary optics, triangles represent Fresnel lens data points. Solid lines connect data points related to $d = 64$ mm, whereas dotted lines connect $d = 128$ mm data.

In this study we introduced a constraint to be able to complete the optimization without the need for measuring plant growth rate as a function of local photon irradiance level.

For each set of factors O, h and d, we determined the dimming level of the lightbars (W) required to set the minimum value of the PPFD distribution at E_{min} =250 µmol· m^{-2}·s^{-1}. It was assumed that E_{min} is equal to the light saturation point of the cultivated crop. The rationale for this approach is that the same growth rate is expected over the crop canopy independently of the position, because all points on the target area are exposed to a PPFD level being at or exceeding the light saturation point. It was also assumed that photodegradation does not reduces crop yield.

The dimming levels setting the minimum PPFD values at the saturation point of 250 µmol· m^{-2}·s^{-1} are listed in TABLE I and plotted in Fig. 10. The lowest values in W are all in the group of $h = 100$ mm with very little difference in absolute value. To make a distinction among the best performing configurations we need to consider other response values as well. Taking the diversity in Fig. 7, configuration #2 (N100_128) has the highest U_d value followed by #7 (F100_64). Looking at the sensitivity of the response values relative the change in parameter h, #7 (F100_64) appears to be the best choice. In Fig. 7 the value of U_d does not change, when h is increased from 100 mm to 200 mm. The same robustness is apparent in Fig. 10, where (F200_64) has the lowest value from the $h = 200$ mm group. Although #8 (F100_128) has the lowest value in W, the dimming level deteriorates faster than in configuration #7 (F100_64).

V. Conclusions

We conducted a designed experiment with 3 factors to determine the optimum PPFD distribution on the surface of a 1 m × 1 m plant cultivation cell. Our objective was to provide a methodology for the optimization of the horticultural lighting system going beyond the procedures copied from general lighting practice. In the experiment we showed that the drop of the photon irradiance at the edges of the illuminated area can be reduced and relatively high uniformity can be achieved across the cultivation cell. We showed that optimization merely for an extreme value based uniformity metric, like U_o carries ambiguity and may not lead to the optimum operation efficiency of the vertical farm. We also showed that the uniformity parameters and the utilization factor are sensitive functions of the mounting height and horizontal position of the luminaires. In practical applications the variable positioning of the fixtures can increase the flexibility and improve the profitability of vertical farms.

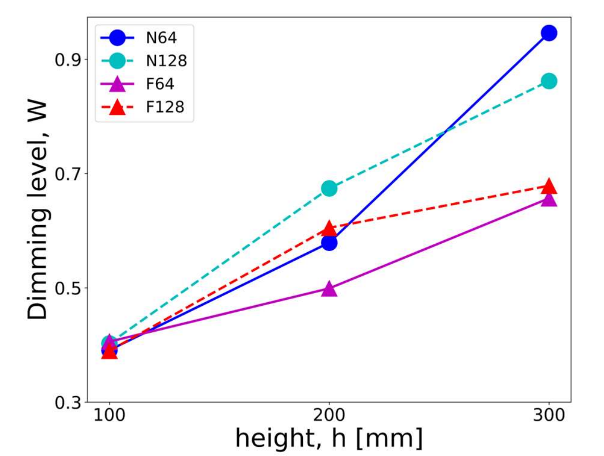

Fig. 10. The dimming level required to maintain the minimum PPFD value of the distribution at 250 μmol m^{-2} s^{-1} as a function of the mounting height of the lightbars, h, for all experimental runs. Circle markers denote no secondary optics, triangles represent Fresnel lens data points. Solid lines connect data points related to $d = 64$ mm, whereas dotted lines connect $d = 128$ mm data.

In this work we did not address many other environmental and economic parameters influencing the productivity of CEA facilities. To fully optimize the lighting systems of indoor crop production, we need to extend our investigation to non-lighting related factors including the light response function of the cultivated crop, electricity cost and sales price of the horticultural product.

References

[1] K. Al-Kodmany, "The Vertical Farm: A Review of Developments and Implications for the Vertical City," *Buildings*, vol. 8, no. 2, Art. no. 2, Feb. 2018, doi: 10.3390/buildings8020024.

[2] F. Kalantari, O. M. Tahir, R. A. Joni, and E. Fatemi, "Opportunities and Challenges in Sustainability of Vertical Farming: A Review," *Journal of Landscape Ecology*, vol. 11, no. 1, pp. 35–60, Jan. 2018, doi: 10.1515/jlecol-2017-0016.

[3] T. Weidner, A. Yang, and M. W. Hamm, "Energy optimisation of plant factories and greenhouses for different climatic conditions," *Energy Conversion and Management*, vol. 243, p. 114336, Sep. 2021, doi: 10.1016/j.enconman.2021.114336.

[4] N. Engler and M. Krarti, "Review of energy efficiency in controlled environment agriculture," *Renewable and Sustainable Energy Reviews*, vol. 141, p. 110786, May 2021, doi: 10.1016/j.rser.2021.110786.

[5] P. Kusuma, P. M. Pattison, and B. Bugbee, "From physics to fixtures to food: current and potential LED efficacy," *Hortic Res*, vol. 7, no. 1, p. 56, Dec. 2020, doi: 10.1038/s41438-020-0283-7.

[6] D. D. Avgoustaki and G. Xydis, "Energy cost reduction by shifting electricity demand in indoor vertical farms with artificial lighting," *Biosystems Engineering*, vol. 211, pp. 219–229, Nov. 2021, doi: 10.1016/j.biosystemseng.2021.09.006.

[7] M. W. van Iersel, "Optimizing LED Lighting in Controlled Environment Agriculture," in *Light Emitting Diodes for Agriculture: Smart Lighting*, S. Dutta Gupta, Ed. Singapore: Springer, 2017, pp. 59–80. doi: 10.1007/978-981-10-5807-3_4.

[8] G. D. Massa, H.-H. Kim, R. M. Wheeler, and C. A. Mitchell, "Plant Productivity in Response to LED Lighting," *HortScience*, vol. 43, no. 7, pp. 1951–1956, Dec. 2008, doi: 10.21273/HORTSCI.43.7.1951.

[9] P. Pinho, K. Jokinen, and L. Halonen, "Horticultural lighting – present and future challenges," *Lighting Research & Technology*, vol. 44, no. 4, pp. 427–437, Dec. 2012, doi: 10.1177/1477153511424986.

[10] "17-29-069 | CIE." https://cie.co.at/eilvterm/17-29-069 (accessed Jul. 02, 2022).

[11] A. Barceló-Muñoz, M. Barceló-Muñoz, and A. Gago-Calderon, "Effect of LED Lighting on Physical Environment and Microenvironment on In Vitro Plant Growth and Morphogenesis: The Need to Standardize Lighting Conditions and Their Description," *Plants*, vol. 11, no. 1, p. 60, Dec. 2021, doi: 10.3390/plants11010060.

[12] D. Llewellyn, T. Shelford, Y. Zheng, and A. J. Both, "Measuring and reporting lighting characteristics important for controlled environment plant production," *Acta Hortic.*, no. 1337, pp. 249–254, Mar. 2022, doi: 10.17660/ActaHortic.2022.1337.34.

[13] L. Balazs and J. Nadas, "Spatial distribution of photon flux density created by LED grow lights," in *2020 IEEE 3rd International Conference and Workshop in Óbuda on Electrical and Power Engineering (CANDO-EPE)*, Budapest, Hungary, Nov. 2020, pp. 000147–000150. doi: 10.1109/CANDO-EPE51100.2020.9337774.

[14] A. J. Both, D. E. Ciolkosz, and L. D. Albright, "EVALUATION OF LIGHT UNIFORMITY UNDERNEATH SUPPLEMENTAL LIGHTING SYSTEMS," *Acta Hortic.*, no. 580, pp. 183–190, Jun. 2002, doi: 10.17660/ActaHortic.2002.580.23.

Development of a Luminaire for Integrative Lighting

Matej Bernard Kobav
Laboratory of lighting and photometry
University of Ljubljana
Ljubljana, Slovenia
matej.kobav@fe.uni-lj.si

Martin Krivec
University of Ljubljana
Ljubljana, Slovenia

Klemen Knez
University of Ljubljana
Ljubljana, Slovenia

Grega Bizjak
University of Ljubljana
Ljubljana, Slovenia

***Abstract* — In recent years science found out that the lighting we are using today provides adequate illumination for vision but not also for non-visual effects of light. To make lighting healthier and to boost also the biological processes in our body some steps toward integrative lighting need to be done. One of them is the development of suitable luminaires. Integrative lighting uses a full spectrum that is close to the spectrum of the sun to affect biological processes in the human body in the same way as natural light. By changing the correlated colour temperature of the light, emitted by the luminaire throughout the day, we can help our body synchronize biological processes with the day and night cycle.**

This project aimed to develop a luminaire for integrative lighting and validate it with help of measurements of the emitted light. The luminaire should be suitable for both residential and working premises. The primary purpose of developing such a luminaire is the improvement of the well-being and productivity of people who spend most of their time exposed exclusively to artificial light. One of the problems in the last decades is the excessive exposure of people to blue light in the evening. With a developed luminaire, we can regulate the amount of blue light to help users sleep better. Another important feature of the luminaire for integrative lighting is that it provides adequate illuminance in the indoor environment. The developed luminaire can adjust the luminous flux and correlated colour temperature of the light. By adjusting the output of the luminaire, we can ensure adequate illuminance and correct correlated colour temperature needed for a specific activity.

The developed luminaire was realized with a set of LEDs, chosen in a way to enable the broad possibility for adjustment of correlated colour temperature at the high colour rendering index. With help of additional optical parts, the luminaire was optimized to achieve compactness, appropriate energy efficiency, adequate light distribution, and flexibility in light adjustment. In the paper, the development of luminaire is described including a selection of LEDs, optimization of optical parts, development of a control program, and measurements of photometrical properties.

Keywords — integrative lighting, luminaire development, LED lighting, adjustable CCT, high CRI

I. Introduction

Light, both visible and invisible to us, is of fundamental importance for the life and existence of living organisms, as it affects the human body in several different ways. Information about light from the environment helps the human body to coordinate the implementation of biological processes. Biological rhythms can take place in very short cycles (milliseconds level) or cycles lasting several years. Biological processes that follow the cycle of day and night or are repeated in approximately 24-hour intervals are also known as circadian rhythms. Circadian rhythms are physiological, behavioural, and biochemical changes in the human body that recur at 24-hour intervals.

We know more than a hundred different processes that take place in circadian rhythms, including the cycle of sleep and wakefulness, fluctuations in body temperature, changes in hormone levels, fluctuations in blood pressure, fluctuations in heart rate and others. In the human body, these processes are controlled by the so-called suprachiasmatic nuclei (SCN) in the brain. SCN regulates the release of melatonin based on light information obtained through light-sensitive cells in the eye [1]. These cells are most sensitive to blue light, which regulates melatonin levels in the body. Melatonin is an important hormone that tells the body that it is night and time for rest and regeneration. During the day, when a large proportion of blue light is present in natural light, the release of melatonin in the body is inhibited. Towards evening, when the proportion of (blue) light decreases, melatonin begins to be released again and the body prepares to rest. Therefore, the adequate concentration of melatonin in the body has a great impact on the well-being of the individual. The release of melatonin and the coordination of other processes that take place in circadian rhythms, therefore, depends on the periodically changing light in the environment.

Integrative lighting is supposed to affect the biological processes in our body in the same way as natural (outdoor) light. With such lighting, we can help the body to better define the phases of rest and activity. Integrative lighting is thus especially suitable for places where people spend a lot of time every day. The most appropriate use of such lighting is in the workplace, in educational and medical institutions, and in nursing homes [2], [3].

II. Influence of Light on Humans

With biological rhythms, the human body adapts to periodic changes in the environment. Although biological rhythms in the body are genetically determined or created by the body naturally, they are also regulated by environmental influences, such as light and temperature [4], [5]. Biological rhythms are taken care of by the biological clock, which is a biochemical oscillator and is the body's innate molecular mechanism. The biological clock creates and controls circadian rhythms. Light can activate and deactivate genes that control the molecular composition of the biological clock. Changing the cycles of darkness and light can speed up, slow down, or reset the biological clock and thus circadian rhythms. SCN have the function of the main biological clock in the human body. SCN is a small area of the brain in the hypothalamus and is responsible for the coordinated functioning of all circadian processes in the body, as shown in Fig. 1. Suprachiasmatic nucleus is made up of about 10,000 nerve cells or neurons, with SCN obtaining light information directly from the eye [1].

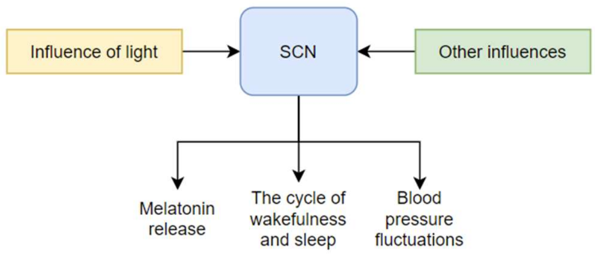

Figure 1: Illustration of the influence of light on biological processes

There are 3 types of photoreceptor cells in the human eye: cones, rods, and intrinsically photosensitive retinal ganglion cells (ipRGC). The cones and rods serve to form the image, while through the ipRGC cells the suprachiasmatic nucleus obtains information about the illuminance at the retina [6]. Light-sensitive ganglion cells have not yet been studied in detail. The fact that light affects the release of melatonin in blind people, confirms the existence of third types of photoreceptors in addition to cones and rods. Nevertheless, according to previous research, rods and cones are not completely ruled out when playing a role in circadian rhythms. Also, research to this date has not confirmed that hitherto known photoreceptors play a primary role in regulating melatonin in the body [7]. The light sensitivity of ipRGC is provided by the photo pigment melanopsin contained in these cells. Melanopsin is most sensitive to light of wavelengths between 460 nm and 484 nm (blue part of the spectrum). Fig. 2 below shows the areas of maximum light sensitivity of melanopsin, rods and cones in relation to wavelength. The white curve illustrates the light sensitivity range of melanopsin. In this range of wavelengths, we can achieve the greatest influence of light on the release of melatonin in the body. In addition to the appropriate wavelength, the angle of incidence of light in the eye and sufficient illumination of the retina are also important. Maximum stimulation of light-sensitive ganglion cells is achieved when light enters the eye by illuminating as much of the retina as possible [8].

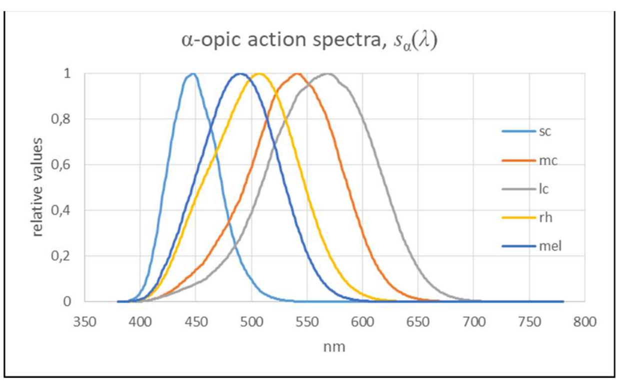

Figure 2: Light sensitivity of photoreceptors [9]

Melatonin is a hormone found in humans, animals and other organisms. It has a significant effect on the processes in the body, is a good antioxidant, strengthens the immune system, lowers body temperature and, among other things, causes fatigue. Exposure to light with high illuminance values has a greater impact on the activation of the nervous system. The release of melatonin during the day, when natural light has the highest intensity and the highest content of the blue part of the spectrum, is limited. In the evening, however, the release of melatonin in the body increases as the body prepares for rest [3]. The suprachiasmatic nucleus sends information to other hypothalamic nuclei and the pineal gland, which secretes melatonin into the human body. Melatonin release is reduced when the retina is exposed to light of appropriate intensity and wavelength. The time of melatonin secretion, on the other hand, is determined by the length of the dark cycle [5]. The discovery of this new light-sensitive system in the human body is the main reason for the beginning of the development of the integrative lighting [10].

A. Usage of the integrative lighting

Studies have shown that by changing the correlated colour temperature (CCT) of light according to activity, we can achieve greater concentration, attention and productivity of students in schools. For work that requires more concentration, one would increase the luminous flux and raise the correlated colour temperature of light, while for more relaxed activities, the latter two parameters should be lowered, as lower CCT values have a more calming effect on humans [8].

Integrative lighting is especially suitable for places where people live, such as nursing homes, where such lighting can improve the lives of both the elderly and staff. Especially in older people, lack of activity during the day can lead to drowsiness during the day and trouble sleeping at night. Older people, due to the yellowing of the lenses in the eyes, also need higher illuminances in rooms [8]. With different profiles of changing luminous flux and correlated colour temperature of light, we can achieve synchronization of circadian rhythms with day and night, as well as improve the productivity of people in certain parts of the day [8] .

Increasing knowledge of the effects of light on the human body is reflected in the increasing use of the integrative lighting in medicine. It is used to treat patients with depression, sleep disorders and chronic fatigue. It also shows good potential in treating Parkinson's disease. One of the symptoms of this disease is the problem of sleeping at night and staying awake during the day [11]. Research on the use of the integrative lighting in patients with dementia also shows positive results regarding sleep problems [12].

The integrative lighting can also help reduce circadian rhythm disturbances due to shift work. An example of such work is working in production in three shifts (morning, afternoon and night shift). Shift work has many negative consequences for health and quality of life. Night workers report mostly problems with insomnia or excessive sleep [13]. Pilots and passengers on intercontinental flights also have problems synchronizing circadian rhythms. On longer flights heading east or west, people travel through multiple time zones in a relatively short amount of time. The result is a time lag between the day and night they experience, which also leads to a time lag in the circadian rhythms.

.

III. MANUFACTURE OF LUMINAIRE

A. Luminaire requirements

The goal is to make a luminaire with a light spectrum as similar as possible to the spectrum of natural light. The light must contain a sufficiently large proportion of the blue light of wavelengths between 460 nm and 484 nm. Adequate luminous flux and proper light distribution are also important, as sufficient retinal illumination in the eye, as already mentioned, reduces drowsiness and increases human concentration [5]. The luminaire must achieve a luminous flux of at least 5000 lm at all settings of correlated colour temperature and have a large luminous surface. The light must enter the eye at a certain angle, as light-sensitive ganglion cells are located at the back of the retina. The optimal angle of incidence is from 45° to 90° in relation to the vertical, while the incidence of light in the eye from below or at an angle greater than 90° is not desirable due to glare. Glare can be eliminated with different types of light diffusers and the position of the luminaire in the room. The luminaire must be capable of adjusting the luminous flux and correlated colour temperature of the light (from 3000 K to at least 8000 K). The value of the colour rendering index should be greater than 80 throughout the range of correlated colour temperature and as constant as possible. It must be possible to automatically set these two parameters according to predefined profiles (for example, simulating changes in intensity and correlated colour temperature of natural light during the day). Due to the desire for a low price of the final product and the cost of production, we try to use as few different LEDs as possible to achieve the above requirements.

B. Choice of the light source

Initially, the magnitude of the luminous flux was the only parameter considered in lighting technology. The only electric light source was a light bulb and other parameters could not be changed. With the advent of fluorescent tubes, two other important light parameters emerged: correlated colour temperature (CCT) and colour rendering index (CRI). Energy-saving or efficiency and lifetime of the light source have also become increasingly important parameters [8, 9]. To design a luminaire for integrative lighting, several approaches are possible regarding the choice of the type of light source. Fluorescent tubes, light-emitting diodes or a combination of both can be used. The approach with a combination of light-emitting diodes and fluorescent tubes enables the achievement of high values of both CCT and CRI, but the main problem with such an approach is the demanding implementation of luminaire control. So it makes the most sense to choose only LEDs. With different types of LEDs, we can create light with high values of CRI and the regulation of CCT and the luminous flux is quite simple. Namely, the LEDs enable the regulation of the luminous flux using the regulation of the electric current through the LEDs. The small dimensions of the LEDs also allow flexibility in choosing the physical shape of the luminaire. When choosing LEDs, we also take into account their angle of light emission, light efficiency, current in the conduction direction and service life.

C. Design of a luminaire for integrative lighting

The program for calculation of light parameters based on the light spectrum served as the basis for selecting the appropriate LEDs and the number of these. In the phase of selecting the appropriate LEDs for the luminaire, we first used multiple spectra from data sheets. Theoretical calculations of the parameters were performed with several different potentially suitable LEDs. The light-emitting diodes, which proved to be potentially suitable for use in the luminaire, were then ordered from the manufacturer and their actual light spectra were measured in the laboratory. The most important parameters in the selection of LEDs were: the high value of the colour rendering index, the correlated colour temperature and luminous flux. It turned out that the combination of three different LEDs already achieves satisfactory results. Since the selected LED driver had four outputs, a fourth LED was added, as the combination of four different LEDs allows for higher resolution when setting the correlated colour temperature and higher luminous flux of the luminaire. Fig. 3 is showing diode spectrum summation algorithm. The input data are measured spectra of individual LEDs. These data are processed and weighted according to the number of LEDs. The possibility of adjusting the luminous flux of individual groups of LEDs as well as all LEDs together has been added. In the last part, the summation and normalization of the spectra are performed. The final spectrum is saved in a graphical form and in the form of a table.

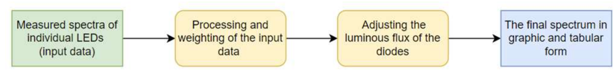

Figure 3: Diode spectrum summation algorithm

In the final version of the luminaire, four different LEDs were selected. The LEDs were selected to meet the above requirements of integrative lighting. LEDs with CCT values of 2800 K and 5500 K ensure adequate values of the CCT in the lower range, while LEDs with CCT values of 6600 K and LEDs with blue light are responsible for adequate values of CCT in higher range. In Fig. 4 we can see the normalized spectra of both types of blue LEDs. For testing purposes, two luminaires with two different types of blue LEDs (one with a peak wavelength at 453 nm and one with a peak at wavelength of 475 nm) were made. The dark blue curve shows the spectrum of a LED with a peak at 453 nm and a light blue curve the spectrum of a LED with a peak at 476 nm.

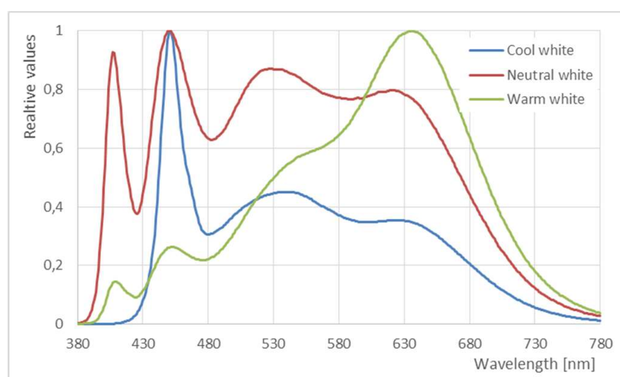

Figure 4: Normalized spectra of white LEDs

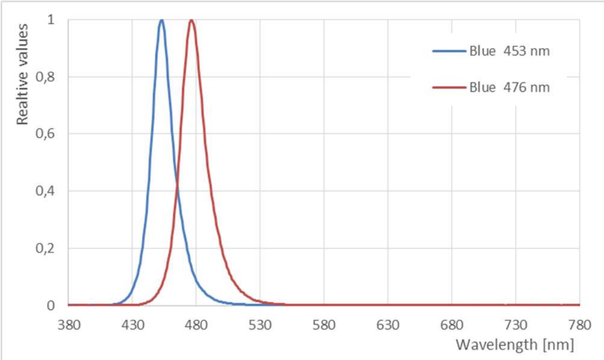

Figure 5: Normalized spectra of both blue LEDs

The luminaire housing is made of painted metal sheet and ensures the mechanical strength of the luminaire. Edge strips are designed to allow the insertion of a light diffuser. The diffuser is built out of two layers. The outer layer has a microprismatic surface and together with the inner opaque layer ensures soft and even scattering of LEDs light. The width and length of the housing are 60 cm, which allows installation in standard ceiling panels measuring 60 cm × 60 cm. The height of the housing is 9 cm. Fig. 5 shows the entire system, which consists of a luminaire in a housing with a light diffuser installed, a LED driver with a connecting cord and an interface for serial communication with a computer. The LED driver is installed in an additional metal housing, which has the option of mounting on an existing luminaire housing and is attached with two screws.

There are 128 LEDs on each printed circuit board, of which 32 are LEDs with blue light, 32 with cool white light, 32 with neutral white light and 32 with warm white light. There are four groups of eight LEDs connected in series on each printed circuit board, which can ensure an even distribution of light over the entire illuminating surface of the luminaire. Four identical printed circuit boards are installed in the luminaire. The total number of LEDs in the luminaire is therefore 512, of which 128 LEDs of each type. A LED driver, which allows an independent setting of the outputs for individual groups of LEDs, was chosen to power the luminaire. Communication is possible via two different inputs: DALI (Digital Addressable Lighting Interface) and DMX (Digital Multiplex protocol). In this case, the DMX512 digital protocol is selected. It is most often used for stage lighting, but it is also increasingly penetrating the field of architectural lighting. The LED driver also allows different profiles and dimming speeds and smooth transitions between different output settings. The input for NTC (negative temperature coefficient) thermistor allows thermal control over the heating of LEDs.

Figure 6: Assembled luminaire with power supply and converter for serial communication

IV. Luminaire analysis

The current of the LEDs at the LED driver output, the temperature at the luminaire components during operation, the light spectrum, the colour rendering index and the correlated colour temperature were measured. To test the luminaire, a program was developed that allows communication with the luminaire driver. The program consists of a part that allows adjusting the total luminous flux of the luminaire and the luminous flux of individual groups of LEDs and a part that allows setting the appropriate CCT value by adjusting the luminous flux of individual groups of LEDs. To achieve lower values of CCT, we need a higher luminous flux of light-emitting diodes with warm white and neutral white light, while to achieve higher values of CCT we need a higher luminous flux of blue and cold-white LEDs. The program allows setting CCT values from 2800 K to 10500 K with a 100 K step, while in the range from 10 500 K to 14 000 K a 500 K step is used. In the last part of the range, the step is larger, as 8-bit communication does not allow a more precise setting.

To achieve different values of CCT, the luminaire was first set based on theoretical calculations. This was followed by laboratory measurements and verification of the accuracy of the saved settings. The results based on the calculations turned out to be largely in line with the measured values. The values of correlated colour temperature deviate on average by 1.2%, and the values of the colour rendering index by less than 1.0%. Despite small deviations, we further optimized the luminaire setting based on measurements. The purpose of the optimization was to achieve more accurate values when setting a correlated colour temperature. Data from the data sheets of individual LEDs were the basis for calculating and adjusting the luminous flux of the luminaire. The calculations in this way are satisfactory, as we were not interested in the actual value of the luminous flux of the luminaire at this stage. However, it was important to maintain a constant magnitude of the luminous flux at different CCT values. The desired deviation of the luminous flux size for individual settings of correlated colour temperature was less than 10% of the maximum value.

A. LED current measurements

To maintain the constant luminous flux of the luminaire at different values of CCT, measurements of the output current of the LED driver are required. The values were measured at different luminous flux settings of individual groups of LEDs. The purpose of the measurements is to determine the linearity of the ratio between the set value and the current at the output of the LED driver, which later serves to ensure a constant magnitude of luminous flux at different settings of correlated colour temperature. *Figure 7* shows the measurement results for all four diodes used.

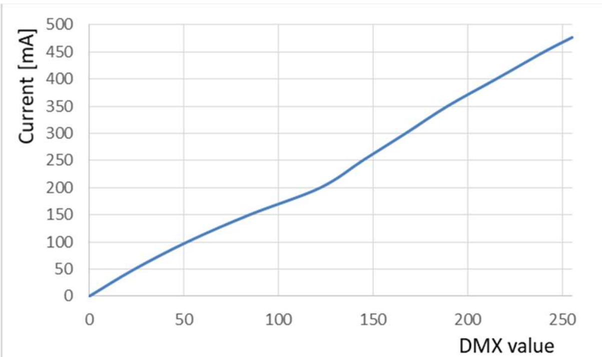

Figure 7: The ratio between the current and the set value for the diodes

B. Colour rendering index measurements

As already mentioned, the colour rendering index tells us to what extent the light of a certain light-emitting diode realistically represents the colours of an object compared to reference light source. Since the goal of developing the luminaire is to ensure the highest possible values of the colour rendering index, LEDs with high values of the colour rendering index were chosen. In particular, we are interested in how the values of the colour rendering index change when combining the light of different LEDs to achieve different values of the correlated colour temperature. The measured values of CRI and CCT of individual LEDs are presented in Table 1.

TABLE 1: MEASURED VALUES OF CRI OF INDIVIDUAL LED

LED	CCT [K]	CRI
Warm white light	2800	97,5
Nutral white light	5500	96,3
Cool white light	6600	95,5

Colour rendering index measurements were performed in the range of 3000 K to 14 000 K. The graph in Fig. 8 shows the values of the colour rendering index for a luminaire with a blue diode with a peak wavelength of 476 nm.

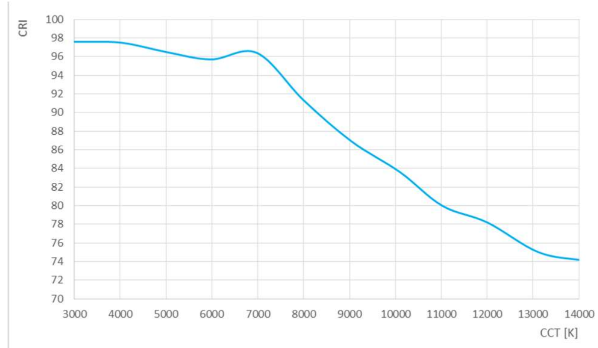

Figure 8: CRI depending on CCT for a luminaire with a blue diode with a peak wavelength of 476 nm

Choosing LEDs with high values of colour rendering index allows us to achieve values of colour rendering index above 95 in the range from 3000 K to 7200 K. At higher values of correlated colour temperature, the colour rendering index begins to decline with the addition of blue light. At a CCT value of 14 000 K, the light of the luminaire has a CRI value of 74.

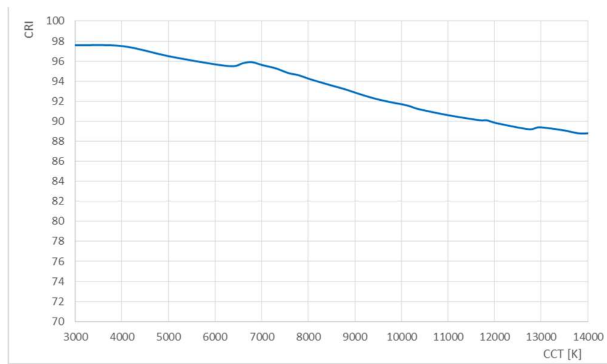

Figure 9: CRI depending on CCT for a luminaire with blue diode with a peak wavelength of 453 nm

Fig. 9 shows the measured values of the colour rendering index for a luminaire with the blue light with a peak wavelength at 453 nm. From the results of measurements of the colour rendering index for a LED with a wavelength of 453 nm, one can see much higher values over the entire range of correlated colour temperature. The disadvantage of using this LED is the lower efficiency of the luminaire in terms of achieving higher light output at wavelengths between 460 nm and 480 nm. The choice of LEDs with blue light is therefore a compromise between achieving better values of the CRI and luminous flux at wavelengths important for the integrative lighting. Given the achievement of satisfactory values of the CRI in both cases, the better choice is a luminaire with blue LEDs with a peak wavelength of 476 nm.

C. Measurements of spectra

Light spectra measurements were performed on all three white LEDs and both types of blue LEDs at different luminaire settings. From the graph in Fig. 4, it can be seen that blue LEDs with a peak at a wavelength of 476 nm are more suitable for a integrative lighting luminaire. The light-sensitive ganglion cells in the human eye are the most sensitive to light wavelengths between 460 nm and 484 nm.

The measurements of the light spectra of the luminaire at different settings of the correlated colour temperature of light are presented below. All values of correlated colour temperature in the range from 2800 K to 14000 K were measured in increments of 200 K. For a better overview, only measurements at selected values are presented, as can be seen in Fig. 10.

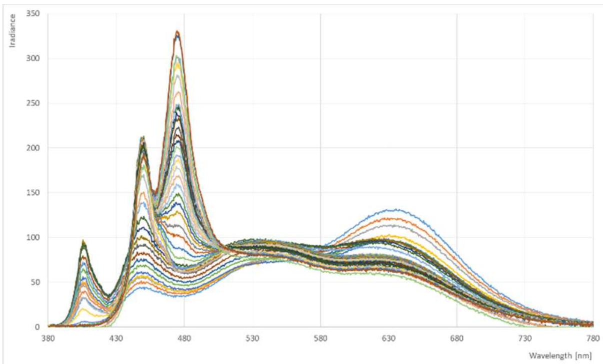

Figure 10: Light spectra from 3000 to 11 000 K

D. Luminaire optimisation

The current version of the luminaire allows achieving approximately 3100 lm luminous flux at the lowest settings of a correlated colour temperature (2800 K). At the highest settings of correlated colour temperature (14000 K), values of around 7000 lm can be achieved. Light-emitting diodes with warm white light are limiting luminaire to achieve higher luminous flux at low CCT values. By installing warm white LEDs with twice the luminous flux, values of approximately 7000 lm could be achieved over the entire range of correlated colour temperature. At the same time, this would increase the efficiency of all LEDs in the luminaire. In the current version, blue LEDs are supplied with only 34.5% of the rated current at the set value of CCT = 14000 K, while cold white LEDs are supplied with 93.7% of the rated current. By using more powerful LEDs with warm white light, we could thus achieve one hundred per cent utilization in terms of rated current. Another option is to use twice as many LEDs with warm white light (2800 K). If reaching a luminous flux of up to 3100 lm is satisfactory, weaker blue LEDs could also be installed, as this would also improve the utilization of all LEDs in the luminaire. We used 8-bit communication to adjust the luminaire. Because the luminaire power supply also provides a 16-bit connection, using a 16-bit converter for serial communication, it could be possible to achieve better results in terms of setting a constant luminous flux and correlated colour temperature. With 16-bit communication, we could also achieve more continuous transitions during the setting of the mentioned parameters, and at the same time, this would enable a more precise setting of the luminaire. For testing purposes, however, 8-bit communication was satisfactory.

Integrative lighting is not only suitable for rooms where only artificial light is available, but also for rooms where natural light is also available. In rooms with windows, the luminaire would serve as a complementary light source. The luminous flux of the luminaire would be adjusted to the amount of natural light entering the room through the windows, as shown in Fig. 11. Such regulation of the luminous flux of the luminaire could provide better tracking of CCT of natural light. Also, the luminous flux would increase if the user uses the blinds on the windows. The reverse would of course apply to sunny days and open shades. Automatic adjustment of the luminous flux of the luminaire is possible with the help of a computer program, light sensors and a control system. According to information obtained from light sensors, the luminaire would adapt in real-time to the current lighting conditions in the room. Adjustment is possible both in terms of luminous flux and correlated colour temperatures, but of course, the user could also adjust the room brightness manually if necessary.

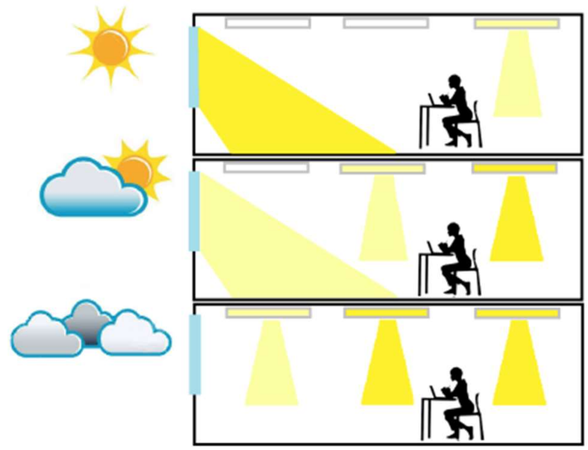

Figure 11: A combination of artificial and natural light

As already mentioned, the goal of integrative lighting is to help synchronize biological processes in the body with respect to day and night. By automatically adjusting correlated colour temperature and luminous flux, we can simulate changing natural light during the day. The problem in modern times is mainly excessive exposure to blue light in the evening when the human body is preparing to rest. In the case of switching on the luminaire in the evening or at night, the luminaire would automatically set the lowest value of a correlated colour temperature, where the amount of light wavelengths between 460 nm and 484 nm is small. The profile of changes in luminous flux and correlated colour temperature during the day could also be adjusted to the changing length of day and night during the year.

V. CONCLUSION

The paper presents several ways in which light affects humans, focusing on the influence of the blue colour of light on human circadian rhythms. To reduce the negative impact of artificial lighting, integrative lighting can be used. The methodology of manufacturing and designing a integrative luminaire was presented, which allows setting a correlated colour temperature from 2800 K to 14000 K. This means that the range of correlated colour temperature is therefore much larger than originally required. The adjustment of the luminous flux was also provided. During the design of the luminaire, a program for communication with the luminaire was developed, which allows the adjustment of individual groups of LEDs independently. This facilitates the further development of the luminaire. The measurement results show that the CRI, when using blue LEDs with a wavelength of 476 nm exceeds 80 in the CCT range from 2800 K to 11000 K. The light contains a sufficient portion of blue light with wavelengths between 460 nm and 484 nm. The light diffuser allows even distribution of light and prevents glare, while the construction of the luminaire allows installation in standard ceiling panels of 60 cm × 60 cm. This design also makes it easy to replace existing luminaires with fluorescent tubes. The next goal in the development of this luminaire will be to achieve a higher luminous flux at lower CCT values, which occurs due to insufficient luminous flux or the number of LEDs with warm white light.

ACKNOWLEDGMENT

We would like to thank company Ledluks d.o.o. (ledluks.com), Vrtojba, Slovenia for the support at producing an integrative luminaire.

REFERENCES

[1] A. P. Patton and M. H. Hastings, "The suprachiasmatic nucleus," Curr. Biol., vol. 28, no. 15, pp. R816–R822, Aug. 2018, doi: 10.1016/j.cub.2018.06.052.

[2] C. Barkmann, N. Wessolowski, and M. Schulte-Markwort, "Applicability and efficacy of variable light in schools," Physiol. Behav., vol. 105, no. 3, pp. 621–627, Feb. 2012, doi: 10.1016/j.physbeh.2011.09.020.

[3] M. Pfeffer, H.-W. Korf, and H. Wicht, "Synchronizing effects of melatonin on diurnal and circadian rhythms," Gen. Comp. Endocrinol., vol. 258, pp. 215–221, Mar. 2018, doi: 10.1016/j.ygcen.2017.05.013.

[4] P. Emery, W. V. So, M. Kaneko, J. C. Hall, and M. Rosbash, "CRY, a Drosophila Clock and Light-Regulated Cryptochrome, Is a Major Contributor to Circadian Rhythm Resetting and Photosensitivity," Cell, vol. 95, no. 5, pp. 669–679, Nov. 1998, doi: 10.1016/S0092-8674(00)81637-2.

[5] R. Leproult, E. F. Colecchia, M. L'Hermite-Balériaux, and E. Van Cauter, "Transition from dim to bright light in the morning induces an immediate elevation of cortisol levels," J. Clin. Endocrinol. Metab., vol. 86, no. 1, pp. 151–157, Jan. 2001, doi: 10.1210/jcem.86.1.7102.

[6] M. T. H. Do and K.-W. Yau, "Adaptation to steady light by intrinsically photosensitive retinal ganglion cells," Proc. Natl. Acad. Sci., vol. 110, no. 18, pp. 7470–7475, Apr. 2013, doi: 10.1073/pnas.1304039110.

[7] "Action Spectrum for Melatonin Regulation in Humans: Evidence for a Novel Circadian Photoreceptor | Journal of Neuroscience." https://www.jneurosci.org/content/21/16/6405 (accessed May 03, 2022).

[8] M. B. Kobav and Bizjak, Grega, "With LEDs toward biologically active lighting," Proc. Balk. Light 2015 16-19 Sept. 2015 Athens Greece, vol. 2015, pp. 429–433, 19. 9 2015.

[9] Cie, "CIE S 026/E:2018 CIE System for Metrology of Optical Radiation for ipRGC-Influenced Responses to Light," International Commission on Illumination (CIE), Dec. 2018. doi: 10.25039/S026.2018.

[10] J. P. Hanifin and G. C. Brainard, "Photoreception for circadian, neuroendocrine, and neurobehavioral regulation," J. Physiol. Anthropol., vol. 26, no. 2, pp. 87–94, Mar. 2007, doi: 10.2114/jpa2.26.87.

[11] Linda Geddes, "Using light to reset the body clock can treat brain disorders," New Scientist. https://www.newscientist.com/article/mg23531335-300-using-light-to-reset-the-body-clock-can-treat-brain-disorders/ (accessed May 03, 2022).

[12] E. van Lieshout-van Dal, L. Snaphaan, and I. Bongers, "Biodynamic lighting effects on the sleep pattern of people with dementia," Build. Environ., vol. 150, pp. 245–253, Mar. 2019, doi: 10.1016/j.buildenv.2019.01.010.

[13] E. M. Wickwire, J. Geiger-Brown, S. M. Scharf, and C. L. Drake, "Shift Work and Shift Work Sleep Disorder: Clinical and Organizational Perspectives," Chest, vol. 151, no. 5, pp. 1156–1172, May 2017, doi: 10.1016/j.chest.2016.12.007.

Practical Usage of UV-C for Surface and Air Disinfection

Seifert, Dirk
Signify GmbH
(former Philips Lighting)
Hamburg, Germany
dirk.seifert@signify.com

Abstract: **The use of UV-C radiation for disinfection purposes has existed since the 1930s. Up to now, it has generally been used for special applications in industry, for example in medicine, pharmacy or food processing, as well as for the disinfection of water or applications in materials technology. Sometimes direct UV-C was used for room air disinfection. The current pandemic situation has made it interesting to use UV-C more widely for surface and air disinfection. The Covid-19 pandemic has put a spotlight like never before on the role of ultraviolet light for germicidal irradiation. However, in my view, professional handling of this technique is necessary to avoid risks and to enable effective application. Here special attention will be given to the application of air disinfection in different practical applications.**

Keywords: Disinfection, UV-C Radiation, Germs, Virus, Upper Air,

I. Introduction Application of UV-C Radiation

We are living with viruses and bacteria's around us. The current pandemic situation has thrown this into a new light – also under the view of reduction. The germicidal effects of short wave ultraviolet (UV-C) radiation were first discovered in 1877 and the 1903 Nobel Prize for Medicine was awarded to Niels Finsen for his use of UV-C against tuberculosis of the skin. The effect of UV-C radiation for purposes of disinfection of air and surfaces was already proven in the 1930s. UV-C for the disinfection of drinking water was already used professionally in 1906 (von Recklinghausen) and 1910 in Marseille. Between 1937 and 1941 upper-room UV-C was used in suburban Philadelphia schools to prevent the spread of measles. Up to now, UV-C has been used for special applications such as in medical technology, pharmacy or food processing as well as for the disinfection of drinking water or different applications in industry. Due to the current pandemic situation it became interesting to use UV-C for surface and air disinfection more broadly. Professional handling of this technology is necessary to ensure a safe and effective application of the UV-C radiation.

The use of ultraviolet radiation has become widespread as it is effective and non-contact in inactivating viruses, bacteria, spores and fungi on surfaces and in the air [1-3]. Since the spectral portion in the UV-C range of solar radiation on Earth is already predominantly absorbed in the atmosphere, living organisms, microorganisms and viruses have not developed natural resistances to this radiation. As the World Health Organization put it: „The virus can also spread in poorly ventilated rooms and/or crowded settings where people tend to spend longer periods of time. This is because aerosols remain suspended in the air or travel further than 1m." [4] Or equally, take these comments from the Centers for Disease Control and Prevention in the US: „Breathing in air when close to an infected person who is exhaling small droplets and particles that contain the virus is a key way the virus is transmitted." [5]

MODE OF ACTION: Absorption of UV-C radiation in cells directly destroys the DNA/RNA in its structure. Thus the reproduction of the cell is prevented and a possible infection ability of microorganisms is stopped. The maximum effectiveness for disinfection is at 265nm (DNA effective spectrum also shown in DIN5031-10 2000-03) [6]. Depending on the type of germ, a certain radiation dose is required for disinfection - determined by irradiation intensity and required irradiation time [in J/m²]. Viruses (common: 6-8J/m² for 90% disinfection rate) are the easiest to deactivate in contrast to bacteria & yeasts (between 6 and 31 J/m²) and fungi (315-488 J/m²) - fungal spores may require about a hundred times the dose for a similar disinfection rate compared to viruses. The effectiveness in air is additionally dependent on the degree of humidity.

Action of UV-C Radiation on DNA & Examples

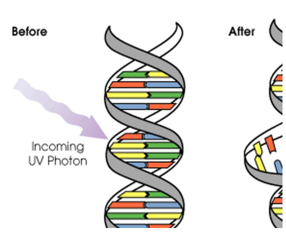

Germ	Dose for log1
Legionella pneumophila	9
Salmonella enteritidis	40
Salmonella typhimuurium	80
SARS CoV 2	**18**
Hepatitis A	73
Influenza Virus	36
Mycobacter.Tuberculosis	60

Examples different germs and needed desinfection Dose for log1 (>90%)

Fig. 1. Action of UV-C on DNA/RNA – destroy stability (inactivation) (Source: Signify/Philips)

Common UV-C lamps typically produce their peak wavelength at 254nm, which is close to the maximum effectiveness of UV-C (265nm). This wavelength is absorbed by organic substances, breaking the nucleobases of DNA of bacteria and viruses etc.

Example output of typical UV-C Low pressure Mercury Discharge lamps

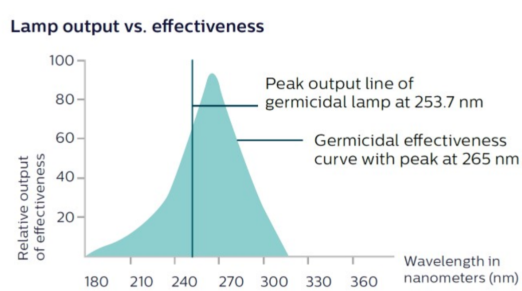

Fig. 2. Lamp output vs. effectiveness (Source: Signify/Philips)

The most common sources of UV-C are gas discharge lamps (low pressure mercury discharge – principe near the Fluorescent lamps) in various formats. They mostly look like traditional fluorescent lamps without the phosphor coating, which produce radiation at a wavelength of 254nm. Other types (such as KrCl) produce radiation at 222nm and there are developments in LED technology that will also produce UV-C. LED UV-C sources now not long time stabil in function.

All bacteria and viruses tested so far respond to UV-C disinfection. And there have been many hundreds over the years, including various coronaviruses [7,8]. Therefore, UV-C radiation can also be used to supplement existing hygiene concepts, for example, in the fight against COVID-19. Further advice and information on this topic can be found in the current ZVEI position paper [9]. In order to avoid risks and to ensure optimal effectiveness, the ZVEI advises expert support in the planning and installation of the devices. UV-C disinfection can be a part of modern disinfection strategy, is without toxic chemicals and can be a simple, sustainable and safety conscious solution. The disinfection effect is directly related to the UV-C dose (measured in Joules/m²).

II. Systems and effectiveness against germs Calculation Principles

UV-C dose - this is the product of the irradiation and the time. The susceptibility of the virus to the UV-C also has to be taken into account by what is known as its k(λ) factor, which varies from virus to virus, and whether it is on a dry surface of in suspension in droplets (ISO15714) [10]. It is also affected by the wavelength of UV-C used.

Dose 1 J/m²= 0,1 mJ/cm² = Irradiance 1 W/m² x Time 1 s

For the irradiation of surfaces, it is possible to use standard lighting software but with units re-calibrated into W/m² instead of lux (UV-C distribution curve instead of light distribution curve).

Example Surface Disinfection in an empty room (no Poeple)

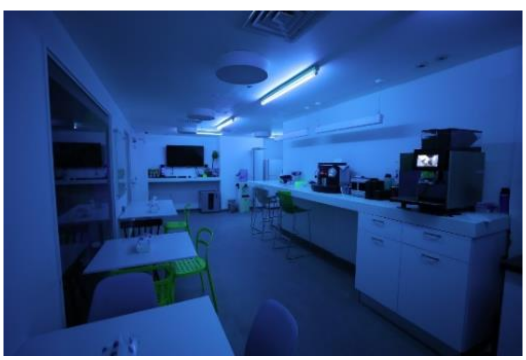

Fig. 3. Surface disinfection from UV-C battens in a laboratory - persons during operation not present (Source: Signify/Philips)

For disinfection in air, it is rather more complex, as we have to think in terms of 'Spherical Irradiance', which has the term 'Fluence Rate' and the Dose is termed 'Fluence'. To calculate the Fluence we need to know how long a virus suspended in a droplet will be in irradiated. This means we have to predict the air movement within a space. Whilst this can be done by computational fluid dynamics, the technique involves complex modelling.

So, when designing air disinfection systems, we usually just calculate the Fluence Rate together with an understanding that there is air movement and mixing in the room.
Another term used is the 'log' reduction. This is simply the % reduction in the virus over a given time. A log1 reduction is 90%, log 2 is 99%, log3 is 99.9% and so on. With a grasp of Irradiance, Fluence, Fluence Rate and Log reduction the lighting designer can transition into a UV-C designer.
For the lighting designer, the shift to calculating with UV-C will see them using similar techniques as they do for light with a few differences. When calculating the surface irradiance, we are looking for the minimum not the average as we want to ensure we can eliminate viruses in all locations.

Example Upper Air Disinfection in an room (People allowed)

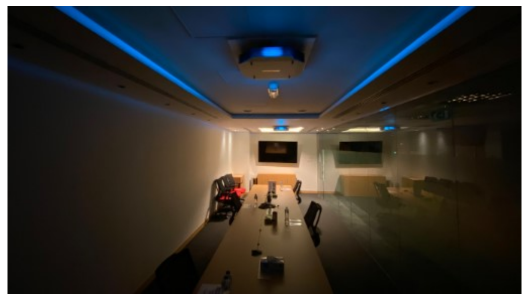

Fig. 4. Upper air UVGI. The small amount of visible blue light in the beam shows where the UV-C is (Source: Signify/Philips)

Also, the reflection properties of surfaces to UV-C are quite different to light and depend on the material. A dark surface, for example, might have a higher UV-C reflection compared to a light one. The table below (figure 5) shows typical values for different surfaces.

Example Reflection Degrees UV-C of different Materials

Reflection factors for UV-C radiation

Material	Reflectance %
Aluminium: untreated surface	40-60
Aluminium: sputtered on glass	75-85
Stainless steel / Tin plate	25-30
Chromium plating	39
Various white oil paints	3-10
Various white water paints	10-35
Aluminium paint	40-75
Zinc oxide paint	4-5
Glass	2
White plastering	40-60
Painted Walls	5-15
Calcium carbonate	70-80

Fig. 5. Typical UV-C reflectance values for different surfaces (Source: Signify/Philips)

There has been much research into the effect of UV-C on viruses such as tuberculosis. Since the start of the pandemic, new research has been carried out to confirm that the Sars-CoV-2 virus responds to UV-C in the same way as other viruses.

For example, research conducted by The National Emerging Infectious Diseases Laboratories (NEIDL) at Boston University demonstrated that a UVC dose of 290

J/m² could achieve a log4 reduction of the Sars-CoV-2 virus on surfaces [8]. Other research has also shown a room with an average Fluence Rate of 40mW/m² gave a log4 reduction in airborne viruses in 10 minutes [11].

In design and calculation always efficiency of disinfection and safety is in the focus. UV-C light should always be used by professionals in accordance with the safety requirements and instructions to avoid humans and animals from being exposed to it since it can damage their skin and eyes.

APPLYING TECHNOLOGY IN PRACTICE
A. SURFACE DISINFECTION

For surface disinfection we can install UV-C in battens over the area to be disinfected. However, only the surfaces in direct sight of the UV-C source will be treated, so anywhere where there are shadows will be missed. It is better to use fewer smaller sources that will create fewer shadows than a single larger one. Under safety view surface disinfection systems not allowed to operate when persons are in the UV-C Beam.

Once this has been calculated, we can work out the duration of the exposure to give the Dose. Disinfection chambers for example can be used for small items such as keys and phones. For room surfaces in rooms (without people during operation) can be used Battens with or without reflector.

Calculating for surface disinfection can be done with any standard lighting software (Dialux, Relux, Visual etc). You just need to use units of mW (UV-C Distribution Curve of the luminaire) instead of lumens and you will get an irradiance in mW/m² in the calculated room. Then multiply by time to get the dose on one point or area.

Below are two images for a washroom application. The grey scale shows the visualization of the space, the colours represent the irradiance values going from yellow (highest) to black (lowest). From this it is easy to see what areas are receiving sufficient irradiation and what are in shadow.

CALCULATION OF SURFACE DISINFECTION IN LIGHTING SOFTWARE

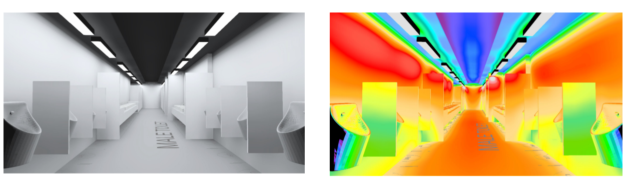

Fig. 6. 3D model & 3D pseudo color represenation of irradiance (Source: Signify/Philips)

APPLYING TECHNOLOGY IN PRACTICE
B. AIR DISINFECTION

Upper air solutions require the system to be operating while the room is occupied to disinfect the air at source. This means that, whilst a high irradiation is required at ceiling height, it must be limited at head height (1.83m) or lower hights. These "upper air" units typically produce a narrow beam, in the order of a few degrees parallel to the ceiling. In these situations, the reflection of the UV-C from the ceiling must be considered as it can make significant contribution to the UV-C at head height. A calcium whitener in a ceiling tile, for example, will cause it to be highly reflective to UV-C, whereas a white acrylic paint will hardly reflect any.

With upper-air solutions, you should also consider how the room is being used. For example, in a typical office it is unlikely that anyone will be standing in the exact spot where the maximum irradiance occurs for eight hours. So, a calculation is also made for the time spent sitting and the total daily dose calculated. For upper air systems we have to calculate both the Fluence Rate, which gives us the effectiveness of disinfection, and check the safe Dose for exposure.

It is recognised that air movement in a room will help disperse airborne viruses and often this is related to **the air changes per hour** (ACH).

The basic ventilation rate required for fresh air, low CO_2 and odor levels is mostly accomplished with 1-6 ACH, sometimes up to 8 ACH. Opening windows gives 1-2 ACH, maybe higher, but with discomfort. Increasing the basic ventilation rate significantly, for example to ACH 15-20, is a well-known method to reduce pathogen levels for disinfection, especially in healthcare applications.

Experiments with upper-air UVGI solutions have shown that the disinfection achieved can be equivalent to up to 50 ACH (eqACH), providing there is basic air movement in the room to start with. Equivalent ACH is related to average Fluence Rate by the following formula:

$$eqACH = E_e m \text{ x } 3.600 \text{ x } k(\lambda) / 1.000$$

where

$k(\lambda)$ is the spectral susceptibility factor
of airborne pathogens (m² /J)

$E_e m$ is the average Fluence Rate (mW/m²)

In his paper Nardell proposes that the economic efficiency of UVGI is over 9x that of HVAC for the same level of disinfection [12].

Calculating for air disinfection requires a 3D grid of points in the volume of the room with spherical irradiance calculated at each. These are then averaged to give the fluence rate.

A separate calculation is made on a horizontal plane(s) at a height of 1.83m* and 1.3m to check maximum the exposure is not exceeded [Security – Standard 13].

*The standard was originally written in imperial units where 1.83m = 8'

CALCULATION OF AIR DISINFECTION IN UV-C SOFTWARE

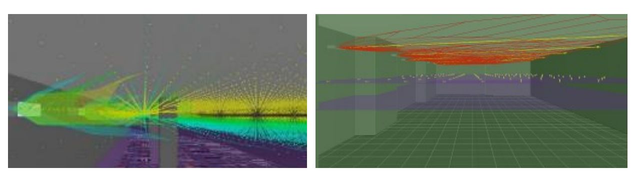

Fig. 7. 3D grid of calculation points in a room & 2D grids of 1,83m and 1,3m hight to check safe exposure of an upper air disinfection system (Source: Signify/Philips)

Before Calculation is to find out the room configuration. Sometimes is to test the UV-C reflection of the ceiling and wall surfaces. UV-C Calculation is possible to make with the program Visual (Acuity Brands Lighting Inc.) and optional with a special UV-C firm-version of Relux program. After

Installation is a security measuring highly recommended before putting the UV-C Upper Air System into operation.

PERMISSED UV-C RADIATION IN WORKING AREAS

Working time in h	Allowable UV-C radiation Irradiance in µW/cm²
12	0,14 (= 1,4 mW/m²)
10	0,17 (= 1,7 mW/m²)
8	**0,20 (= 2,0 mW/m²)**
4	0,40 (= 4,0 mW/m²)
2	0,80 (= 8,0 mW/m²)

Fig. 8. Typical allowable max. UV-C Irradiance by ISO 15858:2016 in h=1,83m (8') security level (Source: Signify/Philips)

III. EXAMPLE AIR DISINFECTION AND VARIOUS SYSTEMS, SAFETY ASPECTS & EXAMPLES OF EXECUTED PROJECTS

Many by UV-C operating systems are today used for various applications.

Open systems / Surface disinfection (no People):
- Free lighting UV-C Tubes (Battens) open UV luminaire
- UV-C Trolleys / robots

Open Systems / Air disinfection:
- Upper Air units for direct disinfection of surrounding air

Closed Systems / Surface disinfection:
- Object Disinfection Chambers for smaller devices

Closed Systems / Air disinfection:
- Units for integration in air conditioning systems
- Mobile Air Cleaner with integrated UV-C units

Other more or less closed Systems:
- Water cleaning and disinfection units
- Systems for industrial processes etc.
- Systems in medical uses

Over the last years where worldwide many projects with different systems realized. Focus for next on air disinfection and some technical and safety aspects.

EXAMPLE PRINCIPE UPPER AIR

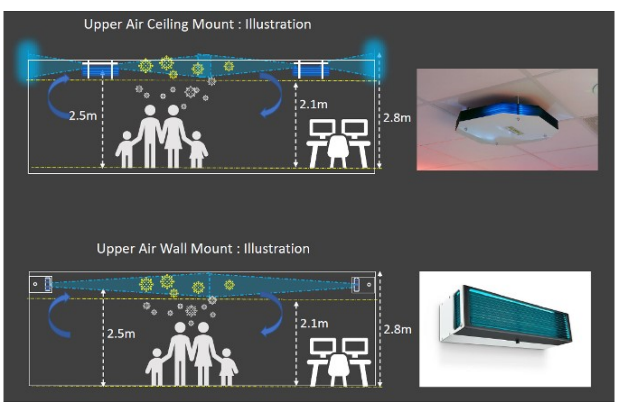

Fig. 9. Air disinfection Upper Air - Principe - persons during operation can be present (Source: Signify/Philips)

The upper room disinfection by direct focused radiation is effective, without noise and need not much energy. By following safety rules its not dangerous in application.

VISUAL MARKING FOR UV SECURITY

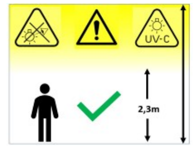

Fig. 10. Visual safety marking for rooms with Upper Air disinfection, security area less then 2,3m (Source: Signify/Philips)

EXAMPLE AIR DISINFECTION TECHNOLOGIES BENCHMARKING

	Natural Ventilation	Mechanical Ventilation	Upper room UV-C
Typical ACH	0-1	1-2	--
Typical eqACH	--	--	6-30+ (*)
Infrastructural costs	low	medium	low
Operational energy costs	medium (additional heating / cooling needed)	medium (additional heating / cooling needed)	low
Discomfort	medium-high (temperature, draught,	medium-high (noise, draught)	very low

Fig. 11. Air disinfection UV-C (Source: Signify/Philips)
(*) UV-C upper air offers flexibility to cover the desired eqACH rate, depending on ceiling height; for rooms with lower ceilings, upper air effectivity is limited because of safety requirements. In such case closed systems could be added

Here some examples from Germany projects.

Studio Skylab Detmold – air disinfection of sport rooms

EXAMPLE FITNES STUDIO UPPER AIR

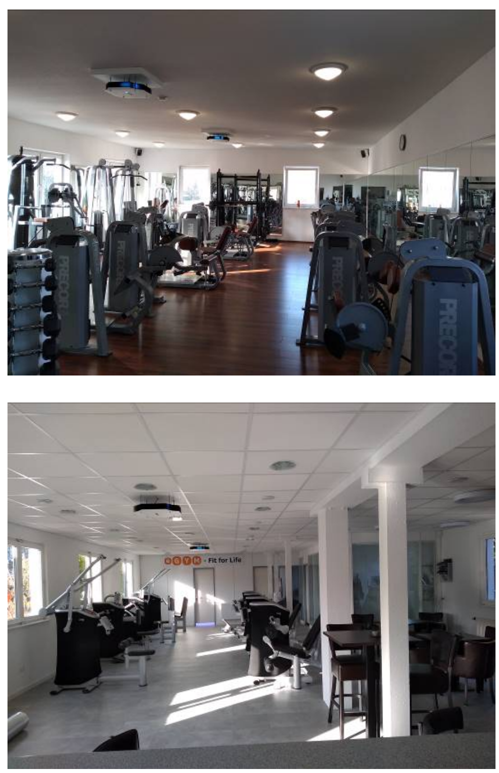

Fig. 12. Upper Air in Skylab Detmold (Source: Seifert Signify/Philips)

In the security level (h=1,83m) under the units was not more then 1,8mW/m² measured. In some areas less then 0,3mW/m².

Various offices, schools, kindergartens were equipped with air purifiers like Upper Air.

EXAMPLES SCHOOLS AND KINDERGARTENS BAD DUERKHEIM

Fig. 13. Air disinfection Upper Air - Principe - persons during operation can be present (Source: Seifert Signify/Philips)

In the security level (h=1,83m) under the units was not more then 0,9mW/m² in the Kindergartens and Schools measured.

EXAMPLE CANTEEN STADTWERKE INGOLSTADT UPPER AIR

Fig. 14. Air disinfection Upper Air - Municipal Services Ingolstadt staff restaurant (Source: Seifert Signify/Philips)

In the security level (h=1,83m) under the units was not more then 0,9mW/m² measured.

Also a successful cinema experiment was made to see – how germs will be reduced by standard air conditioning system with or without UV-C Upper Air units.

EXAMPLE CINEMA WITH UPPER AIR (EXPERIMENT)

Fig. 15. Air disinfection Upper Air in a coinema room Aibling Trifthof (Source: Seifert Signify/Philips)

In the security level (h=1,83m) under the units was not more then 0,4mW/m² measured.

EXAMPLE CONFERENCE ROOM SONAPAR

Fig. 16. Air disinfection Upper Air in a coference room Sonepar Oldenburg (Source: Seifert Signify/Philips)

In the security level (h=1,83m) under the units was not more then 0,3mW/m² measured in this conference room.

Under the view – max. 2mW/m² allowed for an 8h working day – all the solutions are secure.

In compliance with existing regulations and standards, the use of UV-C technology is recommended in all areas of application for protection against pathogenic germs. The use of chemicals can be significantly reduced and also relieves the environment, so UV-C technology is perfectly suited as a supplement to existing hygiene concepts.

The use of UV-C goes beyond the protection of humans, so at the moment the demand in animal breeding is increasing (e.g. because of bird flu).

Today, the use goes far beyond previous "special applications".

Regulations, guidelines and information on the use of such systems, the efficiencies and also the safety should be further specified according to the current state of science and technology.

[1] Darnell, M.E.R. et al. Inactivation of the coronavirus that induces severe acute respiratory syndrome, SARS-CoV. J Virol Methods 121, 85–91, https://doi.org/10.1016/j.jviromet.2004.06.00 (2004).

[2] McDevitt, J.J. et al. Aerosol susceptibility of influenza virus to UV-C light. Appl Environ Microbiol 78, 1666–1669, https://doi.org/10.1128/AEM.06960-11 (2012).

[3] Buonanno, M., et al. Far-UVC light (222 nm) efficiently and safely inactivates airborne human coronaviruses. Sci Rep 10, 10285, https://doi.org/10.1038/s41598-020-67211-2 (2020).

[4] Coronavirus disease (COVID-19): How is it transmitted?', World Health Organization, December 2021, https://www.who.int/news-room/questions-and-answers/item/coronavirus-disease-covid-19-how-is-it-transmitted (2021)

[5] 'How Covid-19 spreads', CDC, (2021) https://www.cdc.gov/socialmedia/syndication/405380/403327.html

[6] DIN 5031-10:2018-03 (E) Optical radiation physics and illuminating engineering - Part 10: Photobiologically effective radiation, quantities, symbols and action spectra (2018)

[7] Fluence (UV Dose) Required to Achieve Incremental Log Inactivation of Bacteria, Protozoa, Viruses and Algae; Revised, updated and expanded by Adel Haji Malayeri, Madjid Mohseni, Bill Cairns und James R. Bolton. With earlier contributions by Gabriel Chevrefils (2006) and Ericn Caron (2006). With peer review by Benoit Barbeau, Harold Wright (1999) and Karl G. Linden.(2019)

[8] Storm, N, McKay, L G A., Downs, S N et al (2020). 'Rapid and complete inactivation of SARS-CoV-2 by ultraviolet-C irradiation'. Scientific Reports 10, 22421 (2020)
In laboratory testing, Signify's UV-C light sources reduced SARS-CoV-2 virus infectivity on a surface to below detectable levels in as few as 9 seconds (Nadia Storm et al, Rapid and complete inactivation of SARS-CoV-2 by ultraviolet-C irradiation, 2020. Report available at https://www.nature.com/articles/s41598-020-79600-8). In this study, an exposure to an UV-C irradiance of 0.849 mW/cm2 for the duration of 9 seconds was applied, resulting in an UV-C dose of 7.64 mJ/cm2. Our UV-C surface disinfection products (fitted with UV-C light sources) will achieve the same level of virus infectivity reduction as long as the same UV-C dose is achieved on each area of surface that is irradiated.
Subject to peer review and available only as a pre-print at https://www.researchsquare.com/article/rs-65742/v2 (2020)

[9] ZVEI Publikation UV-C Anwendungen zur Entkeimung von Oberflächen und Luft, Frankfurt Februar 2021 Link Feb 2021: https://www.zvei.org/fileadmin/user_upload/Presse_und_Medien/Publikationen/2021/Februar/ZVEI-Positionspapier_UV-C-Licht_gegen_Corona/ZVEI-Positionspapier_UV-C-Anwendungen_zur_Entkeimung_von_Oberflaechen_und_Luft_2021-02-18.pdf (2021)

[10] BS ISO 15714:2019: Method of evaluating the UV dose to airborne microorganisms transiting in-duct ultraviolet germicidal irradiation devices, ISO 2019, https://www.iso.org/standard/67814.html (2019)

[11] Efficacy of a wall-mounted UV device against aerosolized SARS-CoV-2', Innovative Bioanalysis, March 2021. Available online at: https://www.assets.signify.com/is/content/Signify/Assets/philips-lighting/global/20210301-innovative-bioanalysis-report-sars-cov-2.pdf (2021)

[12] Nardell E A (2021). 'Air Disinfection for Airborne Infection Control with a Focus on COVID-19: Why Germicidal UV is Essential', Photochemistry and Photobiology, 2021 May;97(3):493-497. Available online at: https://pubmed.ncbi.nlm.nih.gov/33759191/ (2021)

[13] ISO 15858:2016 – UV-C Devices – safety information, information permissible human exposure https://www.iso.org/standard/55553.html
IEC 62471 Photobiological Sanfety of lamps and lamp systems (2002)

Additional Literature - More Informations also here:

[14] W.Kowalski, "Ultraviolet Germicidal Irradiation Handbook, UVGI for Air and Surface Disinfection", Springer Berlin Heidel-berg , 2009 ISBN 978-3-642-01999-9

[15] Global Lighting Association – UV-C Safety Guidelines May 2020 https://www.globallightingassociation.org/images/files/publications/GLA_UV-C_Safety_Position_Statement.pdf

[16] ASHRAE Position Document on Airborne Infectious Diseases, 2020 https://www.ashrae.org/file%20library/about/position%20documents/pd_infectiousaerosols_2020.pdf

[17] CIE Position Statement on Ultraviolet (UV) Radiation to Manage the Risk of COVID-19 Transmission https://cie.co.at/files/CIE%20Position%20Statement%20-%20UV%20radiation%20%282020%29.pdf (2020)

[18] Philips SignifyInformations https://www.signify.com/global/innovation/uv-c

Urban Lighting: Innovative Luminaires Made of an Eco-sustainable, Circular and Corrosion-resistant Material

Alessandro Deodati
Niteko Illuminazione
Montemesola, Italy
alessandro.deodati@niteko.com

Emiliano Petrachi
Niteko Illuminazione
Montemesola, Italy
info@niteko.com

Giuseppe Vendramin
Niteko Illuminazione
Montemesola, Italy
giuseppe.vendramin@niteko.com

***Abstract*— The main causes of corrosion on urban lighting luminaires are represented by marine environments and atmospheric agents. The present research started from studying the Italian territory, a long and narrow peninsula surrounded by seas and rich in rivers, in order to find a solution for a problem affecting many cities across the globe. After analyzing the main consequences of corrosion on aluminum lighting bodies, the conducted study highlights the advantages of using a particular eco-sustainable polymeric material to produce highly resistant luminaires that fully respect the virtuous path of the circular economy. The study focuses on the choice of combining freedom in design, use of secondary raw materials and/or plant-based materials, and low environmental impact production techniques to produce efficient and durable urban lighting luminaires. The thus obtained luminaires are both eco-sustainable and highly customizable. They can fully integrate remote control devices within their lighting bodies – useful in interconnected cities – without any aesthetic consequence for the luminaire. The result is therefore resistant and future-oriented luminaires that really move from a linear macroeconomic model towards a circular one.**

Keywords—sustainability, circular economy, bio-based PE, corrosion, urban lighting

I. INTRODUCTION

Urban lighting luminaires installed close to watercourses are constantly exposed to the corrosive action of both chloride and atmospheric agents in general, as well as big cities and industrial districts are exposed to the corrosion caused by pollutants such as sulfur dioxide.

Corrosion process is slow, yet irreversible. It causes aesthetic and structural damages on the aluminum lighting bodies of traditional luminaires for public lighting.

In coastal marine environments, the resistance of metallic objects is affected by both distance from the coast and action of sodium chloride in the form of salt solution suspended in the air, because the latter feeds the corrosion phenomena under organic coating.

Luminaires installed in these areas thus deteriorate within a few years, and this involves replacement costs and worsening of the related environmental footprint.

II. BACKGROUND AND OBJECTIVES

The study of Italian territory inspired this research. Italy is a long and narrow peninsula surrounded by seas and rich in rivers and lakes where, consequently, the corrosion phenomena on urban lighting luminaires – caused by the action of sodium chloride – are much more common. The objective of the research is to find a solution to this problem by producing durable and corrosion-resistant lighting bodies, which at the same time are unique in design, Made in Italy and follow the circular economy model.

After analyzing the consequences of corrosion on metals, the study – which was conducted in cooperation with an external research organization – highlighted the advantages of using a particular 100% recyclable polymer to produce urban lighting luminaires. The material – based on a particular plant-based and recovered polyethylene – combined with the patent pending manufacturing technique, makes it possible to produce efficient urban lighting luminaires, which are both eco-sustainable and immune to corrosion. In this way, it is possible to achieve the desired goal of a real transition from a linear macroeconomic model towards a circular one.

A. Why and when metal-corrosion occurs: comparison between metals and polymers

Lampposts, luminaires and lighting fixtures are clearly very exposed to atmosphere, and they need to keep their aspect unchanged for decades to resist the attack caused by corrosion mechanism.

Corrosion is a natural and irreversible process, which is present everywhere. It implies a slow and continuous consumption of the material initially involved, where – as a consequence – there is a worsening of its physical properties and of its related mechanical performances. To remedy this situation, it is important to use at source a correct and effective corrosion protection, as it helps to save both money and resources in the long term, even if it requires a higher advance expense and greater environmental impact due precisely to chemical treatments.

It is possible to synthetize the corrosion phenomenon of metallic materials in the following reaction: metal + aggressive agents = corrosion products.

Therefore, corrosion phenomenon occurs when there is the simultaneous presence of a conductive metal, an electrolyte (you only need a slight humidity of the surface) and oxygen to generate the chemical reaction.

The metallic material intervenes in the corrosion process through its chemical composition, that is:

- By its nature (in case of pure metals) or by both its nature and relation with its other constituents (in case of alloys)
- By its structure, where this term is to be understood in a very broad sense, because it includes different properties

such as geometric characteristics, nature, morphology and distribution (and hence position, shape and extension) of the phases that constitute it; but also type and consistency of the existing reticular defects, surface conditions, microstructural characteristics of the grain boundary, effects of mechanical stresses on the material itself, temperature, etc.

To solve the problem from its root, many industrial sectors are choosing more and more often to use polymers which, by their nature, are not subject to the corrosion phenomenon. Polymer materials were introduced with the coming of nanotechnologies. They are significantly less expensive than metals processed with machine tools, but equally reliable, rigid and resistant in many applications. Recently, they were even used instead of stainless steel to produce heart surgery instruments.

When analyzing painted aluminum lighting fixtures for urban lighting, the corrosion phenomenon of main interest is represented by corrosion under organic coating (delamination, blistering) – of which filiform corrosion can be considered its particular case. It is evident that, in such circumstances, maximum resistance to corrosion can be guaranteed by those organic coatings able to both develop the highest barrier protection against aggressive agents (water, oxygen, specific ions) and guarantee an efficient adherence to metallic substrates even in strong humidity conditions.

In fact, in case of organic coatings (especially paints and varnishes) the main problem is related to their intrinsic porosity: in the long term, both atmosphere oxygen and humidity will penetrate by diffusion and they will affect the metallic mass at the interface of the metal/coating. The resulting effect is the typical blistering on the surface of the painted layer: oxygen and atmospheric humidity cause the deterioration of the metal alloy, which means development of corrosion products with high specific volume at the interface, such as to create the swelling of the paint layer. Therefore, by using a same type of paint or varnish, these coatings will give an adequate protection in relation to the thickness used for protecting the material: the greater the thickness of the paint, the longer it takes for the atmospheric aggressive agents to spread within the metal.

In addition, close attention must be paid to the assembly phases of the different metallic components, in order to minimize the possible formation of cracks in correspondence of the joints. This is in order to avoid crevice corrosion phenomena.

It is thus possible to slow down the corrosion process. However, with the use of polymers, such as biopolyethylene and recovered polyethylene, it is possible to eliminate the problem at the root, because these materials are naturally immune to corrosion.

III. METHOD

A. Materials

As described above, the study validated the use of both plant-based polyethylene – known as Green PE – and recovered polyethylene – known as secondary raw material.

- The first case concerns a particular 100% recyclable polyethylene with the same properties as its fossil equivalent. Unlike traditional polyethylene, the ethanol here used for its production does not come from oil, but from sugar cane. By using this renewable raw material, a ton of Green PE can store from the atmosphere up to 3,09 tons of CO_2, thus contributing to reducing harmful greenhouse gas emissions. A negative emission factor is estimated of about 1 kg of CO_2 per kg of bioplastics removed from the atmosphere during the growth of the biomass.
- In the second case, in order to further reduce waste and to encourage the disposal of the products, the research validated the results of using recovered polyethylene – besides the green one – i.e. polyethylene deriving from clean and homogeneous production waste, and selected and post-consumer polyethylene. This kind of materials falls into the so-called "secondary raw materials" category, which includes those materials that transform waste into resources and promote environmental respect, thus avoiding the use of unnecessary raw materials and the resulting diversion of valuable resources away from the planet. Recovered polyethylene contributes to the reduction of greenhouse gas emissions, particularly CO_2. Mechanical recycling of plastics generates no direct emissions, while the indirect emissions are around 0.5 kg of CO_2 per kg of plastic [6].

Mechanical properties of the so obtained luminaires are compliant with the sector-specific standards. In addition, these luminaires are also durable over time, resistant to UV rays and therefore they do not suffer discoloration over time.

The only difference between the two types of materials lies in the resulting surface appearance of the lighting bodies. In case of bio-based polyethylene, the color effect is homogeneous and uniform (Fig. 1). On the contrary, it is more artistic and varied in case of post-consumer polyethylene (in Fig. 2, you can see the example of a luminaire made of recycled bottle tops) or in case of polyethylene deriving from clean and homogeneous production waste (with greater emphasis on the material effect of its finish, as in Fig. 3).

Fig. 1.Example of a bio-based polyethylene luminaire.

Fig. 2. Example of a luminaire made of post-consumer shredded polyethylene.

Fig. 3. Example of luminaires made of polyethylene deriving from clean and homogeneous shredded production waste.

B. Manufacturing technique

The innovation of these new urban lighting luminaires lies in the choice of eco-sustainable materials combined with a patent pending manufacturing technique, which makes it possible to produce both resistant and highly customizable luminaries.

All the studied materials are suitable for rotational molding, a technological process allowing the production of hollow objects with constant thicknesses and without any welding spot. The processing takes place at low pressure. It is based on the adhesion of plastic materials to hollow rotation molds, and it allows the production of stress-free pieces, which is one of the biggest advantages of rotomolding along with extreme ductile process and lower priced molds compared to other molding technologies.

Thanks to this manufacturing technique, it is possible to produce both recessed objects with complicated outlines and multilayer pieces, and it is possible to mold simultaneously different types of products on the same machine.

Rotational molding is a manufacturing technique with low environmental impact, free of annoying smells and toxic vapors, where melting of the powders occurs without direct contact with flames or heat sources. The oven heats the environment, which in turn heats the mold, so the mold heats and shapes the raw material contained in it by induction.

The extreme ductility of the process makes it possible to obtain highly customized designs, which are different from the standard ones. Unlike die-cast aluminum luminaires that need more molds for the final assembly of a single luminaire, a polyethylene lighting fixture produced by rotational molding has a single lighting body and it is batch-dyed. In this way, the final assembly is speeded up.

Hence the high freedom of expression for municipalities and lighting designers when dealing with design. They can choose any shape and see it done.

As an example of different geometries, full and soft volumes characterize the luminaire in Fig. 1-3; while in Fig. 4, you can see a different design obtained by more squared geometric shapes. The result is an urban lighting luminaire merging with branches and giving a touch of design to the place where it is installed, e.g. a tree-lined boulevard (Fig. 5).

It is thus possible to produce different geometries and to avoid all those problems related – for example – to undercuts, which are typical of other molding technologies, such as die-cast aluminum or plastic injection.

It is therefore possible to produce luminaires whose design is characterized by volumes' subtraction (Fig. 6) and by harmonious lines recalling traditional fishing lamps of the ancient maritime environments, which build a bridge between ancient and modern times (Fig. 7).

Fig. 4. Example of a polyethylene luminaire designed starting from the overlapping of two truncated cones and a sphere.

Fig. 5. Example of integration between design and environment. Installation of polyethylene luminaires in the lake city of Sirmione, northern Italy.

Fig. 6. Polyethylene luminaire characterized by volumes' subtraction.

Fig. 7. Polyethylene luminaire whose geometries are symbol of maritime landscapes.

C. *Calculation models*

The aforementioned study made it possible to develop a parametric model allowing the optimization and validation of thicknesses, geometries, and thermo-mechanical performances of the luminaires produced by the polymer described so far, by means of both thermo-fluid dynamic and structural numerical analysis.

In particular, in order to analyze dissipative behavior of both luminaire and its subcomponents, it was developed a thermo-fluid dynamic calculation model allowing the solving of Navier-Stokes equations.

Luminaire's thermal behavior was studied starting from the calibrated thermo-fluid dynamic model and validated by experimental experiences. This model made it possible to determine the volume-power curves for these urban lighting luminaires made of the analyzed polymeric materials. Then, based on the results obtained, luminaire's geometry was optimized from a structural point of view, by developing models that meet resistance checks with a wide margin of safety and make it possible to optimize the thickness of the frames while respecting geometries.

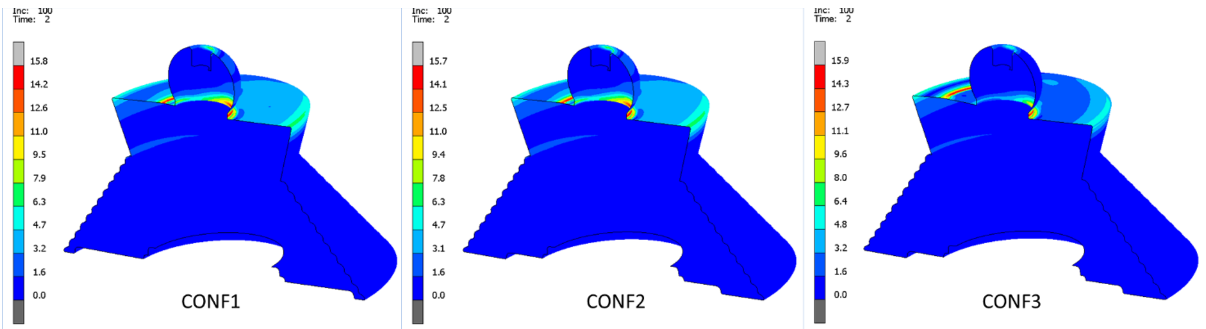

Fig. 8. Contour plot of mechanical stresses in three different constructive configurations.

IV. RESULTS

A. *Lighting results: installation in the Italian city of Sirmione*

Biopolyethylene lighting bodies keep the advantages of the latest LED technology in terms of electric energy consumption and optic efficiency.

In Table 1, it is possible to compare the data concerning the installation in Sirmione - Fig. 5 - of 80 W 24 LED luminaires with biopolyethylene lighting bodies to illuminate a motor traffic road, and 50W 24 LED luminaires to illuminate the sidewalks, which contributed to an annual savings of electricity costs amounting to €14.651 and to annual savings in carbon dioxide emissions of 38 t. The previous lighting system had 24 poles with 125 W mercury vapor lamps – 3 for each pole – and a 250 W metal halide floodlight.

It should be noted that, apart from the huge energy savings, particular attention was focused on adapting lighting to standards and on achieving the best visual comfort by using 3.000 K color temperature LEDs with a minimum color rendering index of 80.

TABLE I.

Annual savings and consumptions of an installation with polyethylene LED luminaires.			
Compared parameters	***Units of measurement***	***Traditional luminaires***	***LED luminaires***
Luminaire's average lifetime (L90B10)	H	9.000	100.000
Number of luminaires	pcs	96	48
Total effective power	kW	16.50	3.12
Hour use per year	dd/yy	365	365
Electricity price	€/kWh	0.25	0.25
Average useful lifetime	yy	2.1	22.8
Annual electricity consumption	kWh/yy	72.270	13.665
Annual emissions of carbon dioxide	t/yy	46.97	8.88
Annual consumption tonnes of oil equivalent	toe/yy	6.21	1.17
Annual savings	%		81.0
Annual savings in electricity consumption	kWh/yy		58.605
Annual savings in electricity costs	€/yy		14.651
Annual savings in carbon dioxide emissions	t/yy		38.09
Annual savings of tonnes of oil equivalent	toe/yy		5.04

Not only an energy but also a qualitative redevelopment, with a significant increase of lighting values achieved by meeting M3 category standards for the road and P1 standards for sidewalks. Plus, the achievement of both overall and longitudinal uniformity values greater than 0.7 and a TI index value of glare lower than 7% by meeting current regulations against light pollution with zero emissions from 90° up.

B. *Summary of the comparative LCA project of urban lighting products whose bodies are made of different materials. Drafted according ISO 14040 and 14044 standards.*

From the comparison of a same kind of luminaire made of five different technologies and compositions, and assuming a durability of 10 years for an aluminum lighting body and a durability of 40 years for an HDPE body in an environment rich in aggressive agents, it appears that:

- Life cycle of HDPE products has lower environmental impact than aluminum products.

- This result comes mainly from the fact that for the aluminum products 4 life cycles have been considered - due to shorter durability of the products – and 1 life cycle has been considered for the HDPE products.

- There are also some small differences between the HDPE products, where those products containing 90% of recycled materials are more eco-sustainable than the fossil and bio ones.

- Concerning the most affected impact categories and excluding the use phase, the most affected categories are those about reduction of mineral resources, climate change, reduction of fossil resources and ecotoxicity of the water.

The report was made by the University of Bari (Italy) through its Industrial Ecology Solutions S.r.l. (IES S.r.l.) spin-off. It describes the results and the technical-scientific aspects of the Life Cycle Assessment study – drafted according ISO 14040 and 14044 (ISO 2021 a, b) standards – of a same urban lighting product with an aluminum lighting body or a polyethylene lighting body made by rotational molding.

C. *Final observations*

Therefore, the urban lighting luminaires obtained by using this bio-based and recovered polyethylene are:

- Immune to corrosion, typical instead of metal lighting fixtures, especially in coastal areas and polluted environments.

- Impact resistant. Lighting fixtures' geometry – combined with thicknesses, mechanical properties and production process – give the luminaires the highest degree of protection against impacts according to CEI EN 62262 (CEI 70-4) standard.

- 100 % recyclable. At the end of the service life of the luminaire, the polyethylene material (both bio-based and recovered) is recycled through mechanical shredding and it can be reused to produce new lighting bodies.

- Totally eco-sustainable and circular. The studied luminaires are 100% eco-sustainable. Polyethylene material is completely green and – combined with the production technology – it contributes to the reduction of carbon footprint during all the manufacturing processes, while recycling makes it possible to transform waste into a new resource, thus respecting the virtuous path of the circular economy.

- UV resistant and batch-dyed. Lighting body's material is immune to discoloration through the use of UV additive stabilizers melted in the base material, which are intended to protect the polymer from the deterioration caused by UV radiations of sunlight with no need for chemical treatments and/or paints.

- Efficient, thanks to LED technology, which guarantees economic saving and allows both energy and qualitative redevelopment, through compliance with current rules on public lighting.
- Transparent to radio signals

Mechanical properties remain unchanged from -60° C to +80° C, with a service life longer than 50 years.

In addition, not only is it possible to choose the design of the luminaire, but also its color, which is highly customizable and adaptable to designer's needs.

The study on the material has also highlighted its "transparency" to radio signals, which are not shielded by the polyethylene, as it occurs in aluminum lighting bodies. This is the reason why it is possible to insert antennas and devices – for example 5G technology – directly within the lighting body, making the luminaires suitable for Smart Cities.

Fig. 9. Example of polyethylene luminaire with custom green color.

Fig. 10. Example of polyethylene luminaire with custom corten effect color.

V. CONCLUSIONS

The use of polyethylene materials for the production of urban lighting luminaires made it possible to meet the original goals of this research, i.e. an eco-sustainable production of circular and highly resistant products to fight the corrosive action of marine environments, atmospheric agents and pollutants in coastal marine environments and heavily polluted cities. Moreover, the use of green and recovered polymers makes it possible to overcome the critical aspects of aluminum recycling, which are associated with the use of thermal treatments at high temperatures (the recast of scrap) that may cause environmental problems due to the production of polluting emissions in the air, associated with the production of POPs (emissions into both the atmosphere and dust). Even if the technologies used in the primary and in the secondary production of aluminum are definitely different, the table of the emissions factors for the main air pollutants (study by ENEA - Italian National Agency for New Technologies Energy and Sustainable Economic Development – from 2002) makes it possible to compare the emissions produced during the electrolysis phase (primary production) and those produced during the pyrolysis phase (secondary production). From the study, it can be noted that – concerning the primary production – the electrolysis phase generates high emissions of CO_2 and PAH (polycyclic aromatic hydrocarbons). Instead, the secondary production is characterized by the emission of heavy metals deriving from the fact that a part of the metals present in the scrap inevitably ends up in the process fumes. Concerning pollutants common to both productions, it can be said that primary production is always more polluting than the secondary one, except for the carbon monoxide and for some substances that are not emitted during the primary production such as antimony, cadmium, chloride, dioxin, vanadium and hexavalent chromium.

Both post-consumer polyethylene and polyethylene deriving from clean and homogeneous production waste allowed the further reduction of waste volumes and the optimization of the resources without exploiting new ones, always getting uniquely designed luminaires with elegant and refined outlines.

The so obtained luminaires make it possible for architects and lighting designers to express their creativity without renouncing the beauty of design because of the resistance, making it possible to combine these two apparently antithetical concepts to create an innovative and future-oriented product.

REFERENCES

[1] A. Deodati and G. Vendramin, "Soluzioni contro la corrosione negli apparecchi di illuminazione urbana," Santarcangelo di Romagna (Italy): Maggioli Editore, pp. 8-26, May 2022.

[2] G. Tassielli, B. Notarnicola and P. A. Renzulli, "Comparative Life Cycle Assessment (LCA) project of urban lighting products whose bodies are made of different materials. Drafted according ISO 14040 and 14044 standards", IES: Industrial Ecology Solutions S.r.l., 2022.

[3] CETMA, Technologies Design and Materials European Research Centre, "Technical report", 2021, unpublished

[4] Tian Xiaogai, Chen Wei and Zhang Jiyong, "Thermal design for the high-power LED lamp", Journal of Semiconductors, 2011.

[5] Rongsheng Chen, Hsin-En Cheng, Chihuang Huang and Ray-Wen Wu, "Optimal Design of Thermal Dissipation for the Array Power LED by Using the RSM with Genetic Algorithm", Modeling and Numerical Simulation of Material Science, 2013.

[6] University of Cambridge Institute for Sustainability Leadership (CISL), "Industrial Transformation 2050", Material Economics, 2019.

[7] V. Veronesi, A.Russo, "Il recupero dell'allumino", in I mercati del recupero – Un'analisi di sistema, curated by S. Pogutz, A.Tencati, Santarcangelo di Romagna (Italy): Maggioli Editore, 2003.

[8] G. Schiona, "Il riciclo e la sostenibilità ambientale dell'alluminio", in the proceedings of the refresher course La gestione integrata dei rifiuti, Polytechnic University of Milan, Milan, Italy, 2008.

[9] M. Piazza, "Il metodo LCA applicato all'alluminio", Bachelor in Engineering, Department of Industrial Systems Engineering and Management, University of Pauda, Padua, Italy, 2013.

[10] A. Mazzetto, "Il ciclo di vita e le attività di riciclo dei principali materiali di imballaggio", Bachelor in Engineering Management, Department of Industrial Systems Engineering and Management, University of Pauda, Padua, Italy, 2013.

From Application to Design: How to Optimise Tunnel Lighting

Filippo Ratti
Arianna SPA
Padua, ITALY
filippo.ratti@ariannaled.com

Lorenzo Trevisanello
Arianna SPA
Padua, ITALY
lorenzo.trevisanello@ariannaled.com

Mauro Cancian
Arianna SPA
Padua, ITALY
mauro.cancian@ariannaled.com

In this work we present the importance of lighting design and development process on TCO (total cost of ownership) and safety, working on optics and application requirements, going through a system approach. Using counter-beam lighting (CBL) and inter-functional correlation between research and development team and lighting designer we demonstrate how to reduce the number of luminaires and the total power consumption, increasing the system efficiency. A complete workflow of a road tunnel lighting project is presented, starting from the following parameters: luminance (L), overall uniformity (U_o), longitudinal uniformity (U_l) and threshold increment (TI), the standard metric for the lighting design evaluation, directly related to the safety of the tunnel as defined in the international standard CIE 88.

Keywords—tunnel lighting, safety, TCO, design, photometry

I. Introduction

LED technology is revolutionizing all the lighting fields. In tunnel application the replacement concerned at the beginning only the nighttime lighting (the inner zone of the tunnel), while the daytime lighting (or entrance zone) relamping has been starting only in recent times due to the higher design complexity.

The reason of this slower adoption process can be mainly ascribed to the complexity of designing high power LED luminaire with better performance and lower costs than a traditional luminaire. On the other hand, improving the performance for entrance lighting luminaire can be really a benefit for the stakeholders and the end user.

The advantages of using LED technology in tunnel lighting systems translate into the following fundamental aspects: a decrease in energy consumption, a lower total cost of ownership (TCO) and, last but not least, an increase in safety. Safety is strictly connected to the optical performance of the luminaire. Firstly, the quality of light in relation to the different colour temperatures (CCT) and the various colour rendering indices (CRI): higher CRI values allow the driver to identify the colour of the marking signals inside the tunnel. Not surprisingly, several road infrastructures companies have included high CRI values in their technical specifications: the Italian ANAS has set CRI 80 [1] as minimum value for the entire tunnel relamping project called Greenlight while the Austrian ASFINAG evaluates the same CRI 80 value as the key feature. In addition to colour quality, the optical configuration has a strong impact on the perceived quality and visual comfort of the user. A recent work by Bartenbach [2] highlights how the different lighting configurations (continuous or discrete; pro-beam, counter-beam or symmetrical light distribution) can influence the reactivity of the driver and their perceived visual comfort, underlining the impact of the age factor on the results.

The international reference standard for lighting design of road tunnel is the Technical Report CIE 88, second edition, published in 2004 [3]. The aim of the report is to provide a guideline for lighting projects, giving a methodology to calculate the usual luminance, uniformity and glare parameters according to project requirements.

The most challenging part is the calculation of luminance value along the tunnel length for the daytime lighting. According to the design speed, that is the maximum speed allowed on the access roads to the tunnel, a luminance curve is defined, in order to allow the perception of contrast of the human eye. The entrance value of the luminance, called threshold luminance (L_{th}), is calculated considering the veiling luminance and the light scenario present outside the tunnel. More details on calculation are available on the standard and several lighting design tools are available to guide the designer in the definition of the luminance curve. The recommendations of CIE 88 have been then revised and rewritten for the different countries, according to their national regulations. The standard UNI 11095 is the regulatory document for Italian road tunnels [4]. It is not unusual to find different minimum luminance values inside national regulations. For instance, a typical requested L_{th} of highway tunnel according to CIE 88 is 180÷200 cd m^{-2}, while UNI standard requires 130÷140 cd m^{-2}, due to different methods of calculating L_{th} from environmental and veiling luminance. Even the inner zone luminance in daytime lighting is different: 1÷10 cd m^{-2} for CIE, 1÷3 cd m^{-2} for UNI. Once the luminance target is defined, the standard focuses on uniformity value, that in tunnel application extends from road surface to wall sides at maximum height of 2 m, since they act as background for traffic. In this case, the prescription is simply defined: $U_o > 0.4$, where U_o is defined as the ratio of minimum to average value of luminance, and $U_l > 0.6$, where U_l is the uniformity calculated along the centre of each lane. Finally, the disability glare is considered and defined using the Threshold Increment (TI) metric, as for standard road lighting design (i.e., CIE 115). Also in this case, the limits change according to different countries: for CIE 88, the limit is 15% for all the tunnel parts, while UNI standard prescribes TI = 20% for entrance zone and 10% for inner zone. For Norwegian Handbook N500:2016 [5] the limit is even lower: TI = 6% for all zones of the tunnel.

The other points of CIE 88 are related to maintenance of tunnel lighting system and method to correctly evaluate the lighting project in the field. Since we are focusing on the optical side of the luminaire development, we will use the lighting parameters just defined.

II. Product development

A. Optical Development

The optical development process stars from tunnel performance requirements. According to our scenario of tunnel lighting with high efficacy requirements, we adopted a reflector based solution instead of TIR lens approach. This technology allows to spread the light on a wider surface, resulting in a lower average luminance on the optical surface and thus a lower discomfort glare generated by the luminaire. In addition, high reflectivity material has been adopted in order to enhance the optical efficiency. This is the reason why a metal based reflector with silver coating has been selected: this material allows up to 98% reflectance. Cut and fold metal sheet process has the important advantage to shorten time to market, since design can be quite fast and time for tooling is not required. This point helps to be flexible in designing application tailored solutions.The only drawback of such solution is the final size of the reflector, that will be always bigger than a flat lens plate solution. However, tunnel lighting fixtures have no special requirements in terms of size, so this technology is compatible with the application. In Fig. 1 an example of reflector and LED module has been reported. The optical design is made by using parametric ray-tracing software, starting from primitive geometries and then increasing complexity. Four different reflectors have been designed in order to create several optical distributions. The four distributions are reported in Fig. 2. We considered only asymmetric distributions with similar but different shapes: further down we will investigate the impact of the shape on lighting parameters.

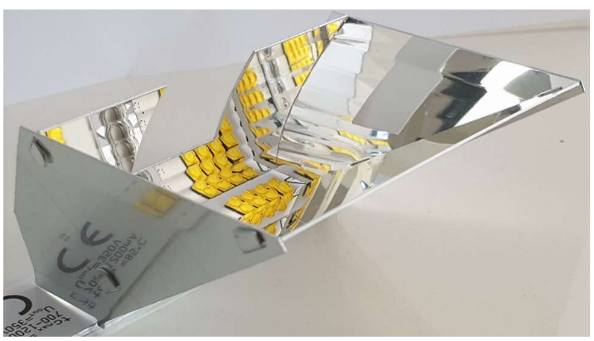

Fig. 1. Picture of reflector

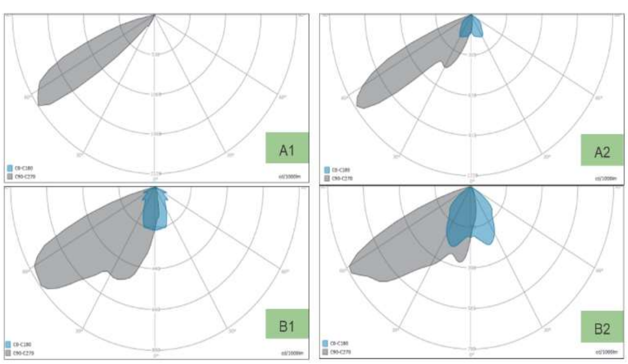

Fig. 2. Optical distribution of asymmetric optics

B. Counter-Beam lighting versus Pro-Beam lighting

There are different strategies to illuminate the entrance zone of the tunnel:

- Pro-Beam Lighting (PBL), where an asymmetric beam is directed in the same direction of the traffic flow, aiming to enhance the positive contrast of a lit object versus dark background;
- Symmetric Lighting (SL), where the beam shape is asymmetric toward both traffic direction and the contrast is always positive;
- Counter-Beam Lighting (CBL), where the asymmetric beam is directed in the opposite direction of the traffic flow, resulting in a negative contrast of the dark object on a lit background.

A simplified scheme of difference between CBL and PBL has been reported in Fig. 3.

The reason to choose different configuration is strictly related to the single project, but some general pro and cons can be inferred: CBL is the more efficient configuration because it enhances the angles of the surface that give an higher luminance result; PBL is the solution that gives best results in terms of glare, since the light source is definitely invisible to the user, but worst results in terms of efficiency; SL is mandatory when the lighting fixtures can be installed only on the sides of the tunnel, and provides good guidance when the luminaire are in a continuous line.

In this work we focused on CBL system since it is widely recognized that the benefit in terms of efficacy is well above the risk of creating disability glare, given that the latter can be well controlled with the LED technology.

The more relevant parameter of an asymmetrical optical distribution is the peak angle on the longitudinal plane. The higher is the peak, the higher will be the luminance but even the glare (TI). This relationship is shown in Fig. 4, where the results of a lighting calculation using optic A2 (see Fig. 2) with an inter-distance of 2 m varying the peak angle have been reported. The results are representative for both CBL and PBL lighting.

As reported in Fig. 4a, the luminance for CBL system is almost 3 times the one obtained with PBL: the developed optic is optimized for CBL installation, but the great advantage of CBL in terms of efficacy is clear.

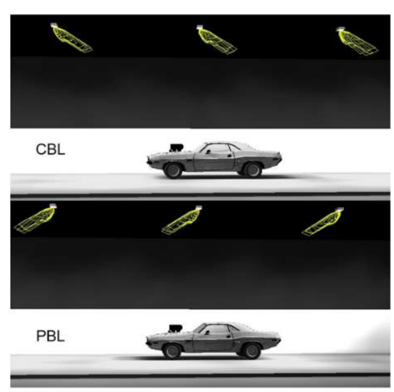

Fig. 3. Schematic of CBL and PBL installation

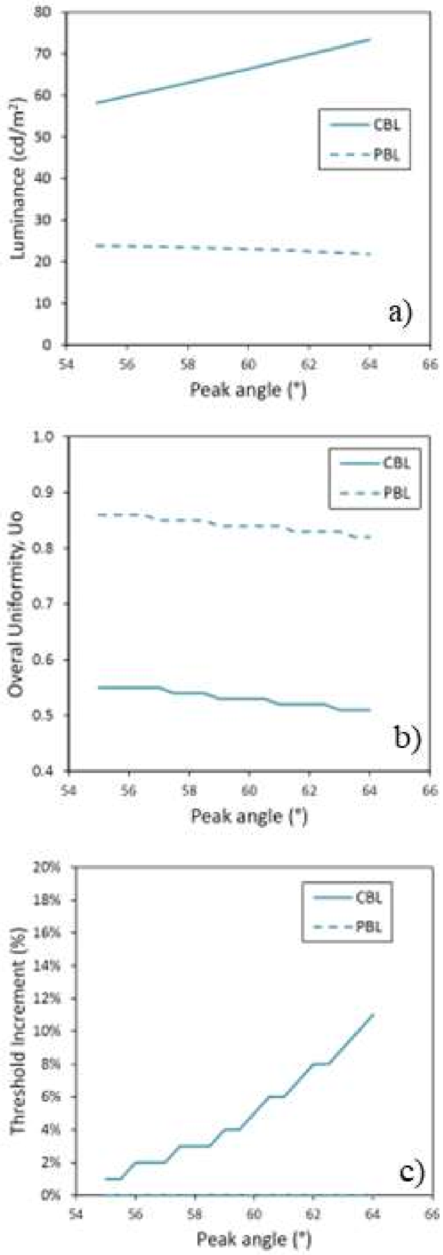

Fig. 4. Variation of project parameters in function of peak inclination for A2 optic: a) Luminance, b) Uniformity and c) TI

Another result in the CBL system is the increase of efficacy (thus luminance) with the increase of the peak angle: with a 9° increase the luminance raises by 25%. The same cannot be said for PBL, where the luminance remains stable with higher angles, since the contribution of surface reflectance on that angles is flat. On the other hand, the PBL system gives better results in terms of uniformity (Fig. 4b) and glare (Fig. 4c): in latter case, the TI is always 0% for PBL, while in CBL configuration is strictly dependent on the peak angle. Just to enhance the concept: the TI limit for CIE 88 is 10%, for Norwegian guidelines is 6%. This is the most challenging part of the optical development of CBL optical systems, where the designer wants to obtain the higher luminance (that means both lower initial costs of installation and maintenance) but with a good margin before ending up outside the avoided glare zone.

III. ANALYSIS AND OPTIMIZATION

A. Light distribution parameters

Once the lighting configuration has been defined, the optical development focuses on the beam shaping phase. For the CBL asymmetric beam, a simple geometrical model can be used to find the best shape that satisfies the initial requirements. The beam can be described by the peak angle and by the opening angle towards longitudinal plane, that we call $FWHM_L$ (considering Fig. 2, the C90-C270 plane). For the 4 optics developed, we report the $FWHM_L$ in Table I. The peak angle impact on lighting parameters has been previously discussed.

There are some correlations between these two parameters and the lighting parameters. In Fig. 5 the dependance of threshold increment and luminance with respect of $FWHM_L$ has been reported. The simulations are made with the same peak angle inclination. The luminance generally decreases with FWHML (squares) increase, mainly because the relative intensity of the peak is lower and the luminance reaction is lower as well. A quite different result is visible for TI (circles): it is quite intuitive that the TI increases together with the FWHML, but this is not true for A1 optic. This one has a FWHML similar to A2 but shows a higher TI. In order to understand this difference, we reported the A1 and A2 intensity distribution on C0-180 plane in Fig. 6: although the peak and width of the two curves are similar, in A1 optic there is a big contribution of flux for angles above the peak: this flux portion contributes to the increase of TI. It would be unfair to say that optic A1 has a bad design: that portion of light that is contributing to increase the TI has the benefit of enhancing the luminance value with respect to similar optic, like A2. Even in this case, the optical development can be tailored to the final application.

TABLE I. GEOMETRICAL CHARACTERISTICS IN TERMS OF $FWHM_L$ OF OPTICAL DISTRIBUTION STUDIES

Optical Model	$FWHM_L$
A1	23°
A2	24°
B1	58°
B2	43°

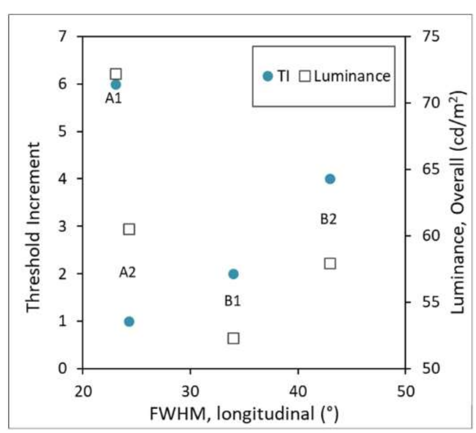

Fig. 5. Project parameters in function of $FWHM_L$ of the beam

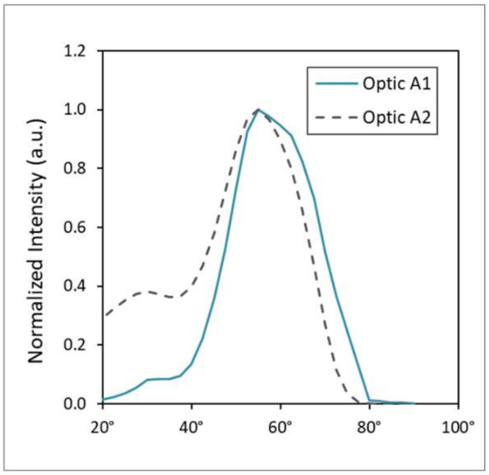

Fig. 6. Trasversal intensity distribution for optic A1 (solid) and A2 (dashed)

B. *Lighting design of road tunnels: project parameters optimization*

The lighting design of a road tunnel has different constrains related to the geometry of tunnel, the status of the paint of the walls, the type of asphalt used, the electrical installation characteristics and consequently the way the fixtures can be attached. Due to the increase of safety requirements and the large use of adaptive lighting controlled with a luminance camera pointing at the entrance of the tunnel, the lighting fixtures need to have a remote-control system on board (DALI, power line communication, wireless control, ...), that is an additional specification of the tunnel project.

In order to find the best trade off in terms lighting performance and energy efficiency, the lighting designers can control the optic type and power of the luminaire, its orientation and the inter-distance of the fixtures, in case the installation geometry allows it. Clearly, more variables available can help the designer. In this section we will show how important is to give a wide range of optics to the designer and how they can impact on the lighting parameters and energy consumption.

In order to show the impact of optic shape in lighting design, two optics with different target have been selected: optic A1 (Fig. 2) has the narrowest beam and the higher luminous intensity, while optic B1 (Fig. 2) shows a wider emission beam and a lower intensity value. In Fig. 7 the plots of luminance, uniformity and TI at different installation distances for both optics have been reported. All the simulations have been done with the same lumen output. As a general comment, higher interdistance always gives worst results in terms of luminance, uniformity and TI. But interdistance has a direct correlation with installation and energy costs, so the first phase of designing a road tunnel lighting consists in finding the best compromise between cost and performance.

However even the optical distribution shape has an impact. The plots shows that a narrow beam (A1) always enhances the luminance, but even the glare, while the uniformity is better with a wider beam (B1). So, the designer has to carefully select the optic type and the interdistance to reach the project target.

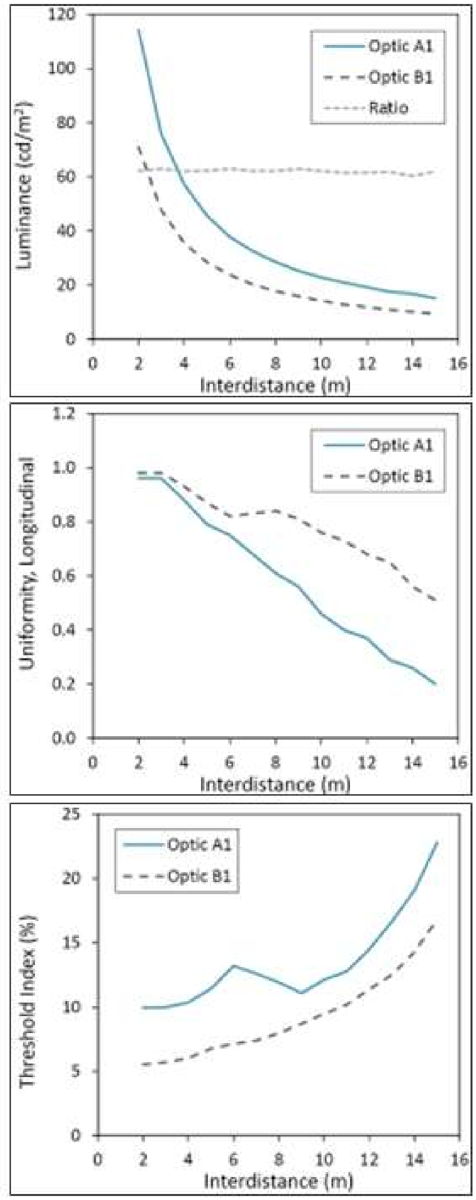

Fig. 7. Variation of project parameters in function of interdistance between fixtures

For instance, starting from luminance plot in Fig 7a, we can reach the same level using fixtures with optic B1 at 8 m distance or with optic A1 at about 14 m distance. The interdistance increase has a negative impact on uniformity (Fig. 7b): while for optic B1 we have a good level of 0.8, optic A1 reaches 0.2, that’s not allowed. We have same results for TI: optic B1 gives 8%, while for A1 reaches 19%, that is not allowed again for CIE 88. This doesn’t necessarily mean that optic A1 is not a good optic: it is very useful for the initial part of the tunnel, where a high level of luminance is requested and can be reached with short distance of fixture, about 2-3 m: in that case, TI and uniformity are well positioned.

The mixing of different optics or a single optimized optic can give more chances to the designers to find the solution with the best TCO, as reported in next paragraph.

C. Energy consumption optimization

In this section we provide an example of lighting design of the entrance daytime section of a reference tunnel. The tunnel section is divided in two main parts: the first from 0 m to 200 m from the entrance, called threshold zone, and the second part from 200 m to 750 m called transition zone. In the next tables we report the results of different lighting scenarios in terms of number of fixtures installed (related to installation costs) and power consumption (related to maintenance costs).

The first attempt is made by using luminaires with optic B1, with wider beam. Results are shown in Table II: as reported in the data, the threshold zone is the most expensive part, since its target is to reach high levels of luminance (130 cd m^{-2}). Using this optic, we need 137 fixtures and about 35 kW of power consumption to reach the lighting requirements.

Switching to a really different optic A1 (the narrowest beam), the results change, as reported in Table III: the energy consumption is reduced by one third, but the number of fixtures is increasing by 15%. The reason is directly connected to the discussion in the previous section: this optic works fine with small interdistance, that is useful in the initial part where high luminance is required, but doesn't make sense in the inner zone, where luminance levels are lower and uniformity and glare requirements are still needed. This configuration is a good solution for energy consumption but shows higher installation costs.

This analysis lets us take into account a mixed situation, where we can use fixtures with optic A1 for the threshold zone, and optic B1 for the transition zone. This solution allows for an energy consumption quite similar to the previous with optic A1, together with a decrease of the total number of fixtures installed: 15% less than optic B1 scenario, 25% less than optic A1 scenario.

Further optimization lies in the design of a new optic which merges both the advantages of A1 for the threshold zone and B1 for the transition zone in term of fixture quantity and power consumption. The optimized optic is A2, data already presented in the Fig.2, Fig.4 and Fig.5. Results are reported in Table IV and Table V.

TABLE II. OPTIC B1 USAGE

Zone	No. luminaires	Power
Threshold	82	33.4 kW
Transition	55	6.0 kW
Total	137	39.4 kW

TABLE III. OPTIC A1 USAGE

Zone	No. luminaires	Power
Threshold	62	22.7 kW
Transition	96	3.6 kW
Total	158	26.4 kW

TABLE IV. OPTIC A2 USAGE

Zone	No. luminaires	Power
Threshold	64	26.0 kW
Transition	52	4.3 kW
Total	116	30.3 kW

TABLE V. OVERALL RESULTS

Optics	No. luminaires	Power
B1	137	39.4 kW
A1	158	26.4 kW
MIX A1+B1	117	28.7 kW
A2	116	30.3 kW

IV. PROJECT VERIFICATION

The final step of lighting design is the verification of the computer aided simulation with real measurements in the field. Lighting standards as UNI 11095 specify how to test the lighting installation in a road tunnel. The preferred way to evaluate the lighting system is using a luminance camera: it is the most fast and versatile measurement and gives luminance results with a good accuracy. In addition, the luminance measurement takes into account of all the environmental variables like reflectance of the road and side walls, giving the definitive results of design project.

In Fig. 8 an example of installation has been reported. The road tunnel in the picture is from a 2016 LED retrofitting of the Goldegg tunnel in Sarntal (BZ), in Italy. The project was designed by Arianna, using their luminaire TESEO (optic A1). In the figure both the photos of the tunnel entrance with daylight system on, and the related false colour map of luminance are reported. The picture is then post-processed and the luminance map of the road surface can be extrapolated, as reported in Fig. 9. The obtained image can be used then to make all the calculation of average luminance and uniformity and validate the whole project.

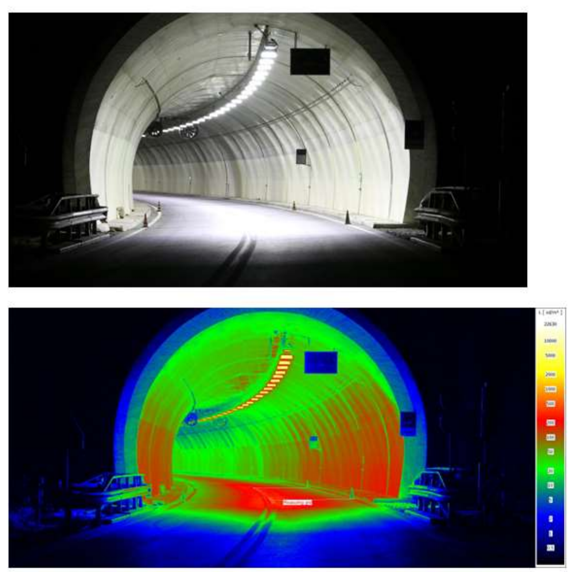

Fig. 8. Example of daylight installation

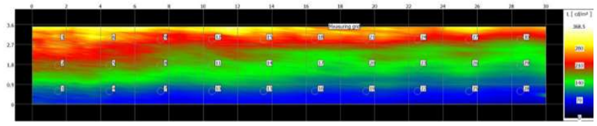

Fig. 9. Extrapolation of road surface luminance from the previous picture

V. CONCLUSIONS

Finally, in this work a complete workflow of a road tunnel lighting design has been presented. Starting from the development of the optical system of the lighting fixture, we showed the technology used for designing the optical system, the importance of selecting the CBL and PBL configuration in order to satisfy the project requirements and how the shape of optical distribution affects the results in terms of lighting performance. Then the focus switched to the lighting design of a road tunnel project, giving an overview of the process through project parameters optimization, energy consumption optimization and the final verification of the project in the field.

The main conclusion can be summarized:

- Custom design of the optical system for tunnel lighting is always an advantage over commercially available solutions as it can be suitably adapted to the needs of the project.
- To obtain the best results in terms of performance and cost savings, an inter-functional connection between the research and development department and the lighting designer is essential.
- The more optical distributions available for lighting design, the more precise and effective the result will be.

REFERENCES

[1] LED Professional [Online, 2017]. Available https://www.led-professional.com/resources-1/articles/technology-challenges-in-professional-tunnel-lighting-applications-1

[2] J. M. Dijon & P. Winkin, Tunnel Lighting: Comparison and Tests of Symmetrical, Counter-beam, and Pro-beam Systems, Transportation Research Record, 1991.

[3] CIE Publication No. 88: Guide for the Lighting of Road Tunnels and Underpasses. International Comitee on Illumination, Wien, Austria, 2004.

[4] UNI 11095: Luce e illuminazione - Illuminazione delle gallerie stradali. Ente Italiano di Normazione, 2021.

[5] N500: Vegtunneler. Staten Vegvesens, 2016.

Preliminary Results on Integrative Lighting in Classrooms: Simulations and Field Measurements

Valerio R.M. Lo Verso
Department of Energy 'Galileo Ferraris', TEBE Research Group
Politecnico di Torino,
Torino, Italy
valerio.loverso@polito.it

Luigi Giovannini
Department of Energy 'Galileo Ferraris', TEBE Research Group
Politecnico di Torino,
Torino, Italy
luigi.giovannini@polito.it

Lodovica Valetti
Department of Energy 'Galileo Ferraris', TEBE Research Group
Politecnico di Torino,
Torino, Italy
lodovica.valetti@polito.it

Anna Pellegrino
Department of Energy 'Galileo Ferraris', TEBE Research Group
Politecnico di Torino,
Torino, Italy
anna.pellegrino@polito.it

***Abstract*— The paper presents results from a study on integrative lighting for real middle school classrooms located in a school building in Turin, Italy, considering the contribution of both daylighting and electric lighting. The research addressed two main objectives: (i) to verify if the circadian values (melanopic equivalent daylight illuminance m-EDI) calculated or measured in the classrooms could meet the reference values reported in recent literature, for instance in the WELL protocol; ii) to assess the influence on integrative lighting (photopic and melanopic illuminances) played by the electric lighting and daylighting and, for this last condition, analyzing the impact of different room orientation and sky conditions.**

Keywords—integrative lighting; lighting in classroom; ALFA simulations; non-visual effect of light; circadian measures

I. Introduction

In the past 25 years research concerning the human responses to light have been largely expanded and currently there is strong scientific evidence that light is not only essential for vision, but it also affects the biological functioning of people and has an important impact for human health and performance [1-2]. Numerous studies have demonstrated that light also influences circadian rhythms, neuroendocrine functions, and neurobehavioral responses [3]. These types of responses have been defined as non-visual and non-image-forming (NIF) effects of light. Non-visual effects are mediated by signals from the retinal photoreceptors, i.e., from circuits of rods, cones, and intrinsically photosensitive retinal ganglion cells (ipRGCs). Particularly, ipRGCs are a type of photoreceptor cells on the retina, discovered in the mammalian eyes about two decades ago. These retinal photoreceptors are specialized ganglion cells that contain the photopigment "melanopsin" and are intrinsically sensitive to light [4-5]. Their peak sensitivity (approx. 460 - 480 nm [6-7]) occurs at shorter wavelength compared to that of rods (at 507 nm) and cones (at 555 nm), suggesting the relevance of the spectral distribution as a factor that influences non-visual effects of light. Indeed, studies demonstrated that NIF effects depend on the spectral power distribution, the quantity, the spatial distribution (directionality), the timing and duration of the light exposure, as well as on person-specific parameters such as circadian phases and history of light exposure [2-8].

Considering the relevant impact of non-visual response to light on humans' health and well-being, huge research has been carried out, which led to the proposition of new, dedicated circadian metrics to estimate and quantify the non-visual effects of light. Currently, three main approaches have been proposed: (*i*) the 'Circadian Stimulus' (CS) model; (*ii*) the 'Equivalent Melanopic Lux' (EML); (*iii*) the 'melanopic Equivalent Daylight Illuminance' (m-EDI).

The 'Circadian Stimulus' model was proposed by Rea and Figueiro [9] and indicates the human response to light in terms of percentage of melatonin suppression. The CS is defined as the calculated effectiveness of the spectrally weighted irradiance at the cornea from threshold (CS = 0.1) to saturation (CS = 0.7), assuming a fixed duration of exposure of 1 hour [10]. According to indications provided by Figueiro et al. [11] a CS value of 0.3 or greater at the eye during the morning is suitable for the promotion of good circadian entrainment. The threshold values are reduced to a maximum of 0.2 in the evening and a maximum of 0.1 during the night [12].

The 'Equivalent Melanopic Lux' (EML) is based on the spectral sensitivity of the melanopsin photoreception of ipRGCs with reference to the illuminant E and is based on studies conducted by Lucas et al. [13] and Enezi et al. [14].

The 'melanopic Equivalent Daylight Illuminance' (melanopic EDI or m-EDI), i.e. an SI-compliant 'alfa-opic' metric defined as illuminance produced by radiation conforming to standard daylight (D65) that provides an equal 'alfa-opic' irradiance as the test source. The m-EDI was recently defined by CIE in its International Standard CIE S 026:2018 [15] to supplement the EML, which did not provide an SI unit for calculating lux. As daylighting is the most natural 'circadian' light, it was assumed as reference for the definition of m-EDI, unlike EML, which refers to an equal-energy spectral power distribution. The EML and m-EDI metrics are thereby correlated by the expression: EML = 1.104*m-EDI. Other than the m-EDI, the CIE S 026:2018 [15] defines the spectral sensitivity functions, quantities, and metrics to describe the ability of optical radiation to stimulate each of the five photoreceptor types that can contribute to retina-mediated non-visual effects of light in humans. Indications from the Second independent expert symposium organized by the CIE in Manchester in 2019 suggested some recommended threshold values, such as at least 250 lx m-EDI throughout the daytime, a maximum of 10 lx 3 hours before bedtime and a maximum of 1 lx during the night [16-17].

The reported framework shows that currently no consensus on non-visual quantification has been reached in the lighting community and no quantitative requirements adopted in a shared international standard have been defined. However, it is equally clear that the issue of health and well-being in the built environment is becoming increasingly important [18] and that light is one of the key physical factors of indoor environmental quality (along with air quality, ventilation, thermal health, moisture, noise, water quality, dust and pests, safety and security) [19] that strongly influence occupants' health, well-being and perception of built spaces. In this frame, some studies have issued recommendations to promote the design of residential buildings [20], offices [21], as well as schools [22], to support the definition of strategies able to respond to multiple physical, physiological, and psychological needs of occupants. On the topic, one of the main references is the International WELL Building Institute (WELL) [23], which proposes a comprehensive approach based on a points-based system organized in Concepts (Air, Water, Nourishment, Light, Movement, Thermal Comfort, Sound, Materials, Mind, Community) and Features with distinct health intents, aimed at supporting the definition of design strategies devoted to prioritizing the health and well-being of users. 'Light' is one of the Concept covered in the WELL Standard, both in terms of the visual and circadian systems. Lighting guidelines to provide appropriate photopic and melanopic light levels, minimize disruption to the body's circadian system, and support good sleep quality are provided.

The awareness about the non-visual effects of lighting plays an important role in all building types, both residential and non-residential, and a new expression, 'integrative light', was introduced within the CIE [24-25] to combine the photopic and melanopic effects on the health and comfort of the occupants of indoor spaces. In fact, nowadays it is well known that within a well-conceived lighting design both visual and non-visual effects of light should be mutually considered and the study of the interaction between light and architecture is fundamental to design comfortable spaces [26].

Integrative lighting is particularly crucial in educational buildings, as it strongly affects the learning process along with physiological growing of young pupils in lower education levels [27]. Regarding the Italian context, the educational building sector has become particularly strategic in terms of architecture interventions over the last decade, through increasing funds for optimizing the building energy performance, as well as the comfort and health conditions for teachers and students. Previous studies demonstrated the significant impact of electric lighting and daylight on visual comfort and on the positive predisposition to learn in educational areas [28-29]. Other studies were focused on the evaluation of both visual and non-visual effects of light, to stimulate a design approach that promote also good circadian rhythm for students. Acosta et al. in 2019 [30] quantified circadian stimulus, promoted by either natural or electric lighting, in typical classroom designs with variable characteristics (window size, position, orientation, reflectance values of the inner surfaces) under three typical sky conditions. Results allowed to compare the impact of architectural design parameters on promoting good circadian rhythm for students. Ezpeleta et al. in 2021 [31] analyzed photopic and melanopic effects of light in four variable teaching environments and optimized an improvement proposal for the classroom lighting in order to address both photopic and melanopic needs.

However, despite the growing knowledge concerning integrative light and NIF effects of light, current design approaches and standards for indoor lighting are mainly intended to ensure visual requirements and to maximize energy efficiency. Consequently, they are usually expressed in terms of photopic quantities, without taking into account non-visual responses to light. Additional efforts are needed to define specific and agreed recommendations that address both photopic and melanopic aspects.

In this frame, this paper presents results from a study on integrative lighting for real middle-school classrooms located in a School building in Turin, Italy. Both electric lighting and daylighting conditions were analysed in the study; as for daylighting, three different orientations (East, South, and West-facing windows) and different sky conditions (clear and overcast) were considered. The study relied on a combination of approaches: (*i*) field measurements, to characterize photopic and melanopic illuminances in the classrooms due to the electric lighting system only; (*ii*) simulations, to evaluate photopic and melanopic illuminances due to daylighting for different time step representative of the different conditions over the year; (*iii*) combination of experimental and numerical results, to analyze the classrooms lighting conditions with the combination of daylight and electric light. The research was conducted with two main objectives: (i) to verify if the circadian values (melanopic equivalent daylight illuminance m-EDI) calculated or measured in the classrooms could satisfy the requirements reported in recent literature, for instance in the WELL protocol; ii) to assess the influence on integrative lighting (photopic and circadian illuminances) played by the different lighting contributions (electric lighting and daylight), the room orientation and the sky condition.

The analyzed case-study, the methods, and the results obtained in the study are described in the following sections.

II. CASE-STUDY

A real educational building was selected as case-study to analyze integrative lighting in classrooms. The case-study is the school "Bernardino Drovetti" and it hosts a kindergarten and a middle school. It is in Turin, Italy (latitude: 45.1°N). The school was built in the 1970s and underwent a renovation in 2016. The building consists of four floors, one of which is partially underground, and has a total area of approximately 10000 m^2, with an outdoor space of 12500 m^2 ca.

In this study, three classrooms of the middle school were selected for the analysis. They have similar geometrical and photometric properties, in terms of room size, size and materials of windows, furniture, finishing, and lighting systems. They are all located on the third floor, but in different areas, thus with three different orientations (East, South, and West-facing windows), with a different obstructing urban setting (Fig. 1).

Each classroom is 6.6 m wide and 7.4 m deep, with a floor-to-ceiling distance of 3.2 m. The lighting system consists of 6 luminaires, each equipped with 2x36W fluorescent tubes, with a parabolic aluminum reflector and anti-glare louvers, plus 2 luminaires equipped with 1x36 W fluorescent tube for the blackboard. The CCT of the lamps is approximately 2880 K and the CRI is 84. They are all ceiling mounted and are located as shown in Fig.2. The luminaires are controlled through two on/off switches.

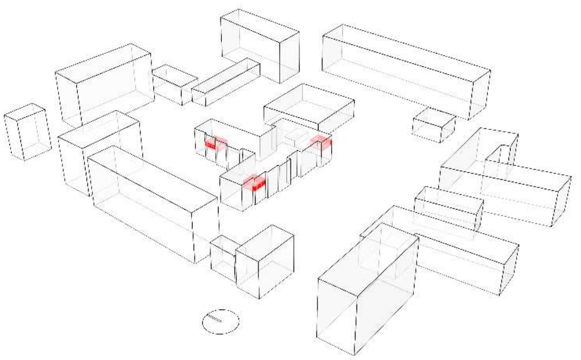

(a)

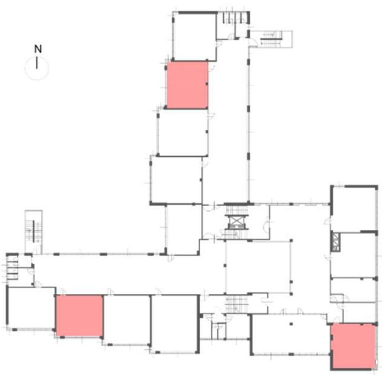

(b)

Fig. 1. Views that show the position of the 3 classrooms analyzed. (a) view from SW; (b) plan view.

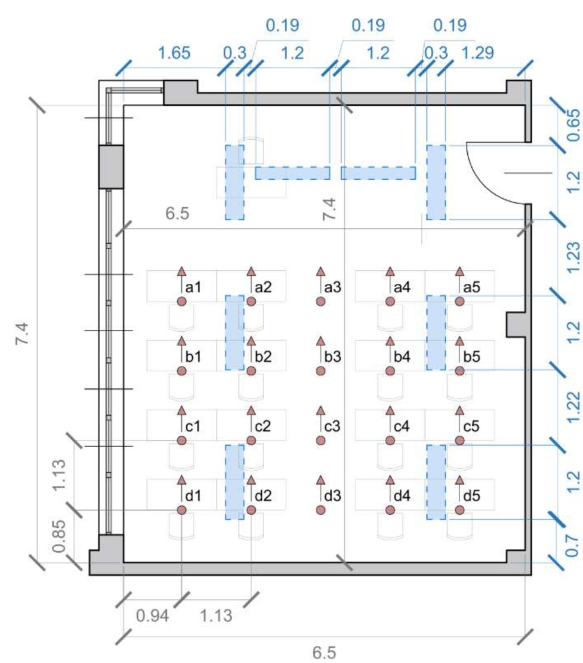

Fig. 2. Position of the points where photopic and melanopic illuminance were measured.

The transparent envelope has a clerestory window with double pane glazing and metal frames. The windows cover the entire width of the façade as well as one of the room corners; they are 1.85 m high, with a sill and a lintel that are 0.97 m and 2.82 above the finished floor, respectively. The resulting window-to-wall ratio is WWR = 0.55 (relative to the main façade, excluding the corner window), while the window-to-floor ratio is WFR = 0.26. The windows are equipped with blinds that are manually operated by the occupants.

An average illuminance of 300 lx was assumed as requirement for the desk plane, in accordance with the Standard EN 12464-1:2011 [32] as the lighting system was designed and installed before the release of the latest version of the standard (2021). The spaces were assumed as occupied in weekdays, from 8:30 until 16:30.

III. METHOD

The research relied on a combination of approaches: (i) field measurements to characterize photopic and melanopic illuminances in the classrooms for electric lighting; (ii) simulations to characterize photopic and melanopic illuminances for daylighting; (iii) combination of results to analyze the integrative lighting due to the combination of daylight and electric light.

For the study, it was decided to refer to the indications set by WELL Building Standard version 2 (WELL v2, Q2 2022) [22]. The document, which operates on a points-based system, provides target reference values for both visual lighting design (Feature L02) and circadian lighting design (Feature L03), which makes it suitable for an integrative lighting analysis.

For what concern the visual requirements, as indicated also by the WELL protocol, the thresholds specified in the Standard EN 12464-1:2011 were assumed for this study [32].

For what concerns the circadian lighting design, the WELL, Feature L03, sets indications and threshold values "*to provide users with appropriate exposure to light for maintaining circadian health and aligning the circadian rhythm with the day-night cycle*". Table I reports the threshold values that are provided for all workstations in regularly occupied spaces to obtain 1 or 3 points.

TABLE I. WELL PROTOCOL INDICATIONS FOR CIRCADIAN LIGHTING

1 point	3 points
at least 136 lux m-EDI;	at least 250 lux m-EDI;
or	*or*
at least 109 m-EDI and 70% of all workstations are within 4.88 m of transparent envelope glazing. Visible light transmittance (T_v) is greater than 40%;	at least 163 m-EDI and 70% of all workstations are within 4.88 m of transparent envelope glazing. Visible light transmittance (T_v) is greater than 40%;
or	*or*
at least 109 m-EDI and average $sDA_{300,50\%}$ is achieved for >75% of regularly occupied floor area.	at least 163 m-EDI and average $sDA_{300,50\%}$ is achieved for >75% of regularly occupied floor area.
The light level must be present on the vertical plane at eye level, to simulate the light entering the eye of the occupant, for at least 4 hours (beginning by noon at the latest) at a height of 0,45 m above workplane.	

Electric lighting

Photopic and melanopic illuminances were measured for a reference classroom in the absence of daylight, using a spectrophotometer with a measurement range of 360–830 nm and a measurement sensitivity of 10 nm (error: ±2.2%). The measurements were taken according to a grid with a spacing of 1 m, set in accordance with a typical layout of student desks (Fig. 2). For each grid point, different quantities were acquired: photopic illuminances were measured at the desk height (horizontal plane), while melanopic and photopic illuminances were measured, at the same grid points, on a vertical plane, set 1.2 m above the finished floor, looking forward to the blackboard, so as to reproduce the most recurring view direction of the students in a classroom. Melanopic measures were taken according to the same grid as photopic horizontal illuminance, thus measuring the circadian contribution at students' eyes in their real position.

Considering that the three classrooms analyzed present the same geometry, materials, and lighting systems, the measurement campaign was carried out in one room only.

Daylighting

Unlike electric lighting, the daylighting amount in the three classrooms changes along time. For this reason, it was decided to simulate daylighting rather than to take measurements, as these latter could not be fully representative of the varying conditions during the course of a year. Three simulation tools were considered: (i) ALFA, a plugin for Rhinoceros 3D developed by Solemma; (ii) Lark, plugin for Grasshopper developed to evaluate circadian lighting by Inanici and ZGF Architects [33]; and (iii) Owl, a plugin for Grasshopper recently developed by Maskarenj et al. [34]. ALFA was eventually chosen as simulation tool: Owl allows the spectral power distribution of a local sky to be simulated starting from local measurements, but it was discarded as in its current version it does not simulate the indirect contribution of spectral daylight that arrives at the eyes of an occupant; besides, as pointed out by Balakrishnan and Jakubiec [35] and by Pierson et al. [36], ALFA yields a higher analysis resolution than Lark, as it uses an extended Radiance engine to render a space 81-color spectra (versus the 9-color spectra rendered by Lark). Furthermore, it calculates EML values for a grid of points (at eye-level) and for up to 8 view directions at each point, thus allowing a full space to be analyzed. The spectral reflectance properties of opaque components as well the spectral transmittance properties of glazing can be simulated, also adding user-defined materials. To use the actual reflectances of the classrooms in simulations, the spectral properties of ceiling, walls, floors, frames, and furniture were measured in-situ using a contact spectrophotometer with a measurement range of 400–700 nm and a measurement sensitivity of 10 nm (error: ±5%). For each sample, the reflectance including the specular component (SCI) and excluding it (SCE) were both acquired by the instrument, for a more consistent simulation of each material in ALFA.

As for the spectral transmittance of glazings and blinds, this was measured as a package *glazing+blind*, using the Gigahertz spectrophotometer described earlier, through the following procedure: (i) the spectral radiation was measured positioning the instrument right behind the blind, with closed window; (ii) the spectral radiation was measured keeping the instrument in the same position but with blinds pulled out and window open; (iii) the spectral transmittance of the package single *glazing+blind* was determined across the range 360-830 nm through the ratio of quantity (i) to quantity (ii).

The spectral transmittance of the *glazing+blind* package was imported in Optics and then exported as a *.usr* file, which is a format read by ALFA to create a new transparent material.

At the end of the process, it was therefore possible to simulate the package as a glazing with the same spectral transmittance as the package *glazing+blind*, but with a specular behavior; it was not possible to measure and to simulate the scattering property of the blind.

Fig. 3 shows the light reflectance and transmittance spectral properties of the main materials measured in-situ.

Considering the different orientations and obstruction context, the three classrooms under analysis were modeled in Rhino, along with the volume of the entire educational building and the urban settings around. The spectral properties of the materials were modeled in ALFA, and simulations were run for the following specific, reference time-steps:

- December 21st, from 8:30 throughout 16:30, with a time interval of 1 h
- March 21st, same range as for December 21st
- June 21st, from 07:30 throughout 15:30 (time interval: 1 h) to account for the daylight-saving time.

The above schedule was selected as representative of the actual occupancy profile of the classrooms, while the three reference days were selected to analyze the melanopic content in the classrooms for the two extreme situations during a year (the two solstices), plus one intermediate condition (the spring equinox, which also represents the fall equinox). Consistently with this logic, simulations were repeated for each time-step assuming two, extreme, sky conditions: clear sky with sun and overcast sky. For the clear sky condition, the possibility of using the blinds to screen sunlight was also considered.

The same grid of sensor points used to measure melanopic illuminances in-the-field under electric lighting was also used for daylighting simulations (see Fig. 4).

Beside ALFA simulations, a set of annual simulations were run using Climate Studio, with two objectives:

- to determine the shading device profile for the three considered days of the year in case of clear sky; for

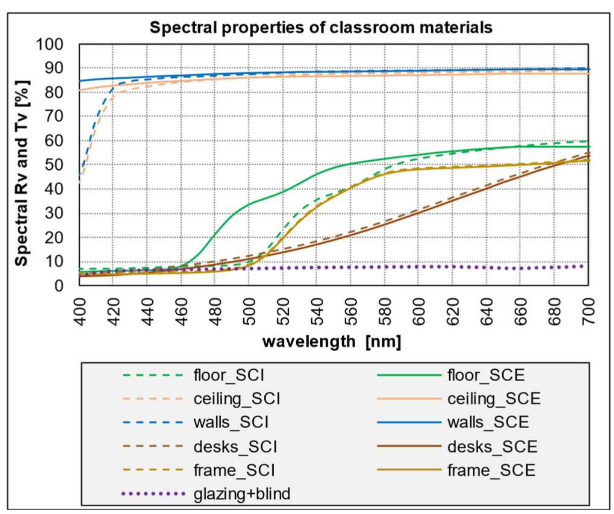

Fig. 3. Light reflectance/transmittance spectral properties of main materials measured in the classrooms.

Fig. 4. Views of the model used to run ALFA (above) simulations.

this purpose, the annual sunlight exposure ASE was calculated, consistently with the criterion set by IES LM-83-12 [37], "*blinds shall close whenever more than 2% of the analysis points receive direct sunlight*"

- to determine the annual values of the spatial daylight autonomy $sDA_{300,50\%}$; as mentioned in Table I, the target m-EDI required by the WELL protocol (Feature L03) can be decreased from 250 lx to 163 lx, and still grant the maximum score of 3 points, if $sDA_{300,50\%} \geqslant 75\%$ of regularly occupied floor area. For this purpose, sDA values were calculated for the same grid used for the melanopic illuminances, which covers the desk area, with a spacing of 30 cm.

Integration of daylighting and electric lighting

Results from electric lighting (measurements) and from daylighting analyses (simulations) were eventually combined to carry out an analysis of the global lighting conditions in the three classrooms.

The goal of this final stage was to define: (*i*) on the one hand, the sufficiency of daylighting (under an overcast and a clear sky, with and without the use of blinds) in meeting both the photopic illuminance requirement (E_{p_wp} = 300 lx on the horizontal workplane) and the melanopic illuminance requirement (m-EDI = 250 lx - or 163 lx if the spatial daylight autonomy in the spaces is higher than 75%); (*ii*) on the other hand, in case of insufficient daylight, the supplementary contribution from electric lighting. The electric lighting was considered switched on when daylight illuminance fell below 300 lux on at least one point on the horizontal workplane. For time-steps when such incompliance occurred, the circadian illuminance on the vertical plane was quantified to verify if the minimum threshold m-EDI ≥ 250 lx (or 163 lx) was also met, with the goal to determine both a workplane-photopic and a vertical-eye level-circadian profile.

IV. Results

Electric lighting

Fig. 5 summarizes the results that were obtained through field measurements in electric lighting conditions. The following data are presented, relative to the area with students' desks: (i) horizontal workplane illuminance, E_{p_wp}; (ii) vertical photopic illuminance at the eyes, E_{p_eye}; (iii) melanopic equivalent daylight illuminance at eyes, m-EDI_eyes; (iv) ratio of the eye vertical to the workplane horizontal illuminance, E_{p_eyes}/E_{p_wp}; and (v) the melanopic ratio at the eyes, M/P_eyes. Besides, the CCT was also measured at the eye-level at each grid point (not displayed in Fig. 5): CCT values were rather warm (values in 2482-2620 K, with an average value of 2551 K), due to the

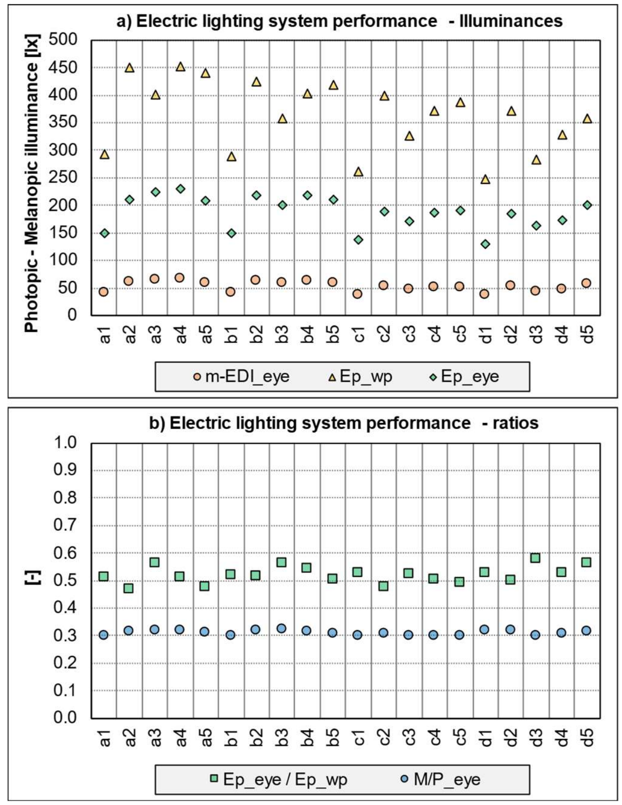

Fig. 5. Results from field measurements for electric lighting.

combination of the spectral content of light sources and the spectral reflectance of materials (shown in Fig. 3).

The following considerations can be stressed:

- as for E_{p_wp}: the average illuminance was 363 lx, with a minimum value of 247 lx and a thus a uniformity of 0.68; these values are compliant with the requirements set by the EN 12464-1:2011 [32]
- as for m-EDI_eyes: the average illuminance was 52.6 lx, with a minimum value of 37.4 lx and a maximum of 66.3 lx; therefore, all values in the classroom are far below the minimum values indicated by the WELL protocol [23]
- as for M/P_eyes: all values are in the range 0.30-0.32, with an average value of 0.31
- as for the ratio E_{p_eyes}/E_{p_wp}: all values are in the range 0.47-0.58, with an average value of 0.52; on average, the vertical illuminance at eye-level is around half of the horizontal illuminance measured at the same location, but on the workplane.

Daylighting and electric lighting

Relative to daylighting, a set of simulations was run using ALFA for the days 21st March (spring equinox), 21st June (summer solstice) and 21st December (winter solstice), for the three orientations considered, under a clear and an overcast sky. The simulations were run with an hourly timestep, from 08:30 to 16:30 for March and December and from 07:30 to 15:30 for June, to account for daylight-saving time.

Prior to running ALFA simulations, a set of annual simulations were run using Climate Studio to calculate the spatial Daylight Autonomy $sDA_{300,50\%}$: these simulations showed that sDA was as high as 99% in all the three classrooms, independently of the orientation. This means that all the spaces qualify for the Feature L05 according to the WELL protocol and therefore reduced m-EDI values of 163 lx are sufficient to get the maximum score of 3 points.

For ALFA simulations, an operable fabric blind was also considered for clear skies, whose utilisation profile is shown in Fig. 6. As one would expect, the blinds are only required in the morning in the classroom with East-facing windows, mainly before 10:30, with the exception of the 21st of December, when they are used until 12:30. Conversely, in the classroom with West-facing windows, the blinds are required in the afternoon only, after 14:30. Differently, for the classroom with South-facing windows, the blinds are used for most of the day in spring and winter, while they are never necessary on the 21st of June, due to the high sun elevation in summer at Turin latitude.

For all skies, the contribution of the electric lighting system was also accounted: it was considered as switched on whenever illuminance fell below the target value of 300 lx in any point of the grid that covers the desks. Fig. 6 shows the electric lighting usage profile for all the days, all the sky conditions, and all the orientations analysed. It is possible to observe how, under a clear sky without blinds, the use of electric lighting is only required on the 21st of December in the early morning and late afternoon. This applies to all the three orientations and is due to the few daylight hours and low daylight availability on winter solstice at Turin latitude. When the blinds are used, the number of hours in which the electric lighting is required increases. It is in fact possible to observe that, besides those moments already highlighted for the clear sky, the electric lighting system needs to be switched on whenever the fabric shade is closed. Finally, for the overcast sky condition, the use of the electric lighting in the winter solstice is required throughout the whole day, while for the summer solstice and the spring equinox this needs to be switched on in early morning hours and in late afternoon hours.

As for the performance of the spaces according to the WELL protocol recommendations, it was verified that, through the integration of daylight and electric lighting the target m-EDI to achieve 1-point (see Table I) is verified for all the classrooms considered, for all the days, the sky conditions and the orientations. Considering then the WELL protocol requirement to achieve 3 points, i.e. a minimum value of 163 m-EDI at eye level for at least four hours per day (starting not later than noon), Fig. 7 shows the space fraction meeting such requirement for all the days, the sky conditions and the orientations considered. The bars edged by a solid line represent the contribution of daylight, while the bars edged by a dashed line show the contribution of electric lighting. Analysing the daylight contribution alone, it is possible to observe how, in a clear sky condition for all the days and orientations, it is enough to satisfy the WELL 3-points requirement at all grid points. When the use of the blinds is considered, daylight alone is not sufficient to meet the requirement for the whole space in the South-oriented classroom on the 21st of March and in the same space, as well as in the East-oriented classroom, on the 21st of December. This is due to the high number of hours, especially in the central part of the day, in which the blinds are kept closed. Finally, under an overcast sky, the WELL requirement to achieve 3-points is not met at any grid point on the winter solstice, for all the three classrooms analysed. This is due to the few daylight hours and the scarce daylight availability around this date at Turin latitude (approx. 8.75 hrs).

Considering then the contribution of electric lighting, it is possible to observe how it improves the performance so as to meet the requirement for the whole space for only three of the above cases, namely South- and East-oriented classrooms on the winter solstice in a clear sky condition with the blinds closed and the East-oriented classroom, again on the winter solstice, but under an overcast sky. For the remaining cases, the performance is improved at a space level, but the melanopic requirement set in the WELL protocol to obtain 3 points is not met. This is due, as shown in the previous section (see Fig. 5), to the poor performance of the electric lighting system in terms of melanopic illuminance. In fact, for those moments in which daylight provides a too scarce melanopic illuminance at eye level, the contribution of the electric lighting is not sufficient to reach the minimum m-EDI of 163. If such moments occur for a significant part of the day, then the contribution of the electric lighting, as it happened, might not be sufficient to meet the daily WELL m-EDI requirement for a 3 points evaluation.

Finally, Fig. 8 shows, for all the days, classrooms and sky conditions, the space fraction in which a minimum horizontal photopic illuminance value of 300 lx on the workplane is reached in all the occupied hours through a combination of daylight and electric lighting. Specifically, the bars edged by a solid line represent the contribution of the daylight, while the bars edged by a dashed line show the contribution of the electric lighting system. The results show how, for all the

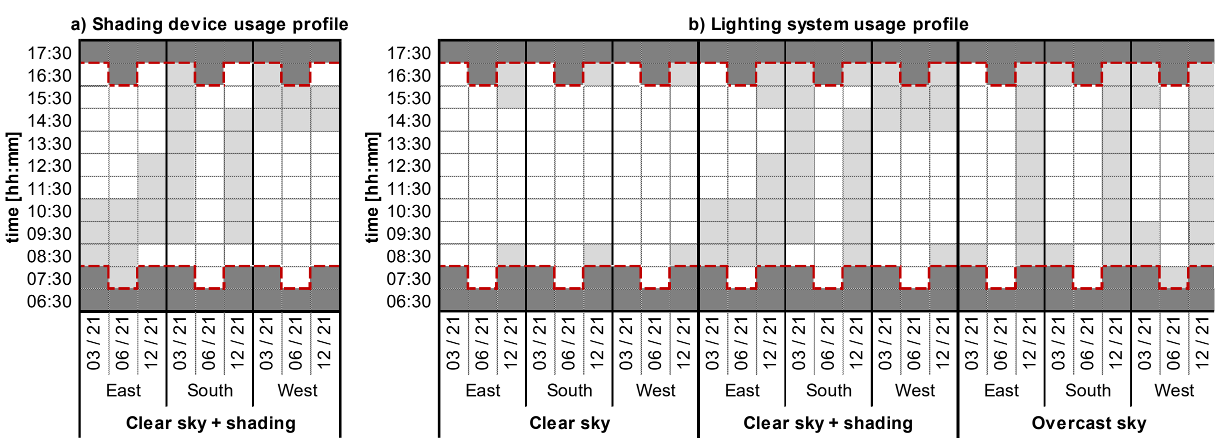

Fig. 6. a) shading utilisation profile (white: shading pulled up, light grey: shading pulled down, dark grey: classroom unoccupied), in clear sky conditions, for all the days and orientations considered; b) lighting system utilisation profile (white: electric lighting off, light grey: electric lighting on, dark grey: classroom unoccupied) for all the sky conditions, days and orientations considered.

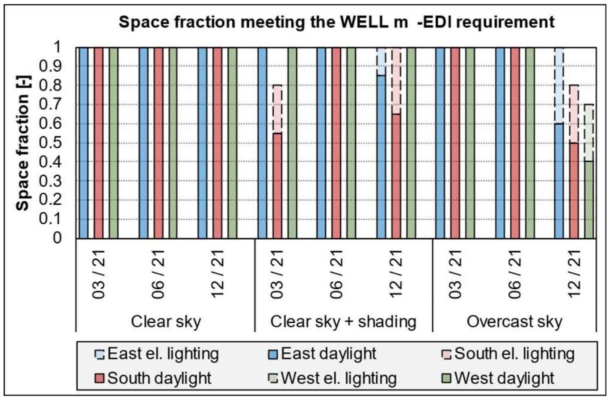

Fig. 7. Daylight and electric lighing contributions to the space fraction meeting the WELL m-EDI daily requirement, for all the days, orientations and sky conditions considered.

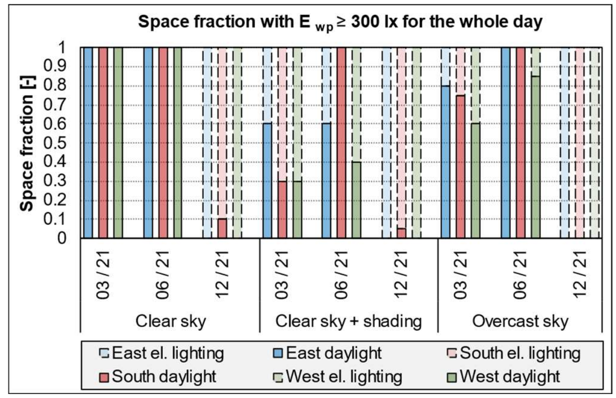

Fig. 8. Daylight and electric lighing contributions to the space fraction meeting the photopic horizontal workplane illuminance requirement, for all the days, orientations and sky conditions considered.

cases analysed, the above requirement is always met in all the points considered. In more detail, if compared to the melanopic performance, the daylight contribution appears weaker, with a higher number of cases in which the electric lighting is required. However, for all these cases, switching on the electric lighting system is sufficient to bring on all the points in the space a workplane illuminance equal to or higher than 300 lx. Observing Fig. 5, it is possible to see that in some points, namely a1, b1, c1, d1 and d3, the lighting system provides on the warplane a horizontal photopic illuminance slightly below the minimum requirement of 300 lx. However, for all the moments analysed a daylight contribution, even if small, was always present, allowing the requirement to be verified for such points as well.

V. Discussion and conclusions

The study presents an analysis on integrative lighting in real classrooms, which considers both the effect of daylighting and electric lighting. For the classrooms analysed, i.e. three similar spaces with different orientations, it was verified what rating could be reached for the circadian lighting Feature (L03), in different days of the year and under different sky conditions, according to the WELL protocol. For all the cases analysed, it was found that it was always possible to reach at least a m-EDI of 109 lux, corresponding to a 1-point rating, through an integration of electric lighting and daylighting. As regards the stricter 3-points rating, it was found that daylight alone was always sufficient to meet the requirements in the spaces and days of the year analysed in a clear sky condition. Conversely, for a cloudy sky condition or if operable blinds are used in clear skies, daylight alone could be insufficient to reach the target m-EDI (163 lux) in some days (mainly on the 21st of December). Out of the 27 combinations *orientation – sky condition – day* considered, the minimum m-EDI to achieve the 3-points rating was not gained by daylight alone in 6 cases, for three of which the use of the electric lighting system allowed the requirement to be still verified. Such a high daylighting performance might be due to the high WWR of the spaces, 0.55, which allows a large amount of daylight to be admitted into the rooms, providing thus high daylight levels also in the points away from the windows.

The study was conducted partly experimentally, mainly for the characterisation of the electric lighting system, and partly numerically, for melanopic and photopic simulations. For this latter part, the main limitation of the study is the reduced number of days (three days of the year) and of sky conditions (only extreme sky conditions were considered, i.e. completely clear and completely overcast sky). Such limitation is due to the impossibility of simulating intermediate sky conditions within ALFA, which makes it impossible to assess the circadian performance of a space on a yearly basis. To overcome this issue, the analysis was performed for three “reference” days of the year, i.e. the two solstices and the spring equinox, in the two extreme sky conditions above. Nevertheless, the validity of such analysis cannot be extended to the whole year, but rather this gives an indication, for the spaces in analysis, of the limit circadian performances during days considered as representative of different seasons of the year.

Moreover, as described in the methodology section, the fabric blind considered was modelled as a specular glazing using the spectral data of the measured *glazing+blind* package. This was necessary because within ALFA it is not possible, to the author’s knowledge, to model a translucent material or to insert a *Bi-directional Scattering Distribution Function* for a shading material. To overcome such limitation, the *glazing+blind* package was modelled as a specular glazing to which the spectral transmittance and reflectance were assigned, based on in-situ measurements. Such modelling assumption may create a bias in the results, since does not allow for that part of the light hitting the blind that gest scattered, i.e. diffused in the indoor ambient. Consequently, the illuminance of the points further from the window may result lower than how this value would actually be, considering also the scattering effect of the shading. Despite this difference, the authors believe that the limitation in the way the fabric blind is modelled is not such as to invalidate the general outcomes of the paper.

As for the case-study, i.e. the three classrooms with different orientations, the results show that the use of the electric lighting system allows the stricter WELL requirement to be met in 3 cases only, out of the 6 in which daylight alone does not satisfy the requirement. Partly, this is due to the light sources the classrooms is equipped with, which have a quite low correlated colour temperature of 2880 K. The environmental circadian performance of the electric lighting system appears thus quite poor, although the system provides adequate horizontal photopic illuminance on the desks plane. This could be explained with the low photopic vertical to horizontal illuminance ratio (E_{p_eyes}/E_{p_wp}) and the low M/P ratio (0.31 considering also the environmental reflections).

Although the results of the study could not be generalized, they provide some indications about integrative lighting in existing Italian school buildings. Despite daylight is the primary light source in classrooms mainly used in the morning and first part of the afternoon, it is not always sufficient to provide the required circadian stimulus, particularly when shading devices are used to control glare, or overcast sky conditions are prevalent. The required vertical m-EDI should be achieved through the electric lighting contribution, but existing electric lighting systems, such as the one analysed in this study, are designed to provide a target illuminance on the horizontal plane and might not be adequate to support a sufficient vertical illuminance at the eye. Furthermore, as shown in the study, the lamps spectral power distribution could be poor in the short wavelengths, thus further lowering the electric lighting contribution to the circadian stimulus.

ACKNOWLEDGEMENTS

The study was carried out within the Agreement between the Department of Energy of the Politecnico di Torino and ITER (Istituto Torinese per una Educazione Responsabile) of the City of Turin (IT) on educational spaces. The authors acknowledge the City of Turin and ITER for making available the spaces of the case-study.

REFERENCES

[1] H. Xiao, H. Cai, X. Li, “Non-visual effects of indoor light environment on humans: A review”, Physiology & Behavior, vol. 228, 2021.

[2] C. Vetter, P. Morgan Pattison, K. Houser, M. Herf, A. J.K. Phillips, K.P. Wright, D.J. Skene, G.C. Brainard, D.B. Boivin, G. Glickman, “A Review of Human Physiological Responses to Light: Implications for the Development of Integrative Lighting Solutions”, LEUKOS, 2021.

[3] K. Houser, P. Boyce, J. Zeitzer, M. Herf, “Human-centric lighting: Myth, magic or metaphor?”, Lighting Research & Technology, 53(2), pp. 97-118, 2021.

[4] D.M. Berson, F.A. Dunn, M. Takao, “Phototransduction by retinal ganglion cells that set the circadian clock”, Science, 295 (5557), pp. 1070–1073, 2002.

[5] S. Hattar, H.W. Liao, M. Takao, D.M. Berson, K.W. Yau, “Melanopsin-containing retinal ganglion cells: architecture, projections, and intrinsic photosensitivity”, Science, 295 (5557), pp. 1065–1070, 2002.

[6] G.C. Brainard, J.P. Hanifin, J.M. Greeson, B. Byrne, G. Glickman, E. Gerner, M.D. Rollag, “Action spectrum for melatonin regulation in humans: evidence for a novel circadian photoreceptor”, J Neurosci, 21(16), pp. 6405–6412, . 2001.

[7] K. Thapan, J. Arendt, D.J. Skene, “An action spectrum for melatonin suppression: evidence for a novel non-rod, non-cone photoreceptor system in humans”, J Physiol. 535 (1), pp. 261–267, 2001.

[8] P. Khademagha, M.B.C. Aries, A.L.P. Rosemann, E.J. van Loenen, “Implementing non-image-forming effects of light in the built environment: a review on what we need”, Build. Environ., 108, pp. 263–272, 2016.

[9] M.S. Rea, M.G. Figueiro, J.D. Bullough, A. Bierman, “A model of phototransduction by the human circadian system”, Brain Research Reviews, 50 (2), pp. 213–228, 2005.

[10] M.S. Rea, M.G. Figueiro, A. Bierman, R. Hamner, “Modelling the spectral sensitivity of the human circadian system”, Lighting Research & Technology, 44 (4), pp. 386–396, 2012.

[11] M.G. Figueiro, M.Kalsher, B.C.Steverson, J.Heerwagen, K. Kampschroer, M.S. Rea, “Circadian-effective light and its impact on alertness in office workers”, Lighting Research & Technology, 51(2), pp. 171-183, 2019.

[12] Underwriters Laboratory, “Design Guidelines for Promoting Circadian Entrainment with Light for Day-Active People”, UL Design Guideline 24480, Edition 1, Northbrook, IL: UL, 2019.

[13] R.J. Lucas et al., “Measuring and using light in the melanopsin age”, Trends in neurosciences, 37(1), pp. 1–9, 2014.

[14] J. Enezi, V. Revell, T. Brown, J. Wynne, L. Schlangen, R. Lucas, “A "melanopic" spectral efficiency function predicts the sensitivity of melanopsin photoreceptors to polychromatic lights”, J. Biol. Rhythms, 26 (4), pp. 314–323, 2011.

[15] CIE. Commission Internationale de l’Eclairage, “CIE system for metrology of optical radiation for ipRGC-influenced responses to light - CIE S 026/E:2018”, Vienna (Austria): CIE Cent. Bur, 2018.

[16] T.M. Brown, “Melanopic illuminance defines the magnitude of human circadian light responses under a wide range of conditions”, J Pineal Res. 69:e12655, 2020.

[17] CIE. Commission Internationale de l’Eclairage, “Position statement on non-visual effects of light. Recommendating proper light at the proper time”, 2nd edition. Vienna (Austria): CIE Cent. Bur., 2019.

[18] S. Altomonte et al., “Ten questions concerning well-being in the built environment”, Building and Environment, vol. 180, 2020.

[19] J.G. Alle et al., “The 9 foundations of a healthy building”, Healthy Buildings Team at Harvard T.H. Chan School of Public Health, 2017.

[20] “Health and wellbeing in homes”, UK Green Building Council, 2016.

[21] “Health, wellbeing & productivity in offices”, UK Green Building Council, 2014.

[22] E. Eitland, L. Klingensmith, P. MacNaughton, J. Cedeno Laurent, J. Spengler, A. Bernstein, J. G. Allen, “Schools for Health: Foundations for Student Success”, Healthy Buildings Team at Harvard T.H. Chan School of Public Health, 2021.

[23] International Well Building Institute, “WELL Building Standard v2”, Q2 2022 Version.

[24] ISO/CIE. International Standards Organization and Commission Internationale de l’Eclairage, “Light and lighting - Integrative lighting - Non-visual effects. ISO/CIE TR 21783”, Under development.

[25] CIE (2016) CIE DIS 017:2016 ILV: International Lighting Vocabulary, 2nd Edition.

[26] L. Bellia, F. Fragliasso, “Good Places to Live and Sleep Well: A Literature Review about the Role of Architecture in Determining Non-Visual Effects of Light”, Int. J. Environ. Res. Public Health, 18, 1002, 2021.

[27] M. Figueiro, D. Overington, “Self-luminous devices and melatonin suppression in adolescents”, Lighting Research & Technology, 48 (8), pp. 966–975, 2016.

[28] V. López-Chao, A.A. Lorenzo, J. Martin-Gutiérrez, “Architectural Indoor Analysis: A Holistic Approach to Understand the Relation of Higher Education Classrooms and Academic Performance”, Sustainability, 11, 6558, 2019.

[29] P. Ricciardi, C. Buratti, “Environmental quality of university classrooms: Subjective and objective evaluation of the thermal, acoustic, and lighting comfort conditions”, Building and Environment, vol. 127, pp. 23-36, 2018.

[30] I. Acosta, M.A. Campano, R. Leslie, L. Radetsky, “Daylighting design for healthy environments: Analysis of educational spaces for optimal circadian stimulus”, Solar Energy, vol. 193, pp. 584-596, 2019.

[31] S. Ezpeleta, E. Orduna-Hospital, J. Aporta, M.J. Luesma, I. Pinilla, A. Sánchez-Cano, “Evaluation of Visual and Nonvisual Levels of Daylight from Spectral Power Distributions Considering Orientation and Seasonality”, Appl. Sci., 11, 5996, 2021.

[32] CEN (Comité Européen de Normalisation). Light and lighting - Lighting of work places - Part 1: Indoor work places. European Standard 12464-1:2011.

[33] Inanici, M. and L. ZGF Architects (2015). Lark spectral lighting.

[34] M. Maskarenj, B. Deroisy, and S. Altomonte. “A new tool and workflow for the simulation of the non-image forming effects of light”. Energy & Buildings 262 (2022) 112012.

[35] P. Balakrishnan, J.A. Jakubiec. “Spectral Rendering with Daylight: A Comparison of Two Spectral Daylight Simulation Platforms”. Proc. of 16th IBPSA Conference, Rome, Italy, Sept. 2-4, 2019, p. 1191-1198.

[36] C. Pierson, M. Aarts, M. Andersen. “Validation of Spectral Simulation Tools for the Prediction of Indoor Daylight Exposure”. Proc. of the 17th IBPSA Conference Building Simulation 2021, Bruges, Belgium, September 1-3, 2021.

[37] Illuminating Engineering Society. IES Lighting Measurements (LM) 83-12, Approved Method: IES Spatial Daylight Autonomy (sDA) and Annual Sunlight Exposure (ASE). IESNA, New York, USA.

Road Lighting as the Backbone of Smart City Networks. Opportunities and Questions

Péter Schwarcz
Senior Lighting and Business Transformation Expert
Tungsram Group
Vice-President
Lighting Society of Hungary
Budapest, Hungary
ptrschwrcz@gmail.com

Abstract—The most of (LED) light sources serve as single endpoints. There is huge potential in turning them to the backbone of smart building and smart cities. However, there are roadblocks slowing down the transformation. This paper highlights some those roadblocks and show potentials.

Keywords—LED lighting, smart cities, smart buildings, LI-FI

I. Introduction

There are approx. 20 billion lampholders installed worldwide, which can (potentially) serve as 20 billion endpoints (or nodes!) for smart systems. Similarly, there are appr. 400 million endpoints at streetlighting networks, which are huge potential for smart road and smart city applications. Road lighting networks could be particularly suitable for being the backbone of a smart network of smart cities. However, the process of transformation seems to be slow. What are the forces to drive them and where the roadblocks are?

II. Evolution of Wireless Telecommunication Technology

The first mobile phones (now, we call them 1G) provided the same functionality as their wired ancestors: they transmitted voice exclusively, but without the restriction of having a wire. It was a revolution in terms of mobility but did not offer any extra functionality beyond voice transmission. 2G technology offered digitally mastered voice, SMS, and other method of transmission of texts. For long time (even today) SMS is the cash cow of the service suppliers. 3G was able to host first applications, transmit voice, videos, and access to the Internet. That is the point, where we could call our communication device as smart phones. 4G made possible HD streaming video-chats and much faster Internet access. The bandwidth, the response time and accessibility of **5G** offers communication platform suitable for billions of IOT device, autonomous cars, Industry 4.0 and **smart cities**.

Fig. 1. The evolution of wireless communication technology. [1]

III. Need for 5G

The main features of 4G and 5G are shown in Table1.

Feature	*4G*	*5G*
Speed, Mbs	20-30	**100-200**
Device density/km^2	2,000	**1,000,000**
Delay, ms	100	**1**
Readiness, %	99,25	**99,999**
Range, m	**1000-5,000**	30-50

Fig. 2. Features of 4G and 5G networks.

Most people remember the increase in speed, but other features are more important in terms of extending number of potential users. The need for increasing the number of IOT devices is evident and 2,000/km2 of 4G is real roadblock, there will be much more endpoints to serve.. Just think about one single autonomous car can have a couple of dozens of endpoints require connection. Similarly, the non-operational ratio of 4G (0,75% equals to 27 sec in every hour) is simply inadequate for autonomous cars, as it runs 450 m within 27 sec at a speed of 60 km/hrs.

There are forecasts with different models about the need for mobile data traffic in the next 10 years. Even pessimistic model forecasts 1,500EB/month, while optimistic model does 6,000 EB/month. Whatever will happen, the need for millions of transmission points for 5G (or 6G later on) and proper bandwidth is evident.

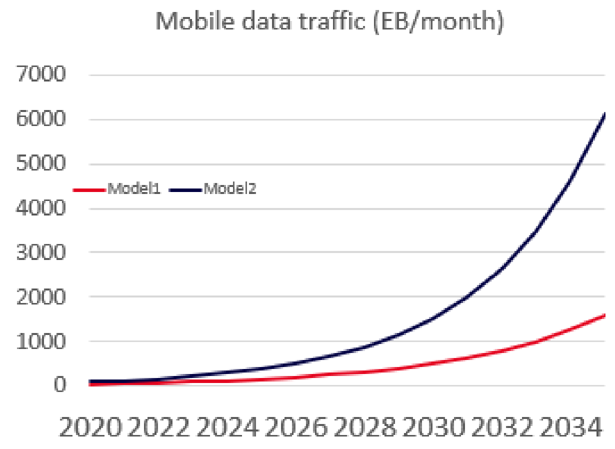

Fig. 3. Foreseen Mobile Data Traffic

IV. ENCREASING ECONOMY POTENTIAL IN IOT

The Internet of Things' large and still growing economic value potential are concentrated in nine settings where the technology is deployed, see Figure 3 [2].

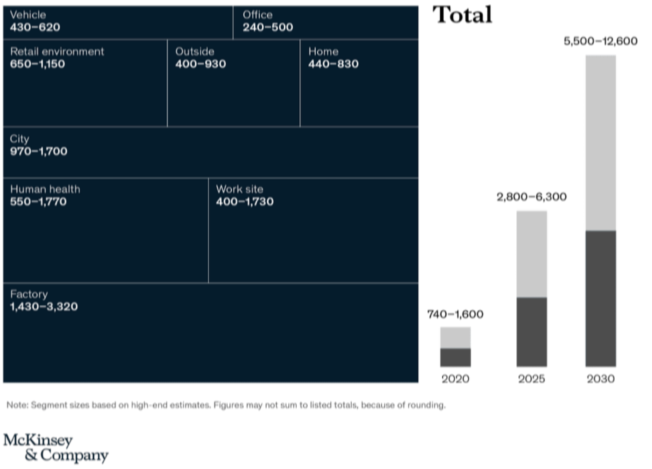

Fig. 4. Estimated 2030 economic value of IOT adoption, by setting, billion USD

The median of the estimated economic value of IOT is 9,050 billion USD. Just comparison, the estimated value of the total lighting market in 2027 is 163 billion USD. Even partial adaption of IOT can give a significant economic boost to lighting industry. [3]

V. POSITION OF LIGHTING ENDPOINTS

The positions of the endpoints of road lighting networks are gaining a real advantage with the progress of 5G (and 6G later) networks. The transmitters of 5G can only cover approx. 50 m, in a built-up area it is even less. The spacing of a typical road lighting network is 20-50 m and endpoints are 6-12 m above the potential users (i.e. pedestrians, cars and street infrastructure elements. Those street lighting positions are ideal for 5G transmitters and as an additional advantage, they can give locations for sensors, which give guidance to self-driven vehicles and other smart devices on the road.

VI. POWER SUPPLY

The power supply for the lamp can supply the smart and communication devices, as well. But it's not that simple, as it looks like. With a few exceptions, today the lighting endpoints are energized only if the lighting function is required. The lighting is controlled from the wall-switch, which cuts the supply of lighting endpoint, as well as the supply of the potential smart device. This is a real disadvantage and significantly reduces the readiness of a smart device. In most of the countries, the streetlighting networks are not energised either during the day. Today, the operators of the streetlighting supply networks are reluctant to give 24 h supply due to the large investment is needed for transformation and increased loss of on the network due longer operation hours. Who is going to cover the huge capital cost of the change to 24/7 operation? It looks like a landlord-tenant trap, and nobody wants to do the first step.

VII. OWNERSHIP

One of the most prominent roadblocks against the marriage of 5G and road lighting network is the complicated ownership structure of a road lighting. Usually, there are independent owners of the control system, the supply network, the supporting structure, and the luminaires. In addition, the most complicated and important issue: who owns the data generated by the system. The ownership structure varies by cities and countries. Rapid expansion of smart city system would require a simplified business process. If it is not solved within a reasonable time, the investors to smart cities will look for alternative backbones or build their own dedicated network.

VIII. SURGE PROTECTION OF LIGHTING NETWORKS

It is well-known that an equipment at the end of the supply network cannot be protected properly against damages surge and over-voltage without the protection of the network itself.

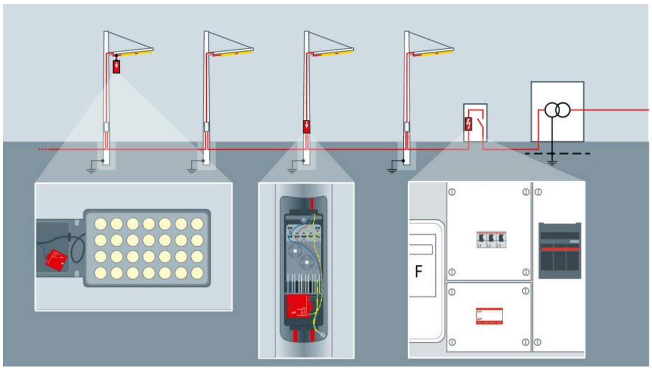

Fig. 5. The recommended locations of the surge protection system, see red boxes. [4]

Today, the full responsibility of surge protection is left to the luminaire suppliers exclusively (the most left red box in Fig. 5). This is not a good approach. The high-level protection requires elements installed at the bottom of the pole and in the distribution cabinet. The sensors, transmitters (of 5G) and other devices of smart cities are also very sensitive for surges and their cost is much higher than that of luminaires. The effective, reliable, and much cheaper surge protection of the network cannot be delayed further. If this is not resolved in short-term, it will once again divert the smart city investors from using the lighting grid as their backbone.

IX. IS THE LIGHTING EQUIPMENT A SINGLE-FUNCTION ENDPOINT OR A SMART PLATFORM?

When LEDs took the lead, lighting industry made a huge leap towards digitization of lighting. The LED lamp and luminaire have become digital inside, but they remained a single-function endpoint for their users. It was a huge leap when we started to use cell phones instead of a landline phone, but we used only one single feature: we called each other and have a voice communication. The real breakthrough was when standard interfaces appeared in the phone on both the software and hardware sides, and ANYONE (not only the producer of the hardware) could install an additional application. That was the point when the cell-phone was transformed from an endpoint to a node of a hub, to a platform. The voice service was (and remained) a must, but not a differentiator anymore.

If lighting devices will be switched from an endpoint to a platform, this would change both user experience and business value chain.

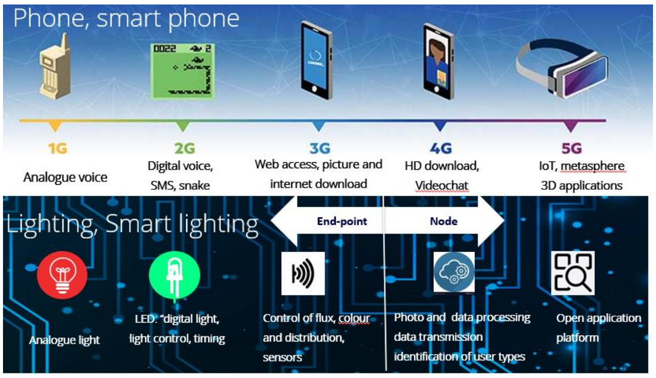

Fig. 6. The foreseen evolution from lighting unit to open application platform for smart building or smart city

The lighting industry is on halfway from single endpoint toward offering a hub. The digital control of light, integration of sensors is quite common, but very few companies offer open platform for smart building or smart cities. However, this platform must be interoperable, safe, and open protocol!

X. VLC and LiFi

LiFi is a wireless communication technology that uses the infrared and visible light spectrum for highspeed data communication. LiFi, first coined in extends the concept of visible light communication (VLC) to achieve high speed, secure, bi-directional, and fully networked wireless communications. [5]

The experimental applications of LiFi can make 1Tb/s. So, it can carry a thousand times more data as 5G. Virtual space will soon change from 2D to 3D, and this will increase the demand for data transfer by orders of magnitude. So far, fundamentally, only people's personal devices have used the bandwidth. The need is limited because of the limited of number of people. With the rapid spread of IoT (Internet of Things), the number of (smart) devices and the amount of data they require and generate will increase the demand almost indefinitely. Just an example: One autonomous vehicle generates 25 GB of data per hour. And to transmit this, data points must be there on the street, on all the streets. Exactly where the endpoints of road lighting networks are now.

The key advantages of a LiFi wireless networking layer are:

- three orders of magnitude enhanced data densities [6];
- unique properties to enhance physical layer security [7];
- use in intrinsically safe environments such as petrochemical plants and oil platforms where RF is often banned;
- with the advent of power-over-ethernet (PoE) and its use in lighting, there exists the opportunity to piggy-back on existing data network infrastructures for the required backhaul connections between the light sources with its integrated LiFi modem, and the Internet.

XI. Summary

The demand for data generation, data processing, and data transmission is growing at an unprecedented rate. Synergy with lighting network seems to be a common sense. The foundation and transformation of technical, economic, and legal environment is in our hands. Whichever industry will arrive first to this space, will carve out a larger slice of the cake. Roadblocks must be removed. The theme is on the street.

Notice

This paper contains certain forward-looking statements. By their nature, forward-looking statements involve uncertainties because they relate to events that may or may not occur in the future. Forward looking statements in this paper are based on current estimates and assumptions that is made to the best knowledge of the author and referenced sources.

References

[1] https://www.digitalrealty.com/blog/5g-how-we-got-here-and-its-impact-on-data-center-infrastructure

[2] https://www.mckinsey.com/business-functions/mckinsey-digital/our-insights/iot-value-set-to-accelerate-through-2030-where-and-how-to-capture-it?cid=other-soc-lkn-mop-mck-oth-2111--&sid=6209212851&linkId=148622620https://www.fortunebusinessinsights.com/industry-reports/lighting-market-101542

[3] K. Kovács, dr: The up-to-date surge protection of LED luminaires, (Kültéri LED-es lámpatestek korszerű túlfeszültség-védelme) (Oral presentation at LED conference organised by Lighting Society of Hungary, 2014.

[5] https://www.led-professional.com/resources-1/articles/lifi-as-a-paradigm-shifting-5g-technology

[6] I. Stefan, H. Burchardt, and H. Haas, "Area spectral efficiency performance comparison between VLC and RF femtocell networks," in IEEE International Conference on Communications (ICC), 2013, pp. 3825–3829

[7] Y. Liang and H. Haas, "Physical-Layer Security in Multiuser Visible Light Communication Networks," IEEE J. Sel. Areas Commun

Lighting business: a competency-based course on business modelling and entrepreneurship in lighting

Frédéric B. Leloup
Light&Lighting Laboratory,
Department of Electrical Engineering (ESAT)
KU Leuven
Gent, Belgium
Frederic.Leloup@kuleuven.be

***Abstract*—This article reports on a new introductory course on entrepreneurship and business modelling in lighting. The course is structured around a real practical issue, for which students have to work out a solution and fit it into a viable business model by aid of a design thinking process. The pedagogical approach is built around the philosophy of competency-based teaching. Stress is thereby laid on the uptake of skills and competences through the entire process. The effectiveness of the course is surveyed by presenting all students with a questionnaire that examines their propensity for entrepreneurship before and after attending the course. The results provide empirical evidence of the positive effect of the course on the students' entrepreneurial mindset. Especially the perception of the feasibility to perform entrepreneurial activities has significantly raised.**

***Keywords*— Entrepreneurship education, design thinking process, competency-based learning**

I. Introduction

Entrepreneurship and innovation play a key role in business environments which rapidly change, such as the lighting industry. Indeed, the development and technological advancement of led lighting has dominated innovation within the industry over the past 15 years. Lighting manufacturers were thereby forced to pivot their business from conventional lighting solutions to the development of new luminaires based on solid state technology. Value was primarily created and delivered through efficiency gains and extended lifetime. Besides the technological advances, the shift was further supported by political decisions and legislative implementations. Today, now that led lighting has matured, the innovation focus shifts towards aspects of sustainability, well-being and the integration of smart applications. As a result, established companies need to review their business model again, and alternative types of business models make their appearance.

Successful start-ups and companies discern themselves from competition by their ability to recognize and to adapt to the changing environment. The relevance and importance of teaching and understanding entrepreneurship principles has therefore gained attention in universities and fields of study other than economics [1], such that many courses or even (under)graduate programmes on the subject have evolved worldwide [2].

While the universal need and importance of teaching entrepreneurship has been recognized [3, 4], the debate has shifted towards the appropriate method of how to teach it in order to be effective. Traditional entrepreneurship programmes focus on operational skill sets and apply an analytical approach of teaching opportunity evaluation, feasibility analysis, and business planning [5]. More recently, proposals were made to shift to a methodological approach which focusses on developing an entrepreneurial mindset, skills and behaviour [6].

This article reports on the development, introduction, and first teaching experiences of a new introductory course on business model innovation and entrepreneurship among engineering and physics students, entitled "Lighting business". The course is incorporated in the lighting track of a new international Erasmus Mundus programme labelled "Master of Science in Imaging and Light in Extended Reality", implemented by a consortium of four universities (see https://imlex.org/).

Adhering to the competency-based perspective [7], the pedagogical approach and specificities of the course are first presented. The key results of a performed student survey to evaluate the general quality and effectiveness of the course are then discussed. Finally, the main findings are considered in relation to the theoretical framework of planned behaviour.

II. Approach

"Lighting business" is included in the lighting track programme of the first year of the IMLEX master, and teached at KU Leuven during the second semester. The first edition of the course was held in academic year '20-'21. Seven resp. 4 students who previously obtained their bachelor degree in physics or electrical engineering enrolled for the programme during the first (academic year '20-'21) resp. second (academic year '21-'22) edition. None of them had prior knowledge of business models or entrepreneurship.

The pedagogical approach of the course is built around the philosophy of competency-based teaching [7], with a focus on methods for developing entrepreneurial attitudes, skills and competences. The course is structured around a real practical issue presented by a lighting company, for which the students have to work out a solution. For this, a design thinking approach is followed, using the "double diamond model" in which creating an understanding and defining the intrinsic problem is considered first, before generating ideas and solutions in a second phase. During each phase, students are presented specific techniques and methods to implement. Stress is laid on the uptake of skills and competences through the entire process, not on the final outcome. As such, the students are graded on how they complete both phases, and on what learnings they have achieved.

Before to start with the practical assignment, student teams are formed consisting of 3 or 4 students. For this, each student first performs a Belbin test [8] to identify his or her specific team role(s). Student teams are then formed in order to guarantee as much team member diversity as possible. Each team is assigned a different case during a first workshop, presented by a representative of the company that developed the problem statement, and who will be available for contact with the team throughout the course.

In the first phase of creating understanding, each group is instructed to collect information about the problem. Interviews are a powerful tool to get a deeper understanding of people's needs and problems. Therefore, each student team is instructed to interview the representative of the company that defined the problem statement, as well as one of the company's affected customers. Theoretical background on how to prepare and conduct an interview is provided beforehand in a lecture.

After collection, the information is analysed with the aim to find underlying problems or needs which typical users encounter. Again, specific techniques and frameworks are provided and explained through practical examples during lectures. For instance, the 5 W's (Who, What, When, Where, Why) and 5 Why's analysis method are exemplified as means for understanding and defining the real problem of a customer, while personas and organisatas are implemented as a tool to identify the typical users in terms of motivations and goals.

To conclude the first phase and before entering the second phase in which stress is laid on the generation and feasibility of ideas, student teams are instructed to present how they have completed the first phase to each other during a workshop. If possible (i.e. when multiple teams have been created), student teams are thereby expected to ask questions and to provide specific thoughts and feedback on the results presented by another team.

After having deepened their understanding of the problem, the teams start with generating solutions in phase 2 of the design thinking process. An obvious technique for generating ideas is brainstorming. To get the teams started, different brainstorming techniques (6 thinking hats, reverse brainstorming, etc.) are explained by aid of practical examples. Each team is challenged to come up with at least 10 solutions for their specific business case.

The viability of the generated business ideas is further on determined through a feasibility analysis. The feasibility analysis includes 4 components: product/service, industry/target market, organizational and financial feasibility [9]. Techniques and frameworks, such as the PESTEL analysis and Porter's Five Forces Model [10], are discussed as a means of conducting the analysis.

Finally, each team retains one solution, and fits it into a viable business model. The business model canvas [11] is thereby used as the theoretical framework, and practical examples of well-known companies applying standard business models (freemium, product as a service, multi-sided platform, etc.) are considered for inspiration. As a final step, the teams pitch their solution and associated business model in front of a jury, composed of the representative of the company, the course co-ordinator, and two additional external experts. These additional experts are business representatives who presented their experiences about a topic of the course during an "inspiring session" earlier in the semester.

As mentioned before, the students are mainly assessed on the learning process. An effective way to capture the learning process has been through a learning or reflection log [12]. Additional to the mid-term presentation and final pitch, each student therefore individually documents his or her own input through the different stages of the design thinking process in a student portfolio. In addition, this student portfolio contains a self-reflection of the most important insights acquired during the course, and a peer evaluation of the other team members. The student portfolio must be submitted 3 weeks after the final pitch.

III. Key insights

As a general quality assessment and to investigate the effectiveness of the course, all students took part in a survey that was further designed to examine their propensity for entrepreneurship before and after attending the course.

The first part of the survey includes 12 statements related to the general structure, overall quality and relevance of the course, for which the respondents have to indicate their agreement on a six-point Likert scale, with 1 representing "I do not agree at all" to 6 representing "I totally agree". The second part of the survey is based on and adapted from the Entrepreneurial Intention Questionnaire (EIQ v3.2), originally including 20 items, designed and developed by [13]. Since this course only forms an introduction to entrepreneurship with the purpose to make the students acquainted with general aspects of entrepreneurship and business modelling, only 16 statements related to the personal attitude toward entrepreneurship (5 questions), the perceived control of entrepreneurial activities (6 questions) and the personal entrepreneurial intentions (5 questions) are retained. Respondents point out their agreement to the 16 statements on a seven-point Likert scale, with 1 representing "totally disagree" to 7 representing "totally agree". This second part of the survey was conducted 2 times: once during the first lecture (pre-test data), and once the course had been completed (post-test data).

Results of the survey indicate that all students were satisfied with the general structure and overall quality of the course. The mean score (M) of all respondents to all questions numbers 5.22, with a standard deviation (SD) of 0.91. More specific, the comprehensive manner in which the subject matter is conveyed ($M = 5.73$, $SD = 0.62$), the accessibility to students ($M = 5.64$, $SD = 0.64$), the quality of teaching ($M = 5.55$, $SD = 0.50$) and the logical structure of the course ($M = 5.45$, $SD = 0.50$) form the most noticeable positive feedback. Not surprisingly, the relevance of the course to the respondents' education ($M = 4.36$, $SD = 1.15$) and the difficulty of the course ($M = 4.82$, $SD = 0.94$) are rated lowest.

To investigate the effectiveness and impact of the course on the entrepreneurial intentions of the students, the difference in responses before and after taking the course was assessed for each of the 3 described factors (attitude, control and intention) by means of a right-tailed dependent t-test for paired samples. The normality assumption was thereby checked based on the Shapiro-Wilk test ($\alpha = 0.05$). The results of each t-test, together with the mean results of all students before and after taking the course, are summarized in Table 1.

Since none of the students had relevant previous knowledge, it forms no surprise that the entrepreneurial intentions before following the course are rather low. On average, the personal attitude toward entrepreneurship after attending the course does not change (incremental increase of only 0.02 units - $M = 3.78$, $SD = 1.61$ after vs. $M = 3.76$, $SD = 1.80$ before). The results of the paired t-test indicate a statistically non-significant difference ($t(54) = 0.080$; $p = .468$). Since the normality assumption is not met ($p = .0072$), a Wilcoxon Signed-Rank test was further performed to test the hypothesis. The result (p = .758) supports the former finding that not enough evidence exists to reject the null hypothesis, i.e., that no significant differences exist between the test results after vs. before attending the course.

Behavioural control refers to the students' perception of the feasibility to perform entrepreneurial activities, as will be discussed further. The potential effect of the course on behavioural control seems to be more explicit than on the attitude towards entrepreneurship, with an increase in average value of 1.57 units, from M = 2.55, SD = 1.55 before to M = 4.12, SD = 1.68 after attending the course. The results of the paired t-test confirm the course effect to be statistically significant ($t(65)$ = 7.33; p < .001). The observed effect size is large (d = 0.90). The normality assumption is again not met (p = .0003). Yet, the therefore further performed Wilcoxon Signed-Rank test supports the alternative hypothesis that the survey results before attending the course are significantly smaller than the results after attending the course (p < .001).

In accordance with the results for behavioural control, the students' entrepreneurial intention also increases after attending the course, on average with 0.51 units from M = 2.85, SD = 1.86 before to M = 3.36, SD = 1.61 after attending the course. The results of the paired t-test confirm the effect to be statistically significant ($t(54)$ = 2.81; p = .003). The observed effect size is small (d = 0.38). Again, since the normality assumption is not met (p = .003), a Wilcoxon Signed-Rank test was performed. The test confirms that the results before attending the course are significantly smaller than the results after attending the course (p = .004).

TABLE I. COMPARISON BETWEEN THE ENTREPRENEURIAL INTENTION OF STUDENTS BASED ON 3 FACTORS (ATTITUDE, CONTROL AND INTENTION) BEFORE AND AFTER ATTENDING THE COURSE, BY MEANS OF RIGHT-TAILED DEPENDENT *T*-TESTS.

	Before		***After***		***t-test for equality of means***	
Factors	***M***	***SD***	***M***	***SD***	***t***	***p***
Attitude toward entrepreneurship	3.76	1.80	3.78	1.61	0.08	.468
Behavioural control	2.55	1.55	4.12	1.68	7.33	<.001
Entrepreneurial intention	2.85	1.86	3.36	1.61	2.81	.003

IV. DISCUSSION AND CONCLUSIONS

The theory of planned behaviour [14] has become the most frequently used theoretical frame in recent studies of entrepreneurial intention. Based on this general theory, several studies claim that entrepreneurial intention, which shapes entrepreneurial behaviour, is determined by three personal factors, i.e., the personal attitude toward, the subjective norm about, and the perceived control of entrepreneurship [15, 16]. Personal attitude refers to the personal impression toward entrepreneurial activities, and is shaped from previous experiences and perceptions formed over life [17]. The subjective norm about entrepreneuship may be defined as a person's own estimate of the social pressure to perform or not perform the entrepreneurial behaviour, which is influenced by the support and acceptance of significant others such as family. Finally, the perceived behavioural control relates to an individual's perception of the feasibility to perform entrepreneurial activities. A positive impression of all three factors enhances the intenions of entrepreneurship [16].

Entrepreneurial education may affect and strengthen the personal attitude towards entrepreneurship [18], and could also impart a higher level of confidence and behavioural control by providing related knowledge, skills and competencies [19].

The results of the survey partially confirm this. The average personal attitude towards entrepreneurship of the students did not significantly increase after attending the course. This might be due to the fact that none of the students had prior knowledge of entrepreneurship and that the course is only a first introduction to the subject, for which emphasis is laid on the acquisition of relevant entrepreneurial skills and competences. This purpose seems to be attained, since the students' perceived behavioural control raised significantly after attending the course. Further assessment of students' perceptions of their entrepreneurial skills indicates that their ability to recognise opportunities, creativity and communication skills in particular have increased. Finally, the increased entrepreneurial intentions of the students further confirm the effectiveness of the course.

In conclusion, the findings of this study provide empirical evidence of the positive effect of the course on the students' entrepreneurial mindset. However, further prove is needed over the coming years. Indeed, the number of participants in this first two editions was too small to generalize the results, and the influences of entrepreneurial learning may not be immediate [20].

REFERENCES

[1] J. Roberts, F. Hoy, J. A. Katz, and H. Neck, "The challenges of infusing entrepreneurship within non-business disciplines and measuring outcomes," Entrepreneurship Research Journal, vol. 4, no. 1, pp. 1-12, 2014.

[2] W. T. Jackson, D. J. Scott, and N. Schwagler, "Using the business model canvas as a methods approach to teaching entrepreneurial finance," Journal of Entrepreneurship Education, vol. 18, no. 2, pp. 99-111, 2015.

[3] A. A. Teixeira and R. P. Forte, "Prior education and entrepreneurial intentions: the differential impact of a wide range of fields of study," Review of Managerial Science, vol. 11, no. 2, pp. 353-394, 2017.

[4] P.Jones and A. Jones, "Attitudes of sports development and sports management undergraduate students towards entrepreneurship: a university perspective towards best practice," Education Training, vol. 56, no. 8/9, pp. 716-732G, 2014.

[5] H. M. Neck and P. G. Greene, "Entrepreneurship education: Known worlds and new frontiers," Journal of Small Business Management, vol. 49, no. 1, pp. 55-70, 2011.

[6] M. H. Morris, D. F. Kuratko, and J. R. Cornwall, Entrepreneurship Programs and the Modern University. Northampton: Edward Elgar, 2013.

[7] J. Tardif, L'évaluation des compétences: documenter le parcours de développement. Montréal: Chenelière Education, 2006.

[8] R. M. Belbin, Team roles at work. Oxford: Butterworth-Heinemann, 2010.

[9] B. R. Barringer and R. D. Ireland, Entrepreneurship: Successfully Launching New Ventures. Harlow: Pearson Education Limited, 2018.

[10] M. E. Porter, "How competitive forces shape strategy," Harvard Business Review, vol. 57, no. 2, pp. 137-145, 1979.

[11] A. Osterwalder and Y. Pigneur, Business Model Generation: A handbook for visionaries, game changers and challengers. Hoboken, NJ: John Wiley and Sons, Inc., 2010.

[12] S. Robinson, H. Neergaard, L. Tanggaard, and N. F. Krueger,. "New horizons in entrepreneurship education: From teacher-led to student-centered learning," Education and Training, vol. 58, no. 7/8, pp. 661-683, 2016.

[13] F. Liñán, D. Urbano, and M. Guerrero, "Regional variations in entrepreneurial cognitions: start-up intentions of university students in

Spain," Entrepreneurship and Regional Development, vol. 23, no. 3/4, pp. 187-215, 2011.

[14] I. Ajzen, "The theory of planned behavior," Organizational Behavior and Human Decision Processes, vol. 50, no. 2, pp. 179-211, 1991.

[15] F. Zhang, L. Wei, H. Sun, and L. C. Tung, "How entrepreneurial learning impacts one's intention towards entrepreneurship. A planned behaviour approach," Chinese Management Studies, vol. 13, no. 1, pp. 146-170, 2019.

[16] T. Kautonen, M. Van Gelderen, and E. T. Tornikoski, "Predicting entrepreneurial behaviour: a test of the theory of planned behaviour," Applied Economics, vol. 45, no. 6, pp. 697-707, 2013.

[17] K. W. Kuehn, "Entrepreneurial intentions research: implications for entrepreneurship education," Journal of Entrepreneurship Education, vol. 11, pp. 87-98, 2008.

[18] E. J. Schwarz, M. A. Wdowiak, D. A. Almer-Jarz, and R. J. Breitenecker, "The effects of attitudes and perceived environment conditions on students' entrepreneurial intent: an Austrian perspective," Education and Training, vol. 51, no. 4, pp. 272-291, 2009.

[19] A. M. F. Do Paço, J. M. Ferreira, M. Raposo, R. G. Rodrigues, and A. Dinis, "Behaviours and entrepreneurial intention: empirical findings about secondary students," Journal of International Entrepreneurship, vol. 9, no. 1, pp. 20-38, 2011.

[20] A. Fayolle, B. Gailly, and N. Lassas-Clerc, "Assessing the impact of entrepreneurship education programmes: a new methodology," Journal of European Industrial Training, vol. 30, no. 9, pp. 701-720, 2006.

The Position of the Luminaire and its Effects on Selected Photometric Parameters of the Lighting System

Marek Mokráň, Roman Dubnička, Peter Janiga, Dionýz Gašparovský
Institute of Power and Applied Electrical Engineering
Faculty of Electrical Engineering and Information Technology STU in Bratislava
Bratislava, Slovakia
marek.mokran@stuba.sk

***Abstract*— Artificial light plays an important role in the work environment. Meeting the qualitative and quantitative lighting parameters increases work productivity. On the contrary, lack of light has several negative effects on people and safety at work. The lighting system meeting all photometric parameters defined by the standard is based on quality lighting design and simulation of the required photometric parameters for a specific space in the computer software. For the correct calculation of the lighting system parameters, it is necessary to know sufficiently accurate parameters entering into the calculation. The position of the luminaires is one of the parameters that can cause differences between the simulated and measured photometric parameters of the lighting system. This article deals with the issue of changing the position of the luminaires after installation, and the problems that result from this change. The investigated photometric parameters were verified by field measurements and simulated in the lighting design software.**

Keywords—interior lighting, lighting system, photometric measurement, lighting design.

I. Introduction

Requirements for artificial lighting are defined in the territory of the Slovak Republic by Decree of the Ministry of Health of the Slovak Republic 206/2011 Coll. which amends Decree 541/2007 Coll. about details and requirements for lighting at work. The level of illuminance required to perform a particular task depends on the visual ability of the person to perform the task. Obviously, this level varies from individual to individual and is affected by age and eye health. The STN EN 12464-1 standard provides detailed instructions for specifying lighting levels for specific tasks and considers the above factors. The illuminance level specified in this standard is the maintained average illuminance level $\bar{E}_m$, which is a level that considers the maintenance factor to ensure that using the lighting system, the illuminance intensity does not fall below this level. On the territory of the Slovak Republic, the level of illuminance set by the standard is verified by measurement. Declaration of compliance with the STN EN 12464-1 standard is very important for the Office of Public Health to allow people to stay in the workplace due to possible health damage due to an incorrect lighting system in the workplace. To avoid a difference between the values in the project and the measurement and the lighting system to meet the normative requirements, the lighting designer must consider a number of input and output parameters in lighting design. Parameters included in the lighting project are, for example, the reflectance of surfaces, luminous intensity distributions curves, dimensions of rooms, maintenance factor, etc. The parameter that enters the realization of the lighting system is the position of the luminaires. This parameter is the output of the lighting design. The difference in position can be caused by e.g. the inaccuracy of mounting the luminaires or, in an extreme case, the luminaires are installed in other positions because other room equipment (air conditioning) is located in the original positions of luminaires. To a certain extent, the designer should consider the difference between the position of the luminaires in the project and the real position in the lighting system when designing this system [1].

II. Experiment

A. Basic Parameters of the Examined Room

The experiment was aimed at determining the change in the average illuminance $\bar{E}$ of the entire space (E_t) and individual areas of work plane 1 – 4 ($E_{w1} - E_{w4}$). The average illuminance was calculated according to the formula:

$$\bar{E} = \frac{\sum_i E_i}{n} \tag{1}$$

where:

- E_i is the illuminance of the i-th measurement point,
- n is the number of measurement points,

The second monitored parameter was the uniformity U_0 of the illuminance calculated according to the following formula:

$$U_0 = \frac{E_{min}}{\bar{E}} \tag{2}$$

where:

- E_{min} is the minimum illumination in calculation points.

These parameters are often compared with the standards, where the normative requirements for average illuminance and uniformity of the illuminance for a specific workplace are defined. A photo of the investigated room is shown in Fig. 1. A visualization of the examined room is shown in Fig. 2. The room had dimensions of 9 m x 7.5 m x 2.8 m, and the height of the photometric head was set at 0.75 m in accordance with the height of the tables in the room. The photometric head was placed on a tripod with a fixed height, and in the case of illuminance measurements on tables, the photometer was placed directly on the table so that a constant height was maintained for the entire room. The lighting measurement points were marked with labels attached to the floor. The spacing of the measurement points was set at 1.86 m x 1.74 m. The distribution of luminaires (starting position), and room equipment, together with the distribution of measuring points is shown in Fig.3.

Fig. 1. Photograph of the examined room

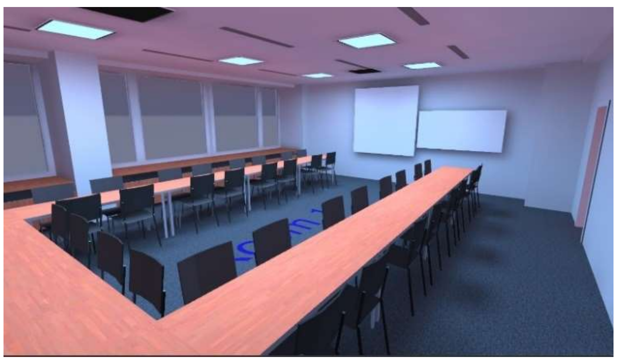

Fig. 2. Visualization of the examined room in lighting design software

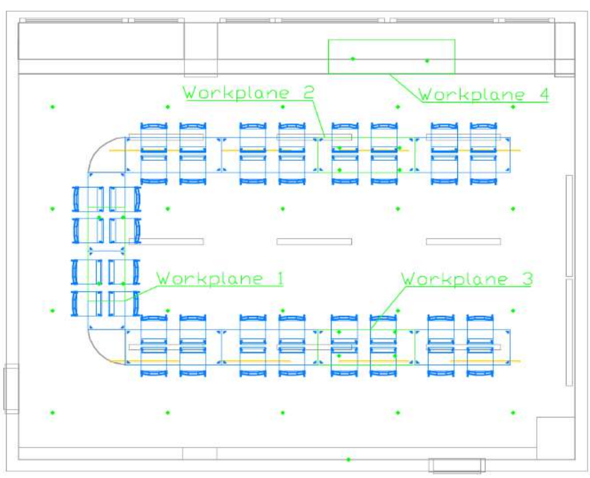

Fig. 3. Layout plan of the room

B. Reflectance of the Surfaces

As can be seen from Fig. 2, the reflectance of the main surfaces together with the reflectance of the room equipment and the permeability of the windows were measured. The measurement was made using a luminance analyser and a luxmeter. In the area with constant luminance, several illuminances were measured, from which the average illuminance and average luminance were subsequently considered to calculate the reflectance of the given surface.

The following relation was used to calculate the reflectance ρ of the surfaces after consideration of the diffuse reflection [1]:

$$\rho = \frac{\pi \cdot L}{E} \tag{3}$$

where:

- L is luminance of the surface,
- E is the illuminance on the surface.

C. Luminous Intensity Distribution Curves

In order to determine the change in illumination due to the change in the position of the luminaires, 2 types of luminaires were chosen. Type 1 was a linear luminaire with a narrow luminous intensity distribution curve (LIDC). LIDC of this type of luminaire is shown on Fig. 5. This type was chosen because such LIDC limits the influence of reflections from the walls and therefore we are mainly considering direct light propagation. There was also achieve a lower uniformity of the illuminance. In this case, a higher relative change in uniformity of the illuminance U_{0rel} is assumed.

Type 2 luminaire was a LED panel with dimensions 600 mm x 600 mm. LIDC of this luminaire is shown in Fig. 6. Such a panel was chosen due to several possible reasons for the mismatch of its location. The first reason comes from the lighting project when it is necessary to define an auxiliary grid and place the luminaires according to it. If this grid is not defined, it is practically impossible to match the positions in the project and in the real lighting system. In addition, the distance between the luminaires will not be the same either. The second reason why this type of luminaire was chosen is that the position of the luminaires depends on the above-mentioned grid (the structure of the lowered ceiling), which the designer very often does not know, and thus the luminaires can have a significantly different position than is considered in the project. In addition, these luminaires cannot be placed in such a way that there is a slight discrepancy in position, e.g., only 1 line of luminaires. With this type of luminaires, we achieved medium and higher uniformity of the illuminance U_0 by considering two layouts of positions of luminaires (Fig. 7). The first layout was 8 active luminaires, and the second layout was 6 active luminaires.

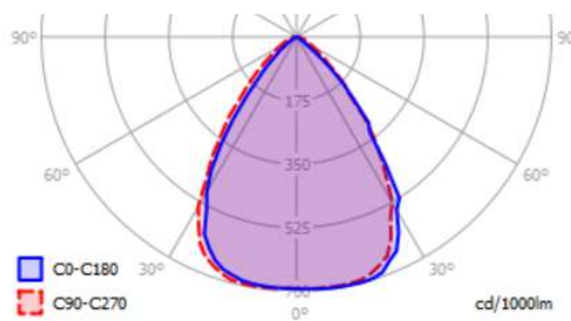

Fig. 4. LIDC of linear luminaire

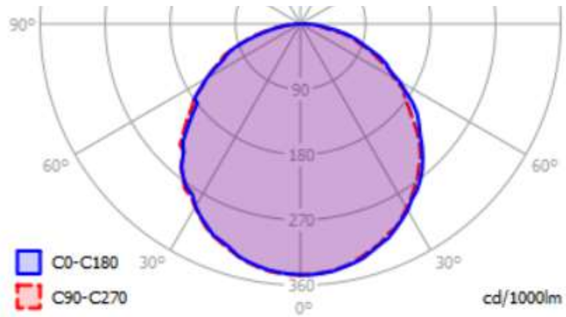

Fig. 5. LIDC of LED panel

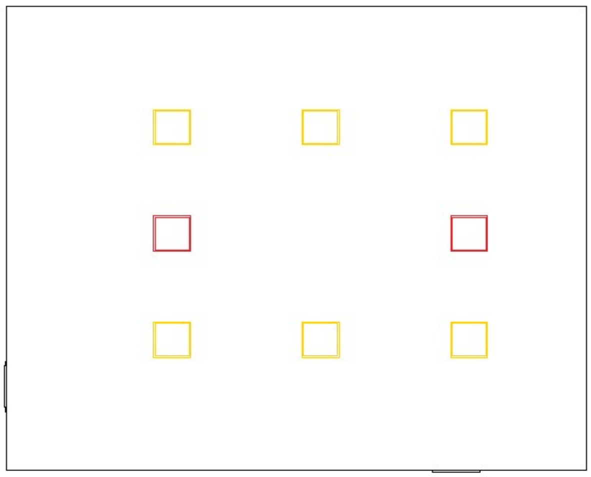

Fig. 6. Layout plan of the LED panels

The measurement of LIDC was performed on a far-field goniophotometer with a rotating luminaire and a fixed photometer in the testing laboratory of light-technical devices according to normative requirements [2] [3]. Each luminaire had its LIDC measured individually. The measurement and evaluation of the measurements were in the C-γ system. The angle intervals for planes C were 15° and for angles γ 2.5°. In order to avoid inaccuracies resulting from LIDC symmetry, no symmetry was considered and each luminaire was measured in all planes and angles. For planes C – γ, the following relationship was used to calculate the luminous flux:

$$\Phi = \int_{\gamma=0}^{\pi} \int_{C=0}^{2\pi} I(C,\gamma) \cdot sin\,\gamma \cdot d\gamma \cdot dC \qquad (4)$$

In tab. 1 shows the measured luminous fluxes Φ of individual luminaires.

TABLE I. MEASURED LUMINOUS FLUX OF LUMINAIRES

Linear luminaire	Φ [lm]	LED panel	Φ [lm]
Luminaire 1	4884	Luminaire 1	4925
Luminaire 2	4868	Luminaire 2	4964
Luminaire 3	4857	Luminaire 3	4986
Luminaire 4	4895	Luminaire 4	5053
Luminaire 5	4906	Luminaire 5	5132
Luminaire 6	4802	Luminaire 6	4916
Luminaire 7	4938	Luminaire 7	5013
Luminaire 8	4827	Luminaire 8	5073

The electrical parameters of the luminaires, the colour rendering index, the correlated colour temperature and the dimensions of the luminaire and its light-active part were also measured. The Eulumdat (ldt.) photometric file was created from the measured data.

III. Results

The determination of the sensitivity of the photometric parameters to the change in the position of the luminaires was carried out for linear luminaires in such a way that 1 line of luminaires was gradually moved with a certain step in the y-axis in both positive and negative. After each change, a measurement was made at all measurement points. In order to find out the possible influence of the type of surface reflectance, the line 2 near the window (mirror reflection) was moved and then the line 1 near the wall (diffuse reflection) was moved too. The starting position of the luminaires was simulated in the computer software to compare the difference between the computer software and the real lighting system at identical positions. In order to achieve this agreement of the starting position as accurately as possible, the luminaires were first installed, their real coordinates were measured, and then a model was created. When using LED panels, a change in the photometric parameters was determined by the change in position so that the position has changed symmetrically (both lines) by 1 length of this fixture. We consider the assumption of a shift of 0.6 m as the worst case, in which it makes sense to solve the change of photometric parameters. A larger difference between the projected position and the real position of the luminaire is considered unacceptable. The results of simulations and measurements are shown in Tab. 2 – 5.

The results of the measurements show that, in the case of using a linear luminaire, significant changes were recorded for the total illuminance E_t = 10.8% in only one case, when was moved the row near the window by 1.2m towards the window. This change can be caused by the fact that a certain part of the light leaked out of the room through the window. The uniformity of the illuminance U_{0t} changes significantly when the luminaire is moved by ± 0.3 m. This change achieved up to 21.6% worse uniformity compared to the original position. The illuminance at individual workplaces changed in a positive or negative direction depending on the position of the luminaires in relation to the specific workplace. These illuminance changes take on critical values also when the position of the linear luminaires is changed only by 0.3 m.

With active 8 LED panels, the illuminance E_t did not change significantly depending on the position of the luminaires. Even in this case, the critical parameter is uniformity, which, in the case of placing the luminaires further apart, turned out to be 18% better than with the original position. In the opposite case, when the luminaires were closer to each other, the uniformity was worse by 17.4%. The results achieved in the case of 6 active LED panels take on greater extremes. The sensitivity of the photometric parameters to a change in position of luminaires in cases with less uniformity of the illuminance is higher.

TABLE II. MEASURED PHOTOMETRIC PARAMETERS WHEN SETTING THE POSITION OF THE LUMINAIRES NEAR THE WINDOWS

	Line 1	Line 2	E_t [%]	U_{0t} [%]	E_{w1} [%]	U_{0w1} [%]	E_{w2} [%]	U_{0w2} [%]	E_{w3} [%]	U_{0w3} [%]	E_{w4} [%]	U_{0w4} [%]
	Δy [m]	Δy [m]										
Meas.	0	1.2	-10.8	-56	-44.4	-45.9	-61.5	-26.7	-0.3	-0.1	357.8	1.9
	0	0.9	-6.2	-50	-40.5	-36.1	-44.5	-23.4	-0.2	-0.3	276.6	3.8
	0	0.6	-2.8	-39.5	-33.3	-18.8	-25.2	-14.7	0	-0.3	168.8	3.8
	0	0.3	0.7	-21.6	-19.3	2	-8.3	-6.5	0.1	-0.2	64.1	2.3
	0	0	0	0	0	0	0	0	0	0	0	0
Sim.	0	0	-0.3	-1.8	1.4	3.8	1.7	2.9	-3.9	-2.8	1.7	2.7
Meas.	0	-0.1	0.6	0.3	10.6	-6.4	1.7	1.9	0	0.1	-15.4	0.6
	0	-0.2	0.1	-6.3	19.9	-8.1	1.8	3.6	0.1	0.2	-29.5	2.7
	0	-0.3	0.7	-16.4	26.6	-12.5	1	1.2	0.2	0.2	-40.7	2.8
	0	-0.4	1	-28.9	37.5	-13.7	-0.5	-1.3	0.8	0.3	-50.2	3.9

TABLE III. MEASURED PHOTOMETRIC PARAMETERS WHEN SETTING THE POSITION OF THE LUMINAIRES NEAR THE WALL

	Line 1	Line 2	E_t [%]	U_{0t} [%]	E_{w1} [%]	U_{0w1} [%]	E_{w2} [%]	U_{0w2} [%]	E_{w3} [%]	U_{0w3} [%]	E_{w4} [%]	U_{0w4} [%]
	Δy [m]	Δy [m]										
Meas.	0	0	0	0	0	0	0	0	0	0	0	0
Sim.	0	0	-0.3	-1.8	0.7	4.2	1.6	2.7	-3.9	-2.8	3.3	2.8
Meas.	-0.1	0	0.9	-2.3	-5	-2.7	2.6	2.8	-2.6	-1.1	1.3	-1.2
	-0.2	0	0.9	-3.7	-10.9	-11.2	0.3	-0.9	-6.1	-3.2	1.5	-1.5
	-0.3	0	-0.1	-5.6	-16.6	-20.7	0.3	-0.9	-11.1	-5.8	1.5	-1.9
	-0.4	0	-0.3	-14.6	-20.8	-26.8	0.3	-1.1	-15.9	-8.2	1.5	-1.9
	-0.5	0	-0.3	-19.9	-22.6	-24.8	0.3	-1.3	-21.7	-10.9	1.9	-2.3
	-0.6	0	-0.9	-30.5	-27	-39.8	0.2	-1.1	-28	-13.8	2.1	-1.2
	-0.7	0	-1.5	-32.5	-27.4	-40.7	0.3	-1.1	-34.4	-16	1.5	-1.5
	-0.8	0	-2.7	-37	-28.6	-43.3	0.4	-1.2	-40.8	-18.6	1.7	-1.2
	-0.9	0	2.4	-41.6	-29	-44.7	0.5	-1	-46.6	-20.1	2.5	-1.6
	-1	0	-2.9	-40.8	-29.5	-45.7	0.6	-1	-52.5	-22.2	2.5	-1.6
	-1.1	0	-3.9	-41.7	-29.3	-46.3	0.9	-0.8	-56.4	-23.2	3	-2
	-1.2	0	-4.2	-42.6	-28.6	-45.9	1	-1	-60.6	-23.5	3.2	-2.2

TABLE IV. MEASURED PHOTOMETRIC PARAMETERS WHEN SETTING THE POSITION OF THE EIGHT LED PANELS

	Line 1	Line 2	E_t [%]	U_{0t} [%]	E_{w1} [%]	U_{0w1} [%]	E_{w2} [%]	U_{0w2} [%]	E_{w3} [%]	U_{0w3} [%]	E_{w4} [%]	U_{0w4} [%]
	Δy [m]	Δy [m]										
Meas.	-0.6	0.6	-4.9	18.1	-16.2	-0.4	-20.5	-5.6	-8.7	1.8	33.3	-0.1
	0	0	0	0	0	0	0	0	0	0	0	0
Sim.	0	0	-3.2	-10.8	-7.5	-1.1	-1.2	-0.4	-1.7	-0.8	1.6	-0.5
Meas.	0.6	-0.6	1.5	-17.4	13.7	2.2	10.3	-4.4	-7.7	-5.2	-28.6	-0.9

TABLE V. MEASURED PHOTOMETRIC PARAMETERS WHEN SETTING THE POSITION OF THE SIX LED PANELS

	Line 1	Line 2	E_t [%]	U_{0t} [%]	E_{w1} [%]	U_{0w1} [%]	E_{w2} [%]	U_{0w2} [%]	E_{w3} [%]	U_{0w3} [%]	E_{w4} [%]	U_{0w4} [%]
	Δy [m]	Δy [m]										
Meas.	-0.6	0.6	-1.8	10.4	-24.1	3.5	-20.3	-3.9	-8.2	-3.4	59.1	0.1
	0	0	0	0	0	0	0	0	0	0	0	0
Sim.	0	0	-3.6	-7.4	-8	0.6	-0.4	-1	-0.8	-0.5	1.5	-0.5
Meas.	0.6	-0.6	2.1	-18.4	38.3	2.2	17.8	-3.7	-8.8	-6.4	-32.6	0.7

IV. CONCLUSION

The results of the experiment show that the photometric parameters are sensitive to the position of the luminaires. Just a small change in position in some cases caused significant changes, mainly in the illuminance uniformity. Therefore, it is necessary to consider certain inconsistencies in the position of the luminaires already during the creation of the lighting project. The ideal procedure is to verify in the lighting project whether the photometric parameters required by the standard will be met even with a slight change in the position of the luminaires. We recommend using auxiliary grids in the design when working with square recessed luminaires.

Acknowledgment

„This publication was created thanks to support under the OP Integrated Infrastructure for the project: International Center of Excellence for Research on Intelligent and Secure Information and Communication Technologies and Systems - II. stage, ITMS code: 313021W404, co-financed by the ERDF“. This work was also supported by the Slovak Research and Development Agency under the contract No. APVV-20-0157.

References

[1] STN EN 12464-1. Light and lighting - Lighting of work places - Part 1: Indoor work places. 2021.

[2] K. Sokanský, a iní. Světelná technika. Praha : České vysoké učení technické v Praze, 2011. ISBN 978-80-01-04941-9.

[3] STN EN 13032-1+A1. Svetlo a osvetlenie. Meranie a vyhodnotenie fotometrických údajov svetelných zdrojov a svietidiel. Časť 1: Meranie a formulár súborov. 2012.

[4] STN EN 13032 - 4 + A1: 2021. Svetlo a osvetlenie. Meranie a vyhodnotenie fotometrických údajov svetelných zdrojov a svietidiel. Časť 4: LED zdroje, moduly a svietidlá. 2021.

Possibilities of Modelling Situations in the Night Traffic Area in Terms of Evaluating the Visibility of Potential Obstacles by the Driver

Tomas Novak, Ondrej Dolejsi, Pavel Valicek
Faculty of Electrical Engineering and Computer Science
VSB – Technical University of Ostrava
Ostrava, Czech Republic
tomas.novak1@vsb.cz, ondrej.neoral@vsb.cz, pavel.valicek@vsb.cz

***Abstract*— On the roads, we constantly encounter situations where the driver is unable to react in time to an obstacle or to a pedestrian in the roadway, and very tragic accidents can occur. The driver's delayed reaction is not only influenced by, for example reduced attention, but by other possible factors. However, if we take into account the vehicle during night driving, one of the main roles here is how well the vehicle's headlights illuminate the road and its additional surrounding spaces in those given situations. The concept of well-lit roads assumes that the driver has sufficient visible space in front of the vehicle due to the permitted speed of the road to be able to react in time to objects in his field of vision. In today's era of modern headlights and road lighting, we should perhaps no longer doubt their precise incorporation, so that the driver has the best possible information about what is happening on the road ahead. Here the question arises whether this is really the case. Using light-technical models, this article outlines what the distribution of luminous flux looks like in the form of an evaluation of different (vertical, horizontal) illuminance in the space in front of the vehicle [1].**

Keywords—Vehicle low beam headlights, Road lighting, Road safety, Night traffic area, Vertical illuminance, Luminous intensity distribution curves (LIDCs)

I. Introduction

The article is focused on the creation of a road model with real parameters in the Dialux software. In the first part a car model with different types of low beam headlights is inserted into the program. The article works with the LIDCs of headlights in low beam mode with LED, H4 and H7 light sources [2]. Using the created model situation with different types of low beam headlights, it is possible to evaluate the light conditions of important areas of the road and its surroundings in the driver's field of view. In the second part of the article, road lighting luminaires, equipped with either high-pressure sodium (HPS) discharge lamps or LED-type light sources, are added to the model situation. The evaluation of the solved areas is carried out for both types of road lighting luminaires and subsequently in combination with low beam car headlights with individual types of different light sources. The solved areas in the model are divided into roadways and adjacent additional surrounding spaces.

The goal is to evaluate the horizontal and vertical illuminance on the road, including additional surrounding spaces at different distances from the vehicle and heights above the road with different combinations of light sources, road lighting luminaires and low beam car headlights. The evaluation is shown using contour charts. The distance of the monitored area from the vehicle is chosen with regard to the safe stopping distance of the vehicle for specific climatic conditions. In this article, a distance of up to 28 m is chosen, which corresponds to the shortest stopping distance of a vehicle at a speed of 50 km/h on a dry road [3]. The height of the monitored area is chosen with regard to the visibility of potential vertical obstacles. A height of 1 m above the road is selected for the evaluation of pedestrian detection. A critical vertical illuminance value of 1 lx was chosen for obstacle detection. For values lower than 1 lx, it is not possible to determine whether an obstacle was seen in the driver's field of view or wasn't. The critical value for horizontal illuminance is also set at 1 lx. This value was also chosen in relation to the possibility of visible light communication (VLC) and its possibility of signal transmission on the luminous flux generated by LED light sources [4].

II. Motivation

Visibility in night traffic has a significant impact on the safety of the driver and other road users/traffic participants. Vehicle's low beam headlights primarily provide visibility on the roads, for the driver, from dusk till dawn. Thanks to good visibility, the driver is able to detect an obstacle earlier and thus gains more time to evaluate the situation and perform an evasive manoeuvre.

The reason for creating the article is to define areas in the traffic space in which obstacles on the road are more difficult to detect. Based on the risk areas defined in this way, it is possible to focus on the proposal of further measures for the elimination of risks.

III. Models Description

A. LIDCs Low Beam Headights

LIDCs of low beam headlights with three light sources (LED, H4 and H7) were used to model the light technical parameters (illuminance) in the driver's field of view at night. Modern LED and cheap halogen bulbs are still the most widespread lighting principles (light sources) in low beam headlights. The LIDCs of the lamps used are shown in Table 1.

TABLE I. LIDCs OF LOW BEAM HEADLIGHTS ACCORDING TO TYPE OF LIGHT SOURCE.

	Low beam headlight with LED	Low beam headlight with H4	Low beam headlight with H7
3D LIDCs	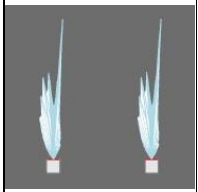	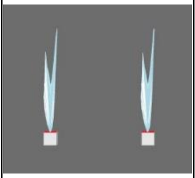	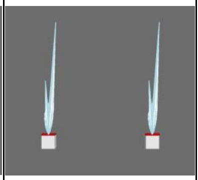
Luminous flux of low beam headlights	2 x 770 lm	2 x 346 lm	2 x 573 lm

B. *LIDCs of Road Light*

The lighting system of road luminaires was modelled using the LIDCs of road lighting luminaires. Luminaires [5] were selected with regard to the most commonly used light sources (HPS and LED), and also have specifications such, that they could be used for M4 class road [6], which is the most advantageous for modelling in terms of their usage frequency on real roads. Both traffic lighting systems were calculated by EN 13201, but for the needing of the enlarged model in case study we have to apply different calculation points (see Figures 1, 2 and 3).

TABLE II. LIDCs OF LUMINAIRES FOR ROAD LIGTING

	Luminaire with HPS discharge lamp	Luminaire with LED light source
LIDCs	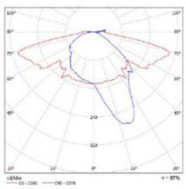	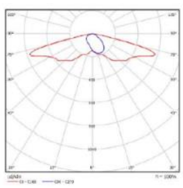
Technical parameters of the luminaire	Luminosity flux: 10 700 lm Tc: 2000 K Ra: 25 η: 107 lm/W	Luminosity flux: 8 235 lm Tc: 4000 K Ra: >70 η: 150 lm/W

C. *Description of the Road Model*

A standard two-way road with a lane width of 3,7 m was chosen for the light-technical modelling. Additional spaces were also considered around the road, within which 2 m were allocated for the sidewalk and 1,3 m for the adjacent greenery were always considered on each side, so that the total width of the investigated area is 14 m, see Figure 1 [7].

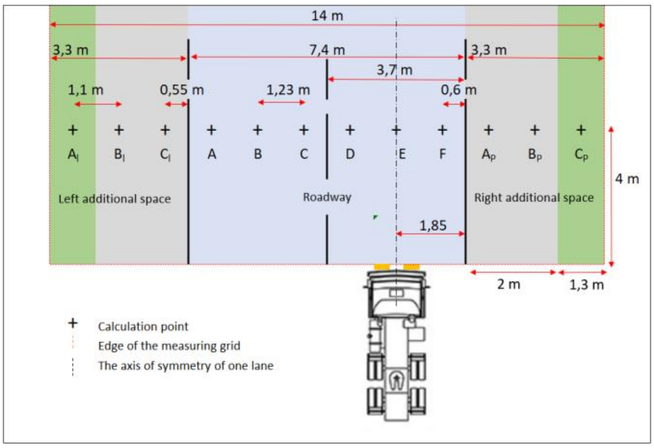

Fig. 1. Grid of calculation points on the model road [7]

This means that the total width of the road is 7,4 m with an additional 3,3 m wide space located on either side of the road. The grid of calculation points of the road model is shown in Figure 2. For it to be possible to model the situation in a sufficient section of the road in front of the driver, a grid with 4 m spacing between calculation points in the longitudinal direction was created, up to a distance of 80 m.

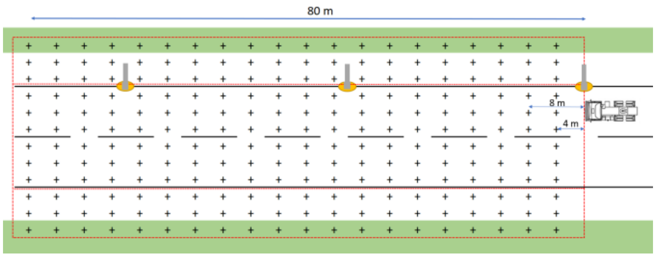

Fig. 2. Distribution of road lighting luminaires with a grid of horizontal and vertical illuminance [7]

Given that the model situation will be illuminated by a combination of road lighting and low beam headlights, it was necessary to determine the parameters of the road lighting luminaires. A one-sided lighting system was chosen for the model with a mounting height of 9 m and a pitch of 35 m see Figure 2. The road model was classified as class M4 and the additional space as class P4. The calculation for the classification of road lighting was, of course, created on the basis of normative requirements [6], i.e. with a spacing of 3,5 m.

In order to evaluate horizontal illuminance, it was necessary to define calculation points not only at the level of road (horizontal illuminance) but also at different heights. These were determined from 0,5 m to 2,5 m with a step of 0,5 m (see Figure 3).

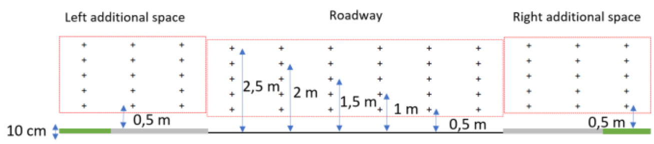

Fig. 3. Perpendicular mesh of points [7]

D. *Description of Different Modeled Situations*

1. In the first model situation, only the horizontal illuminance generated by the low beam headlights with LED sources, H4 and H7, was solved.

2. The second model situation contains the calculation of the vertical illuminance generated with the help of low beam headlights with LED sources, H4 and H7 at a height of 1m above the road.
3. The third model situation solves the illuminance of a vertical grid at a distance of 28 m in front of the vehicle generated only with the help of low beam headlights with LED sources, H4 and H7.
4. Horizontal illuminance of the lighting space with road lighting luminaires and car low beam headlights with LED sources.
5. The fifth model situation contains the calculation of the vertical illuminance generated with the help of low beam headlights with LED sources and road lighting luminaires at a height of 1m above the road.
6. The sixth model situation solves the illuminance of a vertical grid at a distance of 28 m in front of the car, generated with the help of low beam headlights with LED sources, and road lighting luminaires.
7. Vertical illuminance at a height of 1 m with a constant distance of the car and calculation points (28 m), which move, as a whole, with respect to the lighting system of road lighting with a step of 4 m.

IV. Case Study – Horizontal and Verical Illuminance Modelling

A. Horizontal illuminance, space illuminated by low beam headlights

Horizontal illuminance is necessary for the visibility of horizontal road markings. According to the results shown in Figure 4, the LED and H7 sources have a value of 1 lx at the same distance, but the LED source achieves higher illuminance values in additional spaces. The critical value for source H4 was at the shortest distance.

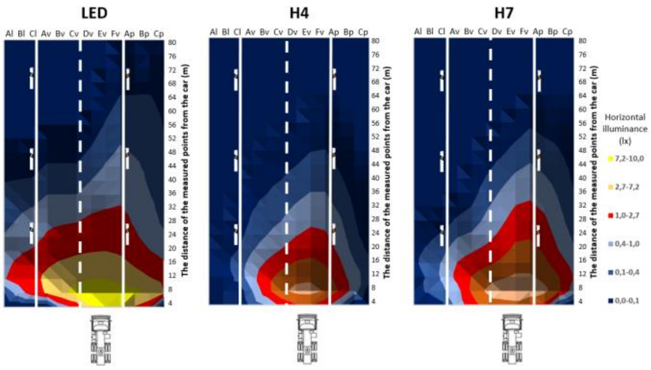

Fig. 4. Horizontal illumination – low beam headlights [7]

B. Vertical illuminance 1 m above the road, space illuminated by low beam headlights

The largest critical distance is reached by the H7 source, approximately 22 m in front of the vehicle. In Figure 4, it can be observed that the critical value of vertical illuminance for all light sources at a distance of 28 m from the vehicle is lower than 1 lx across the entire width of the traffic area. In this situation, there is a risk that the pedestrian would not be spotted in time due to the length of the vehicle's stopping distance.

It is also worth paying attention to the left entrance area of the LED, in which, thanks to the quality optics, the values are the lowest and do not exceed the value of 1 lx at all.

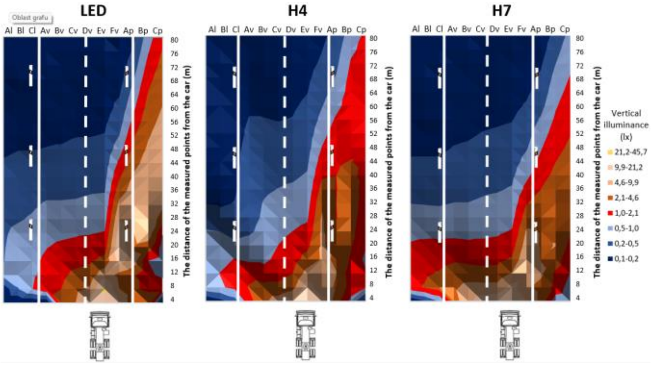

Fig. 5. Vertical illuminance in 1 m – vehicle low beam headlights [7]

C. A vertical grid at a distance of 28 m in front of the vehicle, an area illuminated by the vehicle's low beam headlights

For all compared sources, the critical value of illuminance in the right lane does not exceed a height of 1 m. This phenomenon is caused by an effort to prevent the glare of oncoming vehicles. The worst condition is achieved by source H7, where the critical vertical illuminance in the left boarding area does not even reach a height of 0,5 m. In this part of the area, there will again be a problem with timely reaction to pedestrians. Due to the length of the vehicle's stopping distance, the pedestrian may not be spotted by the driver in time.

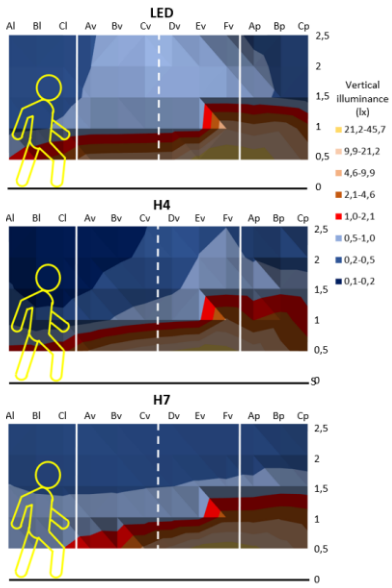

Fig. 6. Perpendicular grid 28 m – front low beam headlights of the vehicle [7]

D. Space Illuminated by road lighting luminaires and vehicle low beam headlights – horizontal illuminance

In Figure 6, it can be observed that in the area of horizontal illuminance, visibility with the contribution of the vehicle's low beam headlights is not significantly affected. In the given model situation, the only thing that happens is that the LED low beam headlights in combination with both LED and HPS road lighting can improve the uniformity in the right boarding area.

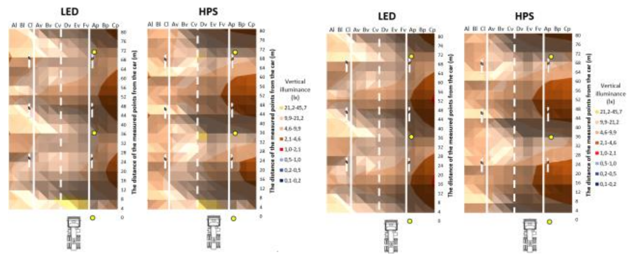

Fig. 7. Horizontal illuminance - LED low beam headlights in combination with road lighting (left picture) and only road lighting (right pisture) [7]

E. Space Illuminated by Road Lighting Luminaires and Vehicle Low Beam Headlights - Vertical Illuminance

The contribution of low beam LED headlights, at the level of 1 m above the road, to the vertical lighting component is visible in the right lane. In order to prevent glare, the low beam headlights do not make a significant contribution to the left part of the traffic area. In this model situation, significant vertical illuminance minima can be traced, especially in the left boarding area. These minimums are more significant in the combination of LED low beam headlights and LED road lighting with high-quality optical systems, when from the driver's point of view, longitudinal uniformity is also significantly reduced in this area. From the left part of the picture, it can be determined that the most dangerous place for crossing the road is entrance from the left with combination of LED low beam headlights and LED road lighting lamp!!!

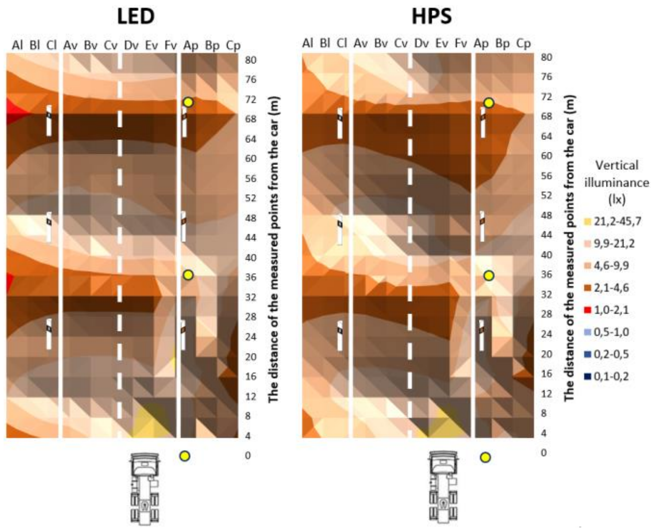

Fig. 8. Vertical illuminance in 1 m – road lighting with LED low beam headlights [7]

F. Area illuminated by road lighting luminaires and LED low beam headlights of the vehicle - horizontal section

A road luminaire with a HPS lamp achieves higher values of vertical illuminance than a luminaire with an LED type source. This model proves the statement from the previous paragraph. Thanks to the "parasitic" luminaires flux from the HPS road lighting, better vertical illuminance values can be achieved in the left boarding area, even in combination with the car's LED low beam headlights at a critical distance of 28 m.

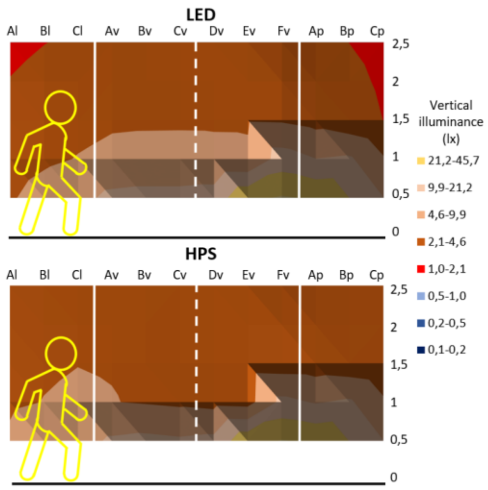

Fig. 9. Perpendicular grid 28 m – vehicle low beam headlights with road lighting [7]

G. Vertical Illuminance 1 m above the Roadway between Street Lighting Luminaires at a distance of 28 m in front of the vehicle, the area illuminated by LED road lighting luminaires and vehicle low beam headlights

The last modelled situation already works with a variant in which the car moves between the road lighting columns and vertical illuminance are evaluated at a critical distance of 28 m.

As part of the modelling, all combinations of low beam headlight and road lighting were carried out, however, from the point of view of comparing the changes in behaviour, the assessment of only two situations appears to be the most important. This is the comparison between least technologically advanced combination of road lighting with HPS and low beam headlights fitted with halogen bulbs and of course the most modern combination of both lighting systems fitted with LED technology. On the vertical illuminance curves in Fig 10, the most important (most critical) area is the left boarding area. If we first evaluate the area of the road itself 28 m in front of the vehicle, we can state that the difference between the combination of conventional technologies and modern technologies is not very striking under road lighting luminaires, it ranges between values of 2,8-3,45 lx, while the maximum between road lighting columns reaches a maximum 10-13 lx. That is that the longitudinal uniformity is above the limit of 0,2. Even better is the situation in the right boarding area, where the minimum values for both variants reach values of 5 lx under the luminaires and less than 9 lx between the luminaires. This results in an excellent longitudinal uniformity higher than 0,6.

However, if we approach the left boarding area, we will find that the differences are significant. With a combination of LED luminaires, the minimum vertical illuminance under the road luminaire is only 1,65 lx, while with a conventional lighting system this value is significantly higher, namely 2,99 lx, which is almost double. An even bigger problem occurs with the variant of LED sources with a longitudinal uniformity that is less than 0,17 compared to the classic combination (H7+HPS) with a uniformity of 0,5. The combination of LED car low beam headlights and LED road lighting can thus create a literally murderous combination of low vertical illuminance and low uniformity under the road lighting, which can lead to the fact that a pedestrian coming from the left will not be detected by the driver in time.

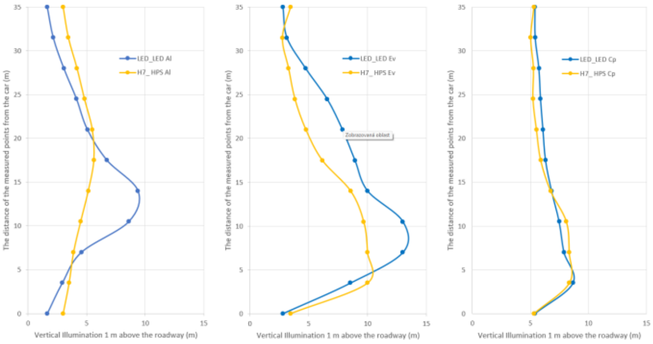

Fig. 10. Selected vertical illuminance 1 m above the roadway between road lighting luminaires at a distance of 28 m in front of the vehicle (from left: left boarding area, center of lane, right boarding area)

V. Conclusion

From the mentioned light-technical models, interesting opinions and especially questions for the future emerge for road safety. If we first look at the conclusions from the mentioned models, we can state that the horizontal illuminance achieved by LED road luminaires are clearly the best not only on the road itself, but also in additional spaces. When evaluating vertical illuminance from the direction of the oncoming driver, however, it is necessary to draw attention to the fact that, thanks to high-quality optical systems and the limitation of potential glare from oncoming vehicles, vertical illuminance in the left entry area are significantly reduced, and thus the visibility of pedestrians entering the road from the left side.

If we add road lighting systems to low beam headlights, in certain situations (see modelling) there may be even greater differences in the values of vertical illuminance on obstacles (pedestrians) in the left boarding area. This phenomenon is further exacerbated by LED road lighting due to their high-quality optical systems (without parasitic light), which de facto do not create any vertical component of luminous flux from the point of view of the oncoming driver in the last third of the pitch of the road lighting luminaires.

VI. Discussion

The above models were made on the basis of interaction with the traffic police, where accidents between pedestrians and cars in cities are increasing, especially in situations of new LED road lighting and modern cars equipped with modern LED low beam headlights. The light-technical models confirmed this trend, because especially in the left-hand entrance area, where the pedestrian is at the level of the road lighting luminaires, he has a false sense of illumination (horizontal lighting is satisfactory) and, especially when entering from the left side of the road, the oncoming driver does not have to see him, because neither road lighting, nor the LED low beam lights of an oncoming car are not able to generate the necessary vertical illuminance that would ensure sufficient contrast and thus the visibility of the given pedestrian at a distance at which the driver is able to safely stop the vehicle.

These models therefore raise the question for the future, whether it will not be necessary for road lighting to address not only the horizontal illuminance of the road, but also the vertical illuminance precisely, because modern lighting systems, thanks to their possibilities of distribution of the luminous flux, completely eliminate the so-called parasitic luminous flux, which in luminaires equipped with halogen bulbs or HPS road lighting lamps was the standard, which was able to ensure at least minimal vertical illuminance in all places of the traffic space and surrounding area being addressed.

VII. Acknowledgment

This work was supported from project SGS SP2022/21 VŠB-TU Ostrava and ERDF „A Research Platform focused on Industry 4.0 and Robotics in Ostrava Agglomeration “, No. CZ.02.1.01/0.0/0.0/17_049/0008425.

VIII. References

[1] T. Novak, P. Becak, R. Dubnicka, J. Raditschova, D. Gasparovsky, P. Valicek and J. Ullman, “Modelling of luminous flux directed to the upper hemisphere from electrical substation before and after the refurbishment of lighting systems,” Energies, 15(1), 2022.

[2] O. Dolejsi, R. Baleja, P. Becak, T. Novak and K. Sokansky, “A Comparison of Light Sources Technologies of Vehicles Headlights Illuminating a Model Road”, 20th International Scientific Conference on Electric Power Engineering (EPE), 169-172, ISBN:978-1-7281-1333-3. ISSN: 2376-5623, 2019.

[3] R. Baleja, O. Dolejsi, P. Becak, K. Sokansky and T. Novak, “The Visibility of Pedestrians in the Traffic Area, Using Different Light Source Technologies of Car Headlights”, 10th International Scientific Symposium on Electric Power Engineering (ELEKTROENERGETIKA). 551-556, ISBN:978-80-553-3324-3, 2019.

[4] T. Novak, J. Latal, S. Hajduk, A. Vanderka, P. Valicek, L. Hajek, P. Becak and M. Slouka, “Case study – Modelling of Visible Light Communication on Luminous Intensity Distribution Curve of LED Low Beam Car Headlamps”, EEDAL-LS-2022: International Conference on Energy Efficiency in Domestic & Light Sources, 2022

[5] P. Becak, J. Wlosokova, J. Picha, T. Novak, K. Sokansky, “Modeling of Luminous Flux Radiation to the Upper Hemisphere from Real Model of Town”, 20th International Scientific Conference on Electric Power Engineering (EPE), pp. 164-168, 2019.

[6] EN 13201 - Road lighting - Part 1-4

[7] O. Neoral, “Road Lighting Modeling and Optimizing to Increase Safety during Night Traffic,” Diploma theses of Faculty of Electrical Engineering and Computer Science, http://hdl.handle.net/10084/143950, 2021.

Candela Realisation Based on LED Standard Lamp and Unfiltered Radiometers at CMI

Petr Kliment
Slovak University of Technology in Bratislava
Bratislava, Slovakia
pkliment@cmi.cz

Petr Kliment
Czech Metrology Institute
Brno, Czech Republic
pkliment@cmi.cz

Marek Šmíd
Czech Metrology Institute
Brno, Czech Republic
msmid@cmi.cz

Geiland Porrovecchio
Czech Metrology Institute
Brno, Czech Republic
gporrovecchio@cmi.cz

Jiří Tesař
Slovak University of Technology in Bratislava
Bratislava, Slovakia
jtesar@cmi.cz

Jiří Tesař
Czech Metrology Institute
Brno, Czech Republic
jtesar@cmi.cz

***Abstract*— The research project „Future photometry based on solid-state lighting products“ (EMPIR 15SIB07 PhotoLED) [1] laid the foundations for photometry based on new measurement techniques of white LED sources. This paper describes the new realization of luminous intensity scale at Czech Metrology Institute (CMI) based on LED standard lamp and an unfiltered broadband radiometer traceable to cryogenic radiometer (CR). The application of an Absolute predictable quantum efficiency detector (PQED) (developed in The Research project "New primary standards and traceability for radiometry" NewStar EMRP SIB57) for totally independent realisation of the unit candela was studied. [2]**

The type A LED-based luminous intensity source (LIS-A) developed in PhotoLED project was calibrated for relative spectra. The trap unfiltered primary photometer (Trap-UPP) based on 3-element trap detector was designed and calibrated to be traceable to the absolute cryogenic radiometer. The luminous intensity of LIS-A was measured, using both the TRAP-UPP and the conventional primary photometer (V(lambda)-PP) traceable to CR. The deviation between these two measurements was less than 0.1 %. It was within the measurement uncertainty and confirmed the reliability of this new measurement technique.

The new independent metrological traceability chain for the detector-based candela realisation was built. The PQED detector was modified to primary unfiltered photometer PQED-UPP and used to calibrate the luminous intensity of LIS-A with uncertainty 0.31 %. The results were compared to the V(lambda)-PP measurements, showing less than 0.1 % difference, which proves the equivalence of this advanced means of realizing the unit of luminous intensity and other derived photometric units. Moreover, it reaches for almost 0.1% lower uncertainty than the conventional method.

Keywords: unfiltered photometer, luminous intensity, LED standard lamp, candela primary realisation, LED photometry, PQED primary photometer

I. INTRODUCTION

The light sources based on LED (Light Emitting Diode) have replaced conventional light sources (tungsten, discharge, fluorescent) in recent years. The modern metrological traceability chains realized in leading national metrology institutes in Europe use absolutely calibrated broadband radiometers to calibrate the primary photometers. The two steps metrology traceability from spectral radiant flux down to photometric units is used. Nevertheless, the specific spectral properties of LED and OLED-based light sources allow to apply the broadband standard radiometers directly as a new primary photometer and thus to significantly shorten the traceability chain.

The aim of this work was to apply a new measurement technique and a new LED Luminous intensity standard source LIS-A were both developed in PhotoLED project for realising a new independent metrological traceability chain for detector-based candela realisation.

The conventional candela realisation uses a V(λ)-filtered primary photometer (V(λ)-PP) traceable to primary standard – absolute cryogenic radiometer (CR). For the metrological traceability chain see Fig. 1. The V(λ)-PP are calibrated against the transfer standard of the total radiant flux of the visible radiation on a primary monochromator facility.

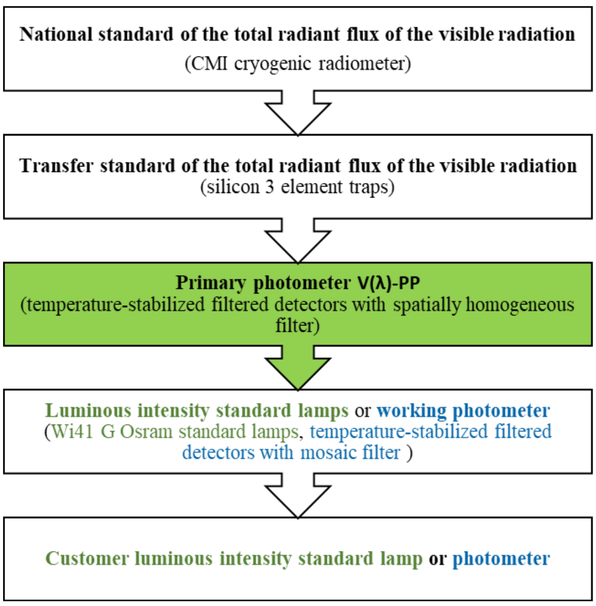

Fig. 1: Conventional candela metrological traceability chain using V(λ)-PP and tungsten lamp

A luminous intensity standard lamp is calibrated with the V(λ)-PP on a photometric bench to realize and transfer the photometric unit candela. The lamp is a Wi41 G type of the Osram producer and its spectral power distribution corresponds with CIE Standard Illuminant A source. [3] The candela or the derived illuminance scale can be transferred to the customers using the working photometers calibrated against V(λ)-PP on a tungsten lamp (CIE Standard Illuminant A source).

Due to the limited spectral bandwidth of white LEDs (approximately 380 nm – 850 nm), the illuminance of a LED standard lamp can be measured with novel detector technology without an optical V(λ) filter. In this case, the photometric weighting can be performed numerically, provided that the LED spectrum is accurately measured. As a result, the replacement of the conventional tungsten standard lamp by LED standard lamp will allow transferring of the luminous intensity unit and illuminance scale from NMIs (National Metrology Institute) to the customers, calibrating photometers and testing SSL (Solid Stay Lighting) products and providing field measurements, with lower uncertainty. [1]

II. Methodology

A. *The new LED-based candela metrological traceability concept*

The conventional candela metrological traceability chain was shown in Fig. 1 and described above. The candela unit is realised by measuring the illuminance at a precise defined distance from standard light source. The luminous intensity is calculated from the measured distance and illuminance values. Instead of using a conventional method and calibrating the tungsten lamp with the V(λ)-PP on a photometric bench, the new technique of measurement of the LED source LIS-A can be applied to realize and transfer the candela unit. The novel technique of measurement uses an unfiltered radiometer as a photometer, so the conventional V(λ)-PP can be replaced by a broadband standard radiometer (three-element silicon trap detector) currently used in the radiometry as a transfer standard for an absolute spectral responsivity scale.

This detector, completed with a precise optical aperture, can be called the Trap Unfiltered Primary Photometer (Trap-UPP). This type of a broadband detector can measure only the luminous intensity or the luminance of light sources with limited spectral distribution, as are white LEDs. For a new LED-based candela metrological traceability chain, see Fig. 2.

As a LED light source, the new LED Luminous intensity standard source LIS-A, developed in PhotoLED project, was chosen. So, the Trap-UPP illuminance responsivity for the particular spectra of the LIS-A source has to be calculated. To do this, the spectral responsivity of the detector and the spectral power distribution of LIS-A has to be calibrated. Then the measured luminous intensity is calculated from the known spectral irradiance responsivity of Trap-UPP, spectral power distribution of LIS-A, irradiance value measured with the Trap-UPP and the distance of the LIS-A to the detector.

The unfiltered method allows to apply a newly realised primary standard for optical power, the Predictable Quantum Efficient Detector (PQED) as a primary unfiltered photometer PQED-UPP. The PQED was developed in the projects iMERA-Plus T1. J2.1 qu-Candela [4] and EMRP SIB57 NEWSTAR [2]. Since then, the PQED detectors have been studied for their time stability, for example within a project

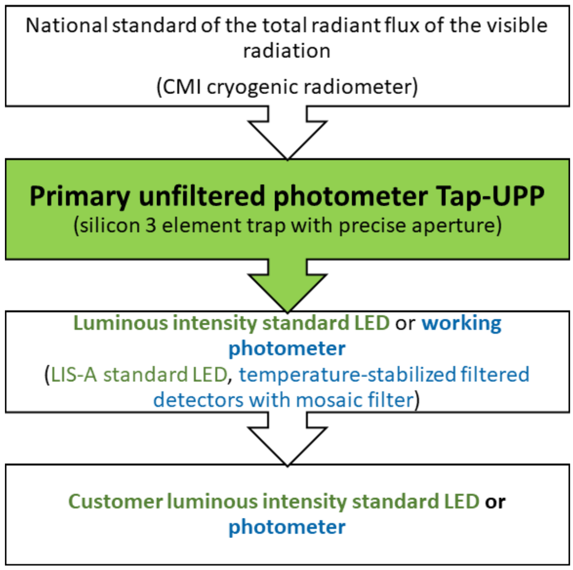

Fig. 2: The candela metrological traceability chain based on LED and Trap-UPP

EMPIR 18SIB10 chipS·CALe [5] .The results have shown a good equivalence between the PQED and CR so far. The PQED has a lot of advantages compared to CR. The PQED is much cheaper, easy to operate and can be applied directly as the unfiltered photometer PQED-UPP. For the newly built independent metrological traceability chain for detector-based candela realisation based on the PQED-UPP and LED see the paragraph III.A.

B. *LED standard lamp LIS-A characteristics*

The new LED standard source (LIS-A) was introduced as an outcome of the European project PhotoLED [1]. The LIS-A corelated colour temperature is about 4100 K and the spectral power distribution is in accordance with the CIE written standard [6]. The standard lists the reference spectra of the white LED illuminants to be used in calibrations of photometers and for computing colorimetric parameters of reflected or transmitted object colours under LED lighting. This particular LED source was used to establish the new LED-based luminous intensity traceability.

The relative spectral irradiance (relative spectral power distribution) of the luminous intensity source LIS-A was calibrated with a spectral irradiance calibration facility based on scanning double monochromator McPherson 2035D which is traceable to the standard spectral irradiance lamp. The measurement was performed in spectral range 360 nm – 1000 nm with 0.8 nm bandwidth.

C. *Trap unfiltered primary photometer development*

The three-element silicon trap detector, usually used in radiometry as a transfer standard, forms a basis of the unfiltered primary photometer. The detector was adopted to measure the irradiance, which is needed to calculate the illuminance and luminous intensity. The precise optical aperture with a diameter of 3 mm was designed, produced and assembled in front of the traps detector optical input aperture to define the reference plain of unfiltered photometer , as well as the area of the optical input. For the picture of the developed Trap-UPP see the Fig.3.

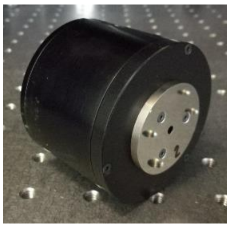

Fig. 3: The developed Trap-UPP

The detector was calibrated against the transfer standard trap detector traceable to the CR. The spectral responsivity was measured on a primary monochromator-based facility in the spectral range 300 nm – 950 nm. The precise aperture was calibrated on an optical CMM (Coordinate Measuring Machine) traceable to the national standard of length. The spectral irradiance responsivity and the illuminance responsivity of the developed trap-based unfiltered primary photometer (Trap-UPP) was calculated for a particular spectral power distribution of the LIS-A source.

D. PQED unfiltered primary photometer adaptation for independent candela realisation

An absolute predictable quantum efficiency detector (PQED) designed as a primary standard for optical power [7] was adopted to measure the irradiance, which is needed to calculate the illuminance and luminous intensity. The precise optical aperture with a diameter of 4 mm was designed, produced and mounted on the front of the detector entrance. The photo of the PQED equipped with front optical aperture is shown in Fig. 4.

The spectral responsivity of the PQED was modelled according to [7] and validated by comparison with the absolute cryogenic radiometer. The precise aperture was calibrated on an optical CMM traceable to the national standard of length. The spectral irradiance responsivity and the illuminance responsivity of the adopted PQED was calculated for a particular spectral power distribution of LIS-A source. This way, the absolute primary standard – PQED-based unfiltered primary photometer (PQED-UPP) was developed for a new independent candela realization.

E. The validation of the realization of the new candela

The SI unit candela is realized by calibrating the luminous intensity of standard light source. The standard light source is then used as a transfer standard do distribute the unit or to realise the derived photometric units.

The validation of the candela realisation based on LED standard lamp and unfiltered radiometers was done by comparing the developed unfiltered photometers with traditional photometer V(λ)-PP using the standard light source LIS-A on a photometric bench, see Fig.5. First, the unfiltered photometer Trap-UPP was compared against the V(λ)-PP to confirm the reliability of this novel measurement technique. Then the measurement results of PQED-UPP and V(λ)-PP

Fig. 4: The developed PQED-UPP

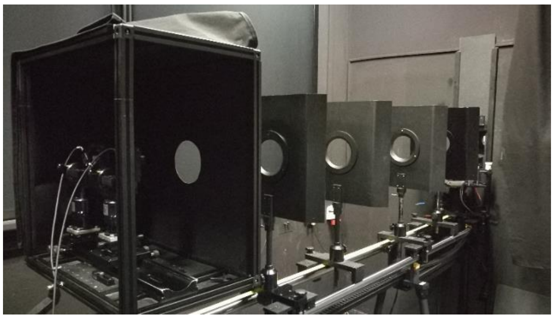

Fig. 5: The photometric bench with the baffles

were compared to validate the new independent metrological traceability chain for candela realisation based on LED standard lamp and absolute PQED-based unfiltered primary photometer.

The measurement of the luminous intensity is derived from the irradiance value measured with the PQED-UPP, Trap-UPP or V(λ)-PP and the distance of the LIS-A to the photometer. The spectral responsivities of all photometers are calibrated or well known as it is in the case of the absolute primary photometer PQED-UPP. To measure the luminous intensity the illuminance responsivity (integral luminous responsivity) of each detector was calculated for a particular spectral power distribution of LIS-A Source.

The luminous intensity measurements were done on the optical bench at the distances of 3 m and 6 m. The average was considered as a final result. The distance was measured with standard uncertainty 1 mm. The luminous intensity source and the detectors were aligned on the optical bench using two parallel alignment lasers facing each other. The optical baffles mounted on the bench were used to reduce a stray light. The LIS-A source is hidden behind the wall in next room to avoid the straylight in the laboratory. as seen in Fig. 6. The first baffle with a circular aperture having a diameter of 12 cm was placed 50 cm in front of the LIS-A. The additional 5 baffles with a 12-cm circular aperture were placed on the photometric bench between the lamp and the detector.

The front surface of the LIS-A was used as a zero point to the distance measurement in the alignment procedure. The light centre (the point used as a zero point for photometric measurements and calculations) was determined during the measurement of the luminous intensity. The relative position of the light centre was calculated from the luminous intensity measurement results for the distance 6 m and 3 m. The relative position of the light centre was 2.05 mm. It was used to reduce the length for photometric measurements and calculations measured from reference plane of LIS-A.

Fig. 6: The source side of the photometric bench

The photocurrent of the two photodiodes in the PQED-UPP was measured with calibrated current-to-voltage converter and digital multimeter. The photodiodes were connected in parallel. No bias was applied because of the low signal currents. A nitrogen flow was used in the PQED-UPP and Trap-UPP to reduce the probability of contamination of the photodiodes. The light source was blocked and the resulting dark currents for all detectors were subtracted from the illuminance measurement currents.

The luminous intensity values measured by each photometer were calculated from the measured photocurrents. The uncertainty budget for each photometer was prepared. The measured luminous intensities and their uncertainties were reviewed see the paragraph III.E.

III. Measurements and Results

A. *The new independent LED-based candela metrological traceability*

The new independent LED-based candela metrological traceability chain for detector-based candela realisation was established, as seen in Fig. 7. The standard LED light source LIS-A is measured by the novel unfiltered method and using the adopted PQED as an absolute unfiltered primary photometer.

The usage of PQED-UPP and LIS-A allowed to reduce the metrological traceability chain length to minimum. And as a result, the total uncertainty of LED-based candela realisation was reduced too. This new independent candela realisation is an equivalent to a conventional realisation using V(λ)-PP traceable to cryogenic radiometer, and has a high potential to replace it in the future.

On the other hand, the Trap-UPP-based metrological traceability, as described in the paragraph II.A, is suitable for the calibration of the customer photometers and luminous intensity standard LED lamps at lower illuminance levels, where the PQED can already have a problem with noise level. The detector is much cheaper and easy to use also for a secondary calibration. However, it is traceable to CR or it has to be always calibrated against a higher standard, which can be the PQED itself. In contrast the PQED-UPP is a kind of absolute primary standard staying on the top of metrological traceability chain. And as such, it allows to realise the unit candela with a lowest uncertainty.

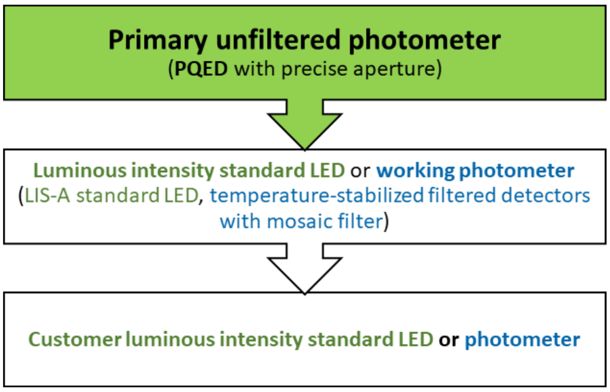

Fig. 7: The new independent candela metrological traceability chain based on LED and PQED-UPP

B. *LED standard spectra measurement*

The relative spectral irradiance of the luminous intensity source LIS-A was calibrated on the spectral irradiance calibration facility in spectral range 360 nm – 1000 nm with the 0.8 nm bandwidth. The relative spectral power distribution data are plotted in a graph, see Fig. 8.

C. *Trap unfiltered primary photometer development*

The three-element silicon trap detector, usually used in the radiometry as a transfer standard, was adopted to the unfiltered primary photometer Trap-UPP. The precise optical aperture with a diameter of 3 mm was designed, produced and mounted on the front of the detector entrance. The picture of the developed Trap-UPP was shown in Fig.3.

The spectral irradiance responsivity (see Fig. 9) was calculated from the spectral responsivity measured on the primary monochromator-based facility in the spectral range 300 nm – 950 nm. The Trap-UPP illuminance responsivity for LIS-A source was calculated to be 9.958E-9 A/lx.

D. *The adaptation of PQED unfiltered primary photometer for an independent candela realisation*

The unfiltered PQED-based primary photometer PQED-UPP was built. The photo of the PQED equipped with front optical aperture was shown in Fig. 4. The spectral responsivity of this detector was modelled according to [7] and is shown in Fig. 10. The PQED-UPP illuminance responsivity for LIS-A source was calculated to be 1.758E-8 A/lx.

E. *The validation of the new candela realisation*

The validation of candela realisation based on a LED standard lamp and an unfiltered radiometer was performed by comparing the newly developed unfiltered photometers with the traditional photometer V(λ)-PP. The photo of the measurement setup of the three compared photometers is

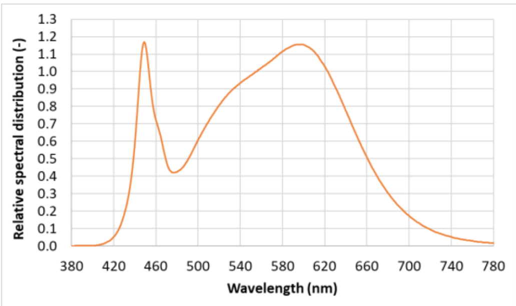

Fig. 8: The relative spectral power distribution of the luminous intensity source LIS-A

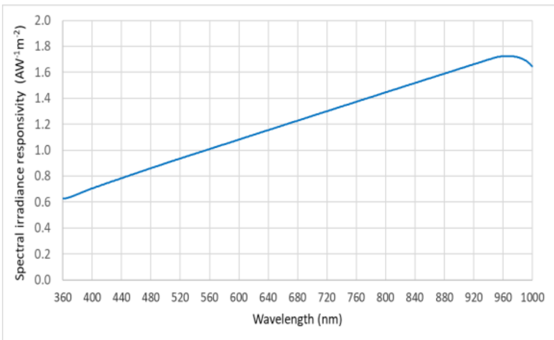

Fig. 9: Spectral irradiance responsivity of the Trap-UPP responsivity

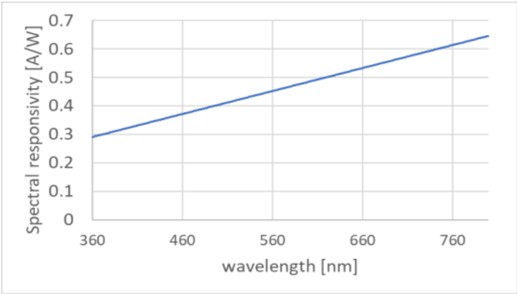

Fig. 10: PQED-UPP modelled spectral responsivity

shown in Fig. 11. In the photo can be seen from the left the Trap-UPP, V(λ)-PP and the PQED-UPP. The comparison was carried out on a photometric bench using the LED-based luminous intensity standard source LIS-A. The LIS-A was allowed to stabilize for 30 minutes before the measurements. The temperature of the reference photometer was allowed to stabilize for 1 hour.

The values of luminous intensity measured with a particular photometer are given in Table I.

Fig. 11: Three compared photometers (Trap-UPP, V(λ)-PP, PQED-UPP)

The relative deviation of the values measured with unfiltered photometers PQED-UPP and Trap-UPP from the value measured with the conventional photometer V(λ)-PP were evaluated. They are given in Table II. For the measurement uncertainty budgets for individual photometers see Table III.

TABLE II. RESULTS OF THE LUMINOUS INTENSITY MEASUREMENTS

Photometer Type	**PQED-UPP**	**Trap-UPP**	**V(λ)-PP**
I [cd]	245.36	245.31	245.37
U (k = 1) [%]	0.16	0.21	0.19

TABLE III. THE UNFILTERED PHOTOMETERS RELATIVE DEVIATIONS FROM THE CONVENTIONAL ONE

Photometer Type	**Relative deviation from V(λ)-PP [%]**
PQED-UPP	0.0031
Trap-UPP	-0.0019

From the results shown above we can see that the agreement between the Trap-UPP and V(λ)-PP is better than 0.002 %, which confirms the reliability of the unfiltered method. Moreover, the agreement of 0.003 % between the PQED-UPP and V(λ)-PP is deep within the measurement uncertainty. So, we can say that the new traceability based on PQED-UPP and LED standard source LIS-A was successfully validated.

TABLE I. UNCERTAINTY BUDGET FOR THE LUMINOUS INTENSITY AND ILLUMINANCE MEASUREMENTS

Description	**Relative Uncertainty [%]**		
	PQED-UPP	**Trap-UPP**	**V(λ)-PP**
Source relative spectral irradiance	0.14	0.14	0.07
Relative responsivity measurement	0.01	0.05	0.03
Repeatability	0.03	0.02	0.03
Aperture area	0.04	0.04	0.04
Straylight	0.02	0.02	0.02
Absolute responsivity at 555 nm	0.01	0.13	0.16
Photocurrent measurement	0.01	0.01	0.02
Drift of the source	0.01	0.01	0.01
LED current setting	0.03	0.03	0.03
Distance measurement	0.02	0.02	0.02
Combined uncertainty	**0.16**	**0.21**	**0.19**
Expanded uncertainty (k = 2)	**0.31**	**0.41**	**0.38**

IV. CONCLUSIONS

The research project „Future photometry based on solid-state lighting products“ (EMPIR 15SIB07 PhotoLED) laid the foundations for photometry based on new measurement techniques of white LED sources. Specific spectral properties of LED and OLED-based light sources allow to apply the unfiltered photometer for both the luminous intensity measurement or the candela realisation. In contrast with traditional V(λ) filtered photometers they do not use any problematic long-term instable optical filters. The photometric weighting is performed numerically and they need to be characterised for the spectral irradiance responsivity in the spectral range corresponding with the spectral power distribution of the measured spectrally limited light sources.

To apply the new unfiltered method the two types of primary unfiltered photometer were developed. The trap-based Trap-UPP and PQED based PQED-UPP. The spectral power distribution of LED based luminous intensity standard source LIS-A was calibrated and used to calculate the illuminance responsivities of these two photometers. Then the two practical LED-based realizations of luminous intensity scale were demonstrated.

At first, the unit candela was realised by calibrating the luminous intensity of standard light source LIS-A using the developed unfiltered photometer Trap-UPP. The candela realisation was validated by the comparison of the Trap-UPP with the traditional photometer V(λ)-PP. The deviation between these photometers was much smaller than the measurement uncertainty, which confirmed the reliability of this novel measurement technique.

The developed Trap-UPP is ideal for secondary calibration of photometers and luminous intensity standard LED lamps also at lower illuminance levels, where the PQED-based unfiltered primary photometer can already have a problem with noise level. Moreover, the trap detector is much cheaper and easy to use. On the other hand, it has to be traceable to the CR or calibrated against a higher standard, which, however, can be a PQED detector itself. In contrast, PQED-based unfiltered photometer is a kind of absolute primary standard staying on the top of metrological traceability chain. And as such, it allows to realise the unit candela with the lowest uncertainty.

Finally, the new independent candela realisation was demonstrated. The absolute primary standard - unfiltered primary photometer (PQED-UPP), based on primary standard for optical power PQED, was developed. Applying the PQED-UPP and the new luminous intensity measurement technique of LED standard source LIS-A a new independent metrological traceability chain for detector-based candela realisation was established. By using the PQED, the metrological traceability chain was maximally simplified, resulting in uncertainty reduction. The uncertainty of LED-based candela realisation dropped to 0.31%.

The new independent candela realisation based on the LED standard lamp LIS-A and the PQED-UPP was validated by comparing with the conventional candela realisation based on the V(λ)-PP traceable to the CR. The deviation between the new and conventional candela realisation was negligible, well below the uncertainty of the measurement. It shows an excellent agreement between the conventional candela realisation based on a tungsten lamp and the new independent realisation based on a LED standard source and PQED-base primary unfiltered photometer.

This new independent candela realisation is an equivalent to the conventional realisation using V(λ)-PP traceable to cryogenic radiometer. Nevertheless, it reaches smaller uncertainty, it is less expensive and time-consuming method. And such that it has a high potential to replace the conventional method in the future when the PQED technology is further explored and expanded.

As a result of this work, CMI keeps now two independent realisations of the unit candela with good agreement. This promotes the robustness and reliability of the whole photometric metrological system maintained at CMI.

ACKNOWLEDGMENT

The work leading to this study is partly funded by the European Metrology Programme for Innovation and Research (EMPIR) Project 15SIB07 PhotoLED “Future Photometry Based on Solid State Lighting Products”. The EMPIR initiative is co-funded by the European Union’s

Horizon 2020 research and innovation programme and the EMPIR Participating States. The project partners would like to thank CIE and the official project collaborators NIM, NRC and IPQ for their support.

REFERENCES:

[1] European Metrology Programme for Innovation And Research „Future photometry based on solid-state lighting products“ EMPIR 15SIB07 PhotoLED

[2] European Metrology Research Programme, “New primary standards and traceability for radiometry” NewStar EMRP SIB57

[3] ISO 11664-2 2007/CIE S014-2:2006 Colorimetry – Part 2: CIE illuminants for colorimetry, 24 p.

[4] implementing Metrology in the European Research Area project iMERA-Plus T1. J2.1 qu-Candela

[5] European Metrology Programme for Innovation And Research, “Self-calibrating photodiodes for the radiometric linkage to fundamental constants”, EMPIR 18SIB10 chipS·CALe

[6] CIE ISO DIS 11664-2:2020, Colorimetry - Part 2: CIE standard illuminants).

[7] Meelis-Mait Sildoja, 2013. Predictable quantum efficient detector: I. Photodiodes and predicted responsivity. Metrologia 50(4):385

Updating the Typical Values of Energy Performance Indicators in Road Lighting

Dionýz Gašparovský
Faculty of Electrical Engineering and Information Technology
Slovak University of Technology in Bratislava
Bratislava, Slovakia
dionyz.gasparovsky@stuba.sk

Peter Janiga
Faculty of Electrical Engineering and Information Technology
Slovak University of Technology in Bratislava
Bratislava, Slovakia
peter.janiga@stuba.sk

Jana Raditschová
Faculty of Electrical Engineering and Information Technology
Slovak University of Technology in Bratislava
Bratislava, Slovakia
raditschova@stuba.sk

***Abstract*— Energy performance of road lighting plays an important role in lighting design and belongs to one of the essential design criteria. Indicators of energy performance are established by European standard but their practical usage is still not widespread. Barriers can be seen in lacking understanding of the approach and correct assessment of values of the indicators. With new edition of the European norm there is chance and intention to update the typical values of energy performance indicators for different combinations of road arrangements, road widths, lighting classes and light source technologies in order to illustrate what benchmarks can be expected using this assessment system. Aim of this paper is to present new typical values prepared for the standard, to discuss factors influencing energy performance and to conclude whether it is appropriate to introduce limiting value requirements and/or ranking systems to label energy performance of road lighting systems.**

Keywords*— *energy efficiency, energy performance, energy savings, lighting control, luminous efficacy, public lighting, road lighting

I. Introduction

Road lighting is provided to residents and visitors of cities, towns, villages and other settlements for the purposes of illuminating public roads, cycle tracks, footways and pedestrian movement areas. Road lighting has to fulfil various functions such as good visual conditions for traffic safety, personal safety and assurance [1], safety to properties, visual performance at amenities other than those used for transportation, and to increase attractivity of urban environment in evenings hours.

Photometric requirements to road lighting are established in CIE 115:2010 [2] which in European countries is implemented in the norm EN 13201-2 [3] while selection of lighting classes is guided by the CEN/TR 13201-1 [4]. For the M lighting classes used for motorized traffic the set of photometric parameters consists of maintained luminance, overall uniformity, longitudinal uniformity, threshold increment TI and edge illuminance ratio EIR. For the P lighting classes intended predominantly for pedestrians and low speed traffic it is essential to assess the maintained average and minimum illuminance and additionally, where applicable, requirements are specified for the maintained minimum vertical and semicylindrical illuminance. For collision sections or areas the C classes based on the maintained horizontal illuminance and overall uniformity should be used. Auxiliary lighting classes HS accounting for hemispherical illuminance, EV for vertical illuminance and SC for semicylindrical illuminance can enhance the quality of lighting in some specific applications.

Careful determination of lighting classes for different periods of the operation time is essential to ensure that only the necessary light level is provided just when it is needed. Classification of road sections and similar structures should take into accounting all relevant circumstances such as visual needs of the users, varying traffic volumes, weather conditions, traffic compositions, background brightness etc.

Criteria specified in European standards for particular lighting classes should be achieved without excessive overlighting and redundant spill light falling outside boundaries of the area to be lit. Luminous flux distribution can be now well controlled by selection of proper optics for luminaires and overlighting can be reduced by variable lighting control. The same principle can be used to compensate for overlighting due to decay of luminous flux emitted from luminaires throughout the lifetime, e. g. by means of control gears with the CLO (Constant Light Output) function.

Besides safeguarding the required photometric parameters it is also important to optimize investment and operational costs, to mitigate adverse impacts on the night-time environment and to benefit from the best energy performance. Environmental impacts comprise broad range of side effects of outdoor lighting such as intrusive light, glare, sky glow or disturbing nocturnal organism. Energy performance is an indicator representing how the required lighting quality and quantity can be achieved with the minimum electricity consumption, CO_2 emissions and light losses in form of unnecessary spill light.

Designing of road lighting system is a complex lighting task. As highlighted by Skoda & Baxant [5], holistically and properly designed lighting is powerful tool helping to reduce the electricity consumption. Besides accordingly designed new lighting installations, refurbishment of obsolete inefficient lighting systems constitutes massive potential for energy savings, emphasized by Boyce et al. [6] as well as by Sokansky & Novak [7]. New simple method for the design of efficient public lighting based on new parameter relationship has been proposed by Rabaza et al. [8].

Assessment of the energy performance of road lighting is established in EN 13201-5:2015 [9] where the performance is described by means of two compound indicators PDI (*Power Density Indicator*) and AECI (*Annual Energy Consumption Indicator*). Yet before publication of the standard EN 13201-5, Pracki [10] dealt with the problems of energy efficiency in road lighting and proposed a particular classification method.

Problem with proper assessment of the energy performance of road lighting is that efficiency of the implemented technologies and performance of the lighting controls compensate each other. It means that systems with energy efficient luminaires operated at full power with no dimming can have similar energy performance rating like some inefficient systems with aggressive dimming strategies. To make the evaluation fair, two key aspects of the energy performance must be split and thus the two mutually dependant indicators should be always evaluated and presented together: PDI (symbol D_P, in $W \cdot lx^{-1} \cdot m^{-2}$) accounts for efficiency of the implemented lighting products as well as how well the lighting system is designed to fulfil various criteria; generally speaking, this indicator is describing the quality of the lighting design from a static perspective. AECI (symbol D_E, in $kWh \cdot m^{-2}$) is accounting for factors influencing the electricity consumption which is the input power and the operation time, both varying in course of operation; this indicator is describing the behaviour of lighting systems in response to lighting controls from a dynamic perspective. PDI should be calculated and presented for all discrete light levels while the AECI is only a single number.

II. Background and motivation

Massive development of advanced LED technology during the last decade leads to the need of more frequent update of technical standards specifying even more stringent requirements to both the quality of light and its energy performance. LED technology in urban lighting has a number of benefits: high luminous efficacy, tailored optics, free choice of colours, dynamic control. Adaptive lighting control is pushing the limits farther towards sophisticated, efficient, sustainable, tailored and integrative (human centric) lighting. By implementation of 'smart lighting' elements, systems and technologies the lighting becomes part of a superior smart city network and tends to integrate with other infrastructural subsystems such as traffic monitoring and control, telecommunication, utility services and others. Interactions influencing target lighting parameters are particularly significant: weather conditions, visibility level, traffic conditions (density, volume, speed), user presence or movement, composition of users etc. Adaptive lighting is the technical precondition to provide lighting on demand – where, when and how much it is needed.

Typical values of PDI and AECI presented in EN 13201-5:2016 are based on lighting products available in Q1/2014. Since that time luminous efficacy of luminaires has been increased, optics improved, selection of light distributions enhanced and tailored to broad range of arrangements. Lighting controls can now dim down the lighting to almost any level and to consider a variety of detectors. It is evident that typical values currently presented in the standard are heavily outdated.

Structure of the tables in EN 13201-5 can be simplified to present values of PDI and AECI only for typical combinations of road widths and lighting classes. It is worthless to provide data for obsolete types of light sources like sodium lamps, metal halide lamps and even mercury vapour lamps. But it is worth to illustrate how developments in lighting affect the value of the indicators. In this respect it is interesting to show the difference in energy performance between LED technologies in span of 8 years (Q1/2014 versus Q1/2022). Note that comparison between different technologies arising for public lighting have been experimentally investigated by Rodrigues et al. [11].

III. Scientific objectives

The paper aims to present typical values of the PDI and AECI indicators for different combinations of road arrangements, road widths, lighting classes and light source technologies to illustrate what benchmarks can be expected using this assessment system. It is also worth to illustrate how developments in lighting affect the value of the indicators. Objectives also comprise discussion on factors influencing the energy performance and recommendation to establish or not limiting values and/or ranking system for energy performance of road lighting.

IV. Methodology

System power (of a lighting installation in a given state of operation) P is total power of the road lighting installation needed to fulfil the required lighting classes as specified in EN 13201-2 in all the relevant sub-areas, and to operate and control the lighting installation during the operation time t.

Assuming finite number of lighting levels in road lighting, annual lighting energy consumption can be calculated as follows:

$$W = \sum_{i=1}^{365} \sum_{j=1}^{M} \left(P_{ij} . t_{ij} \right) \tag{1}$$

where W – is the annual lighting energy consumption (Wh); P_{ij} – is the lighting system power associated with the given lighting level (W); t_{ij} – is the daily operational time of the given lighting level (h); j, M – is the index and number of different pre-set or considered lighting levels.

Power Density Indicator PDI (of a lighting installation in a given state of operation, for an area divided into sub-areas), is value of the system power divided by the value of the product of the surface area to be lit and the calculated maintained average illuminance value on this area according to EN 13201-3 [12]:

$$D_P = \frac{P}{\sum_{i=1}^{n} (\overline{E}_i \cdot A_i)} \tag{2}$$

where D_P – is the power density indicator ($W \cdot lx^{-1} \cdot m^{-2}$); P is the system power of the lighting installation used to light the relevant areas (W); E is the maintained average horizontal illuminance of the sub-area 'i' (lx); A_i is the size of the sub-area '$_i$' lit by the lighting installation (m^2); n is the number of sub-areas to be lit. The PDI indicator should be calculated for each lighting level of the operational profile with associated input power of the luminaires and calculated illuminances of the sub-areas.

Annual Energy Consumption Indicator AECI (of a lighting installation in a specific year) is total electrical energy consumed by a lighting installation day and night throughout a specific year in proportion to the total area to be illuminated by the lighting installation, calculated by the formula:

$$D_E = \frac{\sum_{j=1}^{m} P_j \cdot t_j}{A} \tag{3}$$

where D_E – is the annual energy consumption indicator for a road lighting installation (Wh·m^{-2}); P_j – is the operational power associated with the j^{th} period of operation (W); t_j – is the duration of j^{th} period of operation profile when P_j is consumed, over a year (h); A – is the size of the area lit by the same lighting arrangement (m^2); m – is the number of periods with different operational power P_j.

For calculation of AECI it is indispensary to assume some lighting control profile and in systems with detectors also annual detection probability parameter for each of the lighting levels.

Operation time of road lighting systems is dealt e .g. in [13]. There are typical distinct profiles known in lighting practice. Full power operational profile is typical for many existing lighting installations with simple switching devices like time switchers or photosensors where luminaires operate constantly at full power throughout the night time each day. For this operational profile it is common to take the annual operation time 4 000 hours. In regulated and sensing systems, multi-power detector-driven operational profiles can be used to control lighting levels, like quadri-power profile in the example shown in Fig. 1 (daily course). Here lighting levels must be associated with particular lighting classes specified for a road and given conditions. It is recommended that in period with no traffic at least a minimum lighting level is sustained throughout the night time.

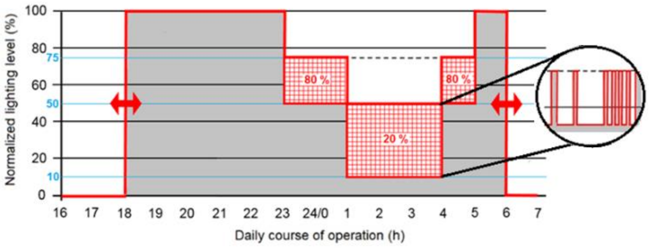

detection probability (%)

Fig. 1. Example of a quadri-power detector-driven operational profile

Estimation of the detection probability can be a hard task particularly for new installations where no historical data are available. The value can be established by comparison with similar and neighbouring installations and/or derivation from higher class major roads. In systems with flat lighting levels without drop downs the probability is 100 % by default.

Values of energy performance indicators PDI and AECI depend on many factors like the actual lighting class, road profile arrangement, width of carriageway and concurrent footpaths, type of the light source and luminaire implemented, spatial distribution of luminous flux from luminaires, etc. Even if the lighting system is optimized according to the target photometric parameters, lighting designs may still differ in energy performance. The lower is the value of PDI and/or AECI, the better is energy performance. Indicative values of energy performance indicators PDI and AECI presented in this paper are based on numerous calculations of lighting systems for different combinations of the above listed factors that are common in practice. Boundary conditions for seeking the optimum geometry of the lighting system are as follows:

- single-sided lighting system arrangement;
- six typical road profile arrangements;
- width of footpaths and grass strips equals to 2 m;
- maintenance factor is set to 0,80 for all cases;
- R3 table is considered for road reflection properties;
- mounting height is optimized within the range 6 m to 12 m in whole number steps;
- spacing of lighting poles is optimized and sought between 20 m to 60 m in 1 m steps;
- arm overhang is ranged from 0 m to 2 m in 0,5 m steps;
- luminaires are not tilted (0°);
- annual operation time 4 000 h at full power.

To minimize energy performance indicators, lighting system geometry has been optimized with preference given to the maximization of spacing and thus the illuminated area. Accounting for the lowest possible installation costs, the mounting height has been sought as minimum in addition to the previously mentioned criteria.

Calculations are based on generic lighting products (luminaires) available in Q1/2022. Average luminous efficacy of LED luminaires is 125 lm/W with very small deviations within the product range (–4 %/+0,8 %). Warm white light sources with T_c = 3 000 K have been used.

Six typical road profile arrangements comprise:

- A: two-lane road for motorized traffic;
- B: road with mixed motorized and pedestrian traffic;
- C: road with footpath on the side of the lighting installation;
- D: road with footpath opposite to the lighting installation;
- E: road with two footpaths on both sides;
- F: road with two footpaths on both sides, separated from carriageway by grass strips (Fig. 2).

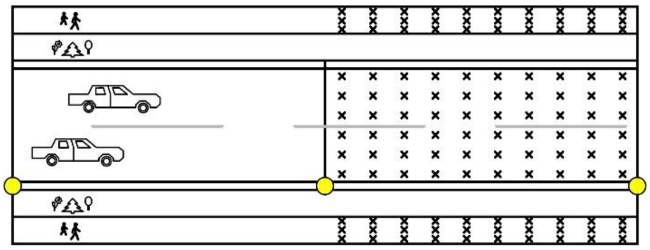

Fig. 2. The most complex road profile F

Range of values for the AECI indicator is presented only in a descriptive way for full power operational profile with annual operation time 4 000 h. To consider different operational profiles it is sufficient to combine the annual operation times of individual lighting levels with the associated system power and the detection probability (in systems with detectors) into a single lighting operation coefficient c_{op}. AECI value for actual operational profile is calculated as full-power AECI multiplied by c_{op}. c_{op} can be used also as a self-standing indicator of energy saving potential of the actual lighting control.

High-pressure mercury vapour lamps (below 45 lm/W), metal halide lamps (70 – 75 lm/W), elliptical and tubular sodium lamps 70 – 120 lm/W, LEDs available in 2014 (100 – 105 lm/W, T_c = 3 000 K) and currently available LED products (2022) are included in the comparison of energy performance indicators for different light sources. Boundary conditions for comparison of different light sources are as follows:

- width of the carriageway 7 m;
- lighting class M4;
- annual operation time 4 000 h at full power.

V. Results and Discussion

A. Typical values of energy performance indicators for contemporary light sources

Road profile A is the simplest arrangement consisting of a single carriageway. Relation between PDI and road width is straightforward. Lower lighting classes are less demanding due to different lighting quality criteria other than luminance. Typical values of PDI are lying around 20 $mW \cdot lx^{-1} \cdot m^{-2}$ with small deviations, as presented in Table 1 with cross section for the 7 m road in Fig. 3. The values of AECI (Table II) for a 7 m road range from 0,32 $kWh \cdot m^{-2}$ for M6 up to 2,70 $kWh \cdot m^{-2}$ for M1. Because AECI is free of reference luminous parameter, the value will strongly depend on lighting class and this is true for all luminance based road profiles. AECI is decreasing with smaller road widths to 0,45 $kWh \cdot m^{-2}$ for 4 m road classified to M6. For wider roads and higher lighting classes the value is also decreasing, for example to 2,35 $kWh \cdot m^{-2}$ for 10 m road and the M1 class and similarly for other situations.

TABLE I. Typical values of the Power Density Indicator D_P ($mW \cdot lx^{-1} \cdot m^{-2}$) for road profile A

Lighting class	Width of carriageway (m)					
	4	5	6	7	8	10
M1				22,4	20,4	19,6
M2				20,6	20,5	20,0
M3			20,6	20,2	20,1	
M4			21,0	21,0	20,2	
M5		20,5	20,1	20,8		
M6	24,1	19,3	20,0	17,4		

TABLE II. Typical values of the Annual Energy Consumption Indicator D_E ($kWh \cdot m^{-2}$) for road profile A

Lighting class	Width of carriageway (m)					
	4	5	6	7	8	10
M1				2,69	2,44	2,35
M2				1,81	1,81	1,76
M3			1,24	1,21	1,21	
M4			0,92	0,92	0,89	
M5		0,61	0,61	0,61		
M6	0,45	0,36	0,37	0,32		

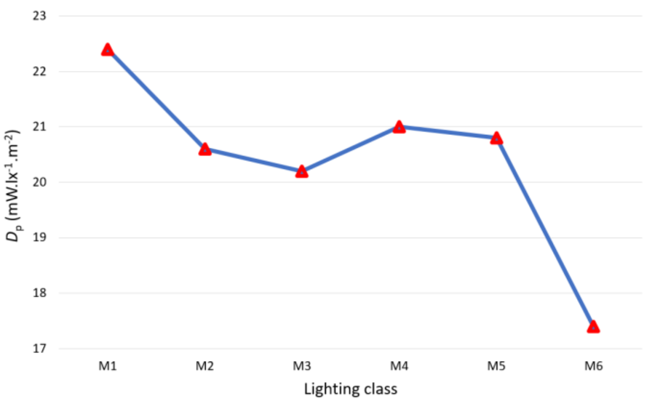

Fig. 3. Typical values of the Power Density Indicator D_P ($mW \cdot lx^{-1} \cdot m^{-2}$) for road profile A and road width 7 m

Road profile B is somewhat unusual compared to the other profiles in that the lighting design is fully based on illuminance and the photometric requirements are associated with C lighting classes. Absence of observer means that complex road surface reflection properties (the *R*-tables) are not applied what makes the design process and the results more predictable. PDI values are presented in Table III. PDI is descending for wider roads where the luminous flux is better used up and losses are smaller (nearby edges). There is almost no or neglectable difference in values across lighting classes what can be seen explicitly in Fig. 4 for an average 7 m road, where span of the values make less than 3 % and this is indeed the worst case. For this reason it is worth to present in the new draft standard only common values for all lighting classes C0 to C5. Graduation of the required illuminance according to the lighting classes is naturally projected to typical values of AECI (Table IV). For the average 7 m road the values are ranging from 0,53 $kWh \cdot m^{-2}$ (class C5) to 3,43 $kWh \cdot m^{-2}$ (class C0) and they are increasing (worse performing) with smaller widths and decreasing (better performing) for wider roads. This clear characteristics is resulting from straightness of the illuminance criterion.

TABLE III. Typical values of the Power Density Indicator D_P ($mW \cdot lx^{-1} \cdot m^{-2}$) for road profile B

Lighting class	Width of carriageway (m)					
	4	5	6	7	8	10
C0				16,5	15,9	14,2
C1				16,6	16,0	15,3
C2			17,9	16,6	16,0	
C3			17,9	16,7	16,0	
C4		19,4	17,9	16,9		
C5	22,5	19,3	17,9	17,0		

TABLE IV. Typical values of the Annual Energy Consumption Indicator D_E ($kWh \cdot m^{-2}$) for road profile B

Lighting class	Width of carriageway (m)					
	4	5	6	7	8	10
C0				3,43	3,38	2,92
C1				2,08	2,00	1,96
C2			1,52	1,41	1,33	
C3			1,14	1,05	1,02	
C4		0,85	0,76	0,68		
C5	0,68	0,61	0,57	0,53		

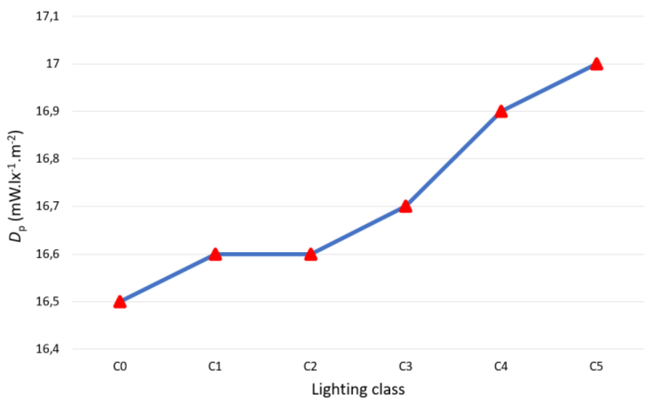

Fig. 4. Typical values of the Power Density Indicator D_P ($mW \cdot lx^{-1} \cdot m^{-2}$) for road profile B and road width 7 m

Road profiles C (Tab. V & VI/Fig. 5), D (Tab. VII & VIII/Fig. 5) and E (Tab. IX & X/Fig 5) can be analysed together and confronted against each other. As shown in Fig. 5, the curves are very similar but the average value of PDI is biased, being around 16 mW·lx^{-1}·m^{-2} for the C profile, slightly higher 17,5 mW·lx^{-1}·m^{-2} for the D profile and only about 14,2 mW·lx^{-1}·m^{-2} for the E profile. For good energy performance it is essential to choose luminaire with luminous flux distribution that suits the actual road profile arrangement, emitting enough light to reach the footpaths. In road profile C this can be away from the carriageway (luminaires emitting light backwards). It is always easier to illuminate footpath on the side of the lighting installation than on the other side due to higher distance (inverse square law) and angles of incidence (cosine law), hence higher (ca 10 %) PDI numbers for the D profile. This principle similarly applies to the E profile but because here the total target area is sum of two sub-areas, the resulting indicator values are shifted downwards (ca 12,5 %) as it can be expected. Behaviour of typical AECI numbers for road profiles C, D and E reflect the same principles. Taking the 7 m road for reference, the AECI values span from about 0,30 to 1,00 kWh·m^{-2} identically for the C and D profiles (the same target area), and from 0,24 to 0,82 kWh·m^{-2} for the E profile (the same area of the carriageway and double area of the footpaths). Variation of the values over widths of carriageways is neglectable.

TABLE V. TYPICAL VALUES OF THE POWER DENSITY INDICATOR D_P (MW·LX^{-1}·M^{-2}) FOR ROAD PROFILE C

Lighting class	Width of carriageway (m)					
	4	5	6	7	8	10
M3/P3			16,0	16,0	16,0	
M4/P4			15,7	15,8	15,8	
M5/P5		15,9	16,0	14,7		
M6/P6	17,8	16,3	16,1	14,7		

TABLE VI. TYPICAL VALUES OF THE ANNUAL ENERGY CONSUMPTION INDICATOR D_E (KWH·M^{-2}) FOR ROAD PROFILE C

Lighting class	Width of carriageway (m)					
	4	5	6	7	8	10
M3/P3			1,00	1,00	1,00	
M4/P4			0,73	0,74	0,75	
M5/P5		0,48	0,50	0,47		
M6/P6	0,31	0,30	0,30	0,30		

TABLE VII. TYPICAL VALUES OF THE POWER DENSITY INDICATOR D_P (MW·LX^{-1}·M^{-2}) FOR ROAD PROFILE D

Lighting class	Width of carriageway (m)					
	4	5	6	7	8	10
M3/P3			17,9	17,7	17,6	
M4/P4			17,5	17,4	17,3	
M5/P5		18,0	17,9	16,8		
M6/P6	19,4	18,4	18,0	16,8		

TABLE VIII. TYPICAL VALUES OF THE ANNUAL ENERGY CONSUMPTION INDICATOR D_E (KWH·M^{-2}) FOR ROAD PROFILE D

Lighting class	Width of carriageway (m)					
	4	5	6	7	8	10
M3/P3			1,00	1,00	1,00	
M4/P4			0,73	0,74	0,75	
M5/P5		0,48	0,50	0,47		
M6/P6	0,31	0,30	0,30	0,30		

TABLE IX. TYPICAL VALUES OF THE POWER DENSITY INDICATOR D_P (MW·LX^{-1}·M^{-2}) FOR ROAD PROFILE E

Lighting class	Width of carriageway (m)					
	4	5	6	7	8	10
M3/P3			14,2	14,4	14,6	
M4/P4			13,9	14,2	14,3	
M5/P5		13,9	14,2	13,5		
M6/P6	14,7	14,2	14,3	13,5		

TABLE X. TYPICAL VALUES OF THE ANNUAL ENERGY CONSUMPTION INDICATOR D_E (KWH·M^{-2}) FOR ROAD PROFILE E

Lighting class	Width of carriageway (m)					
	4	5	6	7	8	10
M3/P3			0,80	0,82	0,84	
M4/P4			0,59	0,61	0,62	
M5/P5		0,38	0,40	0,39		
M6/P6	0,23	0,24	0,24	0,24		

Results for these complex schemes strongly depend on the assumed road profile and lighting class. For example, in real situations the width of footpaths can differ from the assumed value, differently on both sides of the carriageway. It would be beneficial to further study these relations.

Road profile F is even more complicated. Grass strips separating footpaths from the carriageways can be almost arbitrary wide. With currently available lighting equipment it is impossible to avoid light losses on grass strips if all sub-areas are to be illuminated by one lighting installation. From practical experience it follows that widths of grass strips up to 3 m can be acceptable, at 4 – 5 m illumination of concurrent footpaths is inefficient and sometimes also hard to satisfy the lighting requirements; above 5 m it has no sense to consider shared lighting installation and if lighting of footpaths is inevitable or requested then it should be satisfied by a dedicated lighting installation.

TABLE XI. TYPICAL VALUES OF THE POWER DENSITY INDICATOR D_P (MW·LX^{-1}·M^{-2}) FOR ROAD PROFILE F

Lighting class	Width of carriageway (m)					
	4	5	6	7	8	10
M3/P3			22,3	22,4	20,3	
M4/P4			21,8	22,2	20,5	
M5/P5		24,0	21,6	22,3		
M6/P6	27,3	23,8	21,6	22,0		

TABLE XII. TYPICAL VALUES OF THE ANNUAL ENERGY CONSUMPTION INDICATOR D_E (KWH·M^{-2}) FOR ROAD PROFILE F

Lighting class	Width of carriageway (m)					
	4	5	6	7	8	10
M3/P3			0,91	0,93	0,91	
M4/P4			0,67	0,70	0,68	
M5/P5		0,46	0,43	0,47		
M6/P6	0,29	0,28	0,26	0,29		

Typical values of PDI for the road profile F should be deemed as very illustrative due to many assumptions specified for this case. Results are presented in Table XI and cross-section for the 7 m road is unfolded in Fig. 5. Values are spread around 22 mW·lx^{-1}·m^{-2} what is almost 60 % higher than in the case of unseparated footpaths (road profile E). Drop of performance is significant. Typical values of AECI (Table XII) are ranging from 0,29 kWh·m^{-2} (M6/P6) to 0,93 kWh·m^{-2} (M3/P3) with small variations amongst different widths of carriageway.

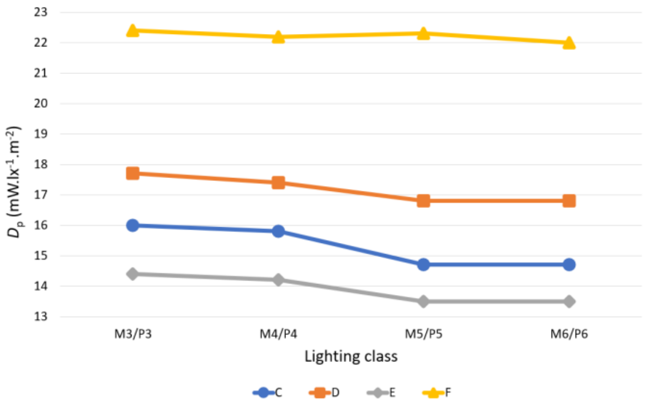

Fig. 5. Typical values of the Power Density Indicator D_P (mW·lx^{-1}·m^{-2}) for road profiles C-D-E-F and road width 7 m

B. Typical values of energy performance indicators for historical light sources

Comparison of energy performance indicators for different light sources taking into account specified boundary conditions in Chapter 4 is shown in Table XII for PDI and Table XIV for AECI. The PDI values are graphically presented in Fig. 12. The data proved that advances in LED technology gained about 10 % in PDI and 20 % in AECI. LED lighting is performing twice better than its sodium technology predecessor and 4,5 times better than the obsolete mercury-based technology. This benefit comes not only thanks to higher luminous efficacy of the lamps (or luminaires) but to much extent it is due to significantly different quality of optics – from modest diffusers in combination with bulky elliptical mercury bulbs through faceted reflectors combined with compact-size sodium lamp burners up to precise Fresnel lens optics attached to tiny LED chips.

TABLE XIII. Typical values of the Power Density Indicator D_P (mW·lx^{-1}·m^{-2}) for different light sources

Road profile	Mer-cury	Metal halide	Sodium elliptical	Sodium tubular	LED (2014)	LED (2022)
A	90	60	41 – 47	34 – 42	23	21
C	73	50	35 – 38	30 – 34	20	16
D	78	48	35 – 40	27 – 35	19	17
E	65	41	33 – 34	26 – 28	17	14
F	71	45	34 – 36	28 – 32	23	22

TABLE XIV. Typical values of the Annual Energy Consumption Indicator D_E (kWh·m^{-2}) for different light sources

Road profile	Mer-cury	Metal halide	Sodium elliptical	Sodium tubular	LED (2014)	LED (2022)
A	5,0	3,1	2,3 – 2,5	1,8 – 2,4	1,1	0,9
C	4,0	2,4	1,8 – 1,9	1,5 – 1,8	0,9	0,7
D	4,0	2,4	1,8 – 1,9	1,4 – 1,8	0,9	0,7
E	3,2	2,0	1,5	1,2 – 1,5	0,7	0,6
F	3,2	2,0	1,5	1,2 – 1,5	1,0	0,7

The tables XIII & XIV are intended only for illustrative purposes to demonstrate how development in light source technology over past decades affects energy performance of road lighting installations. Lamp types presented in the tables are referring to previous lighting techniques and cannot be recommended for new or refurbished lighting systems.

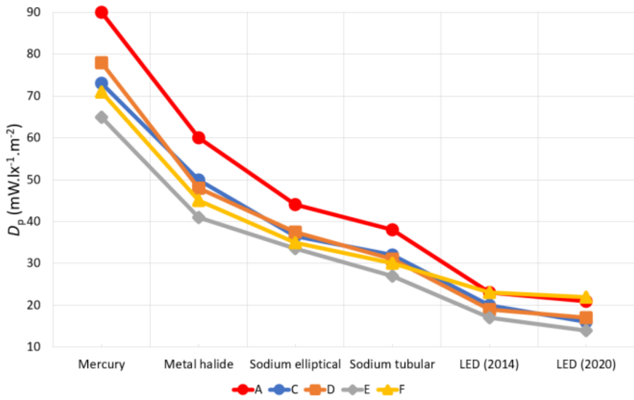

Fig. 6. Typical values of the Power Density Indicator D_P (mW·lx^{-1}·m^{-2}) for different light sources

VI. Conclusions

Typical values well illustrate the behaviour of PDI depending on main influencing parameters which is the road width and the lighting class. Deeper understanding of these relations has been acquired by optimization of road lighting designs in the framework of numerous model calculations, attempting to vary spacing of lighting poles, mounting height and wattage of luminaires amongst others. It has been proved that utilance of an installation is what matters in deed and similar numbers of the performance indicators can be obtained for various lighting system arrangements. It also means that the energy performance expressed through power density (PDI) is appropriate for the purpose in the steady-state operation regime. Hence, to maximize the utilance, proper selection of the luminous flux distribution and adjustment of the absolute value of luminous flux are key points of the lighting design.

Comparison of the indicators showed significant improvement of the performance with upraise of the LED technology, which is twice better than the preceding sodium lamp technology and yet little better than metal halide lamps. Heavily obsolete mercury lamps perform 4,5 times worse than modern lighting products.

Assuming arbitrary setup of the lighting system geometry and arrangement consisting of a single element it is possible to define limit values of PDI as additional criterion within lighting classes. However, this fails when it comes to refurbishment of the system where e. g. replacement of lighting poles is not desired. Moreover, any other road profile arrangement can strongly affect the indicator's value – namely width of concurrent footpaths and grass strips. The situations can be so complex that it is impossible to find a correlation between so many variables and this makes any attempts to define fair limit values and even more a ranking system not feasible. Thus, the indicators should be used only in accordance with the original intention, i.e. to compare different (e.g. alternative, competing in public tenders etc.) lighting designs for the same lighting task – the same road profile and the same boundary conditions.

ACKNOWLEDGMENT

This work was supported by the Slovak Research and Development Agency under the contract No. APVV-20-0157.

REFERENCES

[1] CIE 236:2019, Lighting for Pedestrians: A Summary of Empirical Data

[2] CIE 115:2010, Lighting of roads for motor and pedestrian traffic

[3] CEN/TR 13201-1:2014, Road lighting - Part 1: Guidelines on selection of lighting classes

[4] EN 13201-2:2015, Road lighting - Part 2: Performance requirements

[5] SKODA, J. & BAXANT, P., The reduction in electricity consumption through proper lighting, In proc.: EPE 2009, Brno University of Technology: Brno, pp. 1-4

[6] BOYCE, P.R., FOTIOS, S.,RICHARDS, M., Road lighting and Energy saving, Lighting Research and Technology, 41 (2009), pp. 245-260, ISSN: 1477-0938

[7] SOKANSKY, K., NOVAK, T., Energy savings in public lighting, Przeglad Elektrotechniczny, (2008), No. 8, pp. 72-74. ISSN: 0033-2097.

[8] RABAZA, O., PEŇA GARCÍA, A., PERÉZ OCÓN, F., GOMÉZ LORENTE, D., A new simple method for designed efficient public lighting, based on new parameter relationships, Expert Systems with Applications, (2013), pp. 7305-7315, ISSN: 0957-4174

[9] EN 13201-5:2015, Road lighting - Part 5: Energy performance indicators

[10] PRACKI, P., Proposal to classify road lighting energy efficiency, Lighting Research and Technology, 43 (2011), pp. 271-280, ISBN 978-1-4398-2079-7

[11] RODRIGUES, C., ALMEIDA, P., SOARES, G., JORGE, J., PINTO, D., BRAGA, H., An Experimental Comparison Between Different Technologies Arising for Public Lighting: LED Luminaires Replacing High Pressure Sodium Lamps, IEEE, p. 141-146, ISBN 978-1-4244-9311-1

[12] EN 13201-3:2015, Road lighting - Part 3: Calculation of performance

[13] GAŠPAROVSKÝ, D., Calculation of the Operation Time of Road Lighting, In proc.: CIE Centenary Conference "Towards a New Century of Light", Paris, France, 15-16 April 2013, Vienna: Commission Internationale de l'Eclairage, 2013, pp. 999-1008, ISBN 978-3-902842-44-2

Concept of Prague Public Lighting

Petr Žák
Dept. of Electrical Power Engineering
Czech Technical University in Prague,
Faculty of Electrical Engineering
Prague, Czech Republic
zakpetr@fel.cvut.cz

Roman Koucký
Department of Building Theory
Czech Technical University in Prague,
Faculty of Architecture
Prague, Czech Republic
roman.koucky@fa.cvut.cz

Marek Bálský
Dept. of Electrical Power Engineering
Czech Technical University in Prague,
Faculty of Electrical Engineering
Prague, Czech Republic
balskmar@fel.cvut.cz

Abstract—Prague, the capital of the Czech Republic, through its representatives, decided on a conceptual and systematic approach to the management of the public lighting. On the basis of this decision, a set of documents was submitted for processing under the title *Concept of Prague Public Lighting*. This set of documents is intended to specify what the night image of the city should be, creating through public and architectural lighting. When determining the night appearance of the city, not only the safety of the traffic of people and property, but also the undesirable effects of lighting on the surrounding environment and the effect of lighting on the appearance of public spaces should be taken into account. An integral part of the *Concept of Prague Public Lighting* is also the plan for the renewal and modernization of the public lighting system for the purposes of the city's financial planning. *Concept of Prague Public Lighting* also contains standards of activity and devices that specify requirements for activities related to public lighting and for products that are part of the public lighting system.

Keywords— Concept of public lighting, lighting masterplan, road lighting, architectural lighting, lighting class, environmental zone

I. Introduction

After previous preparations, the capital city of Prague decided at the end of 2019 to proceed with a conceptual and systematic approach to the management of the public and architectural lighting system. On the basis of this decision, it submitted a set of documents for processing under the title *Concept of Prague Public Lighting*. This set of documents consists of three main parts: *Lighting Masterplan, Renewal Plan* and *Standards*.

The *Lighting masterplan* specifies the night image of the city and its purpose is to preserve the defined night appearance of the city through the proposed parameters and rules. The *Lighting masterplan* and its requirements and parameters, are intended to serve as input data for subsequent project documentation.

The second part of the *Concept of Prague Public Lighting* is the *Renewal plan*. This document contains an analysis of the current state of the lighting system of public and architectural lighting in Prague. On the basis of predetermined criteria such as the age, state, power consumption or lighting level of the lighting system, a public lighting renewal schedule is created. It also includes an estimate of the costs of its implementation. This document serves as a tool for financial planning of the city in the field of public and architectural lighting.

The last part of the *Concept of Prague Public Lighting* are the *Standards* related to the activities and products used in public lighting. The *Standards* set requirements for individual activities within public lighting such as design, construction, reconstruction, maintenance and operation. They also set requirements for products such as lamps, light sources, supporting structures, etc., in order to maintain the required quality and limit the number of types of individual devices used in the lighting system.

The following part describes the main principles of the Lighting masterplan.

II. Background

The Lighting masterplan of Prague is understood within the framework of the Concept of Prague Public Lighting as a document that specifies the appearance of Prague at night time. The night time image of Prague is generally shaped by a whole range of artificial light sources (street lighting, buildings, workplaces, sports fields, advertisements). Given that the city of Prague only manages public lighting and architectural lighting, the night image of Prague is primarily described in relation to these two types of lighting systems. As part of the solution to the night time image of the city, aspects related to the safety of traffic, people and property, limiting the adverse effects of artificial lighting on the surrounding environment and the night time appearance of public spaces are taken into account. These viewpoints are assigned lighting parameters that characterize them. At the same time, aspects are structured according to importance and meaning, and limit values are assigned to individual parameters accordingly, or Properties. The lighting masterplan creates a framework of requirements for subsequent project documentation. Its purpose is to maintain a defined idea of the night image of the city during the restoration, reconstruction or new construction of lighting systems of public and architectural lighting.

III. Motivation

The main motivation in the design of the Lighting masterplan was to create a document that would take into account predefined aspects related to public and architectural lighting. The document will include a set of parameters that will be used to describe individual aspects and limit values or properties will be assigned to these parameters. The specified set of parameters will be simple, clear and easy to understand and will allow to create a data model. The proposed data model should be in such a form that it can be easily updated and at the same time integrated into map data (GIS) based on the documents of the Metropolitan Plan of Prague. Data outputs from the data model will be easily accessible and clear.

IV. Analytic Part

An analysis of the current night time picture of the city was carried out before the actual design of the night time picture. The night image of the city can be analyzed in different ways, at different scales and according to different points of view. During the analysis of the night image of the city, an area analysis and a spatial analysis were carried out. The area analysis used aerial views of the city from above, the spatial analysis used night images of significant panoramas.

A. *Area analysis*

A night time photo of Prague was the basis for the area analysis of the night image of the city. In the beginning, there was an effort to acquire night satellite photos, but this effort did not lead to the desired goal. Although several photos were obtained, these images were of insufficient resolution and were not up-to-date. For this reason, nighttime aerial photography of Prague was carried out (Fig. 1). The photography was done at the end of October 2020 from a height of 3 km at a resolution of 0.2 m/px. The resulting file consists of a total of 525 images. The images cover the area of the administrative borders of Prague (459 km^2). Taking into account the segmental nature, the photography was carried out in the time interval from 21:00 to 24:00 so that most of the outdoor lighting systems in the entire territory of Prague were captured. The resulting night image is in the format of an orthogonal map, which is compatible with the daytime orthogonal map and can be used together with map data for spatial planning.

Fig. 1. Night orthogonal image of Prague (city of Prague)

From the nighttime orthogonal photograph, several following insights can be read:

- the main nighttime image of the city is formed by the illuminated surfaces of the transport infrastructure, including roadways, airport areas and railway station areas;
- parking areas of shopping centers have significant lighting levels;
- illuminated roads differ in the level of illumination, related to their function;
- in addition to the lighting level, the color tone of the light sources used (warm white x neutral white) can be distinguished.

An important aspect in the night time image of the city is the structure of the housing development. If the building is continuous (especially the center of the city) then it reflects the light that falls on building facades back onto the road. The lighting of the road in such structure appears to be continuous in contrast to an individual housing development. Individual buildings do not continuously delimit the illuminated space, and the lighting is perceived as a series of bright points.

B. *Spatial analysis*

Photographs of important panoramas and views of Prague are part of the Metropolitan plan of Prague. Their selection was made for the day time. At night, the vast majority of these views and panoramas are not applicable due to the limited range of artificial lighting. For this reason, only those views and panoramas that apply at night were selected and their analysis was performed (Fig. 2).

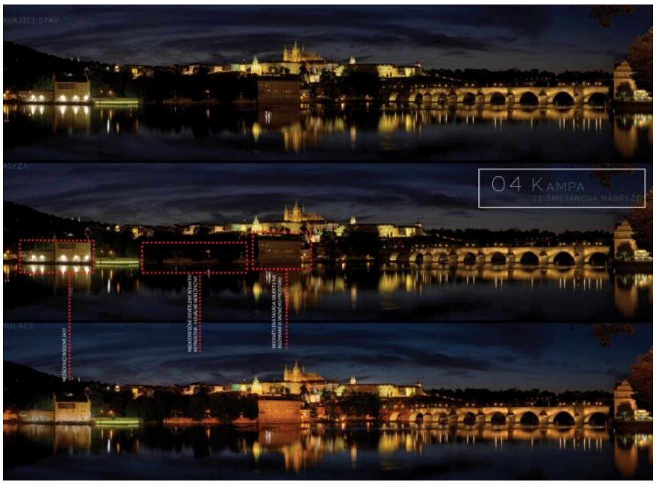

Fig. 2. Analysis of the panorama of Prague Castle (city of Prague)

In addition to the analysis of important panoramas, an analysis of the architectural lighting of the objects was carried out. For objects with architectural lighting, information about the owner of the lighting is important, which can be the local government (city of Prague), the state administration (Czech Republic) or a private owner. As part of the concept, it is possible to primarily work with objects that are illuminated or can be illuminated by the city of Prague. Currently, the city of Prague provides architectural lighting for 145 buildings. As part of the analytical part, an analysis of the current state of lighting at night and the visual application of objects during the day was carried out. Individual objects were classified into one of the following categories:

- monasteries and castles;
- sacred buildings;
- municipal buildings;
- other buildings.

The largest concentration of architectural lighting is in the historical center of Prague (Fig. 3), where there are 80 objects with architectural lighting.

V. Design Part

The Lighting masterplan of Prague sets the requirements for lighting in such a way that it is possible to maintain the proposed night time image of the city of Prague, which is a visual expression of the Lighting masterplan. The Lighting masterplan deals only with public and architectural lighting in its design part, similar to the analytical part.

The primary purpose of public lighting is to ensure safety. The primary purpose of architectural lighting is to create a certain image of the city and its public spaces. In addition to its primary purpose, public lighting also affects the appearance of public spaces at night.

Fig. 3. Architectural lighting is in the historical center of Prague

The primary purpose of public lighting is to ensure safety. The primary purpose of architectural lighting is to create a certain image of the city and its public spaces. In addition to its primary purpose, public lighting also affects the appearance of public spaces at night. At the same time, both mentioned lighting systems can adversely affect the surrounding environment through their operation. The Lighting masterplan in its design takes into account the above facts and is divided into three basic parts:

- safety – the effect of lighting on the safety of traffic, people and property;
- ecology – the effect of lighting on the surrounding environment;
- representation – the effect of lighting on the appearance of the city and public spaces.

A very important requirement for the processing of the Lighting masterplan was the compatibility of the output data with the GIS data environment used by Prague as part of spatial planning. Another essential requirement was that the lighting masterplan be in accordance with the Prague Building Regulations, the Metropolitan Plan and European and national technical standards.

A GIS data layer was chosen for each of the above aspects. Where possible, Metropolitan Plan data layers were used. Attributes have been added to these layers and appropriate values or properties have been assigned to these attributes. This created the basic prerequisites for creating the data model of the Lighting masterplan. The next essential step was the creation of the basic schema of this data model. The basic layer is the safety layer, which sets the minimum requirements for lighting from a safety perspective. The ecology layer complements these requirements with requirements for limiting obtrusive light. The representation layer complements or increases the basic requirements set from the safety point of view and in some exceptional cases mitigates the requirements set from the ecological point of view. The basic structure of the data model is shown in Fig. 4.

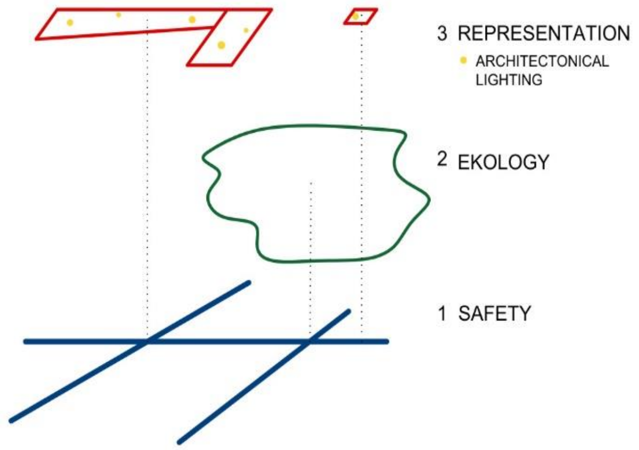

Fig. 4. Schematic representation of data layers of the Lighting Masterplan (R. Koucký)

A. *Safety*

The safety of the transport of people and property as well as the feeling of safety is the primary purpose of public lighting. The basis for the description of this point of view is the line data layer GIS containing roads in the territory of the capital Prague. In this layer, roads are divided into the following five groups, which correspond to their functional use:

I. transit backbone road;

II. urban backbone road;

III. main traffic road;

IV. minor traffic road;

V. non-motorized road;

The length of roads in the line data layer is a total of 7 438 km. The largest share, a total of 5,995 km (80%) is made up of road in groups IV and V. The length of backbone roads (I and II) is 573 km (8%) and the length of main traffic roads is 870 km (12%).

The following three new attributes have been assigned to the specified road groups, namely normal lighting class, adaptive lighting class and operation mode. The assignment of normal and adaptive lighting classes was carried out according to the relevant standard [1], [2]. The assignment of the values of individual attributes to groups of roads is shown in Table I.

TABLE I. ASSIGNMENT OF LIGHTING ATTRIBUTES TO ROAD GROUPS

Groups of roads	normal lighting class	adaptive lighting class	operation mode
I - transit backbone road	M4	M5	A
II - urban backbone road	M3	M4	B
III - main traffic road	M4	M5	B
IV - minor traffic road	P3	P4	C
V - non-motorized road	P4	P5	D

The line layer of roads contains important information about whether a specific section of road is located underground (tunnel, underpass) or on the ground. If the road is underground, the lighting requirements are determined according to a different procedure.

Normal and adaptive lighting classes for roads on the ground were assigned on the basis of standard characteristics (traffic, construction, surroundings) of individual groups of roads according to document CEN/TR 12464-1. However, in practice, the real properties may differ from the standardized ones. For this reason, corrections have been introduced that allow adjusting the lighting requirements if the real characteristics differ from the standardized ones. For this purpose, an auxiliary polygon layer of the "conflict area" was created, which contains intersections and sections of roads with frequent traffic accidents, as well as roads with mixed car and tram traffic. If the given road passes through this area, the requirements for its lighting will increase.

B. *Ecology*

The effect of outdoor lighting on the surrounding environment was labeled with the term ecology. The basic for the description of this point of view is the GIS polygon layer covering the entire administrative territory of Prague, which is based on the Metropolitan Plan, specifically on the layer named "*structure*". Based on this layer, 5 environmental zones were created:

- E0 - natural greenery protected;
- E1 - basic natural greenery;
- E2 - peripheral parts of the city;
- E3 - residential zones, local centers;
- E4 - historical center;

The specified GIS layer has been assigned lighting parameters in accordance with CIE document [3]. These parameters were then assigned limit values for individual environmental zones (Table II). In the area of parameters and their limit values, coordination is currently underway with the newly prepared national standard for reducing the undesirable side effects of outdoor lighting.

TABLE II. ASSIGNMENT OF LIGHTING ATTRIBUTES TO ENVIRONMENTAL ZONE

Zone	**L_b (cd.m^{-2})**	**E_v (lx)**		**R_{UL} (%)**
		Pre-curfew	Post-curfew	
E0	⩽ 0,1	n/a	n/a	⩽ 0
E1	⩽ 0,1	⩽ 2	⩽ 1	⩽ 0
E2	⩽ 5	⩽ 5	⩽ 1	⩽ 2,5
E3	⩽ 10	⩽ 10	⩽ 2	⩽ 5
E4	⩽ 025	⩽ 25	⩽ 5	⩽ 15

C. *Representation*

The influence of public and architectural lighting on the overall nighttime appearance of the city and individual public spaces was marked by the term representation. For this aspect, is worked with two lighting systems, with public lighting and architectural lighting.

1) *Public lighting*

The basic for the description of this point of view is the GIS polygon layer based on the Metropolitan Plan, specifically on the layer named "*hierarchy*". Within this layer, public spaces are divided into four categories:

- metropolitan;
- district;
- territorial;
- local.

The layer hierarchy is supplemented with attributes describing lighting and values are assigned to new attributes for individual categories (Table III).

TABLE III. ASSIGNMENT OF LIGHTING ATTRIBUTES TO CATEGORY OF HIERARCHY

Hierarchy	**Lighting class**	**R_a (-)**	**Evaluation of E_{sc}**	**Operation mode**
metropolitan	+ 2	⩾ 60	yes	extension until 24:00
district	+ 1	⩾ 60	no	extension until 24:00
territorial	+ 0	⩾ 20	no	⩽ 5
local	n/a	n/a	n/a	n/a

2) *Architectural lighting*

A newly created point layer is used for architectural lighting, containing important buildings from the point of view of the night view of the city. These buildings are again divided according to their importance into metropolitan, district, territorial and local categories. Based on these categories, selected buildings are assigned luminance levels and color rendering index (Table IV).

TABLE IV. ASSIGNMENT OF LUMINANCE IN ARCHITECTURAL LIGHTING

Hierarchy	**Luminance L_b (cd.m^{-2})**	**R_a (-)**
metropolitan	20	⩾ 70
district	15	⩾ 70
territorial	10	n/a
local	5	n/a

VI. CONCLUSION

The proposed Lighting masterplan of Prague represents a simple and clear data model that can be easily updated and integrated into the map documents of the Metropolitan Plan used by the capital city of Prague as part of spatial planning. The advantage of the proposed structure of the data model is that it allows the addition of new attributes, or new aspects defined by other GIS data structures. At the same time, the lighting masterplan respects not only requirements for the safety of traffic, people and property, but also requirements for limiting the adverse effects of public and architectural lighting on the surrounding environment and requirements related to the appearance of public spaces.

REFERENCES

[1] CEN/TR 13201-1, Road lighting - Part 1: Guidelines on selection of lighting classes, 2014

[2] EN 13201-2, Road lighting — Part 2: Performance requirements, 2015

[3] CIE (2017). CIE 150-2017 Guide on the Limitation of the Effects of Obtrusive Light from Outdoor Lighting Installations, 2nd Edition. Vienna: CIE

To What Extent are Non-visual Effects of Light Implemented in Current Lighting Design Practice? Findings from an International Survey

Myrta Gkaintatzi-Masouti
Building Lighting Group, Department of the Built Environment
Eindhoven University of Technology
Eindhoven, the Netherlands
https://orcid.org/0000-0003-4864-5556

Juliëtte van Duijnhoven
Building Lighting Group, Department of the Built Environment
Eindhoven University of Technology
Eindhoven, the Netherlands
https://orcid.org/0000-0003-1145-7033

Mariëlle Aarts
Building Lighting Group, Department of the Built Environment
Eindhoven University of Technology
Eindhoven, the Netherlands
https://orcid.org/0000-0003-1562-2489

***Abstract*—This paper presents findings of an online survey on the design practice of lighting professionals and their knowledge about non-visual effects of light. The results showed that there is basic awareness among lighting professionals about the effects of light beyond vision, although discrepancies were noticed. Two thirds of the respondents stated that they have been involved in projects where non-visual effects of light were considered. Vertical illuminance was the most common metric to quantify non-visual effects and uninterested clients was the most common barrier in design practice.**

Keywords—integrative lighting, lighting design, non-visual

I. Introduction

Integrative lighting aims to provide light that supports both visual responses and stimulation of the ipRGC-induced (or non-visual) effects [1]. The visual responses, including visual performance, comfort and perception, are relatively well-understood and implemented in national and international standards. On the contrary, the knowledge of the non-visual responses is fairly novel and has recently also gained the interest of the lighting society. Through the non-visual pathway, light can affect the circadian rhythms, alertness, concentration and performance [2]. Many questions still exist in understanding the mechanism with which light affects the variety of human responses and the interaction between the visual and non-visual pathway. However, experts now agree that brighter days and darker nights, seeking daylight whenever possible, is the best strategy, at least for day-active people [2]–[5].

This has resulted in new recommendations of providing the proper light at the proper time and new metrics to quantify light for non-visual effects. Brown *et al.* [4] recommend a minimum vertical melanopic Equivalent Daylight Illuminance (EDI) of 250lx during daytime and a maximum melanopic EDI of 10lx during the evening for healthy, daytime working adults (aged 18 to 55). The WELL building standard [6] and the Underwriters Laboratory (UL) design guideline 24480 [7] also give recommendations of healthy light levels. WELL describes targets of Equivalent Melanopic Lux (EML) [8] and melanopic EDI to be achieved during the day, which vary based on a point based system. The UL 24480 guideline suggests a Circadian Stimulus (CS) [9] of minimum 0.3 for at least two hours during daytime, maximum 0.2 during the evening and maximum 0.1 at night. Despite the differences, these recommendations aim to urge lighting designers to take non-visual light responses into consideration.

To facilitate the incorporation of these recommendations and metrics in design practice, novel lighting simulation tools have started to emerge. Lark Spectral Lighting [10] and ALFA [11] are two such tools that offer an increased spectral resolution and provide output metrics relevant for non-visual effects of light. Both tools are gaining interest from researchers [12], but their uptake in design practice is unknown.

A few previous studies have investigated lighting design knowledge and practice. Lo Verso *et al.* [13] investigated the daylight knowledge of Italian architectural students in 2019-2020, but decided to leave out knowledge about non-visual effects of light as they considered this topic not mature enough to be taught to students. On the contrary, a 2017 non-peer reviewed magazine survey among 101 American lighting designers stated that 67% of their respondents makes use of testing or simulation to investigate the impact of their design on circadian light metrics (12% answered "always", 24% answered "frequently" and 31% answered "rarely") [14], but it is possible that testing and simulation were broadly interpreted. Previous studies have investigated the use of lighting simulation tools and the barriers to incorporating lighting aspects in the design process [15]–[17], without specifically investigating tools relevant for non-visual effects.

This research aims to investigate whether the insights about non-visual effects of light and the available tools have led to a different lighting design approach in practice and identify possible barriers. This was done through an online survey, distributed to lighting design professionals. The methods, metrics and tools used for incorporating the non-visual effects of light were collected and contrasted with the respondents' typical daylighting and electric lighting design process.

II. Methods

A. Survey development

To gain these insights, an online survey was developed. An initial version of the survey was designed after semi-structured interviews with five building design professionals, recruited through convenience sampling. The topics that were discussed during the interviews were the participants' knowledge about the non-visual effects of light, their experience with lighting simulation tools and, in particular, tools for the simulation of the non-visual effects of light. Moreover, the perceived barriers for applying such tools in their work were discussed and finally, their ideas about the survey development (i.e. whether they thought that questions were missing or difficult to understand and further comments). This resulted in the first draft version of the survey, which was refined after pilot tests among seven other building design professionals (found again through convenience sampling). The aim of the pilot tests was to ensure that the questions were clear for the target group. The pilot tests resulted in rephrasing/ reordering questions and adding/ removing answer options.

The final survey consisted of five categories of questions: 1) general information (demographic and professional), 2) daylighting and electric lighting practice, 3) use of lighting simulation software, 4) respondent's knowledge and experience with non-visual effects of light, 5) use of lighting simulation software particularly for the prediction of non-visual effects of light. The questions were multiple choice with predefined answer options and an additional "other" option with free text input (which was mandatory if the participant selected "other"). In addition, the respondents could provide further comments at the end of the survey. Since non-visual effects of light are referred to with various terms (e.g. non-image-forming effects, ipRGC-induced effects, circadian effects), the following explanation was included to avoid confusion: "…non-visual effects of light (often called circadian lighting, human-centric lighting, integrative lighting or non-image-forming effects of light)".

The survey length depended on the respondents' answers (21 to 52 questions) and the median completion time was 15 minutes. The outline of the survey is presented in Fig. 1.

The survey was distributed in English and was proof-read by a native English speaker. Ethical approval for the study was obtained from the Ethical Review Board of the Eindhoven University of Technology (reference number ERB2021BE32).

B. Survey distribution

The survey was implemented and distributed using the LimeSurvey online survey tool. The survey link was active from July until November 2021. The distribution was done, first, through LinkedIn groups of lighting design professionals, in July and August 2021. Second, email invitations were sent to 898 registered members of the designer directory of the International Association of Lighting Designers (IALD). Of these emails, 872 were successfully delivered and 26 were undeliverable because of invalid email addresses. The emails were send three times (in August, September and October 2021) to all email addresses. Third, the survey was distributed through the website, newsletter and LinkedIn group of the Dutch Association for Lighting (NSVV) in August and September 2021.

C. Data cleaning

After the data was collected, incomplete responses were removed. Additionally, the data from respondents that answered "never" to both the questions "How often do you include daylighting design in your projects at your current job?" and "How often do you include electric lighting design in your projects at your current job?" were excluded from analysis, since they were considered outside of the target group of lighting design professionals. Four duplicate responses were removed by checking the respondents' emails, however 27 respondents did not provide their emails and therefore could not be checked. Finally, comments provided by the participants at the end of the survey were analysed. This was done by deconstructing the free-text comments into themes (or keywords), counting the number of respondents that mentioned a specific theme and identifying the most common ones.

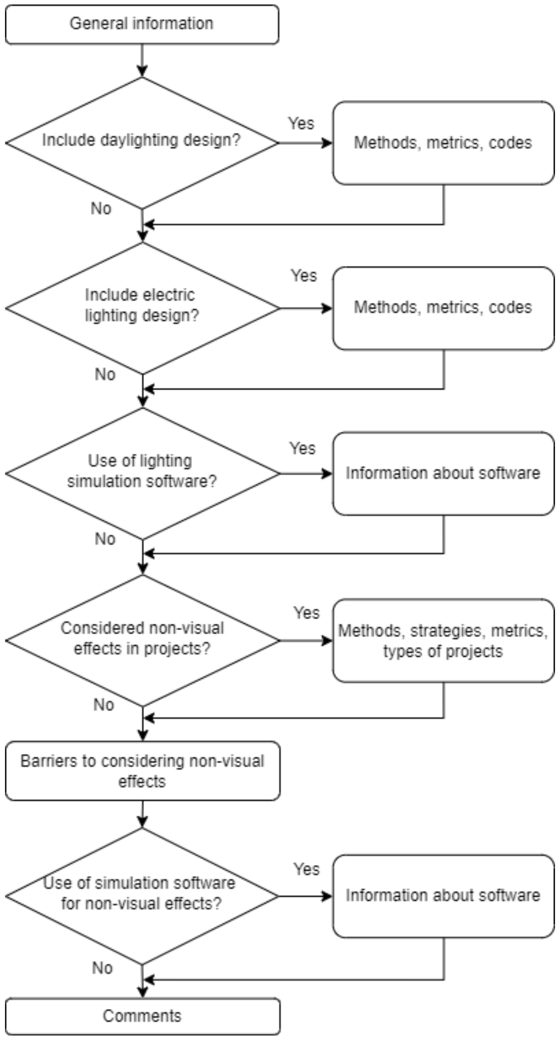

Fig. 1. Outline of online survey.

III. Results

A. General information

A total of 186 responses were included in the analysis. The respondents worked in 36 different countries (Fig. 2**Chyba! Nenašiel sa žiaden zdroj odkazov.**), mostly in the USA (29.5%), the Netherlands (14.5%) and the UK (10%). The participants were 50% male, 49% female and 1% preferred not to indicate their gender. Their mean age was 47 years (SD = 13.5) and three individuals preferred not to indicate their age. Out of the 186 respondents, 78% were *"lighting designers"* and the rest were *"researchers, teachers or academic staff"* (6.5%), professionals in *"sales/ marketing"* (4.5%), *"electrical engineers"* (3%), *"building engineers"* (1.5%), *"architects"* (0.5%), and *"other"* professions (6%). Their most common typical projects were *"residential"* projects (52%) and *"offices"* (50%), followed by *“landscape”* (36%) and *“education”* (34%) (

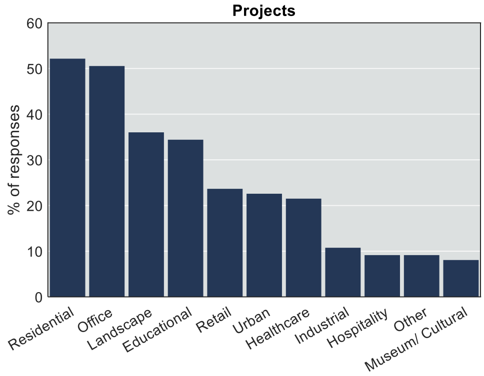

Fig. 3).

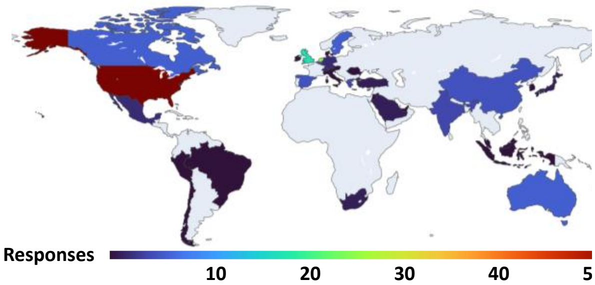

Fig. 2: Responses to the question “In which country do you currently work?”

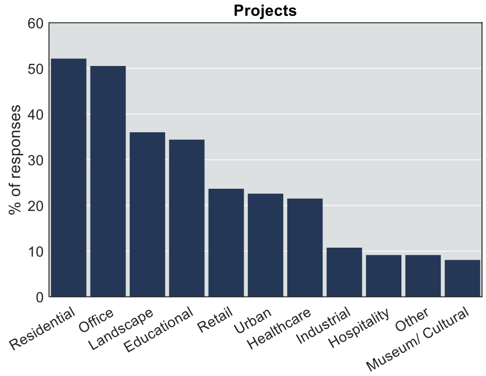

Fig. 3: Responses to the question “What are the typical projects that you work on at your current job?”. Up to 3 options could be selected.

B. *General lighting design*

The frequency of including electric lighting design in projects was *“always”, “usually”* or *“frequently”* for 89% of the respondents, while the same responses for daylighting design were given by only 35% of the respondents (Fig. 4**Chyba! Nenašiel sa žiaden zdroj odkazov.**). Here we clustered these three answer options because they represent the above the middle options of the 7-point scale. This is indicative of the type of work that the majority of the respondents do (mostly lighting designers and not architects or building engineers). When the participants did not indicate *“never”* to the frequency of including daylighting or electric lighting design in their projects, they were asked which methods, metrics and standards they use.

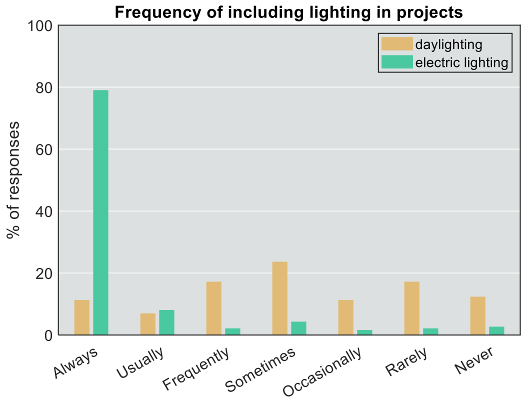

Fig. 4: Responses to the question “How often do you include daylighting/electric lighting design in your projects at your current job?”

Regarding the methods, each participant was given a list of ten predefined options (Fig. 5 and Fig. 6) and the possibility to indicate another method. The three most frequent answers were *“experience”*, *“computer simulations”* and *“design guidelines”* and the three least frequent answers were use of *“formulas/spreadsheets”*, *“scale model measurements”* and *“asking a consultant”* (in addition to *“other”*) for both daylighting and electric lighting design.

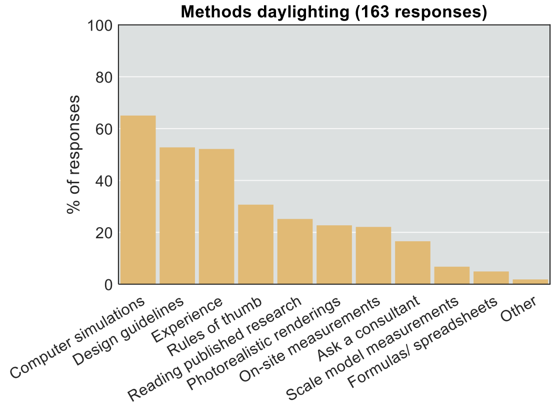

Fig. 5: Responses to the question “Which methods do you use for daylighting design in your projects at your current job?”. Respondents could choose as many as apply.

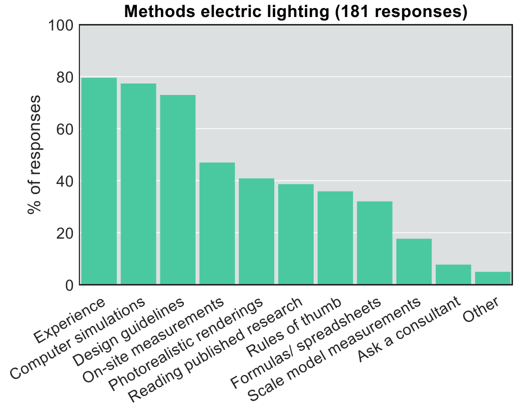

Fig. 6: Responses to the question “Which methods do you use for electric lighting design in your projects at your current job?”. Respondents could choose as many as apply.

For the questions regarding metrics, the participants were given a list of 14 predefined options for daylighting and 11 predefined options for electric lighting and the choice to indicate another metric (

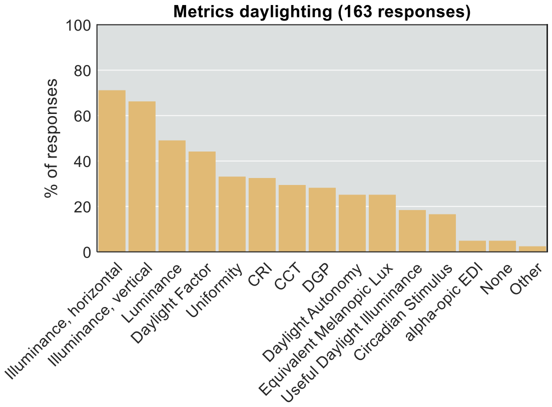

Fig. 7 and Fig. 8). The most used metrics were horizontal and vertical illuminance followed by luminance for daylighting and colour rendering index (CRI) for electric lighting. The metrics that quantify non-visual effects (EML, CS and α-opic EDI) and the metrics for climate based daylight modelling (Daylight Autonomy and Useful Daylight Illuminance) were used the least (in addition to *"other"* and *"none"*).

The participants were also asked which codes, regulations or standards they use to guide their design decisions as an optional free text question. In addition to various country-specific national standards, the LEED and WELL building certification standards were mostly mentioned, by 55% and 43% of the participants that filled in the question for daylight (77 individuals) and 44% and 39% of the participants that filled in the question for electric lighting (110 individuals).

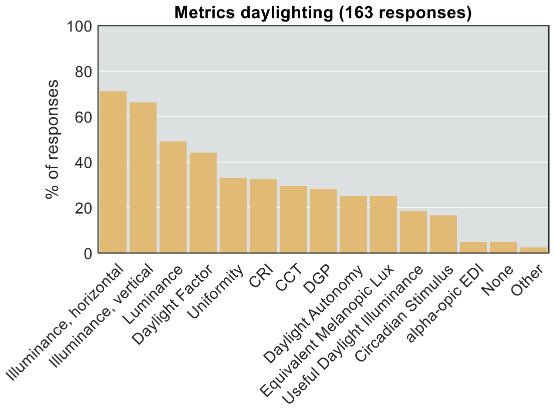

Fig. 11: Responses to the question “Which metrics do you use for daylighting design in your projects at your current job?”. Respondents could choose as many as apply.

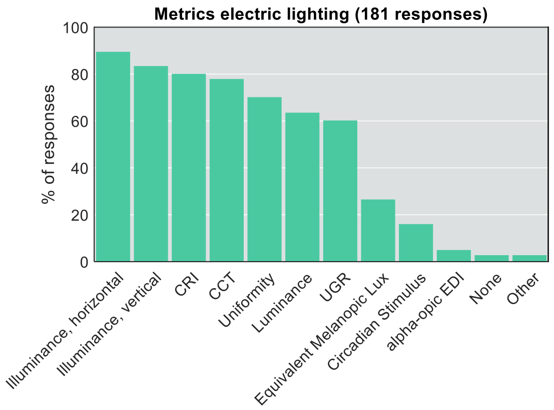

Fig. 12: Responses to the question “Which metrics do you use for electric lighting design in your projects at your current job?”. Respondents could choose as many as apply.

C. *Lighting for non-visual effects*

Approximately two thirds of the participants (126 participants or 68%) indicated that they have been involved in a lighting design project that considered non-visual effects of light. This was 78% of the American participants, 65% of the European participants and 65% of the participants from the rest of the world. Those projects were mostly *“offices”* (74%), followed by *“healthcare”* (54%), *“residential”* (46%) and *“educational”* (40%), as can be seen in

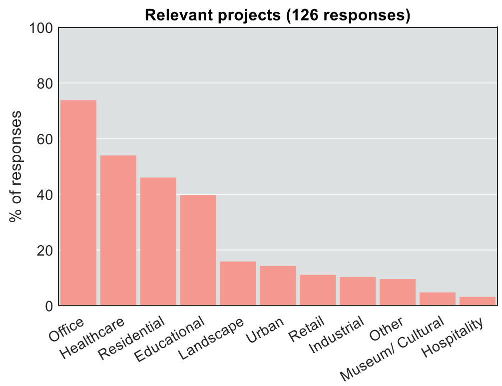

Fig. 9. However, here it should be reminded that residential projects and offices were the most common types of projects that the respondents worked on (selected by 52% and 50% of the participants respectively), whereas healthcare was selected by only 22% of the participants. Relative to the number of typical projects, *“healthcare”* was the most common choice, followed by *“offices”* and *“education”* (Fig. 10**Chyba! Nenašiel sa žiaden zdroj odkazov.**).

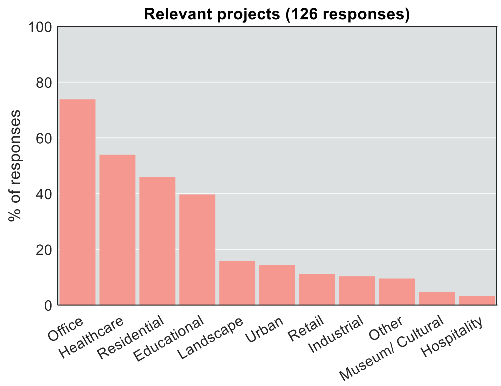

Fig. 7: Responses to the question "In which type(s) of projects did you consider the non-visual effects of light at your current job?". Respondents could choose as many as apply.

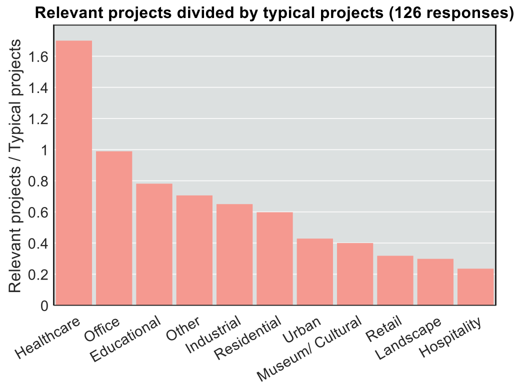

Fig. 8: Relevant projects for non-visual effects relative to typical project types. This is calculated by dividing the number of relevant for non-visual effects projects with the number of typical projects per project type.

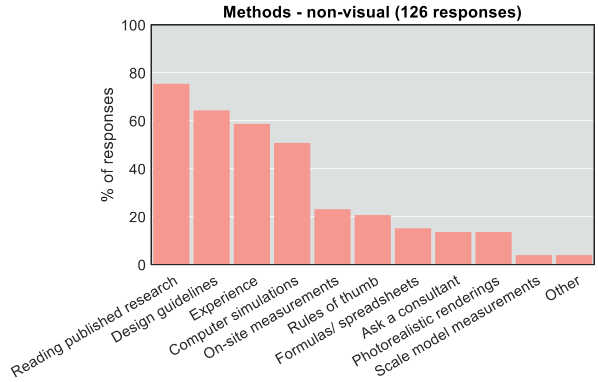

Fig. 9: Responses to the question “Which methods did you use in the project(s) that considered the non-visual effects of light at your current job?”. Respondents could choose as many as apply.

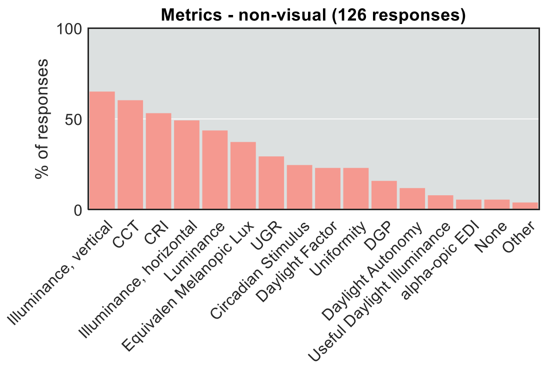

Fig. 10: Responses to the question “Which metrics did you use to quantify light considering the non-visual effects in your projects at your current job?”. Respondents could choose as many as apply.

"Reading published research" was the method that most respondents (75%) indicated to use during projects to guide their design decisions based on non-visual effects of light (Fig. 11**Chyba! Nenašiel sa žiaden zdroj odkazov.**). This was followed by the use of *"design guidelines"* (64%) and *"experience"* (59%).

Vertical illuminance, Correlated Colour Temperature (CCT) and CRI were the most common metrics to quantify light considering non-visual effects, used by 65%, 60% and 53% respectively (Fig. 12). EML and CS were used by 37% and 25% of the participants respectively. The use of these two metrics had a noteworthy geographical variation. EML was used by 43% of the American participants, by 40% of the European participants and 14% of the participants from the rest of the world (including only participants that indicated that they have been involved in a lighting design project that considered non-visual effects of light). CS was used by 45% of the American participants, by 9% of the European participants and 9% of the participants from the rest of the world. Notably, the CIE recommended metric, α-opic EDI, was the least frequent option (excluding "other" and "none"), used only by 5.5% of the participants (3% of American participants, 9% of European participants and 0% of participants from the rest of the world).

A variety of strategies were employed by the survey respondents to design projects accounting for the non-visual effects of light on people (
Fig. 13). *"Selecting light sources based on their colour or spectral power distribution (SPD)"*, *"considering direct and indirect lighting"*, *"control of intensity based on time of the day"*, *"tunable light sources (whose colour/ SPD can be controlled by occupants)"* and *"daylight integration"* were used by 83%, 77%, 74%, 71% and 67% of the respondents respectively.

Almost half of the participants (49%) indicated that a lack of interest from the side of their clients is a barrier for including considerations of the non-visual effects of light in practice (**Chyba! Nenašiel sa žiaden zdroj odkazov.**). The high cost of lighting products and the lack of specific requirements were identified as obstacles by 33% and 28% of the participants respectively. Additionally, a concern related to the absence of sufficient research and case studies was indicated by 22% and 21% of the respondents respectively.

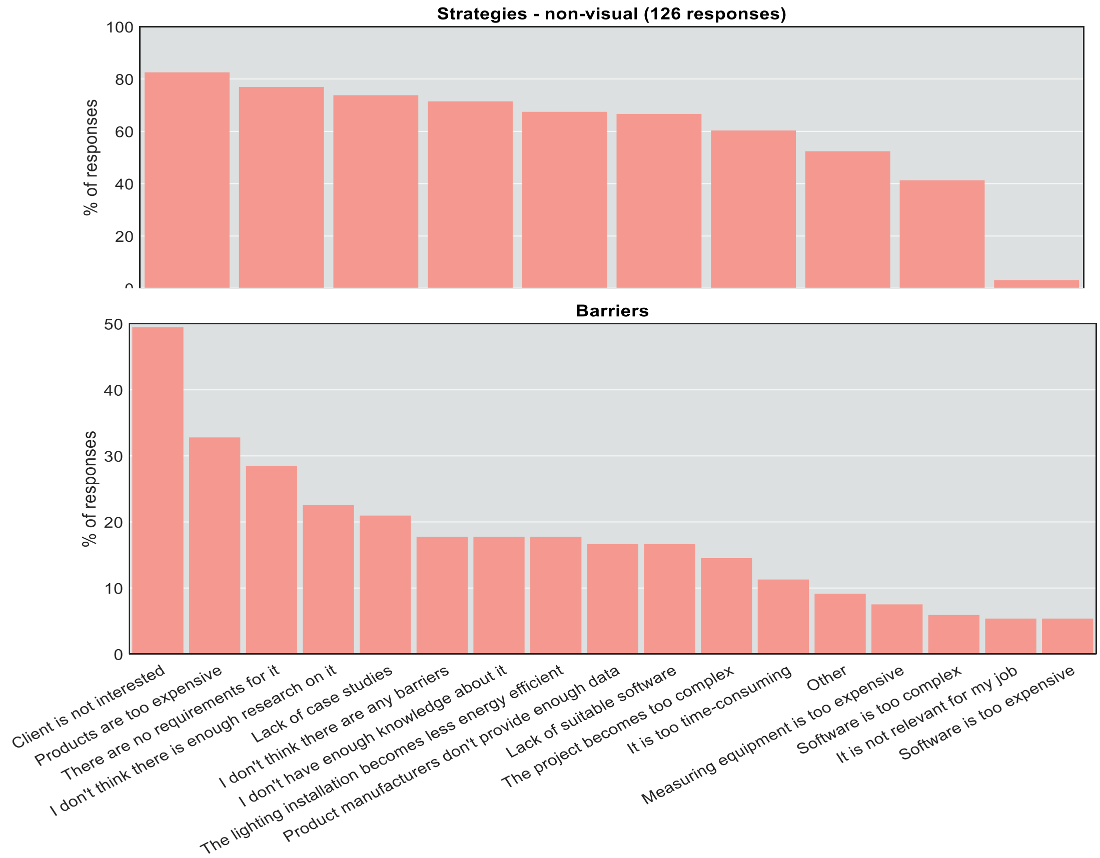

Fig. 13: Responses to the question "What are your main barriers to considering the non-visual effects of light in your projects at your current job?". Respondents could choose as many as apply.

D. Lighting simulation

Lighting simulation software was widely used by the respondents of the survey (92% indicated that they use it for their projects at their current job), but less than a quarter of them used software to estimate the non-visual effect of their lighting design on people (23% indicated that they use it to predict the non-visual effects of light in their projects at their current job). This is approximately a third of the 126 respondents that have been involved in design projects that considered the non-visual effects of light.

The most common lighting simulation tools were Dialux and AGi32 (72% and 29% respectively, Fig. 15), which were also the most popular choices for simulating light considering the non-visual pathway (52% and 28% respectively, Fig. 16). We should note that AGi32 was not a predefined answer option, but it was added because many participants filled it in as *"other"*. The two specialized tools for estimating non-visual effects of light including its spectral composition, namely ALFA and Lark Spectral Lighting, were used by only 14% and 4% of the participants that simulate light considering its non-visual effects.

Lighting simulation was generally used mostly for *"compliance with codes, regulations and standards"* or for *"visualization of a design to a client"* (81% and 76% respectively,

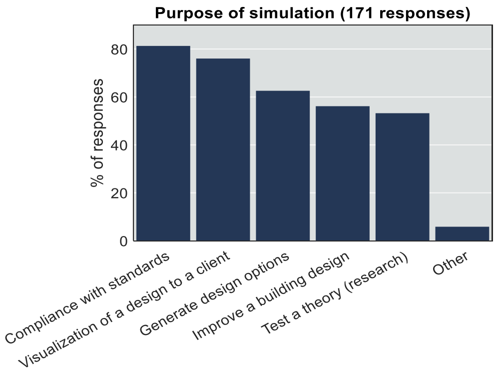

Fig. 17). In relation to non-visual effects of light, *"improve a building design"* was the most common reason for using simulation software (used by 51% of the respondents), closely followed by *"compliance with codes, regulations and standards"* and *"test a theory"* (both used by 48% of the respondents, Fig. 18).

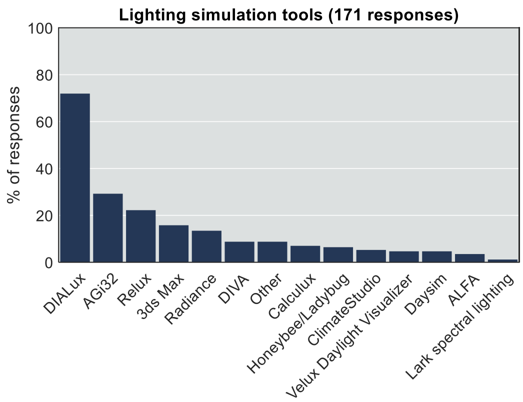

Fig. 17: Responses to the question "Which lighting simulation software have you used in your projects at your current job?". Respondents could choose as many as apply.

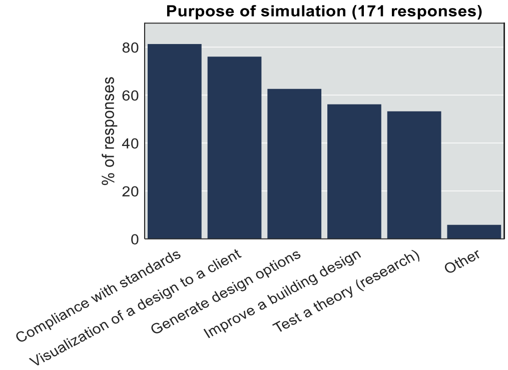

Fig. 15: Responses to the question "For what purpose do you use lighting simulation software in your projects at your current job?". Respondents could choose as many as apply.

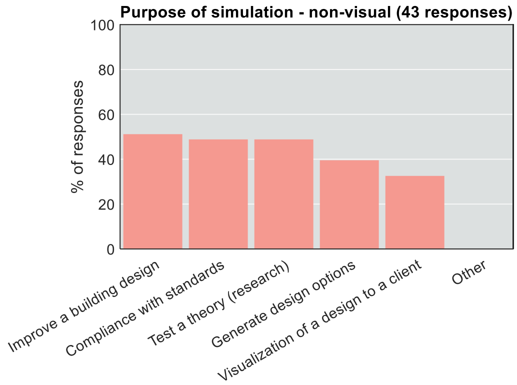

Fig. 16: Responses to the question "For what purpose do you use simulation software for the non-visual effects of light in your projects at your current job?". Respondents could choose as many as apply.

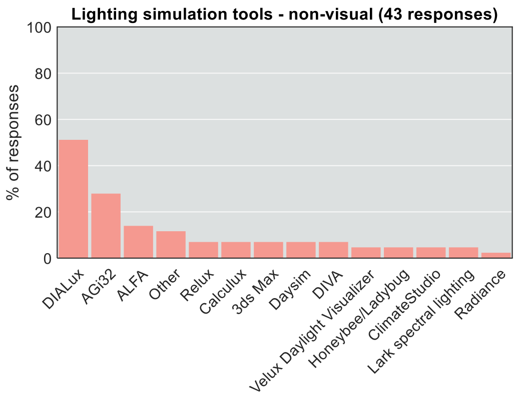

Fig. 18: Responses to the question "Which simulation software for the non-visual effects of light have you used in your projects at your current job?". Respondents could choose as many as apply.

E. Survey comments

The survey respondents were invited to provide their additional comments and suggestions using two free-text questions. The first was after indicating barriers to considering the non-visual effects of light in their projects

(“*What could be a potential solution to the previously mentioned barriers?*”) and the second was at the end of the survey (“*Do you have any additional comments for this survey?*”). Written comments to either of those questions were provided by 96 individuals.

The most common theme of the comments was a desire to create interest and awareness for clients, who often do not see the benefit of using time and resources for additional lighting considerations. Other respondents mentioned the need for further research and realized projects that can be used as case studies. Moreover, the respondents noted the lack of standards and regulations to guide design decisions.

Some unique comments that we found interesting are mentioned here:

- “*Aside from the obvious education needed, the scientific community has not yet settled on a singular metric, which confuses the design community and end user.*”
- “*Software is far too vague, or far too specific for non-visual effects. People move through space and don't act as software assumes.”*
- “*Suggest changing lifestyle rather than changing lighting inside buildings to increase healthy light exposure.”*
- “*In my opinion, ethical lighting design considers the non-visual effects of lighting regardless of programmatic requirements to do so. It would be helpful to have more straightforward ways of evaluating the CS/EML of a space so that it is something we can dovetail into our workflow instead of requiring special add-services for these efforts.*”

IV. Discussion

The responses of the 186 individuals give us an impression of the current lighting design practice and the extent to which non-visual effects of light are understood and implemented. Two thirds of them indicated that they have been involved in projects where non-visual effects of light were considered. This relatively high percentage shows that basic awareness and interest among lighting design professionals on the effects of light beyond vision exists. The relevant projects were mostly offices and healthcare facilities, which is not a surprise considering that healthy lighting might be a higher priority in these kind of spaces and therefore receive more attention by the design team and the clients.

Using design guidelines and personal experience were amongst the three most common options for daylighting, electric lighting design in general and specifically for non-visual effects. Since the WELL standard was widely mentioned, this might be one of the referred design guidelines. In addition, 75% of the respondents that have been involved in projects where non-visual effects of light were considered claimed to read published research to guide their design decisions. It is possible that “published research” was interpreted broadly to include professional articles or information from manufacturers, and not specifically research papers. Nevertheless, this demonstrates an interest of the respondents to keep up with the developments on this relatively new lighting topic.

Horizontal illuminance was the most commonly used metric for both daylighting and electric lighting in general. Specifically to quantify the non-visual potential of a lighting design, vertical illuminance was the first choice, followed by CCT. Both EML and CS were used by less than half of the respondents and α-opic EDI was hardly used. While EML and CS were used with almost equal frequency by American participants, CS was barely used by European participants. Yet, it is clear that these relatively novel metrics are not yet common in design practice. An unexpected result was that Unified Glare Rating (UGR) and Daylight Glare Probability (DGP) were selected by 29% and 16% of the participants respectively. UGR was actually selected more than CS and α-opic EDI, which might indicate that there is confusion to what metrics are appropriate and what is meant by “non-visual effects of light on human”. However, an additional investigation into the participants that selected glare metrics for the quantification of non-visual effects revealed that all of them selected at least one more metric option.

The most frequently used design strategy to achieve non-visual stimulation was selecting light sources based on their colour or SPD followed by considering a combination of direct and indirect lighting. Two thirds of the respondents also selected daylight integration as an effective strategy, even though the main professional focus of most of them was electric lighting design (as shown in Fig. 4). It is difficult to estimate how these strategies were implemented based on the results of the survey. To gain a deeper understanding of this, it would be beneficial to follow this survey with face-to-face interviews.

Clients’ lack of interest was the major barrier to considering non-visual effects in lighting projects. This implies that there is a need for knowledge dissemination and a greater awareness for end users and the entire design team about potential benefits of light. An additional barrier that was noted was the lack of standards to guide design decisions. One participant commented that standards are currently only focusing on “*energy efficiency in buildings instead people's well-being*”. The high cost of lighting products was also stated as a barrier. While this is true for tunable electric light sources and complicated control systems, in most projects an integrated daylight and electric lighting design is the key to bring the cost down and achieve healthy lighting targets.

The results show that lighting simulation is a common design tool, which is in agreement with findings from previous studies [15], [16]. Yet, less than a quarter of the participants claimed to use software to estimate the non-visual effects of their design, with DIALux and AGi32 being the most used simulation tools for this purpose. Specialized tools, such as ALFA and Lark, were hardly used. Both DIALux and AGi32 can calculate illuminance, but require additional post-processing based on the SPD of the light source to calculate EML, CS or melanopic EDI (assuming neutrally colored materials) [12]. The possibility of a direct calculation of these metrics in the mainstream lighting simulation tools might make it easier for professional designers to incorporate them into their workflow.

A. Limitations

The results presented in this paper are based on a small fraction of the international lighting community. Still, our sample size (186 respondents) is similar to the one used by other online international surveys of lighting practice [16], [17]. The respondents were mainly electric lighting designers, and daylight was not the primary focus for most (Fig. 4) which may have been a result of using the IALD database for the survey distribution. This means that the results are primarily reflective of electric lighting design practice. We considered grouping the respondents who answered “always” to the frequency of including electric lighting design in their projects (approximately 80% of them) and analyse their responses separately, but we observed only minor changes in the results and therefore decided that this does not add value.

Moreover, a limitation of online surveys is that we cannot be certain of how the questions are perceived by respondents. Misunderstandings might occur because of phrasing or language barriers. Nevertheless, we strived to reduce these misunderstandings during our interviews and pilot test.

V. Conclusion

This paper presents findings on the design practice of lighting professionals and their knowledge about the topic of non-visual effects of light. A total of 186 responses were collected from 36 countries, via an online survey. The results showed that basic awareness and interest among lighting design professionals on the effects of light beyond vision exist, since two thirds of the respondents stated that they have been involved in projects where non-visual effects of light were considered. These projects were mainly offices and healthcare facilities and the most common strategy for non-visual stimulation was to select light sources based on their colour or SPD.

Discrepancies were noticed in relation to the used methods. Vertical illuminance and CCT were used more than EML, CS and α-opic EDI to quantify light considering non-visual effects (65% and 60% versus 37%, 25% and 5.5% respectively of the respondents who worked with non-visual effects). Although simulation was widely used (by 92% of all respondents), it was not common to use software to estimate the non-visual effects of a lighting design (used by 23% of all respondents). Even when software was used for that purpose, this was mainly software that does not offer increased spectral resolution and direct calculation of relevant output metrics.

The principal barrier to considering non-visual effects in the lighting design process was the lack of interest from clients. This shows that, if integrative lighting is to be the future of lighting design, efforts need to be directed to public awareness. In addition, standards are needed to describe integrative lighting design targets, incorporating both visual and non-visual lighting criteria, since the lack of requirements was identified as a significant obstacle. Finally, the lighting professionals indicated as a barrier that there is insufficient research and case studies that convincingly show the benefits of a lighting design on occupants' well-being.

Acknowledgment

We would like to thank Anneloes de Lange for conducting interviews and drafting the first version of the survey during her master project.

M. Gkaintatzi-Masouti received funding from the European Training Network LIGHTCAP (project number 860613) under the Marie Skłodowska-Curie actions framework H2020-MSCA-ITN-2019.

References

[1] M. Aries, "Human-centred integrative lighting and spill-over effects," *Lighting Research and Technology*, vol. 53, no. 8, p. 699, 2021, doi: 10.1177/14771535211058058.

[2] K. W. Houser and T. Esposito, "Human-Centric Lighting: Foundational Considerations and a Five-Step Design Process," *Frontiers in Neurology*, vol. 12, p. 630553, 2021, doi: 10.3389/fneur.2021.630553.

[3] C. Vetter *et al.*, "A Review of Human Physiological Responses to Light: Implications for the Development of Integrative Lighting Solutions," *LEUKOS - Journal of Illuminating Engineering Society of North America*, 2021, doi: 10.1080/15502724.2021.1872383.

[4] T. M. Brown *et al.*, "Recommendations for daytime, evening, and nighttime indoor light exposure to best support physiology, sleep, and wakefulness in healthy adults," *PLoS biology*, vol. 20, no. 3, 2022, doi: 10.1371/journal.pbio.3001571.

[5] M. Knoop *et al.*, "Daylight: What makes the difference?," *Lighting Research and Technology*, vol. 52, no. 3, pp. 423–442, 2020, doi: 10.1177/1477153519869758.

[6] International WELL Building Institute, "WELL v2 Q4 2021," *WELL Building Standard*, 2021. https://v2.wellcertified.com/wellv2/en/overview (accessed Nov. 30, 2021).

[7] Underwriters Laboratory, *Design Guidelines for Promoting Circadian Entrainment with Light for Day-Active People. UL Design Guideline 24480*. 2019.

[8] R. J. Lucas *et al.*, "Measuring and using light in the melanopsin age," *Trends in Neurosciences*, vol. 37, no. 1, pp. 1–9, Jan. 2014, doi: 10.1016/j.tins.2013.10.004.

[9] M. S. Rea, M. G. Figueiro, J. D. Bullough, and A. Bierman, "A model of phototransduction by the human circadian system," *Brain Research Reviews*, vol. 50, no. 2, pp. 213–228, 2005, doi: 10.1016/j.brainresrev.2005.07.002.

[10] M. Inanici and ZGF Architects, "Lark Spectral Lighting," 2015. https://faculty.washington.edu/inanici/Lark/Lark_home_page.html (accessed Nov. 30, 2021).

[11] Solemma, "ALFA," 2018. https://www.solemma.com/alfa (accessed May 07, 2021).

[12] M. Gkaintatzi-Masouti, J. van Duijnhoven, and M. P. J. Aarts, "Review of spectral lighting simulation tools for non-image-forming effects of light," in *Journal of Physics: Conference Series*, Nov. 2021, vol. 2042, no. 1, p. 012122, doi: 10.1088/1742-6596/2042/1/012122.

[13] V. R. M. Lo Verso *et al.*, "A survey on daylighting education in italian universities. Knowledge of standards, metrics and simulation tools," *Journal of Daylighting*, vol. 8, no. 1, pp. 36–49, 2021, doi: 10.15627/jd.2021.3.

[14] E. Clark and N. Lesniak, "Circadian Lighting Solutions Are Real—Why Aren't They Being Used?," *Metropolis*, 2017.

[15] A. Davoodi, P. Johansson, T. Laike, and M. Aries, "Current Use of Lighting Simulation Tools in Sweden," in *Proceedings of The 60th SIMS Conference on Simulation and Modelling SIMS 2019, August 12-16, Västerås, Sweden*, 2020, vol. 170, pp. 206–211, doi: 10.3384/ecp20170206.

[16] A. D. Galasiu and C. F. Reinhart, "Current daylighting design practice: A survey," *Building Research and Information*, vol. 36, no. 2, pp. 159–174, Mar. 2008, doi: 10.1080/09613210701549748.

[17] C. Reinhart and A. Fitz, "Findings from a survey on the current use of daylight simulations in building design," *Energy and Buildings*, vol. 38, no. 7, pp. 824–835, 2006, doi: 10.1016/j.enbuild.2006.03.012.

Effects of a Personalizable Workplace Lighting Concept on Acceptance, Usability, and Cognitive Performance

Johannes Weninger
Research & Development
Bartenbach GmbH
Aldrans, Austria
johannes.weninger@bartenbach.com

Markus Canazei
Department of Psychology
University of Innsbruck
Innsbruck, Austria
markus.canazei@uibk.ac.at

Wilfried Pohl
Research & Development
Bartenbach GmbH
Aldrans, Austria
wilfried.pohl@bartenbach.com

***Abstract*—As part of two research projects, a workplace lighting prototype was developed to illuminate local vertical and horizontal workplace areas separately with illuminance levels of up to 6,000 lux horizontally and color temperatures between 2,200 and 5,300 Kelvin. In addition, the homogeneity of illumination of the two areas can be varied from selective to uniform. The resulting variety of light settings enables users to personalize their workplace lighting with regards to their individual visual and non-visual lighting needs. Moreover, lighting can be adapted automatically and in real-time to changing work tasks by using sensor technology and neural networks.**

The prototype was evaluated in terms of user acceptance and short-term visual and non-visual effects in a field study with subsequent focus groups and two laboratory studies. The results give first evidence that this workplace lighting concept is well accepted and perceived as useful. In addition, results from the laboratory studies indicate both, inter-individually strongly varying lighting needs at the workplace and acute beneficial non-visual effects of short bright light exposures.

Keywords—Personalized lighting, workplace lighting, non-visual light effects, user satisfaction, performance

I. INTRODUCTION

The 21st century in lighting started with two groundbreaking events: the advancement of the LED from a dim signal lamp to a highly efficient point light source and the discovery of the so called “third receptor” in the human eye.

20 years later, the LED is the unrivaled light source in general lighting. Its efficiency and lifetime exceed every other light source and it allows to design fundamentally new lighting concepts. For example, due to its compact form factor, miniaturized, architecture-integrated lighting can now be implemented that exceeds the achievable illuminance of conventional lighting without additional energy consumption. In addition, the controllability of LED technology makes it possible for the first time to change the emitted light spectrum at the push of a button. As a result, lighting becomes digitized, which, in connection with sensor technologies, forms the basis of integrative lighting [1].

Today, people in Western Europe spend about 90% of the day indoors, of which a third is at work [2]. This typically restricts natural light exposure to 60-90 minutes per day and is particularly problematic during the winter months when outdoor daylight exposure is often absent. The integrative lighting paradigm addresses this problem by implementing biologically effective, dynamic lighting scenarios using automated lighting systems. By stabilizing our circadian rhythm through timed light exposure, these should promote long-term positive health effects.

However, current implementations of such concepts often focus on lighting at room level, which generally does not allow zonal variation of lighting. This makes it impossible to adapt to different individual visual and non-visual lighting needs. In addition, studies have also shown that the comfort of users is substantially restricted by the lack of control over their environment [3] and that the possibility to adjust lighting individually significantly improves user satisfaction in the long term [4-7]. Therefore, room-based lighting systems that do not adequately cover individual needs increasingly lead to dissatisfaction among employees, especially in open-plan offices.

Accordingly, the challenge lies in designing integrative lighting concepts that achieve high levels of vertical illuminance at the eye in a cost- and energy-efficient manner without compromising visual comfort. At the same time, the user and his individual needs should be considered without impairing room ambiance. As part of the research projects Repro-light [8-10] and LessIsMore [11], an innovative workplace lighting prototype was developed based on a large European end-user survey which aimed at deriving requirements for future personalizable workplace lighting systems. The prototype was then evaluated in terms of user satisfaction by means of a 12-week, longitudinal field study and subsequent focus groups.

In addition, two studies were conducted in a controlled laboratory setting. The first study focused on effects of individually adjusted workplace lighting on visual performance and acceptance parameters for older adults (60-70 years), which prove to be very sensitive in terms of visual workplace lighting needs. The goal of the second laboratory study was to quantify short-term effects of several short bright light interventions with a duration of 30 minutes with very high illuminance levels on vigilance, subjective sleepiness, higher cognitive functions, cardiovascular parameters, and visual performance.

Although recently published systematic reviews [12-16] show that bright light during the day acutely increases subjectively perceived wakefulness, objective measures of wakefulness often do not confirm this result. Likewise, the evidence for acute effects of light exposure on higher cognitive functions (e.g., working memory, task switching, decision taking) and mood parameters during the day is currently scarcely documented. In this sense, the present work tries to contribute to close the existing knowledge gap by means of using a novel, user-centered workplace lighting concept, which has been tailored to future requirements through a user-related development process.

II. Understanding User Needs

In 2019, a Europe-wide online survey was conducted with more than 1,100 end users to assess the prevailing user requirements and expectations for future workplace lighting. In addition, a comprehensive literature research and several focus groups with representatives from the professional world along the entire value chain were carried out [17].

The results (Fig. 1) clearly demonstrate the need for improved workplace lighting and the widespread desire for a better user experience. Regarding individual lighting preferences in particular, the study participants stated that they would like to have more influence on their workplace lighting. In addition, the lighting should also be different for different work tasks and the adjustment should be supported automatically, individually, and specifically for varying work contents. Moreover, subjects requested a daytime-related adjustment of color temperatures, which is already a core part of integrative lighting, and asked for forward-looking requirements such as automated lighting based on varying working tasks and individual preferences. Accordingly, users currently perceive their needs as insufficiently fulfilled by lighting solutions and ask for improved interaction possibilities and interfaces, which they are already used to through implementations in other technological areas. It is noteworthy, that these requirements, which originate in information and communication technologies (ICT), were much more pronounced among younger study participants.

III. A new workplace lighting concept

The basic idea of the so-called Personal Table Light (PTL) is to transfer workplace lighting from ceiling lighting to personalizable lighting at the workplace. This not only enables more individuality, but the high illuminance levels required to achieve non-visual effects can also be generated with less power consumption due to its proximity to the user.

In terms of lighting technology, visual comfort and performance are supported by the PTL, as both vertical and horizontal workplace surfaces can be illuminated separately by means of a light engine housing 144 LEDs. The illuminance levels, color temperatures (from 2,200 K to 5,700 K) and light distributions (Fig. 2) can be fully adjusted by the user via a desktop application. In addition, the PTL effectively delivers up to 1,500 lx vertically at eye level and 6,000 lx horizontally at desk level.

User integration is supported by using embedded control technologies and sensor technologies such as a coded-light depth camera to record the user’s gaze behavior (Fig. 3) in order to determine the current work task by using machine learning algorithms [18] or environmental sensors to monitor ambient temperature, daylight availability, and environmental stressors such as carbon dioxide or noise. These features allow the PTL to adjust workplace light settings discreetly and automatically with regards to individual preferences and varying work tasks.

Fig. 1: Results of the end user survey [17] conducted online in 2019 as part of the Repro-light project.

Fig. 2: Independent rear wall and table lighting of the PTL with different color temperatures and light distributions.

IV. Usability and Accessibility Evaluation

In order to evaluate the technology acceptance and usability of the PTL, a user study under natural working conditions was carried out in two European countries (Spain and Austria) over a period of 3 months. Afterwards, focus groups were run with the study participants to measure the impact of the PTL on job performance and wellbeing of users and their acceptance of the technology [19].

A. User study under natural working conditions

The field study was conducted in two open-plan offices of IREC Fundación Instituto de Investigación de la Energía de Cataluña (Barcelona, Spain) and Bartenbach GmbH (Aldrans, Austria) between June and August 2020. The eight study participants (3 Spain, 5 Austria) could freely adjust and change light settings at any time without any restrictions. Scenes were not preconfigured and had to be set by the participants. Before the start of the study, all participants were comprehensively instructed in the functions and operation of the PTL. The instruction also included a description of the sensor technology used (especially the camera system) and the associated data storage and processing procedures. All participants gave their written informed consent before the study started.

Switching times and manually set light settings of the PTL as well as presence at the workplace and categorized work activities (based on gaze data) were recorded over the entire period. In addition, to get an objective indicator of workload, user interactions with the computer mouse and keyboard were continuously recorded. Further, subjective ratings (e.g., current stress level, acceptance level for workplace lighting) were assessed via online-survey every 3 weeks. Ambient parameters recorded by sensors were included as potential confounding parameters. Finally, at the end of the study period, subjects completed an online questionnaire containing 34 questions in 5 categories: sociodemographic data (9 questions); subjective impact assessment (6 questions), system usability (6 questions), and system acceptance (10 questions) based on the Technology Acceptance Model for Luminaires (TAMLIGHT [20]) as outcome measures (Fig. 4); an overall assessment of the PTL with the option of an open comment field. All questions were answered on a 7-point Likert scale ranging from 1 (strongly negative response) to 7 (strongly positive response). All data were summarized after the field study ended and made available as input for the focus groups.

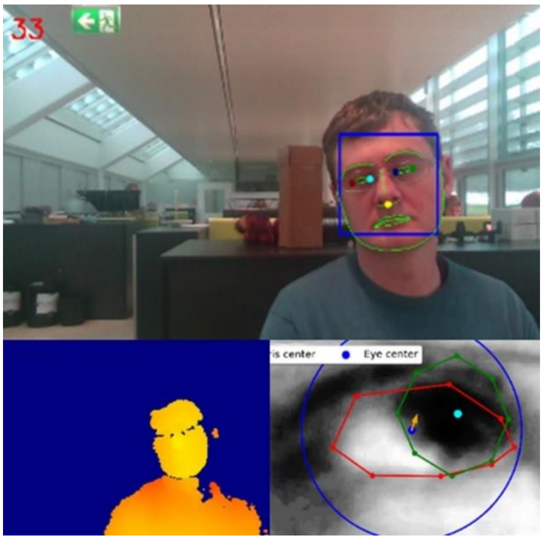

Fig. 4: The PTL's computer vision capabilities include the detection of user presence (top) and gaze direction (bottom right); in addition, presence of a person was obtained using the depth information from the integrated coded-light depth camera (bottom left).

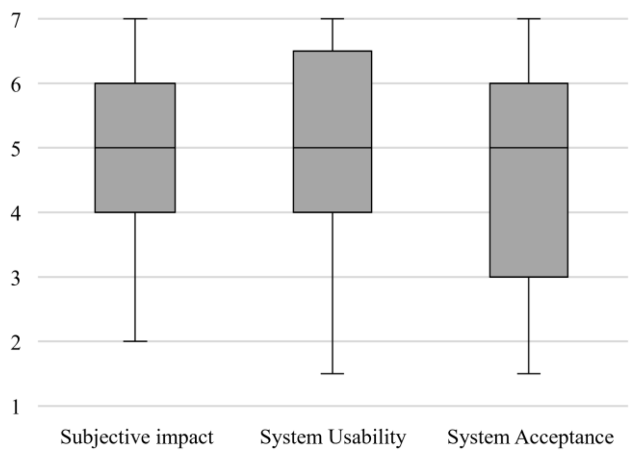

Fig. 3: Responses, summarized in boxplots, in the three primary categories of TAMLIGHT; all questions were answered using a 7-point Likert scale (1 - strongly negative response, 7 - strongly positive response).

B. Focus Groups

To evaluate the acceptance and satisfaction with the new workplace lighting concept, focus groups were conducted with the study participants in Austria and Spain. The information gained from the field study was used as the primary input and discussed in detail with study participants within a structured protocol. The output of the focus groups should both support the interpretation of the data collected within the user study and help to gain detailed insights into the acceptance, usability, and the subjective impact on work performance and well-being. Additionally, the output should help to exploit possible technical improvements.

The focus groups took place in several phases, each supported by templates prepared to guide the process. After an in-depth icebreaker activity [21], the participants first individually gave feedback on the usability of the light control system, the quality of workplace lighting, and the overall impression of the PTL. The results were then discussed at group level. The subsequent impact map activity [22,23] examined whether the lighting system had a perceived impact on performance and well-being compared to the previous lighting system. At the end, participants were asked to name features of the system they wanted to be kept, removed, or added. The participants brainstormed about these aspects individually before the ideas were discussed in the group.

C. Results

The results of the online questionnaire (Fig. 4) show a clear positive response on the perceived impact, system usability, and acceptance. A more granular look at the level of individual questions reveals that study participants were keenly aware of the impact of light on work performance (5.2 ± 1.2), visual quality (5.0 ± 1.8) and overall well-being (5.3 ± 1.3). In contrast, neither positive nor negative responses could be determined with regard to the subjectively perceived influence on sleep quality or mood.

In the analysis of the essential aspects of technology usability, the study participants rated the system positively in all respects. The lighting was perceived as easy to use (5.3 ± 1.5) as well as clear and understandable (5.1 ± 1.4). Participants were able to adjust the light in the workplace to their personal preferences (5.3 ± 1.4) and easily change the light settings for different zones or areas (5.6 ± 1.0) thanks to the intuitive design of the control application, which was also positively highlighted in terms of user acceptance.

The ICT-based integration of the control option by means of the personal computer was not only rated as very easy to handle (5.3 ± 1.9) due to its accessibility and familiarity but was also preferred to both classic control elements (5.1 ± 1.4) and smartphone controls (5.1 ± 1.6). Despite some privacy concerns related to the use of imaging sensors (3.6 ± 1.6), overall trust in the lighting system was high (5.3 ± 1.1). On the other hand, light reflections on horizontal work surfaces, especially on glossy magazines, were rated as disruptive (2.9 ± 1.8).

The focus groups were able to confirm these results. In general, the task-related light adjustment, the presence detection and the easy-to-use technology were particularly emphasized by the users in the group discussions. In summary, it can be said that both the lighting concept and the technology used were well accepted. Five of the eight participants would even want to keep the PTL or recommend it to a friend.

V. EVALUATIONS IN TWO LABORATORY STUDIES

To evaluate the effectiveness of the new workplace lighting concept two controlled laboratory studies were run. Therefore, two identical test rooms, each measuring 3.6 x 4.0 m, were equipped with two PC workstations each. Both rooms had a 1.5 m² window oriented to the north. By means of a shading system, the influence of daylight could be excluded. In addition to the PTL, which was used as workplace lighting, both test rooms used ceiling-mounted lighting systems to provide ambient room lighting with reduced light levels.

A. Effects of preferred lighting conditions on older adults

It is well known that older people require higher illuminances for visual tasks [24-26]. Older people also often suffer from more and stronger asthenopic complaints. As a result, personalization of workplace lighting for older adults might be a necessary feature of future lighting solutions. As part of the first laboratory study, older people (60+ years) could adjust workplace lighting for computer and paperwork. Self-selected lighting was then compared with standard workplace lighting (according to DIN EN 12464-1) in terms of its influence on contrast sensitivity, visual acuity, asthenopic complaints and overall satisfaction with the lighting situation.

Contrast sensitivity was measured on a computer screen with the Freiburg Visual Acuity Test (FrACT) [27] and with a paper-based Letter Comparison Task with Landolt rings. Asthenopic complaints and satisfaction with workplace lighting were rated using a self-developed questionnaire. Each individually set workplace lighting was photometrically documented by measuring illuminance levels and light spectra on the table and rear wall as well as at eye level. A total of 22 people took part in the study (13 female, 9 male). The mean age was 68.5 years (± 6.78 years).

The study protocol contained three phases of 30 to 45 minutes each. In each phase, the entire test battery had to be completed. In the first phase, the participants could familiarize with the setting options of the PTL. In phase 2, lighting condition were set to standard workplace lighting (E_v = 90 lux at eye level; E_h = 500 lux; 4000 Kelvin). In phase 3 the participants had to adjust their preferred light settings for the second time. In each phase, the test battery (visual tests and questionnaires) was presented after a 10-minute lighting adaptation period. Since the first phase was only used for habituation of the subjects, the data were not included in the analysis.

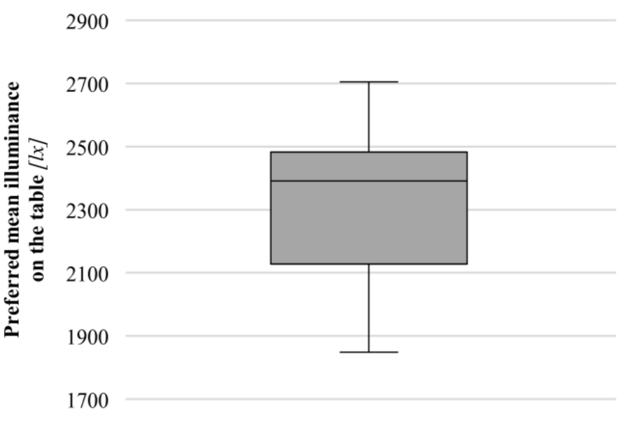

Fig. 5: Boxplots of the individually set horizontal mean illuminance levels on the table.

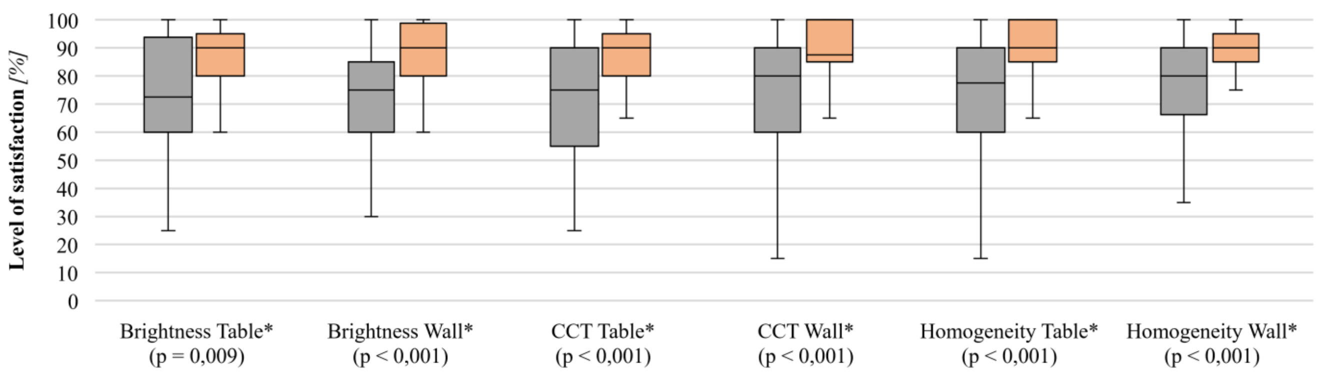

Fig. 6: Boxplots of the reported levels of satisfaction with regard to brightness, color temperature and light distribution on the table and rear wall for both standard (gray) and preferred (orange) lighting conditions; satisfaction could be expressed as a percentage ranging from 0 (completely dissatisfied) to 100 (completely satisfied).

The results show a large variability in the preferred workplace light settings. Moreover, and most importantly, older adults preferred an average of 2,260 lx (± 486 lx) at desk level which is 4.5 times higher than recommend in current lighting standards (Fig. 5). It is further noteworthy that, despite these high workplace illuminance levels, subjects did not report more asthenopic complaints compared to standard lighting but reported a significantly higher satisfaction level with the homogeneity, illuminance, and color temperature of the light setting (Fig. 6). In addition, subjects showed improved visual performance under individually set lighting, as they processed significantly more items in the paper contrast test without increasing the number of errors. Importantly, the FrACT showed no significant differences between the two lighting conditions, indicating no detrimental effects of significantly increased workplace light levels with the PTL. To sum up, this lab study confirms the benefit of individually adjustable workplace lighting for older people.

B. Effects of short bright light interventions on younger adults

Despite clear evidence for bright light effects on various psychophysiological parameters during the night [28,29], findings on non-visual light effects during the day are still inconclusive. In particular, evidence for acute effects of light on work-related cognitive parameters is currently unclear. The aim of the second laboratory study was to investigate effects of the PTL on vigilance and subjective sleepiness parameters, heart rate variability (HRV) and visual performance. Instead of a bright light exposure for several hours, multiple short "light showers" with high vertical and horizontal illuminances (1.360 lux and 5.500 lx at 4000 K respectively) were investigated with a randomized controlled study protocol.

A total of 56 people took part in the study (28 female, 28 male). The mean age was 28.4 years (± 7.43 years). In five study blocks, which lasted 1 hour each containing a 25-minute recovery phase and a 25 minutes light exposure phase, several outcome parameters were recorded: cognitive performance (alertness and the motor inhibition) was examined using the computer-based auditory psychomotor vigilance task (aPVT [30]) and Go/No-Go Task (GNT [31]); visual acuity and potential negative side effects of bright light exposure was examined with the FrACT [27]; questionnaires were used to measure subjective alertness (Karolinska Sleep-piness Scale, KSS [32]), workload (NASA Task Load Index, NASA-TLX [33]), mood (Positive and Negative Affect Schedule, PANAS [34]) and asthenopic complaints; moreover, an electrocardiogram (ECG) was recorded during their stay in the laboratory to derive heart rate variability parameters while performing the two cognitive tests.

In this repeated-measures design, subjects were randomly assigned to start either under the “light showers” or the “placebo light showers” condition; Data collection under each condition lasted for 5.5 hours, started at 7.30 am and took place on two consecutive days. During the “light showers” condition light levels gradually increased within 30 sec from standard light levels to an illuminance of 5,500 lx at the table and 1,360 lx at eye level. In the “placebo light shower” condition illuminances were first dimmed by 50% within 30 seconds without being noticed, and then quickly and noticeably increased within 15 sec to 64% of the light levels within the light shower condition (E_h = 3,520 lx and E_v = 870 lx). Over the next 3.5 minutes, the illuminance was gradually and unnoticeably dimmed to the standard light level (E_h = 500 lx and E_v = 90 lx) again and stayed there while subjects continued to perform the tests and rate the questionnaires. In this way, under the “placebo light shower” condition it was not possible for the subject to notice a difference to the “light shower” condition (all study participants confirmed this statement verbally at the end of the study).

As a further result, HRV analyses indicated an increased parasympathetic activity and analyses of the cognitive tests showed an increased reaction speed for correct answers in the GNT under the “light showers” condition (Fig. 7). However,

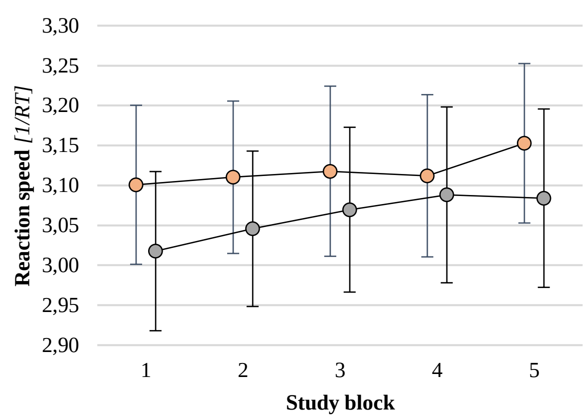

Fig. 7: Reaction speed for correct answers in the GNT in each of the five study blocks for both "light shower" (orange) and "placebo light shower" (gray) condition

TABLE I. REPORTED ASTHENOPIC COMPLAINTS

Asthenopic Complaint	Light condition	
	Light shower	***Placebo***
nausea	1.21 ± 0.60	1.21 ± 0.63
dizziness	1.26 ± 0.66	1.35 ± 0.72
teary eyes	1.28 ± 0.70	1.30 ± 0.60
itching eyes	1.51 ± 0.77	1.44 ± 0.80
headache	1.70 ± 0.96	1.84 ± 1.29
blurred vision	1.88 ± 0.79	1.88 ± 1.14
pain in and around the eyes	1.93 ± 1.24	1.74 ± 1.31
burning eyes	1.91 ± 1.07	2.12 ± 1.20
perception of glare*	2.60 ± 1.48	2.12 ± 1.22
eye strain	2.95 ± 1.34	2.86 ± 1.23

All asthenopic complaints were rated on a 6-point Likert scale ranging from 1 (not noticeable) to 6 (extremely noticeable)

beneficial light effects could not be confirmed on vigilance measured with the aPVT. Moreover, neither perceived workload nor wakefulness showed a significant difference between the lighting conditions. Except for the perception of glare, which was increased in the "light showers" condition, there were no further significant differences in both, asthenopic complaints (Table 1) and visual acuity. However, since all asthenopic complaints were rated as hardly noticeable or not noticeable at all, the significant difference with regard to glare perception appears to be negligible. This is particularly notable given the high level of illuminance.

In summary, although the second lab study could not show acute daytime alerting effects of multiple short bright light pulses, performance in a higher cognitive function task was improved. In addition, we could reveal hardly any effect on asthenopic complaints. The results indicate that short daytime bright light exposure may be beneficial for work performance.

VI. CONCLUSIONS

As results of the Europe-wide survey showed, the demands of end-users on workplace lighting are rising. This does not only affect lighting in terms of quality, but also in terms of the functionality that is made available to the user. However, work-task related and personalizable lighting cannot be implemented with conventional lighting concepts and control solutions. Innovative user-centric new lighting concepts may help to meet these increasing demands. Technologies that are currently available, such as edge computing, artificial intelligence, and imaging sensors, open opportunities to improve lighting solutions in the long term and to offer a large leap forward towards automated personalized lighting. This may not only increase user satisfaction, but also open the possibility of being able to generate visual and non-visual light effects on an individual level.

In this context, the diversity that can be achieved with modern technologies proves to be necessary. In contrast to this, current normative standards appear to be neither expedient nor sensible from this point of view since they cannot cover the required individuality and miss their original basic idea of inclusivity. The high levels of illuminance desired by older people prove to be a relevant example of this, which can, however, also be transferred to the application of immediate, non-visual lighting effects. The exemplary goals of increased alertness or reduced stress level prove to be inseparably linked to individual intrinsic psychophysiological states and require a precise, continuous assessment of current work situations and user states in order to be effective in a target-oriented manner. As the results of the presented studies were able to show, this represents another context in which personalized lighting strategies prove to be fundamentally advantageous.

However, lighting concepts designed in this way require a broad rethinking, in that the currently prioritized spatial reference is reduced in favor of individual workplace-specific lighting requirements. In addition, it is becoming increasingly necessary to understand how machine learning algorithms, modern sensor technologies and lighting control systems help to implement such concepts. Importantly, the resulting relevant specifications are far less deterministic than before, which leads to fundamentally new light designs that first have to find their way into practice. And that will still take some time.

ACKNOWLEDGEMENT

The Repro-light consortium consisted of several European lighting experts, such as the luminaire producer TRILUX and component manufacturers such as BJB, Grado Zero Espace and Rohner Engineering, the lighting design and research and development company Bartenbach and the lighting communication specialist Luger Research, as well as experts in lighting sustainability and life cycle assessment (IREC) and the University of Mondragon. The project was funded by the European Union's Horizon 2020 research and innovation program under grant agreement No. 768780.

The project LessIsMore was funded by the Austrian Research Promotion Agency FFG under application number 861712.

The authors are grateful to Siegmund Staggl (laboratory study on older adults) and Maximilian Dick and Niclas Hubel (laboratory study on younger adults) for study management and data preparation.

REFERENCES

[1] International Standards Organization and Commission Internationale de l'Eclairage [ISO/CIE]. "Light and lighting—Integrative lighting—Non-visual effects", Report No. ISO/CIE TR 21783, Under development, 2022.

[2] World Health Organization. "Combined or multiple exposure to health stressors in indoor built environments: an evidence-based review prepared for the WHO training workshop "Multiple environmental exposures and risks": 16–18 October 2013, Bonn, Germany.", 2014.

[3] Nagy, Z., Yong, F. Y. & Schlueter, A. "Occupant centered lighting control: a user study on balancing comfort, acceptance, and energy consumption", Energy and Buildings, 126, pp. 310-322, 2016.

[4] Despenic, M., Chraibi, S., Lashina, T. & Rosemann, A. "Lighting preference profiles of users in an open office environment", Building and Environment, 116, pp. 89-107, 2017.

[5] Escuyer, S. & Fontoynont, M. "Lighting controls: a field study of office workers' reactions", Transactions of the Illuminating Engineering Society, 33(2), pp. 77-94, 2001.

[6] Fotios, S., Logadóttir, Á., Cheal, C. & Christoffersen, J. "Using adjustment to define preferred illuminances: do the results have any value?", Light & Engineering, 20(2), pp. 46-55, 2012.

[7] Gilani, S. & O'Brien, W. "Modelling and simulation of lighting use patterns in office spaces", Building Simulation, 2017.

[8] Repro-light – Re-usable and re-configurable parts for sustainable LED-based lighting systems. Retrieved 13 June 2022, from https://www.repro-light.eu/

[9] Pohl, W., Weninger, J. & Dick, M. "Repro-light: Sustainable Illumination for People and the Environment", LED Professional Review, 86, pp. 34-43, 2021.

[10] Pohl, W. & Weninger, J. „Repro-light: Die Leuchte der Zukunft – nachhaltig in Produktion und Nutzung", Proceedings of LICHT2021, March 21-24, online, pp. 426-435, 2021.

[11] LessIsMore. (2022). Retrieved 13 June 2022, from https://projekte.ffg.at/projekt/2808056

[12] Cunningham, J. E. A., Stamp, J. A. & Shapiro, C. M. "Sleep and major depressive disorder: A review of non-pharmacological chronotherapeutic treatments for unipolar depression", Sleep Medicine, 61, pp. 6–18, 2019.

[13] Lee, H. J. "Is advancing circadian rhythm the mechanism of antidepressants?", Psychiatry Investigations, 16(7), pp. 479–483, 2019.

[14] Faulkner, S. M., Bee, P. E., Meyer, N., Dijk, D. J. & Drake, R. J. "Light therapies to improve sleep in intrinsic circadian rhythm sleep disorders and neuro-psychiatric illness: A systematic review and meta-analysis", Sleep Medicine Reviews, 46, pp. 108–123, 2019.

[15] Menculini, G. et al. "Depressive mood and circadian rhythms disturbances as outcomes of seasonal affective disorder treatment: A systematic review", Journal of affective disorders, 241, pp. 608–626, 2018.

[16] Terman, M. & Terman, J. S. "Light therapy for seasonal and nonseasonal depression: Efficacy, protocol, safety, and side effects", CNS Spectrums, 10(8), pp. 647–663, 2005.

[17] Tanzer, K. & Rudolph, H. "Repro-light: Modularity, Sustainability & Personalization for the Lighting Industry", Proceedings of the 8th International LED professional Symposium + Expo (LpS), Bregenz, 2018.

[18] Park, S., Spurr, A. & Hilliges, O. "Deep Pictorial Gaze Estimation". Proceedings of the European Conference on Computer Vision (ECCV), 2018.

[19] Lasa, G. et al. "Measuring the User Acceptance: User-centered Methods and Co-creation Processes in Luminaire Development", LED Professional Review, 83, pp. 30-35, 2021.

[20] Lasa, G. et al. "Repro-light Deliverable 2.1: Stakeholder & Technology Acceptance Report", 2018. Retrieved 13 June 2022, from https://ec.europa.eu/research/participants/documents/downloadPublic?documentIds=080166e5bc9e2c98&appId=PPGMS

[21] Almethhib, M. M. "The Impact of Ice Breaking Exercises on Trainees' Interactions and Skill Acquisition: An Experimental Study", Economics and Administration. 23(1), 2009.

[22] Hsu, S. H., Chuang, M. C. & Chang, C. C. "A semantic differential study of designers' and users' product form perception", International journal of industrial ergonomics, 25(4), pp. 375-391, 2000.

[23] Huang, Y., Chen, C. H. & Khoo, L. P. "Products classification in emotional design using a basic-emotion based semantic differential method", International Journal of Industrial Ergonomics, 42(6), pp. 569-580, 2012.

[24] Sagawa, K. & Takahashi, Y. "Spectral luminous efficiency as a function of age", JOSA A, 18(11), pp. 2659-2667, 2001.

[25] Kraft, J. M. & Werner, J. S. "Spectral efficiency across the life span: flicker photometry and brightness matching", In: JOSA A, 11(4), pp. 1213-1221, 1994.

[26] Foutch, B. K. "Luminous efficiency as a function of age and gender", JSM Ophthalmol, 6, pp. 1-6, 2018.

[27] Bach, M. "Freiburg Visual Acuity and Contrast Test", 2021.

[28] Cajochen, C. "Alerting effects of light", Sleep medicine reviews, 11(6), pp. 453-464, 2007.

[29] Kantermann, T., Forstner, S., Halle, M., Schlangen, L., Roenneberg, T. & Schmidt-Trucksäss, A. "The stimulating effect of bright light on physical performance depends on internal time", PLoS One, 7(7), e40655, 2012.

[30] Dinges, D. F. & Powell, J. W. "Microcomputer analyses of performance on a portable, simple visual RT task during sustained operations", Behavior research methods, instruments, & computers, 17(6), pp. 652-655, 1985.

[31] Wright, L., Lipszyc, J., Dupuis, A., Thayapararajah, S. W. & Schachar, R. "Response inhibition and psychopathology: a meta-analysis of go/no-go task performance", Journal of abnormal psychology, 123(2), p. 429, 2014.

[32] Kaida, K. et al. "Validation of the Karolinska sleepiness scale against performance and EEG variables", Clinical neurophysiology, 117(7), pp. 1574-1581, 2006.

[33] Hart, S. G. "NASA-task load index (NASA-TLX); 20 years later", Proceedings of the human factors and ergonomics society annual meeting, 50(9), pp. 904-908, 2006.

[34] Breyer, B. & Bluemke, M. "Deutsche Version der positive and negative affect schedule PANAS (GESIS panel)", 2016.

Field Comparison of Illuminance Meters

Kamil Houdek
Czech Technical University
Department of Electroenergetics
Tecghnická 2, Praha
houdekam@fel.cvut.cz

Zuzana Panská
Czech Technical University
Department of Electroenergetics
Tecghnická 2, Praha
pelanzuz@fel.cvut.cz

Petr Žák
Czech Technical University
Department of Electroenergetics
Tecghnická 2, Praha
zakpetr@fel.cvut.cz

***Abstract*— Illuminance meters used for measuring illuminance related to health protection, environmental protection or safety at work are legally controlled measuring instrument in Czech Republic and are subject to Decree of the Ministry of Industry and Trade No. 345/2002 Coll., item 5.1.2 which specifies measuring instruments for mandatory verification and measuring instruments subject to type approval.**

In the Czech Republic, the legislation defines a period, specified only for legally controlled measuring instrument, that have been type-tested. In the field of illuminance measurement, only a few types of illuminance meters on the market have this type verification. The period of validity of the verification is set by the Decree at 2 years for illuminance meters.

The verification legally controlled measuring instrument is carried out by state or authorized testing institutes. Verification by an authorized metrology center confirms that the legally controlled measuring instrument has the required metrological characteristics in accordance with the procedure laid down by the Ministerial Decree, that the selected decisive parameters correspond to the values indicated by the manufacturer and that they meet the requirements of a measure of a general nature issued by the Czech Metrology Institute. For legally controlled measuring instrument, when they are introduced on the market, a type test is required, which is the verification of all the parameters of the instrument according to the type sheets. Only some important parameters are then checked during the actual verification. The legally controlled measuring instrument is marked with an official mark by the authorized metrology center and subsequently receives a verification certificate in accordance with the Ministerial Decree.

Where illuminance meters are used in situations where the use of legally controlled measuring instrument is not required, calibration is used for their checking, which is also carried out by an authorized center, such as the Czech Metrology Institute. Calibration does not have a set time interval within the legislation when it is carried out. The calibration period is set by the measuring organizations in their own internal regulations. The voluntary national technical standard specifies a maximum interval between calibrations for field measurement illuminance meters of 3 years.

During calibration, the response of the measuring instrument being monitored is determined for a specific standard. The result is a calibration curve from which the 'correct' value relative to a particular standard can be determined.

It is clear from the above description that both verification and calibration can be quite time-consuming matters and, due to the financial cost of the test, are normally only undertaken when necessary. Furthermore, it is common for sites to also own indicating instruments without verification or proper calibration. However, even with these devices, it is necessary to verify, at least in a rudimentary way, the correctness of the quantities indicated. Not every workplace is equipped, for example, with a photometric bench where the instruments can be compared and any deviations in the measured values can be determined. This paper describes the design of an instrument used for comparison of illuminance meters, or field verification of the correct functionality of the illuminance meter, correctness of the displayed measurement results and, if necessary, determination of a simplified correction factor of illuminance values for individual illuminance meters. The device is used to ensure that the same amount of light falls on the two detector of the illuminance meters. The measured values are then read from the illuminance meters and the difference is used to determine a simplified correction factor for the illuminance value.

Keywords— ***illuminance meters, illuminance measurement, field comparision, illuminance meter verification, illuminance meter calibration***

I. INTRODUCTION (*HEADING 1*)

"Measuring illuminance is the most common photometric task. By measuring the distribution of illuminance levels, it can be objectively verified that the basic requirements for the level and uniformity of the illuminance level are met in a given lighting system." (Light and Lighting, 2013, p. 95) A device for measuring illuminance is called a illuminance meter. Illuminance meters consist of a receiver with a corrected, usually silicon photoelectric cell, which is fitted with a cosine attachment, and a measurement and evaluation system with a digital or analogue indicator. (Light and Lighting, 2013, p. 95).

The measurement of the illumination of spaces is regulated by standard ČSN 36 0011.

II. THEORETICAL PART

A. *Method of verification*

Verification (in the case of this work it is an assessment of the condition of the measuring instrument - there is no calibration protocol in the sense of meeting the requirements of MIT No. 345/2002 Coll.) is always carried out on a less accurate device using a more accurate device (illuminance meter) or on an equally accurate device using a newly calibrated or verified illuminance meter. It must be ensured that exactly the same amount of light (illuminance value) falls on both sensors. We have basically two options:

1) Constant illuminance of the sensor during the time

Provide the desired illuminance value at the first illuminance meter sensor, read the value from the evaluation system and then induce the same conditions at the second illuminance meter sensor and read the value again. The advantage here is that we can place the sensors in the same location and thus ensure the same reflection of light from the surrounding environment. However, keep the same level of the luminous flux during the time without laboratory conditions is difficult, if the luminous flux of the source changes during the change of the illuminance meters, this will show up as an error in the measured deviation of the two sensors.

2) Same illuminance for both sensors at the same time

Second possibility is to set the illuminance value for both meters at the same time. The advantage here is that if the luminous flux of the source changes, the change will be reflected on both sensors, so from this point of view we will still measure the true deviation of the two illuminance meters. In real consitions it is not possible to place both sensors in exactly the same place the same time, so it is necessary to ensure as much homogeneity as possible in the surroundings (in our case by making the dome as accurate as possible and by multiple reflections from the inner surface).

The second option was chosen because it was easier to ensure the same illuminance value at two locations in the dome (by reflecting the light) than to ensure an unchanging, unvarying luminous flux from the light source (luminaire).

B. Illuminance meter sensor comparision chamber

Work was inspired by a device called a integrating sphere. The device is spherical and its principle is based on the multiple reflections that occur inside the dome. It is used for laboratory measurements of light sources, specifically to determine their luminous fluxes. The sphere is equipped with a window/hollow with a photocell. The light from the luminaire being measured does not fall directly on this photocell, but in the form of the aforementioned multiple reflection.

The same principle is used by the dome to measure two illuminance meters at diffrent positions at the same time. The light from the luminaire never hits the sensor directly, but is emitted into the dome, where multiple reflection occurs. It is only this reflected light that finally hits the sensor surface of both the one and the other illuminance meter which are placed axisymmetrically inside the dome.

The inner surface of the spherical integrator must be painted with a very high reflectance paint. In practice, barium sulphate ($BaSO_4$) is used for this purpose in professional equipment. Since a barium sulphate coating would be too expensive and difficult to apply, white Primalex high reflectance paint was used as an alternative.

C. Sensor holder bracket

It is absolutely essential that the sensor (or both sensors) has to be always in the right place, same for each measurement, axisymmetricaly placed inside the dome.

Because of the variant where both sensors are illuminated simultaneously was chosen to implement for the device, it is necessary to make a holder that ensures that both sensors are equally far from the dome walls (they will be placed inside the dome mirroring each other).

This holder bracket is designed for Gossen MAVOLUX 5032 B and Gossen MAVOLUX 5032 C illuminance meters. These are professional illuminance meters approved by the Czech Metrology Institute for objective measurement of illumination.

The bracket is also replaceable as it is a separate piece that fits into the chamber floor. This makes the device modular and the dome can be used for other measurements or measurement with another type of illuminance sensors. In case of needs to use different type of illuminance meters, only one part has to be printed again and place instead the original one.

D. Design of light source

It is necessary to use a light source that will provide an unvarying luminous flux. It is required that the luminous flux can be varied according to the needs of the user. There is needed compare the values readings of the sensors accross minimal, average even the high illuminance values.

There are several possible options of light source for this application.

1) Incandescent light source

An incandescent light source has a non-fluctuating luminous flux if we supply it with DC voltage. However, it also has several negative characteristics. It produces a lot of heat and heating the silicon sensor of the illuminance meter can affect the measured values. At the same time, the wavelength spectrum of the light changes if we change the supply voltage, on which the luminous flux of the source is also significantly dependent.

2) Low pressure discharge light source

The fluorescent lamp (low pressure discharge light source) has many unsuitable characteristics. It requires a relatively high voltage, it has inappropriate dimensions, its luminous flux cannot be controlled by the magnitude of the voltage, it takes a very long time (up to tens of minutes) to reach its maximum luminous flux after switching on.

3) High pressure discharge light source

Discharge lamp (high pressure discharge lamp) - the need to use large external starters together with the generally high wattages and unsuitable spectral emission of these lamps make this type unsuitable for use.

4) LED

The LED has a non-fluctuating luminous flux when powered by a constant voltage (not PWM). We can easily vary the luminous flux by the magnitude of the supply voltage, but of course within the positive "linear" part of the VA characteristic. At the same time, the LED is appropriately sized and the wavelength spectrum of the light does not change when the supply voltage is changed. Neither does the colour temperature change.

Color temperature is the colour of light that would be emitted by a perfectly black body heated to this temperature. In luminaires it is given for the main colour emitted. [1]

For the above reasons the LED light source was chosen for the application. 26 pieces of single white LED was placed in the bottom part around the dome. To light up the dome with no direct luminous flux hit the illuminance sensors. Usage of the greater amount of small LED light sources may also help decrease the impact of manufacturing variances between individual LEDs on even distribution of light.

III. PRACTICAL PART

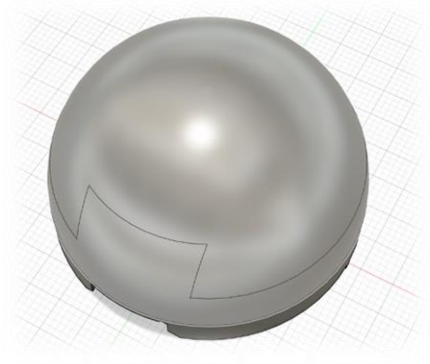

Fig. 2. Complete model of comparision device body

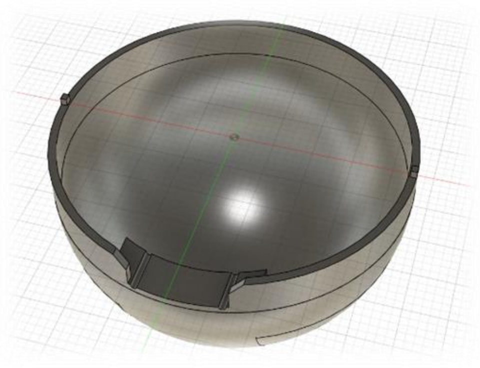

Fig. 1. Model of the top part

A. *Illuminance meter sensor comparision chamber*

Whole device was modeled in Fusion software and than printed out by 3D printer. The body of chamber itself consists of two main parts, the base and the dome. (see Fig. 1 - 3).

The parts fit together so that the chamber can be opened and closed when the sensor is installed inside to be able to make the comparision without any disturbtion light

The bottom part has got preparation for instalation of 26 pieces of LED light sources. The preparation for the LEDs already printed out from the filament ensures uniform distribution of the light flux.

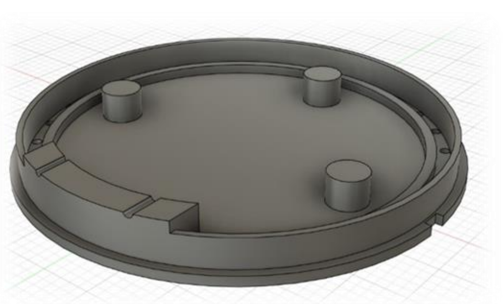

Fig. 3. Model of the bottom part

Due to the technical issues it was not possible to print out the ideal hemisphere. The real printout has got visible individual flat segments. From the inner side it is solved by the painting, which is poured to make rounded surface, from the outer side it has no negative effect for the measurement itself.

Model was printed out by white filament. The dome was printed out using a network of smaller walls with air gaps (geroid). Due to the thickness of the wall and the filament colour unwanted radiation penetrated through the dome. For this reason, the dome was painted black on the outside (see Fig. 4).

B. *Illuminance sensor holder*

The holder is designed for two Gossen MAVOLUX 5032 illuminance meters. It is a circular element that is designed to be inserted into the chamber. The separation of this part from the chamber body facilitates the handling of the light source and also allows the element to be replaced when other types of sensors than those mentioned above need to be assessed. The sensors were originally intended to be secured by the second part. In practice, the part was subsequently found to be redundant and therefore not used (see Figure 5).

Fig. 4. Complete comparision device

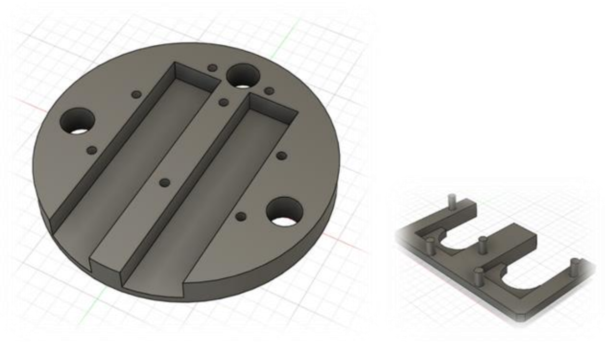

Fig. 5. Illuminance sensor holder model

Power supply

The power supply must be as stable as possible to avoid fluctuations in the luminous flux of the luminaire. At the same time, the entire fixture will be USB powered so that it can be connected easily and anywhere, whether to a mains source (phone charger etc.), power bank or computer. When powered from the USB connector of a computer or mains power supply, voltage stability will also be ensured to some extent. USB 2.0 operates at 5 V with a maximum output current of 2 A. When all 26 LEDs are lit at maximum, their power consumption should not exceed 1.6 A (see below), the Arduino nano needs a power supply of up to 19 mA (see sources/Arduino nano tech specs).

The loss on the operational amplifier can easily reach 1.5 V, the white LED I use here opens fully at about 3 V and some voltage is lost on the biasing resistor of each LED. Therefore both amplifiers are powered from a 12 V supply to ensure sufficient voltage. This is a DC-DC converter powered from 5 V and set to the required 12 V using a trimmer.

Each LED needs a maximum of 25 mA (see sources/gme.cz LED datasheet) and is connected to a maximum of 12 V with its series resistor.

Calculation of the power consumed:

- Luminaire

$$U * I * number\ of\ LEDs = 12 * 0{,}025 * 26 = 7{,}8\ W \quad (1)$$

Where:
U is the maximum voltage across the LED and resistor in series
I is the maximum current drawn by the LED

The theoretical current drawn from a 5V supply is therefore:

$$P/U = 7{,}8/5=1{,}56\ A \quad (2)$$

Where:
P is the power consumed by the LED luminaire
U is the supply voltage of the device

- Display backlight

$$U * I = 5 * 0{,}02 = 0{,}1\ W \quad (3)$$

Where:
U is the supply voltage of the display
I is the current drawn by the display

- Arduino

$$U * I = 5 * 0{,}019 = 0{,}095\ W \quad (4)$$

Where:

U is the supply voltage of the device/Arduino
I is the current drawn by the Arduino Nano microcontroller

This leaves the reserve power of about 2 W:

$$P_{max} – (P_{LED} + P_{disp} + P_{ard}) = 10 – 7{,}995 = 2{,}005\ W \quad (5)$$

This calculations gives room for any losses e.g. on the DC-DC converter of about 20%.

C. Luminous flux control

As mentioned above, all LEDs are connected with their series resistor to a common power supply terminal. So, the current that passes through each LED and hence the luminous flux is determined by the magnitude of the voltage of the common power terminal.

The value of the luminous flux is to be controlled by an Arduino Nano microcontroller, whose analog output is output to the desired voltage level modulated by PWM. Since we require that the luminous flux varies according to the DC voltage level and that the LEDs do not "flash," we must demodulate the PWM. For this purpose, a demodulator with a passive integration cell and an operational amplifier at its output (lm358n) was designed (see Figure 6).

The OZ2 operational amplifier is a TDA2030A power amplifier that provides sufficient power (current) for all light emitting diodes.

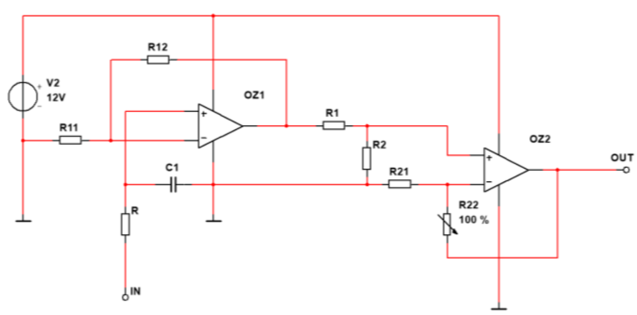

Fig. 6. Circuit scheme diagram

As I mentioned before, the analog output of the Arduino is a PWM signal. The pulse frequency is 490 Hz and the width can vary from 0% to 100%. The width (i.e., the modulation voltage before PWM modulation) is controlled by a program that operates in two modes.

1) Automatic mode

Using a digital sensor with a photoresistor inside the dome, the Arduino receives feedback about the current illumination inside the chamber (dome). Of course, this sensor can in no way compare in accuracy with the illuminance meter we want to calibrate, but it provides a basic idea of the amount of light. According to this, the microcontroller coarsely adjusts the pulse width and thus the value of the luminous flux of the source (LED). To fine tune according to the value on the illuminance meter, a multi-turn potentiometer (see diagram fig.6, resistor R22) is used to adjust the gain of the second operational amplifier. The values that can be automatically adjusted are written in the program and are the illumination values in which calibration is normally carried out.

2) Manual mode

In this mode, any illumination value can be set manually. We manually control the pulse width. (again, of course, fine-tuning is possible with the potentiometer)

The buttons used are push buttons and a voltage is applied to the read pin by software so that the log value is read 0 until the button is pressed.

D. Device control

There are 3 controls for the user. These are two buttons and one potentiometer. In automatic mode, the buttons can be used to switch between preset values. Pressing one button selects a higher or lower value and when it is released the value is automatically set. The display shows the current set value. Pressing both buttons at the same time will switch the mode (automatic/manual). In manual mode, pressing the up/down button moves the output voltage value up/down by one.

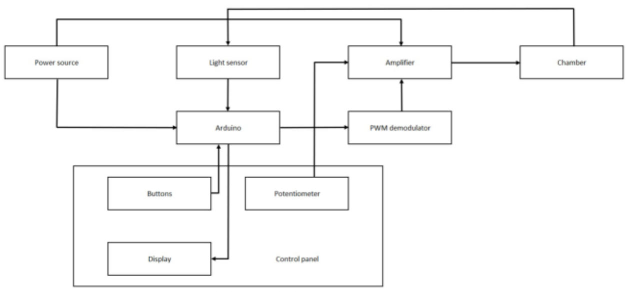

Fig. 7. Block diagram of the whole device

In automatic mode, if you want to adjust the illumination value, use the buttons to select the desired value. We will see the set value on the display as mentioned above. Next, we observe the display of the illuminance meter we want to calibrate and set the exact value using the potentiometer. Once the illuminance meter shows the value we want, we read the value from the other illuminance meter (i.e. the one we are calibrating with) and then we can determine the deviation.

IV. Conclusion

In the course of work on the device and its testing, it was found that the light sensor in the chamber is too inaccurate and therefore its use for monitoring the light inside the chamber is not feasible. For this reason, the voltage levels in automatic mode are fixed in the program.

From a functional point of view, the device meets expectations. During the test measurements, it was found that the difference in measured values between the positions of the illuminance meters in the chamber (left/right) was < 3 %, which is a very satisfactory result.

In particular, the possibility to perform simple comparison/verification measurements of the illuminance meter in the office of the implementation company or in the field, which was not possible before, and the fixtures for such measurements are not a common commercial offer on the market, can be considered as a benefit in the issue of verification of functionality and relative accuracy.

For further improvements, it would be advisable to increase the number of LEDs to achieve higher illuminance (up to 20 klx) and at the same time it would be advisable to connect them in sectors (e.g. create multiple rows) that could be switched off/on separately to achieve lower minimum illuminance.

Acknowledgment

This research was funded by Czech Technical University in Prague grant number SGS20/165/OHK3/3T/13.

References

[1] J. Habel, K. Dvořáček, V. Dvořáček, P. Žák, “Světlo a osvětlování,” Nakladatelství technické literatury. Praha, 2013.

[2] K. Sokanský, T. Novák, M. Bálský, Z. Bláha, Z. Carbol, D. Diviš and kol., “Světelná technika,” Praha, 2011.

[3] ISR-Univerzita, “Základy světla,” Coimra, Portugalsko, 2017.

Preparing the European Survey on Home Lighting

Jana Raditschová
Faculty of Electrical Engineering and Information Technology
Slovak University of Technology in Bratislava
Bratislava, Slovakia
raditschova@stuba.sk

Dionýz Gašparovský
Faculty of Electrical Engineering and Information Technology
Slovak University of Technology in Bratislava
Bratislava, Slovakia
dionyz.gasparovsky@stuba.sk

Magdaléna Kadlečíková
Faculty of Electrical Engineering and Information Technology
Slovak University of Technology in Bratislava
Bratislava, Slovakia
magdalena.kadlecikova@stuba.sk

***Abstract*— The paper is focusing on home lighting, importance of which increased during the COVID-19 pandemy and at the threshold of the anticipated energy crisis. Long-term research in this field aims to fill-in gap in standardization. The paper presents newest data from recent survey and maps the development in home lighting since the previous investigation carried out in Slovakia. To extend harvesting of data to the entire European region and to gather this way more significant information, including international differences, new online questionnaire forms have been prepared.**

Keywords*— *home lighting, residential lighting, interior lighting, lighting audit, lighting survey

I. Introduction

People spend at home considerable part of their lives [1]. Being at workplace during the day, the time spent at home usually falls to early morning and evening hours when little or no daylight is available, even more in the winter season. To support visual functions and to create a cosy atmosphere, proper artificial lighting is needed. Although visual tasks associated with home works is in many aspects similar to those performed at workplaces, light levels are often incomparable lower at households due to lack of professional approach and inappropriate energy saving measures. There are also rooms at home which need to balance some visual performance with relaxed luminous environment, thus different from other interior lighting applications. This applies not only to light levels but also to a range of other luminous parameters and the need of their dynamic variation.

Importance of home lighting is accelerated in recent years by socio-political and socio-economic changes considerably affecting the European region. Pandemic of COVID-19 opened doors to online home education [2] and distant home officing [1], [3]. Now we stand at the threshold of new challenges when expecting the outbreak of energy crisis. This might lead back to study and work from home in order to save energy supplied to public buildings and work places. We should change our look at home lighting as mostly relaxing ambience and only sometimes fulfilling ergonomic roles. Illumination of rooms where demanding visual tasks are to be carried out should resemble workplace lighting, with appropriate lighting control scenarios. Illumination of adjacent rooms are not exempted from changes because too high light levels between rooms should be avoided to reduce the adaptation glare.

Home lighting is underrated from the standardization point-of-view [4], [5]. There is no internationally approved standard, CIE recommendation, technical report or similar normative document on home lighting. From long-term perspective, home lighting is one of the priority topic in the CEN/TC169 roadmap for standardization but barrier to develop a self-standing standard is in lack of experience at European level. The only known national standard on home lighting is STN 36 0452 [6] in Slovakia, which is to be updated in 2022 (works are in progress). Another Slovak national standard on daylighting of residential buildings STN 73 0580-2 [7] is also available but this is out of the scope of this paper. Some recommendations are embedded in the pair of European documents for energy performance of lighting in buildings – EN 15193-1 [8] and CEN/TR 15193-2 [9], however, not specifying any requirements or recommendations to luminous parameters. From the state-of-the-art it follows that to establish a foundation for future European standard on home lighting it is necessary to gather data from all over the Europe.

Designing and installation of a lighting system is thus let to the user as a part of furnishment. To help the public become familiar with current technologies and to help them how to choose the right luminaires and arrange them in the space or outdoors, numerous guidelines are available [10], often provided by national lighting societies or electrical utility companies. However, impact is too low and inhabitants make the lighting on their own. The guidelines, though usually prepared by professionals, lack for discussed and agreed light levels and lighting solutions.

Aim of standardization is not to give prescriptions or restrictions but to intermediate the current level of knowledge and to provide requirements for proper lighting of homes. Solution itself, can incorporate the artistic vision and the same time to create a certain level of illumination.

Importance of normative status in this field increased since private houses and residential buildings are now subjected to the assessment of energy performance of buildings according to the above mentioned European normative documents. However, energy performance should be supported by requirements to quantitative and qualitative photometric parameters [4], [5] including illuminance and uniformity of illuminance, while recommendations how to arrange the lighting systems should be the subject of a technical report or a guideline.

II. Background

Recommendations for luminous parameters in home lighting applications are seldom available [11]. Research studies put focus more on energy related issues [12], [13]. In this respect the LED retrofits play an important role [14]; although this kind of light source does not belong to most efficient lamps, instant replacing of older technology lamps interfaced by standard holder-cap connection makes them so popular. Lamps used in households are subject to product related eco-design and energy labelling requirements [15]. Energy performance of lighting as a system is covered by EN 15193-1 and CEN/TR 15193-2; in domestic sector the current methodology still has many gaps though, suggestions for improvement are nevertheless available [16].

A. *Slovak national standard STN 36 0452*

The standard STN 36 0452 [6] is applicable to illumination of residential buildings of all types. It specifies requirements for lighting with respect to creation of healthy environment. The lighting project shall consider the functional utilization of rooms and designed disposition of interior furniture. Required illuminance values E_{pk} for rooms and task places are in Table 1. E_{pk} stands for average (from an area) and minimum (in time) illuminance which has similar meaning as the maintained illuminance E_m used today. Ratio of the average illuminance from general or localized lighting between neighbouring rooms that have a functional relationship shall not be less than 0,2 (1 : 5) and for areas with occasional usage 0,1 (1 : 10).

From Table I it follows that illuminance levels are in good accordance with the requirements to indoor and outdoor workplaces for the same or similar activities or visual tasks. However, such illuminance levels are barely achieved in real homes.

TABLE I. BASIC RANGE OF ILLUMINANCES AND MINIMUM PERMISSIBLE VALUES OF E_{PK} ACCORDING TO THE STANDARD STN 36 0452

Room / Local place	**E_{pk} (lx)**
Lighting of outdoor areas immediately and operationally related to the residential building	
Courtyards, atria	10
Outdoor entrances	20
Indoor premises for activities where simple orientation or short-time stay is sufficient, domestic communications	
Storage and ancillary premises, domestic communications	20
Inside parts of domestic entrances, lift entrances, ascents	30
Interior parking lots, garages	50
General or localised lighting of inhabited rooms equipped with local lighting, communications in flats	
Inhabited rooms complemented by local lighting	50
Communications in flats	75
General or localised lighting of house facilities	
Inhabited kitchens	100
Bathrooms, toilets, closets	100
Larders, drying rooms and storage room for strollers	100
Lounging rooms, waiting rooms, halls, laundries	150
– occasional reading: Bed header, part of a sofa, armchair	150
General or localised lighting of workplaces without local lighting	
– common dining: dining table	200
Workrooms, ateliers, home workshops, ironing rooms	
– study, writing, drawing: writing desk	300
– food preparation, cooking: kitchen desk	300
– shaving, making-up, hairdressing: vertical illuminance at distance of 40 cm in front of the mirror	300
– playing musical instruments: score	300
– common handworks (stitching, cleaning, minor reparations etc.): task area	300
– ironing: task area	300
Illumination of areas with high visual requirements	
– fine handworks, ironing, sewing, technical drawing, modelling: task area	500

Visual performance, visual comfort and avoidance of fatigue depend on luminances and their distribution in the visual field which shall be safeguarded by appropriate illuminance distribution on surfaces as well as their reflectance. Selection of reflectance and colour of surfaces shall be carried out with respect to lighting requirements as well as architecture of the space and artistic solution of the interior furniture.

Due to favourable colour rendering of the skin, lamps with warm colour appearance (T_C less than 3 300 K) shall be used in living spaces regardless on the illuminance level. For atmospheric lighting, colour temperature of lamps shall respect the artistic intention.

B. *European standard EN 15193-1*

The standard EN 15193-1 [8] does not establish any requirements or recommendations to the maintained illuminance for specific rooms, premises, tasks or activities; the standard is focused on energy efficiency and performance. Standard lighting solutions assume overall efficacy of 15 lm/W while optimized lighting solutions assume overall luminous efficacy 60 lm/W. Table II benchmarks the specific installed power of lighting systems in different kinds of rooms, calculated based on values of installed power and typical room area presented in the standard. Room size (area) is categorized to three levels – small, medium and large, differently for each of the room type. Values are provided here for standard lighting solutions and for general lighting only. Values for local lighting and for optimized lighting solutions are also presented in EN 15193-1 but not shown in this paper.

TABLE II. BENCHMARK VALUES OF SPECIFIC INSTALLED POWER *P/A* (W/M^2) IN RESIDENTIAL BUILDINGS FOR GENERAL AND AMBIENT LIGHTING AND TAKING INTO ACCOUNT STANDARD LIGHTING SOLUTION, BASED ON THE STANDARD EN 15193-1

Premises	**Small room**	**Medium room**	**Large room**
Kitchen	8,6	8,9	10,9
Dining room	10,0	9,6	11,1
Living room	10,0	9,6	11,1
Bathroom and toilet	10,0	10,0	11,1
Bedroom	12,9	11,0	10,0
Entrance hall, corridor, stairs	20,0	15,0	13,3
Storeroom, cellar, laundry	12,0	11,4	13,3

III. SCIENTIFIC OBJECTIVES

Aim of the paper is to present results of home lighting investigation in Slovakia in terms of a survey intending to map the current situation, such as the lamp structure, light levels at different places, preferences of the users and solutions implemented by them as non-professionals. The main goal of this paper is to suggest method for extension of the investigation that can be applied across Europe and which will allow to record essential data such as the geographical latitude, cultural preferences, national habits etc. which are not covered by the current national-level survey. Data collection must allow for simpler approach. Furthermore, research should also cover actual problems of today – home officing and home education, ageing of population, integrative lighting options and deviations for other home-like premises (hotel rooms, jail cells etc.). Additionally, aim of the paper is to present results of the actual trial survey using the new forms.

IV. Methodology

A. *Original questionnaire form (2013)*

Assumptions rely on the fact that what kind of lighting is installed in homes, selected, arranged and installed by the end user, is felt by the user as illumination satisfying his needs in all aspects (aesthetic function, lighting control etc.) albeit this can be biased from the knowledge on visual perception. Up to now, professional questionnaire was the main method of investigation. To achieve the needed level of reliability of data and because measurements of the illuminance are needed, the questionnaire had to be completed by a professional investigator. The questionnaire is based on Excel spreadsheet, see Fig. 1.

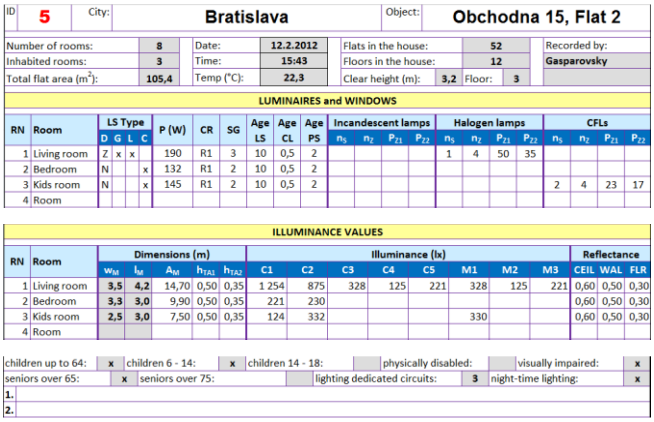

ID	5	City:	Bratislava	Object:	Obchodna 15, Flat 2

Number of rooms:	8	Date:	12.2.2012	Flats in the house:	52	Recorded by:	
Inhabited rooms:	3	Time:	15:43	Floors in the house:	12	Gasparovsky	
Total flat area (m^2):	105,4	Temp (°C):	22,3	Clear height (m):	3,2	Floor:	3

LUMINAIRES and WINDOWS

RN	Room	LS Type				P (W)	CR	SG	Age	Age	Age	Incandescent lamps				Halogen lamps				CFLs			
		D	G	L	C				LS	CL	PS	n_S	n_Z	P_{Z1}	P_{Z2}	n_S	n_Z	P_{Z1}	P_{Z2}	n_S	n_Z	P_{Z1}	P_{Z2}
1	Living room	Z	x	x		190	R1	3	10	0,5	2					1	4	50	35				
2	Bedroom	N			x	132	R1	2	10	0,5	2												
3	Kids room	N			x	145	R1	2	10	0,5	2									2	4	23	17
4	Room																						

ILLUMINANCE VALUES

RN	Room	Dimensions (m)					Illuminance (lx)								Reflectance		
		w_M	l_M	A_M	h_{TA1}	h_{TA2}	C1	C2	C3	C4	C5	M1	M2	M3	CEIL	WAL	FLR
1	Living room	3,5	4,2	14,70	0,50	0,35	1 254	875	328	125	221	328	125	221	0,60	0,50	0,30
2	Bedroom	3,3	3,0	9,90	0,50	0,35	221	230							0,60	0,50	0,30
3	Kids room	2,5	3,0	7,50	0,50	0,35	124	332				330			0,60	0,50	0,30
4	Room																

children up to 64:	x	children 6 - 14:	x	children 14 - 18:		physically disabled:		visually impaired:	x
seniors over 65:	x	seniors over 75:		lighting dedicated circuits:	3	night-time lighting:	x		
1.									
2.									

Fig. 1. Fragments of the original Excel based questionnaire used by professional investigators for survey in 2013

Private houses and flats in residential buildings are distinguished by different types of questionnaire due to significant difference in situation and size. In the questionnaire, emphasize on accuracy of specific information is given while some other information is neglected and/or simplified for the sake of time and effort savings, to make the completion of questionnaire feasible. The questionnaire comprise these pre-defined and fixed type of rooms in order to ease and automatize the evaluation:

- Houses: living room, bedroom, kids room, 3x rooms of a family member, kitchen, dining room, 2x bathroom, 2x WC, hall, 2x corridor, larder, cellar, chamber, stairs, attic, garage, veranda, other
- Flats: living room, bedroom, kids room, 2x rooms of a family member, kitchen, dining room, bathroom, WC, corridor, larder, cellar, stairs, other

Questionnaires are numbered and identified by an unique ID. Data are gathered by visual inspection and measurement. Dataset for individual rooms comprise:

- Room: main dimensions, area, average reflectance of ceiling, walls and floor (estimation), Time elapsed from the last renovation of surfaces
- Occupants: total number, children, elderly (over 65 and over 75 categories), physically disabled, visually impaired
- Lighting system: type (general, local, localized), directionality (direct, mixed, indirect), age, number of lamps/luminaires, time elapsed from the last cleaning of luminaires
- Energy: wattage of the most frequent lamp type, installed power, type of lighting control, number of switching groups
- Daylighting: number and area of windows
- Illuminance: measurement of general lighting and local lighting illuminance in specific (exactly defined) points, including height of the reference planes
- Photo documentation

B. *New questionnaire forms (2021)*

Based on previous experience, new questionnaire forms have been prepared. The original form became outdated and too complicated for gathering larger amount of data. The principal goal was to compose web-based forms accessible to wider range of investigators:

1. **Comprehensive form for investigators** – recording more detailed information and measuring illuminance by calibrated instruments
2. **Simplified form for skilled professionals** – recording essential information and measuring illuminance by broadly available instruments (Fig. 2)
3. **Form adjusted to non-professional usage by amateurs and inhabitants** – recording very basic information and optional measuring of illuminance by mobile phones (Fig. 3)

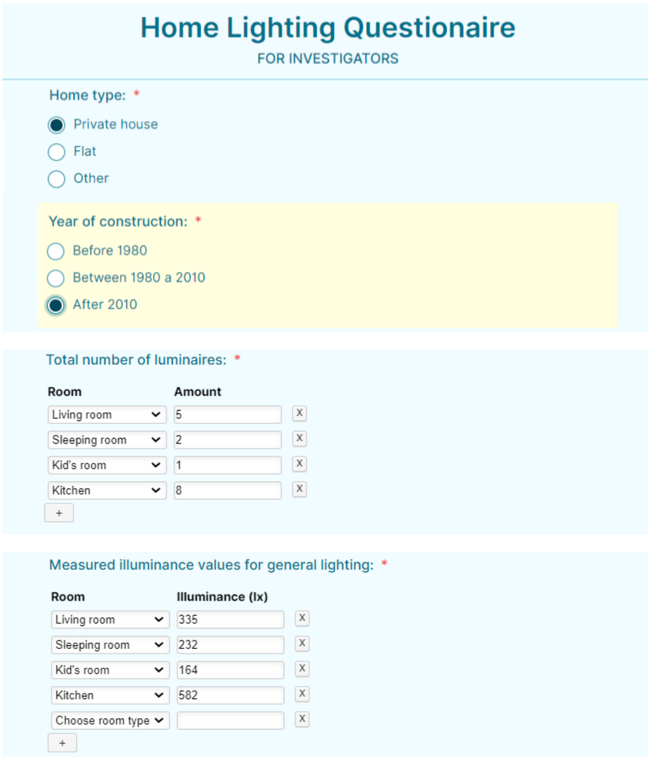

Fig. 2. Fragments of the questionnaire for professional investigators

Questionnaires are created on the Jotform platform benefiting to easy completion and immediate delivery of the forms. Language used in method 3 is adjusted to non-professionals. Interest of the investigation covers questions of both lighting quality and energy efficiency.

Data obtained by three different methods have different level of quality and reliability thus results from different methods should never be mixed. However, altogether they can help to build an illustrative picture of home lighting.

The new forms have been tried and tested in 20 households in Slovakia. Upon testing experience, the forms will be slightly adjusted and prepared for pan-European investigation. Results from European survey are expected to gather significant amount of data and show national specific differences. The survey under preparation should give answer to these essential questions:

- How satisfied is the population with lighting in their homes? What improvement would they appreciate?
- What light levels are common in different rooms and places of interest?
- To what extent is daylight harvested?
- What kind of lighting control is predominantly installed? Are integrative lighting functions incorporated?
- How efficient is the lighting system?

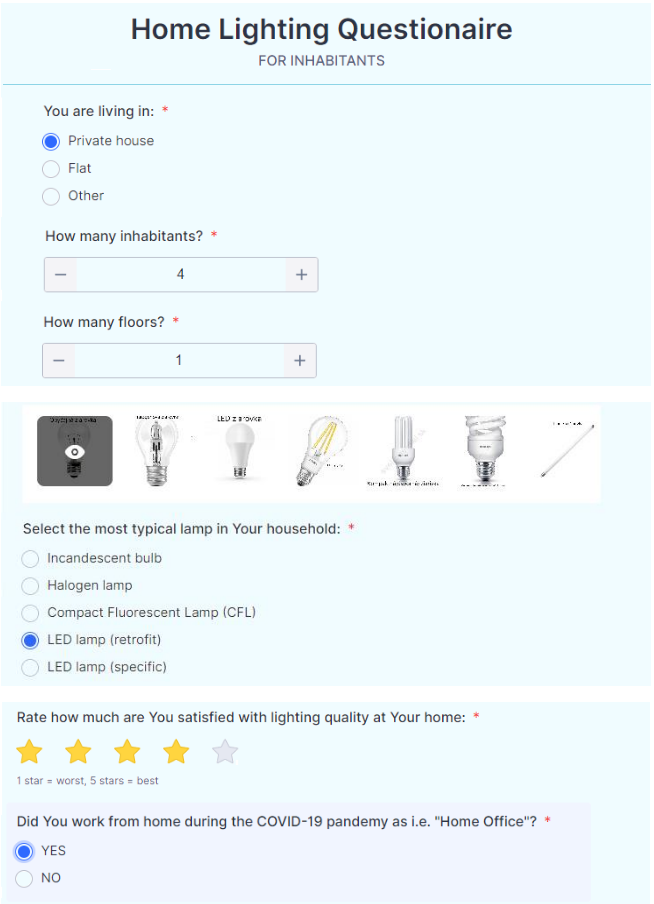

Fig. 3. Fragments of the questionnaire for general public (inhabitants)

V. Results and Discussion

Forms prepared for the consequent pan-European investigation are presented and explained in Methodology (chapter 4). As it follows from the title of this paper, the forms themselves belong to the results fulfilling the defined objectives.

In this part, results from the preliminary (testing stage) investigation carried out in Slovakia using new questionnaire forms are presented, analysed and discussed. This comprise the lamp structure and light levels in different rooms and at typical local points amongst others. The results are compared to previous investigation from 2013 and show how lighting developed withing the past 7 years.

Age of the investigated lighting systems is depicted in Figure 4. In average, age of the lighting systems is between 5 to 10 years what is less than age of flats under investigation. It means that lighting is time to time being renovated. In more recent investigation percentage share of very new lighting systems decreased obviously due to pandemic hiatus.

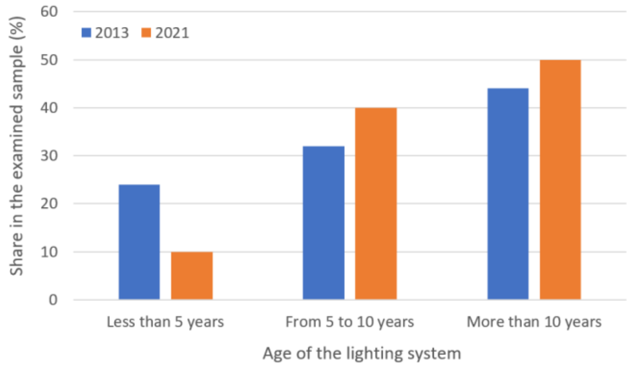

Fig. 4. Age structure of the investigated lighting systems in surveys from 2013 and 2021

Structure of light sources is presented in Table III and Fig. 5. Seven years ago surprisingly there was still big portion of incandescent bulbs including halogen lamps. It was predicted that after phase-out of these lamps from the market, their share will rapidly decrease and the lamps will be substituted by suitable retrofits. Results show considerable deviation towards LED lamps, having now 2/3 of the total share. Results gained from the general public are statistically not significant and should be treated only as illustrative. Results of survey carried out by professionals (Fig. 6) are more relevant but still as interim. In this poll, LED lamps are not distinguished between retrofits and non-retrofits, this will take place in consequent investigations.

TABLE III. Lamp structure in %

Lamp type	**Survey 2013**	**Survey 2021**	**Public 2021**
Incandescent lamps	27,8	18,0	40,0
Halogen lamps	31,1	7,8	29,0
Compact Fluorescent Lamps	20,0	5,4	2,0
Fluorescent tubes	18,2	2,3	24,5
LED lamps	2,9	66,5	4,5

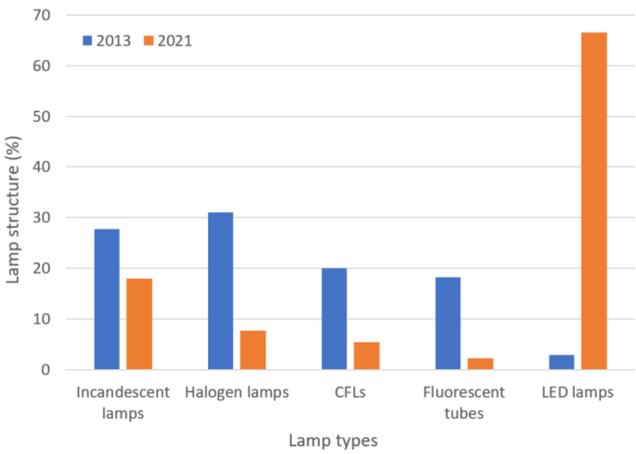

Fig. 5. Lamp structure development between 2013 and 2021

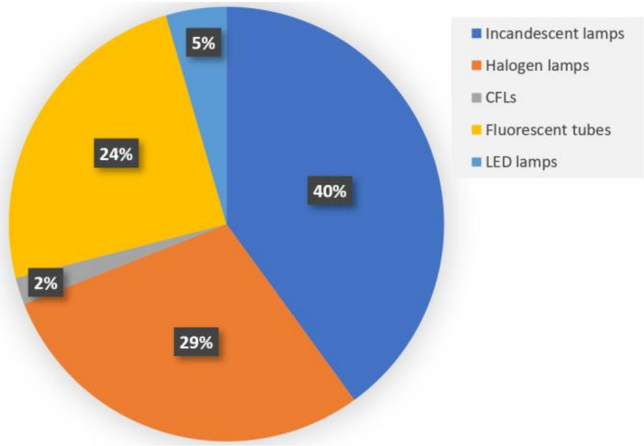

Fig. 6. Lamp structure from public survey 2021

Results of the measurement of illuminance for general lighting in the middle of unobstructed part of the room and at specific local places are in Table IV.

TABLE IV. MEASURED ILLUMINANCE LEVELS IN DIFFERENT KINDS OF ROOMS

Room / Place of measurement	E_{min} (lx)	E_{max} (lx)	E_{av} (lx)	σ
Living room:				
– middle of the unobstucted part	63	198	123,6	39,71
– edges of sofa (average)	45	200	107,1	44,72
– middle of sofa	40	205	111,1	45,51
– armchair	50	238	95,9	49,62
– middle of coffee table	72	212	122,7	39,47
Bedroom:				
– middle of the unobstructed part	35	165	91,0	46,92
– middle of bed	28	210	104,7	54,66
– header of bed 1/2 (average)	30	215	80,5	51,93
– bedside table 1/2 (average)	20	190	58,7	49,55
– middle of table/commode	13	85	41,6	25,97
Inhabited room:				
– middle of the unobstructed part	38	280	133,4	66,57
– middle of bed	27	184	93,3	49,54
– header of bed	35	160	84,7	35,29
– middle of bedside table	30	207	107,7	60,29
Kitchen:				
– middle of the unobstructed part	65	200	119,4	44,5
– work desk edges (average)	32	225	127,8	62,42
– middle of work desk	47	298	162,7	83,95
– cooker	25	122	70,0	28,41
– dining table	60	205	121,3	43,59
Bathroom:				
– middle of the unobstructed part	52	190	114,4	42,47
– washbowl	55	210	106,9	32,64
– middle of bath/shower-tub	20	126	72,5	23,70
– middle of cosmetic table	18	170	87,7	52,82
Corridor:				
– middle of the unobstructed part	22	200	97,7	47,56
– middle of table	36	94	65,4	15,93
WC:				
– middle of WC	50	157	86,3	28,66

Measured data have not been modified by the maintenance factor as it is expected that lighting systems in operation are not new, rather closer to their maintenance cycle period.

For the given set of measured data, three highest and three lowest values have been deleted to avoid extreme peaks. The rest of data have been used to calculate the average value E_{av} (lx) and the standard statistical deviation σ. Minimum and maximum illuminance values are indicated as well. It is hard to assess the measured data against normative requirements presented in Table 1 due to incoherence in the place of measurement. Approach of the investigation is more complex in this aspect.

It can be summarized that in inhabited rooms incl. living room and even bedroom the illuminance in the middle of unobstructed area is about 100 lx. However, variation expressed by the standard deviation is relatively high and low illuminance of about only 40 lx can be found in many rooms of that kind. It is interesting that similar average values are measured for other room types as well, like kitchen, bathroom and corridor. At some local places the measured illuminance is different, e.g. in the middle of the work desk in kitchen it is more than 150 lx.

Table V shows results of the investigation of installed power. The results are not yet related to the technology involved, further analyses are needed in this aspect. Nevertheless the data give imagination on the average installed power P_{av} (W) and specific installed power P_{av}/A (W/m^2) related to the useful area, presented in Table VI. Specific installed power is around 8 – 10 W/m^2 for most of rooms. Higher is the value for stairs and more power demanding rooms comprise bathrooms, toilets and cellars where still incandescents can be obviously found. Comparing the Tables VI and II it can be concluded that there is generally good correlation between benchmark values in the standard and the research results. Supporting by further analyses and data from more questionnaires the benchmark values can be slightly adjusted.

Installed power of flats varies between 200 and 2 600 W, the average is 900 W. This figures can be used to estimate the share of lighting in total energy consumption of residential buildings.

TABLE V. INSTALLED POWER P (W) IN INVESTIGATED RESIDENTIAL BUILDINGS

Room	P_{min} (W)	P_{max} (W)	P_{av} (W)	σ
Living room	20	320	167,4	84,90
Bedroom	50	157	101,3	35,61
Kid's room	67	137	106,3	45,38
Inhabited room	20	180	87,3	46,02
Kitchen	40	150	87,5	40,07
Dining room	108	120	114,0	53,96
Bathroom	40	140	74,5	35,62
WC	35	75	49,8	16,44
Corridor	40	180	89,2	43,30
Chamber	43	60	54,3	24,53
Cellar	60	75	65,0	28,80
Stairs	40	60	43,3	16,66
Entrance	36	60	48,5	21,60

TABLE VI. SPECIFIC INSTALLED POWER P/A (W/M^2) IN INVESTIGATED RESIDENTIAL BUILDINGS

Room	$\mathbf{P_{min}/A}$ **(W/m^2)**	$\mathbf{P_{max}/A}$ **(W/m^2)**	$\mathbf{P_{av}/A}$ **(W/m^2)**	σ
Living room	1,22	16,16	7,94	3,58
Bedroom	1,43	13,33	6,54	3,17
Kid's room	3,38	12,12	7,68	2,94
Inhabited room	1,79	19,05	6,51	4,25
Kitchen	3,51	23,21	9,21	4,68
Dining room	3,86	12,50	8,18	4,32
Bathroom	5,60	155,56	27,59	33,22
WC	13,33	77,92	40,74	20,30
Corridor	2,25	40,00	14,73	9,02
Chamber	5,97	14,81	10,39	4,42
Cellar	6,25	50,00	23,46	19,04
Stairs	2,35	7,50	4,69	1,84
Entrance	9,00	20,00	13,78	4,60

VI. CONCLUSIONS

Home lighting is not only making our living environment comfortable but it is a mean to provide proper conditions for visual needs. Lighting should be tailored according to individual needs and preferences depending on the age, physical disparities, activities and many other factors. Integrative lighting should be the key target to follow at homes. European lighting standard with benchmarks and recommendations has to establish a base ground for good lighting solutions. Development of such a standard must be based on understanding the specific needs of the users. European-wide investigation based on easy-to-access and easy-to-complete forms aims to gather the necessary data and to compose a survey on European home lighting. The forms are already prepared and after careful consideration and adjustment these can be distributed to lighting professionals, enthusiastic amateurs and general public throughout Europe.

ACKNOWLEDGMENT *(Heading 5)*

This work was supported by the Slovak Research and Development Agency under the contract No. APVV-20-0157.

REFERENCES

[1] B. Manav, E.Kaymaz, "Analyses on occupant petterns and energy consumption in residential buildings including the COVID-19 pandemic," in proc. Conference CIE 2021, CIE x048:2021, pp. 280-289, ISBN 978-3-902842-29-9

[2] B.S. Matusiak, C.Amorim, S.Sibilio, J. Martyniuk-Peczek, N. Sokol, Y. Koga, J. Debik, "Home office survey in the scope of the IEA SHC task 61, the lighting conditions for students," in proc. Conference CIE 2021, CIE x048:2021, pp. 300-310, ISBN 978-3-902842-29-9

[3] C.N.D. Amorim, N.G. Vásquez, J.R. Kanno, B. Matusiak, „Lighting conditions in Brazilian and Colombian home offices: a preliminary study based on occupant's perception," in proc. Conference CIE 2021, CIE x048:2021, pp. 280-289, ISBN 978-3-902842-29-9

[4] D. Gasparovsky, R. Dubnicka, J. Raditschova and L. Lipnicky, "Focused on home lighting: What to standardize and what to guide?," in proc. 28th CIE Session 2015, Volume 1, Part 2, Manchester/United Kingdom, pp. 1877-1886, ISBN 978-3-902842-55-8

[5] D. Gasparovsky and J. Raditschova, "Home lighting: A challenge to improve and standardise," in proc. LIGHT-SVĚTLO 2015, Brno/Czech Republic, pp. 69-74, ISBN 978-80-214-5244-2

[6] STN 36 0452:1986 Artificial Lighting of Residential Buildings

[7] STN 73 0580-2:2000 Daylighting of Residential Buildings

[8] EN 15193-1:2017 Energy performance of buildings – Energy requirements for lighting – Part 1: Specifications, Module M9

[9] CEN/TR 15193-2:2017 Energy performance of buildings – Energy requirements for lighting – Part 2: Explanation and justification of EN 15193-1, Module M9

[10] M. Bodart, B. Roisin, A. Deneyer and P. D'Herdt, "Establishment of innovation guidelines for the residential lighting from a relighting project," in proc. Lux Europa 2009, Istanbul/Turkey, 8 p.

[11] D. Gasparovsky and J. Raditschova, "Home Lighting," in proc. LIGHT-SVĚTLO 2013, Podbanské/Slovakia, pp. 194-205. ISBN 978-80-89275-37-3

[12] P. Banwell, J. Brons, J.P. Freyssinier-Nova, P. Rizzo and M.A. Figueiro, "A demonstration of energy-efficient lighting in residential new construction," Lighting Res. Technol. Vol. 36, Issue 2, 2004, pp. 147-164

[13] A. Deneyer, P. D'Herdt, B. Roisin and M. Bodart, "The use of energy efficiency in dwellings – Challenges and potential," in proc. Lux Europa 2009, Istanbul/Turkey, 8 p.

[14] J. Raditschova and D. Gasparovsky, "LED retrofits and their role in transient to the more energy efficient home lighting," in proc. LUMEN V4, Karpacz/Poland, pp. 257-261, ISBN 978-1-5090-3304-1

[15] P. van Tichelen, "Preparatory Studies for Eco-design Requirements of EuPs – Final report – Lot 19: Domestic lighting", 2009, 657 p., http://www.eup4light.net/

[16] D. Gasparovsky and J. Raditschova, "Proposal of a method for assessment of energy performance of home lighting,".in proc. LUMEN V4, Karpacz/Poland, pp. 226-230, ISBN 978-1-5090-3304-1

3D Print of Luminaires

Peter Janiga
Institute of Power and Applied Electrical Engineering
Slovak University of Technology in Bratislava
Bratislava, Slovakia
https://orcid.org/0000-0003-2277-8641

Miloš Grega
Institute of Power and Applied Electrical Engineering
Slovak University of Technology in Bratislava
Bratislava, Slovakia
xgregam3@is.stuba.sk

***Abstract*—The 3D print is implemented in many fields of action. Rapid advancements, availability and good results also open the field also for lighting technology. The aim of this paper is to present the results of two experiments with printed parts of luminaires. The first is focused on printing the mechanical parts, and the second on the optical parts. The second also analyses the impact on the luminous flux from and the impact on the main parameters of standard luminaires. The printed result is compared with ceramic original model by goniophotometer measuring, mathematical formulas, and software tools used for light system modelling.**

Keywords—3D print, luminaire parts, lamp components, comparison of production methods

I. Introduction

The production of luminaires has transformed to LED sources in recent years. Luminaire manufacturers had to adapt to the new conditions to be able to compete with each other. Another novelty in the form of 3D printing is currently appearing in the industry. This technology has place in many industries, and the first benefits appear in the field of lighting technology, too. If we want to understand the potential of 3D printing in the manufacture of luminaire parts and the operation of lighting technology, it is necessary to look at the potential it uses in other industries.

- Consumer goods and marketing - manufacturers are not forced to hold spare parts. If necessary, they can quickly produce the required components. On the other hand, it is possible to produce personalized or customized components, which is popularly used in marketing.
- Automotive and aerospace industries - 3D printing provides the industry with faster and more cost-effective development. Pre-production tasks are carried out faster and dependence on external suppliers is reduced.
- Healthcare and medical industry – currently, 3D printing can also fulfil strict medical criteria. Printing is used to make implants (eg, dental) and support devices (e.g., hearing aids) and accessories (e.g., orthopaedic insoles) exactly and personalised. At present, the printing of skin, bones, tissues and even drugs are already being experimented.
- Construction industry - in the past, 3D printing was used mainly for architectural prototypes. At present, complicated and design elements are commonly printed. There are also the first experiments where 3D printing is the primary construction method for building.
- Education and research - develops creativity in the pedagogical process. Students can quickly create the difficult objects for their projects and it is developing their creativity. It is also possible to speed up research processes.
- Automation and mechanical engineering - the main potential is in the rapid creation of even complex components, while production costs may be lower than in conventional production.

Successful deployment of 3D print technology in practice requires qualified personnel. Currently, there are no fields of study in schools that focus only on 3D printing. You also need to make the most of your experience with technology, which can only be gained through practice. After creating an idea of the current use of 3D printing, the question arises for people working in the field of lighting technology how to use printing in the production, operation, maintenance, and disposal of elements of the lighting system. The results on the experiment of printing LED optics are analysed in [1]. Although there is currently the greatest potential for printing mechanical and optical parts of luminaires, there are also technologies for printing the electrical circuits of luminaires. An example of such a technology is in [2] [3]. The analysis of electromagnetic compatibility of this printed PCB also analysed [5]. For a specific application, it is also possible to print on curved surfaces [4]. But this technology is more difficult and requires specific printers.

II. 3D Printing Technology and Used Materials

There are many 3D printing technologies. They differ in accuracy, speed, materials used, and the way the product is created. This also implies what shapes can be printed and in which industry the technology is optimally used. The schematic illustration shows in the reference [6] the most common printing methods. There is also a comparison and description of the methods.

Each printing technology uses different devices. FDM (Fused Deposition Modeling) technology is the most widespread and available. However, it should be noted that even here experience is required to create a product with the required accuracy, shape, and properties.

III. Lamp Elements Suitable for Print

At present, 3D printing uses rarely in lighting technology. Usually, it is design prototyping, printing parts, or spare parts. There are two main advantages, the speed of production and the production of complex shapes, where the production by traditional methods has been disproportionately demanding. Custom printing is also being carried out when it is possible to use the demanding ideas of designers or creative customers. Transforming ideas into functional luminaires is relatively simple and affordable.

Most large companies use 3D printing like prototyping tools, mainly because it allows them to gather information about the concepts of new luminaires. They do not use it for mass production. Some companies, in cooperation with smaller companies and designers, offer simple stylized elements. The client can adjust the luminaire according to simple preselection based on their own preferences.

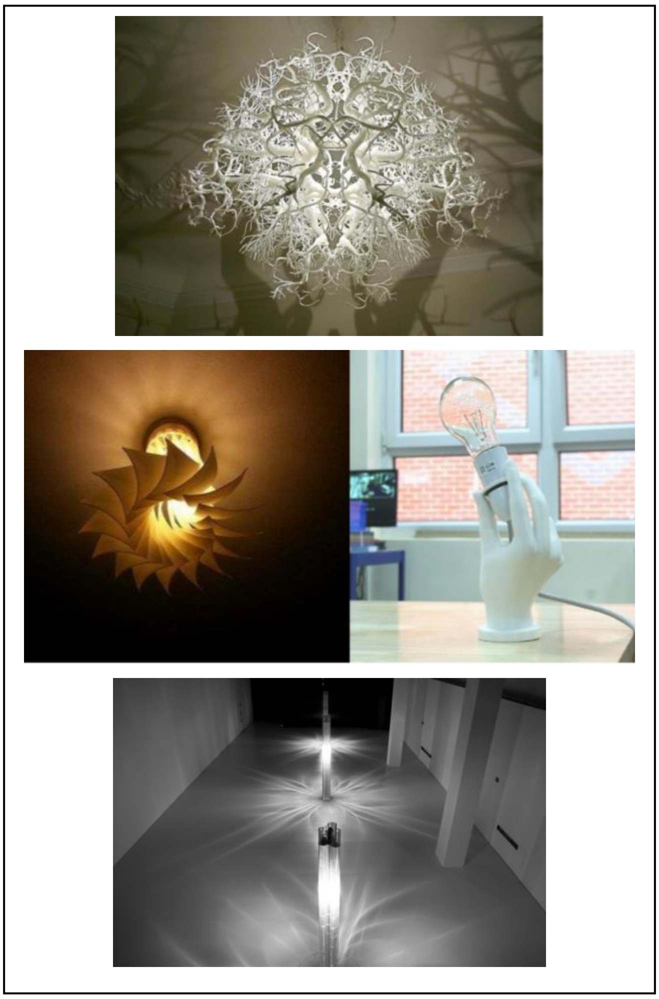

Fig. 1. Examples of printed luminares [9] [8] [7] [11]

Small design studios offer more comfortable and beautiful models than large companies. Luminaires are normally produced in only a few pieces of good quality. 3D printing allows designers not only to create a quick prototype but also to create original models of lighting fixtures, which they then sell online or show off as art.

IV. Experiments

The aim of the experimental part is to show practical experience with printing individual parts of lamps. The commonly available 3D printer Prusa i3 MK3 was used for printing. The printing material was chosen based on the required strength and temperature properties. The printer uses a 0.4mm diameter E3D V6 nozzle for a 1.75mm diameter filament and is capable of printing layers as high as 0.05mm to 0.35 mm. The printer is able to print PLA, ABS, PET, HIPS, Flex PP, Ninjaflex, Laywood, Laybrick, Nylon, Bamboofill, Bronzefill, ASA, T-Glase, and others in various colors.

In the first step, 3D models were created. There are several software tools like Fusion 360, AutoCAD, TinkerCAD, SketchUp , FreeCAD. The models designed for printing were drawn in AutoCAD 2021. The created model is necessary to import to printer in special formats, for example STL, .GCODE or .OBJ. Slicer software like Cura, Simplify3D, Slic3r, and PrusaSlicer use for creating this file. The range of software is wide, and these software are to create an imagine about user difficulty and availability.

A. *Luminaire Prototype I*

A standard table lamp was chosen for printing. The aim was to show which elements can be printed and where the printing limits appear. The drawn model had to be modified so that the printer could print it without deformation and damage on the selected material. It is common for the model to be divided into smaller units because with large overhangs, it would be necessary to push the supports. These must be removed mechanically after printing, which can impair the aesthetic quality of the print.

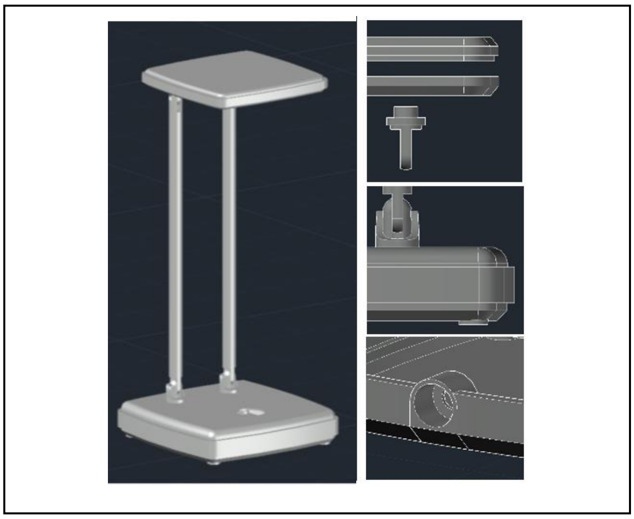

Fig. 2. Model and details of parts

Fig. 3. Original and printed lamp

The yellow PLA material was chosen for printing the selected prototype. It was chosen for its excellent properties and is most suitable for prototyping. The print lasted 3 hours and 45 minutes. When creating a 3D model, print tolerances were forgotten, and overlap problems occurred when assembling the lamp. There was also a lack of deeper experience with a particular material, and aesthetic shortcomings appeared in some components.

B. Luminaire Prototype II

The second element to be printed was the lampshade. It was chosen because of its construction, its complex decorative shape, and the ability to compare lighting features.

Fig. 4. Model and printed part with suport

Fig. 5. Original and printed lampshade

The created 3D model had to be divided to avoid using the supports. The model was divided into 3 parts, which were finalized with pins (approx. Φ 1mm) and glued. Another modification was to extend the bottom part of luminaire by a contact surface to increase the adhesion of this part to the printer table. On the first printing attempt, the bottom part detached and deteriorated during printing. Due to the complex shape, the printing took 8 hours.

V. Comparison Light Distribution Curves

The basic measure of the similarity of luminaires, optical part or shades is the measurement of the luminosity curves, which they then compare. The curves were measured with a goniophotometer at STU in Bratislava and were compared by the method of comparing the luminosity intensity of the two distributions which is described in [12]. The agreement is then determined from the measured light intensity data at all angles of the extruded and glass shades. The intensities in the specific angles of the printed shade are compared with the intensities of the glass shade at the same angles, according to the formula bellow.

$$f_{\text{luminaire,fit}} = 100 \times \left(1 - \sqrt{\frac{\sum_{C=0}^{360}\sum_{\gamma=0}^{180}(I_1(C,\gamma)-I_2(C,\gamma))^2}{\sum_{C=0}^{360}\sum_{\gamma=0}^{180}(I_1(C,\gamma)+I_2(C,\gamma))^2}}\right) \quad (1)$$

The resulting match will be in the range 0 to 100, where 0 means that the different distributions do not resemble at all and 100 means that the distributions are identical. The match between the glass and extruded shade came out 77,8093. The differences are due to the fact that the printed shade consists of a part and is not one piece like a glass shade. The biggest differences are right where the parts are connected. Another difference is the difference in the curve in the C90-270 plane, which is narrower than in the printed piece. This could be due to the fact that the glass shade was rotated during the measurement exactly so that in the C90-270 plane the light went straight between the protrusions in the pattern and not into the cut-out as in the case of the C0-180 plane.

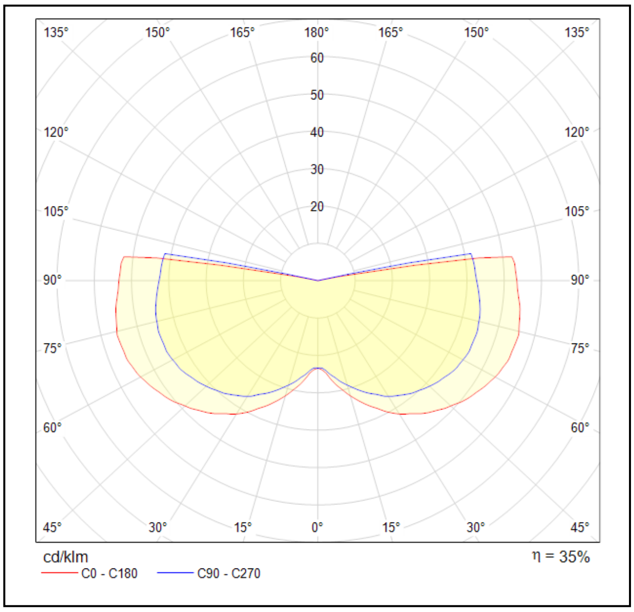

Fig. 6. Light distribution curves original lampshade

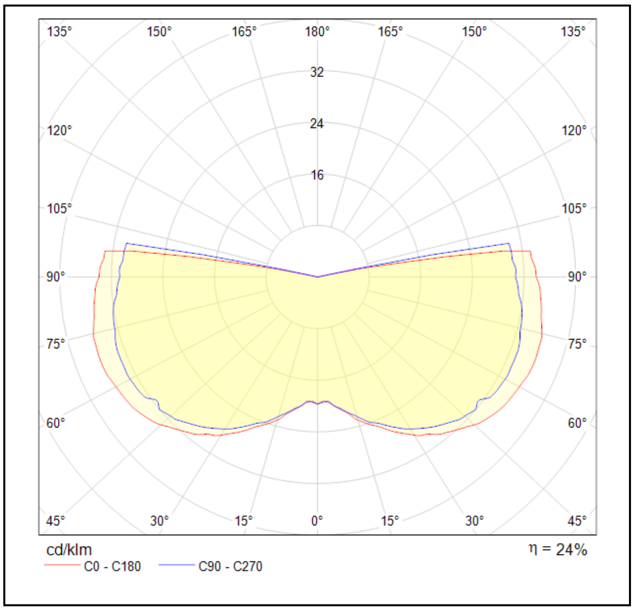

Fig. 7. Light distribution curves printed lampshade

Another reason for the differences is the fact that some printing methods reduce the final product. This is due to the thermal expansion of the material and the fact that the printing takes place at temperatures when the filament is melted. The rate of reduction is difficult to estimate and is not reported by filament manufacturers.

The last identified impact on accuracy, shape, and compliance is due to the use of the FDM printing method. In this method, the filament is applied in layers, and the resulting surface is rough. It contains a slight undulation on the surface. This impact is described in detail in [10].

VI. Conclusions

Most large companies regard 3D printing rather than a prototyping tool as a means of mass production. Mainly because it allows them to gather information about the concepts of new luminaires. However, this does not mean that 3D printed luminaires are not manufactured in such companies. Some companies, in cooperation with smaller companies or designers, offer simple stylized elements, where the client can adjust the luminaire according to simple preferences based on their own preferences.

On the other hand, designers offer more creative and beautiful models than large companies. Lamps are usually produced in only a few pieces and of good quality. 3D printing allows designers not only to quickly prototype but also to create original models of luminaires, which are then sold online or shown as art. art.

Acknowledgment

This paper is supported by the agency VEGA MŠVVaŠ SR under Grant No. VEGA 1/0640/17 „Smart Grids, Energy Self-Sufficient Regions and their Integration in Existing Power System".

References

[1] E. Beckert, F. Kemper, S. Wolleb, M. Reif, I. Wirth and F. Roscher, "3D Inkjet-printed Smart Luminaires," Smart Systems Integration; 13th International Conference and Exhibition on Integration Issues of Miniaturized Systems, 2019, pp. 1-8.

[2] Y. Kim et al., "Optimization of flexible substrate for automotive LED rear-lamp," 2009 11th Electronics Packaging Technology Conference, 2009, pp. 926-929, doi: 10.1109/EPTC.2009.5416410.

[3] K. Afonin, I. Banshchikova, V. Soldatkin, V. Tuev, A. Schkarupo and Y. Yulaeva, "Inkjet-Printed Filament for LED Bulbs," 2019 Ural Symposium on Biomedical Engineering, Radioelectronics and Information Technology (USBEREIT), 2019, pp. 332-335, doi: 10.1109/USBEREIT.2019.8736591.

[4] T. Lee, H. Choi, J. Noh and D. Kim, "EL Display Printed on Curved Surface," 2009 IEEE 22nd International Conference on Micro Electro Mechanical Systems, 2009, pp. 943-946, doi: 10.1109/MEMSYS.2009.4805540.

[5] C. C. Chen, Z. W. Xia, G. C. Wan and M. S. Tong, "Improved Electromagnetic Compatibitity Design for Printed Circuit Board of Automobile Atmosphere Lamp," 2018 Progress in Electromagnetics Research Symposium (PIERS-Toyama), 2018, pp. 760-764, doi: 10.23919/PIERS.2018.8597631.

[6] The Boom in 3D-Printed Sensor Technology. [Online] [May 26, 2022] https://www.researchgate.net/publication/317108041_The_Boom_in_3D-Printed_Sensor_Technology

[7] Sculpteo. Best 3D printed lamps. [Online] [May 26, 2022] https://www.sculpteo.com/en/3d-learning-hub/applications-of-3d-printing/3d-printed-lamps/

[8] Iliopoulos, Andreas. 3D Printed Lamps & Shades: 25 Dazzling Designs. [Online] [May 26, 2022] https://all3dp.com/2/3d-printed-lamps-shades-lights/.

[9] Ilumarco. 3D printed sculpture lamp "Forms in Nature". [Online] [May 26, 2021] http://www.3dprinting.lighting/forms-in-nature-artwork/?fbclid=IwAR1amXfDilCxDCunT2LYQpjRUh3Qb0iCWQkHj3s1HRHQ-vdTYZC1d72CdRc.

[10] Barrios J.M., Romero P.E., "Improvement of surface roughness and hydrophobicity in PETG parts manufactured via fused deposition modeling (FDM): An application in 3D printed self-cleaning parts" (2019) Materials, 12 (15), art. no. 2499, DOI: 10.3390/ma12152499

[11] Glass 3D Printing - Neri Oxman [Online] [June 20, 2022] https://oxman.com/projects/glass-3d-printing

[12] Bergen, A. S. J., A practical method of comparing luminous intensity distributions, 27th Session of the International-Commission-on-Illumination (CIE), JUL 10-15, 2011, South Africa, WOS:000329312800022

Street Light Grid and Charging Stations

Peter Janiga
Institute of Power and Applied Electrical Engineering
Slovak University of Technology in Bratislava
Bratislava, Slovakia
https://orcid.org/0000-0003-2277-8641

Miroslav Murín
Institute of Power and Applied Electrical Engineering
Slovak University of Technology in Bratislava
Bratislava, Slovakia
xmurinm3@is.stuba.sk

Dragan Minovski
Faculty of Electrical Engineering
University Goce Delcev
Stip, North Macedonia
https://orcid.org/0000-0003-0142-8298

***Abstract* — Street light grids are dense and compact networks in all cities. They power the luminaires and elements of smart cities. Recently, they have also been used to power chargers for electric vehicles. The article analyses how charging stations can be connected to public lighting networks. Knowledge about connecting the charger and optimizing operations to increase the power delivered to vehicles. Initial installations show that the combination of luminaires, public lighting networks, and chargers shows specific characteristics. The aim of the paper is to provide knowledge about the implementation of chargers in street light grids. The last part of a the paper presents the results of case study, which is focused on voltage drops and limits for installing charging stations.**

Keywords* — *street lighting, public lighting, charger, charging station, power quality, electric vehicle, lamp, luminaire

I. Introduction

The street light grids (SLG) are the main part of cities and municipalities. They are on all the streets. It is the network that covers the entire city and allows smart city elements to be powered. A specific feature of SLG is that the main appliance (luminaire) is switched on only at night. These properties create possibilities for the use of SLG to power charging stations for electric vehicles. There are already several projects in the world, but there is not enough experience and information on how to build and operate these common networks.

A. *Charging modes*

In relation to the method of connecting the vehicle to the power network, the EN 61851-1 standard defines four possible connection modes.

- Mode 1 - In this case, a standardized socket with a nominal current value not exceeding 16A is used to connect to the AC supply voltage network. It can be a single-phase socket with a nominal voltage of 230V or a three-phase socket with a nominal voltage of 400V, in both cases with a protective earth conductor.

- Mode 2 - In this case, a standardized socket with a rated current value not exceeding 32A is used to connect to the AC supply voltage network. It can be a single-phase socket with a nominal voltage of 230V or a three-phase socket with a nominal voltage of 400V, in both cases with a protective earth conductor. The difference from mode 1, in addition to the rated current, is the need to use a charge control circuit with separate electrical protection in this case. The circuit is integrated directly into the control box of the charging cable, which must be at a distance of 0.3m from the plug, or directly on it.

- Mode 3 - Is charging through a device reserved only for charging electric vehicles. The device is permanently connected to the AC power supply. It is necessary to use a charging control circuit that communicates with the device (charging station) during the entire charging period.

- Mode 4 - In the first three modes, charging was carried out using the vehicle's on-board charger. The fourth mode uses a charger located outside the vehicle's deck to connect the vehicle to the power network. The charger can be powered from an AC or DC network. However, the standard is to be powered by AC current, which must be converted to DC current in a charging station outside the vehicle. Even in this case, communication is necessary, where the charging control circuit communicates with the public charging station, during the entire charging period.

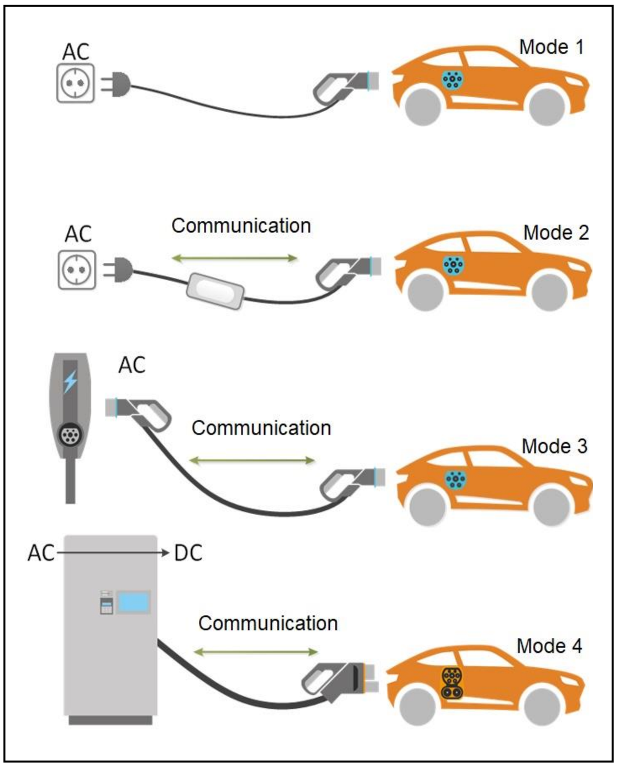

Fig. 1. Charging modes

B. *Charging power and speed of charging stations*

The charging stations are divided into AC and DC. This division determines the output power of the charger. Charging stations with AC current are typically slower than DC stations. Charging with AC current can be divided into two groups: slow charging with a power of up to 3.7kW and accelerated charging with a power of 3.7kW to 22kW. When charging with DC current, we are talking about fast and ultra-fast charging. Fast DC charging is considered to be charging with a power of up to 100kW, while the power of fast charging stations is usually not less than 50kW. Ultra-fast DC charging is charging with a power of more than 100kW.

II. Connecting the Stations to the Street Light Grids

Although the implementation of charging stations in the SLG is a relatively new topic, there are already several ways to connect and control the station. But everything depends on the possibilities and current capacity reserves of the SLG, because public lighting is always a primary functionality that cannot be negatively influenced by other additional appliances.

A. *Implementation of a charging station on a pole*

Connecting the charging station to the public lighting pole can be done in two ways. The first of them is the connection of a charging station in the form of a wallbox to an existing pole. The second is the integration of the charging station directly into the public lighting pole. This solution is better for networks with reconstructed poles, where it is expected to replace the original poles with new ones. This solution is not visually disturbing, and the public lighting pole looks the same as ordinary poles, except that it contains a charging connector. The third solution is to place the charging station in a separate column. This solution is suitable if there is no pole near or for parking spaces. However, there must be a public lighting cable nearby to power the charging station. From the point of view of installation, this solution is suitable for more extensive renovations, where cable lines are also replaced.

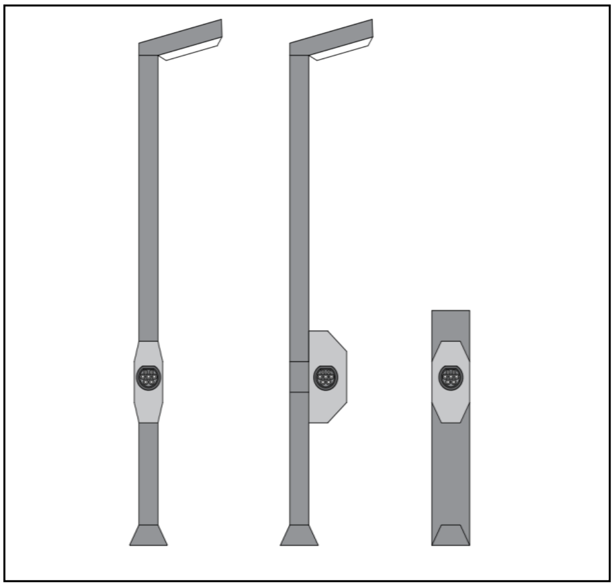

Fig. 2. Charging station integrated to the pole (right), charging station in the form of a wallbox (middle), charging station in a separate column.

In all cases, as with all public AC charging stations, the Type 2 connectors defined in EN 61851-1 are used as standard.

B. *Electrical connection of the charging station*

From the point of view of connecting the power line, there are several ways to implement charging stations in the SLG.

The first of them is the connection of the charging station to the power line that is common to public lighting. In this case, intelligent control is necessary that corrects the maximum power of the charging station based on the current state of the network, so as not to limit the public lighting function. Depending on the possibilities of the network, different capacities of charging stations can be used, up to charging stations with a power of 22kW when supplied from three phases.

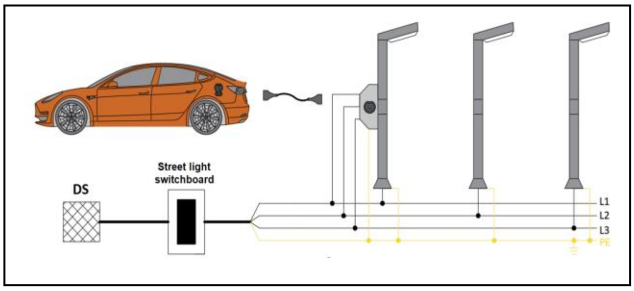

Fig. 3. Connection of the charging station to the power line common with the power supply of the SLG

The second option is to connect the charging station to only one phase of the three-phase system. This phase is reserved for the power supply of the charger and other appliances (e.g. smart city appliances). In this case, public lighting luminaires are powered from the remaining two phases of the three-phase system. A disadvantage with this connection is the unbalanced load on the phase system and a lower charging power for the user, which is around 7kW (for 230 V).

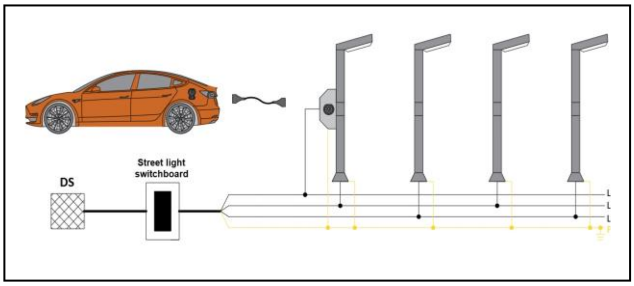

Fig. 4. Connecting the charging station to the reserved one phase of the three-phase system

Another option is the use of two independent three-phase power lines. One is used exclusively to power the public lighting network and the other to power charging stations or other additional appliances. This method is advantageous to realize only in case of complex reconstructions of SLG, where old power lines are replaced with new ones. The advantage is that the maximum charging power is always available. It is given by the maximum current carrying capacity of the branch and the used charging stations. The power of the charging stations is independent of the lights. This, of course, applies if the power line of the public lighting switchboard is sized for the maximum charging power of the lamps and charging stations in the branches.

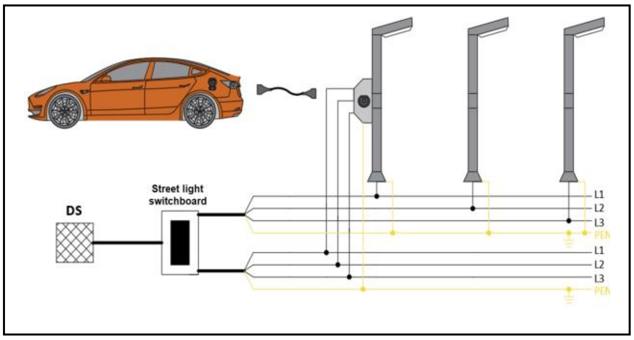

Fig. 5. Charging station powered from a separate power line

A specific case of the previous option is the connection of an SLG line and a line for charging stations at their ends. This creates a two-side power supply system, which can have a positive effect, for example, to reduce voltage drops. But this system requires luminaires with remote switching on system.

III. Voltage Drop

The design of SLG require take care of voltage drop because it has long distance of power line. The same holds for the implementation of charging stations, but the power load is higher. There is no general standard that defined the maximum value of the voltage drop in the SLG. The EN 50160 standard defines a specific voltage deviation of ± 10%, which at a nominal voltage of 230 V is in the range of 207 V to 253 V. However, this standard is only for distribution grids and defines the SLG voltage only at the power supply point. In Slovakia, the STN 332130 standard defines the maximum voltage drops for building lighting installation. Due to the similar indoor appliances and public lighting, it is used in practice as an approximate problem in the calculation of voltage drops in the public lighting network. According to this standard, the voltage drop in SLG does not exceed 4% of the nominal voltage from the switchboard to the appliances.

A. *Calculation of voltage drop*

There are several ways to calculate voltage drops. In the calculations, the simplification is used so that the entire load is at the end of the line. This simplification represents the worst possible situation. For the following calculations, relation (1) from STN 332130 which is for three-phase circuits. This is adjusted to relation (2), because the goal of the calculation is to determine the maximum lengths of the power lines by using standard cable cross-sections and a maximum voltage drop of 4% of the nominal voltage value.

$$\Delta U = \frac{\sqrt{3}\,.l.I.PF}{\gamma\,.\,S} \tag{1}$$

$$l = \frac{\Delta U\,.\gamma\,.S}{\sqrt{3}\,.I.PF} \tag{2}$$

Where:

γ – wire conductivity

ΔU – voltage drop

S – cross-section of wire

l – length of line

I – current in power line

PF – power factor

The result of the calculation is a graph showing the standard copper (CYKY) and aluminium (AYKY) cable lines used in public lighting networks. It is considered with their maximum current capacity and location in the ground.

In the next graph, the CYKY-J 4x10 means the cable with copper core with 4 wires where 3 wires are for phase and one is for PEN (neutral N together with protective earth PE). The cross-section is 10 square millimeters.

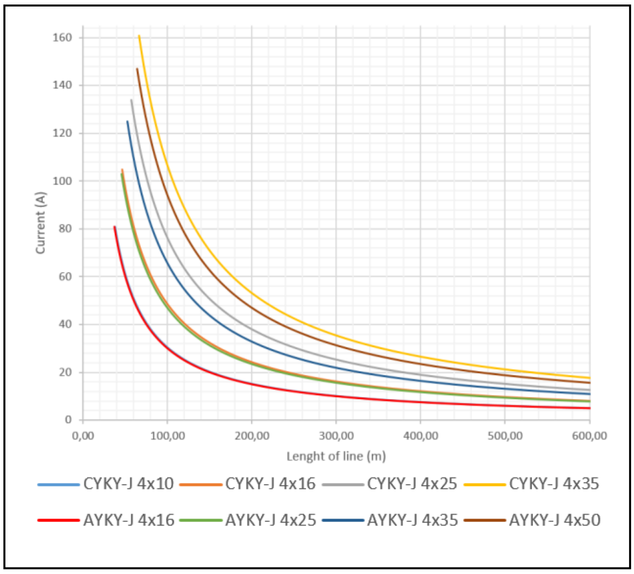

Fig. 6. Dependence between maximum current and lenght of line for 4% voltage drop and variable cables. Copper (CYKY) and aluminium (AYKY)

B. *Case study*

The case study deals with several variants of connecting charging stations to the public lighting network. It determines how far from the SLG switchboard the charging stations can be connected, or how many can be placed in a branch with different cable lines, and the voltage drop is no higher than 4% of the nominal voltage. In this case study, all variants were based on the complex formula (3) to calculate the voltage drop. It takes into account the distribution of the current load I_i in the chosen distances of the branch l_i, based on the sum of the current moments.

$$\Delta U = \frac{\sqrt{3}\,.\sum_{i=1}^{m} I_i\,.l_i\,.PF}{\gamma\,.\,S} \tag{3}$$

In Tab. 1 and Tab. 2 are the maximum lengths of cable lines from switchboard, where the charging station can be placed, and the voltage drop is not exceeded the standard requirements (4%). For the first variants the powering is from one phase according to Fig. 7.

TABLE I. Maximal Lenght of Line – Variant 1

One charger **3.7kW** (1x16A, 230V) connected to one phase without luminaires								
Wire	CU 4x10	CU 4x16	CU 4x25	CU 4x35	AL 4x16	AL 4x25	AL 4x35	AL 4x50
Max. lenght of line (m)	190	304	474	664	188	293	411	587

TABLE II. Maximal Lenght of Line – Variant 2

One charger **7.4kW** (1x32A, 230V) connected to one phase without luminaires								
Wire	CU 4x10	CU 4x16	CU 4x25	CU 4x35	AL 4x16	AL 4x25	AL 4x35	AL 4x50
Max. lenght of line (m)	95	152	237	332	94	147	205	293

In this case the charger uses different phase like luminaires. The current in the phase is independent on luminaires operation. The length is for 7.4kW charger shorter equivalent to the power.

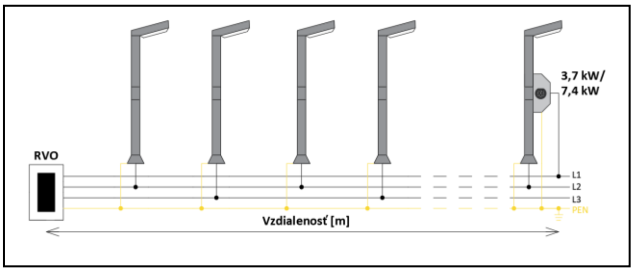

Fig. 7. Connection of charger for variant 1 and 2 (charger use different phase like luminaires)

The third variant is powered according to fig. 8. In this case are luminaires with an input power of 50 W every 25 meter. The charger and luminaires are connected to all three phases. In this case we try to simulate the operation with luminaires. The length is calculated only for one charger with full power.

TABLE III. MAXIMAL LENGHT OF LINE – VARIANT 3

One charger **22kW** (3x32 A) connected to three phases with luminaires every 25m								
Wire	CU 4x10	CU 4x16	CU 4x25	CU 4x35	AL 4x16	AL 4x25	AL 4x35	AL 4x50
Max. lenght of line (m)	94	149	233	326	93	144	202	287

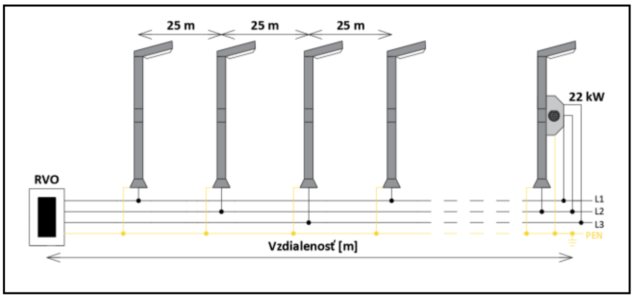

Fig. 8. Connection of charger for variant 3 and 4 (luminares are on)

The fourth variant has the same wiring as the third, but the charging station is located at half the distance compared to the third variant.

TABLE IV. MAXIMAL LENGHT OF LINE – VARIANT 4

One charger **22kW** (3x32 A) connected to three phases with luminaires every 25m**, charger connected in the middle of line**								
Wire	CU 4x10	CU 4x16	CU 4x25	CU 4x35	AL 4x16	AL 4x25	AL 4x35	AL 4x50
Lenght to charger (m)	47	74,5	116,5	163	46,5	72	101	143,5
Max. lenght of line (m)	925	1225	1525	1825	925	1225	1450	1750

C. Case study - discusion

Comparing the second and third variants, we see that the distance difference when using the power line is minimal. So, in the model example, it does not make a significant difference whether the charging station is powered from a dedicated phase that does not power the lights or is powered from a phase that powers the lights in addition to the charging station. The reason is that the power consumption of luminaires is significantly less than the consumption of charger. A more significant difference can occur if the consumption of the lights is comparable to the power input of the charger (e.g. old luminaires with high consumption).

The aim of the fourth variant is to show that the maximum length of the power lines is significantly increasing when the charging station is moved from the end of the branch (variant 3) to half the distance (variant 4). Because the charging station is an appliance with a significantly higher power consumption compared to modern LED luminaires, the total lengths of the branches in variant 4 are in some cases up to 10 times larger than in the case of variant 3.

D. Dependence between the number of chargers and the distance from the switchboard

In terms of load, a 7.4kW charging station connected to one phase is equivalent to a 22kW charger connected to three phases. In both cases, the power per phase is the same. Tab. 5 shows how many chargers can be installed at distances of 50, 100, 200 and 300 meters from switchboard. The consumption of luminaires is not taken into account. In residential areas, the consumption of LED lamps is significantly less than the consumption of the charging station.

TABLE V. NUMBER OF CHARGER WITHOUT LUMINAIRES

Maximum number of charger (7.4kW one phase or 22kW three phase) without luminares								
Wire	CU 4x10	CU 4x16	CU 4x25	CU 4x35	AL 4x16	AL 4x25	AL 4x35	AL 4x50
50m from switchboard	1	3	4	5	1	2	3	4
100m from switchboard	0	1	2	3	0	1	2	2
200m from switchboard	0	0	1	1	0	0	1	1
300m from switchboard	0	0	0	1	0	0	0	0

The closer the charging stations are to the switchboard, the more there can be. Cross-sections CU10 and AL16 are not suitable for maximum load (7.4kW one phase or 22kW) three phase) and it have limited options for powering the light. If it were necessary to install charging stations at distances greater than 200 meters, it would be worth considering the use of even larger cable conductor cross-sections than those shown in the Tab 5.

There is a possibility to increase the number of charging stations in the branch and increase the sum of installed power of charging stations. But this requires intelligent control, that redistribute the available current capacity for the charging stations. During simultaneous charging of electric vehicles from several charging stations in the branch, it is necessary to limit their output power, so that the current capacity of the branch is not exceeded.

The last example is the consideration of a 500m long branch. This branch contains luminaires every 25m. The connection is implemented as in Fig. 8. The first charging station is located at a distance of 25m and each subsequent 25m further.

TABLE VI. NUMBER OF CHARGER FOR 500M LINE

Number of 22kW chargers in 500m line with 100W luminares every 25m. Chargers are connected in distance 25, 50, 100, 150m								
Wire	CU 4x10	CU 4x16	CU 4x25	CU 4x35	AL 4x16	AL 4x25	AL 4x35	AL 4x50
Number of chargers	2	2	3	4	2	2	3	4

The Tab 6 shows how many chargers can be connected to 500m line. When the chargers are every 25m, that means every pole, there can be only 2 to the 4 chargers but relatively close to the switchboard (25m to 100m). The result is that the charger is not easy to connect in a long distance from switchboard on existing SLG.

IV. CONCLUSIONS

Currently, there are several professional and scientific articles focused on charging stations. But the charging stations associated with the SLG operation are addressed minimally. The goal was to provide comprehensive information about charging station operation and implementation methods. It can be connected to existing networks as well as newly built ones. The electrical connection can be single-phase or multi-phase. The choice of a suitable solution depends on the chargers used and also the method of operation of the SLG. This paper provides a description of the theoretical level and a case study focused on the issue of the distance between the charging stations and the switchboard (or power supply point). Because charging stations have a significant consumption compared to luminares, inappropriate placement and connection of the charging station can shorten the power line. The calculations consider the nominal power of the charging stations. By using charge management (reducing the input power of the charger), the number of installed chargers increases, but on the other hand, the charging time increases.

As part of research on this topic, the authors have carried out several measurements. The results are step by step processed and will be published in the following publications. The aim of these measurements will be for provide a base to the theoretical level and show the risks and potential of SLG in connection with charging stations.

ACKNOWLEDGMENT

This paper is supported by the agency VEGA MŠVVaŠ SR under Grant No. VEGA 1/0640/17 „Smart Grids, Energy Self-Sufficient Regions and their Integration in Existing Power System“.

REFERENCES

[1] EN 61851-1 Electric vehicle conductive charging system. Part 1: General requirements

[2] EN 62196-3 Plugs, socket-outlets, vehicle connectors and vehicle inlets - Conductive charging of electric vehicles - Part 3: Dimensional compatibility and interchangeability requirements for d.c. and a.c./d.c. pin and contact-tube vehicle couplers

[3] EN 62196-1 Plugs, socket-outlets, vehicle connectors and vehicle inlets - Conductive charging of electric vehicles - Part 1: General requirements

[4] STN 33 2130 Electric engineering regulations. Internal electric distribution lines

[5] EN 50160 Voltage characteristics of electricity supplied by public electricity networks

[6] T. Novak, J. Sumpich, J. Vanus,K. Sokansky, R. Gono, J. Latal, P. Valicek, „A model for predicting energy savings attainable by using lighting systems dimmable to a constant illuminance“ (2020) Lecture Notes in Electrical Engineering, 554, pp. 860 – 869 DOI: 10.1007/978-3-030-14907-9_83

[7] L. Kuncicky, T. Novak, K. Sokansky, Z. Slanina, „Road Lighting Control Options“ (2019) Proceedings of 44th WILGA Symposium on Photonics Applications and Web Engineering, Wilga, POLAND, MAY 26-JUN 02, 2019, DOI: 10.1117/12.2536886

[8] J. Škoda and M. Motyčka, "Lighting Design Using Ray Tracing," 2018 VII. Lighting Conference of the Visegrad Countries (Lumen V4), 2018, pp. 1-5, doi: 10.1109/LUMENV.2018.8521111.

[9] M. V. Cingoska, V. J. Sarac, S. A. Gelev and V. T. Cingoski, "Efficiency optimization of electrical devices," 2018 23rd International Scientific-Professional Conference on Information Technology (IT), 2018, pp. 1-4, doi: 10.1109/SPIT.2018.8350455.

[10] C. Suarez and W. Martinez, "Fast and Ultra-Fast Charging for Battery Electric Vehicles – A Review," *2019 IEEE Energy Conversion Congress and Exposition (ECCE)*, 2019, pp. 569-575, doi: 10.1109/ECCE.2019.8912594.

[11] T. Chen *et al*., "A Review on Electric Vehicle Charging Infrastructure Development in the UK," in *Journal of Modern Power Systems and Clean Energy*, vol. 8, no. 2, pp. 193-205, March 2020, doi: 10.35833/MPCE.2018.000374.

Lighting of Railway Installations According to EN 12464-1/2

Axel Stockmar
LCI Light Consult International
D-29227 Celle, Germany
a.stockmar.lci@t-online.de

Abstract

In the revised European Standard EN 12464-1:2021 „Light and lighting - Lighting of work places - Part 1: Indoor work places" lighting requirements are given for task areas, activity areas, room and space brightness. One of the more elaborated tables which is accompanied by an informative annex specifies requirements for the lighting of railway installations. The list of task and activity areas comprises the lighting of platforms, underpasses, stairs, maintenance sheds, station halls etc. In a similar table of the European Standard EN 12464-2:2014 "Light and lighting – Lighting of work places – Part 2: Outdoor work places" lighting requirements are given for open and covered platforms, stairs, railway yards, level crossings etc. For the selection of appropriate luminaires, the German Rail has developed a number of lighting design tables for the different task and activity areas which are accompanied by guidelines explaining the proper application of the rail specific regulations, of which examples will be presented.

Keywords

Railway lighting, lighting requirements, platforms, stairs, underpasses, maintenance sheds, railway yards, level crossings

Introduction

In the revised European Standard EN 12464-1:2021 „Light and lighting - Lighting of work places - Part 1: Indoor work places" [1] lighting requirements are given for task areas, activity areas, room and space brightness. One of the more elaborated tables which is accompanied by an informative annex D specifies requirements for the lighting of railway installations. The list of task and activity areas comprises the lighting of platforms, underpasses, stairs, maintenance sheds, station halls etc. The given lighting requirements regarding average illuminances, uniformities, and diversities are dependent on actual usage of the different areas. In a similar table of the European Standard EN 12464-2:2014 "Light and Lighting – Lighting of work places – Part 2: "Outdoor work places" [2] lighting requirements are given for open and covered platforms, stairs, railway yards, level crossings etc.

Special attention is paid to the limitation of glare for passengers, train drivers, and personnel using different methods for the evaluation of disability and/or discomfort glare. Where conventional glare evaluation methods cannot be applied, e. g. to activity areas in maintenance sheds, and direct views towards luminaires are unavoidable, the luminous flux density of the luminaire luminous areas have to be restricted to limit glare under normal viewing conditions. If facial recognition is required the ratio of the vertical to horizontal illuminance along e. g. the centre line of underpasses in the direction of movement should be considered.

For the selection of appropriate luminaires the German Rail has developed a number of lighting design tables for the different task and activity areas which are accompanied by guidelines explaining the proper application of the rail specific regulations.

Platform Lighting

There are about 5400 small, medium or large passenger stations in Germany with 9600 platforms, 900 station buildings, 2000 underpasses, and 3450 platform roofs illuminated by approximately one million luminaires. The stations are located in all different environmental zones classified as E0 to E4 in CIE Technical Report 150.2 [3], i. e. E0 intrinsically dark, E1 dark, E2 low district brightness, E4 medium district brightness, and E5 high district brightness. The lighting requirements in terms of maintained average horizontal illuminances, uniformities, and diversities are specified dependent on the number of expected passengers per day and per platform. According to EN 12464-1 [1] the photometric requirements for fully enclosed platforms are given for a small number (maintained illuminance 50 lx, uniformity 0.40), a medium number (maintained illuminance 100 lx, uniformity 0.40), and a high number of passengers (maintained illuminance 200 lx, uniformity 0.50). In EN 12464-2 [2] similar photometric requirements are listed for open and covered platforms. For open platforms the required maintained illuminance and uniformity are listed for an expected very small number of passengers (train stop, 5 lx/0.20), for a small number (10 lx/0.25), a medium number (20 lx/0.30), and large number of passengers (50 lx/0.40). Covered platforms or covered parts of open platforms require a maintained illuminance of 50 lx or 100 lx depending on a small or large number of passengers associated with uniformities of 0.40 and 0.50 respectively.

In addition, following the German Rail regulations [4], the diversities are also limited; they are not allowed to be smaller than 50% of the corresponding uniformities. These, illuminance related, values apply at platform floor level in a representative reference area. The size of the reference area is given by the width across the platform and the luminaire/pole spacing along the platform. For open platforms with pole mounted luminaires the length of the reference area is defined by the pole spacing. For covered or fully enclosed platforms with ceiling mounted or suspended luminaires the length of the reference area (not being shorter than twice the width) is given as a multiple of the luminaire spacing [5].

Lighting of stairs and underpasses

According to the European Standard EN 12464-1:2021 [1] the photometric requirements for the lighting of stairs and underpasses in fully enclosed (underground) spaces are identical to the requirements for the lighting of the connected platforms, depending in a similar manner on the number of passengers. Stairs leading to the open area (road level) should be illuminated by an adaptive lighting system to ease adaptation during the hours of darkness [4] [6].

The photometric requirements for the lighting of stairs connected to covered platforms (in the open area) are listed in the European Standard EN 12464-2:2014 [2] which is currently under revision. The illuminance levels and uniformities are the same as for the platform floor level.

The requirements for the lighting of stairs connected to open platforms have been elaborated and described in more detail in the regulations of the German Rail [4]. To compensate for the more demanding visual tasks the illuminance levels are twice as high as for the platforms, the uniformities are equal [4] [6].

To provide for sufficient seeing conditions (also for passengers with some visual disabilities) the given requirements [1] [4] [6] have to be fulfilled for every single step.

Where facial recognition is important for adequate visual communication in underpasses the ratio of vertical to horizontal illuminance at a height of 1.6 m above the floor should not fall below 0.20 in the direction of traffic, e. g. along the centre line of an underpass [1] [4] [7].

Lighting of maintenance sheds

The lighting of maintenance sheds comprises the lighting of circulation areas (using ceiling mounted or suspended luminaires with narrow transverse intensity distributions), the lighting of car roofs and car roof level walkways (with luminaires in opposite or staggered arrangements), the lighting of 'vertical' car body surfaces (with asymmetric luminaires mounted under the gantry), and the lighting of inspection pits (usually with luminaires in staggered arrangements at eye height above the pit floor) [8]. Lighting requirements in terms of average illuminances and uniformities, depending on the difficulty of the visual tasks to be performed, are listed in the European Standard EN 12464-1:2021 [1] and in related guidelines on the lighting of maintenance sheds published by the DB AG (in German) [8]. Special attention has to be paid to the colour rendering properties of the light sources. For accurate rendition of colours of objects (e.g. coatings of electric wires) the appropriate special colour rendering index, here the special colour rendering index R9 for saturated red, has to be considered [1] [8].

Lighting of railway yards

The general and specific photometric requirements for the lighting of railway yards are described in the European Standard EN 12464-2:2014 [2]. Average illuminance (10 lx), uniformity (0.40), and diversity (0.20) are specified for marshalling, retarder, and classification yards; for handling areas the average illuminance shall be increased (30 lx). Due to the great variety of possible installation layouts it is advantageous to use standardized luminaire arrangements / reference areas for the selection of appropriate luminaires as described in the guidelines on the lighting of railway yards published by the DB Netz AG (in German) [9]. In addition, there are guidelines available on the evaluation of disability and discomfort glare for train drivers and personal as well as on the limitation of obtrusive light [10].

Lighting of level crossings

Level crossings as points where a railway line and a motor vehicle road intersect at the same level must be illuminated in all cases the road lighting is not sufficient to make the level crossing visible to the road users [11]. In the European Standard EN 12464-2:2014 [2] as well as in the DB Netz AG regulations 954.9103 [12] the photometric requirements are given in terms of average illuminance (20 lx) and uniformity (0.40). In analogy to railway yards a requirement concerning the diversity (0.20) should be added. The size of the level crossing reference area depends on the number of tracks and the total width of the road (carriageway, pedestrian and/or cycle lanes). Where the railway line and the road do not cross at right angles the reference area to be considered has the shape of a parallelepiped [13]. The calculation grid for the evaluation of average illuminances and uniformities has to follow the outline of the reference area; i. e. depending on the crossing angle the grid will be more or less oblique.

Evaluation of glare

Disability and discomfort glare for train drivers, personnel, and passengers should be limited as far as possible. In the table of lighting requirements for task areas, activity areas, room and space brightness of the European Standard EN 12464-1:2021 [1] there are no requirements listed concerning the limitation of glare for the lighting of fully enclosed platforms, stairs, underpasses, and maintenance sheds. The described CIE Unified Glare Rating (UGR) tabular method is not applicable due to the fact that a number of boundary conditions are not met; e. g. no regular luminaire grids with a spacing of 0.25 and in many cases non-symmetric luminous intensity distributions in non-horizontal mounting positions [1]. But in the informative annex D on railway installations guidance is given on the limitation of glare for train drivers and personnel working in maintenance sheds. For relevant positions and viewing directions the threshold increment experienced by train drivers approaching a platform should not exceed 15% based on an adaptation luminance of 10% of the average platform luminance [1]. Where direct views towards luminous parts of luminaires are unavoidable, the luminous flux density of the luminaire luminous areas should not exceed 1000 lm per 300 cm^2 to avoid glare for personnel under normal working conditions in maintenance sheds or for passengers using stairs or underpasses [1]. Further details concerning assumptions and calculation methods are described in the different guidelines [5] [6] [7] [8].

The glare directly caused by luminaires of an outdoor lighting installation shall be determined using the CIE Glare Rating (GR) method. In the table of lighting requirements for outdoor areas, tasks, and activities of the European Standard EN 12464-2:2014 [2] glare rating limits are listed for the lighting of platforms, railway yards, and level crossings. These given limits are valid for passengers on platforms, for personnel working along the tracks in railway yards, and for pedestrians and cyclists moving alongside the road of level crossings [11] [12] [13]. In addition, for train drivers the threshold increment is restricted to 15% either based on an adaptation luminance of 10% of the average platform luminance or on an adaptation luminance which is calculated assuming an average diffuse reflectance of 5% of the different representative reference areas (here railway yards and level crossings) [9] [13].

Calculations and measurements

For the calculation and verification of illuminance values (minimum, average, maximum) a grid system has to be used which is based on a formula giving the maximum grid cell size dependent on the reference area dimensions [1] [2]. The formula has been derived under the assumption that the grid cell size is in proportion to the logarithm of the reference area dimensions [14]. The illuminance values are calculated and measured at the centre points of the grid rectangles [1] [2]. All light sources in the vicinity of the calculation points up to a distance of five times the mounting height have to be taken into account [15]. In case of platform lighting only the light sources installed on a particular platform, not of an adjacent one, have to be considered [4] [5].

The illuminance at points of interest on a calculation plane can be calculated using the inverse square law. However, the inverse square law formula applies only when the luminaires can be regarded as point sources (i. e. small in comparison to the distance between the light source and the point under consideration). Linear and area sources shall be sub-divided into an adequate number of sub-luminaires (of approximately square shape) for which the inverse square law is valid again [14]. In general, inter-reflected light is not calculated, due to a lack of knowledge of the (changing) reflectances of the enclosing surfaces.

When verifying conformity to the illuminance requirements (taking into account the maintenance factor and suppressing the amount of indirect light) the measurement points shall coincide with the calculation points [1]. For subsequent measurements, the same but not necessarily all points shall be used. If odd numbers of points have been used (along and across) a quick check is possible using only the centre point of the one- or two-dimensional grid.

Limitation of obtrusive light

Obtrusive light is defined as light, outside the area to be lit, which, because of quantitative, directional, or spectral attributes in a given context, gives rise to annoyance, discomfort, distraction or a reduction in the ability to see essential information [2] [3]. To safeguard and enhance the night time environment it is necessary to control obtrusive light which can present physiological and ecological problems to surroundings and people. To evaluate the effects of obtrusive light from outdoor lighting installations the methods described in CIE Publication 150:2019 [3] have been included in standards and regulations for the lighting of outdoor work places [2][12]. For the different environmental zones E0 to E4 limits are specified for pre- and post-curfew hours in terms of maximum vertical illuminances on properties, of maximum luminous intensities of individual light sources into potentially obtrusive directions, of maximum average luminances of facades and signs, and of maximum upward light ratios. Furthermore the maximum values of threshold increments for users of nearby roads are considered [2].

The lighting of railway stations - using luminaires for direct illumination at relatively low mounting heights (and no high pole lighting) - will generally not cause problems in terms of vertical illuminances on buildings, of luminous intensities in potentially obtrusive directions, and of the proportion of the luminous flux emitted above the horizontal. The possible reduction of light levels dependent on passenger volume (adaptive lighting) [1] [2] is a further measure to reduce light pollution particularly in intrinsically dark or low brightness areas [2] [3] [4] [5]. Application of energy efficient lighting systems using light sources with higher efficacies, control gear with lower losses, and luminaires providing higher utilances / utilization factors will also help to reduce pollution, obtrusive light, and sky glow.

The amount of (obtrusive) light falling on horizontal, inclined, or vertical (facades) surfaces alongside railway installations could be evaluated in a straight forward manner applying the concept of accumulated utilances as described in the European Standard EN 13032-5:2018 [16]. For luminaires used for the lighting of platforms in the open area, railway yards, and/or level crossings in horizontal mounting position with no upward light it is sufficient to consider the luminous flux onto adjacent surfaces only up to a height equivalent to the mounting height of the luminaires [4] [5] [9] [10] [13].

Lighting design tables

To ease the comparison and selection of appropriate luminaires the German Rail has developed a number of application dependent lighting design tables. In all the different tables pre-calculated photometric values are tabulated for which requirements are specified in standards [1] [2] or regulations [4] [12]. For standardized layouts average illuminances (fixed maintenance factor 0.80), uniformities, and diversities are listed in all cases dependent on the luminaire spacing limiting the representative reference areas and mounting heights. These floor level related values are accompanied by glare describing measures like threshold increments and glare ratings. For train drivers approaching a station platform, moving along a railway yard, or passing a level crossing the appropriate measure is the threshold increment applied to the different observer positions [4] [5] [9] [12] [13]. For passengers on platforms, personnel working between tracks of a railway yards, or passengers moving alongside a level crossing road, the glare rating is the measure to evaluate glare for application specific observer positions and viewing directions [2] [4] [5] [9] [12] [13]. Platform lighting tables provide in addition edge illuminance ratios, i. e. the ratio of the average illuminance along the platform edge (one meter band) to the average illuminance across the platform [1] [4] [5]. For motor vehicle drivers approaching a level crossing disability glare is evaluated using methods well established in road lighting [13] [15]. For lighting installations in the open area (lighting of platforms, railway yards, level crossings) obtrusive lighting is considered and documented in terms of maximum illuminances on nearby facades at application dependent distances from the representative reference areas [5] [9] [13].

Conclusions

Requirements for the lighting of railway installations are specified in a number of European Standards [1] [2] and (in Germany) regulations [4] [11] [12] accompanied by guidelines published by the DB AG. For the different applications – from platform lighting to the lighting of level crossings – standardized installation layouts have been defined for the comparison of suitable luminaires and components. Based on application specific representative reference areas relevant photometric values are evaluated and summarized in lighting design tables which make a quick selection of appropriate equipment possible.

REFERENCES

[1] EN 12464-1:2021 “Light and lighting, lighting of work places – Part 1: Indoor work places “

[2] EN 12464-2:2014 “Light and lighting, lighting of work places – Part 2: Outdoor work places”

[3] "Guide on the limitation of the effects of obtrusive light from outdoor lighting installations", 2nd edition, Technical Report CIE:150, Vienna, 2017

[4] Richtlinie 81305 "Personenbahnhöfe planen und bauen, Beleuchtungsanlagen", DB Station&Service AG, 2020

[5] A. Stockmar, "Leitfaden zur Beleuchtung von Bahnsteigen in Personenverkehrsanlagen (PVA)", DB Station&Service AG, Berlin, 2021

[6] A. Stockmar, "Leitfaden für die Handlauf integrierte Beleuchtung von Treppen in Personenverkehrsanlagen", DB Station&Service AG, Berlin, 2020

[7] A. Stockmar, "Leitfaden zur Beleuchtung von Personenunterführungen", DB Station&Service AG, Berlin, 2019

[8] A. Stockmar, "Leitfaden zur Beleuchtung von Werkhallen", DB Netz AG, München, 2017

[9] A. Stockmar, "Leitfaden Gleisfeldbeleuchtung DB Netz AG", DB Netz AG, Frankfurt am Main, 2014

[10] A. Stockmar, "Blendungsbewertung von Gleisfeld-Beleuchtungsanlagen", DB Netz AG, Frankfurt am Main, 2014

[11] Richtlinie 815.0032 "Bahnübergänge planen und instand halten; Technische Sicherungen an Bahnübergängen anordnen", DB Netz AG, Frankfurt am Main, 2008

[12] Richtlinie 954.9103 „Beleuchtungsanlagen im gleisnahen und/oder sicherheitsrelevanten Bereich", DB Netz AG, Frankfurt am Main, 2018

[13] A. Stockmar, "Leitfaden zur Beleuchtung von Bahnübergängen", DB Netz AG, Frankfurt am Main, 2021

[14] A. Stockmar, "Basic concepts of computer aided lighting design – or how accurate are computer predicted photometric values", Proceedings of the CIE seminar on computer programs for light and lighting, p. 1-3, CIE Vienna, 1992

[15] EN 13201-3:2016 "Road lighting – Part 3: Calculation of performance"

[16] EN 13032-5:2018 "Light and lighting – Measurement and presentation of photometric data of lamps and luminaires – Part 5: Presentation of data for luminaires used for road lighting"

PART II

PR PAPERS

Practical Approach to Application of Radiometer for Measuring and Evaluation Sources with Different Spectral Characteristics of UV Radiation

Marcin Pelko
CARLO Laboratory
GL OPTIC
Puszczykowo, Poland
marcin.pelko@gloptic.com

***Abstract*— Limited information regarding spectrum data of measured source result in difficulties in evaluating it based on radiometric measurement obtained by the device calibrated with specific UV source. Radiometer with individually measured characteristic of the sensor sensitivity, combined with the information characterizing spectrum of the source, allows proper readings to be taken for sources with different spectral characteristics. With the use of the device, radiometric readings can be made for low signals at levels of 0.1 μW/cm2 in relatively short time. This enables fast and more accurate measurements of spatial radiant intensity distribution of UV LED lamps with relatively low signal levels.**

Keywords—radiometer, spectroradiometer, spectrum, sensitivity, SPD

I. Introduction

With the use of individual spectral sensitivity characteristic of the sensor and indication of the source type (peak wavelength) accurate radiometric measures could be performed for different UV sources (sources with different spectrum) based on radiometer with only one measuring probe. Evaluating radiometric performance of a lamp based on measurement done with the device calibrated by another source type, if the spectrum of both lamps is not matching, could lead to incorrect interpretation of result. The impact of both sources may vary due to sensitivity characteristic of the used detector. However, with individually measured characteristic of the spectral sensitivity of the sensor, in combination with the relative data of spectral power distribution of the tested source, proper radiometric results could be obtained for lamps with different spectrum. This can still be measured with the same radiometer and photodiode.

Recalculating measured data can be accomplished automatically by the relevant software associated with the device or based on off-line calculations. The significant advantage of radiometer over most array spectrometers is its sensitivity to low signal levels even below 0.1 μW/cm2 in a relatively short time frame. It also enables fast measurements of spatial radiant intensity distribution of UV LED lamps with low signal levels. Data obtained could be used for evaluating selected impacts (e.g. curing, disinfection,) or for evaluation of photobiological safety. Due to high sensitivity of the device, measurement with high spatial resolution could be performed relatively quickly. Single acquisition is performed at 10 micro seconds, while exposure times needed vary from 10ms to 10s depending on array spectrometers.

Application of individual sensitivity correction of radiometric readings based on spectral characteristic of the sensor and relative spectral data measured at short distance (high signal/noise ratio) with spectrometer, solves variety of measurement issues associated with characterization of UV luminaires in the laboratory, especially in case of low power UV emitter.

II. Use of Radiometers vs. Specroradiometers

Applying calibrated radiometer for irradiance measurements with no additional correction is proper only when spectrum of tested source is in line with the spectrum of the source used for calibration of the device. In case of UVC radiometers, this is often related to Hg mercury discharge lamp (254nm emission line) as typical representative of the UVC product.

As shown in Fig. 1, UVC radiometer with sensitivity characteristic (blue) calibrated at 254nm could not provide proper irradiance reading for other measured UVC sources, even if they overlap with sensitivity range of the sensor.

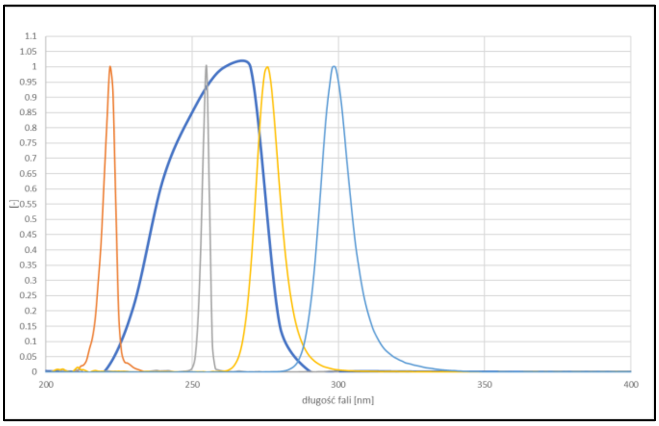

Fig. 1. Spectral sensitivity of tested UVC radiometer – blue vs. SPD of different UV sources

With the change of the spectral power distribution (SPD) or even with the shift of the peak wavelength, reading of the value requires individual correction. With UV LED sources, maximum peak emissions changes not only due to application, but also due to batch-to-batch variation or even operating conditions (forward currents, junction temperatures). This would suggest the need to use a spectroradiometer to allow to measure the correct value for individual sources. However, UV signals that are often used for evaluation of photobiological safety are at levels below 1micro wats which is difficult to properly register with spectroradiometer. This is due to limitation in sensitivity and low signal to noise ratio which is forcing us to apply maximum exposure times. This, in turn, makes it troublesome to distinguish between signal and noise. In addition, we also end up in excessively long measuring times which cause practical difficulties in case of in field testing, or due to changing properties of UV emitters in the time (heating up). As a result, there is no reason not to use the radiometer, which due to technology, is faster and could cover high dynamic range. Still, with the spectral sensitivity characteristic of the detector and data regarding SPD of the tested device, an equivalent correction could be introduced, securing good sensitivity and correct radiometric value. Solution could be achieved by precise calibration of radiometer and proper recalculation of data (spectral correction).

III. Calibration

In order to have radiometer preprepared for correct reading in the defined spectral and dynamic range we need to focus on the following items:

- Spectral responsivity measurement of the photodiode
- Correction of nonlinearity
- Adjustment factor for absolute readings of irradiance

As the first step of calibration for each detector, spectral responsivity of photodiode needs to be measured. The process could be conducted based on double monochromator and reference detector [1]. Depending on the range, Deuterium (UV) and halogen lamps (VIS-NIR) are used. Optical resolution could be adjusted but step of 5nm which seems sufficient in most cases.

For the tested radiometer a wide range silicon photodiode by Hamamatsu: S1337-66BQ was used. No additional filters were planned to be applied, thus, both Deuterium lamp as well as Halogen for VIS_NR range were operated adequately during the test to cover the complete range of the detector.

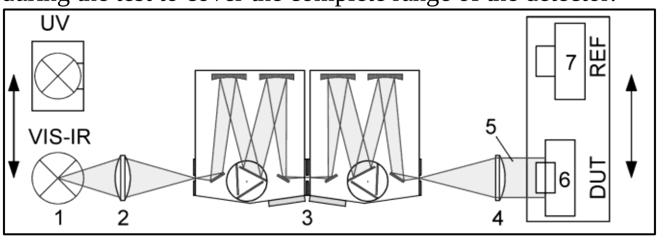

Fig. 2. Measurment set-up for spectral sensitivity measurments

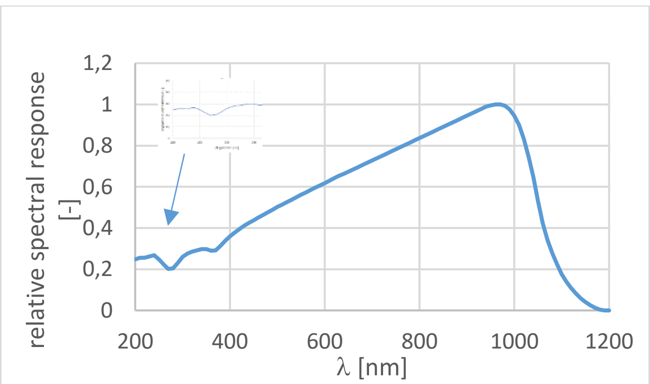

Fig. 3. Measured spectral sensitivity of S1337-66BQ photodiode

Ultimately, we obtained spectral sensitivity characteristic of the individual detector as presented in Fig. 3.
With these measurements, we could define limits for spectral range of the detector, decide on applying filters to limit the range, and link the useful range to the emission spectrum of the lamp which we want to use for any nonlinearity correction. As measurements were intended to be performed in the dark room with no stray, light coming from sources different than measured by one detector was meant to be used for correct radiometric reading in the range from 200nm to 1100nm.

In our case, nonlinearity of the device was adjusted on the photometrical bench with the use of thermally stabilized 3000K white LED. It was possible as the white LED still fits into the sensitivity range of the detector, while at the same time, it was much more practical to obtain wide signal spread for visual source. This would not be the case if UV source was used for non-linearity correction. Signal of the source was changed with the ratio 1:100000 (forward current as well as distance were adjusted).
In case of level adjustments for absolute radiometric measures, again we could refer to sensitivity range and adjustment based on available reference monochromatic LED (thermally stabilized) performance In this case, 650nm red LED was used with known irradiance at given distance and known relative SPD data. Reference lamp could be used as spectrum overlaps with the detector range.

I. Irradiance Measurment

With radiometer sensitivity in the range from 200nm to 1100nm, we could approach irradiance measurements of any source within the range. As sensor is „open" in the wide range, it was critical to perform the measurement in the dark room to avoid stray light coming from different source of radiation which would impact the reading. In case of field measurement, application of filters would be necessary. To properly evaluate functionality of our radiometer (calibrated based on monochromatic 650nm source), irradiance of UVC sources was measured for low pressure mercury discharge lamp as well as for UVC LED with peak wavelength at275nm. Spectral power distribution of tested sources was measured with the use of calibrated reference spectroradiometer. As shown in the table 1, radiometric results of measurements spectrally corrected with the data of spectral sensitivity weighted with the SPD of measured sources are in line with values obtained by the reference device. This would not be the case for non-corrected data as calibration source was of different type as compared to measured one.

As summarized above, tested device could be used for radiometric measurements with any source within the sensitivity range, if results are properly recalculated with available data. Recalculation could be built in the software providing ready results with obtained factors, which makes is intuitive for the user as presented on the samples interface in fig. 4. At the same time, we benefit from speed and high sensitivity characteristic of the radiometer within UV range. Corrected nonlinearity of the device combined with different light source type but still in the wide dynamic range, allows to have reliable measurements even below 0.1µm/cm2

TABLE I. IRRADIANCE MEASURMENTS PERFORMED WITH SPECTRORADIOMETER AND RADIOMETER

Device	Unit	LP Hg	LED 275nm
Reference Spectrometer	[W/m^2]	0.10	0.24
Radiometer w/o correction factor	[W/m^2]	0.0353	0.0791
Radiometer with correction factor (spectrally corrected)	[W/m^2]	0.0993	0.2405

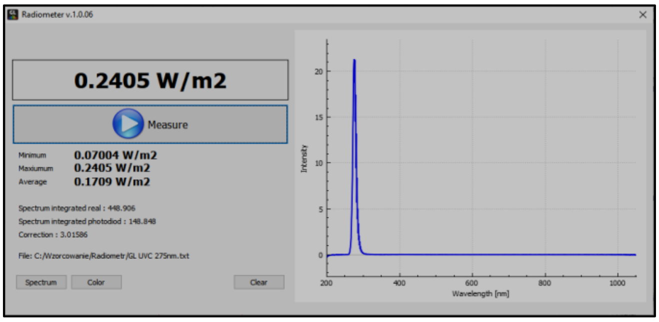

Fig.4. Example of software interface for reading of spectrally corrected radiometric values

II. RADIANT INTENSITY DISTRIBUTION

Increasing popularity of UV LED based applications for curing, disinfection or medical purposes has faced gaps in practical approach for characterizing and validating its performance. There are no standardized radiometric equivalents to photometric files applicable for UV radiant intensity. There are no tools for practical assessment of UVC reflection and degradation properties of materials. There is also no clear need for spectral range and devices used for measurements as well as calculating required UV radiant flux or irradiance based on measured results.

For designing as well as for validation of UV applications radiant intensity distribution data is crucial. In order to have this data available, goniometric measurements are necessary. Spatial model allow to predict potential impact (dose) and to evaluate the application before it is installed. For proper goniometry, measurements adequate to visual measurements exceeding minimum photometric distance are needed between the source and sensor. Since UV LED devices are often generating relatively low signals, using the spectroradiometer could result in a high noise level (long exposure times e.g., 10s for single accusation). This leads to uncertainty levels above 20%, particularly in UVC range, while photobiological safety judgement is critical. In such circumstance, the use of radiometer equipped with proper photodiode would provide a solution. Such a device can handle signals below 0.1µW/cm2 with uncertainty level below 5% for UVC range, while performing the measurement with the sampling rate of 125kHz. (examples of single radiometric measurement of the pulse is presented in fig. 5).

This reduces the total measurement time of the complete 3D radiant intensity distribution by the factor of at least 10, which differs for sampling rate and positioning times of goniometer. It also makes it easier to perform the test with high angle resolution and better accuracy.

For flexible measurement system spectral sensitivity correction must be applied to reading. This needs to be based on individual characteristic of the photodiode as well as on spectral power distribution of device under test (or at least based on peak wavelength data). Still spectrometer could be a perfect supplementary tool as relative SPD could be obtained at short distance for stable operation, where signal to noise ratio is optimal (highest possible level).

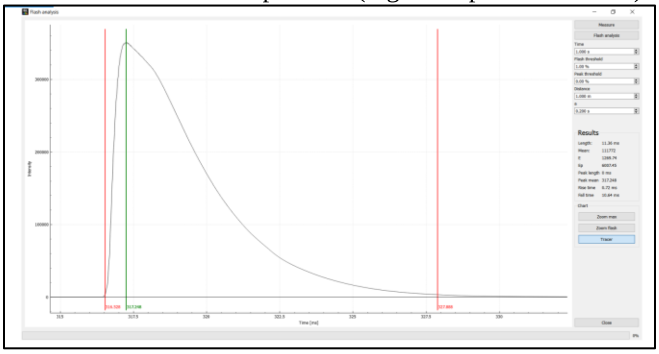

Fig.5. Example of radiometric measurment of the UV pulse at 8µs accusition time

Described measurements would allow to characterize the UV component or luminaire following the pattern used for general lighting solution (fig. 6) and crate equivalent to photometric files with radiometric values used as input for calculation.

Under specified conditions and considering drawbacks associated with lamp or detector performance, available tools can lead to indicative validation of UV effectiveness in the room. They could also be used as a guide for safe design of the upper air installations (verification of permissible exposure times). With photometric files containing radiometric values expressed in mW/sr instead of candelas, lighting design tools could be applied in designing UV application areas based on lighting simulation software.

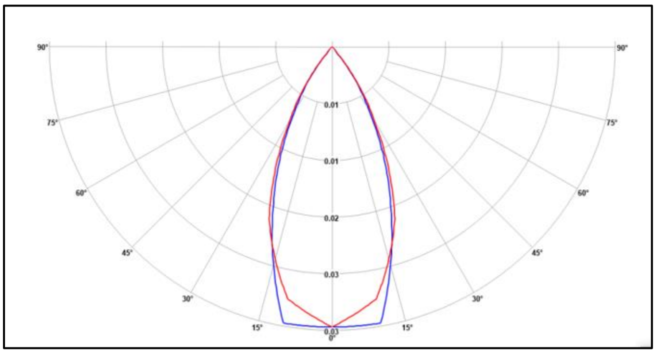

Fig.6. Example of radiant intensity ditribution baed on spectrally corrected radiometric measurment of the UVB device with total radiant flux of 0.02W

III. SUMMARY

Weighting the radiometric reading from properly calibrated device with the individual spectral sensitivity characteristic and relative spectral data is sufficient to increase the application range of radiometer without necessity of changing the measuring probe. At the same time, it allows measurements of sources which are difficult to use during calibration process due to availability or performance instabilities, for example, 222nm UV disinfection lamp. Based on the same probe IR LED could be successfully measured. It is all with uncertainties lower compared to spectral measurements and at relatively high speed. Measurement of different emitters are limited only by the range of photodiode. In case of laboratory application, where measurement could be performed with no background light, spectrally corrected radiometer with 1 measuring probe based on 1 calibration can be successfully used for measurement of sources in the spectral range from 200 to 1100nm and in dynamic range from 0.1μW/cm2 to 1000mW/cm2.

REFERENCES

[1] CIE 202:2011 Spectral responisvity measurmenents of detectors radiometers and photometers

[2] Basic Upper-Room Ultraviolet Germicida; Irradiation Guidelines for Healrhcare Settings

[3] ISO 15714:2019: Method of evaluating the UV dose to airborne microorganisms transiting in-duct ultraviolet germicidal irradiation devices

[4] Ultraviolet Purification Application information. Philips Lighting B.V

Experiences and Challenges Connected with Verification of the Quality of Road Lighting - Part 1: Measurement of Luminance Distribution

Mikołaj Przybyła
M.sc.
GL Optic
Puszczykowo, Poland
mikolaj.przybyla@gloptic.com

Jacek Dylak
M.sc.
GL Optic
Puszczykowo, Poland
jacek.dylak@gloptic.com

Małgorzata Zalesińska
M.Sc., Ph.D.
Poznań University of Technology
Poznań, Poland

Krzysztof Wandachowicz
M.Sc., Ph.D., D.Sc
Poznań University of Technology
Poznań, Poland
Krzysztof.Wandachowicz@put.poznan.pl

***Abstract*— The use of modern LED luminaires in road lighting allows for significant energy savings and can be an opportunity to improve lighting conditions on illuminated road sections. Therefore, cities, municipalities and road managers decide to invest in modern lighting solutions. Optimal use of the advantages of the new LED technology and ensuring proper quality of lighting will be guaranteed by appropriate project brief, proper lighting design and installation as well as, which is equally important, tools to verify the compliance of the investment with the design and assumptions. Practice shows that a lot of effort is made on preparing tender specifications, which are to guarantee the investor the highest quality equipment to be delivered in the investment process. However, the question whether the assumptions and the project were correct arises. Moreover, the issue of whether there were any changes affecting the luminaires performance parameters implemented at the execution stage emerges. And finally, the verification of the luminaries' correspondence to the specification comes up. One of the methods described in the current EN 13201 standard is to measure the distribution of luminance produced on the road. This article will present guidelines for the design of road lighting, methods and instruments of measurement as well as experiences and problems related to the performance of measurements in road lighting. It will also include important information about the research and development project of creating a modern measuring instrument. The project "Development of a system for Imaging luminance measurement system" has been conducted by GL Optic in cooperation with the Poznan University of Technology and it was co-financed by the European Union from the European Regional Development Fund within the Smart Development Programme.**

Keywords—luminance distribution measurements, imaging luminance measuring device

INTRODUCTION

Optimal use of the advantages of the new LED technology and ensuring proper quality of lighting will be guaranteed by appropriate project brief, proper lighting design and installation as well as, which is equally important, tools to verify the compliance of the investment with the design and assumptions.

Practice shows that a lot of effort is made on preparing tender specifications, which are to guarantee the investor the highest quality equipment to be delivered in the investment process. However, the question whether the assumptions and the project were correct arises. Moreover, the issue of whether there were any changes affecting the luminaires performance parameters implemented at the execution stage emerges. And finally, the verification of the luminaries' correspondence to the specification comes up.

One of the methods described in the current PN/EN 13201 standard is to measure the distribution of luminance produced on the road. This article will present guidelines for the design of road lighting, methods and instruments of measurement as well as experiences and problems related to the performance of measurements in road lighting.

WHAT KIND OF ROADS ARE ILLUMINATED AND HOW IS THE QUALITY OF THE LIGHTING VERIFIED?

The European standard EN 13201 Road Lighting provides the basis for the design and assessment of road lighting parameters. In 2014, Technical Committee 169 "Light and Lighting" (CEN/TC169) of the European Commission for Standardization published the first part of the new version of the existing standard - Technical Report, containing guidelines and procedures for the selection of lighting requirements. At the end of 2015, the remaining parts of the updated version of the standard were published, including the latest – the fifth one, concerning the assessment of energy performance of road lighting installations.

The general assumptions concerning both the selection procedures and the quantitative lighting requirements in the new standard are based on the publication of the International Lighting Commission of 2010 entitled "Lighting of roads for motor traffic and pedestrians".

All parts of the new European standard were published between February and March 2016 by the Polish Committee for Standardization. They replace the previous version of the PN-EN 13201:2007 standard Road Lighting. The new PN-

EN 13201:2016 standard Road Lighting consists of five parts (all published in English):

- CEN/TR 13201-1:2016-02 Road lighting - Part 1: Guidelines on selection of lighting classes
- EN 13201-2:2016-03 Road lighting - part 2: Performance requirements
- EN 13201-3:2016-03 Road lighting - part 3: Calculation of performance
- EN 13201-4:2016-03 Road lighting - part 4: Methods of measuring lighting performance
- EN 13201-5:2016-03 Road lighting - part 5: Energy performance indicators

The basic lighting requirements for roads designated primarily for motor traffic at high and medium speeds are based on criteria related to the level and uniformity of luminance of the road itself, its direct surroundings and glare limitation. Properly designed road lighting enhances the safety of drivers and pedestrians on the road.

The luminance method used to assess the quality of road lighting applies for M class roads. M lighting class is intended for use on motorways where medium and high speeds are permitted.

The average luminance Lav should be calculated as the arithmetic mean of the luminance of the points of the measuring field grid. The overall uniformity Uo should be calculated as the ratio of the lowest luminance at each point of the measuring field grid to the average luminance. The longitudinal uniformity Ul should be calculated as the ratio of the least luminance to the highest luminance in the longitudinal direction of the axis of each lane.

The luminance distributions shall be measured in a field which comprises two successive luminaires in the same line. The meter shall be positioned 60 m from the first luminaire (Figure 1). The measuring points shall be evenly spaced.

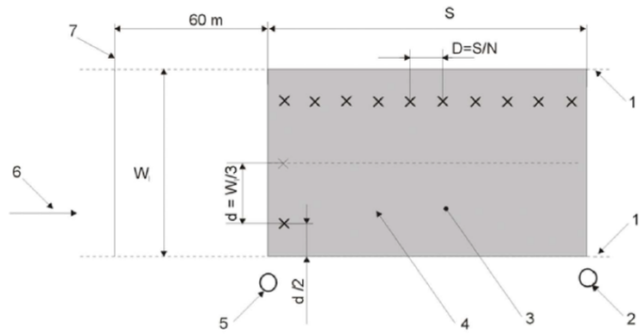

Fig. 1. Calculation field of luminance, positions of calculation points in the lane:

1 - lane edge, 2 - last luminaire in the measuring field, 3 - measuring field, 4 - lane axis, 5 - first luminaire in the measuring field, 6 - direction of observation, 7 - position of luminance meter for longitudinal observation, x - marking of measurement points

TABLE I: . LIGHTING REQUIREMENTS FOR M CLASSES FOR DRY SURFACES

Class	L_{av} [min. use] [cd/m^2]	U_o [min]	U_l [min]
M1	2.00	0.40	0.70
M2	1.50	0.40	0.70
M3	1.00	0.40	0.60
M4	0.75	0.40	0.60
M5	0.50	0.35	0.40
M6	0.30	0.35	0.40

The luminance meter should be at a height of 1.5 m above the road level. In the transverse direction, the meter should be positioned successively in the centre of each lane of the road. The average luminance and the overall uniformity of luminance should be measured for the whole roadway and for each position of the meter. From the driver’s point of view the road area between 60 m and 160 m in front of the vehicle is important. With the driver's level of vision set at a height of 1.5 m above the road surface (or, if measured, from the measuring position), the angle between the optical axis of the measuring device and the road surface changes between 1.5° and 0.5°. Performing measurements in this range requires a precise system which will allow changing the inclination of the meter with high resolution so as to aim the measurement field at the given measurement point located in the distance range described above.

The standard recommends that, in order to obtain a correspondence between the measured and calculated values, location of the measurement points and the observer's position should be the same as the positions used in the calculations. It is recommended that these positions are also in accordance with the requirements of PN-EN 13201-3. The application of such requirements leads to the following problems:

- a very large number of measuring points is created,
- measurement of luminance distributions becomes a difficult task. Problems that may occur in the luminance measurement are rather related only to the large number of measurement points.

On the other hand, the problems occurring during luminance measurements can be presented in the following points:

- the need for a precise and technically advanced luminance meter, which should limit the total angle of the measurement cone to 2 arcminutes on the vertical surface and to 20 arcminutes on the horizontal surface,
- possibility of overlapping of measuring fields from neighbouring points,
- problems with precise targeting of the meter's observation field on the measurement field.

Fig. 2 shows a perspective view of the road with the density of measurement points further away from the observer.

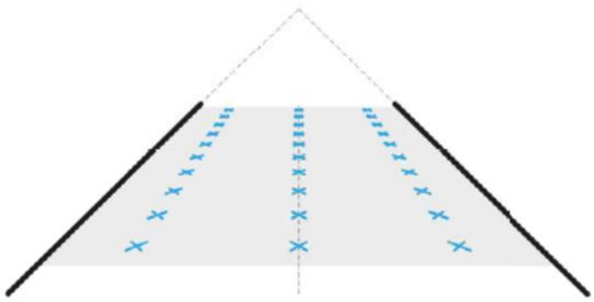

Fig. 2. Density of measurement points

The long lasting experience of the Poznan University of Technology team shows that measurements made with a spot luminance meter make it practically impossible to perform a reliable measurement, especially the distribution of luminance, and, thus, to obtain an objective value of luminance uniformity. The above problems can be solved if a Imaging Luminance Measuring Device (ILMD) is used. The operation of such a meter is similar to that of a digital camera. Professional versions of such meters do not have an optical viewfinder, and the analysed image can be displayed on the screen of a portable computer. Measurements are made by means of

- setting the meter in an appropriate place,
- marking of the measuring field (including its dimensions),
- single recording of the analysed surface image,
- processing of the recorded image outside the place where the measurements were taken.

The team of the Department of Light Technology and Electrothermal Energy of the Poznań University of Technology has many years of experience in performing luminance measurements on roads with the use of both a spot luminance meter and an Imaging Luminance Measuring Device. The use of an ILMD meter makes it much easier to perform measurements and helps to obtain more reliable results allowing for unambiguous assessment of the state of road lighting installation.

The Poznan University of Technology team is in possession of one of the most popular imaging luminance meters. The meter requires connection to a PC on which the software is running. This program can be enriched with an EN13201 Add- On enabling calculation of luminance on the road in accordance with the EN 13201 standard.

After performing a number of measurements with the use of this meter, the Poznań University of Technology team states that the currently available luminance meters are not sufficiently well adapted to perform measurements of luminance distributions on the road.

Meters of this type, produced by different companies, are basically laboratory meters and performing measurements by their means in the field is very cumbersome.

THE PROJECT OF CREATING A MODERN EUROPEAN MEASURING INSTRUMENT

Between 2019 and 2020 the GL Optic company based in Poland, specializing in the production of lighting measurement devices, cooperated with the Poznań University of Technology at the stage of research and development and the industrial research. The project "Development of a system for Imaging luminance measurement system" was co-financed by the European Union from the European Regional Development Fund within the Smart Development Programme. The project is implemented within the framework of the National Centre for Research and Development "Fast Track" programme.

Measurements of the luminance distribution on the road can be made by placing the meter in the centre of the traffic lanes. We may have to deal with a different number of lanes and their different width. One of the tasks of the project was to develop the optical system of the meter, which enables measurements to be made with appropriate angular resolution corresponding with the human eye resolution (resulting from the sharpness of vision of the eye's optical system) under conditions of adaptation to the luminance levels occurring in a road illuminated by artificial light. According to the authors of the project, their decision to work on the new meter was motivated by the fact that the at that time available luminance meters on the market did not take into account the above assumptions.

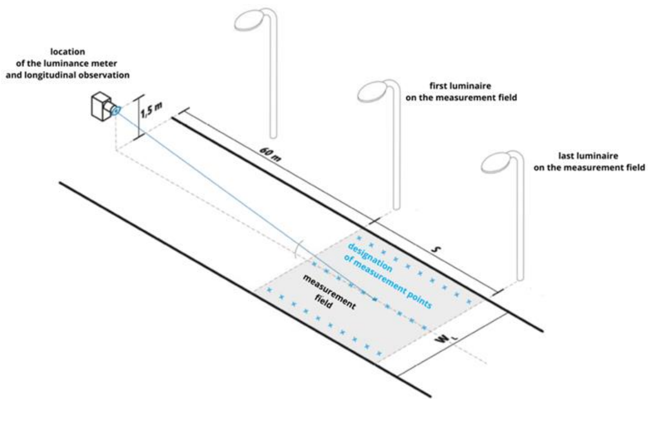

An important task of the project was to develop a measuring system consisting not only of an imaging luminance meter, but also of peripheral devices enabling comfortable measurement of luminance distribution on roads, not requiring specialist knowledge. The imaging luminance meters available on the market are expensive, complicated to operate and not fully adapted to perform luminance measurements on roads in accordance with the requirements of EN 12301. The developed system will enable efficient measurements to be performed by operators who do not have academic expertise.

The newly designed system consists of the following parts:

- a reliable power supply,
- tags enabling the marking of the measurement field,
- optics adapted to the measuring field,
- integrated module enabling efficient and quick setting of the measurement system in a given position by one person, taking into account the requirements of EN 12301,
- convenient system for measuring the distance between the meter and the beginning of the measuring field,
- friendly software enabling efficient, convenient and quick obtaining of results to assess the quality of road lighting according to EN 12301 in real time.

MEASUREMENTS WITH THE IMAGING LUMINANCE MEASURING DEVICE – IMPORTANT ASPECTS

In order to correctly measure the distribution of luminance on the road in accordance with the requirements of the standard, the measuring field between two successive luminaires must be selected. The distance to be measured should be straight. This is rarely the case in practice. Select a distance with as little curvature as possible and, when analysing the measurement results, check that the measuring points do not overlap with the road markings, e.g. the lane dividing lines. In addition, the road behind the measuring field should be illuminated at a distance of at least twelve times the height of the lamp post. The next important step is to mark the measuring field correctly. The markers of the measuring field should clearly indicate the actual boundaries of the area to be measured. This is necessary for the positioning of the calculation points during the analysis of the image recorded with the matrix luminance meter. The next thing to pay attention to is the position of the meter during the measurements. The meter should be positioned in the centre of each lane at a height of 1.5 m above the road surface and 60 m in front of the measuring field, and the optics used must be such that the luminance can be measured over the entire width of the measured road. Finally, before the measurement is taken, the appropriate exposure time must be chosen according to the luminance level of the measuring field.

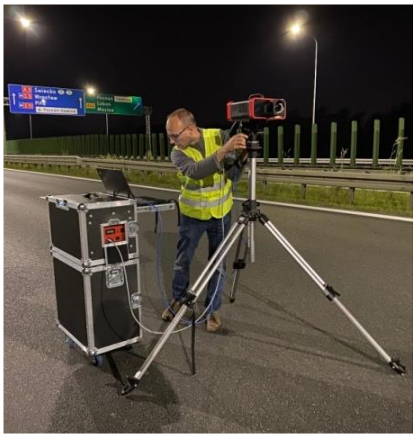

SUMMARY

The use of the new Imaging Luminance Measuring Device GL OPTICAM 3.0 4K TEC allows for performing of reliable measurements and therefore the adequate assessment of lighting parameters on the road is possible thanks to the use of high-class equipment adapted for these purposes. The choice of the meter is particularly important for luminance measurements, as these measurements are difficult, time-consuming and require traffic stops during preparation and measurement. In this situation, the best solution is to use for measurements a measurement system consisting of an imaging luminance meter with appropriately selected optics and friendly software, evaluating the parameters on the road in accordance with the requirements of the EN 13201:2016 standard. Efficient execution of the measurements will be possible if the system is equipped with additional elements, such as: tags for marking the measurement field, a device for measuring the distance between the meter and the measurement field, an integrated module for setting the meter at the appropriate height and position with a computer. The compact form of the measuring system will enable fast and efficient measurement of the luminance distribution on the road by one person only and will minimize the nuisance associated with the reduction of vehicle traffic during measurements, if the measurements are made on the roads in operation.

Advance in 3D Printing Material Offers New Possibility for LED Lighting Technology and Smart Manufacturing

XU Haisheng, Steve Lau, Li Fengjiang.

YD Illumination

Institute of Intelligent Lighting and Control System

Abstract：

Nowadays, because of the advancement of the 3D printing material , 3D printing is widely used in the world. 3D printing technology increasingly used for the education areas, mass customization, in healthcare, automotive industry, aerospace industry, architechture and building, electric and electronic etc. 3D printing or additive manufacturing is the construction of a three-dimensional object from a CAD model or a digital 3D model.Successive layers of material are laid down in different shapes. Traditional machining techniques rely on the removal of material by methods such as cutting or drilling whereas 3D printing layers are added successively. Thus it uses a layering technique where an object is constructed layer by layer until the complete object is manufactured. 3D printing technology has the potential to revolutionize industries and change the production line. In the current market, the conventional 3D printing materials such as PLA, ABS, PETG, TPU and nylon material are used widely. These type of material has limited application usage due to the finished products printed with such materials are prone to aging, fading, deformation and other phenomena when used outdoors, and do not have flame retardancy. Therefore, Institute of new advance materials and lighting research development center of YD Illumination independently developed a new MMLA 3D printing polymer alloy material, which is composed of a variety of polymer materials, solving the technical difficulties of easy aging and poor flame retardancy of materials in the market, and more importantly, it successfully promotes industrial-grade applications and smart manufacturing in the 3D printing industry. 3D printing manufacturing has entered an new era of rapid and smart manufacturing. The printing of parts is being done in a fast and efficient manner thus contributing immensely to the value chain. Customised products are able to be manufactured as customers can edit the digital design file and send to the manufacturer for productions. The personalized creative lamps combined with MMLA printing can be used outdoors or indoors for a long period of time, and it can provide designers with unlimited creative space to realize their design dream. We are convinced that MMLA will bring a revolution in industrial production to the 3D printed lamps and lighting industry.

Keywords：3D Printing, additive manufacturing, flame retardancy, MMLA3D printing polymer alloy material.

1. Introduction:

In recent years, 3D printing technology has been applied in advanced manufacturing as a flexible and powerful technology. 3D printing technology is increasingly used in mass customization, construction sector, healthcare, digital dentistry, education, artificial organs, prosthetics, automotive, locomotive and aerospace industries and lighting industries . The types of 3D printing technologies include Fused Deposition Modelling (FDM), Layered Stacking (GLOM), Stereolithography (SLA), Selective Laser Sintering (SLS), Selective Laser Melting (SLM), etc. Currently on the market, the mainstream 3D printing materials used in the lighting industry are PLA, ABS, PETG, TPU and nylon, etc. There are certain limitations in the application fields. MMLA has strong adaptability and is generally applicable to FDM models on the current market. 3D printing mainstream equipment such as 3D printers.

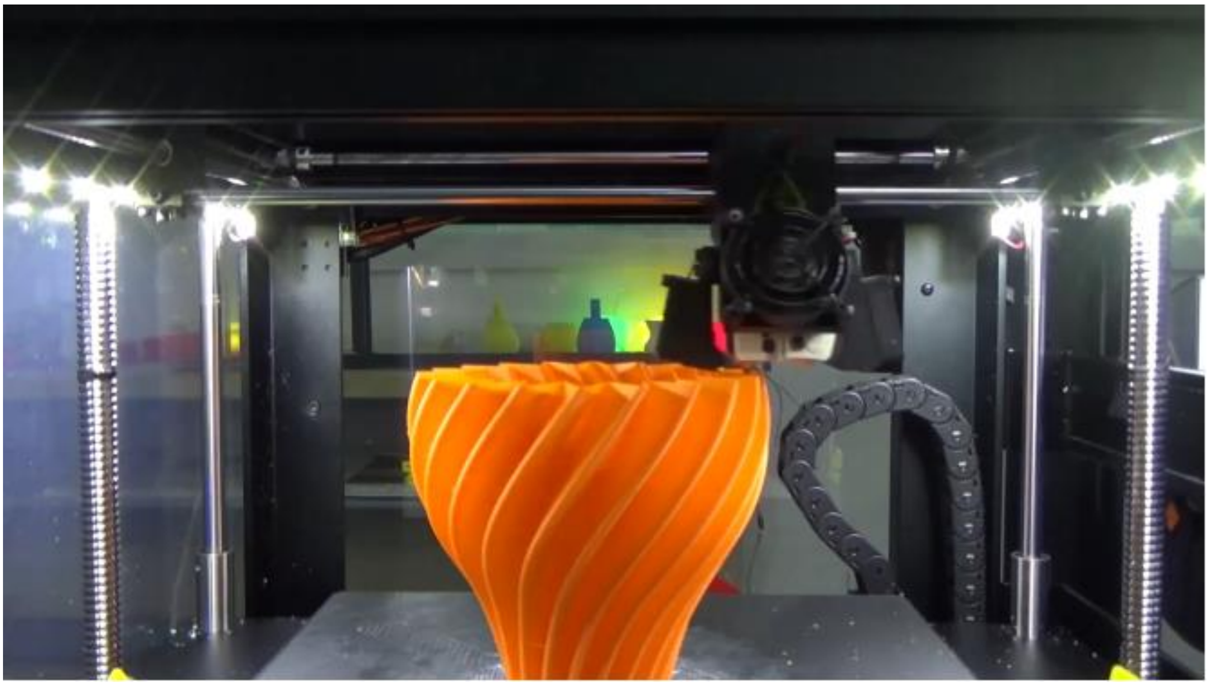

Figure 1: Fused deposition (FDM) is completed by heating and melting layered deposition of fuse type filaments with diameters such as φ1.75mm and φ3m. By reading the cross-section information in the file, the printer prints these cross-sections layer by layer with linear materials, reducing material waste.

2. What is 3D printing and how it works?

Fused Deposition Modelling(FDM) 3D printing is a technology that constructs objects by layer-by-layer printing based on three-dimensional digital model files, using materials such as fuse type filaments. The ideal 3D printing technology can print a solid model of any shape in three-dimensional space, and is not limited by the structural limitation. For product designers, after establishing preliminary design ideas and creative ideas, it is necessary to start the next step to carry out product modelling design or to compose the Computer Aided Diagram (CAD) model. The basic type of design is extracted, and the single elements are arranged and combined in accordance with certain laws or mechanical principles or aesthetic structures. The most basic elements are also composed of points, lines and planes. Considering the nature of modular products and all variety of volumetric requirements, users have freedom and flexibility to stack and combine according to their personal preferences. In general, 3D printing consists of 3 main steps:

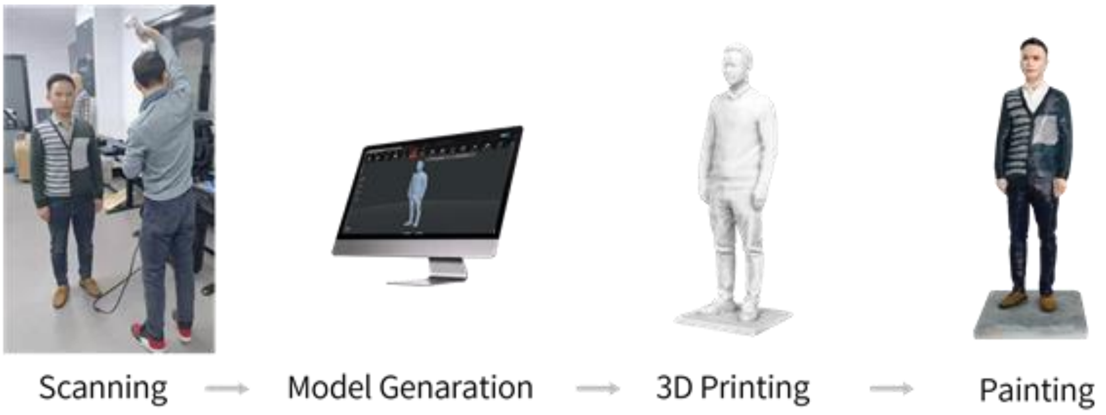

Figure 2: 3D printing process and steps: Scan with 3D scanner, Generation of modeling files, 3D printing, Sample for further processing (painting).

- In the modelling stage, in order to obtain the printed model, the designer can design the product through CAD modelling software, or scan the object to be printed with a 3D scanner or use the original photo of the object, in order to obtain the printed object virtual blueprints. During the process, the product designer can set the shape, texture, size, thickness, and resolution (pixel count) of the sample to be printed.
- During the printing phase, the 3D printer reads the design model or Computer Aided File (CAD) file and deposits layers of material to build the product. Based on 3D digital model files, the technology of constructing objects by layer-by-layer printing using materials such as fuse type wire. With this technique, different objects of various shapes can be created.
- The final stage is to do further processing on the printer sample. In many cases, the finished printed product requires further processing so that the product can achieve the desired outcome. Sometimes, the printed product needs to be further polished to increase the surface smoothness of the product to meet customer needs. If necessary, the product can be further painted to achieve the color desired by the customer, making the printed product more closely resemble the actual physical model.

The invention of MMLA material, combined with 3D printing technology, can directly produce personalized creative lamps that can be used outdoors or indoors for a long period of time, with relative low manufacturing cost. For design needs, it can meet almost any creativity of designers, and save a lot of mold opening costs and manufacturing time. The application of traditional lamps (non 3D printed) in the landscape lighting industry can hardly meet the needs and desires of designers and users, and more and more personalized creative 3D printed luminaires are created. Customizing personalized creative lamps with traditional manufacturing process not only increases pressure on manufacturers (because they can’t make and manufacture it), but also increases engineering costs and processes. The new mold for luminaires needs to be created for the first sample, and it may be repeated several times until the whole process is completed. If it is unsuccessful, it will consume a large quantity of cost and time. Normally it is fine with a large number of orders. If it is a small order, the initial cost of mold opening will be too large, which will inevitably lead to a high average manufacturing cost of lamps and luminaires, which will affect the later operation of the project and cause the engineering company to abandon the project. Sometimes, a lamp designer has a new design idea, the traditional manufacturing process and technology find it hardly to realize the personalized creative lighting that the designer desires even after several attempts, and they could only persuade the designer and the owner to adjust the original design plan. Finally the designer could not achieve the desired effect in the end. In many cases, the engineering company invests a lot of cost in the first sample, and the later the project is abandoned. Using 3D printing technology, personalized and custom made manufacturing in small quantity is very advantageous, and creative lamps that cannot be manufactured by traditional techniques can also be easily created. Some people may also worry that the 3D printing process consumes a lot of time, but compared with the mold opening time of 7-15 days, the printing and manufacturing time can be accelerated with a large number of printing equipment. In short, MMLA combined with 3D printing technology can help to realize the creative dream of designers, make engineering companies more convenient and more beneficial to deal with various projects, and allow project owners to obtain better and more significant project results.

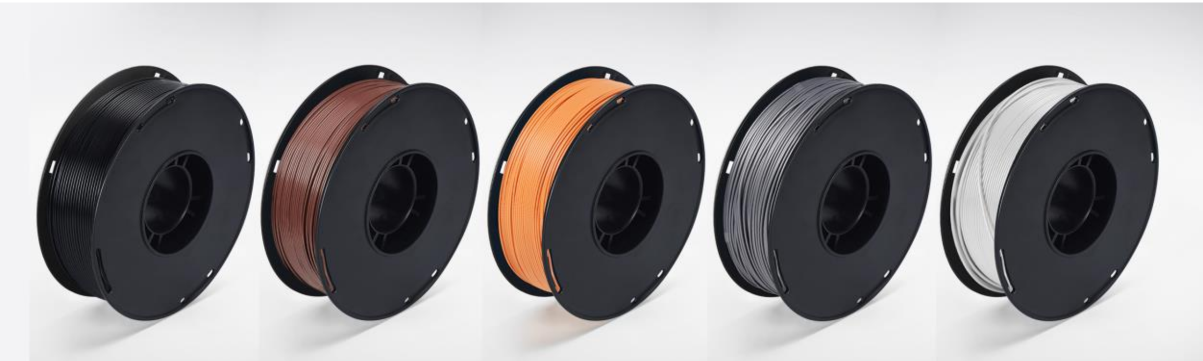

Figure 3: MMLA 3D printing materials can provide a variety of different colors, in addition to the traditional red, green, blue and white, etc., can also be made into other personalized colors such as indigo, pink, orange, etc.

2. MMLA 3D printing polymer alloy consumable material

The new invented MMLA material has superior performance and it breaks through the limitations of 3D printing product applications. It solves the critical limitations of fast aging and poor flame retardancy of 3D printing consumable material in the existing lighting market, making 3D printing process truly industrialized and promoting the development of the 3D printing industry. In addition, the printed product has high strength, good compatibility, and has broad application. The 3D printed product made of MMLA material has high impact strength and high torsional strength, and is fully suitable for long-term use in industrial manufacturing. Because the molecular structure of the polymer material alloy of MMLA contains polar groups and non-polar groups, it has good compatibility with other material like paints, glues and other plastic materials. The main properties of MMLA 3D printing polymer alloy consumable material achieves the following breakthrough:

- Flame retardancy V-0 grade: It has reached the highest flame retardant grade of polymer materials, and improved the fire safety performance for advertising and marked products.
- Passed the ultraviolet aging test: it can be used outdoors for a long time, which improves the service life of advertising logo products.
- The long-term use temperature reaches 75℃: it can be used outdoors in high temperature environment.
- Passed the ROHS certification: it has met the environmental protection requirements of the product.
- The printing speed can be increased by more than 30% compared with traditional 3D printing consumable material, which reduces the manufacturing time and cost.
- It is made of a variety of polymer material alloys, and the finished product has high strength: it reduces the damage rate of the 3D printed product during transportation.
- Has a great cost advantage: On the premise of improving the overall performance, the production cost is close to that of most 3D printing consumable material on the market.
- Stable price: The source of raw materials is abundant, which avoids the price fluctuation caused by the monopoly of some consumable raw materials in the market. It has laid the foundation for the large-scale, industrialized and smart production process of the logo industry.

Table 1： Comparison table for MMLA，PLA， PETG， ABS

Name of Material	Chemical content	Advantages	Disadvantages	Application
MMLA	A variety of polymer alloy materials	Flame retardant, anti-UV (ultraviolet), high strength, high and low temperature resistance, multiple colors (bright), fast printing speed	Slightly poor surface finishing	Support industrialized and smart manufacturing of indoor and outdoor lamp shells, support 3D printing and manufacturing of indoor and outdoor electronic and electrical accessories with complex shapes and structures, production of decorative materials, printing and manufacturing of durable models, printing of indoor and outdoor signs, indoor and outdoor sculpture artworks printing etc.
PLA	It is chemically synthesized using polylactic acid, the product of microbial fermentation, as a monomer.	Low cost, precise size, easy to use, self-degradable	Flammable, prone to oxidative fracture, vulnerable to environmental influences	Disposable models, toys, R&D and printing product molds, models, product packaging, for education purposes etc.
PETG	It is a crystalline saturated polyester resin	Smooth and shiny surface, strong electrical insulation, strong water resistance	Long molding cycle time, high molding shrinkage, and poor dimensional stability	Electronic devices, daily necessities parts, instrument accessories, etc.
ABS	Acrylonitrile (A), Butadiene (B), Styrene (S), is a thermoplastic polymer material	Low cost, strong fluidity, rigidity, high temperature resistance.	Flammable, poor weather resistance (easy to degrade under UV light, poor impact strength)	Car interior accessories, electronic devices, building materials and DIY devices

Figure 4: With MMLA material and 3D printing, customers can freely choose the shape, size, color and texture of their favorite lamps, and truly make their home lamps have an unprecedented experience of unique personalized lamps.

Figure 5: MMLA used as outdoor flame retardant high and low temperature resistant consumable material have excellent performance like high strength of finished products, and can be used in outdoors application for a long period of time, such as garden lawn lamps.

3. MMLA 3D printing materials provide infinite possibilities for LED smart manufacturing

MMLA materials can present a variety of colors, apart from the traditional red, green, blue and white, etc., it can also be made into other personalized colors such as indigo, pink, orange and so on. The invention of

MMLA material, combined with 3D printing technology, can directly produce personalized creative lamps that can be used outdoors or indoors for a long period of time, according to their personal preferences, so as to achieve the designer's favorite color and choice. MMLA production technology can produce a variety of personalized colors lamp covers and then match with LED white light. According to the CIE color mixing principle, it can basically achieve thousands of color matching as the outcome of matching between LED white light and lamp cover, which further strengthens and realizes the designer's uniqueness color selection. When printing the samples of Lux Europa this time, the product designers of YD Illumination choose the two famous scenic spots in Beijing Temple of Heaven and Hangzhou Three Pools Mirroring the Moon. The purpose is to promote these two famous scenic spots to Europe. Attractions, but customers can choose their favorite attractions or patterns, and then print it into a unique luminous surface.

Folk story and history about the Temple of Heaven[1] Park in Beijing and Hangzhou Three Pools Mirroring the Moon:

The Temple of Heaven was built in the Yongle Emperor of Ming Dynasty (1403-1420), and it is a national altar established according to the traditional Chinese etiquette system. Since the nineteenth year of Yongle in the Ming Dynasty, a total of 22 emperors have personally worshipped the GOD devoutly the Temple of Heaven. After the outbreak of the 1911 Revolution, the government of the Republic of China announced the abolition of the ceremonies for worshiping the heavens, and in 1918 the Temple of Heaven was changed to a park. The sacrificial ceremony lasted about five thousand years. In 1961, the State Council announced the Temple of Heaven as a "National Key Cultural Relics Protection Unit". It was recognized as a "World Cultural Heritage" by UNESCO in 1998. On May 8, 2007, the Temple of Heaven Park was officially approved by the National Tourism Administration as a national 5A-level tourist attraction.

Three Pools Mirroring the Moon is one of the ten scenic spots of West Lake in Hangzhou, Zhejiang Province, China and is known as "the first scenic spot in the West Lake". It is the largest island in the West Lake, with beautiful scenery and quiet scenery. The entire Area was declared a UNESCO World Heritage site and has some of the most beautiful landscapes (natural and man-made) in the world. This islet has been created from reclaimed land during the Ming Dynasty, on which three pavilions and pools were built during the Song Dynasty. Because of the beautiful scenery of the Three Pools and the Moon, China put its image on the coins. The first was the one dollar-yuan note Ren Min Bi in the late 1970s, with the emerald green pattern of three pavilions and the moon on the front.

Figure 6: When printing the samples of Lux Europa, the product designers of YD Illumination choose the two famous scenic spots in Beijing Temple of Heaven and Hangzhou Three Pools Mirroring the Moon. The purpose is to promote these two famous Chinese attractions to the European people. You can choose your favourite attractions or patterns, and then print them into unique luminous surfaces.

4. MMLA 3D consumable material meets safety & performance , environmental protection，high light efficiency and reliability requirements：

MMLA is a polymer alloy material that possess flame-retardant V-0 and anti-UV (Ultraviolet) characteristic and it is environmental friendly and has high strength. It is created by blending and combining a variety of polymer materials, and is compatible with most paints and inks. It has good compatibility and suitable for coloring processing. MMLA is an industrial-grade 3D printing consumable. MMLA material can not merely be used as an outdoor flame-retardant and high & low temperature resistant consumable material, it can also can be used as a general-purpose consumable and model consumable material. Among them, MMLA used as outdoor flame retardant high and low temperature resistant consumable material have excellent performance like high strength of finished products, and can be used indoors and outdoors for a long period of time. MMLA used as general consumable material have a wide range of applications, good uniformity, bright colors and smooth surfaces. MMLA used as model consumable material have bright color and good texture of printing models, smooth and delicate. 3D printing polymer alloy consumables MMLA solves the critical limitation of fast aging and poor flame retardancy characteristic in the existing market. With its superior material properties, it breaks through the limitations of the application of 3D printing products and can be widely used in the logo industry, indoor and outdoor lighting industry, construction industry, industrial models, art installations, education and other fields like. industrial grade applications and smart manufacturing. At the same time, MMLA has strong adaptability and is generally applicable to mainstream 3D printing equipment such as FDM mode logos and model 3D printers on the market. Since LED luminaires are installed in public areas, the fire safety of the LED luminaires used is very important. The 3D printed MMLA alloy material can reach the highest flame retardant grade V-0, which is a requirement to ensure fire safety. Not only that, because the outdoor use is exposed to the sun and rain for a long time, the materials used must have good light transmittance, so that the photons are not trapped by the protective layer too much, and must also have anti-ultraviolet performance, anti-oxidation performance, resistance to high and low temperature. In addition, MMLA materials also meet the limit requirements of the above hazardous substances that must be met by the products that enterprises export to the EU, that is, ROHS environmental protection requirements (Directive on the restriction of the use of certain hazardous substances in electrical and electronic equipment). After strict testing by laboratories accredited by CNAS, MMLA materials fully meet the environmental protection requirements of RoHS 1 & RoHS 2.

160002112091
中国认可
国际互认
检测
TESTING
CNAS L0116

检 测 报 告
TEST REPORT

报告编号 REPORT NO. 2013105513A
样品名称 NAME OF SAMPLE 3D 打印户外高分子合金耗材
委托单位 CUSTOMER 杭州勇电照明有限公司
受检单位 INSPECTED ENTITY /
检测类别 TEST CATEGORY 委托检测

国家化学建材质量监督检验中心
STATE CENTER OF SUPERVISION AND TEST FOR CHEMICAL BUILDING MATERIALS

报告编号（Report NO.）: 2013105513A　　第 2 页 共 2 页（Page 2 of 2 ）

检 测 报 告
TEST REPORT

序号 Series Number	检 测 项 目 Test Items	技 术 要 求 Requirement	检 测 结 果 Test Results	单项结论 Item Conclusion	备注 Remarks
1	紫外老化后外观变化（24h，灯型：UVA-340，辐照度：0.76W・m^{-2}・nm^{-1}，暴露方式：60℃辐照 8h；50℃无辐照冷凝 4h）	/	表面无明显变化	/	/
2	塑料氙弧灯老化后外观变化（24h）	/	表面无明显变化	/	/
3	垂直燃烧试验	/	V-0 级	/	/

以下空白 TEST REPORT END

Figure 7: MMLA material meets UV test, plastic aging test, vertical burning test. All tests are carried out in laboratories accredited by CNAS.

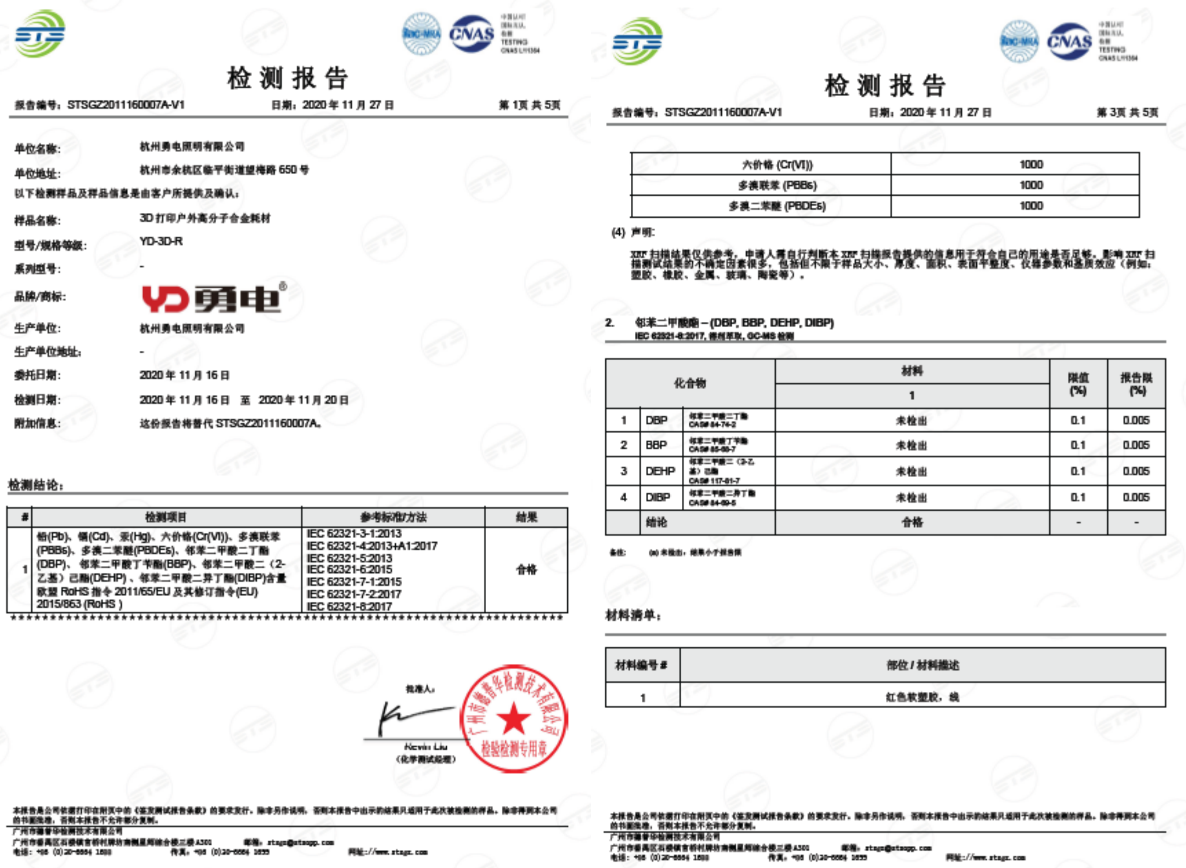

检 测 报 告

报告编号：STSGZ2011160007A-V1　日期：2020 年 11 月 27 日　第 1页 共 5页

单位名称: 杭州勇电照明有限公司

单位地址: 杭州市余杭区临平街道望梅路 650 号

以下检测样品及样品信息是由客户所提供及确认：

样品名称: 3D 打印户外高分子合金耗材

型号/规格等级: YD-3D-R

系列型号: -

品牌/商标: YD 勇电®

生产单位: 杭州勇电照明有限公司

生产单位地址: -

委托日期: 2020 年 11 月 16 日

检测日期: 2020 年 11 月 16 日 至 2020 年 11 月 20 日

附加信息: 这份报告将替代 STSGZ2011160007A。

检测结论：

#	检测项目	参考标准/方法	结果
1	铅(Pb)、镉(Cd)、汞(Hg)、六价铬(Cr(VI))、多溴联苯(PBBs)、多溴二苯醚(PBDEs)、邻苯二甲酸二丁酯(DBP)、邻苯二甲酸丁苄酯(BBP)、邻苯二甲酸二（2-乙基）己酯(DEHP)、邻苯二甲酸二异丁酯(DIBP)含量 欧盟 RoHS 指令 2011/65/EU 及其修订指令(EU) 2015/863 (RoHS)	IEC 62321-3-1:2013 IEC 62321-4:2013+A1:2017 IEC 62321-5:2013 IEC 62321-6:2015 IEC 62321-7-1:2015 IEC 62321-7-2:2017 IEC 62321-8:2017	合格

批准人：Kevin Liu（化学测试经理）

检　测 报 告

报告编号：STSGZ2011160007A-V1　日期：2020 年 11 月 27 日　第 3页 共 5页

六价铬 (Cr(VI))	1000
多溴联苯 (PBBs)	1000
多溴二苯醚 (PBDEs)	1000

(4) 声明:

XRF 扫描结果仅供参考，申请人需自行判断本 XRF 扫描报告提供的信息用于符合自己的用途是否足够。影响 XRF 扫描测试结果的不确定因素很多，包括但不限于样品大小、厚度、面积、表面平整度、仪器参数和基质效应（例如：塑胶、橡胶、金属、玻璃、陶瓷等）。

2. 邻苯二甲酸酯 – (DBP, BBP, DEHP, DIBP)
IEC 62321-8:2017, 溶剂萃取, GC-MS 检测

化合物			材料 1	限值 (%)	报告限 (%)
1	DBP	邻苯二甲酸二丁酯 CAS# 84-74-2	未检出	0.1	0.005
2	BBP	邻苯二甲酸丁苄酯 CAS# 85-68-7	未检出	0.1	0.005
3	DEHP	邻苯二甲酸二（2-乙基）己酯 CAS# 117-81-7	未检出	0.1	0.005
4	DIBP	邻苯二甲酸二异丁酯 CAS# 84-69-5	未检出	0.1	0.005
	结论		合格	-	-

备注: (a) 未检出，结果小于报告限

材料清单：

材料编号 #	部位 / 材料描述
1	红色软塑胶，线

Figure 8: MMLA material meets RoHS1 and RoHS 2 test. ROHS testing is carried out in laboratories accredited by CNAS.

Figure 9: Laboratory technicians are conducting optical tests and UV resistance experiments on MMLA 3D printing materials. The equipment used is calibrated and traceable to the National Metrology Laboratory of China.

5. Summary

3D printing offers the possibility to make creativity into reality in rapid speed. Through 3D printing, lighting product designers have the possibility to create complex object with different shapes, sizes, colors and textures in order to meet the unique needs of customers, which is almost impossible obtained by any existing and conventional manufacturing techniques. A very important advantage of using 3D printing technology to create objects is the reduction of waste. 3D printed materials can be reused and re-printed, which further promotes recycling, energy saving and environmental protection. This paper focuses on the description of the new 3D printing material MMLA, which breaks through the limitations of the application of 3D printing products with its superior performance, and solves the critical limitation of fast aging and poor flame retardancy of the existing 3D printing consumable material in the market. The printed products truly realize industrial application and promote the development of the 3D printing industry. The invention of MMLA, combined with 3D printing technology, can produce personalized creative lamps that can be used outdoors or indoors for a long period of time, and the manufacturing cost is low, and the design can meet almost any creativity of designers. In addition, MMLA is an industrial-grade 3D printing consumable material, which can not merely be used as an outdoor flame-retardant high-low temperature resistant consumable material, but also can be used as a general-purpose consumable material and model consumable material. Therefore, we are convinced that this will further promote the revolutionary and explosive growth of smart manufacturing, which is the future development trend. In the future, the importance and social impact of 3D printing technology will gradually increase, which will bring a significant influence on human life, economy and modern society.

References

1. P. Holzmann, J. Robert, A. Aqeel Breitenecker, Soomro, & J. S. Erich, “User entrepreneur business models in 3D printing,” Journal of Manufacturing Technology Management, Vol. 28, No. 1, pp. 75-94, 2017.
2. L. Jian-Yuan, A. Jia, & K. C. Chee, “Fundamentals and applications of 3D printing for novel materials,” Applied materials today, Vol 7, pp.120-133, 2017.
3. Evans B., Practical 3D Printers: The Science and Art of 3D Printing, Apress Publisher, 2012.
4. Bob Hayward, David Moschella, Jon Schreiber, Simon Wardley, Howard Smith, “3D printing and the future of manufacturing” CSE, the rise of 3D printing.

Xu Haisheng
Institute of Intelligent Lighting and Control System for YD Illumination
Address ： No. 587, Kangxin Road, Linping District, Hangzhou City, Zhejiang, CHina
handphone : +86 18367195915
email : xu.haisheng@china-yd.com

LUX EUROPA COUNCIL

President:

Dionýz Gašparovský	SK	Slovenská svetelnotechnická spoločnosť (SSTS)

Members:

Peter Dehoff	AT	Lichttechnische Gesellschaft Österreichs (LTG)
Frédéric Leloup	BE	Belgian Institute on Illumination (IBE-BIV)
Kiril Kasev	BG	National Committee for Lighting in Bulgaria (NKO)
Mario Rechsteiner	CH	Schweizer Licht Gesellschaft (SLG)
Tomáš Novák	CZ	Česká společnost pro osvětlování (ČSO)
Matthias Hessling	DE	Deutsche Lichttechnische Gesellschaft e.V. (LiTG)
Per Reinholdt	DK	Dansk Center for Lys (DCL)
Manuel Melgosa	ES	Comité Español de Iluminación (CEI)
Heikki Härkönen	FI	Suomen valoteknillinen seura (IES)
Marie-Pierre Alexandre	FR	Association Francaise de l'Éclairage (AFE)
Frangiskos Topalis	GR	Hellenic Lighting Association (HELIA)
Péter Schwarcz	HU	Világítástechnikai Társaság (VTT)
Pat Lehane	IE	Lighting Association Ireland (LAI)
Laura Bellia	IT	Associazione Italiana di Illuminazione (AIDI)
Geertje Hazenberg	NL	Nederlandse Stichting Voor Verlichtingskunde (NSVV)
Katia Valerie Banoun	NO	Lyskultur
Piotr Pracki	PL	Polski Komitet Oświetleniowy SEP (PKO)
Anna Shakhparunyants	RU	Российский национальный комитет МКО (CIE NC RU)
Dorin Beu	RO	Asociația Română de Iluminat (ARI)
Miomir Kostić	RS	Srpsko društvo za osvetljenie (DOS)
Grega Bizjak	SI	Slovensko društvo za razsvetljavo (SDR)
Mehmet Kucukdogu	TR	Aydınlatma Türk Milli Komitesi (ATMK)
Peter Thorns	UK	Society of Light and Lighting (SLL)

BOARD OF DIRECTORS

Chairman:

Dionýz Gašparovský	SK	Slovenská svetelnotechnická spoločnosť (SSTS)

Members:

Peter Dehoff	AT	Lichttechnische Gesellschaft Österreichs (LTG)
Frédéric Leloup	BE	Belgian Institute on Illumination (IBE-BIV)
Mario Rechsteiner	CH	Schweizer Licht Gesellschaft (SLG)
Tomáš Novák	CZ	Česká společnost pro osvětlování (ČSO)
Matthias Hessling	DE	Deutsche Lichttechnische Gesellschaft e.V. (LiTG)
Laura Bellia	IT	Associazione Italiana di Illuminazione (AIDI)
Geertje Hazenberg	NL	Nederlandse Stichting Voor Verlichtingskunde (NSVV)
Piotr Pracki	PL	Polski Komitet Oświetleniowy SEP (PKO)
Grega Bizjak	SI	Slovensko društvo za razsvetljavo (SDR)
Mehmet Kucukdogu	TR	Aydınlatma Türk Milli Komitesi (ATMK)
Peter Thorns	UK	Society of Light and Lighting (SLL)

PROGRAMME COMMITTEE

Chairman:

Dionýz Gašparovský	SK

Members:

László Balázs	HU	Rafał Krupiński	PL
Meike Barfuß	DE	Frédéric Leloup	BE
Laura Bellia	IT	Banu Manav	TR
Dorin Beu	RO	Balázs Vince Nagy	HU
Grega Bizjak	SI	Tomáš Novák	CZ
Urszula Błaszczak	PL	Sermin Onaygil	TR
Constantinos Bouroussis	GR	Anna Pellegrino	IT
Karl Brandstätter	AT	Piotr Pracki	PL
Vladimir Budak	RU	Thomas Römhild	DE
Lambros Doulos	GR	Wouter Ryckaert	BE
Roman Dubnička	SK	Axel Stockmar	DE
Simonetta Fumagalli	IT	Raisa Stolyarevskaya	RU
Catalin Galatanu	RO	Marek Šmíd	CZ
Peter Hanuliak	SK	Peter Thorns	UK
Valéry Ann Jacobs	BE	Frangiskos Topalis	GR
Peter Janiga	SK	Rengin Ünver	TR
Matej B. Kobav	SI	Michal Vik	CZ
Zoltán Kolláth	HU		

SPONSORS

GOLD

SILVER

BRONZE

TABLE OF CONTENTS

PART I

PART II

we bring daylight into dark spaces

Heliobus®

The daylight company

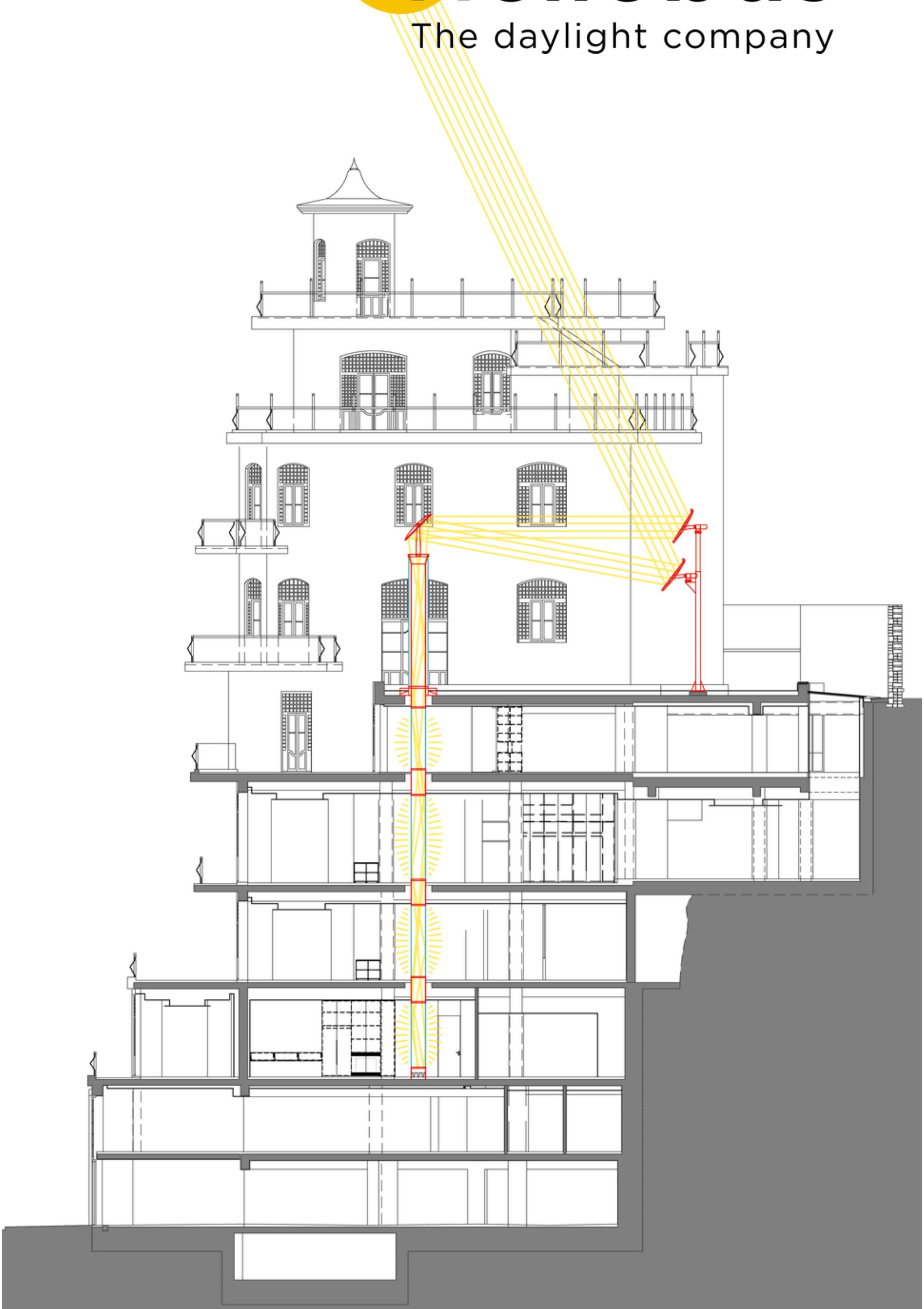

ZUMTOBEL SPECTRUM – WHEN INVISIBLE MATTERS

Even though blue light is not dangerous in everyday life, it can strain the eye. Zumtobel has responded with a new technology that significantly improves visual comfort by changing the LED colour spectrum:

Zumtobel Spectrum.

Light with its visual and non-visual effects has a major impact on our health. The biological, i.e. non-visual, effect is becoming increasingly important. It influences sleep quality, important bodily functions and general well-being. Modern lighting concepts already take account of the non-visual effects of light. Zumtobel now goes one step further and changes the LED colour spectrum within a specific wavelength range in which the eye is particularly sensitive to visual, emotional and biological stimuli. In doing so, Zumtobel is guided by the daylight spectrum.

Adaptation of the LED light spectrum

Zumtobel Spectrum harmonises the light spectrum to get as close as possible to daylight as seen from the human eye. In doing so, the intensities of the blue wavelengths are significantly reduced, while the azure wavelengths are simultaneously increased. The eye does not perceive the difference to regular LED lighting, but it is less strained. At the same illuminance, the pupil diameter of a standard LED light spectrum tends to be larger than in natural daylight. Zumtobel Spectrum reduces the diameter and helps the pupil to stay in its natural size. This reduces the amount of light entering the eye, and the strain on the retina is reduced. The result: the eyes remain relaxed and do not tire so quickly. This not only has a positive effect on concentration but also enables the eye to relax more quickly and easily after strenuous visual tasks.

The standard LED light spectrum usually causes the pupil to have a larger diameter than in natural daylight of the same intensity. The Zumtobel Spectrum reduces the diameter of the pupil, so that the pupil stay in its natural size. This reduces the amount of light entering the eye and reduces the strain on the retina. As a result, the eyes remain relaxed and do not tire as quickly.

About the Zumtobel Group

The Zumtobel Group aims to create wellbeing and improve people's quality of life through light – as a group, and through all its individual brands, Thorn, Tridonic and Zumtobel. As a leading supplier of innovative lighting solutions, the Group offers its customers around the world a comprehensive portfolio, where the focus is invariably on people and their needs. The company's know-how about the effects of light on people, acquired over decades, forms the basis for sustainable and future-oriented lighting solutions that are increasingly energy- and resource-efficient while providing the best possible quality of light. The Group is listed on the Vienna Stock Exchange (ATX Prime) and currently holds a workforce of around 5,800 employees. In the 2021/22 financial year, the company posted revenues of EUR 1,148.3 million. The Zumtobel Group is based in Dornbirn in the Vorarlberg region of Austria. For further information, please visit z.lighting/group.

ZUMTOBEL Group

Light quality control

www.gloptic.com

ISBN 978-80-11-02269-3
EAN 9788011022693